

# THE JOURNAL

OF THE

# INSTITUTE OF METALS

VOLUME LXXVII

1950

EDITOR

N. B. VAUGHAN, M.Sc.

*The Right of Publication and of Translation is Reserved*



*The Institute of Metals is not responsible either for the statements made or  
for the opinions expressed in the following pages*

LONDON  
PUBLISHED BY THE INSTITUTE OF METALS  
4 GROSVENOR GARDENS, S.W.1

1950

*Copyright]*

*[Entered at Stationers' Hall*

## PAST-PRESIDENTS.

Sir WILLIAM HENRY WHITE, K.C.B., LL.D., D.Eng., Sc.D., F.Inst.Met., F.R.S.,  
1908-1910 (*deceased*).

Sir GERARD ALBERT MUNTZ, Bart., 1910-1912 (*deceased*).

Professor WILLIAM GOWLAND, A.R.S.M., F.R.S., 1912-1913 (*deceased*).

Professor ALFRED KIRBY HUNTINGTON, A.R.S.M., 1913-1914 (*deceased*).

Engineer Vice-Admiral Sir HENRY JOHN ORAM, K.C.B., F.Inst.Met., F.R.S.,  
1914-1916 (*deceased*).

Sir GEORGE THOMAS BEILBY, LL.D., D.Sc., F.R.S., 1916-1918 (*deceased*).

Professor Sir HENRY CORT HAROLD CARPENTER, M.A., Ph.D., D.Sc., D.Met.,  
A.R.S.M., F.Inst.Met., F.R.S., 1918-1920 (*deceased*).

Engineer Vice-Admiral Sir GEORGE GOODWIN GOODWIN, K.C.B., LL.D.,  
F.Inst.Met., 1920-1922 (*deceased*).

LEONARD SUMNER, O.B.E., M.Sc., J.P., F.Inst.Met., 1922-1924 (*deceased*).

Professor-Emeritus THOMAS TURNER, M.Sc., A.R.S.M., F.Inst.Met.,  
1924-1926 (*deceased*).

Sir JOHN DEWRANCE, G.B.E., F.Inst.Met., 1926-1928 (*deceased*).

WALTER ROSENHAIN, D.Sc., B.C.E., F.Inst.Met., F.R.S., 1928-1930 (*deceased*).

RICHARD SELIGMAN, Ph.nat.D., F.Inst.Met., 1930-1932.

Sir HENRY FOWLER, K.B.E., LL.D., D.Sc., 1932-1934 (*deceased*).

HAROLD MOORE, C.B.E., D.Sc., Ph.D., F.Inst.Met., 1934-1936.

WILLIAM ROBB BARCLAY, O.B.E., F.Inst.Met., 1936-1938 (*deceased*).

CECIL HENRY DESCH, D.Sc., LL.D., Ph.D., F.Inst.Met., F.R.S., 1938-1940.

The Hon. RICHARD MARTIN PETER PRESTON, D.S.O., 1940-1942.

Lieut.-Colonel Sir JOHN HENRY MAITLAND GREENLY, K.C.M.G., C.B.E., M.A.,  
F.Inst.Met., 1942-1944 (*deceased*).

Sir WILLIAM THOMAS GRIFFITHS, D.Sc., 1944-1946.

Colonel Sir PAUL GOTTLIEB JULIUS GUETERBOCK, K.C.B., D.S.O., M.C.,  
T.D., D.L., J.P., M.A., A.D.C., F.Inst.Met., 1946-1948.

Sir ARTHUR JOHN GRIFFITHS SMOUT, J.P., 1948-1950.



# OFFICERS AND COUNCIL

FOR THE YEAR 1950-1951

---

PRESIDENT:

H. S. TASKER, B.A.

PAST-PRESIDENTS:

SIR WILLIAM GRIFFITHS, D.Sc.

COLONEL SIR PAUL GUETERBOCK, K.C.B., D.S.O., M.C., T.D., D.L.,  
J.P., M.A., A.D.C., F.Inst.Met.

SIR ARTHUR SMOUT, J.P.

VICE-PRESIDENTS:

MAJOR C. J. P. BALL, D.S.O., M.C.  
S. F. DOREY, C.B.E., D.Sc., Wh.Ex.,  
F.R.S.  
PROFESSOR A. J. MURPHY, M.Sc.

PROFESSOR H. O'NEILL, D.Sc., M.Met.  
C. J. SMITHELLS, M.C., D.Sc.  
PROFESSOR F. C. THOMPSON, D.Met.,  
M.Sc.

HONORARY TREASURER:

W. A. C. NEWMAN, O.B.E., B.Sc., A.R.S.M., A.R.C.S.

ORDINARY MEMBERS OF COUNCIL:

JOHN ARNOTT.  
G. L. BAILEY, M.Sc.  
E. A. BOLTON, M.Sc.  
D. F. CAMPBELL, M.A., A.R.S.M.  
MAURICE COOK, D.Sc., Ph.D.  
HARRY DAVIES.  
C. H. DAVY.  
T. M. HERBERT, M.A.  
H. W. G. HIGNETT, B.Sc.

E. H. JONES.  
D. P. C. NEAVE, M.A.  
L. B. PFELL, O.B.E., D.Sc., A.R.S.M.  
A. R. POWELL.  
PROFESSOR A. G. QUARRELL, D.Sc.  
Ph.D., A.R.C.S., D.I.C.  
PROFESSOR G. V. RAYNOR, M.A.,  
D.Sc., D.Phil.

EX-OFFICIO MEMBERS OF COUNCIL:

(Chairmen of Local Sections)

BIRMINGHAM: BERNARD THOMAS.  
LONDON: E. A. G. LIDDIARD, M.A.  
SCOTTISH: H. R. BEAUCHAMP.

SHEFFIELD: H. G. DALE.  
SOUTH WALES: E. A. HONTOIR,  
B.Sc.

---

REPRESENTATIVES OF OTHER BODIES.

The following, in accordance with Article 32, represent Government departments and allied societies at Council meetings for purposes of liaison:

ADMIRALTY:

CAPTAIN (E) L. A. B. PEILE, D.S.O.,  
M.V.O., R.N.

IRON AND STEEL INSTITUTE:

J. R. MENZIES-WILSON, O.B.E.

INSTITUTION OF METALLURGISTS:

E. W. COLBECK, M.A.  
L. ROTHERHAM, M.Sc.

WAR OFFICE:

MAJOR-GENERAL S. W. JOSLIN,  
M.B.E., B.A.

---

SECRETARY:

LIEUT.-COLONEL S. C. GUILLAN, T.D.

ASSISTANT SECRETARY:

MAJOR R. E. MOORE.

EDITOR:

N. B. VAUGHAN, M.Sc.

**CHAIRMEN AND HONORARY SECRETARIES OF THE  
LOCAL SECTIONS.**

at 31 December 1950.

**Birmingham.**

*Chairman* : BERNARD THOMAS, Leigh House, Bradmore Road,  
Wolverhampton.

*Hon. Secretary* : E. H. BUCKNALL, M.Sc., "Ardarroch", 264 Harborne  
Park Road, Harborne, Birmingham 17.

*Hon. Treasurer* : R. CHADWICK, M.A., 5 Fairmead Rise, King's Norton,  
Birmingham, 30.

**London.**

*Chairman* : E. A. G. LIDDIARD, M.A., Fulmer Research Institute, Stoke  
Poges, Bucks.

*Hon. Secretary* : E. C. RHODES, Ph.D., B.Sc., The Mond Nickel Company, Ltd.,  
Development and Research Department, Bashley Road, London, N.W.10.

*Hon. Treasurer* : J. D. GROGAN, B.A., Metallurgy Division, National  
Physical Laboratory, Teddington, Middlesex.

**Scottish.**

*Chairman* : H. R. BEAUCHAMP, Imperial Chemical Industries, Ltd., Metals  
Division, 4 Blythswood Square, Glasgow, C.2.

*Hon. Secretary* : MATTHEW HAY, A. Cohen and Co., Ltd., Craighton Industrial  
Estate, Barfillan Drive, Cardonald, Glasgow, S.W.2.

*Hon. Treasurer* : N. J. MACLEOD, Steven and Struthers, Ltd., 86 Eastvale Place,  
Kelvinhaugh, Glasgow, C.3.

**Sheffield.**

*Chairman* : H. G. DALE, Sheffield Smelting Co., Ltd., Sheffield.

*Joint Hon. Secretaries* : A. J. MACDOUGALL, M.Met., and W. R. MADDOCKS,  
Ph.D., B.Sc., Department of Applied Science, The University,  
St. George's Square, Sheffield 1.

*Hon. Treasurer* : W. R. MADDOCKS, Ph.D., B.Sc., Department of Applied  
Science, The University, St. George's Square, Sheffield 1.

**South Wales.**

*Chairman* : E. A. HONTOIR, B.Sc., Rio Tinto Co., Ltd., Port Talbot.

*Hon. Secretary* : K. M. SPRING, 36 Beechwood Road, Uplands, Swansea.

*Hon. Treasurer* : W. H. GRENFELL, "The Woods", Bryn Terrace, Mumbles,  
Swansea.

**CORRESPONDING MEMBERS TO THE COUNCIL.**

at 31 December 1950.

**Argentina.**

H. N. BASSETT,  
Shell Mex Argentina, Ltd., Casilla Correo 1759, Buenos Aires.

**Australia.**

Professor H. K. WORNER, D.Sc.,  
Professor of Metallurgy, University of Melbourne, Carlton, N.3, Melbourne,  
Victoria.

**Belgium.**

H. P. A. FÉRON,  
Administrateur-Directeur, Visseries et Tréfileries Réunies, 2 Avenue  
Général Leman, Haren, Bruxelles.

**Canada.**

Professor BRUCE CHALMERS, Ph.D., D.Sc.,  
Department of Metallurgical Engineering, University of Toronto, Toronto 5,  
Ontario.

Professor G. LETENDRE, B.A., Ph.D., Professor of Metallurgy and  
Director, Department of Mining and Metallurgical Engineering, Faculty of  
Sciences, Laval University, Boulevard de l'Entente, Quebec City, P.Q.

**France.**

Professor P. A. J. CHEVENARD,  
Directeur Scientifique, Société Anonyme de Commentry-Fourchambault et  
Decazeville, 84 rue de Lille, Paris 7e.

JEAN MATTER, Vice-Président et Directeur-Général, Société Centrale des  
Alliages Légers, Issoire, Puy-de-Dôme.

**India.**

N. P. GANDHI, M.A., B.Sc., A.R.S.M., D.I.C.,  
Kennaway House, Proctor Road, Girgaon, Bombay 4.

**Italy.**

LENO MATTEOLI, Dott.chim.,  
Vice-Director, Istituto Scientifico Tecnico Ernesto Breda, Sesto S. Giovanni,  
Milano.

**Netherlands.**

M. HAMBURGER, Director, N.V. Royal Nederlandsche Lood- en Zinkpletterijen  
voorheen A.D. Hamburger, Leidschekade 30, Utrecht.

**South Africa.**

G. H. STANLEY, D.Sc., A.R.S.M.,  
24 Duncombe Road, Forest Town, Johannesburg, Transvaal.  
Professor L. TAVERNER, A.R.S.M., D.I.C., Professor of Metallurgy and  
Assaying, University of the Witwatersrand, Johannesburg, Transvaal.

**Spain.**

Professor J. ORLAND, M.Sc., M.A., Ph.D., D.D., Head of the Department  
of Metallography and Strength of Materials, Instituto Católico  
de Artes e Industrias, Alberto Aguilera 23, Madrid.



**Sweden.**

Professor CARL BENEDICKS, Fil.Dr., Dr.-Ing.e.h., Dr.Techn.h.c.,  
Drottninggatan 95 B., Stockholm.

Professor AXEL HULTGREN, Professor of Metallography, Kungl. Tekniska  
Högskolan, Stockholm.

**Switzerland.**

Professor A. VON ZEERLEDER, Dr.-Ing., Director, Research Laboratories,  
Société Anonyme pour l'Industrie de l'Aluminium Chippis,  
Rosenbergstrasse 25, Neuhausen a./Rheinfall.


**United States of America.**

Professor R. F. MEHL, Ph.D., Eng.D., Sc.D., Director, Metals Research  
Laboratory, Carnegie Institute of Technology, Pittsburgh, Pa.

Professor C. S. SMITH, Sc.D., Professor of Metallurgy and Director of the  
Institute for the Study of Metals, University of Chicago, Chicago 37, Ill.

Dr. R. A. WILKINS, Vice-President, Revere Copper and Brass Inc., Rome, N.Y.





Digitized by the Internet Archive  
in 2024



H. S. TASKER, ESQ., B.A.  
(President 1950-51)

[Frontispiece, to face p. ix.]

# CONTENTS

MINUTES OF PROCEEDINGS		PAGE
May Lecture, 10 May 1950 . . . . .		xiii
Elections of Members . . . . .		xiii
May Lecture . . . . .		xv
Extraordinary General Meeting, London, 27 June 1950 . . . . .		xv
Annual Autumn Meeting, Bournemouth, 18-22 September 1950 . . . . .		xvii
Visits (18 September) . . . . .		xvii
Autumn Lecture . . . . .		xviii
Official Welcome to Bournemouth . . . . .		xviii
Minutes . . . . .		xviii
Welcome to Members and Visitors from Overseas . . . . .		xviii
Nomination of Officers for 1951-52 . . . . .		xviii
Senior Vice-President for 1951-52 . . . . .		xix
Elections of Members . . . . .		xix
Discussion of Papers (19 September) . . . . .		xxiii
Visit (19 September) . . . . .		xxiii
Civic Reception . . . . .		xxiii
Discussion of Papers (20 September) . . . . .		xxiii
Visits (20 September) . . . . .		xxiv
Dinner . . . . .		xxiv
Discussion of Papers (21 September) . . . . .		xxiv
Votes of Thanks . . . . .		xxiv

PAPERS AND DISCUSSIONS		PAGE
		<i>Papers. Discn.</i>
1238. A Preliminary Study of the Solidification of Castings. By R. W. Ruddle, M.A., A.I.M. . . . .		1
Discussion . . . . .		595
1239. Correlation of Tensile Properties of Aluminium Alloy Plate Castings with Temperature Gradients During Solidification. By R. W. Ruddle, M.A., A.I.M. . . . .		37
1240. Use of Diamond Dust for Polishing Metallographic Specimens of Non-Ferrous Metals and Alloys. By E. C. W. Perryman, M.A., A.I.M. . . . .		61
1241. Atomic Displacements Associated with Elasticity in Plastically Deformed Metals. By W. A. Wood, D.Sc., and N. Dewsnap, B.Met.E. . . . .		65
Discussion . . . . .		597



	PAGE
	<i>Papers. Discn.</i>
1242. Modification in Aluminium-Silicon Alloys. By B. M. Thall, M.A.Sc., Ph.D., and Professor Bruce Chalmers, D.Sc., Ph.D.	79
1243. Presidential Address. By H. S. Tasker, B.A.	99
1244. The Mechanical Properties of Some Wrought and Cast Aluminium Alloys at Elevated Temperatures. By P. L. Thorpe, G. R. Tremain, and R. W. Ridley, B.Sc.	111
1245. The Calculation of the Activation Energies of Recovery and Recrystallization from Hardness Measurements on Copper. By N. Thorley, B.Sc., Ph.D., F.Inst.P.	141
Discussion	611
1246. The Constitution of Magnesium-Rich Alloys of Magnesium and Zirconium. By G. A. Mellor, M.Sc., F.I.M.	163
Discussion	616
1247. The Effect of Applied Load in Micro-Indentation Tests. By W. Rostoker, M.A.Sc., Ph.D.	175
Discussion	621
1248. The Pressure-Welding Characteristics of Some Copper-Base Alloys. By Edwin Davis, M.Sc., F.I.M., and Eric Holmes, B.A.	185
Discussion	630
1249. Stress-Corrosion of Aluminium-7% Magnesium Alloy. By E. C. W. Perryman, M.A., A.I.M., and S. E. Hadden, A.I.M.	207
Discussion	635
1250. A Theory of the Mechanism of Stress-Corrosion in Aluminium-7% Magnesium Alloy. By P. T. Gilbert, Ph.D., A.R.I.C., A.I.M., and S. E. Hadden, A.I.M.	237
Discussion	635
1251. Relationship between the Ageing and Stress-Corrosion Properties of Aluminium-Zinc Alloys. By E. C. W. Perryman, M.A., A.I.M., and J. C. Blade, B.Sc.	263
Discussion	635
1252. Industrial Gas Turbines. Fortieth May Lecture. By H. Roxbee Cox, Ph.D., M.I.Mech.E., F.R.Ae.S., F.Inst.F.	287
1253. Corrosion and Related Problems in Sea-Water Cooling and Pipe Systems in H.M. Ships. By I. G. Slater, Ph.D., C.I.Mech.E., F.I.M., L. Kenworthy, M.Sc., A.R.C.S., F.R.I.C., F.I.M., and R. May, A.R.S.M.	309
Discussion	646
1254. The Jet-Impingement Apparatus for the Assessment of Corrosion by Moving Sea-Water. By R. May, A.R.S.M., and R. W. de Vere Stacpoole	331
Discussion	646
1255. Pitting Corrosion in Copper Water Pipes Caused by Films of Carbonaceous Material Produced During Manufacture. By Hector S. Campbell, B.Sc., A.R.C.S., A.R.I.C.	345
Discussion	646
1256. The New Continuous Brass Mill of the Scovill Manufacturing Company, Waterbury, Conn., U.S.A. By J. J. Hoben and J. F. Mulvey	357
Discussion	658



	PAGE
	<i>Papers. Discn.</i>
1257. <b>The Flow of Zinc Under Constant Stress.</b> By Professor A. H. Cottrell, B.Sc., Ph.D., and V. Aytekin, B.Sc., Ph.D. . . . .	389
Discussion . . . . .	597
1258. <b>Mechanism of Primary Creep in Metals.</b> By W. A. Wood, D.Sc., and R. F. Scrutton, B.Sc. . . . .	423
Discussion . . . . .	597
1259. <b>The Mechanism of Creep as Revealed by X-Ray Methods.</b> By G. B. Greenough, Ph.D., and (Mrs.) Edna M. Smith, B.A. . . . .	435
Discussion . . . . .	597
1260. <b>Some X-Ray Observations on the Nature of Creep Deformation in Polycrystalline Aluminium.</b> By E. A. Calnan, B.Sc., and B. D. Burns, M.Sc. . . . .	445
Discussion . . . . .	597
1261. <b>The Thermodynamics and Kinetics of Precipitation in Solid Solutions.</b> By H. K. Hardy, Ph.D., M.Sc., A.R.S.M., A.I.M. . . . .	457
1262. <b>On the Phases Occurring in Alloys of Aluminium with Copper, Magnesium, Manganese, Iron, and Silicon.</b> By Gösta Phragmén, Lic.Phil. . . . .	489
1263. <b>The Constitution of Uranium-Molybdenum Alloys.</b> By P. C. L. Pfeil, B.Sc., Ph.D. . . . .	553
1264. <b>The Uranium-Iron System.</b> By J. D. Grogan, B.A. With an Appendix: <b>An X-Ray Examination of Uranium-Iron Alloys.</b> By C. J. Birkett Clews, B.Sc., Ph.D. . . . .	571
1265. <b>Deformation Texture of Drawn Face-Centred Cubic Metal Wires.</b> By Walter R. Hibbard, Jr., A.B., D.Eng. . . . .	581
1266. <b>Lattice Parameters of Binary Nickel-Cobalt Alloys.</b> By A. Taylor, Ph.D., F.Inst.P., F.I.M. . . . .	585
Discussion on Paper by Mr. T. H. Rogers: "A Method for Assessing the Relative Corrosion Behaviour of Different Sea-Waters." ( <i>J. Inst. Metals</i> , 1949-50, <b>76</b> , 597) . . . . .	646
Obituary Notices . . . . .	665
Name Index . . . . .	671

# LIST OF PLATES

- Mr. H. S. Tasker, B.A., President. . . . . *frontispiece*
- I-II. Paper by Mr. R. W. Ruddle . . . . . *between pp. 32 and 33*
- III-IV. Paper by Mr. E. C. W. Perryman . . . . . *between pp. 64 and 65*
- V. Paper by Dr. B. M. Thall and Professor  
Bruce Chalmers . . . . . *facing p. 80*
- VI. Paper by Mr. G. A. Mellor . . . . . *facing p. 170*
- VII-IX. Paper by Mr. Edwin Davis and Mr. Eric  
Holmes . . . . . *between pp. 200 and 201*
- X-XIII. Paper by Mr. E. C. W. Perryman and Mr.  
S. E. Hadden . . . . . *between pp. 216 and 217*
- XIV-XVI. Paper by Dr. P. T. Gilbert and Mr. S. E.  
Hadden . . . . . *between pp. 248 and 249*
- XVII-XXI. Paper by Mr. E. C. W. Perryman and Mr.  
J. C. Blade . . . . . *between pp. 264 and 265*
- XXII. Paper by Dr. H. Roxbee Cox . . . . . *facing p. 294*
- XXIII-XXXII. Paper by Dr. I. G. Slater, Mr. L. Kenworthy,  
and Mr. R. May . . . . . *between pp. 318 and 319*
- XXXIII-XXXIV. Paper by Mr. R. May and Mr. R. W. de Vere  
Stacpoole . . . . . *between pp. 334 and 335*
- XXXV-XXXVI. Paper by Mr. Hector S. Campbell . . . . . *between pp. 350 and 351*
- XXXVII-XLII. Paper by Mr. J. J. Hoben and Mr. J. F.  
Mulvey . . . . . *between pp. 372 and 373*
- XLIII-XLIV. Paper by Professor A. H. Cottrell and Dr. V.  
Aytekin . . . . . *between pp. 404 and 405*
- XLV-XLVIII. Paper by Dr. W. A. Wood and Mr. R. F.  
Scrutton . . . . . *between pp. 428 and 429*
- XLIX-LII. Paper by Dr. G. B. Greenough and Mrs.  
Edna M. Smith . . . . . *between pp. 436 and 437*
- LIII-LVI. Paper by Mr. E. A. Calnan and Mr. B. D.  
Burns . . . . . *between pp. 452 and 453*
- LVII-LXXII. Paper by Mr. Gösta Phragmén . . . . . *between pp. 504 and 505*
- LXXIII-LXXIV. Paper by Mr. Gösta Phragmén . . . . . *between pp. 536 and 537*
- LXXV. Paper by Mr. Gösta Phragmén . . . . . *facing p. 555*
- LXXVI-LXXVII. Paper by Dr. P. C. L. Pfeil . . . . . *between pp. 568 and 569*
- LXXVIII-LXXXI. Paper by Mr. J. D. Grogan . . . . . *between pp. 576 and 577*
- LXXXII. Paper by Mr. Walter R. Hibbard, Jr. . . . . *facing p. 584*
- LXXXIII. Discussion on a paper by Mr. Edwin Davis  
and Mr. Eric Holmes . . . . . *facing p. 634*

# THE INSTITUTE OF METALS

## MINUTES OF PROCEEDINGS

### MAY LECTURE

A GENERAL MEETING of the Institute of Metals was held at the Royal Institution, Albemarle Street, London, W.1, on Wednesday, 10 May 1950, at 6.0 p.m., the President, Mr. H. S. TASKER, B.A., occupying the Chair.

The minutes of an Extraordinary General Meeting, held in London on 29 March, 1950, and of the Annual General Meeting held in London on 29, 30, and 31 March 1950, were taken as read and signed by the Chairman.

#### ELECTIONS OF ORDINARY MEMBERS AND STUDENT MEMBERS

The SECRETARY (Lieut.-Colonel S. C. Guilan, T.D.) announced that, since the last General Meeting of the Institute, the following 41 Ordinary Members and Student Members had been elected :

ELECTED ON 27 APRIL 1950

#### *As Ordinary Members*

- ANTELO, Héctor Francisco, B.Sc., Chief of the Laboratories, Fabricá Militar de Aceros, Casilla de Correo No. 2, Sucursal 37, Buenos Aires, Argentina.
- ASHEN, Frederick Charles, Fuel Technologist, Imperial Chemical Industries, Ltd., Metals Division, Witton, Birmingham 6.
- BHADURI, Sukumar, B.Sc., B.Met., Metallurgist, Bhartia Electric Steel Company, 8 Swinhoe Street, Calcutta 19, India.
- CHIAVERINI, Vicente, Engineer, Metallurgical Department, Instituto de Pesquisas Tecnológicas, São Paulo, Brazil.
- CRAIG, George Black, B.A.Sc., Research Student, Department of Metallurgical Engineering, University of Toronto, Toronto, Ont., Canada.
- DODWORTH, Alfred John, Works Manager, Oakes, Turner and Company, Ltd., 75-79 Eyre Street, Sheffield 1.
- HOUSTON, David Arthur, B.Sc., Technical Officer, H. J. Enthoven and Sons, Ltd., 89 Upper Thames Street, London, E.C.4.
- INGHAM, Bertram Hobart, M.Sc., Ph.D., Technical Librarian, Hadfields (Merton), Ltd., Western Road, Mitcham, Surrey.
- JOLLIVET, Léon, Chef du Service des Recherches, Société Minière et Métallurgique de Peñarroya, 12 Place Vendôme, Paris, France.
- KEHL, George Louis, M.S., Associate Professor of Metallurgy, School of Mines, Columbia University, New York 27, N.Y., U.S.A.
- KILLINGWORTH, Donald, B.Sc., Chief Metallurgist, Ruston and Hornsby, Ltd., Sheaf Iron Works, Lincoln.
- PERETTI, Ettore A., D.Sc., Professor of Metallurgy, University of Notre Dame, Notre Dame, Ind., U.S.A.
- RICHARDS, William Gwynfab, B.Sc., Metallurgist, Research Department, Anglo-Iranian Oil Company, Ltd., Chertsey Road, Sunbury-on-Thames, Middlesex.
- SCHARSCHU, Charles A., B.Chem., Chief Metallurgist and Director of Research, Allegheny Ludlum Steel Corporation, Brackenridge, Pa., U.S.A.

- SMURTHWAITE, John William, Deputy Works Manager, Pakistan Government Mint, Lahore, West Punjab, Pakistan.
- DE SOUZA SANTOS, Tharcisio D., Chief Engineer, Metallurgical Department, Instituto de Pesquisas Tecnológicas, São Paulo, Brazil.
- THALL, Burnett M., M.A.Sc., Ph.D., Production Engineer, 80 King Street, Toronto, Ont., Canada.
- THORNELY, Bernard Norman Heath, B.A., Chief Engineer, Northern Aluminium Company, Ltd., Banbury, Oxfordshire.
- TRELA, Edward, M.S., Metallurgist, Apex Smelting Company, Cleveland, O., U.S.A.
- TUCKER, Herbert John Charles, Southern Area Sales Manager, Electric Furnace Company, Ltd., Weybridge, Surrey.
- WAUCHOPE, Kenneth Laird, Student of Metallurgy, University of Toronto, Toronto, Ont., Canada.

*As Student Members*

- AUST, Karl Thomas, M.A.Sc., Graduate Student, University of Toronto, Toronto, Ont., Canada.
- BETHUNE, Albert William, B.A.Sc., Graduate Student, Department of Metallurgical Engineering, University of Toronto, Toronto, Ont., Canada.
- BUNSHAH, Rointan Framroze, B.Sc., Student of Metallurgy, Carnegie Institute of Technology, Box 202, Pittsburgh 13, Pa., U.S.A.
- CHANG, Wen-Hsiang, B.S., Student of Metallurgy, Missouri School of Mines, Rolla, Mo., U.S.A.
- CLARK, Robert, B.A.Sc., Graduate Student, University of Toronto, Toronto, Ont., Canada.
- CURLOOK, Walter, Student of Metallurgy, University of Toronto, Toronto, Ont., Canada.
- EDWARDS, Frank Fryer, Metallurgist, Enfield Rolling Mills, Ltd., Enfield, Middlesex.
- HULME, Kenneth Gretton, Student of Metallurgy, University College, Swansea.
- LAST, Anthony John, Student of Metallurgy, Battersea Polytechnic, London, S.W.11.
- LEE, Morgan Hamilton, Laboratory Assistant, Richard Thomas and Baldwins, Ltd., Landore, Swansea.
- MARTIN, Alfred John, B.Sc., Research Student, Royal School of Mines, London, S.W.7.
- MOODY, John Wentworth, Student of Metallurgy, University of Toronto, Toronto, Ont., Canada.
- RIDLEY, Norman, Student of Metallurgy, King's College, Newcastle-upon-Tyne 1.
- SCARBOTT, Derrick Ronald, Student of Metallurgy, Royal Technical College, Glasgow.
- SYKES, Elwyn Charles, Metallographer, The de Havilland Aircraft Company, Ltd., Hatfield, Hertfordshire.
- SYMONDS, John, Student of Metallurgy, University of Birmingham.
- TEGHTSOONIAN, Edward, B.A.Sc., M.A., Graduate Student, University of Toronto, Toronto, Ont., Canada.
- WENBERG, Fred, B.A.Sc., M.A., Graduate Student, University of Toronto, Toronto, Ont., Canada.
- WINEGARD, William Charles, B.A.Sc., Graduate Student, University of Toronto, Toronto, Ont., Canada.
- WRIGHT, John Charles, Laboratory Assistant, Development and Research Department, The Mond Nickel Company, Ltd., Wiggin Street, Birmingham.



## MAY LECTURE

The PRESIDENT then introduced Dr. H. ROXBEE COX, M.I.Mech.E., F.R.Ae.S., F.Inst.F., who delivered the Fortieth May Lecture on "Industrial Gas Turbines" (see this volume, pp. 287-307).

Sir WILLIAM GRIFFITHS, D.Sc. (Past-President) proposed a hearty vote of thanks to Dr. Roxbee Cox for his lecture. The motion was put to the meeting and carried with acclamation.

The lecturer was afterwards entertained to dinner by the Council at Brown's Hotel.

## EXTRAORDINARY GENERAL MEETING

AN EXTRAORDINARY GENERAL MEETING of the Institute of Metals was held at 4 Grosvenor Gardens, London, S.W.1, on Tuesday, 27 June 1950, when the President, Mr. H. S. TASKER, B.A., occupied the Chair.

The SECRETARY (Lieut.-Colonel S. C. Guilan, T.D.) read the notice convening the meeting.

The CHAIRMAN then put to the meeting the following resolution, which was carried unanimously:

*Resolution*

That the provisions of Clauses 5, 6, 7, 8, 9, 10, 15, 17, 32, 38, 42, 44, 46, 57, 58, 59, 63, and 64 of the Articles of Association of the Institute be altered as follows:

(i) By the insertion in Clause 5 thereof of the words "Junior Members," after the words "Ordinary Members".

(ii) By the substitution in the third paragraph (relating to "Ordinary Members") of Clause 6 thereof of the words "non-ferrous metallurgy" for the words "the metal trades or with the application of non-ferrous metals and alloys, or engaged in their scientific investigation".

(iii) By the addition to Clause 6 thereof after the paragraph relating to "Ordinary Members" of the following new paragraph: "*Junior Members* shall (not being less than twenty-one years of age) be admitted and retained as such within such limits of age as shall be determined from time to time by the Council and/or provided in the Bye-Laws. They shall be either (a) persons engaged in the manufacture, working, or use of non-ferrous metals and alloys; (b) persons of scientific, technical, or literary attainments connected with or interested in non-ferrous metallurgy; or (c) pupils or assistants of persons qualified for Ordinary Membership, whether such persons are members or not. Junior Members shall not be eligible for election on the Council nor shall they be entitled to vote at the meetings of the Institute or to nominate candidates for Ordinary Membership".

(iv) By the substitution in the fourth paragraph (relating to "Associate Members") of Clause 6 thereof of the words "Associate Members shall not be eligible for election on the Council, nor shall they be entitled to vote at meetings of the Institute, or to nominate candidates for Ordinary, Junior, or Student membership" for the words "An Associate Member shall not be entitled to vote at meetings of the Institute or to nominate candidates for Ordinary or Student membership".

(v) By the insertion in the fifth paragraph (relating to "Student Members") of Clause 6 thereof of the words "and allied sciences" after the words "students of metallurgy" and of the word "Junior" after the words "candidates for Ordinary".

(vi) By the insertion in the Form "A" in Clause 7 thereof of the words "Date of Birth" below the word "Qualification".

(vii) By the substitution in the Form "A" in Clause 7 thereof of the words "the above-named applicant" for the words "the said"; and of the words "Signature of applicant" for the words "Name of applicant in full"; and of the words "Private Address" for the word "Address"; and of the words "Appointment and business address" for the words "Business or Profession".

(viii) By the insertion in Clause 7 thereof of the words "if any" after the words "entrance fee".

(ix) By the cancellation of Clause 8 and the substitution of the following new clause therefor: "8. Applications for membership as Ordinary, Junior, Associate, or Student Members shall be submitted to the Council for approval. Before election the names of all applicants shall be exhibited at the offices of the Institute for inspection by members, and published in any other manner as may from time to time be prescribed by the Council. An objection to any candidate whose name is so exhibited or notified to members shall be made in writing to the Secretary within fourteen days of the date when the list shall first be exhibited or published, and such objection shall be brought to the attention of the Council, which shall determine the course of action to be taken. Non-election shall not necessarily prejudice the candidate for election concerned in any future application for election".

(x) By the cancellation of Clause 9 and the substitution of the following new clause therefor: "9. (a) Unless and until otherwise determined by the Council or provided in the Bye-Laws the subscription of each Ordinary Member shall be four guineas per annum, of each Junior Member and Associate Member shall be two pounds and fifteen shillings per annum, and of each Student Member shall be one pound and fifteen shillings per annum. At the discretion of the Council, Ordinary Members, Junior Members, and Student Members may be required to pay an Entrance Fee".

"(b) Rules and/or regulations may be made by the Council from time to time for the transference of members from one class of membership to another class. The fee, if any, to be paid on any such transfer shall be such as the Council may from time to time prescribe. The Council may, in fixing such sum, take into consideration any prior payment of entrance fees by Junior Members and Student Members".

"(c) Subscriptions shall be payable on election and subsequently in advance on the first day of July in each year, or otherwise as shall be determined from time to time by the Council and/or provided in the Bye-Laws".

"(d) No entrance fee or subscription shall be payable in the case of Honorary Members or Fellows".

(xi) By the omission from Clause 10 thereof of the words "in separate columns" and the words "and names of his Sponsors if an Ordinary or Student Member".

(xii) By the substitution in sub-clause (d) of Clause 15 thereof of the word "twelve" for the word "six".

(xiii) By the cancellation of sub-clause (f) of Clause 15 and the substitution of the following new sub-clause therefor: "Junior, Associate, or Student Membership shall cease on the member attaining the prescribed limit of age".

(xiv) By the substitution in Clause 17 thereof of "15 (e)" for "15".

(xv) By the substitution in the second paragraph of Clause 32 thereof of the words "the British Isles or elsewhere" for the words "the British Isles, in British Dominions overseas or in foreign countries".

(xvi) By the addition before the last paragraph of Clause 32 thereof of the words :

“ To appoint and remove such and so many representatives of allied societies or other bodies interested in the promotion of the science and practice of non-ferrous metallurgy as the Council shall think fit, to attend meetings of the Council for purposes of liaison, provided that such persons shall not by virtue of such appointment be entitled to vote either at a meeting of the Council or at a General Meeting of the Institute ”.

“ To appoint and remove, as the Council shall think fit, such and so many members of the Institute as Honorary Corresponding Members in the British Commonwealth and colonies or in foreign countries to advise the Council on the promotion of the objects of the Institute in their respective countries ”.

(xvii) By the substitution in Clause 38 thereof of the words “ four-fifths ” for the word “ all ”.

(xviii) By the insertion in Clause 42 thereof of the letter “ (a) ” before the words “ The President ”.

(xix) By the addition to Clause 42 thereof of the sub-clause “ (b) The Council may nominate Chairmen to preside at General Meetings of the Institute or meetings held jointly with other bodies for the discussion of scientific and technical matters only, but at such General Meetings of the Institute no Resolution shall be discussed or put to the meeting ”.

(xx) By the insertion in Clause 44 thereof of the words “ and shall be conducted in accordance with the provisions of the Companies Act 1948 or any amending Act ” after the words “ United Kingdom ”.

(xxi) By the substitution in Clause 46 thereof of the words “ Twenty-one ” for the word “ Seven ”.

(xxii) By the insertion in Clause 46 thereof of the words “ in writing ” after the words “ shall be given ”.

(xxiii) By the omission from Clause 46 thereof of the word “ general ” after the words “ state the ”.

(xxiv) By the insertion in Clauses 57, 58, and 59 thereof of the words “ or otherwise ” after the words “ by bye-laws ”.

(xxv) By the omission from Clause 63 thereof of the words “ And no person other than a Member of Council shall be entitled to inspection thereof without the consent of the Council ”.

(xxvi) By the insertion in Clause 64 thereof of the words “ or by any amending Act,” after the words “ Companies (Consolidation) Act, 1908 ”.

## ANNUAL AUTUMN MEETING

THE FORTY-SECOND ANNUAL AUTUMN MEETING of the Institute of Metals was held in Bournemouth from Monday to Friday, 18 to 22 September 1950.

### Monday, 18 September

#### VISITS

During the day, visits were paid to the Admiralty Central Metallurgical Laboratory, Emsworth, and the works of Pirelli-General Cable Works, Ltd., Eastleigh, and of John I. Thornycroft and Co., Ltd., Woolston, Southampton.

## AUTUMN LECTURE

In the evening, the Twenty-First Autumn Lecture was delivered in the Hall of the Bournemouth School for Girls, by Mr. EARLE E. SCHUMACHER, B.Sc., on "Communications Metallurgy". The lecture is printed in the *Journal*, 1950-51, vol. 78, pp. 1-23.

A hearty vote of thanks to the lecturer, proposed by Mr. H. W. G. HIGNETT, B.Sc., was carried with acclamation.

## Tuesday, 19 September

The meeting was resumed at St. Peter's Hall, Hinton Road, at 10.0 a.m., the President, Mr. H. S. TASKER, B.A., occupying the Chair.

## OFFICIAL WELCOME TO BOURNEMOUTH

The MAYOR OF BOURNEMOUTH (Councillor S. A. Thomson, J.P.) welcomed the members and delegates, and their ladies, to Bournemouth, and the PRESIDENT replied on behalf of the Institute.

## MINUTES

The minutes of the previous General Meeting, held in London on 10 May 1950, and of an Extraordinary General Meeting held in London on 27 June 1950, were taken as read and signed by the Chairman.

## WELCOME TO MEMBERS AND VISITORS FROM OVERSEAS

The CHAIRMAN welcomed members and visitors from overseas, mentioning in particular: MM. C. Lachaud and M. Tournaire (France); Mr. F. Lodder (Netherlands); Mr. Tore Holth (Norway); Herr R. Goldschmidt (Switzerland); and Mr. Earle E. Schumacher and Mr. J. G. Thompson (U.S.A.).

## NOMINATION OF OFFICERS FOR 1951-52

The SECRETARY (Lieut.-Colonel S. C. Guilan, T.D.) announced that the following members would retire from the Council at the 1951 Annual General Meeting, as required by the Articles of Association:

*President:*

H. S. TASKER, B.A.

*Past-President:*

Sir WILLIAM GRIFFITHS, D.Sc.

*Vice-Presidents:*

S. F. DOREY, C.B.E., D.Sc., Wh.Ex., F.R.S.  
Professor A. J. MURPHY, M.Sc.

*Ordinary Members of Council:*

JOHN ARNOTT  
MAURICE COOK, D.Sc., Ph.D.  
D. P. C. NEAVE, M.A.

He stated that, in accordance with Article 19, Mr. H. S. TASKER B.A., would fill the vacancy as Past-President, and that, in accordance with Article 22, the Council had nominated the following members to fill the other vacancies:



*As President :*

Professor A. J. MURPHY, M.Sc.

*As Vice-Presidents :*

A. B. GRAHAM

P. V. HUNTER, C.B.E.

*As Ordinary Members of Council :*

K. W. CLARKE

H. F. SHERBORNE, M.C., M.A.

CHRISTOPHER SMITH

He reminded the members of their rights, under Article 22, to make other nominations, if desired, before the conclusion of the meeting.

SENIOR VICE-PRESIDENT FOR 1951-52

The SECRETARY announced that, in accordance with Article 42, the Council had elected Dr. C. J. SMITHELLS, M.C., as Senior Vice-President for 1951-52, and that he would be their next nomination for the Presidency.

ELECTIONS OF ORDINARY MEMBERS, JUNIOR MEMBER, AND  
STUDENT MEMBERS.

The SECRETARY announced that since the last General Meeting, the following Ordinary Members, Junior Member, and Student Members, totalling 86, had been elected on 29 May, 28 June, 25 July, and 18 August 1950 :

ELECTED ON 29 MAY 1950

*As Ordinary Members*

- BERTRANDIAS, Jean Antoine George, Ing., Engineer, Research Department, Ets. Bertrandias, 33 rue de Plaisance, La Garenne-Colombes (Seine), France.
- BHATNAGAR, Parmatma Sarup, M.Sc., Assistant Professor, Engineering College, Benares Hindu University, India.
- BOUCHAUD, Peter, Staff Engineer, Société Lorraine de Laminage Continu (SOLLAC), Hayange (Moselle), France.
- BRADSHAW, Francis Julian, M.A., Physicist, British Iron and Steel Research Association, 11 Park Lane, London, W.1.
- CESANA, Giorgio, Chairman and Manager, A. Cesana, 50 via S. Marco, Milano, Italy.
- CHAMBERLAIN, Alan, B.Eng., Research Metallurgist, Gearing Research and Development Department, Vickers-Armstrong, Ltd., Naval Construction Works, Barrow-in-Furness, Lancashire.
- DAS GUPTA, Dhruba Ranjan, B.Sc., Chemist, Sand Testing Laboratories, B.E.S. Company, Ltd., Calcutta, India.
- DICK, Alexander Walter Henry, B.Sc., Chief Chemist, The Delta Metal Company, Ltd., Delta Works, East Greenwich, London, S.E.10.
- DIXON, Wilfred, Technical Publications Officer, Ministry of Supply, Leatherhead Road, Chessington, Surrey.
- EDMONDS, Vincent Louvaine, Estimator, Imperial Smelting Corporation, Ltd., Swansea Vale Works, Llansamlet, Morriston, South Wales.
- FAILONI, Vittorio, Dr. Ing., Consulting Engineer, Corso Italia No. 6, Milano, Italy.

- GIROUDOT, Pierre, Laboratory Chief, Société pour le Forgeage et l'Estampage des Alliages Légers (FORGEAL), Usine du Piat, Issoire (Puy-de-Dôme), France.
- JOHANSEN, Frederick Charles, D.Sc., Director of Research, Avery Research Administration, Ltd., Soho Foundry, Birmingham 40.
- LEHANE, Thomas John, Assistant Works Manager, United Kingdom Chemicals, Ltd., Port Tennant Works, Swansea.
- LIVINGSTON, John A., President, Cerium Metals Corporation, 153 Waverly Place, New York 14, N.Y., U.S.A.
- OLD, Bruce Scott, Sc.D., Director, Arthur D. Little, Inc., 30 Memorial Drive, Cambridge 42, Mass., U.S.A.
- PEARSON, Thomas Gibson, Ph.D., D.Sc., Assistant Director of Research, The British Aluminium Company, Ltd., Chalfont Park, Gerrards Cross, Buckinghamshire.
- PHAILBUS, Theodore, B.Sc., Assistant Engineer, Punjab Government, Public Works Department, Irrigation Branch, Lahore, Pakistan.
- TMM, Harold A., B.Sc., Metallurgical Engineer, Dominion Magnesium, Ltd., Haley, Ont., Canada.

*As Student Members*

- CLARK, John Beverley, B.A.Sc., Graduate Student, Carnegie Institute of Technology, Schenley Park, Pittsburgh 13, Pa., U.S.A.
- DANIEL, Alan Raymond, Student of Metallurgy, Battersea Polytechnic, London, S.W.11.
- DUTT, Asoke Kumer, B.A., Vacation Student, Bhartia Electric Steel Company, Ltd., 8 Swinhoe Street, Calcutta 19, India.
- KENAGHAN, Francis John, B.Sc., Apprentice Metallurgist, Birmingham Small Arms Tools, Ltd., Marston Green, Birmingham.
- MURAD, Abu Bakr, B.Sc., Student of Metallurgy, Royal Technical College, Glasgow.
- PENMAN, Robert Roland, B.S., Graduate Student, Missouri School of Mines and Metallurgy, Rolla, Mo., U.S.A.
- REITER, Stanley F., B.M.E., M.E., Graduate Student, Hammond Metallurgical Laboratory, Yale University, New Haven, Conn., U.S.A.

ELECTED ON 28 JUNE 1950

*As Ordinary Members*

- BARTLETT, Kenneth M., Director of Research, Thompson Products, Inc., 23555 Euclid Avenue, Cleveland 17, O., U.S.A.
- DE BARR, Albert Edward, B.Sc., Leader of Physics Division, Research Laboratories of Elliott Brothers (London), Ltd., Elstree Way, Boreham Wood, Hertfordshire.
- DELBART, Georges Robert, D.Sc., Director, Institut de Recherches de la Sidérurgie, 185 rue Président Roosevelt, St. Germain-en-Laye, France.
- DHAVERNAS, Jean Marie, President, Centre d'Information du Nickel, 41 avenue de Friedland, Paris (8<sup>e</sup>), France.
- FLETCHER, John Thomas, Metallurgist, Clarke, Chapman and Company, Ltd., Victoria Works, Gateshead 8, Co. Durham.
- HUGONY, Eugenio, Dr. Ing., V. Direttore, Istituto Sperimentale Metalli Leggeri, via della Posta 8/10, Milano, Italy.
- JARLEBORG, Martin Holger, Head of Laboratory, Fagersta Bruks A.B. Dannemoraverken, Osterbybruck, Sweden.
- JUETT, Douglas, Supervisor, Heat-Treatment Department, Addressograph-Multigraph, Ltd., 50 Oxgate Lane, Cricklewood, London, N.W.2.
- LLOYD, Lowell Thomas, M.S., Graduate Student, Department of Metallurgy, Carnegie Institute of Technology, Schenley Park, Pittsburgh 13, Pa., U.S.A.

MACKENZIE, David, 7 Waterside Street, Irvine, Ayrshire.

MAYBREY, (Mrs.) Mary Clarke, Managing Director, H. J. MaybreY and Company, Ltd., Worsley Bridge Road, London, S.E.26.

MEUSSNER, Russel Allen, M.Sc., Graduate Student, Department of Metallurgy, Carnegie Institute of Technology, Schenley Park, Pittsburgh 13, Pa., U.S.A.

SIGNORA, Mario, Director of Testing and Research Laboratory, Acciaierie e Ferriere Lombarde Falck, via Mazzini 23, Sesto S. Giovanni, Milano, Italy.

THOMPSON, Thomas, M.Sc., Director, Clarke, Chapman and Company, Ltd., Victoria Works, Gateshead 8, Co. Durham.

WINSTON, John Stanton, A.B., M.A., Instructor, Department of Metallurgical Engineering, Missouri School of Mines and Metallurgy, Rolla, Mo., U.S.A.

*As Student Members*

BALLASS, John Thomas, A.S., Student of Metallurgy, Missouri School of Mines and Metallurgy, Rolla, Mo., U.S.A.

BRUNNER, Hanus, Student of Metallurgy, Battersea Polytechnic, Battersea Park Road, London, S.W.11.

CASSAVETES, Nicholas John, Jr., Student of Metallurgy, Missouri School of Mines and Metallurgy, Rolla, Mo., U.S.A.

FISCHER, Peter, Student of Metallurgy, Eidgenössische Technische Hochschule; temporarily at High Duty Alloys, Ltd., Slough, Buckinghamshire.

HEBERT, Robert Earl, Student of Metallurgy, Missouri School of Mines and Metallurgy, Rolla, Mo., U.S.A.

LOVEDAY, Kenneth William, Student of Metallurgy, Northampton Polytechnic, St. John Street, London, E.C.1.

MASON, Henry Robert, Student of Metallurgy, University of Melbourne, Carlton N.3, Vic., Australia.

PERKINS, Raymond Frank, Laboratory Assistant, British Non-Ferrous Metals Research Association, Euston Street, London, N.W.1.

THORNTON, Philip Challis, Metallurgical Chemist, Chemical Laboratory, Plessey Company, Ltd., Vicarage Lane, Ilford, Essex.

ELECTED ON 25 JULY 1950

*As Ordinary Members*

BORNEMANN, Alfred, Dr.Ing., M.E., Professor of Metallurgy, Stevens Institute of Technology, Hoboken, N.J., U.S.A.

BRAMLEY, George Edward Arthur, Ph.D., M.Sc., Chief Metallurgist, Aluminium Wire and Cable Company, Ltd., Port Tennant Works, Swansea.

COFFINBERRY, Arthur Shotton, B.E., S.D., Group Leader for Physical Metallurgy, Los Alamos Scientific Laboratory, University of California, Los Alamos, N. Mex., U.S.A.

COLLET, Raoul, Sous-Directeur, Compagnie Française des Métaux, Sérifontaine (Oise), France.

HANSER, Klaus, Dipl.Ing., Managing Director, Osnabrücker Kupfer- und Drahtwerk, Osnabrück, Germany.

HOLST, Wilhelm, Dr.Tech., Managing Director, Studieselskapet for Norsk Industri, Munkedamsveien 53B, Oslo, Norway.

JOHNSON, Geoffrey Alan, B.Sc., Vice-President, The Robert Mitchell Company, Ltd., 64 Decarie Boulevard, St. Laurent, Que., Canada.

KAY, Sydney, Director and Chief Engineer, Cooper Roller Bearings Company, Ltd., King's Lynn, Norfolk.

MARKIN, Alan, Officer in Charge, Routine and Research Laboratories, E.M.F. Electric Company (Pty.), Ltd., 991 Rathdown Street, North Carlton, Vic., Australia.

- NOURSE, John Dudley, Metallographer, Bristol Aeroplane Company, Ltd., Bristol.
- QUADT, Raymond A., M.S., Director of Research and Development, Aluminum Division, Hunter Douglas Corporation, Blaine and Pachappa Streets, Riverside, Calif., U.S.A.
- SLOCOMBE, Harry Eric, Plant Layout Engineer, C.A.V., Ltd., Acton, London, W.3.
- SLOOFF, Arnout, Dr.Ir., Chemical Consultant, Orionlaan 92, Hilversum, Holland.
- SWAROOP, M., Works Manager, The Hind Metal Works, Ltd., Khirni Gate, Aligarh, India.
- TIPTON, Clyde Raymond, M.S., Physical Metallurgist, Los Alamos Scientific Laboratory, University of California, Los Alamos, N. Mex., U.S.A.
- TRANIER, Jean Lucien Marcel, Chief Metallurgist, L'Industrielle Métallurgique, S.A.R.L., 13 Boulevard de Vintimille, Marseille, France.

*As Junior Member*

- RANDLE, Keith Charles, B.Sc., Physicist, Research Laboratories, The General Electric Company, Ltd., Wembley, Middlesex.

*As Student Members*

- ABDOU, Abdou Hanna, B.Sc., Postgraduate Student, Sir John Cass Technical Institute, 3 Jewry Street, London, E.C.3.
- CHAPLIN, Norman John, B.A.Sc., Graduate Student, University of Toronto, Ont., Canada.
- DANKO, Joseph Christopher, Student of Metallurgy, Carnegie Institute of Technology, Schenley Park, Pittsburgh 13, Pa., U.S.A.
- DAVIDSON, Roy Campbell, Student of Metallurgy, University of Melbourne, Carlton, Vic., Australia.
- SEATON, Raymond, Student of Metallurgy, Sheffield University, St. George's Square, Sheffield 1.

## ELECTED ON 18 AUGUST 1950

*As Ordinary Members*

- BROWN, Arthur James Stephen, B.Sc. (Eng.), Director in Charge of Production, J. Stone and Company, Ltd., Deptford, London, S.E.14.
- DUVAL, Robert, Ing., Engineer, Anciens Établissements Aubert et Duval, 41 rue de Villiers, Neuilly-sur-Seine, France.
- EBORALL, Robert Kenneth, Works Chemist and Metallurgist, Metal Sales Company (Pty.), Ltd., Box 24, Benoni, Transvaal, South Africa.
- GUEST, Joseph Clifford, B.Sc., Research Metallurgist, T.I. (Group Services), Ltd., Plume Street, Birmingham 6.
- LEVER, Reginald Ernest, Managing Director, Richard Thomas and Baldwins (Argentina), S.A., Reconquista 314 Piso 1, Buenos Aires, Argentina.
- OWEN, Charles Penrhyn, Works Manager, Metal Sales Company (Pty.), Ltd., Box 24, Benoni, Transvaal, South Africa.
- PRESTON, Bryan Wentworth, M.A., Vice-Chairman, J. Stone and Company, Ltd., 1A Cockspur Street, London, S.W.1.
- SHEPPARD, Norman John, Metallurgist, Small Arms Factory, Department of Supply, Commonwealth of Australia, P.O. Box 70, Lithgow, N.S.W., Australia.
- SMITH, Robert, B.Met.E., Lecturer in Metallography, Metallurgy School, University of Melbourne, Carlton, Melbourne N.3, Vic., Australia.

SOLOMON, John Graham, Metallurgist, Small Arms Factory, Department of Supply, Commonwealth of Australia, P.O. Box 70, Lithgow, N.S.W., Australia.

WAGSTAFF, Raymond Claude, B.Sc., Metallurgist, J. Stone and Company, Ltd., Charlton, London, S.E.7.

*As Student Members*

BONDS, John Douglas, Laboratory Assistant, Johnson and Sons (Assayers), Ltd., 74 Hatton Garden, London, E.C.1.

HODGSON, Brian John Rubery, Laboratory Assistant, Bristol Aeroplane Company, Ltd., Bristol.

WALKER, David Gaston, B.Sc., Student, Metallurgy Department, University of Melbourne, Carlton, Melbourne N.3, Vic., Australia.

DISCUSSION OF PAPERS

The following papers were presented and discussed. In each case a vote of thanks to the authors was proposed by the Chairman and carried with acclamation.

"Corrosion and Related Problems in Sea-Water Cooling and Pipe Systems in H.M. Ships," by I. G. Slater, Ph.D., M.Sc., C.I.Mech.E., F.I.M., L. Kenworthy, M.Sc., A.R.C.S., F.R.I.C., F.I.M., and R. May, A.R.S.M.

"A Method for Assessing the Relative Corrosion Behaviour of Different Sea-Waters", by T. Howard Rogers, D.I.C., A.I.M.

"The Jet-Impingement Apparatus for the Assessment of Corrosion by Moving Sea-Water", by R. May, A.R.S.M., and R. W. de Vere Stacpoole.

"Pitting Corrosion in Copper Water Pipes Caused by Films of Carbonaceous Material Produced During Manufacture", by Hector S. Campbell, B.Sc., A.R.C.S., A.R.I.C.

"Stress-Corrosion of Aluminium-7% Magnesium Alloy", by E. C. W. Perryman, M.A., A.I.M., and S. E. Hadden, A.I.M.

"A Theory of the Mechanism of Stress-Corrosion in Aluminium-7% Magnesium Alloy", by P. T. Gilbert, Ph.D., A.R.I.C., A.I.M., and S. E. Hadden, A.I.M.

"Relationship Between the Ageing and Stress-Corrosion Properties of Aluminium-Zinc Alloys", by E. C. W. Perryman, M.A., A.I.M., and J. C. Blade, B.Sc.

VISIT

In the afternoon, a visit was paid to the "Isle" of Purbeck.

CIVIC RECEPTION

In the evening, members and their ladies were the guests of the Mayor and Corporation of the County Borough of Bournemouth, at a civic reception at the Pavilion, Bournemouth.

Wednesday, 20 September

The meeting was resumed at 10.0 a.m., at St. Peter's Hall, the President, Mr. H. S. TASKER, occupying the Chair.

DISCUSSION OF PAPERS

The following papers were presented and discussed. In each case a vote of thanks to the authors was proposed by the Chairman and carried with acclamation.

"Atomic Displacements Associated With Elasticity in Plastically Deformed Metals", by W. A. Wood, D.Sc., and N. Dewsnap, B.Met.E.



"The Flow of Zinc Under Constant Stress," by Professor A. H. Cottrell, B.Sc., Ph.D., and V. Aytakin, B.Sc., Ph.D.

"Mechanism of Primary Creep in Metals", by W. A. Wood, D.Sc., and R. F. Scrutton, B.Sc.

"The Mechanism of Creep as Revealed by X-Ray Methods", by G. B. Greenough, Ph.D., and (Mrs.) Edna M. Smith, B.A.

"Some X-Ray Observations on the Nature of Creep Deformation in Polycrystalline Aluminium", by E. A. Calnan, B.Sc., and B. D. Burns, M.Sc.

"The Calculation of the Activation Energies of Recovery and Recrystallization from Hardness Measurements of Copper", by N. Thorley, B.Sc., Ph.D.

#### VISITS

In the morning, ladies visited the potteries of Messrs. Carter and Co., Ltd., Poole.

In the afternoon, members visited the Admiralty Materials Laboratory, Holton Heath, and the works of Airspeed, Ltd., Christchurch, and Wellworthy Piston Rings, Ltd., Ringwood and Lymington. Other members and ladies took part in a tour of the New Forest.

#### DINNER

In the evening an informal dinner was held at the Royal Bath Hotel, Bournemouth, at which the Mayor and Mayoress of Bournemouth were the principal guests. The Chair was taken by the President, Mr. H. S. TASKER.

#### Thursday, 21 September

The meeting was resumed at 10.0 a.m. at St. Peter's Hall, Hinton Road, the President, Mr. H. S. TASKER, occupying the Chair.

#### DISCUSSION OF PAPERS

The following papers were presented and discussed. In each case a vote of thanks to the authors was proposed by the Chairman and carried with acclamation.

"The New Continuous Brass Mill of the Scovill Manufacturing Company, Waterbury, Conn., U.S.A.", by J. J. Hoben and J. F. Mulvey.

"The Pressure-Welding Characteristics of Some Copper-Base Alloys", by Edwin Davis, M.Sc., F.I.M., and Eric Holmes, B.A.

#### VOTES OF THANKS

The CHAIRMAN moved :

"That the best thanks of the Institute of Metals be, and are hereby, extended to :

(a) The Mayor and Corporation of the County Borough of Bournemouth for their welcome and hospitality.

(b) The Directors of works and laboratories in the Bournemouth, Portsmouth, and Southampton areas for their invitations and for their hospitality.

(c) The Governors of the Bournemouth School for Girls for permission to use the School Hall on the occasion of the Autumn Lecture.

(d) All others who have contributed to the arrangements for this meeting.

The motion was put to the meeting and carried with acclamation.

The meeting then concluded.

#### Friday, 22 September

Members and ladies took part in an all-day tour to Wells and Cheddar.

# A PRELIMINARY STUDY OF THE SOLIDIFICATION OF CASTINGS.\*

1238

By R. W. RUDDLE,† M.A., A.I.M., MEMBER.

(Communication from the British Non-Ferrous Metals Research Association.)

## SYNOPSIS.

Techniques for the measurement of temperatures in solidifying castings are described. These techniques were used to study the mechanism of solidification in cylinder castings made in super-purity aluminium, aluminium alloys containing 4, 8, and 30% copper, phosphor bronze, and aluminium bronze. The effect of small additions of titanium on the solidification of super-purity aluminium and of the aluminium-4% copper alloy was also examined.

The results show that super-purity aluminium and aluminium bronze solidify by "skin formation", and an equation has been deduced for the rate of skin-thickening in a super-purity aluminium cylinder. The aluminium-4% copper alloy and the phosphor bronze, on the other hand, solidify in a "pasty" manner, solid and liquid coexisting throughout the entire casting during the greater part of the freezing period. The mode of solidification of the aluminium-30% copper alloy is obscure, a period being observed during freezing in which the temperature gradients disappear; possible explanations for this are discussed. Addition of 0.1% titanium had little effect on the solidification of the aluminium-4% copper alloy, but inhibited skin formation in super-purity aluminium.

The solidification times of different sizes of geometrically similar cylinders in the aluminium-copper alloys have been calculated, using a method described in an Appendix, and these calculated values were found to be in fair agreement with those measured. The experimental solidification times show that Chvorinov's rule is approximately obeyed by aluminium alloy castings.

## I.—INTRODUCTION.

THIS paper describes some of the first results obtained in a long-term study of the solidification of castings, undertaken in the laboratories of the British Non-Ferrous Metals Research Association. The research aims at producing fundamental information which will enable the foundryman to predict the course of solidification in his castings and hence so to adjust the variables under his control—the method of running, the disposition of feeders, the choice of mould material, and pouring temperature—that the castings solidify in the manner which will lead to the greatest soundness and best mechanical properties.

\* Manuscript received 14 May 1949. The work described in this paper was made available to members of the B.N.F.M.R.A. in confidential research reports issued during 1947 and 1948.

† Head of Melting and Casting Section, British Non-Ferrous Metals Research Association, London.

The solidification of castings can be studied by three methods :

(i) The "pour-out" or "bleeding" method, in which a series of identical castings are poured in open moulds which are subsequently overturned at predetermined intervals after casting.

(ii) The measurement of the temperatures at various points in the casting and mould during the solidification period.

(iii) Utilization of the close analogy between the flow of heat and the flow of electricity to determine the temperatures existing at various points in the casting and mould by comparison with the potentials observed in an electrical reproduction of the casting and mould.

Each of these methods has been discussed at some length in an earlier publication<sup>1</sup> by the present author. Of the three methods, only (ii), the temperature-measurement method, is capable of yielding direct and accurate information on the process of solidification in a casting. Method (iii) gives only inferential information, and method (i), although providing direct information, is liable to yield erroneous results, particularly with alloys which freeze over a range of temperature. For these reasons the temperature-measurement technique was selected as the main line of attack in this research, supplemented where desirable by the other methods and by mathematical analysis.

Before studying any particular branch of the subject in detail, a preliminary survey was made covering the following aspects :

(a) The technique of temperature measurement in castings and moulds.

(b) The mechanism of solidification in a simple casting, with particular reference to the influence of alloy constitution.

(c) The solidification of plate castings in a light alloy, including the influence of section thickness, pouring temperature, and other variables on the solidification gradients, and correlation of these gradients with tensile properties.

(d) The extraction of heat from castings by non-metallic moulds.

The results obtained from the preliminary work on items (a) and (b) are described in Sections II and III of the present paper, work on item (c) being embodied in another paper.<sup>2</sup> The preliminary investigation into item (d) was extended to provide basic information which would be required in the later stages of the research; this study of non-metallic moulds is contained in a third paper.<sup>3</sup>

Published work on the solidification of castings and on related matters has been reviewed at considerable length in an earlier publication<sup>1</sup> and only passing reference to the literature will therefore be made here.

## II.—THE MEASUREMENT OF TEMPERATURES IN SOLIDIFYING CASTINGS.

Since the value of the work depended upon the accuracy of the temperature measurements, a careful study was made of the available techniques. It was clear that the thermocouples employed had to be as small as possible in volume and mass, to keep disturbance of the conditions prevailing within the castings to a minimum, and to ensure rapid response to small changes in temperature. The measuring apparatus had to be capable of recording, in quick succession, readings from a number of thermocouples. After preliminary tests, the following technique was evolved and used in all the experiments described.

The thermocouples were made from either (a) 28-gauge B. & S. (0.38-mm-dia.) Chromel P and Alumel wires (used with aluminium-base alloys), or (b) 0.2-mm.-dia. platinum and platinum-10% rhodium wires (used with copper-base alloys). The thermocouple wires were enclosed in oval-section twin-bore silica tubing of external dimensions  $2.5 \times 1.5$  mm. (0.044 g./cm.) and the exposed hot junctions were protected by a thin wash of alundum or fire-clay cement. This wash also blocked the ends of the protective sheathing and prevented the molten metal from running up the bores. The base-metal thermocouples were welded in a carbon-arc and the rare-metal thermocouples in an oxy-coal-gas flame.

Temperatures were recorded by means of a Tinsley D.C. amplifier with a straight-line characteristic and a high-speed milliammeter pen recorder. The magnification provided by the amplifier was variable in fixed steps and at maximum amplification the output of 20 m.amp. giving full-scale (4 in.) deflection of the recorder was produced by an input of 1 mV., corresponding to about 22° C. for Chromel/Alumel couples, or 100° C. for platinum/platinum-rhodium couples. To obtain high sensitivity the major part of the thermocouple e.m.f. was opposed by a back e.m.f. from a calibrated potentiometer suppressor unit.

A motor-driven switch enabled up to 25 thermocouples to be connected in turn to the D.C. amplifier. When the work was begun the time of response of the equipment was about 3 sec., but improvements were subsequently made which reduced the response time to less than 1 sec., so that it was possible to take up to 60 readings/min.

Tests showed that even without prior calibration of individual thermocouples an absolute accuracy of about  $\pm 2^\circ$  C. was obtainable when maximum amplification was employed. In the greater part of the work described thermal arrests occurred during the solidification



of the castings, which were used to correct differences in calibration between the thermocouples. By calibrating the couples in this way an accuracy of better than  $\pm 1^\circ \text{C.}$  ( $\pm 1.5^\circ \text{C.}$  with the rare-metal couples) was obtained, with, in any one experiment, a relative accuracy between the various thermocouples of  $\pm 0.5^\circ \text{C.}$  ( $\pm 1.0^\circ \text{C.}$  in the case of the rare-metal couples). These figures include the errors inherent in the measuring apparatus, besides the thermocouple errors. Employing full amplification, temperature changes of  $0.25^\circ \text{C.}$  could readily be detected with the base-metal thermocouples.

Experiments were also made to determine the errors due to conduction along the couple wires at different depths of immersion. Using a test casting in super-purity aluminium, the conduction error with both the base-metal and rare-metal thermocouples was found to be about  $2^\circ \text{C.}$  at  $\frac{1}{4}$  in. immersion,  $0.5^\circ \text{C.}$  at  $\frac{5}{8}$  in. immersion, and zero at 1 in. immersion.

In the initial stages of the work considerable difficulty was experienced owing to attack of the couple wires by the molten metal. No sign of such attack was observed in using the methods described above, and they are therefore thought to be suitable for all aluminium- and copper-base alloys. Even under the most severe conditions likely to be met with, namely the solidification of a large phosphor bronze casting containing 1% phosphorus (see p. 28), satisfactory readings were obtained.

### III.—THE SOLIDIFICATION OF CYLINDER CASTINGS.

With a view to obtaining a general qualitative picture of the mechanism of solidification of various alloys when cast into a simple shape, and investigating the kinetics of the solidification process, cylinder castings were made in super-purity aluminium and in a few binary aluminium-copper alloys with which it was thought the experimental difficulties would not be great. It was hoped that the results of these experiments would indicate the mechanism of solidification to be expected in other materials of similar constitution. One or two experiments were also made with copper-base alloys, mainly with the object of developing a temperature-measurement technique suitable for these materials.

#### 1. *Experimental Technique.*

A 5-in.-dia.  $\times$  10-in. cylinder casting was used for the greater part of this preliminary work. This casting was poured down a  $1\frac{1}{2}$ -in. downgate at one end and the thermocouples were introduced into the

mould cavity radially through the side walls of the cylinder so as to avoid conduction errors. A series of cylinders of 2, 3, and 4 in. dia. and geometrically similar to the 5-in.-dia. cylinders were also cast in some of the aluminium-copper alloys.

The moulds were made in synthetic sand bonded with 5% bentonite, using a washed silica sand (Parish's No. 1) of the following sieve analysis :

B.S. Sieve Nos.	Percentage
— 30 + 44	2.7
— 44 + 60	27.9
— 60 + 85	53.6
— 85 + 120	12.6
—120 + 150	1.8
—150	...

All the moulds were dried at about 200° C. before use. The mould hardness before drying was generally from 60 to 70 A.F.S. units, and the permeability after drying was around 180 A.F.S. units.

The materials used in making the castings were super-purity aluminium of 99.99% purity, electrolytic copper of 99.99% purity, and Mellanear refined tin of 99.8% purity; phosphorus was added to the copper-base alloys as a commercial phosphor-copper hardener of 99.9% purity. All the melts were made in a gas-fired furnace. The super-purity aluminium melts were degassed by pre-solidification and the aluminium-copper alloys were degassed with 2 oz. of hexachlor-ethane. The copper-base alloys were not degassed. The aluminium-copper alloys were prepared from the super-purity aluminium and a 50:50 aluminium-copper hardener made from the above materials. In all cases the pouring temperature corresponded to 100° C. superheat.

Except where otherwise stated, the couples were placed with their tips on the central axis of the cylinder, the spacing between the couples varying somewhat according to the material being investigated. The couple-spacing used with the super-purity aluminium castings is shown in Fig. 1. For most of the work with the aluminium-copper alloys and with the bronzes the two thermocouples at the metal/mould interface (couples 1 and 2) were placed as shown in Fig. 1, but only four other couples were used. These were at points  $d/4$ ,  $d/2$ , and  $3d/2$  distant from the end wall, where  $d$  is the dia. of the cylinder (couples 3-6, respectively). Where there were any significant departures from this arrangement mention of these is made in the text.

All the cylinders were cast horizontally, but some of the cylinders made in the aluminium-copper alloys were raised to the vertical immediately after pouring and allowed to solidify in this position.

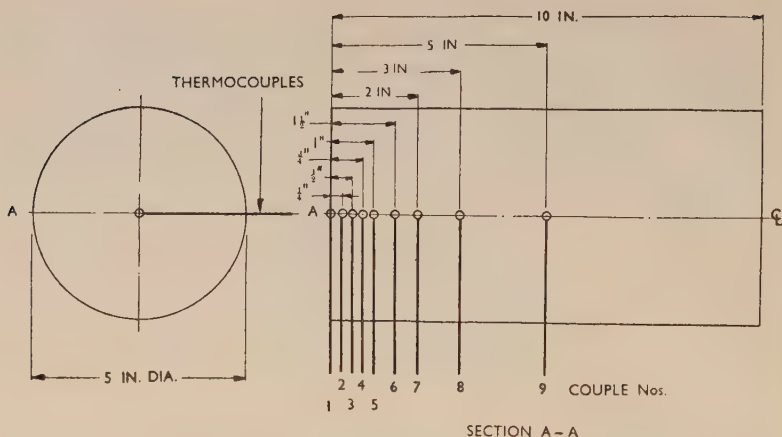


FIG. 1.—Positions of Thermocouples in Pure Aluminium Cylinder Castings.

## 2. *Cylinders Cast in Super-Purity Aluminium.*

The thermocouples were grouped more closely near the end wall of the cylinder opposite to the runner than elsewhere (Fig. 1), because (i) it was thought that solidification in this region would be essentially unidirectional and relatively unaffected by conduction of heat through the corners and radial side walls of the mould, and (ii) solidification was expected to take place most rapidly near the mould wall. Cooling curves obtained from one of the several cylinders cast are presented in Fig. 2. The way in which the temperature indicated by the couple placed at the interface falls past the arrest temperature without any measurable arrest being recorded, shows that freezing was completed at once at this point. It was concluded, therefore, that pure aluminium solidifies by a "skin-forming" mechanism, the casting consisting at any instant during solidification of a zone of completely solid material in contact with an inner region of wholly liquid material. As would be expected with a pure metal, all the castings had columnar macrostructures; the lengths of the columnar crystals, however, varied somewhat from casting to casting. A typical macrostructure of part of a vertical section through the central axis of a cylinder is shown in Fig. 16 (Plate I).

The progress of the solidification front was followed by observing the times at which the thermocouple readings fell below the arrest temperature, and Fig. 3 was thus obtained from one casting. The

thickness  $d$  was plotted against the square root of the time, since the review of published work <sup>1</sup> had indicated that "skin formation" takes place according to a parabolic law. The time  $t$  was reckoned from the moment when the mould was half full. Fig. 3 shows that after an

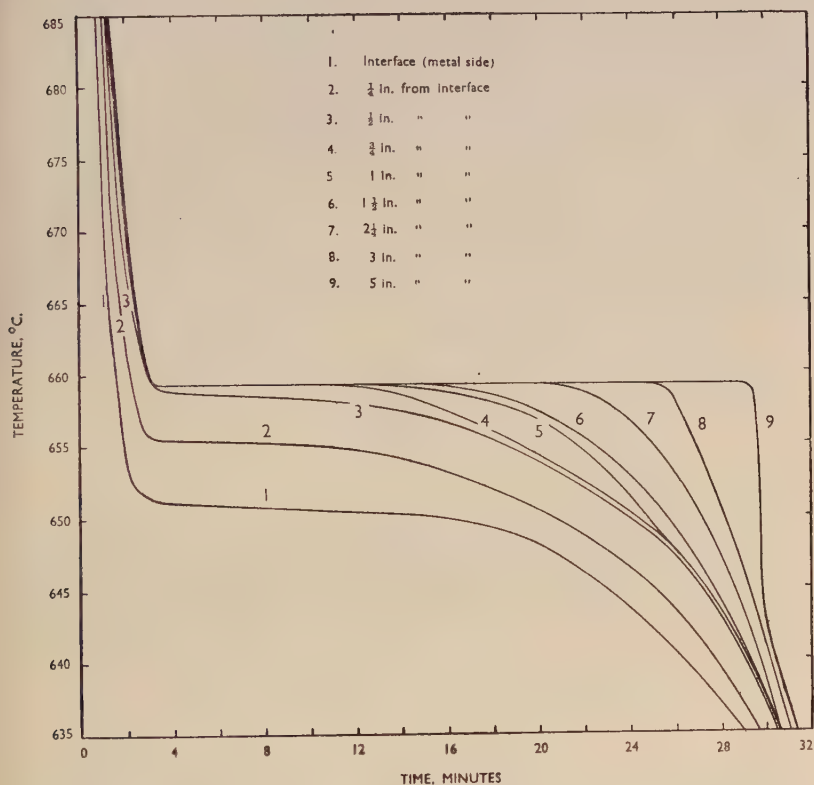


FIG. 2.—Cooling Curves obtained at points on central axis of a 5-in.-dia.  $\times$  10 in. cylinder cast in super-purity aluminium.

induction period of about  $1\frac{1}{2}$  min. solidification begins at a rapid rate but soon slows down to become a parabolic function of time, a relation which is maintained until the skin is over 1 in. thick. The rate of solidification then accelerates and eventually attains a very high value. This high value is obviously due to the fact that the couples more remote from the mould wall were situated in a region where solidification was proceeding inwards from the radial side walls of the cylinder. In



this region solidification is completed when the crystals growing towards each other from the radial walls meet and the entire region probably freezes at almost the same instant.

The apparent non-linearity of the curve near the beginning of solidification is unexpected and the reason is obscure. Possibly the non-linearity, which is dependent on only one experimental point, is not real, but is due to the finite size of the thermocouple placed at the interface.

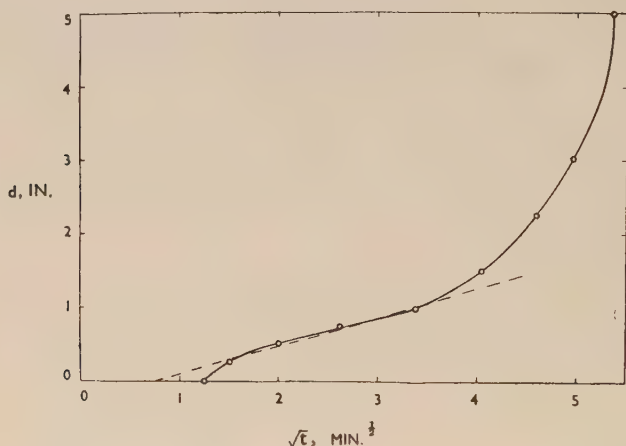


FIG. 3.—Curve showing Rate of Skin Formation in a 5-in.-dia.  $\times$  10 in. cylinder cast in super-purity aluminium.

The straight portion of the curve shown by the broken line in Fig. 3 leads to equation (1) for the rate of "skin formation":

$$d = 0.39\sqrt{t} - 0.32 \quad . \quad . \quad . \quad . \quad . \quad (1)$$

In this equation  $d$  is in inches and  $t$  in minutes. In a duplicate experiment a similar curve was obtained from which the following equation was derived:

$$d = 0.41\sqrt{t} - 0.53 \quad . \quad . \quad . \quad . \quad . \quad (2)$$

which shows reasonable agreement for the value of the constant  $k$  in the general equation:

$$d = k\sqrt{t} - c \quad . \quad . \quad . \quad . \quad . \quad (3)$$

although the figures obtained for  $c$  differ considerably.

The value of  $c$  depends largely upon the pouring temperature and, although every effort was made to keep this constant, a somewhat variable drop in temperature may have occurred between the time at

which the temperature in the pot was measured and the instant at which the metal entered the mould cavity. This factor, together with the unpredictable but probably variable effects of turbulence set up during pouring, may be responsible for the differences in the value of  $c$ .

In further similar experiments the plotted points near the beginning of the curve showed less regularity, and it was found difficult to draw any straight line between them. The reason for these irregularities is unknown, but they may be due to the difficulty of deciding from a cooling curve, the change in slope of which is very gradual, the exact moment at which freezing is completed at a given point in material freezing at constant temperature. An alternative and not unlikely explanation is that the advancing solid front is not plane, the tips of the columnar crystals projecting into the liquid phase. If this condition obtained and if the junctions of some of the couples were near "hills" in the solid front whereas others were in the "valleys", it is evident that the average thickness of the solid skin could not be accurately defined by measurements made with individual thermocouples.

Equation (1) may be compared with the similar equation obtained by Hunsicker<sup>4</sup> in a study of the solidification of aluminium of 99.8% purity cast from 732° C. into a plate 2 × 12 × 12 in. :

$$d = 0.28\sqrt{t} - 0.11 \quad . . . . . (4)$$

Hunsicker used the "pour-out" technique and determined the mean thicknesses of his solidified shells by means of density measurements. The reasons for the discrepancy between the present results and those obtained by Hunsicker are obscure, but may be due to the considerable differences in the experimental methods employed.

### *3. Cylinders Cast in Aluminium-Copper Alloys.*

For the greater part of this work two alloys were employed, an aluminium-4% copper alloy and an aluminium-30% copper alloy. These materials are typical of long-freezing-range and short-freezing-range eutectiferous alloys, respectively. The 4% copper alloy has a freezing range of about 100° C. and when sand-cast normally contains a few per cent. of eutectic; the 30% copper alloy has a freezing range of about 10° C. and consists of eutectic plus a few per cent. of aluminium-rich primary solid solution. One or two experiments were also made with an alloy of intermediate composition containing 18% copper (about 50% eutectic).

Both the 4% and the 30% copper alloys were cast in the whole range of cylinder sizes, but the 18% copper alloy was cast in the 5-in.-dia. cylinder only. As before, a superheat of 100° C. was used, the casting

temperatures being 780° C. for the 4%, 710° C. for the 18%, and 660° C. for the 30% copper alloy.

The results obtained with the different alloys are described separately below.

(a) *Aluminium-4% Copper Alloy.*

The cooling curves obtained from the 5-in.- and 2-in.-dia. horizontal

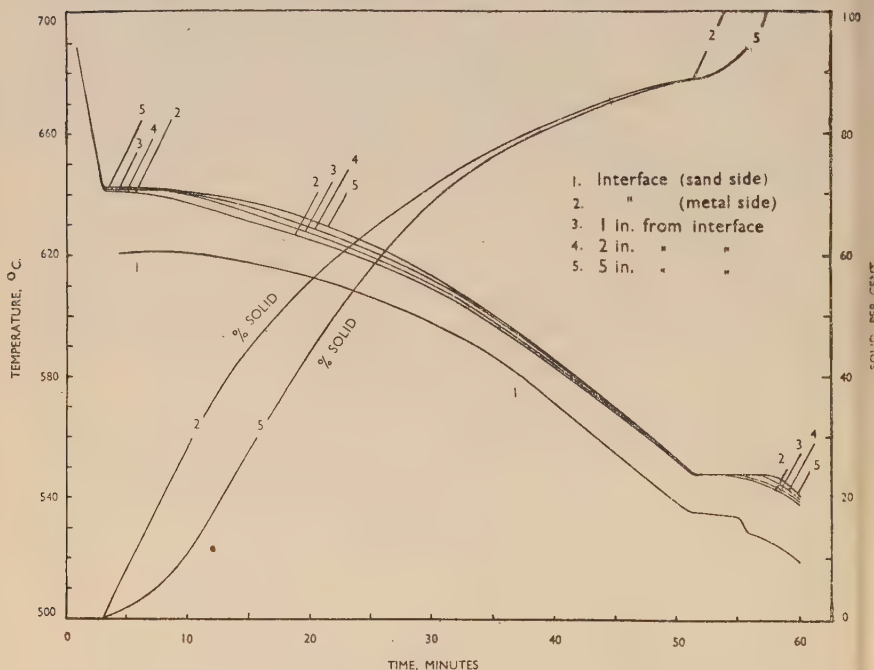


FIG. 4.—Cooling and Percentage-Solid Curves obtained at points on central axis of horizontally cast 5-in.-dia. cylinder in an aluminium-4% copper alloy.

cylinders are reproduced in Figs. 4 and 5. These two Figures show also the percentages of solid material, at different times after pouring, at (i) the metal/mould interface (the position of couple 2) and (ii) the centre of the casting (the position of couple 5). The percentage-of-solid curves were calculated using the equilibrium diagram given by Raynor<sup>5</sup> and assuming that 2.5% copper is retained in solid solution; this figure was deduced by microscopical examination.

Fig. 4 shows that at no time during solidification does the difference between the percentage of metal solid at the surface and at the centre

of the casting exceed 18%, and towards the end of freezing, when interdendritic feeding is taking place, this difference is reduced to a very low figure, so that the eutectic arrest begins within 1 min. at all parts of the casting and ends at the centre of the casting within 2 min. of ending at the surface.

The general picture of solidification is therefore one of freezing

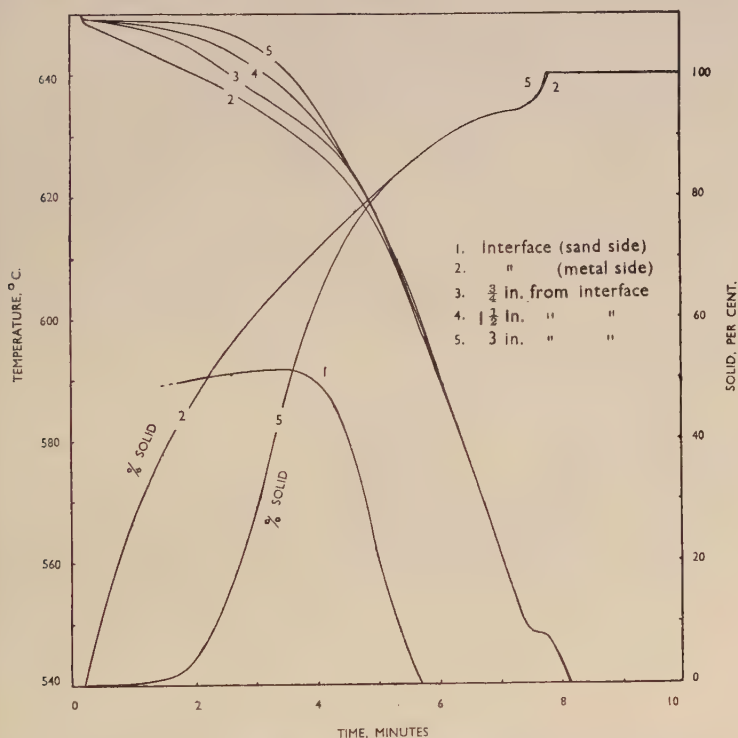


FIG. 5.—Cooling and Percentage-Solid Curves obtained at points on central axis of horizontally cast 2-in.-dia. cylinder in an aluminium-4% copper alloy.

progressing continuously throughout the entire pasty mass, with freezing at the centre lagging behind that at the surface to an extent which becomes less as solidification proceeds. This mechanism of freezing is very different from that in a pure metal, and explains why long-freezing-range alloys of this type have poor feeding properties and are subject to microporosity. In the later stages of solidification all parts of the casting are competing at the same time for the residual liquid, and it is therefore not surprising that the regions more remote



from the heat centre do not receive adequate feeding, and that the shrinkage voids, instead of being concentrated at the heat centre, are more or less uniformly distributed throughout the entire casting.

The results obtained in these experiments show why the "pour-out" method of examining the solidification of castings is unsatisfactory with long-freezing-range alloys, for the method cannot possibly work with a pasty mass such as is formed when the 4% copper alloy solidifies. Hunsicker<sup>4</sup> recently attempted to conduct "pour-out" experiments with an aluminium alloy containing 1.75% copper and found that castings bled soon after pouring gave virtually no shell, practically all the metal running out of the mould; conversely, it proved impossible to bleed castings at a later stage, although they were by no means completely solid.

The curves obtained with the smaller cylinders were closely similar to those for the 5-in.-dia. cylinder, the principal difference being, as Fig. 5 shows, the increased steepness of the temperature (and percent-solid) gradients. The curves from the vertically solidified cylinders were almost identical with those from the corresponding horizontal cylinders.

Average figures for the temperature gradients present along the central axis of the 5-in.-dia. cylinder were: about 2° C./in. in the liquid metal; about 3° C./in. during the early stages of solidification; and about 1° C./in. in the solid immediately after completion of solidification. Gradients of up to 6-7° C./in. were recorded during the solidification of the 2-in.-dia. cylinder. The temperature gradients present before, during, and after solidification in the four different sizes of cylinder are given in Table I, for both the horizontally and vertically cast cylinders.

The fact that the greatest temperature gradients occur during the earlier stages of solidification is probably due to the falling off in the rate of heat extraction by the mould. The rather unusual shape of the liquidus curve in this alloy system, which results in 50% of the 4% copper alloy solidifying in the first 10° C. of the 100° C. freezing range, may also affect the gradients present during solidification. This point is being investigated in current research.

In Fig. 4 the curve showing the temperature on the sand side of the metal/mould interface records a sharp drop of about 5° C. near the end of freezing. This effect has been observed in other experiments (although it does not always occur) and may correspond with the formation of an air-gap between the casting and the mould.

In some of the experiments additional thermocouples were placed in the mould cavity near the runner end, and it was observed that,

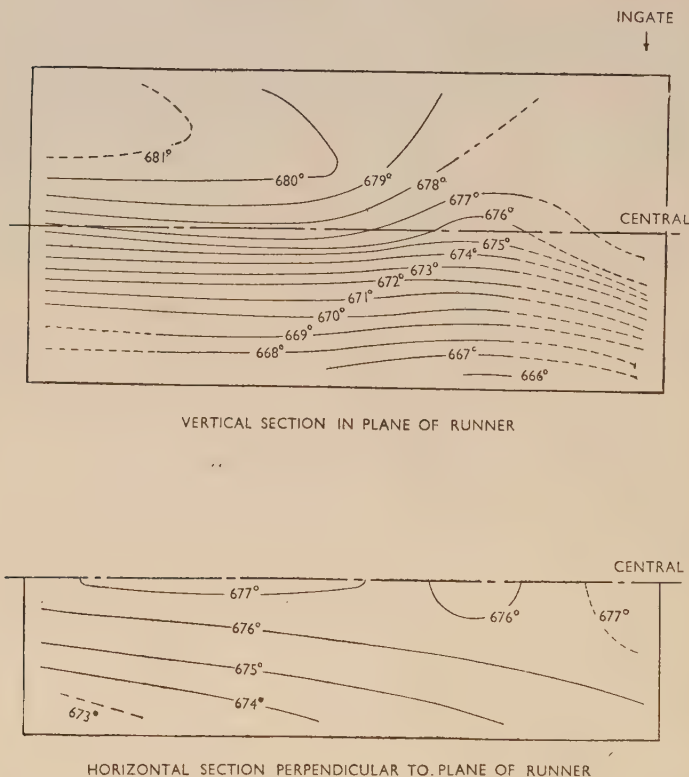
while this end of the casting was one of the last parts to begin solidifying, freezing, once started, proceeded comparatively rapidly. This region was in fact often completely solid some time before the corresponding region at the other end of the casting.

TABLE I.—*Temperature Gradients on Central Axes of Cylinder Castings.*

Alloy	Dia. of Cylinder, in.	Horizontal or Vertical (H or V)	Max. Temperature Gradient in Liquid, ° C./in.	Max. Temperature Gradient during Solidification, ° C./in.	Max. Temperature Gradient at End of Solidification, ° C./in.
Al-4% Cu	5	H	1	3	1
		V	1	2½	1
	4	H	1	3½	1½
		V	3½	3½	1½
	3	H	1	4	1½
		V	...	4	1½
	2	H	...	7	3
		V	...	8	3½
Al-30% Cu	5	H	3	2½	2½
		V	6	2½	4
	4	H	1½	3½	4
		V	8	4½	3
	3	H	1½	3½	4½
		V	...	4	3
	2	H	...	5	6½
		V	11	6	4½

To gain further insight into the way in which these castings solidify, experiments were made in which 5-in.-dia. cylinders were cast with a network of 21 couples introduced into the mould cavity. The results obtained with a horizontal cylinder are shown in Figs. 6 and 7 and similar results obtained with a vertically solidified cylinder are presented in Figs. 8 and 9. These Figures are sectional diagrams showing the approximate positions of the isothermals and isosolids at several

different times after casting. In Figs. 6-9 the first pair of diagrams (Figs. 6 (a) and 8 (a)) corresponds to a time when the entire casting was still liquid, the second (Figs. 6 (b) and 8 (b)), and third (Figs. 7 (a) and 9 (a)) pairs illustrate the isothermals present at various stages of solidifica-

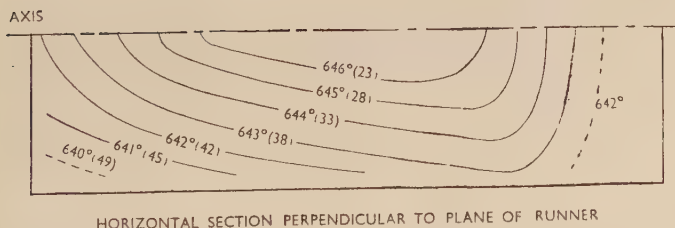
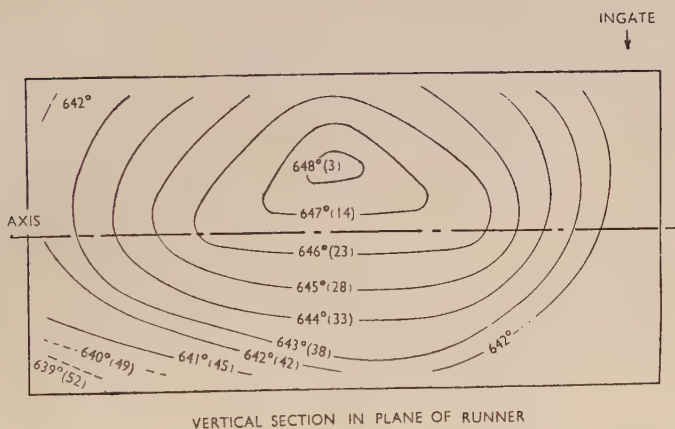


(a) 1 min. after casting.

FIG. 6 (a) and (b).—Isotherms in horizontally cast 5-in.-dia. Cylinder in an

tion, and the fourth pair (Figs. 7 (b) and 9 (b)) show the temperature distribution just before the end of solidification. These diagrams are largely self-explanatory. The marked vertical temperature gradient, especially in the horizontal cylinders, and the steep gradients present in the liquid are particularly interesting. The diagrams also show the way in which solidification proceeds very rapidly at the runner end of the casting. The most likely explanation of this effect is that metal

retained in the gating system solidifies rapidly and then proceeds to act as a heat radiator, thus quickly removing heat from this end of the casting. This rapid heat extraction by the runner displaces the heat centre of the casting away from the geometric centre. The heat centre



(b) 14 min. after casting.

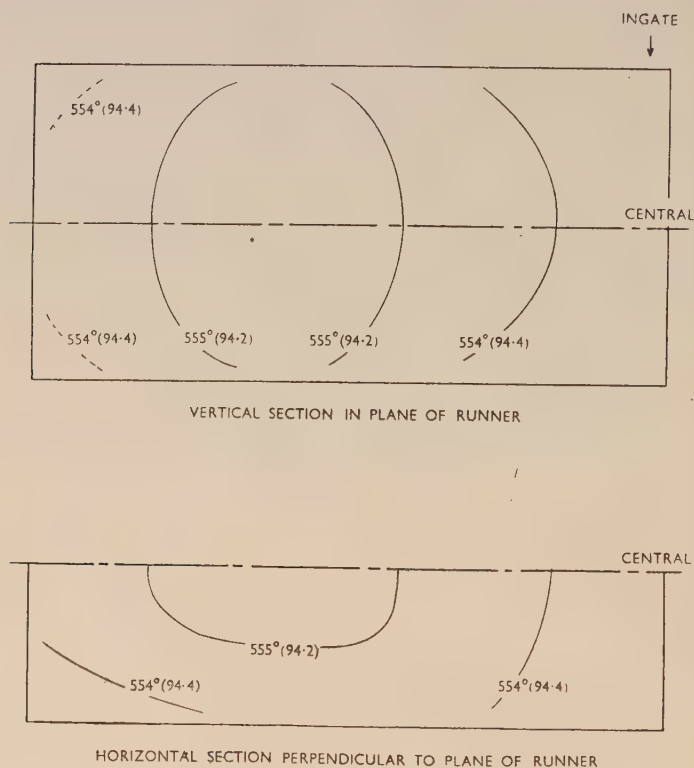
Aluminium-4% Copper Alloy. (Figures in brackets indicate percentage solid.)

is also displaced towards the bottom of the casting during the later stages of solidification, probably owing to the sinking of the top of the casting. The position of the heat centre at the end of freezing corresponded roughly to the position of the shrinkage cavity.

With all the cylinder castings a certain amount of turbulence was evident immediately after pouring, but this soon died away and within about 20 sec. perfectly steady readings were obtained on all the thermo-



couples. It is therefore unlikely that initial turbulence of the liquid metal in the mould exerted an appreciable influence on the solidification of the castings.

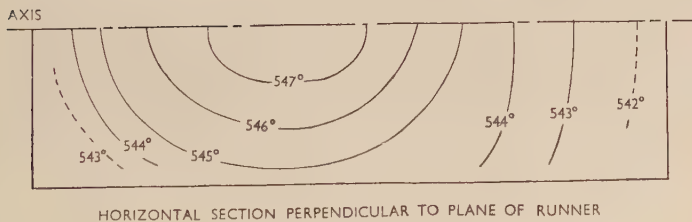
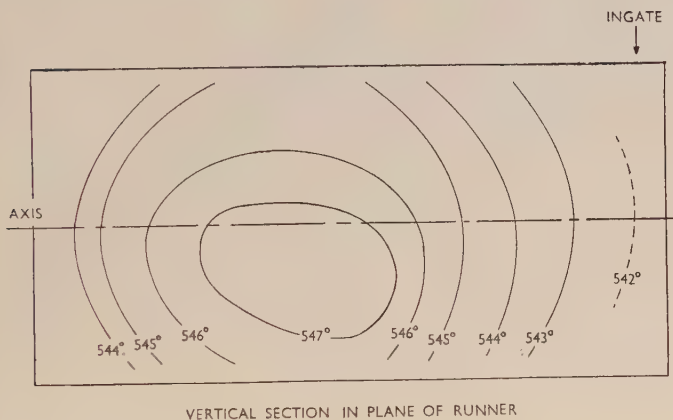


(a) 50 min. after casting.

FIG. 7 (a) and (b).—Isothermals in horizontally cast 5 in.-dia. Cylinder in an

The primary arrest occurred within  $\frac{1}{2}$  min. in all parts of the casting and was always accompanied by undercooling, this being greatest at the surface and least at the centre. The degree of undercooling varied somewhat from casting to casting, figures as high as  $6^{\circ}$  C. at the surface and  $3^{\circ}$  C. in the interior being experienced with some 5-in.-dia. cylinders. In general, undercooling was greatest in the smaller sizes of cylinder. At the surface, recalescence was quite rapid and solidification appeared to proceed immediately after the primary arrest at this point; conversely,

at the centre of the casting recalescence was comparatively slow and freezing was retarded for a few minutes until a temperature gradient was set up in the casting.



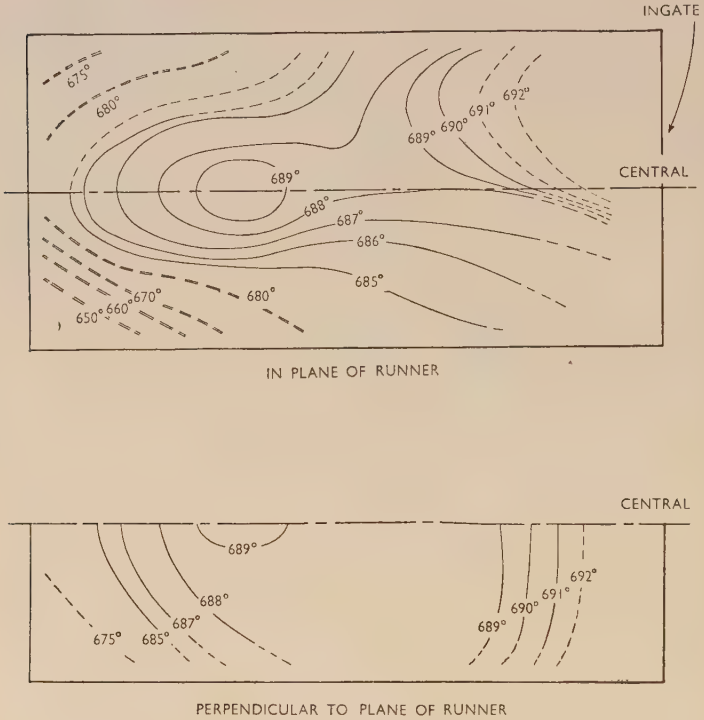
(b) 55½ min. after casting.

Aluminium-4% Copper Alloy. (Figures in brackets indicate percentage solid.)

(b) *Aluminium-30% Copper Alloy.*

This alloy was also cast into cylinders of all the sizes, solidified both horizontally and vertically. The cooling curves obtained with the 5-in.-dia. horizontal cylinder are reproduced in Fig. 10. For about 24 min. during solidification the casting was at the eutectic temperature along the entire central axis (see Fig. 10 and Table II). The mechanism of solidification in this alloy is therefore different from that in either a pure metal or a long-freezing-range alloy, the constant-temperature

period indicating the absence of heat flow within the casting, at least in the direction of the central axis. The temperature measurements were considered to be accurate to better than 1° C. and calculation



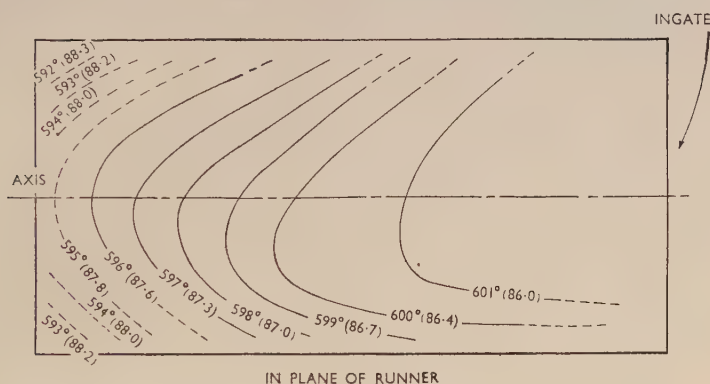
(a) 1 min. after casting.

FIG. 8 (a) and (b).—Isothermals in vertically cast Cylinder in an

TABLE II.—*Eutectic-Arrest Times in a 5-in.-dia. Cylinder Cast in Aluminium-30% Copper Alloy.*

Couple Position, in. from end wall	Time after Casting, min.			Duration of Eutectic Arrest, min.
	Primary Arrest	Beginning of Eutectic Arrest	End of Eutectic Arrest	
0	5.5	10.3	38.5	28.2
1 $\frac{3}{8}$	5.8	12.0	57.5	45.5
2 $\frac{1}{2}$	6.0	13.6	70.0	56.4
4 $\frac{7}{8}$	6.2	14.2	80.9	66.7

shows that the temperature gradient should be about  $2^{\circ}\text{C./in.}$  Furthermore, the thermocouple placed at the interface was at the arrest temperature for about 30 min.; if "skin formation" had occurred



PERPENDICULAR TO PLANE OF RUNNER

(b) 10 min. after casting.

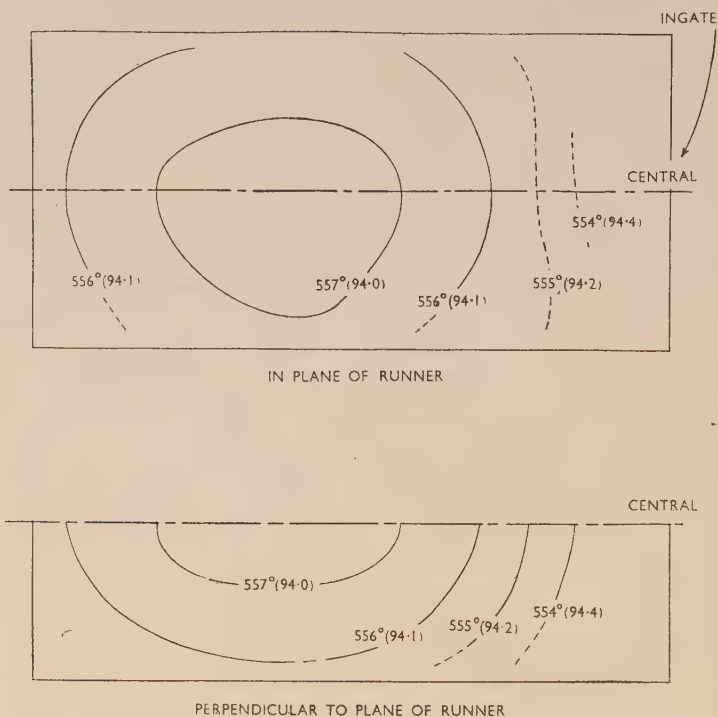
Aluminium-4% Copper Alloy. (Figures in brackets indicate percentage solid.)

in the alloy, this thermocouple should not have recorded an arrest of any appreciable duration, and the temperature at this point should have fallen by about  $2.5^{\circ}\text{C.}$  during the 30-min. period.

To secure further evidence, the temperature gradients along the axis of a 5-in.-dia. cylinder were measured more precisely, using a differential thermocouple. This was calibrated before use by inserting both junctions in a hole drilled in an aluminium block about  $1\frac{1}{2}$  in. in dia.; the block was placed in a furnace the temperature of which was maintained constant at about  $500^{\circ}\text{C.}$  The thermocouple was placed in the mould cavity in such a way that both junctions were on the



central axis of the cylinder, one being contiguous with the mould wall at the end of the cylinder opposite to the runner (position *A*), the other being  $2\frac{1}{2}$  in. inside the casting (position *B*). The e.m.f. generated was measured with the amplifier-and-recorder apparatus, maximum amplification (full-scale recorder deflection for 1 mV. input) being

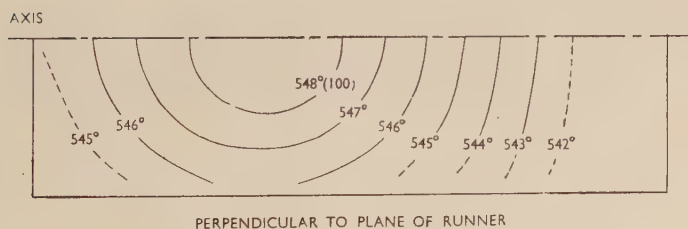
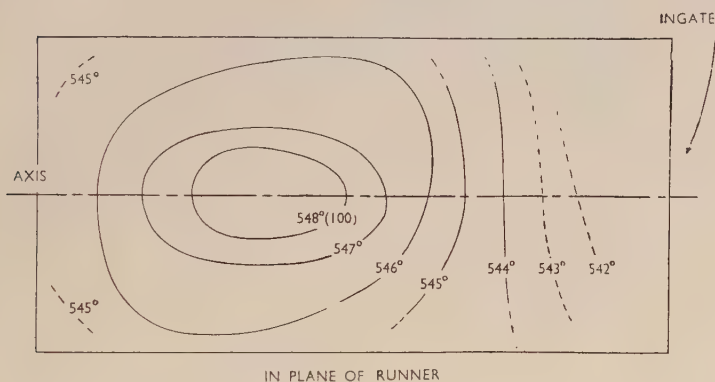


(a) 45 min. after casting.

FIG. 9 (a) and (b).—Isotherms in vertically cast Cylinder in an

employed. Measurements made in this way are considered accurate to better than  $\pm 0.25^\circ \text{C.}$ , so that mean temperature gradients greater than  $0.1^\circ \text{C./in.}$  should have been detectable. The temperature differences recorded by the differential thermocouple are plotted against time in Fig. 11. This shows a complete absence of temperature gradients for about 8 min. when the eutectic temperature was recorded at both positions. Repeat experiments yielded similar results, differing only in detail.

The results of this experiment confirm that a considerable period elapses during the solidification of near-eutectic aluminium-copper alloys in which no measurable temperature gradient is present. The observed "equal-temperature" period was shorter in this instance than in the experiments in which straightforward cooling curves were



(b) 50 min. after casting.

Aluminium-4% Copper Alloy. (Figures in brackets indicate percentage solid.)

taken; this is presumably due largely to the increased sensitivity of measurement. It may be that if still higher sensitivity were employed the constant-temperature period would be found to be of even shorter duration or possibly non-existent; the point is not of great importance, however, for, as shown in the following paragraph, such a gradient as might exist would manifestly be incapable of conducting more than a small fraction of the heat being removed from the mould.

Assuming that the eutectic solidification takes place progressively

on a front advancing from surface to centre, there being a sharp interface of negligible thickness between the liquid and solid regions, the solid shell thus postulated will begin to form as soon as the eutectic arrest occurs at the surface of the casting (i.e. 9 min. after pouring). Consider now the formation of a shell 1 in. thick. Using the thermal

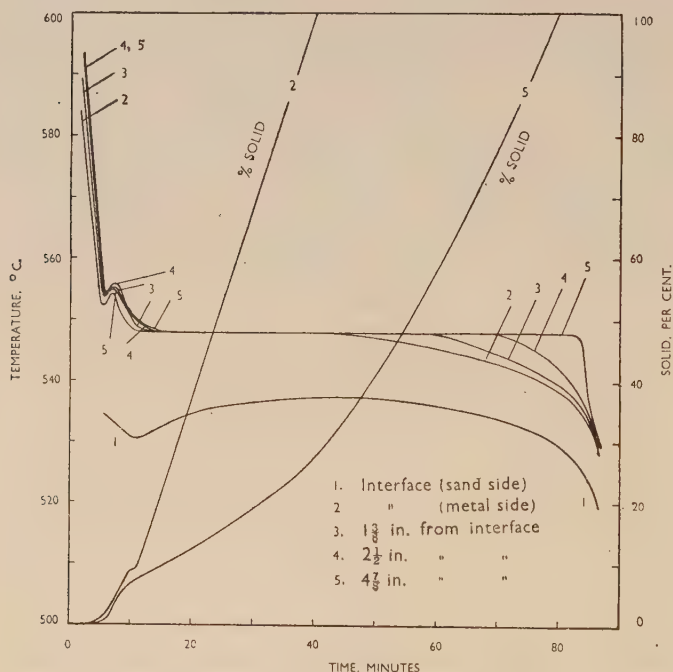


FIG. 10. —Cooling and Percentage-Solid Curves obtained at points on central axis of horizontally cast 5-in.-dia. cylinder in an aluminium-30% copper alloy.

data available\* for the aluminium-copper system, it may be shown that during the formation of this shell about 210 cal. must be conducted away from the casting through each sq. cm. of its surface. Reference to Fig. 6 of the paper by Ruddle and Mincher<sup>3</sup> shows that this amount of heat will be extracted by the mould in about 16 min. (the mould has already been absorbing heat for 9 min.), so that a shell 1 in. thick would exist about 25 min. after casting. Fig. 6 also shows that at this moment the rate of heat extraction by the mould is about 13 cal./min./cm.<sup>2</sup>, and a simple computation yields a figure of

\* See Appendix, p. 33.

approximately  $1.25^{\circ}\text{C./in.}$  for the temperature gradient necessary to conduct this heat through the 1-in.-thick shell. However, at this time (25 min. after pouring) the differential-thermocouple measurements show a temperature difference of, at most, only  $0.25^{\circ}\text{C.}$  over the entire  $2\frac{1}{2}\text{ in.}$ ; even if this difference is assumed to be concentrated in the postulated 1-in.-thick shell of solid metal adjacent to the mould wall, the observed figure is not of the same order as that calculated. It seems clear that a shell- or skin-forming mechanism such as described

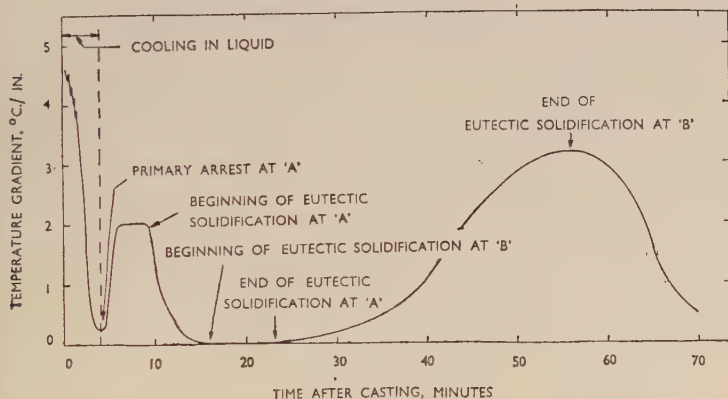


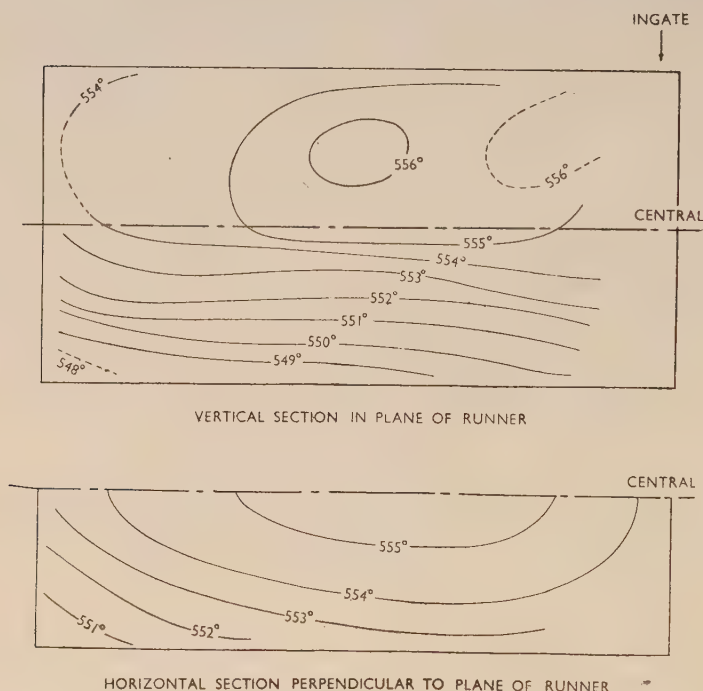
FIG. 11.—Curve showing Variation of Temperature Gradient along central axis of a 5-in.-dia. cylinder in an aluminium-30% copper alloy, from measurements obtained with a differential thermocouple. The approximate times of the principal events during solidification are indicated. ('A' refers to surface of casting, 'B' to a point  $2\frac{1}{2}\text{ in.}$  inside casting.)

above cannot apply in this instance, and solidification must take place in some other way.

The mechanism of heat transfer inside the casting during the constant-temperature period is obscure, but it is tentatively suggested that this might be accounted for by convection or gravity effects. On this hypothesis the mechanism of freezing in the aluminium-30% copper alloy is as follows: freezing begins in much the same way as in the 4% copper alloy, with a primary arrest at which undercooling occurs. Primary crystals are then deposited over a small range of temperature, the rate of deposition slowing down as the eutectic arrest is approached. The eutectic temperature is reached first by the surface of the casting and soon afterwards by the centre. Then follows the period in which no temperature gradients are present along the central axis of the casting. During this period solidification proceeds by the formation



on the surface of the mould of crystals which are then moved by convection and gravity towards the interior, fresh crystals being formed on the vacated surface. After a while the mass of metal becomes too pasty for movement to continue; heat transfer by convection and gravity then ceases and solidification takes place on an advancing front from the outside inwards. The existence of gravity effects is



(a) 8 min. after casting.

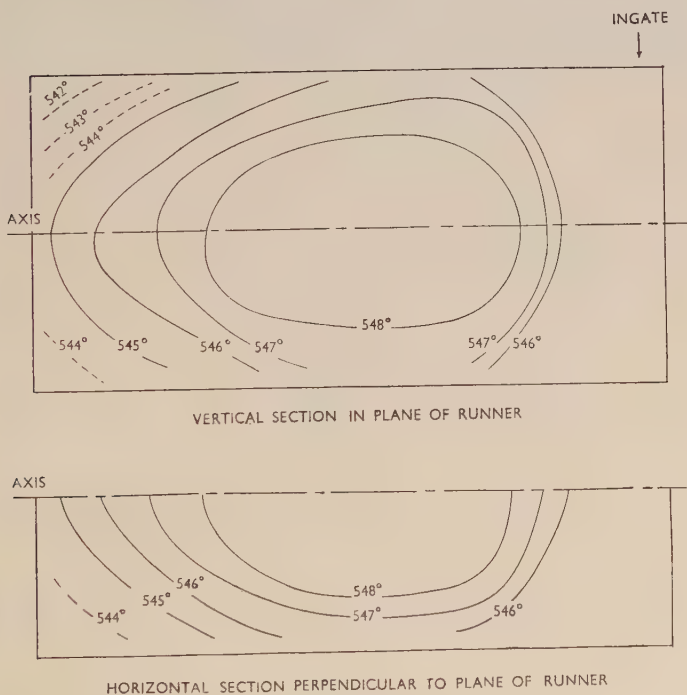
FIG. 12.—Isotherms in horizontally cast 5-in.-dia.

demonstrated in Fig. 17 (Plate II), where a region of columnar eutectic crystallization may be seen at the bottom of the casting. This must be due to flotation of the first-formed primaries, which leaves a region denuded of nuclei on the bottom of the casting; owing to the absence of nuclei the residual liquid of eutectic composition solidifies as columnar crystals growing at right angles to the mould wall. It is interesting to note that the pin-hole porosity present in the casting shown in Fig. 17 is entirely confined to the region of equi-axial crystallization.

The curves shown in Fig. 10 indicate a constant-temperature

period lasting for 24 min. on the central axis, but additional experiments in which a grid of 21 thermocouples was inserted into the mould cavity, revealed that the eutectic arrest ended first at the bottom and corners of the casting. The isothermals and isosolids in this casting at two different stages during solidification have been plotted in Fig. 12.

The curves drawn in Fig. 10 to represent the approximate



(b) 48 min. after casting.

Cylinder in an Aluminium-30% Copper Alloy.

percentages of solid metal at the surface and centre of the casting indicate very much greater differences between these percentages than was the case with the 4% copper alloy. This fact is reflected in the much improved feeding characteristics of the 30% as compared with the 4% copper alloy.

(c) *Aluminium-18% Copper Alloy.*

The curves obtained from a 5-in.-dia. cylinder in this alloy have features in common with both the 4% and 30% copper alloys, but reveal little further of interest.

## 4. The Effect of Grain-Refinement.

In order to discover whether grain-refinement by titanium addition had any marked effect on the mode of solidification, 5-in.-dia. cylinders were made in super-purity aluminium and in the aluminium-4% copper alloy, to both of which about 0.1% titanium had been added. As before, the cylinders were cast with 100° C. superheat.

The cooling curves obtained with the titanium-refined aluminium casting are given in Fig. 13. The presence of the titanium has caused a marked change in the mode of solidification; "skin formation" has

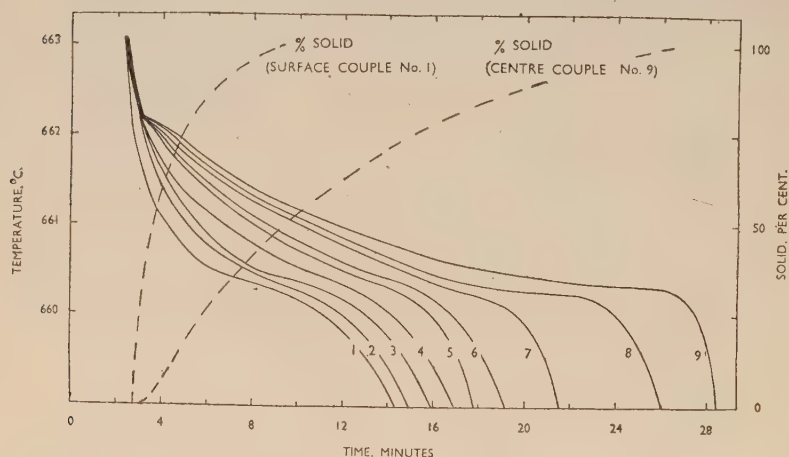


FIG. 13. —Cooling and Percentage-Solid Curves obtained at points on central axis of a 5-in.-dia.  $\times$  10 in. cylinder cast in super-purity aluminium containing 0.11% Ti. Positions of thermocouples: 1, interface (metal side); 2,  $\frac{1}{4}$  in.; 3,  $\frac{3}{8}$  in.; 4,  $\frac{5}{8}$  in.; 5,  $\frac{7}{8}$  in.; 6,  $1\frac{1}{2}$  in.; 7,  $2\frac{1}{8}$  in.; 8, 3 in.; 9,  $4\frac{7}{8}$  in. from interface.

been inhibited and the casting has solidified over a range of about 2° C. in a pasty manner rather like the aluminium-4% copper alloy. Macro-examination showed that in the region of the thermocouple tips the structure consisted of fairly fine equi-axial crystals.

Assuming that solid is deposited uniformly throughout the freezing range,\* the amounts of solid material present at the surface and centre of the casting have been calculated for various times after pouring. These figures are shown plotted against time in Fig. 13. When

\* This assumption is not strictly accurate, but is probably true to a first approximation, as may be seen from the equilibrium diagram for the aluminium-titanium system published by Fink, Van Horn, and Budge.<sup>6</sup> Any attempt to secure higher accuracy is unjustifiable, since the equilibrium diagram is itself not known with sufficient precision.

solidification was just finishing at the surface, the centre of the casting was already about 50% solid. The addition of titanium did not greatly affect the time of complete solidification of the aluminium cylinder, 27 min. being recorded, which is similar to the solidification times of the cylinders in pure aluminium. The macrostructure of the casting revealed other features of considerable interest, especially from the point of view of the theory of grain-refinement of aluminium by titanium. The macrostructure consisted of two regions: a region of columnar crystals at the top of the casting extending downwards for about 1 in., and a region of equi-axial crystallization, rather coarse

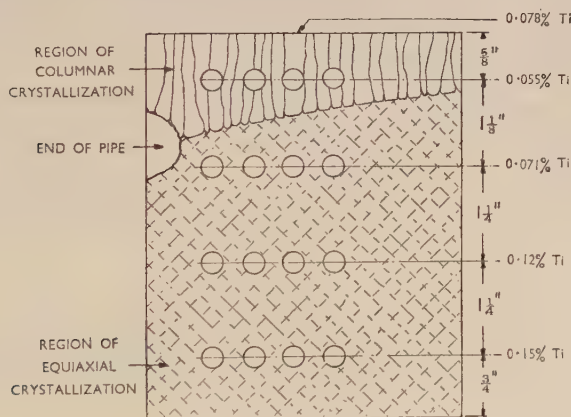


FIG. 14.—Diagram giving Analyses obtained at different locations in a vertical section through part of the cylinder casting in an Al-Ti alloy.

(1–2 mm. dia.) near the boundary with the columnar crystals, but becoming progressively finer in structure (0.5–1 mm. dia.) towards the bottom of the casting. The structure observed has been sketched in Fig. 14. The obvious reason for this effect is that the growing crystallites have sunk under gravity towards the bottom of the casting, producing a fine equi-axial structure and leaving at the top of the casting a region denuded of nuclei which has perforce to solidify by columnar growth. Samples for analysis were taken from various points in the specimen and the results are shown in Fig. 14.

The fact that the titanium content of the alloy increases progressively from top to bottom of the casting (neglecting for the moment the sample from the top surface) supports the view that the effects observed are due to the sinking of the first-formed crystals of aluminium, which



are relatively rich in titanium. The somewhat higher titanium content of the sample taken from the upper surface can be explained by adherence of a few of the first-formed primaries to the upper mould surface. The columnar region contains as much as 0.055% residual titanium, an amount normally sufficient to cause considerable refinement of the structure of pure aluminium. The occurrence, in this instance, of a columnar structure provides strong evidence that the grain-refinement of aluminium by titanium is brought about by the presence of titanium-rich nuclei.

Furthermore, at the temperature of the primary arrest no undercooling occurred in the casting refined with titanium, whereas undercooling of the order of several degrees was found at the surface of the casting made in super-purity aluminium; this observation also supports a nucleation mechanism of refinement.

The curves obtained with the aluminium-4% copper alloy refined with titanium were very little different from those shown in Fig. 4 for the unrefined alloy. The principal effect of the titanium was to suppress undercooling at the primary arrest and to raise the liquidus temperature to about 556° C. as opposed to 550° C. for the unrefined material. The mechanism of solidification was little affected.

#### *5. Solidification of Copper-Base Alloy Castings.*

To test the temperature-measurement technique with copper-base castings, the 5 in.-dia. cylinder was made in a copper-10% aluminium alloy and a phosphor bronze containing 12.5% tin and 1.0% phosphorus.

The cooling curves obtained from the aluminium bronze casting, reproduced in Fig. 15, show that this material has solidified in much the same way as the super-pure aluminium, "skin formation" occurring. The temperature gradients in the casting were rather greater than in the corresponding aluminium cylinders owing to the higher rate of heat extraction by the mould; the gradients were about 6° C./in. in the liquid and up to 11° C./in. in the solid.

The phosphor bronze used has a freezing range of about 300° C. and according to the ternary equilibrium diagram,<sup>7</sup> contains about 15% of the ternary eutectic, so that this material can scarcely be expected to exhibit skin formation. The record obtained was similar to that with the aluminium-4% copper alloy. The temperature gradients present were about 6° C./in. in the liquid and up to this figure during solidification. The macrostructure of the casting consisted entirely of comparatively large equi-axial crystals and a large amount of dispersed porosity was present in the interior.

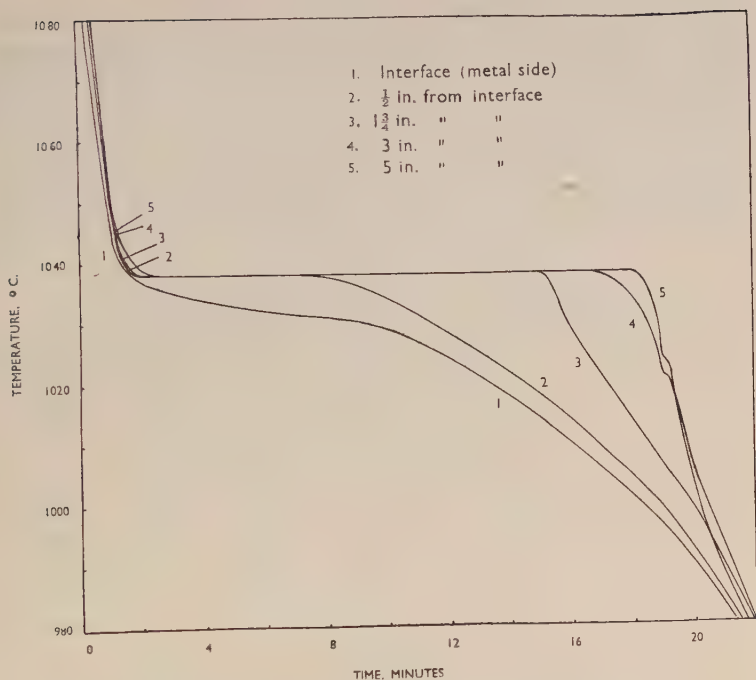


FIG. 15.—Cooling Curves obtained at points on central axis of horizontally cast 5-in.-dia. cylinder in aluminium bronze (10% aluminium).

### 6. Solidification Times.

If corner effects and surface curvature are neglected and a constant interface temperature is assumed, theory shows <sup>8</sup> that the time of complete solidification of castings made under the same conditions in the same material should be proportional to the values of the ratio  $\left(\frac{V}{A}\right)^2$ , where  $V$  is the volume of the casting and  $A$  its surface area. Evidence has been produced by Chvorinov <sup>8</sup> that this rule is accurate for steel castings over a very wide range of sizes, but the work of other authors suggests that this relation can only be regarded as approximate. The question of the solidification times of steel castings has been reviewed by Schwartz.<sup>9, 10</sup>

The solidification times of the cylinder castings were calculated, using the method described in the Appendix to the present paper and data quoted in the paper by Ruddle and Mincher.<sup>3</sup> The observed and calculated solidification times are given in Table III.

In view of the doubtful accuracy of the data for the thermal properties used in making the calculations, the agreement between the calculated and observed times of solidification is reasonably good, if the figures for the aluminium casting are neglected in making the comparison; the tendency for the calculated times to be longer than those observed is probably due to the neglect of corner and curvature effects. While Chvorinov's rule is approximately obeyed, quite large departures do in fact exist; this is particularly true for the 5-in.-dia.

TABLE III.—*Solidification Times of 5-in.-dia. Cylinder Castings.*

Alloy	Dia. of Cylinder, in.	Observed Solidification Time, min. Horizontal	Observed Solidification Time, min. Vertical	Calculated Solidification Time, min.	$\frac{V^2}{A^2}$ , in. <sup>2</sup>
Al-4% Cu	5	62 *	51	67	1.00
	4	41	42	43	0.64
	3	26	21	24	0.36
	2	8.0	9.3	10.7	0.16
Al-30% Cu	5	71 †	68	71	1.00
	4	42	40	45	0.64
	3	22 †	23	25	0.36
	2	9.5	10.8	11.3	0.16
Cu-8.5% Al	5	18	...	20	1.00
Cu-12.5% Sn-1% P	5	108	...	120	1.00
Pure Aluminium	5	26‡	...	36	1.00

\* Mean of 3 determinations.

† Mean of 2 determinations.

‡ Mean of 6 determinations.

cylinder. The reproducibility of duplicate experiments (especially with the 5-in.-dia. cylinders) was only moderate, the solidification times varying by up to 15%. The probable causes of these variations are thought to be :

(i) Heat extraction from the casting by metal solidified in the gating system. It has been shown above that this causes premature solidification of the runner end of the casting and should therefore decrease the solidification time.

(ii) Contraction of the casting away from the mould, thus reducing

the effective surface area. It was observed that the area and depth of the sink at the top of the castings varied considerably from casting to casting, even in duplicate experiments. This factor should tend to increase the solidification time.

(iii) The fall in the temperature of the metal between the time when this was measured in the pot and the instant when the metal enters the mould cavity. It was not found possible to measure accurately this fall in temperature but it is likely that its magnitude varies to some extent.

It is not surprising that the solidification times of the 5-in.-dia. cylinders showed the greatest variability. As solidification proceeds, the rate of heat extraction of the mould decreases according to a parabolic law,<sup>3</sup> so that at long times small changes in the rate of heat extraction involve proportionally large differences in solidification time.

The reason why the freezing times observed with the super-pure aluminium cylinders are so much less than the calculated time, is not clear. The figure given in Table III for the observed time is the mean for six castings; individual values varied between 28.5 and 22.8 min. The freezing time of the vertical 5 in.-dia.-cylinder in the 4% copper alloy was also shorter than that calculated; the reason is again obscure.

It was observed that the pure aluminium cylinders showed little tendency to sink at the top and this may account for the discrepancy between the observed and calculated solidification times. It is possible that all the calculated times are considerably too long owing to the neglect of corner and surface-curvature effects, but that, with the aluminium-copper alloy cylinders, the error due to this neglect is approximately compensated by the reduction in the rate of heat abstraction caused by the formation of the pronounced sink on the top surface. If this is so, the good agreement between the observed and calculated solidification times found with the alloy cylinders is largely fortuitous. Similar reasoning may explain the discrepancy observed with the 5-in.-dia. vertical cylinder in the aluminium-4% copper alloy; although a deep sink was observed in the top surface of this cylinder, the surface area involved was much smaller than with the horizontal cylinders.

### *7. Effect of Casting Temperature.*

The effect of variation of the pouring temperature upon the freezing time and mode of solidification was investigated by casting horizontal 5-in.-dia. cylinders in the aluminium-4% copper alloy from 800°, 750°, 700°, and 660° C. The records obtained were closely similar,

differing only in the times of the beginning and end of freezing and in the magnitude of the temperature gradients present (these varied between about 3.5° C./in., for the cylinder cast at 660° C., and 2° C./in. for the cylinder cast at 800° C.). The solidification times obtained with these four different superheats are given in Table IV, together

TABLE IV.—*The Effect of Casting Temperature on Solidification Time of 5 in.-dia. Cylinders in Aluminium-4% Copper Alloy.*

Casting Temperature, ° C.	Time of Complete Solidification, min.	Calculated Time of Complete Solidification, min.
800	81	79
750	62 *	67
700	56	56
660	47	48

\* Mean of 3 results.

with the calculated times. The agreement between the observed and calculated figures is excellent, except for the cylinder cast from 750° C.; however, in view of the approximate nature of the calculations, it is likely that the very close agreement shown by the solidification times for the other superheats is largely coincidental. According to the theory of heat extraction by a mould, freezing times should be a parabolic function of the superheat, but at long times curvature of the parabola is slight and the curve approximates to a straight line. Plotting the experimental results shows that the times for superheats corresponding to casting temperatures of 660°, 700°, and 800° C., all lie very close to a straight line; the point for 750° C. falls some distance from this line. The approximate linearity of this plot follows from the fact that freezing times of the order of an hour fall on the straighter part of the heat-extraction parabola,<sup>3</sup> but with shorter freezing times this relationship should depart quite considerably from linearity.

#### IV.—SUMMARY AND CONCLUSIONS.

The conclusions reached as the result of the work described in this paper may be briefly summarized as follows:

(1) Experimental techniques capable of measuring temperatures in solidifying non-ferrous castings with an absolute accuracy of better than  $\pm 1^\circ$  C. have been evolved. Changes in temperature of 0.25° C. are detectable using these techniques.

(2) Super-purity aluminium solidifies by a "skin-forming" mechanism in sand moulds. In the cylinder casting studied, and with a



End wall



Centre of  
cylinder

FIG. 16.—Macrostructure of Vertical Section through central axis of Aluminium Cylinder.  $\times \frac{1}{2}$ .

[To face p. 32.]

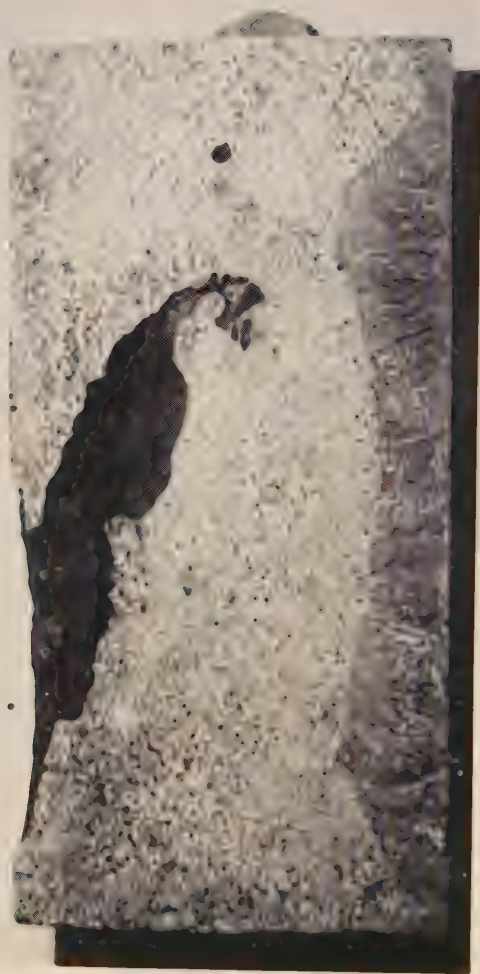


FIG. 12.—Micrograph showing region of solenar crystallization at the bottom of a horizontal section of an Aluminium-30% Copper Alloy.  $\times \frac{1}{2}$ .

pouring temperature of 760° C., the thickness solidified is approximately given as a function of time by the equation :

$$d = 0.4\sqrt{t} - 0.4 \quad . \quad . \quad . \quad . \quad . \quad (5)$$

where  $d$  is the skin thickness in inches and  $t$  is the time after pouring in minutes.

(3) Long-freezing-range alloys, such as the aluminium-4% copper alloy and phosphor bronze, solidify in a "pasty" manner, solidification at the centre of the casting taking place concurrently with, but lagging slightly behind, solidification at the mould walls. During the greater part of the solidification period liquid and solid coexist in all regions of the casting.

(4) The solidification of aluminium containing small quantities of titanium is akin to that of long-freezing-range alloys.

(5) The mode of solidification of near-eutectic alloys is somewhat obscure, but gravity and convection effects may play an important part in transferring heat from the centre of a casting to the mould wall.

(6) The times of complete freezing of simple castings may be calculated from thermal data with fair accuracy. Chvorinov's rule that the freezing times of castings are proportional to their  $\left(\frac{\text{volume}}{\text{surface area}}\right)^2$  ratio is reasonably well obeyed by aluminium-copper alloy castings.

#### ACKNOWLEDGEMENTS.

The author is indebted to the Director and Council of the British Non-Ferrous Metals Research Association for permission to publish this paper. The author's thanks are also due to Dr. A. G. Quarrell, F.I.M., and Mr. W. A. Baker, B.Sc., F.I.M., for much helpful advice and constructive criticism.

#### APPENDIX.

##### *The Calculation of Solidification Times.*

The calculated values, referred to in Section III of the paper, for the solidification times of the cylinder castings were derived by calculating as a function of time the heat extracted from the casting by the mould, and equating the expression obtained for this quantity with the heat content of the casting measured between the casting temperature and the temperature at which the casting became completely solid. In carrying out this calculation, no allowance is made for corner effects or curvature of the casting surface, but it is not thought that the error introduced by this approximation is large; a

greater source of error lies in the values used for the thermal properties, some of which can only be regarded as very approximate.

The expression for the heat extracted by the mould is obtained in the following way.<sup>1,3</sup> At any time  $t$  after casting the temperature  $\theta$  of a point in the mould, at a distance  $x$  from the metal/mould interface, is given by

$$\theta = \Theta \operatorname{erfc} \left( \frac{x}{2\sqrt{\alpha t}} \right) \quad . \quad . \quad . \quad . \quad . \quad (6)$$

all temperatures being referred to the mould's initial temperature, where:

$\Theta$  = the temperature at the metal/mould interface, supposed constant,

$\operatorname{erfc} \left( \frac{x}{2\sqrt{\alpha t}} \right) = 1 - \operatorname{erf} \left( \frac{x}{2\sqrt{\alpha t}} \right)$ , where  $\operatorname{erf} \left( \frac{x}{2\sqrt{\alpha t}} \right)$  is the error function of the expression within the brackets,

and  $\alpha$  = the mean temperature diffusivity\* of the mould material  
 $= K/c\rho$ , where  $K$  is the mean thermal conductivity,  $c$  the mean specific heat, and  $\rho$  the mean density over the temperature range  $\Theta$ .

The rate at which heat is transferred across unit area of the mould/casting interface is given by

$$\frac{\partial Q}{\partial t} = -K \left[ \frac{\partial \theta}{\partial x} \right]_{x=0} \quad . \quad . \quad . \quad . \quad . \quad (7)$$

Using equation (6) and differentiating:

$$\frac{\partial Q}{\partial t} = \frac{K\Theta}{\sqrt{\pi\alpha t}} \quad . \quad . \quad . \quad . \quad . \quad (8)$$

The total heat absorbed by the mould in time  $t$  is found by integrating (8) with respect to  $t$ :

$$Q = \frac{2K\Theta\sqrt{t}}{\sqrt{\pi\alpha}} = \frac{2b\Theta\sqrt{t}}{\sqrt{\pi}} \quad . \quad . \quad . \quad . \quad . \quad (9)$$

where  $b = \sqrt{Kc\rho}$ , the heat diffusivity of the mould material.

The total amount of heat extracted by the mould from the casting in time  $t$  is obtained by multiplying the expression for  $Q$  given by (9) by  $A$ , the surface area of the casting.

If the latent heat of fusion of the metal be  $L$  and the average specific

\* In this country  $\alpha = K/c\rho$  is usually termed the "thermal diffusivity"; in this paper  $\alpha$  is called the "temperature diffusivity" in accordance with German practice, to distinguish it from the related quantity  $b = \sqrt{Kc\rho}$  which is named the "heat diffusivity".

heat over the superheat and freezing range be  $S$ , then the total heat content liberated upon solidification is :

$$W[L + S (\theta_c - \theta_s)]$$

where  $W$  = the weight of the casting,

$\theta_c$  = the casting temperature,

and  $\theta_s$  = the final solidification temperature.

The time for complete solidification is then given by equating the above expression with the expression for  $QA$  :

$$\sqrt{t} = \frac{W\sqrt{\pi}[L + S (\theta_c - \theta_s)]}{2bA \Theta} \quad . \quad . \quad . \quad (10)$$

It will be observed that the above derivation presupposes a constant value for the metal/mould interface temperature. While this is nearly true of castings in pure metals and alloys of small freezing range, in castings of long freezing range the interface temperature may fall through 100° C. or more during the solidification period. Hence, in calculating the freezing time in such instances it is necessary to assume an average figure for the interface temperature. In the calculations carried out here, the figure taken has been the temperature at which the casting has liberated half its latent heat; \* this temperature has been taken correct to the nearest 5° C.

The thermal data used in these calculations were the figures for the specific heats of liquid and solid aluminium, liquid copper, and for the compound  $\text{CuAl}_2$  given by Kelley,<sup>11</sup> and published values for the latent heats of aluminium,<sup>12</sup> copper,<sup>12</sup> and  $\text{CuAl}_2$ .<sup>13</sup> The actual figures used in the calculations were obtained from these values by the use of the mixture law. In the absence of better data, the figures quoted above for copper were used for the calculation for the aluminium bronze and tin bronze cylinders. For alloys freezing substantially at constant temperature the value of the specific heat for the liquid metal was employed; for long-freezing-range alloys a value between that for the liquid and that for the solid (but nearer to the figure for the liquid) was used.

In calculating the freezing times the thermal data for the mould material found experimentally and given in the paper by Ruddle and Mincher<sup>3</sup> were used.

The method of calculation is made clear by the following example for the 5-in.-dia. cylinder in the aluminium-4% copper alloy cast from 750° C. With this casting temperature the alloy has liberated half

\* The heat content due to superheat is included with the latent heat.



### 36 Preliminary Study of the Solidification of Castings

its heat content at 641° C. The "constant" interface temperature was therefore taken to be 640° C. The mould was assumed to be at 20° C. initially.

The thermal data used for the metal were :

$$L = 95 \text{ cal./g.},$$

$$S = 0.255 \text{ cal./g./}^{\circ}\text{C.},$$

and the weight of the casting was 7840 g. The heat content liberated during cooling from 750° C. to 548° C., the final solidification temperature, is therefore

$$= 7840 \times (95 + 0.255 \times 202).$$

Hence, since the surface area of the casting is 1264 cm.<sup>2</sup> and  $b = 0.0204$  C.G.S. units :

$$\begin{aligned}\sqrt{t} &= \frac{7840 \times 1.77 (95 + 0.255 \times 202)}{2 \times 1264 \times 0.0204 \times 620} \\ &= 63.3\end{aligned}$$

so that  $t = 4000 \text{ sec.} = 67 \text{ min.}$

#### REFERENCES.

1. R. W. Ruddle, "The Solidification of Castings: A Review of the Literature", *Inst. Metals Monograph and Rep. Series*, No. 7, 1950.
2. R. W. Ruddle, *J. Inst. Metals*, 1950, **77**, 37.
3. R. W. Ruddle and A. L. Mincher, *J. Inst. Metals*, 1949-50, **76**, 43.
4. H. Y. Hunsicker, *Trans. Amer. Found. Assoc.*, 1947, **55**, 68.
5. G. V. Raynor, *Inst. Metals Annotated Equilib. Diag.* No. 4, 1944.
6. W. L. Fink, K. R. Van Horn, and P. M. Budge, *Trans. Amer. Inst. Min. Met. Eng., Inst. Metals Div.*, 1931, 421.
7. J. Verö, *Z. anorg. Chem.*, 1933, **213**, 257.
8. N. Chvorinov, *Giesserei*, 1940, **27**, 177.
9. H. A. Schwartz, *Trans. Amer. Found. Assoc.*, 1945, **53**, 1.
10. H. A. Schwartz, *Foundry*, 1944, **72**, (12), 80.
11. K. K. Kelley, *U.S. Bur. Mines Bull.* No. 371, 1934.
12. K. K. Kelley, *U.S. Bur. Mines Bull.* No. 393, 1936.
13. G. D. Roos, *Z. anorg. Chem.*, 1916, **94**, 329.

# CORRELATION OF TENSILE PROPERTIES OF ALUMINIUM ALLOY PLATE CASTINGS WITH TEMPERATURE GRADIENTS DURING SOLIDIFICATION.\*

By R. W. RUDDLE,† M.A., A.I.M., MEMBER.

(Communication from the British Non-Ferrous Metals Research Association.)

## SYNOPSIS.

The temperature gradients existing during the solidification of plate castings in an aluminium alloy containing 4.5% copper have been measured and correlated with the soundness and tensile properties of specimens subsequently cut from the plates. The plates were 12 in. long and 6 in. wide and of five thicknesses between  $\frac{1}{4}$  and  $1\frac{1}{2}$  in.; all were run and fed from one end and were rapidly poured. A casting temperature of 700° C. was used for most of the work.

The results show a good correlation between the tensile properties and the longitudinal temperature gradients existing during the later stages of freezing, when interdendritic feeding was occurring. These gradients were steepest in plates  $\frac{1}{2}$  in. thick, the tensile properties of which were considerably superior to those of plates of other thicknesses. A thickness of  $\frac{1}{2}$  in., therefore, appears to be the optimum for the casting conditions used. Sound plates of thicknesses greatly different from the optimum cannot be sand cast when rapidly poured, no matter what size of feeder be employed.

A theoretical explanation is given for the effects observed. Decreasing the pouring temperature produces some increase in soundness and tensile properties, but increasing the pouring temperature causes a marked deterioration in the properties of plates of optimum thickness.

## I.—INTRODUCTION.

THIS paper describes some of the initial work carried out in the British Non-Ferrous Metals Research Association's research into the solidification of non-ferrous castings, the object of which is to provide the quantitative understanding of heat flow in castings and moulds which is necessary for the development of improved casting techniques. A review of the available literature on the subject has been published,<sup>1</sup> and preliminary results on other aspects of the research are embodied in separate papers.<sup>2, 3</sup>

The present paper is concerned with a study of the solidification of

\* Manuscript received 14 May 1949. The work described in this paper was made available to members of the B.N.F.M.R.A. in confidential research reports issued during 1947 and 1948.

† Head of Melting and Casting Section, British Non-Ferrous Metals Research Association, London.

simple plate castings, gated and fed from one end. The principal aim of the work was to establish a correlation between the temperature gradients in the castings during solidification and the tensile properties and soundness of the plates. Plate castings were chosen for the work to minimize possible confusing effects due to convection. As the work was of a preliminary nature, the experiments were confined to a single (aluminium-base) alloy, its mode of solidification being studied concurrently.<sup>3</sup>

## II.—EXPERIMENTAL TECHNIQUE.

### *Metal.*

The material used in this work was taken from two batches (MJS and NJL) of commercial ingot conforming to specification D.T.D. 304 and of the following composition: MJS—copper 4.63, iron 0.11, silicon 0.11, titanium 0.14%; NJL—copper 4.89, iron 0.15, silicon 0.10, titanium 0.10%.

### *Melting and Casting.*

The plates were cast from separate melts, the weights of which varied between about 12 and 24 lb. according to the size of the casting being made. Each charge was rapidly melted in a Salamander crucible in a gas-fired furnace, care being taken to keep the maximum temperature of the melt as low as possible. When the metal temperature reached about 700° C. the melt was degassed with hexachlorethane; during the degassing period the temperature usually rose somewhat, but in most instances remained below 740° C. Each melt was shown to be gas-free by the reduced-pressure test<sup>4</sup> and was then allowed to cool in the furnace to just above the casting temperature. In one or two instances where a high casting temperature was required, the melting temperatures were rather higher than stated above.

Care was taken during pouring to keep the 1¼-in.-dia. downgate full, in order to reduce the pouring time to a minimum and to ensure that all the plates were poured at the same rate. The average pouring time was about 5 sec. For purposes of comparison two D.T.D. test-bars were poured into dry-sand moulds immediately after each plate had been cast. A standard pouring temperature of 700° C. was used for most of the work. Certain of the ½-in. and 1-in.-thick plates were also poured from other temperatures to examine the effect of pouring temperature on the temperature gradients present during solidification and on the tensile properties of the castings.



was a special open feeder, the purpose of which is indicated later. Head B was not used in the present series of experiments.

TABLE I.—*Feeder : Casting Ratios for Plate Castings.*

Plate Thick- ness, in.	Feeder-Head A	Feeder-Head C	Feeder-Head D	Feeder-Head E *
$\frac{1}{4}$	1.72	...	6.18	...
$\frac{1}{2}$	0.96	...	3.34	...
$\frac{3}{4}$	...	...	2.60	...
1	0.58	1.34	1.88	3.08
$1\frac{1}{2}$	...	...	1.39	...

\* Open feeder; see p. 53.

All the plates were cast in dry-sand moulds made from the synthetic sand used for the work on the mechanism of solidification<sup>3</sup> and dried at 200° C.

#### *Temperature Measurements.*

In the majority of the experiments cooling curves were recorded simultaneously from 6 thermocouples located on the longitudinal axis of the plate (couples 1-6 in Fig. 1). In certain cases, to secure fuller information, the arrangement of 12 thermocouples shown in Fig. 1 was employed, and in one or two special experiments a grid of 15 thermocouples was used.

The thermocouples were introduced into the mould cavity in the manner shown in Fig. 1, to minimize errors caused by conduction along the wires. The temperatures were measured to about  $\pm 2^\circ$  C. with the apparatus described in another paper.<sup>3</sup>

#### *Heat-Treatment.*

After removal of the feeder-heads and runners, the plates and their accompanying D.T.D. test-bars were given the following heat-treatment in a small forced-air-circulation electric furnace: Solution-treatment: 16 hr. at 535° C., followed by quenching in cold water; precipitation-treatment: 16 hr. at 140° C.

#### *Examination of Castings.*

All the plates were radiographed after heat-treatment.

Five test-pieces were cut transversely from each plate, these being taken from the  $1\frac{1}{2}$ -in.-wide slices marked *a-e* in Fig. 1. To obtain comparable results from the plates of different thicknesses, the dia. of each test-piece was made equal to half the plate thickness.



The gauge-lengths were chosen so as to maintain the usual  $4 \times \sqrt{\text{cross-sectional area}}$  relationship; the other dimensions of the test-pieces were in conformity with the relations specified in B.S. 18.\* The D.T.D. test-bars were machined into B.S. type C test-pieces of 0.564 in. dia.

The densities of the machined test-pieces were measured, and the percentage voids in each specimen were calculated, assuming that the fully sound material had a density of 2.810 g./c.c. It should be noted that the percentage-voids figures for the  $\frac{1}{2}$ - and  $\frac{1}{4}$ -in.-thick plates are not comparable with the figures given for the other plates. The overall length of the larger test-pieces was the full 6-in. width of the plates, whereas the small test-pieces machined from the  $\frac{1}{2}$ - and  $\frac{1}{4}$ -in.-thick plates were respectively only  $3\frac{1}{2}$  and 2 in. long; the latter were thus machined entirely from the more unsound material at the plate centre and therefore show relatively higher voids.

### III.—RESULTS.

#### 1. Temperature Gradients.

Representative cooling curves are shown in Figs. 2-9, in which, for clarity, only the curves for couples 1, 3, 5, and 6 are included.

In this paper the results observed are related to the temperature gradients present during solidification. The temperature gradients are, however, not of fundamental importance from the point of view of the mechanism of solidification; strictly speaking, the results should have been related to the solidification gradients. Since all the castings studied were made in the same alloy, this point is unimportant in the present instance, but it would be essential to consider solidification gradients rather than temperature gradients, when comparing the solidification of castings made in different alloys.

The scale plotted on the right-hand side of Figs. 2-9 gives the variation with temperature of the percentage of solid metal existing throughout the freezing range of the material. This scale, which is approximate only, was derived in the following way. Cooling curves taken on samples of the ingot material showed the primary arrest to occur at  $649.5^{\circ}\text{C.}$  and the eutectic arrest at  $542.5^{\circ}\text{C.}$  (presumably this is the ternary aluminium-copper-iron eutectic). An approximate freezing point-composition diagram was drawn, using the values given above for the arrests, and making the assumption that the liquidus

\* The parallel lengths of the test-pieces taken from the  $1\frac{1}{2}$ -in.-thick plate were rather shorter than required by the specification, as the plate was only 6 in. wide.

curve was similar in shape to that of the binary aluminium-copper system.<sup>5</sup> It was further assumed that the ternary eutectic contains 32.5% copper,<sup>6, 7</sup> and that 2.5% copper is retained in solid solution under sand-casting conditions. A plot of the variation of the percentage solid with temperature was then made from this diagram.

The mean longitudinal temperature gradients in the plates (i.e. the gradients along their central axes) at certain times after casting, are given in Tables II-IV. In the plates of  $\frac{1}{2}$ -in. thickness and upwards,

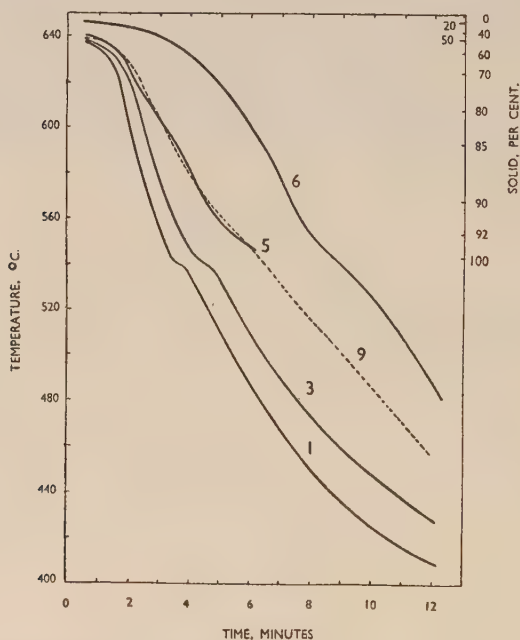


FIG. 2.—Cooling Curves on Central Axis of  $\frac{1}{2}$ -in.-thick Plate Cast with Head A at 700° C. (Feeder : casting ratio 0.96.)

these gradients were fairly small and uniform along the greater part of the plate length, although they steepened somewhat between couple 5 and the feeder-head. In the  $\frac{1}{4}$ -in.-thick plates the steepening of the gradient was very marked in this region. Since all but one of the specimens for tensile test were cut from the portion of the plate between couple 4 and the remote end of the plate, the longitudinal gradients quoted for the  $\frac{1}{4}$ -in.-thick plates are the mean values between couples Nos. 1 and 4, i.e. the gradients are representative of those

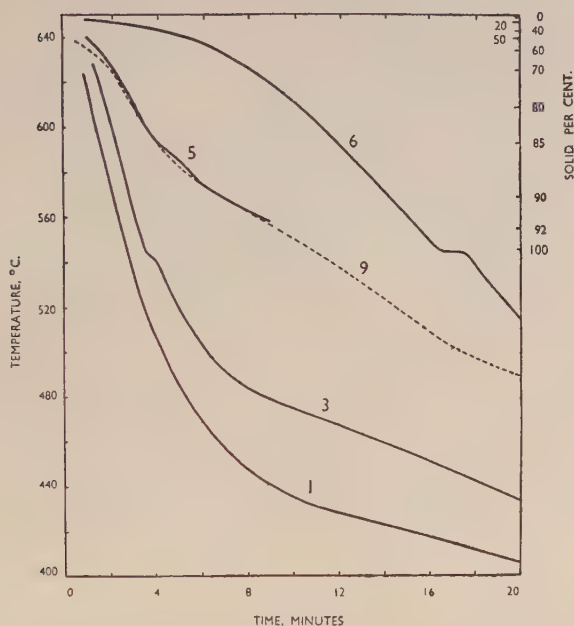


FIG. 3.—Cooling Curves on Central Axis of  $\frac{1}{2}$ -in.-thick Plate Cast with Head D at 700° C. (Feeder : casting ratio 3.34.)

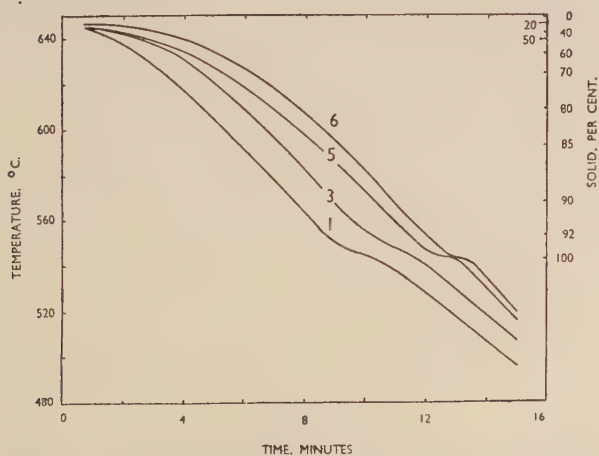


FIG. 4.—Cooling Curves on Central Axis of 1-in.-thick Plate Cast with Head A at 700° C. (Feeder : casting ratio 0.58.)

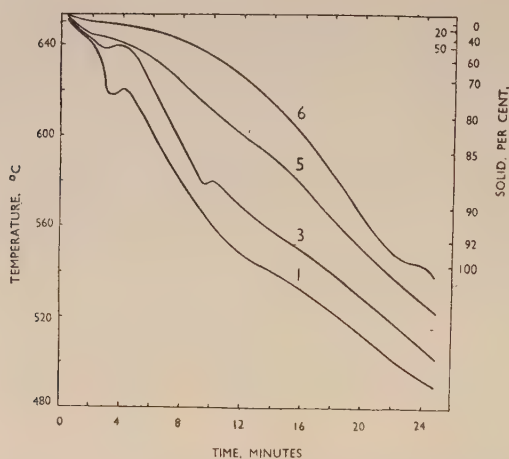


FIG. 5.—Cooling Curves on Central Axis of 1-in.-thick Plate Cast with Head D at 700° C. (Feeder : casting ratio 1.88.)

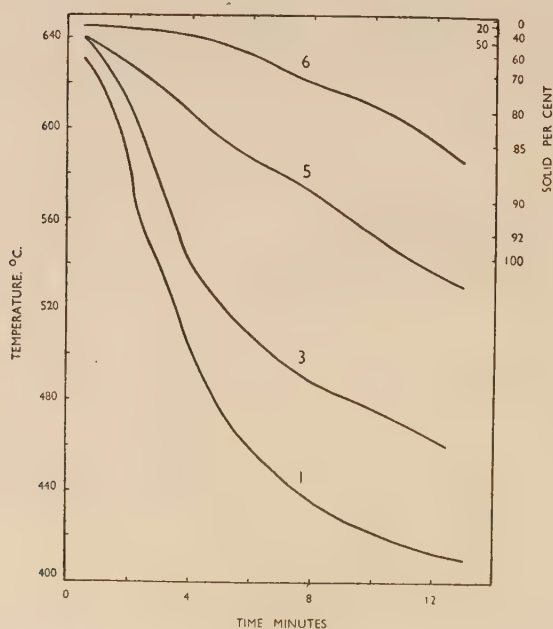


FIG. 6.—Cooling Curves for  $\frac{1}{2}$ -in.-thick Plate Cast with Head D at 670° C. (Feeder : casting ratio 3.34.)

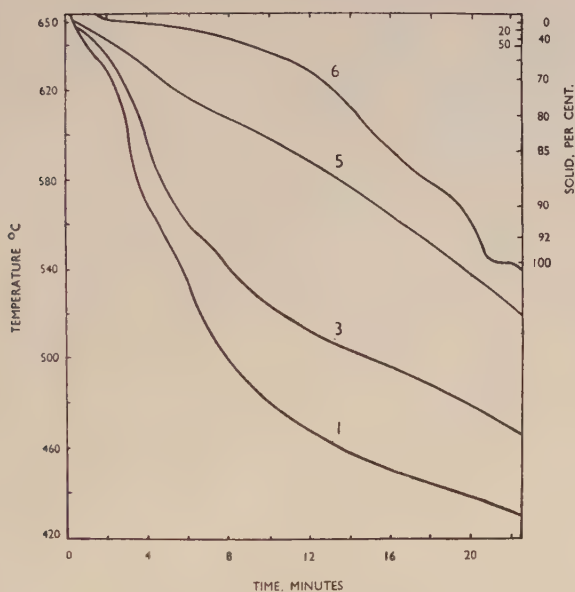


FIG. 7.—Cooling Curves for  $\frac{1}{2}$ -in.-thick Plate Cast with Head D at 760° C. (Feeder : casting ratio 3.34.)

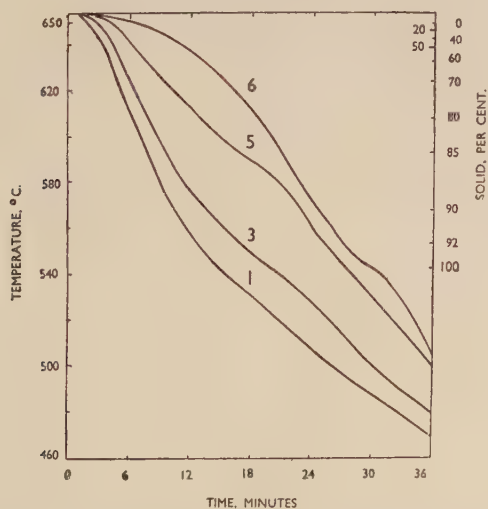


FIG. 8.—Cooling Curves for 1-in.-thick Plate Cast with very heavy Feeder at 700° C. (Feeder : casting ratio 3.08.)



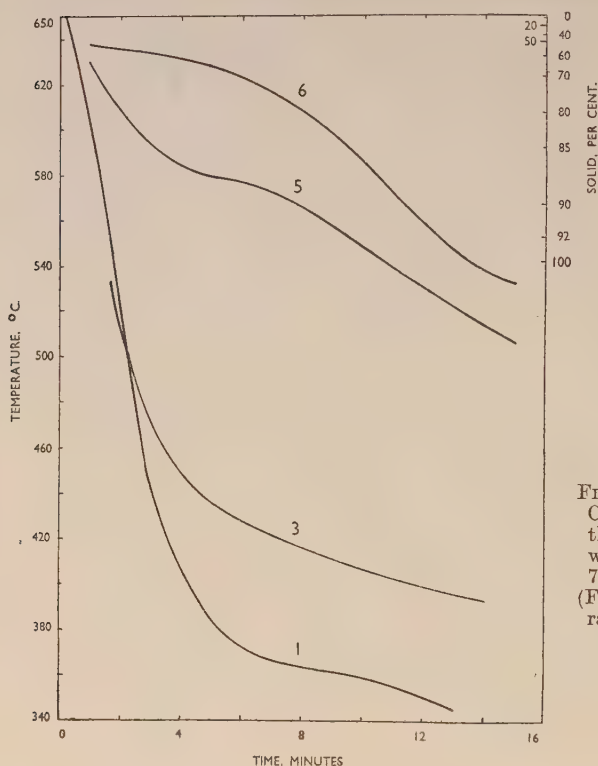


FIG. 9.—Cooling Curves for  $\frac{1}{4}$ -in.-thick Plate Cast with Head D at  $700^{\circ}\text{C}$ . (Feeder : casting ratio 6.18.)

TABLE II.—Effect of Plate Thickness on Longitudinal Temperature Gradients and Ultimate Tensile Strength of Plates Cast at  $700^{\circ}\text{C}$ .

Plate Thickness, in.	Feeder-Head	Feeder : Casting Ratio	Max. Mean Temp. Gradient, $^{\circ}\text{C./in.}$	Mean Temp. Gradient when Solidification just Complete at Couple 1, $^{\circ}\text{C./in.}$	U.T.S., tons/in. <sup>2</sup>
$\frac{1}{4}$	A	1.72	11 *†	3 ‡	11.1
$\frac{1}{2}$	A	0.96	16 $\frac{2}{3}$	8 $\frac{1}{3}$	19.7
1	A	0.58	6	4 $\frac{1}{3}$	16.7
$\frac{1}{4}$	D	6.18	19 *†	3 ‡	10.6
$\frac{1}{2}$	D	3.34	18 $\frac{1}{2}$	12	21.9
$\frac{3}{4}$	D	2.60	15	12	19.2
1	D	1.88	8 $\frac{1}{2}$	8	16.3
1 $\frac{1}{2}$	D	1.39	5 $\frac{1}{4}$	2 $\frac{2}{3}$	15.7

\* Mean gradient between couples 1 and 4; gradient near feeder much higher, viz.  $71^{\circ}\text{C./in.}$  in plate with head D and  $26^{\circ}\text{C./in.}$  in plate with head A.

† Attained after solidification complete.

‡ Mean gradient between couples 1 and 4; gradient near feeder much higher, viz.  $39^{\circ}\text{C./in.}$  in plate with head D and  $15^{\circ}\text{C./in.}$  in plate with head A.

TABLE III.—Effect of Feeder Size on Longitudinal Temperature Gradients and Ultimate Tensile Strength of Plates Cast at 700° C.

Plate Thickness, in.	Feeder-Head	Feeder : Casting Ratio	Max. Mean Temp. Gradient, ° C./in.	Mean Temp. Gradient when Solidification just Complete at Couple 1, ° C./in.	U.T.S., tons/in. <sup>2</sup>
$\frac{1}{2}$	A	0.96	$16\frac{2}{3}$	$8\frac{1}{3}$	19.7
$\frac{1}{2}$	D	3.34	$18\frac{1}{2}$	12	21.9
1	A	0.58	6	$4\frac{1}{3}$	16.7
1	C	1.34	6	$4\frac{1}{2}$	15.9
1	D	1.88	$8\frac{1}{2}$	8	16.3
1	E	3.08	$8\frac{1}{2}$	$8\frac{1}{3}$	17.6

TABLE IV.—Effect of Pouring Temperature on Longitudinal Temperature Gradients and U.T.S. of 1-in. and  $\frac{1}{2}$ -in. Plates Cast with Head D. (Feeder : casting ratios 1.88 and 3.34, respectively.)

Plate Thickness, in.	Pouring Temp., ° C.	Max. Mean Temp. Gradient, ° C./in.	Mean Temp. Gradient when Solidification just Complete at Couple 1, ° C./in.	U.T.S., tons/in. <sup>2</sup>
1	670	$13\frac{1}{2}$	9	18.8
	700	$9\frac{1}{2}$	8	16.3
	760	9	7	15.2
$\frac{1}{2}$	670	21	$12\frac{2}{3}$	22.8
	700	21	12	21.9
	715	21	$12\frac{2}{3}$	20.1
	760	19	$12\frac{1}{2}$	17.6

parts of the plates the tensile properties of which were determined. The gradients varied during the solidification period and, for reasons put forward in the discussion below, the figures given in Tables II–IV (column 5) are those existing in the final stages of solidification (arbitrarily taken as the moment when freezing was complete at couple 1).

The data in Tables II, III, and IV illustrate, respectively, the effects of plate thickness, feeder size, and pouring temperature on the magnitude of the longitudinal gradients.

Figs. 10 and 11 show the approximate positions of the isotherms and isosolids at two different times after casting in  $\frac{1}{4}$ -in.- and 1-in.-thick plates made with feeder-head D. These figures were derived from experiments in which a grid of 15 thermocouples was used. Of these, five were placed with their tips on the centre-line of the plate; three with their tips on the surface of the casting above the central

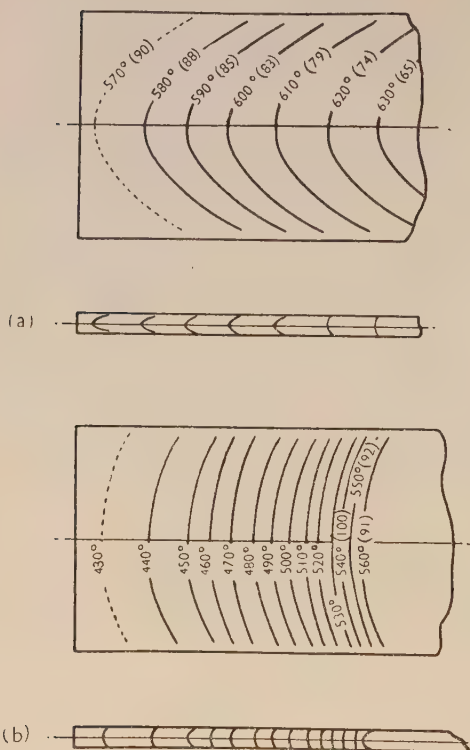


FIG. 10.—Isotherms in  $\frac{1}{2}$ -in.-thick Plate Cast with Head D at  $700^{\circ}$  C. (Feeder: casting ratio 3.34.) Figures in brackets indicate percentage solid.

Sections through centre line show isothermals at (a) 2 min., (b) 10 min. after casting.

TABLE V.—*Temperature Gradients in  $\frac{1}{2}$ -in. Plate Cast with Feeder-Head D.*

Direction of Gradient	Couple Position Nos.	Mean Temperature Gradients Between Positions Indicated, $^{\circ}$ C./in.		
		After 2 min.	After 10 min.	After 15 min.
Longitudinal	1-2	9	$10\frac{1}{4}$	$8\frac{3}{4}$
	2-3	$12\frac{1}{4}$	16	$14\frac{1}{4}$
	3-4	3	$20\frac{1}{4}$	$17\frac{1}{4}$
	4-5	9	30	24
Transverse (across width)	10-11	$8\frac{1}{2}$	2	3
	11-12	8	4	$2\frac{1}{2}$
	12-2	$7\frac{1}{2}$	3	$2\frac{3}{4}$
Lateral (across thickness)	7-1	13	4	6
	8-3	27	8	5
	9-5	3	24	22

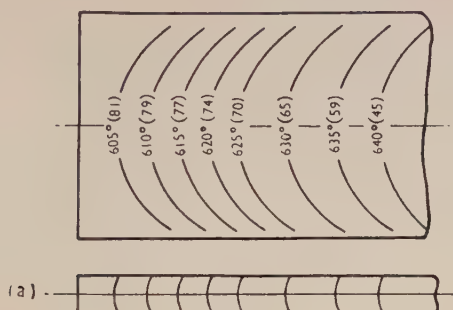


FIG. 11.—Isotherms in 1-in.-thick Plate Cast with Head D at 700° C. (Feeder: casting ratio 1.88.) Figures in brackets indicate percentage solid.

Sections through centre line show isotherms at (a) 5 min., (b) 12 min. after casting.

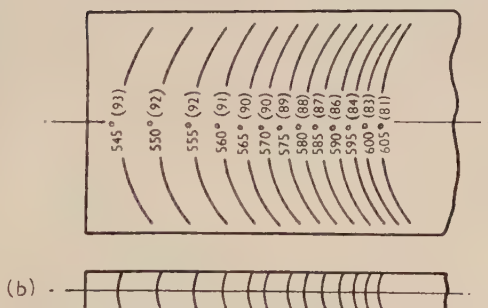


TABLE VI.—Temperature Gradients in 1-in. Plate Cast with Feeder-Head D.

Direction of Gradient	Couple Position Nos.	Mean Temperature Gradients Between Points Indicated, ° C./in.		
		After 5 min.	After 12 min.	After 23 min.
Longitudinal	1-2	6½	5½	4¾
	2-3	5¾	8	5½
	3-4	3½	5½	6¾
	4-5	~3½	~12	~8
Transverse (across width)	10-11	4	1½	½
	11-12	6½	2¾	2
Lateral (across thickness)	7-1	<1	<1	<1
	8-3	<2	<2	8
	9-5	...	...	...

axis; three with their tips in the central (horizontal) plane of the plate, but offset 1 in. from the centre-line; three with the tips similarly in the central plane but offset 2 in. from the centre-line; and one in the estimated heat-centre of the feeder.

Tables V and VI give values for the longitudinal, transverse, and lateral temperature gradients\* in the  $\frac{1}{2}$ - and 1-in.-thick plates (feeder-head D) at various times after casting. In these Tables column 3 shows the gradients present shortly after the beginning of solidification, column 4 the gradients at an intermediate stage, and column 5 the gradients when the feeder end of the plate was almost fully solid.

Similar results were obtained with the other plates, but it was impracticable to measure the transverse and lateral gradients in the  $\frac{1}{4}$ -in.-thick plates.

The main points emerging from Figs. 2-11 and Tables II-VI are summarized below :

(i) The transverse gradients are in general surprisingly small, being of the same order as, and often less than, the longitudinal gradients. (See Tables V and VI.)

(ii) The longitudinal gradients are relatively small immediately after casting, but increase with time to a maximum value and ultimately fall to a low figure. This effect is well-marked in Figs. 3, 5, and 7, and is shown in Tables V and VI.

(iii) The value of the maximum longitudinal gradient (mean for the whole plate) is greatest in the thinnest plates, being roughly proportional to the reciprocal of the plate thickness. (See Table II.)

(iv) The time at which the maximum occurs is not greatly affected by plate thickness; in most instances this time is about 10 min. after casting. (See, for example, Figs. 2-6.)

(v) In the early stages of freezing of any particular plate the steepest gradients exist at the end of the plate remote from the feeder, but as solidification progresses, this point of maximum gradient shifts toward the feeder. (See Tables V and VI.)

(vi) Increase in the feeder : casting ratio causes some increase in the longitudinal gradient. (See Table III.)

(vii) Decrease in the pouring temperature causes an increase in the longitudinal gradient (see Table IV) and a decrease in freezing time. These effects, however, are not large.

Ancillary experiments were made to determine (a) whether up-running had any considerable effect on the gradients present during solidification, and (b) whether the temperatures of the top and bottom

\* Respectively, the gradients along the length and across the width and thickness of the plates.



surfaces of the plates were markedly different. The gradients in down-run  $\frac{1}{2}$ -in. plates, although slightly less steep near the beginning of solidification, were closely similar to those in the corresponding uprun plates; the tensile properties of the downrun plates were almost identical with those of the uprun plates. It was therefore concluded that uprunning was not materially affecting the solidification of the plates at the rapid pouring speed used. The temperatures of the top and bottom surfaces of the plates showed little difference, except close to the feeder, where the top surface was several degrees hotter than the bottom.

## 2. Tensile Properties and Soundness.

The tensile-test and percentage-voids figures obtained from each plate and its accompanying D.T.D. test-bars are summarized in Table VII. The mean ultimate tensile strengths of the plates are also given in Tables II–IV to facilitate comparison with the temperature gradients. In Table VII the figures quoted for the plates are the means of the results obtained with the five test-pieces taken from each plate. Individual test-pieces taken from any one plate showed remarkable uniformity, as is evidenced by the figures given in Table VIII for the  $\frac{1}{2}$ -in. plate.

Radiographic examination showed dispersed porosity extending up to the edges of the plates. The porosity was fine in the plates of high strength and coarser in those possessing poor properties. In all instances the porosity was most severe in regions adjacent to the feeder, and in the  $\frac{1}{4}$ -in. plates a fairly steep porosity gradient was present across the plate width.

Examination of the figures given in Tables VII and VIII leads to the following conclusions:

(i) Decreasing the plate thickness from  $1\frac{1}{2}$  to  $\frac{1}{2}$  in. markedly increases the tensile properties of plates cast at  $700^{\circ}$  C. (see Table II). Further decrease in the plate thickness to  $\frac{1}{4}$  in. results in a sharp fall in strength.\* Thus, under the pouring conditions used, there appears to be an optimum plate thickness conducive to soundness and high strength.

(ii) Increase in the feeder: casting ratio does not have any considerable effect on the tensile properties of the plates (see Table III). The effect appears to be more marked in plates of the optimum thickness ( $\frac{1}{2}$  in.).

(iii) Decreasing the pouring temperature from  $700^{\circ}$  to  $670^{\circ}$  C. improves the strength of the plates, while increasing the pouring temperature to  $760^{\circ}$  C. causes a marked deterioration. (See Table IV.)

\* Specimens cut from the edges of these plates had much higher strength ( $>20$  tons/in.<sup>2</sup>), in conformity with the radiographic evidence.

TABLE VII.—*Tensile Properties of Aluminium-4.5% Copper (D.T.D. 304) Alloy Plates.*

Melt No.	Plate Thickness, in.	Feeder Head	Feeder: Casting Ratio	Casting Temp., °C.	Voids, %	U.T.S., tons/in. <sup>2</sup>	Elongation, %	D.T.D. Test-Bars		
								Voids, %	U.T.S., tons/in. <sup>2</sup>	Elongation, %
NJL119	1	A	1.72	700	1.3 *	11.1 *	7.7 †	0.15	19.9	7.5
NJL118	1	D	6.18	700	1.3	10.6	7.0 †	0.05	18.0	5.0
MJS61	1	A	0.96	700	0.9	19.7	7.1	0.35	19.9	6.5
NJL88	1	D	3.34	670	0.8	22.8	11.6	0.1	20.7	7.0 †
MJS 62	1	D	3.34	700	1.2	21.9	9.6	0.35	19.8	7.0
MJS85	1	D	3.34	715	0.9	20.1	12.4 †	0.0	22.3	8.0
MJS84	1	D	3.34	760	0.9	17.6	5.8	0.6	16.3	5.0
NJL86	1	D	2.60	700	0.5	19.2	5.8	0.2	19.7	4.5
MJS58	1	A	0.58	700	0.6 †	16.7	4.0	0.05	21.4	9.5
NJL56	1	C	1.34	700	0.7	15.9	3.3	0.35	22.2	11.3
NJL90	1	D	1.88	670	0.4	18.8	5.4	0.30	21.4	8.5
MJS57	1	D	1.88	700	0.6 *	16.3	4.9	0.35	20.0	7.0
NJL91	1	D	1.88	760	0.7	15.2	2.3 *	0.75	14.9	3.0
MJS80	1	E	3.08	700	1.3	17.6	5.0 *	0.0	20.8	6.5
MJS60	1½	D	1.39	700	0.9 †	15.7	3.2	0.35	20.5	8.8

Except where otherwise indicated, figures quoted for the plate castings are the mean of 5 results and figures quoted for the D.T.D. test-bars are the mean of 2 results.

\* Mean of 4 results.

† Mean of 3 results.

‡ Single test result.

Note 1.—Percentage voids were calculated on the assumption that the density of fully sound metal = 2.810 g./c.c.

Note 2.—All densities determined on machined specimens. Figures for percentage voids of test-pieces from ¾-in. and smaller plates are therefore not comparable with those for thicker plates.

TABLE VIII.—*Tensile Properties and Percentage Voids for  $\frac{1}{2}$ -in. Plate Cast with Feeder-Head D from 700° C.*

Position of Test-Piece (see Fig. 1)	U.T.S., tons/in. <sup>2</sup>	Elongation, %	Voids, %
<i>a</i>	22.4	9	1.0
<i>b</i>	21.6	8	1.3
<i>c</i>	22.4	9	1.1
<i>d</i>	22.4	13	1.2
<i>e</i>	20.7	9	1.4

(iv) Specimens located close to the feeder tend to show the highest porosity in accordance with the results of the radiographic examination (see Table VIII). The uniformity of the tensile-test results is surprising in view of this.

(v) Under the casting conditions employed, it appears difficult to produce sound plates of thicknesses other than the optimum. This was demonstrated by making the 1-in. plate with a very large feeder (head E); despite the high feeder : casting ratio (3.08) the properties of the plate are considerably below those of the  $\frac{1}{2}$ -in. plates. (See Tables III and VII.)

#### IV.—DISCUSSION.

##### 1. Plates Cast at 700° C.

It is sometimes held <sup>1</sup> that the major factor governing the soundness and strength of a casting is the ratio of the lateral to the longitudinal temperature gradient, a low ratio favouring soundness and high mechanical properties. However, as Tables V and VI show, no correlation exists between this ratio and the tensile properties of the plates studied, and some other explanation was therefore sought for the variation in tensile properties of the plates and in particular for the existence of an optimum plate thickness. The isotherms and isosolids in the  $\frac{1}{2}$ - and 1-in.-thick plates (Figs. 10 and 11) are instructive in this connection. In both plates the isotherms were more or less concentric about the heat-centre provided by the feeder-head, and this being so it is evident that feeding was not prevented by too rapid solidification in the transverse direction. Results obtained with other combinations of plate thickness and feeder size were similar (with the possible exception of the  $\frac{1}{4}$ -in.-thick plates, for which no isothermal diagrams could be prepared).

It is well known that long-freezing-range alloys freeze in a pasty manner, liquid and solid metal coexisting for considerable periods

throughout large regions of the casting. This mode of solidification in relation to the aluminium-4.5% copper alloy is described in some detail in another paper.<sup>3</sup> Baker<sup>4</sup> and others have shown that the freezing shrinkage of castings in these alloys is compensated by two distinct modes of feeding. The first occurs in the earlier stages of solidification; the pasty mixture of solid and liquid is then free to move, if somewhat sluggishly, and this wholesale movement ("mass feeding") continues until the solid crystals grow to an extent such

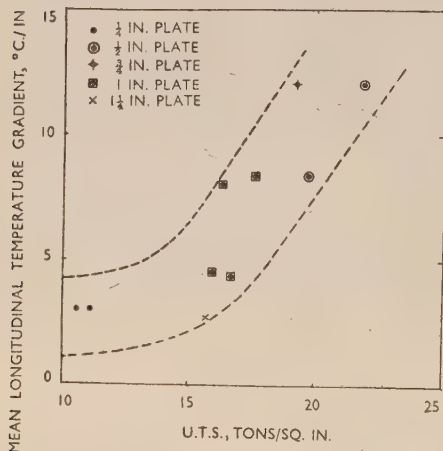


FIG. 12.—Plot of Mean Temperature Gradients during final stage of Solidification against Ultimate Tensile Strength, for Plates Cast at 700° C.

flow occurs. Obviously it takes place more easily and the freezing shrinkage is compensated more completely when the interdendritic channels are relatively short and are steeply tapered, and this condition will be favoured by steep temperature gradients.

If this view is correct the tensile properties and soundness of the plate castings studied should depend on the magnitude of the temperature gradients existing in the later stages of freezing. In Fig. 12 these gradients\* have been plotted against the mean tensile strength of the plates cast at 700° C. There is a good correlation† between

\* The mean longitudinal gradients existing when solidification was just complete at couple 1 (see column 5 in Tables II-IV).

† Statistical examination shows that the probability that the apparent correlation shown in Fig. 12 occurred by chance, lies between 0.01 and 0.001; in statistical practice correlations are generally regarded as significant if the chance probability is less than 0.05.

that they form a coherent mass. —Thereafter, the further volume contraction due to solidification of the interdendritic liquid and to the solid contraction of the dendrites, must be compensated by flow of feeding liquid through the tortuous channels between the growing dendrites. This flow of feeding liquid clearly occurs less readily than the "mass feeding" of the pasty mixture, and in fact, it is generally accepted that the soundness of the final casting depends on the extent to which this interdendritic

these quantities, confirming that the absolute magnitude of the longitudinal gradient at the end of freezing is the principal factor determining the soundness and strength of the plates.

Although (as Figs. 2-9 show) the gradients in all the plates increase to a maximum and then decline, the time after casting at which the maximum gradient is developed, relative to the end of freezing, varies. Thus, in the  $1\frac{1}{2}$ -in. plate (curves not shown) the maximum gradient had been reached and the decline had begun long before freezing was complete at couple 1; but with the  $\frac{1}{4}$ -in. plates (Fig. 9), and to a lesser extent with the  $\frac{1}{2}$ -in. plates (Figs. 2 and 3), the greater part of the plate was solid before the maximum was attained. In the 1-in. plates the maximum approximately coincided with the period of interdendritic feeding (Figs. 4 and 5). It follows, therefore, that the gradient present during the period of interdendritic feeding depends both on the magnitude of the maximum gradient and on its timing relative to the end of freezing. In the castings studied, these two factors are such that plates about  $\frac{1}{2}$  in. thick have the steepest longitudinal gradients in the critical last stages of freezing, and this accounts for the superior properties of plates of this thickness.

These observations may be explained in the following way. The presence of a feeder at one end of the plate, by retarding solidification at the point of the attachment, sets up a temperature gradient along the length of the plate which rapidly becomes steep, since freezing can proceed quickly at the far end of the plate but can only take place slowly near the feeder. The more quickly the far end of the plate freezes (i.e. the thinner the plate), the steeper will be the gradient set up by the feeder. However, the rate at which the mould extracts heat from the casting decreases with the square root of the time and eventually falls to a very low figure.<sup>2</sup> When this happens, heat flow along the plate tends to equalize the temperatures at the two ends, so that the temperature gradients first reach a maximum value and then decrease. The factor introduced by the declining rate of heat extraction of the mould is independent of both plate thickness and feeder size, so that to a first approximation the time in which the maximum gradient is reached should also be independent of plate thickness and feeder size. As noted above, Figs. 2-9 show that this is the case, the maximum being reached in all plates about 10 min. after casting. This explains why a thin plate solidifies before, and a thick plate after, the maximum gradient has been developed. The explanation ignores the gradients set up during pouring, but this is probably justifiable with rapidly poured castings.

A further factor may have influenced the soundness of the  $\frac{1}{4}$ -in.



plates. Since these plates solidified quickly, the transverse and lateral gradients may have been steep, with the isothermals following the contours of the mould wall instead of having the shape depicted in Fig. 10 for the  $\frac{1}{2}$ -in. plate. In this event the shrinkage would tend to take the form of centre-line shrinkage, if the lateral:longitudinal gradient ratio were unfavourable. The radiographic and other evidence suggested that this had in fact happened to some extent.\* Effects of this nature are likely to occur in all castings which freeze quickly, and any factor tending to increase the rate of solidification, for example, a change to a mould material of higher chilling power, should increase the tendency towards centre-line shrinkage.

The reason why it is difficult, if not impossible, to cast sound plates, not of optimum thickness, is readily understandable, since increasing the feeder size cannot alter the time of maximum gradient and can only affect the magnitude of the gradients to a limited extent. It is probable that the only ways of obtaining soundness in such plates are (a) to change the mould material, so as to slow down or increase the rate of solidification, as appropriate, or (b) to pour slowly in order to set up high initial gradients.

The conclusion reached in the present work, that there is an optimum plate thickness, is in agreement with the work of Eastwood and Davis,<sup>8</sup> who found that sound  $\frac{3}{16}$ -in. and  $1\frac{1}{2}$ -in.-thick plates in a magnesium alloy were difficult or impossible to produce, although intermediate thicknesses were readily cast sound.

The optimum plate thickness should be dependent on the thermal properties of both the alloy and the mould material. For example, owing to its lower (volume) thermal capacity, the optimum thickness for a magnesium alloy should be greater than for an aluminium alloy. This has been shown to be the case by Baker<sup>4, 9, 10</sup> who studied the temperature gradients in 1-in.-dia., 11-in.-long sand-cast bars in both aluminium and magnesium alloys. This diameter, ideal for the aluminium alloy, was unsatisfactory for the magnesium alloy, solidification occurring too rapidly. It is interesting to note that a 1-in. bar has the same  $\left(\frac{\text{volume}}{\text{surface area}}\right)^2$  ratio as a  $\frac{1}{2}$ -in. plate, so that it should solidify at about the same rate.<sup>1, 3</sup>

\* The cooling curves for the  $\frac{1}{2}$ -in. plate with head D (Fig. 9) indicate that a reversal in the direction of the temperature gradients took place shortly after pouring (couples 2, 3, and 4 showed reversals with respect to couple 1). This is not altogether surprising, for the initial gradients in very thin plates are likely to be affected by chance variations in metal flow during casting. Such a reversal in the temperature gradient would be an additional reason for the poor properties of the plate.

## 2. The Effect of Pouring Temperature.

The improvement produced by pouring the 1-in.-thick plate from a low superheat (pouring temperature  $670^{\circ}\text{C.}$ ) may be ascribed to the more rapid rate of solidification which, besides increasing the magnitude of the longitudinal gradients, also results in a closer approach between the time of the end of solidification and the time at which the longitudinal gradients are at a maximum. The lower tensile properties of the plate cast at  $760^{\circ}\text{C.}$  may be explained by the smaller gradients and longer solidification times of this plate. However, the D.T.D. test-bars cast with this plate gave unexpectedly poor figures which suggest interference by some other factor. The marked reduction in the properties of the  $\frac{1}{2}$ -in. plate caused by pouring from  $760^{\circ}\text{C.}$  is not explicable in terms of the changes in the temperature gradients during solidification, as Table IV shows. Macro-examination revealed that test-bars and castings poured from  $760^{\circ}\text{C.}$  had large grain-sizes of the order of 3–4 mm. dia., compared with less than 1 mm. for castings poured at  $700^{\circ}\text{C.}$  It is almost certain that this factor was responsible for the poor properties observed, for, as shown in a paper by Cibula and Ruddell,<sup>11</sup> the coarse grain-size resulting from the use of high melting and casting temperatures is associated with an unfavourable type of shrinkage porosity which causes a large reduction in the tensile strength. For example, bars with grain-sizes of 3–4 mm. dia. have an ultimate tensile strength of less than 13 tons/in.<sup>2</sup>, whereas bars with a grain-size of 0.25 mm. dia. give a figure of about 22 tons/in.<sup>2</sup>

The properties of castings, such as the  $\frac{1}{4}$ -in. plate, which solidify too rapidly for the attainment of optimum properties, might be improved by casting from a high superheat, for a high casting temperature, by retarding the rate of solidification, should prevent the completion of solidification before steep gradients are set up.

## 3. General.

Results similar to those found in the present work are only to be expected with sand-castings in alloys of long freezing range which solidify in a "pasty" manner; the longer the freezing range, the more pronounced should be the existence of an optimum section thickness. It is possible that with pure metals and alloys of short freezing range, which solidify by "skin formation" when sand-cast, a different relationship—or no relationship at all—exists between the section thickness and tensile properties of the casting.

Solidification by "skin formation" takes place in a direction perpendicular, or nearly perpendicular, to the mould wall, the isothermals

closely following the contours of the wall. "Pasty" solidification, on the other hand, takes place towards the heat centre of the casting, the isothermals being more or less concentric about this point (see Figs. 10 and 11). Hence, in an alloy of long freezing range, directional solidification is assured provided that the heat centres of the casting are confined to the feeders, and—in contrast with "skin-forming" materials—solidification cannot take place in undesirable directions unless the section is very thin. The heat centre is readily transferred to the feeder—this is exemplified by the 1-in.-thick plate with head A (feeder: casting ratio 0.58)—but, even if solidification is directional, soundness of the casting is by no means certain unless the temperature gradients are substantial. As has been shown, this factor depends on casting size as well as on the feeder: casting ratio. Slow pouring would also assist in setting up steep temperature gradients.

The conclusions reached are directly applicable only to sand-cast plates of the length and width examined, under conditions of rapid pouring. For instance, the suggestion put forward that sound plates not of optimum thickness cannot be cast would obviously be invalid if very slow pouring were employed. However, the optimum plate thickness found in the present work is probably representative of the general case when the thickness of a rapidly poured section is small in relation to its other dimensions.

#### V.—SUMMARY AND CONCLUSIONS.

The main conclusions reached as the result of the work described may be summarized as follows:

(1) The development of high tensile properties in castings made in a long-freezing-range aluminium alloy depends upon the magnitude of the axial (from the feeder to the casting) temperature gradients present during solidification, especially those prevailing during the later stages of solidification when interdendritic feeding is taking place.

(2) In rapidly poured plate castings there is an optimum thickness conducive to good feeding, and hence necessary for the attainment of the maximum tensile properties of which the alloy is capable; for plates of the type studied this is about  $\frac{1}{2}$  in.

(3) The axial temperature gradients present during freezing in a rapidly poured plate are governed by the plate thickness and feeder size, the gradients growing larger with increasing feeder size and decreasing plate thickness. These gradients increase with time after casting. At a later stage, a falling off in the rate at which the mould extracts heat gives rise to a tendency for the gradients to drop. Ulti-

mately, therefore, the gradients reach a maximum value and then decline.

(4) The axial temperature gradient present in a plate during the period of interdendritic feeding is not necessarily the maximum gradient developed. In thick plates the maximum gradient is set up well before the end of freezing; freezing is complete in thin plates before the maximum gradient is attained.

(5) The properties of plates of optimum and greater thickness may be somewhat improved by low pouring temperatures.

#### ACKNOWLEDGEMENTS.

The author is indebted to the Director and Council of the British Non-Ferrous Metals Research Association for permission to publish this paper. His thanks are also due to Dr. A. G. Quarrell, F.I.M., and Mr. W. A. Baker, B.Sc., F.I.M., for much helpful advice and constructive criticism.

#### REFERENCES.

1. R. W. Ruddle, "The Solidification of Castings: A Review of the Literature", *Inst. Metals Monograph and Rep. Series*, No. 7, 1950.
2. R. W. Ruddle and A. L. Mincher, *J. Inst. Metals*, 1949-50, **76**, 43.
3. R. W. Ruddle, *J. Inst. Metals*, 1950, **77**, 1.
4. W. A. Baker, *J. Inst. Metals*, 1945, **71**, 165.
5. G. V. Raynor, *Inst. Metals Annotated Equilib. Diagr.* No. 4, 1944.
6. A. G. C. Gwyer, H. W. L. Phillips, and L. Mann, *J. Inst. Metals*, 1928, **40**, 297.
7. L. F. Mondolfo, "Metallography of Aluminium Alloys". New York: **1943** (John Wiley and Sons).
8. L. W. Eastwood and J. A. Davis, *Trans. Amer. Found. Assoc.*, 1946, **54**, 254.
9. W. A. Baker, *B.N.F.M.R.A. Research Rep.* No. **R.R.A. 661**, 1944.
10. W. A. Baker, unpublished work, B.N.F.M.R.A.
11. A. Cibula and R. W. Ruddle, *J. Inst. Metals*, 1949-50, **76**, 361.





# USE OF DIAMOND DUST FOR POLISHING 1240 METALLOGRAPHIC SPECIMENS OF NON-FERROUS METALS AND ALLOYS.\*

By E. C. W. PERRYMAN,† M.A., A.I.M., STUDENT MEMBER.

(Communication from the British Non-Ferrous Metals Research Association.)

## SYNOPSIS.

A rapid method for the metallographic polishing of non-ferrous specimens containing two or more phases differing greatly in hardness, e.g. electrodeposited and galvanized coatings and multiphase structures, is described. Instead of the usual coarse polishing agents, such as proprietary metal polish,  $\alpha$ -alumina, or magnesia, fine diamond dust ( $0.1\ \mu$ ) is used with the following advantages: (a) reduction of total polishing time, and (b) reduction of relief between coatings or phases differing widely in hardness.

## I.—INTRODUCTION.

ALTHOUGH diamond dust has been used for some considerable time for the final polishing of hard metal carbides, it is only recently that it has been used for polishing metal specimens, and its use for polishing non-ferrous metals and alloys has not been described. Woodside and Blackett<sup>1</sup> in one of the most recent investigations of the use of diamond dust for preparing metallographic specimens found that not only was the preparation time reduced but the surfaces were produced free from relief. Tarasov and Lundberg<sup>2</sup> showed that diamond dust is very satisfactory for preparing metallographic specimens of high-speed steels of the high-carbon, high-vanadium type, and described a technique whereby the usual stages of polishing by emery papers are replaced by polishing with a vitreous-bonded diamond hand hone, the final polishing being done on a rotating pad impregnated with diamond dust.

In general, the use of diamond dust for the preparation of metallographic specimens falls into two classes: (a) polishing very hard materials, e.g. metallic carbides, and (b) polishing metallic specimens containing two or more phases differing greatly in hardness, e.g. electrodeposited and galvanized coatings and multiphase structures. The work described in this paper deals exclusively with specimens of

\* Manuscript received 31 October 1949. The work described in this paper was made available to members of the B.N.F.M.R.A. in a confidential Technical Memorandum issued in September 1949.

† Investigator, British Non-Ferrous Metals Research Association, London.

type (b). The common method for polishing metallographic specimens is to grind down to 0000 emery paper, followed by polishing on cloth charged with a coarse polishing agent (e.g. proprietary metal polish,  $\alpha$ -alumina, or magnesia) and finishing with a finer polishing agent. Such methods commonly give very bad relief after the coarse-polishing stages. Diamond, being much harder than the components being polished, abrades uniformly because the hardness difference between the components is negligible compared with the hardness difference between the components and the diamond. Thus, the use of a very fine diamond dust instead of the usual coarse polishing agents gives a surface finish comparable with that obtained by the normal method, but the relief between the various components is obviated.

## II.—POLISHING TECHNIQUE.

Specimens are mounted in Bakelite in the normal manner and ground down to 0000 emery paper, being turned through  $90^\circ$  after each paper. Specimens of electrodeposited or galvanized coatings, however, are not turned through  $90^\circ$ , the direction of emerying being always parallel to the coating. The specimen is polished on a rotating pad containing diamond dust, the specimen rotating and traversing the pad simultaneously. This pad, 4 in. in dia., is made by sprinkling a very small amount, approximately 25 mg., of diamond dust ( $0.1\text{ }\mu$ ) \* on a dry Selvyt pad, and rubbing the dust in with the fingers. White spirit (light paraffin oil) is used as a lubricant. To avoid loss of diamond during polishing, the pad is surrounded by an ebonite ring projecting above the surface of the pad and fitting tightly over the Selvyt-covered disc. The speed of rotation of the pad does not materially affect the surface finish, though faster speeds decrease the polishing time. On the other hand, if the speed is excessively fast, the diamond dust tends to be thrown off the pad and the process becomes costly. Normally a speed of 120 r.p.m. is used. After polishing on the diamond pad most non-ferrous materials still have fine scratches present, though the specimens are quite suitable for visual examination. Whenever possible specimens are finished by polishing for a short time on a slowly rotating Selvyt pad containing a suspension of  $\gamma$ -alumina in water. It is essential that the polishing time on this pad should be short, for otherwise relief may again appear or staining be produced because of the electrolytic cells set up between the dissimilar metals or phases.

\* Ex Messrs. L. M. Van Moppes.

### III.—RESULTS.

#### 1. *Coatings.*

Galvanized and electrodeposited coatings are normally very difficult to polish owing to the relief obtained between the coating and the underlying metal, caused by the hardness difference between them. By means of the technique described above it is possible to polish this type of specimen quickly with a minimum of relief. An example of a galvanized coating is shown in Fig. 1 (Plate III). It was finished on diamond and etched with nitric acid in amyl alcohol. Points worthy of note in Fig. 1 are : (a) the flatness of field, and (b) the sharply defined alloy layers. A similar application of this technique is for the polishing of electrodeposited coatings. Figs. 2 and 3 (Plate III) show electrodeposited coatings of chromium and nickel on an  $\alpha$  and ( $\alpha + \beta$ ) brass, respectively. Both these specimens were polished on alumina after diamond. Fig. 4 (Plate III) shows a non-adhering electrodeposited coating of nickel on an aluminium-5% silicon alloy. This specimen was finished by polishing on a suspension of magnesia in water. Again, the absence of relief between the various coatings and the underlying metal should be noted, and also the absence of relief between the  $\alpha$  and  $\beta$  phases in Fig. 3 and the aluminium matrix and silicon particles in Fig. 4.

One further use which has been made of this polishing technique for coatings is in the metallographic examination of oxide scales on copper. When polishing these oxide scales by normal methods excessive relief was obtained between the oxide and the underlying copper and, moreover, the thin layer of cupric oxide which is formed on the cuprous oxide became rounded and tended to be dragged away from the underlying cuprous oxide. By using the diamond polishing technique these difficulties were overcome and good results were obtained. In general, the specimens were finished on alumina after polishing on the diamond pad. Fig. 5 (Plate IV) shows a very thin layer of cupric oxide and a thick layer of cuprous oxide formed on tough-pitch copper after annealing at 900° C.

#### 2. *Multiphase Structures.*

If a specimen contains two or more phases, each differing widely in hardness, it is often very difficult to obtain a flat field by normal mechanical polishing methods or by electropolishing. Moreover, if the hard second phase is present in only very small amounts, then, unless the particles are flat, it becomes difficult to decide microscopically whether particles are really present or not. By means of diamond

## 64 *Diamond Dust for Polishing Non-Ferrous Metals*

polishing these difficulties are overcome, and the method has proved extremely useful in the detection of very small hard particles in aluminium and copper alloys. Fig. 6 (Plate IV) shows a specimen of aluminium (hardness approximately 20 V.P.N.) containing hard titanium carbide particles (hardness approximately 1000 V.P.N.) polished by diamond. It was found impossible to polish this specimen by conventional means because of relief between the carbide and aluminium. A further example is given in Fig. 7 (Plate IV), which shows a fracture in a  $\beta$ -brass containing some very hard particles of a second phase. Fig. 8 (Plate IV) shows an example of the use of this technique for polishing an aluminium alloy containing a very hard intermetallic compound; the use of diamond dust considerably reduced the total polishing time.

### IV.—CONCLUSIONS.

It is shown that the coarse-polishing stage in preparing metallographic specimens of non-ferrous metals and alloys can be replaced by polishing on a rotating pad impregnated with diamond dust with the following advantages :

- (i) Reduction of total polishing time.
- (ii) Reduction of relief between coatings or phases differing widely in hardness.

### ACKNOWLEDGEMENTS.

The author wishes to thank the Director and Council of the British Non-Ferrous Metals Research Association for permission to publish the results of this work, and also Mr. P. Grodzinski of the Industrial Diamond Information Bureau, who originally suggested the use of diamond dust for polishing non-ferrous metals and alloys.

### REFERENCES.

1. G. C. Woodside and H. H. Blackett, *Metal Progress*, 1947, **51**, 945.
2. L. P. Tarasov and C. O. Lundberg, *Metal Progress*, 1949, **55**, 183.

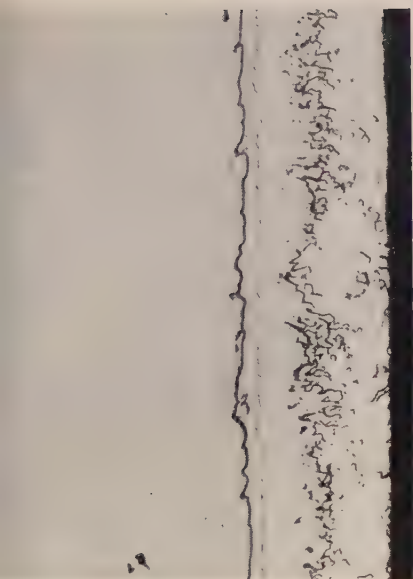


FIG. 1.—Galvanized Coating Containing Aluminium. Etched with nitric acid in amyl alcohol.  $\times 500$ .



FIG. 2.—Defect in Electroplated Chromium and Nickel on  $\alpha$ -Brass.  $\times 1500$ .

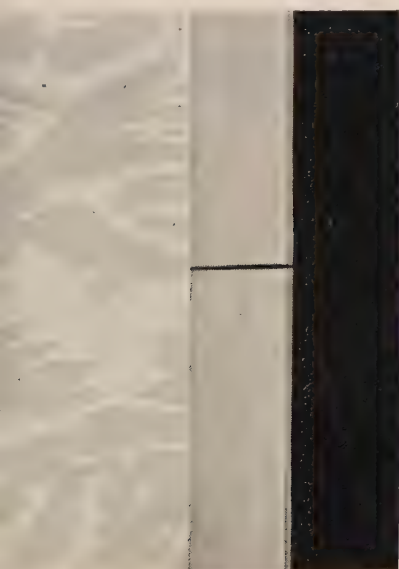


FIG. 3.—Defect in Electroplated Chromium and Nickel on  $(\alpha + \beta)$  Brass.  $\times 500$ .

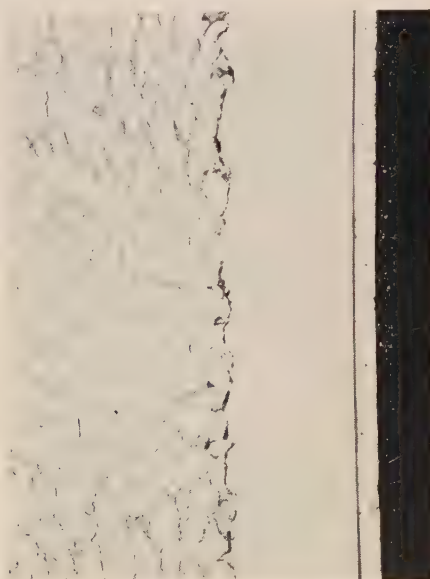


FIG. 4.—Chromium and Nickel Electroplate on Aluminium-5% Silicon Alloy, Showing Lack of Adherence between Nickel and Aluminium Alloy.  $\times 75$ .



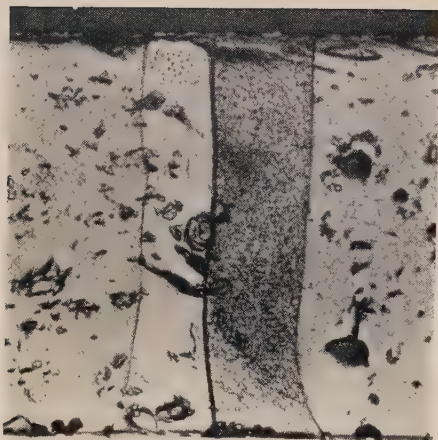


FIG. 5.—Cuprous and Cupric Oxides Formed on Tough-Pitch Copper. Cupric oxide is the uppermost thin white band. Etched in 5% potassium cyanide.  $\times 300$ .

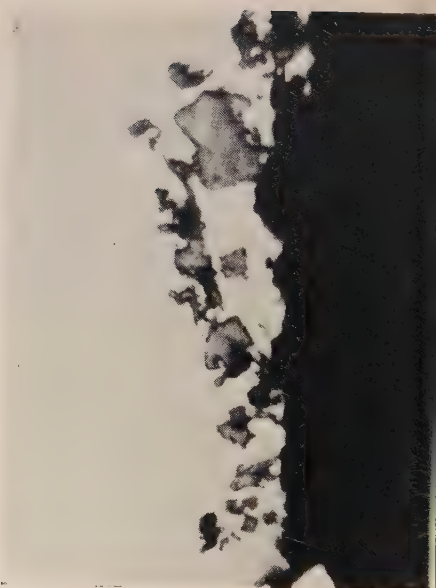


FIG. 6.—Titanium Carbide Particles in Centrifuged Aluminium-0.1% Titanium Alloy.  $\times 2000$ .



FIG. 7.—Hard Particles at Fractured Edge of a  $\beta$ -Brass.  $\times 1500$ .

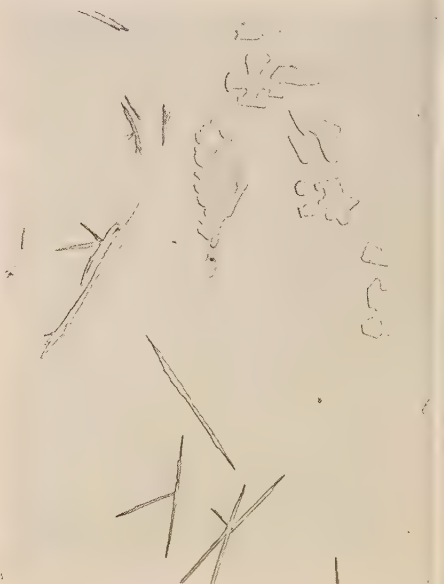


FIG. 8.—Sand-Cast Aluminium-1.5% Tungsten Alloy. Needles of  $\delta$  phase and particles of  $\gamma$  phase.  $\times 150$ .

# ATOMIC DISPLACEMENTS ASSOCIATED WITH ELASTICITY IN PLASTICALLY DEFORMED METALS.\*

1241

By W. A. WOOD,† D.Sc., MEMBER, and N. DEWSNAP,‡ B.Met.E.

## SYNOPSIS.

Determination by the X-ray diffraction method has been made of the magnitude of the internal stresses developed between the grains during the plastic deformation of tensile specimens of iron and aluminium. It is found that in fine-grained specimens the magnitude of the stresses tends to increase in a regular manner with deformation up to a maximum value comparable with the ultimate stress of the material. But as the grain-size becomes coarser and of the same order of size as the section of the test-piece, the intergranular stresses become irregular both in magnitude and direction, and also tend to be smaller. A tentative suggestion is made regarding a mechanism by which the intergranular stresses could arise, otherwise than by the previously recognized mechanism which attributes the stresses to mechanical anisotropy of the metal grain.

## I.—INTRODUCTION.

THE elasticity of a metal must in theory be based on a reversible displacement of the atoms from their normal positions of equilibrium. In practice, X-ray diffraction measurements of the atomic spacings have shown that this simple picture is true in the primitive elastic range only.<sup>1</sup> With the onset of plastic flow various anomalies appear. The spacings may cease to change with increasing applied stress and may not return to their original values when the stress is removed. The actual atomic displacements, therefore, may be considerably modified by the presence of plastic deformation.

The anomalies could be explained by supposing that the actual displacements were the resultant of the external stress and some new internal stress created by the process of plastic flow. This explanation was, in fact, put forward by Smith and Wood<sup>1</sup> as a result of their X-ray work on the subject; they showed also that the stress would need to be on an intergranular scale, possibly differing from grain to grain, and that it must be anticipated even when outwardly the plastic deformation of a metal might appear uniform.<sup>2</sup> Therefore, the presence of such internal stresses would seem to play an essential part in determining the real elastic behaviour of a metal.

\* Manuscript received 14 July 1949.

† Acting Professor of Metallurgy Research, Baillieu Laboratory, University of Melbourne, Australia.

‡ Division of Aeronautics, Council for Scientific and Industrial Research, Melbourne, Australia.

The idea of intergranular stresses is, of course, not new. Thus Heyn<sup>3</sup> pointed out many years ago that they would occur in plastically deformed metals because of the elastic and plastic anisotropy of the grains. These factors also give rise to one aspect of the tessellated stresses considered mathematically in an important series of papers by László.<sup>4</sup> Recently the Heyn stresses have also been put forward by Greenough<sup>5</sup> specifically to explain the above X-ray results. But previous to this X-ray work, no quantitative information has been available whereby these various concepts could be tested.

The present paper is concerned with further such quantitative measurements, and in particular with the variation in magnitude of the stresses from grain to grain. The results may be of some practical interest in showing the surprisingly high values that can be reached. They may also be of theoretical interest, because they suggest that the Heyn stresses do not of themselves appear adequate to account fully for the observations, and that an additional source of stresses should be sought, one possibility being suggested in the paper.

## II.—EXPERIMENTAL WORK.

In principle, the X-ray method measures the elastic strain by determining the change from normal of a given atomic spacing. In practice, the incident beam, which usually has a cross-section of a few sq.mm. only, covers a finite volume of the metal, and the measurements refer to a selection only of the grains in that volume, namely, those grains which are similarly oriented with respect to the incident X-ray beam. The result, therefore, represents the average strain of a similarly oriented set of grains in a small volume of material, and has real significance only if all grains of the same orientation behave similarly throughout the material.

An interesting feature of the early X-ray work was that similarly oriented grains did behave in much the same way from point to point and, for given conditions of stressing, from specimen to specimen of a metal. This work, however, was carried out purposely on fine-grained material, so that the number of operative grains in the volume under examination should be large enough for accidental deviations from the mean strain to cancel themselves out. In the present work, this number has been reduced by using coarse-grained specimens with the object of finding the order of these deviations and thus of measuring the strains when they are more representative of conditions in the individual grain in a polycrystalline aggregate. The experiments therefore involved comparative determinations of the internal stresses developed in fine- and coarse-grained specimens of the same material.

(a) *Specimens.*

The materials used were 99.98% aluminium, a carbonyl iron, and a commercial iron with chief impurities carbon 0.045, manganese 0.29, silicon 0.01, sulphur 0.012, and phosphorus 0.031 wt.-%. The last was employed because similar material had been used in the earlier work, and it provided a standard of comparison with the present work, in which a different mode of deformation was employed. The effects of different grain-sizes were studied mainly on the aluminium and carbonyl iron, from which specimens of various grain-sizes could be prepared easily by the usual method of subjecting annealed specimens to small preliminary deformation and then recrystallizing by heating. The grain-sizes ranged from 0.01 to 2 mm. in the iron and 0.1 to 5 mm. linear in the aluminium specimens.

The specimens were made in the form of flat tensile test-pieces of section 0.04 in. and parallel gauge length  $2\frac{1}{4} \times \frac{1}{2}$  in., obtained from strip material. The aluminium and commercial iron were supplied as strip, but the carbonyl iron strip was prepared from powder. The powder was pressed into cylinders under a stress of 6 tons/in.<sup>2</sup>, partially degassed by heating for some hours *in vacuo* at 1000° C., and then melted in a tungsten arc furnace in an atmosphere of argon, the ingots subsequently being rolled into strip from which the required specimens were obtained.

(b) *Method of Straining and of X-ray Measurement.*

The earlier work was done on specimens subjected to direct loading in order to obtain full systematic "stress-strain curves" for the atomic spacings. For the present purpose of determining mainly residual strains, it was considered sufficient to stretch the specimens in a direct-straining device. In this arrangement the ends of the specimen were held in grips, one of which was fixed and the other movable by a screw along the line of the specimen axis. The device was small enough to be mounted directly on to the table of a back-reflection X-ray spectrometer, and specimens could be examined both while under the tension imposed by the screw and after the tension had been released.

The general procedure involved taking X-ray photographs from an annealed specimen mounted in the straining device, and then after the specimen had been subjected to a known extension. At this extension, the specimen was photographed first under tension and then with the tension released. In both the stressed and unstressed state, for reasons given below, two photographs were taken, one with the incident beam at right angles to the surface and one where the straining device



was rotated on the spectrometer table until the incident beam made an angle of  $45^\circ$  with the surface. The processes were then repeated after progressively greater elongations until the specimen began to neck and fracture.

For iron, cobalt  $K\alpha$  radiation was used, and the photographs recorded the behaviour of the diffraction ring from the (310) planes. For examination of the aluminium both cobalt and copper radiations were used, the former providing reflections from the (420) and the latter from the (511, 333) spacings. All these spacings give reflections at glancing angles of  $80^\circ$ – $81^\circ$ , such large angles being essential for sensitivity to small changes in spacing. With a film-to-specimen distance of 10 cm., which was employed throughout, and the above reflection angles, a change in diameter of 0.1 mm. in the diffraction ring corresponded to an elastic strain or fractional change in spacing of  $\delta d/d = 0.00004$  in the specimen. This would be the order of change produced on application of an external stress of 1–2 tons/in.<sup>2</sup> and represented the limit of measurement.

The X-ray method thus measures the elastic strain from the change in diameter of appropriate diffraction rings. The procedure followed was similar to that described in a recent paper by one of the authors<sup>2</sup> and need not be discussed in detail here.

### (c) *Measurement of the Internal Stresses.*

If the condition of the metal were expressed merely in terms of the directly measured internal strain and left at that, then no exception could be taken. But it is usual to express the results in terms of the stress which would be required to produce an equivalent strain, and so obtain a more graphic representation of the departure of the material from the normal condition. The mode of conversion appropriate to the X-ray measurements has been fully discussed by many authors, particularly by Thomas.<sup>6</sup>

The assumption is made that standard elasticity theory can be utilized, and any observed strain is regarded as due to two principal stresses at right angles in the surface of the specimen. These may be written  $S_x$  and  $S_y$  for a tensile specimen,  $S_y$  being parallel to the axis of the specimen. If measurements of strain are confined to the plane through  $S_y$  perpendicular to the surface, then the strain  $\epsilon$  in the direction making an angle  $\beta$  with  $S_y$  is given by the same standard theory as :

$$E\epsilon = S_y(\cos^2 \beta - \sigma \sin^2 \beta) - \sigma S_x \quad . \quad . \quad . \quad (1)$$

where  $E$  is Young's modulus for the material and  $\sigma$  is Poisson's ratio. If the strain is measured in two directions,  $\beta = 90^\circ$  and  $\beta = 45^\circ$  being



used in the present work, then the values of  $S_x$  and  $S_y$  can be obtained at once.

Strictly, the above procedure is correct only for a homogeneous medium. However, in a metal the elastic strain in a particular direction will depend on the atomic spacing by which it is measured, owing to the anisotropy of the grains. At first sight it might appear that this difficulty would be overcome by using the elastic modulus appropriate to the particular spacing under investigation. But this could be measured accurately only on a single crystal, and there is no guarantee that the crystal would behave in the same way when constrained to deform as one component of a polycrystalline aggregate. Also, as already mentioned, for each direction of the incident beam the X-rays measure the change in the selected spacing only as it occurs in a similarly oriented set of grains, and this set is different for the different directions of incidence employed to obtain the different values of  $\beta$  in the above equation. Therefore the method is to some extent arbitrary. However, so long as this is recognized, no harm is done by expressing the observed strain in the more familiar terms of an equivalent stress system. The results will be adequate for purposes of comparison and will indicate correctly the direction and order of magnitude of the actual stresses.

The measurements of the residual stresses obtained in this way for the iron and aluminium in various conditions are given in the following Sections.

### III.—MEASURED VALUES OF INTERNAL STRESS.

#### (a) *Fine-Grained Iron.*

Table I records the internal stresses measured as a typical specimen was extended and at each extension examined while under the tension

TABLE I.—*Transverse and Longitudinal Principal Stresses,  $S_x$ ,  $S_y$ , Developed During Elongation of Fine-Grained Iron Specimens.*

Specimens under tension.

Elongation, %	$S_x$ , tons/in. <sup>2</sup>	$S_y$ , tons/in. <sup>2</sup>	$S_x + S_y$ , tons/in. <sup>2</sup>
0	...	...	...
9.4	8	7	15
14.3	8	10	18
21.2	1	17	18
26.4	1	17	18
31.5	-2	19	17

imposed by the screw of the straining device. This specimen was of commercial iron with grain-size approximately 0.01 mm., but the results

were similar for carbonyl specimens of comparable grain-size. It might be added that no noticeable alteration in the stresses was observed if a specimen was held in tension for some days; there was no question, therefore, of the results being affected in these experiments by relaxation of the elastic strain with time.

The Table gives the separate calculated values of  $S_x$  and  $S_y$ . Theoretically, on the simple picture of elasticity, the longitudinal stress  $S_y$  should merely increase regularly with extension of the specimen; while the transverse stress  $S_x$  should be zero throughout. In practice, the measurements show no such behaviour. It will be seen that after increasing up to about 21.2% elongation, the value of  $S_y$  ceases to change appreciably with further elongation; and that  $S_x$  exhibits a distinct magnitude in the early stages of deformation, after which it decreases. The sum of the principal stresses,  $S_x + S_y$ , grows up to 14.3% elongation, but thereafter shows little change. These results illustrate clearly, therefore, the anomalous behaviour of the atomic displacements under conditions where they might have been expected merely to increase with the strain-hardening.

Table II records the residual internal stresses observed at various

TABLE II.—*Transverse and Longitudinal Principal Stresses,  $S_x$ ,  $S_y$ , After Elongation of Fine-Grained Iron Specimens and After Tension Released.*

Negative sign indicates compression.

Elongation, %	$S_x$ , tons/in. <sup>2</sup>	$S_y$ , tons/in. <sup>2</sup>	$S_x + S_y$ , tons/in. <sup>2</sup>
0	...	...	...
9.4	— 3	— 5	— 8
14.3	— 4	— 7	— 11
21.2	— 9	— 10	— 19
26.4	— 11	— 10	— 21
31.5	— 11	— 10	— 21
36.5	— 11	— 9	— 20
Neck	— 1	— 2	— 3

stages of elongation after the tension imposed on the specimen was released, and shows more clearly the nature of the anomalies.

Again, on the simple picture of elasticity, the atoms should return to their original positions and no internal stresses should remain, but in practice their behaviour is quite different. Both the longitudinal and transverse components of the stress develop values well beyond any possible experimental limits of measurement. The stresses show interesting features. In the first place they are compressive; the plastic

deformation has tended, therefore, to produce permanent internal stresses opposite in direction to the applied stress. In the second place they are systematic in that they were found to be the same from point to point of the specimen and reproducible for similar elongations from specimen to specimen. Finally, they reach a surprisingly high magnitude. The ultimate tensile strength of the two types of iron used was of the order of 20 tons/in.<sup>2</sup> and the yield stress 10 tons/in.<sup>2</sup> It will be seen that the sum of the internal stresses,  $S_x + S_y$ , actually approaches the ultimate strength. This sum is the appropriate quantity to take for this comparison, since it is directly equivalent to the strain measured under conditions when the angle  $\beta$  in equation (1) is  $90^\circ$ ; that is, it is equivalent to the transverse elastic strain perpendicular to the surface of a specimen. The measured transverse strain, therefore, reaches the same order of magnitude as it would have in the ideally elastic metal subjected to the ultimate tensile stress. Thus, on the grounds of strain alone and apart from considerations of the conversion to stresses, the metal must be in a highly unstable condition.

The high value reached by the internal stress is difficult to explain by the usual concepts of the Heyn stresses. Grains in a given volume must deform under external stress by the same amount in any particular direction if continuity of structure is to be preserved. In view of the plastic and elastic anisotropy, the observed strains in individual grains may be made up of different proportions of elastic and plastic deformation. On release of the external stress the constraints of the more plastically deformed grains will prevent full elastic recovery of the others, and through the volume an average residual strain will be established. This gives rise to the so-called Heyn stresses and must obviously be inevitable in a polycrystalline aggregate. But it is difficult to see how this *average* value could reach the magnitude observed, equivalent to the ultimate stress of the material.

A point of interest arose in connection with measurements of the internal stresses when the specimens began to neck before fracture. Generally, measurements were discontinued as soon as signs of necking appeared, usually at about 40% extension, since such uneven deformation would induce separate macroscopic stresses. For interest, however, some specimens were over-extended. The nature of the stresses then measured in the necked region is recorded in the lower part of Table II. It will be seen that the stresses have dropped to quite low values, suggesting that the macroscopic stresses associated with the necking are such as to relieve the intergranular stresses under investigation.

The main conclusion to be drawn from the above observations, however, is that the plastic deformation of the fine-grained materials

produces a regular form of permanent internal stress, the magnitude of which can approach that of the ultimate tensile strength of the material.

(b) *Fine-Grained Aluminium.*

The results on aluminium of relatively fine grain-size (0.1 mm.) were comparable to the above in that they showed a similar regular development of residual stresses after progressive elongation, reaching values of the order of the ultimate tensile strength, which for this material was 4.5 tons/in.<sup>2</sup> It is unnecessary, therefore, to discuss the results in detail. The values of  $S_x + S_y$  for a typical specimen are recorded in Table III.

TABLE III.—*Sum of Principal Stresses,  $S_x + S_y$ , After Elongation of Fine-Grained Aluminium and After Tension Released.*

Negative sign indicates compression.

Elongation, % . . .	5	10	15	20	25	30
$S_x + S_y$ , tons/in. <sup>2</sup> . . .	-1	-2	-3	-4	-3	-4

(c) *Coarse-Grained Iron and Aluminium.*

In contrast with the measurements on the above fine-grained specimens, those made on coarse-grained material were markedly irregular both in direction and magnitude. They varied from point to point on any one specimen and also from specimen to specimen; nor did they change systematically with degree of deformation.

The irregularity became noticeable as soon as the grain-size became of the same order as the thickness of the specimens. In a fine-grained metal it is known that on the whole the changes in shape of the individual grains follow the external changes of the specimen. It is to be expected that in a coarse-grained specimen, where each grain has one face at or near a free surface, the grains will deform in a less arbitrary manner. The irregular nature of the internal stresses observed in such specimens arises presumably for that reason. It is of interest, however, because in these conditions the only constraints acting on any one grain will be the action of its neighbours, and the stresses arising will be predominantly of the Heyn type. It would appear, therefore, that these Heyn stresses are irregular in nature, confirming the view that they are not of the type to explain the more systematic stresses observed in the fine-grained materials.

The order of the variations for iron is indicated by Table IV. The observed value of  $S_x + S_y$  is given for two typical specimens of carbonyl

TABLE IV.—*Sum of Principal Stresses,  $S_x + S_y$ , After Elongation of Iron Specimens of Relatively Coarse Grain-Size (2 mm.), Showing Variations at Different Positions on a Specimen After Tension Released.*

Negative sign indicates compression.

Specimen	Elongation, %	$S_x + S_y$ , tons/in. <sup>2</sup>			
		Positions			
		1	2	3	4
1	0	...	...	...	...
	12	10	—6	—8	...
	30	0	—8	—14	...
2	30	—6	—2	0	0

iron after various elongations, measurements being made at four different positions on the surfaces. The grain-size was 2 mm. parallel to the surface of the specimens and of the same order as the thickness of the specimens at right angles to the surface. It will be seen that the stresses are quite irregular, but the magnitudes reached are not so high as in the fine-grained material. This latter observation was general for all the specimens examined.

Similar irregularities, as observed on the aluminium specimens, are indicated by Table V. Three ranges of grain-size were studied. The first group consisted of specimens in which the grains were about 5 mm. parallel to the surface, but extending through the thickness of the specimens. It was possible with an incident X-ray beam of 1–2 mm. cross-section to determine the stresses at the centre of such crystals and then at the boundaries. It was found that the stresses in the interior of the grains were invariably too small to measure with any accuracy. Those at the boundaries, however, were usually appreciable but exhibited no regularity. They appeared to be most evident when the grain exhibited a disorientation into mosaic elements or crystallites in the same region of the boundary.

The second group consisted of specimens of grain-size approximately 2 mm. parallel to the surface and two or three grains to the section of the specimen. The measured stresses were appreciable but again exhibited no regularity.

The third group comprised specimens of average grain-size 0.5 mm. The stresses in these finer-grained specimens still showed variations at different points on the surface, but at the same time a definite tendency to regularity. The above results are illustrated by the values recorded in Table V.



The comparison of the behaviour of the specimens of different grain-size thus suggests that at least two types of intergranular stresses may accompany plastic deformation. One is the irregular type observed in the coarse-grained specimens and the other the more systematic stress observed in the finer-grained material. The elastic properties of a polycrystalline metal would normally be measured on a fine-grained test-piece, where deformation would be more uniform. The conclusion to be drawn from the above experiments is that even in such material the

TABLE V.—*Sum of Principal Stresses,  $S_x + S_y$ , After Elongation of Aluminium Specimens of Coarse Grain-Sizes and After Tension Released, Showing Variation at Different Positions.*

Negative sign indicates compression.

Specimen and Grain-Size	Elongation, %	$S_x + S_y$ , tons/in. <sup>2</sup>			
		Positions			
		1	2	3	4
5 mm. Centre of grain } Boundary positions }	15 {	0	...	...	...
		3	1	0	-1
2 mm.	12	1	-2	2	...
	20	1	2	0	...
0.5 mm.	20	0	0	-1	
	24	-1	-1	0	
	24 *	-1	-1	0	
	30	-2	-1	-1	
	30 *	-2	-1	-1	

\* Measured with Cu radiation; remainder with Co radiation.

actual elastic properties will involve a systematic system of permanent internal stresses as soon as deformation extends beyond the primitive elastic range. Departures from Hooke's law are commonly shown, of course, by precise mechanical measurements, becoming evident as mechanical hysteresis loops. It should be added, however, that the X-ray method would not be sufficiently sensitive to show deviations of this kind, and that the internal stresses established by this and previous researches are of quite a different and larger order of magnitude.

#### IV.—DISCUSSION.

The intergranular stresses could be explained qualitatively by considering the anisotropy of the grains, as suggested by various authors in

discussing the earlier results of Smith and Wood.<sup>1</sup> But the later, more detailed observations, such as those described in the present paper, cannot be accounted for adequately in this way. It is difficult, for instance, to explain both an irregular and a systematic stress system on the one hypothesis. Closer examination raises other difficulties.

Consider the small volume under X-ray examination in a test-piece. On applying an external stress, the overall strain in a particular direction will take up a definite value which increases with stress. At each stress this total strain will have a definite value, but will be comprised of strains which in some grains may be wholly elastic and in others partly elastic and partly plastic. The equivalent internal stress from grain to grain will differ in value, and this difference will persist after the external stress is removed. As already mentioned, the X-ray method determines the stress in a similarly oriented selection of the grains, which might be expected to behave similarly. The method, therefore, may indicate a finite intergranular stress where the overall resultant stress is zero. This is the usual explanation.<sup>5</sup>

One difficulty in this explanation is encountered, however, when closer attention is paid to the behaviour of the elastic strains *while the metal is still under stress*. At each value of the external stress the X-rays measure the strain in a similarly oriented set of grains, and this strain appears to have a definite magnitude. Now this magnitude may differ from that exhibited by grains of other orientations but, on the above view, there is no obvious reason why it should not increase continuously with every increment of external stress. In practice, however, as shown by Table I for the quantity  $S_x + S_y$ , the strain tends to a steady value. In previous work with direct loading it was found that actually this tendency to a steady value appeared as soon as the primitive yield of the material was passed. Therefore, the explanations based on consideration simply of the mechanical anisotropy of the grains would need some modifications before they could be regarded as entirely adequate.

It is suggested that explanations of this kind meet difficulties because they tacitly assume that the stress-strain curve for the individual grain in an aggregate is continuous, in the same way as it is for a large homogeneous body. It is considered essential, however, that the atomistic nature of the slip process should be taken into account, and, in this connection particularly, the practical observation that a slip movement is a relatively large discontinuous change which may be "triggered" by a much smaller elastic strain. This latter feature follows from consideration of the very low primitive elastic ranges of single metal crystals.

Thus, consider the classical picture of slip illustrated by Figs. 1 (a) and 1 (b). A crystalline element of side  $a$  under the shear stress  $T$  first exhibits an elastic strain  $\theta = x/a$ , and then at some value of  $T$  the upper half of the block jumps relatively to the lower half by one atomic spacing  $d$ . The strain thus changes abruptly from  $x/a$  to an effective plastic strain of  $d/a$ . As pointed out by Bragg,<sup>7</sup> the jump could occur at any value of  $x > d/2$ . Therefore discontinuous jumps may be produced of values up to  $d/2a$ . Since  $d$  is of the order of  $10^{-8}$  cm., these

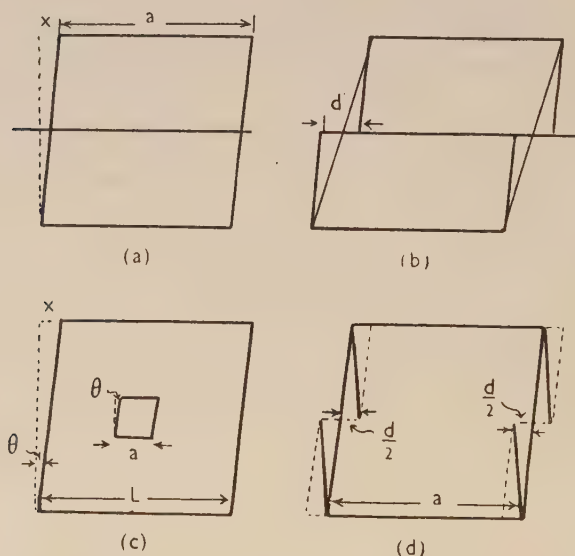


FIG. 1.—Diagrammatic representation of crystal element (a) under elastic strain, (b) after completed slip jump, (c) under elastic strain when in matrix, (d) after slip but with completion of slip jump arrested by constraint of matrix.

jumps would not disturb the apparent continuity of the stress-strain relationship if  $a$  were large, but they would become of the same order as the elastic displacements if  $a$  approached the value of  $10^{-3}$ – $10^{-4}$  cm., the order of a fine grain or mosaic element of a grain.

These considerations then lead to the important part played by the grain boundaries in a polycrystalline aggregate. In the above picture of the slip movement, the element is free to deform. In the polycrystalline metal, however, the element is always part of a larger matrix and the possibility of movement will be determined also by whether the strain associated with the slip jump in one element can be accommodated by simultaneous deformation in others. In general this is unlikely.

In such an event it might reasonably be postulated that at some value of applied stress, as illustrated in Figs. 1 (c) and 1 (d), the internal atomic rearrangement corresponding to that of a completed slip jump should still take place in the element; but that the upper and lower surfaces of the element should remain fixed by the matrix. This condition might be described as an intermediate stage in the slip movement, or a state of "arrested slip". It would be equivalent in effect to a completed slip movement with the element sheared back through the angle  $d/a$ . The final shear in the element would then be  $x/a - d/a$ , which, since  $x < d$ , would be opposite in direction from that before the internal movement.

We should then have, as a result of the discontinuous nature of the slip process, the spontaneous development of an internal strain or internal stress opposite in direction to the external stress on the matrix, *and one which would be produced by an increment in that stress*. Moreover, the internal stress would remain on removing the applied stress. It would thus satisfy the requirements of the experimental work. Stresses arising from mechanical anisotropy might also be present, as first discussed, but the effects associated with the arrested slip would account more easily for a number of the observations.

Thus, as already mentioned, they would account for the relaxation or even reversal of the internal stress in grains subjected to increasing external stress. (Whether the X-ray method measures a decrease or increase in the elastic strain under such conditions will depend, of course, on the actual atomic spacing under measurement, its relation to the direction of plastic flow, and whether it is in the element or the matrix.)

The differences observed in fine- and coarse-grained specimens could also be accounted for. Approximate calculation shows that the reversal of the strain in the element drawn in Fig. 1 (c) would increase the shear in the block by

$$\frac{\delta\theta}{\theta} = -\frac{d}{x} \left(\frac{a}{L}\right)^3 \quad . \quad . \quad . \quad . \quad . \quad (2)$$

where  $L$  is the side of the larger block. It is evident therefore that a number of elements could be in the state of arrested slip if  $a$  were distinctly less than  $L$ . Such conditions would arise in a fine-grained material if  $L$  corresponded with the dimensions of the test-piece and  $a$  with the size of a grain. But the same conditions would not be satisfied in a coarse-grained aggregate. In the latter case, internal stresses in consequence could arise only because of the more accidental macroscopic sources of inhomogeneous deformation, and they might be expected to exhibit irregular values after the manner actually observed.

Further, the relief of the internal stresses observed during necking of the specimens could be explained. For the stability of a test-piece would depend on the proportion and distribution of elements in the condition of arrested slip, and it is to be expected that after heavy deformation the proportion would become sufficiently large to cause a spontaneous relief of the stresses over a large area.

Finally, it will be seen that these intergranular stresses might reach quite high values. The elements contributing to the X-ray diffraction ring of a deformed specimen are known in practice to be small crystallites or mosaic elements of the grains. It has been indicated that the reversed strain of the element would have the value  $(d - x)/a$ . An average value would be  $d/2a$ , corresponding to a shear stress of  $G \cdot d/2a$ , where  $G$  is the shear modulus. If  $a$  is the order of the lower limiting crystallite size for a metal, it has been shown that the shear stress thus estimated is of the same order as the ultimate strength of the metal.<sup>8</sup>

However, in conclusion, it may be reiterated perhaps that the point of main interest is the more general one of the importance of intergranular stresses in determining the technical elastic properties of a plastically deformed metal. The work shows that in practice the atomic displacements in general are considerably more complicated than in the primitive elastic range, and suggests that the deviations are associated inherently with the mechanism of deformation by slip. These considerations do not affect the values of the elastic moduli of the metal, but they do concern the length of the elastic range which can safely be used in practice.

#### ACKNOWLEDGEMENTS.

This work, which was carried out in the Baillieu Laboratory of the University of Melbourne, was part of a research programme undertaken in collaboration with the Division of Aeronautics, Council for Scientific and Industrial Research, Australia.

#### REFERENCES.

1. S. L. Smith and W. A. Wood, *Proc. Roy. Soc.*, 1944, [A], **182**, 404.
2. W. A. Wood, *Proc. Roy. Soc.*, 1948, [A], **218**, 192.
3. E. Heyn, *J. Inst. Metals*, 1914, **12**, 3.
4. F. László, *J. Iron Steel Inst.*, 1943, **147**, 173 p; 1943, **148**, 137 p; 1944, **150**, 183 p; 1945, **152**, 207 p.
5. G. B. Greenough, *Nature*, 1947, **160**, 258.
6. D. E. Thomas, *Inst. Metals: Symposium on Internal Stresses in Metals and Alloys*, 1948, 25. (Monograph and Rep. Series No. 5.)
7. W. L. Bragg, *Nature*, 1942, **149**, 511.
8. W. A. Wood and W. A. Rachinger, *J. Inst. Metals*, 1949, **75**, 571.



# MODIFICATION IN ALUMINIUM-SILICON ALLOYS.\*

1242

By B. M. THALL,<sup>†</sup> M.A.Sc., Ph.D., and PROFESSOR BRUCE CHALMERS,<sup>‡</sup>  
D.Sc., Ph.D., MEMBER.

## SYNOPSIS.

In the modification of aluminium-silicon alloys by small additions of sodium, the properties and structure of the alloys are substantially improved. Various explanations of this improvement have been proposed, none of them entirely adequate; moreover, some of the experimental data on modification are contradictory. In the present work, thermal data on the modified aluminium-silicon alloys have been redetermined, and semi-quantitative determinations of the sodium content have been made by means of a radioactive technique.

The results have led to the formulation of a new theory of modification based on the influence of sodium on the balance of interfacial tensions during solidification. All the experimental facts are accounted for by applying this theory to the mechanism of eutectic solidification.

## I.—INTRODUCTION.

THE aluminium-silicon alloys are of industrial importance largely because of properties which can be obtained as a result of "modification". In the past, the exact nature of modification has not been clearly understood, although much experimental work has been carried out. The work described in the present paper was undertaken in order to resolve certain inconsistencies that appeared in the literature, and it has resulted in the formulation of a new theory to account for modification.

Fig. 4 shows the phase diagram of the aluminium-silicon system.

The eutectic in this system normally consists of lamellæ of silicon in a continuous background of aluminium (Fig. 1, Plate V), but the addition of a small amount of an alkaline fluoride or alkali metal can profoundly affect the structure of the alloys (Fig. 2, Plate V). This structure is then said to be modified.

A similar type of structure can also be produced by rapid solidification. By whichever method the modified structure is obtained, it is accompanied by a depression of the temperature of eutectic solidification and by an increase in the silicon content in the eutectic. The melting point of the eutectic, however, is always the same as in the normal alloy.

\* Manuscript received 16 May 1949.

<sup>†</sup> Lecturer in Physical Metallurgy, University of Toronto, Canada.

<sup>‡</sup> Professor of Physical Metallurgy, University of Toronto, Canada.

The mechanical properties are notably improved by modification, as the microstructure is changed from lamellar to globular (see Table I).

TABLE I.—*Mechanical Properties of an Aluminium-13% Silicon Alloy.*

Condition	Tensile Strength, lb./in. <sup>2</sup>	Elongation, %	Brinell Hardness No.
Normal (Sand cast) . .	18,000	2	50
Modified (Sand cast) . .	28,000	13	58
Normal (Chill cast) . .	28,000	3.6	63
Modified (Chill cast) . .	32,000	8	72

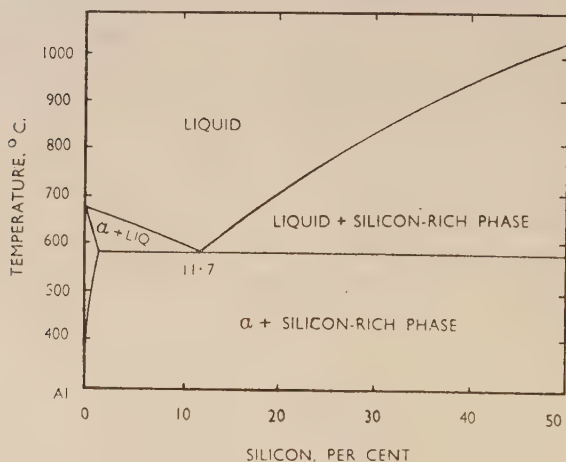


FIG. 4.—Aluminium-Silicon Phase Diagram.

## II.—PREVIOUS WORK.

Until 1900, the addition of silicon to aluminium was considered to be detrimental, and hence the aluminium-silicon alloys were not used. As early as 1891, however, Minet<sup>1</sup> recognized that an abnormal mode of crystallization could occur in the alloys of aluminium and silicon. This discovery received no attention, and it was not until 1920 that the commercial potentiality of these alloys was realized. In that year, Pacz<sup>2</sup> discovered that the mechanical properties of the aluminium-silicon alloys could be materially improved by the addition of a small quantity of an alkaline fluoride. This process subsequently became known as "modification".



FIG. 1.—Normal Aluminium-Silicon Alloy.  
× 300.

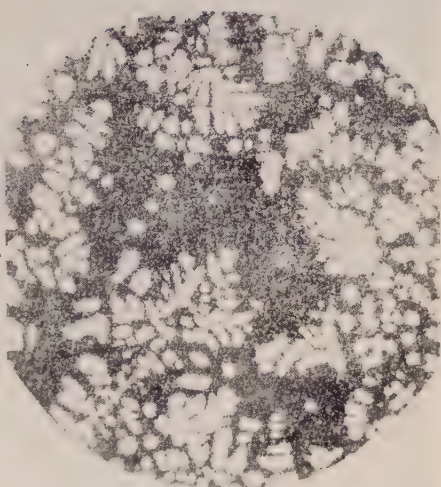


FIG. 2.—Modified Aluminium-Silicon Alloy.  
× 300.

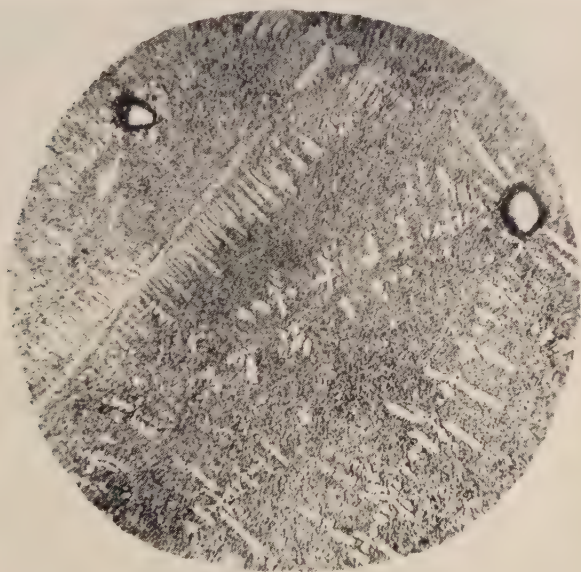


FIG. 3.—Modified Aluminium-Silicon Alloy Showing Both Primary  
Phases. × 300.



Further developments in modification took place in 1922 and 1923 with the introduction of the use of the alkali metals by Edwards, Frary, and Churchill,<sup>3</sup> and of the alkaline earth metals and their oxides and hydroxides by Gwyer and Phillips.<sup>4</sup> The method currently employed to modify the aluminium-silicon alloys is to add pure sodium to the melt just before casting.

Several theories have been proposed to account for the modification phenomenon. The earliest of these was the so-called "true flux theory", proposed by Guillet<sup>5</sup> in 1922. According to Guillet, the modifying agent reacts chemically in such a way as to remove the impurities alumina and silica by reduction. The increased purity of the alloy so obtained was believed to account for the improvement in the mechanical properties.

The possibility that silicon exists in two different allotropic modifications was suggested at about the same time as the true flux theory. It was proposed by Jeffries<sup>6</sup> that two systems of aluminium-silicon alloys exist, one of which is metastable. This theory was quickly abandoned, however, when it was shown by X-ray diffraction methods that the same allotropic modification existed in normal and modified alloys.

Curran<sup>7</sup> suggested an explanation in terms of the ternary aluminium-silicon-sodium system, and Ôtani<sup>8</sup> developed this theory to show how sodium played its part in the production of the modified structure. Schulz<sup>9</sup> has recently attempted to explain the microstructures of modified aluminium-silicon alloys in terms of the ternary theory. In Fig. 5, the ternary diagram is represented by the triangle *ABC*, and three binary diagrams have been constructed on the sides of this triangle.

The binary aluminium-sodium system has two components immiscible in the liquid state; however, a small amount of each component must dissolve in the liquid consisting of the other phase. The silicon-sodium diagram is unknown, but the liquids are probably immiscible, and it is likely that the phase diagram will be similar to that of the aluminium-sodium system. The binary aluminium-silicon system completes the ternary triangle on the side *AB*.

In order to clarify the "ternary" theory, an alloy of the aluminium-sodium binary system (Fig. 6) will be considered. On cooling, either aluminium or  $\beta$  liquid separates from the  $\alpha$  liquid, depending on the composition of the latter. When the monotectic temperature *ab* is reached, aluminium crystallizes out from the  $\alpha$  liquid at constant temperature and  $\beta$  liquid is formed.

The  $\beta$  liquid, under normal cooling conditions, tends to surround the



aluminium; in fact, it isolates the aluminium crystals from the  $\alpha$  liquid, thereby preventing access of the aluminium-rich liquid to the already-formed crystals. Further crystallization can therefore occur only as a result of fresh nucleation. Thus, the  $\beta$  liquid restricts the growth of the aluminium crystals and tends to produce a finer crystal structure.

In Fig. 7, the point  $A'$  represents a typical modified alloy. On cooling, primary crystals of aluminium separate and the composition of the melt changes from  $A'$  to  $h$ . On reaching  $h$ , aluminium and silicon

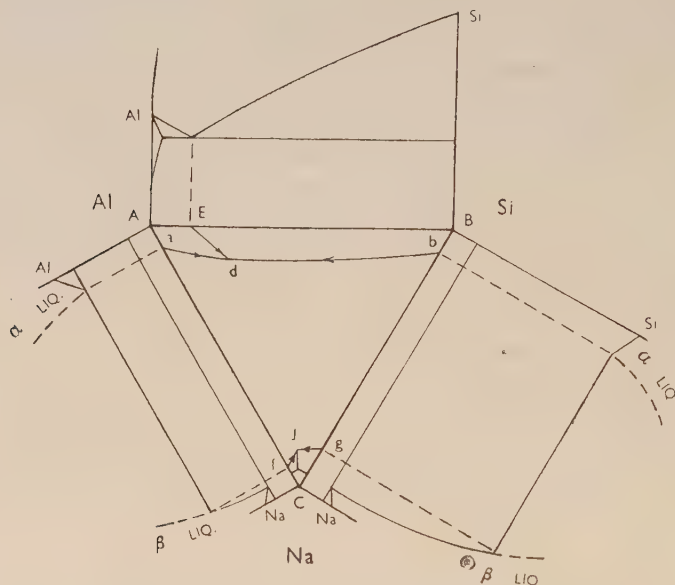


FIG. 5.—Aluminium-Silicon-Sodium Ternary System.

separate simultaneously along  $Ed$  until  $d$  is reached. At  $d$ , the ternary monotectic reaction, which causes the modification of the alloy, takes place at constant temperature. The  $\beta$  liquid behaves in the manner described above, and causes the production of small aluminium and silicon nuclei by hindering the growth of the nuclei already present.

From Fig. 5, it can be seen that the ternary liquid separates into two similar phases corresponding to the  $\alpha$  and  $\beta$  liquids of the two binary systems. The  $\alpha$  liquid is a mixture of aluminium and silicon in which a little sodium is dissolved, and the  $\beta$  liquid is mostly sodium in which a little aluminium and silicon are dissolved. These liquids are stable in



Thus, it was proposed that, in the modified alloys, the modifying agent performs the function of a protector by retarding the rate of coalescence, and thus leads to the fine, modified structure.

The principle of the restriction of growth of a dispersed phase was described by Edwards and Archer,<sup>11</sup> who assumed that, in the modified alloys, sodium separates as a discrete liquid phase just before solidification of the eutectic. This phase was considered to be in a fine state of sub-division similar to that of a colloid. It was further suggested that the fine sodium dispersion hindered crystallization of the silicon and, to a lesser extent, that of the aluminium. The finer structures obtained in the eutectic of the modified alloys are accounted for partly by the obstructing effect of the sodium globules and partly by the rapid formation of silicon nuclei in the undercooled liquid.

### III.—DISCUSSION OF PREVIOUS WORK.

Of the two early theories of modification, viz. the true flux theory and the metastable phase theory, little need be said except to point out that they fail to explain any of the facts associated with modification.

The ternary alloy theory attempted not only to account for the improvement in the properties but also to explain the depression of the eutectic solidification temperature. This theory fails, however, to account for the change in the eutectic composition during modification and for the fact that the modified eutectic melts at the same temperature as the normal eutectic. Nor does the theory account for the presence of both primary phases in modified hyper-eutectic alloys.

It is suggested in the colloidal theory that the modified eutectic structure is formed by the coalescence of colloidal particles. Such a view is not tenable, however, since the growth of crystals in a eutectic does not occur by coalescence of smaller ones; this will be discussed further in Section VI. In order to account for the effect of sodium, the theory depends on the limited solubility of sodium in aluminium and silicon. It thus offers no explanation for the fact that lithium, and to a small extent calcium and magnesium, which are soluble in aluminium-silicon alloys in all proportions, can effect modification.<sup>12</sup> Further, there are metals, such as lead and bismuth, which, like sodium, are partially soluble in aluminium-silicon alloys and yet do not cause modification. Neither the change brought about by rapid chilling of sodium-free alloys nor the presence of both primary phases is accounted for by the colloidal theory.

Examination of the early literature reveals numerous inconsistencies in the results of thermal analyses, the temperature of solidification of the modified eutectic, for example, being reported over the range

576°–560° C. The beginning of primary solidification in modified alloys is variously reported to be above and below the normal temperature.

None of the existing theories, therefore, is able to account for modification, and further progress is only to be expected in terms of new experimental results designed to resolve the discrepancies evident in the literature.

#### IV.—RADIOACTIVE EXPERIMENTS.

Because of the high volatility of sodium and its ease of oxidation, one of the uncertainties in all the earlier work on modification has been the actual sodium content of the alloys. No attempt was made in the present investigation to analyse chemically for sodium because of the difficulties involved in the analytical methods, but it was realized that some method for the estimation of sodium would be necessary in order to study the effects of varying the sodium content added to the melt and of subsequent remelting or superheating.

The only possible alternative to chemical determination appeared to be the use of radioactive sodium. The increased sensitivity offered by the use of radioactive isotopes, where the effect of a single atom can be recorded, over the chemical methods was immediately evident.

When an aluminium-silicon-sodium alloy is exposed to a neutron flux,  $\text{Na}^{23}$  is converted gradually to the radioactive isotope  $\text{Na}^{24}$ , and at the same time other radioactive isotopes are formed from the other elements present. A radioactive isotope is one which spontaneously emits  $\alpha$ -,  $\beta$ -, or  $\gamma$ -rays. In doing so, its chemical identity may be changed. This change is gradual and is characterized by a specific rate, designated by its half-life. In the experiments to be described, it was possible to separate the effects of the various isotopes and to recognize that part due to sodium.

The radioactive isotope  $\text{Na}^{24}$  emits  $\beta$ - and  $\gamma$ -rays having a half-life of 14.8 hr., i.e. the intensity of the radiation will be halved in any period of 14.8 hr. Thus, after a decay period of two half-lives, the intensity is one-quarter of the original intensity. However, the intensity does not decay at this rate if the radiation includes the rays emitted by isotopes other than  $\text{Na}^{24}$ .

The major constituents in the alloys are aluminium and silicon. After neutron irradiation, aluminium emits  $\beta$ -rays with a half-life of less than 2.5 min.; silicon is also a  $\beta$ -emitter, with a half-life of 170 min. The penetrating power of  $\gamma$ -rays is very much greater than that of  $\beta$ -rays, and if it is desired to measure  $\gamma$ -emissions only, therefore, a suitable thickness of absorbing material is interposed between the specimen and the Geiger-Müller counter.

Certain elements develop an extremely high degree of radioactivity because of their large capacity to capture neutrons. If such elements happen to be present as impurities, their effects may be so large compared to the effect of sodium that the latter becomes inappreciable. Under such conditions, the detection of sodium would be difficult. In the present series of experiments, however, these complications did not arise, and the detection of sodium was straightforward.

TABLE II.—*Results Given by Low-Sensitivity Counter.*

Alloy No.	Silicon, %	Sodium Added, %	Condition	$\gamma$ -Counts/Min. After :			
				6 hr.	12 hr.	25 hr.	32 hr.
1	10	0	Cast and air cooled.	750	...	...	...
2	10	0.1	As 1.	12,300	10,300	6,500	4,200
3	10	0.1	As 1, just remelted.	1,700	1,250	850	730
4	10	0.1	As 1, 20° C. super-heat.	1,400	1,300	750	625
5	10	0.1	As 1, 50° C. super-heat.	1,000	950	550	425
6	10	0.5	Cast and air cooled.	10,600	9,200	4,800	3,650
7	10	0.5	As 6, just remelted.	4,600	3,800	1,950	1,440
8	10	0.5	As 6, 20° C. super-heat.	3,750	3,200	1,600	1,250
9	10	0.5	As 6, 50° C. super-heat.	1,370	1,300	800	500
10	20	1.0	Cast and air cooled.	15,600	12,000	7,600	6,000
Background . . . . .				350	300	350	350

In order to explore the possibilities of this radioactive technique, alloys of aluminium and silicon were melted in graphite crucibles and cast into graphite moulds. Of the ten alloys investigated, nine contained 10% silicon and one contained 20% silicon. Sodium was added in amounts of 0.1%, 0.5%, or 1% by weight. Specimens about 1.0 cm. in dia. and 0.5 cm. thick were machined from each alloy, after various heat-treatments (Table II). Through the co-operation of the staff of the National Research Council of Canada, samples of the alloys were irradiated in the pile of the Chalk River Laboratories. After an irradiation of about 30 hr., the samples were removed and the activity was allowed to decay for 4 hr. before the samples were examined. Measurements were then begun, and it was possible by counting only  $\gamma$ -radiation to verify the presence of sodium (Table II).

The apparatus used for the counting was of two types. The first was a low-sensitivity Geiger-Müller counter which gave automatically the number of  $\gamma$ -counts/min. (Fig. 8).



The second counter used was a high-sensitivity Geiger-Müller counter with a considerably shorter specimen-to-counter distance, the results obtained with which are recorded in Table III. Owing to the proximity of the detector to the sample, this more sensitive counting device could not be used until after about two half-lives of  $\text{Na}^{24}$  (i.e. about 30 hr.).

Alloys Nos. 2, 6, and 10 emitted higher counts than the apparatus was designed for and hence are not recorded in Table III. The higher counts recorded in Table III as compared with those of Table II were due to the difference in the geometry of the apparatus. In the second case, the shorter specimen-to-counter distance permitted the counter to respond to a higher proportion of the total radiation emitted.

The variation of  $\gamma$ -ray intensity with time is plotted for some of the specimens in Fig. 9. In the derivation of these decay curves, allowance

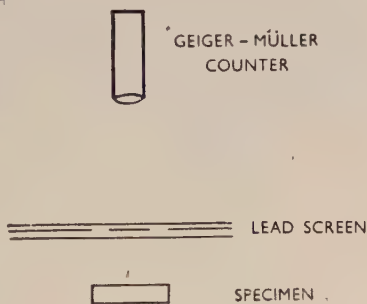


FIG. 8.— $\gamma$ -Ray Counting Apparatus.

TABLE III.—Results Given by High-Sensitivity Counter.

Alloy No.	$\gamma$ -Counts/Min. After :			
	32 hr.	33 hr.	34 hr.	35 hr.
1	1,982	1,835	1,763	1,728
2	...	...	...	...
3	6,681	6,400	6,076	5,960
4	7,000	6,650	6,400	6,322
5	4,600	4,330	4,156	4,000
6	...	...	...	...
7	17,443	16,313	15,940	15,300
8	14,200	13,490	13,000	12,630
9	6,600	6,100	5,823	5,470
10	...	...	...	...
Background	35	50	25	60

was made for the background radiation (see Table III), i.e. the radiation that is detected when no specimen is present. From the curves, it can be seen that the counts/min. are halved in value every 14.8 hr.

From the results of the radioactive experiments, it may be concluded that sodium is present in all the alloys to which it was added, the percentage depending on the amount added to the melt and on the

rate of solidification. Remelting the alloys causes a loss of some but not all of the sodium, and superheating increases this loss.

It is also of interest that the impurities present in the alloys did not change the shape of the decay curves, from which it may be concluded that the impurities were present in very low percentages or had very short half-lives.

From these experiments, it should be possible to calculate the amount

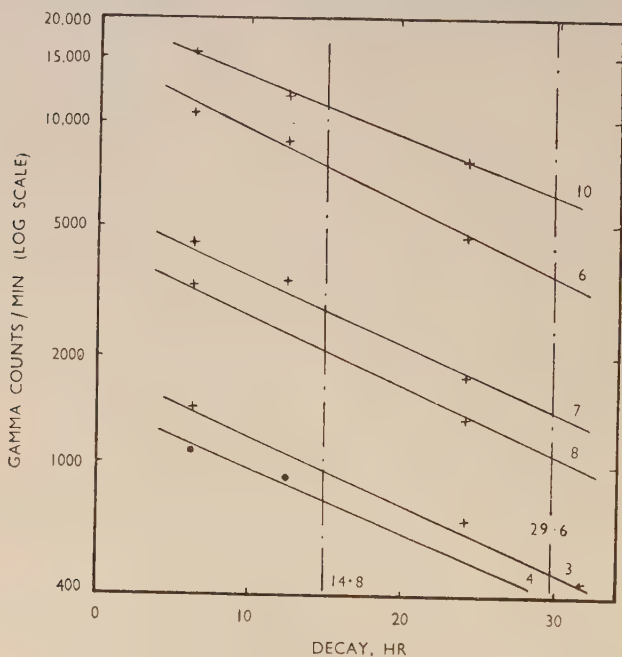


FIG. 9.—Variation of  $\gamma$ -Ray Intensity with Time for 6 Modified Aluminium-Silicon Alloys (for compositions see Table II).

of radioactive sodium in each sample. These calculations would require a detailed knowledge of the geometry of the apparatus and of the efficiency of the counting mechanism. Such a calculation would not, however, yield information regarding the total sodium present, because the ratio of radioactive to natural sodium is unknown. More extensive work would be required to give this information.

#### V.—THERMAL EXPERIMENTS.

Most of the experimental work on the modification phenomenon was carried out over 25 years ago. It was most desirable, therefore, to repeat the thermal experiments using the more modern equipment and

purier metals available to-day, as it was felt that many of the inconsistencies in the early experimental evidence would be clarified in this way.

The alloys used in the experiments were made up from 99.995% aluminium and 99.8% silicon. The apparatus consisted of an electrical resistance furnace, potentiometer, and a rapid-response temperature recorder (Leeds and Northrup, Speedomax Type G). The more sensitive scale of this instrument had a full-scale reading of 8 mV., which corresponds to a temperature range of approximately 200° C. with a Chromel/Alumel thermocouple. Since the important temperature range was about 500°–700° C., it was necessary to arrange for zero deflection to be at 500° C., giving a full-scale deflection for 700° C. This was accomplished by applying an appropriate constant e.m.f. (supplied by the potentiometer) to the thermocouple circuit.

The alloys were melted in graphite crucibles to avoid contamination, and modification was effected by plunging pure sodium, wrapped in paper, below the surface of the melt. The whole melt was then thoroughly mixed to ensure that the sodium was uniformly distributed.

The object of these experiments was to determine the temperature of eutectic solidification and of the beginning of primary solidification for alloys of various compositions, with and without sodium additions. A convenient fixed temperature in the range of the experiments was the eutectic solidification temperature of the normal alloy, and this temperature was used to calibrate the thermocouple. Cooling curves were obtained with various rates of cooling, from furnace cooling to cooling in an air blast.

TABLE IV.—*Thermal Data on Aluminium-Silicon Alloys.*

Silicon, %	Condition	Arrest Points, ° C.		Cooling Rate, ° C./min.
		Primary	Eutectic	
0	Normal	660 ± 0.5	...	40
0	Modified	660 ± 0.5	...	40
10	Normal	588 ± 2	572 ± 0.5	80
10	Modified	588 ± 2	564 ± 0.5	80
10	Modified	...	566 ± 0.5	20
14	Normal	608 ± 5	571 ± 0.5	90
14	Modified	608 ± 0.5	567 ± 0.5	20
20	Normal	...	572 ± 0.5	40
20	Modified	...	566 ± 0.5	15

The results derived from the cooling curves are shown in Table IV.

The conclusions from these and similar results are that: (1) the presence of sodium depresses the temperature of eutectic solidification,

and (2) the presence of sodium does not affect the temperature of primary solidification.

In alloys with more than the normal eutectic silicon content, the

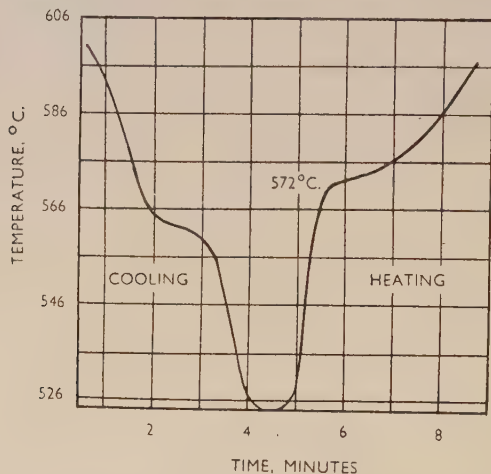


FIG. 10.—Cooling and Heating Cycle of a Modified Aluminium-10% Silicon Alloy.

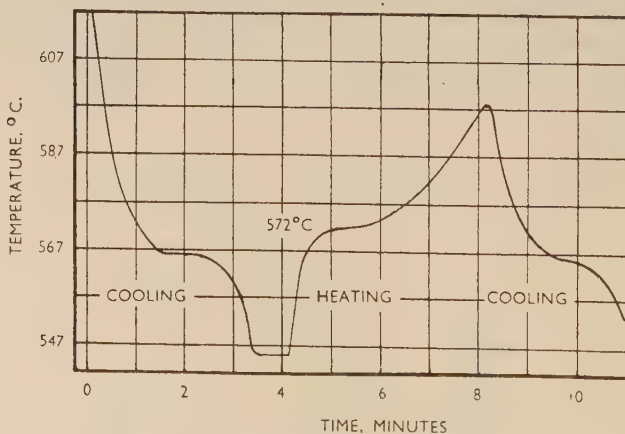


FIG. 11.—Cooling-Heating-Cooling Cycle of a Modified Aluminium-20% Silicon Alloy.

temperature of primary solidification is difficult to determine accurately, especially with high silicon contents. It is suspected that this is the result of variable undercooling of the primary silicon before it solidifies.

Previous investigators had concluded that the sodium burned off

in remelting the modified alloys, since the heating curves of the modified alloys indicated that the modified eutectic melts at the same temperature as the normal eutectic. This observation is confirmed in Fig. 10, which shows the cooling and heating curves of a 10% silicon alloy in the modified condition.

The results of the radioactive experiments showed that sodium was still present after remelting. By taking a second cooling curve of the modified alloy immediately after remelting, it was found that the alloy was still in the modified state (Fig. 11). It follows that the temperature of eutectic solidification is lower than the temperature of melting in modified alloys.

In certain cases, when the sodium content was very low, it was observed that the eutectic solidification took place in two stages, the first at the normal temperature and the second at a lower temperature characteristic of a modified alloy (Fig. 12).

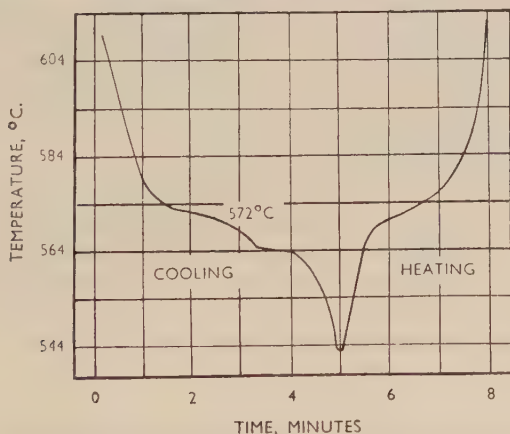


FIG. 12.—Double Eutectic Solidification in Aluminium-Silicon Alloy Very Low in Sodium.

## VI.—EXPLANATION OF MODIFICATION.

It is evident from the experimental results that the presence of a small amount of sodium has a definite effect on the temperature of eutectic solidification and on the eutectic structure. It follows that the process of eutectic solidification is altered by the presence of sodium. These facts may be considered in relation to the mechanism of solidification in eutectics.

Growth of crystals takes place by the addition of atoms to an existing crystal lattice. If no such "seed crystal" exists in the liquid, then solidification can occur only after a crystal nucleus has formed. A



nucleus forms by the chance aggregation of a number of atoms into the appropriate geometric configuration. This happens the more readily the further the temperature falls below the equilibrium freezing point. Thus, in the absence of seed crystals, freezing is not likely to occur until the temperature is below the equilibrium freezing point.

At the eutectic point, the liquid alloy may be in equilibrium with two solids of different composition. The solidification of the two phases must be accompanied by the redistribution of the two kinds of atoms which are present, and this redistribution must take place by diffusion in the liquid.

Two theories have been proposed for eutectic solidification. The first theory <sup>13</sup> is that nucleation and growth of a crystal of one phase so changes the local concentration of the liquid that it becomes supersaturated with respect to the other phase. The second phase then nucleates and forms a crystal. Conditions then become reversed and the result is an alternation of the two phases. This may be described as the intermittent or alternate solidification of two phases.

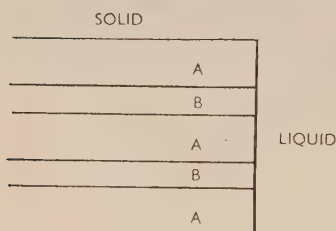


FIG. 13.—Simplified View of Eutectic Solidification.

In the other theory, both phases crystallize simultaneously from the liquid.<sup>14</sup> In the aluminium-silicon series, the aluminium forms a continuous matrix in which is embedded the silicon-rich phase. Intermittent crystallization cannot occur when one of the solid phases is continuous, and the second theory must therefore apply to the eutectic solidification of the aluminium-silicon system.

The simplest view of the solidification of a eutectic is represented by Fig. 13, in which the relative volumes of the two phases are determined by the composition of the eutectic, while the width of each layer depends on the rate of solidification.

The separation of a liquid into two solid phases can take place only by diffusion just before solidification. The distance through which this diffusion can occur depends on the time available, which in turn depends on the rate of solidification. Thus, rapid cooling will allow a short time for diffusion at the liquid-solid interface, and a fine structure will result.

The rate of advance of the interface depends on the balance between rate of heat flow from the liquid to the solid through the interface, and the magnitude of the latent heat evolved during solidification. Under otherwise similar conditions, the interface will advance more rapidly the higher the thermal conductivity and the lower the latent heat of

fusion. The thermal conductivities of aluminium and silicon are 0.53 and 0.20 cal./cm.<sup>2</sup>/cm./° C., respectively; while the latent heats of fusion are 94.6 cal./g. for aluminium and 337 cal./g. for silicon. These figures are probably not strictly correct for aluminium and silicon freezing as eutectics. Nevertheless, because of the very large difference between the values for aluminium and those for silicon, it may be concluded that the aluminium liquid interface will advance more rapidly

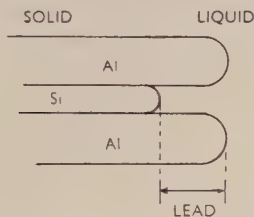


FIG. 14.—Aluminium-Silicon Eutectic Solidification.

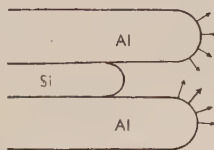


FIG. 15.—Growth of Eutectic in Aluminium-Silicon Alloy.

than the silicon liquid interface. It follows that, during solidification, the solid-liquid interface will not be flat and those parts of the interface where the solid is aluminium will freeze in advance of the parts where the solid is silicon. This "lead" will increase at higher rates of cooling. Thus, a more plausible conception of solidification in the eutectic would be that shown in Fig. 14.

Growth of the aluminium constituent at any point takes place in a

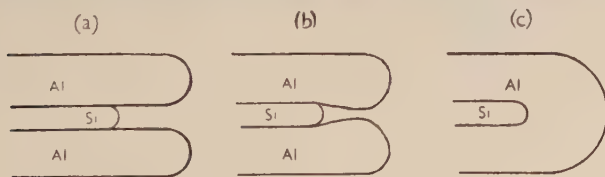


FIG. 16.—Sequence of Solidification of Aluminium-Silicon Eutectic.

direction perpendicular to its surface, as indicated by the arrows in Fig. 15, and therefore, at high rates of cooling, it is possible for the aluminium phase to enclose the silicon crystal, the sequence being as shown in Fig. 16.

This explanation accounts for the change in microstructure and freezing point brought about by the rapid cooling which occurs in chill casting the sodium-free alloys. With slow cooling, each silicon plate continues to grow and supercooling of the liquid is prevented by the presence of seed crystals on which growth can continue. On the other hand, with rapid cooling, where each silicon particle is "sealed off"

from the liquid by the mechanism illustrated in Fig. 16, there are no seed crystals, and solidification of the silicon can occur only as a result of nucleation which takes place at a lower temperature.

The theory proposed to explain sodium modification involves a con-

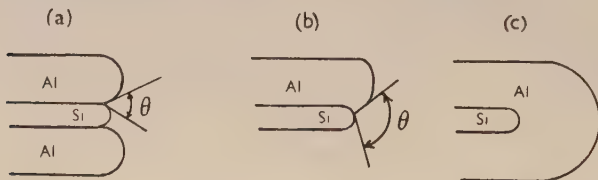


FIG. 17.—Effect of Sodium on Aluminium-Silicon Eutectic Solidification.

sideration of the interfacial angles between the solid aluminium, the solid silicon, and the liquid. In Fig. 17, the angles are governed by surface-tension conditions<sup>15, 16</sup> and at infinitely slow rates of cooling the forces would be in equilibrium.

It is suggested that the effect of sodium is to reduce the surface energy of the aluminium-silicon solid interface, with a resultant increase

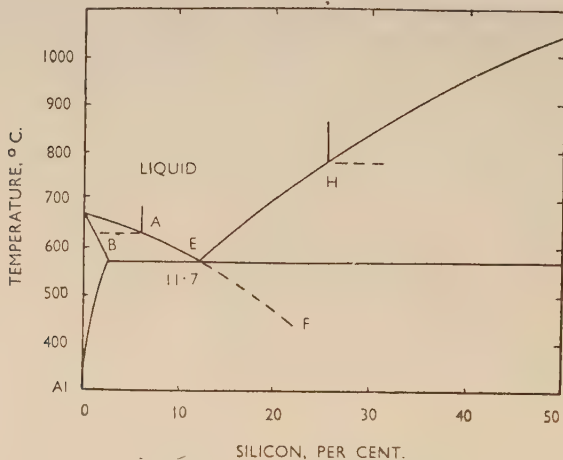


FIG. 18.—Aluminium-Silicon Modified Phase Diagram.

in the angle  $\theta$ , as shown in Fig. 17 (b). Fig. 17 (c) shows a later stage of growth under these conditions. This will result in the suppression of growth of this particular silicon crystal in the manner already described in connection with the rapid cooling of the sodium-free alloys. It may be observed also that this process would not have any influence on the melting point of the eutectic.

In the hypo-eutectic alloys, primary separation occurs with the

appropriate changes as cooling continues until the remaining liquid reaches composition *E* (Fig. 18). In the normal alloys, the eutectic forms at this temperature. It has already been pointed out that, in the modified alloy, undercooling must take place during eutectic solidification. Consequently, primary aluminium solid solution continues to form until a temperature is reached at which nucleation of the silicon is sufficiently rapid for the modified structure to be formed. This will occur somewhere on *EF*, the liquidus line, the exact position depending on the rate of solidification.

With alloys of the eutectic composition, the solidification process is identical with that of a hypo-eutectic, except that primary solidification begins at *E* (Fig. 18) instead of at *A*.

In the hyper-eutectic alloys primary separation of silicon begins when point *H* is reached. The composition of the liquid changes from *H* to *E* on cooling, at which point, if the alloy is modified, primary aluminium solid solution forms and continues to separate out in exactly the same manner as for the modified hypo-eutectic and eutectic alloys. This accounts for the presence of both primary constituents in the alloys of this composition (Fig. 3, Plate V).

Thus, it is possible by making two assumptions to explain the changes in structure and freezing point that occur in the aluminium-silicon system, the assumptions being that a leading phase exists and that a very small sodium content is able to reduce the interfacial tension between the solid aluminium and solid silicon phases. It is well known that a small quantity of a suitable addition may have a profound effect when the surface tension is reduced, but not when it is raised.

The improvement in the mechanical properties of the modified alloys can undoubtedly be attributed to the change in the distribution of the silicon phase. An analogous case is that of the distribution of cementite in steels,<sup>17</sup> where a definite relationship exists between the mean free path in the continuous phase and the mechanical properties (Fig. 19).

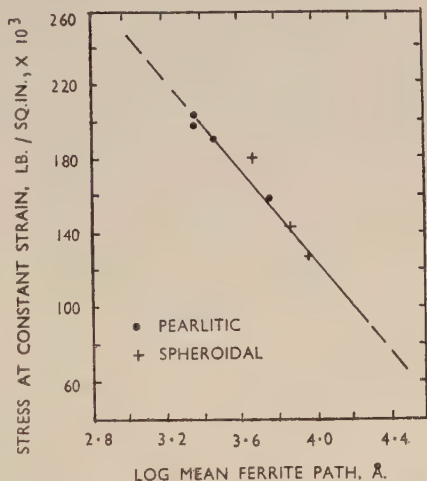


FIG. 19.—Stress at Constant Strain Related to Mean Straight Path through Ferrite in Steel.

It follows from the foregoing that no distinction should be made between modification brought about by the addition of sodium and that brought about by rapid cooling.

#### VII.—CONCLUSION.

It is interesting to speculate as to whether the theory that has been developed for the aluminium-silicon alloys has any wider application. In the present case, significant changes in the structure and properties have been shown to result from a variation in surface-tension equilibria. These changes may be caused by a very small shift in the interfacial surface tensions. A shift of similar magnitude in some other alloy may be insufficient to cause a change from the lamellar to the nodular condition. It is not, therefore, to be expected that all lamellar eutectics could be modified by a minor addition.

It has been suggested that the effect of aluminium on the lead-antimony eutectic is similar to that of the sodium in the aluminium-silicon system. Thermal experiments have, however, demonstrated that the eutectic solidification temperature is the same whether aluminium is present or not.<sup>19</sup> Thus, the mechanism responsible for the changes in the mechanical properties in the lead-antimony-aluminium alloy is not the same as that under discussion.

We are indebted to our colleague, Dr. L. M. Pidgeon, for the suggestion that the modification in normal cast iron to the nodular form brought about by certain additions<sup>20</sup> may be a similar process to modification in aluminium-silicon alloys. An investigation of this possibility is in progress.

#### *Note Added in Proof.*

Further study of the literature on nodular cast iron has shown that the analogy between the nodularization of cast iron and the modification of aluminium-silicon alloys is much closer than was previously realized.

The following conclusions may be drawn from the work of Morrogh and Williams:<sup>20</sup>

(1) Rapid chilling can produce a nodular structure of graphite similar to that obtained by making appropriate additions to the melt.

(2) A lower temperature of solidification is observed when nodularization is effected.

(3) The temperature of melting is the same for normal or nodular cast iron.

(4) The presence of two primary phases was recorded in nodular cast iron.

Existing data indicate that the thermal conductivity of iron is higher



than that of graphite or cementite at the temperature concerned; and that the latent heat of fusion is lower. It is, therefore, to be expected that in cast iron the iron and the carbon will behave like aluminium and silicon respectively in Figs. 15 and 16.

In view of these facts, the authors believe the mechanism of the formation of nodular cast iron to be essentially the same as that described above for modification of aluminium-silicon alloys.

#### ACKNOWLEDGEMENTS.

The authors wish to thank Dr. W. B. Lewis, Director of Research, for permission to conduct the radioactive experiments at the Chalk River Laboratories of the National Research Council of Canada. They also thank Dr. L. Cook, Head of the Department of Chemistry, and Mr. A. Booth, Department of Chemistry, Chalk River, Ontario, for their assistance in these experiments.

The authors acknowledge the assistance rendered by the School of Engineering Research, University of Toronto. They are indebted to Mr. Fred Francis, of Metals and Alloys, Leaside, Ontario, for the chemical analyses of the alloys used in the experiments. The co-operation and encouragement of Dr. L. M. Pidgeon, Head of the Department of Metallurgical Engineering, University of Toronto, is also gratefully acknowledged.

#### REFERENCES.

1. A. Minet, *Compt. rend.*, 1891, **112**, 1215.
2. A. Pacz, U.S. Patent No. **1,387,900** (13 Feb. 1920); Brit. Patent No. **158,827** (26 Jan. 1921).
3. J. D. Edwards, F. C. Frary, and H. V. Churchill, U.S. Patent No. **1,410,461** (27 Nov. 1920).  
R. S. Archer and J. D. Edwards, Brit. Patent No. **171,997** (15 Nov. 1921).
4. The British Aluminium Co., Ltd., and A. G. C. Gwyer, Brit. Patent No. **210,517** (31 Oct. 1922).  
The British Aluminium Co., Ltd., A. G. C. Gwyer, and H. W. L. Phillips, Brit. Patent No. **219,346** (22 Jan. 1923).
5. L. Guillet, *Rev. Mét.*, 1922, **19**, 303.
6. Z. Jeffries, *Chem. and Met. Eng.*, 1922, **26**, 750.
7. J. J. Curran, *Chem. and Met. Eng.*, 1922, **27**, 360.
8. B. Ötani, *J. Inst. Metals*, 1926, **36**, 243.
9. E. Schulz, *Z. Metallkunde*, 1948, **39**, 123.
10. A. G. C. Gwyer and H. W. L. Phillips, *J. Inst. Metals*, 1926, **36**, 283.
11. J. D. Edwards and R. S. Archer, *Chem. and Met. Eng.*, 1926, **31**, 504.
12. E. Scheuer, *Metal Ind. (Lond.)*, 1936, **49**, 557.
13. G. Tammann, "Text-Book of Metallography", p. 182. New York: 1925. (Chemical Catalog Co.).
14. R. Vogel, *Z. anorg. Chem.*, 1912, **76**, 425.
15. C. S. Smith, *Trans. Amer. Inst. Min. Met. Eng.*, 1948, **175**, 15.
16. F. L. Brady, *J. Inst. Metals*, 1922, **28**, 369.
17. M. Gensamer, E. B. Pearsall, W. S. Pellini, and J. R. Low, Jr., *Trans. Amer. Soc. Metals*, 1942, **30**, 983.
18. A. G. C. Gwyer and H. W. L. Phillips, *J. Inst. Metals*, 1926, **36**, 304.
19. R. Clark and R. Eyre, private communication.
20. H. Morrogh and W. J. Williams, *J. Iron Steel Inst.*, 1947, **155**, 321.



## PRESIDENTIAL ADDRESS.\*

1243

By H. S. TASKER,† B.A.

I AM deeply sensible of the honour done to me by the members of the Institute in electing me to the Presidency. Such a sentiment as this is, no doubt, a not uncommon opening to a Presidential Address, but on this occasion it is particularly apposite and keenly felt. The aims of the Institute are those of a learned body, but its founders, in throwing open its membership to a wider community than that of qualified scientific metallurgists, made it possible for many who, like me, cannot claim to be scientists, to play a part in the Institute's affairs. May I, as a representative of the unlearned section of our membership, acknowledge the debt we owe to those pioneers for their broad-minded provision. Still more do I personally owe a debt to my fellow-members who have placed me in this high position.

This Chair has on many previous occasions been occupied by an industrialist, but in these cases scientific eminence has usually marked out these predecessors as well qualified for their duties. I myself can claim no such qualification. Perhaps on this account I am the better able to survey the affairs and problems of the Institute with an eye that, though ignorant, may nevertheless see them with a fresh vision. It is true that I have not served the normal apprenticeship. I have no experience of the local meetings and discussions which, when all is said and done, form one of the main girders in the structure of the Institute's activities. I shall hope, in my year of Presidency, to make modest amends in this regard, but nevertheless I feel keenly the lack of this element of common experience with my fellow-members. Again, I have seen only the financial and not the technical side of our publication work. All the same I have been fortunate enough to play some part in the management of the Institute's affairs, and it is by virtue of this stimulating and satisfying experience that I venture to make some comments on its work.

For my task to-day there is yet another qualification that I lack. I observe with admiration the ability of my scientific friends to deliver, with such ease and authority, learned addresses appropriate to all occasions. Such talents are not possessed by the ordinary industrialist. For the layman the delivery of such an address is usually preceded by

\* Delivered at the Annual General Meeting, London, 29 March 1950.

† Chairman, Goodlass Wall and Lead Industries, Ltd., London.

heavy labour. I can only hope that the generosity of my learned colleagues will prompt in them the kindly tolerance once shown by Dr. Johnson. You may remember the occasion when Boswell mentioned that he had heard a woman preach. "Sir", said the Doctor, "a woman's preaching is like a dog's walking on his hind legs. It is not done well; but you are surprised to find it done at all".

Let me first say a word to my fellow-industrialists and, in particular, to those who are not scientists but whose work and whose livelihood are based also on the non-ferrous metals industry in any of its manifold branches. Some of these may already support the Institute as members. Many others are not members, and it is the attention of these that I would especially seek some means to catch. I am convinced that it is not sufficiently realized by the commercial community in our industry how wide—indeed how world-wide—is the prestige that the Institute of Metals has created for itself and for its publications in its short life of 41 years. In its role as a channel of publication of original work in the field of non-ferrous metallurgy, it stands, I believe, supreme in spite of a great volume of splendid work that is published in other countries. This achievement stands to the credit of British science and is the fruit of the initiative of British scientists as individuals. It is true that many industrial companies have given valuable help with the Institute's finances, but not before the Institute had—in the course of 30 years—built up for itself, unaided, a solid record of achievement. It is by individual members that the Institute has throughout been administered, and I hope it will always be so.

I dwell on this because it should be widely realized how much time and work are devoted, mostly by the scientific members, to an organization of this kind. The arrangement of meetings, both local and central, the educational activities and, most of all, the publication work make heavy demands (quite apart from the assiduous efforts of our staff) on members already fully occupied. No science can be pursued with vitality without the stimulus of discussion or without the facilities for publication of original work of high standard. The British metallurgical industry, in turn, cannot maintain its progress and prosperity unless it is sustained by British supremacy in the field of metallurgical science, pure and applied. This is the measure of the debt owed by the industry to the members of the Institute.

The period of the Institute's development since 1908 has coincided in time with a great expansion in the field covered by metallurgical research and industrial practice. Non-ferrous metals which 40 years ago existed only as laboratory specimens are now in regular commercial use; others have developed from dwarfs to giants, particularly under

the unnatural stimulus of war; knowledge as to the nature of alloys has greatly progressed; the study of metal physics has rapidly increased the understanding of the metallic state; the adaptation of all these advances to the use of non-ferrous metals in their manifold applications, in engineering, in the electrical field, in the enormous variety of contrivances that men and women use and enjoy, has transformed the social scene. Most of our modern technical wonders were unknown when the Institute was founded and, although their identification as blessings or curses may still be in dispute, it is safe to say that, in one way or another, they have all been made possible by developments in metallurgical science.

#### GROUPS WITHIN THE INSTITUTE.

This great expansion has been accompanied by a diversification which, it seems to me, has created problems for our Institute that did not exist in its earlier days. The flow of scientific and technological research in the non-ferrous field, although a strong and rising current, ran in those days in, broadly speaking, one all-embracing channel. As the flow of work has increased it has become ramified and the resulting streams, each in its own bed, have developed so as to stimulate the growth of knowledge in many fields, some of them differing so widely as often to appear to have little in common. To change the metaphor, there was a time doubtless when all metallurgists spoke and understood a common language. The majority of our members in those days could read and appreciate most of the papers published in our *Journal*. Times have changed, and nowadays it affords me, as a layman, not a little consolation when Dr. A, F.I.M., tells me that the paper of Dr. B, F.I.M., is beyond his comprehension. This specialization is no doubt the inevitable result of the scientific method and is, of course, not peculiar to metallurgy. Indeed, if I may digress for a moment, the insulation of the specialists in almost every branch of knowledge from the understanding of the ordinary man—intensified as it is by their proper and peculiar jargons—seems to me to become increasingly a menace to human society. There is being created a high priesthood, whose pronouncements are as incomprehensible and as little to be questioned as those of the oracles and augurs of classical times or of the medicine man of primitive civilizations. Democratic government will find in this one of its hardest practical problems.

However, I refer now to our own problems created by this diversification even in the comparatively restricted field of non-ferrous metallurgy. They find expression, for instance, in comments as to the ultra-theoretical nature of some of the papers published in the *Journal* and in



complaints that the discussions at our General Meetings are not what they were in the old days. There is substance in such statements, and in my view it will be wise for the Institute to modify its policies to meet the changing conditions of the times.

It has, for instance, been somewhat unwilling in the past to countenance, under its broad cover, the formation of groups of those members whose main interest is in one particular branch of the science. Has not the time come when such groups should rather be encouraged? Can we not recognize that, while our scientific members share a fundamental and essential core of interest, many of them are working in widely different fields with highly specialized techniques? Cannot such workers be assisted in joining together under the ægis of the Institute to arrange for such discussions, publications, and activities as will be most helpful to them? Certain provisos are needed. The sphere of interest should be capable of reasonably precise definition; the group must provide a keen and active committee which would initiate and develop its programme under the general survey of the Council. Given such conditions, I am sure that the encouragement of groups within the Institute would be a real practical service to its members. A start has, of course, been made. The successful work of the very active Metal Physics Committee has been well supported and, far from confining itself to esoteric discussions in remote regions of mathematical thought, it has, in arranging such fixtures as the recent Symposium on "Metallurgical Applications of the Electron Microscope", proved its practical usefulness not only to our own members but to a wider circle of scientists both in this country and abroad. It has, moreover, recently commanded my own admiration by attempting to define its own scope and the purpose of its existence—an example worthy of the widest possible imitation, particularly by committees. Quite recently, another Committee, dealing with Metallurgical Engineering, has started work. I know that in raising this subject of group-formation I may be wandering into debatable ground, but if my toes are trodden upon no great harm will be done. My underlying thought is this: that, if a substantial body of members share a desire or need that comes within the aims of the Institute, we should endeavour to satisfy it within the bounds of our powers and resources.

It is in this direction also that the undoubted problems surrounding the arrangement of discussions—particularly at our General Meetings—may, I feel, find their solution. In the old days, so I am told, discussions were lively and controversial; the great men of those days would step down into the arena and belabour each other with gusto, much to the relish of their pupils and subordinates. To what extent this picture

has been magnified by the inverted perspective of Time's glass I do not know. The joys of youth were always the sweetest, although, as a wise man once remarked, they occur far too early in life. But surely the explanation is that in those days everyone talked the same metallurgical language. Most of the members were interested in most of the papers. Times have changed. Papers are more highly specialized, and it will be exceptional if, even where several are grouped together, they give rise to general discussions interesting to all of our members.

As one solution to this problem there was arranged for last year's Annual Meeting a Symposium on "Metallurgical Aspects of Non-Ferrous Metal Melting and Casting of Ingots for Working". There was a valuable and well-attended discussion. A similar Symposium is to be held to-morrow. These are, when all is said and done, special discussions specially designed to assist and interest a certain section of our membership, namely, those concerned with problems of practical technology. But is there any reason why, simultaneously, another and separate discussion should not take place on some widely different theme which would interest a different set of members? Such meetings, designed specifically to meet the needs of defined groups of members, seem to me far more likely to give rise to lively discussion than those at which papers of varied types are presented. I suggest that simultaneous discussions by different groups would be an experiment well worth trying. We rightly aim at bringing together at our General Meetings members of all kinds, often from distant places. A programme which gave them alternatives would avoid wasted days for some of them. I come back again to the root cause of our problem: it is no longer an easy matter to find subjects of current importance which admit of general discussion by the whole body of our members. If that is so, let there be more discussions and, provided that the subjects are of current importance, let them be more restricted in their scope and appeal.

The wider field covered by metallurgical science has helped to create for the Institute another serious problem—that of finance. The volume of our publications has greatly increased and the spread of the Institute's activities has widened. There seems every reason to expect that these tendencies will continue. Simultaneously, the cost of every item of expenditure has risen sharply. It is true that our membership has continuously increased, but, in spite of this, it became necessary in 1947 to increase the rate of subscription by one-third. Now, in spite of the efforts of our Honorary Treasurer, the balance is again substantially on the wrong side. This is not the time for a detailed account of our position, but the fact is that the Institute is caught between the increase

in the volume of its useful activities and the economic conditions now prevailing in this country. Hitherto your Council has laid it down that the former must not be curtailed and, in particular, that every paper submitted for publication must, if it reaches our normal standard, be published. I believe that to be the only possible decision, but it is one that severely limits the opportunities for economies. On the other hand, a further increase in the rate of subscription might well lead to a loss in membership, thus not only undermining our usefulness and influence but also limiting the additional revenue to be expected. Life presses hard on the salaried man to-day and, although membership is a necessary tool in the equipment of every scientist who works in this field, I can well believe that he cannot always easily afford it. The Institute has, thanks to the War-Time Emergency Fund, a brief respite after which, if additional income is not found, its work must be curtailed. To this situation the Council is now, in good time, giving its attention. My own view is that, although we should exercise all reasonable economy, our work should go on and indeed should be expanded in any direction that will assist the progress of metallurgical science. For this new sources of regular income must and will be found.

#### METALLURGICAL EDUCATION.

I would like now to refer to one subject to which in recent years many members of the Institute have devoted considerable attention—metallurgical education. In 1943 the Department of Scientific and Industrial Research appointed a Committee under Dr. (now Sir) Andrew McCance to consider the steps necessary to secure an adequate supply of trained metallurgists in the post-war period. Our Institute was among the organizations invited to give evidence; the task of preparing our evidence was remitted to the Finance and General Purposes Committee, of which at the time I happened to be Chairman, so that it fell to me to reconcile and to condense into coherent form the various views of the Members of Council and others who joined in our deliberations. Anyone less fitted by previous experience for this role could hardly have been found, but I shall always be grateful to Fortune for fastening this duty on me. It chanced that at that same time two other developments occurred. The Board of Education, as it was then, approached the various institutions interested in metallurgy pressing for the establishment of National Certificates in Metallurgy and secondly, among working metallurgists, the demand became active that a qualifying organization concerned specifically with the science and practice of metallurgy should come into being. Neither of these proposals posed a simple problem, but discussions took place with the Iron and Steel

Institute, the Institution of Mining and Metallurgy, and the Institute of British Foundrymen, and ultimately three important results were obtained. The Joint Committee for National Certificates in Metallurgy was formed; the first draft of a constitution for the proposed Institution of Metallurgists was produced; and, lastly, the four metallurgical Institutes combined to set up the standing Joint Committee on Metallurgical Education. National Certificates and the Institution of Metallurgists are now firmly established and the obstacles that once appeared daunting have been happily surmounted. The Education Committee already has a solid record of useful work to its credit, and the Institution of Metallurgists now joins in its labours.

The purpose of all the activity of which I have given a brief review has been the provision, mainly for industry and research, of more and better qualified metallurgists. The planning of the right training for men of graduate standard is far from easy. Metallurgy is in itself a secondary science in that it consists in the application of the fundamental principles of chemistry, physics, and mathematics to the restricted field of substances in the metallic state. I have already indicated the diversity of the mass of knowledge that has developed. If illustration of this is needed, consider the project now under discussion by our Publication Committee for the publication at intervals of progress reports of advances in different fields of non-ferrous metallurgical research and practice. A preliminary survey suggests a minimum of 18 separate and substantial categories, together with 9 sub-categories grouped together under "metal physics". Even after liberal eliminations, it is clear that a well-qualified graduate must cover a very wide area of knowledge and yet a University course allows three or, at most, four years into which some small experience of works' practice must, if possible, be fitted. The weight of your Institute's influence, has, in these circumstances, been exerted solidly in favour of concentration on the three basic subjects—chemistry, physics, and mathematics. We have urged that the metallurgical course should properly be one of four years, and that specifically metallurgical subjects should be introduced only in the later years. We have expressed the view that, as has been the case with some of our greatest metallurgists, a graduate in the basic sciences is likely, if he can take a postgraduate course in metallurgy, to be better qualified, particularly for research, than a metallurgical graduate of equal ability. I am sure that in this emphasis on fundamental grounding, as to which the other metallurgical Institutes have been in full agreement, a contribution to the future well-being of British science and industry has been made.

A supply of University graduates trained purely as scientists does



not, however, fill all the requirements of our industry. These men will not be trained technologists. They must be regarded and used as raw material of good quality, but they are not a finished product. Their employer must spend time and money in forming them into the instruments that he needs, secure in the knowledge that he is shaping well-tempered minds. This is, of course, appreciated by most organizations of substantial size to-day.

#### TRAINING OF TECHNOLOGISTS.

But industry needs, in addition, greater numbers of young men of distinctively technological training, and much discussion has taken place in recent years as to the best way to provide them. There are many students for whom such a training is the most suitable, men whose turn of mind is practical rather than theoretical, but who may nevertheless be of great value in later life, particularly if working alongside men of more fundamental outlook. Moreover, industry in this country, and perhaps particularly the non-ferrous industry in many of its branches, is not preponderantly composed of large companies or groups. The part played by companies of small or moderate size is most important, and for such as these the problem of fitting into the organization a man of purely theoretical university training is often difficult. Many businesses too, have emerged as the creation of practical men of outstanding character and ability to whom the theoretical as opposed to the practical type of recruit makes less appeal. This was well illustrated in a contribution to a recent discussion in which the disadvantages of a University education were happily expressed. "The University man", it ran, "is apt to concentrate his energies on thinking and to leave the practical work to be done by other people". To those of us who spend time searching for men who can think that statement will give pause. Nevertheless the good sense behind the words should be understood and respected. The fact is that the Universities are not fitted and should not be expected to supply the full range of well-trained men that industry requires, and I confess that I view with considerable misgiving the great expansion that has recently taken place in the size of the University Science Schools, largely with the object of increasing the supply not only of scientists but of technologists.

I cannot rid myself of the old-fashioned belief that a University is, and should remain, an establishment for the pursuit and dissemination of knowledge for its own sake; its research, in whatever field, should be unhampered by practical objectives and should follow Truth wherever she may lead; its teaching should be directed to the discipline and



training but not to the technical equipment of the mind. The old toast: "The Higher Mathematics and may they never be of any use to anyone" has, by the inventiveness of man, been robbed of its fulfilment, but it did express the essential purpose of a University foundation. The rise of science has, in the course of a few generations, added an enormous range to the field that a modern University must cover. Many subjects within this range inevitably have aspects which closely affect the material conditions under which we live. This factor in itself must have made it increasingly hard for Professors in scientific subjects to keep ever in view the goal of pure knowledge for its own sake. This difficulty is enhanced in our country to-day when the need is for rapid practical results so that as a nation we may earn our daily bread. Yet it is as true to-day as ever it was that it is from pure research with no practical purpose that the great technical advances of the future may spring. I believe, therefore, that—even on material grounds though by no means on those grounds alone—the Universities should be allowed to fulfil their ancient functions and that no pressure, whether from Government or from industry, should attempt to divert them from the free pursuit of knowledge; otherwise the penalty will ultimately be paid by the people and the industries of this country, and it will not be a light one.

How, then, shall our much-needed technologists be trained and where? I personally have yet to see a better solution than that proposed nearly five years ago by the Percy Committee. The Colleges of Technology then advocated seem to me undoubtedly to be the instruments best suited to produce the well-qualified but practical recruits for whom all branches of our industry are asking. It is to be regretted that the tangible results of the Percy Report are as yet small, for progress on those lines would relieve the present pressure on the Universities. Students of undergraduate age cannot and should not be divided into sharply defined categories, but in time there would take place a rough sorting process so that the different types of men would tend to take the type of training—more fundamental on the one hand or more practical on the other—best suited to their natures. It is worth noting that in this Report emphasis is again laid on the need for a solid basis of fundamental science in a technological, as distinct from a University, course. As for the prestige attaching to a technological training and the standing of these Colleges compared with the Universities, these in the long run will surely depend on the quality of their work and of the men they turn out.

## GENERAL EDUCATION OF THE METALLURGIST.

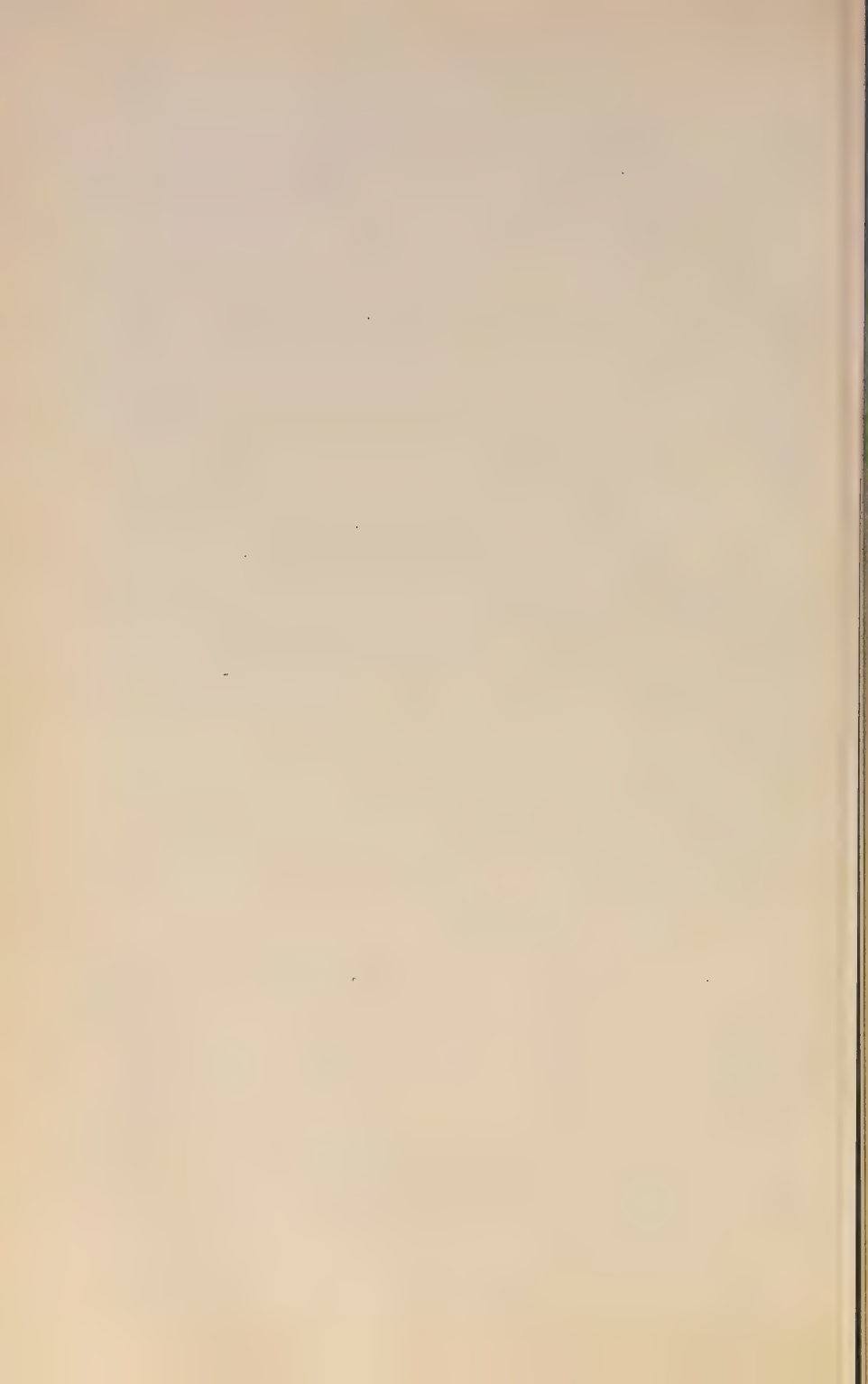
Lastly, I would like to refer to the danger that the increasing demands made by scientific education on the time and energies of the student may crowd out from his mental background that broader culture, that knowledge of the humanities so essential to the full development of character and personality. This question has already received the consideration of our joint educational committee, for in 1948 it published a wise and strong recommendation that the entrant to a University science course should be required to show evidence of culture outside the strictly scientific field. This pronouncement was made specifically as a comment on the Government White Paper on Secondary Education, but I do not doubt that the Committee would go further and agree with me that, during the University course as well, further development of the student on the cultural side is essential. For most of us it is at the undergraduate stage that appreciation of literature and the arts responds most rapidly to stimulus; this is surely the period during which lasting enthusiasms may most readily be kindled. Scientific education, for all its fine mental discipline, cannot provide this cultural impetus. Yet the deeper qualities of character whose development is encouraged by a wider range of intellectual interest will, I believe, be looked for in our scientists no less than in men trained in what are called the more humane studies. Lord Trent said recently "The most important factor in industry to-day is the human. The higher a man rises in industry, the less the technical qualifications count and the more valuable are the human qualities of character, courage and vision." Every young scientist who enters industry to-day should have impressed upon him the truth of those words, and should have encouragement in acquiring the wider horizon which will, as times goes on, thus balance his outlook.

This is no new theme. Recent correspondence in *The Times* showed that it is much in the minds of many leaders in scientific education. Equally is the problem realized by those who speak for history and the classics. The claims of an introduction to history to a place in the so-called modern curriculum have been stressed by G. M. Trevelyan and recently also by A. L. Rowse in his excellent little book "The Use of History". Their essential text is the saying of Bacon: "Histories make men wise". I confess I would like to see inserted in every scientific course as an integral part a weekly lecture dealing each term with History, Classics, Literature, or a similar subject, and designed not to instruct but to stimulate interest. I should hope that there would be in some minds a response that would not otherwise have been aroused

and that these men in later life by their own reading would gather for themselves lasting benefit and satisfaction. (Since this address was drafted, I have read that the science students at Cambridge have recently made a formal request to the English Faculty that special lectures should be provided for them. Clearly the soil is ready for the seed.)

I have mentioned the Classics because the most lofty plea on this subject that I have read is contained in the Presidential Address of Lord Greene to the Classical Association in 1947. He called this "Classics and the Social Revolution of Our Time", and in it he urges that wide familiarity with the Classics should be preserved, not by the study of the classical languages, but by reading for pleasure and in translation. From many tempting quotations I choose this: "If I were asked", he says, "to summarize what lessons have been learnt best in the past from Greece and Rome, as they can be learnt best in the future if taught in a manner suited to the circumstances of the times, I should give this catalogue: integrity of mind, and the habit of following the argument wherever it may lead; accuracy of thought and expression and the impulse to reject what is slovenly or superficial; distrust of the catch-word and all undue simplifications; the habit and method of reasoned criticism which forbids us to accept or reject a proposition merely because it is pleasant to do so or because it saves the trouble of thought; the power to recognize and enjoy beauty in all its forms. I should like to add sublimity of language and, what is both its father and its child, sublimity of thought. Lastly, there is what combines all these qualities in one balanced whole, a conception of humanity in which its capacities can attain their full development and the spirit can reach out in all directions for those delights of reason and of beauty which 'glow before the common steps of life'. These lessons were of course pre-eminently taught by Greece; but they were learnt and passed on to us by Rome, Rome which added lessons of its own."

The young scientist or technologist, contemplating the colossal edifice of material civilization raised by his predecessors in a brief 300 years, may well ponder these words and remember that they are used of the culture developed in a small city-state on the shores of the Mediterranean 3000 years ago. We who are older may well ask ourselves whether our own civilization has learned those lessons and whether we shall hand them on in our turn with added virtues. If we wish to do so we must see to it that our young men and women, in the midst of their material equipment for life, have the opportunity to acquire those finer perceptions which will enable them to know and prefer the good in whatever form it shall appear.



# THE MECHANICAL PROPERTIES OF SOME 1244 WROUGHT AND CAST ALUMINIUM ALLOYS AT ELEVATED TEMPERATURES.\*

By P. L. THORPE,† G. R. TREMAIN,† and R. W. RIDLEY,† B.Sc.  
(Communication from the National Physical Laboratory.)

## SYNOPSIS.

The purpose of the investigation was to provide data on commercial and experimental alloys used in the construction of aero-engines. Results are given of tensile, fatigue, and creep tests at various temperatures in the range 20°–450° C. on seventeen wrought and seven cast alloys, together with results for a form of thermal-strain test on some of the cast alloys. The materials tested included some experimental alloys developed during the last war by the Royal Aircraft Establishment, Farnborough.

The alloys are compared on the basis of their tensile, fatigue, and creep properties at service temperatures. Of those tested at 250° C., R.R. 57 has the greatest resistance to creep, whilst the R.A.E. alloy SA44 has the highest fatigue strength. NA23S has good resistance to both creep and fatigue. Some physical properties of the alloys are given in an Appendix.

## I.—INTRODUCTION.

THE investigation to be described was begun in 1937 at the National Physical Laboratory, in response to a request from the Air Ministry. The information then available to designers of high-speed aero-engines on the creep and fatigue properties of aluminium alloys at high temperatures was very meagre, and a study was required of the thermal stresses associated with the cracking of pistons and cylinder heads during service. The original programme of tests on piston alloys was subsequently revised to include impeller and compressor materials.

Owing to the outbreak of war, with the consequent need for quick results, it was not possible for the investigation to be conducted on as comprehensive a scale as desired; however, it is thought that the information given is reasonably representative of the material, bearing in mind the chemical analysis and particular heat-treatment in each case.

In the earlier stages of the investigation on piston alloys, tensile and fatigue tests were carried out at temperatures ranging from 20° to 450° C., while creep tests were made at two temperatures only, namely, 300° and 400° C. Since, however, it was decided that failures

\* Manuscript received 6 July 1949.

† Engineering Division, National Physical Laboratory, Teddington, Middlesex.





R.A.E. 55 (P)	...	1.73	3.09	0.61	0.40	0.17	0.05	1.55	...	0.26	...	...	98	570° C. for 4 hr., quenched in boiling water; aged for 40 hr. at 160° C., air cooled.
R.A.E. SA34 (P)	...	5.1	1.9	0.5	0.3	10.9	0.1	0.2	...	...	0.2	...	145	500° C. for 3 hr., quenched in hot water; aged for 16 hr. at 175° C.
R.A.E. SA44 (P)	...	5.1	...	0.5 <sub>g</sub>	0.2 <sub>g</sub>	10.7	0.1	0.5	...	...	0.3	...	150	500° C. for 3 hr., quenched in hot water; aged for 16 hr. at 165° C., air cooled.
Duralumin (I)	6L1 and L39	4.10	...	0.73	0.47	0.47	0.09	0.46	...	...	...	...	75 §	495° C. ± 5° C. for 1 hr., quenched in boiling water; aged for 5 days at room temperature.
Y alloy (P)	3L25	3.76	1.85	1.33	0.40	0.45	...	...	...	...	...	...	105	511° C., quenched in fairly hot water; aged at room temperature.
Lo-Ex (P)	D.T.D. 324	1.03	1.02	0.91	0.50	11.80	0.02	0.03	...	...	...	...	120	522° C. for 12 hr., quenched in water; aged for 6 hr. at 136° C., air cooled; final ageing for 4 hr. at 200° C., air cooled.
Ex 275 (P)	...	2.23	2.04	0.83	0.82	0.59	0.15	0.95	...	...	...	...	119	560° C. for 5 hr., quenched in boiling water; aged for 24 hr. at 190° C.
CAST ALLOYS (sand cast unless otherwise stated)														
R.R. 50 (P)	D.T.D. 133B	1.40	0.90	0.12	1.18	2.25	0.19	...	...	...	...	...	70	160°-170° C. for 10 hr., air cooled.
R.R. 53C (P)	D.T.D. 309	1.33	0.87	0.50	1.12	2.42	0.15	...	...	...	...	...	100	530° C. for 2 hr., quenched in water; aged at 160°-170° C. for 15 hr.
R.R. 131D (P)	...	0.30	1.20	1.39	0.30	0.50	0.12	0.44	...	0.18	0.45	0.25	55	160°-170° C. for 10 hr., air cooled.
R.A.E. 40C (P)	...	2.0	5.0	0.5	0.5	0.3	...	3.0	0.4	0.5	...	...	85	Tested in as-cast condition.
R.A.E. 47B (P)	...	1.0	4.0	0.5	0.5	0.2	0.2	3.0	...	...	...	...	{ 80	Tested in as-cast condition.
R.A.E. 47B   (P)	...	1.89	2.90	0.56	0.43	0.21	0.07	1.55	...	0.15	...	...	82	570° C. for 4 hr., quenched in boiling water; aged for 12 hr. at 200° C., air cooled.
R.A.E. 55   (P)	...	...	...	...	0.28	12.0	...	0.29	...	...	...	...	100	510°-518° C. for 4 hr., quenched in cold water; aged at 150°-165° C. for 16 hr.
Alpac-Gamma   (P)	D.T.D. 245	...	...	0.35	0.28	12.0	...	0.29	...	...	...	...	...	...

P and I refer to alloys tested at temperatures and for periods related to piston and impeller service conditions, respectively.

§ Rolls-Royce Experimental Alloy B101; R.R. 57 (stabilized at 215° C.) is a development of B101.

† Figures obtained in a chemical analysis made at the N.P.L. (Figures for all the other alloys were supplied with the material.)

‡ Later batch of R.R. 59 material.

§ Hardness value of material in the softened condition. (Softening treatment 10 days at 250° C.)

|| Chill cast.

around the gudgeon-pin bosses in pistons occurred at temperatures estimated to be in the region of 250° C., most of the later tests were made at this temperature. In the case of some of the impeller and compressor materials, tests were made at 100° and 200° C. in addition to those made at 250° C., the maximum temperature adopted for these alloys.

Tests were also made on three of the alloys in a fully softened condition, such as would be reached after continuous use in the engine. This softening was produced by annealing the materials for 10 days at 250° C.

In order to provide additional data on aluminium alloys, mean values of the thermal conductivity, electrical resistivity, and thermal expansion of several of the alloys are given in Tables XI and XII. These values have been calculated from the results of tests made by the Physics Division of the National Physical Laboratory.

## II.—MATERIALS.

The chemical composition and heat-treatments of the seventeen wrought and seven cast aluminium alloys are given in Table I. These alloys were supplied in bar form, approximately 1 in. in dia. or 1 in. square. They were examined for uniformity by means of hardness tests made at air temperature. As the first alloys tested were of low hardness, a Brinell test using a 10-mm. steel ball and a load of 500 kg. ( $P/D^2 = 5$ ) was employed. This was adopted as a standard for comparison of the alloys. Additional tests were made on some of the harder alloys, using a load of 1000 kg. ( $P/D^2 = 10$ ). The mean values obtained for the hardness of the alloys are given in the right-hand columns of Table I; the values for individual bars were found in general to fall within a range of  $\pm 10$  of the mean, but wherever possible only those bars of hardness number within  $\pm 5$  of the mean were used for the tensile, fatigue, and creep tests.

## III.—TENSILE TESTS.

Tensile tests were carried out at temperatures ranging from 20° to 450° on test-pieces machined to a standard form, with a test portion 0.564 in. in dia., and a gauge-length of 2 in. For the tests at elevated temperatures, the specimen was heated by means of a wire-wound electric furnace. A period of about 2 hr. was taken in heating the specimen to the required temperature, which was then maintained constant for a further 4 hr. before the test was begun. The temperature of the test portion of the specimen was measured by means of three

thermocouples, the temperature along the gauge-length being within  $\pm 2^{\circ}$  C. of the test temperature.

During the tests the load was increased by small increments until the 0.5% proof stress had been passed, when it was applied at a constant rate of approximately  $\frac{1}{2}$  ton/in.<sup>2</sup>/min. until the maximum load was reached.

The extension of the test-piece was measured by means of a rhomb-and-mirror type extensometer, sensitive to a strain of  $5 \times 10^{-6}$ , and the limit of proportionality and proof stresses were calculated from the load-extension diagrams obtained.

The results of the tensile tests are given in Tables II and III and are shown diagrammatically in Figs. 1 and 2.

#### IV.—DIRECT-STRESS FATIGUE TESTS.

The fatigue tests were made mainly on 0.3-in.-dia. test-pieces, in Haigh-type electromagnetic machines of  $1\frac{1}{2}$  tons capacity, operating at a frequency of about 2000 stress cycles/min. Each machine was fitted with a folding-type electric furnace by means of which the test-piece was heated to the required temperature, and controlled to within  $\pm 2^{\circ}$  C. by means of a thermostat.

During each fatigue test, approximate measurements were made of any extension or creep occurring, especially during the fluctuating fatigue stress tests, where a tensile mean stress was used. In only a few cases was any such extension measurable.

The results of the fatigue tests are given in Tables IV, V, and VI, and are shown plotted for several of the more important alloys in Figs. 3, 4, and 5; Fig. 6 illustrates the variation in the estimated endurance limits with temperature.

For the purpose of obtaining the stress ranges given in the Tables, the usual stress-endurance curves were plotted from the individual test results, and the stress ranges estimated for the required endurances.

Owing to the absence of any definite fatigue limit at elevated temperatures, the alloys are compared in Tables IV and V on the basis of the estimated stress for an endurance of  $10^7$  cycles. For the impeller and compressor materials, where the frequencies in service are very high, the stresses are estimated for endurances of  $10^7$ ,  $10^8$ , and  $2 \times 10^8$  stress cycles (see Table VI). The comparison between alternating and fluctuating stresses can also be seen in this Table.

TABLE IIA.—Results of Tensile Tests on Wrought Alloys at Various Temperatures.

Rate of Loading : approximately  $\frac{1}{2}$  ton/in.<sup>2</sup>/min. after 0.5% proof load had been reached.

Material	Test Temperature, °C.	Limit of Proportionality, tons/in. <sup>2</sup>	0.01% Proof Stress, tons/in. <sup>2</sup>	0.1% Proof Stress, tons/in. <sup>2</sup>	0.5% Proof Stress, tons/in. <sup>2</sup>	Ultimate Tensile Stress, tons/in. <sup>2</sup>	Modulus E, lb./in. <sup>2</sup> × 10 <sup>8</sup>	Elongation on 4√area, %	Reduction of Area, %
R.R. 56	20	10.2	16.5	19.9	22.6	28.0	10.5	16	15
	100	10.4	15.6	18.9	20.9	24.7	9.1	23.5	29
	150	4.6	8.8	17.4	19.8	23.3	9.4	18.5	22.5
	200	4.2	8.4	15.2	16.9	18.9	8.9	14	24.5
	250	4.4	7.6	11.5	12.5	13.5	9.0	14	39
R.R. 57	20	4.8	11.4	15.9	18.5	27.3	10.2	10	10
	250	2.4	5.1	8.6	10.5	13.8	8.7	25.5	47
B101	20	12.8	14.7	16.8	18.6	26.1	10.2	15.5	24
	250	3.7	6.0	9.0	11.0	14.5	8.5	23	67
B101 (softened) *	20	6.0	10.8	12.4	14.3	24.1	10.2	13	19
	250	3.0	5.8	8.2	9.7	12.6	9.0	22.5	65
R.R. 59 (L42) †	20	(10.0)	(18.8)	(22.0)	(25.2)	(29.5)	(10.6)	(10)	(19)
	20	10.7	14.2	16.8	20.0	27.2	10.6	17.5	24
	100	8.0	13.4	16.0	18.6	24.9	10.0	15	15
	150	6.1	12.8	15.7	17.8	23.2	10.2	17.5	20.5
	200	3.6	8.0	15.1	16.9	20.4	9.6	14	19
	250	3.2	6.8	10.7	12.2	13.6	9.6	21.5	44.5
	300	(2.4)	(3.3)	(4.1)	(4.8)	(6.3)	(8.5)	(42)	(81)
	400	(0.4)	(0.7)	(1.2)	(1.4)	(2.2)	(5.4)	(81)	(94)
	450	...	(0.3)	(0.6)	(0.8)	(1.5)	...	(130)	(98)
R.R. 59 (L42) (softened) *	20	2.3	4.4	6.7	8.6	14.1	10.9	18.5	40.5
	250	2.1	3.8	4.8	5.4	7.0	9.5	40	71
R.R. 59 (low-Si)	20	12.2	20.8	23.4	25.0	28.7	10.8	14.5	32
	300	2.4	4.4	6.9	8.2	9.7	8.6	> 22.5 ‡	58
	400	0.4	0.7	1.1	1.5	2.2	5.3	112	96
	450	...	0.1	0.7	0.9	1.6	...	228	99
R.R. 77	20	24.5	30.8	34.6	35.6	39.2	10.5	9	11
	100	13.0	23.4	31.4	32.2	37.0	9.8	11	12
	150	10.6	19.2	26.6	27.8	30.3	9.4	15	19.5
	200	7.2	11.0	16.3	17.4	19.3	8.6	21	50
	250	2.5	5.3	7.5	8.2	9.1	8.2	38	73.5
NA23S	20	14.1	15.9	17.8	19.8	29.9	10.3	24	30.5
	250	3.0	7.4	10.1	11.0	12.1	8.8	25	73.5
NA26S	20	13.0	24.2	26.8	28.4	31.2	10.3	13.5	27
	250	3.0	7.0	9.3	10.0	10.7	8.7	27	84
R.A.E. 40C	20	10.4	12.0	13.5	15.8	18.3	11.9	5	7
	300	2.3	3.4	4.9	5.7	7.1	8.3	19	38.5
	400	0.4	0.9	1.5	2.1	3.2	6.8	52	62
	450	...	0.4	0.9	1.3	2.1	...	52.5	64.5



TABLE IIA.—continued.

Material	Test Temperature, ° C.	Limit of Proportionality, tons/in. <sup>2</sup>	0.01% Proof Stress, tons/in. <sup>2</sup>	0.1% Proof Stress, tons/in. <sup>2</sup>	0.5% Proof Stress, tons/in. <sup>2</sup>	Ultimate Tensile Stress, tons/in. <sup>2</sup>	Modulus <i>E</i> , lb./in. <sup>2</sup> × 10 <sup>6</sup>	Elongation on 4√area, %	Reduction of Area, %
R.A.E. 47D	20	6.0	10.4	12.0	13.7	16.5	11.4	8	12.5
	300	1.5	2.0	3.8	4.6	6.1	9.3	37	54
	400	0.7	0.9	1.3	1.7	2.5	6.8	76	73
	450	...	0.3	0.8	1.1	1.9	...	80	80
R.A.E. 55	20	6.5	8.5	10.9	13.3	21.0	11.1	17	27
	250	4.5	6.6	8.0	8.7	10.6	9.5	30	58.5
	300	1.2	2.6	4.0	4.5	6.2	8.8	39	79
	400	0.3	0.6	1.1	1.5	2.5	5.4	65	87
	450	0.2	0.4	0.8	1.0	1.7	5.2	92	93
R.A.E. SA34	20	6.5	17.7	22.3	26.5	29.3	11.8	3.5	4.5
	250	2.7	5.4	8.6	10.0	11.4	10.3	15	32
R.A.E. SA44	20	10.8	20.5	25.3	28.2	30.0	11.5	3	5.5
	250	3.0	5.2	7.7	8.9	10.3	9.5	17	28
R.A.E. SA44 (softened) *	20	2.0	4.0	7.0	10.3	13.8	11.5	11.5	14
	250	1.3	3.2	4.8	5.6	6.8	9.8	37	49.5
Duralumin	20	9.8	13.0	14.4	17.0	27.8	10.4	22	27
	100	6.0	10.4	12.4	14.5	23.8	9.4	25	28.5
	150	4.1	10.2	11.6	13.6	21.0	8.8	27.5	42
	200	2.4	8.0	...	...	17.7	8.7	19.5	55.5
	250	...	5.6	6.9	7.5	8.9	8.6	33	83.5
Y alloy	20	9.0	12.8	14.4	16.5	25.5	10.6	23	23
	300	1.8	3.7	5.1	5.8	7.0	8.6	27	61
	400	...	0.6	0.9	1.3	2.4	...	91	89
	450	...	0.2	0.4	0.7	1.6	...	110	95
Lo-Ex	20	6.1	13.0	19.9	22.0	22.4	12.1	2.5	6
	300	1.0	2.6	3.4	4.1	5.0	8.5	30	44
	400	0.2	0.6	1.0	1.4	2.1	4.6	107	76
	450	...	0.2	0.4	0.7	1.3	...	>110 §	85
Ex 275	20	6.7	14.1	17.9	21.6	26.3	11.2	13.5	18
	250	3.8	8.0	10.0	10.9	12.4	9.3	26	57

\* Softening treatment 10 days at 250° C.

† Values in brackets are for test-pieces from the original batch of R.R. 59 material.

‡ Fracture occurred just inside gauge length : calculated elongation = 26%.

§ Fracture occurred just inside gauge-length : calculated elongation = 134%.

Conversion Factors :

$$1 \text{ ton/in.}^2 = 157.43 \text{ kg./cm.}^2$$

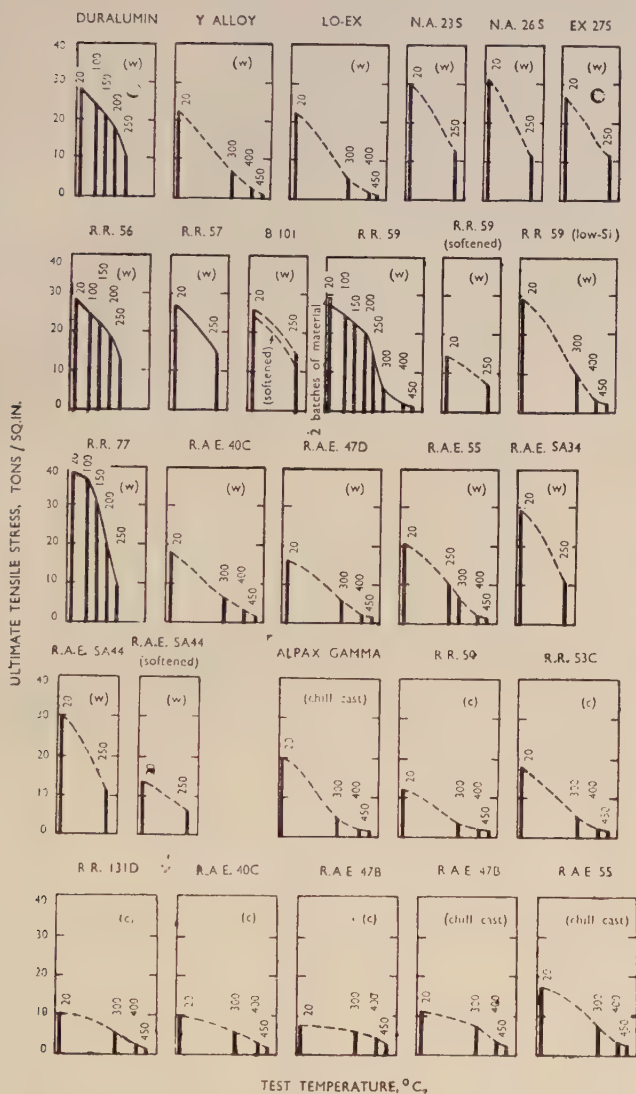
$$1 \text{ lb./in.}^2 = 0.0703 \text{ kg./cm.}^2$$

TABLE IIB.—*Results of Tensile Tests on Cast Alloys at Various Temperatures.*

Alloys are sand cast unless otherwise stated. Rate of Loading : approximately  $\frac{1}{2}$  ton/in.<sup>2</sup>/min. after 0.5% proof load had been reached.

Material	Test Temperature, °C.	Limit of Proportionality, tons/in. <sup>2</sup>	0.01% Proof Stress, tons/in. <sup>2</sup>	0.1% Proof Stress, tons/in. <sup>2</sup>	0.5% Proof Stress, tons/in. <sup>2</sup>	Ultimate Tensile Stress, tons/in. <sup>2</sup>	Modulus E, lb./in. <sup>2</sup> × 10 <sup>6</sup>	Elongation on 4√area, %	Reduction of Area, %
R.R. 50	20	3.6	6.7	9.0	11.0	12.2	10.0	2	2.5
	300	1.8	2.1	2.7	3.1	3.7	6.7	11	17
	400	0.4	0.7	1.1	1.4	1.8	5.4	25	29
	450	0.3	0.5	0.7	0.9	1.5	5.0	35	34
R.R. 53C	20	5.0	12.6	16.0	17.7	17.8	10.1	1	0.5
	300	2.2	3.3	4.1	4.7	5.0	6.5	5	5
	400	0.7	1.1	1.4	1.7	2.2	5.7	22	23
	450	0.2	0.4	0.7	0.9	1.6	5.5	25	29
R.R. 131D	20	3.0	4.6	7.1	8.9	10.3	9.7	2	2.5
	300	1.8	3.0	3.9	4.5	5.3	7.6	4	5
	400	0.6	1.2	1.7	2.0	2.8	6.7	14	17
	450	0.4	0.9	1.3	1.5	1.9	6.0	10	12
R.A.E. 40C	20	2.6	4.7	7.9	...	10.0	11.6	1	<1
	300	1.6	2.8	4.2	5.3	5.6	9.5	1.5	<1
	400	0.6	1.1	1.8	2.4	3.2	8.0	4.5	4.5
	450	0.3	0.9	1.3	1.8	2.4	7.2	6	6.5
R.A.E. 47B	20	2.4	4.1	...	...	7.4	11.4	0.5	<1
	300	1.0	3.0	4.7	6.1	6.2	9.7	0.5	<1
	400	0.6	1.3	2.2	3.0	4.2 <sub>5</sub>	7.2	2.5	2
	450	0.5	1.1	1.8	2.4	3.2 <sub>5</sub>	7.0	4	3
R.A.E. 47B (chill cast)	20	2.6	4.3	7.9	11.5	11.6	11.7	1	1
	300	1.9	3.1	4.4	5.8	7.4	9.2	1.5	2
	400	0.7	1.3	2.0	2.8	3.8	6.4	3	5
	450	0.6	1.1	1.6	2.1	2.8 <sub>5</sub>	5.3	10	20
R.A.E. 55 (chill cast)	20	3.6	9.4	13.6	16.5	17.6	11.2	2	2.5
	300	1.9	3.5	4.6	5.3	7.6	9.7	17.5	10
	400	0.6	1.1	1.6	1.9	3.4	7.0	32.5	49
	450	0.4	0.9	1.3	1.5	2.3 <sub>5</sub>	7.0	32.5	57
Alpax- gamma (chill cast)	20	5.0	11.3	15.6	17.8	20.3	11.1	5	7
	300	1.5	2.5	3.1	3.5	4.5	7.8	35	50
	400	...	0.7	1.1	1.5	2.1	...	66	83
	450	...	0.3	0.5	0.7	1.3	...	89	91

|| Insufficient extension before fracture occurred.



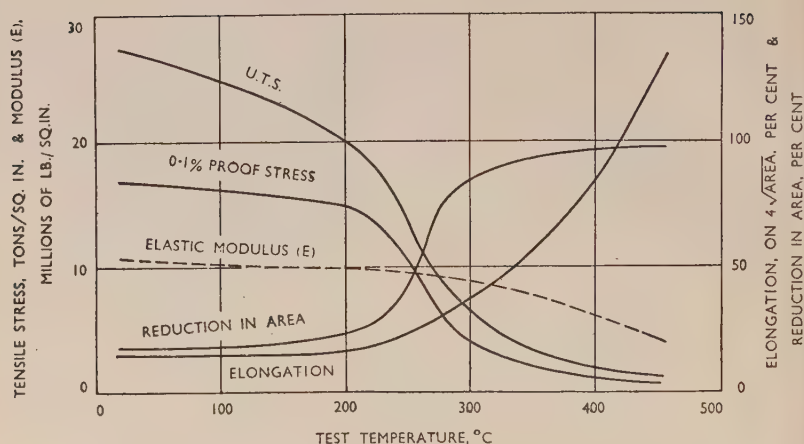


FIG. 2.—Variation in Tensile Properties of Wrought R.R. 59 (L42) with Temperature.

TABLE III.—Comparison Between Tensile Strength of Wrought Aluminium Alloys at 20° and 250° C.

Material	Ultimate Tensile Stress, tons/in. <sup>2</sup>		Ratio B/A
	At 20° C. (A)	At 250° C. (B)	
R.R. 56 . . . . .	28.0	13.5	0.48
R.R. 57 . . . . .	27.3	13.8	0.51
B101 . . . . .	26.1	14.5	0.56
B101 (softened) . . . . .	24.1	12.6	0.52
R.R. 59 . . . . .	27.2	13.6	0.50
R.R. 59 (softened) . . . . .	14.1	7.0	0.50
R.R. 59 (low-Si) . . . . .	28.7	(14.0)	0.49
R.R. 77 . . . . .	39.2	9.1	0.23
NA23S . . . . .	29.9	12.1	0.40
NA26S . . . . .	31.2	10.7	0.34
R.A.E. 40C . . . . .	18.3	(9.0)	0.49
R.A.E. 47D . . . . .	16.5	(8.5)	0.52
R.A.E. 55 . . . . .	21.0	10.6	0.50
R.A.E. SA34 . . . . .	29.3	11.4	0.39
R.A.E. SA44 . . . . .	30.0	10.3	0.34
R.A.E. SA44 (softened) . . . . .	13.8	6.8	0.49
Duralumin . . . . .	27.8	8.9	0.32
Y alloy . . . . .	25.5	(10.0)	0.39
Lo-Ex . . . . .	22.4	(9.5)	0.42
Ex 275 . . . . .	26.3	12.4	0.47

Figures in brackets are values estimated from tests made over the range 20°–300° C.

TABLE IV.—*Alternating Direct-Stress Fatigue Strength of Aluminium Alloys at Various Temperatures.*

Material	Estimated Stress Range for an Endurance of $10^7$ Stress Cycles, tons/in.*						
	Test Temperature						
	20° C.	100° C.	150° C.	200° C.	250° C.	350° C.	450° C.
WROUGHT ALLOYS							
R.R. 56	...	$0 \pm 7.2$	...	$0 \pm 6.1$	$0 \pm 3.9$	...	...
R.R. 57	...	...	...	...	$0 \pm 4.5$	...	...
B101	$0 \pm 8.8$	...	...	...	$0 \pm 4.3$	...	...
(R.R. 59)*	$(0 \pm 10.3)$	...	$(0 \pm 8.0)$	...	$(0 \pm 4.7)$	$(0 \pm 2.6)$	$(0 \pm 1.4)$
R.R. 59	$0 \pm 10.3$	$0 \pm 8.8$	...	$0 \pm 7.0$	$0 \pm 4.5$	...	...
R.R. 59 (low-Si)	$0 \pm 9.8$	...	...	...	...	$0 \pm 2.2$	$0 \pm 1.3$
R.R. 77	...	...	...	$0 \pm 6.9$	...	...	...
NA23S	...	...	...	...	$0 \pm 4.8$	...	...
NA26S	...	...	...	...	$0 \pm 3.7$	...	...
R.A.E. 40C	$0 \pm 8.1$	...	$0 \pm 5.7$	...	$0 \pm 4.5$	$0 \pm 2.5$	$0 \pm 2.1$
R.A.E. 47D	$0 \pm 8.2$	...	$0 \pm 6.4$	...	$0 \pm 4.5$	$0 \pm 2.7$	$0 \pm 1.9$
R.A.E. 55	$0 \pm 5.4$	...	...	...	$0 \pm 4.4$	$0 \pm 2.7$	...
R.A.E. SA34	$0 \pm 10.5$	...	...	...	$0 \pm 3.7$	...	...
R.A.E. SA44	$0 \pm 8.3$	...	...	...	$0 \pm 5.7$	...	...
Duralumin	...	$0 \pm 8.7$	...	$0 \pm 6.8$	...	...	...
Y alloy	$0 \pm 9.0$	...	$0 \pm 7.2$	...	$0 \pm 4.6$	$0 \pm 2.2$	$0 \pm 1.3_s$
Lo-Ex	$0 \pm 9.6$	...	$0 \pm 7.1$	...	$0 \pm 4.5$	$0 \pm 1.9_s$	$0 \pm 1.2_s$
Ex 275	...	...	...	...	$0 \pm 3.8$	...	...
SOFTENED WROUGHT ALLOYS (10 days at 250° C.)							
B101	...	...	...	...	$0 \pm 3.8$	...	...
R.R. 59	...	...	...	...	$0 \pm 3.8$	...	...
R.A.E. SA44	...	...	...	...	$0 \pm 3.8$	...	...
CAST ALLOYS (cc = chill cast, remainder are sand cast)							
R.R. 53C	$0 \pm 2.5$	...	$0 \pm 2.2_s$	...	$0 \pm 2.1_s$	$0 \pm 1.3$	$0 \pm 0.9$
R.R. 131D	...	...	...	...	...	...	$0 \pm 0.9_s$
R.A.E. 40C	$0 \pm 2.6$ (approx.)	...	$0 \pm 2.2_s$	...	$0 \pm 1.7$ (approx.)	$0 \pm 1.8_s$	$0 \pm 1.4_s$
R.A.E. 47B	...	...	...	...	...	...	$0 \pm 1.4$
R.A.E. 47B (cc)	...	...	...	...	...	...	$0 \pm 1.4$
R.A.E. 55 (cc)	$0 \pm 3.9$	...	...	...	...	$0 \pm 1.9$	...
Alpax-Gamma (cc)	...	...	...	...	...	...	$0 \pm 0.9_s$
R.R. 50	$0 \pm 2.0$ to $0 \pm 2.5$	...	$0 \pm 1.9$	...	$0 \pm 1.9$	$0 \pm 1.4$	$0 \pm 1.1$

\* Values in brackets are for the original batch of R.R. 59 material.

## V.—CREEP TESTS.

1. *Comparative Tests at 300° and 400° C.*

In the early stages of the investigation, no comprehensive study of creep properties was attempted, the majority of the tests being confined to 1 ton/in.<sup>2</sup> at 300° C. and 0.5 ton/in.<sup>2</sup> at 400° C., to provide some information on which the creep behaviour of the alloys could be compared. These tests were not continued beyond 400 hr.

A 2-ton-capacity creep machine was used, with a test-piece 0.358 in. in dia. and a gauge-length of 2 in. Two types of extensometer were employed, a micrometer type, sensitive to strains of  $5 \times 10^{-5}$ , and a rhomb-and-mirror type, capable of measuring strains of the order of



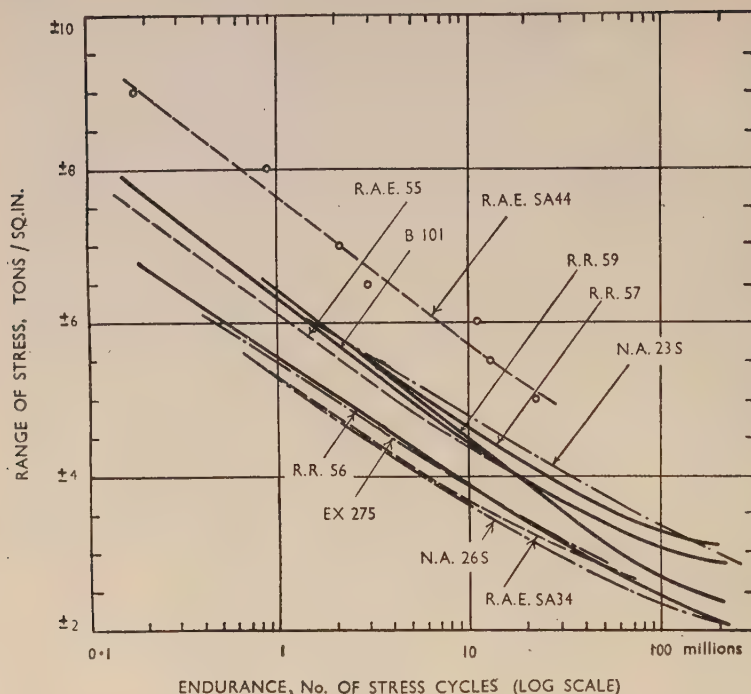


FIG. 3.—Alternating Fatigue Stress-Endurance Curves for Wrought Aluminium Alloys at 250° C. (Zero mean stress.)

Note: For clarity the experimental points have been omitted from the curves, except for R.A.E. SA44.

TABLE V.—*Fluctuating Direct-Stress Fatigue Strength of Wrought Aluminium Alloys at Various Temperatures.*

Material	Estimated Stress Range for an Endurance of $10^7$ Stress Cycles, tons/in. <sup>2</sup>		
	Test Temperature		
	100° C.	200° C.	250° C.
R.R. 56 . . . . .	$6 \pm 7.0$	$6 \pm 5.5$	$3.5 \pm 3.4$
R.R. 57 . . . . .	...	...	$3.5 \pm 4.1$
B101 . . . . .	...	...	$3.5 \pm 3.7$
R.R. 59 . . . . .	$6 \pm 8.2$	$6 \pm 6.5$	$3.5 \pm 3.5$
R.R. 59 (softened) . . . . .	...	...	$3.5 \pm 3.0$
NA23S . . . . .	...	...	$3.5 \pm 4.5$
NA26S . . . . .	...	...	$3.5 \pm 3.4$
R.A.E. SA34 . . . . .	...	...	$3.5 \pm 3.4$
R.A.E. SA44 . . . . .	...	...	$3.5 \pm 3.6$
Duralumin . . . . .	$6 \pm 7.8$	$6 \pm 5.5$	...
Ex 275 . . . . .	...	...	$3.5 \pm 3.8$

TABLE VI.—Comparison Between Alternating and Fluctuating Direct-Stress Fatigue Strength of Wrought Aluminium Alloys at 100°, 200°, and 250° C.

Material	Estimated Stress Range (tons/in. <sup>2</sup> ) for Endurances Indicated.					
	100° C.		200° C.		250° C.	
	A	F	A	F	A	F
10 million cycles						
R.R. 56 . . .	0 ± 7·2	6 ± 7·0	0 ± 6·1	6 ± 5·5	0 ± 3·9	3·5 ± 3·4
R.R. 57 . . .	...	...	...	...	0 ± 4·5	3·5 ± 4·1
B101 . . .	...	...	...	...	0 ± 4·3	3·5 ± 3·7
R.R. 59 . . .	0 ± 8·8	6 ± 8·2	0 ± 7·0	6 ± 6·5	0 ± 4·5	3·5 ± 3·5
R.R. 77 . . .	...	...	0 ± 6·9	...	...	...
NA23S . . .	...	...	...	...	0 ± 4·8	3·5 ± 4·5
NA26S . . .	...	...	...	...	0 ± 3·7	3·5 ± 3·4
R.A.E. SA34 . . .	...	...	...	...	0 ± 3·7	3·5 ± 3·4
R.A.E. SA44 . . .	...	...	...	...	0 ± 5·7	3·5 ± 3·6
Duralumin . . .	0 ± 8·7	6 ± 7·8	0 ± 6·8	6 ± 5·5	...	...
Ex.275 . . .	...	...	...	...	0 ± 3·9	3·5 ± 3·8
Softened alloys :						
B101 . . .	...	...	...	...	0 ± 3·8	...
R.R. 59 . . .	...	...	...	...	0 ± 3·8	3·5 ± 3·0
R.A.E. SA44 . . .	...	...	...	...	0 ± 3·8	...
100 million cycles.						
R.R. 56 . . .	0 ± 5·3	6 ± 5·2	0 ± 4·3	6 ± 4·0	0 ± 2·4	3·5 ± 2·1
R.R. 57 . . .	...	...	...	...	0 ± 3·3	3·5 ± 2·6
B101 . . .	...	...	...	...	0 ± 3·1	3·5 ± 2·3
R.R. 59 . . .	0 ± 7·4	6 ± 5·7	0 ± 5·2	6 ± 4·3	0 ± 2·6	3·5 ± 2·1
R.R. 77 . . .	...	...	0 ± 5·3	...	...	...
NA23S . . .	...	...	...	...	0 ± 3·3	3·5 ± 2·9
NA26S . . .	...	...	...	...	0 ± 2·3	3·5 ± 2·2
R.A.E. SA34 . . .	...	...	...	...	...	...
R.A.E. SA44 . . .	...	...	...	...	...	...
Duralumin . . .	0 ± 6·5	6 ± 6·1	0 ± 4·3	6 ± 3·4	...	...
Ex 275 . . .	...	...	...	...	...	...
200 million cycles.						
R.R. 56 . . .	0 ± 4·7	6 ± 4·7	0 ± 3·7	6 ± 3·6	0 ± 2·1	3·5 ± 1·9
R.R. 57 . . .	...	...	...	...	0 ± 3·1	3·5 ± 2·2
B101 . . .	...	...	...	...	0 ± 2·9	3·5 ± 1·9
R.R. 59 . . .	0 ± 7·2	approx. 6 ± 5·3	0 ± 4·7	6 ± 3·6	0 ± 2·4	3·5 ± 1·9
R.R. 77 . . .	...	...	0 ± 4·8	...	...	...
NA23S . . .	...	...	...	...	0 ± 3·0	3·5 ± 2·6
NA26S . . .	...	...	...	...	0 ± 2·1	3·5 ± 2·0
R.A.E. SA34 . . .	...	...	...	...	...	...
R.A.E. SA44 . . .	...	...	...	...	...	...
Duralumin . . .	0 ± 5·8	6 ± 5·6	0 ± 3·6	6 ± 2·8	...	...
Ex 275 . . .	...	...	...	...	...	...

A = alternating stress,

F = fluctuating stress.

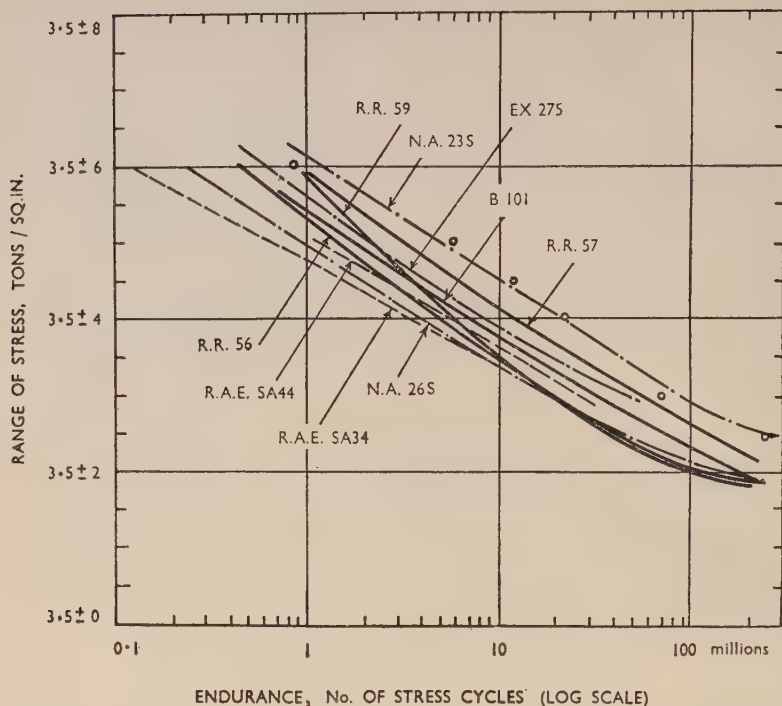


FIG. 4.—Fluctuating Fatigue Stress-Endurance Curves for Wrought Aluminium Alloys at 250° C. (Mean stress = 3.5 tons/in.<sup>2</sup>)

Note: For clarity the experimental points have been omitted from the curves, except for NA23S.

$10^{-5}$ , the former being used for higher creep rates. The temperature of the test-piece was maintained throughout the test within  $\pm 2^{\circ}$  C. of the required temperature.

## 2. Impeller and Compressor Materials and Piston Alloys.

Creep tests were continued for 1000 hr. for the impeller and compressor materials, and 400 hr. for the piston materials, unless fracture had previously occurred. Three of the piston alloys were tested in a fully softened condition.

Larger test-pieces were used, 0.564-in. in dia. and with a 5-in.-gauge-length. The tests were made in machines of 5 tons capacity, in which creep strains of the order of  $10^{-6}$  can be measured by means of a mirror-and-rhomb type extensometer. Each machine was fitted with an electric furnace, in which the test-piece was heated up to the test

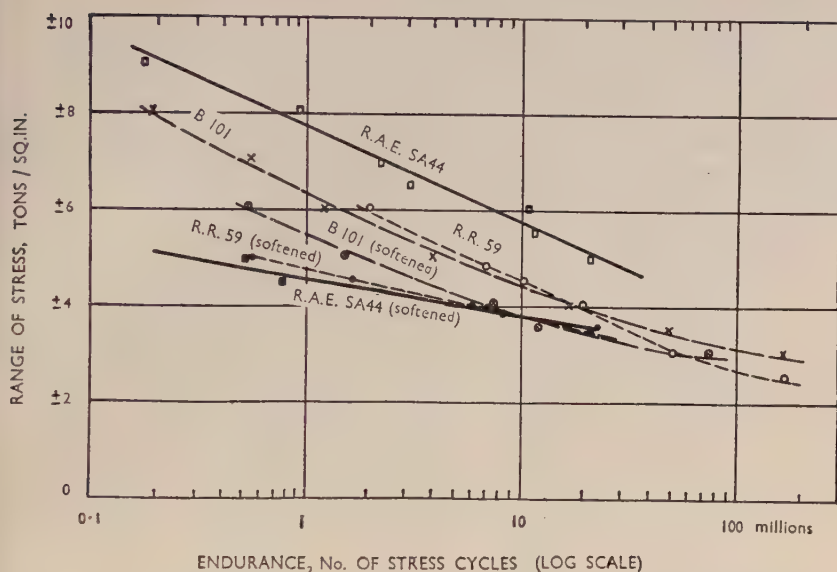


FIG. 5.—Effect of Softening on Fatigue Strength of Three Wrought Aluminium Alloys at 250° C. Alternating fatigue stress-endurance curves.

temperature over a period of about 6 hr. The test-piece was then held at this temperature for a further 18 hr. before the load was applied. The temperature was determined by means of three thermocouples tied to the middle and ends of a 5-in. gauge-length of the test-piece; the variation in temperature along this length did not exceed  $\pm 1^\circ$  C. The test temperatures were maintained constant to within  $\pm \frac{1}{2}^\circ$  C.

The results of tests on wrought and cast alloys at 300° and 400° C. are given in Table VII in the form of creep strains for 100, 200, and 400 hr.

Data for creep tests at 100°, 200°, and 250° C., are set out in Table VIII, and are shown plotted in Figs. 7–10 for temperatures of 200° and 250° C. The results in Table VIII were obtained from creep strain-time curves plotted for various temperatures; from these curves, corresponding stress-log time curves for 0.1–0.5% creep strain were obtained.

Fig. 11 shows the stress-creep strain curves for several of the alloys at 250° C.

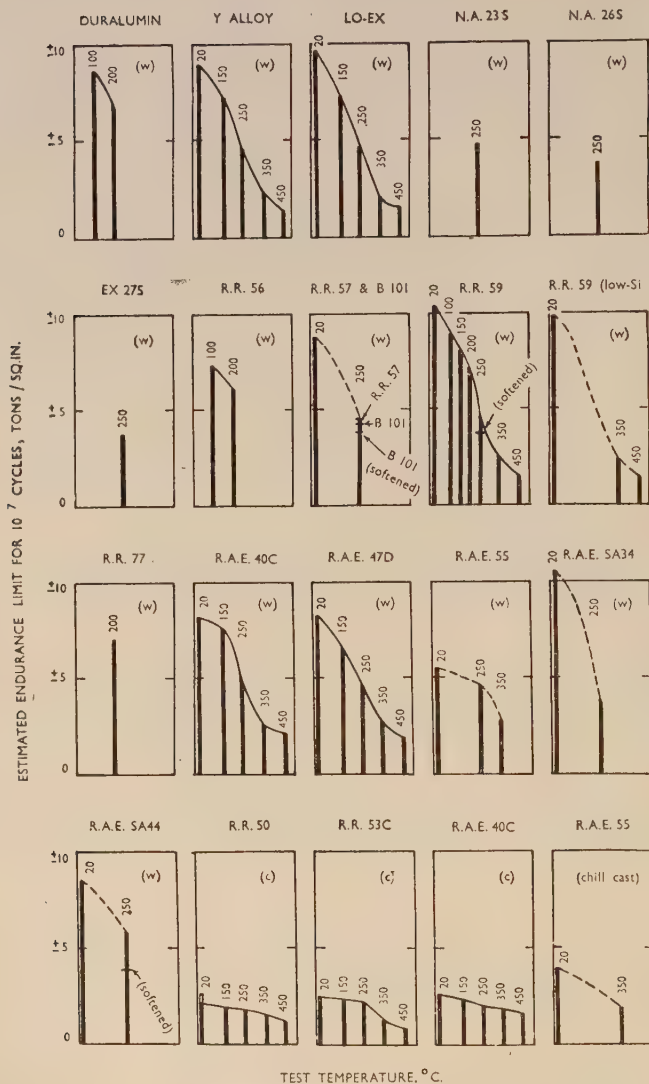


FIG. 6.—Variation in Alternating Fatigue Strength of Aluminium Alloys with Temperature. (Zero mean stress.)

(w = wrought and c = sand-cast alloys)



TABLE VII.—Results of Creep Tests at 300° and 400° C. on Wrought and Cast Aluminium Alloys.

Material	Stress, tons/in. <sup>2</sup>	Creep Strain, %		
		100 hr.	200 hr.	400 hr.
Wrought Alloys at 300° C.				
R.R. 59 . . .	1.0	0.029	0.041	(Discontinued after 300 hr.)
R.R. 59 (low-Si)	1.0	0.087	0.118	0.163
R.A.E. 40C . .	1.4	0.034	0.053	0.078
" . . .	1.0	0.022	0.031	0.036
R.A.E. 47D . .	1.0	0.005	0.005	0.005
R.A.E. 55 . . .	1.0	0.031	0.042	0.052
Y alloy . . .	1.0	0.058	0.098	(0.070% at 1000 hr.)
Lo-Ex . . .	1.0	0.104	0.152	0.190
				...
Cast Alloys at 300° C.				
R.R. 50 * . . .	1.4	0.075	0.140	0.290
" . . .	1.0	0.021	0.035	0.070
R.A.E. 40C * . .	1.0	0.020	0.028	0.040
R.A.E. 55 † . .	1.0	0.018	0.023	0.029
				(0.042% at 1000 hr.)
Wrought Alloys at 400° C.				
R.R. 59 . . .	0.5	Broken 160 hr. (42% elongn. on 2 in.)	...	...
" . . .	0.3	0.260	0.380	0.670
R.R. 59 (low-Si)	0.5	Broken 78 hr. (47½% elongn. on 2 in.)	...	...
R.A.E. 40C . .	1.0	Broken 75 hr. (26% elongn. on 2 in.)	...	...
" . . .	0.7	0.330	0.510	1.080
" . . .	0.5	0.075	0.090	0.115
R.A.E. 47D . .	0.5	0.045	0.060	0.065
R.A.E. 55 . . .	0.5	0.023	0.031	0.040
				(0.052% at 1000 hr.)
Y alloy . . .	0.5	20.7 in 27 hr.	...	...
" . . .	0.3	2.65	3.75	...
Lo-Ex . . .	0.5	4.45 in 70 hr.	...	...
Cast Alloys at 400° C.				
R.R. 50 * . . .	0.5	0.790	3.03	...
" . . .	0.3 <sub>5</sub>	0.160	0.270	0.425
R.A.E. 40C * . .	0.5	0.025	0.045	0.057
R.A.E. 55 † . .	0.5	0.016	0.019	0.021
				(0.023% at 1000 hr.)

\* Sand cast.

† Chill cast.

TABLE VIII.—Stresses for Specific Creep Strains, and for Fracture, in 300 hr. and 1000 hr., for Solution-Treated Wrought Aluminium Alloys at 100°, 200°, and 250° C.

Material	Test Temperature, ° C.	Stress for Creep Strain or Fracture in 300 hr., tons/in. <sup>2</sup>					Stress for Creep Strain or Fracture in 1000 hr., tons/in. <sup>2</sup>						
		0.1%	0.2%	0.3%	0.4%	0.5%	Fracture	0.1%	0.2%	0.3%	0.4%	0.5%	Fracture
R.R. 56	100	...	...	...	...	20	9.6 <sub>5</sub>	7.1	7.8	...	...	8.5	...
	200	7.7	9.0 <sub>5</sub>	4.6	4.7	9.5 <sub>5</sub>	4.9	3.4 E	3.7 <sub>5</sub> E	...	...	4.1	4.2
R.R. 57	250	3.8	4.4	6.3	6.5	4.7 <sub>5</sub>	...	4.6	5.8	3.9	4.0 <sub>5</sub>	6.3	6.6
B101	250	5.2	6.1	4.7	5.0	5.2	...	...	...	6.0	6.2	...	...
B101 (softened)	250	3.9	4.2 <sub>5</sub>	4.1	4.3	4.4	...	...	...	...	...	...	...
R.R. 59	100	...	...	...	...	19	...	...	...	...	...	...	...
	200	7.8	9.6 <sub>5</sub>	...	...	10.1	10.2	6.7	7.5	...	...	8.3	8.7
	250	2.7	3.2	3.5	3.7	3.8	4.2	2.3	2.6	2.7 <sub>5</sub>	2.8	2.8 <sub>5</sub>	3.1 E
R.R. 59 (softened)	250	...	Results very variable					...	...	...	...	...	...
R.R. 77	100	...	...	...	...	26	...	3.2	3.7	...	...	4.0	4.9
	200	3.8	4.4	...	...	5.3	6.3 <sub>5</sub>	...	...	...	...	...	...
NA28S	250	3.9	4.2 <sub>5</sub>	4.4	4.5	4.5 <sub>5</sub>	4.7	...	...	...	...	...	...
NA26S	250	3.0	3.3	3.4 <sub>5</sub>	3.5	3.5 <sub>5</sub>	...	2.8 E	2.9 <sub>5</sub>	3.0 <sub>4</sub>	3.0 <sub>8</sub>	3.1 <sub>2</sub>	...
R.A.E. 55	250	2.8 E	3.1	3.1 <sub>5</sub>	3.2	3.2	3.3 E	...	...	...	...	...	...
R.A.E. SA34	250	3.0	3.1	3.1	3.2	3.3	...	2.9 <sub>5</sub> E	3.0	3.0 <sub>4</sub> E	3.0 <sub>7</sub> E	3.1 E	...
R.A.E. SA44	250	3.0	...	...	...	3.0-3.5	...	...	...	...	...	...	...
R.A.E. SA44 (softened)	250	3.05	3.25	3.3	3.3 <sub>5</sub>	3.4	...	...	...	...	...	...	...
Duralumin	100	...	...	...	...	15	...	...	...	...	...	...	...
	200	6.6 <sub>5</sub>	7.2	...	...	7.6	8.1	5.7	6.2	...	...	6.5	6.9
Ex 275	250	3.2	3.4	3.4 <sub>5</sub>	3.5	3.6	...	2.9 <sub>5</sub> E	3.1 <sub>5</sub>	3.2	3.2	3.2 <sub>5</sub>	...

The stresses in italic type are probable values, the materials supplied being somewhat variable in creep strength at 250° C.  
E = Extrapolated values.

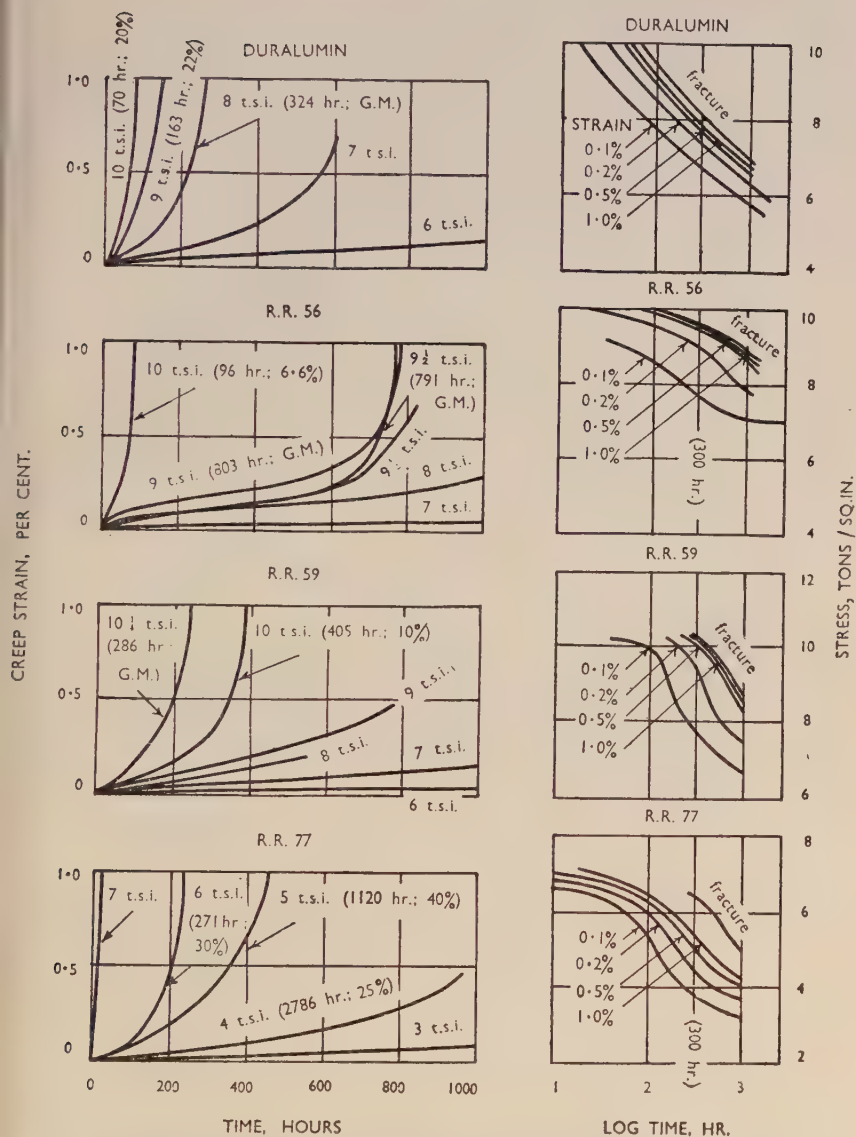


FIG. 7.—Creep Tests at 200° C. on Impeller and Compressor Materials. Time for fracture is given in brackets followed by elongation % at fracture. G.M. = fractured at gauge mark. t.s.i. = tons/in.<sup>2</sup>

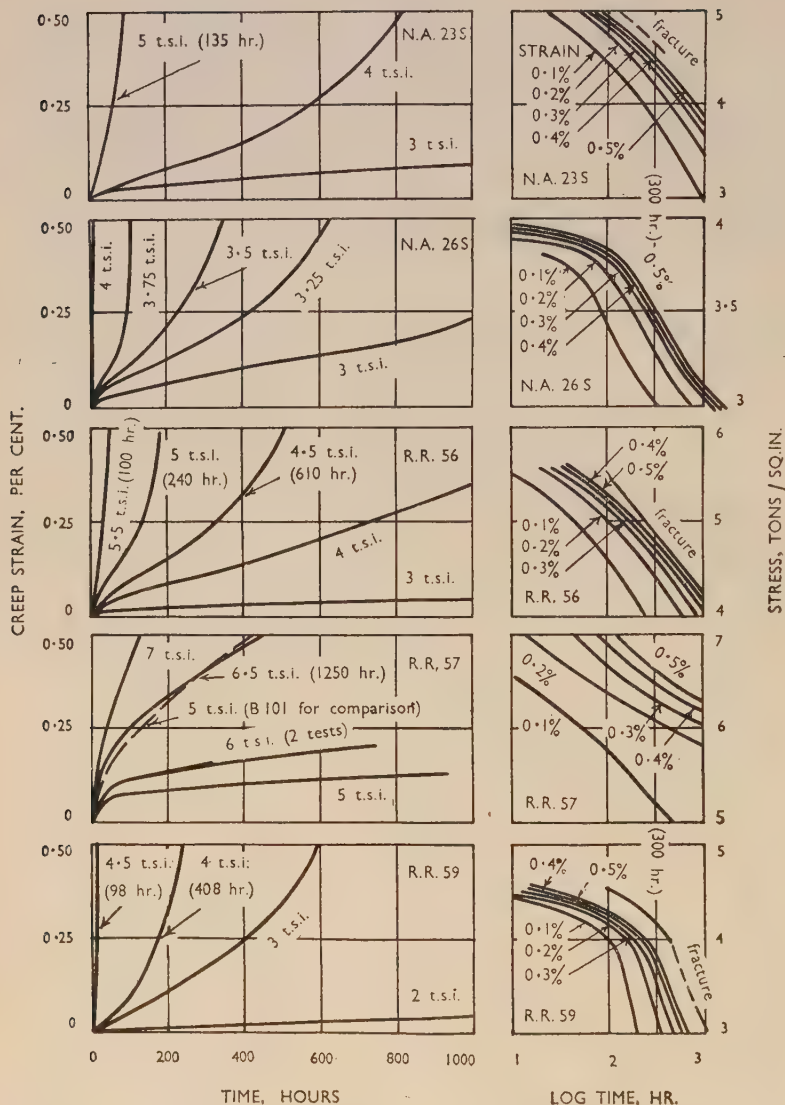


Fig. 8.—Creep Tests at 250° C. on Impeller and Compressor Materials.

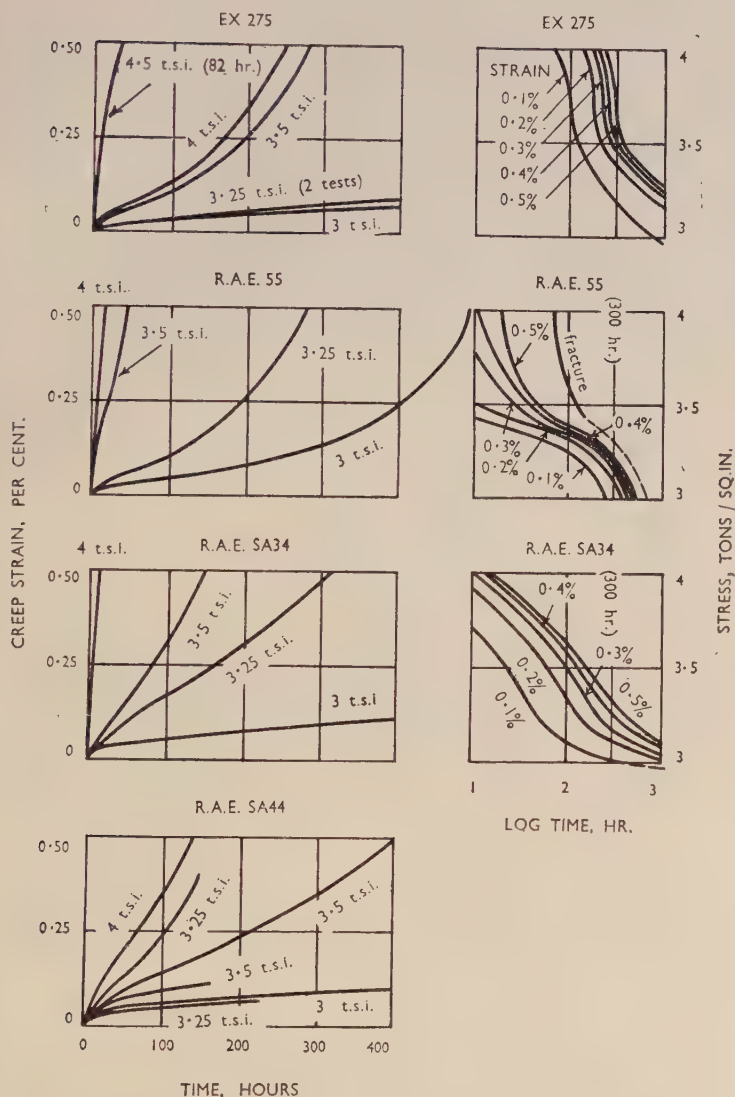


Fig. 9.—Creep Tests at 250° C. on Piston Materials. Owing to inconsistent creep curves for R.A.E. SA44 alloy, no stress-log time curves have been drawn for this alloy.



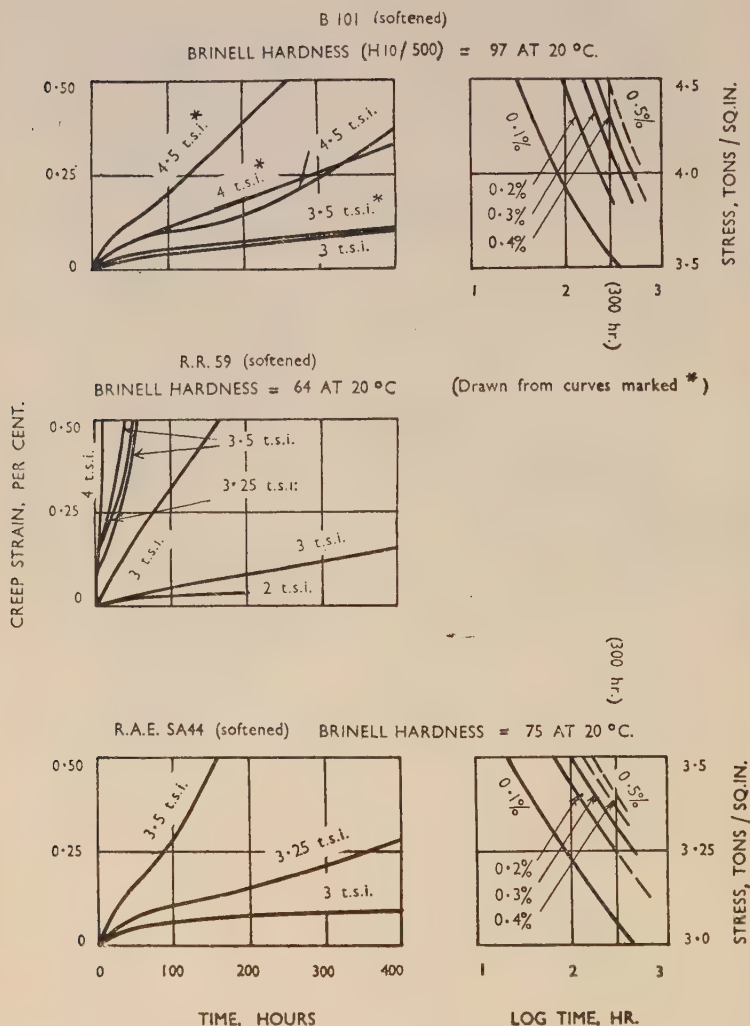


FIG. 10.—Creep Tests at 250° C. on Softened Aluminium Piston Alloys. Owing to inconsistent creep curves for softened R.R. 59 alloy, no stress-log time curves have been drawn for this alloy.

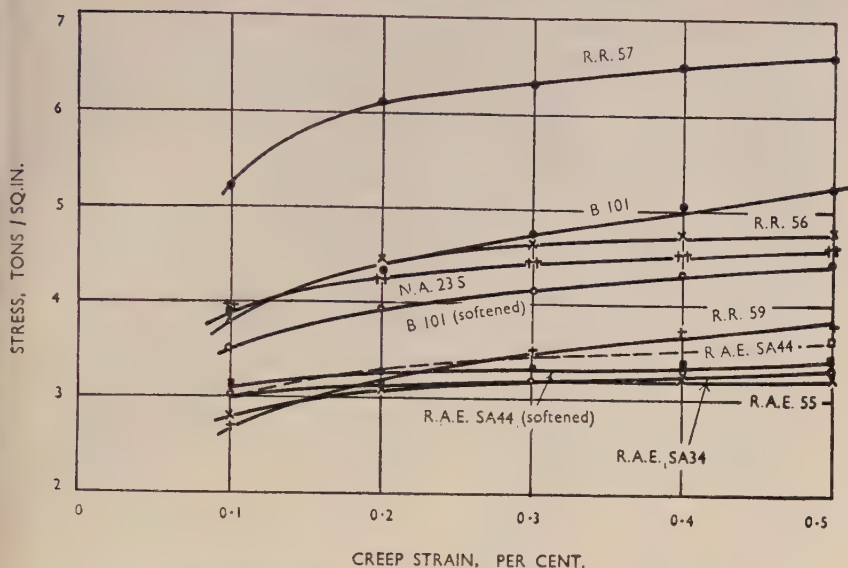


Fig. 11.—Stress-Creep Strain Curves for Wrought Aluminium Alloys held for 300 hr. at 250° C.

## VI.—THERMAL-STRAIN TESTS.

This type of test was used only in the case of some of the earlier cast aluminium alloys, where service failures had occurred in cylinder heads of aero-engines owing to complex stresses induced in the materials by the temperature gradient present. The test is of an empirical nature and was devised to examine the tendency of a cast alloy to crack as a result of the stresses arising from thermal gradients in a water-cooled cylinder block.

The test-piece, which was about 4 in. long with a reduced section at the middle  $\frac{1}{4}$  in. in dia., was inserted in a rigid frame consisting of two steel blocks held apart by steel bolts, as shown in Fig. 12. The ends of the test-piece were screwed into the two steel blocks and clamped with lock nuts. With the test-piece in position, the frame was placed in an electric furnace and the temperature raised to the test temperature in about 3 hr. The frame was then allowed to cool in the furnace to room temperature, the rate of cooling from 400° C. being about 80° C./hr.

It will be seen that the stiffness of the frame relative to the test-piece is such that the latter is forced to accommodate a compressive strain when hot, owing to its coefficient of expansion being about

double that of the steel. Any plastic yielding of the aluminium alloy test-piece occurring during the heating period, which may be expected

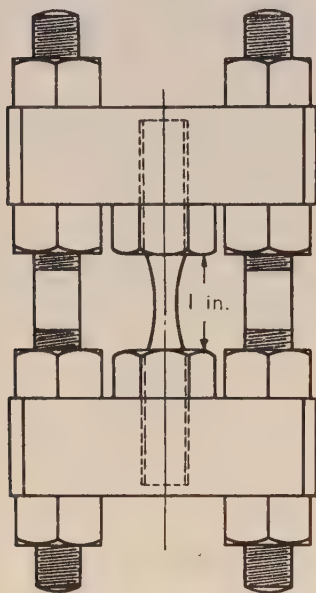


FIG. 12.—Arrangement of Test Apparatus for Thermal-Strain Tests on Aluminium Alloys at Elevated Temperatures.

The curves in Fig. 2 illustrate the variation in tensile properties of R.R. 59 with temperature. The general form of the stress curves shows several distinct trends. From 20° to 200° C. there is a gradual decrease in strength, followed by a rapid drop between 200° and 300° C. As the temperature is further increased to 450° C., the fall in strength gradually diminishes again. The curve for the modulus of elasticity exhibits a gradual fall which becomes more rapid as the temperature is increased.

The tensile values given in Tables II and III, and illustrated in Fig. 1, show clearly that materials with a high strength at room temperature may have a low tensile strength at higher temperatures; this is especially so in the case of R.R. 77. At 250° C., R.R. 56 and R.R. 59 have the highest proof stresses, but they have a slightly lower ultimate strength than either B101 or R.R. 57 at this temperature. In the softened condition, B101 is considerably stronger than either R.R. 59 or R.A.E. SA44 at 250° C.

from its low resistance to creep, will be followed by a corresponding tensile strain on cooling, and this may set up sufficient stress to cause a crack, if the ductility of the material is low. The compressive creep and subsequent tensile stress would be concentrated at the neck of the specimen, and cracking, if any, would be expected to occur there.

After test, the central portion of each test-piece was examined under a microscope. The results of these examinations are shown in Table X.

## VII.—DISCUSSION OF RESULTS.

### 1. *Tensile Properties of Wrought Alloys.*

In the early stages of the investigation, the tensile tests on both wrought and cast alloys were made at 20°, 300°, 400°, and 450° C.; for reasons already stated, later tests were confined to the two temperatures 20° and 250° C.

TABLE IX.—Comparison Between the Tensile, Fatigue, and Creep Strength of Wrought Aluminium Alloys at 250° C.

Material	Ultimate Tensile Stress, tons/in. <sup>2</sup> (A)	Estimated Alternating Fatigue Stress for $4 \times 10^7$ Cycles (300 hr. approx.), tons/in. <sup>2</sup> (B)	Estimated Creep Stress (tons/in. <sup>2</sup> ) for 0.1% and 0.5% Strain in 300 hr.		Ratio B/A	Ratio C/A	Ratio B/C
			0.1% Creep Strain (C)	0.5% Creep Strain			
R.R. 56 . . . . .	13.5	0 ± 3.0	3.8	4.7 <sub>5</sub>	0.22	0.28	0.79
R.R. 57 . . . . .	13.8	0 ± 3.7	5.2	6.6	0.27	0.38	0.71
B101 . . . . .	14.5	0 ± 3.5	3.9	5.2	0.24	0.27	0.90
B101 (softened) *	12.6	0 ± 3.1	3.5	4.4	0.25	0.28	0.89
R.R. 59 . . . . .	13.6	0 ± 3.3	2.7	3.8	0.24	0.20	1.22
R.R. 59 (softened) *	7.0	0 ± 3.1	...	3.0	0.44	...	...
NA23S . . . . .	12.1	0 ± 3.9	3.9	4.5 <sub>5</sub>	0.32	0.32	1.00
NA26S . . . . .	10.7	0 ± 2.8	3.0 <sub>5</sub>	3.5 <sub>5</sub>	0.26	0.29	0.92
R.A.E. 55 . . . . .	10.6	0 ± 3.3	2.8	3.2	0.31	0.26	1.18
R.A.E. SA34 . . . . .	11.4	0 ± 3.1	3.0	3.3	0.27	0.26	1.03
R.A.E. SA44 . . . . .	10.3	0 ± 4.5	3.0	between 3 and 3.5	0.44	0.29	1.50
R.A.E. SA44 (softened) *	6.8	0 ± 3.3	3.0 <sub>5</sub>	3.4	0.49	0.45	1.08
Ex 275 . . . . .	12.4	0 ± 3.1	3.2	3.6	0.25	0.26	0.97

The stresses in italic type are probable values, the materials supplied being somewhat variable in creep strength at 250° C.

\* Softening treatment 10 days at 250° C.

### 2. Tensile Properties of Cast Alloys.

Table II<sub>B</sub> shows the R.A.E. alloys to have relatively high strength values at 400° and 450° C., but, with the exception of alloy 55, they have low ductility at these temperatures. Chill-cast Alpac-Gamma, while possessing the highest tensile strength at room temperature, has the lowest strength at 450° C. None of the cast R.R. alloys has outstanding strength at the higher temperatures.

The limit of proportionality was not always well defined and values for the 0.01%, 0.1%, and 0.5% proof stresses are therefore included in Table II.

### 3. Fatigue Strength.

The alternating fatigue stress results in Table IV indicate an appreciable difference in the fatigue strength of the wrought alloys at room temperature. At 250° C., with the exception of the high value of 5.7 tons/in.<sup>2</sup> for SA44, the remainder of the alloys fall roughly into two groups: those with a fatigue strength of about 4.5 tons/in.<sup>2</sup> and those with about 3.8 tons/in.<sup>2</sup>

The effect of the prolonged softening treatment at 250° C. and

TABLE X.—Results of Thermal-Strain Tests on Cast Aluminium Alloys.

Material	Max. Temp. of Cycle, ° C.	Number of Cycles	Remarks on Examination of Specimen under the Microscope
R.R. 50 :			
Specimen 1 .	400	1	Surface crack observed.
" 2 .	400	12	Surface cracked.
" 3 .	500	1	Surface crack observed.
" 3 .	500	13	Considerable surface cracking.
R.R. 53C :			
Specimen 1 .	300	1	Definite cracks observed.
" 2 .	400	1	No definite cracks observed.
" 2 .	400	2 and 3	Cracking occurred at each cycle. There were a few small blow-holes in the test-piece and cracks showed a tendency to start at these holes.
" 3 .	400	1	Definite cracks observed.
R.A.E. 40C .	400	1, 5, and 12	No cracks observed.
Alpax-Gamma .	300	1	No cracks observed.
(same specimen)	400	4	"
"	500	12	"

subsequent testing at this temperature is to reduce the fatigue strength of each of the three wrought alloys B101, R.R. 59, and SA44 to approximately 3.8 tons/in.<sup>2</sup> Fig. 5, which shows the form of the stress-endurance curves for the three solution-heat-treated and the three softened materials, indicates that after several million reversals of stress, the limiting stress tends to converge to a common value. This suggests that the safest stress to use for design purposes, where the metal is likely to be subjected to prolonged stresses at elevated temperatures, is that obtained from the tests made on the material when softened at the temperature which is likely to occur in service.

The effect of superimposing an alternating stress on a static tensile stress (i.e. fluctuating stress) varies considerably with the material. For instance, considering nine of the wrought alloys tested at 250° C. at an endurance of 10<sup>7</sup> cycles (Table VI), the estimated stress range is reduced by amounts varying from 37% for R.A.E. SA44, to only 3% for Ex 275. It will also be seen from Table VI that the softened alloy R.R. 59 shows a further drop in fatigue strength at 250° C. from  $\pm 3.8$  tons/in.<sup>2</sup> to  $\pm 3.0$  tons/in.<sup>2</sup>, when a mean stress of 3.5 tons/in.<sup>2</sup> is applied.

A further point to be observed is that SA44, which was superior to all the other alloys under alternating stressing, loses this superiority



when a mean stress of 3.5 tons/in.<sup>2</sup> is used at 250° C. The effect of prolonged endurance to 200 million stress cycles is shown in Table VI, and also in Figs. 3 and 4; both types of stress (alternating and fluctuating) show a steady decrease in strength, at a particular temperature, as the endurance is increased.

#### 4. Creep.

Test results on wrought alloys at 300° C. and 1 ton/in.<sup>2</sup> (Table VII) show that the R.A.E. experimental alloy 47D is by far the best (0.005% strain in 200 hr., compared with 0.031% for R.A.E. alloy 40C). R.A.E. 55 and R.R. 59 come next and are closely similar, with 0.042 and 0.041% strain in 200 hr., respectively. Of the cast alloys, R.A.E. 55 is the best, being slightly better than R.A.E. 40C (0.023 and 0.028% strain in 200 hr., respectively). These two alloys were tested in both the wrought and cast conditions, and in both cases the cast material was slightly superior to the wrought.

At 400° C. the R.A.E. alloys 40C, 47D, and 55 are better than the commercial alloys R.R. 59, R.R. 50, and Y alloy, and again the cast alloys are superior to the wrought.

As regards the creep tests on the wrought alloys at lower temperatures, Table VIII gives the stresses for creep strains of 0.1–0.5%, and for fracture in 300 and 1000 hr. for a number of the alloys at 100°, 200°, and 250° C. Results at 100° C. are available for Duralumin, R.R. 56, R.R. 59, and R.R. 77, the stresses for 0.5% strain in 300 hr. being given; R.R. 56 and R.R. 59 are almost identical and somewhat superior to Duralumin.

Values at 200° C. are given for Duralumin, R.R. 56, R.R. 59, and R.R. 77. Again there is very little difference between R.R. 56 and R.R. 59, either at 300 or 1000 hr., the stress for 0.1% strain in 300 hr. being 7.7 tons/in.<sup>2</sup> for R.R. 56 and 7.8 tons/in.<sup>2</sup> for R.R. 59. Duralumin comes next with 6.65 tons/in.<sup>2</sup>, and R.R. 77 gives 3.8 tons/in.<sup>2</sup>

R.R. 77, which exhibited very high tensile strength at room temperature and reasonably high tensile strength at 200° C., was not tested in creep at 250° C. on account of its poor creep-resistance at 200° C.; similarly, no creep tests were made at 250° C. on Duralumin. Comparing the alloys tested at 250° C. it will be seen that R.R. 57 is far superior to any of the others; the stress for a creep strain of 0.1% in 300 hr. being 5.2 tons/in.<sup>2</sup>; the corresponding value for alloys R.R. 56, B101, and NA23S is approximately 4 tons/in.<sup>2</sup> There seems to be very little difference between the other alloys tested; they all give values of about 3 tons/in.<sup>2</sup> for 0.1% strain in 300 hr.

B101, R.R. 59, and SA44 were tested at 250° C. in the fully softened

condition and the creep curves are given in Fig. 10. The sets of curves do not form very good families owing to a lack of uniformity in the materials. In the case of B101, the scatter of results is no worse than in the heat-treated and aged condition, while the softened material is slightly less resistant to creep. It was impossible to obtain consistent results for R.R. 59 in the softened condition, and no estimates are included in Table VIII for the stresses to produce specific creep strains. The three test results for SA44 in the softened condition seem to conform to a family, but are not sufficient to reveal whether or not non-uniformity exists similar to that obtained for the heat-treated and aged material.

Generally speaking, the softened materials are slightly less creep-resistant than the heat-treated and aged materials, but owing to the variation in the results, it is not possible to make a strict comparison. It may be useful to compare the tensile, fatigue, and creep values obtained at a constant temperature of 250° C., and for this purpose Table IX has been included. It will be seen that the fatigue stress is estimated for an endurance of 40 million stress cycles or approximately 300 hr. This endurance corresponds with the period for which the 0.1 and 0.5% creep strains are calculated, thus enabling a direct comparison to be made. The 300-hr. period has also been chosen as a reasonably useful life for a material in service.

The results given in Table IX show that the creep strength is approximately related to the ultimate tensile strength of a material, but that there is apparently no definite relation between either the tensile or the creep strength and the fatigue values obtained in this investigation. As an example, B101 has a high tensile strength and creep-resistance, but does not possess high resistance to alternating fatigue stressing.

### *5. Thermal Strain.*

The results given in Table X show the cast alloy R.R. 53C to be poor in resistance to thermal-strain cracking. It is true that in one test at 400° C. cracking originated at small blow-holes, but even so this material shows a marked tendency to crack under these conditions.

R.R. 50, although possessing higher tensile ductility than R.R. 53C, also cracked in tests at 400° and 500° C. Results for R.A.E. 40C and Alpax-Gamma, which both resist cracking in this test, are interesting, since the former alloy has little ductility, whereas the latter is very ductile at all temperatures (see Table II). It is probable that, owing to its relatively high creep-resistance at 400° C., R.A.E. 40C yields very

little under the compressive stress in this test and consequently the tensile stress on cooling is correspondingly small.

With regard to the more ductile alloy Alpax-Gamma, although appreciable creep probably occurs at 400° C., it no doubt yielded on cooling sufficiently to prevent the development of a tensile stress high enough to cause cracking.

#### VIII.—CONCLUSIONS.

*Tensile Properties.*—Considering the 0.5% proof stress alone, the wrought alloys R.R. 56 and R.R. 59 are superior in tensile strength to the other aluminium alloys tested at 250° C. in the normal heat-treated condition. B101, however, has the highest ultimate tensile stress at this temperature, but exhibits lower proof stresses than the former alloys. Alloy R.R. 57 is not exceptional in tensile strength at this temperature.

In the fully softened condition, B101 is superior to R.R. 59 or SA44 in tensile properties at 250° C.

At the highest temperatures the cast R.A.E. alloys are the strongest of those tested.

*Fatigue Strength.*—With regard to fatigue properties, there appears to be no great difference between the wrought alloys at 250° C., with the exception of R.A.E. SA44, which is superior to the others tested. In the softened condition, B101, R.R. 59, and SA44 all have the same fatigue-resistance at 250° C.; at the highest temperatures, 350° and 450° C., the R.A.E. alloys are stronger than the others. With a mean tensile stress in the fluctuating fatigue stress tests the fatigue range is only slightly reduced relative to the alternating type of stressing.

*Creep Strength.*—R.R. 57 is found to possess the highest creep-resistance at 250° C. of all the wrought alloys tested. It is, however, not exceptional as regards its tensile or fatigue properties. NA23S has good resistance to both creep and fatigue. The R.A.E. alloys are the strongest of those tested at the higher temperatures, the superiority being particularly marked at 400° C.

*Resistance to Thermal Strain.*—The cast alloys R.A.E. 40C and Alpax-Gamma both resist cracking in the thermal-strain test.

#### ACKNOWLEDGEMENTS.

The work described above was carried out in the Engineering Division of The National Physical Laboratory on behalf of the Ministry of Supply. This paper is published by permission of the Director of the Laboratory and with the approval of the Director, Aircraft Research and Development, Ministry of Supply.

The authors acknowledge the advice and encouragement given by Mr. H. J. Tapsell, A.C.G.I., M.I.Mech.E., of the Engineering Division, N.P.L., and the continuous interest shown in the work by Dr. H. Sutton, Deputy-Director, Aircraft Research and Development, Ministry of Supply, during the course of the investigation.

#### APPENDIX.—*Physical Properties of the Alloys.*

For design purposes, mean values of the thermal conductivity, electrical resistivity, and thermal expansion for several of the aluminium alloys used in this investigation are given in Tables XI and XII. (Alloys were all stabilized at 300° C.) These are based on the results of tests made by the Physics Division of the National Physical Laboratory and published separately.<sup>1</sup> Additional data on the physical and mechanical properties of some aluminium alloys have been published in America.<sup>2, 3</sup>

TABLE XI.—*Mean Values of Thermal Conductivity and Electrical Resistivity of Wrought and Cast Aluminium Alloys.*

Temperature, ° C.	Condition of Alloy	Thermal Conductivity, cal. cm./cm. <sup>2</sup> sec. ° C.	Electrical Resistivity, microhm. cm. <sup>2</sup> /cm.
20	Wrought	Range 0.38 (0.31–0.43 <sub>5</sub> )	Range 4.4 (3.5–5.45)
	Cast	0.32 (0.20–0.45)	6.0 (3.8–9.0)
300	Wrought	0.41 (0.36–0.46 <sub>5</sub> )	8.2 (7.0 <sub>5</sub> –9.2)
	Cast	0.35 (0.26 <sub>5</sub> –0.42)	10.5 (7.8 <sub>5</sub> –13.3)

TABLE XII.—*Mean Values of Thermal Expansion of Wrought and Cast Aluminium Alloys.*

Temperature, ° C.	Condition of Alloy	Mean Coefficient of Linear Expansion per ° C.
20–300	Wrought	Range $22.7 \times 10^{-6}$ ( $20.6$ – $25.4 \times 10^{-6}$ )
	Cast	$22.8 \times 10^{-6}$ ( $21.3$ – $24.4 \times 10^{-6}$ )

Mean specific gravity of aluminium alloys = 2.80 (2.76–2.86).

Mean density of aluminium alloys = 0.101 lb./in.<sup>3</sup> (0.100–0.103 lb./in.<sup>3</sup>).

#### REFERENCES.

1. R. W. Powell, M. J. Hickman, and C. R. Barber, *Metallurgia*, 1949, **41**, (241), 15.
2. *U.S. Nat. Bur. Stand. Circ. C 447*, 1943, pp. 22–63.
3. S. L. Hoyt, "Metals and Alloys Data Book", pp. 225–230. New York: 1943.



# THE CALCULATION OF THE ACTIVATION ENERGIES OF RECOVERY AND RECRYSTALLIZATION FROM HARDNESS MEASUREMENTS ON COPPER.\*

By N. THORLEY,† B.Sc., Ph.D., F.Inst.P.

## SYNOPSIS.

The changes which take place in the crystallites of a metal when it is cold worked and then annealed are reviewed, and suggestions are made for observing these changes directly, using X-ray line-broadening measurements, in an investigation of the fundamental processes of annealing.

Cook and Richards's two-stage theory of recrystallization for an isothermal anneal (*J. Inst. Metals*, 1947, **73**, 1) is extended, and a new equation obtained which fits their experimental results for the hardness of copper better than previous equations. It is found that the process followed by hardness measurements is one in which strain release and recrystallization both begin at zero time and proceed simultaneously in different parts of the specimen until annealing is complete.

The experimental results of Cook and Richards on the hardness of copper are analysed in some detail, and a direct method is developed whereby the activation energies of both the recovery and recrystallization processes are obtained separately. The calculated values are of the same order, so that recovery and recrystallization may be the same energetically and in this sense alone the whole anneal could be described as a single-stage process. Physically, there would still be two manifestations of this single activation energy, namely, removal of strain and growth of crystallites from freshly-formed nuclei.

As used at present, the words "recovery" and "recrystallization" are given meanings which often imply that the latter begins in the specimen when the former is complete, whereas the present paper shows that strain release and recrystallization take place simultaneously in the metal. An appeal is therefore made for a complete revision of the nomenclature, and it is hoped that formal definitions of the more common expressions will soon be agreed upon.

## I.—INTRODUCTION.

It has long been known that a cold-worked metal is unstable and will gradually return to its original soft state at any temperature, given sufficient time. This time-period may be millions of years at ordinary or low temperatures, and is actually minutes or even seconds at sufficiently high temperatures. During this softening process there is a corresponding increase in the size of the crystal grains of the metal which can be correlated with the decrease in mechanical strength. In the case of indentation-hardness measurements it is found that there is

\* Manuscript received 9 August 1949.

† Lecturer in Physics, King's College, Newcastle-upon-Tyne.



no appreciable decrease in hardness until new, soft crystals are observed under the microscope, but there are other properties which start to change in the early stages of annealing before the hardness begins to decrease. Among these properties are electrical conductivity and thermo-electromotive force. It is quite obvious, then, that there is some radical change in the condition of the metal, structural or otherwise, which is not necessarily revealed by strength tests. The time-period of an isothermal anneal can therefore be divided into two separate parts, as a result of experimental observation :

(i) a period in which there is a change in some properties but no readily observable change in the microstructure of the metal, or appreciable change in its mechanical properties; and

(ii) a period in which there is a rapid decrease in the strength properties of the metal accompanied by the formation of new crystals, i.e. by observable recrystallization.

The first of these periods has been called "recovery" and the second "recrystallization". A third period, namely that of grain growth, follows the recrystallization period. As has already been pointed out,<sup>1</sup> there is a certain amount of vagueness and confusion in the meaning and interpretation of these terms, due, no doubt, to attempts to give theoretical reasons for this empirical division of the whole annealing cycle.

Since any change in the condition of the metal must be the result of atoms shifting from one position to another, i.e. by the destruction of old lattice planes and the formation of new, it has been suggested that the two processes of recovery and recrystallization are simply different stages in the same fundamental rearrangement process which is motivated by the same energy of activation throughout. This is the one-stage theory as supported by the experiments of Balicki,<sup>2</sup> Brindley,<sup>3</sup> and Varley<sup>4</sup> on various metals. Alternatively, the two processes may be further distinguished by the fact that their activation energies are different. Such a view is held by Cook and Richards<sup>5</sup> for copper, and is referred to as the two-stage theory.

The evidence in support of either of these theories seems to be very conflicting, and it is the object of this paper to stimulate interest in the situation and to attempt to clarify the meanings of the terms "recovery" and "recrystallization", as applied to the annealing process in metals.

## II.—THE STRUCTURE OF A COLD-WORKED METAL.

When a soft metal is cold worked there is a general increase in its strength properties and a corresponding decrease in the size of the

mosaic crystals of the metal. Wood <sup>6</sup> has suggested that there is a lower limit to the size of crystallites so formed—a limit peculiar to the element of the metal—but work by Stokes, Pascoe, and Lipson <sup>7</sup> and by Megaw and Stokes,<sup>8</sup> on filed metals, has shown that lattice distortion, causing small variations in lattice parameters, leads to the same type of X-ray line-broadening as that observed by Wood. It is now believed that for metal filings, at least, lattice distortion makes a greater contribution to line-broadening than do crystallite dimensions. This does not absolutely preclude the possible existence of crystallites of an average dimension of  $10^{-5}$  cm., but it does mean that the X-ray method is not sufficiently sensitive to detect crystallite sizes of this order when the crystallites are severely strained.

A fully cold-worked metal consists of an aggregate of strained crystallites of sizes of the order of  $10^{-4}$  cm. or less, in which some, at least, of the atomic planes are severely distorted, bent, twisted, and irregularly placed relative to each other so that the regular geometry of the lattice, which traces out the unit cell, is lost completely in the highly strained localities. The distribution of the crystallites is not necessarily crystallographically random, but there may be preferred orientation related to the method of cold working.

Even in the individual blocks of the mosaics, which may show almost a perfect lattice, there are atomic misfits in the lattice framework. These are the “atomic dislocations” of Taylor, Orowan, and others which have given rise to so much discussion and mathematical theory. In the region of any dislocation or distortion—in fact anywhere where the atoms have been forced out of their equilibrium positions—there will be local strain and a corresponding increase in the internal energy. If this strain energy is sufficiently high it will break up the crystallites still further. The number of dislocations will depend on the degree of cold work and also on the number of foreign atoms present in the form of impurities. The existence of these dislocations is a very plausible hypothesis, which, although it finds some substantiation as interpreting certain observed properties of metals, suffers from the fact that it cannot be put to a direct experimental test in annealing techniques; the hypothesis of dislocations may be supported by the results of gliding and strength experiments on single crystals, but not by annealing experiments devised to study recovery and recrystallization.

In addition to the individual crystallites there are further important regions where the atomic array is irregular and the lattice parameters are not peculiar to the unit cell of the annealed metal. These are :

- (a) inter-crystallite or inter-grain boundaries, and
- (b) inter-subcrystallite boundaries within the larger crystallites.

These regions can be studied by internal-friction methods, and their properties can be expected to be different from those of the unstrained crystallites themselves. It has been recorded that the melting point of the intergranular region is slightly lower than that of the rest of the lattice, showing that the atoms are more tightly bound within the crystallites when the metal is near the melting point. Also, when a metal is fractured at room temperature it fractures across the metallic grain, so that the intergranular region is the stronger, whereas at temperatures nearer the melting point the fracture takes place between the grains, showing that this region is now the weaker, with its correspondingly lower melting point.

### III.—THE EFFECT OF ANNEALING.

The important feature of the annealing treatment, from the structural point of view, is that the return to the soft state by annealing is not structurally the reciprocal process of the hardening of the metal by cold work. A given large grain of the soft metal is broken up completely by cold work, but the crystallites so produced do not rejoin along the same boundaries to give the same parent grain on annealing. Fresh crystallites are formed, very small at first, by growth around nuclei newly constituted within or between the old crystallites. These new crystallites gradually supersede the old, which therefore lose their entity completely. Hence the annealed metal is structurally different from the original soft metal before it was cold worked, at least in relation to the disposition of the grains relative to one another. Annealing a work-hardened metal gives birth to a new family of crystallites, whose growth into the final grains is the process known as recrystallization.

Before recrystallization begins, some of the strain in the regions where the lattice is warped is gradually removed by the increasing effect of the thermal vibrations with increasing temperature. This "loosening up" of the strained lattice before the onset of recrystallization constitutes the so-called "recovery" process, whereby some atoms which are out of their equilibrium positions are forced back into them by the increased thermal motion. There is very little change in mechanical properties at this stage, and no change in the size, structure, or orientation of the crystallites has been recorded. Since a metal in which the strain has been almost completely removed can still provide nuclei for later recrystallization, and if these nuclei are actually formed in regions of local inhomogeneity, it is evident that the so-called "recovery" process does not mean that all possible types of internal strain are removed, but that some forms of dislocation have a much higher internal energy than others and so remain for nucleation.

At a later stage in the anneal, which is a function of both time and temperature, submicroscopic nuclei are therefore produced. This represents the true onset of recrystallization, which then proceeds and can eventually be observed by several experimental methods. The exact mechanism of the formation of nuclei, by the movements of atomic dislocations, has been the subject of many theoretical papers, but it is sufficient to say here that it bears little relationship to the observed results of annealing. It is, as yet, impossible to predict by means of dislocation theory alone exactly the behaviour of a metal in terms of its physical properties during annealing. For this reason it seems necessary to obtain as much experimental evidence as possible on annealing-sensitive properties before a general theory can be applied.

It is possible that in some metals the release of strain before recrystallization may be accompanied by changes in the average lattice parameters which, although probably quite small, may just be detectable by using the modern X-ray methods<sup>9</sup> which are now capable of giving an accuracy of 1 in 100,000 for a spacing measurement.

#### IV.—EXPERIMENTAL METHODS.

To show experimentally the difference between the two processes just described has always been one of the main difficulties of this work. Changes in mechanical properties are really only indirect effects. The physicist has used the X-ray method of detecting the change in crystal-lite dimensions, since the Debye-Scherrer lines first become "spotty" at about  $10^{-3}$  cm. average crystal size, as the crystallites grow. So far, growth up to  $10^{-3}$  cm. has not been extensively studied during the annealing treatment.

Cook and Richards<sup>5</sup> have plotted the fraction  $x$  of the metal recrystallized, as observed and assessed microscopically, against the diamond pyramid hardness (D.P.H.) of the metal. They find a linear relation of the form :

$$x = \frac{H_0 - H_x}{H_0 - H_1},$$

or, better :

$$x = 0.1 + 0.9 \frac{H_0 - H_x}{H_0 - H_1},$$

where  $H_x$  = hardness when fraction  $x$  is recrystallized,  $H_0$  = maximum initial hardness, and  $H_1$  = final end-point hardness. In their isothermal annealing curves there is a sudden decrease in the hardness which corresponds to  $x = 0$  or 0.1, as the case may be, but this must not be confused with the *true* onset of recrystallization as it shows only that the



crystallites have now grown to the minimum size which will affect the hardness. Also, Cook and Richards have themselves recorded the appearance of new recrystallized metal long before the hardness decreases. Similarly, the first appearance of spots on an X-ray line, the criterion used by Varley,<sup>4</sup> merely indicates that some crystallites have grown to  $10^{-3}$  cm., but gives no information regarding their life previous to this point in the anneal. Since the recrystallized metal is soft, it is assumed that all the newly-formed crystallites are soft, but this is not necessarily so, since the methods hitherto used to detect these changes have never isolated a single crystallite for individual study.

The true onset of recrystallization, the possible division in time and temperature of the two periods, when the crystallites are of the order of  $10^{-5}$  cm. or less, cannot possibly be detected by these methods. Any measurement of a property after observable recrystallization measures the combined effect of the new, soft crystals and the old, harder and strained crystallites. Hardness itself cannot be simply and wholly concerned with the new recrystallized material and cannot therefore offer a highly accurate measure of the amount of such material present. Indentation methods cannot be used without introducing further strain, and the same argument applies to determinations of ultimate tensile strength. These methods must therefore be regarded as indirect, and this fact should be borne in mind when deductions of the properties of the actual crystals are made from them.

If, in a severely cold-worked metal, the crystallites are of the order of  $10^{-4}$  cm. or less, the new crystallites formed within or between them during annealing must be smaller still and so cannot give "spots" on the Debye-Scherrer lines until they have grown larger than the parent crystals. It would seem better to investigate such changes fundamentally rather than to rely on secondary effects. If X-ray line-broadening is studied carefully, the lines should first sharpen as the initial strains are removed, then, as small, new, strain-free crystallites are formed, a second broadening should follow. This will occur only in the absence of strain-distortion broadening in the region being studied, and if the crystallites are less than  $10^{-4}$  cm. in size. There is already some evidence of this given in the paper by Megaw and Stokes.<sup>8</sup> As the new material supersedes the old and the crystallites grow, the lines should sharpen again and finally become "spotty" at about  $10^{-3}$  cm. It should be noted that the appearance of spots on the photograph is the last effect to be observed, not the first, and so cannot indicate the true onset of recrystallization.

So far, X-ray methods have been used incidentally as a guide to structural changes in many investigations dealing primarily with



technological aspects of annealing. These investigations have yielded valuable results, but until the phenomena of recovery and recrystallization are specifically studied by X-ray methods, and not in conjunction with a study of commercial annealing, it is felt that the whole situation will remain comparatively obscure. It would also be worth while to devise apparatus to measure the changes in X-ray line breadths *during* annealing rather than on specimens quenched from the annealing temperature.

### V.—THEORY.

The relevant theory has already been discussed at length,<sup>3, 5</sup> so that it is unnecessary to reproduce it in detail here. If  $x$  is the fraction of the metal recrystallized after annealing time  $t$ , there are two possible ways of relating  $x$  to  $t$ , depending on whether recovery and recrystallization have the same or different activation energies. For the one-stage theory (hereafter referred to simply as I) the following equation is obtained :

$$\ln \frac{1}{1-x} = At \exp. \left( -\frac{B}{RT} \right) \quad . \quad . \quad . \quad (1)$$

whereas, for the two-stage theory (hereafter referred to as II), the corresponding equation is :

$$\ln \frac{1}{1-x} = Ct^2 \exp. \left( -\frac{D}{RT} \right) \quad . \quad . \quad . \quad (2)$$

where  $A$ ,  $B$ ,  $C$ , and  $D$  are constants, independent of time, and the other symbols have their usual meanings.

Equation (1) was given by Krupkowski and Balicki,<sup>2</sup> but (2) is preferred by Cook and Richards, who show that it gives a curve more nearly parallel to the observed isothermal annealing curves than (1). A simple test to differentiate between equations (1) and (2) is to plot  $\log \ln \frac{1}{1-x}$  against  $\log t$  for an isothermal anneal, since the slopes of the curves so obtained from (1) and (2) are unity and two, respectively. This criterion has been used by Brindley.<sup>3</sup>

It has already been pointed out that a direct and accurate measurement of  $x$  is almost impossible, but if any property  $X$  can be correlated with  $x$  so that  $X = X_0(1-x)$  the two formulæ become :

$$\ln \frac{X_0}{X} = k_1 t \text{ for I,}$$

and

$$\ln \frac{X_0}{X} = k_2 t^2 \text{ for II,}$$

where  $k_1$  and  $k_2$  are temperature-dependent constants. Hence, the

first and obvious curves to plot are  $\ln X_0/X$  against  $t$  and  $t^2$ , to see which relation is linear.

In Cook and Richards's development of II it is assumed that, if  $w$  is the fraction of the metal remaining unrecovered after time  $t$ , then  $w = \exp.(-\beta t)$  and, to a first approximation, the fully recovered material is  $\beta t$ , where  $\beta$  is a temperature-dependent constant and  $\beta t$  is small. It is this approximation which gives the  $t^2$  term in equation (2). Now if this approximation is due solely to small values of  $t$ , it is automatically assumed that the recovery period is small compared with the full annealing time and is therefore complete in the early stages of the recrystallization process. Put in another way, it means that on Cook and Richards's assumptions theory II, and hence equation (2), is only true when  $\beta t$  is small,  $1 - w$  is small, and  $w$  is large, *not* small as stated by Brindley. Since the amount of recovered material must inevitably become large, it seems that the approximation is valid only very early in the anneal and not for its full duration. Indeed, as will be shown later,  $1/\beta$  is of the order of the incubation period  $t_L$ , and since the approximation can only be valid for  $\beta t \sim 0.1$  then it only holds for  $t \sim 0.1t_L$ , which is about one-fiftieth of the whole annealing period. Therefore, equation (2) cannot hold when there is an observable change in  $X$  or  $x$ , and if  $\ln \frac{1}{1-x}$  is linear with  $t^2$  experimentally, it is due to some cause other than the approximation  $\exp.(-\beta t) = 1 - \beta t$  for  $\beta t$  small.

Following Cook and Richards:

$$\frac{dx}{dt} = a(1-x)(1-w) \exp.\left(-\frac{Q}{RT}\right),$$

$$w = \exp.(-\beta t), \beta = b \exp.\left(-\frac{P}{RT}\right)$$

where  $a$  and  $b$  are constants independent of time, and  $P$  and  $Q$  are the activation energies of the recovery and recrystallization processes respectively.

Writing  $A = a \exp.\left(-\frac{Q}{RT}\right)$ :

$$\begin{aligned} \frac{dx}{dt} &= A(1-x)(1-w) \\ &= A(1-x)\{1 - \exp.(-\beta t)\} \end{aligned}$$

$$\therefore \frac{dx}{1-x} = A\{1 - \exp.(-\beta t)\}dt$$

Integrating,  $\ln \frac{1}{1-x} = A\left\{t + \frac{1}{\beta} \exp.(-\beta t)\right\} + \text{constant.}$

Since at  $t = 0$ ,  $x = 0$ , this equation becomes

$$\ln \frac{1}{1-x} = A \left\{ t + \frac{1}{\beta} [\exp. (-\beta t) - 1] \right\} \quad (3)$$

which contains no approximations for  $\beta t$ . If  $t$  is very small in equation (3), so that  $\exp. (-\beta t) \rightarrow 1 - \beta t$ , then  $x = 0$  and there will therefore be a short initial period for which the amount of recrystallized material is almost zero and the rate of increase of  $x$  is small. For large values of  $t$ ,  $\exp. (-\beta t) \rightarrow 0$ , and (3) becomes :

$$\ln \frac{1}{1-x} = A(t - t_0) \quad (4)$$

where  $t_0 = \frac{1}{\beta}$ .

Equation (3) thus predicts :

(i) a short initial period in which  $x$  increases very slowly and

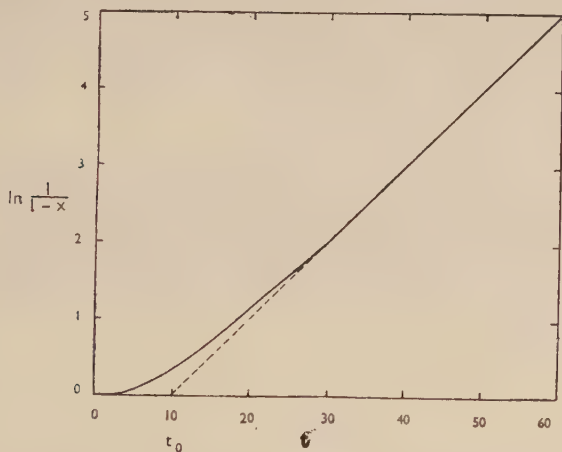


FIG. 1.—Curve calculated from equation (3) for  $A = 0.1$  and  $\beta = 0.1$ .

$\ln \frac{1}{1-x}$  is almost zero, i.e. an incubation period ; and (ii) a later period in which  $\ln \frac{1}{1-x}$  is linear with  $t$ , as in equation (4), and the rate of growth of the crystals is higher than in (i).

Both  $A$  and  $t_0$  will depend on the temperature and condition of the metal, but the general shape of the  $\ln \frac{1}{1-x}$ ,  $t$  curve will be as shown in Fig. 1.

*Calculation of Activation Energies P and Q.*

From the linear part of the  $\ln \frac{1}{1-x}$ ,  $t$  curve, given by equation (4), both  $A$  and  $t_0$  can be found. Now since  $A = a \exp.\left(-\frac{Q}{RT}\right)$  it will depend on recrystallization only, and

$$\ln A = \ln a - \frac{Q}{RT}.$$

Similarly,  $\beta = b \exp.\left(-\frac{P}{RT}\right)$  depends on recovery only, and

$$\ln \beta = \ln b - \frac{P}{RT}$$

or

$$\ln t_0 = \frac{P}{RT} - \ln b.$$

Hence, if equation (3) is true, the curves of  $\ln A$  and  $\ln t_0$  against  $1/T$ , for various annealing temperatures  $T$ , should be linear, and their slopes should yield  $P$  and  $Q$ . The importance of this is that the activation energies are thereby derived separately, and not added together as in Cook and Richards's treatment.

## VI.—ANALYSIS OF PREVIOUS EXPERIMENTAL RESULTS.

Brindley<sup>3</sup> has measured the thermo-electromotive force  $E$  of samples of cold-rolled copper against a standard annealed copper strip. He finds that the experimental isochronal annealing curves can be calculated by means of an equation such as (1), and that the isothermal curves of Brandsma<sup>10</sup> gave a slope of almost unity when  $\log \ln \frac{E_0}{E}$  was plotted against  $\log t$ . Brindley therefore concludes that the decrease of  $E$  with increasing temperature is a single-stage process throughout. It is the opinion of Richards,<sup>11</sup> however, that the effect could be attributed to the non-contribution of the small "islands" of recrystallized metal to  $E$ , and hence is due to recovery only. Brindley calculates  $P = 21,600$  cal. from Brandsma's measurements and 11,500 cal. from his own.

Cook and Richards<sup>5</sup> have measured the variation of diamond-pyramid hardness of copper sheets with time, in an isothermal anneal, having shown that the D.P.H. number is a linear function of the degree of recrystallization as judged by microscopic examination. They find  $H_x = H_0(1-x) + xH_1$ , where  $H_0$  is the initial maximum hardness, and  $H_1$  is the final "end" hardness corresponding to complete re-

crystallization of the whole specimen. No figures are given for the actual sizes of the crystallites while  $x$  is increasing.

Following the argument of Section V  $\ln \frac{1}{1-x}$  is plotted against  $t$  and  $t^2$ , using Cook and Richards's empirical correlation equation:

$$x = 0.1 + 0.9 \frac{H_0 - H_x}{H_0 - H_1} \quad . \quad . \quad . \quad . \quad . \quad (5)$$

to find  $\ln \frac{1}{1-x}$ . Calculated values of  $\ln \frac{1}{1-x}$  are plotted against  $t$  and  $t^2$  in Figs. 2 and 3, for specimens A4 and B4 which have undergone

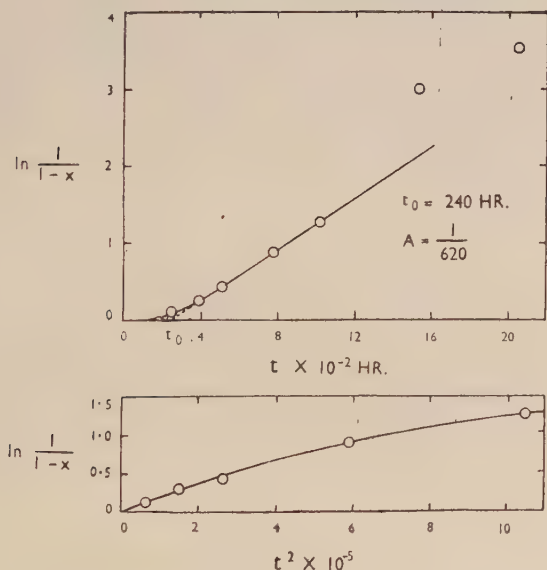


FIG. 2.—Experimental curves for specimen A4 annealed at 27° C.

97.5% reduction, the hardness figures for 27° C. being taken from Table V in Cook and Richards's paper.<sup>5</sup> In the  $t$  curves there is an unmistakable resemblance to Fig. 1 as deduced from equation (3). Also it is found that  $t_0 \sim t_L$ , the incubation period. In the  $t^2$  curve there is an initial linear part which passes through the origin, as required by equation (2), but the linearity extends far beyond the time period for which  $\beta t$  can be reckoned as small. Hence, it does not follow that because  $\ln \frac{1}{1-x}$  is fairly linear with  $t^2$  Cook and Richards's analysis is correct.



The constants  $A$  and  $\beta$  can be obtained from the slope and intercept of the  $\ln \frac{1}{1-x}$ ,  $t$  curve, and using these values in equation (3) values of  $x$  can be calculated for any assumed value of  $t$ . Equation (5) then gives the calculated value of  $H_x$  at any time, and so the calculated  $H_x$ ,  $t$  curve can be compared with the observed isothermal curve. This comparison is made in Figs. 4 and 5, from which it is seen that the agreement is fairly good.

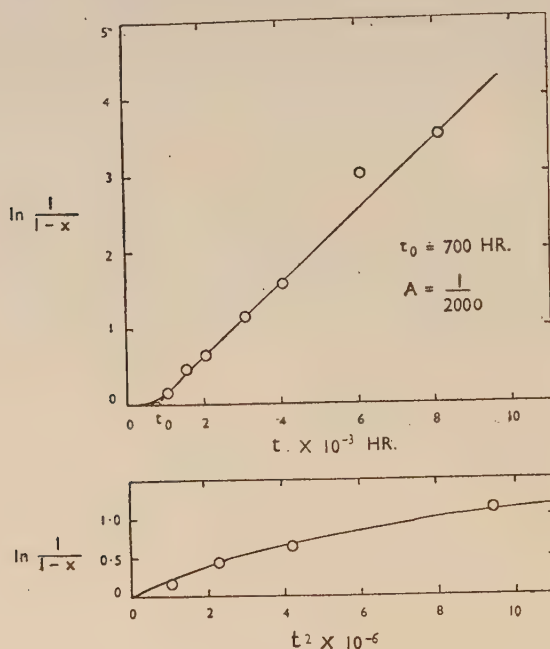


FIG. 3.—Experimental curves for specimen B4 annealed at 27° C.

In order to compare the validity of an equation of the form  $\ln \frac{1}{1-x} = Kt^2$ ,  $K$  must first be calculated from the experimental curve. From this it is then possible to calculate  $x$  and  $H_x$  for any given value of  $t$ . This has been done for two values of  $K$ , one for a small value of  $t$  and the other for a larger value, and the curves are compared with the experimental curves in Figs. 4 and 5. The first value of  $K$  gives general agreement for the initial stages of the anneal, but deviates seriously at the higher values of  $t$ , the deviation increasing with  $t$ . The second value of  $K$  gives less agreement. This brings out the weak-

ness in an equation such as (2), for which  $C$  should be independent of time.

It has been indicated in Section V that the activation energies  $P$  and  $Q$  are obtainable from graphs of  $\ln A$  and  $\ln t_0$  against  $1/T$ , which

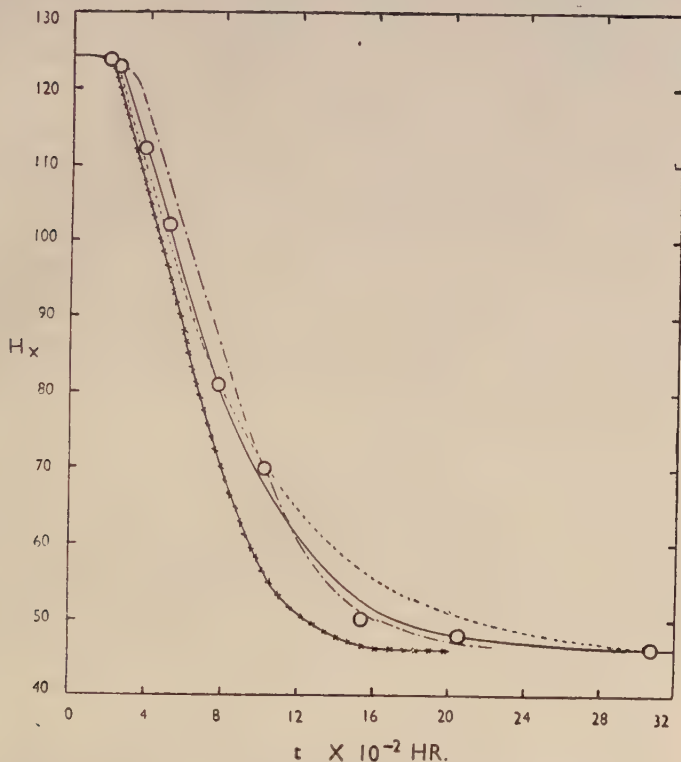
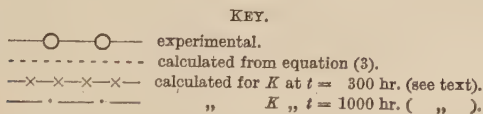


FIG. 4.—Relation between D.P.H. values  $H_x$  and time, for specimen A4 annealed at  $27^\circ\text{C}$ .



should both be linear. Fig. 6 shows the curves obtained for sample A4, and the linearity of these curves justifies equations (3) and (4) and the deductions made from them. The slopes of these curves give  $P = 21,600$  cal. and  $Q = 19,500$  cal., showing that the activation energies of the two processes are nearly equal. This may explain why

there has been so much controversy about the single- and double-stage theories of recovery and recrystallization. However, the importance of the present method lies in the fact that  $P$  and  $Q$  can now be obtained separately.

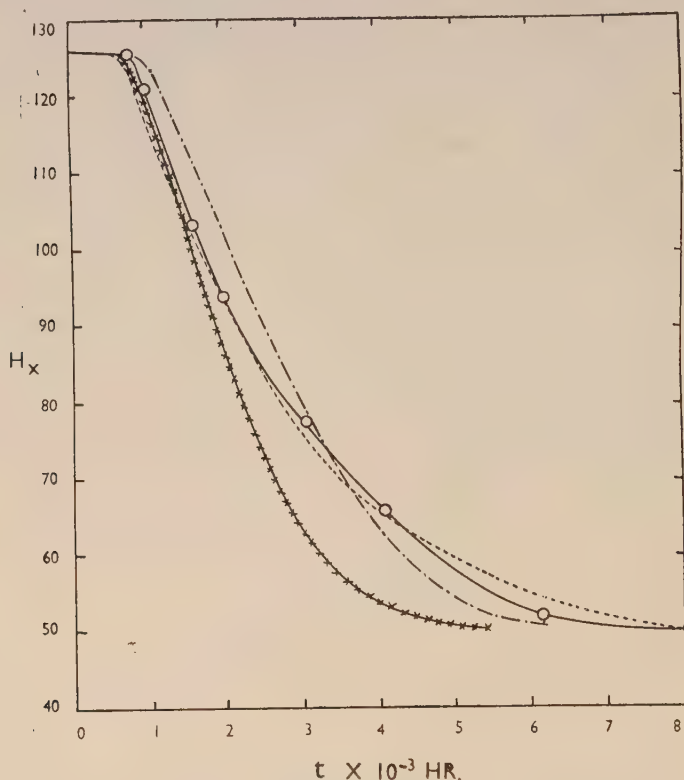


FIG. 5.—Relation between D.P.H. values  $H_x$  and time, for specimen B4 annealed at 27° C.

KEY.  
 —○—○— experimental.  
 - - - - - calculated from equation (3).  
 —x—x—x—x— calculated for  $K$  at  $t = 1000$  hr. (see text).  
 — · — · — · — calculated for  $K$  at  $t = 3000$  hr. ( " " ).

Cook and Richards plot log half-softening times against  $1/T$  to obtain  $(P + Q)$ . It may now be seen that this gives a straight line only because the point selected is on the linear portion of the  $\ln \frac{1}{1-x}, t$  curve, and  $P \sim Q$ , so that  $\exp. (P - Q)/RT \sim 1$ . Thus all Cook and

Richards's results for  $(P + Q)$  are really approximate values of  $2Q$  from which  $Q$  can be deduced.

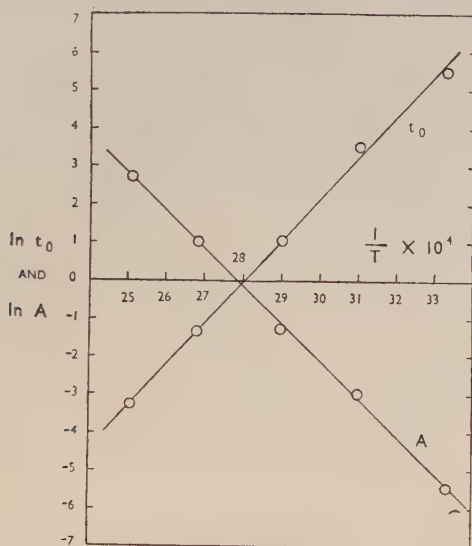


FIG. 6.—Graphs showing linearity between  $\ln t_0$  and  $\ln A$  and  $1/T$  for specimen A4.

From slopes,  $P = 21,600$ ,  $Q = 19,500$  cal./mol.

The results obtained from all Cook and Richards's measurements on copper are collected in Table I, and it is interesting to note that there is good agreement with Brandsma's results and with Cook and

TABLE I.—Activation Energies Calculated from Cook and Richards's <sup>5</sup> Measurements on the Hardness of Copper.

Specimen	Recovery $P$ , cal./mol.	Recrystallization $Q$ , cal./mol.	Cook and Richards' Values of $\frac{1}{2}(P+Q)$ , cal./mol.
A2	20,000	24,400	22,200
B2	24,800	23,200	24,000
A3	22,400	22,800	22,300
B3	22,400	20,800	23,300
A4	21,600	19,500	21,900
B4	23,200	21,200	23,400
A5	21,600	18,000	21,000
B5	21,600	19,200	22,200

Richards's values of  $\frac{1}{2}(P + Q)$ . This confirms Richards's suggestion that the thermo-electromotive force responds only to recovery (strain-

release) and not to recrystallization and growth of crystallites, and that this property follows a single-stage process of annealing.

*Direct Use of Hardness Figures.*

It has already been suggested that a direct plot of  $\ln \frac{H_0}{H_x}$  against  $t$  and  $t^2$  might be instructive as a comparison with the corresponding

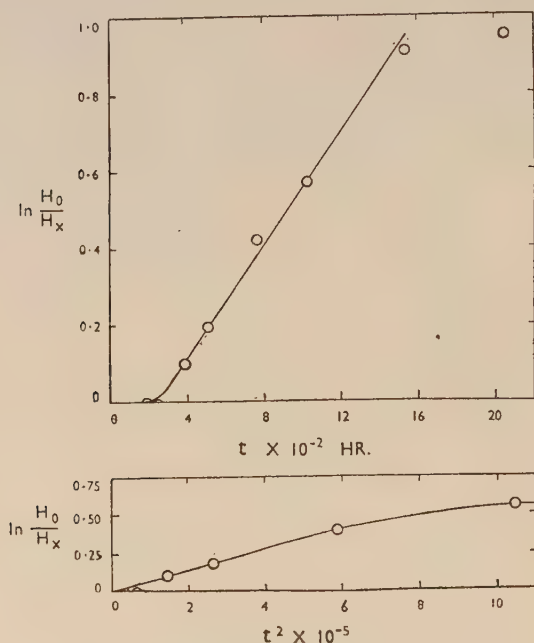


FIG. 7.—Relation between  $\ln H_0/H_x$  and time for specimen A4 annealed at 27° C. Compare Fig. 2.

$\ln \frac{1}{1-x}$  plots. This has been done in Fig. 7 for specimen A4 at 27° C., and there is an obvious similarity between these curves and the corresponding  $\ln \frac{1}{1-x}$  curves for this specimen (see Fig. 2).

Following the previous treatment the slope and intercept of the curve gives  $A$  and  $\beta$  in the equation corresponding to (3), viz.:

$$\ln \frac{H_0}{H_x} = A \left\{ t + \frac{1}{\beta} [\exp. (-\beta t) - 1] \right\} \quad . \quad . \quad (6)$$

By plotting  $\ln A$  and  $\ln t_0$ , where  $t_0 = 1/\beta$ , against  $1/T$  as before, the



activation energies can be obtained. This is shown in Fig. 8 for specimen A4, and the values obtained are  $P = 20,800$  cal. and  $Q = 19,900$  cal., agreeing fairly well with those obtained for the same specimen from the  $\ln \frac{1}{1-x}, t$  curves. It seems, from this agreement, that while the overall correlation between  $H_x$  and  $x$  may be as in equation (5), the hardness responds to changing  $x$ , in the steep part of the annealing curves at any rate, as though  $H_x = H_0(1 - x)$ .

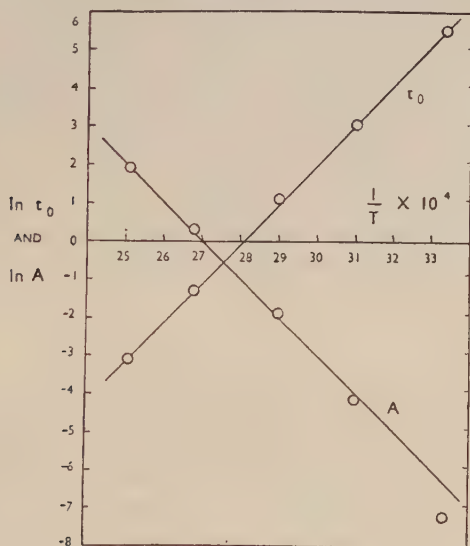


Fig. 8.—Graphs showing linearity between  $\ln t_0$  and  $\ln A$  and  $1/T$ , where  $A$  and  $t_0$  are calculated directly from  $H_x$ , for specimen A4.

From slopes,  $P = 20,800$ ,  $Q = 19,900$  cal./mol.

It is not necessary, therefore, to calculate degrees of recrystallization in order to estimate the activation energies, since it is experimentally true that over the part of the annealing curves where  $H_x$  decreases rapidly, the equation connecting  $H_x$  and  $t$  is of the form :

$$\ln \frac{H_0}{H_x} = \text{const.} (t - t_0).$$

This is true irrespective of any theoretical consideration, and the majority of the curves show this linearity quite well.

### The Incubation Period.

The incubation period may be defined as the initial stage of the anneal when there is no observable change in the property being

measured. From the theoretical equations (1) and (2) there is no true incubation period for  $x$ , but such a period is observed for  $H_x$ . This may be the result of:

(i) A very slow rate of recrystallization at the beginning of the anneal, increasing later; and/or

(ii) a very slow response of  $H_x$  to changes in strain and crystallite growth when the crystallites are very small.

Equation (3) is the only equation which predicts an incubation period for  $x$ .

For higher-temperature anneals the incubation period, which is of the order of  $t_0$ , is always very short, as can be deduced from the  $\ln t_0, 1/T$  curves. Even as low as  $100^\circ$  C. the incubation period is only about 15 min., and at  $150^\circ$  C. it is less than 30 sec. It is not surprising, therefore, that an incubation period has not been observed by Anderson and Mehl<sup>12</sup> for aluminium with 90% deformation at  $325^\circ$  C., or by Varley<sup>4</sup> for aluminium with about 75% deformation at temperatures above  $200^\circ$  C., although Anderson and Mehl observe an incubation period for aluminium with low deformation.

## VII.—DISCUSSION.

A full analysis of Cook and Richards's results for the hardness of cold-rolled copper supports the theory that strain-release (recovery) and recrystallization take place simultaneously throughout the whole period of the anneal, each starting at zero time. Recrystallization starts immediately in the regions where the strain is already sufficiently low. The evidence supporting this is provided by the determination of  $P$  and  $Q$  separately by a less arbitrary method than has previously been possible, and the agreement between the theoretical and experimental  $H_x, t$  curves. On no account can a formula of the type (I) (see p. 147) be made to fit the experimental facts. It must be emphasized, however, that these remarks apply only to the hardness of copper rolled in a special way, and need not be taken as universally applicable. Further and more extensive experimental work is required to test the main theories to see whether one of them is predominantly true.

Suggestions have been made for following the changes during annealing by the measurement of X-ray line breadths. It is considered that this is the most fundamental approach to the problem, and work is continuing on these lines.

In an isochronal anneal, or in any process in which the temperature is a variable, the temperature at which the recrystallized metal is first observed has been called the recrystallization temperature, and it is

always pointed out that this temperature depends on so many variables that it cannot be rigidly defined. Since, in any case, the true recrystallization temperature, corresponding to the true onset of recrystallization when the first nuclei are just formed, can never be observed and may be at zero time, it might be better to avoid the use of this term altogether or to use it only when describing works or plant processes of fabrication where the term may have a technically important meaning. Its use in describing physical changes on an atomic scale should be discouraged.

If the term "recovery" is used to mean the initial release of strain before the formation of new crystallites at any time in any particular region, the following points arise :

(i) Does recovery take place *fully* in small regions before recrystallization nuclei can be formed? If so, are these regions or patches separate in time and space? If they are separate in space the profile of the X-ray lines should alter slightly with the position of the beam relative to the specimen. If they are separate in time, the profile of the X-ray lines from the same part of the specimen should alter with time. Micro-beam methods will probably be required here.

(ii) Does "rate of recrystallization" mean rate of formation of nuclei, rate of growth of crystallites after formation, or rate of increase of volume of new material? In these experiments it seems to mean the last.

(iii) Do the two processes of recovery and recrystallization start together at zero time and proceed simultaneously until the recovery of the whole specimen is complete, leaving recrystallization to proceed alone, or do the two processes proceed simultaneously throughout the whole time of annealing, or are the two processes completely separate in time?

(iv) Assuming that both processes take place by the movements of atoms in or across the lattice planes, are they therefore two different results of the same single process energized throughout by the same activation energy, or are they different processes with separate and distinct activation energies?

Obviously, these points are all interrelated and need careful consideration before a clear picture of the annealing process on an atomic scale can be given. The present paper suggests that where the hardness of copper is taken as the measure of degree of recrystallization the two processes start at zero time and proceed simultaneously until the anneal is complete, i.e. the whole of the metal specimen is not fully recovered until it is also fully recrystallized. Considering individual micro-

regions of the metal, this means that in some regions the strain is so low that recrystallization can commence immediately at zero time, whereas in others partial recovery precedes the onset of recrystallization. The net rate of recrystallization is therefore low at first and increases rapidly as the anneal proceeds.

From the point of view of the specimen as a whole there is no evidence that recovery takes place uniformly throughout the metal until it is complete, after which recrystallization begins at favourable places, and if it does take place in patches the metal contained in such a patch need not necessarily be fully recovered, i.e. completely strain-free, before recrystallization of the patch can begin. There may be levels of strain energy, and recrystallization may start at any one of them, depending on the local conditions. In a recovering patch, for example, there may be micro-regions only a few lattice parameters in diameter which are fully recovered, and neighbouring micro-regions in the same patch which are only partially recovered to different degrees. Once a nucleus of recrystallization has been formed in such a micro-region, it grows by capturing neighbouring micro-regions as soon as they have sufficiently recovered.

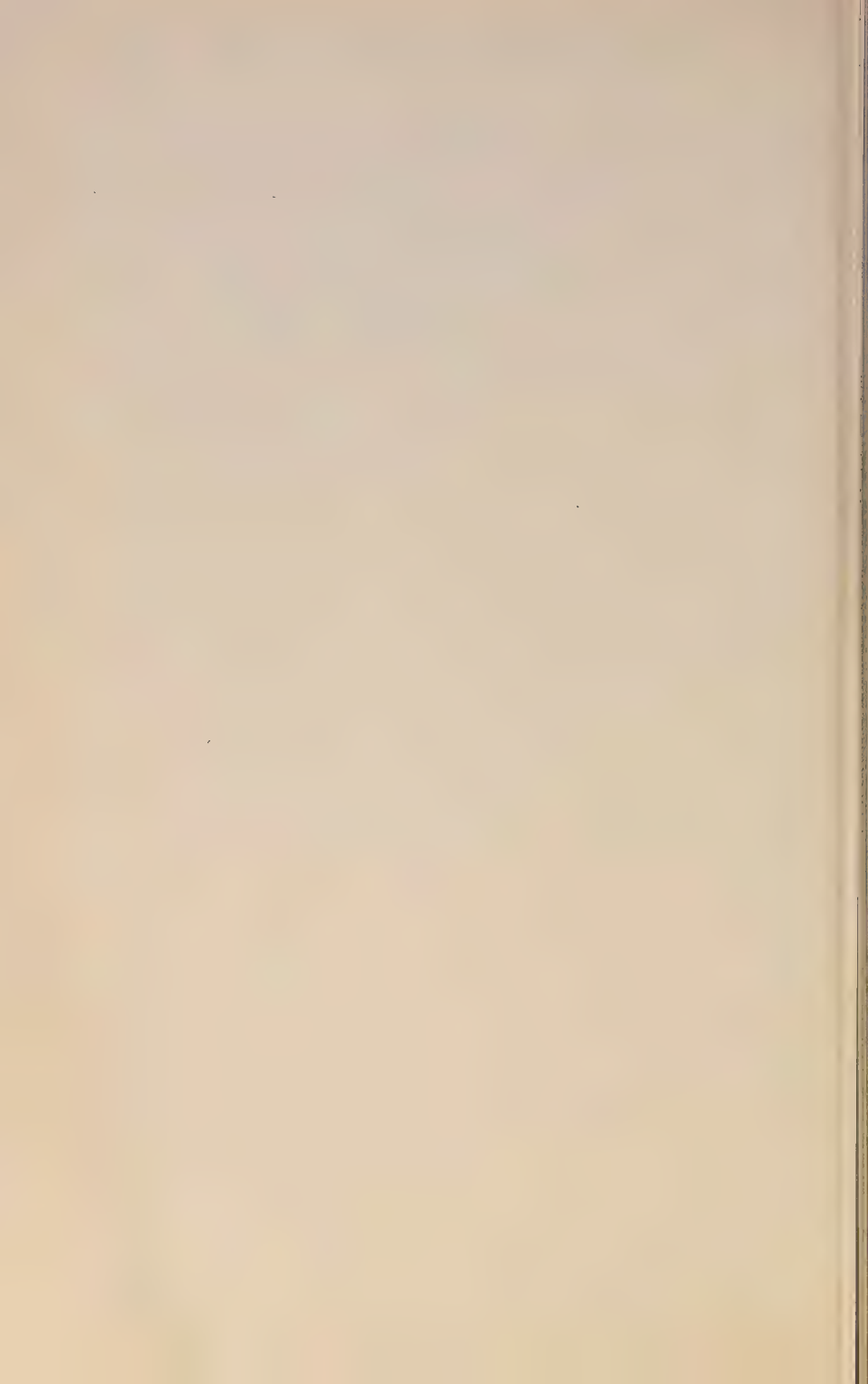
If the term recovery is to retain its present meaning, i.e. the change which may take place in a property of the metal during the initial stages of the anneal and before recrystallization is observed, further terms are required to describe the release of strain in an individual region which immediately precedes the formation of a recrystallization nucleus in that region, and also for the complete process whereby any original property is eventually regained after the specimen has been cold worked. Recrystallization would then mean the changes which take place in the structural properties of the metallic crystallites themselves while the physical property of the specimen as a whole is being regained.

The desirability of a theory of recrystallization which is comprehensive and applicable to all metals in all conditions, and the need for a clear understanding of the processes involved, shows that the whole problem requires careful consideration based on correctly designed experiments before any further pronouncements can be made. It is hoped that the present paper will arouse more academic interest in the fundamentals of annealing techniques, that the nomenclature will be thoroughly revised, and that strict and formal definitions of the commoner terms will be agreed upon.

REFERENCES.

1. N. Thorley, *J. Inst. Metals*, 1948-49, **75**, 1038 (discussion).
2. M. Balicki, *J. Iron Steel Inst.*, 1945, **151**, 181 p.  
M. Balicki, *J. Inst. Metals*, 1947, **73**, 705 (discussion).  
A. Krupkowski and M. Balicki, *Ann. Acad. Sci. Tech. Varsovie*, 1937, **4**, 270.
3. G. W. Brindley, *Phys. Soc. : Rep. Conf. on Strength of Solids*, 1948, 95.
4. P. C. Varley, *J. Inst. Metals*, 1948-49, **75**, 185.
5. M. Cook and T. Ll. Richards, *J. Inst. Metals*, 1947, **73**, 1.
6. W. A. Wood, *Proc. Roy. Soc.*, 1939, [A], **172**, 231.  
W. A. Wood and W. A. Rachinger, *J. Inst. Metals*, 1948-49, **75**, 571.
7. A. R. Stokes, K. J. Pascoe, and H. Lipson, *Nature*, 1943, **151**, 137.
8. H. D. Megaw and A. R. Stokes, *J. Inst. Metals*, 1945, **71**, 279.
9. D. E. Thomas, *J. Sci. Instruments*, 1948, **25**, 440.
10. W. F. Brandsma, *Z. Physik*, 1928, **48**, 703.
11. T. Ll. Richards, *Phys. Soc. : Rep. Conf. on Strength of Solids*, 1948, 105 (discussion).
12. W. A. Anderson and R. F. Mehl, *Trans. Amer. Inst. Min. Met. Eng.*, 1945, **161**, 140.





# THE CONSTITUTION OF MAGNESIUM-RICH ALLOYS OF MAGNESIUM AND ZIRCONIUM.\* 1246

By G. A. MELLOR,† M.Sc., F.I.M., MEMBER.

(Communication from the National Physical Laboratory.)

## SYNOPSIS.

An investigation into the constitution of magnesium-zirconium alloys containing up to 0.7% zirconium is described. During the experimental work true equilibrium conditions were difficult to establish owing to: (1) the high vapour pressure of magnesium, (2) the chemical activity of zirconium, and (3) the presence of inclusions.

It was found that the liquidus rises 1.5° C. from the melting point of pure magnesium at 649° C. to a peritectic horizontal. From a peritectic point at approximately 0.5% zirconium the liquidus rises steeply, passing through 800° C. at 0.6% zirconium and 900° C. at 0.67% zirconium. The solid solubility appears to be about 0.3% at 300° C., 0.4–0.5% at 400° C., and over 0.6% at 500° and 600° C.

## I.—INTRODUCTION.

FOR more than a decade it has been known that small amounts of zirconium confer useful properties on certain magnesium alloys, but it is only as a result of patient research that satisfactory methods of production have been developed.<sup>1</sup> The difficulties met with in making sound and usable alloys have also been encountered in attempts to determine the constitution, and little work has consequently been published.

Nowotny, Wormnes, and Mohrnhelm<sup>2</sup> claimed to have made up alloys with 0.99.4% zirconium, but their zirconium was stated to contain 3% of metallic impurities and 9% of oxide, so that their conclusions may be open to doubt. Other investigators, British and American, have not been able to introduce more than about 0.7% zirconium into magnesium, and this is now considered to be the upper limit. In an alloy of higher zirconium content compounds of zirconium with elements other than magnesium may be present, or zirconium particles may be held in a mechanical mixture with magnesium, but such is not considered a true alloy. Nowotny, Wormnes, and Mohrnhelm<sup>2</sup> gave the limits of solubility at the magnesium end of the diagram as 0.8% at 700° C. and 0.3% at 300° C., and they postulated a compound  $Mg_2Zr$ . Sauerwald<sup>3,4</sup> produced a diagram of the magnesium-rich end of the system showing a peritectic at a temperature slightly higher

\* Manuscript received 12 September 1949.

† Metallurgy Division, National Physical Laboratory, Teddington, Middlesex.

than the melting point of pure magnesium, a steeply mounting liquidus, and a solid solubility rising to 4.52% zirconium at 645° C. In arriving at a figure of 4.52% Sauerwald assumed that the zirconium soluble in hydrochloric acid was identical with the zirconium soluble in magnesium. It has since been found that in a magnesium-zirconium alloy some of the zirconium not in solution in magnesium is nevertheless dissolved in hydrochloric acid, so that Sauerwald's figure of 4.52% is almost certainly too high. Beck,<sup>5</sup> quoting his own and Siebel's unpublished results, gave the peritectic point as 0.26% zirconium and the solid solubility as not less than 0.8% at 500° C. and less than 0.1% at 400° C. Siebel<sup>6</sup> has since published figures for the solubility of zirconium in molten magnesium, and these are discussed below.

It seemed probable, therefore, that there was a peritectic in the system very close to the magnesium end of the diagram, that there was a limited solubility in the solid state, and that the liquidus rose steeply from the peritectic point. It was decided to test the truth of these hypotheses and, if possible, to obtain an accurate estimation of the position of the liquidus, peritectic line, and of the limit of solid solubility.

## II.—PREPARATION OF ALLOYS.

Two batches of magnesium were used, and their chemical analyses are given in Table I.

TABLE I.—*Chemical Analysis of Magnesium.*

	Si, %	Fe, %	Mn, %	Ni, %	Cu, %	Al, %	Zn, %
Batch 1	0.004	0.01	0.005	trace	nil	nil	n.d.
Batch 2	0.0035	0.0052	0.0037	<0.0004	0.0004	0.013	0.0056

The high vapour pressure of magnesium and its inflammability are complicating factors in all melting and casting operations. When attempts are made to add zirconium other problems arise, namely :

(1) Hydrogen is normally present in magnesium alloys and, according to Busk and Bobalek,<sup>7</sup> may amount to as much as 50% by volume. Such hydrogen, and hydrogen from other sources, readily combines with zirconium to form a hydride insoluble in magnesium. Sauerwald<sup>8</sup> reported that the zirconium content of a magnesium-zirconium alloy was reduced from 0.63 to 0.04% on treating with hydrogen at 750°–780° C. for  $\frac{1}{2}$  hr. A similar reduction was found to take place at 600° C. in the present work.

(2) Zirconium forms other insoluble compounds with oxygen, nitrogen, carbon, iron, aluminium, and silicon, as described by Kroll

and Schlechten.<sup>9</sup> Contamination by these elements must therefore be reduced to a minimum.

(3) Any retention in the alloy of particles of insoluble compounds of zirconium or of soluble salts used in alloying leads to a fictitiously high zirconium content as determined by chemical analysis. A comprehensive study of the types of non-metallic inclusions and insoluble zirconium-rich particles which can occur in magnesium-zirconium alloys has been made by Emley.<sup>10</sup>

The first method of alloy preparation tried in the present investigation was the addition of pure anhydrous double fluoride of zirconium and potassium prepared in the laboratory to molten magnesium contained in an iron crucible. The reaction was violent and the temperature of the melt was not easily controlled. Chemical analyses of the resulting alloys showed varying amounts of zirconium and the microstructures generally revealed inclusions. Attempts to make up alloys by pressing and sintering powders of magnesium and zirconium were not successful, and no evidence of diffusion was found. The addition of zirconium powder to the molten magnesium was likewise unsuccessful.

Some degree of success was achieved by using a method, developed by Magnesium Elektron, Ltd.,<sup>11</sup> of adding in lump form 12% of the dry double chloride of zirconium and sodium to magnesium at 760°–800° C. A number of alloys containing about 0.6% zirconium were made in this way and were used in attempts to determine the liquidus, the peritectic horizontal, and the solid solubility of zirconium in magnesium. No alloy could be relied upon, however, to be completely free from flux.

An attempt was made to enrich an alloy containing 0.57% zirconium by distilling off some of the magnesium. The alloy was placed in a closed steel tube evacuated to about 0.1 mm. of mercury and held at 700° C. for 5 hr. Magnesium condensed in the cooler part of the tube and the residue at the bottom was an alloy containing 0.73% zirconium, which was large enough in amount for thermal analysis but not for other experiments. In addition, a sponge-like residue was found which was identified as pure zirconium by X-ray examination. This suggests that zirconium in equilibrium with magnesium exists as pure zirconium and not as a compound. There has been no indication in the present work of the compound  $Mg_2Zr$ , which confirms the finding of Emley.<sup>10</sup>

After the investigation had been begun Magnesium Elektron, Ltd., developed the "chloride-master-alloy" process of adding zirconium to magnesium. The "master alloy", consisting of a mixture of magnesium, zirconium, and dense flux, is brought to a semi-

molten state in an iron crucible at about 600° C. Solid magnesium is added, with more dense flux for protection, and the temperature is raised to 780°–820° C. After stirring with an iron rod for 1 min. the charge is allowed to stand for 5 min. in this temperature range and is then ready for casting. The most important feature of this process is that the “master alloy” at the bottom of the crucible acts as a reservoir of active zirconium and any loss of zirconium due to the formation of insoluble compounds is made good. The dense flux cleans the metal and the resulting alloy is free from inclusions and contains 0.6% zirconium. After consultation with Magnesium Elektron, Ltd., this method was adopted for the latter part of the work, and spectrographic examination showed that no detectable impurities were introduced from the flux or the “master alloy”.

### III.—EXPERIMENTAL RESULTS.

#### 1. *The Peritectic.*

An alloy containing 0.73% zirconium was used for thermal analysis and arrests were determined from two heating and two cooling curves. The alloy showed arrests at an average temperature of 650.5° C. compared with 649° C. for the melting point of pure magnesium, indicating a small but significant rise to a peritectic. The fact that it has not been found possible to make up alloys containing more than about 0.7% zirconium would suggest that there is a very limited solubility of zirconium in molten magnesium in the temperature range 650°–800° C. The higher temperature of arrests found by means of thermal curves in zirconium-containing alloys is therefore much more likely to be due to a rise of the liquidus to a peritectic point than to the gradual rise occurring in a system where there is a wide range of solubility.

#### 2. *The Liquidus.*

A 0.6–0.7% zirconium alloy would contain such a small proportion of solid zirconium at temperatures above the peritectic horizontal that no arrest would be observed in passing through the liquidus. It was therefore necessary to find some method of determining the liquidus other than by thermal analysis.

The use of a closed pressure vessel seemed a promising method, in that it would eliminate volatilization and burning and obviate the necessity for flux. Cylinders of the alloys were machined to fit mild-steel pressure vessels with welded lids. Such “bombs” were held at temperatures of 700° and 800° C. for 24 hr., a time estimated to be sufficiently long for the excess zirconium to settle. For higher temperatures, graphite linings were at first used in order to avoid con-



tamination by iron, but as it was found that zirconium carbide was formed, magnesia linings were substituted. After rapid cooling, the top of the ingot was analysed and the resulting figure for zirconium content was expected to give the limit of solubility. The figures obtained from the magnesia-lined "bombs" showed an increase in solubility with temperature, but after holding at 800° C. the zirconium found at the top of the ingot amounted to only 0.35%. It was difficult to see how an alloy containing 0.6% zirconium could be produced at 800° C. by the chloride-master-alloy process, if in fact the solubility at that temperature was only 0.35%. It was concluded, therefore, that in these "bomb" experiments losses of zirconium had occurred, mainly through the presence of moisture or hydrogen or through iron contamination during the long treatment.

Another means of approaching the problem was suggested by the fact that the liquidus at the magnesium-rich end of the magnesium-manganese system had been determined by Grogan and Haughton<sup>12</sup> by holding molten alloys at fixed temperatures sufficiently long for the excess manganese to sink. Chemical analysis of a dip-sample gave the limit of solubility at the temperature selected. It was necessary, of course, to start with an alloy of higher manganese content than that at the limit of solubility. With the adoption of the chloride-master-alloy process it was possible to carry out a modification of the dip-sampling technique, for the master alloy at the bottom of the crucible formed a source of excess zirconium. Alloys were therefore made up by the chloride-master-alloy method and held for different times at 675°, 800°, or 900° C. Table II shows the results of chemical analyses of dip-samples taken at these various temperatures, or of chill-cast bars.

It is clear from the Table that very little zirconium was lost through holding at 800° or 675° C. for 30 or 60 min. It was necessary to cut down the time of holding at 900° C. in order to reduce contamination by iron from the crucible. Excessive burning took place at this temperature unless a stream of chlorine was used to protect the metal on pouring.

The average compositions given in Table II indicate a liquidus rising from a peritectic point at approximately 0.5% zirconium and passing through about 0.58% zirconium at 800° C. and 0.67% zirconium at 900° C. In view of the experimental difficulties mentioned earlier in the paper it would be unwise to claim that the above figures are accurate to limits closer than  $\pm 0.03\%$  zirconium.

The results obtained by Siebel<sup>6</sup> by dip-sampling (see Table III) are similar to those obtained by the author in the mild-steel bomb

TABLE II.—Zirconium Contents of Alloys.

Alloy No. :	Zirconium, %														Average
	75	76	83	90	99	100	101	102	102	102	102	102	102	102	
Held at 900° C. :															
5 min. . .	...	...	...	...	...	...	...	...	...	...	...	...	...	...	0.67
Held at 800° C. :															
5 min. . .	0.58	0.58	0.54	0.55	0.57	0.63	0.63	0.61	0.59	0.60	0.62	0.60	...	...	0.58
30 min. . .	...	...	...	...	0.56	0.61	0.56	...	...	...	...	...	...	...	
60 min. . .	...	...	...	...	0.55	0.59	0.55	...	...	...	...	...	...	...	
Held at 675° C. :															
30 min. . .	0.53	0.57	0.48	0.48	...	...	...	...	...	...	...	...	...	...	0.51
60 min. . .	...	0.53	0.48	0.48	...	...	...	...	...	...	...	...	...	...	

\* Chill-cast bars.

experiments. Siebel gives no details of any method of providing excess zirconium during the experiments or of precautions taken to prevent loss of zirconium at temperatures above 800° C., so that his figures may be expected to be low.

TABLE III.—*Solubility of Zirconium in Magnesium*  
(from Siebel <sup>6</sup>).

Temperature, ° C. .	655	700	750	800	850	900	950
Zirconium, % .	0.21	0.23	0.25	0.27	0.29	0.35	0.45

### 3. Solid Solubility.

#### (a) *Microscopical Analysis.*

Heat-treatment of magnesium alloys for subsequent microscopical examination is liable to result in volatilization of the magnesium, oxidation, and absorption of hydrogen. It was found that sealing specimens in argon in heat-resistant glass tubes did not prevent loss by volatilization, and the most satisfactory method of protection was eventually found to be to coat specimens with a proprietary mixture consisting mainly of boric acid.

It was realized at the start of the investigation that the identification of limiting quantities of very small particles of zirconium in the microstructure would present some difficulty. In the cast alloy zirconium is identified by the characteristic coring which surrounds a very small particle of zirconium, as shown in Fig. 1 (Plate VI). Coring can often be seen, even if the plane of the microstructure does not include the zirconium particle. Alloys of varying zirconium content were quenched after holding at temperatures of 300°, 400°, 500°, and 600° C., and an attempt was made to determine whether certain specimens did or did not show particles of zirconium in the microstructure. It was found, however, that on heat-treatment at the above-mentioned temperatures the characteristic coring was converted into clusters of dots (see Fig. 2, Plate VI) suggesting that zirconium in the cored region came out of solution as particles. Once formed, the clusters could not be redissolved by treatment at a higher temperature. For example, an alloy containing 0.55% zirconium was water quenched after 24 hr. at 600° C., and clusters of dots could be seen. Further heat-treatment at 640° C. for 72 hr. produced no evidence of re-resolution of the dots. Chemical analysis showed that there had been a reduction of 0.03% in the amount of zirconium soluble in 15% hydrochloric acid, so that the true reduction of zirconium dissolved in magnesium was probably

greater than 0.03%. It therefore appears that, on annealing a cast specimen, a certain amount of insoluble compound of zirconium is likely to form from the zirconium previously in solution.

These experiments on heat-treatment and microscopical examination seem to indicate that (i) the complete elimination of hydrogen during annealing is extremely difficult, (ii) the formation of characteristic clusters of dots is partly due to zirconium coming out of solution and partly to the formation of hydride, and (iii) annealing with subsequent microscopical examination is not a reliable method of determining the limit of the solid solubility.

(b) *Electrical-Resistivity Method.*

The solid solubility was determined by measuring the electrical resistivity of duplicate test-pieces of four alloys quenched after different periods of time at various temperatures. The measurements were made by the Electricity Division of the N.P.L. on specimens 1 cm. in dia.  $\times$  15 cm. long. Batches of test-pieces for heat-treatment were protected by coatings of a mixture consisting mainly of boric acid. The results of the resistivity determinations are given in Table IV.

TABLE IV.—*Electrical Resistivity of Four Magnesium-Zirconium Alloys at Room Temperature (20° C.).*

Batch	Heat-Treatment	Resistivity, microhms/cm. <sup>3</sup>			
		0.23% Zr Alloy	0.35% Zr Alloy	0.53% Zr Alloy	0.60% Zr Alloy
G	As rolled	5.34	5.56	5.76	5.82
E	24 hr. at 600° C., water quenched	{ 5.42	5.78	6.34	6.64
		{ 5.42	5.76	6.30	6.62
F	90 hr. at 500° C., water quenched	{ 5.30	5.74	6.36	6.62
		{ 4.98	5.52	6.32	6.60
F	168 hr. at 500° C., water quenched	{ 5.24	5.68	6.32	6.64
		{ 4.66	5.42	6.28	6.62
E	216 hr. at 400° C., water quenched	{ 5.30	5.60	6.10	6.36
		{ 5.28	5.60	6.06	6.34
E	480 hr. at 400° C., water quenched	{ 5.28	5.62	6.12	6.38
		{ 5.22	5.58	6.10	6.34
E	40 hr. at 600° C., water quenched	{ 5.28	5.62	6.26	6.54
		{ 5.26	5.64	6.24	6.52
F	528 hr. at 300° C., water quenched	{ 5.18	5.42	5.88	6.06
		{ 4.62	5.28	5.82	6.00

The electrical resistivity at room temperature of pure magnesium was found to be 4.52 microhms/cm.<sup>3</sup>, and specimens of magnesium-zirconium alloys, after holding at 600° C., gave a regular increase of resistivity with zirconium content, as shown in Table IV. It will be

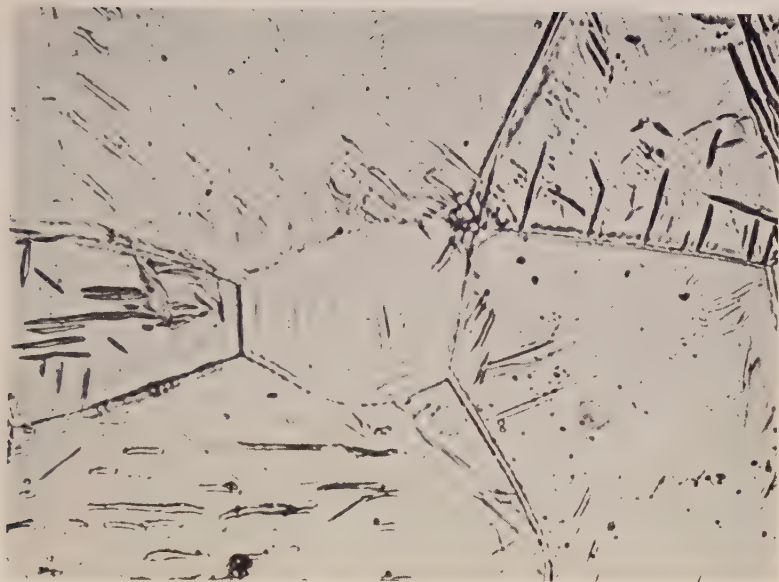


FIG. 1.—Magnesium-0.53% Zirconium Alloy, As Cast, Showing Coring.  $\times 750$ .

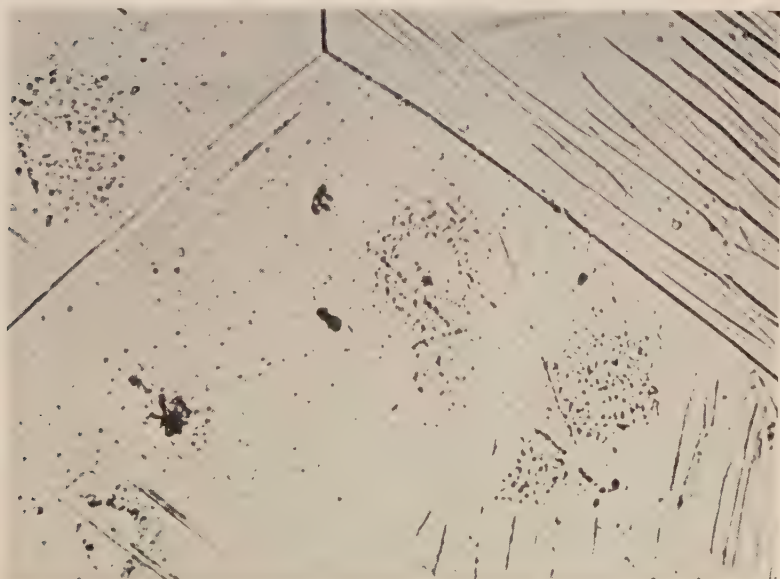


FIG. 2.—Magnesium-0.53% Zirconium Alloy, Heat-Treated 24 hr. at  $600^{\circ}\text{C}$ . and Water Quenched, Showing Clusters of Dots.  $\times 750$ .





observed that on heat-treatment there was in many cases a reduction in resistivity due to (a) zirconium, as such, coming out of solution, or (b) the formation of insoluble hydride in a specimen which was insufficiently protected during heat-treatment or which already contained some dissolved hydrogen. When a batch was re-heat-treated at 600° C. an incomplete restoration of the original resistivity showed that some insoluble hydride had been formed. It has therefore been considered legitimate to regard the higher value of each pair of results shown in Table IV as the true figure, lower figures being generally due

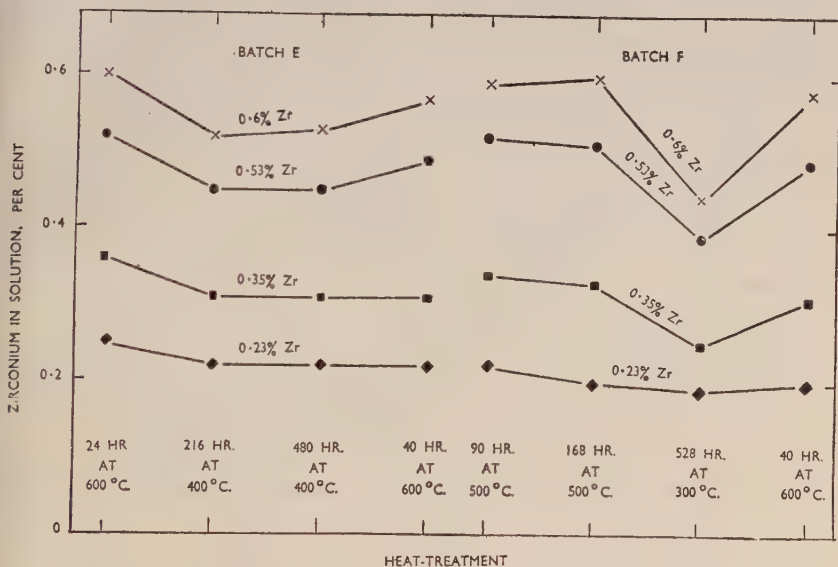


FIG. 3.—Variation, due to Heat-Treatment, of Zirconium in Solution.

to hydride which is not re-dissolved at 600° C. The regular increase in resistivity after solution-treatment at 600° C. from 4.52 microhms/cm.<sup>3</sup> for pure magnesium to 6.64 microhms/cm.<sup>3</sup> for a 0.6% zirconium alloy has been used in deducing the percentage of zirconium in solution in samples from other heat-treatments, and the results are set out in Fig. 3.

No significance should be attached to differences of less than 0.02% zirconium, for the limits of accuracy of chemical analysis are of that order, and readings of electrical resistivity are accurate only to 0.5%.

Heat-treatment of the rolled rods of batch E at 600° C. (see Fig. 3), resulted in a regular increase of the amount of zirconium in solution, indicating that the limit of solubility at that temperature was not less

than 0.6%. Batch F gave almost identical values of resistivity after treatment at 500° C. for 90 hr. No significant change occurred on increasing the time of heat-treatment to 168 hr., so that it may be assumed that equilibrium conditions had been reached after 90 hr. It follows that the solubility at 500° C. is not less than 0.6% zirconium.

Batch E was treated at 400° C. for 216 hr. and 480 hr. Each alloy showed some loss of soluble zirconium, and on reheating to 600° C. the values originally obtained for the 0.53 and 0.60% alloys were almost fully restored. In the alloys of 0.23 and 0.35% zirconium the loss at 400° C. was small and was not restored at 600° C., indicating the formation of insoluble compounds. It appears, therefore, that the limit of solubility at 400° C. must lie below 0.53% zirconium and is probably above 0.35%.

Treatment of batch F for 528 hr. at 300° C. led to a marked decrease in resistivity in the 0.35, 0.53, and 0.60% alloys, but only a slight decrease in the 0.23% alloy. The final treatment of this batch at 600° C. gave a higher resistivity, indicating a substantial increase in the amount of zirconium in solution except in the case of the 0.23% alloy. The limit of solubility at 300° C. may therefore be expected to lie between 0.23 and 0.35% zirconium.

Electrical-resistivity values for four chill-cast alloys, together with the figures for zirconium in solution derived from these values, are given in Table V.

TABLE V.—*Zirconium in Solution in Cast Alloys.*

Zr, % by chemical analysis	Resistivity, microhms/cm. <sup>3</sup>	Zr, % in solution (derived from resistivity values)
0.26	5.16	0.18
0.43	5.38	0.24
0.53	5.56	0.29
0.60	5.54	0.29

The small amount of zirconium in solution would be expected in a chill-cast alloy with insufficient time for re-solution of zirconium below the peritectic temperature during cooling.

#### IV.—DISCUSSION.

It has been found that the magnesium-zirconium diagram at the magnesium-rich end contains a peritectic horizontal at a temperature slightly higher than the melting point of pure magnesium and a liquidus rising steeply from a peritectic point, and that there is a limited solid solubility of zirconium in magnesium. The diagram based on the

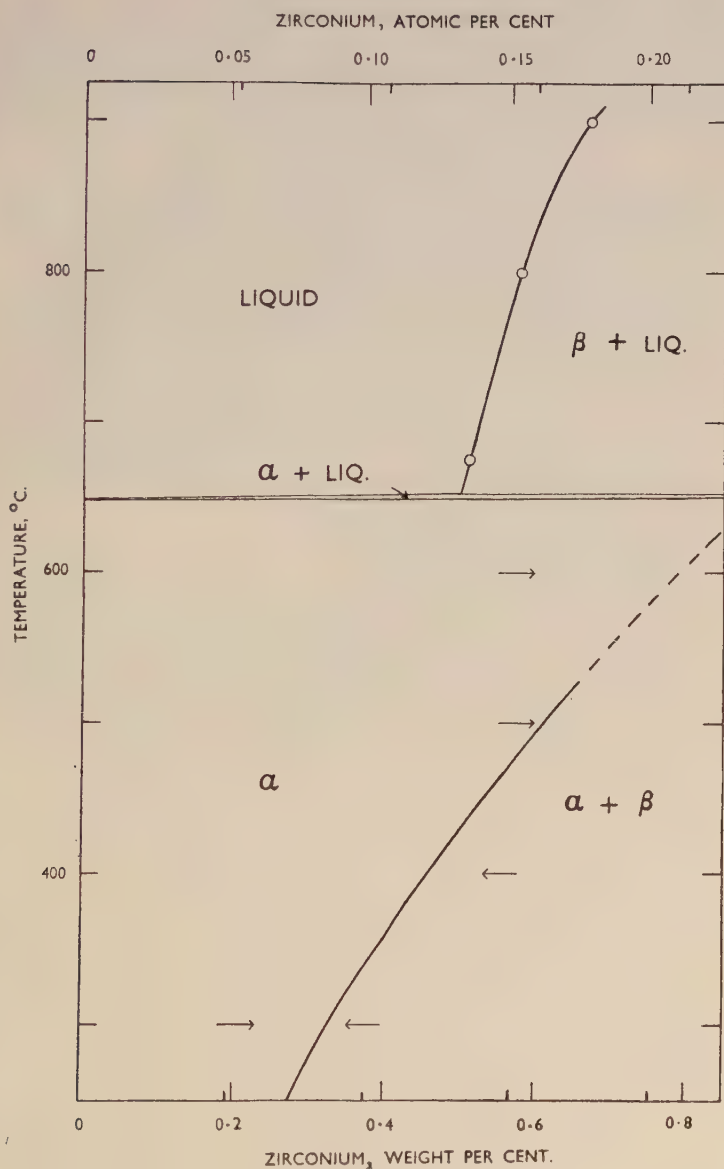


FIG. 4.—The Magnesium-Zirconium Diagram.

present work is given in Fig. 4. The author has not found the liquidus to lie in the same position as that given by Siebel,<sup>6</sup> and the limits of solid solubility as determined by electrical resistivity are somewhat different from those put forward by Beck<sup>5</sup> and by Nowotny, Wormnes, and Mohnheim.<sup>2</sup>

#### ACKNOWLEDGEMENTS.

The author desires to acknowledge the assistance rendered by Mr. P. G. Ward, B.Sc., in carrying out chemical analyses, and by Mr. E. G. Sutherland, B.Sc., in the experimental work.

The work described was carried out in the Metallurgy Division of the National Physical Laboratory on behalf of the Ministry of Supply, by whose permission this paper is published.

#### REFERENCES.

1. C. J. P. Ball, *Aluminum and Magnesium*, 1946, 3, (1), 20; (2), 12; and *Metallurgia*, 1947, 35, 125, 211.
2. H. Nowotny, R. Wormnes, and A. Mohnheim, *Z. Metallkunde*, 1940, 32, 39.
3. F. Sauerwald, *Z. anorg. Chem.*, 1947, 255, 212.
4. F. Sauerwald, *Z. Metallkunde*, 1949, 40, 41.
5. A. Beck, "The Technology of Magnesium and Its Alloys", p. 77. London: 1940 (F. A. Hughes & Co., Ltd.).
6. G. Siebel, *Z. Metallkunde*, 1948, 39, 22.
7. R. S. Busk and E. G. Bobalek, *Trans. Amer. Inst. Min. Met. Eng.*, 1947, 171, 261.
8. F. Sauerwald, *I.G. Farbenind. Research Rep. No. 30*, 1941.
9. W. J. Kroll and A. W. Schlecten, *U.S. Bur. Mines, Inform. Circ. No. 7341*, 1946.
10. E. F. Emley, *J. Inst. Metals*, 1948-49, 75, 481.
11. Magnesium Elektron, Ltd., British Patent No. 533,264, 1941.
12. J. D. Grogan and J. L. Haughton, *J. Inst. Metals*, 1943, 69, 241.



# THE EFFECT OF APPLIED LOAD IN MICRO-INDENTATION TESTS.\*

By W. ROSTOKER,† M.A.Sc., Ph.D.

## SYNOPSIS.

Experiments have been conducted with a Bergsman microhardness tester to study the variation of apparent hardness with small applied loads in relation to the metallurgical condition of the material under test. It has been found that the apparent hardness decreases continuously with decreasing load, and that the rate of decrease is dependent on the capacity of the material for cold work. Thus, the "rule of similarity" which is normally applicable to pyramidal indenters breaks down.

A new Meyer exponent can be derived which behaves in a similar but reverse manner to the exponent derived from tests using a ball indenter and large applied loads.

## I.—INTRODUCTION.

IN recent years much interest has been centred on the development of instruments which will measure the hardness of very small regions. The size of the region predetermines the permissible indentation size, and the microhardness tester achieves its purpose by using sufficiently small applied loads. It is manifestly necessary to establish that calculated hardnesses are independent of impression size or, if not, to show in what manner hardness, impression size, and pretreatment of the specimen are interrelated.

The literature, to date, contains a large amount of conflicting data on microhardness testing, showing the effect of applied load on the hardness number. Three investigators <sup>1, 2, 3</sup> report that hardness numbers increase with decreasing indenter load; two <sup>4, 5</sup> maintain that, as with the Vickers testing machine, hardness numbers are essentially independent of load; and yet another group of authors <sup>6</sup> give evidence that hardness numbers definitely decrease with decreasing load. Thibault and Niquist <sup>1</sup> and Tate <sup>2</sup> deal largely with the Knoop indenter, and the rest used the familiar pyramid indenter with 136° apex angle.

Until now, it had been thought that the area of impression bore a constant relation to the applied load for any material, provided that the angle included by the opposite edges and the bottom of the impression was independent of the depth. This is generally known as Kick's

\* Manuscript received 23 August 1949.

† Research Fellow, Department of Industrial Metallurgy, University of Birmingham.

"rule of similarity", and the condition of adherence is fulfilled by pyramidal and conical indenter shapes. Previous investigators have taken for test random samples of often unknown metallurgical history. The confident and intelligent use of microhardness testing instruments requires that observed deviations from this "rule" be shown to be not peculiar to the instrument, or to the samples tested, but to be related to the metallurgical condition of the test-piece.

Many years ago, Meyer showed that the diameter of the Brinell ball impression varied with the applied load in the manner :

$$P = a \cdot d^n,$$

where  $P$  is the applied load,  $d$  is the diameter of the ball impression, and  $a$  and  $n$  are constants. The exponent  $n$  was furthermore shown to be related to the metallurgical condition of the test-piece, namely, as a parameter which represents capacity for cold work. Since then, numerous investigators into hardness phenomena, in particular Kokado,<sup>7</sup> have shown that the Meyer equation is a more general relation associating the applied load or force with any measured resultant parameter characteristic of hardness.

Preliminary tests with a microhardness tester showed that hardness numbers decreased, for any particular material, with decreasing applied load. It therefore seemed advisable to examine microhardness measurements to determine their conformity with the Meyer equation, i.e. to show a linear relation between the logarithm of the load  $P$  and the logarithm of the diagonal of the indentation  $d$ . Onitsch<sup>3</sup> attempted this analysis and reports the  $\log P$ - $\log d$  plots to be linear, but, contrary to the present author's results, having slopes less than two.

## II.—EXPERIMENTAL METHODS.

Since microhardness testing is a relatively new practice, some space will be devoted to the conditions of testing and preparation of the specimen. The instrument used in these experiments was a Bergsman microhardness tester, mounted on the stage of a Vickers projection microscope. This particular tester works on the balanced-beam principle, common to a number of other such instruments. No attempt will be made to give details of construction, as these are adequately covered in an article by the designer.<sup>4</sup> The instrument is of simple construction and, for all practical purposes, free of inertia.

The indentations were made with a standard diamond-pyramid indenter (136° apex angle) set in an objective holder. In the test procedure, the desired field was located with a microscope objective, and then, to make the impression, the objective was replaced by the

diamond. With a little adjustment, the diamond could be set to give impressions in the centre of the field located by the objective. Examination of the indenter by shadow comparator at a magnification of 30 disclosed no defects, although the apex angle seemed to be a few degrees larger than  $136^\circ$ . Under a magnification of 300, the tip appeared sharp; there was no chisel-type tip as reported by Campbell, Henderson, and Donleavy.<sup>6</sup>

Making the actual impressions requires care, as there are a number of variables which can have a serious effect on the results. The rate of loading is a very critical factor, and every attempt must be made to apply the load as slowly as possible. The rack and pinion, for the fine focus of the microscope, is sensitive enough to permit careful loading. To provide assurance that the electrical-contact points do not impede the penetration of the indenter, it is desirable, after making contact between specimen and indenter, to lift the sample several microns above the fixed contact. The time of application of the load is not critical, and in these experiments a 30-sec. period was used. It has been found important to locate the centre of gravity of the applied weight directly above the axis of the indenter. Provision is made for this with the Bergsman instrument. With the instrument as described, the author experienced difficulty in preventing a double-indentation effect when using loads of less than 25 g., or when the diagonal of the impression was less than  $10\ \mu$ . This may have been due to loose alignment in one of the mechanical systems involved.

Undoubtedly the most critical stage in microhardness testing is the precise and accurate measurement of the dimensions of the impression. The effect of an error in measurement of  $1\ \mu$  can be appreciated by consideration of the following :

$$H = b \cdot \frac{P}{d^2}$$

$$\Delta H = -2b \cdot \frac{P}{d^3} \Delta d$$

$$\text{If } \Delta d = 1\ \mu$$

$$\frac{\Delta H}{H} = -\frac{2}{d}$$

where  $H$  is the diamond pyramid hardness number (D.P.H.),  $P$  is the load applied,  $d$  is the diagonal of the impression, and  $b$  is a constant.

Thus, with a material whose D.P.H. = 50, the error in hardness would be 5 units for a diagonal measurement of  $20\ \mu$ ; while, for a material whose D.P.H. = 500, under similar conditions, the hardness number could be in error by 50 units. In the present experiments,

indentations were measured by projecting their image, at 1000 times magnification using a 4-mm. objective, on to a millimeter-grid screen. An engraved standard scale of 1 mm. divided into one hundred divisions was used to calibrate the magnification. Under these conditions, measurements were made to the nearest micron.

It has been maintained that the preparation of the surface of the specimen is of the utmost importance. A number of investigators have blamed erratic or inexplicable results on the possible existence of a layer of disturbed metal produced by mechanical polishing of the specimen. For these experiments, copper and brass specimens were electropolished. By way of comparison, a piece of annealed copper was hand polished, using no more care than is usual for ordinary metallographic examination. A light etch serves to disclose any scratches which have been flowed in during polishing and, provided that the polishing has been sufficiently careful to prevent this effect, there seems to be no difference in the hardness of the specimens prepared by the two methods. Furthermore, it might be expected that the hardness numbers from small indentations would be anomalously high owing to the cold-worked polish layer. Quite the opposite effect, however, was systematically noted in iron and steel specimens, which were all mechanically polished. Examination of the hardness impressions is preferably carried out in the unetched state, as etching introduces dark regions which may mask the corners of the impressions.

The precision of any single measurement is a subject worthy of consideration. Standard deviations are calculated from the large amount of data available to lie between 0.5 and 1.5  $\mu$ , tending to the smaller value at small indentation sizes. This may be an indication of the disturbing effect of grain boundaries. In view of the considerable error introduced by a small error in measurement, it is necessary to take a number of impressions before deciding on a hardness value. All measurements in this paper are arithmetic averages of ten indentations.

### III.—MATERIALS EXAMINED.

To study the effect of cold work, mild-steel wire (about 0.05% carbon), high-conductivity copper wire, and an ( $\alpha + \beta$ ) brass wire were drawn to various reductions in area. The wires were examined in longitudinal section. Copper sheet was rolled to a similar reduction. Tests showed that there was no variation in hardness between rolled and drawn materials.

The effect of heat-treatment was studied on a plain carbon steel (0.9% carbon) in the quenched condition and after subsequent tempering at 250°, 450°, and 650° C.



## IV.—MICROHARDNESS MEASUREMENTS.

Table I summarizes the measurements of the variation of diamond pyramid hardness with applied loads from 200 g. to 25 g. for copper, iron, and brass which had been cold worked by amounts up to 94% reduction in area. Fig. 1 illustrates that, in each case, the measured hardness decreases with decreasing load, and that the greater the initial degree of cold work in the specimen, the more rapid is the decline of the hardness curve.

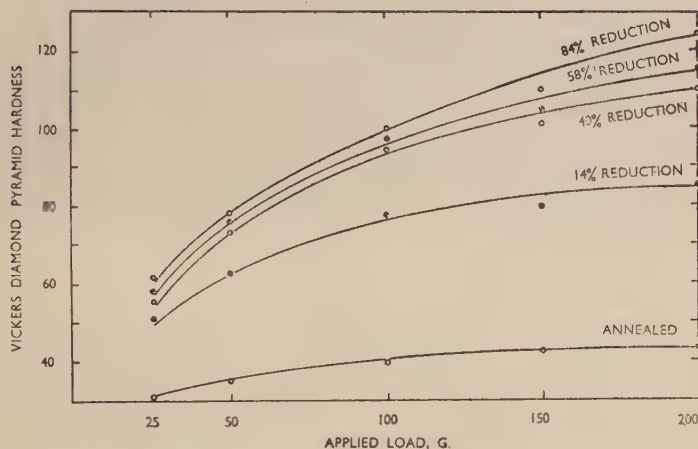


FIG. 1.—The Effect of Applied Load on the Measured Diamond Pyramid Hardness for Copper in Various Stages of Cold Work.

The variations of indentation diagonal with applied load have been plotted on a log-log scale for the various degrees of cold work. An example of such a series is shown in Fig. 2. The slopes of these straight lines, i.e. the Meyer exponent  $n$ , have been measured, and they have been plotted as a function of the percentage reduction in area in Fig. 3.

It will immediately be seen that the Meyer exponent derived from microhardness measurements is a continuous function of the degree of cold work, and that the function seems to be common to all three materials tested. The values of  $n$  for the annealed states show some scatter. The same is true for exponent values derived using ball indenters. The initial high hardness of the annealed brass suggests insufficient preparatory heat-treatment.

In contrast to these results, the Meyer exponent as derived from macrohardness tests with the Brinell ball varies from about three for the annealed state to two for high degrees of cold work. An example of such



results is given by O'Neill.<sup>8</sup> We are thus faced with an unusual situation, that the pyramidal indenter, with small applied loads, behaves in a similar but reverse manner to a ball indenter with very high loads.

The effect of applied load on the D.P.H. number for a 0.9% carbon steel in the quenched and tempered states is shown in Table I. It will be noted that a martensitic structure indicates a capacity for cold work which is much less than that of severely strained materials. This is more in keeping with reality than the surprising value of 2.7 for  $n$  obtained by O'Neill<sup>9</sup> with a diamond ball indenter set in a Brinell tester. Interpreted on the basis of the usual trend of the Meyer exponent, this would mean a high capacity for cold work, which is not borne out by other physical tests.

The tempered structures seem to possess similar capacities for cold work independent of the tempering temperature. This is in accordance with drawing practice for high-carbon steel wire, where a patented structure possessing a fine carbide dispersion and a relatively high initial hardness can undergo surprisingly high degrees of strain without requiring annealing.

#### V.—DISCUSSION.

The results given in this paper indicate that the apparent size of the impression produced by a pyramidal indenter is related to the metallurgical condition of the material under test; and that a new parameter can be derived from micro-indentation measurements which is indicative of capacity of the material for cold work. A real understanding of this behaviour is beyond the scope of the present paper. Indeed, our understanding of the more orthodox hardness tests is still far from satisfactory. But the author would present certain observations which suggest that the process of surface penetration under the action of very light loads involves factors which are not apparent in heavy-load tests.

Some comment on the appearance of micro-indentations may be of interest. Around the smaller impressions, a large disturbed region, circumscribing the impression, is always apparent. This region can extend from the edge of the impression by as much as the length of the edge itself. In general, the relative magnitude of the disturbed zone increases with decreasing size of the impression. Tolansky and Nickolls<sup>10</sup> have recently shown by interferometric examination that this region represents the "piling-up" effect familiar in macrohardness testing. There do not seem to be any cases of the "sinking-in" effect. For example, on the surface of a hardened steel, the impression made by a 5-kg. load shows the sides bulging in towards the centre of the impression, which is typical of the "sinking-in" effect; however, the

TABLE I.—Diamond Pyramid Hardness of Copper, Iron, and Brass, Subjected to Varying Degrees of Cold Work.

Material	Treatment	Diamond Pyramid Hardness Numbers (Diagonals of Impressions in Microns are given in Brackets)					n
		200-g. load	150-g. load	100-g. load	50-g. load	25-g. load	
Copper	Annealed	43 (93.0)	43 (80.5)	40 (68.1)	34 (52.2)	31 (38.7)	2.3
	14% R.A.	86 (65.6)	80 (59)	77.5 (49.0)	62 (38.6)	52 (29.9)	2.6
	40% R.A.	110 (58.1)	102 (52.2)	93.5 (44.5)	73 (35.6)	57 (28.5)	2.95
	58% R.A.	116 (56.6)	105 (51.5)	97.5 (43.6)	76 (35.0)	59 (28.0)	3.05
	84% R.A.	125 (54.5)	110 (50.4)	100 (43.1)	78.5 (34.4)	62 (27.3)	3.05
Iron	Annealed	115 (56.8)	113 (49.6)	120 (38.0)	112 (29.8)	102 (21.4)	2.05
	11% R.A.	151 (49.5)	143 (43.8)	140 (36.4)	115 (28.4)	100 (21.5)	2.54
	45% R.A.	190 (44.2)	185 (38.8)	175 (32.6)	132 (26.6)	102 (21.4)	3.0
	61% R.A.	200 (43)	192 (38.1)	185 (31.6)	140 (25.8)	105 (21.0)	3.1
	86% R.A.	213 (41.7)	202 (37.1)	185 (31.6)	140 (25.8)	110 (20.5)	3.1
	94% R.A.	223 (40.7)	215 (36.0)	185 (31.6)	146 (25.2)	118 (19.8)	3.0
	Annealed (?)	110 (58.1)	113 (49.6)	106 (41.8)	85 (33)	77 (24.6)	2.34
Brass ( $\alpha + \beta$ )	10% R.A.	145 (50.6)	140 (44.6)	118 (39.8)	98 (30.7)	82 (23.8)	2.70
	21.5% R.A.	153 (49.2)	150 (43.1)	129 (38.0)	107 (29.4)	86 (23.2)	2.85
	71% R.A.	205 (42.5)	192 (38.0)	178 (32.2)	135 (26.2)	99 (21.6)	3.05
Aluminium (99.99%)	Annealed	23.8 (125.0)	21 (115.0)	23.8 (88.3)	25 (61.0)	23.2 (44.6)	2.0
Steel (0.9% carbon)	Water quenched	900 (20.3)	775 (19.0)	665 (16.7)	500 (13.6)	...	3.34
	Tempered 250° C.	665 (23.6)	630 (21.0)	550 (18.4)	480 (13.9)	...	2.85
	" 450° C.	435 (29.1)	410 (26.1)	360 (22.7)	270 (18.5)	...	2.85
	" 650° C.	245 (38.9)	230 (34.9)	205 (30.0)	160 (24.1)	...	2.85

R.A. = Reduction in area.



impression made by a 50-g. load on the same surface gives distinct evidence of "piling-up" around the sides. A number of Bergsman's photographs <sup>4</sup> show the same effect.

Relatively low hardness numbers or, in effect, excessively large impressions when using light applied loads might conceivably be due to one or more of the following causes :

(a) Inertia of the instrument, which constitutes an effective increase in the applied load appreciable only at low loads.

(b) The presence of a thin, softer layer on the surface of the impression due to preparation.

(c) A kinetic-energy effect due to the rate of application of the load.

(d) Gross distortion of the impression by elastic recovery.

The inertia of the instrument beam-bearing was investigated. The beam was balanced so that, at equilibrium, the electrical contacts were about 1 mm. apart. Successively smaller weights were placed at the opposite end of the beam and the new equilibrium point noted. It was found that as little as 50 mg. would appreciably displace the point of equilibrium. Therefore, inertia cannot be a significant influence.

Suggestion (b) is extremely unlikely. A harder layer has been more widely postulated and, in any case, electrolytic polishing must have removed any abnormal surface layers. Suggestion (c) is also unlikely. The load is applied by manual adjustment, and if any such effect were operative, it must necessarily be inconstant and lead to erratic results. These have not been observed.

The subject of elastic recovery deserves some consideration. Actual experiments to study the change in shape and dimensions of an impression are difficult with macro-impressions, and with micro-impressions well-nigh impossible. Discussion of this subject must necessarily be of an inferential nature. O'Neill <sup>10</sup> reports that elastic recovery can reduce the initial depth of penetration of a conical indenter by as much as 50%. This, in itself, cannot influence the hardness numbers calculated from measurements of the diagonal of the square image at the surface, unless the upward movement of the base were to cause a lateral thrust tending to widen the sides of the square impression at the surface. This action might also be the cause of the "piling-up" effect.

Some experiments by Kokado <sup>7</sup> on the height of rebound of a steel ball are of interest. The rebound of a ball impinging on a surface is due to the combined elastic reaction of both the ball and the surface. The height of rebound is a direct function of the elastic recovery of the material immediately surrounding the impression produced by the impact. In Fig. 4, data have been taken from Kokado's tests on a mild

steel to plot the fraction of energy recovered in the rebound against the initial energy of impact. In the actual plot, height is used instead of energy as the two differ only by a constant. It is seen that the proportion of energy converted to elastic strain becomes rapidly greater when the initial energy of impact becomes very small, and at large values of initial energy the proportion is essentially constant. Tabor,<sup>12</sup> using the coefficient of restitution as his ordinate, shows the same effect for cast steel and wrought brass. It is reasonable to assume that,

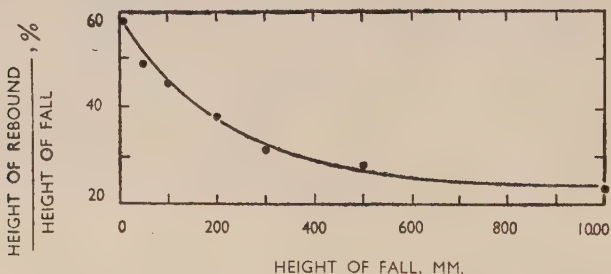


FIG. 4.—Relationship between Height of Fall and Height of Rebound of a Steel Ball, from Kokado's data for mild steel.<sup>7</sup>

under conditions of static loading, the ratio of elastic strain to total strain should behave in a similar fashion.

Of the four possible causes of the phenomena reported here, only the last, elastic recovery, seems to have any basis for credibility. Finally, it might be pointed out that in every case a large decrease in apparent hardness is associated with a material of high elastic-strain capacity.

#### ACKNOWLEDGEMENTS.

The author wishes to express his thanks to the Uddeholm General Agencies of Birmingham for the loan of the Bergsman microhardness tester.

#### REFERENCES.

1. N. W. Thibault and H. L. Niquist, *Trans. Amer. Soc. Metals*, 1947, **38**, 271.
2. D. R. Tate, *Trans. Amer. Soc. Metals*, 1945, **35**, 374.
3. E. M. Onitsch, *Berg- u. hüttenmänn. Monatsh. montan. Hochschule, Leoben*, 1948, **93**, 7.
4. E. B. Bergsman, *Metal Progress*, 1948, **54**, 183.
5. E. W. Taylor, *J. Inst. Metals*, 1948, **74**, 493.
6. R. F. Campbell, O. Henderson, and M. R. Donleavy, *Trans. Amer. Soc. Metals*, 1948, **40**, 954.
7. S. Kokado, *Technol. Rep. Tôhoku Imp. Univ.*, 1927, **6**, 201.
8. H. O'Neill and J. W. Cuthbertson, *J. Inst. Metals*, 1931, **46**, 288.
9. H. O'Neill, *Proc. Inst. Mech. Eng.*, 1944, **151**, 125.
10. S. Tolansky and D. G. Nickolls, *Nature*, 1949, **164**, (4159), 103.
11. H. O'Neill, *Carnegie Schol. Mem., Iron Steel Inst.*, 1926, **15**, 239.
12. D. Tabor, *Proc. Roy. Soc.*, 1947, [A], **192**, 260.



# THE PRESSURE-WELDING CHARACTERISTICS OF SOME COPPER-BASE ALLOYS.\* 1248

By EDWIN DAVIS,† M.Sc., F.I.M., MEMBER, and ERIC HOLMES,† B.A.,  
STUDENT MEMBER.

## SYNOPSIS.

The pressure-welding characteristics of deoxidized copper and nine commercial copper-base alloys have been determined by making butt welds with  $\frac{1}{2}$ -in.- or  $\frac{5}{8}$ -in.-dia. rod, the efficiency of jointing being assessed by tensile testing and micro-examination. Heating to welding temperature was effected by means of an oxy-acetylene ring burner, and pressure was applied by a hydraulic press of 10 tons capacity. The joint strength was influenced by the surface condition before welding, mechanical preparation proving most suitable, and by the deformation taking place during welding. Welding time, pressure, and temperature were of importance only in so far as they affected deformation, provided that the welding temperature exceeded the recrystallization temperature of the material. With each alloy welded joints were made of a strength equal to the inherent strength of the annealed material, and welding took place by recrystallization across the interface. Taking as the criterion of weldability the minimum deformation required to produce maximum joint strength, the order of merit was: deoxidized copper; 70:30 and 80:20 cupro-nickel; 93:7 and 91:9 phosphor bronze; 85:15 brass;  $\alpha/\beta$  brasses; silicon bronze and aluminium bronze.

## I.—INTRODUCTION.

RECENTLY, much interest has been aroused in the jointing of metals by pressure welding, which, if carried out under proper control, yields a welded joint superior to those that can be made by other welding processes, particularly in respect of homogeneity. As pressure welding does not involve the melting of the parent metal or of a filler rod or electrode, there is no cast metal in the joint. The possible complications attendant on the use of fusion welding, such as absorption of gas in the molten metal, and its subsequent rejection in the form of pores on solidification, the formation of shrinkage cavities, shrinkage cracks, the trapping of slag inclusions, and inadequate fusion of the parent metal cannot arise in pressure welds. Although pressure welding is not, of course, of universal application, it is being successfully used to an increasing extent when conditions permit.

Apart from the age-old welding of wrought iron in the smithy, which is not true pressure welding because of the presence of a liquid slag that plays a not unimportant part in forming the weld, the first use of

\* Manuscript received 16 September 1949.

† Technical Officer, Imperial Chemical Industries, Ltd., Metals Division, Birmingham.

pressure welding seems to have been associated with mild steel. The water-gas welding of mild steel, in which overlapping areas are heated and subsequently deformed either mechanically or manually, has been employed for many years, and in some, though probably not all instances, pressure welding takes place without any local fusion. Since 1943<sup>1</sup> pressure welding of pipe-lines end to end has been a constant practice in the U.S.A., and the manufacture of stainless steel rings by pressure welding two semi-circular pieces has been described by Rustay *et al.*<sup>2</sup> Dowson,<sup>3</sup> in 1945, recorded the application of pressure welding to the construction of portions of chemical plant in silver, and Tylecote<sup>4, 5, 6</sup> has covered in a number of papers the pressure-welding characteristics of many commercial aluminium alloys. The pressure welding of aluminium alloys has not yet been developed to any great extent, though patents have recently been applied for in respect of tools, &c., for pressure welding these and other alloys at room temperature.<sup>7</sup> Cook and Davis<sup>8</sup> in 1947 investigated the pressure-welding characteristics of H.C. copper, and indicated that other copper-base alloys appeared to respond to this method of jointing, while Kinzel<sup>9</sup> also gave a few details in 1944. One other reference to pressure welding of a copper-base alloy, brass, was made in 1944, when Carl<sup>10</sup> gave particulars of welding which took place as a result of extensive deformation during an explosion.

The present paper deals with the pressure-welding characteristics of deoxidized copper, three brasses, two tin bronzes, two cupro-nickel alloys, aluminium bronze, and silicon bronze, the investigations being carried out by making butt welds with  $\frac{1}{2}$ - or  $\frac{5}{8}$ -in.-dia. rod. The influence upon joint strength of the surface condition before welding, the relationship between the strength of pressure welds and the deformation taking place in forming the joint, and the welding conditions, temperature, pressure, and time of application of pressure, necessary to give optimum joint strength, have been established. Throughout, efficiency of jointing has been assessed by tensile testing and microscopic examination of the welds. Although the treatment has not been exhaustive, the information given is sufficient to permit an appraisal to be made of the weldability by pressure methods of the alloys considered, and of the possible application of pressure welding to their fabrication.

## II.—EQUIPMENT.

Fig. 12 (Plate VII) gives a general view of the apparatus employed for the work, showing the modified 10-tons-capacity laboratory press set up for making pressure welds. The test-bars to be welded were held in

dies bolted to the two platens of the press, as shown in Fig. 1, the position of the lower die being adjustable to permit accuracy of location. Heating was effected by means of an oxy-acetylene ring burner (Fig. 13, Plate VIII), held at diametrically opposite points in such a way that one support was always at a fixed distance from the upper platen, and the other at a fixed distance from the lower. Thus during pressing the plane of the burner tilted slightly, but the six jets continued to be directed upon the line of the interface.

Welding pressure was read directly from the calibrated pressure-gauge attached to the press, while the temperature at the interface was determined indirectly from the temperature indicated by the thermocouple in the shoulder of the specimen and the relevant correlation curve. This indirect method of temperature measurement was adopted as the most satisfactory after much experimental work, although a separate calibration was required for each material. This calibration was made with dummy test-bars set up as for welding, but in the lower bar two thermocouples were inserted, one as indicated in Fig. 1 and the second located in a drilled hole which ended only 0.005 in. from the interface. These samples were heated in stages between 300° and 1000° C., or less for alloys of lower melting point, and the correlation curve for the particular material was established. Throughout the paper the references given to welding temperatures are those at the interface obtained from the relevant correlation curve.

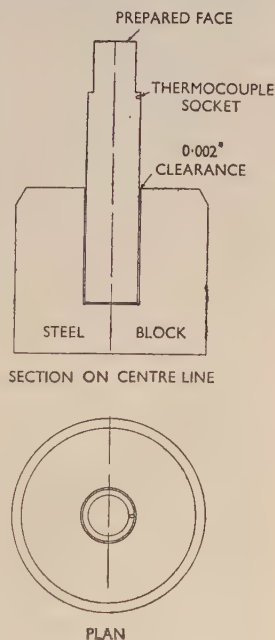


FIG. 1.—Lower Specimen and Holder for Pressure Welding.  $\frac{1}{2}$  natural size.

### III.—TECHNIQUE, MATERIALS, AND ASSESSMENT OF WELDS.

After suitable cleaning, as described below, the specimens were assembled in the press, that carrying the thermocouple being placed on the lower platen. The thermocouple was held in contact with the sample by asbestos string, which also served to protect it from direct flame impingement; further protection was afforded by a sheet of asbestos. The lower specimen was adjusted so that it registered ac-

curately with that held in the upper pressure-block, and a light load was applied to ensure good contact at the interface. A strictly neutral flame was employed in order, on the one hand, to inhibit oxidation and, on the other, to prevent carbon deposition. Heating was rapid at first, but when the temperature was about 100° C. below that required, the gas flow was reduced to assist in the attainment of steady conditions at the operating temperature. After some little experience had been gained, steady temperatures could be maintained without much difficulty for the period of time required. Pressure was then applied and was maintained for a predetermined time, varying between  $\frac{1}{4}$  and 8 min. Deformation took place under the load and, since this tended to relieve the pressure, adjustment was effected by use of the hand-pump, which, however carefully used, tended to cause some pressure fluctuations.

The materials whose pressure-welding characteristics were studied included deoxidized non-arsenical copper, 85 : 15 gilding metal, 60 : 40 brass, 57 : 40 : 3 leaded brass, 70 : 30 and 80 : 20 cupro-nickel, phosphor bronzes containing 7 and 9% of tin, a 7% aluminium bronze, and a 96 : 3 : 1 copper-silicon-manganese alloy. Details of composition are given in Table I.

The degree of success of the experimental pressure welds formed was assessed by tensile tests or micro-examination, welds for these purposes being made in duplicate under each set of conditions. Standard tensile test-pieces were machined from the welded bars (to a dia. of 0.282 in.), whilst two sections were prepared from each of the duplicate samples, and the extent of recrystallization and the incidence of oxide films or particles were assessed.

Early in the investigation it became apparent that, as in other work on pressure welding, the amount of deformation at the weld zone was of primary importance, and this was expressed numerically by the formula :

$$\text{Deformation \%} = \frac{\text{Final area} - \text{Original area}}{\text{Final area}} \times 100.$$

Fig. 14 (Plate VIII) illustrates the appearance of test-bars which had been deformed 44, 60, and 72%, respectively.

#### IV.—SIGNIFICANT VARIABLES IN PRESSURE WELDING.

The significant factors influencing pressure welding include surface condition, time of application of pressure, temperature, and pressure, and exploratory work was carried out with a view to standardizing, if possible, the first two factors and so reducing the number of variables.

TABLE I.—*Composition of Alloys.*

Alloy	Chemical Analysis												
	Cu, %	Sn, %	Pb, %	Ni, %	Al, %	Zn, %	P, %	Mn, %	Fe, %	Sb, %	Bi, %	As, %	Si, %
Deoxidized non-arsenical copper	99.89	nil	trace	about 0.01	nil	nil	0.045	trace	> 0.005	trace	trace	about 0.005	nil
85 : 15 Gilding metal	85.05	trace	trace	trace	nil	remain-der	nil	nil	nil	nil	trace	<0.005	nil
60 : 40 Brass	59.94	<0.01	trace	trace	nil	remain-der	nil	trace	0.02	nil	trace	trace	nil
Lead brass	57.81	0.02	3.12	trace	nil	remain-der	nil	trace	0.02	nil	nil	nil	nil
93 : 7 Phosphor bronze	93.11	6.71	<0.01	trace	trace	trace	0.12	0.01	about 0.02	trace	0.001	<0.005	trace
91 : 9 Phosphor bronze	91.14	8.70	<0.01	trace	trace	trace	0.10	0.01	about 0.02	trace	0.001	<0.005	trace
70 : 30 Cupro-nickel	67.56	trace	<0.01	30.45	nil	0.05	nil	1.01	0.88	trace	nil	trace	trace
80 : 20 Cupro-nickel	79.95	about 0.01	<0.01	19.74	nil	0.10	trace	0.09	about 0.07	nil	nil	about 0.01	0.05
Aluminium bronze	92.01	trace	trace	about 0.01	7.68	about 0.03	trace	0.20	about 0.05	nil	nil	<0.005	0.02
Silicon bronze	96.95	trace	trace	trace	nil	about 0.02	trace	1.02	about 0.05	nil	nil	trace	2.94



Earlier work had indicated that the most satisfactory surface preparation for pressure welding H.C. copper was to etch the surfaces to be welded for 10 sec. in nitric acid, wash in water, and dry in alcohol. Test welds with the surfaces to be joined prepared in this manner were made with all the alloys under review, and a similar series of welds was made with the surfaces prepared with 0 emery paper while the specimen was being rotated in a lathe, and afterwards washed in acetone.

For deoxidized copper, etching was the more satisfactory method of surface preparation before pressure welding, for there was evidence on the samples prepared mechanically that joint formation was adversely affected by the presence of emery particles not removed by washing. With the other materials the efficiency of joint formation was not significantly affected by either of the two surface preparations given to the bars before welding, but in view of the fact that after etching stains sometimes formed, which interfered with welding, and the simplicity of the mechanical preparation, the latter was adopted for all the materials other than deoxidized copper.

There was, however, greater difficulty in making strong pressure welds with the aluminium bronzes and silicon bronzes than in the cases of the other alloys studied, and it was considered that this might be bound up with surface condition before welding. Accordingly, more extensive tests were made to determine the effect of surface condition upon weldability with these two alloys. With the silicon bronze, welds were made with a deformation of some 40% at a temperature of 725° C., after the surfaces had been prepared in various ways. The degree of roughness of the surface, as indicated by the Talysurf machine, the etching reagents, and the time of immersion in the reagent were all varied and the results are summarized diagrammatically in Fig. 2. The most satisfactory welds, however, were obtained with surfaces prepared on emery paper, and trials made with the aluminium bronze gave similar results.

The effect of the time of application of welding pressure at temperature was studied, using silicon bronze, by making a number of joints at constant pressure and temperature; the results are shown in Table II. It was apparent that time, up to the maximum considered, was important only in so far as its effect upon deformation was concerned, both deformation at the interface and joint strength increasing with time. The magnitude of the effect, however, was slight provided that the welding time did not exceed about 5 min. During the remainder of the work, therefore, time at temperature was maintained constant at 1 min. unless otherwise indicated.

Pressure and temperature are interrelated variables in pressure

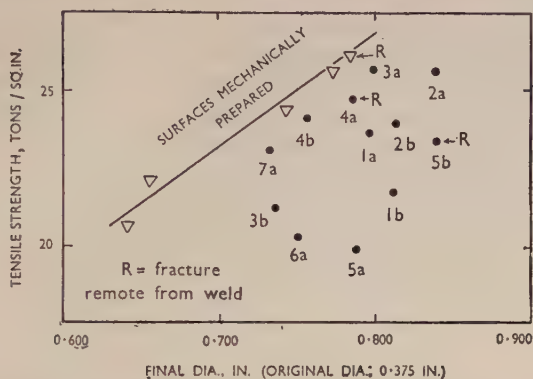


FIG. 2.—Tests on Cleaning and Degreasing Agents for Surface Preparation of Silicon Bronze.

KEY.

Number	Cleaning Agent
1	50% Nitric acid
2	Hot 10% sulphuric acid
3	None
4	50% Warm hydrochloric acid
5	Warm 5% acid solution ferric chloride
6	Ammonium persulphate
7	Ammonia and hydrogen peroxide
Letter	Degreasing Agent
a	Acetone
b	Alcohol

welding, and to determine their effect upon weld strength two series of joints were made with the silicon bronze alloy, one at constant pressure and varying temperature and a second at constant temperature and varying pressure. The results of these tests, which are shown in

TABLE II.—Effect of Time of Application of Load on Pressure Welding of Silicon Bronze.

Temperature 700° C. Pressure 4 tons/in.<sup>2</sup>

Pressure Time, sec.	Deformation, %	Ultimate Tensile Strength, tons/in. <sup>2</sup>
15	45	10.7
30	45	11.0
120	47	10.1
240	50	10.7
300	50	10.8
480	62	12.0
600	68	18.0

Table III, indicated that no definable relationship existed between the welding pressure and the strength of the welds when the temperature was constant, or between the temperature and the weld strength when the pressure was constant. Since, however, marked differences in deformation resulted from minor variations in temperature or pressure, poor correlation between pressure or temperature and joint strength was readily explained, and from the data it was apparent that the weld strength was closely related to deformation. As the work progressed it became evident that deformation at the weld interface was the main significant variable, other factors, except surface condition, influencing the joint strength only in so far as they affected deformation.

TABLE III.—*Temperature/Pressure/Weld-Strength Relationship for Silicon Bronze.*

Welding time constant at 30 sec.

Temperature, °C.	Pressure, tons/in. <sup>2</sup>	Deformation, %	Ultimate Tensile Strength, tons/in. <sup>2</sup> †	Elongation on 4√A, %
440	17.9	62	...	...
575	2.02	28	...	...
585	6.08	68	...	...
600	6.82	45	...	...
620	6.82	56	14.4	4
640	5.68	68	18.4	11
640	6.08	68	16.1	7
645	6.82	45	13.4	4
656	4.54	39	7.2	1
660	3.41	28	...	...
665	4.54	45	11.2	2
665	5.68	50	14.4	4
665	6.82	62	18.1	10
670	2.02	34	...	...
670	6.08	74	12.0	4
675	2.43	50	10.7	2
690	4.54	39	12.4	4
690	5.68	50	11.4	3
700	2.27	50	...	...
700	3.41	50	12.2	8
725	2.02	45	10.4	4
725	6.82	58	16.2	8
745	6.82	68	16.7	12
770	2.27	50	11.9	6
770	6.82	68	19.2	21
775	1.14	34	...	...
800	1.71	39	...	...
800	2.27	39	10.4	3
845	1.14	34	9.6	4
850	9.09	79	26.1	48 *

\* Fracture remote from the weld.

† Where no tensile-strength values are given, the joint was insufficiently strong to withstand machining.

The joint strength throughout has, therefore, been related to the deformation at the weld; pressure and temperature, though detailed in the relevant tables, are regarded as subsidiary factors.

The diameter of the test-piece can also influence the apparent tensile strength of a joint if, as may well be the case, welding is not uniform over the whole cross-section of the joint, owing to the difference in relative flow over the section under pressure. To estimate this effect, three welds were made in silicon bronze under conditions known to give incomplete recrystallization, and hence low strength, and test-pieces 0.500, 0.400, and 0.325 in. in dia., respectively, were machined therefrom. The weld strength varied only from 8.4 to 8.6 tons/in.<sup>2</sup>, and thus it was apparent that provided the tensile test-piece did not contain any of the oxide film which always occurred around the perimeter of a joint, the strength was uniform across the whole weld interface.

#### V.—PRESSURE-WELDING TESTS ON COMMERCIAL ALLOYS.

##### *Copper.*

The deformation/tensile strength relationship for pressure welds in deoxidized non-arsenical copper is shown in Fig. 3, compiled from results given in Table IV. Strong joints were formed without difficulty at temperatures above about 300° C.; and at 400° C. and over, the amount of deformation required was between 5 and 10%, which indicates the ease with which this material responds to pressure welding. The welding pressure needed for the necessary deformation fell from some 10 tons/in.<sup>2</sup> at 400° C. to about 0.5 ton at 500° C. The results obtained were similar to those reported by Cook and Davis in 1947,<sup>8</sup> regarding the pressure welding of H.C. copper. Joint formation was the result of recrystallization across the interface, and the extent to which this had taken place in any sample was related directly to the strength of the weld. In those welds having tensile strengths of 14.5 tons/in.<sup>2</sup> or more, recrystallization across the interface was complete, and in many instances the line of the weld could not be detected with certainty.

##### *Brasses.*

At temperatures below 600° C. joints made in 85 : 15 brass were of poor quality, even when the pressures used were sufficiently high to effect deformations as great as 65%, but with similar deformations at 800° C., the joints formed were clean and strong. This amount of deformation (65%) seemed to be the minimum required for the production of strong joints in this alloy, as indicated by the deformation/strength

TABLE IV.—*Deformation/Weld-Strength Relationship for Deoxidized Non-Arsenical Copper.*

Welding Conditions		Deformation during Welding, %	Weld Strength, tons/in. <sup>2</sup>	Elongation on $4\sqrt{A}$ , %
Temperature, °C.	Pressure, tons/in. <sup>2</sup>			
300	10.0	11.1	6.5	12.0
	10.0	12.0	4.0	3.0
400	5.0	4.0	6.0	6.0
	5.0	4.0	9.3	12.5
	10.0	23.0	14.2	42.5
	10.0	24.0	15.1	48.0
500	2.5	4.0	6.0	4.0
	2.5	4.0	6.5	5.0
	5.0	10.0	11.4	18.0
	5.0	10.0	12.8	22.0
	7.5	34.0	14.4	42.5
	7.5	35.0	14.6	48.0
600	2.5	5.0	10.6	14.5
	2.5	5.0	11.1	19.0
	3.0	5.0	13.6	32.0
	4.0	23.0	14.4	42.5
	4.0	24.0	14.0	41.0
700	0.5	2.0	6.0	7.0
	1.0	2.0	10.6	9.0
	1.0	2.0	11.1	10.0
	0.5	3.0	7.0	10.0
	1.5	6.0	14.8	40.0
	1.5	6.0	15.1	42.0
	2.0	7.0	14.4	48.0
	2.5	28.0	14.4	46.0
800	0.25	1.0	6.5	9.0
	0.25	1.0	7.5	8.0
	0.5	7.0	10.0	14.0
	0.5	9.0	11.4	19.5
	1.0	12.0	14.5	40.0
	1.0	14.0	14.4	38.0
	1.5	28.0	14.2	37.0
	1.5	33.0	14.0	44.0
900	0.25	2.0	10.7	10.0
	0.25	2.0	11.2	12.0
	0.5	6.0	13.1	30.5
	0.5	7.0	14.5	46.0
	1.0	20.0	14.4	48.0

curve in Fig. 4 (Table V). Fracture on tensile testing usually took place through the joint, even though the strength of the joint was that of the fully annealed parent metal, and as a result of this mode of failure, elongation values were lower than those for annealed stock,



Welds made under optimum conditions had recrystallized completely across the interface, and only small well-dispersed traces of oxide indicated the line of the joint (see Fig. 15, Plate IX).

$\alpha/\beta$  Brasses are more suitable for hot working than  $\alpha$  alloys, a feature reflected by the ease with which quite high deformation could be obtained under light pressures at temperatures as low as 475° C., in pressure-welding trials with 60 : 40 brass. Joint strength, however, was poor at temperatures below about 525° C., when joints made with deformations of 50–60% failed on tensile testing through the joint area, because recrystallization across the interface was not complete. In the temperature range 525–660° C., sound, strong welds were formed

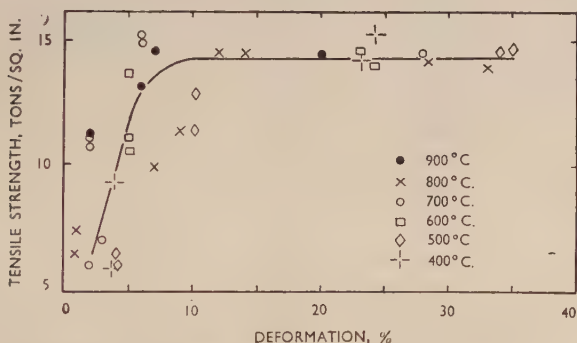


FIG. 3.—Pressure Welding of Deoxidized Non-Arsenical Copper. Deformation/weld-strength relationship.

with deformations of the order of 70% and data relating to these joints are given in Table VI and Fig. 5. Recrystallization was complete, and the location of the joint was not readily visible, either in micro-sections (see Fig. 16, Plate IX) or on tensile testing. Kinzel<sup>9</sup> has stated that pressure welding is facilitated if phase changes occur during the temperature cycle of the pressure-welding operation, and it may therefore be significant that with the  $\alpha/\beta$  alloys, pressure welds were more easily made at temperatures above 525° C., at which quite significant changes in the  $\alpha : \beta$  ratio take place. In pursuing this matter further, attempts were made to pressure weld the 60 : 40 alloy at about 800° C., where only the  $\beta$  phase exists, but owing to the method of heating adopted, marked volatilization of zinc and local overheating occurred, and satisfactory joints could not be made.

In general, the pressure-welding characteristics of the leaded brass were not significantly different from those of 60 : 40 brass; full joint strength was obtained with deformations of some 70%, and the minimum

TABLE V.—*Deformation/Weld-Strength Relationship for 85 : 15 Brass.*

Welding Conditions		Deformation during Welding, %	Weld Strength, tons/in. <sup>2</sup>	Elongation on $4\sqrt{A}$ , %
Temperature, ° C.	Pressure, tons/in. <sup>2</sup>			
525	16.0	63.0	Failed in machining	
575	16.0	65.0	Failed in machining	
630	12.0	60.0	10.2	4.0
	12.0	65.0	10.9	5.0
	12.5	72.5	18.4	25.0
685	8.0	48.5	8.6	3.0
	9.5	61.0	12.3	7.0
	9.5	67.0	17.0	23.0
735	8.0	51.0	Failed in machining	
	8.0	59.0	11.7	7.0
	8.5	67.0	17.2	43.0
	9.5	70.0	17.8	19.0
	9.5	78.0	17.9	16.0
790	3.0	43.0	7.7	4.0
	3.2	51.0	13.9	5.0
	4.0	52.5	13.9	7.0
	4.0	55.5	13.2	7.0
	5.0	63.0	15.7	6.0
	5.0	63.5	16.8	17.0
	5.5	72.5	17.6	19.0
	6.5	76.0	17.1	20.0
	6.5	76.5	17.2	21.0
840	1.2	47.0	15.0	19.0
	1.5	60.0	17.4	60.0 *
	1.5	63.5	16.6	30.0
	3.0	71.0	17.3	25.0
	3.0	71.0	17.4	20.0
	3.0	74.0	17.6	28.0

\* Fracture remote from weld.

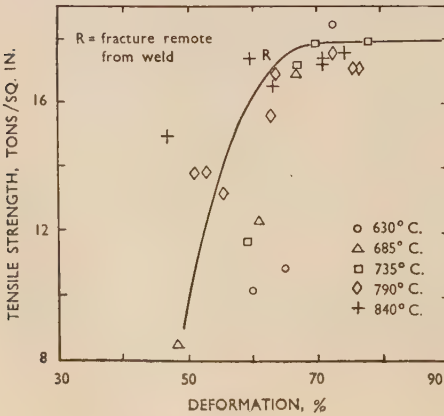


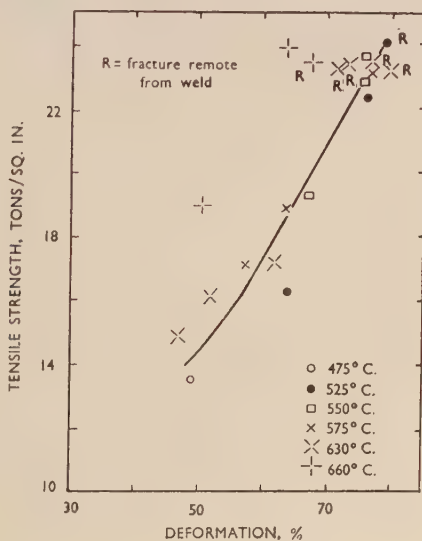
FIG. 4.—Pressure Welding of 85 : 15 Brass. Deformation/weld-strength relationship.

TABLE VI.—Deformation/Weld-Strength Relationship for 60 : 40 Brass.

Welding Conditions		Deformation during Welding, %	Weld Strength, tons/in. <sup>2</sup>	Elongation on $4\sqrt{A}$ , %
Temperature, °C.	Pressure, tons/in. <sup>2</sup>			
475	6.5	49.0	13.5	2.0
525	9.0	63.5	16.3	9.0
	9.5	76.0	22.4	18.0
	9.5	79.0	24.1	20.0 *
550	6.0	67.0	19.4	12.0
	6.5	75.5	22.9	33.0
	6.5	76.5	23.7	45.0
575	4.5	57.0	17.1	10.0
	5.0	64.0	18.9	20.0
	5.0	76.5	23.3	43.0
630	1.0	34.0	Broke before testing	
	1.2	47.0		
	1.5	52.0	14.9	4.0
	1.5	61.5	16.1	4.0
	3.0	71.5	17.2	11.0
	3.0	72.0	23.4	43.0 *
	3.0	76.5	23.4	43.0 *
	3.0	79.0	23.6	46.0 *
660	1.0	50.5	23.3	43.0 *
	1.5	63.5	19.0	6.0
	1.5	67.5	24.0	11.0
			23.6	30.0 *

\* Fracture remote from weld.

FIG. 5.—Pressure Welding of 60 : 40 Brass. Deformation/weld-strength relationship.



temperature to permit joint formation was around 500° C. (Table VII and Fig. 6). Recrystallization took place across the interface, and the lead distribution and particle-size were not markedly affected by heating to welding temperature. Fracture on tensile testing often occurred remote from the weld, with joint strengths similar to that of the annealed parent metal.

TABLE VII.—*Deformation/Weld-Strength Relationship for Leaded Brass (Copper 57, Zinc 40, Lead 3%).*

Welding Conditions		Deformation during Welding, %	Weld Strength, tons/in.*	Elongation on $4\sqrt{A}$ , %
Temperature, °C.	Pressure, tons/in.²			
475	3.0	59.0	17.2	3.0
500	3.0	58.0	18.4	4.0
	3.0	62.5	21.4	6.0
	3.0	68.5	23.2	7.0
	3.2	70.5	27.2	15.0
	3.5	81.0	26.3	17.0 *
525	1.2	41.0	13.6	2.0
	1.5	52.0	17.3	3.0
	1.5	60.0	21.9	9.0
	2.5	67.5	24.6	14.0
	2.5	74.0	26.6	21.0
	3.5	77.5	27.1	21.0 *
	3.5	80.5	26.2	19.0 *
550	1.0	45.0	15.0	3.0
	1.0	48.5	15.5	3.0
	1.5	60.0	20.0	6.0
	1.5	61.0	18.9	5.0
	1.5	67.5	23.0	10.0
	2.5	72.0	25.3	14.0
	2.5	72.5	24.0	7.5 *
	2.5	74.0	25.4	9.0
	2.5	78.0	25.6	19.0 *

\* Fracture remote from weld.

#### *Phosphor Bronzes.*

Both the 93 : 7 and 91 : 9 phosphor bronzes responded readily to pressure welding, and, with the alloy lower in tin, deformations of the order of 50% produced joints the strengths of which exceeded 20 tons/in.², although high welding pressures of some 20 tons/in.² were required. Despite the high joint strength of welds made under these conditions, recrystallization was not complete, and superior joints were produced at higher temperatures. Optimum results for the 7% tin alloy, both in respect of joint strength and recrystallization, were associated with

deformations between 50 and 60%, irrespective of temperature over the range 525°–685° C. investigated, as shown in Fig. 7 and Table VIII. Welds made under these conditions, which always required welding pressures of 6 or more tons/in.<sup>2</sup>, fractured away from the joint on testing, with strength values between 24 and 26 tons/in.<sup>2</sup> The microstructure of a typical joint in the 93 : 7 alloy is shown in Fig. 17 (Plate IX). With the 91 : 9 alloy (Fig. 8 and Table IX) somewhat higher deformations

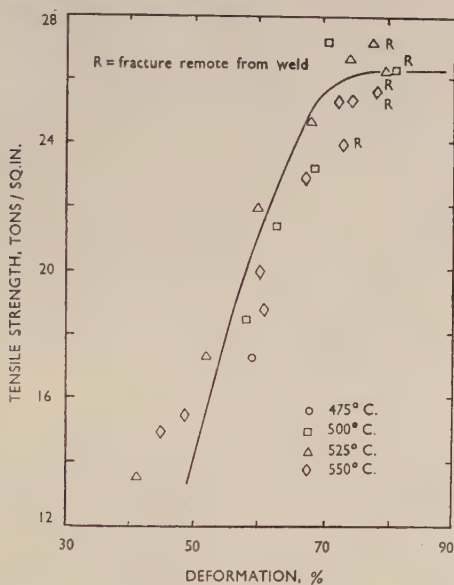


Fig. 6.—Pressure Welding of a Leaded Brass. Deformation/weld-strength relationship.

of 60% were required to develop full joint strength, and here pressures needed to ensure adequate deformation, and therefore high joint strength, were 8 tons/in.<sup>2</sup> or more.

### Cupro-Nickels.

With the cupro-nickel alloys containing 20 and 30% of nickel, preliminary trials indicated that appreciable deformation could be obtained only under very high pressure, unless the temperatures were raised to 1000° C. Above 1000° C., with the 70 : 30 alloy, weld strengths of 24–25 tons/in.<sup>2</sup> were readily obtained with deformations varying from 17 to 24% (see Table X and Fig. 9). In all instances, strong joints were associated with complete recrystallization across the interface



TABLE VIII.—*Deformation/Weld-Strength Relationship for 93 : 7 Phosphor Bronze.*

Welding Conditions		Deformation during Welding, %	Weld Strength, tons/in. <sup>2</sup>	Elongation on $4\sqrt{A}$ , %
Temperature, °C.	Pressure, tons/in. <sup>2</sup>			
420	20.0	17.0	17.2	7.0
	20.0	41.0	23.6	25.0
470	18.0	22.0	14.4	3.0
	18.0	34.0	23.8	25.0
525	14.0	26.0	18.6	5.0
	16.0	45.0	25.3	62.0 *
	18.0	50.0	24.8	26.0
	18.0	52.5	24.5	63.0 *
	18.0	59.0	25.4	60.0 *
	18.0	67.0	25.6	62.0 *
580	12.0	26.0	20.1	16.0
	12.0	26.0	19.7	16.0
	14.0	39.0	22.3	26.0
	16.0	56.0	24.9	57.0
	16.0	58.0	24.7	60.0
	16.0	60.0	24.5	24.0
630	6.0	14.0	11.3	4.0
	6.4	26.0	21.2	29.0
	8.0	34.0	21.6	29.0
	9.6	52.5	25.1	70.0 *
	9.6	56.0	24.5	65.0 *
	12.0	60.5	24.6	47.0
685	6.4	37.0	22.1	31.0
	6.4	62.5	25.1	70.0 *

\* Fracture remote from weld.

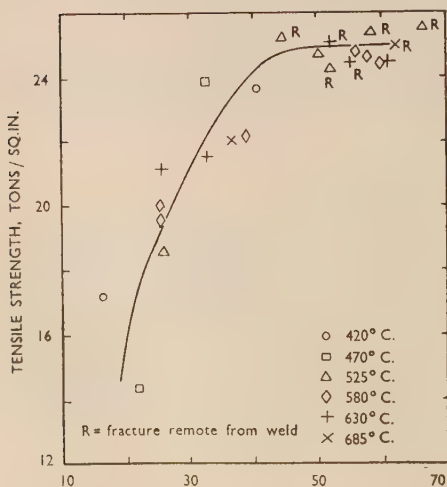


FIG. 7.—Pressure Welding of 93 : 7 Phosphor Bronze. Deformation/weld-strength relationship.

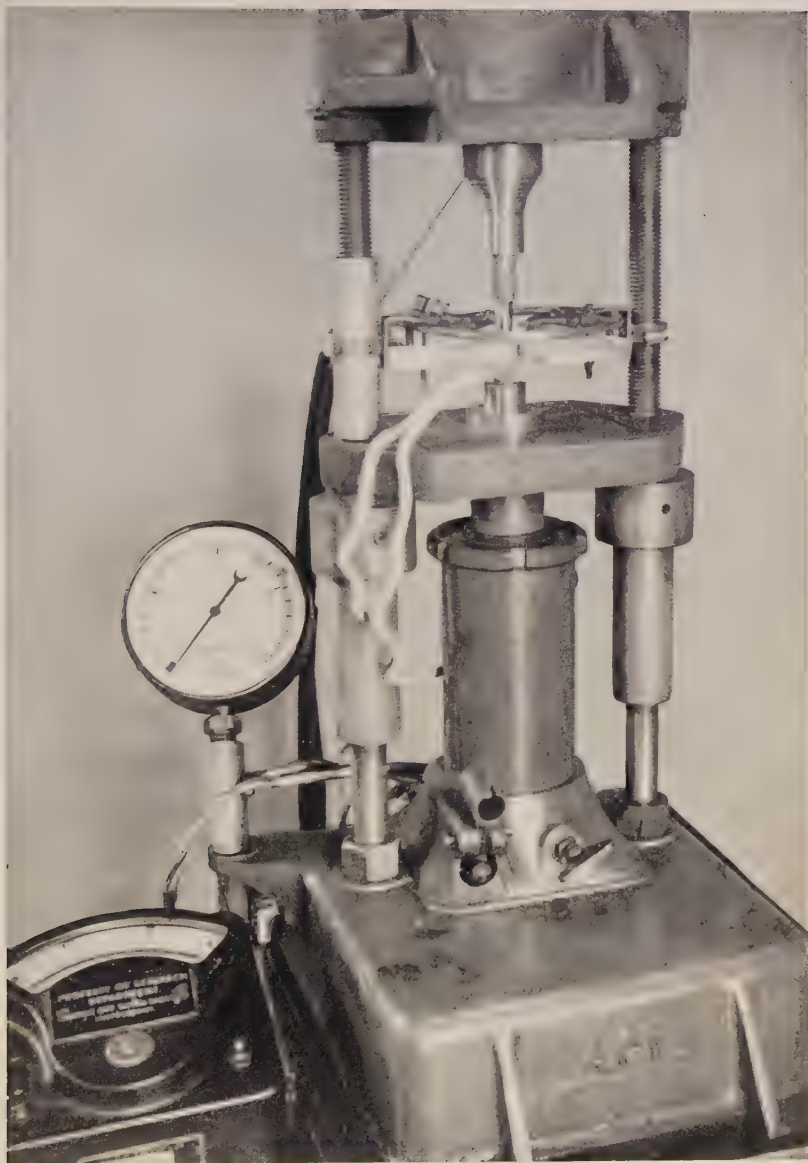


FIG. 12.—General Arrangement of Equipment for Pressure Welding.

[To face p. 200.]



FIG. 13.—Oxy-Acetylene Burner for Heating Test-Pieces.

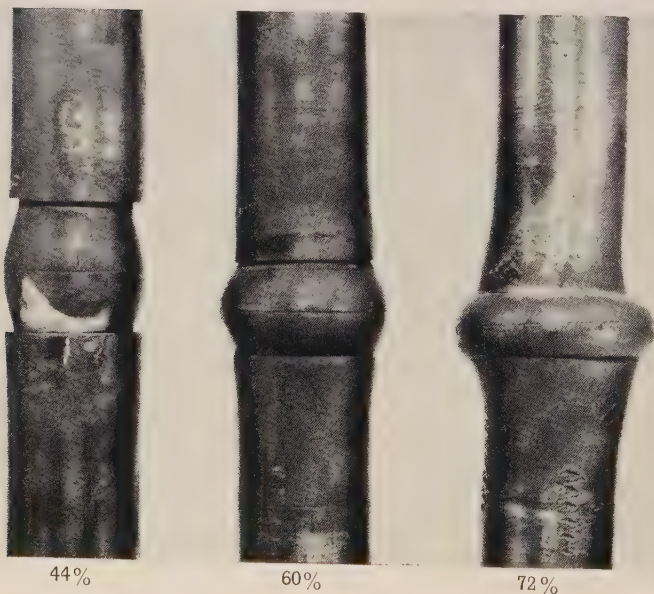
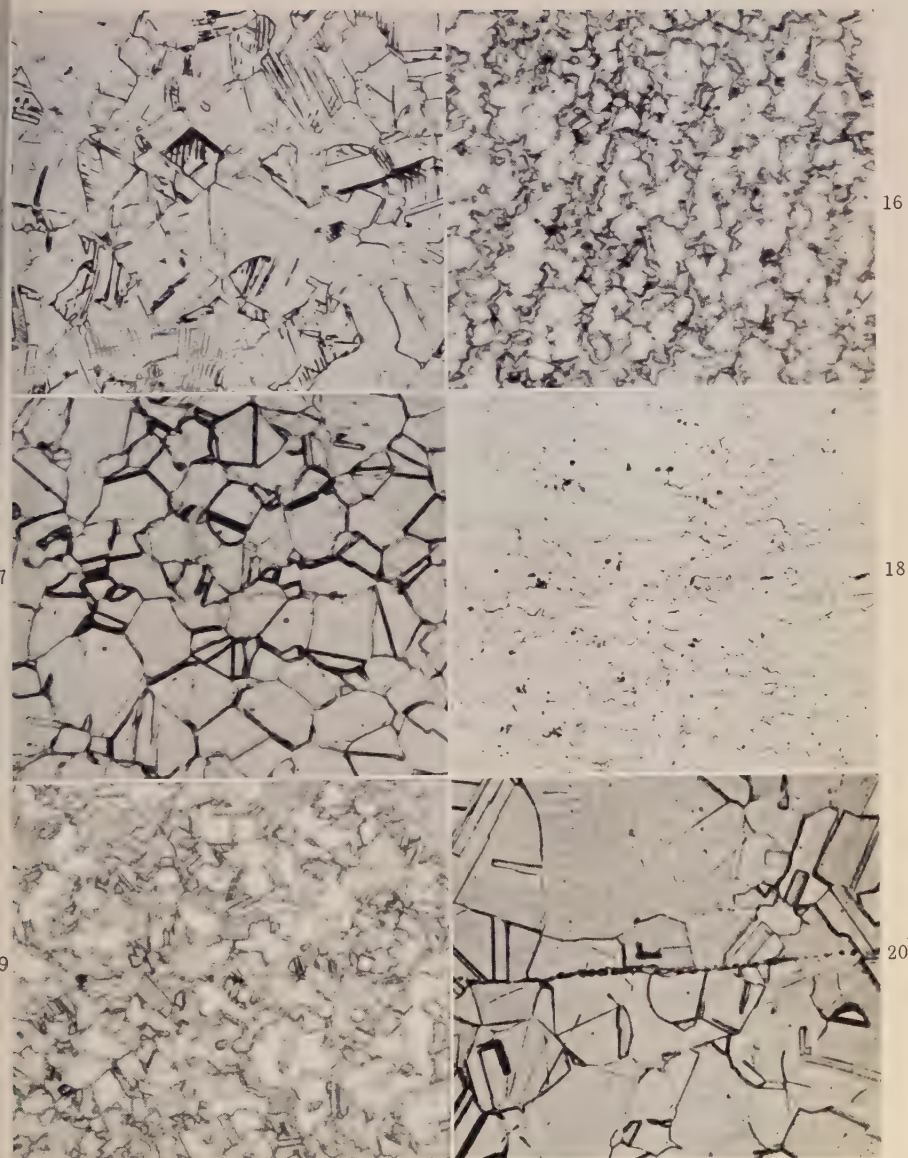


FIG. 14.—Examples of Deformation in Pressure Welding.



FIGS. 15-20.—Structures of Pressure Welds in Copper-Base Alloys.  $\times 200$ .

FIG. 15.—85 : 15 Gilding metal.

FIG. 17.—93 : 7 Phosphor bronze.

FIG. 19.—Silicon bronze.

FIG. 16.—60 : 40 Brass.

FIG. 18.—70 : 30 Cupro-nickel.

FIG. 20.—93 : 7 Aluminium bronze.





TABLE IX.—*Deformation/Weld-Strength Relationship for 91 : 9 Phosphor Bronze.*

Welding Conditions		Deformation during Welding, %	Weld Strength, tons/in. <sup>2</sup>	Elongation on $4\sqrt{A}$ , %
Temperature, °C.	Pressure, tons/in. <sup>2</sup>			
615	10.0	61.0	27.4	55.0
	10.0	65.5	28.0	60.0
	10.5	69.5	27.1	53.0 *
	10.5	73.5	27.3	48.0
680	6.0	31.0	19.5	16.0
	6.0	31.0	21.8	24.0
	6.5	52.0	22.5	22.0
	6.5	57.5	26.4	58.0
	7.0	65.0	25.9	54.0 *
	8.0	65.5	28.0	60.0
	8.0	68.0	27.2	52.0
	8.0	69.0	25.0	77.0
	8.0	73.5	26.7	70.0

\* Fracture remote from weld.

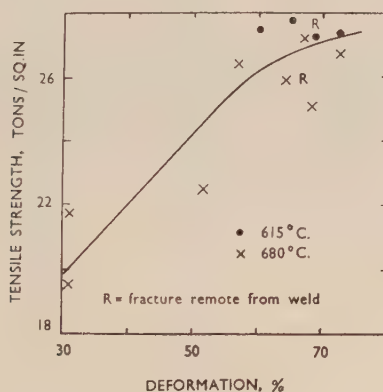


FIG. 8.—Pressure Welding of 91 : 9 Phosphor Bronze. Deformation/weld-strength relationship.

(see Fig. 18, Plate IX), which took place at temperatures between 1025° and 1125° C. with welding pressures varying with temperature from 1.5 to 18 tons/in.<sup>2</sup> The amount of work carried out on the 80 : 20 alloy was more restricted in scope, but again the results indicated that joints could be made at temperatures of 1050° C. or more, with deformations of the order of 30% (Table XI and Fig. 9).

TABLE X.—*Deformation/Weld-Strength Relationship for 70 : 30 Cupro-Nickel.*

Welding Conditions		Deformation during Welding, %	Weld Strength, tons/in. <sup>2</sup>	Elongation on $4\sqrt{A}$ , %
Temperature, °C.	Pressure, tons/in. <sup>2</sup>			
975	10.0	39.0	} Failed in machining	
	12.0	44.0		
	13.0	48.0		
1025	1.5	7.5	18.1	10.0
	1.5	17.0	24.2	34.0
	5.5	33.0	24.6	40.0 *
	6.5	43.0	25.0	44.0 *
	10.0	48.0	25.8	42.0 *
1035	12.0	57.0	25.1	38.0 *
1075	1.5	14.0	23.7	44.0 *
	1.5	17.0	22.9	18.0
	2.5	38.0	24.3	39.0 *
	3.0	44.0	24.4	44.0 *
	5.0	55.0	25.1	44.0 *
	6.5	59.0	25.0	43.0 *
	10.0	63.0	25.0	38.0 *
1100	5.0	54.0	24.5	41.0 *
	6.5	57.0	24.0	35.0 *
	6.5	60.0	25.1	46.0 *
	7.0	68.5	25.2	37.0 *
1125	2.0	29.0	24.1	41.0 *
	3.0	44.0	24.7	41.0 *
	4.0	52.5	24.5	39.0 *
	5.0	59.0	24.7	37.0 *
	5.0	62.0	25.1	36.0 *
	6.5	64.0	24.5	39.0 *
	6.5	68.0	24.8	40.0 *
	7.0	71.5	24.9	38.0 *
	8.0	74.0	24.3	...
1160	10.0	80.0	24.0	8.0 *

\* Fracture remote from weld.

*Silicon Bronze.*

Joint strengths of pressure welds in silicon bronze exceeded 20 tons/in.<sup>2</sup> when the deformation was 70% or more (Fig. 10 and Table XII). Welding took place at temperatures of 650° C. or over, and the welding pressure required to form strong joints decreased as usual with the increase in welding temperature. At temperatures lower than 650° C. complete recrystallization was rarely obtained, but at higher tempera-

TABLE XI.—*Deformation/Weld-Strength Relationship for 80 : 20 Cupro-Nickel.*

Welding Conditions		Deformation during Welding, %	Weld Strength, tons/in. <sup>2</sup>	Elongation on $4\sqrt{A}$ , %
Temperature, ° C.	Pressure, tons/in.*			
1050	4.0	29.0	20.8	24.0
	6.0	46.0	22.1	32.0
	6.0	57.0	21.2	21.0
	6.5	66.0	21.7	34.0 *
1100	6.0	66.0	20.9	16.0
	6.0	72.0	22.2	28.0
	6.0	78.0	21.8	32.0 *
	6.0	78.0	21.9	32.0 *
1200	4.0	80.0	22.2	29.0 *

\* Fracture remote from weld.

tures, and with suitable deformation, recrystallization across the interface was complete (see Fig. 19, Plate IX), although there was often some slight indication of the interface.

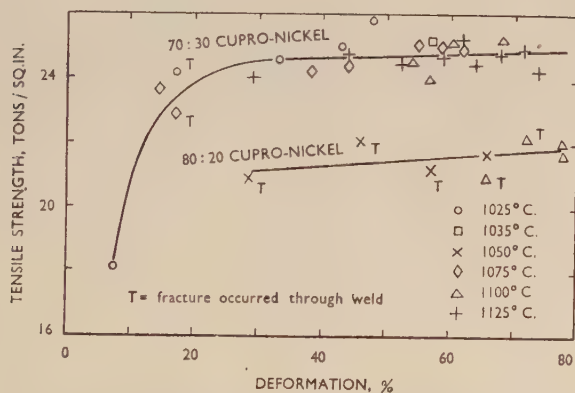


FIG. 9.—Pressure Welding of 70 : 30 and 80 : 20 Cupro-Nickel. Deformation/weld-strength relationship.

### Aluminium Bronze.

Of the alloys included in the investigation, aluminium bronze was the least responsive to pressure welding, and the erratic nature of the tensile-test results on joints made in this material is well illustrated by

TABLE XII.—*Deformation/Weld-Strength Relationship for Silicon Bronze.*

Welding Conditions		Deformation during Welding, %	Weld Strength, tons/in. <sup>2</sup>	Elongation on $4\sqrt{A}$ , %
Temperature, °C.	Pressure, tons/in. <sup>2</sup>			
615	20.0	66.5	15.7	7.0
	20.0	73.0	21.1	23.0
	28.5	79.0	24.1	27.0
650	12.9	66.0	20.7	9.0
	15.7	67.5	22.1	28.0
	15.7	74.0	24.3	43.0
	15.7	76.5	25.7	48.0
	15.7	77.0	26.1	54.0 *
	15.7	80.0	24.2	51.0 *
700	14.3	79.0	24.9	54.0 *
725	6.4	63.0	16.6	12.0
	8.1	68.0	20.8	18.0
	9.9	73.0	22.0	20.0
	9.9	73.0	22.4	24.0
	6.4	74.0	24.6	48.0
	6.4	77.0	24.2	45.0
	10.7	77.0	25.3	38.0
750	3.2	38.0	7.77	2.0
	2.4	54.0	13.0	12.0
	3.2	63.5	16.9	21.0
775	2.4	50.5	11.0	3.0
	2.4	56.0	11.5	8.0
	3.2	56.0	11.7	7.0
	2.4	61.5	14.9	16.0
	2.4	62.0	14.3	18.0
	3.2	63.0	15.6	16.0
	8.9	78.0	26.1	48.0 *
800	2.4	35.5	6.85	0.5
	2.4	48.0	9.68	5.0
	2.4	50.5	8.80	5.0
	2.4	52.0	7.8	8.0
	2.4	56.5	10.6	7.0
	2.4	56.5	11.1	9.0
	2.4	56.5	12.8	13.0
	2.4	61.0	16.4	19.0
	2.4	65.0	15.9	16.0
	2.4	67.0	16.6	19.0
	3.2	70.0	20.3	28.0
	4.8	72.5	21.2	66.0
	4.8	80.0	25.7	58.0 *
820	6.4	73.0	22.1	14.0

\* Fracture remote from weld.

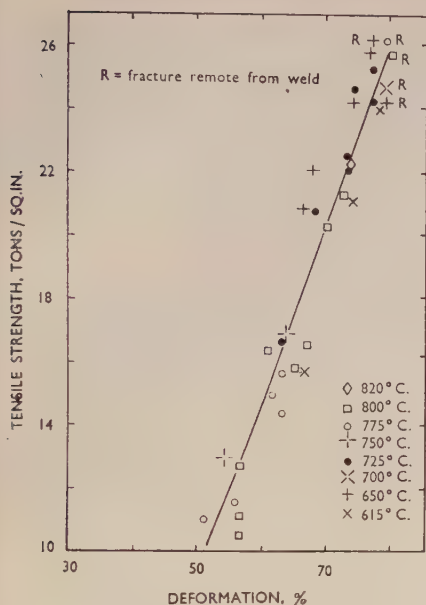


FIG. 10.—Pressure Welding of Silicon Bronze. Deformation/weld-strength relationship.

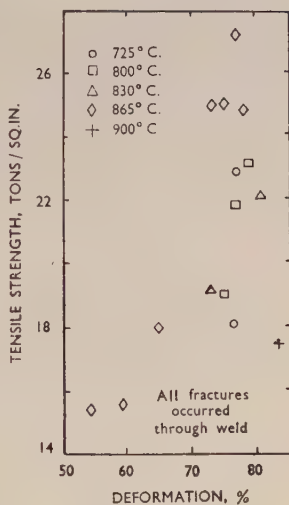


FIG. 11.—Pressure Welding of 97:3 Aluminium Bronze. Deformation/weld-strength relationship.

TABLE XIII.—Deformation/Weld-Strength Relationship for 97:3 Aluminium Bronze.

Welding Conditions		Deformation during Welding, %	Weld Strength, tons/in. <sup>2</sup>	Elongation on $4\sqrt{A}$ , %
Temperature, °C.	Pressure, tons/in. <sup>2</sup>			
725	25.0	76.5	18.1	6.0
	25.0	77.5	22.9	6.0
800	17.0	75.0	19.1	6.0
	17.0	77.0	21.9	6.0
	20.0	79.0	23.2	8.0
830	17.0	74.0	19.4	6.0
	22.0	81.0	22.1	4.0
865	11.0	28.0	No joint	
	11.0	42.0		
	12.0	54.5	15.4	14.0
	12.0	59.0	15.6	10.0
	12.5	65.0	18.1	18.0
	14.0	73.5	25.1	36.0
	14.0	75.0	25.1	8.0
	14.0	77.0	27.2	36.0
	14.0	78.5	24.8	6.0
900	14.0	84.0	17.5	7.0



Fig. 11 and Table XIII. In all instances failure on tensile testing occurred through the weld, and this could be attributed to the presence of oxide inclusions at the interface, the primary cause of the formation of unreliable welds. Recrystallization, in fact, took place only where there was no oxide film, as indicated in Fig. 20 (Plate IX), which is in complete contrast with the other illustrations of pressure welds.

#### ACKNOWLEDGEMENT.

The authors wish to acknowledge with gratitude the helpful advice they have received from Dr. Maurice Cook, in the course of the work described in this paper.

#### REFERENCES.

1. A. L. Forbes, *Petroleum Eng.*, 1943, **14**, (6), 190A.
2. A. L. Rustay, A. Crowell, S. M. Jablonski, and C. J. Burch, *Weld. J. (J. Amer. Weld. Soc.)*, 1947, **26**, 129; also *Steel Processing*, 1946, **32**, 782; and *Steel*, 1947, **120**, (2), 88.
3. A. G. Dowson, *J. Inst. Metals*, 1945, **71**, 205.
4. R. F. Tylecote, *Trans. Inst. Weld.*, 1945, **8**, 163.
5. R. F. Tylecote, *Weld. Research* (in *Trans. Inst. Weld.*), 1948, **2**, (5), 94r.
6. R. F. Tylecote, *Weld. Research* (in *Trans. Inst. Weld.*), 1949, **3**, (1), 2r.
7. British Patent Application Nos. 11275/48, 17340/48, 24765/47, 11011/47.
8. M. Cook and E. Davis, *Trans. Inst. Weld.*, 1947, **10**, 178.
9. A. B. Kinzel, *Weld. J. (J. Amer. Weld. Soc.)*, 1944, **23**, 1124.
10. L. R. Carl, *Metal Progress*, 1944, **46**, 102.

# STRESS-CORROSION OF ALUMINIUM-7% MAGNESIUM ALLOY.\*

1249

By E. C. W. PERRYMAN,† M.A., A.I.M., STUDENT MEMBER, and  
S. E. HADDEN,‡ A.I.M., MEMBER.

(Communication from the British Non-Ferrous Metals Research Association.)

## SYNOPSIS.

The stress-corrosion properties of commercial-purity aluminium-7% magnesium alloy have been determined after various ageing treatments. It is shown that there is a close correlation between the continuity of the grain-boundary  $\beta$  precipitate and the stress-corrosion susceptibility when sprayed with 3% sodium chloride solution, maximum susceptibility occurring when this precipitate is apparently quite continuous. It is possible, however, for the material to be susceptible when the precipitate at the grain boundaries is present as separated lakes, though this has only been found to occur after ageing at high temperatures.

Cold work before ageing increases the rate of precipitation and has a profound effect on the stress-corrosion susceptibility. Internal strains set up during precipitation are shown to play no important part in the stress-corrosion mechanism and, moreover, once a continuous grain-boundary network of the  $\beta$  phase is formed, change in the magnesium concentration of the solid solution has little effect. Small additions of zinc decrease the rate of precipitation; once a continuous grain-boundary network is formed, however, the zinc additions have little or no influence on the stress-corrosion susceptibility. Compressive stresses do not promote the advancement of a stress-corrosion crack as do tensile stresses. The rate of penetration of a stress-corrosion crack was found to increase rapidly just before the specimen failed. The stress-corrosion life can be lengthened by cold working the specimen surface after ageing (e.g. buffing, shot-peening, wet-blast, &c.) and an increase is also brought about by reducing the magnesium content at the surface before ageing.

It is shown that stress-corrosion cracking occurs more rapidly when specimens are sprayed with 3% sodium chloride solution than when totally immersed, and that the stress-corrosion life decreases with increasing concentration of sodium chloride. Dissolved oxygen is necessary for stress-corrosion to occur in the aluminium-7% magnesium alloy.

## I.—INTRODUCTION.

THE published work on the stress-corrosion of wrought aluminium-magnesium alloys is largely that of German authors. Many stress-corrosion failures have been produced under laboratory testing conditions, but very few service failures have been reported. Mention should be made, however, of the failures in rivets of aluminium-5% magnesium alloy described by Metcalfe<sup>1</sup> and by George and Chalmers.<sup>2</sup>

\* Manuscript received 24 September 1949. The work described in this paper was made available to members of the B.N.F.M.R.A. in a series of confidential research reports issued over the period 1943-49.

† Investigator, British Non-Ferrous Metals Research Association, London.

‡ Research Assistant, British Non-Ferrous Metals Research Association, London.

From the published work it is clear that in certain structural conditions the aluminium-magnesium alloys are susceptible to stress-corrosion and also to intercrystalline corrosion in the absence of stress. In most of the experiments described in the present paper the aluminium-7% magnesium alloy has been deliberately treated to produce such susceptibility; the results therefore do not apply to the commercially produced alloy, which is relatively immune from susceptibility to stress-corrosion and has given satisfactory service for many years.

The aluminium-7% magnesium alloy has attractive mechanical properties, and the first stages of the work now described were planned to determine the conditions under which advantage could be taken of these properties without fear of stress-corrosion. With this in mind, commercially produced sheet was submitted to stress-corrosion tests after cold working and heat-treatment to simulate a wide range of service conditions. As the investigation proceeded, however, interest in the more fundamental aspects of stress-corrosion increased, and it became desirable to work on material which was originally in the solution-treated condition, rather than in the less easily defined "commercially annealed" state. The present paper summarizes the experimental work; the results form the basis of a detailed theory of the stress-corrosion of aluminium-7% magnesium alloy given in a separate paper.<sup>3</sup>

There is general agreement that structural changes brought about by heat-treatment control the sensitivity of this alloy to stress corrosion.<sup>4, 5, 6</sup> In particular, precipitation of the  $\beta$  phase ( $\text{Mg}_2\text{Al}_3$ )\* in the form of continuous films at the grain boundaries leads to extremely rapid failure in laboratory tests. Althof<sup>7</sup> investigated the relationship between susceptibility to stress-corrosion and the time and temperature of ageing for solution-treated (i.e. supersaturated solid solution) alloys. He showed that ageing times in excess of 4-5 hr. at temperatures in the range 100°-250° C. produced a structure giving extremely rapid failure. Other workers<sup>8, 9</sup> have produced structures giving rapid failure by ageing at temperatures as low as 75° C. for periods up to 14 days or at 50° C. for 81 days.

The stress-corrosion behaviour of solution-treated material not aged at low temperatures is reported to be good.<sup>4, 7</sup> However, the instability of such a structure has led to the development of other more stable structures. German workers have advocated the "string-of-pearls" type of heterogeneous structure as being most resistant to

\* It has been found by X-ray examination that the precipitate formed during ageing at low temperatures is unstable, but is only transformed to the stable form after prolonged ageing.

alteration by low-temperature ageing. In this the  $\beta$  phase is in the form of globules at the grain boundaries as distinct from apparently continuous films. Brenner and Roth<sup>6</sup> have shown that by cooling aluminium-9% magnesium alloy from the solution-treatment temperature at about 30° C./hr. a structure is obtained which is not susceptible to stress-corrosion and which moreover is not altered by further ageing.

Many attempts have been made to obtain structures resistant to stress-corrosion by the addition of various elements. Favourable results are reported, especially with alloys containing about 1% zinc<sup>10</sup> and 0.5% chromium.<sup>6</sup> Althof<sup>7</sup> states that stress-corrosion is not completely prevented by zinc and chromium additions, that chromium is less efficient than zinc, and that the efficiency of zinc additions decreases if the zinc content exceeds 2%.

Another method of increasing the stress-corrosion-resistance is by cladding with an aluminium alloy not affected by elevated temperatures, such as aluminium-zinc alloys containing up to 5% zinc or aluminium-magnesium alloys with less than 3% magnesium.<sup>10</sup> Vosskühler<sup>11</sup> has suggested reducing the magnesium content at the surface by diffusion, thus producing a zone with a low magnesium content which will not be affected by subsequent ageing.

#### *Definition of Stress-Corrosion.*

In this paper the definition of stress-corrosion given in a letter to the *Monthly Journal* of the Institute of Metals by Sutton, Liddiard, Chalmers, and Champion<sup>12</sup> has been adopted. The definition is as follows: "The term stress-corrosion implies a greater deterioration in the mechanical properties of the material through the simultaneous action of static stress and exposure to corrosive environment than would occur by the separate, but additive, action of those agencies".

The German workers seem to have adopted the view that stress-corrosion is merely corrosion in the presence of stress, and their definite statements that stress-corrosion takes place in the aluminium-magnesium alloys must be viewed in this light.

In much of the published work stress-corrosion tests have been carried out by forming strips of material into loops and testing to destruction, with no record of the progress of intercrystalline corrosion in unstressed control specimens in the same corrosive medium.

In the present work unstressed controls have been exposed, so that when a stressed specimen fractured, a corresponding control specimen which had been subjected to corrosion for the same time was removed and its mechanical properties measured. The difference between the ultimate tensile stress of the corroded unstressed control

specimen and the testing stress then gave the loss of strength due to stress-corrosion. Similarly, if a stressed specimen was removed from test before failure, the difference between its residual strength and the residual strength of an unstressed control removed after the same period gave the loss due to stress-corrosion. The difference between an uncorroded specimen and one corroded without stress gave the strength loss due to ordinary corrosion. All ultimate tensile stress measurements were calculated using the original dimensions of the uncorroded test-pieces.

## II.—EXPERIMENTAL DETAILS.

### 1. *Materials Employed.*

Various 18 S.W.G. commercially produced sheets which had been given a heat-treatment at the works to reduce the stress-corrosion susceptibility were used. Chemical analyses are given in Table I.

TABLE I.—*Analysis of Aluminium-7% Magnesium Alloy Sheets.*

Alloy Mark	Mg, %	Mn, %	Fe, %	Si, %	Cu, % *
JQW 1 . .	6.90	0.31	0.32	0.26	0.02
NFO . . .	6.84	0.18	0.20	0.08	0.01
LXU 2 . .	6.70	0.30	0.24	0.15	0.07
MNY . . .	7.40	0.20	0.34	0.16	0.03
KEN . . .	7.34	0.24	0.30	0.20	0.02

\* Determined spectrographically.

When solution-treated material was needed the treatment given was 3 hr. at 420° C. followed by quenching in water at room temperature. All ageing treatments were carried out in an air oven, controlled to  $\pm 2^\circ$  C.

### 2. *Corrosion-Testing Methods.*

#### (a) *Direct Loading.*

Standard 2-in. flat tensile test-pieces (B.S.S. No. 485 (1934), type A) were cut with the long axis perpendicular to the final rolling direction. Except in certain experiments described later, no surface preparation was given other than degreasing by acetone. The specimens were then painted with a chromated lanolin solution except for the 2 in. gauge-length.

Springs which had previously been calibrated on a testing machine were used to stress the specimens. The method is shown in Fig. 1, 32 specimens being carried on each rigid angle-iron frame. The steel springs used were capable of taking maximum loads of 500 or 1000 lb.



without permanent extension, and to prevent corrosion by the salt spray they were coated with chromated lanolin solution. During test the distance between the datum marks on the springs was checked from time to time and changes of more than 0.02 in. (corresponding to 0.05 and 0.1 ton/in.<sup>2</sup> in the specimen for the 500-lb. and 1000-lb. springs, respectively) were corrected. Such adjustments were rarely necessary.

The specimens were sprayed with 3% sodium chloride solution twice daily. Unless otherwise stated, all the stress-corrosion life tests were carried out in an unheated building with doors and windows open, so that although the specimens were protected from rain they were exposed to the natural fluctuations of atmospheric temperature and humidity. Thus in humid weather specimens remained wet continuously, whereas in dry spells they became dry soon after spraying. Further, relatively few failures occurred in dry weather, but when the weather changed and a period of high relative humidity succeeded a dry spell, an unusually large number of specimens failed. Such difficulties were overcome by :

(1) Starting comparative tests at the same time.

(2) Arranging, whenever possible, that the load was such that the failure time was of reasonable length and so likely to include both wet and dry periods.

(3) Exposing specimens in triplicate or quintuplicate.

Unstressed control specimens were exposed at the same time as the stressed specimens.

(b) *Loop Tests.*

Strips cut perpendicular to the final rolling direction were machined to  $5\frac{1}{2} \times \frac{1}{2}$  in., and were bent to the shape shown in Fig. 2 (a). When under test the two ends of the strip were pressed together as shown in

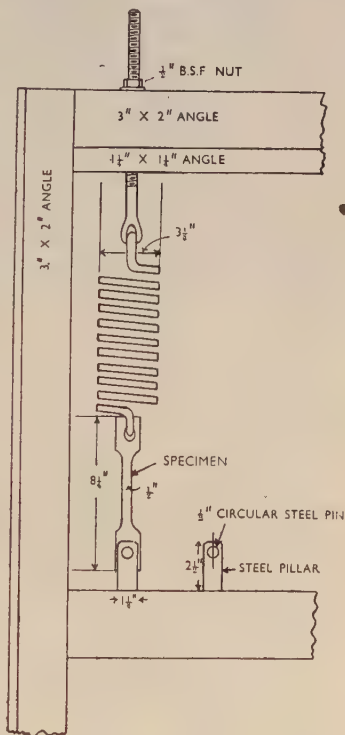


FIG. 1.—Method of Spring-Loading Specimens.

Fig. 2 (b) so that region (a) was in the condition of plastic deformation plus elastic stress and region (b) received an elastic stress with little plastic deformation, the elastic stress decreasing as the distance from (a) increased.

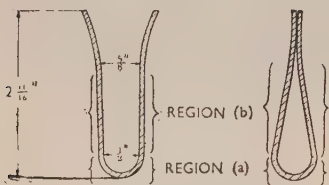


FIG. 2.—(a) Completed Loop.  
(b) Loop with Ends Compressed for Tests.

Unless otherwise stated, the loops were formed after solution-treatment (if any) but before low-temperature ageing treatment, and were corroded either by immersion in 3% sodium chloride solution or by spraying with that solution twice daily.

### (c) *Four-Point Bending.*

In certain experiments specimens were stressed by four-point bending as shown in Fig. 3, the upper surface thus being in tension and the lower surface in compression. The advantage of this method

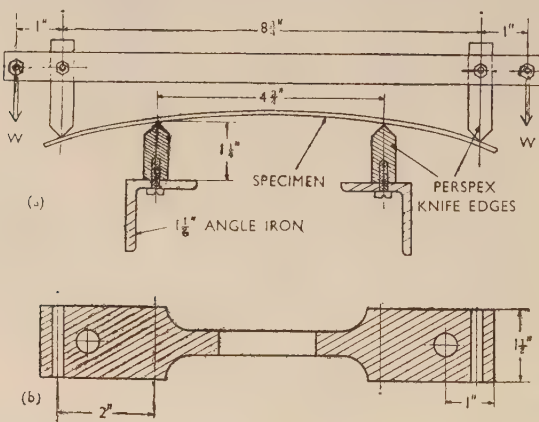


FIG. 3.—(a) Method of Stressing by Four-Point Bending. (b) Diagram of Specimen. Shaded area is painted.

of bending is that between the two centre supports there exists a constant bending moment and hence a constant surface stress if the cross-section is constant. The specimens used were similar to ordinary tensile specimens except that the ends were  $\frac{3}{4}$  in. longer to allow the Perspex knife edges to be located on the wide ends. The specimens were painted with chromated lanolin solution except for the exposed gauge-length. The paint was removed from the parts of the specimen

in contact with the knife edges, and a small quantity of lanolin softened with benzene applied to these areas, in order to reduce friction while still giving protection against corrosion.

The loads required to give various surface stresses were calculated by means of the usual flexural formulæ,<sup>13</sup> and consequently involved all the assumptions on which these formulæ are based.

### III.—EFFECT OF VARIOUS FACTORS ON STRESS-CORROSION SUSCEPTIBILITY.

#### 1. Time and Temperature of Heat-Treatment.

In order to simulate service conditions commercially annealed (as-received) aluminium-7% magnesium sheet was overstrained 10%, given various heat-treatments, and tested for stress-corrosion susceptibility by spring loading at an initial tensile stress of 9.5 tons/in.<sup>2</sup> and spraying with 3% sodium chloride solution. Three stressed and two unstressed specimens in each condition were exposed; one control specimen was removed when the first, and the other when the third stressed specimen failed.

The mechanical properties of specimens in various conditions are given in Table II and the results of the stress-corrosion tests on material aged at temperatures of 100° C. or lower in Table III.

TABLE II.—*Mechanical Properties of As-Received Aluminium-7% Magnesium Alloy After Different Ageing Treatments.*

Each result is the mean of two determinations.

Alloy Mark	Treatment	U.T.S., tons/in. <sup>2</sup>	0.1% Proof Stress, tons/in. <sup>2</sup>	Elongation on 2 in., %
LXU	None	21.2	9.1	25.8
"	10% overstrain	24.0	19.5	14.5
"	" + 24 hr. at 125° C.	22.2	13.3	19.6
"	" + 8 hr. at 200° C.	23.5	11.8	20.0
"	" + 8 hr. at 250° C.	22.7	9.9	18.5
NFO	10% overstrain + 1 week at 175° C.	23.3	10.1	15.8
"	" + 1 week at 200° C.	22.5	8.4	15.5
"	" + 1 week at 212° C.	21.6	8.3	14.9
"	" + 1 week at 225° C.	21.1	8.1	15.5
"	" + 1 week at 250° C.	21.3	8.3	16.3
"	" + 1 week at 267° C.	21.2	8.5	17.1
"	" + 1 week at 284° C.	21.3	8.9	19.3
"	" + 1 week at 300° C.	21.5	9.1	21.8
"	" + 1 week at 350° C.	21.3	8.4	23.3

As the temperature of ageing increased, the time of ageing necessary to produce rapid failure decreased (Table III). Also for a constant

ageing time the susceptibility to stress-corrosion increased with increasing temperature.

Metallographic examination of these specimens showed that as the ageing time or temperature increased the precipitate at the grain boundaries became more continuous, suggesting that the material must be in the heterogeneous condition for stress-corrosion to occur. This is confirmed by the fact that material solution-treated and overstrained 10% withstood a stress of 10 tons/in.<sup>2</sup> (i.e. 88% of the limit of proportionality) for 365 days without any significant loss of strength due to stress-corrosion.

TABLE III.—*Stress-Corrosion Behaviour of As-Received Aluminium-7% Magnesium Alloy LXU After 10% Overstrain and Various Ageing Treatments.*

Initial tensile stress 9.5 tons/in.<sup>2</sup>

Heat-Treatment after 10% Overstrain		Average Life of Specimens Corroded under Stress, days	U.T.S. of Unstressed Corroded Control Specimens, tons/in. <sup>2</sup>	U.T.S. of Unfailed Stressed Specimens, tons/in. <sup>2</sup>	Approx. Loss of Strength due to Stress- Corrosion, tons/in. <sup>2</sup>
Temp., °C.	Time				
20	25 months	No failures up to 382 days	17.5 *	16.5	1.0
50	32 hr.	No failures up to 382 days	17.0	16.7	0.3
"	1 week	"	15.5 *	16.9	nil
"	1 month	"	18.0	16.4	1.6
"	6 months	257	18.3	...	8.8
75	8 hr.	No failures up to 382 days	17.9	17.2	0.7
"	32 hr.	"	17.5	15.9	1.6
"	1 week	536	16.7	...	7.2
"	1 month	24	23.0	...	13.5
100	2 hr.	No failures up to 382 days	18.0	15.7	2.3
"	8 hr.	"	18.5	15.6	2.9
"	32 hr.	335	17.1	...	7.6
"	1 week	19	22.6	...	13.0

\* One control specimen only.

Experiments were also carried out using higher ageing temperatures than those given in Table III. The effect of increasing the ageing temperature for a constant ageing time of 1 week is shown in Fig. 4; as the ageing temperature rises the stress-corrosion life decreases to a minimum and then increases. On raising the temperature still further, a new region of susceptibility appears. To confirm this result a further series of tests was made on another sheet, with the results shown by the dotted line in Fig. 4. The large difference in the behaviour of the two sheets (LXU and NFO) is not necessarily due to

the small difference in magnesium content, for the two sets were not tested at the same time. The results confirm, however, that there is a region of renewed susceptibility after ageing at about 250° C.

The effects of ageing times other than 1 week were also investigated, and in all cases graphs similar to those in Fig. 4 resulted. Complete graphs were not obtained, and it is not possible to say whether regions of renewed susceptibility at higher ageing temperatures occur for ageing periods of other than 1 week. There were indications that this was so for 8-hour ageing periods, though the temperature at which

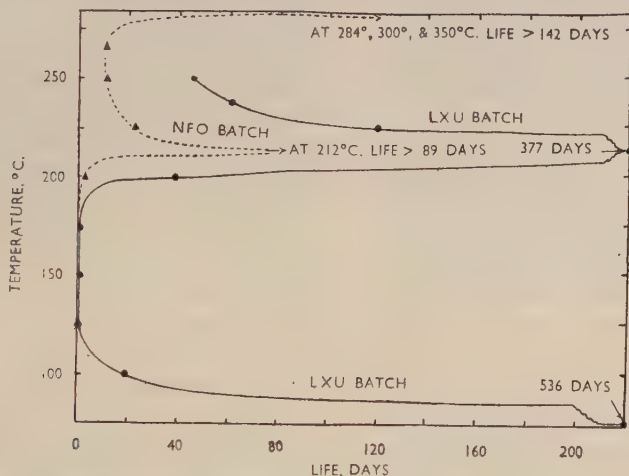


FIG. 4.—Stress-Corrosion Tests of Aluminium-7% Magnesium Alloy after 1 week's artificial ageing. Initial tensile stress 9.5 tons/in.<sup>2</sup>

the renewed susceptibility occurred was higher than for the ageing period of 1 week.

Fig. 4 consists of two loops, and for convenience each loop will be considered separately:

*Ageing Treatments up to 212° C. for 1 Week.*—Metallographic examination showed clearly that as the ageing temperature approached 125°–175° C., the range producing extreme susceptibility, the grain-boundary network of the  $\beta$  phase became more nearly continuous (Fig. 12, Plate X), thus providing a better path for corrosion. On raising the ageing temperature to 200° C. a certain amount of spheroidization occurred, making the grain-boundary network less continuous, and producing a large amount of precipitate within the grains. On increasing the ageing temperature to 212° C. the structure shown in Fig. 13 (Plate X) was obtained, in which there is a very



dense precipitate within the grains, but the grain boundaries themselves are only outlined in a fragmentary way. The increase in life as the  $\beta$  becomes more discontinuous is no doubt due to the time taken to corrode the solid-solution bridges at a relatively slow rate.

*Ageing Treatments above 212° C. for 1 Week.*—In material treated for 1 week at temperatures between 225° and 267° C. the total amount of  $\beta$  precipitate was less than at 212° C., and precipitate at the grain boundaries was again present, not as a continuous film but in the form of small, separated "lakes" (Fig. 14, Plate X). At still higher temperatures the amount of  $\beta$  precipitate decreased, little remaining after treatment at 350° C.

Thus, for ageing temperatures of 212° C. and below, the stress-corrosion susceptibility can be closely correlated with the continuity of the  $\beta$  phase at the grain boundaries, but for temperatures greater than 212° C. this correlation no longer seems to exist. For example, assessing purely on the basis of apparent discontinuity in the  $\beta$  at the grain boundaries, a specimen with the structure shown in Fig. 15 (Plate X) would be expected to have a similar or shorter stress-corrosion life than a specimen with the structure shown in Fig. 14. Instead, the lives were 335 days and 46 days, respectively.

However, material with the structure shown in Fig. 14 has been found to undergo intercrystalline corrosion in the absence of stress (see Fig. 16, Plate XI), and the solid-solution bridges appear to be fairly easily corroded, though the reason for this is unknown. The mechanism of stress-corrosion in material aged at 250° C. for 1 week is probably essentially similar to that in material aged at lower temperatures, the short life being due to (i) the solid-solution bridges being comparatively readily corroded, and/or (ii) the  $\beta$  phase at the grain boundaries being much more continuous than is apparent from a microsection.

From graphs similar to Fig. 4 (for different ageing times) it has been found that for a constant stress-corrosion life the logarithm of the time of ageing is proportional to the reciprocal of the ageing temperature (° K.) (see Fig. 5). The overall activation energy derived from Fig. 5 is 18,000 cal./g.-mol., and the stress-corrosion susceptibility is clearly governed by one or more activation processes. As the stress-corrosion life is dependent on the continuity of the  $\beta$  precipitate at the grain boundary, precipitation within the grains having no effect, each line in Fig. 5 corresponding to a constant stress-corrosion life will represent an equivalent state in the precipitation process at the grain boundary. It therefore appears that the process leading to precipitation at the grain boundaries has a lower activation energy than that for the

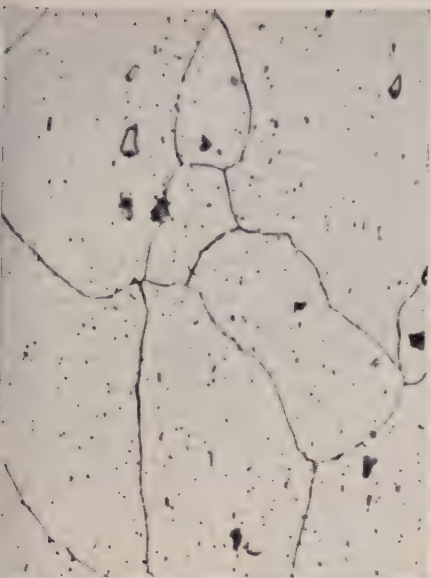


FIG. 12.—As-Received, overstrained 10%, and aged at 125° C. for 1 week. Average life 3 days.  $\times 1000$ .

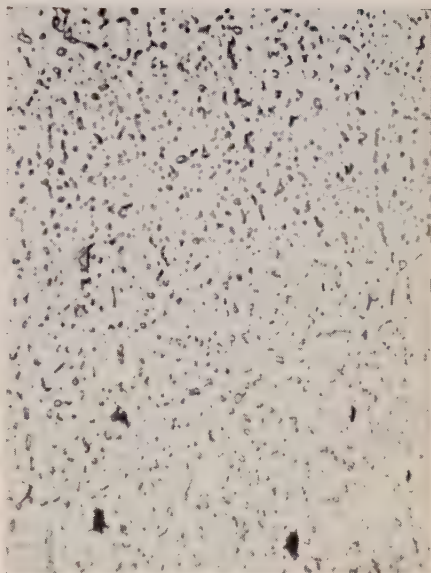


FIG. 13.—As-Received, overstrained 10%, and aged at 212° C. for 1 week. Average life 377 days.  $\times 1000$ .



FIG. 14.—As-Received, overstrained 10%, and aged at 250° C. for 1 week. Average life 46 days.  $\times 1000$ .



FIG. 15.—As-Received, overstrained 10%, and aged at 100° C. for 32 hr. Average life 335 days.  $\times 1000$ .

ALUMINIUM-7% MAGNESIUM ALLOY.

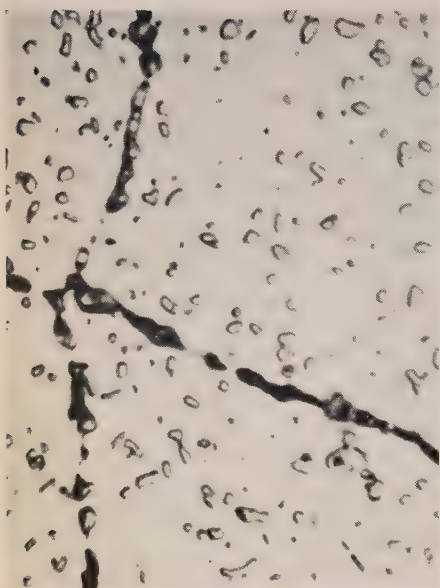


FIG. 16.—Same as Fig. 14, corroded unstressed in 3% sodium chloride for 33 days.  $\times 2000$ .

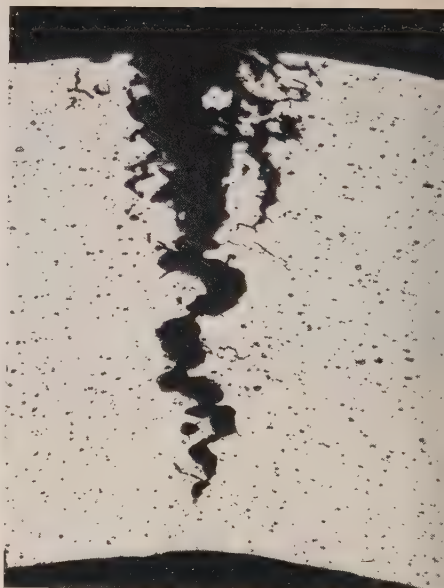


FIG. 17.—Stressed Loop with intercrystalline crack at bend. Alloy JQW1 solution treated, bent, and aged at  $125^{\circ}\text{C}$ . for 24 hr. Immersed in 3% sodium chloride for 45 days.  $\times 50$ .

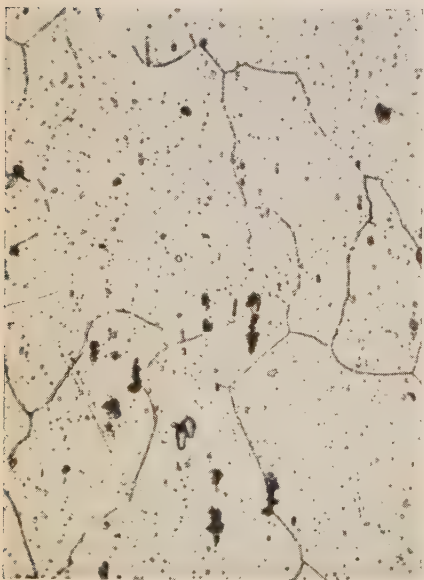


FIG. 18.—Solution-Treated and aged at  $125^{\circ}\text{C}$ . for 24 hr.  $\times 550$ .



FIG. 19.—Solution-Treated, overstrained 2%, and aged at  $125^{\circ}\text{C}$ . for 24 hr.  $\times 550$ .

ALUMINIUM-7% MAGNESIUM ALLOY.

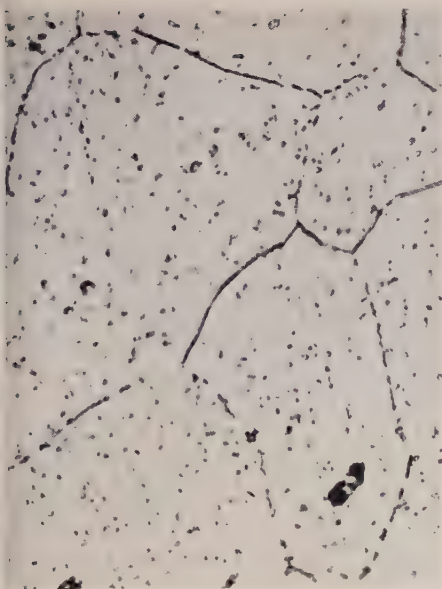


FIG. 20.—Solution-Treated and aged at 200° C. for 16 hr.  $\times 1100$ .

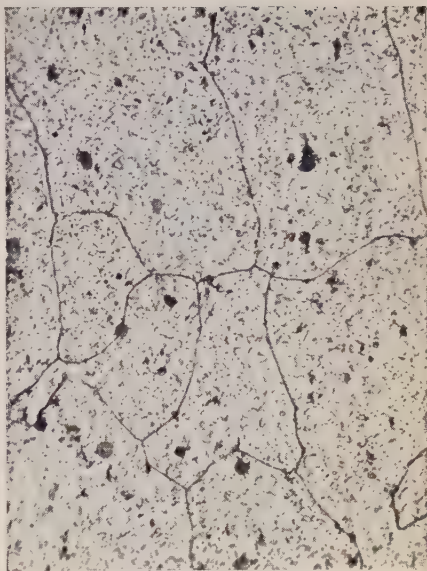


FIG. 21.—Solution-Treated and aged at 200° C. for 24 hr.  $\times 550$ .

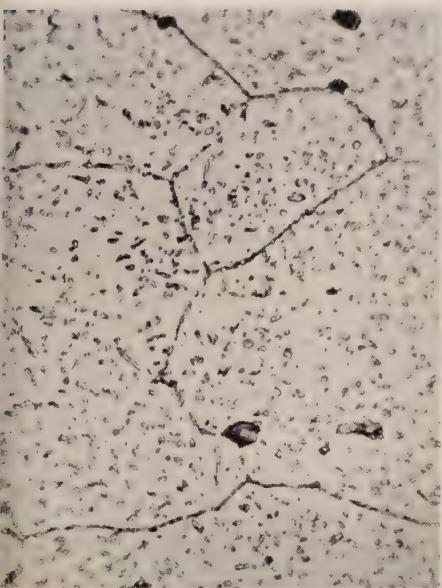


FIG. 22.—Solution-Treated and aged at 200° C. for 2 days.  $\times 1100$ .

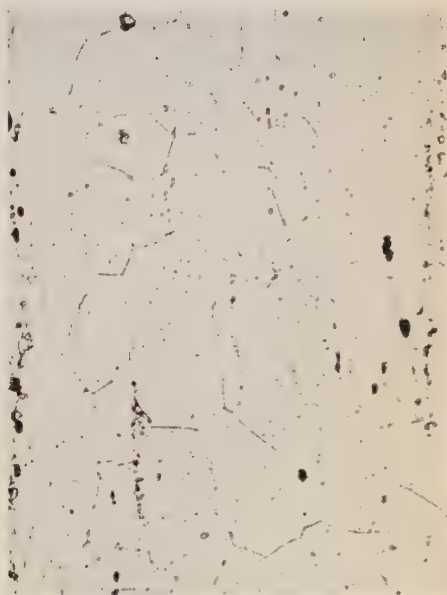


FIG. 23.—Zinc-Free Alloy, solution-treated and aged at 75° C. for 1 day.  $\times 500$ .



ALUMINIUM-7% MAGNESIUM ALLOY.



FIG. 24.—Alloy with 0.5% Zinc, solution-treated and aged at 75° C. for 1 day.  $\times 500$ .



FIG. 25.—Alloy with 1% Zinc, solution-treated and aged at 75° C. for 1 day.  $\times 500$ .



FIG. 26.—Zinc-Free Alloy, solution-treated and aged at 100° C. for 2 days.  $\times 500$ .



FIG. 27.—Alloy with 1% Zinc, solution-treated and aged at 100° C. for 2 days.  $\times 500$ .



diffusion of magnesium in pure aluminium (38,500 cal./g.-mol),<sup>14</sup> leading to precipitation within the grains. This is in agreement with the well-known observation that during the ageing of this alloy precipitation takes place first at the grain boundaries.

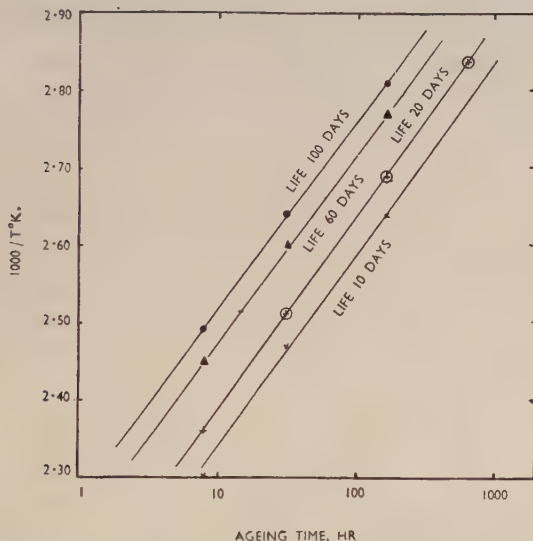


FIG. 5.—Relation Between Reciprocal of Ageing Temperature and Logarithm of Ageing Time for Various Stress-Corrosion Lives. Aluminium-7% magnesium alloy LXU2 overstrained 10% after commercial annealing.

The points plotted are interpolated from graphs of life against temperature for various ageing times (e.g. Fig. 4), except the three ringed points on the 20-day curve which are actual experimental points.

## 2. Corrosive Conditions.

### (a) Concentration of Corrosive Agent.

Loops made from material that had been solution-treated, overstrained 10% in tension, and then aged at 125° C. for 24 hr. were pickled for 4 min. in 10% caustic soda at 60° C., stressed, and immersed in sodium chloride solution of different concentrations. Fig. 6 shows that as the concentration increased the stress-corrosion life decreased, until a concentration of 9% was reached, after which the life remained constant.

### (b) Comparison of Total Immersion with Spraying.

Stress-corrosion loop tests by spraying with 3% sodium chloride solution twice daily and by immersion in 3% sodium chloride solution which was renewed every 4 weeks, gave the results shown in Table IV.

In all cases the cracking was found to be intercrystalline. Fig. 17 (Plate XI) illustrates an intercrystalline crack at the apex of a loop which had been immersed in 3% sodium chloride for 45 days. The material had been solution-treated, bent, and aged for 24 hr. at 125° C., and had an almost continuous grain-boundary  $\beta$  network. Table IV shows that spraying causes more rapid stress-corrosion than

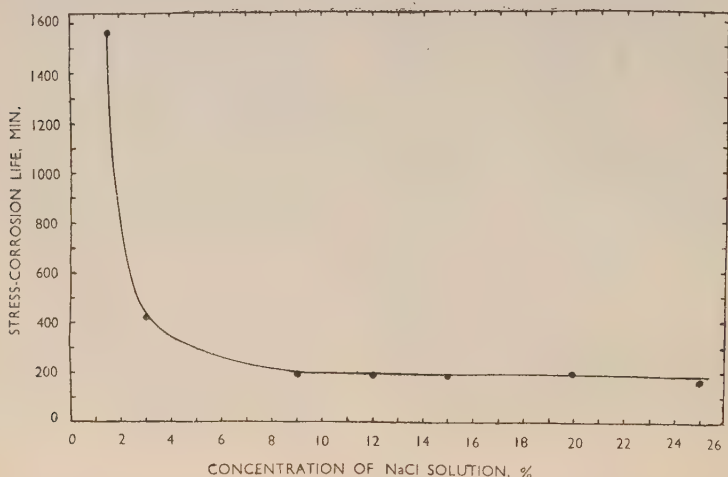


FIG. 6.—Effect of Concentration of Sodium Chloride Solution on Stress-Corrosion Life of Aluminium-7% Magnesium Alloy.

immersion, and this has been confirmed by direct-loading stress-corrosion tests. This difference between immersion and spraying may be because (i) there is more ready access of oxygen to the specimen during spraying than during immersion, and/or (ii) there is an increase in the concentration of the sodium chloride solution as the sprayed specimens dry (see Fig. 6).

TABLE IV.—*Relative Effects of Immersion in and Spraying with 3% Sodium Chloride Solution on Stressed Loops.*

Condition of Alloy Tested	Immersion	Spraying
As received, bent into loop, 24 hr. at 125° C.	Both specimens unfailed after 365 days.	Both specimens failed (in 51 and 59 days, respectively).
Solution-treated, bent into loop, 24 hr. at 125° C.	All three specimens failed, each in 45 days.	All three specimens failed (in 23, 23, and 33 days, respectively).

(c) *Humidity.*

It has been mentioned earlier that at high relative humidities when the specimens remained wet they tended to fail more rapidly than when the corrosive agent dried on the specimens. To determine the magnitude of this effect specimens were tested in a controlled-humidity room. The specimens were solution-treated, overstrained 10% in tension, and then aged for 24 hr. at 125° C., giving continuous grain-boundary  $\beta$  films and high susceptibility to stress-corrosion. All the specimens were tested at a load corresponding to an initial stress of 4.4 tons/in.<sup>2</sup>, with the results given in Table V.

TABLE V.—*Effect of Humidity on Stress-Corrosion of Aluminium-7% Magnesium Alloy NFO.*

Relative Humidity, %	Individual Lives of Specimens, days	Average Life, days
81	2½, 2½, 2½	2½
73-77 *	6, 3, 5	5
71	8, 6, 7	7

\* During the first 3 days the humidity was 73%, and thereafter increased to 77% and remained constant.

Although humidities greater than 81% have not been tried in the controlled-humidity room, tests have been carried out in a small Perspex cabinet with the relative humidity kept at 100%. Few failures occurred under these conditions and then only after long periods. This could be due to the fact that 3% sodium chloride solution becomes diluted at relative humidities greater than 98%, since the stress-corrosion life increases with dilution (see Fig. 6). The rapid failures at relative humidities between 71 and 81% can be explained by the increase in concentration of sodium chloride solution between sprayings. The longer life at relative humidities between 71 and 77% than at 81% (see Table V) is probably due to the fact that below 75% relative humidity the sodium chloride solution dries.

(d) *Oxygen Dissolved in Corrosive Agent.*

To determine whether oxygen dissolved in the corrosive agent was playing a part in the stress-corrosion process, loop tests were carried out in aerated and deaerated 3% sodium chloride. The loops were made from commercial 18 S.W.G. aluminium-7% magnesium sheet which had been solution-treated, overstrained 10% in tension, and aged at 125° C. for 24 hr., which, as noted above, gives a condition very susceptible to stress-corrosion. Deaeration of the solution was carried

out by a method of alternate exposure to reduced pressure and saturation with commercial oxygen-free nitrogen, the pressure over the solutions being reduced by means of a water pump.

Deaeration inhibited cracking; for example, loops failed in aerated solution in a few hours, but in deaerated solution did not fail in 94 days. When air was later drawn over the deaerated solution the loops failed in a few hours. Such experiments show that removal of dissolved oxygen can prevent or greatly retard stress-corrosion. Fuller details of experiments on the effect of dissolved oxygen have been given and the significance of the results discussed by Gilbert and Hadden.<sup>3</sup>

### 3. *Exposed Area.*

To investigate the effect on stress-corrosion life of variation in area of the specimen exposed to corrosion, three sets of specimens were prepared with either 2 in., 1 in., or  $\frac{1}{2}$  in. of the 2-in. gauge-lengths exposed, the remaining surface area being protected by painting. The specimens were cut from as-received sheet, overstrained 10% in tension, and then aged for 24 hr. at 130° C. The load during corrosion corresponded to an initial stress of 9.5 tons/in.<sup>2</sup>, i.e. approximately three-quarters of the 0.1% proof stress. The results are given in Table VI.

TABLE VI.—*Effect of Exposed Area on Stress-Corrosion of Aluminium-7% Magnesium Alloy LXU 2.*

Area Exposed	Individual Lives of Specimens, days	Mean Life, days	Standard Deviation
Set A 2 in. of gauge-length	9, 10, 10, 10, 10, 10, 10, 12	10	0.84
Set B 1 in. of gauge-length	10, 10, 12, 14, 10, 13, 14, 19	13	3.06
Set C $\frac{1}{2}$ in. of gauge-length	10, 12, 12, 28, 10, 16, 44, 45	22	15.0

Statistical analysis of the figures in Table VI shows that the means are significantly different for sets *A* and *B* and for sets *A* and *C*, but the significance is doubtful for sets *B* and *C*. Therefore, under the testing conditions employed, the life becomes greater and the scatter of the results increases as the exposed area decreases.

The most likely explanation of these results is that there exists

on the surface a certain distribution of points at which the susceptibility to stress-corrosion is greater than elsewhere. These may be places where the  $\beta$  phase at the exposed grain boundaries is more continuous or where the grain boundary is more nearly perpendicular to the surface and to the applied stress. The probability of such points occurring in the exposed area will decrease as the exposed area decreases, and thus the stress-corrosion life would increase as the exposed area is decreased. If, however, one of these susceptible points existed in the smallest exposed area, the specimen should fail as quickly as the most susceptible specimen with the largest exposed area. These conclusions are borne out by the results given in Table VI. Set *A* establishes the life of a specimen as 10 days when the largest area, presumed to contain the greatest number of susceptible points, is exposed. Set *B* contains 3 and Set *C* contains 2 specimens which have failed in the same time. Since the number of highly susceptible points will be a linear function of the exposed area, this number will be in the ratio  $2 : 1 : \frac{1}{2}$  or  $8 : 4 : 2$ . Considering specimens with lives of 10 days it is interesting to note that they occur in the ratio  $7 : 3 : 2$ , in good agreement with the ratio of the exposed areas.

#### 4. Surface Condition.

In all experiments so far described the surfaces of the specimens have been degreased with acetone, but otherwise untreated. De Brouckère<sup>15</sup> has shown that after the solution heat-treatment of 3 hr. at 420° C., the surface film on aluminium-magnesium alloys is one of magnesia superimposed on alumina; these oxide films may well play a part in the early stages of stress-corrosion. Also many workers<sup>16, 17</sup> have claimed that shot-peening increases the stress-corrosion life by leaving the surface in a state of compression.

A series of tests was therefore carried out in which the specimen surfaces were treated by various methods, some of which cold worked the surface. Before surface treatment the specimens were solution-treated, overstrained 10% on a 2-in. gauge-length in tension, and then aged at 125° C. for 24 hr. The specimens were stressed during corrosion at a load corresponding to an initial stress of 4.5 tons/in.<sup>2</sup> The surface conditions tested and the results are shown in Table VII.

Specimens of groups 1-8 had relatively short lives, and those of groups 9-13 (except 10) relatively long lives, the latter being the specimens with cold-worked surfaces. A separate experiment on another batch of material showed that specimens metallographically polished but unetched gave a life comparable with the long life of a specimen longitudinally polished with emery paper.



The small but significant difference between the lives of the unworked chemically prepared surfaces (including the as-heat-treated surface) indicates that the initial film on the material has some effect on the stress-corrosion life. It is likely that different times will be taken for various films to break down during corrosion in 3% sodium chloride solution and so open the way for stress-corrosion. This is confirmed by the observation that stressed loop specimens immersed\* in 3% sodium chloride solution crack more quickly if they have been pickled in caustic soda than if tested with an unprepared surface.

TABLE VII.—*Effect of Surface Finish on Stress-Corrosion Life of Aluminium-7% Magnesium Alloy MNY.*

Group No.	Surface Condition	Time to Failure, days	Average Life, days *
1	As heat-treated	1 $\frac{3}{4}$ , 1 $\frac{3}{4}$ , 3 $\frac{3}{4}$ , 4	3
2	Metallographically polished and etched (H <sub>3</sub> PO <sub>4</sub> )	$\frac{5}{16}$ , 1 $\frac{3}{4}$ , 3 $\frac{3}{4}$ , 5 $\frac{3}{4}$	3
3	Electrolytically polished (Jacquet's solution)	1 $\frac{3}{4}$ , 1 $\frac{3}{4}$ , 1 $\frac{3}{4}$ , 2 $\frac{3}{4}$	2
4	Pickled in NaOH	$\frac{1}{2}$ , $\frac{1}{2}$ , 1 $\frac{3}{4}$ , 1 $\frac{3}{4}$	1
5	Pickled in 10% HNO <sub>3</sub>	1 $\frac{3}{4}$ , 1 $\frac{3}{4}$ , 4, 4 $\frac{3}{4}$	3
6	Macro-etched (HNO <sub>3</sub> + HCl + HF)	$\frac{1}{2}$ , $\frac{1}{2}$ , $\frac{1}{2}$ , $\frac{1}{2}$	$\frac{1}{2}$
7	Chamfered edge (flat) (otherwise untreated)	4 $\frac{3}{4}$ , 4 $\frac{3}{4}$ , 5 $\frac{3}{4}$ , 19	8 $\frac{1}{2}$ (5)
8	Chamfered edge (round) (otherwise untreated)	1 $\frac{3}{4}$ , 5 $\frac{3}{4}$ , 8 $\frac{1}{2}$ , 8 $\frac{1}{2}$	6 (7 $\frac{1}{2}$ )
9	Polished with emery paper (longitudinally)	20, 21, 23, 60	31 (21)
10	Shot-peened " (transversely)	3 $\frac{3}{4}$ , 4, 4, 4 $\frac{3}{4}$	4
11	Buffed	8 $\frac{1}{2}$ , 11, 11, 16	11 $\frac{1}{2}$
12	Wet blasted (with alumina)	10 $\frac{3}{4}$ , 11, 21, 60	26 (14)
13		11, 82, 136, (a)	> 73

\* The figures in brackets are the means neglecting the extreme value in each set.  
(a) The fourth specimen was unfailed at 64 days, but was then spoiled.

A marked improvement in the stress-corrosion life results from cold working the surface (e.g. shot-peening, &c.); this is most probably due to the setting up of compressive stresses in the surface which oppose the applied tensile stress. Such compressive stresses need only occur in a thin surface layer, as shown by the fact that specimens metallographically polished but unetched gave a long life, whilst similar specimens that were micro-etched had a much shorter life, almost the same as that of untreated material. The longer life of specimens polished longitudinally with emery paper as opposed to specimens transversely polished, suggests that the compressive stress set up is parallel to the direction of rolling.

To confirm the view that longitudinal polishing with emery paper sets up surface compressive stresses and thus prolongs the stress-

corrosion life, further specimens (material KEN) were tested after the following treatments :

(a) Polished longitudinally with emery paper, solution-treated 3 hr. at 420° C., overstrained 10%, aged 24 hr. at 125° C.

(b) Not polished with emery paper, otherwise as (a).

(c) Solution-treated, overstrained, and aged as (a) and then longitudinally polished with emery paper.

The stress-corrosion lives at 4.4 tons/in.<sup>2</sup> averaged 49, 27, and > 140 days, respectively, these being the means of five test results in each case.

The actual lives are not strictly comparable with those quoted for another material (MNY) tested at another time (Table VII). However, it is clear that solution-treatment after polishing with emery paper largely eliminated the effect of this surface treatment on the stress-corrosion life, as would be expected if the compressive stresses introduced by the surface treatment are largely relieved during solution-treatment.

In the course of the work some specimens were solution-heat-treated, in air, for an unusually long time (1 week), and after overstraining and ageing in the usual way, these had much longer stress-corrosion lives than specimens solution-treated for only 3 hr. For example, specimens of material NFO, solution-treated for 3 hr., overstrained 10%, and aged for 24 hr. at 125° C., had lives averaging 9 days, while specimens solution-treated for 1 week but otherwise treated similarly and tested at the same time, had lives averaging 49 days (triplicate tests at 4.5 tons/in.<sup>2</sup> in each case).

Specimens given the short and long solution-treatments were examined by the back-reflection X-ray method between successive etching treatments which progressively removed the surface layers. The lattice parameters at various depths below the surface were determined in this way and the results are plotted in Fig. 7. From the lattice parameter/composition curve given by Lacombe,<sup>18</sup> it appears that the concentration of magnesium in the outermost layers of the specimens heat-treated for 1 week was lowered by about 1.3%.

It seemed likely that this magnesium impoverishment of the surface layers was responsible for the longer stress-corrosion life of material solution-treated for 1 week, and this view is supported by the fact that such specimens had shorter lives when approximately 0.001 in. was removed from the surface by pickling before the stress-corrosion test. For example, in strictly comparable tests, pickled specimens lasted 22 days, and those not pickled, 63 days (duplicate tests).

To summarize these observations, it is clear that treatments that affect the composition or condition of the extreme surface layers of the material may have a considerable effect on its susceptibility to stress-corrosion.

It should be pointed out that treatments which cold work the surface can have two opposing effects: (i) a beneficial effect due to compressive stresses; and (ii) a detrimental effect due to an increase in the rate of precipitation of the  $\beta$  phase if ageing occurs subsequently.

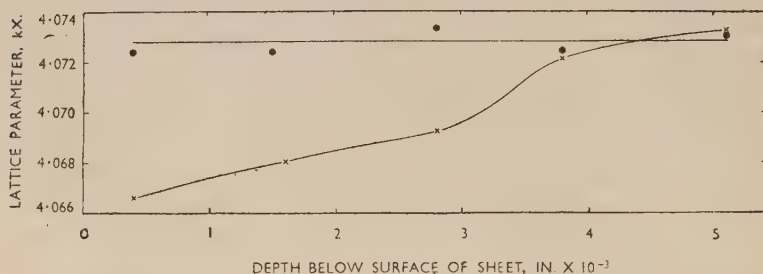


FIG. 7.—Change of Lattice Parameter with Distance Below the Surface of Aluminium-7% Magnesium Wrought Alloy Sheet after Short and Long Periods of Solution-Treatment at 420° C.

● 3 hr. at 420° C. } Overstrained 10% and aged 24 hr. at 125° C.  
 x 1 week at 420° C. }

The overall effect in any instance will depend on the balance between these two factors. In the tests described in the present paper the beneficial effect has usually predominated, since the  $\beta$  phase was already heavily precipitated at the grain boundaries in all the specimens owing to overstraining 10% before ageing at 125° C. for 24 hr. It is possible that the stress-corrosion life may be decreased if ageing occurs after cold working the surface.

##### 5. *The Rate of Stress-Corrosion of Aluminium-7% Magnesium Alloy.*

During the course of the work it was noticed that, after one specimen of a triplicate set had failed, the other specimens, if these were unloaded and the mechanical properties determined, were usually found to have lost very little strength. Also no visible cracking was noticed during stress-corrosion tests until a short time before actual fracture. These observations suggested that a specimen under test probably lost most of its strength towards the end of its life.

To confirm this, direct-tensile stress-corrosion tests were carried out on material solution-treated, overstrained 10% in tension, and

aged at 125° C. for 24 hr. The specimens had an ultimate tensile stress of 23.6 tons/in.<sup>2</sup>, 0.1% proof stress 14.2 tons/in.<sup>2</sup>, and an elongation of 22%. Specimens were tested at an initial tensile stress of 5 tons/in.<sup>2</sup>, the usual unstressed controls also being exposed, and at regular intervals specimens were unloaded and their tensile strengths determined. Five specimens were kept on test until failure, the average failure time being 16½ days. The loss of strength due to stress-corrosion after various times of exposure is shown in Fig. 8. The equation of this curve is :

Loss of strength due to stress corrosion =  $0.0053t^{2.83}$  tons/in.<sup>2</sup>,

where  $t$  is the time of exposure in days.

The effect of stress in increasing corrosion damage is therefore most marked in the last stages of a specimen's life. The results in Fig. 8 are supported by the results of deflection measurements made during the four-point-bending tests described in the next Section

(Fig. 9). This type of curve is to be expected, since as penetration proceeds the stress on the remaining uncorroded section is continuously increasing. The experiment shows that in order to gain a true assessment of stress-corrosion susceptibility it is necessary to expose some specimens until failure.

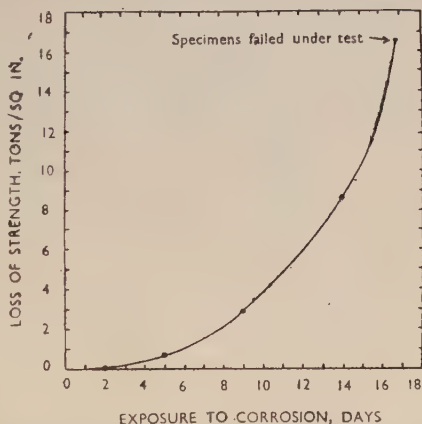


FIG. 8.—Loss of Strength due to Stress-Corrosion. Initial stress 5 tons/in.<sup>2</sup> in all cases.

Exposure : 2 5 9 14 16½ days  
Loss of strength : 0.04 0.60 2.8 8.53 16.48 tons/in.<sup>2</sup>

## 6. Tensile and Compressive Stresses.

It has frequently been stated that for stress-corrosion to occur, a tensile stress is necessary. Robertson<sup>19</sup> has shown that compressive stresses do not promote stress-corrosion in the alloy 24S, and to see if this was true for aluminium-7% magnesium alloy, specimens: (a) solution-treated, overstrained 10% in tension, and aged at 125° C. for 24 hr.; or (b) as-received, overstrained 10% in tension, and aged at 200° C. for 8 hr., were stressed by four-point bending as shown in Fig. 3. The specimens were painted, leaving only the gauge-length on one side of the specimen exposed. The unpainted gauge-length

was exposed uppermost for the "tensile" specimens and downwards for the "compression" specimens, and was sprayed with 3% sodium chloride twice daily.

During the test, deflections of the specimens were measured with a micrometer. The change of deflection due to weakening of specimens by ordinary corrosion was assessed by temporarily loading the unstressed specimens at the same stress as the continuously stressed specimens.

Specimens (a) when stressed in tension at an initial stress of 9 tons/in.<sup>2</sup> gave an average life of 7 days, while similar specimens subjected to an equal compressive stress did not fail in 41 days. Specimens

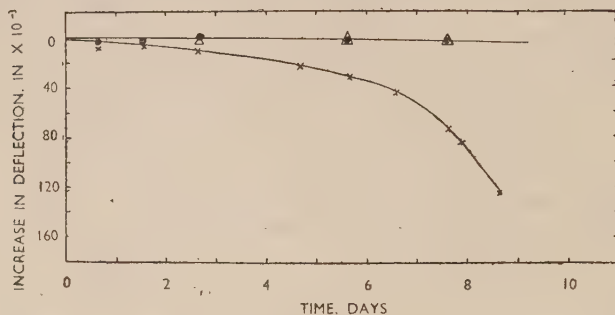


Fig. 9.—Deflection Produced in 4-Point Loading Test in Aluminium-7% Magnesium Alloy, Solution-treated, Overstrained 10%, Aged at 125° C. for 24 hr. Initial surface stress 9 tons/in.<sup>2</sup>

● Unstressed specimen.                      Δ Compression specimen.  
× Tension specimen.

(b) gave similar results, the failure time being 11 days for those subjected to a tensile stress of 9.5 tons/in.<sup>2</sup>, while no failures were obtained in 91 days for those subjected to compressive stress. The residual mechanical properties of the unbroken compression specimens were in most cases slightly lower than those for unstressed specimens exposed to corrosion for a similar period. It is doubtful whether this was really a weakening due to compressive stress, since corrosion had occurred under the paint at the edges of the specimens, causing small cracks to form at the edges of the tensile (painted) surface.

Microscopic examination of sections of the various specimens showed that the type and amount of intercrystalline corrosion was approximately the same for the "compression" specimens and the unstressed controls. Shallow areas of intercrystalline corrosion could be seen, but the cracks showed no tendency to penetrate across the specimens. In contrast to this, the specimens stressed in tension



showed single cracks which penetrated deep into the specimen in a direction roughly at right-angles to the stress.

As shown in Fig. 9, unstressed specimens and those stressed in compression gave hardly any change in deflection. On the other hand, the deflection for specimens stressed in tension increased continuously until fracture occurred, the rate of increase becoming greater towards the end of the life. The significance of this has already been discussed.

### *7. Cold Work before Low-Temperature Ageing.*

Plastic deformation before low-temperature ageing has been shown <sup>4, 6</sup> to be a most important factor in determining the rapidity of stress-corrosion failure. Dix <sup>5</sup> found that with aluminium-10% magnesium alloy the effect of cold work was greater for short than for long ageing times at 100° C., and also that for a constant ageing time the effect was more marked for small than for large amounts of cold work. Metcalfe <sup>1</sup> has shown that aluminium-5% magnesium alloy rivets suffer stress-corrosion after prolonged exposure to marine and tropical conditions, the cold-worked heads being particularly liable to such failure.

Specimens of solution-treated aluminium-7% magnesium alloy sheet were overstrained in tension to extensions of between 0 and 10% on a 2-in. gauge-length. After overstraining, one set of specimens was aged at 125° C. for 24 hr. and another set at 200° C. for 24 hr., both sets being then tested for stress-corrosion susceptibility at an initial tensile stress of 7 tons/in.<sup>2</sup>

As shown in Fig. 10, the effect of the cold work is to decrease the stress-corrosion life; furthermore, the magnitude of this decrease for a given increment is greater for the smaller than for the larger amounts of overstrain. By increasing the ageing temperature from 125° to 200° C. the stress-corrosion life is markedly decreased, and is further decreased by plastic deformation before ageing, though the effect is much less for 200° C. ageing than 125° C. ageing.

### *Metallographic Examination.*

Figs. 18 and 19 (Plate XI) show the microstructures of specimens without and with 2% overstrain followed by ageing at 125° C. for 24 hr.; the specimens were etched in 10% phosphoric acid for 30 min. The precipitated  $Mg_2Al_3$  occurs at more of the grain boundaries and is more continuous in the overstrained (Fig. 19) than in the material not overstrained (Fig. 18). In material overstrained 2% the grain-

boundary network appears practically continuous, but careful examination at high magnifications revealed small discontinuities, and the effect of further overstrain before ageing was to decrease these discontinuities both in magnitude and number. The change in microstructure brought about by the application of 1 or 2% overstrain was, however, much more apparent than the difference between, say, 5 and 7%.

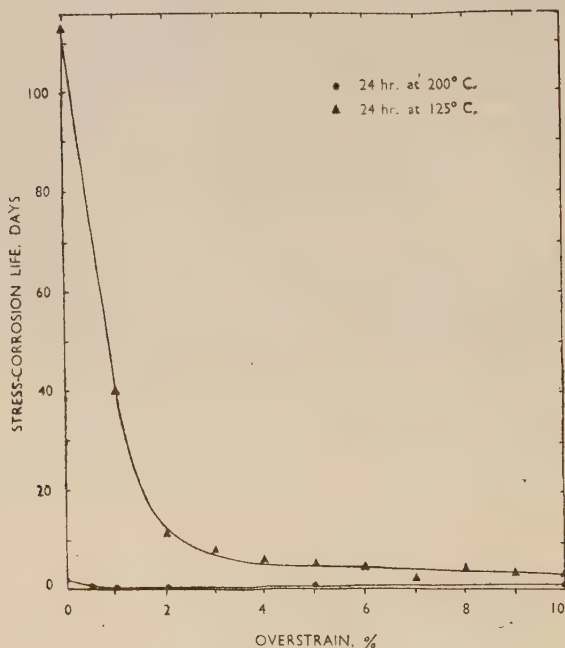


FIG. 10.—The Effect of Pre-Overstrain on the Stress-Corrosion Life of an Aluminium-7% Magnesium Alloy.

Specimens aged at 200° C. showed two main differences from those aged at 125° C.; (a) there was much more general precipitation within the grains, and (b) an almost continuous network existed in the specimen which had not been overstrained (see Fig. 21, Plate XII). Overstraining caused a decrease, both in magnitude and number, of the small discontinuities that existed in the specimen not overstrained, though no appreciable difference was observed between specimens overstrained by 2–10%. General precipitation within the grains did, however, increase with increasing amounts of overstrain. It is therefore confirmed that a more or less continuous grain-boundary network

of the precipitated  $Mg_2Al_3$  is necessary for rapid stress-corrosion. The effect of cold work before ageing is to increase the continuity of this network by increasing the rate of precipitation.

### 8. Microscopic Internal Strains.

As a result of a few *ad hoc* experiments it seemed that there might be some relation between the stress-corrosion susceptibility of aluminium-7% magnesium alloy and the diffuseness of the X-ray diffraction pattern obtained from the material. Gayler<sup>20</sup> has already put forward

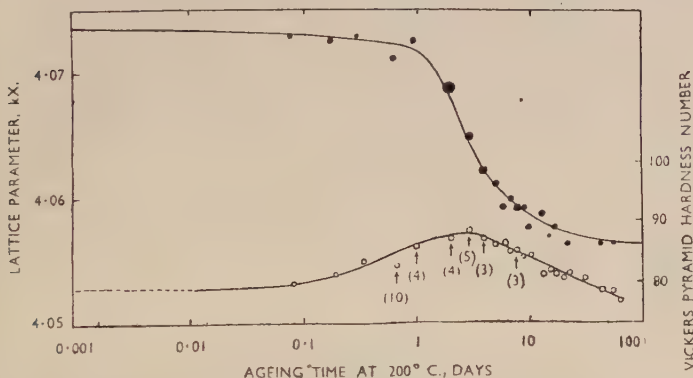


FIG. 11.—Variation of Lattice Parameter (upper curve) and Vickers Diamond Pyramid Hardness Number (lower curve) with Ageing Time at 200° C. for Aluminium-7% Magnesium Alloy.

the idea that internal stresses set up during precipitation might play an important part in determining the stress-corrosion susceptibility of the material. This possibility was explored by determining the ageing properties of the alloy by hardness and X-ray measurement, and then by testing the stress-corrosion susceptibility of specimens after various ageing treatments.

Fig. 11 shows the variation of hardness and lattice parameter with time of ageing at 200° C. after first solution-treating. The size of spot on the lattice-parameter curve represents the degree of diffuseness of the diffraction lines, a small spot indicating a sharp and a large spot a diffuse pattern. As the hardness increased so did the diffuseness of the diffraction lines, and there was a general decrease in the lattice parameter which began after visible precipitation had taken place. The arrows in Fig. 11 indicate ageing treatments used for stress-corrosion tests at an initial tensile stress of 6.2 tons/in.<sup>2</sup>, and the figures beside the arrows give the stress-corrosion lives in days. The micro-

structures of all these specimens had equally continuous grain-boundary networks of the  $\beta$  phase, except the specimens aged for 16 hr. in which the grain boundaries were not so continuous (see Figs. 20 and 22, Plate XII). The most noticeable feature of the microstructures was that the amount of precipitate within the grains increased with ageing time.

The results of the stress-corrosion tests are given in Table VIII.

TABLE VIII.—*Stress-Corrosion Tests on Aluminium-7% Magnesium Alloy after Various Times of Ageing at 200° C.*

Time of Ageing at 200° C.	Mg in Solid Solution, % *	Stress-Corrosion Life, days	Loss of Strength due to Stress-Corrosion, tons/in. <sup>2</sup> †	Loss of Strength due to Corrosion for 5 days Without Stress, tons/in. <sup>2</sup>
16 hr.	6.2	7 $\frac{3}{4}$ , 8 $\frac{3}{4}$ , 12 $\frac{3}{4}$ (10)	12.3	3.5
1 day	6.0	4 $\frac{1}{2}$ , 4 $\frac{1}{2}$ , 3 (4)	13.8	3.1
2 days	5.1	4 $\frac{1}{2}$ , 4 $\frac{1}{2}$ , 3 (4)	14.5	4.2
3 days	4.6	4 $\frac{1}{2}$ , 4 $\frac{1}{2}$ , 6 $\frac{3}{4}$ (5)	13.8	6.3
4 days	4.0	4 $\frac{1}{2}$ , 2, 2 $\frac{1}{2}$ (3)	14.0	7.1
8 days	3.4	2 $\frac{3}{4}$ , 2 $\frac{3}{4}$ , 4 $\frac{1}{2}$ (3)	14.5	5.8

\* Obtained from the curve of lattice parameter against magnesium content given by Lacombe.<sup>18</sup>

† Obtained from the curves giving the U.T.S. of unstressed corroded specimens against time of corrosion.

There is no significant difference in the stress-corrosion life after ageing at 1, 2, 3, 4, or 8 days at 200° C., although on the basis of X-ray and hardness measurements (Fig. 11) the internal stresses are at a maximum at about 2 days. The longer life of the specimen aged for 16 hr. is probably due to the grain-boundary  $\beta$  networks being less continuous than in the other specimens tested. It follows that the internal strains set up during precipitation of the  $\beta$  phase do not play an important part in the stress-corrosion mechanism. Robertson<sup>21</sup> similarly found no correlation between the stress-corrosion susceptibility and the ageing curve for an aluminium alloy containing 4.5% copper and 1.5% magnesium. The results in Table VIII also show that when an apparently continuous grain-boundary network of the  $\beta$  phase is present, the stress-corrosion life is not significantly affected by the magnesium content of the solid solution. However, the loss of strength due to ordinary corrosion increases as the magnesium content of the solid solution decreases and the amount of  $\beta$  increases.

### 9. Small Zinc Additions.

Many authors<sup>22, 23, 24, 25</sup> have claimed that small additions of zinc improve the stress-corrosion properties of aluminium-magnesium alloys, though none has shown the reason for this improvement. To

investigate this in more detail chill-cast ingots of alloys containing 0,  $\frac{1}{2}$ , 1, and 2% zinc were prepared from commercial-purity materials, and rolled to 18 S.W.G. sheet. Analyses of the sheets are given in Table IX.

TABLE IX.—*Analysis of Aluminium-7% Magnesium Alloys Containing Zinc.*

Alloy Mark	Mg, %	Zn, %	Mn, %	Fe, %	Si, %	Al, %
NEE . .	7.80	...	0.21	0.25	0.11	Remainder
NEF . .	7.44	0.51	0.15	0.20	0.11	„
NEG . .	7.73	1.06	0.21	0.20	0.11	„
NEH . .	7.54	2.01	0.13	0.20	0.11	„

(a) *Metallographic Examination after Ageing at 75°, 100°, and 125° C.*

The material was solution-treated and aged for various times at 75°, 100°, and 125° C., some of the specimens having been given 10% overstrain in tension before ageing. At all ageing temperatures the  $\beta$  precipitate came out at the grain boundaries first; the rate of precipitation was greater for overstrained than for un-overstrained material, and increased with increase in temperature. As the ageing time increased, the precipitate at the boundaries became more continuous, and at the same time the amount of precipitate within the grains increased, this effect being more marked in the zinc-bearing alloys than in the plain aluminium-7% magnesium alloy. The most important effect of zinc was to decrease the initial rate of precipitation at the grain boundaries (see Figs. 23-27, Plates XII and XIII). This agrees with the statement by Bollenrath and Bungardt,<sup>23</sup> that zinc decreases the rate of diffusion of magnesium in aluminium. With increasing zinc content precipitation was slower, in agreement with Brenner and Roth's finding,<sup>6</sup> and more precipitate appeared in the grains relative to the amount at the grain boundaries (see Figs. 26 and 27). The latter effect doubtless results from the decrease in solid solubility of magnesium in aluminium caused by the additions of zinc. For example, at 200° C. the solubility of magnesium in aluminium is reduced from about 3% to 1% by the addition of 0.5% zinc.<sup>26</sup>

(b) *Stress-Corrosion Tests.*

Solution-treated material was aged for various times at 100° C., with and without prior 10% overstrain in tension, and then bent into loops. Three stressed loops and one unstressed loop in each different condition were sprayed twice daily with 3% sodium chloride. The results are given in Table X.



Examination of the unstressed corroded loops showed that the zinc-containing alloys suffered more general corrosion than the plain aluminium-7% magnesium alloy.

When considering the results of the stressed-loop tests it must be remembered that the stress developed in the loop will depend upon the mechanical properties of the material. It was found during this work that the zinc-bearing alloys age-hardened much more than the plain aluminium-7% magnesium alloy, and that the magnitude of hardening was greater the higher the zinc content; thus the stresses in the loops tested were by no means equal. As the hardness of the zinc-bearing alloys is greater than the plain aluminium-7% magnesium

TABLE X.—*Stress-Corrosion Tests on Solution-Treated Aluminium-7% Magnesium Alloy with and without Additions of Zinc, Aged at 100° C.*

Ageing Time at 100° C., After Solution-Treatment and 10% Overstrain	Ageing Time at 100° C., After Solution-Treatment	Average Life of Loop, days			
		NEE 0% Zn	NEF ½% Zn	NEG 1% Zn	NEH 2% Zn
...	2 days	5	111	>240	>127
...	3 "	3½	2	220	111
...	6 "	1	$\frac{3}{4}$	5	17
...	10 "	$\frac{3}{4}$	$\frac{3}{4}$	$\frac{3}{4}$	$\frac{3}{4}$
...	16 "	$\frac{3}{4}$	$\frac{3}{4}$	$\frac{3}{4}$	$\frac{3}{4}$
8 hr.	...	6	136	>240	>60
1 day	...	$\frac{3}{4}$	$\frac{3}{4}$	2½	3
3 days	...	$\frac{3}{4}$	$\frac{3}{4}$	$\frac{3}{4}$	$\frac{3}{4}$
6 "	...	$\frac{3}{4}$	$\frac{3}{4}$	$\frac{3}{4}$	$\frac{3}{4}$
16 "	...	$\frac{3}{4}$	$\frac{3}{4}$	$\frac{3}{4}$	$\frac{3}{4}$

alloy, it is not unreasonable to assume that the stresses developed in them would be greater, which would tend to give a shorter stress-corrosion life. Different stresses in the loops are therefore not responsible for the differences obtained, since in several cases the zinc-bearing alloy loops lasted much longer. The results are clearly due to the differing microstructures (Figs. 26 and 27, Plate XIII), and once a continuous or nearly continuous grain-boundary network is formed there is no improvement due to the addition of zinc. Table X shows the profound effect of cold work before ageing on the stress-corrosion susceptibility; for example, the 1% zinc alloy aged at 100° C. for 3 days lasted 220 days, whereas if aged after overstraining 10% the life was  $\frac{3}{4}$  day.

Zinc additions, therefore, are beneficial in delaying the development of a susceptible condition, but are of no value if the conditions of service are such as to cause precipitation in a dangerous form.

(c) *Electrochemical Study.*

Electrode potential measurements (against the *N*-calomel electrode) were carried out in 3% sodium chloride on the four solution-treated alloys and the  $\beta$  phase, this being cast to the composition of 64% aluminium, 36% magnesium. The results are given in Table XI.

TABLE XI.—*Electrode Potentials in 3% Sodium Chloride of Aluminium-7% Magnesium Alloy with and without Additions of Zinc.*

Alloy Mark	Zn, %	Steady Potential of Solution-Treated Material, V.	Difference in Potential between Solid Solution and $\beta$ Phase, V.
NEE . . .	0	-0.800	0.400
NEF . . .	0.5	-0.858	0.342
NEG . . .	1	-0.962	0.238
NEH . . .	2	-1.000	0.200
Mg <sub>2</sub> Al <sub>3</sub> . . .	...	-1.200	...

Table XI shows that as the zinc content of the solid solution increases the electrode potential becomes more anodic. This is not surprising in view of the observation that the alloys with the higher zinc contents suffer much more from general corrosion (i.e. attack of the solid solution) than the plain aluminium-7% magnesium alloy. This variation in the potential difference between  $\beta$  and the solid solution was not reflected in the lives of the corresponding loop specimens, showing that once the grain-boundary network of  $\beta$  phase is apparently complete, such changes in electrochemical relationships have only a secondary effect upon stress-corrosion behaviour.

## IV.—CONCLUSIONS.

It has been confirmed that for stress-corrosion to occur in aluminium-7% magnesium alloy the material must be in a heterogeneous condition. There is a close correlation between the continuity of the grain-boundary  $\beta$  precipitate and the stress-corrosion susceptibility, the maximum susceptibility occurring when this precipitate is apparently quite continuous. It is possible, however, for the material to be susceptible when the precipitate at the grain boundaries is present as separated lakes, though this has only been found to occur after ageing at high temperatures.

The rate of decomposition of the supersaturated solid solution increases with temperature, and precipitation starts at the grain boundaries forming a fine apparently continuous network, this occurring without any measurable change in the lattice parameter. As the time

of ageing is raised precipitation takes place within the grains, this being accompanied by a decrease of lattice parameter. With the higher ageing temperatures the precipitate at the grain boundaries coagulates and grows in size. Cold work before ageing increases the rate of precipitation, and small amounts of cold work before ageing at 125° C. have a profound effect on the stress-corrosion susceptibility. The internal strains set up during precipitation of the  $\beta$  phase do not play an important part in the stress-corrosion mechanism; moreover, once a continuous grain-boundary network of the  $\beta$  phase has been formed, the magnesium concentration of the solid solution has little effect.

Compressive stresses did not promote the advancement of a stress-corrosion crack as did tensile stresses. The rate of penetration of a stress-corrosion crack was found to increase rapidly just before a specimen failed.

The mechanism of stress-corrosion cracking in aluminium-7% magnesium alloy is at least partially electrochemical, as is shown by (a) the effect of oxygen dissolved in the corrosive agent, and (b) the effect of concentration of the agent. Closely connected with these two effects is the fact that spraying a given material gives more rapid cracking than immersion in a similar solution. A large potential difference exists between the supersaturated solid solution and the  $\beta$  phase, the latter being the anode. There is little doubt that this is the reason why intercrystalline corrosion occurs in unstressed material with continuous films of precipitate at the grain boundaries.

Small additions of zinc to aluminium-7% magnesium alloy decrease the rate of precipitation, thus increasing the time at any one temperature necessary for the formation of a continuous grain-boundary network. Once such a network has been formed, however, zinc additions have little or no effect on the stress-corrosion susceptibility. The most suitable addition for delaying precipitation appears to be 1%.

By cold working the specimen surface after ageing, e.g. buffing, shot-peening, wet blast, &c., a considerable extension of the stress-corrosion life can be obtained. An increase in life can also be brought about by reducing the magnesium content of the specimen surface.

#### ACKNOWLEDGEMENTS.

The work recorded in this paper was undertaken as part of a research on the stress-corrosion of light alloys carried out for the Principal Director of Scientific Research (Aircraft), Ministry of Supply.

The authors wish to thank the Chief Scientist, Ministry of Supply, and the Director and Council of the British Non-Ferrous Metals Research

Association for permission to publish the results of this work, and also to thank various colleagues who have helped at different stages in the investigation.

## REFERENCES.

1. G. J. Metcalfe, *J. Inst. Metals*, 1946, **72**, 487.
2. C. W. George and B. Chalmers, *Symposium on Stress-Corrosion Cracking of Metals (A.S.T.M.-A.I.M.E.)*, 1944, 345.
3. P. T. Gilbert and S. E. Hadden, *J. Inst. Metals*, 1950, **77**, 237.
4. K. Matthaes, *Jahrb. Lilienthal-Ges. Luftfahrtforsch.*, 1936, 404.
5. E. H. Dix, Jr., *Trans. Amer. Inst. Min. Met. Eng.*, 1940, **137**, 11.
6. P. Brenner and W. Roth, *J. Inst. Metals*, 1948, **74**, 159.
7. F.-C. Althof, *Luftfahrtforsch.*, 1938, **15**, 60.
8. G. Siebel, *Jahrb. deut. Luftfahrtforsch.*, 1938, (I), 511.
9. A. Mühlenbruch and H. J. Seemann, *Z. Metallkunde*, 1939, **31**, 293.
10. P. Brenner, *Metallwirtschaft*, 1938, **17**, 1272.
11. H. Vosskühler, *Z. Elektrochem.*, 1943, **49**, 204.
12. H. Sutton, E. A. G. Liddiard, B. Chalmers, and F. A. Champion, *Monthly J. Inst. Metals*, 1945, (Aug.), xxii.
13. J. Case, "Strength of Materials", p. 159. 3rd edition. 1938: London (Edward Arnold).
14. F. Seitz, "The Physics of Metals", p. 180. 1943: New York (McGraw-Hill Book Co., Inc.).
15. L. de Brouckère, *J. Inst. Metals*, 1945, **71**, 131.
16. L. J. Wieschhaus, *Product Eng.*, 1947, **18**, (8), 122.
17. H. A. Knight, *Materials and Methods*, 1947, **26**, (5), 83.
18. P. Lacombe, *Rev. Mét.*, 1944, **41**, 180, 217, 259.
19. W. D. Robertson, *Trans. Amer. Inst. Min. Met. Eng.*, 1948, **175**, 428.
20. M. L. V. Gayler, *J. Inst. Metals*, 1947, **73**, 681.
21. W. D. Robertson, *Trans. Amer. Inst. Min. Met. Eng.*, 1946, **166**, 216.
22. G. Siebel and H. Vosskühler, *Z. Metallkunde*, 1940, **32**, 298.
23. F. Bollenrath and W. Bungardt, *Z. Metallkunde*, 1940, **32**, 303.
24. P. Brenner, *Jahrb. Lilienthal-Ges. Luftfahrtforsch.*, 1936, 431.
25. W. Mulfinger, *Z. Metallkunde*, 1940, **32**, 311.
26. W. L. Fink and L. A. Willey, *Trans. Amer. Inst. Min. Met. Eng.*, 1937, **124**, 78.





# A THEORY OF THE MECHANISM OF STRESS-CORROSION IN ALUMINIUM-7% MAGNESIUM ALLOY.\*

By P. T. GILBERT,† Ph.D., A.R.I.C., A.I.M., MEMBER, and S. E. HADDEN,‡  
A.I.M., MEMBER.

(Communication from the British Non-Ferrous Metals Research Association.)

## SYNOPSIS.

A detailed theory is put forward of the mechanism of stress-corrosion in aluminium-7% magnesium alloy, based partly on work covered in the paper and partly on work described elsewhere (*J. Inst. Metals*, 1950, 77, 207).

The commercially produced alloy is not susceptible to stress-corrosion, but after heat-treatments which lead to preferential precipitation of the  $\beta$  phase at the grain boundaries the alloy is liable to suffer rapid intercrystalline failure when stressed in, say, sodium chloride solution.

The theory postulates that in stressed specimens stress concentrations are built up at the tip of crevices formed by preferential attack of the  $\beta$  ( $\text{Al}_3\text{Mg}_2$ ) phase. When the stress concentration at the tip of the most advanced crevice is sufficiently high, a sudden partial mechanical fracture between  $\beta$  and the solid solution leads to progress of the crack along the grain boundary. Rapid corrosion of the bare  $\beta$  surfaces so exposed then occurs, with the evolution of hydrogen. This intercrystalline attack quickly slows down as corrosion films re-form on the electrodes and then proceeds by oxygen absorption. Eventually the conditions leading to mechanical disruption are again built up. It is thus visualized that slow corrosion by oxygen absorption, partial mechanical intercrystalline failure, and a short period of rapid corrosion with hydrogen evolution follow each other in turn until the fracture is complete; or, in the case of a specimen under constant load, until the ultimate tensile stress of the residual metal is exceeded.

Experiments related to the electrochemical and mechanical aspects of the stress-corrosion process are described and discussed.

## I.—INTRODUCTION.

DURING recent years research on the stress-corrosion of light alloys has been carried out for the Principal Director of Scientific Research (Aircraft), Ministry of Supply, by the British Non-Ferrous Metals Research Association. In the course of this work much information has been obtained on the rate of failure of wrought aluminium-7% magnesium alloy, and its relation to the metallurgical condition of the material

\* Manuscript received 24 September 1949. The work described in this paper was made available to members of the B.N.F.M.R.A. in a confidential research report issued in 1948.

† Head of Corrosion Section, British Non-Ferrous Metals Research Association, London.

‡ Research Assistant, British Non-Ferrous Metals Research Association, London.

and to the test conditions. The more important of these findings are published in another paper.<sup>1</sup> With the aid of this extensive background a theory was developed of the mechanism of stress-corrosion of aluminium-7% magnesium alloy, although certain additional experiments, the results of which are given, were necessary before the theory could be formulated in detail in the present paper.

It must be emphasized that the aluminium-7% magnesium alloy in the as-manufactured condition is not susceptible to stress-corrosion.<sup>1</sup> By certain heat-treatments it can be rendered susceptible, and such specially treated material was used in the present work.

## II.—PREVIOUS WORK.

A number of theories of the mechanism of stress-corrosion have been put forward, many of them based on the assumption that a local stress concentration is built up at the base of a narrow crevice formed by corrosion, the initial production of such a crevice being due to some kind of selective attack, usually along grain boundaries. Such a view was advanced by Dix<sup>2</sup> in 1940, and later in more detail by Mears, Brown, and Dix.<sup>3</sup> It is worth quoting the following passage from the latter paper :

“ If attack penetrates preferentially along a narrow path, it would appear axiomatic that a component of tensile stress normal to the path would create a stress concentration at the base of the localized corroded path. The deeper the attack and the smaller the radius at the base of the path, the greater would be the stress concentrations. Such a condition would act to pull the metal apart along these more or less continuous localized paths. At sufficient concentration of stress, the metal might start to tear apart by mechanical action. Since it has been observed that a scratched metal surface is anodic to an unscratched metal surface, the tearing action described above would expose fresh metal, unprotected by films, to the action of the corrosion environment. Because this freshly exposed metal is more anodic, an increase in current flow from the base of the localized path to the unaffected surface would be expected, and hence there would be an acceleration of corrosion. Further corrosion would result in further tearing of the metal, and as a result, increased rate of penetration would occur because of the mutual effect of the corrosion environment and the tensile stress.”

This appears to give a good general picture of the process, though the mechanical effects of the stress concentration and the part played

by the exposure of unfilmed metal are not explained in detail (bearing in mind that, if an anodic path is assumed to exist at the grain boundaries, two phases are probably present at the base of the crevice). In the present paper a theory of this type is developed in more detail for the special case of aluminium-7% magnesium alloy.

Keating,<sup>4</sup> who also assumes that mechanical damage occurs by the action of the stress concentration at the base of a crevice, goes one step further than Mears, Brown, and Dix; he suggests a reason why the mechanical disruption at the base of the crack, once started, does not immediately cause the complete failure of the specimen. He states that "each advancing section of the crack, in time, encounters an obstacle in the form of a non-metallic inclusion, lattice discontinuity, or unfavourably orientated grain boundary. In each case, the result may be reduction in the stress-concentration effect to a level at which crack-ing cannot proceed." Keating also assumes that "the supply of fresh corrodent to the vicinity of the point of the crack will be slow, and will not keep pace with a propagating crack", so that only when the mechanical propagation is temporarily arrested will the corrosive agent be able to diffuse to the tip of the crack and produce corrosion which will eventually lead to further mechanical disruption.

It is generally recognized that when aluminium-magnesium alloys are in a condition seriously susceptible to stress-corrosion, more or less continuous films of the  $\beta$  phase ( $\text{Al}_3\text{Mg}_2$ ) exist at the grain boundaries,<sup>5, 6, 7</sup> this  $\beta$  phase being anodic to the solid solution in chloride solutions. Extensive work on the effect of various metallurgical treatments on the form of the  $\beta$  precipitate and on the relationship between structure and susceptibility to stress-corrosion has been published, for instance, by Brenner and Roth,<sup>8</sup> and by Perryman and Hadden.<sup>1</sup> In susceptible aluminium-7% magnesium alloy the anodic phase is already present before the stress-corrosion test begins, and therefore there appears no need to introduce the concept of Waber, McDonald, *et al.*<sup>9</sup> that one effect of stress concentration at the base of a narrow crevice is to cause or hasten precipitation of an anodic phase.

In general the susceptibility to stress-corrosion in this alloy depends on the degree of continuity of the  $\beta$  phase at the grain boundaries, and over certain ranges the susceptibility (for constant stress-corrosion conditions) has been found to be quantitatively related in a simple way to the time and temperature of ageing,<sup>1</sup> showing that the life is determined by the ageing treatment given before the stress-corrosion test. The increase in life as the  $\beta$  phase becomes more discontinuous is probably largely due to the time taken to corrode the solid-solution bridges between the  $\beta$  particles at a relatively slow rate. Perryman and

Hadden<sup>1</sup> have shown, however, that there are apparent exceptions to this rule and have discussed the reasons why material aged at 250° C. for 1 week is highly susceptible to stress-corrosion, although the grain-boundary precipitate appears to be relatively discontinuous. There is, however, no reason to believe that the mechanism of stress-corrosion in this material is essentially different from that in material aged at lower temperatures.

### III.—THEORETICAL CONSIDERATIONS.

Since the stress-corrosion behaviour of the alloy is closely associated with grain-boundary  $\beta$  networks, the mechanism of stress-corrosion must involve this  $\beta$  precipitate. It is likely that the presence of  $\beta$  will affect the mechanical as well as the electrochemical stages of the stress-corrosion process. Assuming that a stress concentration sufficient to cause some mechanical disruption has been built up at the tip of a crevice, there are several ways in which this may lead to the rapid propagation of the crack :

(i) Mechanical breakdown of the metal may cause advancement of the crevice either along the grain boundary or in some other direction. This process would probably be influenced by the presence of the brittle  $\beta$  phase at the grain boundaries.

(ii) The mechanical advancement by breakdown of the metal may be negligible, but breaking of corrosion films on the metal may cause acceleration of the rate of penetration as compared with the rate due to ordinary intercrystalline corrosion.

(iii) Accelerated penetration may be due to the combination in any proportions of processes (i) and (ii).

Since the breaking of corrosion films may be an important factor in the stress-corrosion process, it is necessary to consider the possible ways in which this could occur :

(a) If the solid solution were sufficiently strained, the corrosion film on it would break, exposing bare metal. This might increase the rate of corrosion of the  $\beta$  by increasing the rate of the cathodic reaction.

(b) Although the  $\beta$  corrodes preferentially, the rate of attack may be restricted by films and the breaking of such films might increase the corrosion rate considerably. Since the  $\beta$  may be as brittle as the corrosion film on it, it is possible that the film could not be broken unless the  $\beta$  itself were fractured.

(c) The highest rates of attack might not occur unless both solid solution and  $\beta$  were bared, as might happen, for instance, if the stress concentration caused the  $\beta$  to be torn from the solid solution along the grain boundary.



These considerations have determined the general direction of the experimental work described in the next Section.

#### IV.—MATERIALS AND METHODS.

Several batches of commercial 18-S.W.G. aluminium-7% magnesium alloy wrought sheet were used, analyses of which are given in Table I. Material susceptible to stress-corrosion was produced by solution-treating at 420° C. for 3 hr., overstraining 10%, and ageing at 125° C. for 24 hr. This material was bent into loops and stressed in the manner described by Perryman and Hadden,<sup>1</sup> the loops being then supported in the centre of 500 c.c. wide-necked flasks containing 400 c.c. of 3% sodium chloride solution. This stressed-loop test was the normal stress-corrosion test used in the present work.

The time of failure of such loops varied to some extent with (i) the batch of material, and (ii) the surface treatment. Table I shows the varia-

TABLE I.—*Analysis of Materials Used and Normal Cracking Time for Stressed Loops in 3% Sodium Chloride Solution.*

Alloy Mark	Chemical Analysis				Approx. Time for Beginning of Cracking, hr.
	Mg, %	Fe, %	Si, %	Mn, %	
MNY . . .	7.4	0.33	0.16	0.20	20
NFO . . .	6.85	0.20	0.08	0.18	20 *
LXU . . .	6.7	0.24	0.15	0.30	2½

\* Single experiment only.

tion for the three batches of material used, when surface treatment other than degreasing was omitted. There is no apparent correlation between the time for cracking and the analysis; the material containing the least magnesium cracked most rapidly.

Material MNY was used unless otherwise stated, and the usual procedure was to give specimens no surface treatment except degreasing with acetone. In some cases, however, the specimens were electropolished using Jacquet's acetic anhydride/perchloric acid solution, or pickled in 10% sodium hydroxide solution. Such treatments decreased the time for cracking, e.g. loops of material MNY with electropolished or pickled surfaces began to crack in about 1 hr.

#### V.—ELECTROCHEMICAL EXPERIMENTS.

The behaviour of loops undergoing stress-corrosion, including the change in electrode potential, was observed closely and is described below. Tests were also performed (a) in deaerated solutions, to de-



termine which cathodic reactions are important during stress-corrosion, and (b) in acid and alkaline solutions to determine the effect of pH. Measurements were made of the corrosion currents flowing in various circumstances between massive electrodes of the phases believed to be present in susceptible aluminium-7% magnesium alloy.

Deaeration of solutions was carried out by alternate exposure to reduced pressure and saturation with commercial oxygen-free nitrogen. A water pump which reduced the pressure over the solutions approximately to that of the vapour pressure of water at room temperature was used. Under optimum conditions the dissolved oxygen content was probably reduced to very low values, but no analyses were made. The nitrogen used was stated by the suppliers to contain not more than 0.0005% of oxygen.

All electrode potentials given in the paper are with respect to the normal calomel electrode.

### 1. *Effect of Oxygen.*

Oxygen is found to be necessary for the stress-corrosion of aluminium-7% magnesium alloy in the susceptible condition. Cracking of stressed loops does not begin in the absence of oxygen, and if oxygen is removed during cracking the process is arrested. Admission of oxygen to uncracked or partially cracked stressed loops immersed in deaerated solution results in rapid cracking. The following experiments are representative of a number carried out :

*Experiment (i).*—A loop was immersed in deaerated solution for 94 days, during which period no cracking occurred. At the end of this time the potential of the specimen was  $-0.91$  V. Air was drawn over the surface of the liquid, and the potential rose to  $-0.81$  V. After 1 hr. signs of cracking were observed, a definite crack being apparent after 84 min., when the potential was  $-0.90$  V. 220 min. after admitting air the loop had cracked completely across, and its potential was still  $-0.90$  V. Table I shows that loops in aerated solution normally begin to crack in about 20 hr.

*Experiment (ii).*—In this experiment the loops were not of the usual construction. Instead of being supported in the centre of the flask, the ends were riveted together, and the loop was laid on the bottom of the flask in a deaerated solution. After 21 days the specimen was removed and placed in a fresh deaerated solution. This procedure was repeated after 75 days.

After 97 days there was no sign of cracking of the loop. Oxygen was then passed into the solution, and in 43 min. the specimen had cracked completely across. The pH of the solutions was measured

at various stages, and varied between 6.4 and 7.9, though it did not appear to have any great significance. When oxygen was admitted after 97 days the electrode potential of the specimen was initially  $-0.84$  V. On completion of cracking the potential was  $-0.89$  V. A similar loop in aerated solution did not fail in 14 days, but when the solution was then renewed the loop cracked completely across within 75 min. A third loop of this type (but of material NFO) cracked after  $2\frac{1}{2}$  days in the original aerated solution.

*Experiment (iii).*—An electropolished loop in deaerated solution began to crack after 17 days, and the crack was about two-fifths of the way across the face after 27 days. Owing to inadequate pressure of water used in operating the pump, the deaeration in this experiment was not efficient. A similar electropolished loop immersed in aerated solution began to crack in 35 min., and cracked completely across the face in 2 hr.

*Experiment (iv).*—A stressed loop immersed in aerated solution began to crack after 28 hr. The solution was then deaerated and no development of the crack occurred for the next 31 days. During the following 3 days the crack proceeded slowly, and it was noticed that during this time abnormally high day-time room temperatures of about  $31^{\circ}$ – $32^{\circ}$  C. occurred. Development of the crack later ceased again, and it had made no further progress when the total time of immersion reached 73 days. At this time air was passed through the solution, and after 30 min. cracking began again, the crack travelling right across the specimen in some time less than about 12 hr. (overnight). In another experiment cracking started after 13 hr. in aerated solution and was then arrested for 3 days by deaeration. On re-admission of air cracking proceeded completely across in 8 min.

*Experiment (v).*—Two loops were immersed in solutions through which air and oxygen respectively were continuously bubbled. In the solution saturated with air the crack began in 15 hr., and in that saturated with oxygen in 31 hr.

Another loop was immersed in a solution through which pure oxygen was passed after first evacuating to remove dissolved gases initially present. The specimen had not started to crack after 19 hr., but was completely cracked across after 66 hr. (In ordinary aerated solution the usual time for cracking to begin was about 20 hr. for this material.)

These experiments indicate that the rate of cracking in solutions saturated with oxygen may be a little slower than in solutions saturated with air, though the evidence is not conclusive. It is also shown that minor constituents in the air, such as carbon dioxide, are not essential for cracking.

### 2. Appearance of Hydrogen Gas During Cracking.

During active stress-corrosion cracking of aluminium-7% magnesium alloy a stream of fine gas bubbles rises from the crack. Samples of this gas have been analysed and found to consist essentially of hydrogen. The time at which bubbles begun to appear has been closely correlated with the potential/time graph for a cracking specimen (see below). When cracking is arrested by deaerating the solution, evolution of bubbles ceases. In those experiments where cracking proceeded at a slow rate in deaerated solution (probably owing to inefficient removal of oxygen), evolution of bubbles occurred at a much slower rate than usual.

Specimens of (a) aluminium-7% magnesium alloy, either homogenized or with the  $\beta$  phase heavily precipitated, (b) massive  $\beta$ , and (c) pure aluminium, were scratched with a glass point under 3% sodium chloride solution. In each case numerous bubbles of gas were visible along the line of the scratch, most appearing to come from the edges of the scratch although fine bubbles seemed to arise from the area within the boundary of the scratch. The bubbling ceased almost immediately scratching was stopped.

### 3. Potentials of Cracking Specimens.

While specimens with unprepared surfaces always have potentials of about  $-1.3$  to  $-1.4$  V. on initial immersion, specimens with electro-

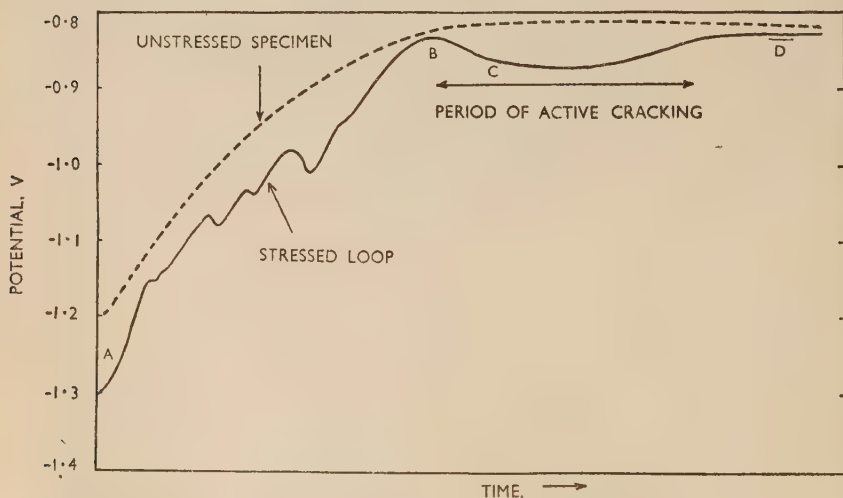


FIG. 1.—Typical Potential/Time Curve for Stressed Aluminium-7% Magnesium Alloy Loop in 3% Sodium Chloride Solution.

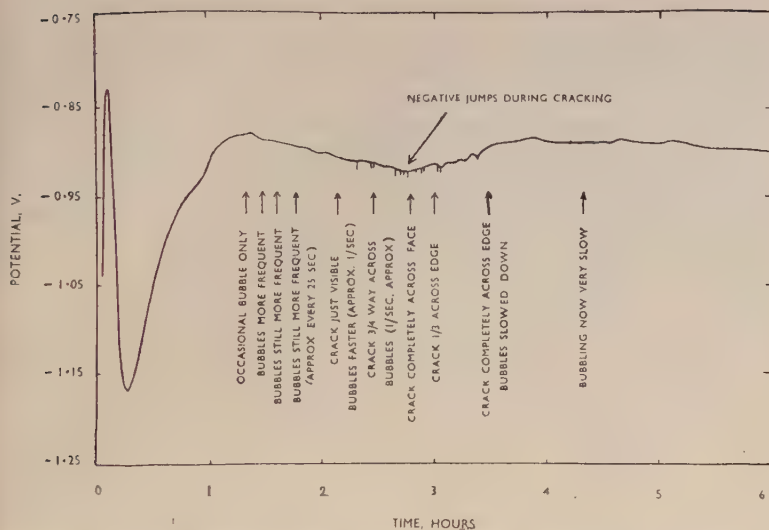


FIG. 2.—Graph of Potential against Time for Stressed Aluminium-7% Magnesium Alloy Loop (prepared from material pickled 4 min. in 10% NaOH).

polished or pickled surfaces have more cathodic values of about  $-0.8$  to  $-1.0$  V. The form of potential/time graph found for stressed loops is shown in Fig. 1. Although specimens with untreated surfaces must have a relatively thick oxide film resulting from the heat-treatments,<sup>10</sup> it appears that this film must be porous in view of the anodic value of the potential on initial immersion. The portion of the graph *AB* indicates that this film becomes built up and consolidated during the initial period of immersion. Specimens with an electropolished surface probably have a thinner film, which nevertheless seems to be much less porous, since the potential on initial immersion is more cathodic (about  $-1.0$  V.).

Very soon after point *B* is reached (Fig. 1), occasional bubbles of hydrogen are observed coming from a point on the surface. These increase in number as the section *BC* of the graph is followed, and usually at about point *C*, a crack becomes visible to the eye. Rapid evolution of bubbles from the crack continues while cracking proceeds, and the potential remains relatively constant. When cracking is complete, evolution of bubbles ceases and the potential becomes more cathodic again (point *D*, Fig. 1). A recorded curve of the potential of a loop prepared from material pickled for 4 min. in 10% sodium hydroxide solution is given in Fig. 2. A noteworthy feature is the occurrence of small and fairly frequent anodic kicks during the period of active cracking.

For an unstressed specimen the potential changes steadily during the initial period *AB* (Fig. 1) and then remains steady. The potential of stressed specimens fluctuates considerably during the period *AB*.

#### 4. *Effect of Variation of pH of Corroding Solution.*

A series of loops prepared from material which had been pickled in sodium hydroxide were immersed in 3% sodium chloride solution, the *pH* of which had been adjusted to various values by the addition of suitable amounts of hydrochloric acid or sodium hydroxide. The results are given in Table II.

TABLE II.—*Time for Cracking in Solutions of Various pH Values.*

Initial <i>pH</i> of Solution	<i>pH</i> after Test	Time for Cracking Completely across Face
0	...	< 13 min.
1.0	...	5 "
2.97	3.03	45 "
5.0	5.8	56 "
6.26	6.6	70 "
8.1	6.9	70 "
9.8	8.7	26-45 hr.
10.7	9.3	> 2 months

A loop was also tested in *N*-hydrochloric acid containing no sodium chloride, and this cracked completely across the face in about 8 min. Another loop was immersed in deaerated 3% sodium chloride solution with hydrochloric acid added to bring the *pH* to 1, and this began to fail in about 40 min., and was still not completely cracked after 3½ hr. Another loop was tested in 1% sodium hydroxide solution (*pH* approximately 13.5), and in this case the specimen dissolved away and no cracking occurred.

In general the time of cracking decreases as the acidity of the solution increases. In the more acid solutions there was much general intercrystalline attack of the specimens as well as the intercrystalline stress-corrosion failure. In the more alkaline solution there was rapid general attack but no stress-corrosion.

#### 5. *Measurement of Corrosion Currents.*

A cell was constructed using a piece (approximately 4 cm.<sup>2</sup>) of solid solution of 7% magnesium in aluminium (material LXU) as one electrode, and a piece (approximately 1 cm.<sup>2</sup>) of  $\beta$  cast to the composition  $\text{Al}_3\text{Mg}_2$ \* as the other electrode. Arrangements were made for de-

\*  $\beta$  Cast to composition  $\text{Al}_3\text{Mg}_2$  has a different structure, as shown by X-ray investigation, from the  $\beta$  which is present at the grain boundaries after ageing aluminium-7% magnesium alloy at 125° C. for 24 hr. It is not considered likely, however, that the electrochemical properties of the two forms are greatly different.



aerating the cell, and for scratching either electrode, or both simultaneously, with glass points. Corrosion currents flowing between the electrodes were measured, the electrolyte being 3% sodium chloride solution. The results obtained are summarized in Table III. Essentially similar results were obtained on repetition of these experiments.

Noteworthy facts emerging are that: (i) very large currents flowed when the  $\beta$  was scratched, whether the solid solution was simultaneously scratched or not, and whether in aerated or deaerated solution; (ii) on scratching the solid solution only, the current reversed, showing that the filmed  $\beta$  phase was cathodic to the partly bare solid solution; and (iii) in all cases the large currents flowing during scratching decreased

TABLE III.—Corrosion Currents Flowing Between  $\beta$  and Solid Solution in 3% Sodium Chloride Solution.

Experimental Procedure	Corrosion Current,* $\mu$ amp.	Remarks
(1) Cell Aerated.		
Steady current after standing overnight.	31	...
Cell shaken.	40 †	...
$\beta$ only scratched.	575 †	H <sub>2</sub> evolved from $\beta$ , but no visible H <sub>2</sub> evolution from S.S.
Steady current $\frac{1}{2}$ hr. later	34	...
S.S. only scratched.	-4 †	Copious evolution of H <sub>2</sub> from scratch lines on S.S. continuing after scratching had ceased when current temporarily increased to +60 $\mu$ amp.
Steady current $2\frac{1}{2}$ hr. later.	32	Still a little H <sub>2</sub> from S.S.
$\beta$ only again scratched.	600 †	...
Both electrodes scratched simultaneously.	575 †	...
Steady current $2\frac{1}{2}$ days after scratching.	7	...
(2) Cell Deaerated.		
Steady current 3 hr. after deaerating.	2	...
$\beta$ only scratched.	545 †	No visible H <sub>2</sub> evolution from S.S.
S.S. only scratched.	-68 †	Much H <sub>2</sub> evolved from S.S., ceasing after 10 min.
$\beta$ only again scratched.	835 †	H <sub>2</sub> evolved from S.S. on side which had previously been scratched, but not from other side.
Both electrodes scratched simultaneously.	800 †	...

S.S. = solid solution.

\* Normally  $\beta$  was the anode. A negative sign indicates that  $\beta$  was the cathode.

† Maximum current observed.

almost immediately to their previous values when scratching was stopped, indicating a very rapid polarization of the scratched areas. When the cell was in the steady state deaeration caused the corrosion current to drop from 7 to 2  $\mu$ amp.

## VI.—EXPERIMENTS RELATED TO MECHANICAL ASPECTS.

### 1. *Failure of Notched Specimens.*

Notches 0.07 in. deep and approximately 0.006 in. wide were made in each side of the gauge-length ( $\frac{1}{4} \times \frac{1}{4} \times 2$  in.) of a tensile test-piece of aluminium-7% magnesium alloy which had been solution-treated, overstrained 10%, and annealed for 24 hr. at 125° C. followed by 5 days at 150° C., giving apparently continuous grain-boundary  $\beta$  networks.

When the ultimate tensile stress of this specimen was determined, parts of the fracture were intercrystalline, and no deformation of the crystals was apparent (see Fig. 5, Plate XIV). The breaking stress of the material between the notches was 25% greater than that of an unnotched specimen.\* The gross deformation and transcrystalline fracture in an unnotched specimen are shown in Fig. 6 (Plate XIV).

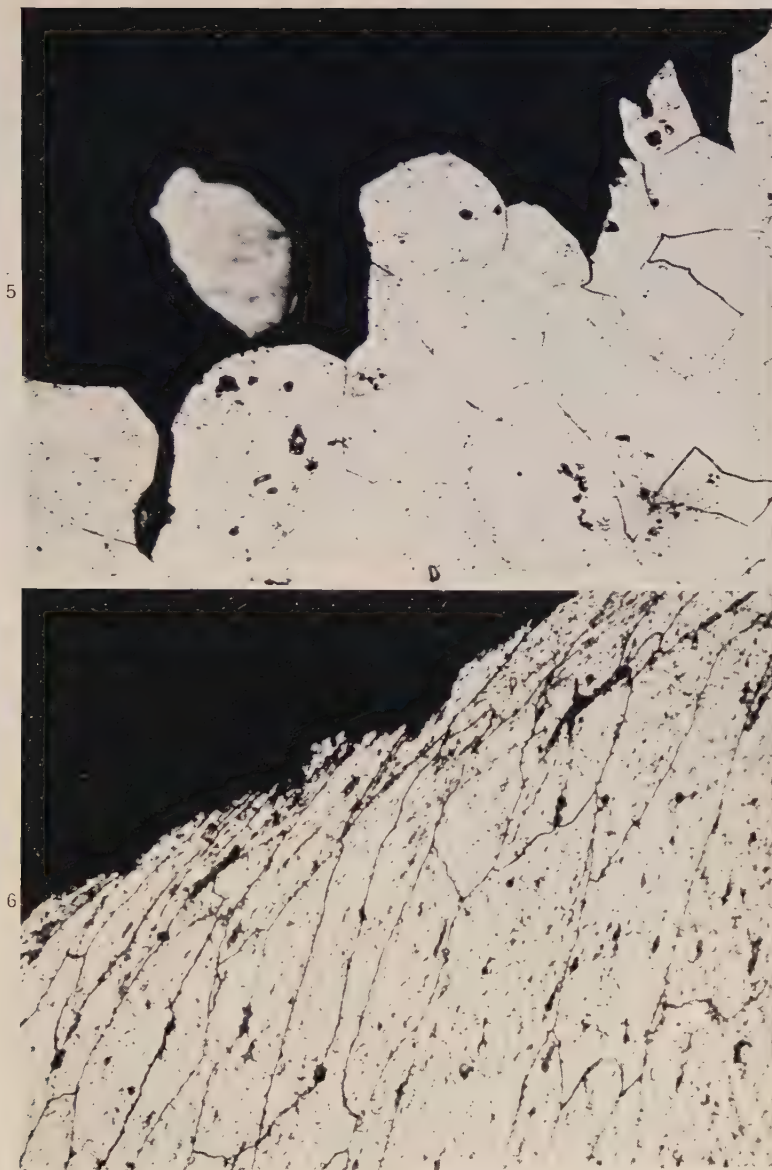
### 2. *Creep Tests.*

A test-piece of solution-treated material NFO was loaded at room temperature at 20.7 tons/in.<sup>2</sup> (the ultimate tensile stress of the material being 21.3 tons/in.<sup>2</sup>, 0.1% proof stress 8.3 tons/in.<sup>2</sup>, and elongation 24%). The specimen failed after 440–510 hr., with an extension at fracture of 40%. The fracture was completely transcrystalline, and no sign of intercrystalline cracking could be seen anywhere in the specimen.

A second test-piece was homogenized and aged for 8 days at 200° C. and then loaded at 21.5 tons/in.<sup>2</sup> (the ultimate tensile stress of the material being 22.4 tons/in.<sup>2</sup>, 0.1% proof stress 6.9 tons/in.<sup>2</sup>, and elongation 18%). The specimen, which had a grain-boundary network of  $\beta$  particles resolvable at high magnifications, failed in 383 hr., the extension at fracture being 21%.

Parts of the fracture of this aged specimen were intercrystalline, although the greater portion was transcrystalline. There was intercrystalline cracking in the body of the material (see Fig. 7, Plate XV). There was some intercrystalline cracking in a similar specimen pulled for determination of mechanical properties, but much less than in the creep specimen, indicating a difference between a short-time and a relatively long-time test.

\* In subsequent experiments increases in breaking stress of up to 60% have been observed.



FIGS. 5-6.—Aluminium-7% Magnesium Alloy, Solution-Treated, Overstrained 10%, and Aged for 1 day at 125° C. followed by 5 days at 150° C. Etched in 5%  $H_3PO_4$ .

FIG. 5.—Part of Mechanical Fracture in Notched Specimen.  $\times 500$ .

FIG. 6.—Mechanical Fracture in Unnotched Specimen.  $\times 500$ .

[To face p. 248.

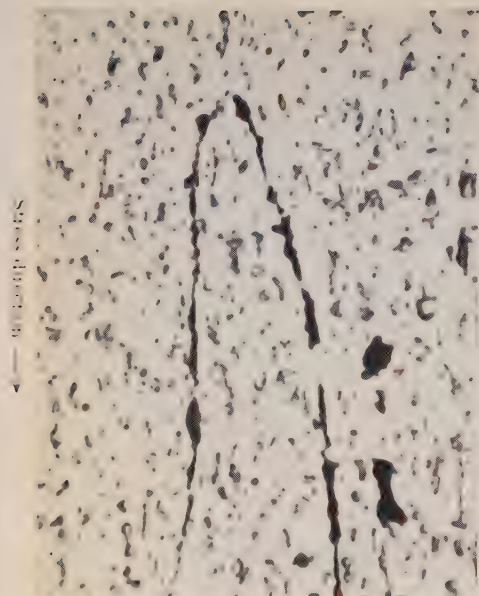


FIG. 7.—Aluminium-7% Magnesium Alloy, Solution-Treated and Aged 8 days at 200° C. Intercrystalline cracking in creep specimen in area near creep fracture. Etched in Wassermann's reagent.  $\times 2000$ .

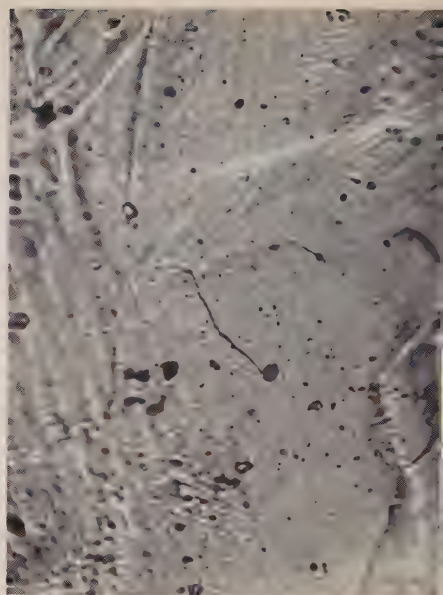


FIG. 8.—Aluminium-7% Magnesium Alloy, As Received, Aged 3 days at 125° C. Surface crack in polished, stressed tensile specimen. Unetched.  $\times 500$ .



FIG. 9.—Aluminium-7% Magnesium Alloy, As-Received, Aged 3 days at 125° C. Surface crack in stressed tensile specimen. Specimen shown in Fig. 8, repolished and lightly etched in Wassermann's reagent.  $\times 500$ .



FIG. 10.—Aluminium-7% Magnesium Alloy, Solution-Treated, Overstressed 10%, and Aged 1 day at 125° C. Uncorroded stressed loop specimen showing intercrystalline cracks. Etched in 10% NaOH at 55° C.  $\times 350$ .



Stress-corrosion crack.

FIG. 11.—Aluminium-10% Magnesium Alloy, Solution-Treated, Overstrained 10%, and Aged 1 day at 125° C. Showing stress-corrosion crack in stressed loop specimen immersed in 3% NaCl solution. Etched in 10% NaOH at 55° C.  $\times$  2500.





### *3. Effect of Gradually Increasing Stress.*

One surface of a tensile test-piece cut from sheet and aged for 3 days at 125° C. was polished and observed under the microscope while an increasing stress was gradually applied. Intercrystalline cracks began to appear in the surface at about 3% overstrain, and at about 11% overstrain transcrystalline cracks also appeared. Fig. 8 (Plate XV) shows an intercrystalline crack in the specimen after the strain had been relieved. The specimen was repolished and given a light etch; this proved that the cracks were intercrystalline (see Fig. 9, Plate XV).

### *4. Mechanical Cracks in a Stressed Loop.*

A stressed loop (material NFO) was mounted in Bakelite while still stressed, polished, and the edge of the loop examined. Many short intercrystalline cracks were observed, chiefly in the outer layers of the loop, and although there was a tendency for more to occur at the point of maximum stress, i.e. the tip of the loop, there were also cracks in the sides at points where the stress in the outer layers must have been much less than at the tip. The cracks were in various directions, though the general tendency was for cracking to be perpendicular to the loop surface (see Fig. 10, Plate XV).

These experiments demonstrate that intercrystalline fractures occur in notched tensile specimens and in creep and other suitably stressed aluminium-7% magnesium alloy specimens in a condition susceptible to rapid stress-corrosion. It is not easy to demonstrate by photomicrographs the occurrence of mechanical disruption caused by the stress concentration at the base of a corrosion crevice, owing to the difficulty of distinguishing between penetration due to corrosion and that due to mechanical breakdown. Fig. 11 (Plate XVI) possibly shows mechanical disruption at a grain boundary at the tip of a stress-corrosion crack. The experiment next described, however, gives good evidence for the occurrence of mechanical disruption during stress-corrosion.

### *5. Discontinuous Nature of Stress-Corrosion in a Loop.*

A loop was prepared from material NFO in the usual way except that it was made by bending round a former  $\frac{3}{4}$  in. in dia. instead of  $\frac{1}{2}$  in. To an arm fixed at one side of this loop was attached a small mirror which reflected a beam of light on to a scale 110 cm. away. Movement of the side of the loop, such as always occurs when loops collapse during stress-corrosion, was thus magnified and indicated by movement of the

light-spot on the screen, the light-spot being viewed through a lens. The loop was immersed in 6% sodium chloride solution.

The light-spot began to move after about an hour, and during the next hour it moved steadily. By this time a crack had appeared, and a series of small jumps of the light-spot began. During the next 2 hr. at least twenty of these rapid small jumps were observed, each of about  $\frac{1}{2}$  mm. on the screen, corresponding to a movement of the side of the loop through an angle of approximately  $45''$ . The jumps were sharp definite movements such as would be expected if the metal underwent a series of limited mechanical fractures. The slow gradual movement of the light-spot continued between the sudden kicks.

After about 5 hr. cracking was complete and movement of the light-spot ceased. The total movement of the side of the loop was about  $1.5^\circ$ .

#### VII.—DISCUSSION OF RESULTS.

Some of the main facts which a theory of the mechanism of stress-corrosion in aluminium-7% magnesium alloy must explain are as follows :

(1) For constant-load tests the rate of stress-corrosion increases with the applied load.

(2) The rate of loss of strength of tensile specimens under constant load due to stress-corrosion increases with time <sup>1</sup> (see Fig. 3).

(3) Failure can occur rapidly at applied loads well below the limit of proportionality of the material; e.g. material with a limit of proportionality of 8.8 tons/in.<sup>2</sup> can fail rapidly when the initial stress is 4.4 tons/in.<sup>2</sup> (Perryman and Hadden <sup>1</sup>).

(4) Oxygen dissolved in the corrosive agent is necessary.

(5) Hydrogen is evolved from the crack during stress-corrosion.

(6) The rate of cracking increases as the pH falls, and decreases as the pH rises. There is no cracking at pH values greater than about 11.

(7) The stress-corrosion process is a discontinuous one.

These and other observed facts appear to be explained by a theory along the following lines :

##### 1. *General Outline of Theory.*

When aluminium-7% magnesium alloy in a susceptible condition, i.e. with more or less continuous networks of  $\beta$  phase at the grain boundaries, is stressed and immersed in a neutral solution such as 3% sodium chloride solution, electrochemical corrosion takes place, attack being concentrated on the  $\beta$  at the exposed grain boundaries. Inter-

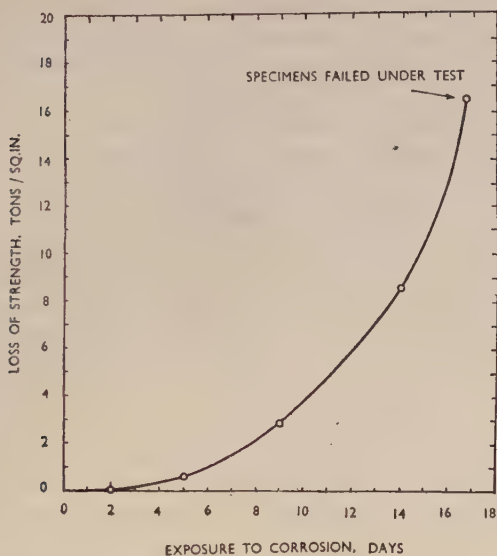


FIG. 3.—Loss of Strength of Aluminium-7% Magnesium Alloy due to Stress-Corrosion. Material solution-treated, overstrained 10%, and aged at 125° C. for 24 hr. Graph gives difference in strength loss between stress-corrosion specimens and corresponding unstressed control specimens, after various periods of exposure.<sup>1</sup> Initial stress 5 tons/in.<sup>2</sup> in all cases. Specimens sprayed twice daily with 3% NaCl solution.

crystalline crevices are thus slowly produced, the cathodic reaction being chiefly oxygen absorption. Owing to locally favourable conditions one crevice advances beyond the others, and as it deepens and sharpens, the stress concentration at its base increases. When this stress concentration reaches a critical value mechanical disruption occurs at the base of the crevice, causing a sudden extension of the crevice along the grain boundary and exposing bare  $\beta$  surfaces, and probably also bare surfaces of solid solution.

The precise nature of this mechanical disruption is not certain, but it is thought to proceed along grain boundaries because of the presence of films of the  $\beta$  phase. This mechanical propagation of the crack is soon arrested, e.g. when an unfavourably orientated grain boundary is encountered (a number of other possible reasons are discussed later).

The results are that :

- (i) The crevice is suddenly extended mechanically.
- (ii) The local high stress is temporarily relieved.
- (iii) Corrosive agent is immediately drawn down the crevice by

capillary action and atmospheric pressure, and rapid attack on the bare  $\beta$  surfaces occurs, thus deepening the crevice further.

(iv) Hydrogen is evolved from the bare metal surfaces.

Extension of the crevice occurs by (i) and (iii), and it would be difficult to distinguish the penetration due to either of these two factors. A period of relatively fast corrosion will occur when bare  $\beta$  surfaces are exposed, but the proportion of the penetration due to corrosion as compared with that due to mechanical breakdown is unknown.

(v) After the local breakdown at the base of the crevice and the ensuing period of rapid corrosion, films re-form on the bare electrodes and the rate of corrosion quickly decreases as the  $\beta$  becomes re-filmed. The reason for the filming is probably the production of alkali at the nearby cathodes, which raises the pH of the minute amount of liquid at the tip of the crevice.

(vi) Corrosion of the  $\beta$  proceeds slowly, being now controlled by anodic polarization, the cathodic reaction being oxygen absorption at the metal surfaces at which oxygen is available, possibly outside the crevice. Ordinary intercrystalline corrosion is in fact again occurring.

(vii) The crevice is thus deepened relatively slowly until the conditions again produce a stress concentration sufficient to cause further mechanical disruption. The whole cycle of events is then repeated.

It is thus visualized that slow intercrystalline corrosion, mechanical disruption, and fast intercrystalline corrosion follow each other in turn. However, the crack will not be propagated at a uniform rate across its advancing front, and small elements in the crevice, possibly of similar dimensions to the solid-solution grains, will at any one time be at different stages of the cycle. As a result, a continuous stream of hydrogen will come from the crack as it progresses. Moreover, it will be possible to prevent or arrest cracking indefinitely by deaerating the solution, since, if the stage of slow corrosion by oxygen absorption is prevented for each element, succeeding stages cannot occur, and the process must come to a stop.

This qualitative picture will apply for all types of stressed specimen, and there is no reason to think that it will be essentially different if the specimen is sprayed with 3% sodium chloride solution instead of being completely immersed.\* Most of the experimental observations have been made using loop specimens, which are easily handled experimentally, but the conditions in such specimens are complicated, since the operating stress changes as stress-corrosion proceeds. It is of interest therefore to apply the theory to the simpler case of tensile

\* The effect of changes in the corroding environment is discussed by Perryman and Hadden.<sup>1</sup>



specimens under constant applied load. In this case, since the stress concentration at the base of a crevice increases as the radius of curvature at the base decreases and the depth of crevice increases, on the average the amount of corrosion necessary between successive mechanical disruptions will decrease as the crevice penetrates into the specimen. This will probably be true whatever the precise nature of the mechanical disruptions (see Section VII. 2 below).

For an element in the stress-corrosion crevice the graph showing rate of corrosion against time would be of the form shown in Fig. 4. The initial period of slow corrosion with electrodes filmed, before stress-corrosion begins, is represented by *AB* in Fig. 4. The first mechanical

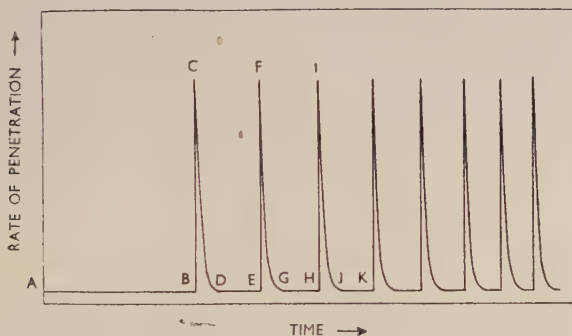


FIG. 4.—Theoretical Curve for Rate of Corrosion in Crevices during Stress-Corrosion of Aluminium-7% Magnesium Alloy Tested under Constant Tensile Load.

disruption results in a period of rapid corrosion occurring between *B* and *D*, which is followed by a slow period *DE* when the surfaces become filmed. The next mechanical disruption causes another period of rapid attack between *E* and *G*, and the succeeding slow period *GH* follows. *GH*, however, is of shorter duration than *DE*, since the crevice is now deeper, and less penetration is needed before the stress concentration becomes sufficient to cause mechanical disruption. Similarly, *JK* is shorter than *GH*, and so on, and the process is continually accelerating. Summation of this process for all the elements of the crevice shows that a specimen should lose its strength at an ever-increasing rate. This has been demonstrated experimentally<sup>1</sup> (see Fig. 3). Finally, the ultimate tensile stress of the residual metal is exceeded and the specimen breaks mechanically.

Much of the experimental evidence on which the theory outlined above is based is readily apparent, e.g. the necessity of oxygen for cracking (Section V. 1), the evolution of hydrogen during cracking

(Section V. 2), and the occurrence of mechanical intercrystalline cracks of limited extent in suitably stressed material (Sections VI. 2, 3, and 4, and Figs. 7-10, Plate XV). The corrosion-current measurements (Section V. 5 and Table III) suggest that the production of bare  $\beta$  during stress-corrosion will lead to much more rapid intercrystalline corrosion than occurs in unstressed material (in which bare  $\beta$  is never present) and also show that such rapid attack is likely to be quickly reduced by the formation of films. Sudden jumps in the potential of a cracking loop and in the rate of movement of its arm, both of which occur during the stage of active cracking, show the discontinuous nature of the process.

In the following Sections, certain aspects of the process are discussed in more detail. In Section VII. 2 the nature and effects of the mechanical processes occurring during stress-corrosion are considered. Section VII. 3 (a) deals with the electrochemical aspects, including in particular the nature of the cathodic reaction, and Section VII. 3 (b) with the effect of change in the pH of the corroding environment.

## 2. *Mechanical Processes During Stress-Corrosion.*

Before considering mechanical processes occurring during stress-corrosion it should be stated that stress may have an effect additional to that suggested in the theory described. It is possible that stress can cause a metal to become more anodic merely on account of the greater energy content of stressed as opposed to unstressed metal. Since there is stress concentration at the base of crevices, it is possible that these regions would be more anodic for this reason apart from any other. In the absence of adequate experimental evidence it is not possible to ignore this factor in any theory of stress-corrosion, and it may cause an increase in the rates of corrosion in addition to the mechanism outlined above.

It has been postulated that when a crevice formed by intercrystalline corrosion becomes sufficiently sharp and deep, the stress concentration at the tip causes some mechanical disruption. It has been pointed out that this disruption might be sufficient only to break corrosion films, or, on the other hand, it may cause mechanical breakdown of the metal, so that an appreciable part of the penetration during the stress-corrosion process could be purely mechanical. The sudden movements of the arm of a loop during stress-corrosion (Section VI. 5, p. 249), which were thought to be too abrupt to be accounted for by periods of rapid corrosion, are good evidence for the occurrence of a series of limited local mechanical breakdowns.

Intercrystalline cracks were produced mechanically in suitably

stressed aluminium-7% magnesium alloy in several experiments (see Figs. 7-10, Plate XV). These were of limited extent and did not lead to complete fracture of the specimen. Similar intercrystalline cracks of limited extent may be produced at the tip of the crevice during stress-corrosion, and a possible mechanism of their formation is given below. To be acceptable, this mechanism should explain why in stress-corrosion failures there is little or no plastic deformation of the crystals surrounding the fracture, while in a normal fracture in tension there is severe deformation and a transcrystalline fracture (Fig. 6, Plate XIV). On the other hand, intercrystalline fracture with little or no deformation of the surrounding crystals was produced when a specimen containing fine notches was pulled in a tensile test (Section VI. 1 and Fig. 5, Plate XIV).

These facts may be explained by assuming that at the tip of a sharp crevice approximately perpendicular to the direction of applied stress, there exists locally a stress condition which prevents fracture by shear and the accompanying plastic deformation, even though the material as a whole is ductile. Such a state of hydrostatic tension, or system of triaxial stresses<sup>11</sup> may exist at the base of sharp notches in a ductile metal and, if so, fracture in this limited region can only be brittle. Stress-corrosion cracks in aluminium-7% magnesium alloy are wholly intercrystalline, and therefore any mechanical fractures which occur at the tip of the crevice during stress-corrosion proceed along grain boundaries. Any such weakness of the grain boundaries under these conditions is probably due to the presence of films of the  $\beta$  phase.

There are several reasons why local mechanical fractures occurring during stress-corrosion, once started, should stop after making limited progress :

(a) The formation of subsidiary crevices in the vicinity of the main crevice would reduce the stress concentration.

(b) The stress concentration may be reduced owing to an increase in the radius of curvature at the tip of the crevice; this could occur for a number of reasons, e.g. encountering an obstacle such as an inclusion.

(c) The fracture might stop when an unsuitably orientated grain boundary was reached, because only a component of the stress at the tip of a crevice is acting to cause fracture along a grain boundary not perpendicular to the stress direction.

(d) If the stress concentration necessary to cause fracture along a grain boundary containing  $\beta$  is less than that necessary to cause fracture along a boundary not containing  $\beta$ , it is possible that fractures may be stopped when a gap in the  $\beta$  at the grain boundary is encountered.

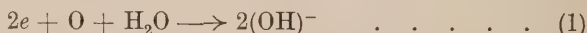
When the mechanical fracture stops, penetration will proceed first

by rapid corrosion of the bare  $\beta$  surfaces exposed during the mechanical breakdown, and then by slower corrosion. Eventually the stress concentration will be sufficient for a further partial mechanical failure. The proportions of the penetration due to corrosion and to mechanical breakdowns probably depend on the operating stress.

### 3. *Electrochemical Aspects of Theory.*

#### (a) *Neutral Solutions.*

In the case of a stressed specimen immersed in a neutral solution, such as 3% sodium chloride solution, corrosion will initially occur mainly by oxygen absorption, i.e. the reaction at the cathodic areas (the solid solution in the grain bodies) will be chiefly :



The reversible potential for hydrogen evolution is given by :

$$E = \frac{RT}{F} \log_e [H^+] - 0.284 \quad . \quad . \quad . \quad . \quad (2)$$

and for 3% sodium chloride solution, the pH of which is about 6.5,  $E = -0.66$  V. The overvoltage at an aluminium surface is about 0.5 V. for current densities up to about 100  $\mu\text{amp./cm.}^2$ , and it will probably be little different for the solid solution of 7% magnesium in aluminium (the overvoltage for pure magnesium is about 0.6 V.). As the current densities involved are unknown, the exact overvoltage is also unknown, but it will probably not be less than 0.5 V. Therefore appreciable hydrogen evolution from aluminium-7% magnesium alloy in 3% sodium chloride solution will not occur if the potential is more positive than  $-(0.5 + 0.66)$  V., i.e.  $-1.16$  V. But the potential of the unstressed alloy in aerated 3% sodium chloride solution becomes steady at about  $-0.8$  V., and hydrogen evolution is therefore not to be expected. Corrosion will therefore proceed by oxygen absorption, and lack of oxygen should inhibit the corrosion of a stressed specimen from the outset, so that stress-corrosion should never begin. It has been confirmed experimentally that no cracking occurred in deaerated solution after periods of immersion of the order of a hundred times as long as was necessary for cracking to begin in aerated solution.

However, some hydrogen evolution, insufficient to form visible bubbles, can occur at less negative potentials, particularly at points of low overvoltage (due to impurities, &c.). For instance, when oxygen is admitted to a specimen which has for some time been in a deaerated solution, the potential is found to be approximately at point B (Fig. 1). This suggests that the process of consolidation of the



is an anodic solution causes the potential to rise from  $d$  to  $E$ , as shown in decreased solution. The process is therefore probably associated with hydrogen evolution, whereby gas and voids in the film become clogged with corrosion product, and potential rises to potentials more positive than  $-1.15$  V. Although it was that about 10% of the corrosion of pure aluminum is due to chloride evolving in due to hydrogen evolution. Some of corrosion corrosion of commercial aluminum  $Ti$  magnesium was shown in  $Ti$ , which corrodes without forming that which plate is decreased without time but appear to give rise to excellent attack, some stress-corrosion, but not occur in the case of oxygen. This may be explained in part by the observation that  $W$  was noted that with continuous wetting in distilled water most of corrosion occurring by hydrogen evolution is very small  $I$  when oxygen is removed.

During anode stress-corrosion the overall potential of a large specimen is about  $-1.05$  V, see Fig. 2, but although the  $W$  will move to that the value  $-1.15$  V, hydrogen comes from the metal. It is likely that at the anode when mechanical disruption occurs the metal is polished in the anode. The overall potential remains approximately. The anode takes (Fig. 2) are indication of the speed of response of the anode and was previously noted to enable the maximum reading to be observed during the changes. In the experimental cell specimen  $W$  is the potential coupled electrodes was never more cathodic than about  $-1.15$  V, hydrogen evolution was possible whether the cell was stressed or not. Large currents flowed when the  $W$  was connected to an anodic or decreased solution, and in both cases hydrogen evolution took place at the cathode. It is interesting to note, however, that the  $W$  was first connected, before the solid solution had been etched, a current of the order of 100–500 amp. was sufficient to cause very visible hydrogen bubbles at the cathode in order stressed solution. When the  $W$  was connected after or while the anode was stressed, visible bubbles came from the anode and at the cathode but there was only a slight increase in the current at the stressed cell and about 10% increase in the decreased cell. Hydrogen evolved during cracking may therefore come from sources, viz. cathodic parts of the large cracks, areas of bare solution, areas of thinly etched solid solution, or, if the current is sufficiently high, from normally etched solid solution.

Stress and evolution of hydrogen will cease when the  $W$  becomes an anode and the potential rises again. This is likely to happen quickly



since the large corrosion currents produced in the experimental cell when the  $\beta$  was scratched, dropped very rapidly when the scratching was stopped, in either aerated or deaerated solution. The reason for the filming of the  $\beta$  and the consequent fall in the corrosion rate is probably the production of alkali at the nearby cathodes when the rapid attack is occurring, and the rise in the pH of the minute amount of liquid at the tip of the crevice. Diffusion of oxygen into the crevice is not likely to be the chief reason for the filming of the  $\beta$ , since the large corrosion current on scratching  $\beta$  decreased rapidly when scratching was stopped, even in deaerated solution.

During the periods of slow corrosion that succeed each period of rapid attack, corrosion currents must flow from the  $\beta$  at the tip of the crevice to cathodic areas where depolarization by oxygen can occur.

When it is possible to arrest by deaeration a crack already started, the periods of rapid corrosion cannot deepen the crevice sufficiently for mechanical disruption to occur again without intervening periods of slow attack by oxygen absorption. It is possible, however, that during the later stages of the failure of a direct tensile specimen, cracking is proceeding so rapidly that no slow stages intervene, and during this time it would not be possible to stop the crack by deaeration.

The experimental results show that readmission of oxygen to a deaerated solution containing a specimen which was initially partly cracked in aerated solution, results in very rapid failure of the specimen, the rate of cracking during this stage being considerably greater than for a loop immersed in aerated solution throughout its life. This can be explained by assuming that dissolved oxygen can diffuse to the tip of a crevice during continuous immersion in aerated solution. This would decrease the rate of slow corrosion, since the corrosion current in a cell with the cathode fully aerated and the anode partially aerated would be less than that in a similar cell with the cathode fully aerated and the anode completely deaerated.

It should be pointed out that some caution has to be exercised in interpreting the results obtained from cells constructed of massive electrodes. Such cells obviously do not imitate the conditions at the base of crevices in all respects. As an example, the potential of aluminium-7% magnesium alloy with  $\beta$  at the grain boundaries is about  $-0.8$  V. in 3% sodium chloride solution, but when electrodes of massive  $\beta$  and solid solution are coupled together in this solution a resulting potential more positive than about  $-1.2$  V. has never been observed, even when the ratio of the areas of solid solution to  $\beta$  was as large as 50 : 1.

(b) *Acid and Alkaline Solutions.*

Cracking is much slower in alkaline solution, and much faster in acid solution, than it is in neutral solution (Table II).

On immersion in strongly acid solution oxide films will dissolve and the main reaction is likely to be hydrogen evolution. Thus, at pH 0 the potential for hydrogen evolution will be approximately  $-(0.5 + 0.28)$  V., i.e.  $-0.78$  V. The potential of stressed aluminium-7% magnesium alloy specimens in *N*-hydrochloric acid is found to be about  $-0.87$  V., and there is much hydrogen evolution. Stress-corrosion cracking still occurs, however, and in much shorter times than in neutral solution. In acid solutions it is to be expected that the initial intercrystalline corrosion will be more rapid than in neutral solutions, and the time before stress-corrosion begins will be correspondingly less.

In these conditions dissolved oxygen is likely to be relatively unimportant. If the rate of attack of  $\beta$  in strongly acid solution were sufficiently greater than that of unfilmed  $\beta$  in neutral solution, it would be possible for a crack to proceed completely through a specimen at the rapid rate with no intervening slow periods. This would occur if the crevice deepened sufficiently for further mechanical disruption to take place before the  $\beta$  became filmed. This is apparently not so, however, since even in 3% sodium chloride solution adjusted with hydrochloric acid to pH 1, oxygen has some effect. When such a solution was open to air a loop in it cracked completely across in about 5 min. (Table II), but when oxygen was excluded, cracking of a similar loop did not begin until after about 40 min., and was only three-quarters of the way across after 200 min.

Even in strongly acid solution it is conceivable for the pH at the tip of a narrow crevice to rise to a value high enough to cause filming of the  $\beta$ . Since the time taken for the pH to rise from 0 to that necessary for film formation would be expected to be considerably longer than that taken in rising from 7 to the same value, the periods of rapid corrosion would probably be longer in acid solution than in neutral, and the necessary periods of slow attack correspondingly shorter. It is possible that efficient enough deaeration would completely prevent cracking in acid solutions. On the other hand, when the  $\beta$  at the base of the crevice is filmed, the cathodic reaction in acid solution is probably still chiefly hydrogen evolution. Complete removal of oxygen might therefore only slow down but not prevent corrosion during this stage, and in this case deaeration would not prevent cracking in acid solutions.

In alkaline solutions, on the other hand, it is to be expected that the

rate of cracking will be slower, since bared  $\beta$  will film more quickly, the periods of fast corrosion will be shorter, and periods of slow attack correspondingly longer. In very alkaline solutions (e.g. 1% sodium hydroxide) the process changes entirely, the alloy is dissolved away generally, and stress-corrosion cracking no longer occurs. In sufficiently alkaline solutions massive  $\beta$  electrodes are found to become cathodic to solid-solution electrodes. This is in agreement with the observations of Akimov and Clark,<sup>14</sup> and occurs presumably because a film of magnesium hydroxide forms on the  $\beta$  while the aluminium oxide or hydroxide on the solid solution is soluble. Thus, in sufficiently alkaline solution, intergranular attack will not occur, since corrosion of the solid solution with the formation of aluminates and much hydrogen is faster than the corrosion of the  $\beta$  phase.

#### VIII.—STRESS-CORROSION IN OTHER MATERIALS.

It appears probable that, for stress-corrosion to occur, some path for selective corrosion must exist, which may be either intercrystalline or transcrystalline. This path may be due to a second phase, but can conceivably be present for other reasons. It is possible that even in a pure metal the grain boundaries may in some environments be sufficiently anodic to the grain bodies for intercrystalline attack to take place. The danger of stress-corrosion is likely to be greatest if the path for selective attack is an anodic one, but it is conceivable that stress-corrosion could occur as a result of preferential attack close to a continuous cathodic path through the metal.

A good instance of the important part played by electrochemical factors in stress-corrosion is provided by certain magnesium alloys which can suffer intercrystalline or transcrystalline failure according to the nature of the corrosive environment.<sup>3</sup>

When crevices are produced by selective attack, stress-concentration effects can then lead to localization and acceleration of attack, so that eventually failure occurs at a few (or even only one) isolated cracks.

The mechanism of stress-corrosion will depend on the mechanical as well as the electrochemical nature of the selective path. It has been found<sup>15</sup> that alloys having material at the grain boundaries which is more ductile than the material in the grain bodies, are liable to fail when stressed (at, say, about 0.1% proof stress) in air or some inert environment. This inherent intercrystalline weakness has been demonstrated for a number of alloys. In such cases the presence of a corrosive environment accelerates the failure. To provide a complete

picture it is necessary to explain the mechanical failure, before the combined effects of stress and corrosion can be considered.

The detailed theory given in the present paper applies to the stress-corrosion of aluminium-7% magnesium alloy. This mechanism may have points in common with the mode of failure in other alloys, but the exact nature of the stress-corrosion process is likely to depend on the material in question. The type of mechanism given would be expected to apply fairly closely in the case of any other aluminium-base alloy containing grain-boundary films of an anodic second phase, unless this phase is more ductile than the grain body, when, as already stated, other factors have to be taken into account.

In general, it appears that stress-corrosion depends on a combination of metallurgical, electrochemical, and mechanical factors, and that the mechanism of the process is likely to vary from alloy to alloy, though certain broad principles may apply to many cases.

#### ACKNOWLEDGEMENTS.

The authors wish to thank the Chief Scientist, Ministry of Supply, and the Director and Council of the British Non-Ferrous Metals Research Association for permission to publish this paper. They also wish to thank a number of their colleagues for many helpful discussions.

#### REFERENCES.

1. E. C. W. Perryman and S. E. Hadden, *J. Inst. Metals*, 1950, **77**, 207.
2. E. H. Dix, Jr., *Trans. Amer. Inst. Min. Met. Eng.*, 1940, **137**, 11.
3. R. B. Mears, R. H. Brown, and E. H. Dix, Jr., *Symposium on Stress-Corrosion Cracking of Metals (A.S.T.M.-A.I.M.E.)*, 1944, p. 323.
4. F. H. Keating, *Inst. Metals: Symposium on Internal Stresses in Metals and Alloys*, 1948, p. 311. (Monograph and Rep. Series No. 5.)
5. U. R. Evans, "Metallic Corrosion, Passivity and Protection", pp. 463, 466. London: 1946 (Edward Arnold and Co.).
6. M. Hansen, *J. Inst. Metals*, 1939, **64**, 77 (discussion).
7. F.-C. Althof, *Luftfahrtforsch.*, 1938, **15**, 60.
8. P. Brenner and W. Roth, *J. Inst. Metals*, 1948, **74**, 159.
9. J. T. Waber and H. J. McDonald, *Corrosion and Material Protection*, 1945, **2**, (8), 13; (9), 13; 1946, **3**, (3), 13; (4), 13.  
J. T. Waber, H. J. McDonald, and B. Longtin, *ibid.*, 1946, **3**, (1), 13; (2), 13.  
R. D. Misch, J. T. Waber, and H. J. McDonald, *ibid.*, 1946, **3**, (5), 13.
10. L. de Brouckère, *J. Inst. Metals*, 1945, **71**, 131.
11. E. Orowan, *Trans. Inst. Eng. Ship. Scotland*, 1946, **89**, 165.
12. F. A. Champion, *Trans. Faraday Soc.*, 1945, **41**, 593.
13. R. B. Mears, *Symposium on Corrosion (Amer. Soc. Refrig. Eng.)*, 1943.
14. G. V. Akimov and G. B. Clark, *Trans. Faraday Soc.*, 1947, **43**, 679.
15. E. C. W. Perryman and J. C. Blade, *J. Inst. Metals*, 1950, **77**, 263.





# RELATIONSHIP BETWEEN THE AGEING AND 1251 STRESS - CORROSION PROPERTIES OF ALUMINIUM-ZINC ALLOYS.\*

By E. C. W. PERRYMAN,<sup>†</sup> M.A., A.I.M., STUDENT MEMBER, and  
J. C. BLADE,<sup>‡</sup> B.Sc., STUDENT MEMBER.

(Communication from the British Non-Ferrous Metals Research Association.)

## SYNOPSIS.

The changes in microstructure which take place on ageing aluminium-10% zinc alloy at room temperature and at temperatures up to 125° C. have been investigated and the results correlated with the stress-corrosion properties. Alloys containing 8 and 13% zinc were also examined. Age-hardening data have been determined and are given in an Appendix.

On ageing the aluminium-10% zinc alloy between room temperature and 100° C. hardening took place with the formation at the grain boundaries of zinc-rich particles and a "light phase" which is considered to be the aluminium solid solution stable at the temperature of ageing. At ageing temperatures above 100° C. no "light phase" was found. It is considered therefore that at and below 100° C. the precipitation process is discontinuous and above 100° C. continuous. The same structural changes accompanied the age-hardening of the 8 and 13% zinc alloys, except that with the 13% zinc alloy the light phase was found at higher ageing temperatures than was the case with the 10% zinc alloy. The rate of hardening and of precipitation increased with increasing zinc content.

Specimens of the 10% and of the 13% zinc alloy, solution-treated and aged at room temperature, were found to fail with an intercrystalline fracture when subjected to a sustained tensile stress in a non-corrosive environment. Moreover, the type of fracture was dependent upon the rate of straining, rapid rates giving transcrystalline fractures. It is considered that the aluminium solid solution stable at the temperature of ageing is responsible for this delayed intercrystalline fracture, and a mechanism of fracture, depending upon creep in the grain-boundary ductile phase, is discussed. Results of similar tests carried out on an aluminium-4% copper alloy, aged to an extent such that the stable solid solution was precipitated at the grain boundaries, are given as support for this view of the mechanism of fracture.

Stress-corrosion tests on the aluminium-zinc alloys carried out by spraying with 3% sodium chloride solution showed that the corrosive environment enhances the rate of intercrystalline fracture, and that the stress-corrosion susceptibility increases with the zinc content. A mechanism of stress-corrosion is put forward in the light of the electrochemical properties of the precipitated phases.

---

\* Manuscript received 24 September 1949. The work described in this paper was made available to members of the B.N.F.M.R.A. in a confidential research report issued in 1949.

<sup>†</sup> Investigator, British Non-Ferrous Metals Research Association, London.

<sup>‡</sup> University of Durham; formerly Bursar, British Non-Ferrous Metals Research Association, London.

## I.—INTRODUCTION.

IN general, aluminium alloys susceptible to stress-corrosion contain two or more phases differing widely in electrochemical properties. Aluminium-zinc alloys are apparent exceptions and are of theoretical interest because :

(a) Stress-corrosion failures have been reported in allegedly homogeneous alloys of this type;<sup>1, 2, 3</sup> and

(b) In 3% sodium chloride solution the difference in potential between the solid solution and the equilibrium precipitate (zinc containing up to 0.4% aluminium) is very small.

Stress-corrosion and electrochemical tests supplemented by metallographic examination, have therefore been carried out on aluminium-10% zinc alloy after various heat-treatments. The age-hardening properties of the alloy have been determined and are given in an Appendix (see p. 282).

Stress-corrosion failures and intercrystalline failures in stressed specimens in non-corrosive environments have been reported by several investigators not only in alloys of the aluminium-zinc system but also in alloys such as aluminium-8% zinc-2% magnesium.

Grogan and Pleasance<sup>1</sup> carried out stress-corrosion tests on high-purity aluminium alloys containing 10, 15, and 20% zinc, and also on an alloy containing zinc 20 and copper 3%. Specimens were tested under sustained stress in air and in 5% sodium chloride solution after air-cooling from 450° C. At 6 tons/in.<sup>2</sup> the 15 and 20% zinc alloys failed in air with an intercrystalline fracture; all the alloys failed with an intercrystalline fracture when stressed in 5% sodium chloride solution. Grogan and Pleasance suggested that the zinc content was a controlling factor in the intercrystalline failure of these materials.

The French workers Chaudron and Hérenguel<sup>2, 3</sup> have conducted a considerable amount of research on aluminium-zinc solid solutions with and without additions of magnesium. Chaudron<sup>2</sup> by electrolytic polishing revealed intercrystalline cracks and slip-bands in these alloys aged at room temperature, though no stress was applied. He suggested that the slip-bands indicated internal stresses proportionate to the time of ageing. No trace of precipitation was found, whatever the period of ageing, using the anodic-oxidation method which he claims to be very sensitive in revealing precipitation. It was not possible to restore the mechanical properties by a further solution-treatment after ageing in air, whereas this was possible after ageing *in vacuo*. Tensile tests in air or *in vacuo* gave intercrystalline cracks.

FIGS. 1-4.—HIGH-PURITY ALUMINIUM-10% ZINC ALLOY.



FIG. 1.—Solution-treated and aged at room temperature for 16 days. Electrolytically polished.  $\times 1500$ .



FIG. 2.—Solution-treated and aged at room temperature for 198 days. Electron micrograph of electrolytically polished surface.  $\times 9400$ .



FIG. 3.—Solution-treated and aged at room temperature for 4 months. Mechanically polished and etched in 4% alcoholic  $\text{HNO}_3$ .  $\times 1500$ .



FIG. 4.—Same field as Fig. 3, after further etching in Wassermann's reagent.  $\times 1500$ .

FIGS. 5-8.—HIGH-PURITY ALUMINIUM-10% ZINC ALLOY.



FIG. 5.—Same field as Figs. 3 and 4, electrolytically polished.  $\times 1500$ .



FIG. 6.—Solution treated and aged at room temperature for 396 days. Mechanically polished and etched in 25%  $\text{HNO}_3$  at  $70^\circ \text{C}$ .  $\times 2000$ .



FIG. 7.—Same field as Fig. 6, after further etching in Wassermann's reagent.  $\times 2000$ .



FIG. 8.—As solution treated. Electrolytically polished.  $\times 1000$ .

FIGS. 9-12.—HIGH-PURITY ALUMINIUM-10% ZINC ALLOY.



FIG. 9.—Solution-treated and aged at room temperature for  $2\frac{1}{2}$  days. Electrolytically polished.  $\times 1500$ .



FIG. 10.—Solution-treated and aged at  $50^{\circ}$  C. for 12 days. Electrolytically polished.  $\times 1500$ .

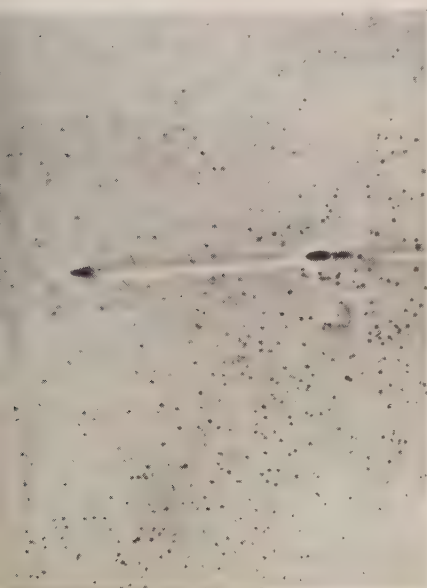


FIG. 11.—Solution-treated and aged at  $100^{\circ}$  C. for 13 days. Electrolytically polished.  $\times 1500$ .



FIG. 12.—Solution-treated and aged at  $125^{\circ}$  C. for 96 days. Electrolytically polished.  $\times 1500$ .



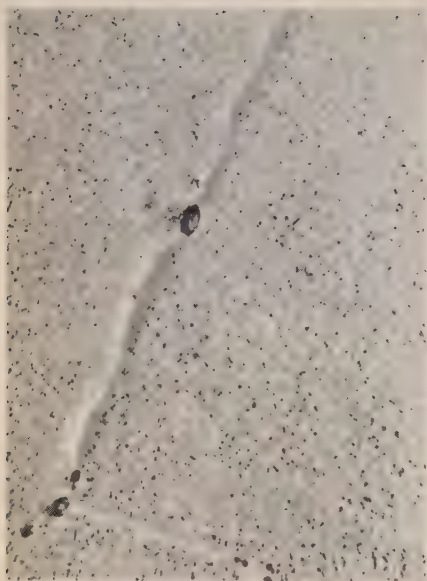


FIG. 13.—Aluminium-13% Zinc Alloy, solution-treated and aged at 125° C for 67 days. Electrolytically polished.  $\times 1500$ .



FIG. 14.—Aluminium-8% Zinc Alloy, solution-treated and aged at room temperature for 60 days. Electron micrograph of electrolytically polished surface.  $\times 14,000$ .

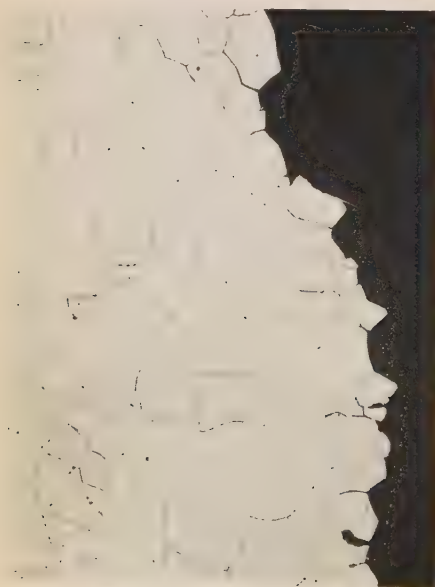


FIG. 15.—Part of Stress-Corrosion Fracture in Aluminium-10% Zinc Alloy.  $\times 15$ .

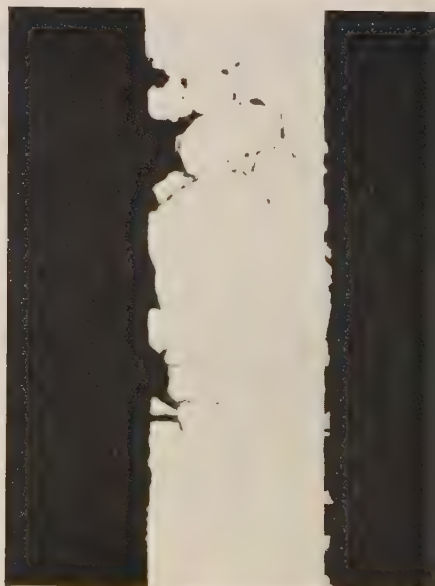


FIG. 16.—Aluminium 10% Zinc Alloy aged at room temperature. Corroded unstressed in 3% NaCl for 110 days.  $\times 20$ .



FIG. 17.—Inter crystalline Crack in Aluminium-10% Zinc Specimen stressed in dry air at 10 tons/in.<sup>2</sup>  $\times$  1500.

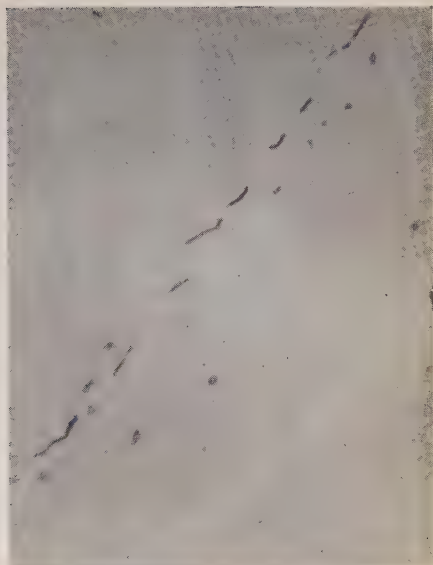


FIG. 18.—Aluminium-4% Copper Alloy, solution-treated and aged at 150° C. for 2 days. Mechanically polished and etched in 25%  $\text{HNO}_3$  at 70° C.  $\times$  2000.



FIG. 19.—Same field as Fig. 17, after further etching with Wassermann's reagent.  $\times$  2000.



FIG. 20.—Aluminium-10% Zinc Alloy aged at room temperature. Electrolytically polished and corroded in 3%  $\text{NaCl}$ . Note that corrosion follows interface of old and new solid solutions.  $\times$  1500.



Chaudron suggested that oxygen or moisture might be playing a part in the intercrystalline failure.

Hérenghuel<sup>3</sup> has shown that the tendency to intercrystalline failure in these alloys increases with the ageing time at room temperature. The tensile strength and elastic limit increased with the ageing time until brittleness set in, when the values became very scattered. The elongation decreased slowly at first and then rapidly as the brittleness developed. No grain-boundary film of precipitate to which the brittleness could be attributed was found. Since the failure under stress took place in a vacuum or with specimens covered with various protective coatings, Hérenghuel concluded that corrosion was not the primary cause of failure, but only a subsidiary factor. Commercial-purity alloys of this type had much longer lives than pure alloys, and additions of copper, chromium, zirconium, and silver had important stabilizing effects. Where the zinc content was high, a combination such as copper and chromium was necessary to produce any stabilizing effect.

Recently, Finlay and Hibbard<sup>4</sup> have reported intercrystalline fractures in short-time creep tests at 100° C. on aluminium-12% zinc alloy using an initial stress of 5.1 tons/in.<sup>2</sup>

## II.—EXPERIMENTAL PROCEDURE.

### 1. *Preparation of Alloys.*

Chill-cast ingots,  $9 \times 4 \times 1$  in., were made from super-purity aluminium (>99.99%) and high-purity zinc (>99.99%). The head of each ingot was sawn off and samples representative of the cross-section were taken for analysis. In addition, some  $\frac{3}{8}$  in.-dia. rods of aluminium-3% zinc alloy, made from the same high-purity materials, were cast for use in electrochemical experiments.

The ingots were annealed for 16 hr. at 450° C. and hot rolled to 18 S.W.G. sheet according to the following schedule: (i) cross rolled to approximately 0.4 in. in 0.02 in. passes and then rolled down to approximately 0.07 in. in 0.02 in. passes, with intermediate anneals of  $\frac{1}{2}$  hr. at 450° C. after every 40-50% reduction; (ii) rolled to 18 S.W.G. in 0.01 in. passes. The rolls were heated to 60°-80° C. The sheets obtained were free from cracking.

### 2. *Composition of Alloys.*

The compositions of the alloys are given in Table I.

*3. Heat-Treatments.*

All specimens were solution-treated at 450° C. for 3 hr. and quenched in water at room temperature before ageing. Ageing treatments at 50°, 100°, and 175° C. were carried out in air, and at 85° and 125° C. in an oil bath.

TABLE I.—*Composition of Alloys.*

Mark	Zn, %	Fe, %	Si, %	Mg, %	Cu, %
NPY 1 .	10.8	<0.01 *	~0.005 *	≤0.005 *	<0.01 *
NPY 2 .	10.2	<0.01 *	~0.005 *	≤0.005 *	<0.01 *
NPY 3 .	10.2	0.005 *	~0.005 *	≤0.005 *	<0.01 *
NPY 5 .	7.9	<0.005 *	~0.005 *	≤0.005 *	~0.01 *
NPY 6 .	13.4	<0.005 *	~0.005 *	<0.005 *	~0.04 *
NTL .	2.7	<0.01 *	~0.005 *	<0.005 *	<0.01 *
Al-Cu .	n.d.	0.0045	0.002	n.d.	4.10

\* Determined spectrographically.

n.d. Not determined.

*4. Preparation for Metallographic Examination.*

Specimens were usually prepared by electrolytic polishing, though for comparison some specimens were mechanically polished. For any one ageing temperature the same specimen was used for all examinations.

The solution used for electropolishing contained 200 c.c. of absolute alcohol and 50 c.c. of 60% perchloric acid.<sup>5</sup> A vertical aluminium cathode was used, 5 cm. away from the specimen, and the voltage across the cell was maintained at 10 V. Before electrolytic treatment the specimens were polished with commercial metal polish. During polishing the surface of the specimen became covered with a black film which peeled off after 1-1½ min. After a further minute the specimen was removed, washed in a strong jet of water, and dried with acetone; a polished and partially etched specimen was thus obtained. Increasing the voltage above 12 V. caused a blue film to be formed on the surface, which under the microscope appeared as a brown stain. Decreasing the voltage below 9 V. gave specimens which were heavily etched but not polished. It was sometimes necessary to give a short etch in Wassermann's reagent, which consists of equal parts of 0.5% hydrofluoric acid and of a mixture containing 2 c.c. hydrochloric acid, 20 c.c. nitric acid, and 50 c.c. 10% potassium dichromate. The etching characteristics of this reagent are similar to 0.5% hydrofluoric acid, except that a stain-free surface is produced.



## III.—RESULTS.

## 1. Metallographic Examination.

## (a) Identification of Phases.

On electropolishing specimens aged at room temperature, pits were found at the grain boundaries, in conjunction with another phase which appeared as "loops" in the grain boundary (see Fig. 1, Plate XVII), and which lit up when the focus was altered. The pits were usually found in the advancing edge of this "looped" phase or in the unchanged grain boundary. Fig. 2 (Plate XVII) is an electron micrograph prepared from a Formvar replica showing that the light phase is raised relative to the grains, with pits in the advancing boundary. This structure is similar to the "light phenomenon" that Gayler<sup>6</sup> found during the ageing of an aluminium-4% copper alloy and which she attributed to the precipitated new solid solution in equilibrium at the temperature of ageing.

In order to identify the light phase and to ascertain the cause of the pits, a specimen of the aluminium-10% zinc alloy that had been aged for several months at room temperature was mechanically polished and etched with 4% alcoholic nitric acid, which is known to attack zinc. After etching, pitting could be seen in some of the grain boundaries (see Fig. 3, Plate XVII), indicating the presence of zinc-rich zones. It should be noticed that grain boundaries free from pitting and the advancing edges of the light phase are also revealed. It has been shown by Gayler<sup>6</sup> that the new solid solution, that is, the solid solution in equilibrium at the temperature of ageing, formed as a result of discontinuous precipitation, can be revealed in the aluminium-4% copper alloy by etching with  $\frac{1}{2}$ % hydrofluoric acid. Further etching of the aluminium-zinc alloy with Wassermann's reagent revealed the straight boundary and delineated the advancing boundary more clearly (see Fig. 4, Plate XVII). The pits shown in Fig. 4 are larger than those in Fig. 3 (because hydrofluoric acid attacks zinc also), but their positions coincide exactly with those in Fig. 3. This suggests that the light phase is the new solid solution formed as a result of discontinuous precipitation, the pits indicating the zinc-rich zones. The same field after electropolishing is shown in Fig. 5 (Plate XVIII). Figs. 6 and 7 (Plate XVIII) represent a specimen that was first etched in aqueous 25% nitric acid at 70° C. instead of the 4% alcoholic nitric acid solution. Etching for longer times in the 25% nitric acid reveals the complete looped structure. The light phase will henceforward be called the new solid solution; it is presumed to contain approximately 3% zinc at room temperature.

Geisler, Barrett, and Mehl,<sup>7</sup> on ageing aluminium-25% zinc alloy at 100° C. and etching in 25% nitric acid, found a looped phase at the grain boundaries which was outlined but not attacked. They interpreted this structure as coarse particles of non-coherent zinc, but this seems unlikely since zinc would be attacked by 25% nitric acid, and the looped phase shown is probably the new solid solution. The same alloy aged to an extent such that the zinc-rich precipitate was observable by X-rays, was found, after etching with 0.5% hydrofluoric acid, to contain only precipitate particles which were either stained black or attacked by the etching reagent. Nitric acid, in addition to attacking zinc, etches the advancing edge of the new solid solution (see Figs. 3 and 6), while Wassermann's reagent also reveals the boundary from which the new solid solution advances (see Figs. 4 and 7).

It is inferred from these results that the orientation of the new solid solution is closely related to that of the neighbouring grain, but not to that of the grain into which it grows. This orientation relationship between the new and the old solid solution agrees with Gayler's<sup>8</sup> observations on the "light phenomenon" in the aluminium-4% copper alloy. In view of the above, the lattice misfit at boundaries of the new and old solid solution will be greater at the advancing edge than at the straight edge; hence conditions will be more favourable for the formation of zinc-rich concentrations at the advancing edge. These concentrations will cause pitting, and will migrate with the advancing boundary of the new solid solution until zinc-rich particles are formed which will arrest the growth of the new solid solution. It will be shown later that this in fact occurs. The new solid solution has not been obtained in sufficient quantity after any of the ageing treatments to be detectable by X-ray examination, although in any case this would be difficult because of the small difference in lattice parameter between the solid solutions containing 3 and 10% zinc.

(b) *Examination of Aluminium-10% Zinc Alloy.*

(i) *Solution-Treated.*—After solution treatment at 450° C. for 3 hr. and quenching in cold water, the alloy was completely homogeneous (see Fig. 8, Plate XVIII).

(ii) *Furnace-Cooled from 450° C.*—On furnace-cooling from 450° C. to room temperature in approximately 8 hr., the alloy appeared completely homogeneous on microscopic examination. This treatment had not entirely stabilized the alloy, however, since hardening occurred on standing at room temperature, and metallographic examination after 35 days revealed a small amount of new solid solution at some grain boundaries.

In an attempt to obtain complete equilibrium, a specimen was solution-treated and then cooled from 450° to 210° C. in 1 day and from 210° C.—this being above the solid-solubility line—to room temperature in 12 days. Electropolishing revealed pitting in both the grains and the grain boundaries. Lattice-parameter measurements and the small amount of pitting present indicated that, even after such prolonged cooling, the alloy was not in equilibrium; this view was supported by the appearance of some new solid solution after standing at room temperature for 53 days.

(iii) *Room-Temperature Ageing*.—The first sign of change in the structure on room-temperature ageing after solution-treatment was the appearance on electropolishing of fine pits in some of the grain boundaries after approximately 20 hr. After 1 day one boundary was found to contain some new solid solution in addition to the pitting, but only after 2½ days did this become more generally apparent (see Fig. 9, Plate XIX). Subsequently both the number of grain boundaries containing new solid solution and the size of the new solid-solution areas increased, but at a diminishing rate until, after 16 days, the rate of growth was very small. The new solid solution did not appear in every grain boundary, and no completely continuous network was formed. This suggests that precipitation at the grain boundaries depends on the orientation of the neighbouring grains, an observation which has been made by Forsyth *et al.*<sup>9</sup> in other alloy systems.

(iv) *Elevated-Temperature Ageing*.—On ageing the alloy at 50° C. a few small pits were detected at the grain boundaries after ½ hr., and the appearance of the new solid solution in the grain boundaries occurred much more rapidly than at room temperature, being quite pronounced after 9 hr. As at room temperature, the amount and size increased for some time and then remained constant. Although the new solid solution was more massive (Fig. 10, Plate XIX), no continuous network was formed, and no precipitation within the grains was observed.

On ageing at 85° C., grain-boundary pitting was detected after 1 hr. and the new solid solution after 2 hr. The latter took a rather different form at this temperature, occurring more frequently as thin threads, although sometimes it still appeared in the looped form; more grain boundaries seemed to contain it, though little change was detected in the amount or size after 2½ days. After 75 days there were indications that precipitation was beginning within the grains, since pitting was observed when the electropolished specimens were etched with Wassermann's reagent.

On ageing at 100° C., pitting was again detected in the grain

boundaries during the early stages, but the new solid solution was not easily discernible and appeared as threads in the grain boundaries. After 13 days fine pitting was visible within the grains (see Fig. 11, Plate XIX). This pitting was not always revealed by electropolishing, etching with Wassermann's reagent sometimes being necessary.

Grain-boundary pitting was detected in the early stages of ageing at 125° C., but no new solid solution could be definitely identified in the grain boundaries. Pitting within the grains could be seen after 5½ days. Fig. 12 (Plate XIX) shows the structure of an electropolished specimen aged at 125° C. for 96 days. It consists of zinc particles in a matrix of the equilibrium solid solution.

After ageing at 175° C. for periods up to 10 days, pitting in the grain boundaries was obtained, but little or none within the grains. Some of the pits in the boundaries were quite large. Lattice-parameter measurements showed that equilibrium had been obtained after 10 days at 175° C. No new solid solution was found at this ageing temperature.

(c) *Examination of Aluminium-13% Zinc Alloy.*

(i) *Room-Temperature Ageing.*—The change in structure was similar to that of the aluminium-10% zinc alloy, the main differences being: (a) the precipitate was visible after shorter periods of ageing, and (b) in general the new solid solution appeared as thin threads at the grain boundaries, as was observed with the 10% zinc alloy on ageing at 100° C.

(ii) *Ageing at 125° C.*—In contrast to the 10% zinc alloy, this material showed the presence of new solid solution (generally in the form of thin threads at the grain boundaries), together with pits. Precipitation was more rapid, e.g. pitting within the grains was apparent after 2 days' ageing compared with 5½ days for the 10% zinc alloy. Fig. 13 (Plate XX) shows the presence of new solid solution at the grain boundaries together with irresolvable precipitate within the grains.

(d) *Examination of Aluminium-8% Zinc Alloy.*

(i) *Room-Temperature Ageing.*—There appeared to be no change in structure after ageing at room temperature, though some grain boundaries, under low-power examination, seemed to be etched more heavily than others. Examination of a specimen, aged at room temperature for 60 days, by the electron microscope did, however, reveal the presence of pits and small particles of the light phase at the grain boundaries (see Fig. 14, Plate XX). It therefore appears that



the structural change in this alloy is the same as that in the 10 and 13% zinc alloys, except that the change is much slower.

(ii) *Ageing at 125° C.*—On ageing at 125° C. pits were observed at the grain boundaries after 8 days though, as with the 10% zinc alloy, no new solid solution was apparent. After ageing for longer times (up to 67 days) the only detectable change in structure was the appearance of a few lozenge-shaped particles (presumably zinc) in addition to the pits.

From the above results it is clear that for a constant zinc content low ageing temperatures favour the formation of the new solid solution; also, if the zinc content is increased, the new solid solution appears at higher ageing temperatures than in the case of the alloys of lower zinc content. These observations agree with those of Gayler and Carrington,<sup>10</sup> in that high ageing temperatures favour continuous precipitation and low temperatures discontinuous \* precipitation.

Intercrystalline cracking during ageing, as recorded by Chaudron, Héréguel, and Lacombe,<sup>2</sup> has not been observed during this work.

## *2. Electrochemical Investigation.*

### *(a) Potential Measurements.*

Strips of the sheet material were solution-treated at 450° C. for 3 hr., quenched, and an area approximately  $1\frac{1}{2} \times \frac{1}{2}$  in. polished down to 0000 emery paper, the specimen being finally degreased with acetone. The surrounding area was covered with a 1 : 1 mixture of Chatterton's compound and vacuum wax, and the exposed area was completely immersed in the electrolyte.

Cast rods of aluminium-3% zinc alloy, the equilibrium solid solution at room temperature, were hammered and then solution-treated. The width of the area exposed as above was slightly under  $\frac{1}{2}$  in.

The electrode potentials of specimens in 3% sodium chloride solution were measured with a Cambridge pH meter, against a *N*-calomel half-cell.

\* Discontinuous precipitation is said to take place when the supersaturated-solid-solution lines in the X-ray spectra decrease in intensity and, at the same time, new lines appear corresponding to the solid solution in equilibrium at the temperature of ageing. These new lines increase in intensity until the lines of the original solid solution disappear. In general, discontinuous precipitation starts at the grain boundaries and spreads into the grains. Continuous precipitation is said to take place when the X-ray lines from the supersaturated solid solution gradually move from their original position to the position corresponding to the equilibrium composition at the temperature of ageing. In general, when continuous precipitation occurs the precipitate takes the form of the Widmanstätten structure.



The steady potentials are given in Table II.

Each specimen was vigorously scratched with a sharp glass point while immersed in the solution and the effects on the potentials were observed. Times for specimens to refilm are given in Table II. Potentials of specimens partly immersed in 3% sodium chloride solution were similar to those in Table II, except that the values were slightly more cathodic.

TABLE II.—*Electrode Potentials of Aluminium-Zinc Alloys and Pure Zinc Immersed in 3% Sodium Chloride Solution (N-calomel Scale).*

Alloy Mark	Zinc, %	Final Steady Potential, V.	Max. Potential on Scratching, V.	Time for Film to Re-form on Scratched Area
NPY . .	10.8	—1.026	—1.266	8 min.
NTL . .	2.73	—0.998	—1.360	12 min.
Pure zinc . .	>99.99	—1.095	—1.128	Approx. 6 hr.

Table II shows that in the filmed state the 10% zinc solid solution is more anodic than the 3% zinc solid solution, whereas in the unfilmed state the reverse is true. These results are in agreement with those of Akimov and Clark.<sup>11</sup> On scratching, the aluminium-rich solid solutions became more anodic and refiled quickly, while the zinc was little affected by scratching and took a long time to refile.

(b) *Measurement of Corrosion Currents.*

Three cells were made by immersing in 3% sodium chloride solution the following electrodes, each pair being connected by a microammeter of 500 ohms resistance and a sensitivity of 2  $\mu$ amp. per small division :

- (i) Aluminium-10% zinc solid solution and pure zinc.
- (ii) Aluminium-3% zinc solid solution and pure zinc.
- (iii) Aluminium-10% zinc solid solution and aluminium-3% zinc solid solution.

When a steady current through the cell had been reached, one of the electrodes was scratched with a glass point until no further change in current occurred. Scratching was then stopped and the cell allowed to reach a steady current again. This procedure was repeated by scratching the other electrode and then both electrodes simultaneously. The results are given in Table III.

Scratching the zinc electrode had little effect, which agrees with the potential measurements; when one of the solid solutions was scratched, that solid solution became the anode and a large corrosion current

flowed. If, however, both solid solutions were scratched simultaneously, the 3% zinc solid solution became the anode, which also agrees with the potential measurements (Table II). The large currents obtained by scratching the solid-solution electrodes rapidly decreased to the steady values when scratching was stopped, indicating a very rapid polarization of the scratched areas.

TABLE III.—*Corrosion Currents in 3% Sodium Chloride Solution.*

Electrodes	Condition	Current, $\mu$ amp.	Anode
Al-10% Zn solid solution and zinc	Steady rate	0 *	...
	S.S. scratched	180-200	S.S.
	Zinc scratched	0 *	...
	Both scratched	170	S.S.
Al-3% Zn solid solution and zinc	Steady state	2	Zn
	S.S. scratched	170-180	S.S.
	Zinc scratched	3	Zn
	Both scratched	290	S.S.
Al-10% Zn solid solution and Al-3% Zn solid solution	Steady state	0 *	...
	10% S.S. scratched	60	10% S.S.
	3% S.S. scratched	70	3% S.S.
	Both scratched	70	3% S.S.

S.S. = Solid Solution.

\* Currents smaller than about 1  $\mu$ amp. could not be measured by the micro-ammeter used.

### 3. *Mechanical Properties.*

The mechanical properties after various ageing treatments are given in Table IV.

From the results in Table IV it is clear that the ultimate tensile stress and 0.1% proof stress increased with increasing zinc content, while the elongation decreased; for the aluminium-10% zinc alloy the elongation decreased as the ageing temperature increased to 100° C. and thereafter increased. At temperatures above 100° C. no new solid solution was found on subsequent microscopic examination; the decrease in elongation may therefore be associated with the presence of the new solid solution. All the specimens gave transcrystalline fractures, except those of the aluminium-13% zinc alloy which gave intercrystalline fractures.

### 4. *Stress-Corrosion Tests.*

Direct-tensile stress-corrosion tests were carried out using standard sheet tensile specimens cut at right-angles to the final rolling direction. The specimens were stressed by means of a calibrated spring, as

TABLE IV.—*Mechanical Properties of Aluminium-Zinc Alloys.*

Alloy	Heat-Treatment after Solution-Treatment	U.T.S., tons/in. <sup>2</sup>	0.1% Proof Stress, tons/in. <sup>2</sup>	Elongation on 2 in., %
Al-10% Zn	None *	13.2	8.3	14
"	10 days at room temp.	13.4	8.1	13
"	10 " 50° C.	13.0	7.6	12
"	10 " 100° C.	11.1	6.3	11
"	10 " 125° C.	7.7	4.8	15
"	10 " 175° C.	9.5	2.1	23
"	Furnace-cooled from 450° C.†	11.0	4.5	15
Al-13% Zn	10 days at room temp.	17.1	10.6	9
Al-8% Zn	10 " "	11.9	6.7	14

\* These specimens were tested as soon as possible after quenching, but it is obvious from the results that ageing had occurred (see Appendix and Fig. 21).

† Specimens were cooled from 450° to 210° C. in 1 day and from 210° C. to room temperature in 12 days.

described by Perryman and Hadden,<sup>12</sup> and sprayed with 3% sodium chloride solution twice daily. In general three stressed and two unstressed specimens were exposed. One of the unstressed specimens was removed when the first stressed specimen broke, and the other when the last broke, and their residual mechanical properties were determined.

Specimens of aluminium-10% zinc alloy were tested after the following treatments :

- (a) Solution-treated.
- (b) Solution-treated and aged for 16 days at room temperature.
- (c) Furnace-cooled from 450° C. in 8 hr.

The heat-treatments were so arranged that all specimens were tested at the same time, and moreover the solution-treated specimens were tested directly after quenching. The tests were planned to demonstrate the effect on stress-corrosion life of the various phases that can be present. The solution-treated specimens would be initially homogeneous, but during the test would age with the formation of the same phases as were present after treatment (b), namely, old solid solution, new solid solution, and zinc. The furnace-cooled specimens, if the cooling was slow enough, should be in equilibrium and consist of two phases only, the equilibrium solid solution at room temperature and zinc.

Tests were also carried out on the 8 and 13% zinc alloys after ageing at room temperature for 10 days.

The results are given in Table V.

TABLE V.—*Stress-Corrosion Tests on Aluminium-Zinc Alloys.*

Alloy	Heat-Treatment	Initial Applied Stress, tons/in. <sup>2</sup>	Time to Failure	Mean Life	Loss of Strength due to Stress-Corrosion, tons/in. <sup>2</sup> †
Al-10% Zn	Solution-treated	7	5½, 9½, 2½ days	6 days	6.0
"	Solution-treated and aged at room temperature for 16 days	7	5½, 5, 4½ days	5 days	6.0
"	Furnace-cooled from 450° C.*	7	35, n.f., n.f.	>89 days	...
Al-13% Zn	Solution-treated and aged at room temperature for 10 days	10 8	2, 3, 3 hr. 4, 2, 3 hr.	3 hr. 5 hr.	7.0 8.7
Al-8% Zn	"	10 8	3, 4, 10 days >13,‡ 27 days	6 days ...	1.0 2.7

n.f. No failure had taken place in 118 days. These specimens were taken down and pulled for residual mechanical properties. It is not possible to give figures for the loss of strength due to stress-corrosion because ageing had proceeded during the test. As the residual properties (U.T.S. 11 tons/in.<sup>2</sup>, elongation 10%) were near those of specimens aged at room temperature after solution-treatment, it is inferred that little strength was lost during corrosion.

\* The time taken to cool from 450° C. to room temperature was 8 hr.

† Figures in this column were obtained by subtracting the initial applied stress from the residual U.T.S. of the unstressed control specimens.

‡ This specimen broke at grip.

All specimens failed with an intercrystalline fracture (see Fig. 15, Plate XX). Table V shows that the stress-corrosion life for the 8% zinc alloy is very much greater than that for the 13% zinc alloy.

There was little difference between the stress-corrosion life of aluminium-10% zinc specimens solution-treated and specimens solution-treated and aged, but those which were furnace-cooled had a much longer life. The furnace-cooled specimen which failed in 35 days was microscopically examined after failure and a small amount of the new solid solution was detected at the grain boundaries. This must have been formed during the test, because previous examination had shown that directly after furnace-cooling the alloy was apparently homogeneous. It appears therefore that the furnace cooling was not slow enough for equilibrium to be attained. Some zinc was precipitated in the initial stages of cooling, but thereafter the cooling was fast enough to be considered as a quench. Presumably the supersaturated solid solution, containing less than 10% zinc, then slowly aged and ultimately the new solid solution was formed. In general, therefore, the new solid solution was present in all specimens which failed.

Unstressed control specimens lost little strength during corrosion over short periods, but Fig. 16 (Plate XX) shows that severe intercrystalline corrosion can take place in the absence of stress over longer periods.

## 5. Tests on Specimens Stressed in Air.

Specimens of the aluminium-10% zinc alloy were (a) solution-treated, and (b) solution-treated and aged for 16 days at room temperature; they were covered with lanolin to protect them from corrosion, and subjected to an initial stress of 7 tons/in.<sup>2</sup> The solution-treated specimens did not fail in 100 days; the stress was then raised to 10 tons/in.<sup>2</sup>, and the two specimens failed with a partly intercrystalline fracture in a further 3 and 7 days, respectively. Similarly, the solution-treated and aged specimens did not fail in 65 days, after which the stress was raised to 10 tons/in.<sup>2</sup> and failure occurred in 3 and 6 days. Specimens of the aluminium-13% zinc alloy, solution-treated and aged at room temperature for 10 days, covered with lanolin and subjected to an initial stress of 8 and 10 tons/in.<sup>2</sup>, failed with an intercrystalline fracture in 7 and 0.5 days, respectively. Similar results were obtained on the 8% zinc alloy, the failure times being >51 and 2 days at 8 and 10 tons/in.<sup>2</sup>, respectively.

Specimens of the aluminium-10% zinc alloy which had been solution-treated and aged for 2 days at room temperature were then tested at 10 tons/in.<sup>2</sup> in (a) air dried with a mixture of calcium chloride and silica gel, (b) wet air maintained by surrounding, but not touching, the specimen with a cylinder of damp blotting paper, and (c) reduced pressure (approx. 0.1 mm.). The results are shown in Table VI.

TABLE VI.—Tests on Aluminium-10% Zinc Alloy in Various Atmospheres at 10 tons/in.<sup>2</sup>

Testing Medium	Life, days
Reduced pressure . . . .	*9½, 3
Dry air . . . . .	10, 6½
Wet air . . . . .	<2½, <2¾

The lives in dry air and in air under reduced pressure were of the same order, whereas the life in wet air was shorter. A similar effect has been observed by Wassermann<sup>13</sup> for an alloy containing zinc 6, magnesium 3, and manganese 1%. All the fractures in specimens tested in air at 10 tons/in.<sup>2</sup> were intercrystalline. Fig. 17 (Plate XXI) shows an intercrystalline crack in a specimen stressed in dry air; the crack has a tendency to follow the interface between the new and old solid solutions, and some of the new solid solution particles have fallen out.

## IV.—SUMMARY.

On ageing the aluminium-10% zinc alloy at temperatures below 100° C. and electropolishing, pitting occurred at the grain boundaries,



probably due to the presence of zinc-rich zones, and the equilibrium solid solution at the temperature of ageing was revealed. At ageing temperatures above 100° C. no new solid solution was found. Similar structural changes occurred on ageing the aluminium-8% zinc alloy but much more slowly. The aluminium-13% zinc alloy also behaved similarly to the 10% zinc alloy, except that the new solid solution also appeared on ageing at 125° C.

Electrochemical measurements show that in the unfiled state the new solid solution (3% zinc) is the most anodic phase present, and it could provide the path for intercrystalline corrosion with the super-saturated solid solution and zinc as cathodes.

Stress-corrosion tests have shown that susceptibility is dependent upon the zinc content, and have indicated that the presence of the new solid solution in the grain boundaries is responsible for the rapid stress-corrosion of this material. Intercrystalline fractures have also been obtained by stressing specimens at reduced pressure, and in dry and wet air at atmospheric pressure. Tests under sustained tensile stress in non-corrosive conditions have shown that the failure-time decreases with increasing zinc content.

#### V.—DISCUSSION OF RESULTS.

For convenience the discussion will be divided into two parts: (a) intercrystalline failure in air, and (b) intercrystalline failure in 3% sodium chloride.

##### (a) *Intercrystalline Failure in Air.*

From the foregoing it is reasonable to suppose that the intercrystalline fracture in air is due to the precipitate formed during ageing. When this intercrystalline fracture occurs there exist at the grain boundaries zinc-rich zones and new solid solution. The latter, at least, will be more ductile than the supersaturated solid solution, composing the remainder of the grain, which has hardened during ageing. Thus an explanation is required as to why a ductile phase at the grain boundaries causes intercrystalline cracking and why this cracking is delayed. Following Orowan,<sup>14</sup> let us consider a synthetic specimen made from two metal blocks *A*, between which a thin layer of another metal *B* is sandwiched, *B* being more ductile than *A*. If this specimen is stressed beyond the yield point of *B* but below that of *A*, the stress being perpendicular to the thin layer of *B*, then the metal *B*, if free to do so, would deform plastically. However, as *B* is joined to *A* and is very thin, no transverse plastic contraction can take place, and since during plastic deformation the volume must remain constant, axial

plastic extension is also prevented. This means that a transverse stress is set up which, together with the applied axial stress, causes a state of hydrostatic tension, so that the fracture, if any, will be brittle. Orowan<sup>14</sup> has carried out experiments on such specimens, using tin welded between two blocks of iron, and specimens were found to withstand stresses  $5\frac{1}{2}$  times the ultimate strength of the tin which, it was confirmed, constituted the centre of the sandwich. The fracture always occurred at the tin/iron interface and not in the tin itself.

The conditions in the aluminium-zinc alloy specimens aged at room temperature are very similar to those described above for the synthetic specimen, except that in the polycrystalline alloy only a few of the ductile layers are at right-angles to the stress. Three main types of boundary must be considered :

(i) Boundaries lying parallel to the applied stress with neither shear stresses in their plane nor transverse tensile stresses acting on them.

(ii) Boundaries lying perpendicular to the applied stress, which are in hydrostatic tension as explained above.

(iii) Boundaries lying at some angle to the applied stress and which will be subjected to some component of shear stress.

The resolved shear stress along a number of the boundaries of type (iii) will, if the applied stress is more than a certain value, be sufficient to cause creep in the ductile phase (new solid solution). There will thus be stress relaxation along these boundaries, and a large stress will be built up on boundaries of type (ii). As shown above, plastic deformation is prevented at this type of boundary because of the constraint exerted by the grain on the new solid solution, and so brittle fracture will occur. The load will then be carried again by the boundaries of type (iii), and these will fail progressively.

To initiate intercrystalline failure only a small movement will be needed, and this can be accomplished either by a long time at low temperature (creep test) or a short time at high temperatures (ordinary tensile test), in either case at a stress such that deformation of the hard matrix is negligible. On the other hand, in an ordinary tensile test at room temperature the stress will rise sufficiently to deform or rupture the hard grains before the movement at the boundaries can be accomplished and so a transcrystalline fracture will result. Supporting this is the fact that all the fractures of ordinary tensile test specimens of the aluminium-10% zinc alloy have been transcrystalline and also Finlay and Hibbard's<sup>4</sup> observation that an aluminium-12% zinc alloy gave an intercrystalline fracture when tested at 5 tons/in.<sup>2</sup> and 100° C.

It is clear that the tendency to intercrystalline fracture will increase if the hardness of the matrix relative to that of the new solid solution increases. This is probably the reason for the intercrystalline fracture of the aluminium-13% zinc alloy in the ordinary mechanical test. It is also possible that the form in which the new solid solution was precipitated (i.e. thin threads at the grain boundaries) may have had an effect.

The more rapid failure observed in moist air may be caused by the effect described by Benedicks,<sup>15</sup> who proved that the tensile strength of a metal could be raised or lowered by contact with a liquid and that water lowered the tensile strength of steel.

Gayler<sup>6</sup> has shown that if aluminium-4% copper alloy is aged at elevated temperatures the solid solution in equilibrium at the temperature of ageing is precipitated at the grain boundaries. If, therefore, the theory described above is correct, the aluminium-4% copper alloy, suitably aged, should suffer intercrystalline fracture when stressed in air or any inert environment.

Specimens of a high-purity aluminium-4% copper alloy were accordingly tested for ordinary mechanical properties and also by prolonged stressing in air. Two conditions were tested (a) solution-treated (3 hr. at 535° C. and quenched in cold water) and aged at room temperature for 15 days, and (b) solution-treated and aged at 150° C. for 2 days. Material in the former condition was microscopically homogeneous, while in specimens aged at elevated temperatures copper-rich areas and the new solid solution were present at the grain boundaries. Fig. 18 (Plate XXI) shows the presence of copper-rich areas. Fig. 19 (Plate XXI) shows the same field after further etching in Wassermann's reagent, revealing the new solid solution. The results are given in Table VII.

TABLE VII.—*Results for Aluminium-4% Copper Alloy in Tensile and Sustained-Stress Tests.*

Heat-Treatment	Ordinary Mechanical Properties			Initial Applied Stress, tons/in. <sup>2</sup>	Time to Failure, days
	U.T.S., tons/in. <sup>2</sup>	0.1% Proof Stress, tons/in. <sup>2</sup>	Elongation on 2 in., %		
Solution-treated and aged at room temp. for 15 days	17.5	8.3	16	17	n.f.
Solution-treated and aged at 150° C. for 2 days	19.6	13.2	8	16, 17½	13, 19

n.f. No failure in 50 days; test discontinued.

The fractures of the specimens aged at elevated temperature were intercrystalline both in the ordinary tensile and sustained-stress tests, whilst those of specimens aged at room temperature were transcrystalline and there was appreciable necking. The results are thus in keeping with the theory outlined for the intercrystalline fracture of the aluminium-zinc alloys.

(b) *Intercrystalline Failure in 3% Sodium Chloride Solution.*

It is clear that cracking takes place much more rapidly in sodium chloride solution than in air. For example, specimens of the aluminium-10% zinc alloy tested at 7 tons/in.<sup>2</sup> failed in 6 days when sprayed with 3% sodium chloride solution, while specimens covered with lanolin did not fail in 100 days at that stress. Increasing the stress on specimens covered with lanolin to 10 tons/in.<sup>2</sup>, however, caused intercrystalline fracture. Similarly, specimens of the 13% zinc alloy tested at 8 tons/in.<sup>2</sup> failed in a few hours when sprayed with 3% sodium chloride, while specimens covered with lanolin failed in 7 days at that stress.

It seems likely that in the tests at the lower stress in 3% sodium chloride solution failure is initially by stress-corrosion, proceeding until the stress on the residual cross-section is sufficient to cause mechanical failure by the mechanism outlined above.

When the aluminium-zinc alloys are corroded unstressed in 3% sodium chloride solution, corrosion takes place at the grain boundaries (Fig. 15, Plate XX). During this corrosion it is probable that the effective anode would be the zinc-rich zones, with either of the solid solutions acting as cathode (see Tables II and III), though the old solution, having the largest area, would probably be the more effective cathode. Support for this is given by Fig. 20 (Plate XXI) which shows an electropolished surface after corrosion in 3% sodium chloride. The corrosion is localized at the junction of the new and old solid solutions, leaving the new solid solution uncorroded. It was not found possible to decide whether the corrosion was localized at the advancing edge of the new solid solution or at the straight edge. If the specimen is stressed, this type of localized corrosion will go on until one of these intercrystalline crevices is sufficiently deep for the stress concentration to cause mechanical rupture. Fig. 17 (Plate XXI) indicates that this would involve a tearing apart of the new solid solution from the old thereby exposing unfilmed electrode surfaces to the corrosive agent; another possibility is that the stress concentration could crack the corrosion films by straining the metal at the tip of the crevice without rupturing it. When the electrodes are unfilmed, the new solid solution is likely to be the effective anode



with either the zinc-rich zones or old solid solution as cathode (see Tables II and III). The old solid solution will be the more effective cathode during this stage for the reasons given below.

During the stress-corrosion cracking of loops made from the aluminium-zinc alloys, bubbles of gas, presumably hydrogen, can be seen coming from the stress-corrosion crack, indicating that corrosion of the hydrogen-evolution type is occurring. The reversible potential for hydrogen evolution is given by the equation :

$$E = \frac{RT}{F} \log_e [H^+] - 0.284.$$

For 3% sodium chloride solution, whose pH is about 6.5,  $E = -0.66$  V. (*N*-calomel scale). However, the overvoltage at an aluminium surface is given as 0.5 V. at current densities up to about 100  $\mu\text{amp./cm.}^2$ , and at a zinc surface as 0.72 up to 1000  $\mu\text{amp./cm.}^2$ . The overvoltage of the aluminium-zinc solid solutions will probably be little different from that of aluminium. Thus, appreciable hydrogen evolution will not occur at an aluminium surface whose potential is more positive than  $-(0.5 + 0.66)$  V., i.e.  $-1.16$  V., nor at a zinc surface whose potential is more positive than  $-(0.72 + 0.66)$  V., i.e.  $-1.38$  V. Since the zinc cannot have a potential as negative as  $-1.38$  V. (see Table II), no hydrogen could be evolved from a zinc cathode, but hydrogen evolution could occur from the solid-solution cathode. It seems, therefore, that during the rapid localized corrosion, when the electrodes are bare, the anode and cathode are the new and old solid solutions respectively. This rapid stage of corrosion would probably lead to a rounding off of the crack tip with a resultant decrease in the stress concentration and further intercrystalline corrosion would proceed until the stress concentration was once more sufficient to cause the exposure of bare electrodes. This process would be repeated until failure occurred by the mechanical process; towards the end of the stress-corrosion period, creep would already be occurring in suitably orientated boundaries containing the ductile new solid solution. As similar conditions exist in aged aluminium-copper alloys, it is likely that a similar mechanism of stress-corrosion may apply.



## APPENDIX.

## AGE-HARDENING OF ALUMINIUM-ZINC ALLOYS.

1. *Previous Investigations.*

Aluminium alloys containing more than 5% zinc have been found to harden at room temperature,<sup>16, 17, 18, 19</sup> the precipitate, when formed, being zinc containing up to 0.4% of aluminium in solid solution. Hérenghuel and Chaudron<sup>19</sup> have shown that an alloy containing 10% zinc hardens very rapidly at room temperature after quenching from the solution-treatment temperature. The maximum Brinell hardness number of 91 is almost reached within a few minutes of quenching, the maximum itself being attained after 3 hr. at room temperature. By extrapolation, Hérenghuel and Chaudron obtained a Brinell hardness number of 26 immediately after quenching. Iron was found to diminish the degree of hardening at ordinary temperatures, whereas magnesium additions reduced the rate of hardening but increased the maximum hardness.

Geisler, Barrett, and Mehl<sup>7</sup> found that an aluminium-25% zinc alloy hardened rapidly at room temperature, but on ageing at 100° and 229° C. softening took place. This was most probably due to the alloy being hardened at room temperature before ageing at the elevated temperatures.

2. *Experimental Procedure.*

All heat-treatments were carried out in the same way as that described earlier and, unless otherwise stated, specimens were air-cooled from the ageing temperature. Hardness determinations were made using a 5-kg. load, a minimum of five hardness impressions being made for each determination. The same specimen was used for all the determinations at any one ageing temperature, except in the case of specimens aged at room temperature for short times. In this case the hardness immediately after quenching was determined from the mean of six single impressions, each on a separate specimen. The time taken to make an impression was approximately 30 sec.

3. *Results.*(a) *Ageing at Room Temperature.*

The ageing curve at room temperature for the aluminium-10.8% zinc alloy is given in Fig. 21. The Vickers diamond pyramid hardness number 25 sec. after quenching was 46, increasing rapidly to 87 within 2 min. of quenching. The Vickers hardness then increased less rapidly, a value of 90 being reached after approximately 15 min. There was no further change in hardness up to 193 days. Extrapolation of the

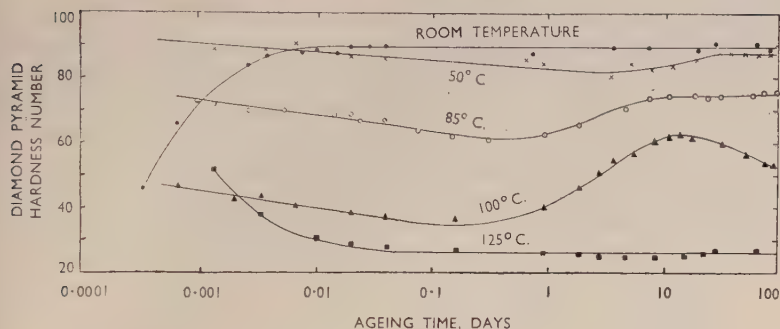


FIG. 21.—Ageing Curves for Aluminium-10.8% Zinc Alloy.

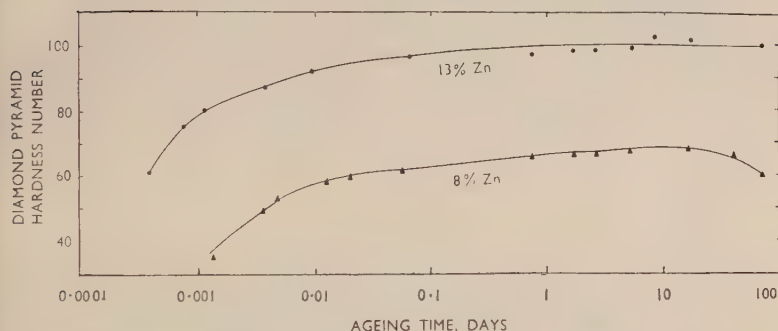


FIG. 22.—Ageing Curves for Aluminium-8% Zinc and Aluminium-13% Zinc Alloys at room temperature.

hardness-time curve for the rapid-hardening stage gave a Vickers hardness of 32 for the as-solution-treated material, which is slightly higher than the estimated Brinell number of 26 given by Hérenghuel and Chaudron.<sup>16</sup> Curves for the 8 and 13% zinc alloys are given in Fig. 22. The final hardness and rate of hardening increase with increasing zinc content.

#### (b) Ageing at Elevated Temperatures.

Age-hardening curves for the aluminium-10.8% zinc alloy at 50°, 85°, 100°, and 125° C. are given in Fig. 21. At all temperatures except 125° C., an initial drop in hardness is followed by a rise which occurs earlier with increasing temperature. The initial softening is probably due to relief of strain set up, or to re-solution of nuclei formed during the room-temperature ageing which inevitably occurred during transference of the specimens from the quenching bath to the heat-treatment bath or oven. Although this delay was only 2 or 3 min.,

appreciable hardening would have taken place (see Fig. 21). Ageing curves for the 8 and 13% zinc alloys at 125° C. are given in Fig. 23. It is interesting to note that in contrast to the 8 and 10.8% zinc alloys aged at 125° C., the 13% zinc alloy shows appreciable hardening, the maximum being reached in approximately 4 days. It appears, therefore, that whenever hardening occurred the new solid solution was always present. These results thus support the view put forward by

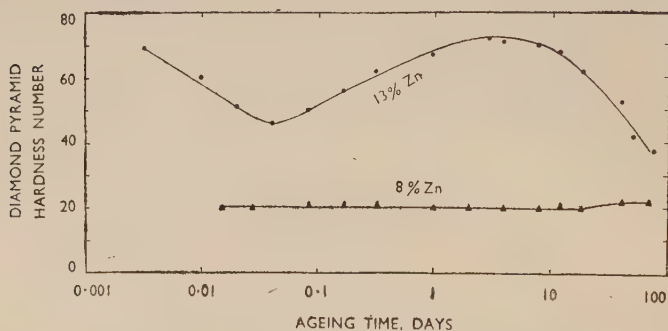


FIG. 23.—Ageing Curves for Aluminium-8% Zinc and Aluminium-13% Zinc Alloys at 125° C.

Hardy<sup>20</sup> that the amount of lattice strain is the principal factor deciding whether precipitation is continuous or discontinuous.

To find out whether the initial decrease in hardness on ageing at an elevated temperature (see Figs. 21 and 23) was due to previous ageing at room temperature while the specimen was transferred to the ageing bath, or while the hardness measurements were being carried

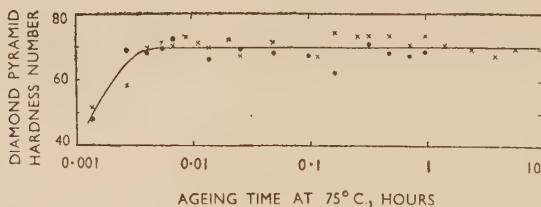


Fig. 24.—Ageing Curve for Aluminium-10.8% Zinc Alloy.

out, specimens were solution-treated and quenched in water at the ageing temperature. After ageing for a certain time the specimen was quenched into liquid oxygen, so that no age-hardening would take place whilst the specimen was transferred to the Vickers hardness

machine which was 2 or 3 minutes' walk away.\* The specimen was removed from the liquid oxygen and the hardness impression made just as the ice on the specimen had melted, thus ensuring that the hardness was determined at an approximately constant temperature (0° C.). After the hardness had been recorded the specimen was transferred to the liquid oxygen and then to the ageing bath. Results for the aluminium-10.8% zinc alloy aged at 75° C. are given in Fig. 24. Hardening has started directly after solution-treatment, indicating that the initial softening in Figs. 21 and 23 is due to room-temperature ageing before ageing at the elevated temperature.

#### 4. Discussion of Results.

On ageing at room temperature the structural changes which accompany the hardening are similar to those found by Gayler<sup>6</sup> for the aluminium-4% copper alloy. The main difference between the two alloy systems appears to be the rate of hardening. X-ray work by Geisler, Barrett, and Mehl<sup>7</sup> and by Guinier<sup>21</sup> has shown that during the initial stages of ageing coherent zinc-rich platelets are formed on the (111) matrix planes, and Fink and Van Horn<sup>17</sup> found that on ageing aluminium-zinc alloys at room temperature there was a rapid initial increase in electrical resistance. It seems therefore that the age-hardening at room temperature is due in the case of the aluminium-zinc alloys to the formation of coherent zinc-rich zones, the resulting lattice strains leading to the increase in hardness and electrical resistance.

#### ACKNOWLEDGEMENTS.

The work recorded in this paper was undertaken as part of a research on the stress-corrosion of light alloys carried out for the Principal Director of Scientific Research (Aircraft), Ministry of Supply.

The authors wish to thank the Chief Scientist, Ministry of Supply, and the Director and Council of the British Non-Ferrous Metals Research Association for permission to publish this paper, and also Mr. R. Eborall, Dr. P. T. Gilbert, and Dr. M. L. V. Gayler for many helpful discussions.

\* That no age-hardening occurred at the temperature of liquid oxygen is shown by the fact that measurements made on specimens which had been immersed in liquid oxygen overnight gave the same hardness as they did before immersion.

#### REFERENCES.

1. J. D. Grogan and R. J. Pleasance, *J. Inst. Metals*, 1939, **64**, 57.
2. G. Chaudron, J. Hérenghuel, and P. Lacombe, *Compt. rend.*, 1944, **218**, 404.
3. J. Hérenghuel, *Rev. Mét.*, 1947, **44**, 77.

4. W. L. Finlay and W. R. Hibbard, Jr., *Metals Technol.*, 1948, **15**, (6); *A.I.M.M.E. Tech. Publ.* No. **2470**.
5. Private communication from The British Aluminium Co., Ltd.
6. M. L. V. Gayler, *J. Inst. Metals*, 1946, **72**, 243.
7. A. H. Geisler, C. S. Barrett, and R. F. Mehl, *Trans. Amer. Inst. Min. Met. Eng.*, 1943, **152**, 201.
8. M. L. V. Gayler, private communication.
9. P. J. E. Forsyth, R. King, G. J. Metcalfe, and B. Chalmers, *Nature*, 1946, **158**, 875.
10. M. L. V. Gayler and W. E. Carrington, *J. Inst. Metals*, 1946, **73**, 625.
11. G. V. Akimov and G. B. Clark, *Trans. Faraday Soc.*, 1947, **43**, 679.
12. E. C. W. Perryman and S. E. Hadden, *J. Inst. Metals*, 1950, **77**, 207.
13. G. Wassermann, *Z. Metallkunde*, 1942, **34**, 297.
14. E. Orowan, *Trans. Inst. Eng. Ship. Scotland*, 1946, **89**, 165.
15. C. Benedicks, [*Proc.*] *Pittsburgh Internat. Conf. on Surface Reactions (Electrochem. Soc.)*, **1948**, 196.
16. J. Hérenguel and G. Chaudron, *Rev. Mét.*, 1944, **41**, 33.
17. W. L. Fink and K. R. Van Horn, *Trans. Amer. Inst. Min. Met. Eng.*, 1932, **99**, 132.
18. H. Nishimura, *Mem. Coll. Eng. Kyōtō Imp. Univ.*, 1924, **3**, 133.
19. J. Hérenguel and G. Chaudron, *Métaux, Corrosion, Usure*, 1943, **18**, 105.
20. H. K. Hardy, *J. Inst. Metals*, 1948-49, **75**, 707.
21. A. Guinier, *Métaux, Corrosion, Usure*, 1943, **18**, 209.



## INDUSTRIAL GAS TURBINES.

FORTIETH MAY LECTURE TO THE INSTITUTE OF METALS,  
DELIVERED 10 MAY 1950.

By H. ROXBEE COX,\* Ph.D., M.I.Mech.E., F.R.Ae.S., F.Inst.F.

## SYNOPSIS.

The lecture is of an introductory character and particularly refers to British efforts.

The present activity in industrial gas turbines in Great Britain is seen as the consequence of the success of the aircraft gas turbine here and of the progress made with industrial applications in Switzerland. Swiss achievements are noted and industrial engines at work and under construction here are referred to. The various possible fuels and the difficulties attendant upon their use—the vanadium problem with residual oil, the ash problem with coal, and the moisture problem with peat—are discussed. The three lines of attack on the design of the coal-burning gas turbine and the interesting case of the design of a gas turbine to use “firedamp” in mine upcasts as fuel are described.

The advantages which the gas turbine offers for use in power stations in this country if it can be made to run consistently on indigenous fuel, its possibilities in rail and road traction, and the ways in which it can be applied as a component in industrial processes are briefly reviewed.

Reference is made to the relative merits of closed- and open-cycle systems and of axial and centrifugal compressors, and the lecture concludes with some notes on the demands which will be made on metallurgists for cheaper materials, higher-temperature materials, and materials in forms specially suitable for cooling.

## 1.—INTRODUCTION.

I WANT first of all to record my appreciation of the honour done to me by the Council of the Institute of Metals in inviting me to give the Fortieth May Lecture. It is indeed a great privilege to be added to the list of my distinguished predecessors.

The gas turbine is being applied to duties on the land, on the sea, and in the air. Its range is so extensive that, when I was asked to lecture on “Gas Turbines”, I realized that I could not profitably attempt to deal with the subject in its widest sense. I decided, therefore, to confine myself to the land applications of the gas turbine, as it is with these that I have been for the past eighteen months most closely concerned. Even with this restriction, I cannot hope in a short paper to present a comprehensive picture—the canvas is still too

\* Chief Scientist, Ministry of Fuel and Power.

vast—but I propose to offer some observations on recent developments, current problems, and future prospects which I trust will be of interest.

The history of the gas turbine appears to begin with John Barber's patent of 1791. Its practical development belongs wholly to this century.<sup>1</sup> The widespread activity in gas turbines to-day can fairly be thought of as mainly a development of the past 15 years. Members of this Institute can take great pride in the fact that they made this development, prodigious in extent and promise as it is, possible. To examine whether metallurgical progress stimulated the gas-turbine designers, or the gas-turbine designers the metallurgists, is as profitless as the parallel exercise on the priority of the chicken and the egg, but of the magnitude of the metallurgical contribution to the rapid progress in the current gas-turbine epoch there can be no doubt. All gas-turbine engineers salute your inspired alchemy: may your cauldrons seethe with ever more potent earths.

Appearance is apt to vary with the point of observation. That is as true for history as it is for everything else except a sphere. Being conscious of that, I am conscious that in seeing the present state of the gas-turbine art as mainly the consequence of British and Swiss endeavours, I may not be fairly assessing the notable contributions to progress from France, Germany, America, Sweden, and Hungary. For us here, however, I think it is true.

It was in 1936 that Whittle's great effort, which resulted in the jet-propulsion gas turbine for aircraft, truly got under way. It was in the same year that serious experiment on axial compressors was put in hand at the Royal Aircraft Establishment. The way in which, in this country, the movement so begun gathered a momentum of invention, research, and development has been told already.<sup>2, 3</sup> The point of interest to note here is that until after the end of the war the movement was directed solely towards the aircraft gas turbine.

Also in or about 1936, serious interest in the gas turbine was reviving on the Continent. Except in Germany, the industrial gas turbine was the main objective. Development towards this objective was largely frustrated by the war everywhere but in Switzerland, where progress has been uninterrupted. The result is that Swiss progress in the industrial field has been as significant as our own in the aircraft field.

Soon after the war ended, it was possible to conclude that through this country's intensive attack on the aircraft gas turbine objective, we had built up a store of thermodynamic, aerodynamic, mechanical, and metallurgical knowledge which would be of the utmost value applied to the problems of the industrial and marine gas turbines; that

these gas turbines were of more importance to the national economy than the more spectacular aircraft gas turbines; that the Swiss were leading the rest of the world by several years in the industrial field; and that in consequence we should be wise, while maintaining our lead in aircraft gas turbine technology, to try to achieve a similar position in the industrial and marine spheres.

These views steadily gained acceptance, and to-day, I would suppose, are widely held. That this is so is indicated by the work done since the war, the work in hand, and the work projected in this country on industrial and marine gas turbines. Dr. T. W. F. Brown has fairly recently given a full account<sup>4</sup> of the marine part of this work, and it is of the industrial part of it that I intend to give a brief account in this lecture. In so doing I shall refer briefly to the Swiss achievements, which have undoubtedly provided a tremendous stimulus to the effort here.

## 2.—GAS TURBINES FOR GENERATING ELECTRICAL POWER.

Probably the first modern\* gas turbine to go into service in a power station was the 4000 kW. stand-by set built by Brown, Boveri

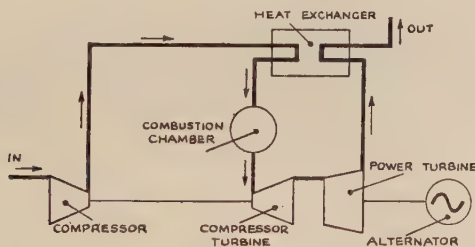


FIG. 1.—Diagram of a Simple Open Cycle.

and Co., Ltd., of Baden, Switzerland, and installed in 1938 at Neuchâtel. This, like all Brown, Boveri gas turbines, works on the open cycle, a simple form of which is illustrated diagrammatically in Fig. 1. In all, this company has received orders for twelve gas-turbine sets for electrical power generation, and has delivered six of them. Some of these run on gaseous fuel, but the majority on liquid fuel. The company's greatest achievement so far is the new power station at Beznau in Switzerland, where one 13,000 kW. set and one 27,000 kW.

\* The modern gas turbine works on the constant-pressure cycle. A Holzwarth gas turbine, working on the constant-volume cycle (the explosion-type gas turbine), was built by Brown, Boveri of Mannheim in 1925 for Muldenstein power station.

set are installed as base load plant. They run on an Anglo-Iranian fuel of 225 seconds viscosity (Redwood No. 1) at 100° F. (38° C.). This is probably the heaviest oil yet used regularly in service in a gas turbine.

The Escher Wyss Engineering Works, Ltd., of Zürich, has con-

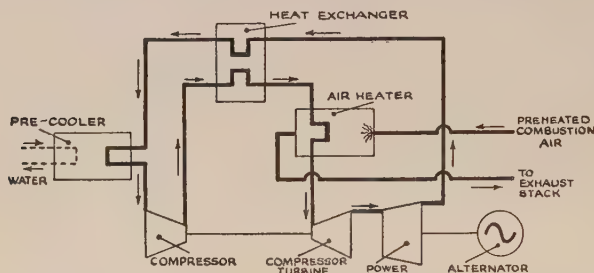


FIG. 2.—Diagram of a Simple Closed Cycle.

centrated on the closed-cycle gas turbine, simply illustrated in Fig. 2. This company's major work so far is the 12,500 kW. set now being installed in the St. Denis power station near Paris.

Sulzer Bros., of Winterthur, have completed a 7500 h.p. experimental marine set and a 20,000 kW. power station set at Weinfelden.

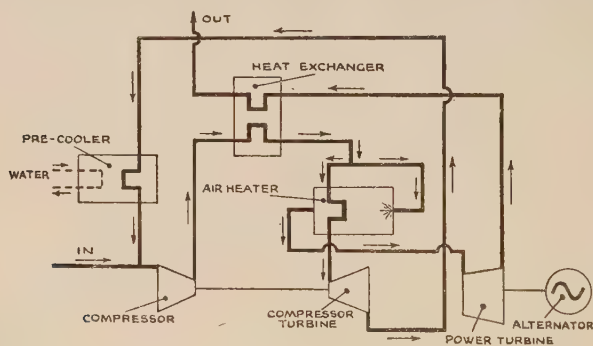


FIG. 3.—Diagram of a Simple Mixed Cycle.

These machines are designed on a mixed cycle—partly open and partly closed—which is simply illustrated in Fig. 3, from which it will be seen that the open-cycle part is associated with the power turbine and the closed-cycle part with the compressor turbine.

There are already running four small plants in this country. C. A. Parsons and Co., Ltd., have a 500 h.p. experimental open-cycle set of

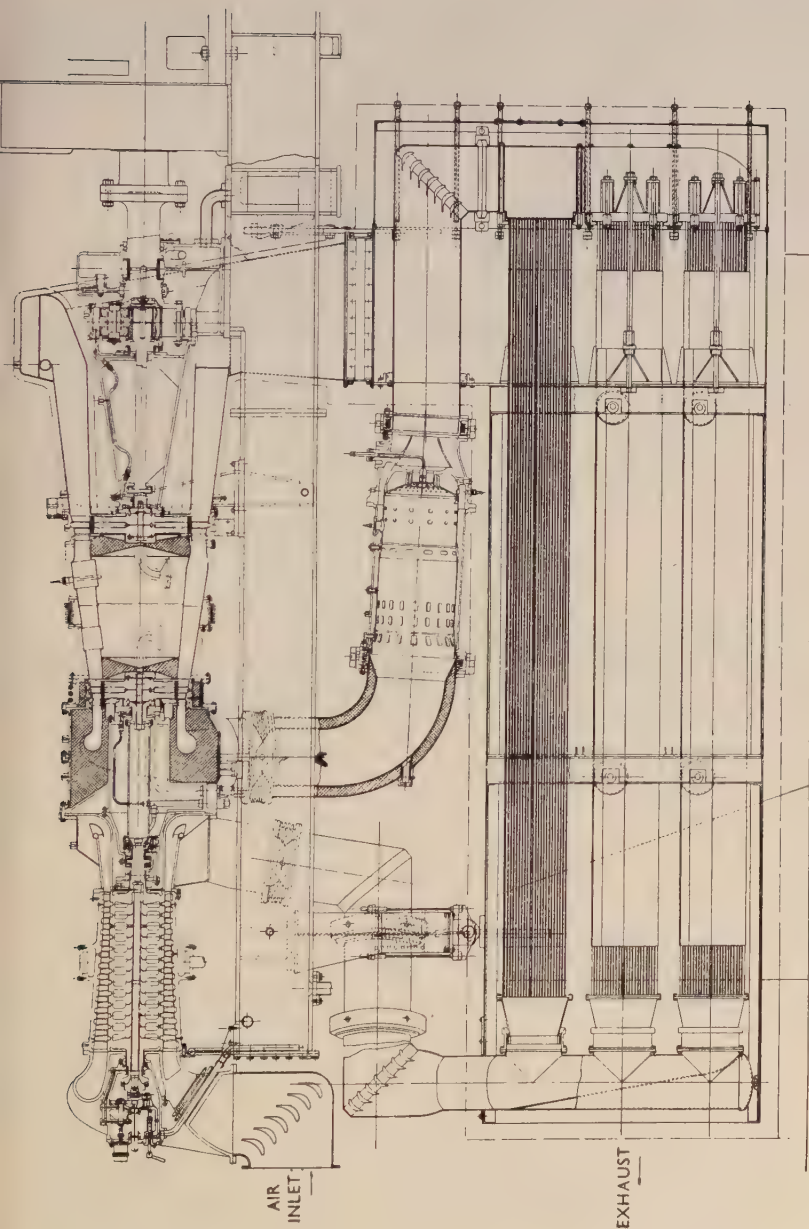


FIG. 4.—Sectional Arrangement of Ruston and Hornsby 750 kW. Gas Turbine with Alternator.



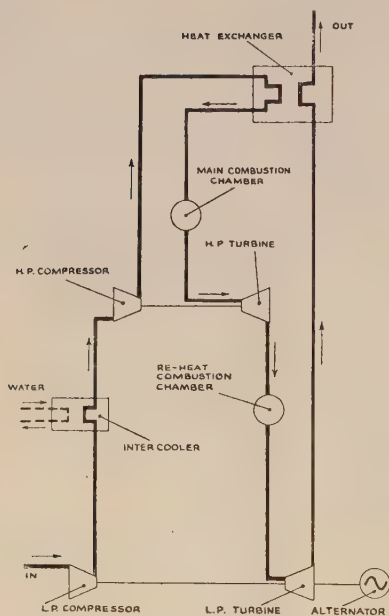


FIG. 5.—Cycle Diagram for Metropolitan-Vickers 15,000 kW. Open-Cycle Set for the British Electricity Authority.

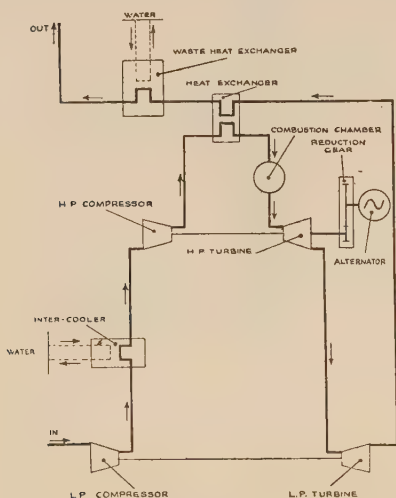


FIG. 6.—Cycle Diagram for C. A. Parsons 10,000 kW. Open-Cycle Set for the National Gas Turbine Establishment.

their own design, John Brown and Co., Ltd., a 500 h.p. experimental set, designed originally by Pametrada\* as an open-cycle machine and recently converted by John Brown to the closed cycle. The Metropolitan-Vickers Electrical Co., Ltd., have made a 2000 kW. open-cycle set on which experiments with a variety of liquid fuels have been carried out. The latest of the smaller industrial gas turbines is the neat 750 kW. set built by Ruston and Hornsby, Ltd., which is shown in Fig. 4. In the 2000 kW. class, three gas turbines have been ordered by the Metropolitan Water Board for stand-by duties.

There are four quite large electricity generating plants now under construction in this country. Two of them, each of 15,000 kW. capacity, are to the order of the British Electricity Authority, one from C. A. Parsons and the other from Metropolitan-Vickers (Fig. 5). C. A. Parsons are also making a 10,000 kW. plant for the National Gas Turbine Establishment (Fig. 6). These are all open-cycle gas turbines. The fourth is a 12,500 kW. set being made by John Brown on the Escher Wyss closed-cycle plan

\* Parsons and Marine Engineering Turbine Research and Development Association.



developed to run on cheap fuel. One obvious possibility is residual oil. The others, likely to appeal even more to industry in this country, are our only indigenous fuels, coal and peat.

### 2.1. *Residual oil.*

A certain amount of running on residual oil has already been accomplished in Switzerland, but the general problem is still far from being solved. Experimental running in this country has clarified the nature of the problem. There is no difficulty in burning the heaviest residual oil; the removal of solid particles from the products of combustion is a problem which can be solved mechanically; the heart of the matter is to neutralize the effects of the corrosive dispersed products of combustion, the most intractable of which is vanadium pentoxide. Such extended running as has yet been achieved is probably with residual oils low in vanadium content. In the general case, there is no doubt about the severe and rapid corrosive action, which is illustrated in Fig. 8 (Plate XXII), and no dependable solution of the difficulty has yet been suggested. The metallurgist who produces a material for combustion chambers, blading, and heat-exchanger tubes which is resistant to vanadium attack will make a major contribution to gas-turbine engineering.

### 2.2. *Coal.*

There are three ways in which coal may be consumed in a gas turbine:

First of all, there is direct internal combustion of pulverized coal in the open-cycle gas turbine.

Second, there is two-stage internal combustion of coal in the open-cycle engine. By this I mean the gasification of coal in a gas producer and the internal combustion of the gas produced. This is most desirably achieved by employing a gas producer which works at the gas-turbine cycle pressure or higher.

Third, there is external combustion of coal in either open- or closed-cycle engines.

With direct internal combustion the major problem is to find how to deal with the combustion ash. This is a mechanical problem. There seems to be no chemical problem comparable with the vanadium problem of residual oil. A considerable body of work has been put in hand. Combustion research is in progress at the Fuel Research Station on two forms of combustion chamber. One is a simple cylindrical chamber with a multijet burner (Fig. 9) and the other a so-called vortex chamber (Fig. 10). In the vortex chamber the fuel particles



FIG. 8.—Turbine Blade, showing corrosive action due to vanadium content of residual oil.

[To face p. 294.]





are burned while held in suspension between the inward component of the velocity of injection and the outward component of the rotational velocity imparted to the charge. At the British Coal Utilisation Research Association, research is proceeding on a cyclone combustion chamber. In this type of chamber (Fig. 11), the charge velocity is designed to throw the particles on to the walls, where they burn, leaving most of the ash in the form of liquid slag which can be withdrawn.

C. A. Parsons are adapting their experimental 500 h.p. gas turbine to run on pulverized coal, and the English Electric Co., Ltd., are beginning work on a 2000 kW. gas turbine, the cycle diagram for which is shown in Fig. 12, with which it is hoped to demonstrate and experiment with coal as a fuel on a practical scale, using ultimately all the types of chamber I have mentioned.

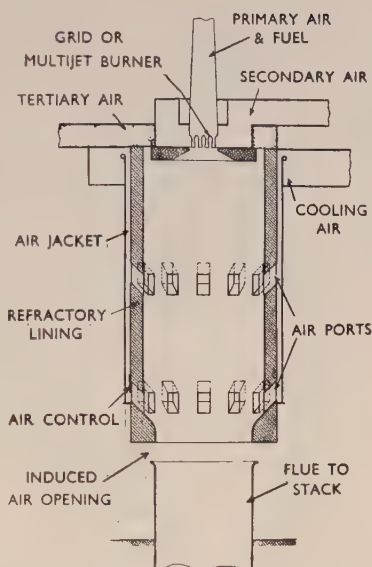


FIG. 9.—Tubular Combustion Chamber.

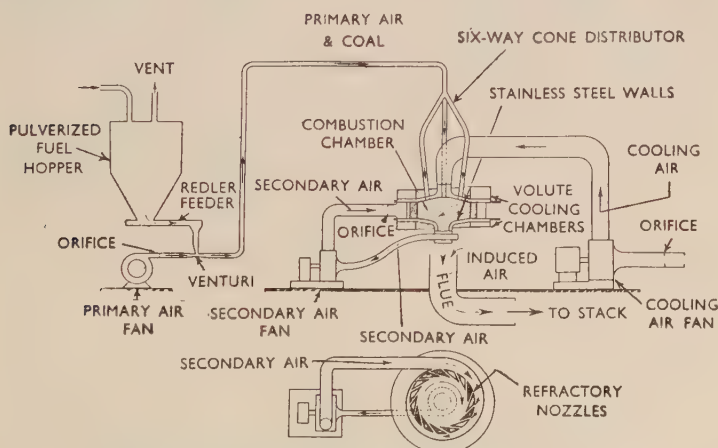


FIG. 10.—Diagrammatic Arrangement of Experimental Vortex Combustion-Chamber Unit,

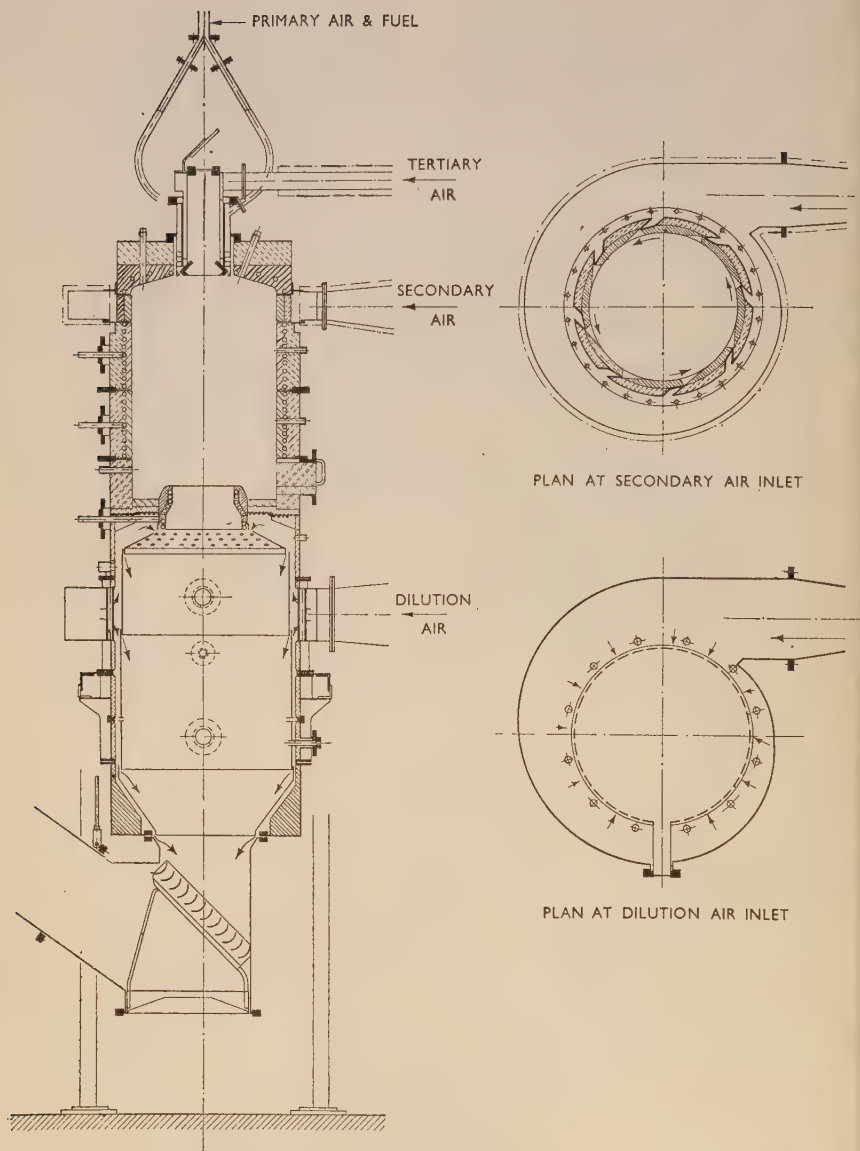


FIG. 11.—Sectional Arrangement of B.C.U.R.A. Experimental Combustion Chamber for Burning Coal at Atmospheric Pressure.

In the case of two-stage internal combustion, we visualize a gas producer of cyclone form operating at ash-slugging temperature and capable of dealing with pulverized low-grade coal. It requires a high degree of blast preheat (about  $1000^{\circ}\text{C}.$ ). This preheat is provided by a ceramic heat exchanger which also cools the gas products. The gas turbine associated with the gas producer has itself no particularly novel features.

In the case of direct internal combustion, it is necessary to clean the whole throughput of the engine. In the two-stage system, however, it is clearly only the output of the gas producer that has to be cleaned. It is of interest to note that the successful development of the gas-producer part of the system will provide a "total gasification" method of considerable interest quite apart from gas-turbine applications.

A plant on the lines described, and illustrated in Fig. 13, has been ordered. The gas turbine is being provided by Metropolitan-Vickers and the gas-producer part by the Incandescent Heat Co., Ltd., and Joseph Lucas, Ltd., working in collaboration.

The possibility of ash causing deterioration of the turbine blading makes the idea of using a cycle in which the ash does not pass through the blading particularly attractive. It is possible to arrange the open cycle to achieve this by heating the air in a "boiler" instead of by internal combustion (Fig. 14). The maximum possible use is made of the heat in the air after expansion through the turbine by using some of it as the air for combustion of the fuel in the boiler. Even so, the cycle cannot be very efficient (15–20%), and its charm lies in its simplicity. Simplicity is not unfortunately an invariable concomitant of elegance, and in this cycle the heat exchanger of the air boiler is likely to obtrude unpleasantly if tubing of, say,  $\frac{3}{4}$  in. or 1 in. outside dia. is used, or else is likely to consist of a very large number of small tubes (e.g. of  $\frac{1}{4}$  in. outside dia.) which are difficult to clean. Nevertheless, the scheme is worth most serious consideration for duty with coal of high ash content.

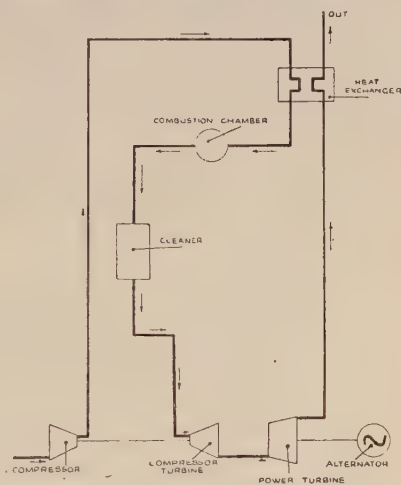
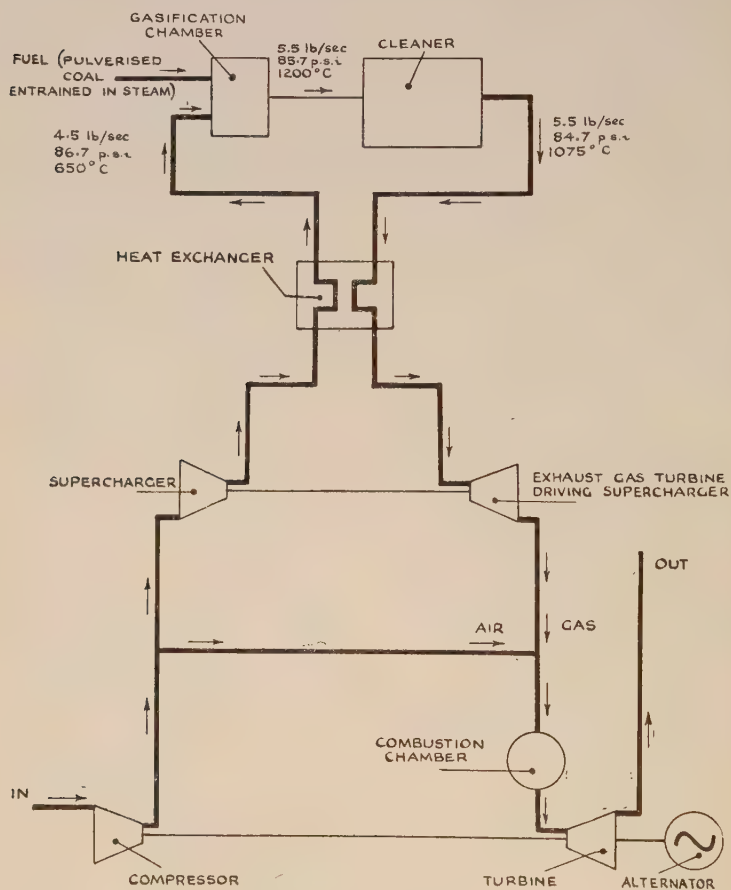


FIG. 12.—Cycle Diagram for English Electric 2000 kW. Coal-Burning Gas Turbine.

The closed cycle offers similar advantages without the disadvantage of low efficiency. So far, however, the large closed-cycle engine has generally been assumed to employ a pressurized air boiler, because an



NOTE :- ALL FIGURES SHOWN ARE APPROXIMATE.

FIG. 13.—Cycle Diagram for Gas-Producer Gas Turbine.

atmospheric air boiler would be unattractively large both on æsthetic and economic grounds. With the pressurized air heater, the advantage of avoiding passing ash through the main turbine would be largely neutralized by its having to pass through the turbine for supercharging

the pressurized air heater. There is, therefore, much to be gained by an atmospheric air heater, and John Brown and Co., Ltd., have now designed one which appears to be no larger than the pressurized one which it replaces. The principle which leads to this advance is the use in the atmospheric heater of radiant heat. Even with the atmospheric heater, there is still the problem of avoiding deleterious action of ash on the tubing of the heater. There are some experts who regard this as presenting as serious a problem as the action of ash on blading, and there are others who do not. It is in any case obviously sensible to pursue both approaches to the problem of clean working gas—via internal and via external combustion—simultaneously. That is in fact being done, and John Brown and Co. are building a special coal-burning air heater to use with their 500 h.p. experimental engine.

### 2.3. Peat.

Peat as a gas-turbine fuel was first suggested by C. H. Secord in 1947, and the idea has had a particular appeal in Scotland where large quantities are available. Peat, like coal, can be used in both open- and closed-cycle engines, and with both of these there is the possibility of using the peat in a wet state. Peat, when cut, is generally more than 90% water, and is ordinarily air dried—a long and hence relatively expensive process—to about 30% moisture content for use. It can be taken into the gas turbine in a much wetter state, and the heat generated in the cycle can be used to dry it to the condition for ready combustion.

The first steps towards the closed-cycle peat-gas turbine are being taken by John Brown, who are making an air heater for their 500 h.p. set to take peat of 30% humidity.

Ruston and Hornsby, Ltd., are making a version of their 750 kW. set to run on peat. In the first instance, the cycle will be as shown in Fig. 15. It is hoped that in a later version of the cycle the steam generated in the drying process will be used to augment the power of

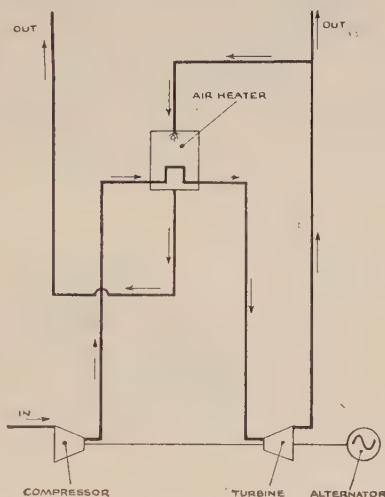


FIG. 14.—Diagram of Open Cycle with External Combustion.



the turbine. It appears possible to quadruple the power for a given size of plant by this means.

There is, of course, with peat, as with coal, an ash problem, and similar means of cleaning are envisaged. As peat ash seems likely to be somewhat less abrasive than coal ash, it is possible that a somewhat lower standard of cleaning may be permissible.

#### 2.4. Gas.

It would seem that to use gas as a gas-turbine fuel would avoid some of the difficulties attendant upon the use of residual oil and solid fuel. Natural gas, blast-furnace gas, town's gas, and gas from petroleum-cracking plants are all possible fuels. Brown, Boveri have built a number of gas turbines to run on natural gas in oil fields, and two of the latest of these will shortly be

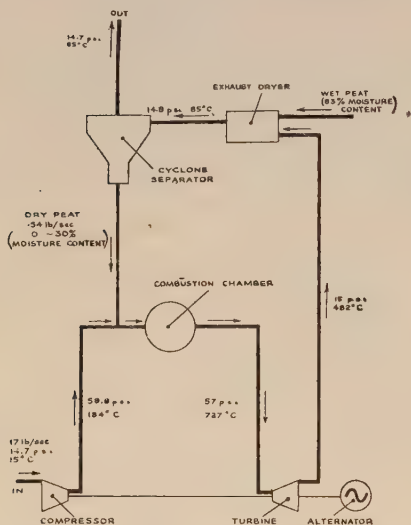


FIG. 15.—Cycle Diagram for Simple Peat-Gas Turbine.

delivered to the Anglo-Iranian Oil Company for use in Iran. The same Swiss company have also in hand a 5400 kW. set for Luxembourg to run on blast-furnace gas.

In this country, there are few appreciable sources of natural gas, and town's gas, while perfectly suitable technically, is too expensive to use as a gas-turbine fuel. Gas turbines to run on blast-furnace gas and petroleum-cracking gas could be made if required. There are, however, two other sources of gas which may ultimately provide sources of energy of much greater magnitude. One is the gas from underground gasification of coal. If the experiments on underground gasification now in hand lead to success, we shall certainly consider utilizing the gas in gas turbines.

The other source is the "firedamp" or methane in mine upcast air. If this methane could be fully used in efficient engines it could generate all the power our collieries require. The fact that methane rarely occurs in the upcast air in concentrations higher than 1% is not basically a disadvantage, as an air : fuel ratio of 100 : 1 is of the

right order for a gas turbine. To get such a mixture to burn, however, a considerable amount of preheating is necessary. Sir Alfred Egerton has found that for a 1% concentration, about 980° C. preheat is required. It follows that the cycle of the firedamp gas turbine must provide preheating of this order (Fig. 16). A gas-turbine plant of this kind is being designed and will be built. The Ministry of Fuel and Power have ordered the gas turbine proper from the English Electric Co., Ltd. The National Coal Board will provide the site and installation. The plant is being designed for a concentration of about 1%. If it were used in conditions where the concentration exceeds this figure, the upcast air would be diluted with fresh air. If, as is very likely, it is used in conditions where the concentration falls below 1%, then auxiliary fuel will be used to bring the equivalent concentration back to 1%. Clearly, this auxiliary fuel must be cheap, if possible, even though the main fuel, the methane, costs nothing. Coke-oven gas is an interim possibility, but the ultimate aim is to bring together two lines of experiment—the firedamp work on the one hand and the coal-burning gas turbine work on the other. The target is a gas-turbine plant which consumes both firedamp and the colliery fines available at pitheads.

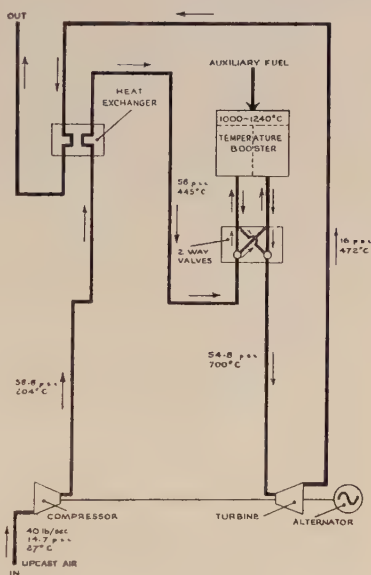


FIG. 16.—Cycle Diagram for Firedamp Gas Turbine.

2.5. *Prospects of the Gas-Turbine Power Station.*

The gas turbine is issuing its challenge to the steam turbine as a base-load plant. The steam turbine is a very efficient machine and represents a high standard of achievement. Its further development must, however, be limited in scope, whilst the gas turbine is still not far from its beginnings. On the grounds of thermal efficiency, we may be encouraged by, say, the 34% of the 27,000 kW. set at Beznau, an efficiency which few steam stations can equal. But the Beznau

plant runs on oil, whereas in England to compete generally with the steam turbine, the gas turbine will have to run on coal. A great deal of development will have to be done before this is achieved on a practical scale.

Those of us who have been closely associated with the gas turbine believe that its thermal efficiency can be raised as high as 40%. At such an efficiency, and burning a cheap fuel, it will be very attractive indeed. But looking again on the debit side, we realize that to compete with large steam turbines, readily provided in 100,000 kW. units, gas turbines will have to be developed to much larger sizes than any yet made or projected, or else an economic case for smaller units must be proved.

If large units are demanded, then I think that they will be most conveniently provided on the closed-cycle plan. I say this because, power for power, the rotors of the closed-cycle plant will be smaller than those of the open-cycle plant. Rotor size is more likely to be the limiting factor in size than any other factor. On the other hand, the open-cycle plant as normally designed needs little or no water, and independence of water gives a degree of freedom in choice of site which is very attractive indeed. There would not seem to be any chance of one type ousting the other; both will be used, depending on the conditions of service and the designer's tastes.

In addition to high thermal efficiency, the gas-turbine power station has other attractions. It has no component equivalent in bulk to the steam-turbine boiler. In other words, for a given output, the gas turbine is much smaller than the steam turbine, and this should be reflected not only in the relative costs of the two kinds of plant, but in the relative costs of the buildings to house them.

There is another interesting comparison to be made between them when the power station is considered as a source of heat for so-called "district heating". If a steam power station of, say, 30% efficiency, is made to use its rejected heat in a hot-water heating system, then though the overall thermal efficiency of the power-plus-heating system may be as high as 80%, the efficiency of power generation will be reduced to about 23%. If a 30% efficient gas-turbine station is made to use its rejected heat similarly, then though the overall efficiency is not likely to be more than 75%, its efficiency in power generation is unaffected. It may be noted that the exhaust heat of the 10,000 kW. set of Fig. 6 is used for "district heating".

### 3.—GAS TURBINES FOR TRACTION.

All the applications of the gas turbine to which I have so far referred are applications for the generation of electrical power. Power generated in this way could, of course, be used to drive trains on electrified lines. The gas turbine can, however, be used more directly for locomotion.

The first gas-turbine locomotive was built by Brown, Boveri and Co., Ltd., for the Swiss railways, and began to run in 1942. This engine has since run about 150,000 miles, mostly in regular service, in Switzerland and in France. It employs a gas turbine of 2200 h.p. of 18% efficiency and electric drive. It normally runs on a blended oil of 200 seconds viscosity (Redwood No. 1) and has given very little trouble. With the Swiss railways almost entirely electrified, there is little opportunity for the gas-turbine locomotive in Switzerland, but the Brown, Boveri Company see the possibilities of such machines for export. They in fact built their second gas-turbine locomotive to the order of the Great Western Railway, and it was delivered in January of this year to the British Railways (Western Region). This engine is of 2500 h.p. and 18% thermal efficiency, and is at present running on oil of 950 seconds viscosity (Redwood No. 1) which requires pre-heating to 100° F. (38° C.). A second gas-turbine locomotive was ordered by the G.W.R. from Metropolitan-Vickers, and this should start its trials about the end of this year.

The world's second gas-turbine locomotive, however, started its trials in January 1949 in the U.S.A. This is a 4800 h.p. engine of 17% efficiency designed and built by the General Electric Company of Schenectady.

All these locomotives are oil burners. At the present time, the oil-burning locomotive does not, except for special duties, appear very attractive on economic grounds in this country. Our natural inclination is to use coal as the main railway fuel, whether the policy be steam engines, electrification, or gas turbines. If the gas-turbine locomotive is to have a future in this country, there is a strong presumption that it will have to run on coal. In this connection, the coal-burning gas-turbine experiments to which I have referred are of considerable interest. Success with either the pulverized-coal engine or the gas-producer engine would represent the first step towards the locomotive.

Our policy in this country is to make the gas turbine run successfully on coal before beginning to adapt it to locomotive duty. The geometrical restrictions and operational requirements of the locomotive



would, in my view, have a crippling effect on progress if imposed at the outset. This has, I believe, also been the view in the U.S.A., where the efforts of the Locomotive Development Committee and their research engineer, Mr. Yellott, have been devoted since 1945 to the problems of producing a gas-turbine locomotive running on pulverized coal. A bench-test engine—not that for the chassis—is now running on the test bed on coal.

This locomotive engine, like the oil burners, is planned for electrical transmission. In this, the gas turbine has so far followed the Diesel engine, for which, because of its poor starting torque, electric drive is difficult to avoid. There does not appear, however, to be any compelling reason for the gas turbine, with adequate starting torque, to use electric transmission, and I confidently look forward to seeing a gas-turbine locomotive with direct mechanical drive.

For the gas-turbine locomotive, even though running on coal, to become standard equipment in this country, it will have to show itself economically superior to electrification. Main-line electrification has long had its adherents, and now the gas-turbine locomotive has its champions. Comparison of the two systems is a difficult and complex matter, and a great deal of careful and dispassionate estimation and analysis remains to be done before a critical evaluation can be made. I would not care to guess which will show up the better when the comparison is complete. If electrification proves superior for this country, however, there will still be opportunities for export which British gas-turbine locomotive makers will, I hope, be ready to seize. In countries where the low traffic density makes electrification unattractive, where improvement on steam-locomotive efficiency is worth while, and where water is scarce, the gas-turbine locomotive is a potential boon.

The other obvious possibility is to use the gas turbine for road transport. This possibility is being explored by more than one British company, and in March last the Rover Co., Ltd., demonstrated the first gas-turbine automobile in the world. The engine is a straight-forward open-cycle type, with a single-stage centrifugal compressor of maximum pressure ratio 4:1, driven by a single-stage turbine at 40,000 r.p.m. maximum, with a separate single-stage power turbine running at 34,000 r.p.m. maximum.

The engine was designed to give 200 h.p., and is intended for commercial vehicles and marine applications as well as for use in private cars. It has given so far 90% of its rated power. The lay-out is such as to provide for the incorporation of a heat exchanger, which is still under development.



There is a fair prospect of developing such small gas turbines to efficiencies comparable with those of the conventional automobile engine, and if at the same time they are developed to run on Diesel-type, or, better still, residual oils, they would be very attractive alternatives.

#### 4.—GAS TURBINES IN INDUSTRIAL PROCESSES.

The gas turbines I have so far mentioned have been straightforward prime movers, but the gas-turbine cycle can conveniently be used in combination with other cycles and with industrial processes. It was in such auxiliary roles that the earliest gas turbines of the present epoch were used. For example, in Brown, Boveri's Velox boiler of 1932, the gas turbine running on the boiler combustion products is used to supercharge the air supply to the boiler. In 1938 the gas turbine was first used as part of the Houdry oil-cracking process. In this process cracking takes place on the surface of a catalyst which in time becomes covered by a layer of carbon. By using two catalytic chambers, the carbon is burned off one whilst the other is in use, and the heat of combustion of the carbon is used to drive the gas turbine. The power generated is used to drive other auxiliaries. Brown, Boveri have built at least 29 of these specialized gas turbines.

A gas turbine may be used for generating power from such heat as is liberated from reactions in chemical works, and which might otherwise be wasted or used less effectively. A gas turbine of this character has been commissioned from John Brown and Co., Ltd., for the Coventry gasworks at Foleshill. In this case, the flue gases from continuous vertical retorts provide, by external combustion, the heat source for a closed-cycle gas turbine of 700 kW. These flue gases could alternatively have been used under steam boilers, and the choice of method is dependent on circumstances.

The gas turbine can be used in a number of ways in combination with an exhaust-heat boiler to produce shaft power and process steam with high overall efficiency.

It can also be used as an exhaust-driven supercharger for a prime mover and as a source of compressed air for blast furnaces and steel furnaces, taking the furnace gases as its fuel.

#### 5.—DESIGN PROBLEMS.

Nearly all the gas turbines I have mentioned employ axial compressors. The design of axial compressors has progressed steadily in the last few years under the pressure of aeronautical demands, and to-day a 6:1 pressure ratio with 10 stages of compression and an

adiabatic efficiency of 85% presents no difficulty. The axial compressor, with its hundreds of fixed and moving blades, is, however, quite an expensive article to design and make, and its performance is sensitive to fouling of the blades, which, also, are liable to damage if any foreign body finds its way into the compressor. Consequently, some thought has been given to the possibilities of the centrifugal compressor which, though common in aircraft gas turbines, has been employed in few industrial designs, among them the 1000 kW. experimental engine of the Oerlikon company in Switzerland, and the Rover car.

The centrifugal compressor is not as efficient as the axial, but it should be cheaper to make and it is very robust. This last quality is of the greatest importance now that we are considering the gas turbine for work in which toughness is sometimes more important than efficiency.

Whether to use an axial or a centrifugal compressor in a particular case will always depend upon the circumstances of that case. Centrifugal compressors for aircraft of 4:1 compression ratio and 80% adiabatic efficiency have been made and the Oerlikon company have shown that when the space restrictions of the aircraft do not apply and intercooling is used, 87% is possible. The present domination of the industrial gas turbine field by the axial compressor does not therefore appear to be indicative of the relative merits of the two forms of compressor, and there is a strong case for trying to develop industrial centrifugal compressors of high efficiency to give designers the maximum choice in designing the engine most suitable to the job.

Broadly, the efficiency of the gas turbine increases with the increase of the maximum gas temperature permissible. In the case of the turbine rotor and blading, higher temperatures become possible with the development of methods of cooling and the development of materials capable of bearing stress at still higher temperatures than the present ones. Both these lines of development provide problems for the metallurgist. For example, the so-called sweat cooling of blading requires the development of sintering methods to produce a blade of adequate strength sufficiently porous to permit the passage through it of clean air to form a continually refreshed insulating layer of air on the blade. Internal cooling by the passage of air or water through ducts inside the metal is another alternative which also demands the development of constructional methods.

The development of metallic materials to work at higher and higher temperatures has been steadily pursued since the aircraft gas turbine first appeared, and this development must continue. The demand does not come only from the turbine disc and turbine blading. For

example, material properties at present limit the maximum temperature in recuperative heat exchangers to about 800° C., and advance beyond this figure is highly desirable. It is not surprising that research has begun into materials which are partly metallic and partly ceramic, a development which will, I hope, be taken as a challenge by pure metallurgists.

Even if gas-turbine designers were content with present temperature standards, the programme facing their material suppliers would be sufficiently onerous. Cheaper materials are needed. This does not necessarily mean new alloys: there are the possibilities of cladding and enamelling. Cheaper constructional methods are needed. This suggests a drive for more weldable alloys and the development of welding techniques.

#### 6.—CONCLUSION.

This has been a brief review of some aspects of the industrial gas turbine with particular reference to and emphasis on the British contribution and effort. It may possibly serve as an introduction to the more technical and specialized literature of the subject and emphasize, what most metallurgists probably already recognize, the immense extent of the new field which is claiming their wares. Confidence in the gas turbine is no longer restricted to its pioneers, and metallurgists, who have played so big a part in bringing it safely through infancy, have an even bigger part to play in guiding it, with due regard to economy, through its adolescence—always a difficult time.

I acknowledge with gratitude the help I have received in preparing this lecture from Mr. D. G. Tobin, my oldest gas-turbine colleague.

#### REFERENCES.

1. (Sir) Claude Gibb and A. T. Bowden, *J. Roy. Soc. Arts*, 1946-47, **95**, 265.
2. F. Whittle, *Proc. Inst. Mech. Eng.*, 1945, **152**, 419.
3. H. Roxbee Cox, *J. Aeronaut. Sci.*, 1946, **13**, (2), 53.
4. T. W. F. Brown, *Trans. N.E. Coast Inst. Eng. Ship.*, 1948-49, **65**, 117.



# CORROSION AND RELATED PROBLEMS IN 1253 SEA-WATER COOLING AND PIPE SYSTEMS IN H.M. SHIPS.\*

By I. G. SLATER,† Ph.D., M.Sc., C.I.Mech.E., F.I.M., MEMBER,  
L. KENWORTHY,‡ M.Sc., A.R.C.S., F.R.I.C., F.I.M., MEMBER,  
and R. MAY,§ A.R.S.M., MEMBER.

## SYNOPSIS.

A study is presented of corrosion and related problems that were encountered in sea-water cooling systems during war-time service. Details are given of the deterioration liable to occur in the component parts of the system, such as inlets, valves, gratings, pumps, trunking, condenser doors, tube-plates, ferrules, condenser tubes, and piping. Impingement attack and deposit attack were the two most prominent types of corrosion encountered. It is shown that the main factors which influence these are water speeds with related eddies and turbulence, entangled air bubbles, tube obstructions, and contamination of the water. Remedial and palliative measures are discussed in relation to the corrosion-resistance of the materials and protective coatings available; the use of different alloys in the same system; modifications of design for minimizing the severity of the conditions; and the importance of maintenance routines.

Laboratory tests, and especially the jet-impingement apparatus, are shown to be of great value in indicating the probable service behaviour of materials, provided certain precautions are observed.

## I.—INTRODUCTION.

For many years, the corrosion of condenser tubes presented the biggest problem in marine cooling systems, and its importance was realized as early as 1910 when the Council of the Institute of Metals appointed a Committee to study it under the chairmanship of the late Sir Harold Carpenter. As a result of the investigation carried out under the guidance of that Committee, largely by the late Dr. G. D. Bengough and one of the authors of the present paper (R. M.), much information was collected about the causes of the various types of corrosion experienced. (Of the several papers published, attention is particularly directed to references 1 and 2.) It was found that the incidence of tube corrosion depended not only on the properties of the metal used and on those of the cooling water, but also to a remarkable extent

\* Manuscript received 27 October 1949.

† Director of Research and Development, T.I. Aluminium, Ltd., Birmingham; formerly Royal Naval Scientific Service.

‡ Royal Naval Scientific Service.

§ Corrosion Adviser and Senior Investigator, British Non-Ferrous Metals Research Association, London.



upon the working conditions in the plant. The effects of these conditions on the tube alloys then available varied appreciably, so that, by taking advantage of the knowledge gained, it was sometimes possible to control corrosion by adjustment of working conditions to a point where one or other of the alloys could safely be used. Control, however, gradually became more difficult and the risk of failure greater with the advance in condenser efficiency required by engineering progress. Later work led to the development of more resistant alloys, and these have proved so successful for condenser tubes that unless and until changes in design bring about a marked increase in the severity of the operating conditions the condenser-tube problem may be considered to be virtually solved.

Experience in the last war, however, revealed that severe corrosion was liable to occur in other parts of cooling systems in H.M. ships, where attack had not been expected. This problem assumed serious proportions and, since it threatened to affect the serviceability of ships at a critical period, an investigation was at once started by the Admiralty with the help of the British Non-Ferrous Metals Research Association, in the hope of finding a rapid solution. After a number of inspections of H.M. ships had been carried out and experiments made with certain remedial measures, it was possible to issue to the Fleet a Book of Reference to guide ships' officers, repair authorities, and designers in identifying the types of corrosion, realizing the factors responsible, and putting into effect such methods to overcome or minimize the troubles as at that time could be recommended.

The investigation was far from complete at this stage (1943), however, when its further pursuit came within the terms of reference of the then newly-formed Non-Ferrous Corrosion Sub-Committee of the Admiralty Corrosion Committee, of which all three authors of the present paper were members while this project was receiving active consideration. During this period, a considerable amount of additional experience was gained, and it is now thought that many of the observations and results accumulated in the course of the investigation would be of sufficient interest to warrant their wider circulation. The present paper has therefore been written with this object.

## II.—CORROSION IN COOLING SYSTEMS.

### 1. *Salient Features of Arrangement.*

The general arrangement of the main condenser and cooling-water systems of many naval vessels has for some time tended towards the single-pass straight-through type previously confined to destroyers

(Fig. 1). In this diagram a sloping inlet tube is depicted, although in some ships there may be more or less streamlined modifications of the earlier inlet box. Conditions differ from those in merchant ships largely because the whole system has to be designed for a very high maximum power output, combined with the greatest possible efficiency under the much lower power that will be used for most of the running time. To save pump power, the quantity of cooling water is varied according to requirements. Thus the average water speed in the system may at times be as low as 3 ft./sec., when mud deposits may tend to build up, and at other times as high as 12 ft./sec., when there is an ever-increasing risk of excessive local turbulence and much higher local speeds, both extremes being undesirable from the point of view of corrosion. Moreover, the water entering the system may be of varying quality according to place and circumstance. Thus, it may be brackish in estuarine waters and contaminated in and around ports;

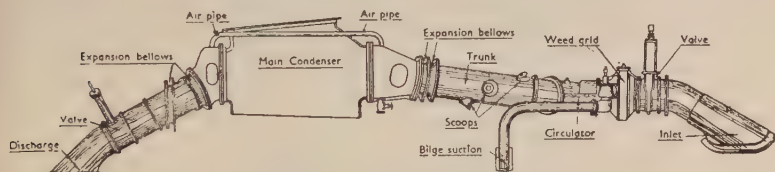


FIG. 1.—Diagram of the Main Cooling System.

or it may contain sand or mud in shallow waters, while in-shore seaweed and other marine organisms and their decomposition products may be present in quantity, especially in some localities and at certain seasons of the year. Air bubbles are practically inevitable and require special mention because of their importance in certain types of corrosion.

Additional to the main condenser system, a number of smaller cooling systems are installed which may be fed either from branches on the main cooling-water trunking or from separate inlets. These systems may include smaller condensers, as, for example, the drain cooler, turbo-generator, air ejector and distiller condensers, and coolers of various kind such as those in the lubricating-oil and refrigerator systems. Besides the units themselves, the piping leading to and from the various units constitutes an important item, and so does the great length of piping involved in the system of fire mains throughout the ship. Each of these may show trouble of a similar nature to those of the main system, and some of them have peculiarities and problems of their own, as will be explained in the following Section.

## 2. *Deterioration Encountered in Component Parts.*

### (a) *Shipbuilder's Inlet Tubes and Inlet Boxes.*

These are usually formed from steel plating, either riveted or welded, and in more recent designs are arranged to encourage scoop action and to give a reasonably smooth flow of water direct through the system with a minimum of pumping when the ship is steaming ahead. Earlier designs making use of scoop action, of which Fig. 1 may be taken as an example, were less satisfactory, the flow up the large convergent inlet often being excessively turbulent. Before undocking, the inlets receive the same protective treatment with paints as does the remainder of the under-water plating, namely, one or more coats of protective paint composition with a final coat of anti-fouling composition. In less satisfactory designs of inlet, the protective coats of paint may be eroded away rapidly, leaving bare steel exposed which may show rapid wastage and ultimate penetration by corrosion. Areas thus attacked often lie at the crown of the tube or at other points where there is a sudden change in the direction of flow, leading to impingement of rapidly moving water against the surface. Fig. 3 (Plate XXIII) demonstrates the effects of a rotary motion which may develop.

In addition, substantial areas of non-ferrous metals are located inboard adjacent to the steel tube, and these tend to accelerate attack of the upper end of the tube by galvanic action (see Fig. 4, Plate XXIII). It is normal practice to fit zinc protector slabs on the steel immediately adjacent to the gun-metal valve casting, and there is little doubt that this lessens the tendency for galvanic attack on the steel, as long as the zinc lasts or is in metallic contact with the steel. This practice, however, is not free from the danger of mechanical damage to parts of the circulator and sometimes to the condenser ferrules in ships not fitted with a weed grid, owing to large pieces of zinc coming adrift and being carried in the water stream. Consideration has recently been given to the use of better-quality protective paints (conveniently known as high-duty compositions) on the steel tube, and to the possibilities of lining the tube with rubber or other resistant material.

### (b) *Valves.*

These are almost invariably made of gun-metal\* in Service ships and are singularly trouble-free on this account. Corrosion is sometimes encountered with the slide-operating spindle, if made of rolled naval brass (Fig. 5, Plate XXIV), as this is liable to suffer dezincification, especially by contact in sea-water with the more noble gun-metal.

\* The chemical composition of the various alloys referred to throughout the paper will be found in Table I, p. 320.

(c) *Inlet Gratings and Weed Grids.*

It is usual to fit some form of grating to exclude flotsam which might damage the circulators or prevent the closing of valves. In some cases this is built up of mild-steel slats, running fore and aft, fitted over the bottom end of the inlet and flush with the outer bottom plating. Troubles encountered with this type of grating are usually associated with an insufficiently robust design, which allows vibration and so results in subsequent failure of the slats by corrosion-fatigue. The design of grating very considerably affects the degree of turbulence

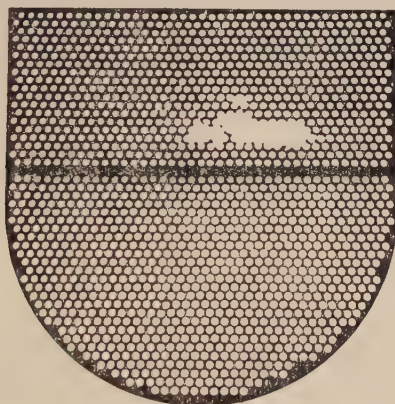


FIG. 2.—Naval Brass Weed Grid, showing extensive wastage due to impingement attack over an area coinciding with the most turbulent water flow. Approx.  $\times \frac{1}{12}$ .

in the water stream, and although later designs are better in this respect, the ideal grating has yet to be designed.

In destroyers and smaller ships, a weed-grid is also fitted in an athwartships box between the inlet valve and the circulator, comprising a non-ferrous plate drilled with holes. Rolled naval brass has been commonly used for this component and very many cases of rapid deterioration have been encountered, as illustrated in Fig. 2. The corrosive attack is usually of the impingement type resulting from high water speeds, excessive turbulence, and entangled air bubbles. The example shown indicates that conditions favouring impingement attack were at a maximum above and to the right of the centre and may well have been associated with a vortex motion initiated in the shipbuilder's tube as illustrated in Fig. 3, a matter which is discussed in Section III. 2. Often, long strands of weed lodge across the bridge of metal between



adjacent holes and give rise to a "sawing" action by their fluttering movements, producing narrow grooves resembling saw cuts. Some of these weeds can be seen in the tube-plate in Fig. 14 (Plate XXVIII). There is not much doubt that the action is mainly due to corrosion localized by the wearing away of the protective film. Other marine debris and flotsam lodging in the grid may give rise to similar effects or to deposit attack which, it should be noted, can remain active even when the system is shut down if the deposits are not removed. Parts adjacent to the weed-grid are usually of cast gun-metal which, before it becomes covered with scale, introduces galvanic effects to the further detriment of naval brass grids. Gun-metal grids which eliminate these effects and have great resistance to impingement attack have been found to give much more satisfactory service; the extra expense has been well justified where severe conditions of impingement are encountered. Another method to ensure longer life has been to paint the rolled brass grids with high-duty compositions at regular intervals, an improvization which was found useful during the stress of war-time refits and for the purpose of economy in gun-metal. Incidentally, this procedure afforded a most excellent method for testing the relative durability of different high-duty compositions.

(d) *Sea-Water Pumps and Main Circulators.*

The pump impeller is the main sufferer in these components and is liable to impingement attack and to sand erosion and perhaps even to cavitation-erosion. A typical example of an impeller of a fire-main pump is shown in Fig. 6 (Plate XXIV). Phosphor bronze, which is commonly used for such impellers, normally gives reasonable service. Alternative alloys for more severe conditions are Monel metal and stainless steel, though perhaps with some risk to adjacent parts owing to the highly cathodic nature of these alloys.

(e) *Main Trunking.*

In older designs this was of cast gun-metal which is almost trouble-free, but in cases where copper had been introduced for reasons of weight-saving and ease of fabrication, substantial deterioration arose when war-time conditions of running were encountered, because of the lower inherent resistance of copper to impingement attack. Such deterioration is particularly prone to occur at areas of turbulence, as in the wake of flanged joints or of scoops where water is drawn off into auxiliary pipe-lines, or at bends where the direction of water flow is changed abruptly.



(f) *Expansion Bellows.*

These thin copper components, which serve to take up imperfections in alignment and to allow for a certain amount of flexure or deformation of the hull structure without the transmission of undue stresses to vital parts of the machinery, were among the first to show corrosion failures when war conditions demanded higher water speeds for long periods. The attack was again of the impingement type (see Fig. 7, Plate XXIV), often accentuated by galvanic effects due to adjacent gun-metal parts, and kept active by deposit attack during stand-by periods. Protection by tinning was worse than useless, and paints invariably failed. Fitting steel wastage pieces alongside the copper bellows diminished the rate of deterioration, but was by no means a complete cure. A permanent protection was eventually found by bonding sheet rubber to the bellows, and this has now become standard practice.

(g) *Main Condenser Water-Boxes (Condenser Doors).*

Before the war these were nearly always made of gun-metal (most of the exceptions being in certain minor ships where cast iron was used), and were trouble-free except for a little highly localized attack at the air holes between the inlet and outlet sections of two-pass condensers which occurred as a result of excessive local impingement. Consequent on metal shortages, recourse was made to doors of fabricated steel, which even more than cast iron requires adequate protection, owing to the adjacent large cathodic area of the tube plate and tubes. Attempts to find a suitable high-duty protective paint for the steel, which can be relied upon under all conditions of service to remain intact for a substantial period of time (say, 6–12 months), have so far proved abortive. One of the drawbacks to the use of paint is that local failure of the paint film at a pin-point may lead to intense pitting at the exposed area. Up to date, the complete coating of the water side of the door with rubber appears to be the most promising solution, but there is not yet enough practical experience to draw final conclusions from trials which are in progress. Some early experiments in which imperfectly bonded rubber linings became detached and stopped the flow of water are still remembered. Cast iron appears to have a lower rate of deterioration than mild steel, possibly owing to the semi-protective nature of the graphite-bearing layer which is left behind as the material undergoes progressive corrosion and graphitization. Its use, however, in ships subject to modern warfare can be a serious danger because of its inherent rigidity and poor shock-resistance.

*(h) Condenser Tube-Plates.*

The rolled naval brass tube-plates commonly employed seldom show rapid deterioration unless corrosive conditions have been exceptionally severe. Cases in point have been in two-pass condensers where the division plate had not bedded-down on the tube-plate and had provided an "easy" path for some of the water, the local high velocity and turbulence causing impingement attack (see Fig. 8, Plate XXV). The same type of attack has also been experienced in turbo-generator condensers with water passages of poor design, which have been operated for long periods at water speeds greatly in excess of requirements. The tube-plates of drain coolers sometimes suffer considerable dezincification, especially those of insufficient capacity which run consistently hot. A section of a tube-plate which has deteriorated in this way is shown in Fig. 9 (Plate XXV).

Another more frequent form of attack, though generally not of very serious proportions, occurs when the system is standing idle with perhaps a few inches of water lying stagnant against the tube-plate. Consequent upon the accumulation of marine debris and the decomposition of organic matter contained in it, a form of deposit attack may be set up leading to slight overall wastage with shallow pitting in these areas. An acute form of this trouble can arise, however, as experienced in certain designs of air-ejector condensers in which, owing to imperfect circulation, a stagnant zone may exist in the second pass. The lower naval brass tube-plate then undergoes rapid dezincification under the accumulated debris, accelerated by the presence of the cathodic gun-metal water box and cupro-nickel tubes, and also by the increased temperature due to the faulty circulation. Figs. 10 and 11 (Plate XXVI) show an air-ejector tube-plate which has been affected in this way.

It is usual to fit steel protector slabs, spaced about 2 ft. apart, on the inlet-end tube-plate of main condensers, and these provide useful galvanic protection to the tube-plate and ferrules when the water-boxes are of gun-metal. In addition, these protectors provide a continuous supply of iron corrosion products, some of which become incorporated in the protective film on condenser tubes and other parts, thereby materially improving their resistance to many forms of corrosive attack. In one case examined, zinc protector slabs had been fitted in error (in a new ship). These had rapidly disintegrated, leaving the brass tube-plate subjected to the full galvanic effects of the gun-metal condenser door, with the result that dezincification to a depth of up to a quarter of an inch had taken place over the whole plate.

(i) *Ferrules.*

Naval brass or Admiralty brass ferrules were commonly employed in pre-war years, but it soon became apparent in new designs involving higher water speeds and under the stress of war-time operation, that such ferrules were liable to rapid and severe wastage, as illustrated in Fig. 12 (Plate XXVII). Moreover, the deterioration tended to affect the tube ends, mainly because the corrosion products spreading from the ferrules interfered with the formation of protective films even on the most resistant condenser-tube alloys. An example is shown in Fig. 13 (Plate XXVII).

Occasionally, the lower rows of ferrules are more severely corroded as a result of recurring deposit attack caused by marine debris, as mentioned above. Entanglement of weed between tubes, as illustrated in Fig. 14 (Plate XXVIII), also accelerates deterioration, mainly by abrading the naturally-formed protective layers and exposing bare metal to impingement conditions. It has often been noted that ferrules immediately behind iron protector slabs are relatively un-attacked, whereas others elsewhere show substantial deterioration. Both galvanic protection and shielding from impingement may be involved in these instances.

Cupro-nickel ferrules (composition given in Table I) have now replaced brass ferrules in many important instances and have given excellent results; they will eventually become standardized in all H.M. ships. Aluminium brass ferrules, which have shown good service in merchant vessels, have also given equally satisfactory results in trials made in Service ships. Where naval brass or Admiralty brass ferrules have been fitted, coatings of high-duty protectives over the tube plate and ferrule ends provide moderate success, but fall short of the performance offered by cupro-nickel or aluminium brass ferrules.

(j) *Condenser Tubes.*

In days when 70 : 30 brass or Admiralty brass were practically the only condenser-tube materials, it could be fairly said that the corrosion of condenser tubes was the most serious marine corrosion problem. Failures were mainly due to impingement attack, often set up by partial obstruction, as shown in Fig. 15 (Plate XXVIII), or to dezincification as shown in Fig. 16 (Plate XXIX). The advent, between the wars, of newer alloys for condenser tubes, such as cupro-nickel, containing small amounts of iron and manganese, and aluminium brass, containing a small amount of arsenic (see Table I for compositions), has completely changed this, and tube troubles are indeed rare. Occasional failures in

aluminium brass are usually due to deposit attack, assisted by decomposing organic matter and by excessive local turbulence where a foreign body has lodged (see Fig. 17, Plate XXIX); or to mechanical abrasion of the protective film by a partly loose obstruction, such as a mussel, flapping in the water stream. As previously noted, cases of attack of tube ends in both alloys have been met following ferrule failures (Fig. 13, Plate XXVII).

Cupro-nickel tubes have been employed more extensively than aluminium brass in naval vessels, and they are possibly more reliable under the widely varying conditions in which such vessels must operate. Aluminium brass, which in future is to be used chiefly for distillers, may show to advantage where higher temperature conditions are encountered; on the other hand, cupro-nickel is less damaged by partial obstructions and deposits of decomposing organic matter. Both alloys are about equally resistant to impingement attack under the conditions of flow at present in use. Aluminium brass possesses better thermal conductivity properties than cupro-nickel, but the significance of this difference in a condenser is still being investigated.

#### (k) *Auxiliary Piping.*

Copper piping used for fire mains and for supplying salt water to auxiliary cooling systems may show wastage mainly by impingement attack, typical instances being given in Figs. 18 and 19 (Plate XXX). As in the case of other copper components, the attack is mainly associated with disturbances of flow, which in this case are particularly numerous because of the many bends, valves, and connections. To make matters worse, many of the pipes are too small and inaccessible for the application of protective compositions at regular intervals of time. Moreover, in some of the pipes the conditions may be almost stagnant for long periods, during which fouling organisms may develop to an astonishing degree and by their eventual decomposition liberate various harmful sulphur compounds into the water. During stagnant periods such compounds readily encourage pitting or larger areas of corrosion, which are then subjected to the scouring action of the turbulent water, thereby giving a particularly virulent attack.

Methods for jointing copper piping by brazing or welding merit careful thought from the corrosion point of view when the jointing alloy is exposed to sea-water. A case in point is illustrated in Fig. 20 (Plate XXXI), where two lengths of piping were brazed with 60:40 brass which crumbled away as a result of severe dezincification. Failure would have been delayed considerably by making the joints with a large overlap, so that the dezincification would have had to penetrate



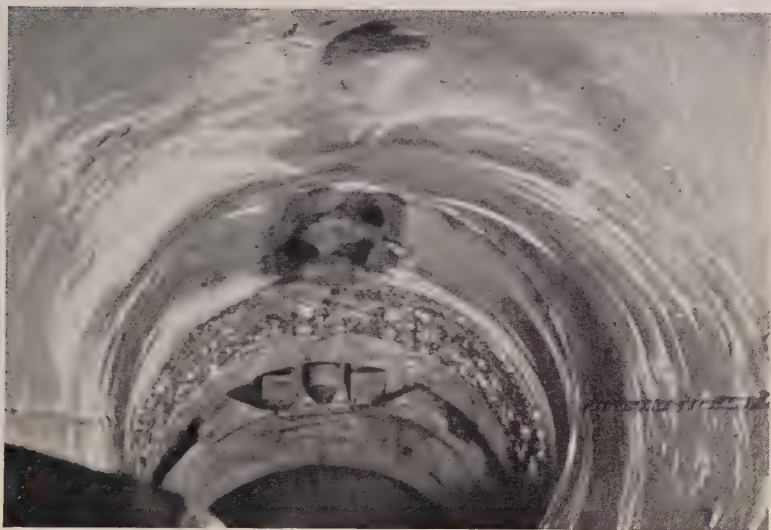


FIG. 3.—Steel Main Inlet Trunking (Shipbuilder's Tube), looking inward, showing rust streaks indicative of turbulence in the water stream.

Steel



Gun-Metal

FIG. 4.—Steel Main Inlet Trunking (Shipbuilder's Tube), adjacent to gun-metal valve housing, showing severe wastage to rivet heads.  $\times \frac{1}{2}$ .

[To face p. 318.





FIG. 5.—Naval Brass Valve Spindle from fire-main system, showing impingement attack.  $\times 1$ .



FIG. 6.—Fire-Pump Impeller Wheel (Phosphor Bronze Casting) with badly eroded vanes and faces showing extensive impingement attack.  $\times \frac{1}{2}$ .

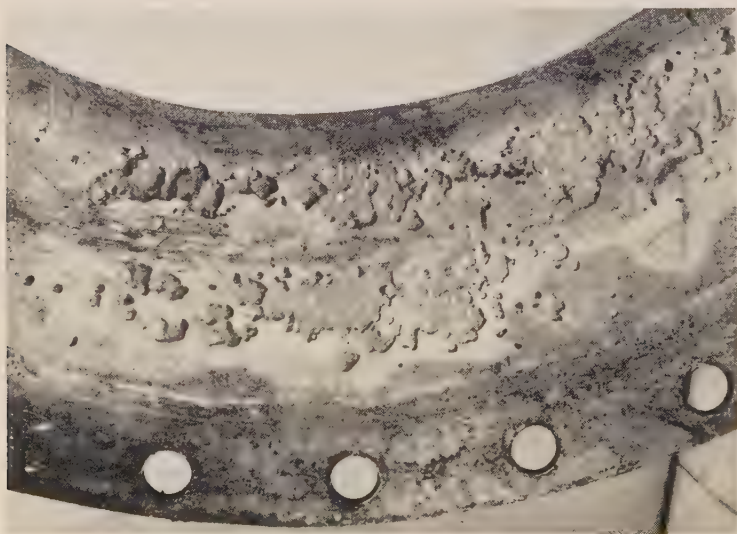


FIG. 7.—Portion of Copper Bellows Piece severely affected by impingement attack at radius of leading face.  $\times \frac{1}{2}$ .

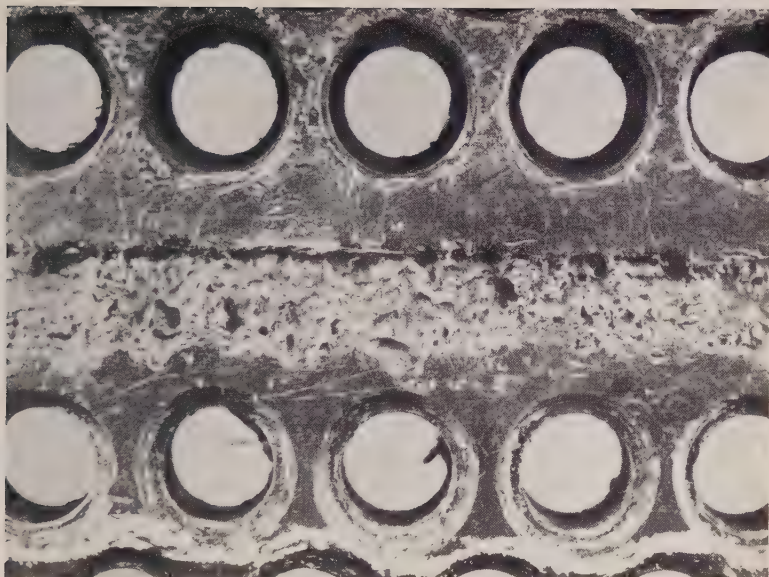


FIG. 8.—Impingement Attack of Turbo-Generator 2-Pass-Type Condenser-Tube Plate (Naval Brass) immediately in way of division plate under which water has passed in a turbulent manner.  $\times 1$ .

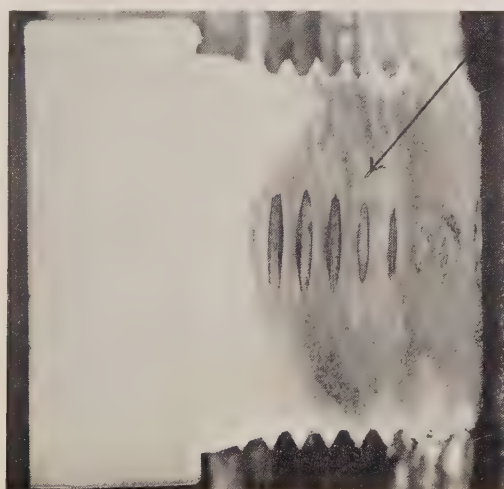


FIG. 9.—Cross-Section of Drain-Cooler Condenser-Tube Plate (Naval Brass) showing extensive dezincification.  $\times 2$ .

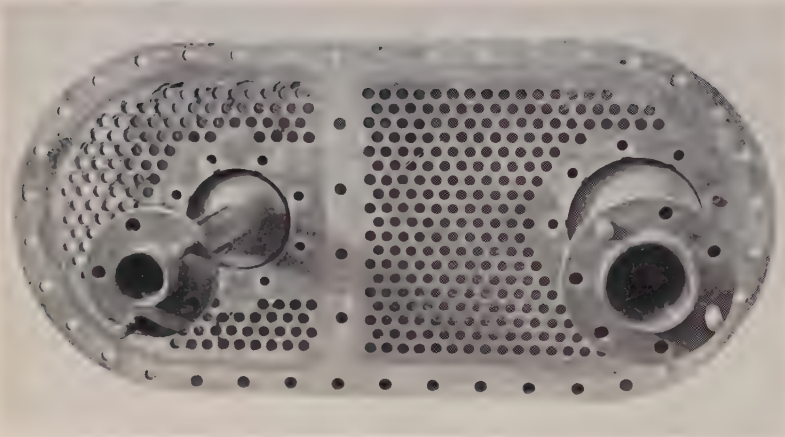


FIG. 10.—Lower Tube-Plate (Naval Brass) of Air Ejector, showing attack in second pass (left of photograph) which had taken place under an accumulation of debris resulting from faulty circulation.  $\times \frac{1}{11}$ .



FIG. 11.—Enlarged View of Corroded Portion of Tube-Plate shown in Fig. 10.  $\times 1$ .





FIG. 12.—Typical Example of Impingement Attack and Wastage of Admiralty Brass Ferrules in Condenser Tube-Plate.  $\times 1$ .

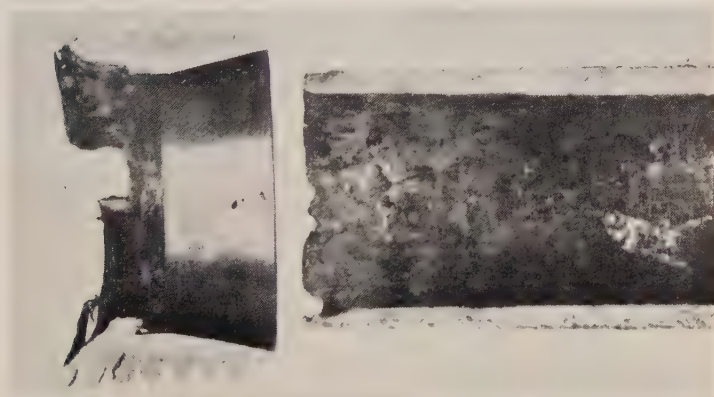


FIG. 13.—Section of Badly Corroded Admiralty Brass Ferrule, together with corresponding aluminium brass tube end which had been attacked in consequence. (Packing removed.)  $\times 2$ .

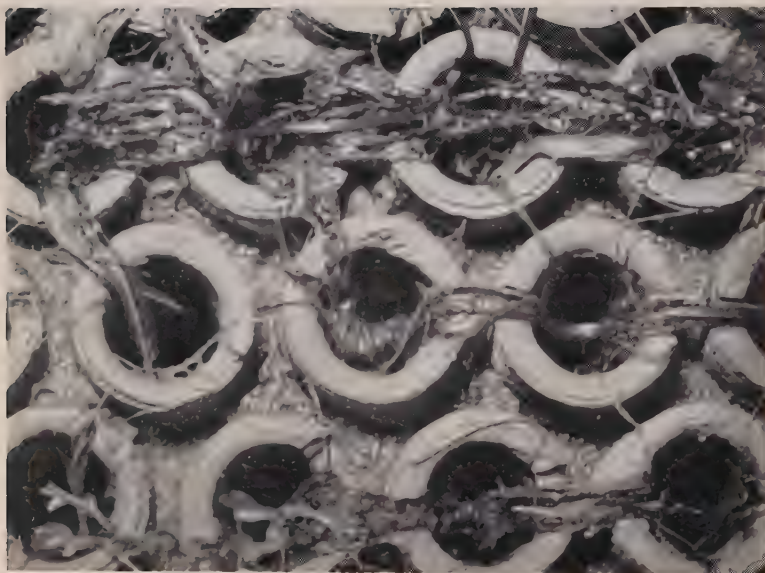


FIG. 14.—Section of Condenser-Tube Inlet Plate as opened up, showing weed entrapped between adjacent tube ends. The strands of weed flutter in the water stream and abrade the protective film on the ferrules.  $\times 1$ .



FIG. 15.—Perforation of an Admiralty Brass Condenser Tube. Attack of this nature is usually associated with deposits in the tube.  $\times 3$ .



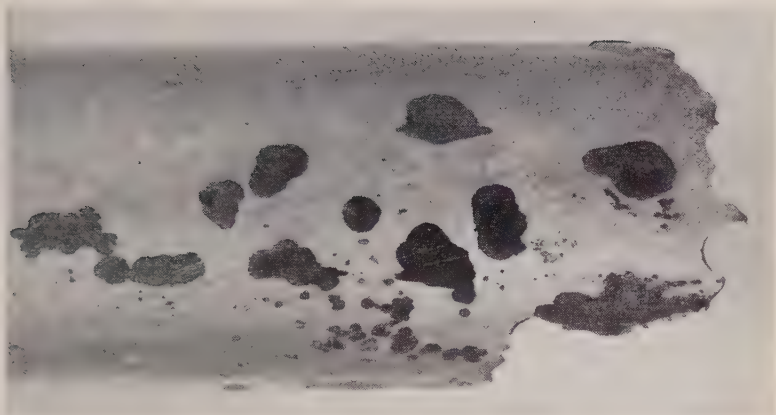


FIG. 16.—External Surfaces of 70:30 Brass Condenser Tube, showing severe dezincification which has penetrated the tube wall.  $\times 3$ .

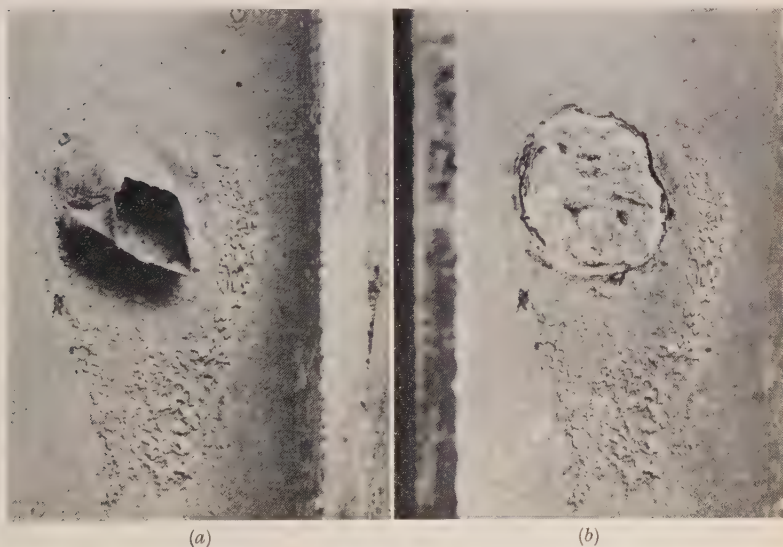
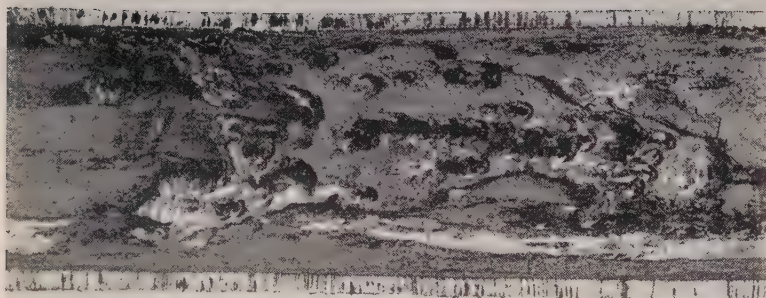


FIG. 17.—Deposit Attack in an Aluminium Brass Condenser Tube caused by a large barnacle. The decomposition products from the dead barnacle have attacked the protective film, whilst the shell itself has given rise to deposit attack and has also set up local turbulence in the water stream.  $\times 3$ .

(a) Dead barnacle in position.

(b) Barnacle removed showing attack beneath.



← Direction of water flow

FIG. 18.—Typical Impingement Attack in a Copper Pipe, showing characteristic “horse-shoe” form of pits.  $\times 1$ .

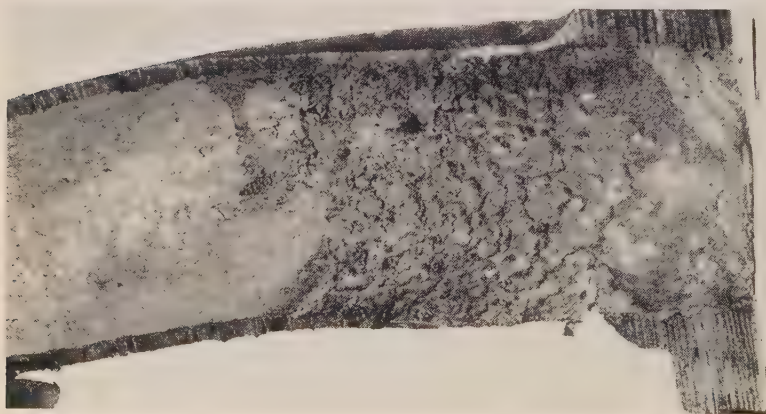
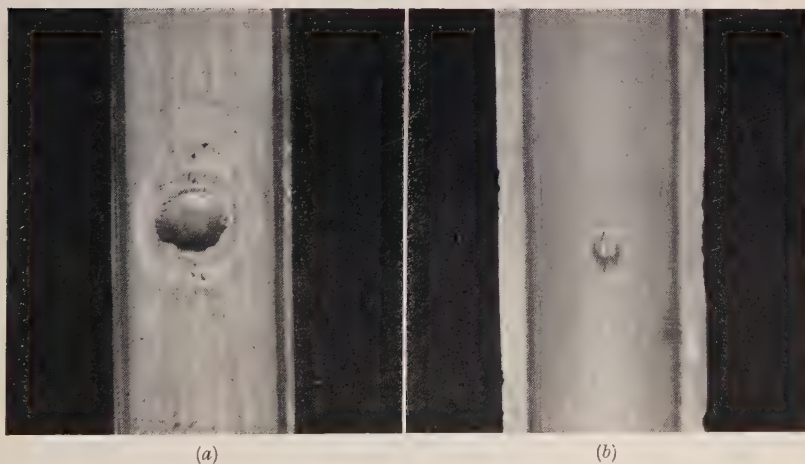


FIG. 19.—Copper Pipe, showing extensive wastage by impingement attack immediately adjacent to the flanged end, where the water flow has been more turbulent.  $\times 1$ .



FIG. 20.—Section of Flame-Welded Joint in a Copper Fire Main. The filler metal (60 : 40 brass) has suffered severe dezincification.  $\times 3$ .



FIGS. 21 (a) and (b).—Portions of Jet-Test Specimens, showing condition of surface opposite the jet after 28 days' test at a water speed of 17 ft./sec. with 3% entrained air.  $\times 2$ .

(a) Admiralty Brass, deeply pitted.

(b) 70 : 30 Cupro-Nickel containing manganese and iron, slightly pitted.



FIG. 22.—Sectioned Pipes, showing condition after carrying sea-water at 16 ft./sec. with 2% entrained air for 3 months in experimental apparatus.  $\times 1$ .

along a film of the brazing alloy before leakage or serious weakening of the joint occurred. The use of tin-free copper-zinc brazing alloys is, however, to be deprecated; the aim should be to secure a brazing alloy in the actual joint containing not less than 60% copper with 1% tin. Alternatively, silver solders to B.S. Specification 206, Grade B (typical composition: silver 50, cadmium 20, copper 15, zinc 15%) or Grade C (typical composition: silver 43, copper 37, zinc 20%) have given extremely satisfactory results.

The care with which the joints are made is also of importance. Many failures have occurred in piping close to joints as a result of adjacent ends of piping not being correctly butted and consequently setting up severe local turbulence.

Galvanized mild steel has been used in some ships for fire mains, but not with much success. The zinc coating is fairly rapidly removed in fast-moving sea-water, after which penetration of the piping soon occurs.

In certain high-class merchant-ship practice aluminium brass has been employed for piping, but up to the present it has not been used for this purpose in H.M. ships.

### III.—PRACTICAL ASPECTS AND REMEDIAL MEASURES.

It might be said immediately that there were two forthright solutions to the problem: either to use an alloy such as cupro-nickel for the whole system, or to modify the operating conditions and design to minimize the harmful forms of turbulence and aeration of the moving water so that less-resistant materials might be safely used.

The questions of availability of materials in time of war as well as cost enter strongly into the picture as regards the first of these, whilst modifications of operating conditions and design are matters for much more extensive thought and investigation. Fabrication problems are formidable enough with existing materials, and nearly all piping has to be bent to the intricacies of the layout. Many added complications are inseparable from the vital requirement that replacements or repairs must be possible immediately, wherever the ship happens to be.

Design aspects involve considerations of weight, space, and efficiency, as well as factors that are significant in reducing liability to attack. The latter can be listed conveniently for discussion as follows:

- (1) Relative corrosion-resistance of available materials.
- (2) Conditions of water movement and aeration.
- (3) Miscellaneous details of design which affect corrosion.



1. *Relative Corrosion-Resistance of Materials.*

The three most prominent types of corrosion deterioration encountered in sea-water cooling systems are impingement attack, pitting, and deposit attack, and a rough guide to the relative resistance of various materials is given in Table I.

TABLE I.—*Approximate Resistance of Materials to Impingement, Pitting, and Deposit Attack as Observed in Service.*

Material	Average Water Speed (ft./sec.) at which Risk of Impingement Attack Generally Arises under Practical Conditions	Resistance to Pitting.	Resistance to Deposit Attack
Tough-Pitch Copper	6	Moderate *	Moderate
Deoxidized Copper			
Arsenical Copper (0.3-0.5% As)	7	Moderate	Moderate
Admiralty Brass (70% Cu, 29% Zn, 1% Sn)			
Naval Brass (60% Cu, 39% Zn, 1% Sn)	10	Moderate	Moderate
Cupro-Nickel (30% Ni, 0.5-1.5% Mn, 0.4-1% Fe)	15	Good †	Good †‡
Aluminium Brass (76% Cu, 22% Zn, 2% Al, with 0.01-0.05% As)	15	Good/moderate §	Very good/moderate §
Cast Gun-Metal (B.S.S. 382 : 88% Cu, 10% Sn, 2% Zn; or B.S.S. 1023 : 86% Cu, 7% Sn, 5% Zn, 2% Pb)	20	Very good	Very good
Phosphor Bronze    (90% Cu, 10% Sn, 0.3% P)	Approaching 20	...	...
Rubber	Immune	Immune	Immune

\* Though attack may be considerable it tends to be widespread and shallow.

† Attack, if any, is usually widespread and shallow.

‡ Cupro-nickel is less affected by decaying organic matter than other materials.

§ Aluminium brass may be badly affected by decaying organic matter.

|| The authors have had but limited experience of this material in cooling systems.

The water speeds given in Table I in relation to liability to impingement attack refer to the ordinary conditions of turbulence and aeration associated with most of the present designs, and it is necessary to consider lower speeds if these conditions are intensified at any point or if there is an unfavourable combination of different metals in contact at points of impingement. Thus, for Admiralty brass under the least favourable conditions involving excessive aeration, impingement attack will occur at water speeds as low as 6 ft./sec. On the other hand, higher average speeds might be safe in some cases if special

precautions could be taken to eliminate rotation of the water stream as well as the local concentration of air bubbles, as discussed in the following Section. A further significant point is the relative "newness" of the system. If good natural protective films have formed upon the metal surfaces, e.g. during favourable conditions in early service, the resistance to impingement attack is substantially greater, and it has been found that troubles are usually more evident during the early history of a ship and tend to die away in the course of time for this reason. It would appear that differences in the rates of protective-film formation on the various materials can give rise to critical periods in which one reaches a highly cathodic stage to the detriment of an adjacent material on which the film is not yet fully protective. In due course the main cathodic areas, such as a gun-metal condenser door, tend to become passivated or even insulated by scale formation. A film of calcium carbonate from the sea-water—the characteristic "cathodic chalking"—is perhaps the most common, but films containing calcium sulphate and corrosion products such as iron rust from protector slabs are important.

## *2. Conditions of Water Movement and Aeration.*

### *(i) Water Speed.*

It must be emphasized that, in general, impingement attack is not caused directly by a high average water speed but by much higher local speeds often assisted by local concentration of entangled air bubbles. Both of these factors depend on various forms of additional turbulence superimposed on that normally associated with flow at the average speed. Unfortunately, in many cooling systems such excess turbulence is present, varying directly with the average speed, with which therefore impingement attack has an indirect connection. However, if by accident or design excess turbulence is small, both average speed and aeration can be higher without impingement attack taking place.

### *(ii) Rotation of the Water Stream.*

The most harmful forms of excess turbulence can arise if a rotational motion is imparted to the main water stream so that large vortices develop. These can produce impingement conditions of great severity by the high local speed brought about by the rapid rotation at the centre of the vortex and also by causing the small air bubbles present in the water to collect together and coalesce by centrifugal action. Such rotation is easily imparted by unsatisfactory design of the inlet system, as previously mentioned. Unsuitable scoops in the trunking or certain designs of bends can occasion similar rotation on a smaller scale. If

undisturbed, the rotational motion can pass through long lengths of pipe without causing trouble, but a sudden change of section, an abrupt bend, a partly-closed valve, or even a projecting gasket, can cause the rotation to break down and release the stored energy together with the air concentrated at the centre. This gives a local onset of excessive turbulence often resulting in severe impingement attack. Antiquated designs and water-boxes which cause rotation over the face of the tube-plate are no longer fitted to main condensers, but may still be found in a few auxiliary condensers.

(iii) *Eddies and Turbulence.*

Local disturbance of flow tends to destroy the stability of the boundary layer and give intermittent impingement or "scrubbing" action at certain areas, which may show corrosive effects, particularly if the metal is copper, and if air bubbles are also present. Smoothness of contour is all-important in this respect, as is shown by the undoubted success of bell-mouthed ferrules; and every effort should therefore be made to ensure that joints butt accurately and concentrically and that gaskets do not project. Scoops can also give rise to troubles of the same kind, and the best practical solution is to avoid their use as far as possible or at least to restrict their size. The large number of valves fitted in auxiliary piping presents a difficult problem, because many of them are used to control flow and are as a rule only partly open. The result is that piping on the discharge side of the valve may be subject to varying degrees of excess turbulence, which calls for a far more resistant material than copper. For the worst cases, the design of valves to incorporate some form of energy-absorbing grid on the downstream side might be worth considering. A scheme at present much used is to fit a replaceable length of thick steel pipe, and renew this as often as required. Division plates in two-pass condensers must be fitted properly, using a rubber joint to ensure a tight fit on to the tube-plate. Where the division plate is fitted horizontally, air-escape holes should be provided to avoid trapping air under the plate, but they should be so placed that the stream of water and air passing through them does not impinge on the tube-plate or ferrules.

(iv) *Tube Obstructions.*

Partial obstructions in tubes are another potent cause of excessive local impingement. The effect arises when the presence of an obstruction reduces the flow through a tube to a fraction of the normal amount, so that the tube friction becomes small and nearly the whole pressure drop is available to drive water past the obstruction. In a cooler with long tubes it is easily possible with a nominal water-speed of 10 ft./sec.

for a local speed of 30 ft./sec. to occur at an obstruction, with most unfavourable results. If the obstruction contains decomposing organic matter, even the most resistant tube alloys might well fail. In some ways the danger of partial obstructions is one of the chief factors which limits the use of higher water-speeds, so that the design of weed-grids or strainers is a matter worthy of considerable thought.

(v) *Entangled Air Bubbles.*

It is safe to assume that even under normal running, the water passing through a cooling system will always contain air bubbles from the turbulent layer on the ship's hull. The complete removal of this air would reduce but not eliminate impingement attack in the case of copper, which at the present level of water speeds would still be liable to attack at points of local impingement. Admiralty brass and naval brass would benefit to a much greater extent, laboratory tests indicating that in the complete absence of air bubbles the most violent impingement at about 12 ft./sec. has little effect on these materials. However, this approach to the problem is mainly of academic interest because of the very small quantity of air necessary to maintain impingement attack of these susceptible alloys. About 1% by volume is sufficient, and in practice much less can produce severe local attack if the bubbles are collected together by rotatory motions as previously described.

Although there is little hope of achieving complete absence of air bubbles, there is much to be gained by reducing the amount in every possible way and by ensuring that the remainder are kept uniformly disseminated in the water. In order to deal with large gulps of air which might enter the system, air-escape pipes are essential at the top of the water-boxes, particularly at the inlet end; it is sometimes useful to lead these over to the outlet end to ensure a continuous action and freedom from overflow, the pipe being made large enough to pass any object which can get through the weed-grid. It must be realized, however, that the proportion of air which separates out so that it can be carried away by the air-escape pipes is small compared with that which remains entangled in the water; the time available for a bubble to separate out instead of making its small contribution to the total of damage is only 2 or 3 sec. The location of sea-water inlets in the ship's hull can have a large effect on the entry of air bubbles, but other considerations usually decide where the inlets are actually placed. It is not uncommon to find auxiliary inlets immediately below the bilge keels, which is almost the worst possible location as regards entangled air bubbles. Even some main inlets are poorly placed in this respect.



### 3. *Details of Design Affecting Corrosion.*

#### (i) *Steel Protectors.*

The value of steel protectors fitted to the tube-plate is unquestioned; they should be as large as possible and spaced with considerable care to ensure a proper distribution of the protective action with a minimum disturbance of flow. To avoid eddies and turbulence over the tube-plates and ferrules, the protectors should be placed end-on to the water stream and as much use as possible should be made of parts of the tube-plate bare of tubes, e.g. in way of the steam lanes. To ensure good metallic contact, they should be secured with a heavy brass nut, washer, and bolt.

#### (ii) *Accessibility.*

Successful maintenance depends in great measure on making water-boxes accessible by means of well-sited manhole doors clear of a mass of adjacent pipe-work and fittings. A hand-hole door is essential at the lowest point to ensure complete drainage and to enable all sludge and foreign matter to be swilled away. Regular and systematic hosing down is essential to remove all debris effectively, particularly dead fish, weed, slime, and mud, which on decomposition can give rise to significant attack which is often most active when the condenser is not working.

### IV.—VALUE OF LABORATORY TESTS IN INDICATING SERVICE BEHAVIOUR.

It will be noted from the foregoing survey that most of the available metals and alloys are not regarded as perfect; the majority have their weaker points and tend to undergo some corrosion of one type or another, if the specific factors or conditions to which the material is sensitive make their appearance in the corrosive environment. This tendency has to be considered along with the better properties of each material. Of such properties, a natural protective film which only breaks down slowly even under the worst conditions and quickly forms again when these have passed is perhaps the most valuable in practice and is more likely of attainment than is complete resistance.

The elimination of the less satisfactory materials either by laboratory, semi-scale, or service trials is relatively simple. In the case of the more resistant materials, however, it is essential to realize that the specific factors which may cause their failure are so elusive that they may arise only in a small minority of cooling-water systems and may then be of intermittent occurrence depending on the precise sequence of operating conditions. For these reasons it is essential that service



trials should be carried out in an adequate number of systems, in order to ensure an acceptable probability that some of them will involve potentially damaging conditions.

### *1. Simulation of Service Conditions.*

As regards laboratory tests, present knowledge now permits their use not only for preliminary sorting but also for simulating a number of the rarer and more damaging types of corrosive attack. In this manner much time and effort can be saved before embarking upon expensive field trials. Unfortunately, some factors which may be responsible for practical corrosion troubles have not yet yielded to laboratory reproduction with certainty; the seasonal contamination of the water with various corrosion-accelerating agents liberated by decomposition of organic matter is a notable example.

One important reason for using laboratory tests is to save time in obtaining information on the behaviour of materials. Such information would inspire little confidence, however, if tests were speeded up by introducing conditions never encountered in practice, or even by undue exaggeration of any of the known factors responsible for corrosion troubles. The principle which has now been in use for a number of years is to take the maximum rate of attack observed in practice as a standard, and to arrange test conditions so that when using the same material this rate is approached, but not exceeded. It is also considered important that the essential factors introduced to obtain this rate of attack should be, so far as possible, the same as those which operate to produce the same type of corrosion in practice, and furthermore, that none of them should be exaggerated much beyond what would occur under the worst practical conditions. Fortunately, these limitations do not make the tests unduly slow, for although the maximum rates of attack in practice are extremely high, the conditions which produce them usually occur intermittently, whereas in the laboratory they can be maintained continuously if need be. For example, under the worst conditions of practice, i.e. when maximum attack occurs continuously, failures of 70 : 30 brass condenser tubes in 3 weeks or less have frequently been observed and hence this rate may be duplicated in laboratory tests without going beyond "legitimate conditions".

Some types of corrosion, of which dezincification is an example, usually progress slowly in practice because of their nature or because the factors which might cause acceleration rarely occur in the cooling systems concerned; no attempt is made to speed these up in laboratory tests for the evaluation of resistant materials for such systems. Usually it is sufficient to note the initiation of the corrosion and to estimate its

rate by comparison with known check specimens tested at the same time. Other types may be slow in causing failures and their importance may be under-estimated because the factors which stimulate them are of infrequent occurrence in a particular class of cooling system. The excessive attack that can occur if conditions change and if the stimulating factors are present for a large proportion of the time, was amply demonstrated in parts of the cooling systems of naval vessels during the recent war, as described in this paper. Obviously, it is essential to know the effect of such changes on any new material, and laboratory tests with this object can be arranged so that the changes occur as required and in the proper sequence to imitate what might occur in practice.

## 2. *Jet-Impingement Test.*

In a corrosion test intended to reproduce practical conditions in a cooling system, factors that must obviously be included are water movement and the presence of entangled air bubbles, both of which play an essential part in impingement attack, which is responsible for the majority of failures in cooling systems at the present time. One way of obtaining the required combination of factors is to use the jet-impingement test,<sup>2</sup> in which a jet of sea-water carrying the desired amount of air in the form of bubbles impinges against samples of materials to be tested. A water-speed at the jet of 17 ft./sec. with 3% by volume of entangled air is mostly used. This gives a rate of attack which represents fairly closely the local maxima that can occur in a cooling system with an average water speed of about 12 ft./sec., when there is a considerable amount of turbulence and a local concentration of air bubbles due to rotating motions of the water stream. The test is run continuously for 28 days, during which the samples can be examined and compared, the depth of penetration being measured at the end of the test. The present form of jet-test equipment used in the B.N.F.M.R.A. laboratories is illustrated in the paper by May and Stacpoole,<sup>3</sup> and typical specimens after test are shown in Fig. 21 (Plate XXXI).

The optimum conditions for producing maximum impingement attack at the jet are critical; the main essential is that the impingement must cause the bubbles to break up into many smaller bubbles at the point of impingement. This is not difficult to ensure if the mixing of the air and water takes place under conditions of velocity and turbulence considerably less than at the jet, so that the bubbles remain large enough to be broken further when they reach the jet. Another more troublesome requirement is that there must be little air present in very fine bubbles before impingement, as these have a cushioning effect greatly reducing the intensity of impingement attack. For this reason, it is

necessary in the test apparatus to remove the fine bubbles produced by impingement with a filter, so that they are not re-circulated. This action of fine bubbles, whilst noticeable with susceptible alloys such as 70 : 30 brass, becomes of increasing importance with resistant alloys which require the maximum intensity of impingement to test them properly.

When a test has been started, it is important that there should be no accidental stoppage or changes in the conditions, such as failure of the air-bubble supply, otherwise film formation may overtake film removal and impingement attack may stop. To ensure that mishaps of this kind do not remain undetected, at least one check specimen of a material of known susceptibility to such attack is included in each test. In the event of there being no attack of the check specimen in the first 7 days, it is still possible to obtain valuable information from the test if a scratch is made through the protective film on all the specimens at the area of maximum impingement, and this may be repeated at intervals if desired. Consistent healing of the scratch under these conditions indicates corrosion-resistance of a high order, unless, of course, the check specimen also heals, in which case it must be concluded that something has gone wrong with the test. For example, a partial obstruction which causes the bubbles to be broken up before they reach the jets can have this effect.

For this laboratory test to be of practical value, it is at present necessary to use natural sea-water, and because of its varying corrosive properties, this means that the test is not reproducible in the way usually demanded of a laboratory test. Thus, the results of any one particular test only represent practical conditions in cooling systems using that particular sea-water, so that further tests with other waters are needed before general conclusions can be drawn as to the value of an alloy. It should be remembered that variations in the corrosive properties of the water are a major factor in the practical behaviour of cooling systems, and it could hardly be expected that this could be represented by a single test with one sample of water. However, there is some prospect that before long it may be possible to shorten the testing by using a water in which any gradation of properties up to the worst that occur in practice can be assured by accurately controlled additions of the correct agents.

### *3. Pitting, Deposit Attack, and Galvanic Attack.*

Although originally intended as a test for impingement attack, the jet test has proved a useful method of detecting pitting properties in a water due to contaminating substances and in comparing the resistance of materials to such a water. If pitting is going to take place it becomes

evident in the course of a test running under the ordinary conditions. The pits may develop very close to the jet, as in the case of aluminium brass, or may be distributed over the surface under small blisters or localized at the points of contact with the holder, as with cupro-nickel, or occur on the back of the specimens remote from the jet, as with Monel metal and stainless steel. Pitting does not emerge very definitely with ordinary brasses or copper because these materials show impingement attack in any case, and this probably eliminates any small pits that start to develop.

Useful information on the resistance of materials to deposit attack is often obtained by examining samples from the jet test at places where they have been in contact with the ebonite holders. Alloys susceptible to deposit attack often exhibit deep corrosion at these areas. However, as a rule it is advisable to supplement this information by stagnant tests in which samples are suspended horizontally in beakers of sea-water, with a small heap of clean sand on the surface of the sample. It has been found an advantage to run these tests at about 40° C., which helps deposit attack to start within a reasonable time.

It will be appreciated that, as cooling systems are often made from a number of different materials, the testing of a new alloy is not complete until its behaviour when coupled with others under conditions of impingement and aeration has been checked. A good deal of information can be obtained from jet tests on coupled specimens, but it is often desirable to have more widespread and uniform impingement, and for this purpose the C.R.L.\* rotor test<sup>4</sup> has advantages. In this test, the samples connected together as required are all attached to the circumference of an ebonite rotor immersed in a tank of sea-water and rotated at a suitable speed.

Much useful information may be obtained by the use of small experimental condensers and by model circulating systems installed in the laboratory, and these have the advantage of providing an important link between the laboratory tests previously described and large-scale trials. The results obtained by an experimental apparatus using 1-in.-bore pipes are illustrated in Fig. 22 (Plate XXXII). The large quantities of sea-water required for this class of test unfortunately present a serious drawback, especially for inland laboratories, but in one of the Admiralty laboratories where this difficulty can be overcome, extended use is to be made of model circulating systems.

#### V.—DISCUSSION AND CONCLUSIONS.

Of the various factors concerned with corrosion in sea-water cooling systems, the authors have been particularly impressed by the signi-

\* Chemical Research Laboratory, Teddington.



ficance of excessive local turbulence, which may often result in damage and which is frequently caused by relatively minor design features. The use of so many different metals and alloys in the same system, especially in juxtaposition, is also a disturbing feature and probably accounts for the significantly inferior performance of systems during the early history of many ships, as a result of galvanic attack and its effect in promoting other forms of corrosion. It is fortunate that sea-water will deposit an insulating scale on the offending cathodic areas in due time and thus permit the formation of the natural protective film on the other metal surfaces. Stagnant periods when marine muds activated by decomposing organic matter settle on the metal surfaces and destroy the natural protective films, are yet another of the major problems.

The proper use of steel protectors merits particular mention, for they can do much to limit attack of immediately adjacent non-ferrous components. They can also play an important role by providing iron corrosion products which become incorporated in the protective film on condenser tubes and other parts, thereby improving resistance to attack. Protection for a limited time can be secured by suitable paint coatings, and there is an obvious need for much further research and development in this field. Sheets of natural rubber "tailored" and bonded to the metal are proving very durable, although such protective techniques are, of course, limited to the larger and more accessible parts of the system.

As regards materials for future installations, a major problem is the search for alternative and better alloys for sheet and piping which have to be shaped and bent to form. In this connection, a copper alloy containing small percentages of nickel and iron, which has been developed by the B.N.F.M.R.A., has given most promising results and is now going into service to replace copper for certain piping prone to impingement attack. Its superiority to copper under these conditions is illustrated in Fig. 22 (Plate XXXII). As regards condenser tubes, whilst two very acceptable alloys for present operating conditions are available in cupro-nickel and aluminium brass, future designs may call for much higher water speeds and even better alloys.

As in most fields of human endeavour, good housekeeping is a corollary of success, and it is vital that strict attention should be regularly paid to maintenance routines. This is particularly so when cooling systems are laid off for either long or brief periods; simple procedures of hosing away debris and mud must not be neglected.

Laboratory testing procedures have been shown to be of very great value in aiding the selection of suitable alloys and in forecasting the



probable effects of changes in design. These tests require very careful selection and control of conditions or misleading results may be obtained. Above all, it is essential to avoid either introducing conditions that are not encountered in practice or exaggerating any of the factors that are normally present.

In conclusion it may be stated that this investigation has demonstrated that the problems of corrosion and deterioration in sea-water cooling systems involve a large number of factors, and the basic patterns of behaviour can only be approached by careful and continued observation of service performance. In particular, it should be appreciated that naval practice demands high-powered units where flexibility and irregular operating intervals are the rule; damage and deterioration are all too often initiated during these periods of either high demand or idleness. Moreover, sea-water is far from being a homogeneous or uniform fluid and a ship's cooling system has to take all that comes its way, from air bubbles to the manifest unpredictables of marine muds, flora, and fauna, and all that sinks or floats therein.

It has been shown that questions of design and layout play an important part in the problem, whilst the immensely practical considerations of cost, workability, and fabrication strongly enter the picture in the selection of desirable materials. It is clear that both designer and operator need all the information the scientist can provide if corrosion troubles are to be reduced to a minimum, and to this end the authors have endeavoured to bring out the more salient features of design which may influence performance, to suggest minor modifications which will ensure greater durability, and to indicate the characteristics and limitations of the available materials.

#### ACKNOWLEDGEMENTS.

This paper is published with the approval of the Lords Commissioners of the Admiralty, but the responsibility for any statements of fact or opinions expressed rests solely with the authors.

The authors record their appreciation of the assistance afforded by their respective scientific colleagues and by their friends in industry. They finally wish to pay tribute to the Engineer Officers of the Royal Navy, who, in the stress of war, inspired and made possible much of the work, not only by affording facilities to see, discuss, philosophize, and experiment, but also by having faith in the scientists' prognostications.

#### REFERENCES.

1. G. D. Bengough and R. May, *J. Inst. Metals*, 1924, **32**, 82.
2. R. May, *ibid.*, 1928, **40**, 141.
3. R. May and R. W. de Vere Stacpoole, *ibid.*, 1950, **77**, 331.
4. F. Wormwell, T. J. Nurse, and H. C. K. Ison, *J. Iron Steel Inst.*, 1948, **160**, 247.

# THE JET-IMPINGEMENT APPARATUS FOR 1254 THE ASSESSMENT OF CORROSION BY MOVING SEA-WATER.\*

By R. MAY,† A.R.S.M., MEMBER, and R. W. DE VERE STACPOOLE.‡

(Communication from the British Non-Ferrous Metals Research Association.)

## SYNOPSIS.

Failure of condenser-tube and sea-water pipes occurs largely as a result of the corrosive-erosive action of impinging air bubbles carried in the water stream. A jet-impingement apparatus which reproduces the condition favourable for this type of attack is described. The construction of apparatus, running of tests, and assessment of results are discussed.

## I.—INTRODUCTION.

In 1924 Bengough and May<sup>1</sup> investigated the corrosive-erosive action of rapidly moving aerated sea-water upon condenser-tube materials, using various forms of apparatus, including one in which the essential conditions were produced by the impingement of jets of the water containing carefully controlled air bubbles. In 1928 May<sup>2</sup> described a more or less standardized type of jet-test apparatus, and showed how it could be used to evaluate condenser-tube materials without having to employ conditions of velocity or aeration beyond those known to be possible in existing condenser systems. Although the jet test is often described as an accelerated corrosion test, it differs from others in this category in that all possible precautions are taken to keep corrosion-accelerating factors at the same level as in practice, with the one exception that the desired conditions are maintained continuously, whereas in practice conditions of maximum severity are often separated by longer periods in which the conditions are comparatively mild.

Since the development of the original "Jet Test" the design has been improved and modified to keep pace with the changing conditions of practice. New units embodying these alterations have been built for use in the B.N.F.M.R.A. laboratory; the most recent is capable of

\* Manuscript received 27 March 1950. The work described in this paper was made available to members of the B.N.F.M.R.A. in a confidential technical memorandum issued in February 1950.

† Corrosion Adviser and Senior Investigator, British Non-Ferrous Metals Research Association, London.

‡ Research Assistant, British Non-Ferrous Metals Research Association, London.

producing water velocities up to three times that of the original and has twice the testing capacity.

## II.—FUNDAMENTAL CONSIDERATIONS.

### (a) *Impingement Attack.*

The well-known phenomenon of impingement attack, which can be of such serious consequence in condenser systems whether in ships or ashore, results from the corrosion-erosion effects of a turbulent, aerated water stream impinging against a metal surface; with a non-resistant metal it can occur at water velocities as low as about 6 ft./sec. Primarily it is associated with the continuous local breakdown and removal of protective films from the metal surface by impingement, the effect of which is greatly increased by the breaking at the surface of suitably-sized air bubbles entrained in the water. With the local removal of films and exposure of the basis metal conditions favourable to corrosion are initiated. Thus, a small area of a condenser tube is rendered anodic to adjacent areas and suffers rapid corrosive attack. While the mechanical impingement of air bubbles removes the corrosion products and ensures that the anodic areas remain active, the impinging aerated water has an equally important effect in causing intense depolarization of the film-covered cathodic areas closely adjacent to the anodes, so that ideal conditions for electrochemical corrosion are maintained.

### (b) *Simulation in the Laboratory.*

In order to assess the resistance of a material to this type of attack<sup>1</sup> it is necessary to subject it to the action of moving sea-water containing air bubbles of such a size that they will break on the metal surface under the conditions of impingement chosen. The quantity of such bubbles must be identical for each test specimen so treated, and the time required to produce a useful degree of attack must not be unduly long. Further discussion of the value of laboratory testing is given by Slater, Kenworthy, and May.<sup>3</sup>

## III.—APPARATUS.

### (a) *General Description.*

The above conditions are fulfilled by the apparatus shown on p. 165 of May's paper.<sup>2</sup> This consists of a centrifugal pump driven by a variable-speed motor (shunt- or compound-wound D.C.) for circulating water at the required speed. The pump lifts sea-water from a tank and delivers it at a suitable pressure to a manifold into which a con-

tinuously measured quantity of air is fed through an injector. The resulting air/water mixture then passes out through rubber tubes to a series of specimen-holders where the air/water mixture emerges through a standard jet to impinge against the specimen.

### (b) Design.

The objective in view is to produce controlled conditions of turbulence at the jet equivalent to the most severe found in practice. Any turbulence greater than that at the jet must be eliminated from the circulating system by maintaining lower water velocities in the rest of the apparatus than at the jet orifice. Undue turbulence in the apparatus produces bubbles of air smaller than those capable of producing impingement attack, either by premature breaking of the injected air bubbles or by bringing air out of solution in a fine state of division; such small bubbles, if present in sufficient quantity together with those of the optimum size, will "cushion" the impingement of the latter so that the amount of impingement attack is greatly reduced.

The size and shape of the jet must be carefully standardized in order to produce optimum and uniform conditions at each specimen. The jet orifice chosen is 2 mm. in dia., which is small enough to ensure that the effect of a velocity gradient across the jet is not pronounced; also the quantity of water delivered by such a jet is not unduly great, and this enables the size of the pumping system to be kept within reasonable limits (a  $\frac{1}{2}$  h.p. motor is sufficient for 24 jets of this size with water velocity 30 ft./sec.). It has been suggested<sup>2</sup> that the best shape for such a jet is probably that which most nearly approximates to a hole in a thin sheet, and the designs used are the nearest practicable approach to such a condition. The dimensions are: a 2-mm.-dia. orifice, 1 mm. in length, joining the  $\frac{3}{16}$ -in.-dia. supply passage by a 1-mm. radius (see Fig. 1).

When the jet is running under water the maximum disruption of air bubbles occurs at from 1 to 3 dia. from the jet. The specimens

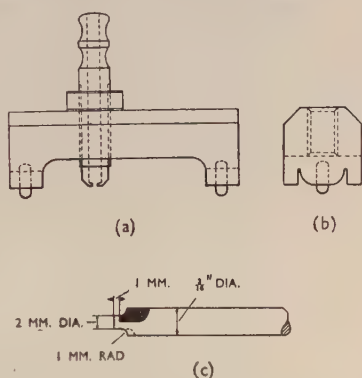


FIG. 1.—Jet and Specimen-Holder.

(a) Longitudinal cross-section.

(b) End view.

(c) Special reamer for shaping jet.



are therefore held 2 mm. from the jet orifice and, since they are normally about 2 mm. thick (14 S.W.G.), impingement attack can cause complete penetration of a specimen before distance from the orifice becomes a limiting factor.

These dimensions have been experimentally verified by using two jets, one having the dimensions given and the other having the same 2-mm. orifice, but being about 4 mm. long. By substituting a glass slide for a specimen and viewing the point of impingement through a low-power microscope with the aid of an intermittent light source, it was observed that in the case of the jet 4 mm. long the bubbles of air were too small and too numerous to be fully effective in producing impingement attack, and flowed from the periphery of the jet. With the jet 1 mm. long, however, continuous, violent disruption of air bubbles occurred across the full jet diameter. Confirmation has been obtained by actual tests using standard condenser-tube materials subjected to the action of the two types of jets described.

The correct functioning of a jet can be roughly ascertained by placing a finger beneath it, when the true turbulent action will produce a tingling sensation, and a continuous low crackle can also be heard from the breaking bubbles.

The jet is held normal to the surface of the specimen, although this condition would rarely be found in practice; experimental work<sup>1</sup> has shown that the angle of incidence of the jet has little effect on the degree of attack above angles of approximately 30°.

All parts in contact with the sea-water must necessarily be made of corrosion-resistant material. Therefore, the pump, manifold, specimen-holders, jets, and main piping are made of ebonite, and the container is of glazed porcelain.

#### IV.—DETAILED DESCRIPTION OF APPARATUS.

##### (a) *Specimen-Holder and Jet.*

Fig. 1 shows the holder at present in use; the jet screws through the body of the specimen-holder enabling its distance from the specimen to be varied and adjusted as required. The holder will accommodate specimens cut from either tube or sheet material.

The jet is made by machining ebonite rod to the required external dimensions and then, after centring in the lathe, first drilling the larger hole and then the 2-mm. jet orifice, both holes being drilled from the same end. The internal shape is hand-finished, using a special reamer (Fig. 1 (c)).



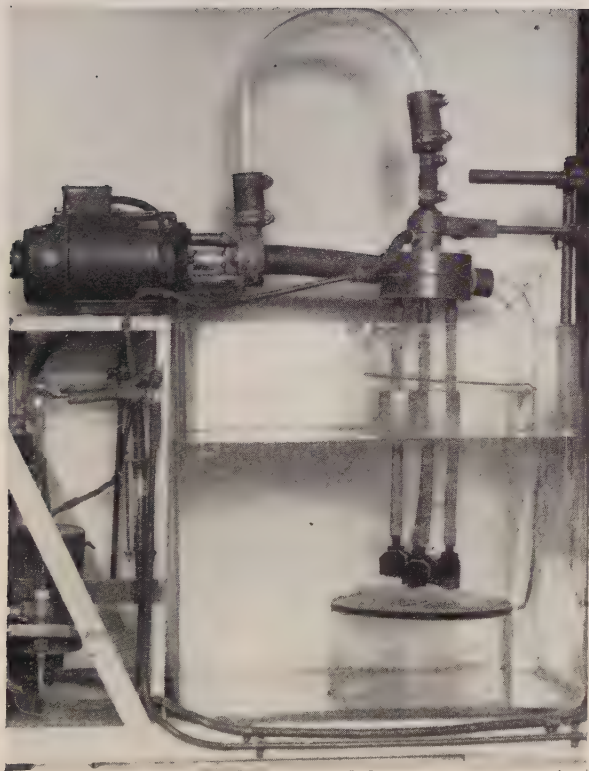


FIG. 6.—4-Unit Jet-Impingement Apparatus, showing mixing manifold with inlet from pump and outlets to jets at opposite sides. Separation of air is effected by means of the beaker.



FIG. 7.—24-Unit Jet-Impingement Apparatus (water velocity 15 ft./sec.). The mixing manifold is on the same side as the outlets to the jets. Water is delivered to the inlet by rubber tubing rising through a hollow ebonite pillar in the centre of the stoneware vessel.

(b) *Mixing Manifold.*

The original type of mixing manifold (see May's paper,<sup>2</sup> p. 165) has now been superseded by that shown in Fig. 2. This pattern is rather more simple in design than the original and consequently is easier to modify for different water velocities and testing capacity.

Water from the pump flows through the inlet tube (A) at a velocity of not more than 6 ft./sec. Air enters through (B), being delivered at a pressure of 20 lb./in.<sup>2</sup> through an injector nozzle (H) which just projects into an annular groove (C) machined at a point where the bore of the inlet tube is enlarged by  $\frac{1}{16}$  in. Thus the incoming water passes through a large-bore jet at an average velocity of 6 ft./sec. and entrains in itself a predetermined quantity of air. The mixture of air and water then flows into the main manifold (D) consisting of two circular discs of ebonite (E) and (F) clamped together by phosphor-bronze screws (G). One disc (E) has a flat machined surface, whilst the other (F) is recessed to a suitable depth, so that a constant water velocity is maintained from the centre to the point where the water outlets (J) are situated. The air/water mixture passes through these outlets, still at a velocity of 6 ft./sec., to the jets.

The outlets may be situated in either disc depending upon the construction of the apparatus—(see Figs. 6 and 7, Plates XXXIII and XXXIV). By ensuring uniform water velocity not greater than 6 ft./sec. between the point where air is injected and the jet orifices, undue breaking of the air bubbles is avoided while there is still sufficient turbulence to obtain :

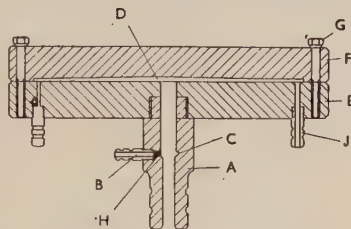


FIG. 2.—Mixing Manifold.  
(For key see text.)

- (i) Uniform mixing of air with the water flowing from the pump.
- (ii) Equal distribution of the air/water mixture to each of the jets.

If it is necessary to increase the working speed of a jet-impingement apparatus above its designed figure, the water passages in the mixing manifold must be suitably modified to avoid water velocities much greater than about 6 ft./sec., otherwise the conditions favouring impingement attack at the jet fall below the optimum.

*(c) Pump.*

Provided that continuous adequate water circulation is maintained, the pump need not be specially designed if a suitable commercial model can be obtained constructed of corrosion-resistant material which will introduce no contamination into the sea-water. Although large rubber-lined pumps are on the market it is difficult to obtain the small sizes (300 gal./hr.) required. It is the practice to

design and construct in the B.N.F.M.R.A. workshops the pumps for the apparatus now in use.

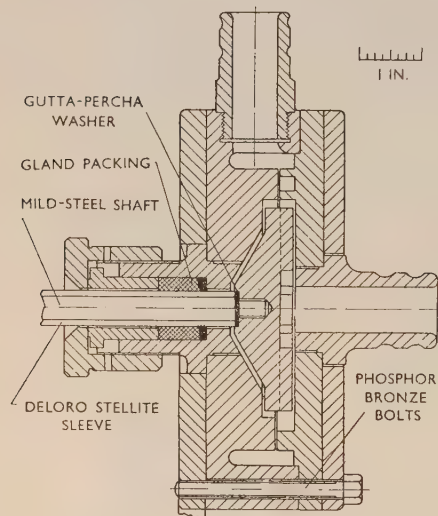


FIG. 3.—Centrifugal Pump.

The circulating pumps used are of the centrifugal radial-flow type, based upon standard design procedure. Owing, however, to the fact that they are constructed entirely of ebonite, certain compromises have to be made in the design of the impeller and guide vanes, to allow for the low strength of this material.

A sectional view of such a pump is shown in Fig. 3. The impellers are solid conical blocks of ebonite with slots cut in their bases to serve

as water passages, thus avoiding the thin vanes which would be normal for a metal impeller. In the case of low-speed pumps, i.e. those producing water velocities at the jets of 15 ft./sec. or under, it was found to be satisfactory to compromise between the inlet and outlet angles and have straight slots machined in the impeller, even though this resulted in some loss of efficiency. At jet velocities greater than 15 ft./sec., however, in order to increase the pumping efficiency and keep the rotational speed at a reasonable level, larger impellers with curved slots were introduced which maintained approximately correct inlet and outlet angles (see, for example, Fig. 4 (a), the volute passages in the stator being shown in Fig. 4 (b)).

The pump shaft is driven through a universal joint which supports it at the outer end and which also transmits the pump thrust to the

bearing. The shaft is thus free to centre itself in the water-lubricated packing, a Deloro Stellite sleeve on the shaft forming the rubbing surface. This somewhat unorthodox system was developed in the first instance to allow for the inaccuracies of ceramic sleeves which

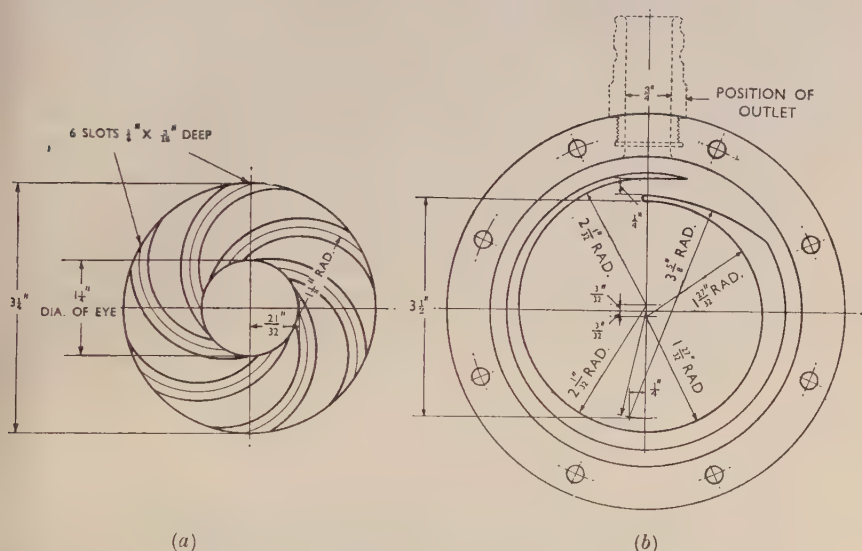


FIG. 4.—Details of Centrifugal Pump.

(a) Passages in rotor.

(b) Volute passages in stator.

were used originally, and has many advantages over a rigidly supported shaft in small high-speed pumps of this type. A clearance of about  $\frac{1}{64}$ – $\frac{1}{32}$  in. is provided between the face of the impeller and the body of the pump, and this is adjusted by large nuts on the bearing housing. The volute passages are of standard design, converting the impeller-outlet water velocity to a pressure of about 10–15 lb./in.<sup>2</sup>

#### (d) Air Supply.

The injected air is supplied at a pressure of 20 lb./in.<sup>2</sup> It must be filtered free from oil, and this is done by means of a 2-in.-dia. steel cylinder, 2½ ft. long, capped at both ends and fixed in a vertical position. Air is introduced half-way along its length and passes through a packing of cotton wool in the top half of the cylinder. A tap in the bottom cap facilitates occasional removal of the oil and water which collect in the sump. After filtration the air passes through a capillary-tube



flow-meter calibrated to measure the percentage of air introduced into the water stream. A needle-type control valve is placed between the gauge and mixing manifold, together with some convenient form of non-return valve which prevents water being pumped back into the air-supply line in the event of failure of the air supply.

If the apparatus is run from a high-pressure (50–60 lb./in.<sup>2</sup>) air supply reduced to the required 20 lb./in.<sup>2</sup>, the air delivered will often be too dry. This causes the injector nozzle in the mixing manifold to become blocked with salt by local evaporation of the sea-water, and the air should therefore be passed through a suitable humidifying tank to overcome this difficulty.

(e) *Separating Fine Air Bubbles before Re-Circulation.*

As already explained, if a large percentage of very fine bubbles is present (such as produce a milky appearance in the water) then the breaking of the larger injected air bubbles against the specimen surface is “cushioned”, and thus the severity of the test is considerably decreased.

These fine air bubbles are produced as a result of :

- (i) Undue turbulence in the water, particularly in the pump.
- (ii) Presence of undissolved air in the suction intake to the pump.
- (iii) Impingement of the air/water mixture on the specimen.

(i) can be eliminated by designing the apparatus to maintain suitable water velocities in the passages, as already mentioned; while (ii) is partly due to (iii), but can also be caused by insufficient depth of immersion of the suction pipe.

At low water speeds the fine bubbles can be removed by fitting a suitable filter consisting of a bag of medium-weave cloth, such as dairy filter cloth, which permits the passage of water but not of air. This system of filtration is satisfactory when the water in the container is completely circulated in not less than 4 min. Difficulties arise, however, at jet velocities of 30 ft./sec. or more, when this rate of circulation is exceeded (unless the size of the tank is increased), or when it is desired to test alloys in the presence of rusting iron, the corrosion products of which assume a gelatinous form in sea-water thus blocking the filter bag. A more satisfactory method for separating the air in these cases has been devised as follows :

The jets and specimen-holders are contained in a second vessel the outflow from which is arranged in the form of a shallow weir, thus enabling even fine air bubbles to rise to the surface of the water. Figs. 5 and 6 illustrate two forms of this device. Fig. 6 (Plate XXXIII)

is a photograph of a small apparatus (4-jet) in which the second container is a beaker with the air/water mixture flowing over the side. Fig. 5 shows diagrammatically the type of construction for a 24-unit high-speed apparatus. The specimens are contained in the upper vessel (A) which is connected to the lower vessel (B) by a wide-bore ebonite "weir" tube (C) fashioned in a U-shape. The upper end of this tube (C) is perforated, as shown, with a number of holes about  $\frac{5}{16}$  in. in dia. An ebonite tube (D) is situated at the mid-point of the U-bend and, by projecting above the water level, continuously bleeds air which tends to flow round the inside of the bend.

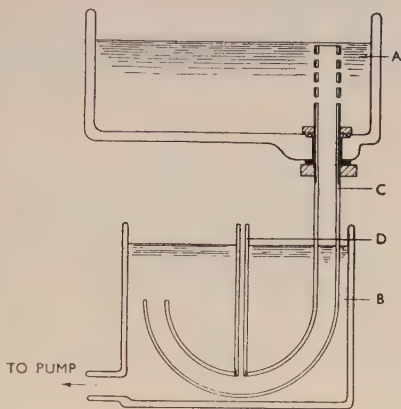


FIG. 5.—Method of Air Filtration for 24-Specimen High-Speed Apparatus. (Not to scale.).

#### (f) Cooling.

Early experiments showed that at elevated temperature, i.e. 30–50° C., films highly resistant to impingement attack were formed. Therefore to ensure that materials are tested under the correct conditions it is necessary to fit a cooling coil to the jet-impingement apparatus to keep the water temperature at 20° C. or less. Results obtained at all times of the year will then be related to normal practice. Lead pipe to British Standard No. 602 is suitable for this purpose; a double coil has been found sufficient with a slow rate of flow of cooling water.

### V.—ASSEMBLY.

In setting up the apparatus there are several points to which particular attention must be paid :

#### (a) Pumping System.

Before assembly all machined ebonite parts should be thoroughly degreased using a detergent (Teepol X) and cleared of all traces of swarf. All ebonite joints and ebonite-to-rubber joints must be made watertight. This can be done by using a sealing compound such as "Hermetite" for the manifold and its concomitant parts and for

the various parts of the pump. The tubing joining the pump to the manifold may be  $\frac{1}{8}$ -in.-wall rubber for low-speed apparatus, but must be canvas-insert hose for high speeds, all joints being made with jubilee clips. The tubes connecting the jets to the manifold may be ordinary rubber pressure tubing and do not need clips if the internal diameter of the tubes is the same as that of the manifold outlets.

(b) *Air Supply.*

All connections in the air lines are made of pressure tubing which is wired on to the piping—glass or metal—after wrapping with insulating tape as protection. The flow gauge is filled with medicinal paraffin diluted with a light paraffin oil so that it flows freely and coloured by a dyestuff such as Congo Red. In no circumstances should mercury be used, since any trace of contamination in the apparatus would render the tests useless.

#### VI.—STANDARDIZATION : INITIAL TEST.

Before any routine experiments can be undertaken the apparatus must be standardized for water velocity, percentage of air and uniformity of jets, and distribution of air to the jets.

(a) *Measurement of Water Velocity at Jet.*

This may be done with sufficient accuracy by measuring the volume of water delivered by each jet in a given time. This must be done with all jets connected and running normally.

The quantity of water delivered per minute by a jet is given by :

$$Q = 60 av$$

where

$Q$  = quantity of water in c.c.

$a$  = cross-sectional area of jet in cm.<sup>2</sup>

$v$  = velocity of water in cm./sec.

The standard figure for the normal 2-mm.-dia. jet working at 15 ft./sec. is 860 c.c./min. The motor-pump speed is adjusted until one jet gives approximately the correct delivery, then all the jet deliveries are measured. For a velocity of 15 ft./sec. jets delivering in the range 860 c.c./min.  $\pm$  20 c.c. are accepted, but those delivering amounts outside this range are reamed to 2 mm. dia., as shrinkage may have occurred after machining, or if necessary replaced. It is helpful to have a jet accurately made in stainless steel as a standard.

(b) *Measurement of Injected Air.*

The total quantity required for all the jets is calculated and measured by normal displacement methods at the end of the air line which connects to the manifold. A suitable-bore capillary must be chosen by trial and error for the flow-meter in order to obtain a reasonable difference in the indicator liquid level.

(c) *Jet Distance.*

With the type of jet and specimen-holder shown in Fig. 1 the standard distance between jet and specimen (2 mm.) is easily adjusted with the aid of a gauge consisting of a specimen cut from either a tube or sheet (depending on the type of specimens to be tested), with a rivet or stud fixed in the appropriate place so that it projects 2 mm. from the surface. The gauge is held on the specimen-holder and the jet screwed down until it touches the stud, when it is locked in position by the nut provided.

(d) *Check Run.*

After calibration a check run should be performed using as test material an alloy known to undergo impingement attack under the conditions being used (e.g. with water speed 15 ft./sec. and 3% injected air, 70:30 low-iron cupro-nickel). Measurement of the depth of penetration after test and low-power microscopical examination will show any non-uniformity as between jet and jet due to unequal distribution of air or differences in rate of delivery.

## VII.—PREPARATION FOR TEST.

(a) *Specimens.*

Material to be tested is cut into specimens measuring  $3\frac{1}{4} \times \frac{1}{2}$  in. Two holes are drilled in each specimen, with the aid of a jig, to fit the pegs on the holder. In the case of sheet material the surface is filed to remove all scale and then abraded on emery paper, finishing on 240x emery paper with A.R. benzene (thiophene-free) as a lubricant. Tube specimens usually need only sufficient emery abrasion to remove the surface film. A metallographic polish or "flowed layer" must be avoided as it produces very variable results.

After the final abrasion the specimens are degreased by immersion in three successive baths of A.R. acetone before putting on test.

*(b) Apparatus.*

After each run the apparatus must be cleaned of all corrosion products and bacterial contamination. It is first emptied of sea-water, filled with tap-water to which 50 c.c./40 l. of concentrated hydrochloric acid are added and run for 12 hr. The treatment is then repeated, using sodium hypochlorite in place of acid, followed by two washes with clean tap-water.

The container is then filled with sea-water strained through a cloth filter and run with the correct percentage of air for 24 hr. before putting the specimens on test.

*(c) Start of Test.*

The apparatus is switched off and the specimens are put on the holders and held in position by sulphur-free rubber bands which have been boiled in dilute acid and thoroughly washed.

## VIII.—ASSESSMENT OF RESULTS.

The testing of materials for resistance to sea-water corrosion can only be a matter of comparison, since there is no absolute criterion for assessing the behaviour of any material when subjected to impingement attack. Owing to variations in the corrosive characteristics of sea-waters<sup>4</sup> it is never possible to conduct experiments in which every factor is under control.

In order to assess the corrosion-resistance of an alloy by means of the Jet-Impingement Apparatus, the following procedure is recommended. In each set of specimens tested, two check specimens should be included of a material which is attacked under the impingement conditions employed and whose behaviour is well known. The alloy usually employed is 70 : 30 cupro-nickel with an iron content less than 0.05%. The necessity of using such a material must be stressed, since if a set of alloys is tested in a moderately contaminated water and no attack is produced, this may be (i) due to a fault in the apparatus, or (ii) because they are highly resistant. Whether (i) or (ii) is the cause can only be shown by means of a check alloy. Two specimens of each material are tested together and each set of materials tested at least three times (using fresh specimens) in sea-water samples each having different characteristics. It is helpful in the latter respect to use the Copper Corrosion Index test<sup>5</sup> for assessment of the sea-waters.

By the above procedure three or more sets of specimens, each



including the check alloy, will be obtained; from these may be deduced the behaviour of each alloy in different types of sea-water.

The individual assessment of each specimen is carried out by measurement of depth of attack and by low-power microscopical examination as follows:

(a) *Depth of Impingement Attack.*

This is measured using a millimetre micrometer fitted with a needle point on the moving arm. Four readings are taken on the unattacked metal around the point of impingement attack and the results averaged. The difference between this figure and the *lowest* reading obtained in the jet area gives the depth of penetration.

(b) *Low-Power ( $\times 30$ ) Microscopical Examination.*

The specimens are examined under a bench microscope—preferably binocular.

(1) First the jet area is examined to determine the degree of impingement attack, which may be highly localized, i.e. 2 mm. in dia. (the same as the jet orifice), or very widespread. Also with certain alloys tested in contaminated sea-waters pitting may occur in the jet area. This is sometimes difficult to detect if corrosion products which normally fill the pits have been swept away by the impinging jet. Impingement attack, however, produces a bright regular area of attacked metal, whilst pitting produces highly irregular attack, the basis metal being filmed and the bottom of the pits containing corrosion product.

(2) The film which has formed on the specimen is examined. It may be protective or non-protective, adherent or non-adherent, thin, thick, or scale-like and easily detached (by needle point or probe), and with or without general attack underneath. It may have blistered with pitting action proceeding under the blisters.

(3) Attack at shielded areas, i.e. parts of specimen in contact with the holder, should be noted as, although of doubtful practical significance, evidence of such attack can help in estimating the overall corrosion-resistance.

The above notes give only a brief outline of some of the types of attack which may be found; a complete description of the various degrees and types of attack found in the many alloys used in sea-water-carrying systems is beyond the scope of this paper. The results of tests can only be successfully interpreted in the light of experience gained from examination of many sets of specimens, as well as actual service failures.

## ACKNOWLEDGEMENTS.

The authors are indebted to the Director and Council of the British Non-Ferrous Metals Research Association for permission to publish this paper, and their thanks are due to the many colleagues who have contributed to the practical development of the test.

## REFERENCES.

1. G. D. Bengough and R. May, *J. Inst. Metals*, 1924, **32**, 81.
2. R. May, *ibid.*, 1928, **40**, 141.
3. I. G. Slater, L. Kenworthy, and R. May, *ibid.*, 1950, **77**, 309.
4. T. H. Rogers, *ibid.*, 1948-49, **75**, 19.
5. T. H. Rogers, *ibid.*, 1949-50, **76**, 597.

# PITTING CORROSION IN COPPER WATER 1255 PIPES CAUSED BY FILMS OF CARBON- ACEOUS MATERIAL PRODUCED DURING MANUFACTURE.\*

By HECTOR S. CAMPBELL,† B.Sc., A.R.C.S., A.R.I.C.

(Communication from the British Non-Ferrous Metals Research Association.)

## SYNOPSIS.

A number of cases of rapid failure of copper water pipes by pitting corrosion in one town has been investigated. All the samples of tube that had failed which were examined were found to contain films of carbonaceous material. Moreover, a close connection was found between the weight of carbon present as film and the presence or absence of pitting in sixteen copper water pipes taken from houses in the same town, where failure had not occurred. It was concluded that the pitting corrosion experienced in this area was due to carbonaceous films formed from drawing-lubricant residues during annealing in manufacture.

One hundred and twenty-one samples of copper water pipes, which had been submitted at various times to the British Non-Ferrous Metals Research Association for examination, after service in areas where pitting is known to occur, were re-examined and the quantity of carbon in each determined. The results indicated that at least 75% of failures of copper cold-water pipes by pitting were due to carbonaceous films formed during manufacture. The influence of such films upon pitting corrosion in hot-water pipes has not been established.

## 1. *Introduction.*

IN the course of research into the corrosion of copper water pipes carried on for some years by the British Non-Ferrous Metals Research Association, it has become apparent that pitting corrosion of copper occurs only in a few districts, and that, in those districts, only a relatively small number of pipes is affected. It is obvious that the incidence of pitting corrosion depends upon the character of the local supply water. The differences between waters in which pitting corrosion may occur and those in which it does not are difficult to discover, but recent unpublished work by the Association suggests that most supply waters contain traces of natural inhibitor which prevent pitting corrosion of copper, and that pitting occurs only in waters which do not contain inhibitor.

\* Manuscript received 28 March 1950. The work described in this paper was made available to members of the B.N.F.M.R.A. in a confidential research report issued in February 1950.

† Investigator, British Non-Ferrous Metals Research Association, London.

It is significant that even in districts where failures have been reported, many of the pipes installed show no tendency towards pitting corrosion but give a normal long service life. The present paper seeks to explain the vast differences in behaviour of apparently similar copper pipes in districts where the supply water does not contain inhibitor and in which pitting is therefore possible.

## *2. Rapid Failures of Copper Water Pipes.*

In February 1949 the Association was asked to investigate cases of rapid failure of copper cold-water pipes by pitting in a town in Lincolnshire. The local Borough Council was erecting on six sites a total of 350 prefabricated steel houses, with all the water services in copper, apart from galvanized-steel cold storage tanks. The first houses to be completed were occupied in January 1948 and by February 1949 twelve failures in copper cold-water pipes had occurred, all taking place within nine months and most within six months of installation.

### *(a) Presence of Black Film.*

The corrosion pits in the samples examined of pipes that had failed were larger and contained more cuprous chloride and less cuprous oxide than those commonly found in cold-water pipes where failure has occurred after periods of the order of ten years. There was a general scale of nodular calcium carbonate stained green with copper oxy-chlorides, and mounds of basic copper carbonate, oxy-chlorides, and calcium carbonate covered the pits. There was also some ferric oxide among the corrosion products and in the general scale. An unusual feature was a glossy black wrinkled film beneath the general carbonate scale. This film was in contact with the copper, but fine crystalline cuprous oxide had formed beneath it under some of the wrinkles and in the neighbourhood of the pits. Fig. 1 (Plate XXXV) is a photograph of part of one of the pipes showing the wrinkled film with nodules of calcium carbonate upon it.

Between February and May 1949 thirteen samples of copper pipe that had failed in prefabricated steel houses in the town in question were examined, and in every case a black wrinkled film was present. Up to this time 25 failures had taken place in 21 different houses, all in cold-water pipes of  $\frac{1}{2}$  or  $\frac{3}{4}$  in. dia. All the copper tube used in the houses was of phosphorus-deoxidized non-arsenical copper.

### *(b) Identification of Black Film as Carbon.*

The black wrinkled film, which was considered to be probably responsible for the rapid failure of the tubes, was thought at first to consist of copper oxide. In April 1949, however, a sample of copper

water pipe was received which had failed after ten months' service in a brick cottage in the same town, and which contained a black wrinkled film similar to those observed on the previous samples, but thicker and tending to peel away from the metal. The black film in this tube looked like carbon and could easily be detached for examination. It was insoluble in acids and alkalis; organic solvents extracted a certain amount of oil from the film but left it otherwise undissolved; on igniting on platinum foil, the film glowed and left only a minute quantity of ash—apparently consisting of ferric oxide. These observations supported the belief that the film on this pipe consisted essentially of carbon, and the nature of the film on the samples previously examined was therefore investigated.

Samples of the black wrinkled film, together with the carbonate scale and other corrosion products, were scraped from some of the earlier tubes and treated with concentrated hydrochloric acid. The black film remained undissolved and had the same properties as the thicker black film described above. A sample of the film separated in this way was subjected to X-ray analysis. After 3 hours' exposure a very weak pattern on a low-intensity background was obtained. The pattern was due to copper, with the strongest line of cuprous chloride, cuprous oxide, and graphite also present. From the low intensity of the background it was considered unlikely that more than 2% of copper was present, and probable that the bulk of the specimen consisted of an amorphous substance of very low X-ray absorption, such as carbon.

Further confirmation of the nature of the black film was obtained by measuring electrode potentials. The carbonate scale was carefully scraped off a sample of tube, leaving the black wrinkled film beneath intact. The back and edges of the specimen were painted with insulating varnish and the specimen was suspended in a dilute sodium chloride solution containing 40 p.p.m. of chloride. A sample of copper coated with graphite, and another of copper with a hot-formed oxide scale, were suspended in the same vessel, and the potentials of all three against a silver/silver-chloride electrode were recorded. After 3 hr. the potentials settled to steady values, those of the specimen with the black wrinkled film and the graphite-coated specimen being identical and 25 mV. more cathodic than that of the oxide-coated specimen.

#### *(c) Responsibility of Carbonaceous Films for Corrosion.*

The evidence described above was considered sufficient to establish that the black wrinkled film on the corroded pipes was composed principally of carbon, and it was next necessary to determine whether the film was responsible for the corrosion that had occurred. In co-



operation with the Copper Development Association, arrangements were made with the Borough Engineer concerned to have samples of pipe taken from the cold-water systems of sixteen prefabricated steel houses in the town where trouble was being experienced, and sent, filled with water, to the Association's laboratories for examination. The samples were 4-ft. lengths of  $\frac{3}{4}$ -in.-dia. pipe, taken, in each case, from the horizontal run between the storage tank and bathroom; up to May 1949 40% of the failures had occurred in this position. The houses concerned had been occupied for from 8 to 18 months with no report of failures. The samples were replaced by selected lengths of copper tube, eight of which were arsenical and eight non-arsenical, four of each grade being pickled and four being of good scale-free stock. It is hoped to have these back for examination after about 12 months' service.

Representative pieces of each pipe removed from service were photographed and all but two are reproduced in Fig. 2 (Plates XXXV and XXXVI), while the nature of attack is more fully described in Appendix I. The two pipes (OLN and OMP) that are not reproduced, owing to lack of space, were similar to that marked OLM and were unattacked. The weight of carbon in the scale on the photographed pieces was determined gravimetrically by the method given in Appendix II, and the tubes were examined metallographically for inclusions and differences of grain structure. Table I summarizes the results of these tests and gives the spectrographic analyses of the tubes.

In 6 of the 16 tubes examined there were large corrosion pits, similar to those in the tubes that had failed; in another there was a large number of small pits, and the remainder showed no pitting. The extent of attack in each case may be judged from the photographs in Fig. 2. Table I shows that all the tubes were of phosphorus-deoxidized non-arsenical copper, there being only small differences of composition which are clearly not related to the occurrence of pitting. Nor was pitting associated with grain-size or metallographic cleanliness of the metal. There was, however, a close connection between the weight of carbon in the samples and the presence or absence of pitting. Thus, excluding three tubes which had been protected by films of oily matter, there was a clear division between 6 tubes which had 0.4 mg. of carbon per dm.<sup>2</sup> or less and were not corroded, and 6 which had from 1.9 to 4.5 mg. of carbon per dm.<sup>2</sup>, and were pitted. The sixteenth tube was pitted although there was little carbon present. There was a thick, even, vitreous-looking scale of hot-formed cuprous oxide inside this tube, however, which may have caused the pitting in the absence of a carbonaceous film.

TABLE I.—*Examination of Samples of Copper Water Pipes Taken from Service.*

B.N.F. Mark	Service, months	Corrosion (Pitting) (see also Appendix I)	Metallographic Examination		Carbon in Scale, mg./dm. <sup>2</sup> ‡	Spectrographic Analysis										Other Elements ¶		
			Inclusions *	Grain-Size †		Sb, %	As, %	Bi, %	Fe, %	Pb, %	Mn, %	Ni, %	Sn, %					
OLM	18	Nil	1	X	0.2	0.0008	n.d.	n.d.	0.0002	0.001	n.d.	0.0003	0.0005	0.0001	0.0003	0.0005	0.0001% Co, 0.0004% Zn	...
OLN	18	Nil	4	Y	0.2	n.d.	0.003	0.0006	0.02	0.008	0.001	0.002	0.0003	0.0005	0.0001	0.002	0.0005	...
OLO	18	Nil	2	X	0.4	0.0002	n.d.	n.d.	0.0002	0.0005	n.d.	0.0003	0.0005	0.0001	0.0003	0.0005	...	
OLP	18	Large pits	5	Y	2.8	n.d.	0.005	0.0006	0.0005	0.002	0.001	0.001	0.001	0.002	0.003	0.003	0.0001	...
OLQ	15	Nil	2	Z	2.4 §	n.d.	0.005	0.0006	0.0002	0.004	n.d.	0.003	0.003	0.003	0.003	0.003	0.001	...
OLR	15	Large pits	3	Y	1.9	0.0002	0.002	0.0006	0.003	0.01	0.001	0.002	0.002	0.003	0.003	0.003	0.001	...
OLS	15	Large pits	3	Y	3.5	0.0008	n.d.	n.d.	0.0002	0.0005	n.d.	0.0003	0.0005	0.0005	0.003	0.003	0.0005	...
OLT	15	Large pits	2	X	0.4	n.d.	0.002	0.006	0.0002	0.002	0.001	0.003	0.002	0.002	0.003	0.003	0.001	...
OLU	14	Large pits	4	X	1.9	0.0005	0.005	0.0003	0.06	0.008	0.001	0.002	0.003	0.008	0.003	0.003	0.0001% Co	...
OMM	12	Many small pits	2	X	2.4	n.d.	0.002	0.001	0.0002	0.0003	n.d.	0.002	0.003	0.003	0.003	0.001	0.001	...
OMN	14	Nil	2	Y	0.2	0.0005	n.d.	0.001	0.0002	0.0003	n.d.	0.002	0.003	0.0003	0.003	0.0005	Trace only P	...
OMO	12	Nil	5	X	2.8 §	n.d.	0.01	0.0003	0.03	0.01	0.001	0.003	0.003	0.001	0.003	0.001	...	...
OMP	8	Nil	2	X	0	n.d.	0.003	0.0006	0.0002	0.0003	0.001	0.002	0.003	0.007	0.001	0.003	...	...
OMQ	8	Large pits	3	X	4.5	0.0005	0.01	0.0003	0.03	0.01	0.001	0.003	0.003	0.001	0.003	0.001	...	...
OMR	12	Nil	1	X	0	0.0002	0.002	0.001	0.0002	0.0003	0.001	0.002	0.003	0.001	0.002	0.001	...	...
OMS	12	Nil	1	X	1.5 §	0.0005	0.002	0.001	0.0002	0.001	0.001	0.002	0.003	0.001	0.002	0.001	...	...

## Notes :

\* 1 = clean, 2 = fairly clean, 3 = fairly dirty, 4 = dirty, 5 = very dirty. Inclusions in all cases probably slag.  
 † X = fine grain equi-axial, Y = slightly coarser equi-axial, Z = coarser elongated grain showing slight recrystallization. All microspecimens were axial sections through wall of tube.

‡ 1 dm.<sup>2</sup> = internal area of approx. 6½ in. of ½-in. nominal-bore tube.

§ Interior of tube protected by film of oil.

|| Thick coherent scale of crystalline cuprous oxide present.

¶ Tellurium, zinc, and cobalt not detected unless otherwise stated. Silver about 0.002–0.004% in all pipes. Phosphorus present in all cases. n.d. = not detected.

The evidence afforded by the 16 pipes taken from service and the 14 failures previously examined is considered to justify the conclusion that the pitting corrosion experienced in these tubes was due to carbonaceous films, or perhaps in a few cases to oxide scales, formed during manufacture.

### 3. *Mode of Formation of Carbonaceous Films.*

The source of carbonaceous films such as those described above is almost certainly residual drawing lubricant, which is decomposed during the annealing of the tubes before their final draw. The final draw is usually effected by hollow sinking, with no tool inside the tube, and carbonaceous films would be wrinkled but not stripped off by this process. Oily matter was always associated with the carbonaceous films in the tubes examined, as would be expected if the films were formed from drawing lubricant in the manner suggested; in three cases sufficient oil or grease had remained on the surface of the tube after annealing to prevent its being wetted by the water. In a few laboratory experiments carbonaceous films were produced on copper by annealing in a neutral atmosphere tubes coated with a thick layer of drawing lubricant, but these films were rather different in appearance from those found in practice. It is thought that experiments using a full-size furnace, followed by hollow sinking, would be necessary to produce the correct type of film.

### 4. *Action of Carbonaceous Films in Producing Pitting.*

The action of carbonaceous films in producing corrosion in copper tubes is probably twofold. The most obvious effect of the film is to provide a large and efficient cathodic surface which acts in conjunction with small anodic areas situated where cracks in the film expose the copper beneath. It has been mentioned above that a copper specimen with a carbonaceous film had a potential in dilute chloride solution equal to that of a graphite-coated specimen and 25 mV. more cathodic than copper covered with an oxide scale. Inspection of the pipes which had failed and which contained carbonaceous films indicated that the films had in fact acted as cathodes, for in each case the entire film bore a typical cathodic scale consisting of rounded nodules of calcium carbonate.

The second effect of the carbonaceous film is to act as an oxygen screen for the copper under the wrinkles. The film at these points contains small pores and cracks through which water can seep, but the rate at which oxygen can diffuse through to the copper surface from the bulk of the water is small. Protective cuprous oxide films are therefore not laid down on the metal and sparingly soluble cuprous

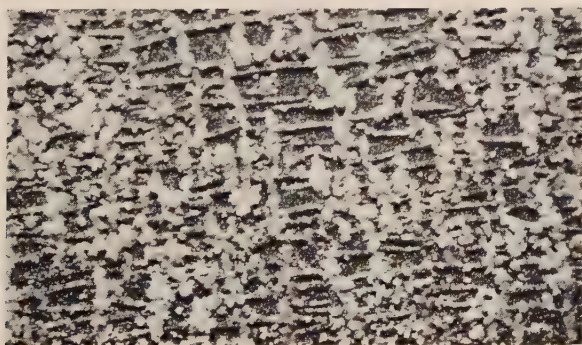


FIG. 1.—Wrinkled Carbonaceous Film under Nodular Carbonate Scale in a Copper Water Pipe.  $\times 25$ .

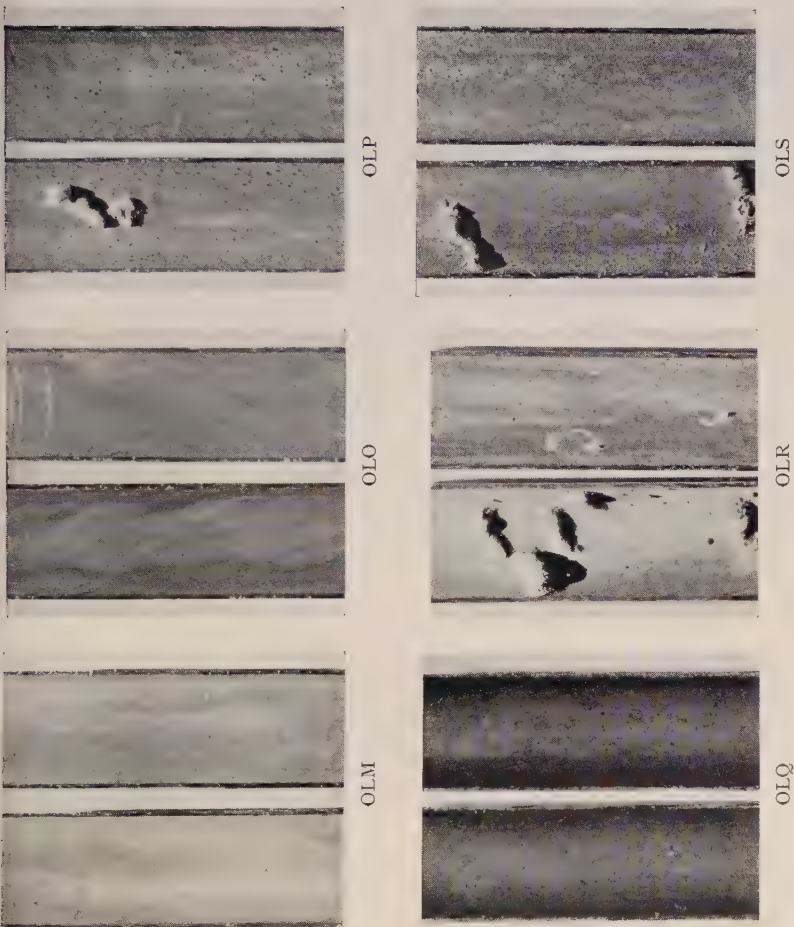


FIG. 2.—Copper Water Pipes taken from service, showing extent of corrosion attack (continued on Plate XXXVI).



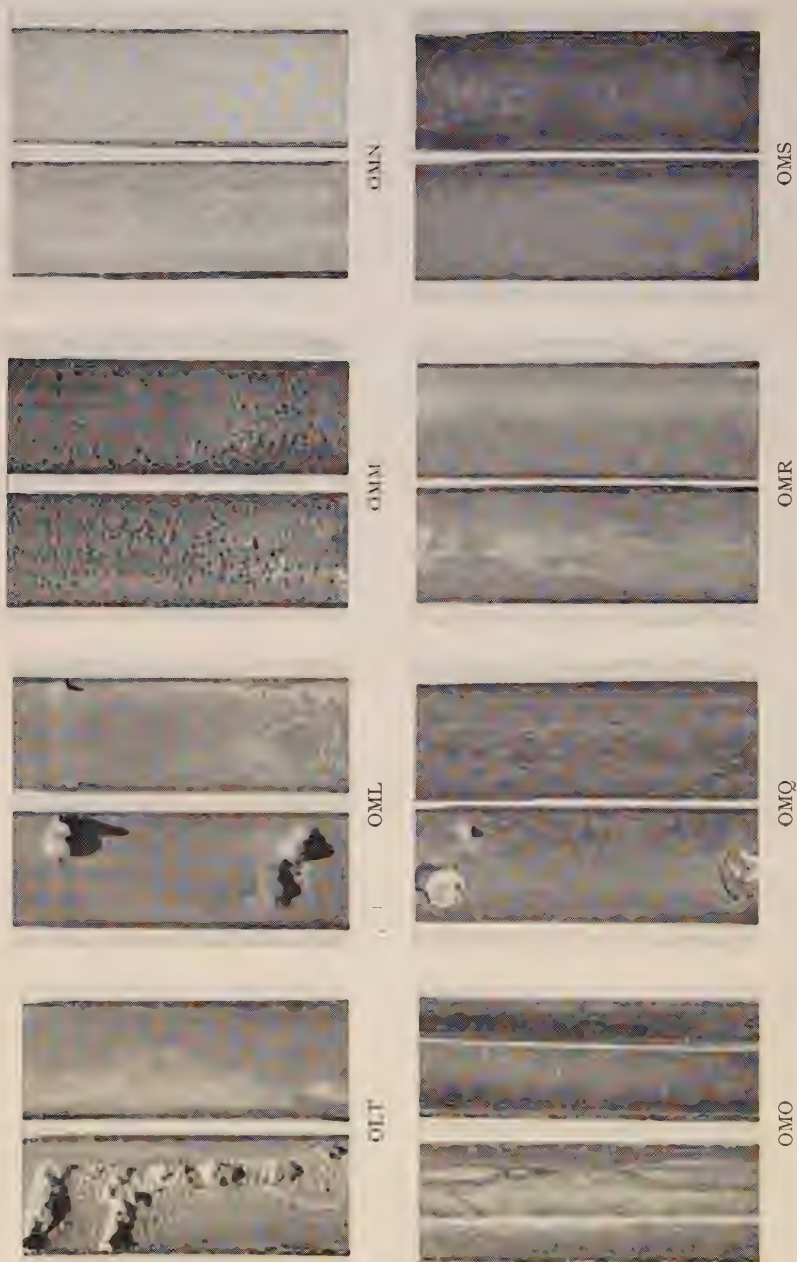


FIG. 2.—Copper Water Pipes taken from service, showing extent of corrosion attack (continued from Plate XXXV).



chloride—the primary product at these anodic areas—is not oxidized to soluble cupric salts as quickly as it is formed. This cuprous chloride acts as an anodic depolarizer by keeping the copper-ion concentration low at the copper surface. For pitting to proceed, the water in the tube must be one which does not contain sufficient natural inhibitor to stifle the anodic reaction. Many waters contain such an inhibitor and pitting would not be expected to take place in them even in the presence of carbon films.

The mechanism suggested above would produce a large number of small pits corresponding to the large number of wrinkles in the film, as in fact occurred in one of the tubes shown in Fig. 2 (Plate XXXVI) (OMM). In practice, however, the usual result is the formation of a small number of larger pits which, in horizontal tubes, are usually in the lower half. Some of the possible pits under wrinkles in a carbonaceous film are obviously likely to start off more quickly and more vigorously than others, e.g. those at less oily parts of the tube, or where the ratio of the size of the film wrinkle to the size of the pores in it is most favourable. Such pits, once established, would protect the nearby surface and prevent the formation of other pits in the vicinity. It is not obvious, however, why pits in a horizontal pipe are usually in the lower half. Possibly the carbonaceous film renders the tube particularly sensitive to deposit attack in some way, but no sign of deposits associated with the pits has been observed in most of the pipes examined. This aspect of the effect of carbonaceous films needs investigation.

#### *5. Other Cases of Pitting Caused by Carbonaceous Films.*

It has been shown that pitting corrosion in copper cold-water pipes in the town mentioned above was due to carbonaceous films. Six other cases of failure of copper cold-water pipes after less than 2 years' service have been reported to the Association. In five of these cases carbonaceous films of the type shown in Fig. 1 (Plate XXXV) were present in the corroded tubes, while a vitreous-looking scale of cuprous oxide was present in the remaining case.

Such rapid failure of copper water pipes is rare, the more usual period of service of pipes that fail being of the order of 10 years. Table II gives the results of the determination of carbon in the scale on samples of all copper water pipes which have been submitted to the Association after service in areas where pitting is known to occur. This Table includes the 16 tubes described in Table I, with the exception of the three oily tubes which had not been in actual contact with water.

The division into three classes representing very little carbon, an

TABLE II.—*Occurrence of Carbon in Copper Water Pipes.*

Weight of Carbon in Scale, mg./dm. <sup>2</sup>	No. of Cold-Water Pipes Examined		No. of Hot-Water Pipes Examined	
	Pitted	Unpitted	Pitted	Unpitted
Less than 1.0 . . .	7	12	3	1
1.0-1.9 . . .	10	1	8	0
More than 1.9 . . .	63	0	13	3

intermediate quantity of carbon, and an excessive quantity of carbon is arbitrary but affords valuable information.

Out of 80 pitted cold-water pipes, 63 had more than 1.9 mg./dm.<sup>2</sup> of carbon and only 7 had less than 1.0 mg.; while out of 13 cold-water pipes not pitted all but one had less than 1.0 mg. (this one having 1.0 mg.). Thus, at least three-quarters of the total number of failures of cold-water pipes examined can be attributed to carbonaceous films. Some, at least, of the remainder can be attributed to oxide scales produced during manufacture. Work on the question of oxide scales continues, but it seems probable that carbonaceous films and oxide scales are responsible, between them, for practically all the cases of failure of copper cold-water pipes which have been investigated.

No definite association between carbonaceous films and pitting in hot-water pipes has yet been established. The figures for hot pipes in Table II suggest some such association, but they must be viewed with caution. The method used for the determination of carbon does not distinguish between carbon in carbonaceous material produced during manufacture and carbon in organic matter deposited during service. In the case of cold-water pipes there is no doubt that the figures given in Table II closely represent weights of carbon produced during manufacture, since the carbon can be seen as a black flaky or powdery residue in the dilute acid which is used to separate the scale from the copper pipe. The deposits in hot pipes, however, usually contain silt and sparingly soluble manganese oxide, and it is not possible, in most cases, to see whether black carbon particles are included in the bulky residue which is obtained.

An interesting illustration of the influence which carbonaceous films have upon pitting corrosion has recently come to light. Several cases of failure by pitting have taken place during the last few years in a certain large building with its own deep-well supply. Failures have all been in horizontal water pipes and have been attributed to corrosion under deposits. A run of some 40 ft. of 1½-in.-dia. pipe perforated by corrosion in many places was recently replaced after about 10 years'

service, and portions of the old pipe have been examined. One section, about 4 ft. long, was completely free from corrosion at one end and had suffered slight pitting at the other; while a second piece, about 2 ft. long, although perforated along the entire length was more severely pitted at one end than at the other. The weights of carbon in the scales on samples from each end of each tube are given in Table III.

TABLE III.—*Corrosion and Carbonaceous Scale in Copper Water Pipes.*

Sample	Composition	Weight of Carbon in Scale, mg./dm. <sup>2</sup>	
		Uncorroded end. Slightly corroded end.	0·4 2·6
OOG/S	Phosphorus-deoxidized non-arsenical copper.		
OOG/C	Phosphorus-deoxidized arsenical copper.	Severely corroded end. Less severely corroded end.	8·0 21·5

These figures support the view that corrosion in a single pipe occurs only where sufficient carbonaceous film (say, not less than 2 mg./dm.<sup>2</sup>) is present; they also suggest that the severity of attack increases with increasing quantity of carbon present, only up to a point. When a tube contains very large quantities of carbon it is often present in lumps and may then be less effective than a smaller quantity present as a continuous film.

#### 6. *Types of Carbonaceous Film.*

The form in which carbon is present in a tube is clearly important, and two main types of carbonaceous film have been observed. The first type has already been described; it is continuous but wrinkled as shown in Fig. 1 (Plate XXXV) and is usually associated with rapid pitting leading to failure of the tube in less than 2 years—sometimes in as little as 2 months. This type of film comes away in sheets when undermined with nitric acid. The second type of carbonaceous film is more powdery and is believed to be discontinuous; it comes away as a powder when undermined with acid and has been found in tubes that have failed after about 10 years' service.

#### ACKNOWLEDGEMENT.

The author thanks the Director and Council of the British Non-Ferrous Metals Research Association for permission to publish this paper.

APPENDIX I.—*Details of Examination of Copper Water Pipes from Service.*

The 16 specimens of tube taken from service were inspected by looking down them, and a short length of each was selected, on which corrosion was typical of the whole pipe. The selected portions were then carefully sawn in two axially and photographed (see Fig. 2, Plates XXXV and XXXVI). They were examined under a low-power binocular microscope and appeared as follows :

*Tube OLM.*—An even scale of calcium carbonate covered the whole surface. There was a little green corrosion product along shallow score lines but no pitting. Ferric oxide was associated with the green corrosion product and was found at some other points on the surface. No carbonaceous scale was visible.

*Tube OLN.*—Similar to OLM. (Not reproduced.)

*Tube OLO.*—One half was similar to OLM but had a small area of slight local attack associated with an isolated patch of carbonaceous film. The other half had several patches of green corrosion product on the carbonate scale but no pitting.

*Tube OLP.*—A nodular scale of calcium carbonate, stained bright green with copper corrosion products, had been deposited on a carbonaceous film which covered the tube. There was one large pit and many very small ones, all with mounds of carbonate and chloride above and cuprous chloride and oxide within.

*Tube OLQ.*—A light brown oily film, with patches of carbon beneath, covered the tube. The metal had not been in contact with water at all, although the tube had been in service for 15 months. At one end of this tube the oily film had been partly carbonized.

*Tube OLR.*—A scale of calcium carbonate had been formed on top of a thin carbonaceous film and a coherent cuprous oxide scale. There were five large nodules, consisting of carbonate and chloride, covering pits containing cuprous chloride and oxide. There were considerable deposits of ferric oxide, but mostly away from the pits.

*Tube OLS.*—There was a heavy carbonaceous film with calcium carbonate deposited on it, and a considerable quantity of ferric oxide. Two large pits similar to those in other tubes were present.



- Tube OLT.*—A long run of deep pitting along the tube was covered by two mounds of corrosion product. A calcium carbonate scale with deposits of ferric oxide and, beneath it, a compact, vitreous-looking scale of cuprous oxide covered the rest of the tube. No carbonaceous film was observed.
- Tube OML.*—Two large pits and a few very small ones were present, and a carbonaceous film with calcium carbonate scale on top covered the rest of the tube.
- Tube OMM.*—A thin carbonaceous film covered the tube, with a calcium carbonate scale on top, and a large number of small pits were present.
- Tube OMN.*—A few minute spots of local corrosion were distributed over a general scale of calcium carbonate with no carbonaceous film visible.
- Tube OMO.*—A patchy carbon scale was covered by a film of oil. The oil had not completely prevented water reaching the tube as there was a little calcium carbonate scale stained green with copper corrosion product present, but it had obviously protected it considerably.
- Tube OMP.*—Similar to OLM. (Not reproduced.)
- Tube OMQ.*—A very heavy carbonaceous film showed a network of wrinkles instead of the usual wrinkles parallel to the axis of the tube. A nodular calcium carbonate scale had been deposited on the film and there were two large pits, one small one, and a number smaller still. The mounds of corrosion products above the large pits were cracked off when the sample was cut and do not appear in the photograph.
- Tube OMR.*—Similar to OLM.
- Tube OMS.*—Some carbon was present under a film of oil which had prevented the tube coming in contact with the water.

## APPENDIX II.—*Determination of Carbon in Scales on Copper Pipes.*

A short section of tube, in which the corrosion was typical of the whole sample, was selected and the outside machined, dry, or filed to remove dirt. The length required for carbon determination (3 in. of  $\frac{3}{4}$ -in.-bore tube or in the same ratio to the bore for other sizes) was carefully cut, without cracking off any of the scale, and placed in a 250-ml. beaker. 25% nitric acid was added to cover it and the beaker covered with a watch glass and left at room temperature until all the scale had dissolved or been detached from the surface of the tube.



Any carbonaceous film came away from the inside of the tube and remained suspended in the acid. As the outsides of the tubes had been cleaned by machining or filing no insoluble residue came from the outside.

The scale-free copper tube was lifted out of the acid with glass forceps and washed down into the beaker with distilled water. The contents of the beaker were heated almost to boiling and filtered on ignited asbestos in a Gooch crucible or through a silica crucible with a fused-in disc of sintered silica. The residue on the filter was washed with hot distilled water until free from copper and then with acetone until free from oil, which was present in considerable quantity in heavy carbon deposits.

The crucible containing the washed residue was dried in an oven at 110° C. and then transferred to a combustion furnace in which it was ignited at 800° C. in a current of carbon dioxide-free oxygen. The carbon dioxide produced was absorbed in a U tube containing soda-asbestos which was weighed before and after the combustion. The weight of carbon in mg./dm.<sup>2</sup> was calculated from the increase in weight of the absorption tube and the internal area of the sample.

# THE NEW CONTINUOUS BRASS MILL OF THE 1256 SCOVILL MANUFACTURING COMPANY, WATERBURY, CONN., U.S.A.\*

By J. J. HOBEN † and J. F. MULVEY.‡

## SYNOPSIS.

A detailed description is given of a recently installed continuous plant in an American brass mill. Metal melted in 1000-kW. Ajax-Scomet induction furnaces is cast into 2000-lb. slabs in a continuous-casting machine of the Junghans-Rossi type. The  $2\frac{1}{2}$ -in. thick slabs are broken down in a large two-high cold-rolling mill and, after annealing, the rolling is completed, with more annealing, in two four-high mills. Annealing is carried out in four continuous, roller-hearth, propane-fired furnaces, equipped with spray-cooling chambers. Spray pickling in acid bichromate solution is effected in two machines capable of handling brass strip 29 in. wide at rates up to 600 ft./min. Finally, the wide strip is slit on one of three machines, depending on its thickness, and inspected on both sides at a rate of 60–240 ft./min. Vacuum-handling equipment is extensively used in the plant.

## I.—INTRODUCTION.

THE Scovill Manufacturing Company is one of the oldest brass-producing companies in America, its business having been established in the Naugatuck Valley in Connecticut in 1802. Through the intervening years the manufacturing operations have changed with the demands of the times, so that from humble beginnings as a manufacturer of metal buttons, Scovill was, by the late 1820's, casting and rolling brass, and to-day possesses the most modernly equipped continuous brass mill in the world.

Some of the important factors in the early growth of the Scovill business can be traced to the skill of the British craftsmen who were first engaged in 1821. A Mr. James Croft of Birmingham was able to help, especially in problems of button gilding and finishing, and it was this gentleman who was instrumental in obtaining other Birmingham workmen for Scovill, including toolmakers and burnishers whose handling of the bloodstone gave a better finish to the brass buttons.

At about that same time, Scovill sent Israel Holmes to Birmingham to persuade Wm. Eaves to come to Waterbury. Eaves was a friend of Croft's and reputed to be a master of both toolmaking and die-sinking

\* Manuscript received 26 May 1950.

† Works Manager, Mills Division, Scovill Manufacturing Co., Waterbury, Conn., U.S.A.

‡ Assistant Works Manager, Mills Division, Scovill Manufacturing Co.

and "possessed a knowledge of how to keep a factory moving". Holmes also had the job of finding a caster and a brass roller. Legend has dramatized his visits to England. It is a treasured tradition that Birmingham manufacturers raised so many objections to Holmes's activities that he was forced to smuggle his "recruits" out of the country in barrels! At least, so goes the tale!

It did not take very many years, with the Company's rapid growth, for brass casters to gain a position of prestige. In fact, by the close of the century, the brass caster was "King Among Labour" in the Naugatuck Valley, hiring his own help, and setting his own terms. His casting methods were closely guarded secrets, passed on only from father to son, and any outsider who ventured into this field served a long and weary apprenticeship, without pay, considering it a privilege to be initiated into this very select profession.

The prestige of this group received a shattering blow when pit fires were replaced by oil furnaces, and the final blow came when their individual skills bowed to organized methods of production with standard procedures made possible by the introduction of electric furnaces and by 20th century demands which necessitated the huge present-day continuous-casting machines.

Scovill were pioneers in this latter development, and purchased the first continuous-casting machine to be brought to the United States. Improvements effected by its engineers resulted in the continuous-casting process reaching a degree of perfection which enabled a high output to be achieved to meet the demand for armaments for World War II.

With the end of the war and the final development of Scovill's continuous flat-metal casting machine—the only one in the country continuously casting rectangular-section brass bars weighing a ton or more each—Scovill, at a cost of over  $10\frac{1}{2}$  million dollars, have designed and brought into operation a single plant incorporating all the equipment for producing cold-rolled brass, from continuous casting of large bars to finished mill products packaged for delivery.

The continuous strip mill occupies an area 1400 ft. long by 140 ft. wide. This area is divided into two bays, one 80 ft. wide and the other 60 ft. wide. While material transportation is generally accomplished by means of conveyors, overhead cranes are necessary to service the equipment, i.e. change rolls, cutters, &c., and in a few instances transport material where backtracking could not be avoided. To satisfy these requirements, the 80-ft. bay is equipped with one 15-ton crane and three 10-ton cranes. The 60-ft. bay is equipped with two 10-ton cranes and one  $7\frac{1}{2}$ -ton crane. The small amount of material transfer which must

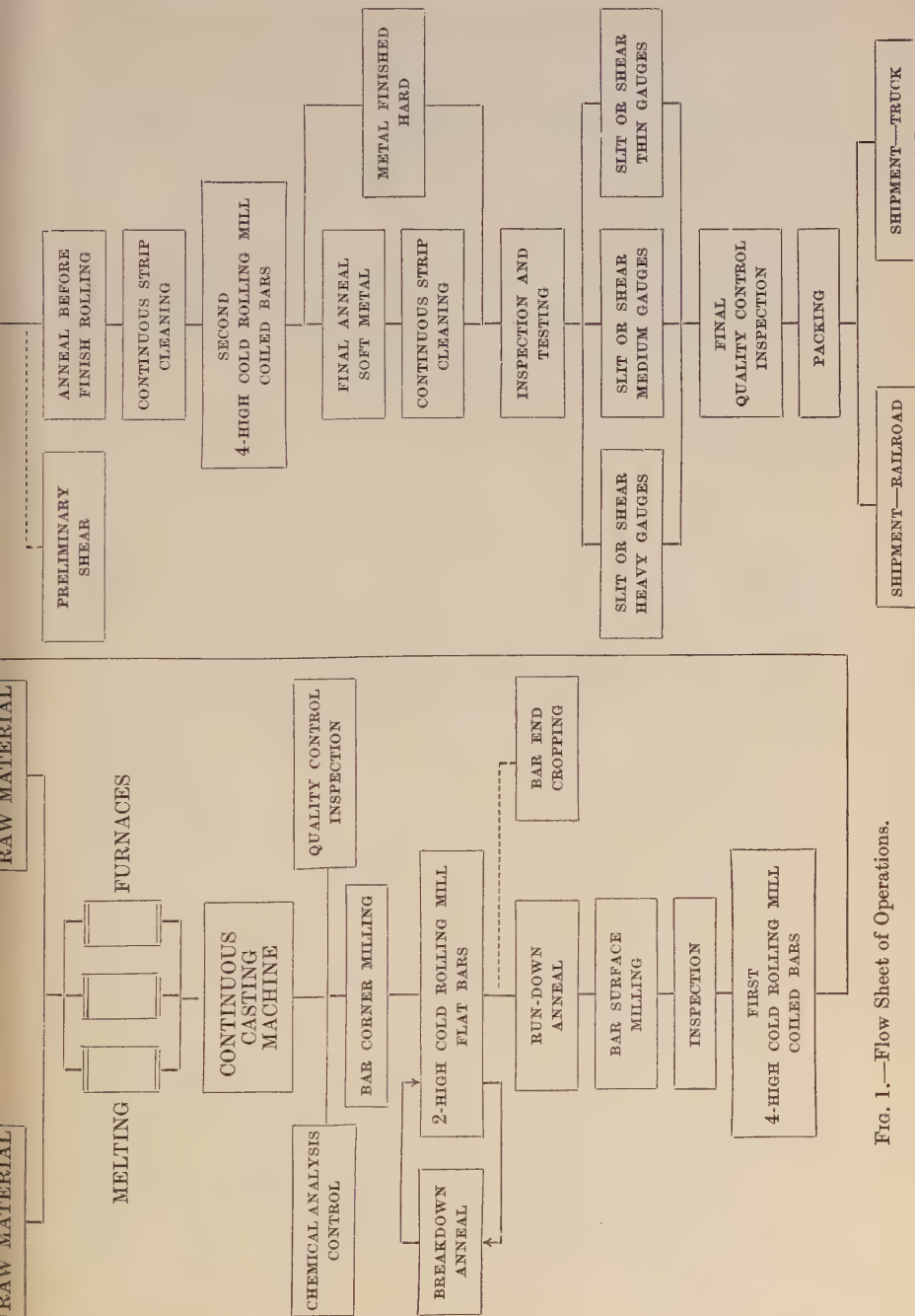


Fig. 1.—Flow Sheet of Operations.

take place between bays is accomplished by means of two transfer cars which are mounted on rails and are motor driven.

The general flow of work through the area starts at one end, where the breakdown mill is located, and flows through the successive operations as shown in Fig. 1, to the packing and shipping area at the opposite end, where it is loaded on to trucks or loaded into railroad cars which are located on a siding inside the building. This arrangement is regarded as affording the nearest practical approach to straight-line production of brass-mill products.

All this equipment is serviced by a machine room adjacent to the 80-ft. bay, which covers an area 385 by 77 ft. and which is equipped with the most modern equipment for grinding rolls, overhauling cutters, &c.

The 2000-lb. slabs that constitute the raw material of the strip mill are cast in an adjacent building which houses the Ajax-Scomet melting furnaces and the continuous-casting machine.

## II.—MELTING FURNACES.

The Junghans-Rossi continuous-casting machines require a large amount of molten metal per hour, and when the new continuous strip mill was projected the Scovill Company was confronted with the problem of melting the required amount of metal in the fastest, most economical manner. After a very careful investigation of all the problems involved, it was decided to install three Ajax-Scomet furnaces of 1000 kW. each. All three are now in operation, and have the following characteristics :

Rated capacity.—1000 kW. each.

Power supply.—575 V., 60 cycles, three phase, with all phases balanced.

Holding capacity.—Maximum 22,000 lb.

Melting rate.—About 10,000 lb. of brass per hr.

Temperature control.—Automatic with permanently inserted thermocouple and with high-low change of power.

Tilting.—Mechanical with an electric motor, speed reducer, and two chains.

The furnace, which is shown in Fig. 2, consists of a steel drum (*A*) provided with a refractory lining (*B*), made of prefired shapes and standard bricks. Three detachable inductor units (*C*, *D*, and *E*) are fastened to the lower part of the drum. In these inductor units, each rated at 333 kW., the heat is generated within the melting channels (*F*, *G*, *H*, and *K*), which form two secondary loops, interlaced with two primary coils (*L* and *M*). This circuit must be considered as the



secondary winding of a short-circuited transformer. A current of many thousands of ampères flows through these melting channels. The heat is dissipated to the cold metal charged into the drum by the well-known movement caused by electromagnetic forces, which is present in all low-frequency induction furnaces. The two primary windings (*L* and *M*) surround a closed transformer core (*N*).

As stated above, the inductor units (*C*, *D*, and *E*) can be detached and replaced without interrupting the operation of the furnace. In order to change one of the inductors it is necessary to turn the drum in the manner described below to bring the inductor which has to be changed above the molten metal line, to discharge the metal content of one of the inductors while keeping the metal hot with the two remaining inductors, to take the damaged inductor out and to replace it with a new one. Each inductor unit has two powerful blowers (*O*), suitable for cooling the transformer core (*N*) and the primary windings (*L* and *M*). These blowers, which are attached to each inductor, are powered with a 3-h.p. motor and have a capacity of 1250 cu. ft./min.

For rotating the drum, a motor-driven speed reducer (*P*) and two chains (*Q*) are used. On both ends of the drum two tyres (*R*), supported by pinions (*S*) are provided. With this device it is possible to turn the drum in all directions, so that any of the three inductors, including the lower one, can be emptied for the purpose of replacing them, as described above. The rotating device is also used to discharge metal from the drum over the pouring spout (*T*).

The furnaces described above are the largest ever made for the melting of brass. The efficiency, according to present experience, is higher than has been obtained with any other type of furnace, due to the fact that a great amount of power is concentrated in a small space. The metal-holding capacity of the furnace has been reduced as much as possible in order to facilitate the rapid change of alloys, which is a requirement of no little importance in a brass mill. Fig. 4 (Plate XXXVII) shows one of the furnaces from the pouring end, and makes clear how the pouring spout is located in such a way that molten metal can be discharged into 5000-lb. capacity ladles, which are used to transfer the metal to the Junghans-Rossi continuous-casting machine. The three furnaces are able to supply about 30,000 lb. of metal per hour to the continuous-casting machine (Fig. 5, Plate XXXVII).

The advantages obtained with the use of the three large furnaces and the automatic charging machine are as follows :

- (1) Greatest uniformity in chemical composition of castings.
- (2) Ease of operation, because the charging machine permits the dumping of large amounts of material containing virgin metal and

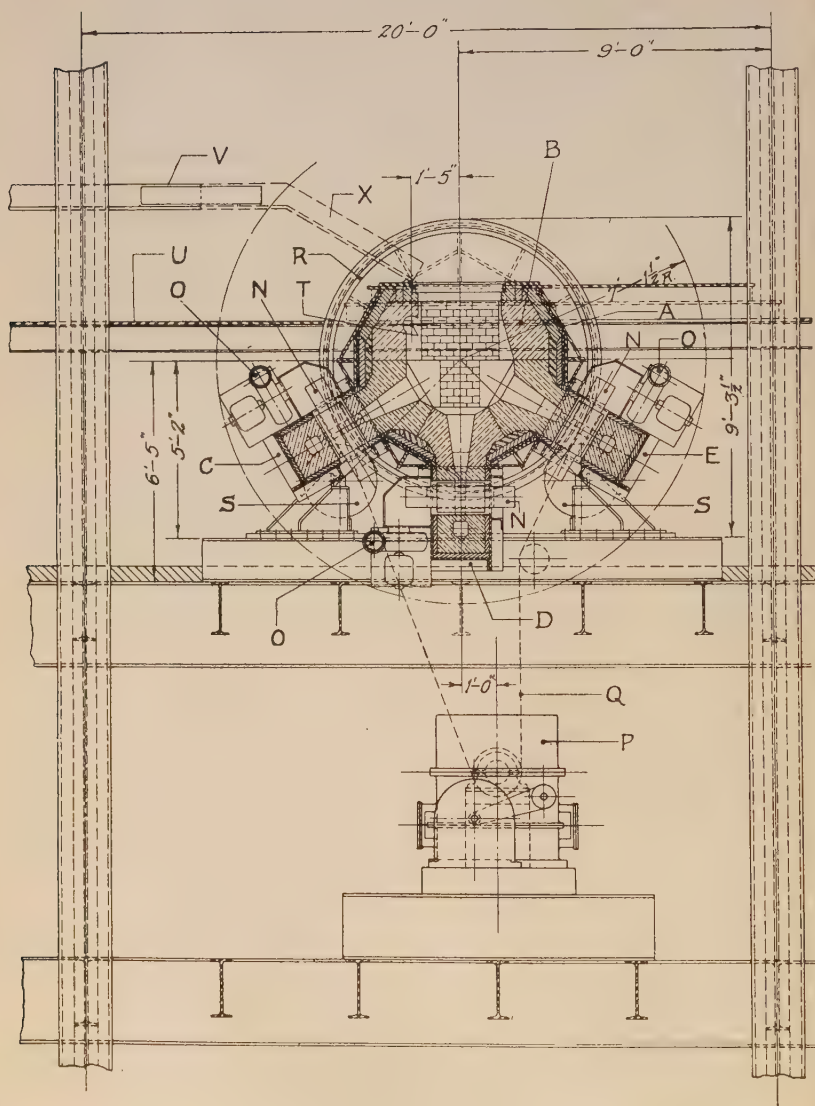
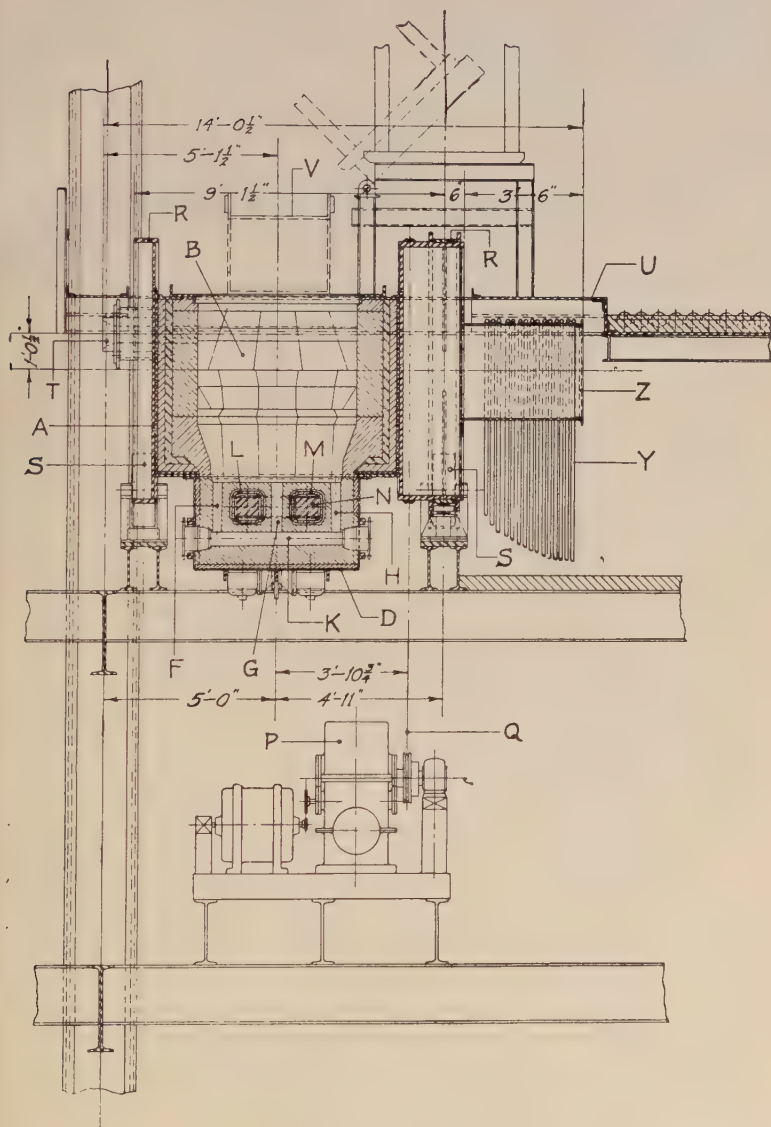


FIG. 2.—Ajax-Scomet 1000-k.w.



Induction Melting Furnace.

scrap of all kinds into the furnace. With this arrangement it is possible to operate two furnaces with two men.

(3) The automatic temperature control assures not only uniformity of temperature but also eliminates the necessity of manually switching the power supply on and off.

(4) The large amount of metal contained in the drum facilitates the rapid melting of the cold metal charged into the furnace through a large opening at the top.

(5) Because the melting channels are straight, they can be cleaned from time to time to prevent clogging or obstruction of the melting circuit.

(6) Although the furnace is provided with a high power rate, a change of alloy is not difficult because the furnace can be completely emptied.

### III.—CONTINUOUS CASTING.

The holding or reservoir furnace located at the top of the continuous-casting machine has a bath capacity of 9000 lb. and has a 120-kW. Ajax induction unit to maintain the molten metal at the desired temperature. The furnace is equipped with two diametrically opposite sets of spouts, each set consisting of a pouring downspout, a receiving funnel, and an emergency dump spout. When the machine is running, the furnace is tipped  $25^\circ$  and the front downspout is submerged in liquid metal in the mould. When not running, both downspouts are sticking out of the horizontal furnace at  $25^\circ$  from vertical and above the liquid metal line in the furnace. Fig. 3 shows the general lay-out of the continuous-casting unit for casting slabs of varying widths up to 29 in. by  $2\frac{1}{2}$  in. thickness.

The downspout is an inverted T with holes in the bottom for proper distribution in the mould. The pouring rate of the molten metal through the downspout is controlled by a needle valve through the top of the holding furnace. If trouble is encountered at pouring, the machine is tipped back to horizontal (stopping casting) and revolved  $180^\circ$  in order to bring into use the reserve downspout; the furnace is then tipped again, and the machine resumes casting. A water-cooled copper mould reciprocates up and down, the down stroke being synchronized with the discharge rate of the bar; the up stroke operates at three times that rate. The bar or slab is brought down from the mould at a constant speed by a set of withdrawing rolls, the speed of the rolls and the descent of the mould being synchronized.

The slabs are cut to the desired length—which, of course, may be standardized as required for rolling-mill operations—by a 30-in. saw

which is mounted on a platform capable of being elevated or lowered. During the sawing operation it is clamped to the bar and its speed of descent is synchronized with that of the bar. The sawing time required for a  $25 \times 2\frac{1}{2}$ -in. bar of non-leaded material is approximately 35 sec. (Fig. 9, Plate XL).

### *Sequence of Operations.*

A 5000-lb. unit charge of metal is assembled on the first floor, hoisted to the fourth or casting shop floor, and dumped into a vibrating hopper that automatically feeds it into one of the Ajax-Scomet melting furnaces at a controlled speed and at predetermined intervals.

When ready to pour, the metal is transferred via  $2\frac{1}{2}$ -ton ladles to the holding furnace feeding the casting machine, as shown in Fig. 5 (Plate XXXVII). The metal is poured from the bottom of the holding furnace through a chrome-iron distributor into the mould in a continuous stream which maintains the pool at a constant level at all times. A constant gas flame at the top of the mould prevents excessive oxidation of the surface of this pool of molten metal. As the metal moves down through the mould, which is 25 in. long, it freezes and emerges as a solid bar, goes through the withdrawing rolls, and is cut to length by the saw. The bars or slabs are inspected, tested, and sent to the continuous strip mill for cold rolling (Fig. 6, Plate XXXVIII).

## IV.—ROLLING MILL EQUIPMENT AND OPERATION.

### *1. Breakdown Mill.*

The breakdown operations on the bars are performed on a two-high cold mill, built by Farrel-Birmingham Co., Inc., of Ansonia, Conn., which is believed to be the largest manufactured so far for the non-ferrous industry (Fig. 8, Plate XXXIX). The two-high mill has roll sizes of  $30 \times 36$  in. and with the unique handling equipment, also built by Farrel-Birmingham, the production efficiency is high.

Completely mechanized handling makes it possible for two operators to manipulate the bar on both sides of the mill and also regulate the roll speed and gauge, all from two control desks, one placed on each side of the mill on opposite sides of the roller tables. The system employs the use of vacuum pilers and unpilers travelling over the entry, delivery, and transfer tables. These units each consist of a series of suction discs mounted on a structural supporting member, which is operated hydraulically. By means of these suction devices, the ton-weight pieces are easily moved from point to point. On the feed side, the routine processing procedure is to lift the bars from the transfer table to the



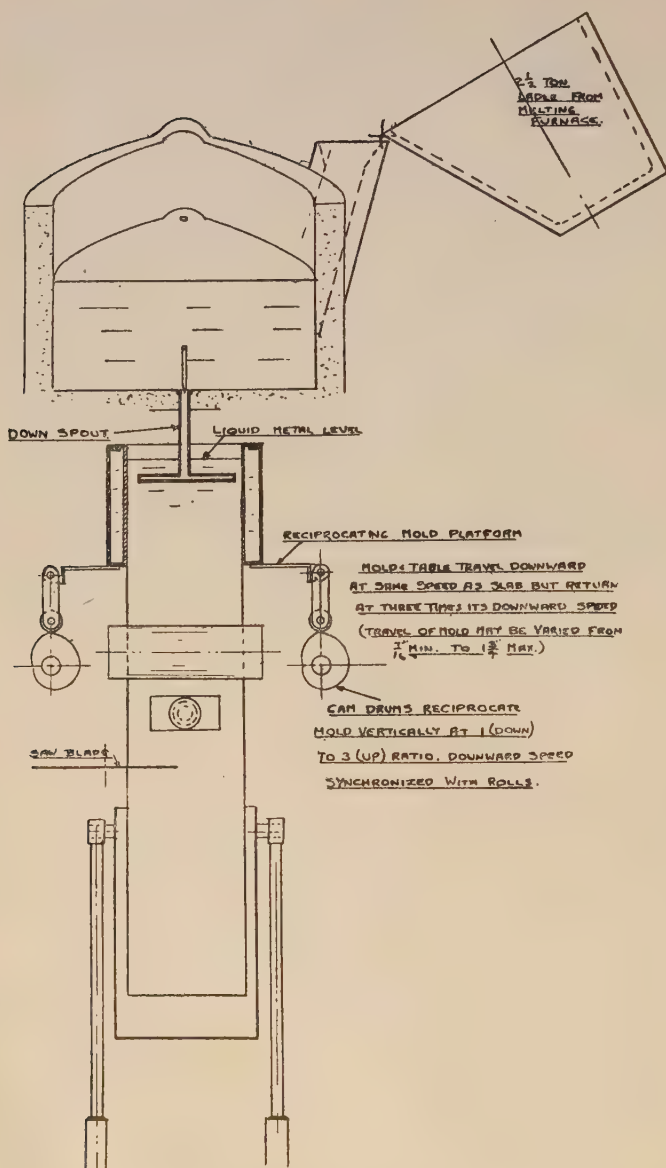
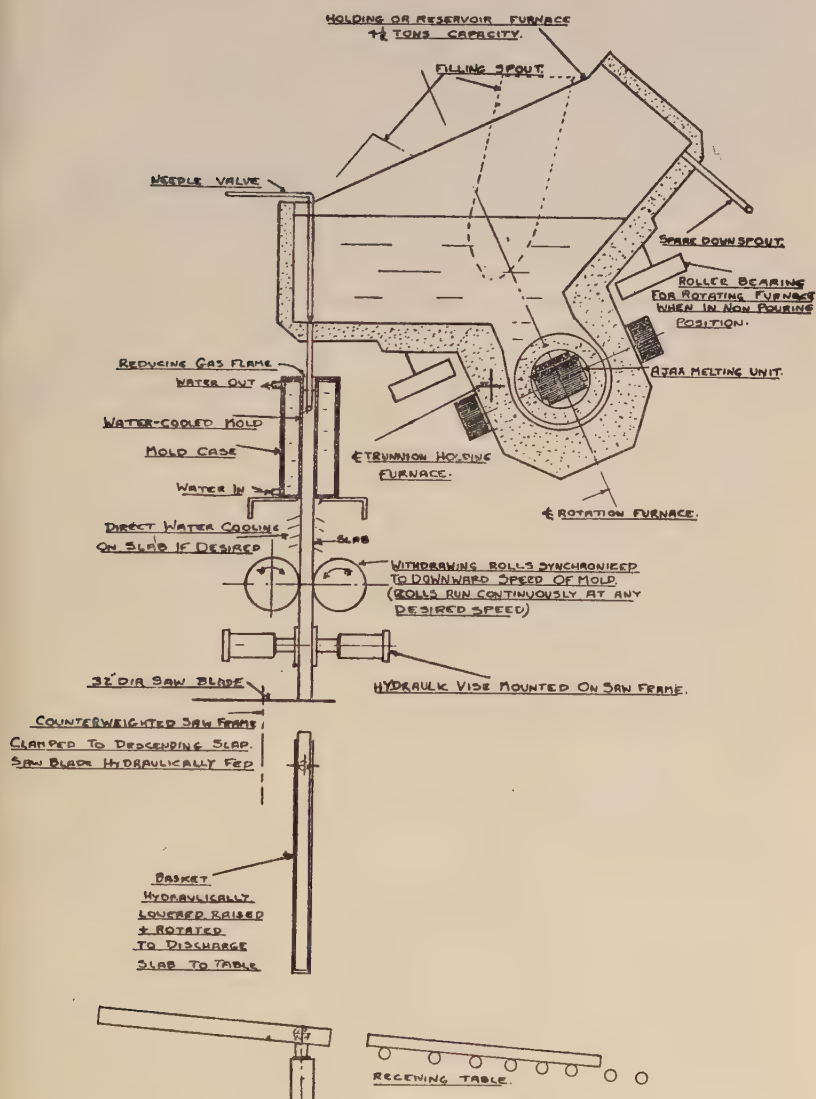


FIG. 3.—Continuous



Slab-Casting Machine.

entry table of the mill where a hydraulic sticker is installed to assure positive entry of each bar into the roll bite. On the delivery side a kick-off device removes the bar after the pass to one of the transfer tables located on either side of the delivery table. To accommodate varying lengths of bar, there are eight of these air-operated kicker arms set on different centres, all mounted on a shaft beneath the table. From either of the transfer tables on the delivery side of the mill, the bars are stacked by vacuum pilers and the stacks later returned by chain transfer to the entry side of the mill for a succeeding pass, or delivery made to the annealing oven. Limit switches interlock the tables on both sides of the mill to prevent accidents.

The cold-rolling mill itself is of conventional Farrel-Birmingham design, although some new features have been introduced. The frames are cast steel, proportioned for great strength and mounted on cast-steel stringer bedplates. The double motor screwdown of the mill is equipped with a magnetic clutch which provides for the independent operation of either screw or the simultaneous adjustment of both. Two large dial indicators are mounted on the housings at the entry side for gauge readings, each having two hands, one for thousandths and one for fractional divisions of an inch. In addition, Selsyn units on the entry control desk indicate roll opening in thousandths of an inch.

The two mill rolls are made of forged steel, and the journals are supported in Morgoil sleeve bearings. The top roll is hydraulically counter-balanced by means of cylinders located on the under-side of the mill housings, which support the roll against the adjusting screws through lifter rods. The system includes a nitrogen-loaded accumulator maintained at a predetermined pressure by a positive displacement pump.

To facilitate the changing of rolls, an electrically driven roll-changing rig is recessed in the floor on the side of the mill opposite the drive. In preparation for roll removal, spacers are used to support the upper roll chocks on the lower ones, and the rolls, still in their bearing boxes, are easily removed from the mill as a pair and a new set quickly installed in like manner.

Universal spindles are used to connect the rolls to the pinion stand, and these units are simply but effectively designed to eliminate shock, looseness, and end thrust. The spindle assembly support is of new design which abandons the use of a heavy cast housing. Instead, 2½-in.-dia. solid steel rods serve for the upper spindle support, and for horizontal alignment two hollow steel bars are used which pivot in brackets attached to the housing of the pinion stand.

The 2000-h.p. combination drive and pinion stand, which is equipped

with gearing manufactured in the Farrel gear plant at Buffalo, N.Y., drives the mill at either 90 or 180 ft./min.

The first reduction gears and the mill pinions are of the Farrel-Sykes continuous-tooth herring-bone type, while the second reduction consists of split (divided) double helical gears. This makes a compact arrangement which distributes the load uniformly and requires minimum floor space. A unit-type pressure lubricating system with separate motor-driven pump, provides a continuous spray of oil at the mesh line of all gears and pinions and force-feed lubrication to all anti-friction bearings. The pinion stand housing is of cast Meehanite metal and the base and cover for the drive are substantial steel weldments.

The 2000-lb. cast bars enter this mill at 2.500 in. thickness and are rolled to 1.380 in. in four passes. Then they are annealed and rolled to 0.790 in. in two passes, followed by further annealing and rolling to 0.415 in. in two passes on the two-high breakdown mill. They are then annealed and overhauled and are ready for the four-high run-down mill.

## *2. Cold Run-Down Mill.*

The cold run-down mill is a 16- and 34-in.  $\times$  34 in. mill operating at a speed of 0/400/1000 ft./min., and is capable of rolling 2000-lb. bars 29 in. wide (maximum) and  $\frac{3}{8}$  in. thick (maximum) by 68 ft. long (maximum) down to coils 0.050 in. thick, using an upcoiler after the mill (Fig. 7, Plate XXXVIII).

The equipment consists of a vacuum-cup crane to place bars on an entry driven feed table which transports the bar to an entry feed pinch roll unit in front of the mill. An upcoiler on the delivery side of the mill receives the bar and creates a coil. These coils can be wound with or without a tail, depending upon subsequent routeing of the coils. The handling of the coils is done by means of conveyor systems with gravity rollers, brakes and escapements, side tilters, and pallet-type driven conveyors, with exits to annealing furnaces and entrances back again to the mill, or around the conveyor system if subsequent rolling is to be done without annealing. The whole conveyor system, which forms a storage area, is one of the most complete and modern coil-handling units ever to be installed, and is mostly automatic in operation, with fully interlocking features for sequence operation of equipment as the coils progress around the mill. After coils have once been formed, subsequent rolling is in coil form. The front end of the mill is provided with a charging car to take coils from the conveyor system and deposit them in a coil box to be fed to the mill through pinch rolls and sticker entry guides.

This mill is also arranged to operate as a finishing mill, with an expanding pay-off reel on the entry side which receives coils from the same charging car as that mentioned above. A wedge-type expanding and collapsing reel is located on the delivery side of the mill, which is equipped with a belt wrapper for starting the front end of the coil around the reel at mill speed. A pallet-type driven conveyor receives coils from the reel stripper and deposits them on the general conveyor system.

### *3. Cold Finishing Mill.*

The finishing mill is the same size and of the same design as the run-down mill and operates at 0/400/1000 ft./min., handling the same coils as the run-down mill except in lighter gauges on the upcoiler. The reel is for metal down to 0.011 in. thick. It is provided with the same equipment and conveyor system as the other mill, except that it has not a vacuum-cup crane and driven roller table as it is used for coils only.

Both mills have a common oil cellar in which are located the roll-coolant systems, the metal lubrication system, the oil lubrication system for gear-drive units, the lubrication system for the mill bearings, and the hydraulic system. The roll coolant is arranged with two systems so as to be able to use different solutions on the two mills. Either system is of sufficient capacity to supply both mills when they are operating on the same solution, and the piping and valves are so arranged that either system can supply either mill stand. These systems are of the latest design and are provided with alarm signals should pressures drop below a pre-determined point. This immediately warns the operators that a certain system requires immediate attention to safeguard the proper performance of the mechanical equipment. All manual hydraulic valves are operated by transmitter-receiver units for ease of operation. The roll balance hydraulic systems have been located on the mill floor adjacent to the respective mills. Both mills are provided with individual automatic grease systems.

### *4. Electrical Equipment.*

The electrical equipment for the two four-high mills is among the most modern and up to date ever installed by the Westinghouse Electric Corporation. The main drive equipment for each of the mills is essentially duplicate in character, with only minor differences in the auxiliaries. The drive for each mill consists of the following:

1 1250 h.p., 600 V., 0/400/1000 r.p.m., D.C. motor for the mill drive.



1 5 h.p., 230 V., 400/1000 r.p.m., D.C. motor for the wiper roll drive.

1 75 h.p., 230 V., 300/1200 r.p.m., D.C. motor for the blocker drive.

1 50 h.p., 230 V., 400/1200 r.p.m., motor for the upcoiler drive.

These motors are operated as part of a special adjustable-voltage mill drive. The speeds of each motor require close co-ordination to assure the proper speeds and proper tensions during normal operation as well as during acceleration and deceleration. These functions are furnished by special characteristics built into the motors and control and by use of Rototrol rotating regulators.

The 1250-h.p. mill-driving motor which drives the work rolls is supplied with power from a 1000-kW., 600-V., D.C. generator to form an adjustable voltage drive system. The 5-h.p. wiper roll motor, the 75-h.p. blocker motor, and the 50-h.p. upcoiler motor are supplied with power from a separate 75-kW., 230-V., D.C. generator as part of a variable voltage system. The speeds of these motors are co-ordinated with the speed of the main drive by means of Rototrol regulating exciters. The blocker and upcoiler are alternative methods of operation and will not be run at the same time. The metal is coiled in the upcoiler until its thickness is such that it can be reeled, at which time the upcoiler is disconnected and the blocker put into operation. A Rototrol regulating exciter controls the tension on the blocker so that it is maintained essentially constant during normal running operation as well as during acceleration and deceleration. Special means for inertia compensation are provided to assure constant tension under conditions of acceleration and deceleration.

Ventilation of the main drive machines is provided by a unique layout designed to provide maximum convenience and saving of floor space. The main motor-generator sets are ventilated from a separate fan located in the basement and arranged to force air through the machines and discharge it into the mill area. The 1250-h.p. main drive motors are each ventilated by individual recirculated systems. The system consists of special endbells for the motor and a cooler and fan for cooling and recirculating the ventilating air. The tension reel and upcoiler motors are ventilated by individual motor-mounted blowers with filters which take the air from the room, filter it, and exhaust it to the room through the machine.

Both the auxiliary and the main drive are controlled from conveniently located master panels which are located and arranged for maximum operator convenience.

## V.—ANNEALING.

All annealing in the mill is done in four continuous furnaces which are heated with propane gas. As the trend is towards the use of larger-size bars, the muffles were designed to take bars up to 29 in. in width.

The first furnace, designated the short-bar furnace, was designed to handle bars ranging from 9 ft. 9 in. to 42 ft. 3 in. in length, and to anneal at thicknesses varying from 0.40 to 1.75 in. Normal widths used are 16, 24, and 29 in., although other widths might also be handled. With 16-in.-wide bars, it is contemplated that three of them will be handled across the width of the short-bar annealing furnace. With 24- or 29-in.-wide bars, these will be handled two in width across the hearth of the furnace.

The capacity of the new short-bar continuous annealing furnace, which is propane-fired, is approximately 37,000 lb./hr., with a normal expected capacity of approximately 33,000 lb./hr.

In order to reduce the overall length of the furnace to a minimum, its performance was implemented by the addition of a preheating chamber. The furnace equipment is 117 ft. in length. This length, however, does not include the loading and unloading extensions, with the handling equipment for handling the bars on to the loading extension and the handling equipment for unloading the bars from the discharge extension. Each is approximately 45 ft. in length, including a 5 ft. charging extension, the flame impingement or preheat chamber, the conventional furnace chamber, the spray-quench chamber, and a 5 ft. discharge extension. The floor-space requirements, if the above new-type preheat chamber had not been employed, would have been increased by approximately 53 ft., making the length of the equipment between the loading and unloading mechanisms approximately 170 ft. instead of the present length of 117 ft.

The major portion of the heating is done in the preheat chamber, with the long conventional heating chamber being used to equalize and take care of the final heating of the bars to the desired annealing temperature. In actual operation this has proved to be a very desirable feature of this equipment.

The equipment is provided with a spray chamber for quickly cooling the bars from the annealing temperature to enable them to be handled as soon as they are delivered to the discharge table.

Since the major portion of the production is copper-base alloys containing zinc, which would cause discoloration, there was no justification for full atmosphere control. Furthermore, this is unnecessary because the bars are to be overhauled at approximately 0.40 in. gauge.

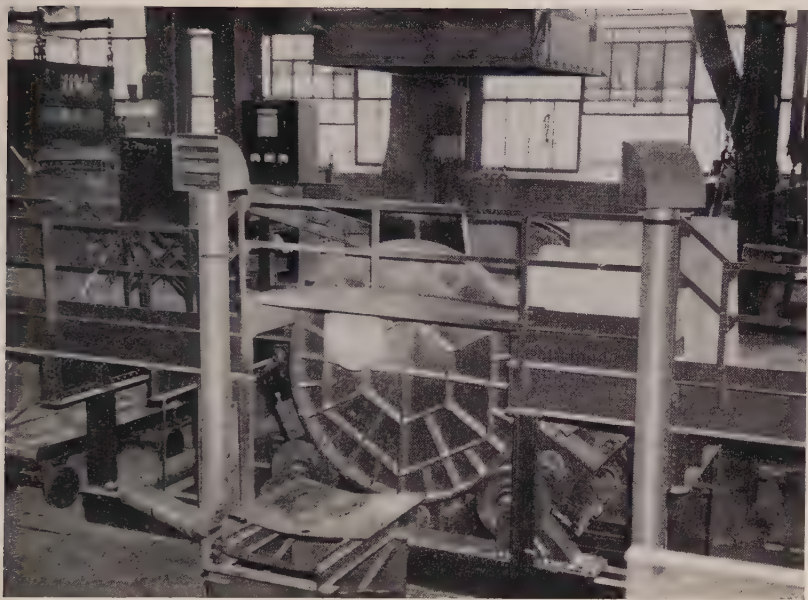


FIG. 4.—Pouring Side of Ajax-Scomet Melting Furnace.



FIG. 5.—Transferring Molten Metal by Ladle to the Continuous-Casting-Machine Holding Furnace.

[To face p. 372.]



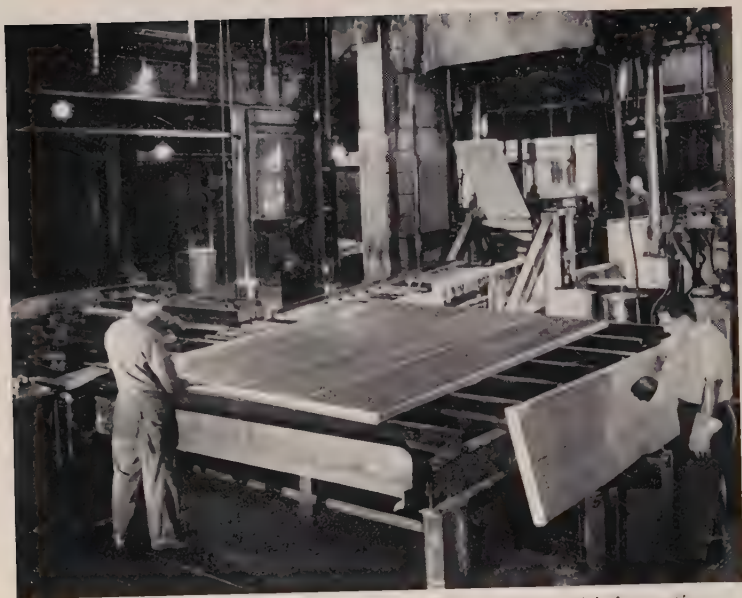


FIG. 6.—Discharge End of Continuous-Casting Machine, with Inspection.

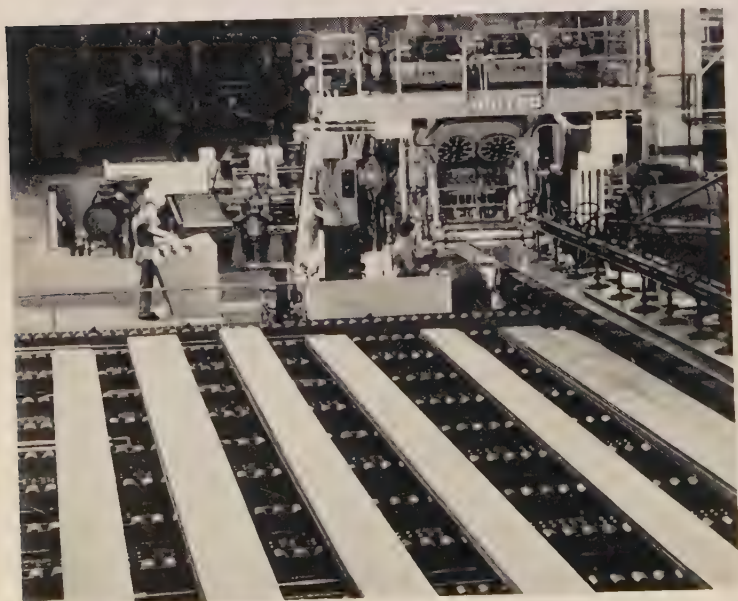


FIG. 7.—Entry Side of Four-High Cold Run-down Mill.

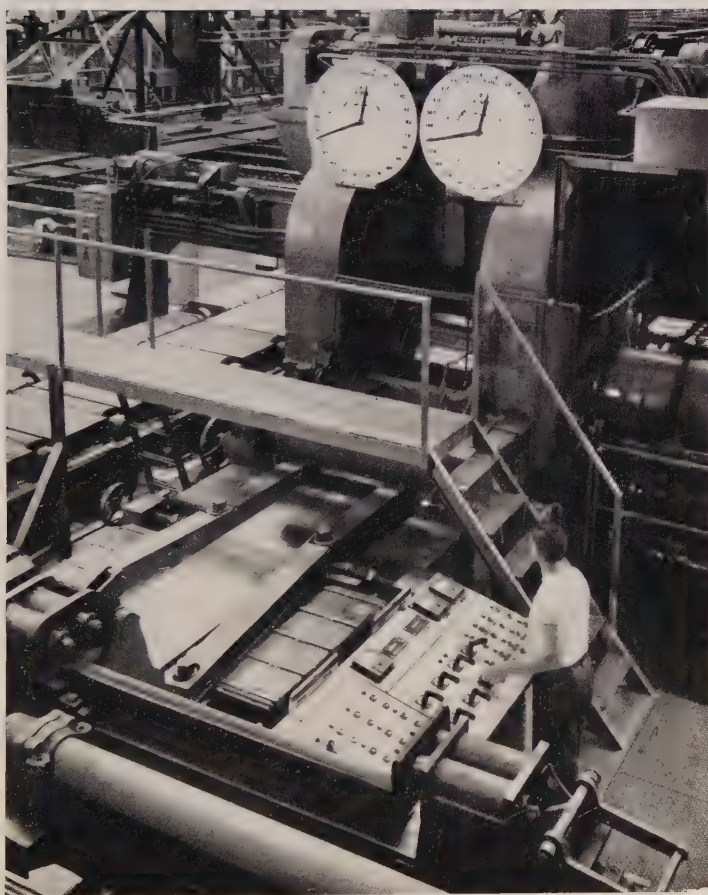


FIG. 8.—Two-High Cold-Rolling Mill, 30 × 36 in.



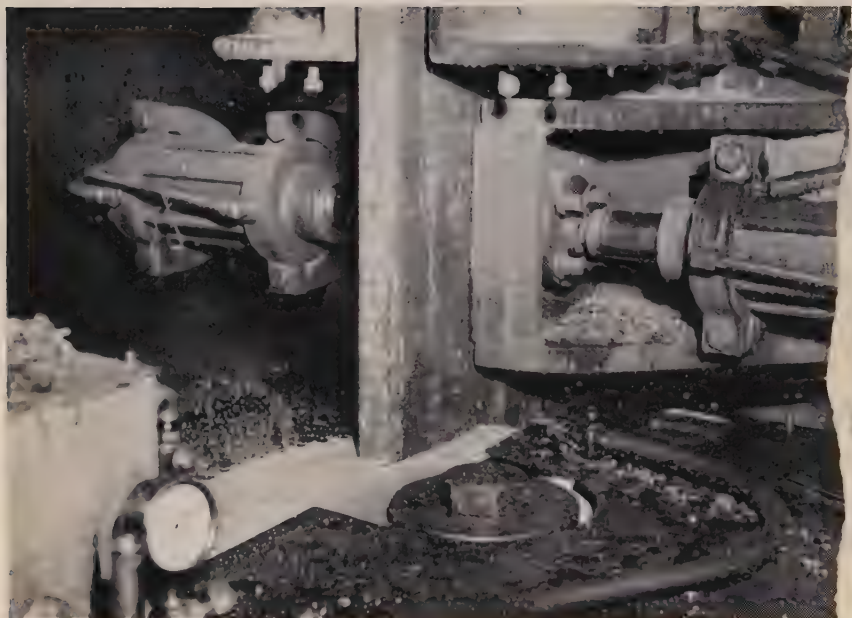


FIG. 9.—Sawing of Cast Slabs to Required Lengths.

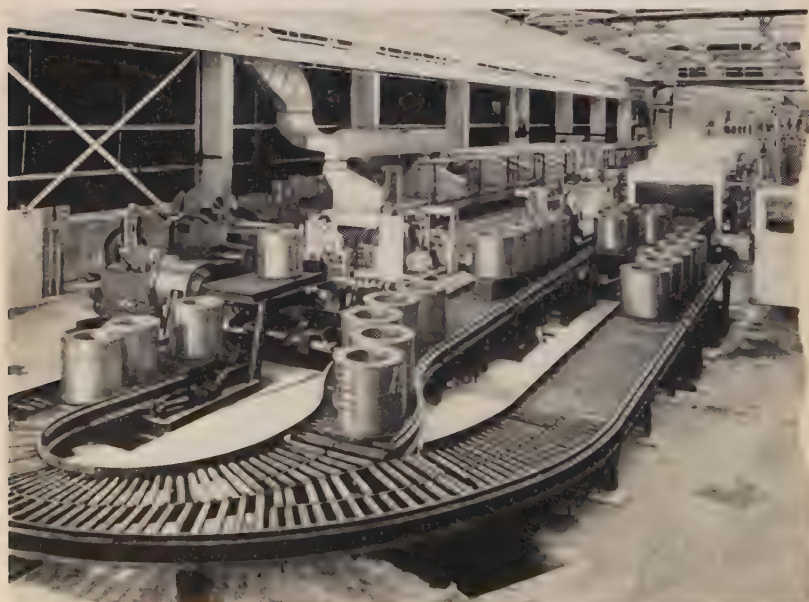


FIG. 10.—Continuous Annealing Furnace for Brass Coils, two abreast.

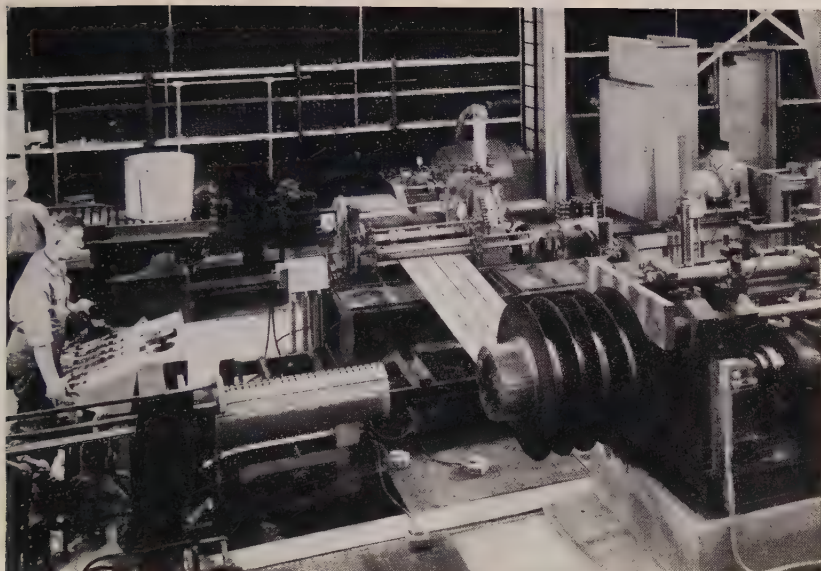


FIG. 11.—Light-Duty Slitting Machine.

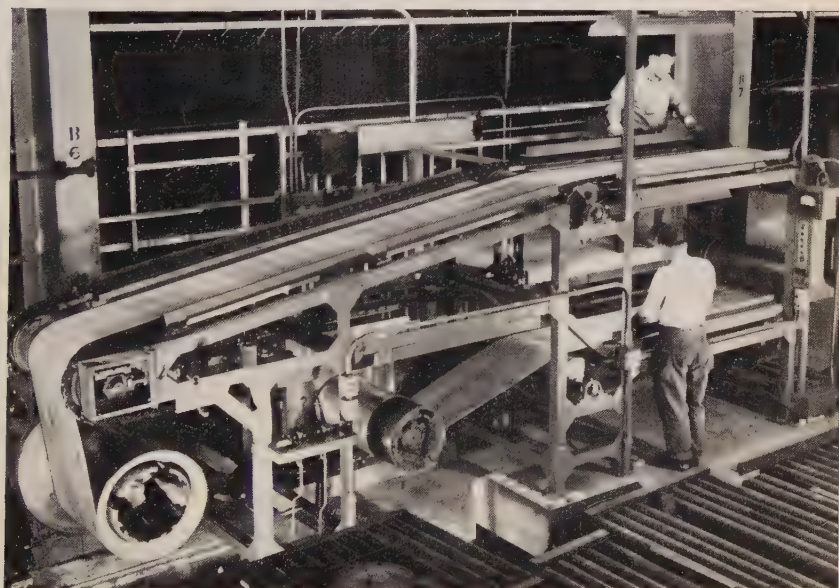


FIG. 12.—Inspection Machine for Metal Strip.

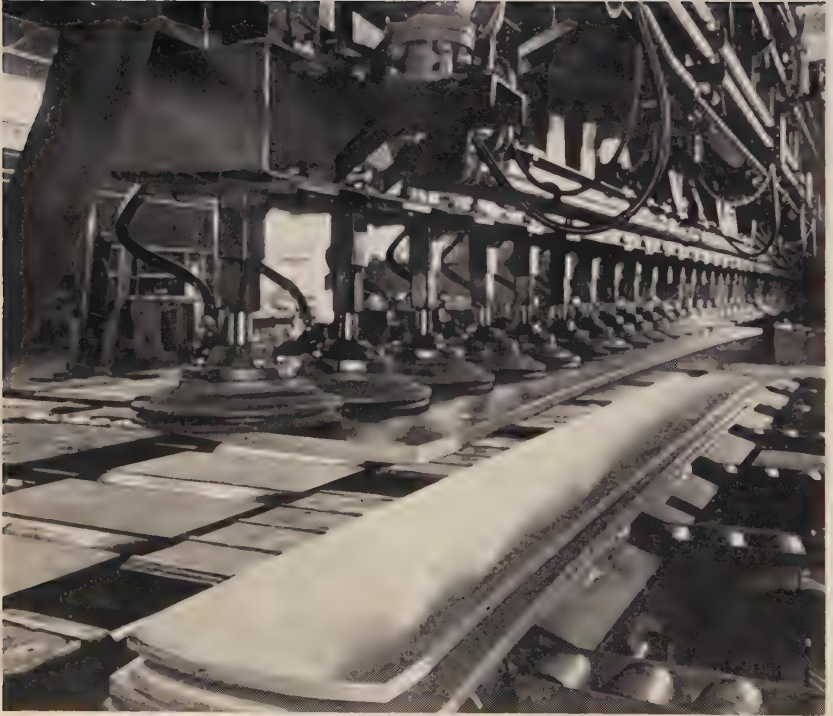


FIG. 13.—Vacuum-Cup Handling Equipment.



Extreme care was taken in selecting the proper size of burners for the various zones of the furnace equipment, so that the turndown condition during normal operation would be such, with the type of burners selected, as to give the closest control on the ratio of gas : air. By means of auxiliary burners in the last two zones, it is also possible to heat all zones of the furnace equipment to operating temperature at approximately the same rate after a shutdown period.

The equipment is designed to shut off gas and air in case of failure of either the gas or electric service. Also, if an interruption of electric service should occur, the equipment is provided with a gasoline engine operating on propane gas, to drive the rolls and to protect the furnace equipment.

The drive mechanism from the actual drive shaft to sectionalized sets of rolls is further protected in case there is a failure of the drive chains for a given group by the sounding of an alarm to notify the furnace operator that a given set of rolls is not operating, so that this condition can be rectified at the earliest possible moment.

In this high-production continuous strip mill, equipped with a large-capacity furnace unit, every precaution has been taken in order to ensure a minimum of interruption in operating time.

The remaining three furnaces were designed and built by the Surface Combustion Corp., Toledo, O., and are of the direct-fired roller-hearth continuous-annealing type. They burn propane gas and are designed for production capacities of about 32,500 lb./hr. of coiled sheet to 36,700 lb./hr. of ingot bars.

One of these furnaces, referred to as the long-bar furnace, is a unique assembly composed of a heat chamber joined together with a specially constructed high-capacity preheater, cool chamber, and quench tank. It is designed to take bars from 0.400 to 1.750 in. thick in lengths up to 65 ft.

The preheat chamber is about 14 ft. long and contains air-cooled, power-driven, Inconel conveyor rolls similar to those in the main heating section of 69 ft. length and the slow-cool section of 5 ft. length. The stainless steel spray-quench chamber is 12 ft. long and has water-cooled brass conveyor rolls. This constitutes a furnace over 100 ft. in length with an added driven charge table and a receiving table. Each roller is chain-driven through one counter-shaft drive running the entire length of the furnace.

The other two furnaces are of the same type. They are duplicates, within limits—one unit can handle coiled sheet and bars while the use of the other furnace is restricted to coils—but do not incorporate the preheater found in the modified unit (Fig. 10, Plate XL).

Material is handled in the form of slab or bar stock 16 or 24 in. in width weighing 2000 lb., or as-coiled sheet stock measuring 23–30 in. in outside dia. and of the same weight. The work travel pattern is 2 or 3 parallel rows of bars, 2 high, or 2 parallel single rows of coils.

While the furnace is designed for maximum production at temperatures up to 800° C. and uniform annealing conditions at temperatures as low as 250° C., in actual production the bar stock is annealed at 750° C. and the coiled sheet stock at 570° C. The metal being annealed is conveyed through the heating chamber, then through a quench section, and is discharged on to delivery tables. The furnace speed ranges from 1.8 to 7.8 ft./min. and the pass line is approximately 3 ft. above floor level.

The continuous coil furnaces are both divided into two main work sections—the heating chamber and the cool and spray-quench portion. The 100-ft. heating chamber in both furnaces is further divided into five heat zones for flexibility of heating cycles. This permits the changing of alloys or furnace temperatures by merely leaving an empty zone between different charges and thus eliminating the necessity for resorting to the costly and time-consuming operation of clearing the entire furnace. The burners, approximately 100 in number, are of the surface-combustion, low-pressure, automatic proportioning, velocity type, burning propane gas. They are located in the side walls and are staggered to fire above and below the work. Automatic heat-demand controls for each zone are built into this furnace and facilities for removal of burner units without furnace shutdown are also provided.

To realize an even distribution of heated gases through the charge, especially during the annealing of sheet coils, thirteen recirculating fans are situated in the ceiling of the furnace chamber. The fans, which have water-cooled bearings, have 36-in. blades, and are driven by individual 3-h.p. motors with separate push-button controls.

Adjacent to the discharge end of the furnace is the refractory-lined slow-cool chamber and the stainless steel spray-quench chamber. Water is sprayed on the work in an efficient cooling pattern and the floor is sloped in the direction of the work travel in order to minimize run-back of the quench water into the slow-cool chamber. The slow-cool chamber, about 6 ft. long, is directly connected to the 12-ft. spray-quench chamber.

Because of the weight requirements encountered in continuous brass annealing, the power rollers used in the heat chamber and in the slow-cool chamber are spaced 10 in. on centres and are fabricated of extruded Inconel. They have an outside dia. of 7 in. with a  $\frac{7}{16}$ -in. wall, and have a rated capacity of 2000 lb. per roll at 800° C. They extend



through the furnace side walls and are supported by means of anti-friction-type self-aligning bearings. The bearings are attached to stand-off plates to provide necessary cooling by ambient air.

Power is obtained from a sprocket-and-chain arrangement on the outside of the furnace, geared through a 3-h.p. conveyor-drive motor and double transmission. The quench-tank rollers are made of brass to avoid rusting and are water cooled. An auxiliary gaseous propane engine is provided in case of motor failure. Both of the continuous-coil furnaces measure about 116 ft. in length, including cooling and spray chambers.

A prepared-atmosphere gas is not used in any of these furnaces, it being a generally accepted fact in the industry to-day that the properly controlled direct flue products of combustion in a direct-fired furnace are suitable for the annealing of copper and many copper-base alloys.

#### VI.—STRIP PICKLING.

The first strip-pickling machines for brass rolling-mill operations ran at relatively low speed, namely, up to 100 ft./min. Experience indicated that this method of handling the material would be quite satisfactory, with some minor modifications, for operating at much higher speeds, and spray pickling was recognized as far superior to any of the older methods.

In co-operation with the engineering staff of the Scovill Manufacturing Company, the Metalwash Machinery Corporation have designed and built two spray-pickling machines to handle strip up to 29 in. wide at speeds up to 600 ft./min.

One of the major problems in this project concerned the carry-over of solution from one section to another. In order to investigate thoroughly the possibility of controlling this carry-over, an experimental machine was built to simulate the conditions found in actual production, and the engineering staffs of both Scovill and Metalwash devoted considerable time and experimental work to determine the best method of controlling the carry-over. This experimental machine contributed much to the solution of this problem and enabled the Scovill engineering staff to satisfy themselves that carry-over could be adequately controlled before fabrication of the equipment commenced.

The above is only one of a score or more details that required thorough investigation to ensure that the machines would be capable of handling cold-rolled brass strip at high speeds in continuous operation.

Another unusual feature of this machine is the manner in which the coil is threaded through the machine. In the conventional strip pickler

the "lead" end of one coil is attached to the tail end of the preceding coil by stitching or some other method. This operation makes it necessary to stop the machine before the tail end has entered it, which means that a portion of the strip is exposed to the action of the acid for a longer period of time than is necessary to clean it. For this reason that portion of the strip may be over-pickled or etched.

In order to eliminate this possibility, the "leader bar" method of threading was developed. This "bar" is simply a stainless steel frame, the weight of which develops sufficient friction between the conveyor rolls of the machine and itself to carry it through the machine. In operation it works as follows:

The "leader bar" is placed on the rolls of the entry table. A spring-loaded clamp or jaw on the tail end of the "bar" is opened; the "lead" end of the coil is inserted; the clamp is closed on the strip, and the machine is started. As the "bar" emerges from the discharge end of the machine, it passes between open pinch rolls and on to the discharge table. At this moment the pinch rolls close on the strip and the "leader bar" automatically releases its grip. The speed of the rolls on the discharge table is greater than that of the pinch rolls which now control the speed of the strip. This means that the "leader bar" runs away from the strip on to a section of the table which rotates 90° upward, using one edge of the section as an axis. This motion carries the "bar" out of the path of the strip and changes the plane of the "bar" from a horizontal position to a vertical position. At this point, rollers which are built into the edge of the "bar", engage a rail which slopes back to the entry side of the machine and serves as a gravity conveyor to return the "bar" in time to service the next coil. In the meantime the section of table which disposed of the "bar" has returned to its original position before the end of the strip has reached that point on its way to the block or coiler. With this method, the strip or sheet moves continuously through the machine with no stops, thus eliminating the possibility of over-pickling or etching in patches.

The fact that spray pickling is much faster than the immersion type of pickling makes it possible to operate at high speeds with a relatively short machine. If this same equipment were to be constructed for use with the immersion type of pickling, the equipment would be approximately twice as long, assuming that the same cycle of operations was to be used. In addition, the scrubbing action of the high-velocity sprays turns out brass strip having a much better appearance and surface condition than can be obtained by any other known method and eliminates the necessity of brushes, which are a constant source of maintenance trouble and expense.

While the Metalwash Machinery Corporation has constructed many spray-pickling machines since the first units nine years ago, none has been designed and built to handle such a wide variety of gauges at such high speeds as these machines in the new Scovill cold-rolling mill.

As these machines constitute a striking change from previous strip-pickling designs, the following details are submitted :

(1) *Capacity* : Up to 600 ft./min.

Acid strength : 10% sulphuric acid by volume at 140° F. (60° C.).

Acid bichromate : 10% sulphuric acid by volume plus 3% bichromate at room temperature.

(2) *Cycle of Operations* :

(a) Warm  $H_2SO_4$  power spray pickle.

(b) Warm bichromate power spray pickle.

(c) Cold fresh water spray rinse to sewer.

(d) Warm  $H_2SO_4$  power spray pickle.

(e) Recirculated power spray cold water rinse combined with fresh water rinse.

(f) Recirculated power spray soap rinse.

(g) Cold fresh water spray rinse to sewer.

(h) Cold air blast.

(i) Hot air blast.

(3) *Construction* : All stainless steel. Type 316 stainless up to and including (e) above. Type 304 for the remainder. Structural supports and pump mountings are stainless.

(4) *Pumps* : With the exception of the soap pump, the pumps are made of Worthington Worthite. The soap pump is of the Ingersoll-Rand type, but made of cast iron. The capacities of the pumps are as follows :

First pickle (2 pumps each)	.	.	350 gal./min. at 60 ft. total head.
Bichromate pickle	.	.	200 " " " "
Second pickle	.	.	200 " " " "
Recirculated rinse pump	.	.	125 " " " "
Soap pump	.	.	125 " " " "

(5) *Air Strip Nozzles* : Seven Spencer turbo-compressors each having a capacity of 1350 cu. ft./min. at a pressure of 32 oz. and driven by a 20-h.p., 3600-r.p.m. motor provide air to the upper and lower strip nozzles between each section of the machine.

(6) *Hot Air Blower* : Has 6 blowoff nozzles, 3 above and 3 below the sheet. Air for these nozzles is furnished by a Spencer turbo-compressor having a capacity of 2550 cu. ft./min. at 16 oz. pressure, which is powered by a 20-h.p., 3600-r.p.m. motor. The air is heated by forcing it across a steam-heated Young heat-exchanger.

(7) *Conveyor*: Consists of a series of  $1\frac{1}{2}$ -in.-dia. stainless steel shafts on which are moulded 4-in.-dia. Ryertex coverings. These shafts are mounted in Ryertex block bearings which are lubricated by the liquors in the machine.

(8) *Motors*: These are all totally enclosed, fan-cooled, wound for 220-440 V., 3-phase, 60 cycle, with a horse-power schedule as follows:

		h.p.	r.p.m.
First pickle (2) each 10 h.p.	. . . . .	20	1800
Bichromate . . . . .	. . . . .	$7\frac{1}{2}$	1800
Second pickle . . . . .	. . . . .	$7\frac{1}{2}$	1800
Recirculated rinse . . . . .	. . . . .	5	1800
Soap pump . . . . .	. . . . .	2	1200
Air stripper (7) each 20 h.p.	. . . . .	140	3600
Hot blast dryer . . . . .	. . . . .	20	3600

Total horse-power required for operation of unit: 202.

Each strip pickler has the following auxiliary equipment with the power indicated:

	h.p.	r.p.m.	V.	Motor
Pay-off Reel . . . . .	$3\frac{5}{8}$	690/2300	230	D.C.
Straightener . . . . .	25	850/1700	230	D.C.
Pickle Tank Conveyor . . . . .	15	850/1700	230	D.C.
Feed Roll (used for threading only) . . . . .	2	...	440	A.C.
Coiler (for heavy strip) . . . . .	25	850/1700	230	D.C.
Winder (for light strip) . . . . .	20	500/1250	230	D.C.

Adjustable voltage power is furnished by a General Electric motor-generator set with a 50-kW. main generator and a 10-kW. booster for use with the winder-motor tension regulator.

The coiler used with heavy strip is a combination three-roll bender and a windup reel. Interlocking provides for coiling either with no tail or with a 4-ft. straight tail with automatic coil kick-off when coiling with straight tails. The winder used with light strip is of conventional design with expanding mandrel. The winder control includes an amplidyne tension regulator.

## VII.—SLITTING OR SHEARING OPERATIONS.

The slitting of the wide bars into narrower sheet and strips is performed on equipment built by the Waterbury Farrel Foundry and Machine Co., of Waterbury, Conn. There are three lines of slitters. A heavy-, a medium-, and a light-duty line.

### 1. *Heavy-Duty Slitting Line.*

This slitting line will handle  $\frac{3}{8}$ -in. metal, hard or annealed, up to 30 in. in width.



*Coil Box.*—The first unit in the line is the coil box or holder, which has a capacity for coils up to 33 in. in dia. and 2000 lb. in weight. The machine is driven by a 5-h.p. gear-motor and is fitted with geared anti-friction rollers for supporting the coil. These rollers are chain-driven from the motor, through an over-running clutch, to provide free-wheeling for the coil. The side plates are individually adjustable by handwheels to suit the width of coil, and the side guides are of the vertical roller type, adjustable and air-operated. The coil pin or arbor is pneumatically withdrawn for loading. The coil box is equipped with wheels for supporting the unit on rails; this provides the necessary sliding movement for sticking the tail of the coil into the feed rolls of the straightener, which is the next unit in the line. This movement is derived from an air cylinder, located below the floor line.

*Straightener.*—The metal next passes to a 5-roll straightener, equipped with feed rolls. This machine is driven by a 40-50-h.p. motor. A tachometer generator is direct-connected and is mounted on the motor; a voltmeter, calibrated in ft./min., and a visual Weston instrument are mounted on the control desk for indicating the strip speed in ft./min. The straightener is equipped with a pneumatic metal wiper, actuated by a 4-way solenoid valve through a limit switch. The wiper remains up until the coil box has been rolled forward and the metal passed to the feed rolls. After straightening, the metal passes over a guide table on the outgoing side of the machine, and thence to the gang slitter. The guide table can be shifted laterally to suit requirements; this movement is derived from an air cylinder.

*Slitter.*—In a slitting line, the capacity and speed of the slitter govern the output. The No. 6 heavy-duty gang slitter employed in this installation has a capacity for 30-in.-wide metal and can make up to five cuts on  $\frac{3}{8}$ -in. brass at a speed of 150 ft./min. With metals of lighter gauge either the number of cuts or the slitting speed can be increased in a proportionate manner. The slitter is driven by a 100-125-h.p. motor through a speed reducer. The cutter spindles turn in roller bearings and are equipped with 16-in.-dia. cutters, sleeve-mounted. The upper spindle is adjustable vertically by means of the large hand-wheel shown. Entering side guides are of the vertical roller type, air-operated and adjustable. The tailstand is retractable electrically on to an extension of the bed. This bed extension is mounted on a pedestal that is supported on anti-friction bearings, so that the tailstand can be manually swung out of position by the operator for convenience in setting up the cutters and sleeves.

*Scrap Cutter.*—A rotary scrap cutter, with feed rolls, is located directly behind the slitter. It will cut  $1\frac{1}{2}$ -in.-wide scrap into 2-in.



lengths, and is independently driven by V-belts from a 10-15 h.p. motor. The rotor is of two-piece construction with central bearing, each section having two cutter blades  $180^\circ$  apart, assembled so that only one piece of scrap is cut at a time. The upper feed roll is pivoted and spring-loaded, and is driven by friction from the lower roll as the metal passes through. The scrap is carried away by a conveyor under the base of the machine. A removable table, mounted on rods, extends from the slitter over the scrap cutter to the entering side of the up-cut shear, which is the next unit in the line. Similar tables span the space between various units in the slitting line, wherever a guide is required to support the metal.

*Shear.*—Next in line is an up-cut shear used to square the tail ends or to cut the strips to length, if so desired. The cutter blade has a  $\frac{5}{8}$ -in./ft. shear and the up-stroke of the slide is  $3\frac{1}{2}$  in. The shear is back-gearred and is driven by a 5-h.p. motor. This machine is provided with a solenoid 3-way air valve for operating a single-cycle clutch mechanism, and is equipped with centralized lubrication.

*Coiler.*—Finally, the metal strips pass over a guide table leading to the feed rolls of a 3-roll coiler, the function of which is to re-coil the strips. This machine is driven by a 40-50-h.p. motor at a speed of 100-300 ft./min. The coiler rolls are 6 in. in dia. by 34 in. long, the upper roll being vertically adjustable by a handwheel, as is also the upper feed roll. The tailing device and the coil kick-off mechanism are pneumatically actuated from an air-cylinder, through a solenoid valve.

## 2. *Medium-Duty Slitting Line.*

This slitting line may be used for either conventional slitting, in which the metal is fed through, or for "pull through" slitting. It is designed to handle hard or annealed brass strip or sheet not over  $\frac{1}{8}$ -in. thick and 30 in. wide, in coils up to 2000 lb. in weight, which is the capacity of the pay-off stand.

*Pay-Off Stand.*—This unit has a speed range of 100-1000 ft./min., depending on the thickness of metal. It is driven by a 5-h.p. motor with an air-cooler for high speeds. The motor speed is regulated to give a back tension to the metal as it is unwound from the drum. The drum is of the 4-piece hydraulically-operated expanding type,  $13\frac{1}{4}$  in. in dia. when collapsed and 17 in. when expanded. There is an 8-in. lateral movement provided for lining up the coil with the straightener, by means of a motor-operated screw located at the left-hand end of the machine. The pay-off is slideably mounted on a base which is retractable hydraulically for "sticking" (i.e. feeding to the straightener rolls) by means of a 4-in.-dia. cylinder located below the floor line,

*Straightener.*—This machine, second in the line, runs at 450 ft./min. for  $\frac{1}{8}$ -in. metal and proportionately faster for thinner gauges, being driven by a 20-h.p. motor. It is equipped with adjustable air-operated roller-type entry-side guides and a metal wiper, also air-operated, located behind the slide guides. The metal wiper remains up until the pay-off is moved forward for "sticking". The upper feed roll and the two upper straightener rolls are separately adjustable vertically by crank handles. A roll unit at the rear regulates the strip speed. It consists of two rubber-covered rolls which are driven by friction only, as the metal passes between them. The upper roll is spring-loaded; it is raised or lowered by means of a 2-in.-dia. air-cylinder, operated through a solenoid air valve. A tachometer generator, chain-driven from the lower roll, is connected to a voltmeter which is calibrated in ft./min.

*Shear.*—The metal next passes over a removable metal table to the up-cut shear. This machine, which trims the tails or cuts the strip, as required, is similar to the shear employed in the  $\frac{3}{8}$ -in. slitting line (previously described), except that it is not back-gearred. It is driven by a 3-h.p. motor.

*Roll Feed.*—Between the above shear and the gang slitter, there is a retractable roll-feed unit, driven by a 3-h.p. gear-motor through an over-running clutch. The rolls are  $5 \times 32$  in. The feed unit is provided with a 6-in.-dia., 1-in.-stroke air-cylinder for raising and lowering the upper roll, and has adjustable roller-type, air-operated side guides. The unit is mounted on rolls and is retractable laterally on rails by means of an air-cylinder. A removable metal table spans the space between the feed unit and the slitter, which is the next machine in the line.

*Slitter.*—This is a No. 3 size machine, having a maximum slitting capacity of five cuts on  $\frac{1}{8}$ -in. metal at 450 ft./min. The number of cuts and the speed can, of course, be increased proportionately for thinner metal. The machine is driven by a 50-h.p. motor, through a herring-bone speed reducer and a coupling-type over-running clutch. For conventional slitting, this clutch is locked; for "pull-through" slitting, it is released.

The spindles are  $4\frac{1}{2}$  in. in dia.; they turn in roller bearings and are fitted with 9-in.-dia. cutters, sleeve-mounted. The upper spindle bearings are simultaneously adjustable by a handwheel. The tailstand is movable laterally by rack and pinion by means of a manually-operated ratchet wrench, and it can be readily swung out of position for convenience in assembling the cutters and sleeves. The slitter is equipped with front and back finger bars and also with adjustable side-guides at the entry side for light-gauge metals only, operated by individual hand-wheels.

Mounted behind the slit on the pedestal is a burring-roll unit, driven from the lower spindle by a sprocket and chain, through a slip friction. The burring rolls are fitted with anti-friction bearings, and the upper roll, which is spring-loaded, is adjustable by means of a hand-wheel. The clutch is also handwheel-adjusted and is provided with a hand-operated quick release.

*Rotary Scrap Cutter.*—This unit is located directly behind the slit. It is able to cut 1-in.-wide scrap into  $2\frac{1}{2}$ -in. lengths, at a slitting speed of 450 ft./min., and is independently driven by V-belts from a  $7\frac{1}{2}$ -h.p. motor. The rotor is one-piece with three cutter blades. The scrap is removed by a conveyor beneath the base of the unit.

The last two units in the line, a winder and a coiler, are both retractable, so that if the strips are to be re-coiled the winder is moved out of line. Otherwise, the coiler is retracted and the metal passed directly to the winder drum. In either case, the usual removable table serves to guide the metal from the slit to the final unit.

*Coiler.*—This coiler is similar to that described in the  $\frac{3}{8}$ -in. slitting line, except for size. It is driven by a 15–20-h.p. motor at a speed of 100–450 ft./min. and is equipped with feed rolls on the entering side. The coiler rolls are 4 in. in dia. and 34 in. long, the upper roll being vertically adjustable by a handwheel, as is also the upper feed roll. Both the coil kick-off and the tailing device are pneumatically operated. The machine is mounted on a sliding base and is moved in and out of line, hydraulically, by means of a 4-in.-dia. cylinder located below the floor line.

*Winder.*—This machine will wind 0.090-in.-thick metal at 1000 ft./min. and is driven by a 60-h.p. motor. The three-piece, 12-in.-dia. drum has a capacity for 30-in. coils up to 2000 lb. in weight, and it can be increased to 16 in. dia. by means of fillers. It is manually expanded and collapsed, the coils being stripped from the drum hydraulically. The winder is mounted on a sliding base and is moved hydraulically in and out of line. The hydraulic power unit for the winder, coiler, and pay-off was supplied by Vickers, Inc.

### 3. *Light-Duty Slitting Line.*

This line is designed to slit hard or soft brass 0.032–0.005 in. thick, 30 in. wide, in coils weighing up to 2000 lb. The coils travel on a conveyor to an hydraulically operated down-ender which places them on an hydraulically motor-driven pay-off reel. This reel is equipped with a four-piece hydraulically expanded type drum, which is 13 in. in dia. when collapsed and 16 in. when expanded (Fig. 11, Plate XLI).

The pay-off unit has a lateral movement of 8 in. for lining up the

strip with the centre line of the slitter by means of a motor-operated screw. It is also mounted on a sliding base which is retractable hydraulically in the pass line by means of a 4-in.-dia. cylinder located below the floor line. The pay-off reel can be jogged in either direction of the strip line by a push-button control to facilitate feeding.

*Tachometer Roll Unit.*—This unit consists of a pair of rubber-covered rolls, the bottom roll being connected to the tachometer generator which in turn is connected to a tachometer voltmeter and a Weston indicator. The upper roll is raised and lowered by an hydraulic cylinder to permit free entry of the strip. The complete unit has a lateral movement in and out of the pass line to facilitate the tooling of the slitter and the adjustment of the strip guide fingers. A constant-displacement piston-type fluid pump is connected to the bottom rubber-covered roll, which in turn controls the strip speed. This slitting line is not equipped with a straightener, because of the thin gauges of metal.

*Slitter.*—This machine has a slitting capacity of 25 cuts on 0.032 gauge and will trim metal up to  $29\frac{1}{2}$  in. finished width. The slitter is of the "pull-through" type using  $6\frac{1}{4}$ -in.-dia. cutters. It is driven by a 5-h.p. gear-head motor to a coupling-type overrunning clutch which is connected to a herring-bone speed reducer driving the slitting cutter arbors. When the strip base speed of 300 ft./min. is exceeded, the overrunning clutch is disengaged and the line is then of the conventional "pull-through" type. The upper spindle bearings are simultaneously adjusted by a handwheel and the tail stand is movable laterally for convenience in assembling the cutters and sleeves.

The slitter is equipped with front and back finger bars, and also with adjustable side guides at the entry side.

Mounted on the delivery side of the slitter is a burring-roll unit which is driven from the main spindle drive by sprocket and chain through a slip friction clutch. Burring rolls are fitted with anti-friction bearings and the upper roll, which is spring loaded, is adjustable by means of a handwheel. The clutch is also handwheel-adjusted.

*Scrap Conveyor.*—The scrap conveyor is of a special design which receives the edge scrap from the slitter guides into a box-type compartment. This compartment, which is approximately 9 ft. long, is provided with retractable pins mounted on an endless chain, which is driven by a 2-h.p. motor. As the pins enter the scrap compartment, they come in contact with the accumulated scrap and carry the same to the exit end of the scrap compartment where the pins are automatically retracted, thereby stripping the scrap from the pins.

*Winder.*—This unit is driven by an hydraulic motor connected to a herring-bone reduction unit on which a 3-piece, 12-in.-dia. hydraulically



collapsible and expansible winding drum is mounted. This unit is also provided with an hydraulically operated stripper for stripping full-width or multiple-width coils from the drum after the drum has been collapsed. The unit is mounted on a sliding base and is moved hydraulically in and out of the pass line. The hydraulic motor driving the winder unit can be jogged by push-button control from zero to base speed for threading. The hydraulic motor also provides variable speed at a base of 300 ft./min. to a maximum of 1500 ft./min. Constant tension is provided throughout the strip-speed range by the hydraulic motor.

The hydraulic motor on the pay-off unit and the hydraulic motor on the winder unit are supplied by two Vickers constant-displacement fluid pumps driven by a 50/60-h.p., 250/1200-r.p.m., 230-V., D.C. motor.

The hydraulic supply for expanding and collapsing the pay-off drum and winder drum, raising the upper rubber-covered tachometer roll and traversing the units in and out of the pass line is from a Vickers variable-delivery pump with handwheel control, driven by a 3-h.p., 1200-r.p.m., 440-V., 3-phase, 60-cycle motor.

#### VIII.—STRIP-INSPECTION MACHINE.

This machine is designed to handle coiled metal 12-30 in. wide, 0.004-0.050 in. thick, in coils weighing up to 2000 lb., it being possible to inspect both sides of the strip at speeds from 60 to 240 ft./min. (Fig. 12, Plate XLI).

The pay-off unit is driven by a 5-h.p., 230-V., D.C. ball-bearing motor suitably braked. The pay-off stand is not retractable. The drum of the pay-off is of the four-segment type, expanded and collapsed hydraulically. At the back of the drum is mounted a large-diameter adjustable drag brake.

The coils are fed to the inspection line on a gravity roll conveyor. Individual coils are selected and placed on an hydraulically operated traversing down-ender provided with an hydraulically operated stripper to pay the coil on to the pay-off unit. The drum is then expanded. By jogging the 5-h.p. motor, enough metal is released to attach the end to a bar clamp which is attached to two side-threading chains. The strip-threading drive is powered by a 3-h.p., 1800-r.p.m., gear-head motor with a ratio of 120 : 1.

This unit is controlled by a push button to carry the strip up over idler rolls convenient for inspection of one side or outer surface of the metal. Continuing to jog, the threading motor carries the strip downward over other idler rollers and to the winder unit. This provides a



convenient location for inspecting the other side of the metal, or the inner surface of the coil.

The threading bar is then released and the end of the bar is attached to the winder drum.

The winder unit consists of a gear-reduction unit on which is mounted a three-segment, 12-in. collapsible block. The block is expanded and collapsed hydraulically. This unit, which is powered by a 10-15 h.p., 230-V., D.C. motor with a motor-mounted magnetic brake, has a variable speed of 60-240 ft./min. The winder is provided with an hydraulically operated stripping plate to remove coils from the drum.

#### IX.—FLAT-METAL VACUUM-HANDLING EQUIPMENT.

One of the major items of consideration in designing a cold-rolling mill for non-ferrous strip and sheet is the handling and storage of metal in the process of production. This is especially so in the first, commonly referred to as breakdown, stages of rolling while the stock is still in the form of flat bars.

The wide variation in specifications covering metal in the non-ferrous industry does not permit synchronizing the various rolling, annealing, shearing, and slab-milling operations. To overcome, as far as possible, this condition, and in order to provide for more economical operation and production efficiency in the new continuous strip mill, a system of roller conveyors was installed connecting essentially all of the flat-bar processing equipment. Conservation of floor space and the desirability for reducing to a minimum the handling time by means of overhead cranes requires the stacking of bars on the roller-conveyor system.

Bars are fed into and discharged from equipment, one at a time, and it was this combination of both multiple and individual handling that necessitates provision for piling and unpling the bars. Various factors, such as speed in handling different starting or rolled sizes of bars, the requirement for annealing several such different sizes of bars, and prevention of damage to metal surfaces, influenced the decision to adopt vacuum handling for transfer of the flat bars in preference to other types of handling equipment.

Basically, vacuum-handling equipment for this type of service consists of a load-carrying beam, supporting a series of rubber cups, attached to suitable supports arranged so that the load beam with cups can be moved laterally a sufficient amount to permit removing one bar at a time from a delivery table and forming a stack adjacent thereto, or removing one bar at a time from a stack and depositing it on an

entry table. The vacuum cups have individual hose connections to a pipe header connecting to a motor-driven exhauster which creates the required vacuum for supporting a bar while it is being transferred (Fig. 13, Plate XLII).

The lifting power of a given size of cup is dependent on the degree of vacuum or pressure pushing the bar against the cup. For this class of service the general practice is to use a design pressure of approximately 7 lb./in.<sup>2</sup> This, for example, means that a vacuum cup having an area inside the rubber seal ring of 50 in.<sup>2</sup> would have a theoretical lifting capacity of 350 lb. Thus ordinary room air pressure is used to lift a 2000-lb. flat bar when a line of vacuum cups are affixed simultaneously to such a bar.

Two types of supports for the load-carrying beam are in general use: one consisting of a travelling structural bridge arranged with trucks at the ends, similar to a travelling bridge crane, and supported on runway rails above the bars to be handled; the other a series of stands and arms pivoted at the stands to which the load-carrying beam is attached. In the former type the load beam may be arranged for longitudinal as well as lateral movements, and these movements are usually accomplished by hydraulic cylinders, although it is possible to use electric motors or pneumatic cylinders. The vertical movement for raising and lowering the bars is usually by means of pneumatic or hydraulic cylinders, with preference for the pneumatic type to avoid oil dripping from hydraulic cylinders on to the metal. In the latter type, the supporting stands are equipped with vertical cylinders for elevating the load bar and horizontal cylinders for swinging the arms about the stands after picking up a bar. The cylinders for both movements are operated hydraulically.

The first type requires more head room than the second type, yet it occupies less floor space and is far more flexible in that the lateral travel can be much greater where required to accomplish certain results, and it can be arranged for longitudinal travel with a separate control for this movement, which in some cases is required, while this feature cannot readily be accomplished with the second type.

The equipment described here is of the first type, and was manufactured by the Wean Engineering Company, Inc. It is installed at the entry and delivery sides of the two-high cold-rolling breakdown mill, ahead of and also beyond the up-cut shear, at the entry and delivery ends of the bar-annealing furnaces and at the entry end of the slab-milling equipment. The vacuum equipment is designed for continuous operation 24 hr./day, and each unit has sufficient capacity to lift and transfer flat bars 16-29 in. in width, weighing 2000 lb. and upwards each.

Depending upon the pass in the rolling schedule, bars also vary in length from about 9 to 64 ft. and in thickness from  $2\frac{1}{2}$  to 0.400 in.

The bridge, constructed of structural-steel shapes welded together and mounted on forged steel wheels that travel on the end structural supports, is traversed laterally by means of two hydraulic cylinders. Alignment of the bridge is maintained by a rack-and-pinion equalizing mechanism. The bridge supports a load-carrying beam upon which the rubber cups are mounted. Each of the cups has a lifting and holding capacity of approximately 400 lb. They are so spaced and grouped on the carrier beam that a sufficient number will engage any length of bar within the capacity of the equipment served. Any cups not in contact with the bar may be rendered inactive either locally or from the operator's control station. The carrier beam upon which the cups are mounted may be hydraulically traversed in a longitudinal direction, if required, to compensate for the travel of bars through the furnace when annealing two bars in height.

The lifting and lowering of the vacuum-cup assembly is accomplished by two air cylinders mounted near each end of the carrier beam.

Although, fundamentally, all of the units are similar, the following description applies specifically to the unpling unit at the entry end of the short-bar furnace. This unit has a maximum bridge travel of 7 ft.  $5\frac{3}{8}$  in., a maximum cup lift of 18 in., and a carrier-beam longitudinal traverse of 18 in. The unpiler frame has a span of approximately 47 ft. between supports. The equipment is designed to transfer flat bars of various widths from a single position on the storage roller conveyor adjacent to the furnace and place them at different locations on the furnace-entry table. This condition at the furnace-entry table precludes a completely automatic cycle of operation.

The cycle of operations is started with a flat bar on the cups and with the cup-carrying beam raised to the up position above the pile of bars. The operator manipulates manual valves which control the stroke of the hydraulic cylinders provided to traverse the bridge and thereby position the bar at the proper location cross-wise over the furnace-approach table. The carrying beam, with bar attached, is then lowered to the desired height over the approach table by manual operation of the valves controlling the pneumatic cylinders and, if necessary, also traversed longitudinally by a manually controlled hydraulic cylinder. The bar is in the desired position over the furnace table and the operator now presses a push button, starting the automatic cycle. With the operation of the push button, the operator removes his hands from the manual valves controlling the vertical and horizontal operations. In so doing, the valves automatically return to their neutral positions,

placing these functions under control of electrically operated valves which perform the following functions in this order :

The vacuum is released, allowing the bar to drop, and the carrier beam is simultaneously raised to its top position. At this point contact is made with a limit switch which energizes a valve applying hydraulic pressure to the traverse cylinders moving the bridge to a position over the stack of bars. Vacuum is now automatically restored and the cup-carrying beam is lowered to the stack where the cups, having made contact with the bar, are automatically raised to the top position carrying a bar, thereby completing the automatic portion of the cycle, and the equipment is ready for the operator to make the next transfer. An adequate system of interlocks and controls is provided to ensure the proper sequence of operations and to prevent, as far as possible, injury to personnel or damage to either the equipment or the metal being handled or transferred.



# THE FLOW OF ZINC UNDER CONSTANT STRESS.\* 1257

By Professor A. H. COTTRELL,† B.Sc., Ph.D., MEMBER, and V. AYTEKIN,‡  
B.Sc., Ph.D., MEMBER.

## SYNOPSIS.

Part A describes a general study of the flow of single crystals of pure zinc, under constant shear stress on the glide planes, and of polycrystalline specimens, under constant tensile stress. With the exception of single crystals having basal planes inclined at angles greater than  $45^\circ$  to the axis of tension, both types of specimen gave curves of a standard shape which could be resolved into transient and steady-state components. Andrade's  $t^{1/3}$  law was accurately obeyed by the transient component. The rate of steady-state flow of both types of specimen varied exponentially with stress and with the reciprocal of temperature, although the values of the parameters in the relation were quite different in the two cases. Flow of the single crystals occurred by slip, while that of polycrystalline specimens involved at least four processes, slip, twinning, cell-formation, and displacement along grain boundaries.

In Part B, the nature of steady-state flow in single crystals has been examined from the point of view of the recovery theory of creep. Orowan has suggested that, in recovery creep, the rate of flow ought to be related to the rate of recovery and the coefficient of strain-hardening; also that reducing the load suddenly on a specimen in the steady state should produce an induction period in which the rate of flow is small or zero. These effects have been observed on crystals undergoing steady-state flow. Application of the theory to the softening of strain-hardened crystals during annealing experiments leads to the conclusion that the yield strength should decrease according to a logarithmic time relation. Measurements of the recovery of zinc crystals have given results consistent with this relation and the values of the parameters in the recovery equation agreed with those obtained from the creep experiments.

## PART A.—GENERAL EXAMINATION OF SINGLE-CRYSTAL AND POLYCRYSTALLINE SPECIMENS.

### I.—INTRODUCTION.

AN important development in the understanding of creep has been the realization that it is usually made up of several distinct mechanisms of flow, operating either simultaneously or consecutively. The compound nature of creep is not really surprising, because a specimen under load will make use of every available process that enables it to give way to the load, and the many effects which can be called upon, e.g. slipping, twinning, recovery, recrystallization, grain-boundary and constitutional

\* Manuscript received 12 October 1949.

† Professor of Physical Metallurgy, University of Birmingham.

‡ Ankara, Turkey; formerly Research Student, University of Birmingham.



changes, must provide many such processes. Failure always to appreciate this point has led to some confusion in the past; for example, theories put forward to explain the results of experiments where one process has dominated have sometimes been unjustifiably applied to other experiments where different mechanisms have operated.

It is thus necessary, when investigating the nature of creep, first to separate and classify the various component processes contributing to the flow, after which each of these can be studied as a distinct phenomenon. In the present investigation an attempt has been made to follow this programme by the study of the flow of single crystals and polycrystals of pure zinc under constant stress. Zinc was chosen for study because it is readily available in a state of high purity, because single crystals can be grown easily, and because these crystals have a simple slip system.

## II.—MATERIAL.

Throughout the investigation, a single sample of spectroscopically pure zinc was used; it was kindly supplied by the National Smelting Company, Ltd., and drawn to 1-mm.-dia. wire by Messrs. Johnson, Matthey and Company, Ltd. Spectroscopic analysis of the finished wire showed the presence of traces of lead, cadmium, iron, and copper, but not in amounts large enough to be measured reliably.

## III.—APPARATUS.

*Maintenance of Constant Stress.*—Unless the plastic strain is small, it is important in a creep test to include a device which will maintain a constant stress on the specimen, rather than constant load, since the creep curve will otherwise be distorted. In tensile-creep experiments on polycrystalline specimens a constant tensile stress is required, so that the problem is to reduce the applied load progressively in proportion with the diminishing area of cross-section. In the present work a lever device of the beam balance type used by Andrade and Chalmers<sup>1</sup> was adopted for this purpose; full details of this device have been given by Andrade and Chalmers and will not be repeated here.

In the case of single crystals the device has to satisfy a different law of relaxation of load. Since the resolved shear stress on the glide planes in the glide direction controls plastic glide in single crystals, it is this, rather than the tensile stress, which must be constant. In a metal with a single glide plane, such as zinc, the area of this plane is constant during slip so that no compensation for the change of the area of cross-section is required. However, the glide plane rotates towards the axis of extension as the specimen extends, and this causes the resolved

shear stress per unit load to increase. From the well-known geometrical laws of slip <sup>2, 3, 4</sup> it is easily shown that, for constant load, the resolved shear stress increases with extension according to the formula :

$$\frac{\tau_1}{\tau} = \left( \frac{1 - (l^2 \sin^2 \lambda)/l_1^2}{1 - \sin^2 \lambda} \right)^{1/2} \quad . \quad . \quad . \quad (1)$$

where  $\tau$  is the shear stress acting when the (initial) length of the specimen is  $l$ ,  $\tau_1$  is the value associated with a (subsequent) length  $l_1$ , and  $\lambda$  is the initial angle between the glide direction and the axis of pull.

For crystals where  $\lambda$  is small, approximately constant resolved shear stress can be obtained by simply applying a constant load, as was suggested and used by Andrade and Roscoe.<sup>4</sup> In general, however, the load must be relaxed. This has been accomplished in the present work by using a beam device exactly similar to that of Andrade and Chalmers,<sup>1</sup> except that it was designed to relax the load according to equation (1) instead of in proportion to the area of cross-section.<sup>5</sup> Since equation (1) contains the initial orientation,  $\lambda$ , it is necessary strictly to use a different beam for each crystal orientation. Actually, only seven beams were constructed, corresponding to values of  $\lambda$  of 22°, 30°, 35°, 40°, 44°, 47°, and 50°. With crystals of intermediate orientations, beams with the nearest values of  $\lambda$  were used; in this way it was always possible to hold the shear stress constant to within 1%. Crystals with  $\lambda < 22^\circ$  could either be tested with the 22° beam or by constant loading; those with  $\lambda > 50^\circ$  were unsatisfactory for the reason discussed in Part A, Section V, and were not used.

*Description.*—A diagram of the apparatus is shown in Fig. 1. All components are attached to the heavy vertical steel column *A*, and this in turn is supported on the floor by a heavy baseplate and joined to a wall through shock-absorbing rubber joints. A brass plate *B* serves as the main platform carrying the specimen and the loading device. The load produced by weighting the pan *C* is transmitted to the beam *D*

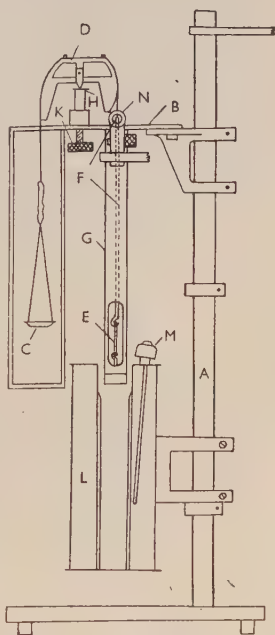


FIG. 1.—The Apparatus for Creep Experiments. (For key see text.)

by means of a rubber band and silk thread, and from the beam to the specimen *E* by a silk thread and a thin, but rigid, steel wire *F*. The specimen is held vertically by two hooks, the upper one of which is attached to the steel wire and the lower one is screwed into the bottom of a steel tube *G*. This tube is suspended rigidly from the brass platform. The beam is pivoted by two gramophone needles in adjustable supports which rest on a small glass-topped table *H*. This table may be raised or lowered by a screw *K*, thus making it possible to bring the beam into a horizontal position before starting an experiment.

A cylindrical furnace *L*, closed at its lower end, can be moved vertically by means of brackets which attach it to the main column and can thus be brought round the tube carrying the specimen. The furnace, which is resistance-wound, is controlled by means of a Sunvic thermostat, *M*, to  $\pm 0.5^{\circ}$  C., and is provided with a copper tube which serves to reduce the temperature gradient along its length. Provision is made for a thermocouple to be mounted close to the specimen.

The extension of the specimen is measured with a travelling microscope *N* attached to the main column and sighted on the top of the steel wire. Since the wire provides a rigid connection with the top of the specimen, displacement of the latter is transmitted directly to the top of the wire, where it can be measured. Extensions could be measured in this way to  $5 \times 10^{-4}$  cm.

#### IV.—PREPARATION OF SPECIMENS.

*Single-Crystal Specimens.*—All single-crystal specimens were prepared from 1-mm.-dia. wire by the fusion method of Andrade and Roscoe.<sup>4</sup> During growth, the wires were loosely supported in horizontal silica tubes and enclosed in an atmosphere of argon. The travelling furnace was designed to have a peak temperature of  $15^{\circ}$  C. above the melting point of zinc and to travel over the wires at a speed of 2 cm./hr.; in this way a 100% yield of single crystals having clean smooth surfaces was produced.

Owing to their extreme softness the crystals had to be handled with very great care, and auxiliary apparatus was constructed which enabled the operations of extracting, cutting, and mounting in grips to be performed with the minimum risk of distortion. Specimens were cut from the single-crystal wire with the aid of a pin-point flame, care being taken to protect the rest of the wire during this operation. The crystals were too soft to be mounted in ordinary testing grips or pin-chucks, and a method recommended by Orowan<sup>6</sup> was used, in which small loops of copper wire were soldered to the ends of each

specimen; this proved very successful and, by fastening these loops on the hooks of the creep apparatus, a specimen could easily be mounted for testing. The beams for maintaining constant stress were designed on the basis of an initial gauge-length of  $l = 5$  cm. It was observed, however, that the restraining effect of the copper loops prevented plastic flow extending right to the soldered ends of the specimen; preliminary experiments showed that undeformed regions 1.5–2 mm. in length extended inwards from each loop. Accordingly, the actual length of each specimen between the loops was fixed at 5.4 cm., thus providing an effective gauge-length of 5 cm.

The crystallographic orientation was determined in each case on a separate short specimen cut from the same crystal. This was etched to develop etch-pits by the reagent recommended by Barrett,<sup>7</sup> and its orientation then determined by the optical method of Barrett and Levenson.<sup>8</sup> The angles  $\lambda$  and  $\chi$  (the angle between the basal plane and the wire axis) could be measured in this way with an accuracy of about  $1^\circ$ .

*Polycrystalline Specimens.*—These were prepared from 1-mm.-dia. wire by soldering copper loops to their ends in the same manner as described above. Before testing, the specimens were annealed for 15 hr. at  $120^\circ\text{C}$ .

#### V.—THE STRAIN/TIME CURVE.

*Single-Crystal Specimens.*—Since single crystals of zinc deform at low stresses by glide on the basal plane, all the results of the present work are expressed in terms of the shear strain on the glide plane in the glide direction.

In the early stages of the investigation two types of creep curves could be distinguished, (i) curves having an S-shape of the type observed by Burghoff and Mathewson<sup>9</sup> on brass, and (ii) curves of a shape similar to those observed by Andrade.<sup>10</sup>

Figs. 2 and 3 show examples of the two types. In the case of the S-shaped curves it was observed that the specimens deformed inhomogeneously, intense slip occurring in a few isolated regions. This type of curve usually occurred with crystals having high values of  $\chi$  and  $\lambda$  (e.g.  $\chi > 45^\circ$ ), and in tests at high temperatures ( $> 120^\circ\text{C}$ .) and at slow rates of strain. These facts suggest that the occurrence of S-shaped curves in the present work was due to the geometric softening effect,<sup>4</sup> in which the increase of resolved shear stress resulting from the lattice rotation accompanying glide more than counteracts work-hardening, so that the first regions to deform behave as if they had become softer; deformation thus tends to confine itself to these regions. Because of the inhomogeneity of the deformation, the S-shaped curves

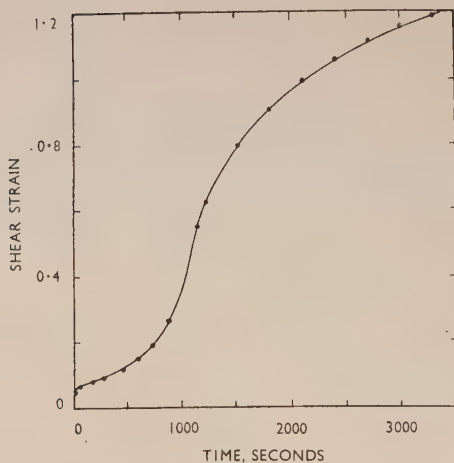


FIG. 2.—S-Shaped Creep Curve on a single crystal of zinc ( $\chi = 47^\circ$ ,  $\lambda = 48^\circ$ ,  $T = 93^\circ \text{C.}$ ,  $\tau = 45 \text{ g./mm.}^2$ ).

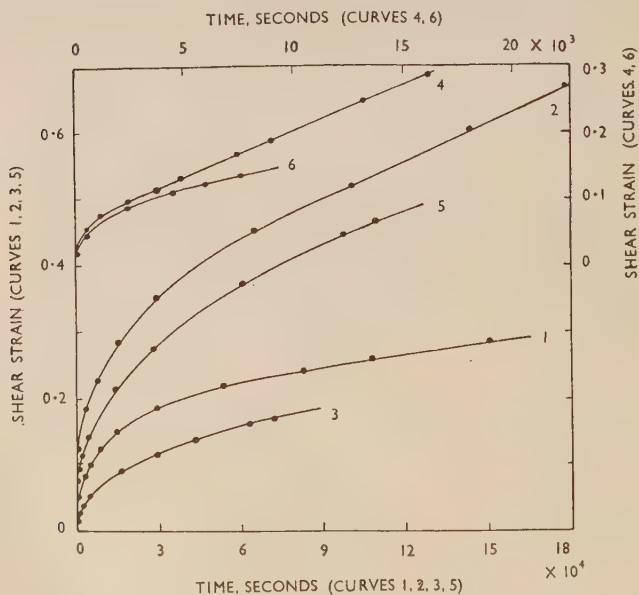


FIG. 3.—Creep Curves on Single Crystals under constant resolved shear stress. (The curves and specimens are numbered as in Table I.)



did not provide a strain/time relation under constant shear stress, and efforts were made in later experiments to avoid them. By confining the investigation to crystals with  $\chi < 45^\circ$  and to temperatures below  $120^\circ \text{C}$ . homogeneous deformation and the second type of creep curve could almost always be obtained.

Fig. 3 shows that the second type of curve possesses the usual features of a creep curve. After a virtually instantaneous extension accompanying loading, a fast flow occurred the rate of which steadily decreased until a stage of constant rate of flow was reached. This flow at constant rate then continued indefinitely, even in experiments which were prolonged for several weeks. No final stage of accelerating flow was ever observed and no specimen ever fractured.

Andrade<sup>10</sup> first showed that creep curves of this type could be resolved into three components: (i) instantaneous extension, (ii)  $\beta$ -flow or transient flow, which is predominant in the early part of the curve and obeys the law  $\gamma \propto t^{1/3}$ , where  $\gamma$  is the strain and  $t$  the time, and (iii)  $\kappa$ -flow or steady-state flow, predominant in the later stages and obeying the law  $\gamma \propto t$ . Andrade introduced an exponential factor into his final creep equation to allow for the increase of gauge-length with extension. In the present work, however, where the results are expressed in terms of strain, the exponential factor is unnecessary, and it was considered<sup>5</sup> that the most suitable form of Andrade's equation for application to these results is:

$$\gamma = \gamma_0 + \beta t^{1/3} + \kappa t \quad . \quad . \quad . \quad . \quad . \quad (2)$$

where  $\gamma$  is the total shear at time  $t$ ,  $\gamma_0$  is the instantaneous shear accompanying loading, and  $\beta$  and  $\kappa$  are coefficients of flow.

The continuous curves of Fig. 3, determined by selecting the best values of  $\gamma_0$ ,  $\beta$ , and  $\kappa$ , show that this equation can be fitted closely to the experimental results. A more critical test of the  $t^{1/3}$  law can be made by subtracting the steady-state component from each set of results and examining the variation of the remaining part,  $\gamma - \kappa t$ , with  $t^{1/3}$ . Fig. 4 shows that this is linear, thus confirming the law. Equation (2) was therefore adopted as the standard form of expression for the experimental results and the parameters  $\gamma_0$ ,  $\beta$ , and  $\kappa$  were determined on every specimen. A representative selection of these is given in Table I, together with the details of the experiments. Although the parameters were not reproducible from specimen to specimen, no systematic variation with crystal orientation was observed.

*Polycrystalline Specimens.*—A similar series of experiments was made on polycrystalline specimens under constant tensile stress. Much higher stresses had, of course, to be applied to produce measurable

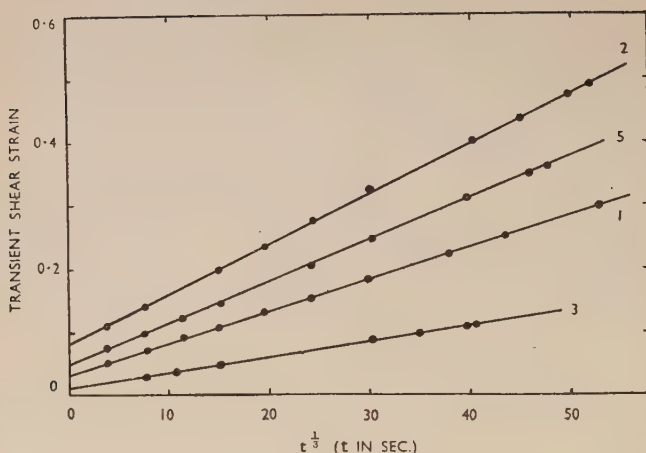


FIG. 4.—Verification of the  $t^{1/3}$  Law for the transient flow of single crystals. The points are derived from those of Fig. 3 by subtracting the steady-state strains.

TABLE I.—The Parameters  $\gamma_0$ ,  $\beta$ , and  $\kappa$  in Equation (2) for the Shear Strain of Single Crystals.

(Time in Seconds.)

Specimen No.	Shear Stress, g./mm. <sup>2</sup>	Temperature, °C.	$\alpha$	$\lambda$	$\gamma_0$	$\beta$	$\kappa$
1	58.0	11.5	13°	14°	0.030	0.00520	$<5 \times 10^{-9}$
2	59.0	11.5	14°	27°	0.080	0.00780	$8.7 \times 10^{-7}$
3	37.0	59.5	5°	12°	0.010	0.00230	$8.0 \times 10^{-7}$
4	45.0	23.0	36°	36°	0.004	0.00105	$3.2 \times 10^{-7}$
5	59.0	22.5	9°	28°	0.045	0.00675	$11.0 \times 10^{-7}$
6	59.0	22.5	43°	44°	0.021	0.00410	$47.0 \times 10^{-7}$
20	40.0	23.0	27°	28°	0.001	0.00225	$1.1 \times 10^{-7}$
21	40.0	23.0	20°	33°	0.001	0.00685	$0.5 \times 10^{-7}$
22	40.0	23.5	51°	53°	0.002	0.00035	$0.3 \times 10^{-7}$
23	40.0	23.5	10°	31°	0.025	0.00420	$6.9 \times 10^{-7}$

rates of flow; whereas the single crystals flowed rapidly under tensile stresses of about 100 g./mm.<sup>2</sup>, stresses exceeding 1000 g./mm.<sup>2</sup> were necessary before the polycrystalline specimens flowed at comparable rates. The tensile strain  $\epsilon$  was determined as a function of time and curves were obtained very similar to those of Fig. 3. Accordingly, the equation:

$$\epsilon = \epsilon_0 + \beta t^{1/3} + \kappa t \quad . \quad . \quad . \quad (3)$$

was tried and found to fit the experimental results. As an example,

the continuous curve of Fig. 5 is traced from equation (3), with suitable values of the parameters, and the points represent observed results. Some numerical values of the parameters are given in Table II.

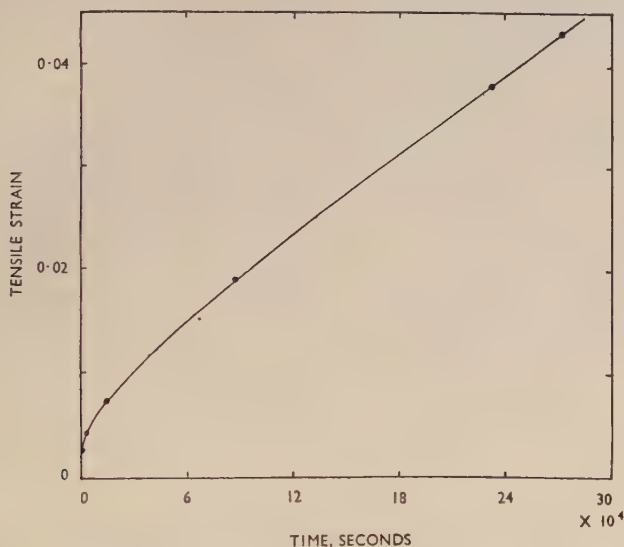


FIG. 5.—Creep Curve on Polycrystalline Zinc under constant tensile stress.  
( $T = 121.5^{\circ}\text{C.}$ ,  $\sigma = 828\text{ g./mm.}^2$ )

TABLE II.—*The Parameters  $\varepsilon_0$ ,  $\beta$ , and  $\kappa$  in Equation (3) for the Tensile Strain of Polycrystalline Specimens.*  
(Time in Seconds.)

Specimen No.	Tensile Stress, g./mm. <sup>2</sup>	Temperature, °C.	$\varepsilon_0$	$\beta$	$\kappa$
1P	828	121.5	0.00028	0.00022	$1.1 \times 10^{-7}$
2P	828	131.0	0.00063	0.00019	$1.7 \times 10^{-7}$
3P	1020	108.0	$< 5 \times 10^{-5}$	0.00035	$1.5 \times 10^{-7}$

## VI.—DEPENDENCE OF STEADY-STATE FLOW ON STRESS AND TEMPERATURE.

*Reproducibility.*—To examine the effect of a variable such as stress or temperature, it is necessary to make either separate measurements on each of a series of specimens or a series of measurements on a single specimen. A series of specimens can be used if the behaviour is closely reproducible from one specimen to the next; the results summarized

in the previous section showed that this was not so, which meant that the second method had to be adopted. This method can be used in the case of a flow which is independent of the mechanical history of the specimen. It was therefore expected that transient flow could not be studied because its rate depends on time and hence on the mechanical history. A few experiments were made in which the stress and temperature were altered during the early part of the test, but the resulting changes in the rate of transient flow were erratic and unreproducible; this part of the investigation was therefore discontinued. However, the fact that the rate of steady-state flow is constant suggested that this flow should be independent of mechanical history and controlled only by the instantaneous values of stress and temperature. Experiments to examine this were carried out by making temporary changes in the stress or temperature on a specimen flowing almost entirely by steady-state flow. Between each change, the stress or temperature was returned to its initial value and the rate of steady-state flow determined to see whether the initial value was reproduced; transient effects were produced at each change, and it was necessary to wait until a steady state was attained before reliable measurements of the rate could be made. Table III gives the results of such an experiment and shows that the steady-state flow is sufficiently reproducible.

TABLE III.—*Reproducibility of the Rate of Steady-State Flow on a Crystal Subjected to Various Shear Stresses.* ( $\chi = 38^\circ$ ,  $\lambda = 46^\circ$ ,  $T = 23.5^\circ \text{C.}$ )

Order of Test	Shear Stress, g./mm. <sup>2</sup>	$\kappa$ , sec. <sup>-1</sup>
1	40.0	$2.42 \times 10^{-7}$
2	37.5	$1.28 \times 10^{-7}$
3	40.0	$2.32 \times 10^{-7}$
4	34.5	$0.58 \times 10^{-7}$
5	40.0	$2.45 \times 10^{-7}$
6	33.0	$0.36 \times 10^{-7}$
7	40.0	$2.77 \times 10^{-7}$

*Single-Crystal Specimens.*—From several experiments of this type it was observed that, at constant temperature, the coefficient,  $\kappa$ , of steady-state flow varied with the shear stress  $\tau$  according to the relation :

$$\kappa = Ae^{B\tau} \quad . \quad . \quad . \quad . \quad . \quad . \quad (4)$$

where  $A$  and  $B$  are constants. The verification of this relation is shown in Fig. 6. An exponential increase of strain rate with stress was first observed by Ludwik,<sup>11</sup> on polycrystalline materials. Since equation (4) predicts a finite rate of flow at zero stress, it must break down at very

low stresses and  $\exp(B\tau)$  must be an approximation to a more complex function. An attempt to detect a deviation from the exponential law at low stresses proved unsuccessful; this was not unexpected, for the rate of flow was only large enough to be measured when the exponent itself was large, i.e. when  $B\tau > 10$ .

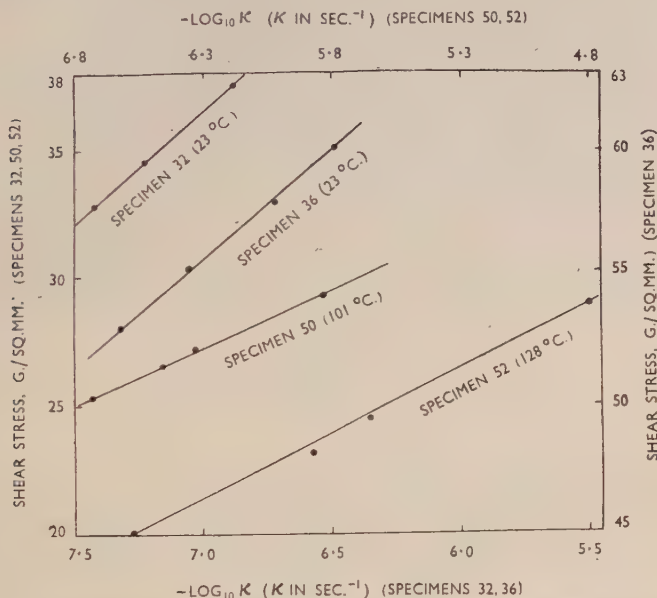


FIG. 6. —Variation of Rate of Steady-State Flow of single crystals with stress.

The constant  $A$  was observed to increase strongly with increasing temperature;  $B$  appeared to decrease slightly, although this could not be determined accurately. Experiments at various temperatures, with a constant shear stress, showed that the dependence of  $\kappa$  on temperature was consistent with:

$$\kappa = Ce^{-Q/RT} \quad . \quad . \quad . \quad . \quad . \quad (5)$$

as may be seen from the linear variation of  $\log \kappa$  with  $1/T$  in Fig. 7. The quantity  $Q$  represents an activation energy for the flow.

To combine equations (4) and (5) into a single equation for the dependence of the rate of flow on stress and temperature, it is necessary to know how the parameters in equation (5) depend on stress. An attempt was made to determine this, but the accuracy with which  $C$  and  $Q$  could be measured was insufficient to allow their dependence on stress to be studied quantitatively. However,  $Q$  appeared to de-



crease slightly with increasing stress, and no systematic variation of  $C$  was observed. It was therefore considered reasonable to assume that the applied stress affects the rate of flow by altering the activation energy. If  $Q(\tau_0)$  represents the activation energy corresponding to a

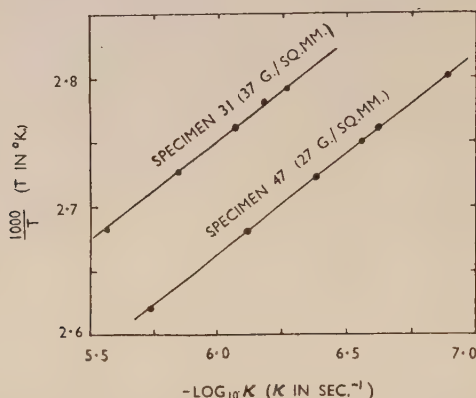


Fig. 7.—Variation of Rate of Steady-State Flow of single crystals with temperature.

selected stress,  $\tau_0$ , then, for any neighbouring value  $\tau$  of the stress, the activation energy can be written as :

$$Q = Q(\tau) = Q(\tau_0) - b(\tau - \tau_0) + \dots$$

where  $b = -dQ/d\tau$ . Hence, substituting into equation (5),

$$\kappa = Ce^{-\frac{Q(\tau_0) + b\tau_0}{RT}} e^{\frac{b\tau}{RT}} \dots \dots \dots (6)$$

which, with  $b = BRT$  and  $A = Ce^{-\frac{Q(\tau_0) + b\tau_0}{RT}}$

is the required combination of equations (4) and (5).

TABLE IV.—Values for the Parameters  $C$ ,  $Q$ , and  $b$  in Equation (6) for the Steady-State Flow of Single-Crystal and Polycrystalline Specimens of Zinc.

Specimen	Range of Stress, g./mm. <sup>2</sup>	$C$ , sec. <sup>-1</sup>	$Q$ , cal. g.-mol.	$b$ , cal. g.-mol. · mm. <sup>2</sup> g.
Single crystal	20–50 (shear stress)	$10^{10}$ – $10^{13}$	28,000–30,000 ( $\tau_0 = 35$ g./mm. <sup>2</sup> )	150–300
Polycrystal	800–1200 (tensile stress)	0.1–10	11,000–13,000 ( $\sigma_0 = 1000$ g./mm. <sup>2</sup> )	4–6

Since, for practical reasons, measurements of the rate of flow can only be made within a fairly narrow range of stress, the complete activa-

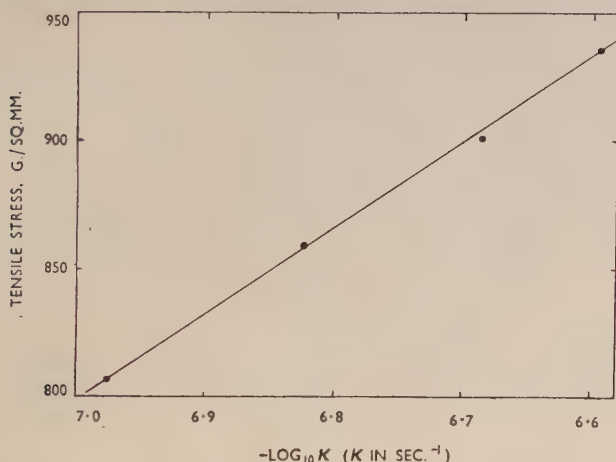


FIG. 8.—Variation of Rate of Steady-State Flow of a polycrystalline specimen with stress. ( $T = 121.5^\circ \text{C.}$ )

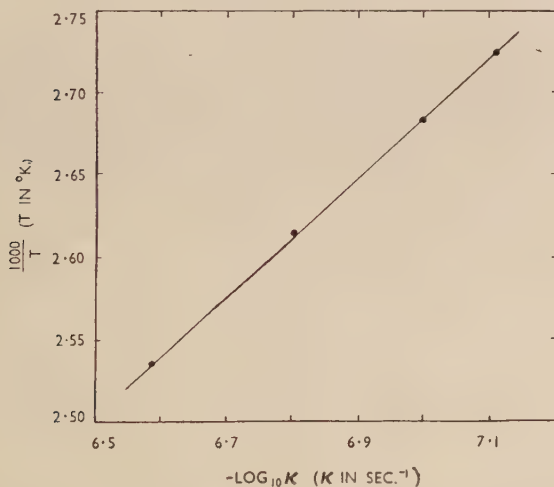


FIG. 9.—Variation of Rate of Steady-State Flow of a polycrystalline specimen with temperature. ( $\sigma = 955 \text{ g./mm.}^2$ )

tion energy function  $Q(\tau)$  cannot be determined. This means that the activation energy at zero stress cannot be found by substituting  $\tau_0 = 0$  in equation (6), for there is no *a priori* reason to assume that  $Q$  is a linear

function of stress. It is only possible to quote the value of  $Q(\tau_0)$  for a stress  $\tau_0$  chosen within the range studied experimentally. The values of  $C$ ,  $Q$  (for  $\tau_0 = 35$  g./mm.<sup>2</sup>), and  $b$  have been determined on several crystals and lie in the ranges given in Table IV.

*Polycrystalline Specimens.*—A similar investigation on polycrystalline specimens showed that the steady-state flow in this case also could be represented by equation (6), with tensile stress  $\sigma$  replacing shear stress  $\tau$ . Figs. 8 and 9 show the linear variation of  $\log \kappa$  with stress and reciprocal of temperature, respectively, and average values of the constants of the flow are given in Table IV (taking  $\sigma_0 = 1000$  g./mm.<sup>2</sup>). All three constants are much smaller than those for single crystals.

## VII.—METALLOGRAPHIC STUDIES.

*Single-Crystal Specimens.*—Although the steady-state flow of polycrystalline metals has often been studied, little or no attention has been

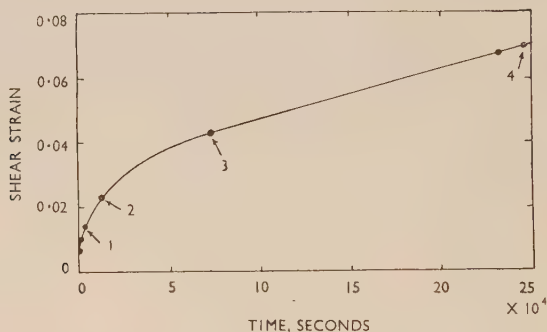


FIG. 10.—The Creep Curve of a Single Crystal at room temperature.  
( $\chi = 39^\circ$ ,  $\lambda = 40^\circ$ ,  $\tau = 35.5$  g./mm.<sup>2</sup>)

given to that of single crystals. The widely held and well-founded view that steady-state flow is intimately connected with quasi-viscous sliding along grain boundaries,<sup>12, 13, 14, 15</sup> derives from the work on polycrystals and can hardly be related to the corresponding flow of single crystals. Indeed, it is difficult to see how, in a homogeneously deformed zinc crystal, any process could give rise to a large-scale flow except one which allowed slip to continue on the glide planes.

To investigate this point, some creep tests were made at room temperature. The furnace was removed for these experiments and replaced by a low-power microscope for observing and photographing a crystal while it was under test. Before testing, each specimen was lightly electropolished with the aid of the chromic acid solution recom-

mended by Rodda.<sup>16</sup> The creep curve of one such specimen and photomacrographs taken at the stages marked 1, 2, 3, and 4 on the curve are shown in Fig. 10 and Fig. 11 (Plate XLIII), respectively. These show that the slip-bands became more prominent as flow progressed, and hence that the process of slip continued throughout the test.

It was also observed, from orientation determinations taken on crystals with initial values of  $\chi$  and  $\lambda$  in the range  $20^{\circ}$ – $40^{\circ}$  and extended 5–10% in creep, that the rotation of the glide plane and glide direction towards the axis of extension was always about  $2^{\circ}$ – $3^{\circ}$ , irrespective of the relative amounts of transient and steady-state flow. There were no indications of crystal fragmentation or recrystallization in these specimens.

*Polycrystalline Specimens.*—Hanson and Wheeler<sup>13</sup> showed that useful information on the creep of polycrystalline aluminium could be gained by metallographic examination. A similar examination of polycrystalline zinc seemed desirable. Since a specimen of cylindrical form is unsuitable for such work, some wire specimens were prepared by polishing flat longitudinal faces on them with fine polishing papers followed by electrolytic polishing in chromic acid.

Fig. 13 (Plate XLIV) shows the microstructure of a specimen before testing. At fast rates of strain the flow was characterized mainly by the formation of slip bands and twin crystals; these are shown in Fig. 14 (Plate XLIV) taken from a specimen which extended 0.54% in 8 min. After slower rates of strain the thick black boundaries associated with sliding along grain boundaries were observed, as shown in Fig. 15 (Plate XLIV); this specimen extended 9.5% in 71.5 hr., most of the flow being due to the steady-state component. Fig. 16 (Plate XLIV) shows the same specimen after electropolishing and etching in HCl; twin bands can be seen.

A fairly common feature of those specimens extended at slow rates was the formation of a cell structure within the original grains, similar to that observed by Wilms and Wood<sup>17</sup> on aluminium. An example is shown in Fig. 12 (Plate XLIII), taken from a specimen that extended 6.85% in 43 hr., most of this extension being due to steady-state flow. It will be noticed that slip bands cross the sub-boundaries without interruption and with a very small change of direction, and that the sub-boundaries are less heavily marked than the initial grain boundaries. This shows that neighbouring cells in the substructure have almost the same orientations and, therefore, that they can hardly have formed by recrystallization in the usual sense of the term. Additional evidence was given by X-ray back-reflection photographs, which agreed with the

X-ray observations of Wilms and Wood in that the original spots were observed to split into several discrete, but closely grouped, parts, showing that the grains had broken into a small number of well-defined fragments closely oriented with each other. The fact that it (i) occurs after plastic deformation, particularly at slow rates of strain, (ii) shows sub-boundary structures, and (iii) produces a splitting of X-ray spots, makes it very probable that the cell-formation effect is an example of the phenomenon called *polygonization* by Cahn<sup>18</sup> and by Guinier and Lacombe.<sup>19</sup>

It may thus be concluded that at least four distinct processes, slipping, twinning, cell-formation, and movement along grain boundaries, are involved in the creep of polycrystalline zinc. At fast rates of strain, and low temperatures, slipping and twinning predominate and there is little movement at the grain boundaries; on the other hand, in prolonged tests, particularly at high temperatures, cell-formation and intense grain-boundary movements occur, although some slipping and twinning is observed in all cases.

#### VIII.—DISCUSSION.

*Analysis of the Creep Curve.*—It has been shown that Andrade's resolution of the strain/time curve into transient and steady-state components, increasing as  $t^{1/3}$  and  $t$ , respectively, can be applied successfully to the flow of both single crystal and polycrystalline specimens of zinc. It may be asked whether these components have an independent physical significance or whether they merely represent the two leading terms of a series expansion for the strain due to a single process. The different properties of transient and steady-state flow support the widely held view that they are in fact different processes.<sup>10, 15</sup> For example, steady-state flow is strongly dependent on temperature and, below a certain temperature range, becomes too slow to be detected. Transient flow, on the other hand, can always be produced by taking the stress above the elastic limit of the material, even at the lowest temperature.<sup>10, 15</sup>

*Transient Creep.*—An intriguing feature of transient creep is the consistency with which Andrade's  $t^{1/3}$  law is obeyed by a wide range of materials. It has long been known that several polycrystalline metals, of various crystal structures, follow the law. The present work has shown that single crystals of one metal, at least, also follow the law with considerable accuracy. What is perhaps even more striking is the observation of Filon and Jessop<sup>20</sup> that Andrade's law fits the transient creep of celluloid much more closely than any other of the several functions that they tried.



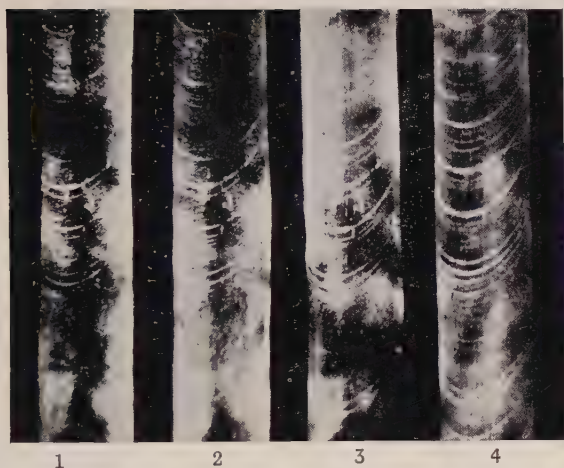


FIG. 11.—Photomicrographs of Zinc Single Crystal, showing slip bands observed at stages 1, 2, 3, and 4 of Fig. 10.  $\times 11$ .



FIG. 12.—Photomicrograph of Polycrystalline Zinc Specimen after 6.85% extension in 43 hr., showing formation of cell structures. ( $T = 100^{\circ}\text{C}$ .,  $\sigma = 1100\text{ g./mm.}^2$ ) Unetched.  $\times 350$ .

[To face p. 404.



FIGS. 13-16.—Photomicrographs of Polycrystalline Zinc Specimens in various stages of creep testing.

FIG. 13.—Structure before test. Etched in HCl.  $\times 130$ .

FIG. 14.—After 0.54% extension in 8 min. ( $T = 108^{\circ}\text{C.}$ ,  $\sigma = 1200\text{ g./mm.}^2$ ) Unetched.  $\times 140$ .

FIG. 15.—After 9.5% extension in 71.5 hr. ( $T = 108^{\circ}\text{C.}$ ,  $\sigma = 1050\text{ g./mm.}^2$ ) Unetched.  $\times 85$ .

FIG. 16.—As Fig. 15, but electropolished and etched in HCl.  $\times 360$ .

It might be argued that such agreement is fortuitous, and that insufficient precision in the determination of creep curves allows some latitude for roughly fitting an empirical formula of the right qualitative form. This seems unlikely. Filon and Jessop had no success with their other formulæ, all of which were of the right qualitative form. Moreover, the linear variation of the transient flow of zinc crystals with the cube root of time (cf. Fig. 4) shows that the true function must lie very close to  $t^{1/3}$ , even if it does not actually coincide with it.

If the validity of Andrade's law is accepted, then the wideness of its range of application must mean that the dependence of transient flow on time is determined by very general factors and not by the detailed internal structure of the specimen. Orowan<sup>15</sup> recognized this point and attempted to construct a theory of transient creep based on the very general assumptions that the specimen hardens linearly with strain, during the transient stage, and that this causes the activation energy for flow to increase, thereby slowing down the rate of flow. While this theory successfully and convincingly explained the occurrence of transient creep at very low temperatures, in terms of a vanishingly small activation energy at the start of flow, it was unable to account for the  $t^{1/3}$  law without the introduction of additional and less convincing assumptions. Recent attempts to refine Orowan's theory in other directions have also not led to Andrade's law.<sup>21, 22</sup> This raises what is perhaps the central difficulty facing the theory of transient creep. The wide application of Andrade's law shows that the theory must be cast in very general terms, involving only those factors such as work-hardening and thermal agitation which are common to all or most solids, and yet the form of the law,  $t^{1/3}$ , is not easily reconcilable with the exponential or logarithmic type of expression that usually results from such theories.

*Steady-State Creep.*—The wide occurrence of steady-state creep, characterized by a constant rate of flow, is not surprising since this type of flow must result whenever a material maintains a constant mechanical state during flow, and there are some very general ways in which this could happen. For example, it must happen whenever the internal structure of the material is unaffected by flow, as in the case of simple liquids; alternatively, changes in internal structure caused by flow (e.g. strain-hardening) may be balanced by spontaneous changes in the opposite direction (e.g. thermal softening), as envisaged in the recovery theory of creep.

Because of its very general character, steady-state creep in different materials, or even in different forms of the same material, cannot be assumed to be produced by the same underlying atomic processes.



It is more reasonable to expect that several processes can exist, which differ from each other except in the common characteristic of maintaining a constant mechanical state. This is borne out by the present work on single-crystal and polycrystalline specimens. Although equation (6) for the coefficient of flow is obeyed in both cases, the constants are quite different in magnitude. Furthermore, while in single crystals the flow is associated with glide on the slip planes, the essential feature in the case of polycrystalline specimens appears to be the displacement of neighbouring grains by slip along grain boundaries.

The occurrence of at least four processes, slip, twinning, cell-formation, and grain-boundary movements, makes the steady-state creep of the polycrystalline specimens much more complicated than that of the single crystals, and it is doubtful whether much can be gained by comparing the two cases. Twinning must take place in polycrystalline zinc if the structure is to accommodate a plastic strain, greatly exceeding the elastic strain, without fracturing; the number of orientations of shear by glide on the basal planes is insufficient to allow the grains to remain joined together when the metal is deformed by slip. Thus it was found necessary to apply (tensile) stresses of about  $1000 \text{ g./mm.}^2$ , which is in the range where twinning occurs in zinc<sup>23</sup> before the polycrystalline specimens could be made to flow freely, although the single crystals flowed rapidly under (shear) stresses of  $30\text{--}50 \text{ g./mm.}^2$ . In addition to introducing twinning and grain-boundary movements, the polycrystalline structure can affect the behaviour of the metal in a third way. Owing to the interference of neighbouring grains with each other, homogeneous deformation will hardly ever occur and in most grains lattice bending will be produced. Cahn<sup>18</sup> showed that single crystals of zinc only became polygonized on annealing if they had previously been bent; homogeneously deformed crystals did not show the phenomenon. The occurrence of the cell structure in polycrystalline creep specimens can therefore be understood as a consequence of the mutual interference of neighbouring grains.

## PART B.—STEADY-STATE FLOW AND RECOVERY OF SINGLE CRYSTALS.

### I.—INTRODUCTION.

Of the different kinds of flow observed in Part A, the steady-state flow of single crystals promised to be the easiest to understand. It is simpler than transient flow because it is defined by a constant rate of strain, at constant stress and temperature, implying that the mechanical

properties of the material remain constant during the flow. Furthermore, it appears to involve only slip on the basal planes, whereas in the corresponding flow of polycrystalline specimens several processes can be identified. It was thus decided to make a more detailed study of the steady-state flow of single crystals in the hope of determining the underlying mechanism.

## II.—THEORIES OF STEADY-STATE FLOW.

### 1. *The Constant-Barrier Theory.*

Two formal theories of plastic flow have been proposed which can be applied to the steady-state flow of a single crystal under constant stress. The first of these, which will be called the "constant-barrier" theory, has been proposed in various forms,<sup>24, 25, 26</sup> but in all cases is based on an argument of the kind used in the theory of the rates of chemical reactions;<sup>27</sup> it is also very similar to the early Becker theory of crystal plasticity.<sup>28</sup>

Suppose that, before an elementary unit of flow can take place, the atoms involved must pass through a configuration of higher free energy; also, that the activation energy  $U$  associated with this barrier is lowered by an amount  $a\tau$  in the direction of flow, when a stress  $\tau$  is applied, and raised by the same amount in the opposite direction. If  $a\tau$  is sufficiently large, the probability of flow occurring in the backward direction is negligible compared with that of forward flow. In this case, if each successful attempt to overcome the energy barrier causes, on average, the same amount of flow, the rate of strain will be :

$$\frac{d\gamma}{dt} = \nu e^{-\frac{U - a\tau}{RT}} \quad . \quad . \quad . \quad . \quad . \quad . \quad (7)$$

where  $\nu$  depends on the frequency of the attempts to overcome the barrier and upon the size of a unit of flow. This equation obviously resembles the empirical equation (6). However, it may reasonably be objected that, if the stress is large enough to make the backward flow negligible, one ought not to assume that it is so small as to affect the activation energy only through a linear term. It is preferable to replace  $U - a\tau$  by the undetermined function  $U(\tau)$ . The procedure used in deriving equation (6) may then be followed, giving the rate of strain as :

$$\frac{d\gamma}{dt} = \nu e^{-\frac{U(\tau_0) + a\tau_0}{RT}} e^{\frac{a\tau}{RT}} \quad . \quad . \quad . \quad . \quad . \quad . \quad (8)$$

where  $U(\tau_0)$  is the activation energy corresponding to the stress  $\tau_0$ .

The theory gives a constant rate of flow, at constant stress and



## 2. The Recovery Theory.

[illegible]

### 3. *A Unified Theory.*

Objections can be raised against both of the above theories. The assumption of an inherently constant energy barrier does not seem

reasonable. The simplest physical interpretation of the barrier is that it is caused by internal stresses, created by previous flow, which oppose the external stress. But these stresses ought to increase with increasing deformation in the absence of recovery, thereby increasing the energy barrier and slowing down the flow. Transient rather than steady-state flow is thus to be expected; in fact, this same idea has now become the starting point for recent theories of transient creep.<sup>15, 21, 22</sup>

On the other hand, the recovery theory contains the assumption that the yield stress is affected only by strain hardening and thermal softening. Orowan<sup>30</sup> has shown that the occurrence of certain dynamical effects in short-time tests, in particular the dependence of the yield stress on the rate of straining, contradicts this assumption. To explain such effects a theory of the constant-barrier type is required in which stress and rate of strain are directly related; thus Orowan was able to show that Becker's theory could explain the effects rather convincingly.

The nature of these objections suggests that a unified theory can be formulated, free from these difficulties, by starting from the constant-barrier theory and taking the simple step of regarding the barrier as being not inherently constant, but dependent on both strain-hardening and thermal softening.

Let  $\tau_i$  represent the mean internal stress and suppose for the moment that no softening can take place, i.e. that the rate of recovery :

$$r = - \left( \frac{\partial \tau_i}{\partial t} \right)_{\dot{\gamma}=0} \quad . \quad . \quad . \quad . \quad . \quad (10)$$

is zero. If a constant stress  $\tau \gg \tau_i$  is applied to the specimen, flow can occur without the aid of thermal fluctuations and the specimen will deform rapidly; thus  $\tau_i$  can be regarded as the "yield stress" of the material.<sup>15, 21</sup> As the specimen deforms strain-hardening will occur and  $\tau_i$  will increase at a rate determined by the coefficient of hardening :

$$h = \left( \frac{\partial \tau_i}{\partial \gamma} \right)_{\tau=0} \quad . \quad . \quad . \quad . \quad . \quad (11)$$

and the rate of strain. Thus  $\tau_i$  will increase above  $\tau$  so that an energy barrier  $U(\tau_i, \tau)$  will be created. This energy barrier has to be overcome with the aid of thermal fluctuations if flow is to continue, and the rate of flow will then be controlled by a Boltzmann relation of the type :

$$\frac{d\gamma}{dt} = \nu e^{-\frac{U(\tau_i, \tau)}{RT}} \quad . \quad . \quad . \quad . \quad . \quad (12)$$

The barrier  $U$  will increase with increasing strain so that successful fluctuations will become increasingly rare and the creep rate will

decrease. Thus, for a constant applied stress both the rate of creep,  $(\partial\gamma/\partial t)_{r=0}$ , and the rate of hardening,  $(\partial\tau_i/\partial t)_{r=0}$ , will decrease as  $\tau_i$  increases.

So far, this is essentially Orowan's theory of transient creep. Recovery is introduced into the theory by assuming that  $r$ , defined by equation (10), is not zero. Hence, when both strain-hardening and thermal softening are present :

$$\frac{d\tau_i}{dt} = \left(\frac{\partial\tau_i}{\partial t}\right)_{r=0} + \left(\frac{\partial\tau_i}{\partial t}\right)_{\dot{\gamma}=0} \quad . \quad . \quad . \quad (13)$$

Remembering that the rate of recovery increases with increasing strain-hardening, it will be observed that the terms on the right-hand side of this equation have opposite signs and vary in opposite directions with  $\tau_i$ . Thus a value  $\tau_1$  of  $\tau_i$  can be found at which  $d\tau_i/dt = 0$ . When the internal stress reaches this value a pure steady-state flow will occur, and equation (13) becomes equation (9) of the recovery theory, as can be seen by writing :

$$\left(\frac{\partial\tau_i}{\partial t}\right)_{r=0} = \frac{d\gamma}{dt} \left(\frac{\partial\tau_i}{\partial\gamma}\right)_{r=0} = \kappa h \quad . \quad . \quad (14)$$

Equation (13) also shows that a specimen which is not in the steady state will automatically adjust its rate of flow until the steady state is reached. For example, suppose that  $\tau_i < \tau_1$  in which case the rate of flow is faster than the steady-state value. Then :

$$\left(\frac{\partial\tau_i}{\partial t}\right)_{r=0} > -\left(\frac{\partial\tau_i}{\partial t}\right)_{\dot{\gamma}=0}$$

so that  $d\tau_i/dt$  is positive and  $\tau_i$  will increase; the rate of flow will therefore decrease and approach the steady-state value as  $\tau_i$  approaches  $\tau_1$ . The theory thus describes the transition from transient to pure steady-state flow. A similar argument can be applied to the case where  $\tau_i > \tau_1$  and shows that the rate of flow will increase towards the steady-state value.

#### 4. Theoretical Predictions.

When applied to short-time tests where recovery can be neglected, the unified theory is able to explain Orowan's dynamical effects in the same way that they can be explained from the constant-barrier theory; this follows from the fact that Becker's formula, which Orowan<sup>30</sup> used to explain the dynamical effects, is a special form of the more general expression for the rate of flow given in equation (12).

On the other hand, the unified theory becomes almost indistinguishable from the simple recovery theory when applied to steady-state flow, and equation (9) remains as the basic equation for recovery creep. The main difference is that the "yield stress" is now considered to be somewhat greater than the applied stress, during steady-state flow, instead of equal to it. This slightly modifies Orowan's prediction of an induction period after a small reduction in the applied stress. If  $\tau$  is suddenly reduced, the thermal vibrations are given the task of providing more intense stress fluctuations than before, in order to produce flow, so that the rate of flow will be reduced, in some cases practically to zero. However,  $d\tau_i/dt$  is now negative and  $\tau_i$  will slowly fall by recovery. As  $\tau_i - \tau$  diminishes, less intense stress fluctuations are required and the creep rate will increase, gradually approaching the steady-state value. Thus a smooth increase in the creep rate is to be expected rather than a sharp change from zero to the full steady-state value.

A feature of the theory is that two separate processes of thermal activation are required for producing steady-state flow. Flow actually occurs when the energy barrier  $U(\tau_i, \tau)$  is overcome, but a second thermal activation is required to produce the internal changes, associated with recovery, which keep the barrier constant. In the absence of a detailed theory of the atomic mechanisms involved it cannot be assumed that the activation energy is the same for both processes, or even that the processes are closely related. Which process actually controls the rate of steady-state flow? This can be decided by observing that the height of the barrier  $U(\tau_i, \tau)$  is not an independent variable during steady-state flow. Pure steady-state flow can only be obtained when the two expressions for the rate of flow, equations (9) and (12), are equal; if they are not equal, transient flow will occur until  $\tau_i$  and  $U(\tau_i, \tau)$  have changed to the steady-state values  $\tau_1$  and  $U(\tau_1, \tau)$ . Thus, whatever changes of temperature or stress are made, the final steady rate will always be determined by the value of  $r/h$ . Hence, for a fixed hardening coefficient, the rate of steady-state flow is controlled by the rate of recovery, and, unless  $h$  is strongly dependent on temperature, the activation energy for the flow should be the same as for recovery.

### *5. An Equation for Recovery.*

If the theory of steady-state flow is correct, it should be possible to derive an equation for recovery, giving the softening of a strain-hardened specimen in terms of the degree of hardening and the time and temperature of annealing, by applying the theoretical equations to the empirical

equation (6). For this purpose we first rewrite equation (6) in the form :

$$\kappa = Ae^{\frac{b\tau_i}{RT}} \quad . \quad . \quad . \quad . \quad . \quad . \quad . \quad . \quad (15)$$

where :

$$A = Ce^{-\frac{b\tau_0}{RT}} e^{-\frac{Q(\tau_0)}{RT}} e^{-\frac{b(\tau_i - \tau)}{RT}}.$$

There are theoretical reasons for expecting  $\tau_i - \tau$  to be small,<sup>15, 21</sup> and this conclusion is confirmed by experiments in which  $\tau$  is suddenly increased by a small amount during steady-state flow;<sup>31</sup> in the present work, for example, it has been observed that a sudden small increase in  $\tau$  ( $\simeq 5\%$ ) always produced a small instantaneous plastic extension, showing that  $1 < \tau_i/\tau < 1.05$ . Taking  $\tau_i - \tau \simeq 2$  g./mm.<sup>2</sup>,  $\exp[-b(\tau_i - \tau)/RT]$  is about 0.5; since  $C$  can be determined experimentally only in order of magnitude, it is thus a sufficient approximation to write :

$$A = Ce^{-\frac{b\tau_0}{RT}} e^{-\frac{Q(\tau_0)}{RT}} \quad . \quad . \quad . \quad . \quad . \quad . \quad (16)$$

Substituting  $\kappa = -\frac{1}{h} \left( \frac{\partial \tau_i}{\partial t} \right)_{\dot{\gamma}=0}$  into equation (15) gives a differential equation for  $\tau_i$ , which has the solution :

$$\tau_i(t) = -\frac{RT}{b} \log_e \left[ \frac{bAh}{RT} (t + t_0) \right] \quad . \quad . \quad . \quad (17)$$

where  $\tau_i(t)$  is the yield stress of the material at time  $t$ , and  $t_0$  is an integration constant. This equation should describe the softening of a strain-hardened specimen during an annealing experiment. The physical interpretation of  $t_0$  is made clear by substituting  $t = 0$  in the equation, i.e. :

$$\tau_i(0) = -\frac{RT}{b} \log_e \left( \frac{bAh}{RT} t_0 \right) \quad . \quad . \quad . \quad . \quad (18)$$

Since  $\tau_i(0)$  represents the initial yield stress of the hardened specimen, before any recovery has taken place,  $t_0$  is determined by the initial degree of strain-hardening. Introducing  $\tau_i(0)$ , equation (17) can be reduced to :

$$\tau_i(t) = \tau_i(0) - \frac{RT}{b} \log_e \left( \frac{t}{t_0} + 1 \right), \quad . \quad . \quad . \quad (19)$$

which is the simplest form for the equation of recovery. This shows that the yield stress should decrease logarithmically with the time of annealing, starting from the value  $\tau_i(0)$ ; the rate of softening is controlled by the factor  $t_0$ , the magnitude of which depends upon the temperature of annealing, the degree of strain-hardening, and the properties of the





The first curve gives the creep of crystal *A* under a shear stress of 43.2 g./mm.<sup>2</sup>. At the point *P* the stress was reduced to 40.5 g./mm.<sup>2</sup>, and the behaviour of the specimen after this is given by curve 2; here a new origin has been taken, for convenience, starting from *P*. Fig. 18 shows similar curves taken on specimens *B* and *C* after reducing the stress. The details of the experiments are given in Table V.

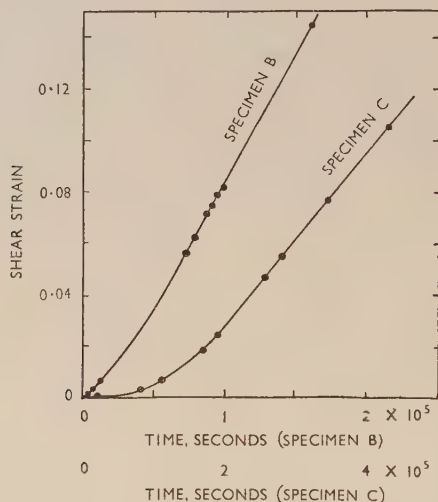


FIG. 18.—Strain/Time Curves on Specimens *B* and *C* after reducing the stress.

TABLE V.—Details of Experiments on the Reduction of Stress During Creep.

Specimen	$\alpha$	$\lambda$	$T, ^\circ\text{C.}$	Resolved Shear Stress, g./mm. <sup>2</sup>	
				Initial Value	Reduced Value
A	33°	41°	20	43.2	40.5
B	44°	45°	36.5	49.5	46.5
C	14°	23°	82	27.7	26.3

The results of these and similar experiments showed that reducing the stress during the steady-state stage caused the rate of flow to fall instantly to a much lower value and then to increase again gradually until a new steady state was reached. A smooth increase to the steady state was always observed and, because of this, the ends of the induction periods were too indefinite to allow the lengths of these periods to be measured with accuracy. Rough measurements showed that between

5 and 20 hr., depending on the reduction of stress, were needed for the steady state to be recovered at room temperature.

Induction periods of a very similar kind have been observed recently by Carreker, Leschen, and Lubahn,<sup>31</sup> when studying the effects of sudden changes of stress on the creep behaviour of lead and copper.

*Approximate Rates of Recovery.*—By using the relation  $r = h\kappa$  to calculate the rate of recovery from the creep rate, an estimate can be made of the expected length of an induction period. Comparison with observed periods thus allows the relation to be roughly tested.

It is first necessary to know the magnitude of  $h$ . From published results,<sup>2</sup> it can be deduced that  $h$  is about 240 g./mm.<sup>2</sup> for zinc crystals. A few tensile experiments were made on some of the present specimens and, from the slopes of the stress/strain curves, values of  $h$  in the range 200–400 g./mm.<sup>2</sup> were observed. No doubt  $h$  depends on temperature, but this should be negligible in comparison with the great temperature dependence of  $\kappa$ ; accordingly, a standard value of  $h = 250$  g./mm.<sup>2</sup> will be assumed.

The mean rate of steady-state flow for the curves of Fig. 17 is  $3 \times 10^{-7}$  sec.<sup>-1</sup>. With  $h = 250$  g./mm.<sup>2</sup>, the equivalent rate of recovery is  $r = 7.5 \times 10^{-5}$  g./mm.<sup>2</sup>/sec. The induction period should be approximately the time required for the yield stress to fall, with recovery, by the same amount as the applied stress. In the case of Fig. 17 the stress was reduced by 2.7 g./mm.<sup>2</sup>, thus giving an expected induction period of  $2.7/(7.5 \times 10^{-5})$  sec., i.e. 10 hr., which is in fair agreement with the observed one. Similar computations for specimens *B* and *C* give induction periods of 3 and 5 hr., respectively.

Thus, although this method does not allow the relation to be rigorously tested, it shows that the rate of recovery is of the right order of magnitude to account for the observed rates of steady-state flow.

#### IV.—EXPERIMENTS ON RECOVERY.

*Method.*—To test the theory further a series of experiments was made on the recovery of strain-hardened crystals. The critical shear stress, defined as that resolved shear stress in the glide plane along the glide direction at which plastic deformation can be first detected in a standard tensile test, was chosen as the most suitable property to measure for determining the recovery. The procedure adopted was to harden a crystal a standard amount by extending it in tension until its glide plane was subjected to a certain shear stress; the crystal was then unloaded, annealed at a standard temperature for a certain time, and tested in tension to determine its critical shear stress. This procedure was re-

peated several times on the same specimen, using different times and temperatures of annealing, until enough information on the recovery of the specimen had been gained. Making a complete set of measurements on the same specimen had the advantage of eliminating errors due to lack of reproducibility from one specimen to another, but meant that, in order to make as many tests as possible, the total strain and hence strain-hardening applied in any one test had to be kept small.

All tests were made on a small tensile machine, constructed specially for work on single crystals, which was based on the machine designed by Polányi.<sup>33</sup> An approximately constant rate of extension of about  $10^{-4}$  in./sec. could be applied, and the stress and extension could be measured to within  $0.5$  g./mm.<sup>2</sup> and  $10^{-4}$  in., respectively. All tests

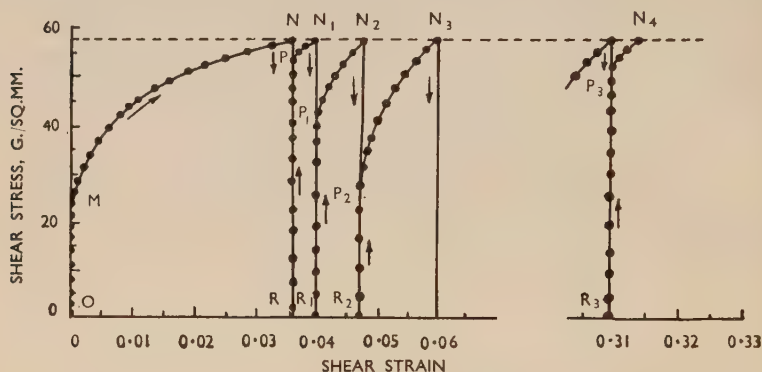


FIG. 19.—Stress/Strain Curves after different annealing treatments (see text).

were made at room temperature. During annealing the specimens remained mounted on the machine and were immersed in paraffin in a Dewar flask. The annealing temperature was held constant to within  $1.5^{\circ}$  C.

Fig. 19 shows the type of results obtained. The primary stress/strain curve of the crystal is given by  $OMN$  which shows that the critical shear stress,  $M$ , was initially  $23$  g./mm.<sup>2</sup> At the point  $N$  the crystal was unloaded to  $R$  and immediately reloaded, giving in this case the curve  $RPN_1$ . It should be noticed that the critical shear stress,  $P$ , of the hardened crystal was only  $54$  g./mm.<sup>2</sup>, in spite of the fact that the crystal was loaded up to  $58$  g./mm.<sup>2</sup> This effect is common in tensile testing. Orowan<sup>30</sup> has argued that it is not due to thermal softening because there is not enough time for this to occur, but is a dynamical effect which can be explained from a flow equation of Becker's type (cf. equation (12)).

After unloading to  $R_1$  the crystal was annealed for 5 min. at  $56^\circ \text{C.}$ ; the subsequent curve  $R_1P_1N_2$ , shows that it had partly recovered as a result of this treatment. More extensive annealing, for 30 min. at  $170^\circ \text{C.}$ , gave the curve  $R_2P_2N_3$  which shows that the specimen then regained its original critical shear stress. It is to be noted that, although the specimen had fully recovered its critical shear stress, the stress/strain curve is steeper than the original one. This effect has been observed previously<sup>32</sup> and explained by assuming the existence of different activation energies for recovery in different parts of the specimen; some parts remain fairly hard while others become fully softened.

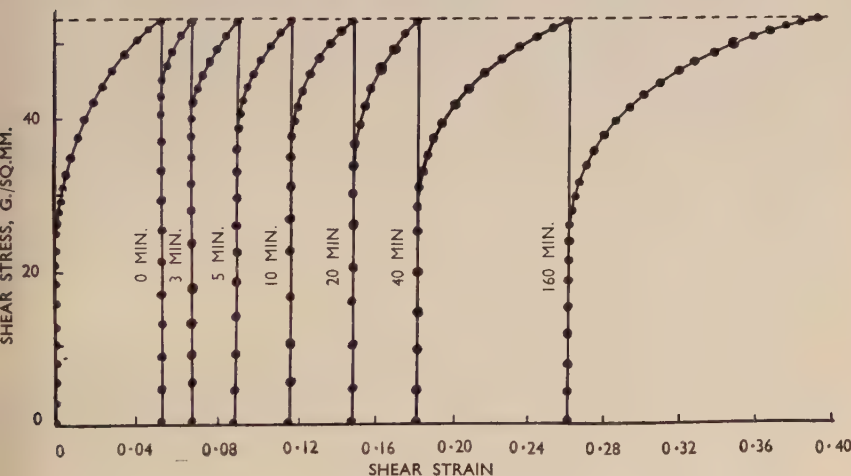


FIG. 20.—Effect of Time of Annealing at  $60^\circ \text{C.}$  on the stress/strain curve of a hardened crystal.

The final curve,  $R_3P_3N_4$ , was taken after the fifteenth test on the crystal and shows that the dynamical softening effect is reproducible.

**Results.**—As an example of the influence of time of annealing on the stress/strain curve, Fig. 20 shows a set of curves taken after various periods of recovery at  $60^\circ \text{C.}$  It will be observed that recovery is rapid at first and slows down as the specimen becomes softer.

Figs. 21 and 22 show the variation of the critical shear stresses of two crystals with time of annealing at different temperatures. The experimental points in each diagram have been brought into approximate coincidence by suitably adjusting the time scales, through their  $t_0$  values, for the two annealing temperatures. The continuous curves have been constructed from equation (19) by choosing suitable values for the parameters  $\tau_i(0)$ ,  $b$  and  $t_0$ ; these values are given in Table VI.



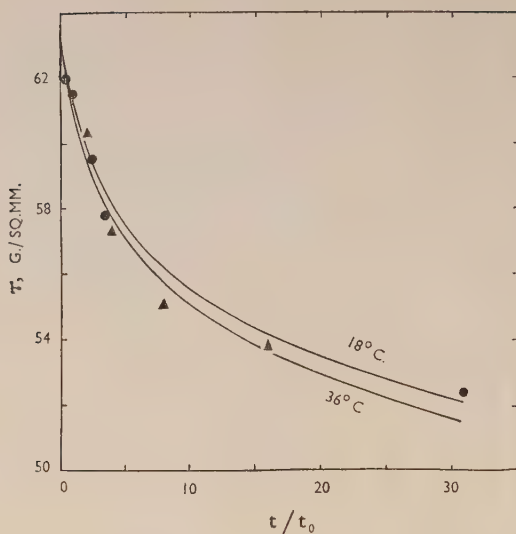


FIG. 21.—Recovery of the Critical Shear Stress with time of annealing.

● 18° C. ( $t_0 = 30$  min.).      ▲ 36° C. ( $t_0 = 2.5$  min.).

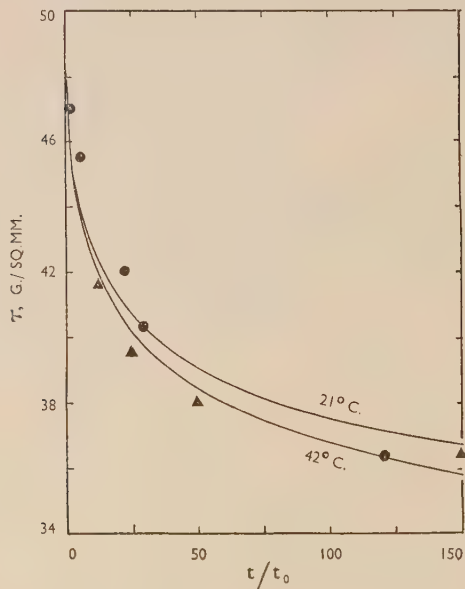


FIG. 22.—Recovery of the Critical Shear Stress with time of annealing.

● 21° C. ( $t_0 = 8.5$  min.).      ▲ 42° C. ( $t_0 = 0.4$  min.).

TABLE VI.—Values of Parameters for Fitting Equation (19) in Figs. 21 and 22.

Fig. No.	$\tau_0(0)$ , g./mm. <sup>2</sup>	$b$ , $\frac{\text{cal.}}{\text{g.-mol.}} \cdot \frac{\text{mm.}^2}{\text{g.}}$	T, °K.	$t_0$ , min.
21	64	185	$\begin{cases} 291 \\ 309 \end{cases}$	$\begin{matrix} 30 \\ 2.5 \end{matrix}$
22	48	260	$\begin{cases} 294 \\ 315 \end{cases}$	$\begin{matrix} 8.5 \\ 0.4 \end{matrix}$

It is to be noted that the presence of the factor  $RT/b$  in equation (19) makes it necessary to construct a separate curve for each temperature; the equation cannot be represented by a single master curve.

*Quantitative Comparison with Steady-State Flow.*—The approximate agreement with the experimental results in Figs. 21 and 22 provides some justification for using equation (19) as the equation for recovery. In this case it should be possible, starting from the numerical values of the constants in the equation, to derive a set of parameters for recovery equivalent to those for steady-state flow in equation (6). In the first place, the parameter  $b$  is the same in both equations, and the two values, 185 and 260, obtained from the recovery experiments (cf. Table VI) lie within the range, 150–300, derived from the creep experiments.

The activation energy for recovery can be deduced from the values of  $t_0$  at different temperatures. By substituting for  $A$ , defined as in equation (15), equation 18 can be rewritten in the form :

$$\log_e \left( \frac{t_0}{T} \right) = \frac{Q(\tau_0) + b(\tau_0 - \tau)}{RT} - \log_e C - \log_e \left( \frac{bh}{R} \right) \quad (21)$$

Over the narrow range of temperature studied  $\log(bh/R)$  can be regarded as constant, so that :

$$\log_e \left( \frac{t_0'}{T'} \cdot \frac{T''}{t_0''} \right) = \frac{Q(\tau_0) + b(\tau_0 - \tau)}{R} \left( \frac{1}{T'} - \frac{1}{T''} \right) \quad (22)$$

where  $t_0'$  and  $t_0''$  are the values of  $t_0$  corresponding to the temperatures  $T'$  and  $T''$ . Substituting for  $t_0$ ,  $T$ ,  $b$ , and  $\tau$  from Table VI, and taking  $\tau_0 = 35$  g./mm.<sup>2</sup> (as in the case of the creep results), thus enables  $Q$  to be determined. Applying this procedure to the two sets of results in Figs. 21 and 22 gives in both cases the value 30,500 cal./g.-mol. for the activation energy associated with a stress of 35 g./mm.<sup>2</sup> This agrees well with the range of values, 28,000–30,000 cal./g.-mol., determined from the creep experiments.

The frequency factor  $C$  can be found by substituting numerical

values for the various quantities in equation (21) and values of  $C$  in the range  $10^{14}$ – $10^{15}$  sec.<sup>-1</sup> are then obtained. These are rather higher than the values,  $10^{10}$ – $10^{13}$ , given by the creep results, but this difference is of little significance in view of the fact that the order of magnitude of  $C$  can be changed by a small error in  $Q$ . Thus, since  $Q$  can only be accurate to about 10%,  $C$  cannot be determined to within two powers of ten.

#### V.—DISCUSSION.

The agreement which has been obtained between the results of the creep and the recovery experiments, together with the evidence on induction periods, justifies the view that the steady-state flow of zinc crystals is a result of a balance between strain-hardening and thermal softening.

It is interesting to consider some of the factors in the empirical equation (6) for steady-state flow from the point of view of the recovery theory. The frequency factor  $C$  is very large. It would not be easy to explain its magnitude on a theory of the constant-barrier type, where  $C$  would have to be interpreted as the expression of the frequency of attempting to overcome the barriers opposing glide and of the size of the elementary glide process produced by each successful attempt. In the recovery theory, however,  $C$  is a derived constant, determined from the rates of recovery and strain-hardening; it is not limited in magnitude by, or even simply related to, the frequency of attempting to overcome the obstacles to glide. If a specimen is to flow at a steady rate, then the recovery theory requires that it should always flow fast enough for the rate of strain-hardening to keep up with the rate of softening, quite independently of whether there is a limit to the frequency with which glide processes can be generated. If there is such a limit then one would expect the rate to be no longer controlled by the rate of recovery in the case of extremely fast steady-state flows. Under ordinary testing conditions, however, the limiting factor is the slowness of the recovery process. This means that the barriers remain sufficiently high to ensure that only a few of the attempts to scale them are successful.

The part played by the applied stress in steady-state flow deserves some attention. The stress will undoubtedly affect the height of the barriers, as envisaged in the constant-barrier theory, and it is through this kind of action that transient effects caused by sudden changes of stress can be explained. However, it is not in this way that the stress affects the rate of steady flow because, during this flow, the height of the barriers is controlled ultimately by the rate of recovery and the co-efficient of strain-hardening. The action of the stress on the steady-

state flow appears to be indirect, working through its action on the rate of recovery. Even in the case of recovery there is no evidence for a direct action of the stress. According to the present interpretation of the theory, the stress merely determines the intensity of strain-hardening in the material, and it is the latter rather than the stress itself which controls the rate of recovery, and hence the rate of steady flow.

The recovery theory of creep is a formal theory in the sense that it makes no assertions concerning the details of the atomic mechanisms involved, but instead is concerned with showing how a complex process, steady-state flow, can be resolved into two separate and simpler processes, strain-hardening and thermal softening. It thus suggests that further progress towards an understanding of steady-state flow is more likely to be made by studying the processes of hardening and softening separately, rather than by studying the creep process itself, where they occur together.

#### ACKNOWLEDGEMENTS.

This research was carried out in the Metallurgy Department of the University of Birmingham, under the general supervision of Professor D. Hanson, to whom the authors' thanks are due for his interest and support. The authors must acknowledge the useful advice they have received from Dr. E. Orowan and Dr. S. Harper concerning the preparation and handling of single crystals, and the assistance of Dr. B. A. Bilby and Mr. H. Hatton, who designed and constructed the apparatus for making tensile tests. Generous financial assistance has been given by the Department of Scientific and Industrial Research and by the Director-General, Sumer Bank, Ankara.

#### REFERENCES.

1. E. N. da C. Andrade and B. Chalmers, *Proc. Roy. Soc.*, 1932, [A], **138**, 348.
2. E. Schmid and W. Boas, "Plasticity of Crystals, with Special Reference to Metals" (translation of "Kristallplastizität"). London: 1950 (F. A. Hughes & Co., Ltd.).
3. C. F. Elam, "Distortion of Metal Crystals". Oxford: 1936 (Oxford University Press).
4. E. N. da C. Andrade and R. Roscoe, *Proc. Phys. Soc.*, 1937, **49**, 152.
5. A. H. Cottrell and V. Aytekin, *Nature*, 1947, **160**, 328.
6. E. Orowan, private communication.
7. C. S. Barrett, "The Structure of Metals". New York: 1943 (McGraw-Hill Book Co., Inc.).
8. C. S. Barrett and L. H. Levenson, *Trans. Amer. Inst. Min. Met. Eng.*, 1940, **137**, 76, 112.
9. H. L. Burghoff and C. H. Mathewson, *Trans. Amer. Inst. Min. Met. Eng.*, 1941, **143**, 45.
10. E. N. da C. Andrade, *Proc. Roy. Soc.*, 1910-11, [A], **84**, 1; 1914, [A], **90**, 329.
11. P. Ludwik, *Physikal. Z.*, 1909, **10**, 411.
12. W. Rosenhain and J. C. W. Humphrey, *Proc. Roy. Soc.*, 1909-10, [A], **83**, 200.

13. D. Hanson and M. A. Wheeler, *J. Inst. Metals*, 1931, **45**, 229.
14. D. Hanson, *Trans. Amer. Inst. Min. Met. Eng.*, 1939, **133**, 15.
15. E. Orowan, *J. West Scotland Iron Steel Inst.*, 1946-47, **54**, 45.
16. J. L. Rodda, *Min. and Met.*, 1943, **43**, 323.
17. G. R. Wilms and W. A. Wood, *J. Inst. Metals*, 1948-49, **75**, 693.
18. R. W. Cahn, *Phys. Soc. : Rep. Conf. on Strength of Solids*, 1948, 136 (discussion).
19. A. Guinier and P. Lacombe, *Métaux et Corrosion*, 1948, **23**, 212.
20. L. N. G. Filon and H. T. Jessop, *Phil. Trans. Roy. Soc.*, 1928, [A], **223**, 89.
21. N. F. Mott and F. R. N. Nabarro, *Phys. Soc. : Rep. Conf. on Strength of Solids*, 1948, 1.
22. C. L. Smith, *Proc. Phys. Soc.*, 1948, **61**, 201.
23. R. F. Miller, *Trans. Amer. Inst. Min. Met. Eng.*, 1936, **122**, 176.
24. W. Kauzmann, *Trans. Amer. Inst. Min. Met. Eng.*, 1941, **143**, 57.
25. F. Seitz and T. A. Read, *J. Appl. Physics*, 1941, **12**, 100, 170, 470, 538.
26. S. Dushman, L. W. Dunbar, and H. Huthsteiner, *J. Appl. Physics*, 1944, **15**, 108.
27. H. Eyring, *J. Chem. Physics*, 1936, **4**, 283.
28. R. Becker, *Physikal. Z.*, 1925, **26**, 919.
29. R. W. Bailey, *J. Inst. Metals*, 1926, **35**, 27.
30. E. Orowan, *Z. Physik*, 1934, **89**, 614.
31. R. P. Carreker, J. G. Leschen, and J. D. Lubahn, *Trans. Amer. Inst. Min. Met. Eng.*, 1949, **180**, 139.
32. D. Kuhlmann, G. Masing, and J. Raffelsieper, *Z. Metallkunde*, 1949, **40**, (7), 241.
33. M. Polányi, *Z. techn. Physik*, 1925, **6**, 121.



## MECHANISM OF PRIMARY CREEP IN METALS.\*

1258

By W. A. WOOD,† D.Sc., MEMBER, and R. F. SCRUTTON,‡ B.Sc.

## SYNOPSIS.

Previous work on the deformation of metals at elevated temperatures had shown that the grains dissociated into a sub-structure of elements whose size tended to an equilibrium value depending on the temperature of deformation and rate of strain, and this equilibrium condition was identified with secondary creep. The process of breakdown itself appeared therefore to be associated with primary creep, and the details of this process have been studied in the present work on annealed aluminium. It is shown that the mode of breakdown is determined by the rate of strain. At the higher rates, the dissociation of the grain is accompanied by a disordering of the structure which is then removed on continued deformation to reveal the fundamental sub-structure; this is referred to as a two-stage recovery mechanism and is associated with a progressive softening of the metal. At the lower rates, the dissociation of the grain proceeds directly without intermediate disordering; this is referred to as the cell mechanism and is associated with a progressive hardening of the initially annealed grains until the equilibrium of the secondary phase is reached. The actual primary creep curve is regarded as the resultant of the two mechanisms.

## I.—INTRODUCTION.

IN recent papers, evidence has been advanced for the view that plastic deformation reduces the metallic grain to a sub-structure of elements whose size largely determines the mechanical strength.<sup>1</sup> At temperatures and stresses leading to creep, it has been found that the size of the elements approaches an equilibrium value that depends on the temperature and rate of deformation; and the attainment of this equilibrium is identified with the onset of secondary creep.<sup>2, 3</sup> It follows that the preceding breakdown in the grains should be associated with primary creep, and that a detailed study of the process should throw some light on the mechanism of this initial phase of creep. The present experiments have been made with that object in view.

It was desired also to compare this sub-structure, formed while the metal is under stress at an elevated temperature, with the type of sub-structure revealed on heating a metal that has been stressed previously by cold working, which has been studied in particular by Crussard,<sup>4</sup> Cahn,<sup>5</sup> and Guinier and Lacombe.<sup>6</sup> The sub-structure formed by this

\* Manuscript received 29 December 1949.

† Acting-Professor of Metallurgy Research, Baillieu Laboratory, University of Melbourne, Australia.

‡ Baillieu Laboratory, University of Melbourne, Australia.

two-stage process, in which deformation and heat-treatment are applied in sequence, has been attributed to the disruptive action of heat on regions of marked lattice bending or distortion produced in the previous deformation, an effect for which Orowan has proposed the self-descriptive term *polygonization*. It has been suggested that the same process gives rise to the sub-structures observed in creep.

This type of explanation, however, raises obvious difficulties and is likely to lead to confusion. For there is no reason to suppose that hot working produces the same form of distortion as cold working, if indeed it produces any at all. In fact in aluminium, on which most of this work has been done, the X-ray line-broadening that is supposed to be the sign of lattice distortions in the cold-worked metal does not occur at the usual temperatures of creep testing. Further, it is difficult to see how the irregularity that must characterize the distortion of a cold-worked polycrystalline metal can give rise to the regular size of sub-structure observed in creep, especially a size that depends on the rate of strain. Finally, the mechanism of deformation itself alters with temperature; for as the temperature is increased and the rate of strain decreased, it is found that the elements of the sub-structure systematically become larger; and with increasing size of the elements, the slip lines become more widely spaced until they disappear altogether. Thus the slip process is superseded by a different mode of deformation, which has been termed the "cell mechanism".

These considerations suggest strongly that the sub-structure associated with this mechanism can hardly be that associated with slip, or with what might be termed a polygonized slip structure; that, in fact, the cell mechanism is a distinct process. It is evident, however, that this issue would be clarified by comparison of the formative stages of the two types of sub-structure under comparable experimental conditions, and such comparisons therefore are included in the present investigations.

## II.—EXPERIMENTAL METHODS.

The test material was aluminium of 99.98% purity, similar to that used in the previous work, and the procedure, as before, involved X-ray diffraction and metallographic examination of specimens deformed progressively at various temperatures. The arrangements differed, however, in that in the present experiments this examination could be made while the specimens were still deforming at the test temperature.

For this purpose a compact tensile-testing apparatus was constructed and mounted before the window of an X-ray tube. For the creep tests, a constant load was applied to the specimen through a

lever system; and the specimen was surrounded by a small furnace, which contained one aperture through which an X-ray back-reflection photograph could be taken from the front of the specimen, and a second aperture on the opposite side through which the rear surface of the specimen could be observed by a microscope. The temperature of the specimen was controlled by means of thermocouples; but the actual value was determined from measurement of the lattice spacing and knowledge of the coefficient of thermal expansion. The temperature could be measured to  $\pm 2^\circ$  C., and variations could be detected well within this limit; but the main advantage of the method was that the region on the surface that defined the temperature was also the region in which the structural changes were observed. The specimens themselves were in the form of flat tensile specimens with parallel gauge-length  $1\frac{3}{4} \times 0.2$  in. and 0.06 in. thick, and for most of the work they had an average grain-size of  $10^{-3}$  cm.

An essential requisite was that the specimens should be initially in the annealed condition and that the grains should give sharp reflection spots that were clearly separated on the diffraction rings; otherwise the elongation of the spots into arcs, which accompanies deformation, led to undue overlapping and obscured the fine structure developed in the arcs as the grains broke down. It was necessary therefore to adjust the size of the incident beam to the grain-size of the specimen, and it was also helpful to limit the number of reflecting grains by using a stationary specimen; the specimen could be oscillated, however, when it was desired to measure the diameter of the diffraction rings accurately for lattice-spacing determinations.

Another feature was that the apparatus was fixed, relatively to the X-ray tube, so that the same region on the specimen was continually under observation; thus the same reflections often appeared in the X-ray photographs until continued extension of the specimen caused too great a change in orientation of the reflecting grains. Similarly, in the metallographic examination, for which the specimens were electropolished before testing, the observations were made on the same grains by using a microscope which also was fixed relatively to the apparatus. The possibility of viewing progressive changes in given grains by both X-ray and the microscope greatly facilitated interpretation of the observations. It might be added that the X-ray photographs required exposures of  $\frac{1}{4}$ – $\frac{1}{2}$  hr. and therefore represented an average of the changes over a period of deformation; but since these changes occur slowly at the creep rates that are of interest, this point was not important in practice.

## III.—MODES OF FORMATION OF SUB-STRUCTURES.

In this Section the development of a sub-structure by the two-stage recovery process is contrasted with the formation of a sub-structure by creep. The former process has already been studied by other workers, but in order to make the required comparisons it was desirable to produce the effect under the present conditions of experiment. It is illustrated, therefore, by relevant photomicrographs and X-ray photographs, the latter showing the (420) back-reflections obtained with cobalt  $K_\alpha$  radiation at a specimen-film distance of 10 cm.

It is convenient to consider the recovery process first, and to emphasize the two separate stages.

(a) *The Normal Two-Stage Process of Recovery.*

(i) *Cold-Worked Stage.*—The effects of this first stage are shown in the X-ray photographs by an elongation of the initially sharp reflection spots into diffuse arcs. This process is now well known, but it is important to recognize the extent of the change even in the earliest stages of deformation. The magnitude is evident from Figs. 2-5 (Plate XLV), which correspond respectively to a specimen in the initial state and after 1%, 3%, and 5% extension.

It is interesting also to note the changes in corresponding reflection spots. Not all reflections persist in the above photographs because the intervals in the extensions are too large, but some that do so are marked by arrows. These suffice to indicate that in practice the initial reflections usually split into strong and often sharp reflection spots, which then are linked by the diffuse continuous arc. The spread of the arcs thus formed proves, of course, that each of the original grains breaks down into a disoriented structure that reflects over an extended angular range; but the irregular intensity distribution and particularly the strong spots indicate that the broken-down grain includes relatively perfect fragments. The accompanying diffuse line, due presumably to the material between these fragments, would be attributed by many workers to a distorted but continuous connecting lattice; but as far as the photographic effects are concerned, it could be explained equally well by an intermediate debris of crystallites of size  $10^{-4}$ – $10^{-5}$  cm. In order to avoid a precise distinction for the time being, it will be convenient to include both these alternatives in the general term of "disordered" material.

Then, in the first stage, the first feature of special significance is the evident magnitude of the disordered material that accompanies quite small extensions of a test specimen. The second feature, which



it is hardly necessary to emphasize, is that this extensive type of disordering is inevitably accompanied by the usual sharp and closely spaced slip lines in the microstructure; Fig. 7 (Plate XLV) is a typical example for the present material.

(ii) *Recovery Sub-Structure.*—The second stage of the normal recovery process is the heat-treatment that reveals a sub-structure in the original cold-worked grains. The explanation depends on the manner in which the previously deformed state is pictured. If the disordered material is associated with a bent but continuous lattice, then the explanation of polygonization might apply. If, however, the disordered material is associated with a crystallite formation, the sub-structure would be revealed as a result of the progressive absorption of crystallite debris into the coarser fragments that are also formed in the early stages of deformation, and to which, therefore, the sub-structure should roughly correspond.

As noted by the authors already mentioned, this second stage is shown by the formation in the continuous diffraction arcs of separate reflection spots that appear to grow in intensity at the expense of the background of continuous line, and thus to stand out in greater contrast as the test specimen is progressively heated. Under the back-reflection conditions standardized for the purpose of the present comparisons, the effect is illustrated by Figs. 5 and 6 (Plate XLV); these correspond to a specimen extended 5% at room temperature and then heated for 2 days at 350° C. It will be seen from the latter figure, however, that the continuous diffraction line is not completely removed, with the result that the reflection spots appear diffuse. It is the present authors' experience that this peripheral diffusion is never completely removed before recrystallization; a residual disordering of the structure always appears to accompany the sub-structures obtained by the two-stage process of recovery from deformation by slip at room temperature. This point is of interest in comparison with the sub-structures involved in the cell mechanism.

The recovery process, as normally understood, therefore involves in effect the formation by the slip mechanism of a considerable proportion of disordered material as a first stage; and then, as a second stage, the partial removal of this disordering in such a way as to form, or possibly merely to reveal, relatively perfect elements of a sub-structure in the grain.

(b) *Development of Sub-Structure by Simultaneous Deformation and Heating.*

It is next possible to compare the above two-stage process with the processes involved in development of a sub-structure when de-



formation and heating occur simultaneously, as in creep. These processes were studied by choosing given temperatures, which were comparable with the temperatures used in recovery experiments, and considering the structural changes in specimens under loads that produced primary creep at different average rates. The observations led to the following conclusions.

(i) The first or disordered stage is progressively inhibited as the average rate of primary creep is smaller. When the rate is sufficiently small there is no disordered state at all; the grain dissociates into a sub-structure direct.

(ii) As the initial disordering becomes less marked with the decrease in creep rate, the slip lines become fewer and more irregular in direction; and when there is no initial disordering, the slip process is replaced by the "slip-less" cell mechanism of deformation.

(iii) Unless the creep rate is very rapid, any initial disordered state is removed by the time the primary phase of creep is completed, and further deformation can proceed without any disordering whatsoever. The final sub-structure, whether preceded by disordering or not, is always larger and more perfect than that associated with the recovery process from deformation at room temperature, whatever the recovery temperature.

The evidence for the above points is illustrated by photographs showing the structural changes in three specimens that typify, respectively, a relatively rapid, a medium, and a slow average rate of primary creep at 290° C. These are the specimens that correspond to the primary creep curves marked *A*, *B*, and *C* in Fig. 1. Observations were made on other specimens and at other temperatures of testing, but they fall into the same general pattern as those discussed below.

*Specimen A* (Rapid rate, load 941 lb./in.<sup>2</sup>, temperature 290° C.).—Fig. 8 (Plate XLVI) is the X-ray photograph of the annealed state and illustrates the initial sharpness of the reflection spots. Fig. 9 (Plate XLVI) indicates the state of the specimen after some 5% extension in 1 hr.; it shows that the sharp spots have become short irregular arcs, and therefore that a distinct disordering has developed. Fig. 10 (Plate XLVI) then shows that continued deformation, here to 6% in 3 hr., removes the disordering and results in a clearly marked sub-structure. It will be noted, however, that the disordering which preceded this sub-structure is less marked than that which characterizes comparable deformation at room temperature. Thus this series serves to demonstrate the beginning of an inhibition of the factor of disordering. This change is also reflected significantly in the microstructure, which

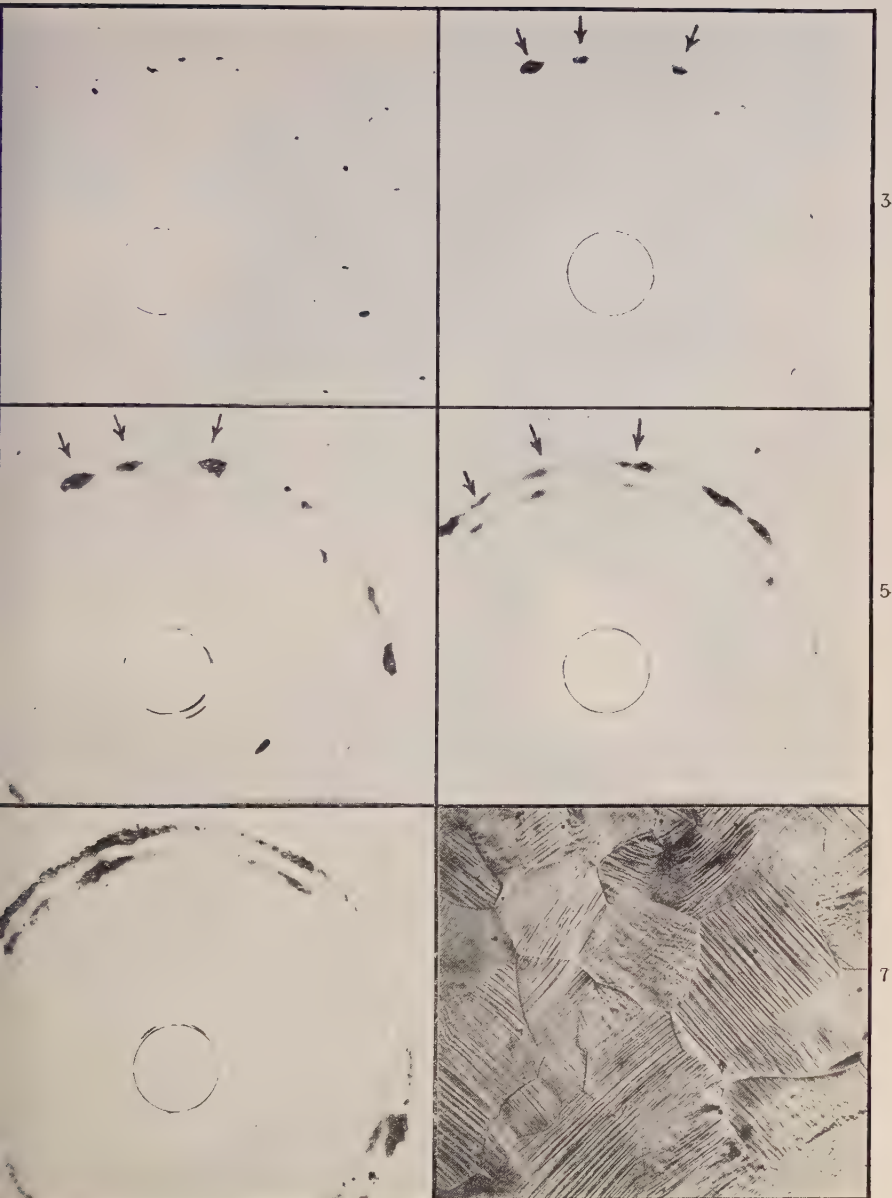


FIG. 2.—Annealed specimen before extension.

FIGS. 3, 4, 5.—After 1%, 3%, and 5% extension cold.

FIG. 6.—After 5% extension cold and heating for 2 days at 350° C.

FIG. 7.—Microstructure after 5% extension.  $\times 100$ .

[To face p. 428.

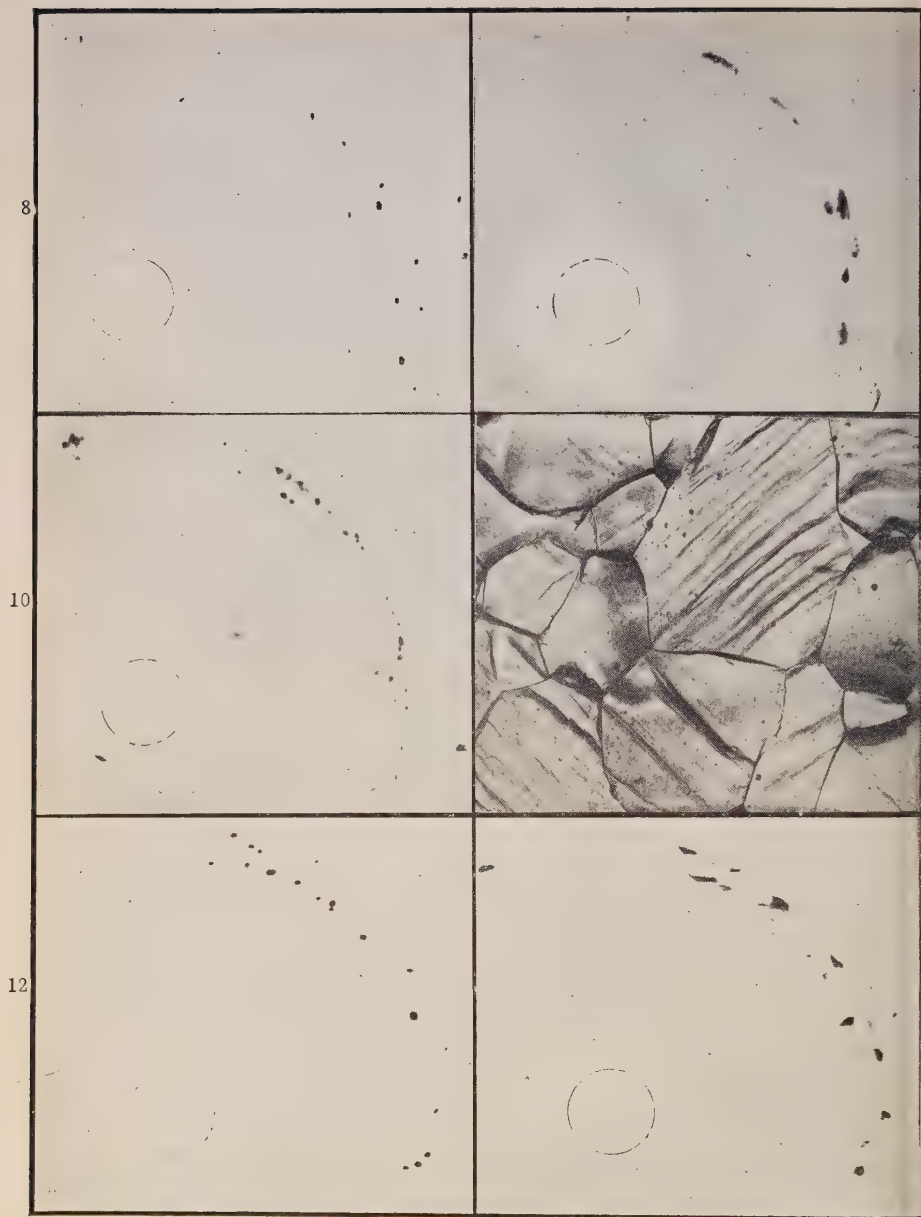


FIG. 8.—Annealed state of Specimen *A* (see text, p. 428).

FIG. 9.—After “rapid” creep to 5% in 1 hr. at 290° C.

FIG. 10.—After continued extension to 6% in 3 hr.

FIG. 11.—Final microstructure of Specimen *A*.  $\times 100$ .

FIG. 12.—Specimen *B* (see text, p. 429) after “medium rate” creep to 4% in 2 hr. at 290° C.

FIG. 13.—After continued extension to 4.3% in 3 hr.

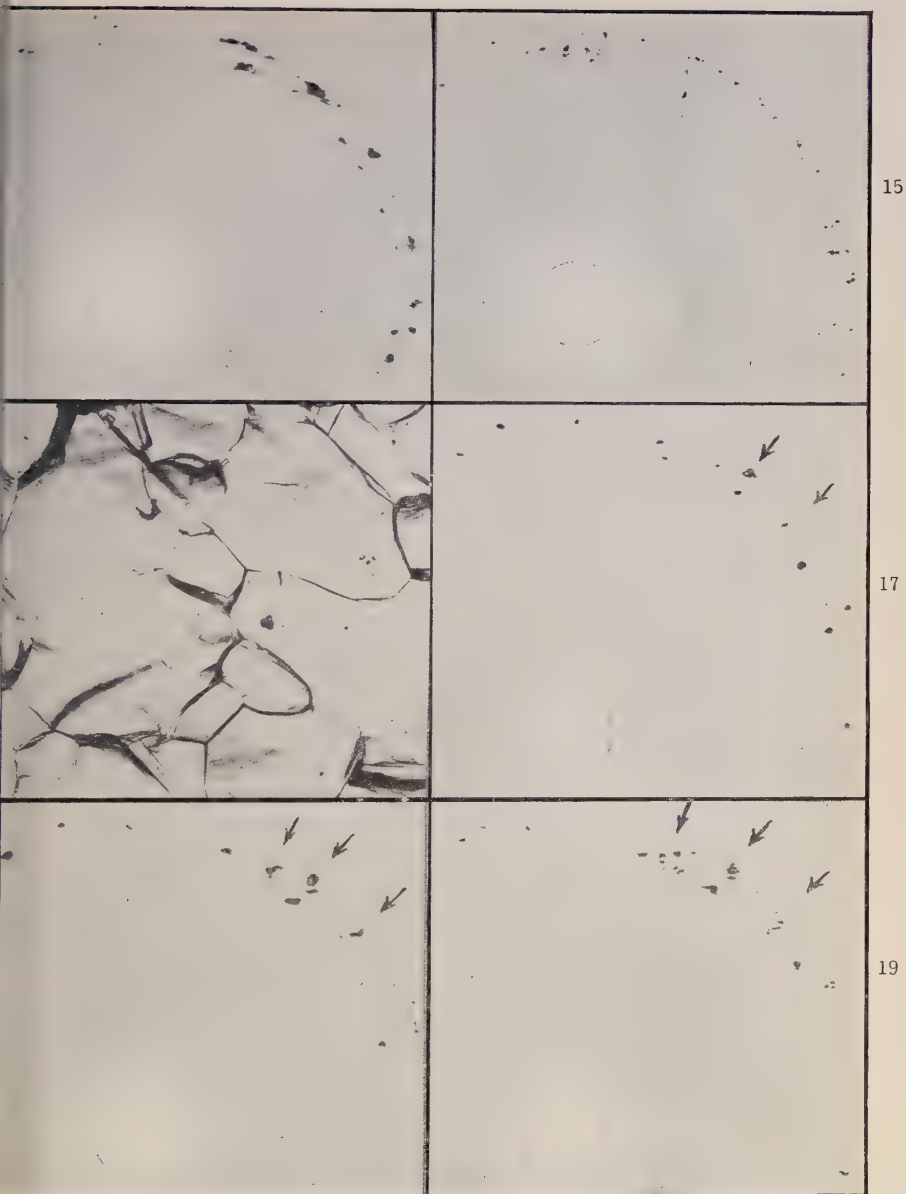


FIG. 14.—After continued extension to 4.7% in 4 hr.

FIG. 15.—After continued extension to 6% in 17 hr.

FIG. 16.—Final microstructure of Specimen B.  $\times 100$ .

FIG. 17.—Specimen C (see text, p. 429) after "slow" creep to 1% in 1 hr. at 290° C.

FIG. 18.—After continued extension to 3% in 120 hr.

FIG. 19.—After continued extension to 5% in 287 hr.

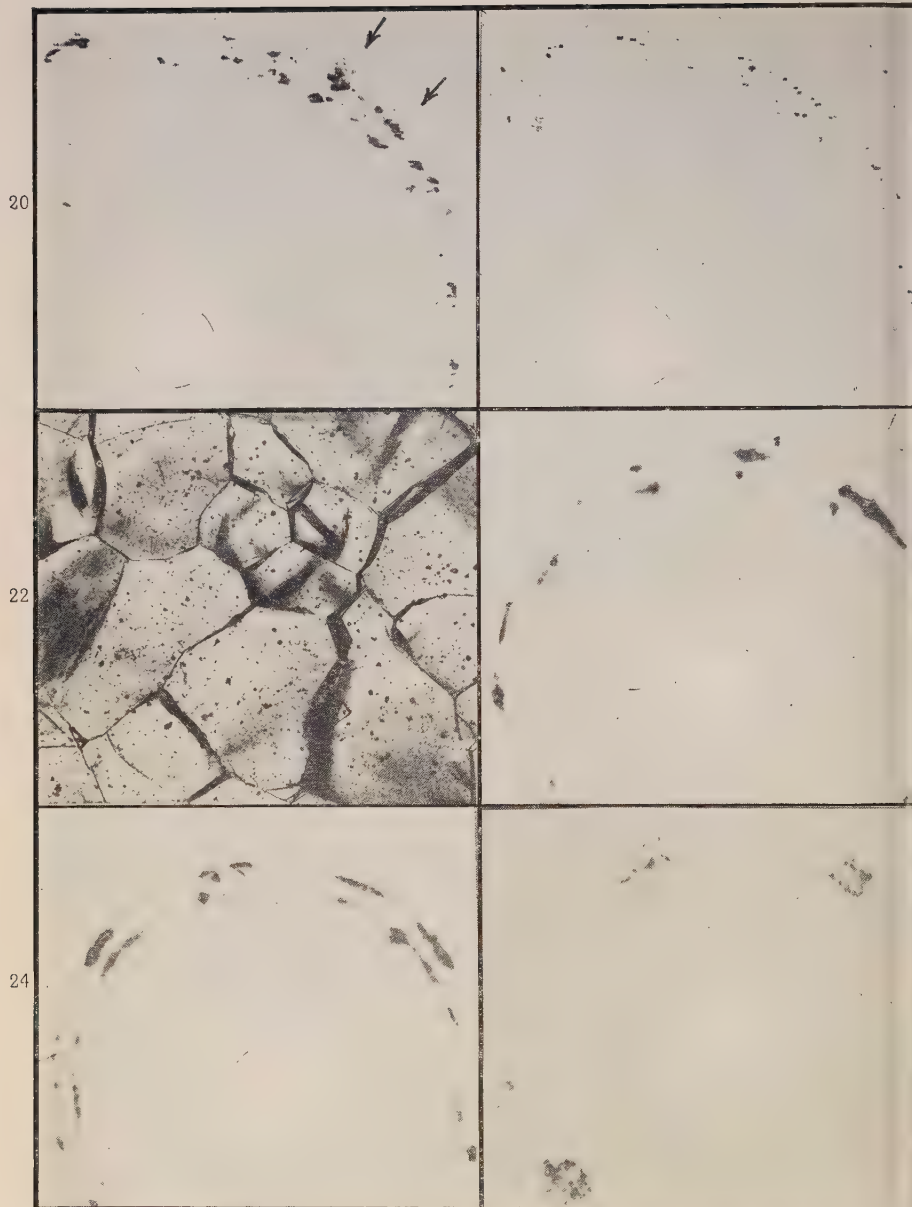


FIG. 20.—After continued extension to 6.5% in 455 hr.

FIG. 21.—After continued extension to 9.5% in 920 hr.

FIG. 22.—Microstructure of Specimen C after 10% extension in 1035 hr.  $\times 100$ .

FIG. 23.—Specimen D (see text, p. 431) after 3.5% extension cold.

FIG. 24.—Same specimen after heating unloaded for 10 days at 250° C.

FIG. 25.—Similar specimen extended 3.5% cold, after heating loaded for 68 hr. at 250° C.



(Fig. 11, Plate XLVI) now exhibits much coarser slip formations than those typical of cold deformation and shown by the previous Fig. 7.

*Specimen B* (Medium rate, load 652 lb./in.<sup>2</sup>, temperature 290° C.).—The X-ray photograph of the initial state is not reproduced since it contains only the standard sharp reflection spots already illustrated. The other photographs of this specimen show that the reduction in strain rate, compared with the Specimen A, results in further inhibition of the disordering that precedes the sub-structure. Thus Fig. 12 (Plate XLVI), obtained after 4% extension in 2 hr., shows much less diffusion of the reflections than Fig. 9, which corresponds to roughly the same extension at the faster rate. Fig. 13 (Plate XLVI), after

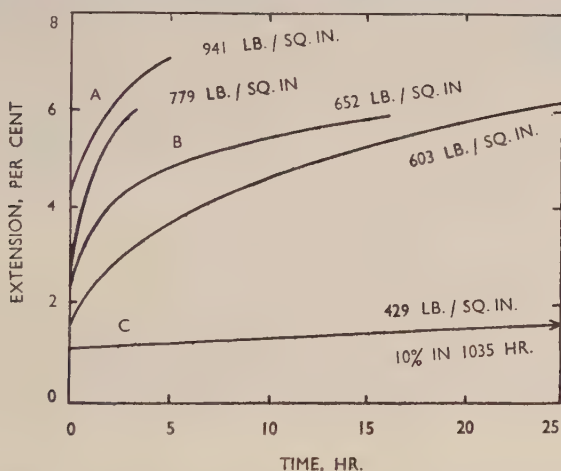


FIG. 1.—Creep Curves at 290° C. Curves A, B, and C refer to specimens described in the text as creeping at relatively rapid, medium, and slow rates.

4.3% extension in 3 hr., and Fig. 14 (Plate XLVII), after 4.7% extension in 4 hr., demonstrate that continued deformation and heating produced no appreciable further disordering; instead the reflections begin to break up into the secondary spots indicative of the beginning of the sub-structure. The sub-structure is then rapidly formed; it is evidently completed after 6% extension in 17 hr., as shown by Fig. 15 (Plate XLVII). The further inhibition of the previous disordering is again reflected in the microstructure, which, as illustrated by Fig. 16 (Plate XLVII), now shows traces only of slip formations.

*Specimen C* (Slow rate, load 429 lb./in.<sup>2</sup>, temperature 290° C.).—It will be evident from the above that further decrease in strain rate should rapidly reduce the disordering of the structure to negligible

dimensions. This is confirmed by Fig. 17 (Plate XLVII), obtained after 1% extension in 1 hr., and Fig. 18 (Plate XLVII), after 3% extension in 120 hr.; these show very little diffusion of the reflections, and such diffusion as there is arises rather from the clumping of the secondary reflection spots already formed within the parent reflections but not scattered sufficiently to be separately visible. This point is illustrated by Fig. 19 (Plate XLVII), after 5% extension in 287 hr., when the discrete reflections are well separated. The effect of continued deformation is then to scatter the reflections more widely, as shown by Fig. 20 (Plate XLVIII), after 6.5% extension in 455 hr., and Fig. 21 (Plate XLVIII), after 9.5% in 920 hr. In addition, the microstructure (Fig. 22, Plate XLVIII), obtained after 10% extension in 1035 hr. proves the further point that when the sub-structure is formed without observable disordering in the X-ray photographs then there are no signs in the photomicrographs of deformation by slip.

Finally, the clarity and separation of the above secondary reflections associated with creep may be contrasted with the imperfection and residual diffusion of the reflections in Fig. 6 (Plate XLV), which was typical of the most distinct form of sub-structure obtainable by the usual two-stage process of recovery from deformation at room temperature. The difference confirms that different mechanisms are involved in the breakdown of the grains to the two types of sub-structure.

The above observations therefore show that as the rate of strain is reduced, the two-stage process of recovery is replaced by a single-stage process in which the grain dissociates directly into a sub-structure without any complex intermediate disordering of the structure. The full development of the sub-structure, as shown by the previous work, is associated with the onset of true secondary creep. The present results now show that this sub-structure may be reached in one of two ways according to the rate of strain, either by direct sub-division of the grains or by way of a preliminary disordered phase of the structure. The significance of this lies in the implication that there are two forms of primary creep, because the manner in which the metal exhibits strain-hardening will be quite different in the two cases. This aspect is discussed more fully later. At the moment it is desired merely to draw attention to the underlying feature that the *mechanism* of breakdown, as well as the resulting sub-structure, is a function of the rate of deformation.

#### (c) *Accelerating Effect of Stress on Recovery.*

The following experiments demonstrate a further interesting difference between the production of a sub-structure by the normal recovery

process and by actual deformation at an elevated temperature. This is the observation that the removal of the preliminary disordered phase by heat-treatment is accelerated by concurrent deformation or stressing; the combination of heat-treatment and deformation is more effective in removing the disordered structure than heat-treatment alone.

This inference was evident from the tests described in the preceding Section, because it was known that the test temperature there employed was too low for recovery effects to be produced merely by heating specimens that had been deformed by comparable amounts at room temperature. Confirmation was obtained, however, by direct experiments of which the following is typical.

Two similar specimens (*D*) were deformed at room temperature by the same amount of 3.5% in order to produce a distinct disordered structure of the type already discussed; this cold-worked stage gave rise to the photograph in Fig. 23 (Plate XLVIII). One specimen was then heated unstressed at 250° C., and X-ray photographs were taken at intervals and examined for traces of break-up of the diffuse arcs that would indicate signs of recovery. No evidence whatever could be seen after 10 days, as shown by Fig. 24 (Plate XLVIII); and it was clear that recovery at this temperature was not likely to occur within practical times of heating. The second specimen was heated at the same temperature of 250° C., but subjected at the same time to a constant load of 1000 lb./in.<sup>2</sup>, under which it proceeded to creep. In this case, the disordering was in process of removal after 1 hr. After 68 hr., during which it extended by 3.5%, removal was practically complete and a distinct sub-structure developed, as shown by Fig. 25 (Plate XLVIII).

It may be concluded that during creep the grains tend to form a sub-structure whether they are initially in an annealed state or a disordered state; and that although the formation may be facilitated by temperature, the main operative factor is not temperature but the action of deformation itself.

#### IV.—APPLICATION TO PRIMARY CREEP.

It is of interest next to utilize the above results in a consideration of primary creep. The actual shape of the creep curve obviously depends on the rate at which a test specimen exhibits strain-hardening. The interesting aspect of the above results is that the hardness in the phase of primary creep depends on two opposing mechanisms, which can be described in terms of structure. The mechanisms are dis-

tinguished by the two distinctive ways in which they cause the grain to become dissociated into a sub-structure. These are as follows :

(i) *The Cell Mechanism*.—Its characteristic is that in effect the grains break down directly to a sub-structure without appreciable preliminary disordering; and the result is that, as far as this mechanism is concerned, the grains will harden progressively during the whole process of breaking down. This hardening is to be expected on both experimental and theoretical grounds for two reasons: Firstly, because of the reduction in size from the relatively large, perfect annealed grains to the smaller but internally perfect elements of the sub-structure<sup>1, 3</sup>—a change roughly equivalent to that from a coarse- to a fine-grained specimen; and secondly—a less fundamental reason—because of the dispersal in orientation of the elements during progressive deformation. For if the orientations remained parallel, the parent grain would remain virtually a single crystal, which even with a mosaic structure constitutes a soft state of the metal; while on the other hand, if the orientations were random, each grain would be reduced in effect to a fine-grained polycrystalline matrix, which is known to constitute a relatively hard state. Therefore both the breaking down of the grain and the partial disorientation will lead to progressive hardening, until the equilibrium condition that characterizes the secondary phase of creep is reached. Thus breakdown by the cell mechanism might be expected to lead in the simplest manner to the shape of a normal primary creep curve, indicating progressive hardening from first loading though at a diminishing rate.

(ii) *The Two-Stage Recovery Process*.—In this case there is an initial marked disordering of the structure followed by recovery to a coarse sub-structure. It will be generally agreed, whatever detailed views of the process are held, that the initial disordering would give rise to considerable hardening, and that the subsequent "cleaning up" by recovery to a relatively perfect sub-structure would then constitute a softening process. If this two-stage mechanism alone were involved in primary creep, then the creep rate would accelerate from the beginning of a test, and the normal creep curve would be inverted. It is of interest to note that in special cases such continuously accelerating creep does occur, examples having been observed by Greenwood and Worner<sup>7</sup> in work on lead, so that conditions in which the two-stage recovery process is predominant are not impossible. The characteristic of the second mechanism therefore, in contrast to the first, is initial hardening followed by progressive softening.

The normal primary creep curve, however, is one that shows progressive strain-hardening. Before passing to the explanation most



consistent with the observations, reference should perhaps be made to the suggestion sometimes made, that creep reflects a running balance between strain-hardening and recovery. The results lend no support to this assumption. On the contrary they show that the disordering associated with marked strain-hardening in general is removed once for all in the early stages of deformation; there is no evidence whatever that disordering and recovery alternate in the manner implied by the concept of a running balance. The recovery process would appear incidental, rather than fundamental, to the creep process.

The mechanism of primary creep, as indicated by the observed structural changes, appears therefore to be the resultant of the two distinct and, as far as strain-hardening is concerned, opposing processes of the cell mechanism and the recovery mechanism. Physically, of course, these two extreme mechanisms must combine in the general case into an intermediate process, which would appear to be as follows. At the beginning of deformation the grains start to dissociate into a sub-structure, and the size of the elements tends rapidly to that typical of the ultimate secondary creep rate; this breakdown will lead to progressive strain-hardening until the latter equilibrium is attained. Superposed on this direct dissociation is a disordering of the structure presumably at the sub-boundaries; this adds to the hardness at first, but the effect is rapidly removed with continuing deformation. The removal of this latter factor should cause some softening of the metal, but the actual shape of the primary creep curve will depend on the extent to which this incidental softening is appreciable in comparison with the more fundamental hardening associated with dissociation to the cell structure. In general, presumably, it is not appreciable, and the curve will take the normal course.

Mathematically, it might be possible to express the primary creep curve as the sum of two strength/time curves: one, due to the cell mechanism, showing increase in hardness; and one, due to the recovery process, showing a decrease in hardness with time. Creep curves have been analysed mathematically into components, particularly by Andrade<sup>8</sup> and by Orowan;<sup>9</sup> and it might be of interest to relate such analysis to the structural changes observed here. It is hoped to follow this point in other work, but there is the obvious difficulty of making allowance in such analysis for the main physical feature that is brought out by the present observations, namely, that the actual mechanism of breakdown and deformation continually changes with rate of deformation.

In conclusion, it will be seen that the observations also clarify the second object of the investigation, which was to determine whether



the sub-structures formed in creep are associated with polygonization. Apparently at higher rates of strain a two-stage process is involved, and in that range the concept of polygonization might apply, although the authors prefer the alternative view that the sub-structures become evident because of the absorption of finer crystallite debris into the main fragments formed by deformation. Whatever view is taken, however, it is clear that at the usual slow rates of strain there is no question of polygonization, because the grains dissociate without any intermediate disordering of the structure.

## REFERENCES.

1. W. A. Wood and W. A. Rachinger, *J. Inst. Metals*, 1948-49, **75**, 571.
2. G. R. Wilms and W. A. Wood, *J. Inst. Metals*, 1948-49, **75**, 693.
3. W. A. Wood and W. A. Rachinger, *J. Inst. Metals*, 1949-50, **76**, 237.
4. C. Crussard, *Rev. Mét.*, 1944, **41**, 111.
5. R. W. Cahn, *Phys. Soc. : Rep. Conf. on Strength of Solids*, 1948, 136 (discussion).
6. A. Guinier and P. Lacombe, *Métaux et Corrosion*, 1948, **23**, 212.
7. J. N. Greenwood and H. K. Worner, *J. Inst. Metals*, 1939, **64**, 135.
8. E. N. da C. Andrade, *Proc. Roy. Soc.*, 1914, [A], **90**, 329.
9. E. Orowan, *J. West Scotland Iron Steel Inst.*, 1946-47, **54**, 45.

# THE MECHANISM OF CREEP AS REVEALED 1259

## BY X-RAY METHODS.\*

By G. B. GREENOUGH,† Ph.D., and (Mrs.) EDNA M. SMITH,† B.A.

### SYNOPSIS.

A hypothesis is put forward to explain in terms of dislocation theory the recent observations of Wilms and Wood (*J. Inst. Metals*, 1948-49, **75**, 693) and of Wood and Rachinger (*J. Inst. Metals*, 1949-50, **76**, 237) in relation to the mechanism of the deformation of metals. This mechanism is considered to be closely allied to that of the polygonization phenomenon observed by Cahn (*J. Inst. Metals*, 1949-50, **76**, 121), and the hypothesis incorporates many of his ideas. Some new X-ray observations are presented which offer experimental evidence in favour of the hypothesis.

### I.—INTRODUCTION.

THE application of X-ray diffraction methods to the study of deformation in polycrystalline aluminium at various temperatures by Wilms and Wood <sup>1</sup> and by Wood and Rachinger,<sup>2</sup> and their use by Cahn <sup>3</sup> in the study of the recovery of deformed single crystals during annealing, has led to results of very great interest. Cahn has employed the term *polygonization* to describe his observations, and explains them in an entirely satisfactory manner using the concept of dislocations. On the other hand, Wood and his collaborators, although they consider that Cahn's observations may be a special case of the phenomena which they studied, do not seek an explanation in terms of what they describe as "the somewhat abstract theories of slip and dislocations which have been put forward by physicists in recent years".

It appeared to the present authors that some explanation of the results of the experimental work on creep should be attempted, since full use of the observations can only be made if the physical reasons behind them are understood. It also seemed that future experimental work would be of greater value if designed to test a particular hypothesis than if it were carried out with no theoretical basis. The most promising explanation is of the type suggested by Cahn, and it is the main purpose of this paper to put forward an explanation of the results of the X-ray diffraction investigations of creep which is consistent with theories of dislocations and of creep.

In order to make the paper as concise as possible the experimental

\* Manuscript received 18 April 1950.

† Royal Aircraft Establishment, South Farnborough, Hants.

work is described first, and this is then discussed together with the work of Wood and his collaborators, and that of Cahn.

## II.—EXPERIMENTAL WORK.

The experimental work here described falls into two parts. Firstly, some work on three separate materials was undertaken to determine whether the same difference was observed in all cases in the X-ray diffraction photographs from specimens deformed rapidly and slowly. Secondly, the effect of an applied stress on the rate of "recovery" of cold-worked high-purity aluminium was investigated; this was undertaken specifically to test the hypothesis put forward to explain the previous results.

Since the details of the experimental work are, in general, very similar to those described by Wood and his collaborators, only the main outline is given. The results of a series of experiments of one type are illustrated by reproducing the X-ray photographs from a number of typical specimens, and the history (e.g. strain rate, load, &c.) of each specimen is recorded in the figure caption rather than in the text. Where X-ray diffraction photographs were taken of any specimen at various stages, they were always taken from approximately the same position, but the siting was not precise. Throughout the work, the unfiltered radiation from a cobalt target operating at 48 kV. and a film-specimen distance of 7 cm. were employed. The X-ray photographs have been reduced slightly in reproduction.

### 1. *Effect of Speed of Deformation.*

#### (a) *High-Purity Aluminium.*

This material was studied principally because it corresponded most closely to that used by Wood and his collaborators and so would serve as a useful reference with which to compare future work. The analysis of the aluminium was as follows: Fe 0.02, Si < 0.005, Mn < 0.005, Ni < 0.02, Cu 0.02, Mg < 0.01, Ti < 0.005, Al (by difference) 99.92 wt.-%.

All tests were carried out at 300° C., and the strain rates used were: for the "fast" rate about 2%/min., obtained by step-loading, and for the "creep" rate an average of about 0.2%/hr., under constant load. Specimens were cooled down to room temperature as quickly as possible after the completion of the tests, taking 5 min. to reach 200° C. After examination the rapidly pulled specimen was annealed at 300° C. for a time approximately equal to that required for the corresponding creep test and then re-examined. A few specimens were also examined microscopically after the various tests.

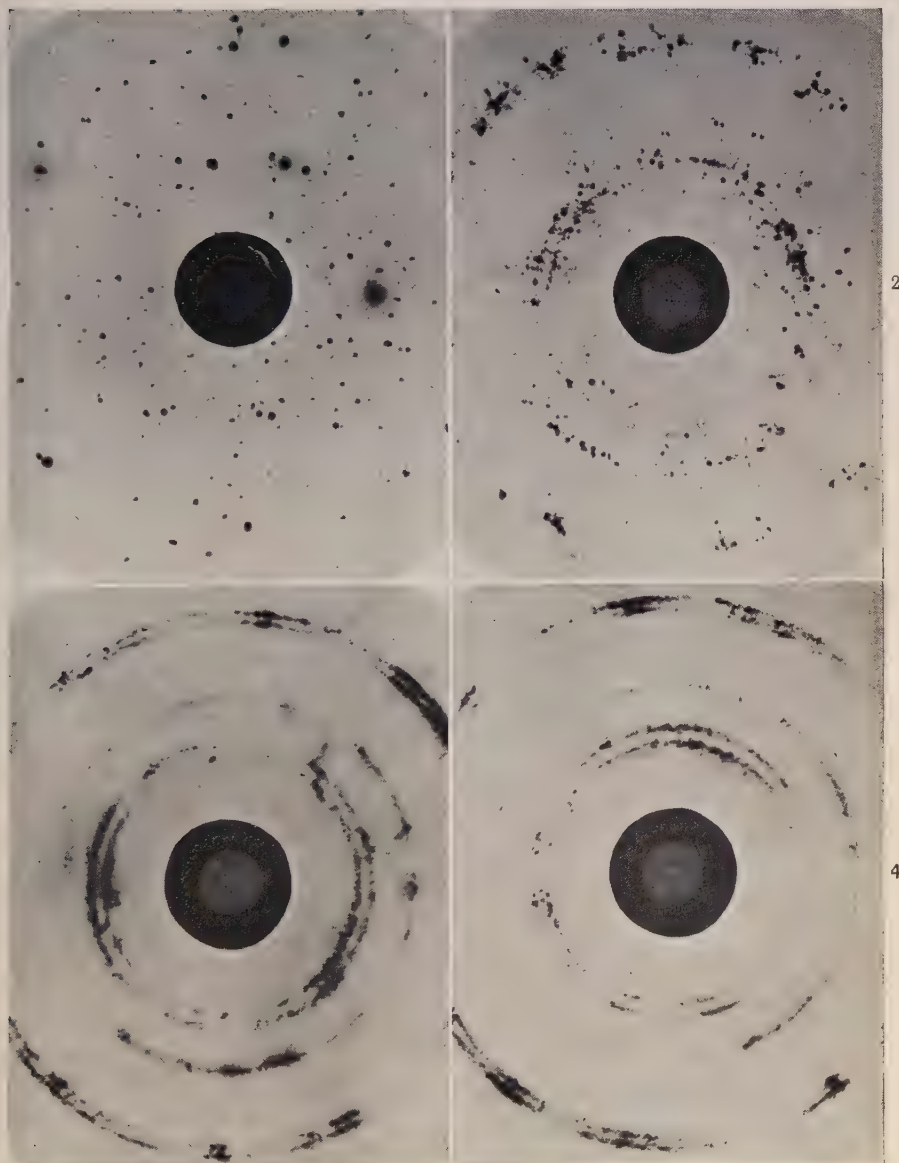


FIG. 1.—Annealed state.

FIG. 2.—As Fig. 1 after creep of 8.9% in 44 hr. at 300° C. (450 lb./in.<sup>2</sup>).FIG. 3.—As Fig. 1 after extension of 10.6% in 3½ min. at 300° C. (step-loaded up to 1660 lb./in.<sup>2</sup>).

FIG. 4.—As Fig. 3 after a further 50 hr. at 300° C. without load.

## 99.25% ALUMINIUM

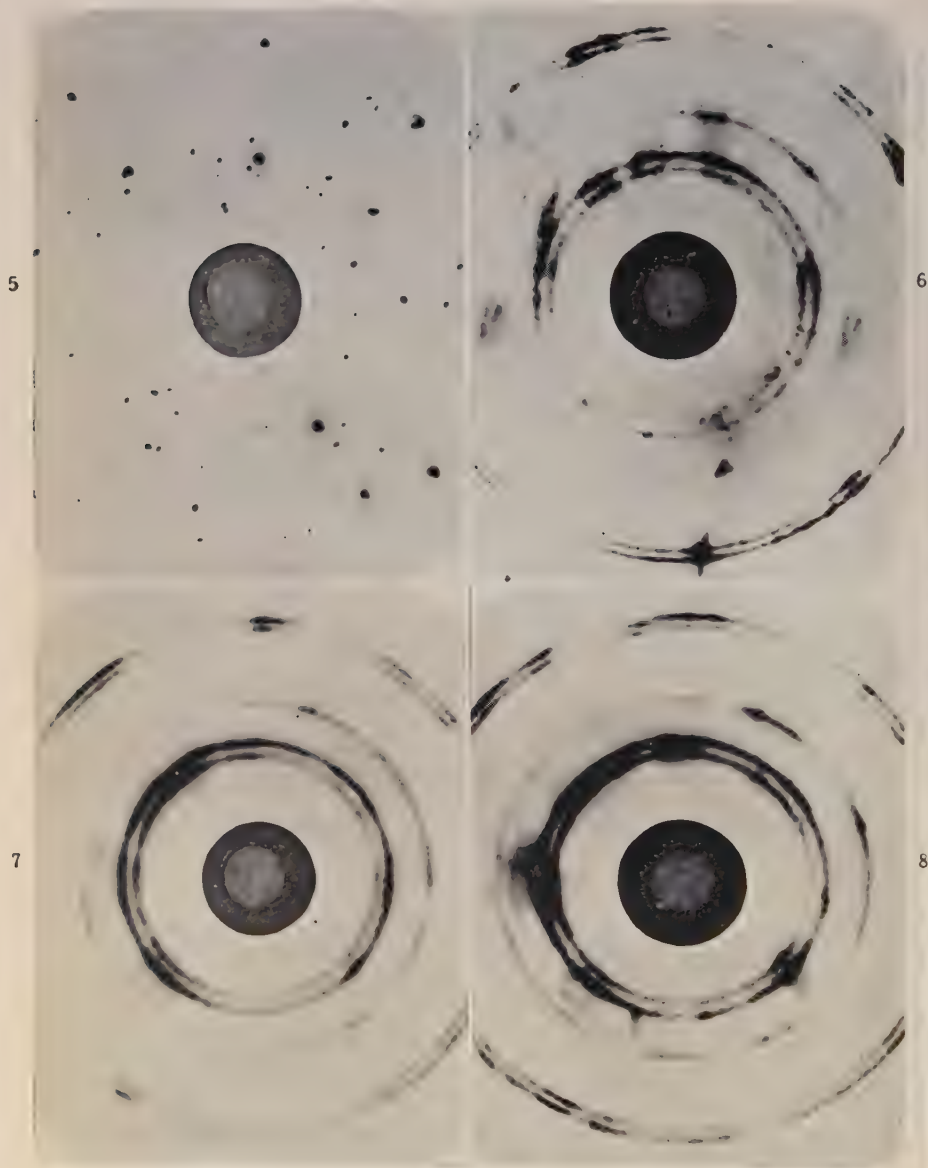


FIG. 5.—Annealed state (large-grained specimen).

FIG. 6.—As Fig. 5 after creep of 10% in 52 hr. at 300° C. (2690 lb./in.<sup>2</sup>).

FIG. 7.—As Fig. 5 after extension of 11.5% in 12 min. at 300° C. (step-loaded up to 4680 lb./in.<sup>2</sup>).

FIG. 8.—As Fig. 7 after a further 90 hr. at 300° C. without load.



## 99.25% ALUMINIUM.

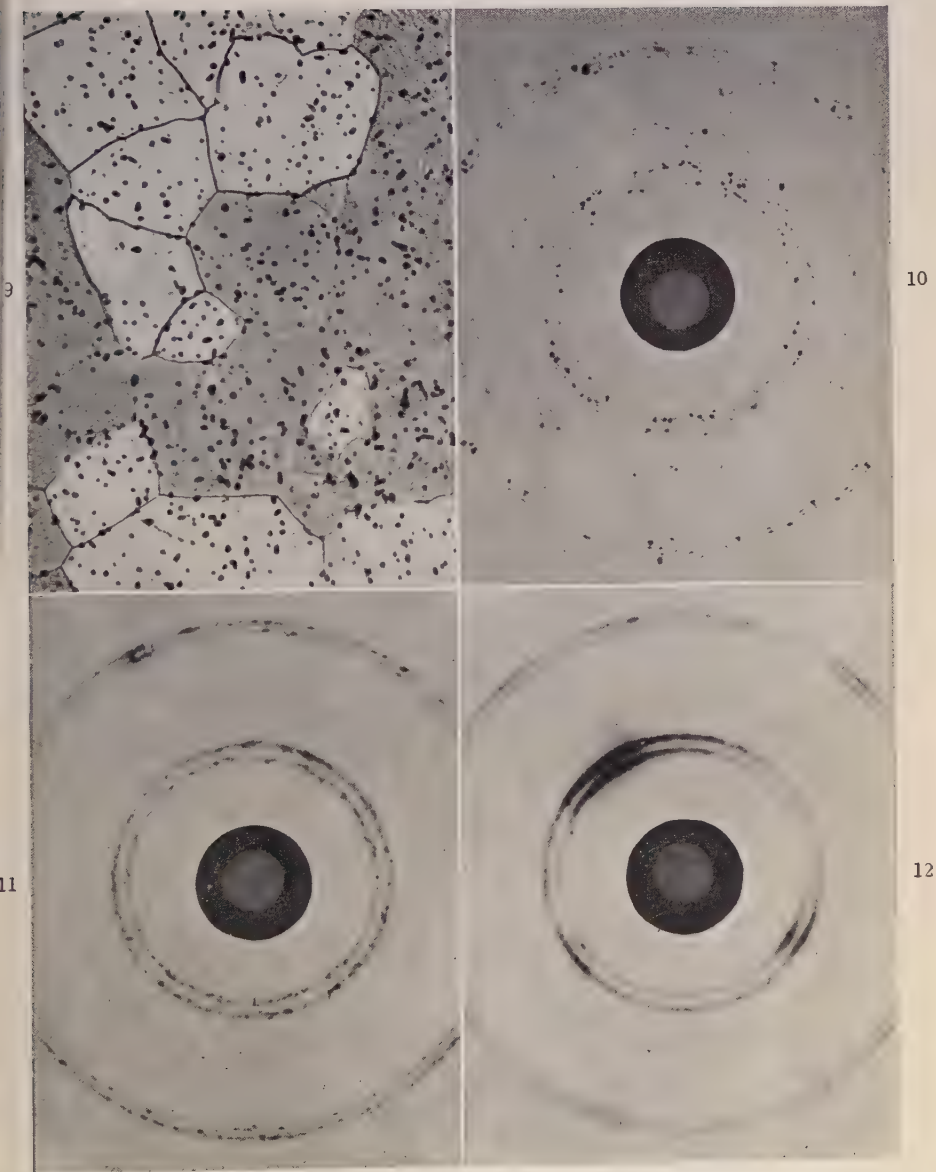


FIG. 9.—Photomicrograph of large-grained specimen.  $\times 200$ .

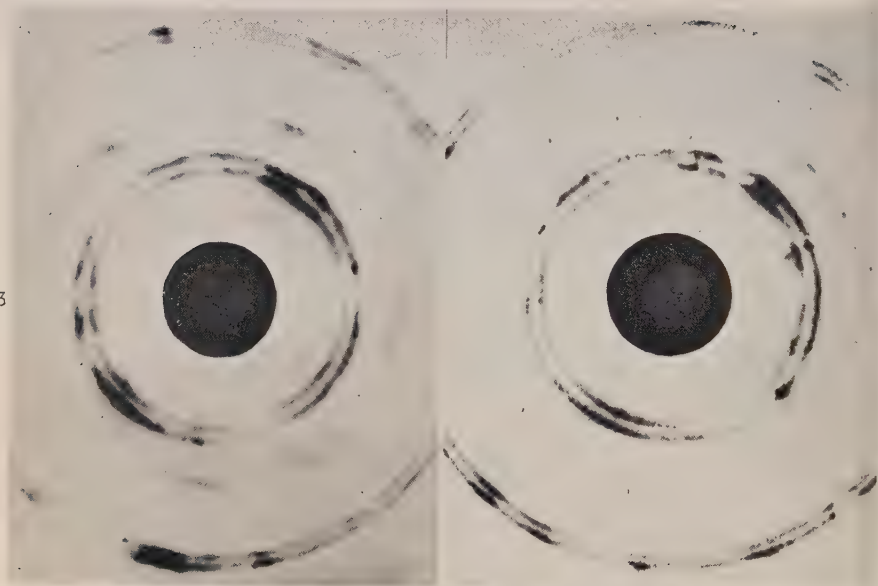
FIG. 10.—Annealed state (small-grained specimen).

FIG. 11.—As Fig. 10 after creep of 14% in 3 hr. at 300° C. (1200 lb./in.<sup>2</sup>).

FIG. 12.—As Fig. 10 after extension of 14% in 3 min. at 300° C. (step-loaded up to 3500 lb./in.<sup>2</sup>), followed by 24 hr. at 300° C.

## 99-92% ALUMINIUM

13



15

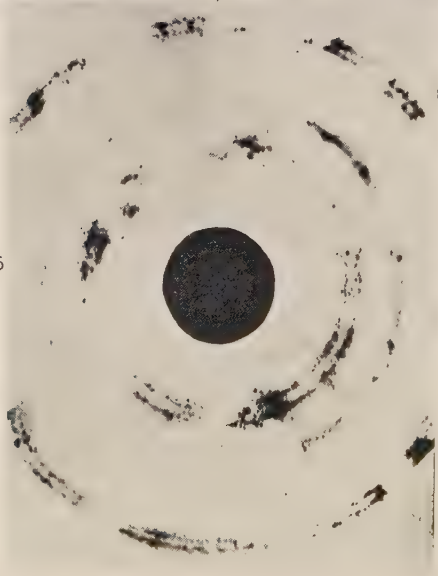


FIG. 13.—As Fig. 1 (Plate XLIX) after extension of 6.75% in 2 min. at 20° C. (stress gradually increased up to 5500 lb./in.<sup>2</sup>).

FIG. 14.—As Fig. 13 after 69 hr. at 300° C. without load.

FIG. 15.—As Fig. 13 after creep of 2.3% in 69 hr. at 300° C. (450 lb./in.<sup>2</sup>).

Figs. 1-4 (Plate XLIX) show the X-ray photographs from a typical series of specimens. It will be seen that the results of Wood and his collaborators are completely confirmed, in that the rapidly extended specimen shows mainly diffuse diffraction spots, whereas the creep specimen shows sharp diffraction spots which are smaller and more numerous than those obtained from an annealed specimen. The results also confirm that allowing the rapidly extended specimen to soak at 300° C. produces little or no change in the diffraction pattern. Lastly, the microscopical investigation confirmed Wood's conclusion that none of the effects was due to recrystallization by a process of nucleation and growth.

(b) *Commercial-Purity Aluminium.*

The analysis of this aluminium (to specification L.34) was : Fe 0.42, Si 0.18, Mn 0.02, Ni 0.05, Cu 0.04, Mg 0.02, Ti 0.02, Al (by difference) 99.25 wt.-%. By different working and annealing treatments a large and a small grain-size were obtained in the annealed specimens, yielding the X-ray photographs shown in Fig. 5 (Plate L) and Fig. 10 (Plate LI). Fig. 9 (Plate LI) is a photomicrograph of the large-grained material. It can be seen that the impurities occur mostly in the form of small precipitated particles scattered throughout the crystals; there is little tendency for grain-boundary segregation.

As with the high-purity aluminium, the tests were all carried out at 300° C., and X-ray diffraction photographs were taken of creep specimens, of rapidly extended specimens, and again of the latter after a period of annealing at 300° C. Figs. 6-8 (Plate L) and Figs. 11 and 12 (Plate LI) are typical examples of the results obtained.

It is apparent that again less diffuseness of the X-ray reflections is caused by the slow deformation than by the rapid extension, and that the length of time spent at 300° C. without an applied stress, subsequent to rapid extension, has little effect on the diffraction pattern. But a comparison of the photographs with those of the high-purity aluminium shows that for any rate of deformation the X-ray reflections of the commercial aluminium exhibit much more diffuseness. Most marked is the difference between the effects of a creep extension on the two materials; whereas in the pure aluminium there are few, if any, diffuse reflection spots, the commercial aluminium shows spots which are almost entirely diffuse. The same kind of difference is also apparent in the rapidly extended specimens; in the pure aluminium the spots have become diffuse, but they do not merge into each other sufficiently to give the continuous ring shown by the commercial aluminium.

(c) *Lead.*

The analysis of the lead was : Bi 0.002, Cu 0.01, Sb 0.09, Sn trace, Fe trace, Zn trace, Pb (by difference) 99.9 wt.-%. Experiments were made on this material at room temperature in a manner analogous to that described above. The rates of extension employed ranged from 4% in 28 hr. to 10% in 1½ min. The X-ray photographs after these tests all showed blurred diffraction rings, and there was no significant difference in the photographs from the rapidly extended specimens and those extended by creep.

## 2. *Recovery of Specimens Showing Diffuse Reflections.*

This work was undertaken to check whether in the case of the high-purity aluminium, after a deformation causing considerable diffuseness of the X-ray reflections, "recovery" at 300° C. was appreciably affected by the presence of a stress. The initial annealed state of the material is shown in Fig. 1 (Plate XLIX). Specimens were first subjected to a known deformation by extending them 5–10% at room temperature. They were then maintained at 300° C. for several hours and during this time a stress of sufficient magnitude to produce a small creep strain was applied. X-ray photographs were taken before and after creep, as previously described, and the amount of recovery in each case was compared with that of a reference specimen which had undergone a similar initial extension and had been allowed to recover at 300° C. for a comparable time without load. Figs. 13–15 (Plate LII) are typical of the general behaviour.

It is clear that the specimen subjected to a stress during the recovery interval gives diffraction spots which are much sharper than those given by the cold-worked specimen. On the other hand, the same period at 300° C. without applied load has little effect and still leaves the diffraction spots in a very diffuse condition. It is also interesting to compare Fig. 15 (Plate LII) with Fig. 2 (Plate XLIX), when it can be seen that the sharp spots formed during recovery appear to be smaller than those exhibited by specimens deformed entirely by creep at 300° C.

## III.—DISCUSSION.

All the X-ray observations made by Wilms and Wood,<sup>1</sup> and by Wood and Rachinger,<sup>2</sup> may be interpreted as indicating that in high-purity aluminium, as the speed of deformation is progressively reduced and/or the temperature of deformation raised, the crystals of the annealed metal break down into fragments which become progressively larger and less distorted. The difference between a creep deformation and a

rapid deformation at about 300° C. is very marked indeed; after the former the fragments are almost entirely perfect, while after the latter they show considerable strain. The results described above for commercial aluminium show that no such marked effect occurs in this case. With the impure material, X-ray reflections from creep specimens are less blurred than those from specimens which have undergone rapid deformation, but there is no evidence of a breakdown of the crystals into perfect fragments. The rapid deformation, too, causes considerably more distortion in the commercial than in the pure aluminium.

Wood and Rachinger have correlated the size of the "cells" observed with the yield stress of the material, but it must be pointed out that the yield stress is a *consequence* of the cell-size and not a *cause* of it. They do not explain why the rate and temperature of deformation is so important in determining the size of the fragments. Before seeking such an explanation it is useful to consider the results that might be expected from general dislocation theory and to review the explanation given by Cahn of polygonization phenomena.

### 1. Deformation and Dislocation Theory.

In terms of dislocation theory, which has recently been surveyed by Mott,<sup>4</sup> normal plastic deformation may be considered as due to the motion of dislocations through the metal under the influence of the applied stress. The rapid motion of the dislocations through the lattice, and the effect of the applied stress at points of stress concentration in the metal, produce many more dislocations during the deformation. These dislocations tend to become trapped in the lattice where the potential energy of the dislocations is a minimum, e.g. when they are so placed as partially to relieve their mutual strain energy or the strain energy round a foreign atom. Before they can move further, these dislocations must be pulled out of their potential-energy troughs by the applied stress, and this process is assisted by thermal fluctuations of the dislocation positions. The probability of the occurrence of a thermal fluctuation large enough to enable the applied stress to pull any particular dislocation out of its potential hole increases with both temperature and time. It would therefore be anticipated that the number of dislocations remaining trapped in the lattice, and hence the diffuseness of the X-ray diffraction spots, would decrease as the temperature of deformation was raised or the strain-rate decreased.

This agrees with the observation of Wood and his collaborators that, in general, rapid deformation causes more blurring of the diffraction spots as the temperature of deformation is reduced. The results obtained by the present authors for commercial aluminium are also



readily explained on this basis. On the other hand, the experimental results for high-purity aluminium at, say,  $300^{\circ}$  C. are contrary to expectation; the creep deformation causes little or no diffuseness of the X-ray diffraction spots, and the sole effect of the deformation seems to be to break the annealed grains into perfect fragments. The effect is much as if the distorted crystals had polygonized during the creep process in the manner described by Cahn. This is discussed more fully later.

## 2. *Polygonization.*

The salient experimental feature of polygonization is that when a metal is annealed after plastic bending, the diffuse streaks of the X-ray diffraction photograph break up into a series of sharp reflections. Cahn concludes from his own results, and those of other workers, that a number of metals show the effect, that high-temperature annealing is required, that polycrystal aggregates show a small effect, that single crystals show a very marked effect after inhomogeneous deformation, but that if the deformation is at too low a temperature polygonization is not observed after subsequent annealing.

The explanation, in terms of dislocations, is as follows. During the plastic deformation, dislocations become scattered through the crystal lattice and the resulting distorted lattice gives a blurred diffraction spot. When the distorted lattice is annealed, the dislocations of like sign on the different slip planes attract each other and arrange themselves in rows along lines perpendicular to the slip planes. Such rows of dislocations constitute the boundaries between crystals with perfect lattices and of slightly different orientations. It should be noted that the explanation requires that the dislocations remaining in any particular region of the lattice after deformation are predominantly of one sign; these repel each other if on the same glide plane, but attract each other when on different planes and arrange themselves so that the line joining them is perpendicular to the glide plane. Dislocations of opposite sign hinder the process.

The similarity between the polygonization phenomena described by Cahn and the observations made during the creep researches is obviously very close, but there are three main points of difference. The first is that a temperature considerably greater than  $300^{\circ}$  C. is necessary to cause the aluminium single crystals to polygonize. This point is confirmed by the researches of Wood and his collaborators, and by the authors of the present paper, since the polycrystal specimens rapidly extended and then maintained at  $300^{\circ}$  C. show little, if any, tendency to polygonize. Secondly, the explanation of polygonization postulates

that the dislocations are free to move under their own attractive forces; the position must be somewhat different if a stress is applied at the same time. These two points are satisfactorily explained by the hypothesis put forward below, and form an essential part of it.

The third difference is that the single crystals used by Cahn were given an extremely inhomogeneous deformation; it is difficult to imagine that the deformation of grains in a polycrystalline aggregate is inhomogeneous to the same degree. This difference is fundamental, since the whole process of dislocations moving from a random distribution in the crystal to a regular array dividing it into large perfect fragments can only take place when there is a preponderance of dislocations of one sign. However, it is interesting to note that Nye <sup>5</sup> has recently made observations on polycrystalline silver chloride specimens which indicate that after a uniform plastic extension of the aggregate there are always more dislocations of one sign than of the other left in each crystal. It is possible, of course, that in the polycrystalline metal specimens the regions in which dislocations of the same sign are predominant are smaller than the crystals, and that any particular crystal could be curved in different directions in different regions.

#### IV.—EXPLANATION OF OBSERVATIONS.\*

In creep, the initial extension produces dislocations. These move under the influence of the applied stress, helped by thermal atomic movements, until they reach a relatively stable position. In a pure metal there are few impurity atoms in the crystal to act as dislocation traps, consequently the most stable position tends to be reached when the dislocations are arranged so that their mutual free energy is a minimum. Assuming that there is a local excess of dislocations of one sign, an array is formed, as in polygonization. It is probable that the effect will occur at a lower temperature when a load is applied than under no load, because the stress assists the motion of the dislocations, whereas in polygonization they must move solely under the influence of their own attractive forces. However, the stress must not be large enough to pull dislocations away from their stable array, or at least only rarely, and further deformation must take place by some other mechanism than by the motion of dislocations, for instance by viscous

\* *Note added in proof:* The authors were not present at the Institute of Metals meeting held in Paris during October 1949, and were unaware of the remarks then made by Professor Crussard on the paper by Wilms and Wood until they were published (*J. Inst. Metals*, 1948-49, 75, 1125) when the present paper was already in proof. Professor Crussard has advanced an explanation of the phenomena which is broadly similar to that described here.

flow<sup>6</sup> as in secondary creep. In a rapidly extended specimen, the applied stress would be large enough to move the dislocations away from a stable array and consequently none is formed.

It has now been explained how the crystals of the metal become broken down into smaller perfect fragments under certain conditions, and it is clear why the temperature and rate of deformation are so intimately connected with the formation of these "cells". As already shown in Section III. 1, the number of dislocations remaining in the lattice after a given deformation is decreased as the temperature of deformation is raised or the strain rate decreased. If the conditions are such that polygonization will occur, it seems likely that the fewer dislocations there are to be accommodated in the array, the further apart will be the lines of dislocations, i.e. the larger will be the cell-size. This is in agreement with the trend of the results of Wood and Rachinger in the range where "cell formation" occurs.

The difference in the results obtained from the high- and low-purity aluminium can also be immediately explained on the basis of the hypothesis put forward above. If a metal contains foreign atoms dissolved in the lattice, or precipitated particles occurring in the crystals, then these will act as effective dislocation traps. This means that after any given plastic deformation there will be more dislocations left in the lattice than in the case of the pure metal, which explains the increased diffuseness of the X-ray diffraction spots. Further, the mutual attraction of the dislocations is relatively less important than the interaction of the dislocations with the stress fields of the foreign atoms, and it is less likely that, at a given temperature, the polygonized structure will form.

With regard to the results obtained for lead, it is possible that the similarity in the effects of fast and slow rates of strain is due either to the temperature of test being too low or to the impurity of the lead.

It also follows from the explanation given above that if dislocations are introduced at random into a pure metal, say, by deforming it rapidly at room temperature, then a small load applied at 300° C. should enable these dislocations to form themselves into an array. This array will not form at that temperature if there is no applied stress. The experiments described in Section II. 2 were carried out specifically to test this point, and the results were entirely as expected. The photographs show that the perfect fragments obtained in this way are smaller than those formed during creep from a strain-free state, but this is to be expected since there are more dislocations to accommodate in the array.

## V.—CONCLUSION.

By following the accepted dislocation theories of plastic deformation, and by adopting the theory of polygonization put forward by Cahn, it is possible to explain all the observations made by Wilms and Wood, and by Wood and Rachinger. Only one assumption has to be made, that the deformation of the crystals in a polycrystalline aggregate is inhomogeneous and that particular regions of each crystal are left with a preponderance of dislocations of one sign, and this has some experimental justification. The explanation has the merit that deductions may be drawn from it which can be checked by experiment; so far there are no experimental results available which contradict the explanation.

## ACKNOWLEDGEMENTS.

Acknowledgement is made to the Chief Scientist, Ministry of Supply, and the Controller of H.M. Stationery Office for permission to publish this paper.

## REFERENCES.

1. G. R. Wilms and W. A. Wood, *J. Inst. Metals*, 1948-49, **75**, 693.
2. W. A. Wood and W. A. Rachinger, *J. Inst. Metals*, 1949-50, **76**, 237.
3. R. W. Cahn, *J. Inst. Metals*, 1949-50, **76**, 121.
4. N. F. Mott, *Research*, 1949, **2**, 162.
5. J. F. Nye, *Proc. Roy. Soc.*, 1949, [A], **200**, 47.
6. E. Orowan, *J. West Scotland Iron Steel Inst.*, 1946-47, **54**, 45.





# SOME X-RAY OBSERVATIONS ON THE 1260 NATURE OF CREEP DEFORMATION IN POLYCRYSTALLINE ALUMINIUM.\*

By E. A. CALNAN,† B.Sc., and B. D. BURNS,‡ M.Sc., MEMBER.

(Communication from the National Physical Laboratory.)

## SYNOPSIS.

Back-reflection Laue patterns have been taken from the same series of locations on a large-grained aluminium test-piece after successive amounts of creep deformation at 250° C. From the analysis of the asterism and the movement of the reflection spots relative to the stress axis it appears that, under the conditions of the present experiments, the creep deformation up to about 3% extension in 170 hr. is associated with slip processes. During this stage the striking feature of the deformation is its inhomogeneity not only from grain to grain but also within the grains themselves, so producing in many cases a comparatively coarse sub-structure. The later stages are characterized by the presence of numerous fine units or cells which are formed from the previously distorted material.

## I.—INTRODUCTION.

IN recent years there has been considerable theoretical speculation on the nature of creep deformation and a measure of success has been achieved in accounting for the earlier stages of creep, particularly for transient creep, in terms of dislocation theory. Such theoretical work has not involved any detailed consideration of the crystallographic aspects, and the criterion of its adequacy has generally been its success in predicting the shape of the creep curve. This is the only correlation possible between theory and experiment, owing to the lack of experimental evidence of the precise deformation processes involved in creep.

Earlier work at the National Physical Laboratory by Wood and Tapsell and the researches at Melbourne under Wood have involved the use of characteristic radiation in the X-ray work. This method, yielding a general picture of the slow deformation in polycrystalline material, shows that it proceeds without the occurrence of the extensive diffuseness of the X-ray reflections associated with normal rates of strain. The characteristic-radiation technique, however, is limited in scope and the present work was undertaken to provide more detailed information, possibly quantitative, on the behaviour of individual

\* Manuscript received 25 April 1950.

† Metallurgy Division, National Physical Laboratory, Teddington.

‡ Formerly Metallurgy Division, National Physical Laboratory; now at Metallurgical Branch, Armaments Research Establishment, Woolwich.

grains within a polycrystalline mass, and to study any grain-boundary interaction effects.

For the detailed examination of a small number of grains in deformation studies the Laue technique, where the grain-size is large enough to make this possible, is to be preferred to characteristic-radiation patterns. In both cases the state of internal strain is deduced from the spread of the diffraction spots.

With the characteristic radiation, information on the ranges of orientation is limited to those which produce a spread in the circumferential direction of the diffraction ring; for the changes in blackening in the radial direction, some of them abrupt, depend on the range of parameters present, the energy distribution in the immediate neighbourhood of the characteristic X-ray peak, and on the absorption edges of the photographic material. In the Laue method, however, subject to the wave-length condition discussed below, the spread in any direction on the pattern corresponds to a range of orientation, and from the directions of the spread detailed crystallographic deductions may be made.

The range of wave-lengths desirable in employing the Laue method may be estimated in the following manner. In the transmission technique, with a range of orientation of, say,  $10^\circ$  of a particular set of planes of spacing  $d$  inclined at  $\theta = 15^\circ$  to the X-ray beam, a range of wave-lengths  $2d \sin 20^\circ$  to  $2d \sin 10^\circ$  is required, assuming radial extension of the spot, i.e.  $0.68d$  to  $0.35d$ . In the back-reflection technique, however, with  $\theta = 75^\circ$ , wave-lengths from  $1.97d$  to  $1.88d$  are required. The short-wave limit of the radiation at an operating voltage of 55 kV. is  $0.23 \text{ \AA}$ ., and the main white radiation peak extends from approximately  $0.3$  to  $0.6 \text{ \AA}$ .. Thus the danger of the recorded range of orientation being reduced on the short-wave side occurs for planes of spacing less than  $1 \text{ \AA}$ . in the case of transmission and for those of spacing less than  $0.15 \text{ \AA}$ . in the case of back-reflection. For the higher-spacing net planes the incident wave-length fulfilling the reflection condition in the latter case will be of comparatively low intensity, but the reflected intensity will be augmented by additional high-order reflections.

## II.—EXPERIMENTAL.

The material used was 99.4% commercially pure extruded aluminium rod containing iron 0.33, silicon 0.21, manganese 0.03, magnesium 0.02, and titanium 0.02%. Ideally, specimens of normal grain-size and a microbeam technique would be employed, but in the first instance it was thought that useful information could be obtained

using large-grain specimens and a conventional Laue technique. Cylindrical test-pieces of gauge dia. 0.4 in. (1 cm.) were used. These were carefully machined to avoid any deep working and annealed for 2 hr. at 400° C. They were then given 10% extension at room temperature and annealed for 4 hr. at 450° C. In this way a controlled and uniform grain-size of between 1 and 2 mm. was obtained. This uniformity was checked on sections by microscopic and X-ray examinations.

The specimens were not subjected to X-ray examination simultaneously with creep deformation, since the exposure time was 2 hr., but they were removed from the creep machine and examined at various stages. Radiation from a rhodium target at 55 kV. was used. In order to facilitate precision location of the specimen for each examination a central band roughly 2 cm. long was etched to reveal the grain structure. Two pairs of adjacent grains were selected and a very fine fiducial mark was impressed with a needle point near each grain pair. The specimen was located vertically in a Pye Universal goniometer, the centring and alignment being carried out with a low-power microscope. The position of the various points to be irradiated could then be specified accurately by an angular co-ordinate relative to the fiducial mark. By this method any particular point could be reset in the X-ray beam with an error not exceeding 10'. For each grain pair a sequence of five X-ray photographs ranging from the centre of one grain across the grain boundary to the centre of the adjacent grain, was taken at each stage in the deformation process. With a grain dimension of 2 mm. and a beam dia. of 0.4 mm. at the point of incidence, it was possible to make these observations without any significant overlapping of the irradiated areas. It should, however, be noted that the grain-boundary observations refer to an area extending roughly 0.2 mm. on either side of the boundary itself.

The creep extension was carried out by the Engineering Division of the Laboratory. The straining conditions were selected on the basis of continuous deformation results obtained with specimens of the same material and condition, and were designed to provide a deformation/time curve with well-defined transient, secondary, and tertiary creep stages leading to failure within 500 hr., so that the crystallographic changes could be correlated with the recognized stages of creep deformation. The load employed was 0.65 tons/in.<sup>2</sup> (1.0 kg./in.<sup>2</sup>) at a controlled temperature of 250° C. X-ray observations were made at the following points :

Time, hr.	.	.	0	0.5	4	100	170	2000	2500
Strain, %	.	.	0	0.3	0.55	1.7	3.2	9.0	13.0

The preliminary continuous deformation/time curve was thus not repeated under conditions of interrupted stressing, and the deformation curve shows some irregularities, although earlier work by Wood and Tapsell <sup>1</sup> had shown that the creep characteristics of fine-grain specimens were not seriously affected by intermittent examinations at room temperature.

The two grain pairs studied have been designated pair *A* and pair *B*, with component crystals *A*1, *A*2, and *B*1, *B*2, respectively.

### III.—OBSERVATIONS.

Before describing the observations in detail it is convenient to consider them in general terms.

(1) Quite definite diffuseness and elongation of the Laue spots was observed after attaining a strain value of 0.55%, and in some instances even after the first strain value of 0.3% there was a suggestion of asterism. The method therefore is quite sensitive, and it is probable that by using a microbeam technique with suitable fine-grain single-coated films greater sensitivity could be attained.

(2) Different reflections in a single pattern of deformed material show a markedly different appearance (Figs. 1 (*a*) and (*b*), Plate LIII). Although this will be discussed later in terms of the direction of the axes of inhomogeneous rotation due to slip processes, it must be mentioned here, since it is essential that in the comparison of successive patterns the same reflections should be considered throughout.

(3) There were very marked differences in the type and extent of the rotation effects in different grains, as would be expected in any polycrystalline material. These differences ranged from the relatively simple unidirectional spreading of the Laue spots for grain *A*1 to the complex general spreading observed in some parts of grain *A*2 (Fig. 3 (*c*), Plate LIV; Fig. 4 (*b*), Plate LV).

(4) The differences in type and extent of the rotation effects at different locations in the same grain were almost as marked as the differences from grain to grain. Generally the grain-boundary regions exhibited a greater complexity of breakdown than the grain centres, but the patterns from the intermediate positions also showed significant differences compared with the grain-centre patterns (Figs. 3 (*c*), (*d*), (*e*), Plate LIV).

(5) In the grain-boundary patterns a relative shift of the two superimposed patterns occurs with extension. This relates to the centre of the observed range of orientations, and measurement of these changes of orientation is possible only while the reflections are reasonably sharp (Figs. 1 (*c*) and (*d*), Plate LIII).



(6) In the later stages of the test (9% and 13% extension) the spread of orientation was very great and reflections due to the characteristic rhodium  $K_{\alpha}$  radiation are contained in some of the spots. Nevertheless, the initial configuration of Laue spots was still discernible (Fig. 5, Plate LVI).

It may be remarked that the spread of X-ray reflections during deformation was far less than that usually observed after normal tensile tests at room temperature, particularly for strain values up to 3.2%.

#### IV.—DETAILED DESCRIPTION.

The spread of the most extended spots in each pattern was measured with a Greninger<sup>2</sup> hyperbolic chart appropriate to the specimen-film distance of 2 cm. This gives the angular range of the normals to the planes reflecting. The angle corresponding to the size of the initial strain-free spot, which in this experimental arrangement depends almost entirely on the size and divergency of the X-ray beam, was subtracted from the measured value and these corrected values are listed in Table I. On account of the diffuse nature of the spots these measurements are only approximate, especially so in the case of the very diffuse reflections at 9 and 13% extension. In three grains the linear spread is greater at the boundaries than at the centres, but grain A1 shows that this is not always so, for here the unidirectional spread at the centre is markedly greater than anywhere else.

TABLE I.—*Variation of Linear Spread of Crystal Orientation with Extension.*

Extension, %	Linear Spread of Crystal Orientation, Degrees							
	Grain A1		Grain A2		Grain B1		Grain B2	
	Centre	Boundary	Centre	Boundary	Centre	Boundary	Centre	Boundary
0.55	0.7	0.5	0.3	0.7	0.3	0.5	0.3	1
1.7	1.7	1.3	0.3	1.3	0.3	1	0.7	1.5
3.2	3.3	2	0.7	2	1.3	2	1.3	2.5
9	7	3	4	4	2	7	4	7
13	9	9	7	9	4	9	7	9

The analysis of the changes of orientation in the early stages (up to 3.2% extension) falls into two parts. First, for the analysis of the directions of spread of orientation in each pattern, the extended Laue spots were plotted on a standard stereographic projection together with the position of the stress axis. The axes for rotation on the basis of



(i) Taylor crystallite "rollers" (rotation about an axis lying in the slip plane and perpendicular to the slip direction), (ii) isolated single-crystal rotation (rotation about an axis perpendicular to the direction of stress and the slip direction), and (iii) rotation about the slip plane normal (Collins and Mathewson,<sup>3</sup> and Heidenreich and Shockley<sup>4</sup>) were then added and the directions of spread compared with those which would be produced by the operation of these axes.

Secondly, there is the general shift or bulk rotation to which reference has already been made. Since the total rotation involved was

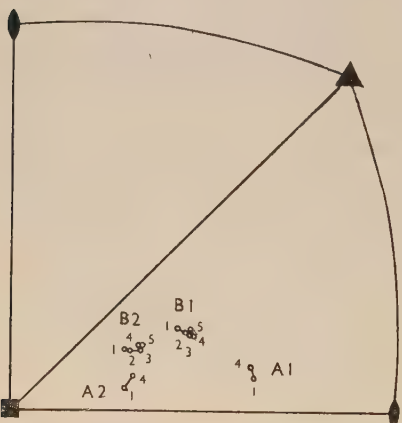


FIG. 7.—General Lattice Rotation of the Grains. Stress-axis positions drawn as circles of  $0.3^\circ$  radius.

#### KEY.

- Original position 1.
- Subsequent position 2 after 0.3% extension.
- Subsequent position 3 after 0.55% extension.
- Subsequent position 4 after 1.7% extension.
- Subsequent position 5 after 3.2% extension.

only one or two degrees, as high an accuracy as possible was required in the measurement of the X-ray films. This was achieved by the construction of a tenfold enlargement of the Laue pattern geometrically, showing only three selected reflections from each grain, and by devising a triangulation method of checking that the measured distances on the film were mutually consistent. From these measurements the position of the stress axis for each grain could be fixed on a standard stereographic projection. Simple manipulation of the Wulff net was not sufficiently accurate for this operation and geometrical constructions were instead used throughout. As the orientations

of the two grains of each pair were derived from the same grain-boundary pattern it was considered that the geometrical construction gave their relative orientations to within  $\pm 0.3^\circ$ . In Fig. 7 the stress-axis positions after various extensions for grains B1 and B2 show general trends of rotation, which suggests that the experimental error in relating the stress-axis position to successive patterns was not appreciably greater than this amount.

In the case of grain A1 the bulk rotation is that of an isolated single crystal in tension, that is, the stress axis shown in the stereographic projection (Fig. 7) moves towards the opposite (110) pole which is the operative direction. From the Schmid-Boas<sup>5</sup> formula  $l_1 \sin x_1 = l_0 \sin x_0$

(where  $l_0$  and  $l_1$  are the initial and final lengths of the crystal in the stress direction and  $x_0$  and  $x_1$  are the initial and final angles between the slip directions and the stress axis), the calculated rotations after 1.7% extension for the three slip directions of highest resolved shear stress ( $x_0 = 49^\circ, 58^\circ, 67^\circ$ ), are  $1.1^\circ, 1.6^\circ$ , and  $2.1^\circ$ , in reasonable agreement with the observed value of  $1.5^\circ$ . Patterns from the intermediate and grain-boundary positions of this grain showed development of a more complex type of spot (Fig. 3, Plate LIV).

The patterns from the centre of grain *A2* after 1.7 and 3.2% extension (Figs. 4 (*a*) and (*b*), Plate LV), show a definite splitting of the reflections into a series of more or less discrete spots. Part of the 110 zone is illustrated, and it will be observed that these discrete spots are evenly spaced along this zone hyperbola, and hence the splitting could be accounted for by the rotation of sub-structure units about this axis. However, the presence of the quite definite transverse asterism precludes the assumption that this is the unique operative axis of rotation. Fig. 4 (*c*) (Plate LV) shows the same zone recorded from the intermediate position of this grain after 1.7% strain and reveals a far more complex spreading of the spots with finer and less regular sub-structure. The structure is notable for the fact that one unit of sub-structure is well removed from the remainder of the units. The reflection from this unit is marked by arrows. The splitting effect is frequently observed, for example after 1.7% strain the spots on the pattern from the intermediate position of grain *B2* showed a complex splitting into two principal components with striations in each, while after 3.2% strain the patterns showed a greater separation of these two components with a more or less discrete spot sub-structure within each component (Figs. 6 (*a*) and (*b*), Plate LVI). The corresponding pattern from the grain centre was notable in showing a discrete reflection some  $4^\circ$  from the main spot.

After strain values of 9 and 13% the majority of patterns were characteristically different from those of earlier stages. They showed far more extensive and general spreading of the original spots, so much so that although the initial configuration of Laue spots was discernible, it was no longer possible to speak of a sub-structure of the spots, and in some cases the hyperbolæ corresponding to the direction of principal asterism became almost continuous broad zones. The coarse sub-structures of the earlier stages were no longer in evidence and the relatively few sub-structure units had disintegrated into a widespread distribution of numerous very much finer spots which varied widely in definition (Figs. 2 (*a*) and (*b*), Plate LIII, and Fig. 5, Plate LVI). Where crystal components were oriented to reflect the characteristic

radiation, the Debye-Scherrer arcs were frequently recorded as fairly sharp well-defined spots, with an angular separation of plane normals of a few minutes of arc only. The spot formations on some Debye-Scherrer arcs were very similar to the observations made by Wilms and Wood.<sup>6</sup>

### V.—DISCUSSION.

Of considerable significance in the interpretation of the observations is the mechanism causing the bulk rotations of the grains relative to one

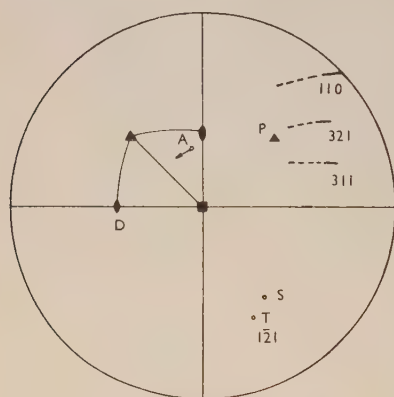


FIG. 8.—Asterism and Bulk Rotation of Grain A1.

#### KEY.

- A. Stress axis and direction of bulk rotation.
- D. Operative slip direction
- P. Operative slip plane
- T. Taylor crystallite "roller" axis.
- S. Axis  $\perp A$  and  $\perp D$ .

Directions of asterism are shown for the (110), (321), and (311) reflections, together with parts of the rotation circles about S.

another. These are sometimes ascribed to some form of viscous flow at the grain boundaries. The existence of grain-boundary flow appears to have been established by the work of Kê<sup>7</sup> who associates it with constant-rate (secondary) creep. Since the rotations were measurable in the earliest stages, that is, even after 0.3% strain, it is reasonable to conclude that these bulk rotations were caused by the operation of glide systems rather than by grain-boundary flow. This conclusion that the deformation during transient creep proceeds by glide processes is in accord with the metallographic observations of Hanson and Wheeler.<sup>8</sup>

It is perhaps significant that in grain A1, which displayed a predominantly simple asterism of the Laue spots, the bulk rotation up to a strain of 1.7% was within the limits of measurement consistent with a single axis of rotation and with the total amount of strain observed. The undirectional extension of the Laue spots on the grain-centre patterns which occurs at the same time may be attributed to rotation about an axis lying in the slip plane perpendicular to the operative slip direction, that is the Taylor crystallite "roller" effect. It may be stated, however, that in this particular case it might equally well be due to inhomogeneous single-crystal rotation, i.e. rotation about an axis perpendicular to the stress axis and the operative slip direction, since these two axes were quite close (Fig. 8).

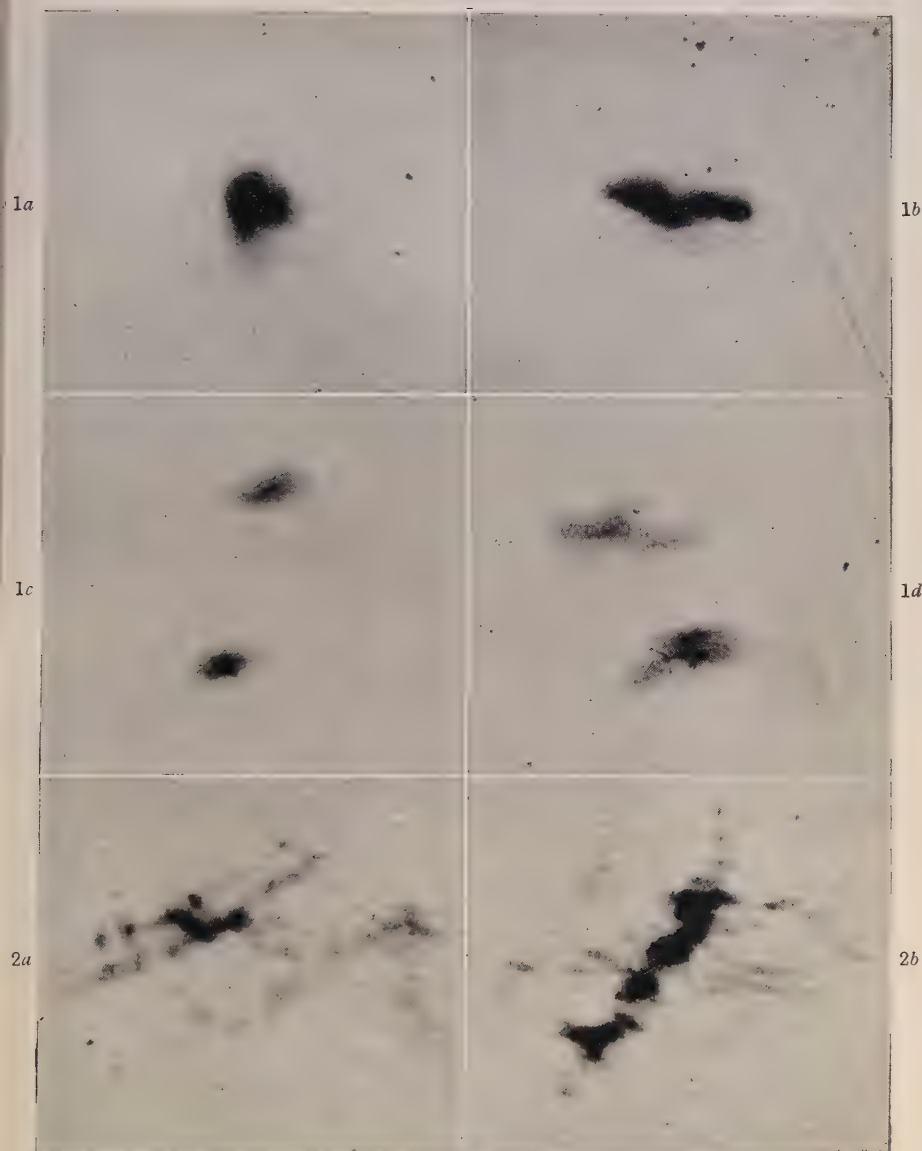


FIG. 1 (a).—Grain B2. Midway to boundary; after 1.7% extension. (110) reflection.  
 FIG. 1 (b).—Grain B2. Midway to boundary; after 1.7% extension. (211) reflection.  
 FIG. 1 (c).—B1/B2 Boundary; initial state. (110) reflection of B1; (211) reflection of B2.  
 FIG. 1 (d).—B1/B2 Boundary; after 1.7% extension. (110) reflection of B1; (211) reflection of B2. All  $\times 10$ .  
 FIG. 2 (a).—Grain A1. Centre; after 9% extension.  
 FIG. 2 (b).—Grain B2. Centre; after 9% extension. Both  $\times 10$ .

→ stress axis.

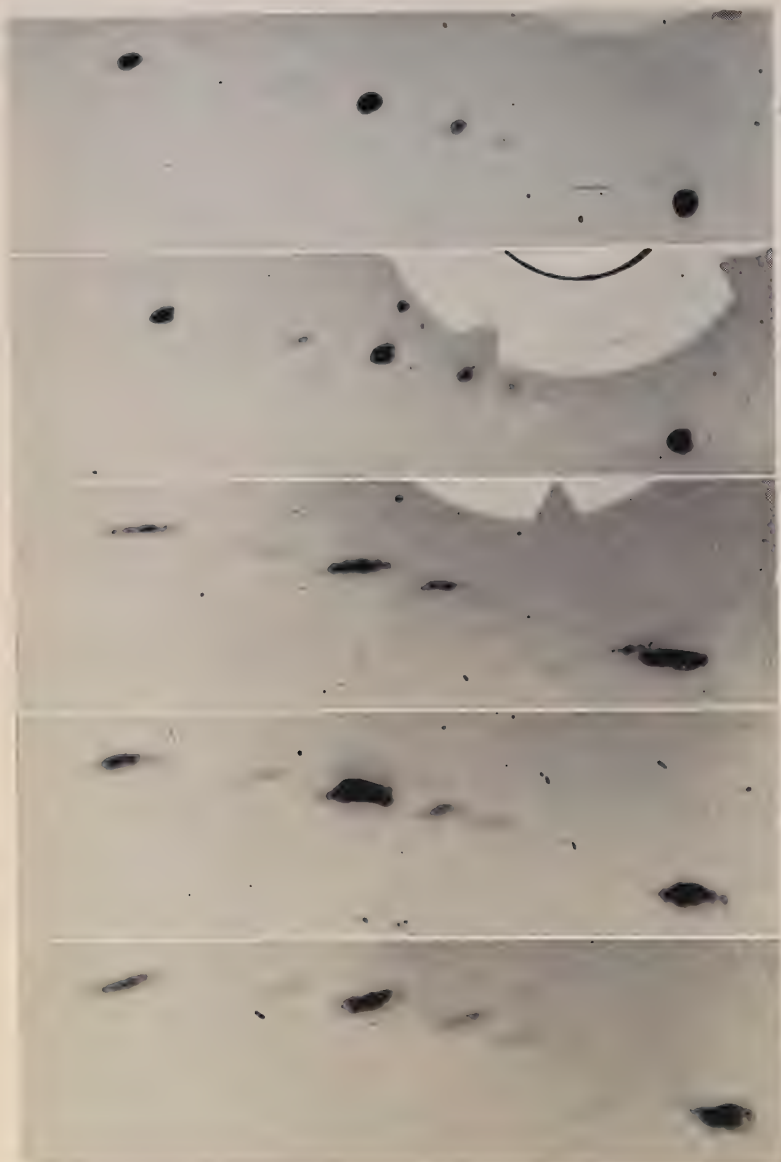


FIG. 3.—Grain A1.  $\times 3\frac{1}{2}$ .

- (a) Midway to boundary; initial state.
- (b) Centre; after 0.3% extension.
- (c) Centre; after 3.2% extension.
- (d) Midway to boundary; after 3.2% extension.
- (e) Boundary; after 3.2% extension.



—→ stress axis.

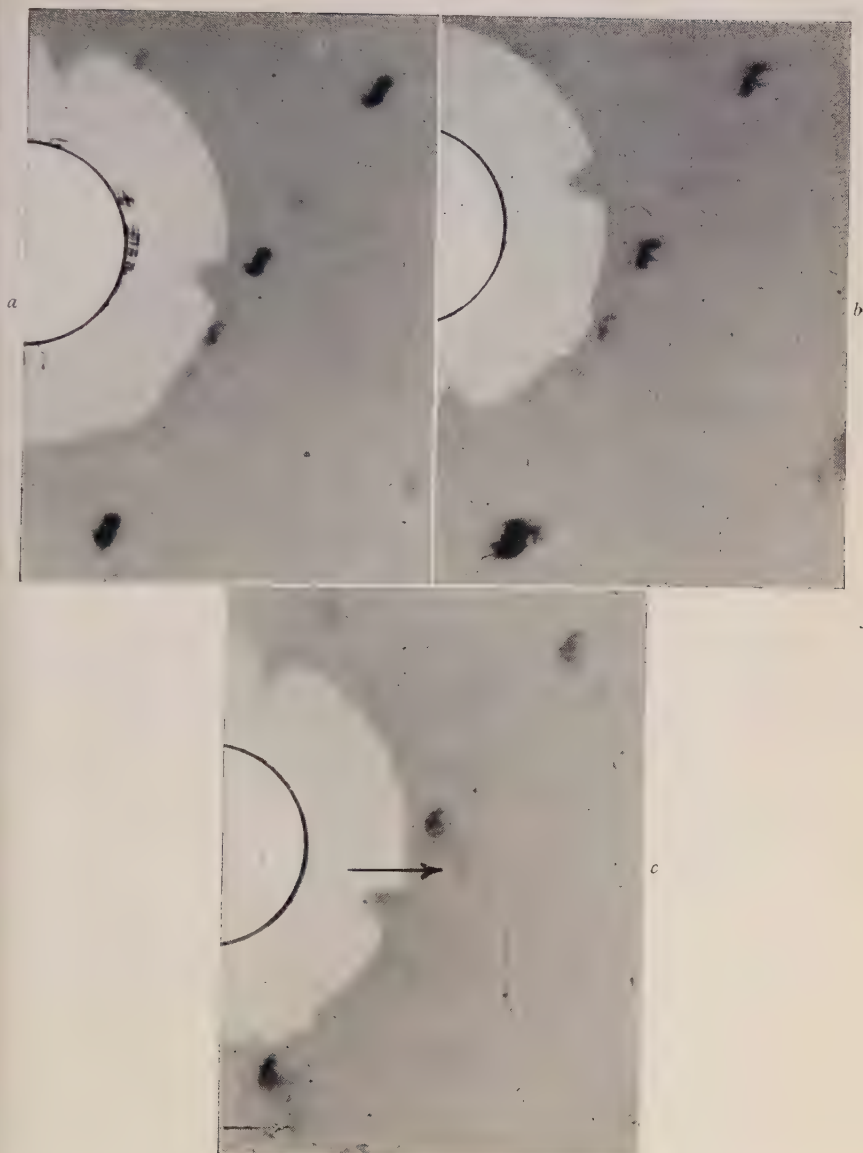


FIG. 4.—Grain 42.  $\times 3\frac{1}{2}$ .

- (a) Centre; after 1.7% extension.
- (b) Centre; after 3.2% extension.
- (c) Midway to boundary; after 1.7% extension. Arrows show unit of substructure well removed.

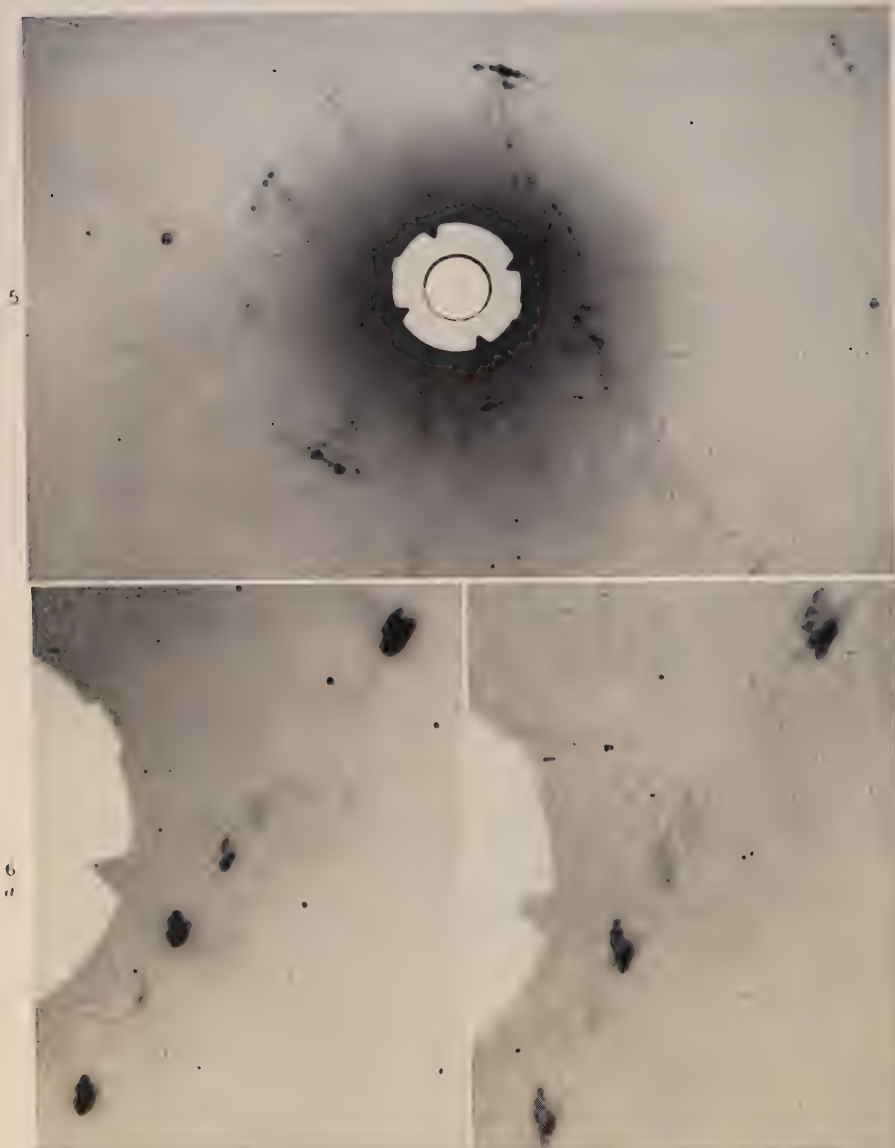


FIG. 5.—Grain A1. Centre; after 13% extension. Actual size.  
 FIGS. 6 (a) and (b).—Grain B2.  $\times 3\frac{1}{2}$ .

(a) Midway to boundary; after 1.7% extension.  
 (b) Midway to boundary; after 3.2% extension.

The analysis of the complex directions of spread found in grains other than *A1* is open to some doubt, first because in general the amount of linear spread was considerably less than in *A1*, and secondly because the splitting of the reflections is not necessarily the result of a single rotation. At 1.7 and 3.2% extension splitting was observed in five out of the ten irradiated positions. Assuming a single operative rotation axis it was possible to explain the directions of splitting in four of these cases by either Taylor crystallite rotation or rotation about a slip plane normal, and in the other case by inhomogeneous single-crystal rotation or rotation about a slip plane normal. Thus, in this last case only could the splitting be due to rotation about a single axis in the transverse section of the test-piece. Barrett and Levenson<sup>9</sup> concluded from X-ray work on a carefully compressed crystal that the directions of spread of orientation did not conform to the Taylor crystallite roller theory. Accepting this, the splitting would appear, on the assumption of a single rotation axis, to be due to rotation about the slip plane normal. On the other hand, it would be possible to propose several combinations of simultaneously operative rotation axes that would give the same effect.

One point, however, is indisputable, namely that in adjacent areas of the same grain the apparent directions of splitting are quite different, implying either different rotations or different relative amounts of rotation of the few large sub-structure units irradiated by the X-ray beam. It is possible that this sub-structure is connected with the interaction of adjoining grains, but since very similar splitting of reflections has been observed in single-crystal specimens at room temperature (Yen and Hibbard<sup>10</sup>), it is more likely to be due either to a macroscopic inhomogeneity inherent in the crystal and associated with its previous history or to the deformation process itself. This inhomogeneity may be connected with the malformation of the Laue spots of some of the patterns from the unstrained specimen, where the disorientation between the units of sub-structure would amount to only a few minutes of arc.

It has already been mentioned that the sub-structure units after 9 and 13% extension are considerably smaller than the units just discussed from which they may have been formed by further sub-division. On the other hand, they may be the result of a polygonization process, as described by Orowan, Cahn, Guinier, and others.

On the current hypotheses transient creep is considered as a slip process thermally activated in the presence of an applied stress nearly great enough to cause instantaneous slip. The decreasing rate is associated with exhaustion of the dislocations and, at higher stresses, with

physical hardening, namely the multiplication of dislocations and their locking together. Secondary creep is considered by Nowick and Machlin <sup>11</sup> to depend on the equilibrium between the exhaustion of the dislocations and their generation by thermal activation, but Mott <sup>12</sup> associates it, at higher stresses and temperatures, with viscous grain-boundary effects due to the melting of small groups of atoms in the boundary regions. On the experimental side, Wilms and Wood <sup>6</sup> deduce from X-ray and micrographic examination on material subjected to a constant rate of strain that transient creep is associated with the crystallite formation due to slip within the grains, while quasi-viscous creep is a result of much coarser cell formation, the cells having undistorted crystal structure and the deformation proceeding by their relative displacement and rotation. The results of the present investigation agree with their fundamental observation that cell formation or polygonization is present during secondary creep, but are at variance with their explanation of the origin of the cells. Wilms and Wood conclude that the cells form by direct division of the parent grains into substructure units whose size depends on the temperature and rate of deformation. In the work reported here, however, it has been shown that there is a marked variation of the size of the units throughout the extension. First a comparatively coarse sub-structure is formed, by processes apparently consistent with slip mechanisms, to be followed by increasingly complex deformation until the state is reached which is characterized by the presence of the numerous fine units or cells. The exact part which these latter units play in the continued deformation is not yet clearly demonstrated.

In conclusion it may be stated that under the conditions of the present experiments the creep deformation in the stage up to about 3% extension is accompanied by slip processes of which the striking feature is their inhomogeneity, not only from grain to grain but also within the grains themselves. In the later stages it proceeds by a mechanism associated with the formation of fine sub-structure units, believed to be the cells observed by Wilms and Wood, from the material previously deformed.

#### ACKNOWLEDGEMENTS.

The authors desire to acknowledge the advice of Mr. H. J. Tapsell and his assistance in arranging for the creep tests to be carried out in the Engineering Division of the Laboratory.

The work has been carried out as part of the Research Programme of the National Physical Laboratory, and this paper is published by permission of the Director of the Laboratory.

REFERENCES.

1. W. A. Wood and H. J. Tapsell, *Nature*, 1946, **158**, 415.
2. A. B. Greninger, *Trans. Amer. Inst. Min. Met. Eng.*, 1935, **117**, 75.
3. J. A. Collins and C. H. Mathewson, *Trans. Amer. Inst. Min. Met. Eng.*, 1940, **137**, 150.
4. R. D. Heidenreich and W. Shockley, *J. Appl. Physics*, 1947, **18**, 1029.
5. E. Schmid and W. Boas, "Plasticity of Crystals, with Special Reference to Metals" (translation of "Kristallplastizität"). 1950: London (F. A. Hughes and Co., Ltd.).
6. G. R. Wilms and W. A. Wood, *J. Inst. Metals*, 1948-49, **75**, 693.
7. T.-S. Kê, *J. Appl. Physics*, 1949, **20**, 274.
8. D. Hanson and M. A. Wheeler, *J. Inst. Metals*, 1931, **45**, 229.
9. C. S. Barrett and L. H. Levenson, *Trans. Amer. Inst. Min. Met. Eng.*, 1940, **137**, 112.
10. M.-K. Yen and W. R. Hibbard, Jr., *Trans. Amer. Inst. Min. Met. Eng.* (in *J. Metals*), 1949, **185**, 710.
11. A. S. Nowick and E. S. Machlin, *J. Appl. Physics*, 1947, **18**, 79.
12. N. F. Mott, *Research*, 1949, **2**, 162.





# THE THERMODYNAMICS AND KINETICS OF 1261 PRECIPITATION IN SOLID SOLUTIONS.\*

By H. K. HARDY,† Ph.D., M.Sc., A.R.S.M., A.I.M., MEMBER.

## SYNOPSIS.

The factors governing diffusion, fluctuations, and nucleation are briefly outlined to show the manner in which the precipitation process is controlled by the free-energy/composition and free energy/structure relationships. Various precipitation phenomena can be accounted for by the shape of the free energy/composition curve, from which the energy changes on precipitation can be derived. These energy changes control the mechanism of precipitation, and the rates of the various processes are determined by the energy barriers which have to be surmounted.

Description of the precipitation process in terms of a hypothetical free energy/composition curve shows that stable segregates of solute atoms are to be expected as the first stage of the breakdown from high initial concentrations. These segregates possess the structure of the parent lattice and are formed by uphill diffusion. On the other hand, at low initial degrees of supersaturation stable segregates do not occur and a "transient-steady" size distribution of embryos of the new phase is set up by downhill diffusion. These possess the lattice structure and composition of the new phase and attain stability as the true precipitate when the critical nucleus size has been reached. Alloys quenched and aged to give segregates may, on further ageing, form precipitates from the larger segregates provided that the process is structurally continuous or directly from the matrix if the process is not structurally continuous. In either case, the remaining segregates will be forced to redissolve in an attempt to maintain the matrix composition in equilibrium with them. The solute atoms from the segregates are deposited on the precipitate by normal downhill diffusion. The type of free energy/composition curve chosen leads directly to a theory of reversion. Segregates formed on ageing at a low temperature may redissolve when the alloy is raised to a temperature at which they are not normally formed and represent an unstable condition.

The time taken to set up the steady size distribution is the incubation period, and once this has been completed the critical nucleus size exerts a dominant effect on the rate of precipitation at low degrees of supersaturation. A check has been made of the Becker theory of rates of precipitation in lead-tin alloys and hence of the analysis setting up the Becker theory as defining the rate-controlling factor. The thermodynamic quantities for these calculations were obtained by methods used by Borelius in considering the same alloys, but from a different point of view.

## I.—INTRODUCTION.

THERMODYNAMIC theory, as normally applied, describes strictly equilibrium conditions. It can be used to define the initial and final

\* Manuscript received 18 October 1949.

† Head of Physical Metallurgy Section, Fulmer Research Institute, Stoke Poges, Bucks.

states, but gives little information about intermediate stages. That thermodynamics and kinetics do not require any exact model of the process is of advantage in presenting a generalized picture, but of disadvantage in that specific details of the process cannot be deduced. However, under the conditions peculiar to greatly supercooled materials, such as quenched alloys, the thermodynamic conditions of intermediate stages can be deduced and a descriptive account may be given of the mode of decomposition of the alloys.

The work described in this paper has had the following objectives:

(1) To present a general picture of precipitation from the viewpoint of classical thermodynamics and kinetics.

(2) To account for the occurrence of various intermediate states of the precipitate and, in particular, to find whether structures such as Guinier-Preston zones could be accounted for thermodynamically, as no adequate explanation of their possible existence had been offered previously. In this sense the paper arises from the account of the descriptive theories of precipitation given earlier.<sup>1</sup>

The free energy/composition curve of alloy systems has been taken as the starting point. The thermodynamic factors influencing diffusion, compositional fluctuations, and the formation of nuclei are briefly set out. These factors and their derivation are available in several textbooks on physical chemistry, but references to them are infrequent in metallurgical literature.

Although considerable work has been carried out on various thermodynamic aspects of precipitation, no complete account has been given previously of the process in terms of the free energy/composition curve for all degrees of supersaturation.

## II.—THE FREE ENERGY/COMPOSITION CURVES OF SOLID SOLUTIONS.

The stable alloy structure is that in which the thermodynamic potential,  $G$ , is at a minimum, where:

$$G = U - TS + pV \quad . \quad . \quad . \quad . \quad . \quad (1a)$$

$U$  being the internal energy,  $T$  the absolute temperature,  $S$  the entropy,  $p$  the pressure, and  $V$  the volume. In condensed alloy systems, the term  $pV$  is very small in comparison with  $(U - TS)$  and may be neglected, so that the condition for equilibrium is:

$$F = U - TS \quad . \quad . \quad . \quad . \quad . \quad (1b)$$

where  $F$  is the Helmholtz free energy and is in these circumstances practically identical with  $G$ .

The free energy will vary with composition and, since the stable

structure is that of lowest free energy, equilibrium diagrams may be accounted for in terms of the free energy/composition curves of the different phases.<sup>2</sup>

In assessing the variation of free energy of a solid solution with composition, allowance must be made for the thermodynamic potentials of the pure components, the deviation from an ideal solution, and the thermal and positional entropies of the components.<sup>3-6</sup> Entropy is a measure of the degree of randomness, so that the thermal entropy is an assessment of the distribution of atomic vibrations about their mean value, and the positional entropy measures the degree of disorder of the atoms in the parent lattice. An ideal solution may be defined as one which obeys Raoult's law so that the partial pressure is directly proportional to the concentration of the component over the whole range of concentrations and at all temperatures. No metallic solid solutions are strictly ideal, but they may be considered to be "regular" solutions, which is a solution in which the positional entropy is that of an ideal solution.<sup>3</sup>

By considering the internal energy as a function solely of the interaction energies of nearest neighbours<sup>7</sup> in the atomic assembly Becker<sup>8</sup> gives the free energy as:

$$F = ZNVx(1-x) + RTx \ln x + RT(1-x) \ln (1-x) \quad . \quad . \quad (2)$$

where  $N$  is Avogadro's number,  $Z$  is the co-ordination number (number of nearest neighbours), and  $V = V_{AB} - \frac{1}{2}(V_{AA} + V_{BB})$ ,  $V_{AA}$ , &c., being the interaction energies between neighbouring atoms,  $x$  is the atomic concentration, the last two terms are the positional entropy and  $R$  is the gas constant.

Consider the equilibrium diagram, Fig. 1 (a), of a hypothetical system of alloys which solidifies to give a continuous series of solid solutions, and in which this single solution breaks up into two phases at a lower temperature and over a limited range of compositions. For such a system the Becker equation (equation 2) will, by a suitable choice of the value for  $V$ , give a free energy/composition curve for a temperature  $T_1$  similar to that in Fig. 1 (b). It can be shown that an alloy of composition  $QR$  will, on cooling to a temperature  $T_1$ , break up into a mixture of two phases of composition  $x_1$  and  $x_2$ , and that this mixture will have the lowest possible free energy  $F_R$ , the condition being that the points  $F_{x_1}$ ,  $F_R$ , and  $F_{x_2}$  lie along the common tangent to the two portions of the free-energy curve. It follows, therefore, that the condition for the phase boundaries is that:

$$\frac{\partial F_1}{\partial x_1} = \frac{\partial F_2}{\partial x_2} \quad . \quad . \quad . \quad . \quad . \quad . \quad . \quad . \quad (3)$$

where  $F_1$  and  $F_2$  are the free energies of the two phases. Where the two components  $A$  and  $B$  can form, at least hypothetically, a continuous series of solid solutions, it is reasonable to make the free-

energy curve continuous between the two phases.

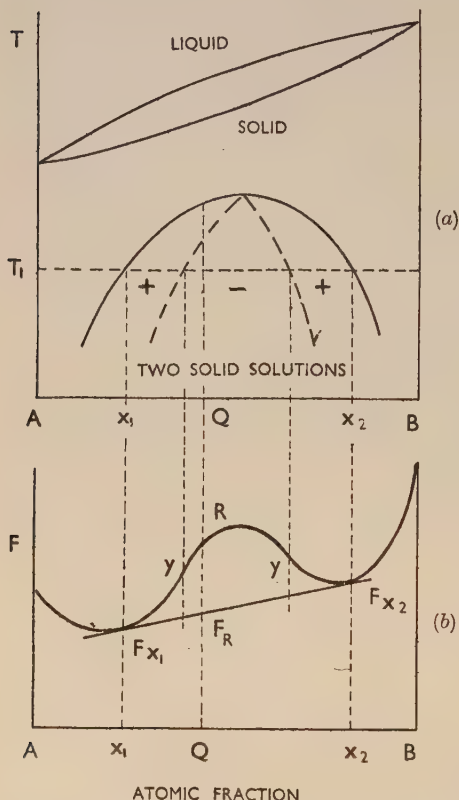


Fig. 1.—(a) Equilibrium diagram of system solidifying to a continuous series of solid solutions which break up into two solid solutions at a lower temperature. (b) The free energy/composition curve at  $T_1$  for the hypothetical diagram of (a).

An alloy quenched from the single-phase into the two-phase region may be regarded as having the free energy which would be possessed by the single-phase alloy of the same composition, could it exist at the quenching temperature. Thus the portion  $F_{x_1}-R-F_{x_2}$  of the free energy-curve of Fig. 1 (b), lying above the common tangent, gives the free energy of the alloys quenched to the temperature  $T_1$  which still retain the single-phase structure. It may be noted that in this region a portion of the free energy/composition curve is convex to the composition axis, and this may be expressed by saying that the second differential  $\partial^2 F / \partial x^2$  is negative (see Figs. 1 (a) and (b)).

In Fig. 1 (a) dotted boundaries have been inserted to correspond with the points of inflection of the supersaturated portion

of the free-energy curve. They thus indicate the compositions and temperatures at which the second differential coefficient  $\partial^2 F / \partial x^2$  changes from positive to negative.

The quenched alloy will tend to change to the most stable structure, i.e. that given by a mixture of the stable phases, and the precipitation theory is an account of the mechanism by which this change takes place.



## III.—DIFFUSION FOR PRECIPITATION.

The decomposition of the quenched alloy will not take place unless it is possible for diffusion to occur, and the rate of diffusion will be one of the factors controlling the rate of precipitation.

Fick's first and second equations for one-dimensional flow along the  $y$  axis are :<sup>9</sup>

$$P = -D \frac{\partial x}{\partial y} \quad \text{and} \quad \frac{\partial x}{\partial t} = \frac{\partial}{\partial y} \left( D \frac{\partial x}{\partial y} \right) \quad . \quad . \quad . \quad (4)$$

where the flow  $P$  is expressed as proportional to the concentration gradient  $\partial x/\partial y$  and  $D$  is the diffusion coefficient.  $\partial x/\partial t$  in the second equation represents the quantity transferred per unit time.

If, instead of the concentration gradient, the driving force for diffusion is taken to be the free-energy gradient,<sup>10, 11, 12 \*</sup> the diffusion equations may be written :

$$P = -D^0 D^T \frac{\partial x}{\partial y} \quad \text{and} \quad \frac{\partial x}{\partial t} = \frac{\partial}{\partial y} \left( D^0 D^T \frac{\partial x}{\partial y} \right) \quad . \quad . \quad . \quad (5)$$

where  $D^0$  is the simple diffusion coefficient and  $D^T$  is a dimensionless thermodynamic factor based on the free energy/composition gradient.

For a regular binary solution this factor works out as :

$$D_{ab}^T = \frac{x_a x_b}{RT} \frac{\partial^2 F}{\partial x_a^2}$$

where  $x_a$  and  $x_b$  are the atomic concentrations of the components,  $F$  is the free energy of the solid solution, and  $R$  is the gas constant. For an ideal solution  $D_{ab}^T$  is equal to unity. It was first pointed out by Dehlinger<sup>10</sup> that the sign of  $\partial^2 F/\partial x^2$  determines the sign of the diffusion equation through its effect on the sign of  $D_{ab}^T$ . When the sign  $\partial^2 F/\partial x^2$  becomes negative any concentration differences will be accentuated, leading to segregation of like atoms or "uphill" diffusion against the concentration gradient. The point of inflection on the free energy/composition curve in the supersaturated region gives the boundary between positive and negative values of  $\partial^2 F/\partial x^2$  (see Figs. 1 (a) and (b)), and is thus of fundamental significance in precipitation theory. An alloy quenched into a region of negative  $\partial^2 F/\partial x^2$  may be expected to show segregation of like atoms.<sup>†</sup>

\* Other views are also possible, cf. references Nos. 12 and 13.

† Cottrell<sup>14</sup> suggests that Fick's law cannot be applied in regions where  $\partial^2 F/\partial x^2$  is negative because of the smallness of the numbers of atoms involved. This is correct when considering the detail of the segregation process, but is equally true when considering the detail of normal downhill diffusion. It is, however, permissible to apply the Fick equations to obtain an overall picture of diffusion in either direction.

## IV.—FLUCTUATIONS IN SOLID SOLUTIONS.

Although nominally disordered statistically, all solid solutions will show fluctuations within small regions from the mean value of the composition. Such fluctuations, either retained on quenching or formed in the supersaturated material, will have an important bearing on the decomposition of the solid solution.

The probability of an atom having an energy  $\Delta F$  higher than the average is proportional to :

$$e^{-\Delta F/kT} \quad . \quad . \quad . \quad . \quad . \quad . \quad . \quad . \quad . \quad . \quad (6)$$

where  $k$  is Boltzmann's constant and  $T$  is the absolute temperature. A fluctuation is defined as the square of the difference from the mean, i.e.  $(x - x_0)^2$ . The probability of a fluctuation is a Gaussian function and may be put proportional to : <sup>5, 6, 15</sup>

$$e^{-(x - x_0)^2 (\partial^2 F / \partial x^2) / kT} \quad . \quad . \quad . \quad . \quad . \quad . \quad . \quad . \quad . \quad . \quad (7)$$

Laurent <sup>16</sup> has attempted to apply fluctuation theory to the precipitation process. However, the integrals are extremely complex and it is probably better to draw only very general conclusions.

The significance of expression (7) in relation to precipitation theory is that this probability factor influences the formation of fluctuations in those regions of the diagram in which  $\partial^2 F / \partial x^2$  is positive, in other words over a range of compositions extending up to the point of inflection in the free-energy curve <sup>15</sup> (point  $y$  in Fig. 1 (b)). Beyond this composition, where  $\partial^2 F / \partial x^2$  becomes negative, this probability becomes unity and no activation energy is required for segregation within the parent lattice other than that for diffusion. Such segregates are also known as clusters.

Borelius <sup>15</sup> has interpreted two branches to the rate of precipitation/composition curve in gold-platinum alloys <sup>17</sup> as indicating a transference from a positive to a negative value of  $\partial^2 F / \partial x^2$ . But, since the possibility of a change from continuous to discontinuous precipitation was neglected, this cannot be taken as proved. For lead-tin alloys, however, Borelius, Larris, and Ohlsson <sup>18</sup> have calculated the ageing temperature at which  $\partial^2 F / \partial x^2$  becomes negative for a given composition and correlated it fairly satisfactorily with the rates of ageing. These experiments are discussed more fully below.

## V.—THE WORK OF FORMATION AND THE MINIMUM STABLE SIZE OF NUCLEI.

A new phase is formed by the creation of a nucleus capable of growth and possessing an interface with the parent matrix. A nucleus

smaller than the minimum critical size for stability and growth will be termed an "embryo". Phase transformation takes place with a drop in free energy, some of which is used to provide the interfacial energy of the nucleus. The conditions are :

*Cubical Nucleus.*

*Spherical Nucleus.*

$$\Sigma F_p = -\frac{a^3 \Delta F}{N} + 6a^2 \sigma \quad \Sigma F_p = -\frac{4}{3} \pi a^3 \frac{\Delta F}{N} + 4\pi a^2 \sigma \quad . \quad . \quad . \quad (8)$$

where  $\Sigma F_p$  is the free-energy change on the formation of a nucleus (or an embryo) of the precipitate,  $-\Delta F$  is the free-energy reduction/g.-atom of the new phase,  $N$  is Avogadro's number,  $\sigma$  is the interfacial energy per atom, and  $a$  is a measure of the size of the nucleus.

The variation of  $\Sigma F_p$  with  $a$  in a supersaturated solution is shown in Fig. 2. The critical nucleus size is at  $a_0$ ; nuclei above this size are capable of growth with a fall in free energy. Differentiation of equations (8) and equating to zero gives the position of the maximum on the curve as :

*Cubical Nucleus.*

*Spherical Nucleus.*

$$a_0 = \frac{4N\sigma}{\Delta F} \quad a_0 = \frac{2N\sigma}{\Delta F} \quad . \quad . \quad . \quad (9)$$

Embryos smaller than the critical size will tend to redissolve rather than to grow.

The activation energy or the work of formation for the surface,  $A_0$ , which has to be supplied to produce a nucleus of the critical size,<sup>8, 19</sup> is :

*Cubical Nucleus.*

*Spherical Nucleus.*

$$A_0 = 2a_0^2 \sigma \quad A_0 = \frac{4}{3} \pi a_0^2 \sigma \quad . \quad . \quad . \quad (10)$$

Thus the work of formation is equal, for cubic and spherical nuclei respectively, to one-third of the surface energy term associated with the critical nucleus size, which is Gibbs' equation.<sup>20</sup>

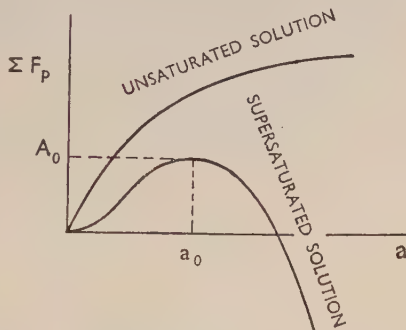


FIG. 2.—Variation of  $\Sigma F_p$  with size of embryo for unsaturated and supersaturated solutions.

The activation energy can also be expressed independently of  $\alpha_0$ , viz.:

$$\begin{array}{ll} \text{Cubical Nucleus.} & \text{Spherical Nucleus.} \\ A_0 = \frac{32\sigma^3 N^2}{\Delta F^2} & A_0 = \frac{16}{3} \pi \frac{\sigma^3 N^2}{\Delta F^2} \end{array} \quad (11)$$

It will be seen from equations (11) that the activation energy which has to be supplied is inversely proportional to the square of the free-energy change per atom of precipitate. It also follows from equations (9) that the critical nucleus size is inversely proportional to the free-energy change per atom of precipitate. Since  $\Delta F$  can be estimated from the free energy/composition curve, these relationships are of importance in determining the size and rate of formation of the precipitate.

For solid solutions it is also necessary to allow for the strain energy due to volume changes. This will introduce an additional positive term into equations (8) so that they become:

$$\left. \begin{array}{l} \text{Cubical Nucleus.} \\ \Sigma F_p = -\frac{a^3 \Delta F}{N} + 6a^2 \sigma + a^3 \varepsilon \\ \text{Spherical Nucleus.} \\ \Sigma F_p = -\frac{4}{3} \pi a^3 \frac{\Delta F}{N} + 4\pi a^2 \sigma + \frac{4}{3} \pi a^3 \varepsilon \end{array} \right\} \quad (12)$$

where  $\varepsilon$  is the strain energy per atom of the precipitate and is independent of the size of the particles.<sup>21</sup>

The maximum on the curve for the free energy plotted against size of nucleus is now at:

$$\begin{array}{ll} \text{Cubical Nucleus.} & \text{Spherical Nucleus.} \\ a_0 = \frac{4N\sigma}{\Delta F - N\varepsilon} & a_0 = \frac{2N\sigma}{\Delta F - N\varepsilon} \end{array} \quad (13)$$

Thus, the inclusion of a strain-energy term reduces the effective free-energy change but, since it does not influence the form of the equation, it will be neglected in the subsequent treatment.

The existence of a critical nucleus size depends on the existence of the surface-energy terms. The first and third terms on the right-hand side of equations (12) could not in themselves give rise to a maximum for  $\Sigma F_p$  plotted against  $a$ .

## VI.—THE INCUBATION PERIOD.

It is frequently found that the property changes associated with ageing reach their maximum rate of change some time after the beginning of the transformation. The cumulative curve for the extent of

decomposition then has the typical shape shown in Fig. 3. The initial stage where the rate of change is small is usually called the incubation period. There are two ways in which an incubation period may arise. Firstly, an incubation period is to be expected when a distribution of nuclei has been inherited from a previous treatment. This applies to processes such as recrystallization, where the relatively few points of highest free energy have the greatest probability of transformation but where the maximum rate is determined by the very much larger number of points of slightly lower free energy. This gives rise to an apparent incubation period which is a function of the particular distribution. Secondly, an incubation period is to be expected where no nuclei are inherited and atomic re-arrangements and energy fluctuations are necessary to initiate the transformation. This represents a real incubation period and applies to the formation of particles of precipitate.

The only satisfactory basic account of the incubation period has been derived by Frenkel for reactions not involving a change of composition.<sup>22, 23</sup> This treatment will be adopted here, since it forms a necessary preliminary to the discussion of the precipitation process in which allowance has to be made for a change in composition. Frenkel's discussion of pre-transitional effect<sup>22, 23</sup> has been used by Fisher, Hollomon, and Turnbull<sup>24</sup> to give the following explanation of the incubation period.

The energy change involved in the formation of an embryo of the new phase in the quenched material has been given for a nucleus of cubic shape as :

$$\Sigma F_p = -\frac{a^3 \Delta F}{N} + 6a^2 \sigma \quad . \quad . \quad . \quad . \quad . \quad (8)$$

where  $-\Delta F$  is the energy reduction on the formation of the new phase,  $a^3$  is the number of atoms in the embryo, and the volume strain-energy term of equation 12 has been neglected. An embryo is regarded as having the lattice structure as well as the composition of the new phase, but is smaller than the critical nucleus size.

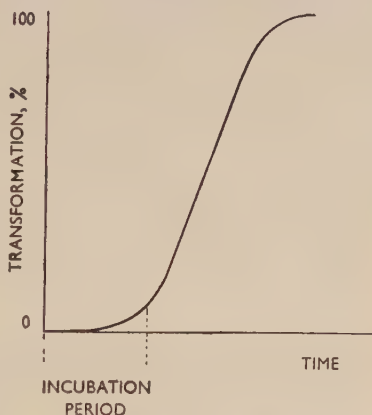


FIG. 3.—Cumulative transformation curve in the presence of an incubation period.



Likewise the energy change involved in the formation of an embryo in the solid-solution single-phase region may be put as :

$$\Sigma F_p = \frac{a^3 \Delta F}{N} + 6a^2 \sigma \quad . \quad . \quad . \quad (14)$$

This differs from equation (8) in that the first term on the right-hand side is no longer negative, as it is in the case of material quenched into the two-phase region of the equilibrium diagram. A phase change in a single-phase unsaturated region would require an increase in energy, and in this case  $\Sigma F_p$  increases continuously with size of the hypothetical embryo, as shown in Fig. 2.

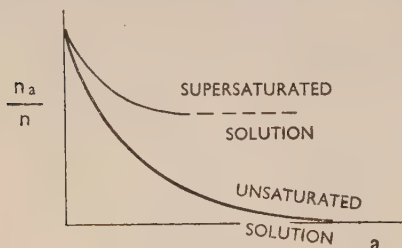


FIG. 4.—Steady size distribution for embryos in supersaturated and unsaturated solutions.  $n_a/n$  is the number of embryos containing  $a$  atoms out of all the embryos.

The individual embryos (equation (14)) possess a higher energy than the mean, and will have a greater tendency to redissolve than to grow indefinitely. But there will be a steady size distribution, considered statistically, of embryos which individually

are in the process of growth and re-solution. This is termed a "transient-steady" size distribution,<sup>24</sup> and will also apply to the rising part of the  $\Sigma F_p$  curve (equation (8)) for the supersaturated solution in Fig. 2.

The probability of an embryo containing  $a^3$  atoms being formed is proportional to :

$$e^{-\Sigma F_p/kT} \quad . \quad . \quad . \quad (15)$$

where  $\Sigma F_p$  is the additional energy required for its formation. The number of such embryos containing  $a^3$  atoms out of all the embryos is :

$$\frac{n_a}{n} = e^{-\Sigma F_p/kT} \quad . \quad . \quad . \quad (16)$$

The steady size distribution of embryos of different sizes may be derived from Fig. 2, and is given in Fig. 4. The incubation period now represents the time for the steady size distribution of embryos to change from that characteristic of the high-temperature unsaturated solution to that characteristic of the supersaturated quenched material. This process has been analysed by Turnbull<sup>25</sup> with the assumption that the growth of the embryos is by unit changes involving the excess additions of one atom over the removals of one atom at a time over all

the embryos. Embryos arise initially by an energy fluctuation involving the smallest possible number of atoms having the precipitate composition. Such groups of atoms are inherent in the statistical distribution within a solid solution. When the embryos have grown to a size equal to  $a_0$  (Fig. 2) they will be removed from the "transient-steady" size distribution as stable nuclei. Any embryo in the unsaturated solution larger than the critical size  $a_0$  will immediately transform on quenching without any incubation period.

## VII.—THE FREE-ENERGY CHANGE ASSOCIATED WITH PRECIPITATION.

The free-energy change associated with precipitation is readily obtained from the free energy/composition curve. In Fig. 5 an alloy of composition  $x$  with free energy  $f$  is precipitating a phase  $\beta$  of composition  $x_2$  and free energy  $f_2$  and forming a matrix  $\alpha$  of composition  $x_1$  and free energy  $f_1$ . In the supersaturated condition the alloy is on the free-energy curve at  $B$ , whilst  $AC$  is the common tangent. On complete precipitation  $x$  forms  $\frac{x-x_2}{x_1-x_2}$  parts of  $\alpha$  and  $\frac{x_1-x}{x_1-x_2}$  parts of  $\beta$ .

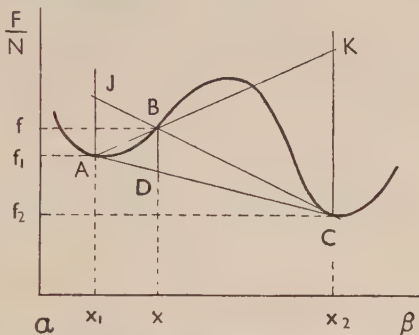


FIG. 5.—Free-energy changes for complete precipitation.

The free-energy change on complete precipitation is :

$$\Delta f = f - \frac{x-x_2}{x_1-x_2} f_1 - \frac{x_1-x}{x_1-x_2} f_2 \quad . \quad . \quad . \quad (17)$$

where  $f_1$  and  $f_2$  are the free energies of the stable phases  $\alpha$  and  $\beta$ . It is easily shown geometrically that this reduces to :

$$\Delta f \text{ per atom of alloy} = f - f_1 - \frac{\partial f_1}{\partial x_1} (x_1 - x) \quad . \quad . \quad (18)$$

which is equivalent to  $BD$  in Fig. 5.

If the free-energy change per atom of alloy is divided by the atomic fraction of  $\beta$ , the quotient gives the free-energy change per atom of  $\beta$ . It is then easily shown geometrically that :

$$\Delta f \text{ per atom of } \beta = [KC] \text{ (see Fig. 5)} \quad . \quad . \quad . \quad (19)$$

The condition at the beginning of precipitation, when  $x$  and  $x_1$  can be taken as infinitely close together, is shown in Fig. 6 for the

precipitation of an intermetallic compound of composition  $x_2$ .  $f_2$  is the point of contact of the common tangent to the two free-energy curves. When  $x$  and  $x_1$  lie infinitely close together,  $x_1xK$  is the tangent

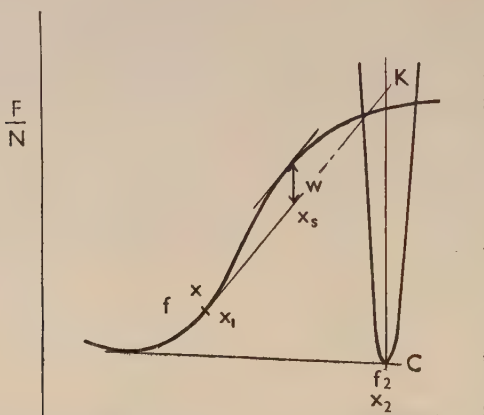


FIG. 6.—Free-energy change at the beginning of precipitation =  $[KC]$  per atom of precipitate.  $w$  per atom is the energy of activation which would be required to allow segregation of solute atoms to occur from  $x$  to  $x_2$ .<sup>26</sup>

to the curve at  $x$ . The free-energy change per atom of the initial precipitate is now :

$$\Delta f/\text{atom of ppte.} = \left[ f - f_2 + \frac{\partial f}{\partial x}(x - x_2) \right] = [KC] \quad . \quad . \quad (20)$$

and is equal to  $KC$  in Fig. 6.

Thus, by comparison with nucleation theory (Section V), the critical nucleus radius is inversely proportional to  $[KC]$  and the activation energy is inversely proportional to  $[KC]^2$ . These can be calculated if the free energy/composition relationship can be established.

## VIII.—PRECIPITATION IN TERMS OF THE FREE ENERGY/COMPOSITION CURVE.

### 1. Previous Treatments.

There have been several previous treatments, but no general account has been provided showing the variations for all degrees of supersaturation. Becker<sup>8, 19</sup> has described the effect of the surface energy of the nucleus in giving rise to the activation energy for nucleation. Borelius<sup>26</sup> has considered the influence of an activation energy for segregation. Hobstetter,<sup>27</sup> although attempting to rationalize the

Becker and Borelius approaches, actually gave a refinement of the Becker treatment showing the effect of slight variations in nucleus composition on the free-energy drop and hence on the activation energy for nucleation. The actual composition of the nucleus was more critical the lower the degree of supersaturation. By using Takagi's calculations<sup>28</sup> on free energy in terms of the Bethe interactions and Becker's equation (2), Laurent<sup>29</sup> has calculated the condition that an energy drop should accompany segregation. The resulting expression is very complicated and not easy to interpret in terms of a physical picture. These approaches are each applicable only to specific degrees of supersaturation.

## 2. *Present Treatment.*

The results obtained in the foregoing Sections allow an account to be given of an alloy undergoing precipitation in terms of its free-energy compositional and structural relationships.

One object of the analysis is to determine the conditions under which decomposition occurs by the formation of segregates or of precipitate. A segregate is taken to be formed by a change of composition within the parent lattice and without change of structure. Segregates of solute atoms are also termed clusters, but the former expression will generally be used here. A precipitate is taken to be a region possessing a composition and structure different from that of the matrix. The precipitate may be either coherent or non-coherent with the lattice of the matrix but possesses an energy term proportional to its surface area. Embryos are regions of precipitate structure and composition which are below the minimum critical size for a stable nucleus.

The following assumptions have been made in the initial analysis: (1) the volume of the segregate or cluster of solute atoms has been taken as that possessing the mean composition of the precipitate; (2) all processes are structurally continuous. This implies that a segregate can change to a precipitate and that intermediate precipitate can change to more stable forms by allotropic transformations.

The effect of removing these restrictions is discussed later.

## 3. *Free-Energy Drop and Stable Nucleus Size for Precipitation.*

Fig. 7 (a) shows the free-energy change per atom of the nucleus on initial precipitation from various parts of the free energy/composition curve.  $f_2$  is the free energy of a coherent intermediate precipitate possessing a form of interface with the matrix which gives rise to a strain-energy term proportional to the surface area.  $F_2$  is

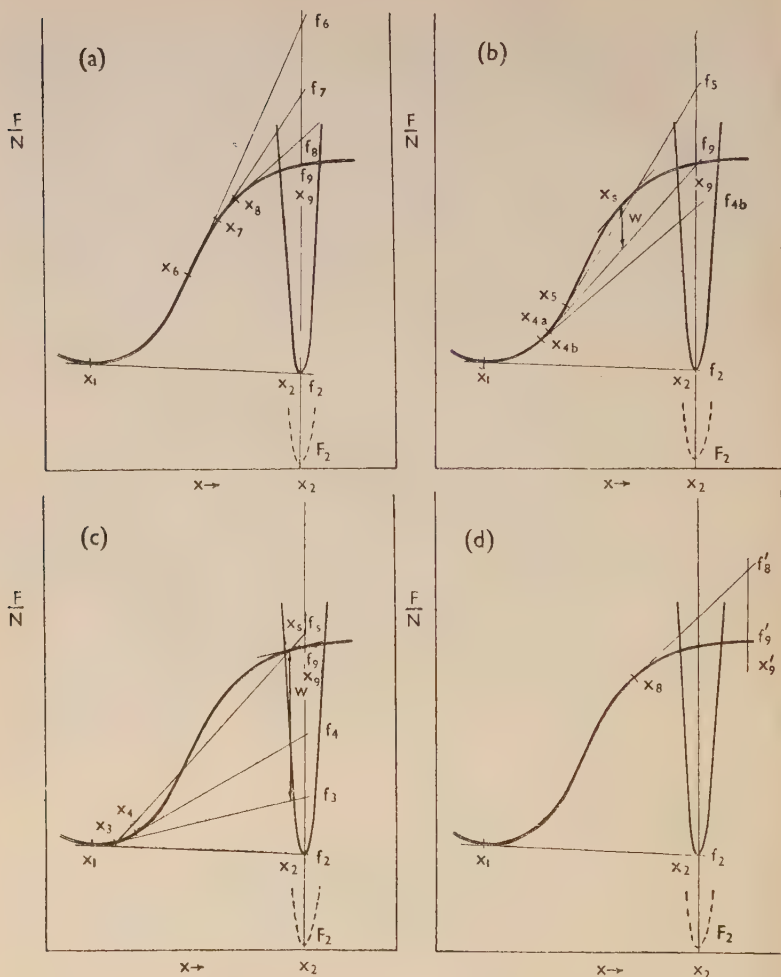


FIG. 7.—Free-energy changes on decomposition from various degrees of super-saturation. The straight lines are tangents to the free energy/composition curve at the concentrations indicated. The corresponding energy drop per atom of precipitate is given by the vertical distance at the precipitate composition, e.g. from  $x_5$  this is  $f_5 - f_9$ , or  $f_5 - f_2$ , or  $f_5 - F_2$ , depending on the precipitate formed.

(a)–(c) cover alloys quenched to the part of the free energy/composition curve in which the probability of a change is proportional to  $\exp[-Q/RT]$  (a);  $\exp[-(Q + W)/RT]$  (b); and  $\exp[-(Q + A)/RT]$  (c).

(d) gives the conditions should segregation occur beyond the  $x_2$  composition.

$Q$  is the activation energy for diffusion.  
 $W$  " " " segregation.  
 $A$  " " " nucleation.



the free energy of the equilibrium precipitate formed from the intermediate precipitate by an allotropic change.  $f_9$  is the free energy of the supersaturated solid solution of the same composition as the precipitate.  $x_8$  lies at the point of inflection of the free energy/composition curve and is thus also the concentration representing the change from a positive to a negative value of  $\partial^2 F / \partial x^2$ .  $x_{4a}$  (see Fig. 7 (b)) is the point of contact with the curve of a tangent drawn from  $x_9 f_9$ .

The free-energy drop per atom of the intermediate precipitate is given by the vertical distance between  $f_2$  and the tangent from any

TABLE I.—*Minimum Nucleus Size,  $a_0$ , and Activation Energy,  $A_0$ , for the Formation of the Intermediate Precipitate for the Initial Concentrations Shown in Fig. 7.*

Initial Concentration	$a_0$ proportional to :	$A_0$ proportional to :
$x_8$	$\frac{1}{f_8 - f_2}$	$\left( \frac{1}{f_8 - f_2} \right)^2$
$x_7$	$\frac{1}{f_7 - f_2}$	$\left( \frac{1}{f_7 - f_2} \right)^2$
$x_6$	$\frac{1}{f_6 - f_2}$	$\left( \frac{1}{f_6 - f_2} \right)^2$
$x_5$	$\frac{1}{f_5 - f_2}$	$\left( \frac{1}{f_5 - f_2} \right)^2$
$x_{4a}$	$\frac{1}{f_{4a} - f_2}$	$\left( \frac{1}{f_{4a} - f_2} \right)^2$
$x_4$	$\frac{1}{f_4 - f_2}$	$\left( \frac{1}{f_4 - f_2} \right)^2$
$x_3$	$\frac{1}{f_3 - f_2}$	$\left( \frac{1}{f_3 - f_2} \right)^2$
$x_1$	$\infty$	$\infty$

particular concentration, points  $f_3$  to  $f_9$ . At concentrations lower than  $x_{4a}$  (Figs. 7 (b) and (c)), the free-energy drop on precipitation, e.g.  $f_{4b} - f_2$ , will be less than the value  $f_9 - f_2$ . It will be noted that at concentrations higher than  $x_6$  the free-energy change per atom of precipitate begins to diminish. This does not, of course, apply to the total-energy change which continues to increase.

The minimum nucleus size and activation energy for the formation of the stable initial nucleus of the intermediate precipitate are proportional to the values shown in Table I.

#### 4. Decomposition from High Initial Concentrations.

At concentrations higher than  $x_6$  (Fig. 7 (a)) all segregations of like atoms are accompanied by a decrease in overall free energy and will

occur provided that the energy is available for the diffusion mechanism. The energy drop per atom of segregate is, for example,  $f_7 - f_9$ .

Segregates do not possess an interface with the matrix, but they will possess a strain-energy term due to differences in atomic size. Part of this strain energy is associated with the steep concentration gradient between segregate and matrix, and can thus be regarded as analogous to an interfacial energy. This part of the strain energy will then be proportional to the equivalent surface and gives rise to an equation similar to equation (8), namely:

$$\Sigma F_s = -a^3 \Delta f_s + 6a^2 \sigma \quad . \quad . \quad . \quad . \quad . \quad . \quad (21)$$

the minimum stable size being given by:

$$a_{0s} = \frac{4\sigma}{\Delta f_s} \quad . \quad . \quad . \quad . \quad . \quad . \quad (22)$$

where  $-\Delta f_s$  is the energy drop on segregation and  $\sigma$  is equivalent to the interfacial energy per surface atom. Since the segregates are continuous with the lattice,  $\sigma$  will depend on particle size. But, as this will be very small initially,  $a_{0s}$  will be very small and segregation can occur within a region of negative  $\partial^2 F / \partial x^2$  with no activation energy except that for diffusion.

The probability of segregation is thus proportional to:

$$e^{-Q/RT} \quad . \quad . \quad . \quad . \quad . \quad . \quad (22a)$$

where  $Q$  is the activation energy for diffusion and no activation energy is required for segregation.

The smallest stable nucleus of the intermediate precipitate would be formed by a direct fluctuation from the  $x_6$  composition. The condition for the intermediate precipitate of minimum stable size  $a_{0i}$  (see Fig. 8 (a)) is:

$$a_{0i} = \frac{4S}{\Delta f_i} \quad . \quad . \quad . \quad . \quad . \quad . \quad (23)$$

where  $S$  is the interfacial energy per surface atom of the precipitate and  $\Delta f_i$  is the free-energy change per atom of the intermediate precipitate. The probability of the direct formation of the stable nucleus is proportional to:

$$e^{-\frac{(Q + A_0)}{RT}} \quad . \quad . \quad . \quad . \quad . \quad . \quad (23a)$$

where  $A_0$  is the additional activation energy required for nucleation (see Fig. 2).

Comparison of equations (22a) and (23a) shows that segregation within the parent lattice will be preferred to the formation of a new

phase with a different lattice structure. Such segregates, say of composition  $x_9$ , will remain stable until they have reached a critical size  $a_{0(s \rightarrow i)}$  at which they will transform to the intermediate precipitate by an allotropic change assuming that the process is structurally continuous. The condition for this change is given by :

$$a_s = a_{0(s \rightarrow i)} = 6 \frac{(S - \sigma)}{f_i - f_s} = 6 \frac{(S - \sigma)}{f_9 - f_2} \quad (24)$$

at which stage a particle of the intermediate precipitate will be formed.

These relationships are shown diagrammatically in Fig. 8 (a).  $\Sigma F_s$

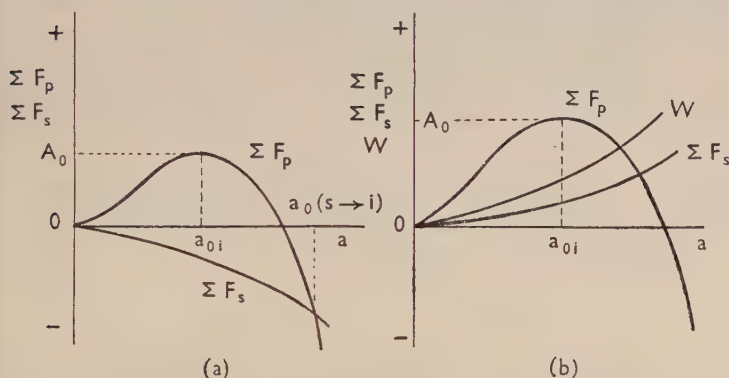


FIG. 8.—Relation between  $\Sigma F_p$  for the formation of the intermediate precipitate and  $\Sigma F_s$  for the formation of segregates from different initial concentrations.

(a) High initial concentrations, such as  $x_6$  in Fig. 7 (a), or moderate concentrations, such as  $x_5$  in Fig. 7 (b). In the latter case there will be an activation energy for segregation, cf. Fig. 9 (a). Transfer of segregates to precipitates occurs at  $a_{0(s \rightarrow i)}$  provided that the process is structurally continuous.

(b) Moderate initial concentrations, such as  $x_{4b}$  in Fig. 7 (b). The activation energy for segregation,  $W$ , is small compared with the activation energy for nucleation, cf. Fig. 9 (c).

for the formation of a segregate is given by equation (21) and decreases monotonically with increasing size of segregate, because the strain-energy term  $\sigma$  in this equation is very small in relation to the first term.  $\Delta F_p$  for the formation of the intermediate precipitate (equation (8)) shows the humped curve with a maximum at  $a_{0i}$ . The segregate may transform at any size greater than  $a_{0i}$ , but the probability of this will increase with size and becomes unity when the curve for  $\Sigma F_s$  crosses  $\Sigma F_p$  in Fig. 8 (a) at  $a_{0(s \rightarrow i)}$ .

Thus, for all concentrations greater than  $x_6$  the energy drop on the formation of a nucleus of the intermediate precipitate from a segregate is independent of composition. Any variation in the stable

nucleus size of the intermediate precipitate with matrix composition in this region will depend on the interfacial-energy terms. A term for the volume strain energy should also be included in equation (24); for the present purpose this can be regarded as affecting only the value of  $f_9 - f_2$  (see equation (13)). The formation of the stable precipitate from the intermediate precipitate is governed by a relationship similar to equation (24), although it is possible for several intermediate precipitates to exist in practice.

Within the region where  $\partial^2 F / \partial x^2$  is negative segregation can be regarded as occurring in either direction. For instance,  $x_7$  can be looked upon as segregating towards  $x_9$  or  $x_6$ . There is no *prima facie* reason why the segregate composition cannot go beyond  $x_9$  to a value such as  $x_9'$  (Fig. 7 (d)) before true precipitation begins. It is, however, convenient to consider the size of a segregate or a nucleus as being that which gives it a mean composition similar to the precipitate composition.

There will be a strong tendency for the decomposition to slow up when diffusion has reduced the matrix composition to  $x_6$ . Under conditions where true precipitation does not occur and the segregate has the composition  $x_9$  the matrix will have a composition between  $x_6$  and  $x_{4a}$ .

### 5. *Decomposition from Moderate Initial Concentrations.*

Segregations or fluctuations of composition from initial concentrations lower than  $x_6$  will occur only when accompanied by an initial addition of free energy. Borelius<sup>26</sup> has recently associated the slowness of precipitation under these conditions with the activation energy  $w$  per atom in Figs. 6 and 7 (b), which would have to be provided to enable a fluctuation to pass the  $x_s$  composition. The free-energy curve at  $x_s$  has the same slope as the tangent to the initial concentration ( $x$  in Fig. 6,  $x_{4a}$  in Fig. 7 (b), and  $x_3$  in Fig. 7 (c)). Given this energy fluctuation, segregation, which will occur by unit processes, will give rise to the formation of aggregates of composition  $x_9$  with a free energy less than that of the matrix (Fig. 9 (a)). Once this initial segregation has occurred, the free-energy conditions with varying size of segregate and embryo are again as shown in Fig. 8 (a) and stable segregates will be formed.

Since additional energy has to be provided for segregation, the probability of initial decomposition by segregation from moderate initial concentrations may be put proportional to :

$$e^{-(Q + W)/RT} \quad . \quad . \quad . \quad . \quad . \quad . \quad (25)$$

where  $W$  is the activation energy for segregation and

$$W = Na^3w \quad . \quad . \quad . \quad . \quad . \quad . \quad (26)$$

Once a segregate has been formed under these conditions its further growth is possible by downhill diffusion. But it must be noted that this only applies when the matrix composition is between  $x_6$  and  $x_{4a}$ .

The energy barriers to be overcome for precipitation from  $x_5$ ,  $x_{4a}$ , and  $x_{4b}$  in Fig. 7 (b) are shown diagrammatically in Fig. 9. The base line in Fig. 9 represents the energy level of the quenched alloy. The alloys can give rise to segregates by overcoming the energy barrier  $W$  of equation (26) (see Fig. 6 and Fig. 7 (b)). Depending on the initial

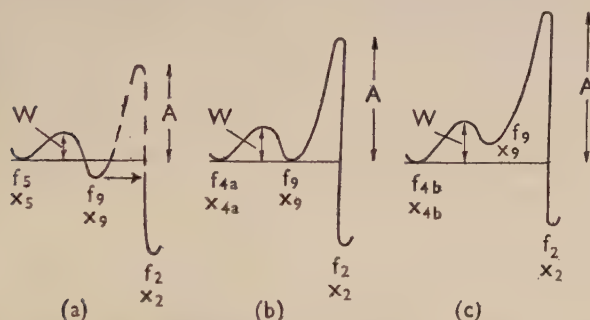


FIG. 9.—Diagrammatic representation of the energy barriers for decomposition from initial concentrations  $x_5$ ,  $x_{4a}$ , and a composition  $x_{4b}$  between  $x_{4a}$  and  $x_4$  in Fig. 7. The base line represents the energy of the initial supersaturated solution in each case.

concentration, the segregates of composition  $x_9$  will possess a free energy lower, equal to, or higher than the quenched alloy. The second energy barrier,  $A$ , is for the formation of the intermediate precipitate and is a function of the energy drop available.

$x_{4a}$  has been chosen such that its tangent cuts the free energy/composition curve at  $x_9$  in Fig. 7 (b). This means that the segregate of composition  $x_9$  has the same energy as the matrix from which it has been formed by surmounting the energy barrier  $W$  (Fig. 9 (b)).

$x_{4b}$  is only slightly less supersaturated than  $x_{4a}$  so that  $W$  is still small compared with  $A$ . In this case the segregate has a higher energy than the matrix after surmounting the energy barrier  $W$  (Fig. 9 (c)). No accumulation of segregate is to be expected from this composition since the probability of flow in the reverse direction is so much greater.

The effect of size variation on the free-energy factors for precipita-



tion from compositions such as  $x_{4b}$  is shown in Fig. 8 (b).  $W$  and  $\Sigma F_s$  increase continuously with size of segregate.  $\Sigma F_p$  shows the normal maximum.

Some segregates of composition  $x_9$  will, nevertheless, occur by fluctuation from composition  $x_{4b}$  and, as in the case of the incubation period, their steady size distribution will be given by the expression:

$$\frac{s_a}{s} = e^{-\Sigma F_s/kT} \quad . \quad . \quad . \quad . \quad . \quad (27)$$

where  $s_a$  is the number of segregates containing  $a^3$  atoms out of all the segregates.

Under these conditions there will be a "transient-steady" size distribution of segregates from which the larger will be removed as stable nuclei of the intermediate precipitate, assuming full structural continuity.

#### 6. *Decomposition from Low Initial Concentrations.*

At low degrees of supersaturation, such as  $x_3$  (Fig. 7 (c)), the activation energy for segregation is given by  $w$  per atom. This is equivalent to  $f_s - f_3$  per atom of the segregate of composition  $x_9$ . The point  $f_s$  is obtained by extending the straight line  $x_3 x_s$  to intersect the  $x_9$  vertical in  $f_s$ , where  $x_s$  is the contact point of the tangent to the free-energy curve parallel to  $x_3 f_3$ . To a first approximation  $f_s$  will be treated as coinciding with  $f_9$  and, whilst this is not strictly accurate, the results are quite applicable to the case where  $W$  is large compared with  $A$ .

Precipitation from compositions such as  $x_3$  can be regarded as occurring directly. In this case:

$$\Sigma F_p = -a^3 \frac{\Delta F}{N} + 6a^2 S \quad . \quad . \quad . \quad . \quad . \quad (8)$$

is equivalent to

$$\Sigma F_p(3 \rightarrow 2) = -a^3(f_3 - f_2) + 6a^2 S \quad . \quad . \quad . \quad (28)$$

Precipitation may also be regarded as occurring via the formation of segregates as in the case of high degrees of supersaturation. In this case the segregates of  $x_9$  composition would require an increase of energy:

$$\Sigma F_s(3 \rightarrow 9) = a^3(f_9 - f_3) \simeq a^3 w \quad . \quad . \quad . \quad . \quad (29)$$

but on precipitation they would give up energy according to

$$\Sigma F_p(9 \rightarrow 2) = -a^3(f_9 - f_2) + 6a^2 S \quad . \quad . \quad . \quad (30)$$

Nuclei of precipitate would not, however, be formed unless they were above the minimum size given by equation (28).

These factors have been set out in Fig. 10 which has been drawn for  $(f_3 - f_2) = \frac{1}{3}(f_9 - f_2)$ , the curves for which are in the correct relative positions, and may be compared with Fig. 8 for the cases where  $W = 0$  or is small compared with  $A_0$ .

It will be seen that over most of the size distribution  $\Sigma F_s$  (or  $W$ )

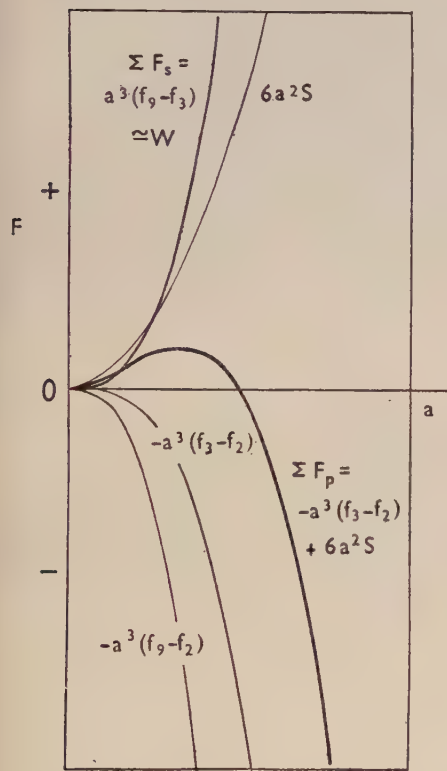


FIG. 10.—The variation with size of nucleus of factors involved in precipitation from composition  $x_3$  (see Fig. 7 (c)), assuming two possible mechanisms.  $\Sigma F_p$  is the summed curve for direct precipitation, a “transient-steady” size distribution of embryos being set up initially during the incubation period.  $\Sigma F_s$  ( $\approx W$ ) is the energy term for simple segregation and, since this is higher than the  $\Sigma F_p$  curve, this process of segregation and subsequent precipitation is unlikely for the conditions when  $W$  (cf. Fig. 7) is large compared with  $A$ . Under these conditions the quenched alloy forms embryos which grow to stable nuclei by unit processes. The embryos possess the lattice of the new phase.

is large compared with  $\Sigma F_p(3 \rightarrow 2)$  (Fig. 10). The steady size distribution of segregates can be set as :

$$\frac{s_a}{s} = e^{-\Sigma F_s/kT} \quad . \quad . \quad . \quad . \quad . \quad . \quad (31)$$

whilst the steady size distribution for an embryo possessing the structure of the precipitate is :

$$\frac{n_a}{n} = e^{-\Sigma F_p(3 \rightarrow 2)/kT} \quad . \quad . \quad . \quad . \quad . \quad . \quad (16)$$

where  $\Sigma F_s$  and  $\Sigma F_p$  are the additional energies required in each case.



forced to redissolve to maintain the matrix composition as the precipitate grows. This mechanism of decomposition automatically

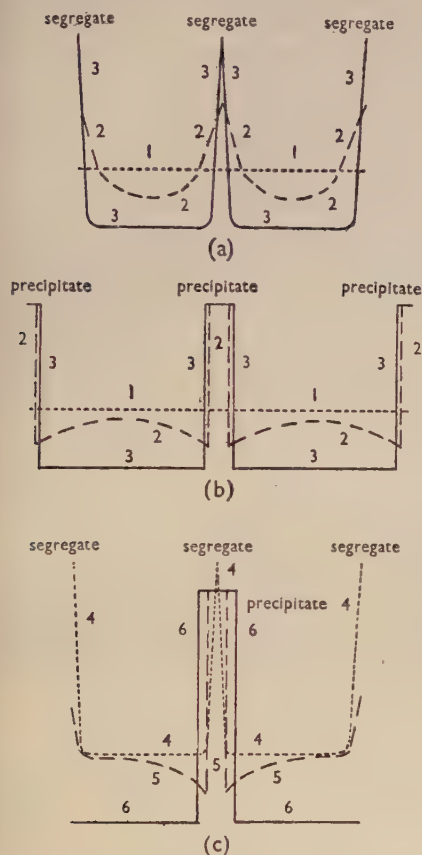


FIG. 11.—Diagrammatic representation of the solute concentration during decomposition.

(a) Formation of segregate by uphill diffusion: (1) Statistically uniform distribution when quenched. (2) Uphill diffusion has occurred. (3) Final distribution; segregates separated by regions of lower solute concentration.

(b) Formation of precipitate by downhill diffusion: (1) Statistically uniform distribution when quenched. (2) Downhill diffusion to regions possessing the new structure. These form stable nuclei when the critical size has been reached. (3) Final distribution: precipitate separated by regions of lower solute concentration.

(c) Formation of precipitate from segregates: (4) As in (a) (3). (5) Particle of precipitate formed from segregates. This leads to downhill diffusion in its immediate vicinity and causes neighbouring segregates to re-dissolve to maintain the metastable equilibrium concentration around them. (6) Final distribution; precipitate separated by regions of lower solute concentration.

removes the necessity for closely defining the size of the segregate to give the same composition as the precipitate.

### 8. Reversion.

An alloy quenched and aged to contain segregates may be raised to a higher temperature at which segregates would not normally form. The larger segregates may transfer directly to the intermediate precipitate, if the process is structurally continuous. In general, the segregates will redissolve, because a suitably chosen increase in tem-

perature will have the effect of transferring the supersaturation below the  $x_{4a}$  composition (Fig. 7) where segregation does not lead to a decrease in the free energy of the alloy. This is equivalent to transferring the free-energy size of segregate relationships from those of Fig. 8 (a) to those of Fig. 8 (b) and leads directly to a thermodynamic theory of reversion.

This theory is more satisfactory than one based on the variation in minimum critical nucleus size with temperature.<sup>1</sup> The latter predicts clear reversion effects in all alloy systems, whereas in practice large effects are confined to only a few systems. All these show ageing in several stages of which the first could well be segregation.<sup>1</sup> The slow rate of re-ageing after partial reversion would be accounted for since an activation energy for segregation might be required by the new matrix composition.

## IX.—RATE OF PRECIPITATION.

### 1. *Measurement.*

The rate of precipitation is generally estimated by measuring the time to a certain property change, such as a maximum on a hardness/ageing curve, or the time for half the electrical-resistance change. These changes often show an exponential relation<sup>30</sup> such that :

$$\log t = \frac{C}{T} + B \text{ or } t = Be^{C/T} \quad . \quad . \quad . \quad (33)$$

where  $t$  is the time to the property change under consideration,  $T$  the absolute temperature, and  $B$  and  $C$  are constants.

### 2. *Precipitation Rate from Nucleation Theory.*

There have been two approaches to the semi-quantitative account of the rate of precipitation, that of Becker<sup>8, 19</sup> and that of Borelius.<sup>18, 26</sup> As mentioned in the previous Section, Borelius accounts for the decreasing rate of precipitation and departure from equation (33) by the additional energy term  $w$  (Fig. 6) beginning to play an important part. He and his co-workers have investigated the ageing of lead-tin alloys and calculated<sup>18</sup> the temperature for various alloys at which  $\partial^2 F / \partial x^2$  for the free energy/composition curve became negative. Borelius<sup>26</sup> later made an estimate of the height of the energy barrier to segregation.

Becker views precipitation in terms of an activation energy arising from the formation of an interface and which increases rapidly with decreasing supersaturation. This theory has been applied to account for precipitation rates in gold-platinum alloys. The initial rate of reaction is put as :

$$N = Ke^{-(Q+A)/RT} \quad . \quad . \quad . \quad . \quad (34)$$



where  $Q$  is the activation energy for diffusion,  $A$  the activation energy for nucleation (see Section V), and  $K$  is a constant. It will be noted that this predicts a constant rate per unit volume of untransformed material and there should be no incubation period according to this theory.

It has been pointed out in the previous Section that the Borelius activation energy is operative only over a very limited composition. It does not apply at high degrees of supersaturation and decomposition at low degrees of supersaturation is by the formation of embryos of the new phase. Once the "transient-steady" size distribution of embryos has been set up, the Becker activation energy should apply.

Data for testing the Becker rate of precipitation, and hence the analysis in Section VIII, against ageing-rate curves on lead-tin alloys<sup>18</sup> may be obtained by using the Borelius method for calculating the free energy/composition curve. The activation energy for nucleation and the minimum critical nucleus size can then be calculated by comparison with one of the Becker equations.<sup>19</sup> The details of the method are given in the Appendix (p. 486).

The logarithm of the time for half the resistance change on ageing lead-tin alloy wires at different temperatures<sup>18</sup> is shown plotted in Fig. 12. This is a straight line at low temperature, but turns towards the horizontal as the ageing temperature approaches the solubility limit. These curves have the same shape as the top half of the  $S$  curves for steel.<sup>31</sup> The advantage of taking the time to half the

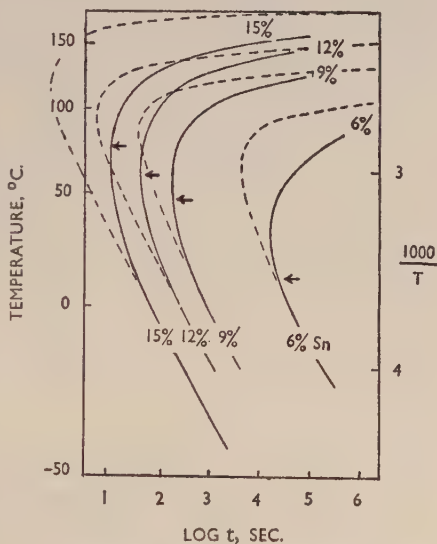


FIG. 12.—Comparison of Borelius's experimental curves (full lines) for log time to half the resistance change of lead-tin alloys on ageing, plotted against  $\frac{1000}{T}$ , and curves (dotted lines) calculated from nucleation theory based on the original concentrations.

$Q = 10,400$  cal./g.-atom.

$t$  = time to half resistance change.

← denotes temperature for change from positive to negative value of  $\partial^2 F / \partial x^2$

property change is that it minimizes the effect of the incubation period, which is an incalculable quantity.

The equation of the straight-line portion of Fig. 12 is :

$$\log t = \frac{Q}{2.3RT} + B \quad . \quad . \quad . \quad . \quad . \quad (35)$$

where  $Q = 10,400$  cal./g.-atom. This is taken as the activation energy for diffusion, since it applies in a region where  $\partial^2 F / \partial x^2$  is found to be negative by calculation.

The values of the minimum critical nucleus size for various alloys ageing at different temperatures are shown in Table II. The corre-

TABLE II.—*Effect of Ageing Temperature on the Critical Nucleus Size of Lead-Tin Alloys.*

The values are in terms of atomic distances, the figures in parentheses are values of  $a_0^3$  and indicate the nucleus size in terms of atoms. The blank spaces above the figures indicate the region of solid solubility. The blank spaces at the foot of the 12, 15, and 18% columns are for a region with negative  $\partial^2 F / \partial x^2$ .

Temperature, ° K.	Tin Content, wt. %					
	4.5	6	9	12	15	18
450	...	...	...	...	...	12.1 (1,770)
440	...	...	...	...	23.9 (13,650)	6.85 (320)
430	...	...	...	...	9.65 (898)	4.4 (85)
420	...	...	...	14.2 (2,860)	6.1 (227)	3.8 (55.9)
410	...	...	23.4 (12,800)	7.5 (422)	4.4 (85)	3.1 (29.8)
400	...	...	9.5 (860)	5.0 (125)	3.5 (43)	2.6
380	50.6	8.8 (720)	4.3 (80)	3.0 (27)	2.4 (14)	1.94
360	6.1 (230)	3.9 (64)	2.7 (20)	2.2	1.82	1.57
340	3.1	2.5 (15)	2.0	1.65	...	...
327	2.47	2.05	1.7	...	...	...

sponding values of  $A_0$ , the activation energy, are given in Table III and have been put into equation (35) so that :

$$\log t = \frac{(Q + A_0)}{2.3RT} + B \quad . \quad . \quad . \quad . \quad . \quad (36)$$

The value of  $t$  calculated from this equation has been plotted in Fig. 12 as a dotted extension to the straight lines. The dotted lines thus show the theoretical time for half the property change, assuming a rate of precipitation typical of that of the initial supersaturated solution, i.e. assuming no change in matrix composition.

In view of the simplifying assumptions which have been made in the calculations for the free-energy changes, the minimum nucleus size, and the activation energy, the agreement is not unsatisfactory. Whilst complete proof of the accuracy of the analysis of the mode of precipitation was not to be expected, the results are sufficiently good

TABLE III.—Effect of Ageing Temperature on the Activation Energy (cal./g.-atom of precipitate) for Nucleation of Lead-Tin Alloys.

Temperature, ° K.	Tin Content, wt. %					
	4.5	6	9	12	15	18
450	...	...	...	...	...	13,850
440	...	...	...	...	53,200	4,470
430	...	...	...	...	10,070	1,860
420	...	...	...	24,550	4,020	1,390
410	...	...	77,000	6,910	2,095	930
400	...	...	12,590	3,080	1,325	650
380	441,000	12,400	2,610	1,210	638	370
360	6,400	2,435	1,027	597	362	240
340	1,640	1,100	567	341	...	...
327	885	690	411	...	...	...

to encourage the conclusion that the discrepancy between theory and actuality is not large.

#### X.—SIGNIFICANCE OF THE THERMODYNAMIC ANALYSIS IN RELATION TO PRECIPITATION THEORY.

Modern descriptive theories of precipitation are of two main types, and these have been discussed in a previous paper.<sup>1</sup> One type includes a pre-precipitation stage involving the collection of solute atoms within the parent lattice as an essential part of the process. The second type postulates that the first step is essentially the formation of a precipitate, i.e. a region in the matrix with a markedly different lattice spacing.

No deductions can be drawn from the general thermodynamic study to give an explicit picture of the process of precipitation or of the number of stages in any particular alloy system. But this study has shown that there is a sound thermodynamic basis accounting for the possibility of an association of solute atoms during the precipitation process. A system having thermodynamic characteristics similar to those assumed may certainly be expected to show pre-precipitation phenomena at high degrees of supersaturation. In systems where only comparatively lower degrees of supersaturation can be produced, the change will be directly to the embryo and the new phase.

Borelius *et al.*<sup>32</sup> have derived an equation for the free energy of the aluminium-copper solution :

$$\frac{F}{R} = [3300x - 1200x^2 + T(x \ln x + (1 - x) \ln (1 - x))]. \quad (37)$$

Whilst this involves a considerable over-simplification, it does agree

with measured values of the energy liberated on ageing,<sup>32, 33</sup> and it gives an inflection in the free energy/composition curve at about 4% copper at 225° C.

Thus, the thermodynamic approach provides no reasons for querying the hypothesis that segregation of copper atoms is an integral part of the mode of decomposition of the aluminium-4% copper alloy. By showing the theoretical possibility of this mechanism it can, in fact, be taken as backing up the experimental observations,<sup>34</sup> which can best be accounted for by the hypothesis of segregation of copper atoms forming Guinier-Preston zones. An examination is being made of the ageing mechanism in aluminium-copper alloys from the view-point of the present analysis.

Guinier has stated that the first stage in the decomposition of aluminium-silver<sup>35</sup> and aluminium-zinc alloys<sup>36</sup> is by the formation of spherical clusters of solute atoms. Full structural continuity would not be expected in those cases where the precipitate is in the form of platelets.<sup>37-39</sup> Trotter and McLean<sup>40</sup> have very recently observed the collection of carbon atoms as an early stage in the tempering of martensite. These processes are all understandable on the present basis if the appropriate free energy/composition curve possesses a region concave to the composition axis.

## XI.—SUMMARY AND CONCLUSIONS.

An analysis of the decomposition of supersaturated solid solutions in terms of the free energy/composition and free energy/structure relationships has shown that precipitation may proceed by different mechanisms depending on the degree of supersaturation. Segregates or clusters of solute atoms may be formed by uphill diffusion whilst embryos of precipitate are formed by downhill diffusion.

At high initial degrees of supersaturation, in a region of negative  $\partial^2 F / \partial x^2$ , the first stage in the decomposition is by the accumulation of stable segregates rich in the solute. These form a true precipitate when the correct size has been attained, provided that structural continuity is possible. With no structural continuity, nuclei of precipitate arise in the matrix, as described for lower initial degrees of supersaturation. The remaining segregates are forced to redissolve in either case.

At moderate initial degrees of supersaturation accumulation of segregates is also possible, but there is an additional activation energy for the initial segregates. At very slightly lower concentrations there is no accumulation of segregates but a "transient-steady" size distribution

is set up from which the larger segregates are removed by the formation of the true precipitate, assuming structural continuity.

At low initial degrees of supersaturation there is neither accumulation nor "transient-steady" size distribution of segregates and the change is directly to embryos of the new phase. Under these conditions, where the activation energy for nucleation is much lower than the activation energy of segregation, a "transient-steady" size distribution of embryos with the lattice structure of the new phase is set up. The embryos grow by unit process and when the steady size distribution has been attained (the incubation period) the probability of nucleation is given by the Becker (Volmer-Weber) relation.

This Becker theory and thus the analysis of the mode of decomposition at low degrees of supersaturation has been tested against ageing rates of lead-tin alloys. The results are in sufficiently good agreement to encourage the conclusion that the underlying analysis has been correct.

The finding that the first stage of decomposition at high degrees of supersaturation is by segregation lends weight to theories of precipitation involving pre-precipitation processes leading to the collection of solute atoms in certain systems. This process is not to be expected where the thermodynamic characteristics are unsuitable, the easiest mode of decomposition being chosen by any particular system. The thermodynamic approach used here successfully predicts that marked reversion effects are to be expected when an alloy quenched and aged to form segregates is raised to a suitable higher temperature.

#### ACKNOWLEDGEMENTS.

The author's thanks are due to Dr. M. L. V. Gayler, Professor G. V. Raynor, and to his colleagues at the Fulmer Research Institute, Dr. P. Gross and Dr. A. H. Sully, for helpful discussion of the subject matter of the paper.



## APPENDIX.

## CALCULATION OF MINIMUM CRITICAL NUCLEUS SIZE AND ACTIVATION ENERGY FOR PRECIPITATION IN LEAD-TIN ALLOYS.

Borelius *et al.*<sup>18</sup> take the free energy :

$$F = U - TS = U + RT(x \ln x + (1 - x) \ln (1 - x)) \quad (38)$$

as dependent only on composition. The internal energies of the pure metals are both put as zero. Differentiation of equation (38) and integration for values of  $x$  along the solid-solubility curve gives :

$$\frac{U}{R} = \int_0^x \left[ -T \ln \frac{x}{1-x} \right]_b dx + \int_0^x \left[ \frac{\partial F/R}{\partial x} \right]_b dx. \quad (39)$$

where  $b$  signifies a boundary value of  $x$  and  $T$ . Graphical integration of the boundary values of  $\ln \frac{x}{1-x}$  gives a first approximation of  $U/R$ . A second approximation putting  $U_{\text{Sn}} \propto (1-x)$  is made leading to  $\left[ \frac{\partial F/R}{\partial x} \right]_b$  and inserted to give the values of  $U/R$  at the lead solid-solution boundary. By inserting these values of  $U/R$  in equation (38) the value of  $\left[ \frac{F}{R} \right]_b$  was obtained along the solubility curve. From these values the temperature was calculated at which  $\partial^2 F / \partial x^2$  becomes negative for a given composition. This is indicated by the arrows in Fig. 12, and shows the points at which the Borelius activation energy for diffusion starts to play a part.

In another paper<sup>26</sup> Borelius obtained the variation of free energy with the temperature for a given composition from :

$$\left[ \frac{1}{R} \frac{\partial F}{\partial x} \right]_T = \left[ \frac{1}{R} \frac{\partial F}{\partial x} \right]_b + T_b \left[ \ln \frac{1-x}{x} \right]_{x_b} - T \left[ \ln \frac{1-x}{x} \right]_{x_b} \quad (40)$$

since  $\frac{\partial U}{\partial x}$  cancels as  $U$  has been taken independent of temperature.

The value of  $\left[ \frac{\partial F}{\partial x} \right]_T$  at the new temperature  $T$  is now inserted in equation (39) and  $\left[ \frac{U}{R} \right]_T$  again obtained graphically. This value of  $U$  is placed in equation (38) so that  $F$  can be calculated. By this means the free energy/composition curve can be calculated within the limitations imposed by the basic assumptions.

The limiting solubilities at low ageing temperatures have been estimated by extrapolating a plot of  $\log$  (concentration lead) against  $1/T$ . The necessary free energy values were then calculated from these compositions using the methods of equations (38)-(40).

The energy drop on precipitation  $\Delta F$  can be estimated since :

$$\Delta F = a_0^3 \left[ F - F_2 + \frac{\partial F}{\partial x} (x - x_2) \right] \quad . \quad . \quad . \quad (41)$$

where  $a_0^3$  is the number of atoms in the nucleus, of composition  $x_2$ , which is assumed to be the tin-rich solid solution stable at the ageing temperature.

By considering the internal energy as a function of the interaction energies of nearest neighbours Becker <sup>8</sup> gives the free energy as :

$$F = ZNVx(1-x) + RT [x \ln x + (1-x) \ln (1-x)] \quad . \quad (42)$$

where  $N$  is Avogadro's number,  $Z$  is the co-ordination number (number of nearest neighbours) and  $V = V_{AB} - \frac{1}{2}(V_{AA} + V_{BB})$ ,  $V_{AA}$ , &c., being the interaction energies between neighbouring atoms.

In terms of interaction energies Becker <sup>19</sup> obtains the following expression for the minimum critical nucleus size :

$$a_0 = \frac{4V(x-x_2)^2}{\Delta F} \quad . \quad . \quad . \quad . \quad (43)$$

$\Delta F$  is given by equation (41) and is obtained from the previously calculated free-energy values. A comparison of equations (38) and (42) allows the value of  $V$  to be obtained from the calculated values of  $U$  since :

$$V_{(Tx)} = \frac{U_{(Tx)}}{x(1-x)Z} \quad . \quad . \quad . \quad . \quad (44)$$

$Z$  has been taken as 12 for the face-centred cubic lead lattice and a cubical nucleus has been assumed. In view of the other assumptions being made, this is sufficiently close to reality to be of minor importance.

All the values required for the calculation of  $a_0$  are then available and the results are given in Table II.

The activation energy for nucleation can now be calculated, since : <sup>19</sup>

$$A_0 = 2a_0^2 S = 2a_0^2 V(x - x_2)^2 \quad . \quad . \quad . \quad . \quad (45)$$

and these values are given in Table III.

The results in Tables II and III show the trends expected with large values close to the solubility curve.

## REFERENCES.

1. H. K. Hardy, *J. Inst. Metals*, 1948-49, **75**, 707.
2. H. Lipson and A. J. C. Wilson, *J. Iron Steel Inst.*, 1940, **142**, 107 p.
3. J. H. Hildebrand, "The Solubility of Non-Electrolytes". New York: 1936 (Reinhold Publishing Corp.).
4. S. Glasstone, "Textbook of Physical Chemistry", 2nd edn. New York: 1946 (D. Van Nostrand Co.).
5. L. Landau and E. Lifshitz (translated by D. Shoenberg), "Statistical Physics". Oxford: 1938 (Oxford University Press).
6. J. C. Slater, "Introduction to Chemical Physics". New York: 1939 (McGraw-Hill Book Co., Inc.).
7. H. A. Bethe, *Proc. Roy. Soc.*, 1935, [A], **150**, 552.
8. R. Becker, *Z. Metallkunde*, 1937, **29**, 245.
9. R. M. Barrer, "Diffusion In and Through Solids". Cambridge: 1941 (Cambridge University Press).
10. U. Dehlinger, "Chemische Physik der Metalle und Legierungen". Leipzig: 1939 (Akademische Verlagsgesellschaft m.b.H.).
11. L. S. Darken, *Trans. Amer. Inst. Min. Met. Eng.*, 1948, **175**, 184.
12. C. E. Birchenall and R. F. Mehl, *Trans. Amer. Inst. Min. Met. Eng.*, 1947, **171**, 143.
13. J. C. Fisher, J. H. Hollomon, and D. Turnbull, *Trans. Amer. Inst. Min. Met. Eng.*, 1948, **175**, 202.
14. A. H. Cottrell, "Theoretical Structural Metallurgy". London: 1948 (Edward Arnold and Co.).
15. G. Borelius, *Ann. Physik*, 1938, [v], **33**, 517.
16. P. Laurent, *Rev. Mét.*, 1945, **42**, 22.
17. C. G. Wictorin, *Ann. Physik*, 1938, [v], **33**, 509.
18. G. Borelius, F. Larris, and E. Ohlsson, *Arkiv. Mat., Astron. Fysik*, 1944, [A], **31**, (10).
19. R. Becker, *Ann. Physik*, 1938, [v], **32**, 128.
20. M. Volmer and A. Weber, *Z. physikal. Chem.*, 1926, **119**, 277.
21. F. R. N. Nabarro, *Proc. Roy. Soc.*, 1940, [A], **175**, 519.
22. J. Frenkel, *J. Chem. Physics*, 1939, **7**, 200.
23. J. Frenkel, *J. Chem. Physics*, 1939, **7**, 538.
24. J. C. Fisher, J. H. Hollomon, and D. Turnbull, *J. Appl. Physics*, 1948, **19**, 775.
25. D. Turnbull, *Trans. Amer. Inst. Min. Met. Eng.*, 1948, **175**, 774.
26. G. Borelius, *Arkiv Mat., Astron. Fysik*, 1945, [A], **32**, (1).
27. J. N. Hobstetter, *Trans. Amer. Inst. Min. Met. Eng.*, 1949, **180**, 121.
28. Y. Takagi, *Proc. Phys. Math. Soc. Japan*, 1941, [iii], **23**, 44.
29. P. Laurent, *Compt. rend.*, 1947, **224**, 1431.
30. C. H. M. Jenkins and E. H. Bucknall, *J. Inst. Metals*, 1935, **57**, 141.
31. E. S. Davenport and E. C. Bain, *Trans. Amer. Inst. Min. Met. Eng., Iron Steel Div.*, 1930, 117.
32. G. Borelius, J. Andersson, and K. Gullberg, *Ing. Vetensk. Akad., Handl. No.* **169**, 1943.
33. G. Borelius and L. Ström, *Arkiv Mat., Astron. Fysik*, 1945, [A], **32**, (21).
34. M. L. V. Gayler, *J. Inst. Metals*, 1946, **72**, 243.
35. A. Guinier, *J. Phys. Radium*, 1942, [viii], **3**, 124.
36. A. Guinier, *Métaux, Corrosion, Usure*, 1943, **18**, 209; *Bull. Laboratoire d'Essais*, 1947, No. **23**.
37. C. S. Barrett, A. H. Geisler, and R. F. Mehl, *Trans. Amer. Inst. Min. Met. Eng.*, 1941, **143**, 134.
38. A. H. Geisler, C. S. Barrett, and R. F. Mehl, *Trans. Amer. Inst. Min. Met. Eng.*, 1943, **152**, 182.
39. A. H. Geisler, C. S. Barrett, and R. F. Mehl, *Trans. Amer. Inst. Min. Met. Eng.*, 1943, **152**, 201.
40. J. Trotter and D. McLean, *J. Iron Steel Inst.*, 1949, **163**, 9.

# ON THE PHASES OCCURRING IN ALLOYS OF 1262 ALUMINIUM WITH COPPER, MAGNESIUM, MANGANESE, IRON, AND SILICON.\*

By GÖSTA PHRAGMÉN,† Lic.Phil.

## SYNOPSIS.

By means of a microscopic and X-ray crystallographic study of aluminium alloys containing copper, magnesium, manganese, iron, and silicon, and by a critical survey of previous work, the phases which may form a eutectic with solid aluminium have been determined. The results are shown in diagrams for systems of three, four, five, or six components. In the diagrams for quaternary, quinary, and senary alloys the relative amounts of the alloying constituents are shown. The four-component systems are represented as triangular diagrams, the five-component systems as solid models, and the system with six components in a series of three-dimensional sections.

The phases which, according to these diagrams, occur in some commercially important alloys of aluminium with copper, magnesium, manganese, iron, and silicon are discussed. The alloys in question all belong to a group having copper and magnesium as the chief alloying components. Generally, manganese constitutes a further intentional component of these alloys, and in certain cases silicon also is deliberately added. The colours of the phases in ordinary and polarized light, their etching properties, crystal system, crystal form, the parameters of the unit cell, and in some instances the densities, are listed in tables. Some information is also given about two phases, denoted *t*-AlFeSi and *z*-AlCuMgMn, which do not form eutectics with aluminium.

## I.—INTRODUCTION.

A HEAT-TREATABLE aluminium alloy in its soft condition consists of a matrix of almost pure aluminium and of particles of one or more phases which contain the main part of the alloying components. During heat-treatment the alloy is first held at a temperature slightly lower than that of incipient fusion, and then quenched. Afterwards it is either stored at room temperature for several days or heated at a comparatively low temperature for many hours. During the first heating the matrix may take a considerable amount of the alloying components into solid solution. The quenching prevents re-precipitation of the constituents, and the matrix at room temperature thus consists of a supersaturated solid solution. This is called solution-

\* Manuscript received 13 June 1949.

† The author, who was Director of the Metallografiska Institutet, Stockholm, died in 1944. The paper has been prepared for publication by some of his Swedish colleagues. Editorial footnotes have been inserted where subsequent work by other authors has provided additional information regarding certain alloys.

treatment. The matrix is not appreciably harder after the solution-treatment than before, but it is no longer stable. During the second part of the heat-treatment process, which involves ageing at room temperature or at a somewhat higher temperature, the hardness is considerably increased.

The alloying content of the material is generally so high that many of the phases present will remain undissolved after the solution-treatment. These phases are hard and brittle and have therefore a direct influence on the properties of the heat-treated alloy. The aluminium-rich matrix, however, forms the predominant part of the alloy, and the properties of this matrix are chiefly dependent on its composition, i.e. on the amount of dissolved alloying components. The solubility of a given element in the aluminium-rich phase depends largely on the concentration of other alloying elements present simultaneously. Thus, aluminium in equilibrium with  $\text{Mg}_2\text{Si}$  at  $500^\circ\text{C}$ . may contain magnesium 1.0 and silicon 0.2%, or magnesium 0.6 and silicon 0.4%,<sup>1</sup> whereas if the aluminium-rich phase, at the same temperature, is in equilibrium with free silicon alone, its silicon content is 0.8%.<sup>2</sup>

For the study of the relation between the composition and the properties of an aluminium alloy it is therefore important to know which phases may be present, and the amounts of the different alloying components that it is possible to dissolve in the aluminium phase. For instance, an alloy of pure aluminium with 4% copper may be hardened by means of solution-treatment followed by ageing at room temperature. An alloy with the same content of copper and with 0.3% iron, however, will not harden appreciably at room temperature,<sup>3, 4</sup> because the iron combines with part of the copper to form a phase with low solubility.<sup>5, 6, 7</sup> Alloys with a copper content lower than 4% harden to a lesser degree or not at all. It has also been found that an aluminium-copper alloy containing iron has a higher electrical conductivity after solution-treatment than an iron-free alloy with the same copper content, which shows that the content of alloying components in the aluminium-rich phase is lower if the alloy contains iron. It is thus important to ascertain which iron- and copper-containing phases may be present in the alloys. Once this is known, the question of solution equilibria can be elucidated. If yet another alloying element is added, e.g. silicon, this element might conceivably bind the iron into a still less soluble phase, which would decrease the influence of the iron.

As early as 1926 Dix and Keith<sup>8</sup> published a schedule for identifying, by etching, the phases present in commercial aluminium alloys. Keller and Wilcox<sup>9</sup> later published an etching table with photomicrographs,



which was subsequently revised by Schrader<sup>10</sup> and reproduced in this form by Berglund.<sup>11</sup> These etching tables have, however, not been found to be entirely correct. A new study of the etching properties was therefore considered desirable for the purposes of the present paper, and the data obtained are set out in Table XXVII (Plate LXXV).

The investigation now described was planned with special reference to the well-known group of wrought alloys in which copper and magnesium are the main alloying components. Manganese is also added to this type of alloy. The first heat-treatable aluminium alloy, developed by Wilm<sup>12</sup> and later known as Duralumin, contained copper 4, magnesium 0.5, and manganese 0.6%. Certain of these alloys also contain silicon as an intentional addition, but in any case silicon is usually a normal component, as the virgin aluminium generally contains appreciable amounts of this element. For the same reason some iron is always present in the alloys. The investigation therefore involves an alloy system with six components. A systematic study of such a system must start with an examination of the subsidiary systems with two components, and then continue with a similar survey of the three-, four-, and five-component systems. In the commercial alloys concerned, aluminium is always the main component. The field may therefore be limited to those systems in which aluminium is one of the components, as follows :

Al-Cu	Al-Cu-Mg	Al-Cu-Mg-Mn	Al-Cu-Mg-Mn-Fe	Al-Cu-Mg-Mn-Fe-Si
Al-Mg	Al-Cu-Mn	Al-Cu-Mg-Fe	Al-Cu-Mg-Mn-Si	
Al-Mn	Al-Cu-Fe	Al-Cu-Mg-Si	Al-Cu-Mg-Fe-Si	
Al-Fe	Al-Cu-Si	Al-Cu-Mn-Fe	Al-Cu-Mn-Fe-Si	
Al-Si	Al-Mg-Mn	Al-Cu-Mn-Si	Al-Mg-Mn-Fe-Si	
	Al-Mg-Fe	Al-Cu-Fe-Si		
	Al-Mg-Si	Al-Mg-Mn-Fe		
	Al-Mn-Fe	Al-Mg-Mn-Si		
	Al-Mn-Si	Al-Mg-Fe-Si		
	Al-Fe-Si	Al-Mn-Fe-Si		

The investigation is also restricted to the aluminium-rich parts of these systems and is principally concerned with those phases which form a eutectic with solid aluminium.

## II.—METHODS OF INVESTIGATION.

### 1. *Representation of the Systems.*

The equilibrium conditions in a binary system may be represented on a two-dimensional diagram, and those in a ternary system by a solid model. Compositions in a ternary system are generally plotted on a diagram in the shape of an equilateral triangle, the sides of which correspond to the three subsidiary binary systems. This triangle forms

the base of the complete concentration/temperature diagram. Sections at right angles to the temperature axis form triangular diagrams, which may be used to illustrate isothermal equilibria. It is also possible to project the liquidus and solidus surfaces on to the basal plane, thus obtaining a triangular diagram which represents the solidification process without regard to temperature. In such a diagram, the binary systems forming the vertical faces of the model project into the sides of the triangle.

Vogel<sup>13</sup> has introduced the term "polythermal" for the latter type of diagram. In the present work only polythermal diagrams will be used.

Just as a ternary system may be represented by a two-dimensional diagram, so a quaternary system may be described by a solid model. A four-component system has four subsidiary systems with three components. Alloy compositions in each of these may be plotted on triangular diagrams, and the quaternary system may in turn be represented by a regular tetrahedron, the faces of which are the triangular diagrams of the four subsidiary ternary systems. This method of describing the composition of a quaternary alloy was suggested by Roozeboom in 1894,<sup>14</sup> and has been used mainly in discussion of isothermal equilibria. Polythermal tetrahedral diagrams were first used by Parravano and Sirovich<sup>15,16</sup> in 1912.

If the content of one of the components in a four-component system is constant, the contents of the other components may be represented by means of an equilateral triangle, which forms a section through the complete concentration tetrahedron. The temperature axis may then be erected at right angles to the triangle mentioned. Such a scheme has been proposed by Schrader and Hanemann.<sup>17</sup>

A polythermal diagram for a quaternary system may be constructed as follows. Let *ABCD* (Fig. 1) represent a system of four phases all of which form eutectics. *E* represents the binary eutectic of *A* and *B*, *G* that between *A* and *C*. In the ternary system *ABC* the area *AELG* represents the field of separation of primary *A*, and *EL* and *GL* the binary eutectics *AB* and *AC*, *L* being the ternary eutectic of the three phases *A*, *B*, and *C*. Similarly, *K* represents the ternary eutectic of *A*, *B*, and *D*; *M* that between *A*, *C*, and *D*. In the space model the region having apex *A* and base *LGMP*, *FMPK*, *ELPK*, represents the region in which primary *A* is in equilibrium with the liquid; the surface *LGMP* that in which liquid is in equilibrium with *A* and *C*; *FMPK* that in which liquid is in equilibrium with *A* and *D*; and *ELPK* that in which liquid is in equilibrium with *A* and *B*. The three lines *LP*, *MP*, *KP* represent liquid in equilibrium with three solids,

whilst  $P$  is the quaternary eutectic in which liquid is in equilibrium with  $A$ ,  $B$ ,  $C$ , and  $D$ .

To obtain a plane diagram the surfaces and their lines of intersection may be projected, using the  $A$  corner of the tetrahedron as vertex, on to the face  $BCD$ . Thus the binary eutectic  $E$  projects into the point  $B$ , its extension into the ternary system  $A$ - $B$ - $C$  into the line  $BL_1$  and the ternary eutectic  $L$  into the point  $L_1$ . Hence  $KP$ ,  $LP$ , and  $MP$  project into the three lines  $K_1P_1$ ,  $L_1P_1$ ,  $M_1P_1$ , respectively, meeting in  $P_1$  the projection of the quaternary eutectic, whilst the area  $BK_1P_1L_1$  is the projection of the binary eutectic surface in which liquid is in equilibrium with solid  $A$  and  $B$ .

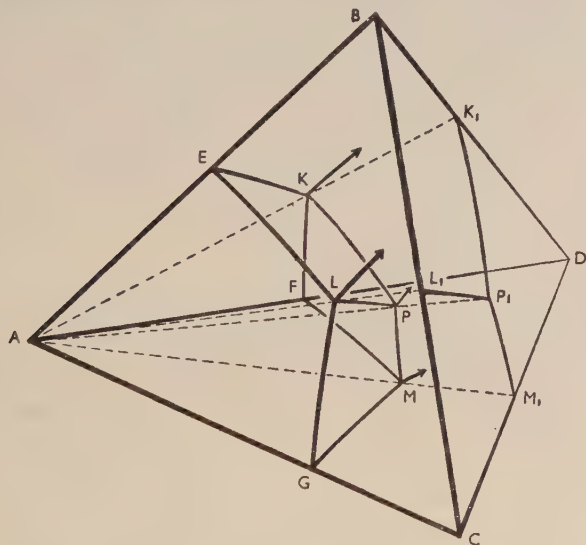


FIG. 1.—Schematic Diagram Showing Method of Plotting Quaternary Diagrams.

In such a projection the  $A$  content of the melt is not represented, the co-ordinates being the relative concentrations of the three components  $B$ ,  $C$ , and  $D$ . If the tie-lines for the equilibrium between  $A$  and melt were to coincide with "rays" from the  $A$  corner of the tetrahedron (e.g. if the alloying constituents were completely insoluble in solid  $A$ ), the separation of  $A$  from the melt would be without effect on the relative contents of the alloying constituents  $B$ ,  $C$ , and  $D$  remaining in the melt. If the solubility is limited, and the amount of primary separation small, the discrepancy from the ideal case may be neglected. There is a complete analogy between such a projection for a quaternary system and the ordinary triangular diagram for a ternary system,

relative and not absolute concentrations being used as co-ordinates. These projections are used in this paper for describing those portions of the quaternary systems in which aluminium is the primary constituent, the aluminium apex of the tetrahedron being used as the vertex of projection.

Similarly, the projection of the five-component system becomes a regular tetrahedron, the faces of which correspond to the projections of the four subsidiary systems of aluminium and three alloying constituents. For a certain relative content of one alloying element a section may be cut through such a projection of a five-component system. This section will be an equilateral triangle.

A system of aluminium with five alloying components has five subsidiary systems of aluminium and four alloying elements. Of these subsidiary systems, four have one alloying element as a common component. Sections through projections of four such subsidiary systems with a certain relative content of the common alloying element may be represented as equilateral triangles, and correspondingly a section through a projection of the six-component system for the same relative content of the component mentioned can be reproduced as a regular tetrahedron, the faces of which correspond to the sections through the projections of the four subsidiary systems.

## *2. Identification of Phases and Determination of Composition.*

The phases present in the various alloys have been identified microscopically. For this identification the use of polarized light proved of great value. Where possible the phases have been separated and their chemical composition determined; in some cases crystals were picked out from cavities in the centre of the ingots, while in other cases the aluminium-rich matrix was dissolved and crystals of the phase in question picked out from the residue. Different phases in the residue were sometimes separated by means of heavy liquids.

In several cases the crystal structures of the phases isolated were studied by X-ray methods at Stockholm University in collaboration with Professors A. Westgren and H. Perlitz. The determination of the lattice spacings of a phase is often a necessary means of identification, as etching reactions are frequently influenced to a considerable extent by elements present in solid solution. In many cases the occurrence of a solid solution may be directly proved by a determination of the unit-cell dimensions. In some instances it was possible to determine the exact positions of the atoms in the unit cell, and in these cases the chemical formula corresponding to the structure is given. It should be emphasized that the actual chemical composition may differ from this



formula, since some lattice points may not be completely occupied, or may be occupied by more than one kind of atom.

### 3. *Nomenclature of Phases.*

In those cases where the crystallographic structure has been exactly determined, the chemical formula corresponding to the structure has been used to define the phase, e.g.  $\text{Al}_2\text{Cu}$ ,  $\text{Mg}_2\text{Si}$ ,  $\text{Al}_7\text{Cu}_2\text{Fe}$ ,  $\text{Al}_2\text{CuMg}$ . Although the structures of the Al-Fe and Al-Mn phases which may occur in equilibrium with the melt and solid aluminium are not known, these phases have been called  $\text{Al}_3\text{Fe}$  and  $\text{Al}_6\text{Mn}$ , respectively, to conform with general practice. With the single exception of an unstable phase in the Al-Cu-Mg-Mn system, the crystal systems of all phases studied have been determined. Where no definite chemical formula is available, therefore, it is convenient to indicate the crystal symmetry in the designations. The letters *c*, *t*, *h*, *r*, and *m* thus indicate cubic, tetragonal, hexagonal, orthorhombic, and monoclinic symmetry in such ternary and quaternary phases as *c*-AlCuMg, *t*-AlFeSi, *h*-AlCuMgSi, *r*-AlCuMn, *m*-AlFeSi. The phase of unknown symmetry is designated *z*-AlCuMgMn. The formula  $\text{Al}_8\text{Mg}_3\text{FeSi}_6$  for one of the phases referred to will probably be considered somewhat complicated for general use and the designation *h*-AlMgFeSi may therefore be substituted. The only binary phase which could not be given a chemical formula is called  $\beta$ -AlMg. In equilibrium reactions solid aluminium is described as  $\alpha$ -Al.

The designations used by other authors are mentioned in the text, and a correlation between different nomenclatures will be found in Table XXVII (Plate LXXV).

### 4. *Preparation of Alloys.*

The alloys were melted in crucibles of Acheson graphite in a Tammann furnace and, in general, were cast in a mould made of "Sil-o-Cel", a refractory brick ( $120 \times 120 \times 70$  mm.). The mould consisted of a 50-cm.-deep hole in the form of a truncated cone with basal planes of 60 and 40 mm. dia., respectively, giving ingots of approximately 180 g. weight. In some cases the castings were made under conditions of more rapid or less rapid cooling than with the above technique. Thus, some alloys were cast in a cast-iron mould, which was either cold or preheated to  $400^\circ$ – $500^\circ$  C., and had a wall thickness of 10 mm. and internal dimensions  $10 \times 50 \times 120$  mm. The largest dimension lay in the vertical direction during casting. Some melts were cast in graphite crucibles, and these also solidified relatively rapidly. Very slow solidification and cooling were obtained by casting in preheated



refractory-brick moulds, which were allowed to cool slowly in the furnace. Only in one special case, mentioned below, was an alloy annealed for any considerable time.

Some alloys were prepared from ordinary virgin aluminium, containing 99·8% aluminium, with iron and silicon as the main impurities. Other alloys, in cases where especially low contents of iron and silicon were required, were prepared from electrolytically refined aluminium (99·99%).

Copper was added as electrolytically refined copper, and magnesium as metal with a purity of 99·9%, the chief impurities being aluminium and iron.

Manganese was either added as metallic manganese\* or as an aluminium-rich master alloy containing 20% manganese. The main impurities of the master alloy were iron and silicon; spectrographic analysis of one such alloy gave iron 0·46 and silicon 0·18%. Master alloys of aluminium and manganese with especially low contents of iron and silicon were made from crystallized manganous chloride of composition  $\text{MnCl}_2 \cdot 4\text{H}_2\text{O}$  and electrolytically refined aluminium, using a method, described by Wöhler,<sup>18</sup> in which manganous chloride reacts with molten aluminium, forming aluminium chloride, which evaporates, and manganese, which dissolves in the aluminium melt. Spectrographic analysis of an alloy prepared by this method and containing 25% manganese showed that the iron and silicon contents were each less than 0·01%, the copper content below 0·005%, and the magnesium content below 0·002%.

Iron was added either directly as very soft sheet of low-carbon rimming steel or as master alloys prepared from this sheet and virgin aluminium. For such a master alloy containing 25% iron, chemical analysis gave a silicon content of 0·35%.

The alloys containing silicon were prepared from a 50 : 50 aluminium-silicon alloy, the purity of which was 99·5% for aluminium plus silicon. Where a higher degree of purity was necessary, a master alloy made from electrolytically refined aluminium and refined silicon was used. The refined silicon was prepared by washing with nitric acid the residue obtained on dissolving the 50 : 50 aluminium-silicon alloy in hydrochloric acid. A master alloy with 10% silicon made in this way was found to have a content of aluminium plus silicon of 99·99%.

Some of the alloys have been analysed, partly chemically and partly spectrographically. To avoid segregation, the test-pieces for analysis

\* The editors of this paper have not been able to ascertain the quality of the manganese metal.

were cast in special metal moulds intended for the casting of spectrographic-analysis electrodes.

### III.—BINARY SYSTEMS.

The features of the binary systems which are of particular importance to the present work are summarized in Table I.

### IV.—TERNARY SYSTEMS.

Triangular diagrams, which are projections of the liquidus surface on the basal plane, have been used to represent the ternary systems. The primary phases separating over the various regions of the diagrams have been indicated, and arrows are used to show the direction of solidification in the binary separations. The compositions suggested for the various phases are indicated by open circles, or, where an extended homogeneity range has been shown to exist, by an area enclosed by a curve. In each case the symbol of the phase is given in quotation marks.

In most cases the diagrams are those published by earlier investigators. Where these have been checked by the author, the compositions of the alloys studied and the phases which appear to be primary have been indicated by appropriate symbols.

#### 1. Al-Cu-Mg.

In this system two phases besides those belonging to the subsidiary systems Al-Cu and Al-Mg have been observed. These phases will be designated *c*-AlCuMg and Al<sub>2</sub>CuMg (see Table XXVII, Plate LXXV). According to Laves, Löhberg, and Witte<sup>37</sup> *c*-AlCuMg is cubic ( $a_1 = 14.2$  kX.); in the present investigation the parameter value 14.28 kX. was found. The positions of the atoms in the unit cell are unknown, and it is not possible to decide whether the composition of *c*-AlCuMg corresponds to the formula Al<sub>6</sub>CuMg<sub>4</sub>, suggested by Laves and his collaborators,<sup>37</sup> or to Al<sub>5</sub>CuMg<sub>4</sub>, as suggested by Nishimura.<sup>38</sup> Crystals of *c*-AlCuMg form rhombic dodecahedra, i.e. they have the form {110}, sometimes slightly blunted by faces belonging to the {100} group. The crystals are white, but darken slightly on polishing and are not birefringent.

Perlitz and Westgren<sup>40</sup> have shown that Al<sub>2</sub>CuMg has orthorhombic symmetry ( $a_1 = 4.00$ ,  $a_2 = 9.28$ , and  $a_3 = 7.14$  kX.). The unit cell contains 8 aluminium, 4 copper, and 4 magnesium atoms. The atomic arrangement is given in an Appendix (p. 552). The formula Al<sub>2</sub>CuMg for this phase is thus confirmed. Crystals form white prismatic needles with faces belonging to the {010} and {021} groups. The phase darkens

TABLE I.—*Characteristics of the Binary Systems.*

System	Phase in Equilibrium with $\alpha$ -Al	Crystal Structure	Lattice Spacing, kX.	Crystal Habit	Behaviour in Polarized Light	Appearance in Ordinary Light	Remarks	Additional References
Al-Cu	Al <sub>2</sub> Cu	Tetragonal, with 12 atoms/unit cell (20), (21).	$a_1 = 6.052$ } (20), (21) $a_2 = 4.878$ }	Tetragonal needles of form {110}.	Strongly birefringent giving strong colour effects.	White to pale pink.	Actual composition of Al <sub>2</sub> Cu is better represented by Al <sub>2</sub> Cu <sub>0.97</sub> (19).	...
Al-Mg	$\beta$ -AlMg	Hexagonal (30).	$a_1 = 11.38$ } (30) $a_2/a_1 = 1.57$ }	Dendritic.	No birefringence.	White.	The hexagonal crystal structure was deduced from powder photographs, which is unreliable where the unit cell is large. The cubic structure is based on single-crystal measurements.	(9), (22) to (29).
		Cubic (31).	$a_1 = 28.13$ (31)					
Al-Mn	Al <sub>6</sub> Mn	Orthorhombic (32).	$a_1 = 6.51$ } (33) $a_2 = 7.57$ } $a_3 = 8.87$ }	Rhombic needles of form {110}.	Crystals show brown to blue-grey polarization colours.	Light grey.	...	(32).
			$a_1 = 6.485$ } Present $a_2 = 7.525$ } work. $a_3 = 8.840$ }					
Al-Fe	Al <sub>3</sub> Fe	Orthorhombic (34).	$a_1 = 47.6$ } (34) $a_2 = 15.49$ } $a_3 = 8.11$ }	Flat rhombic needles of forms {110} and {100}.	Weak birefringence.	Grey.	Al <sub>3</sub> Fe is reported (35) to decompose on slow cooling into Al <sub>7</sub> Fe <sub>3</sub> and Al <sub>3</sub> Fe <sub>2</sub> . X-ray photographs of Al <sub>7</sub> Fe <sub>3</sub> and Al <sub>3</sub> Fe are very similar and it is not definitely established that they are different phases.	...
			$a_1 = 48.04$ } Present $a_2 = 15.59$ } work. $a_3 = 8.10$ }					
Al-Si	Silicon	Cubic.	$a_1 = 5.4173$	Octahedra.	No birefringence.	Dark violet.	Solid silicon from an Al-Si alloy has a lattice spacing of 5.4176 kX., showing negligible solubility for aluminium.	(36).

*Note.*—The numbers in parentheses relate to the references at the end of the paper.

on polishing, but less easily than *c*-AlCuMg. The crystals are strongly birefringent and in polarized light appear violet to orange.

The liquidus surfaces of the two phases mentioned have previously been investigated by Nishimura,<sup>38</sup> whose results agree well with those of the present investigation, which are summarized in Fig. 2. Both the compositions,  $\text{Al}_6\text{CuMg}_4$  and  $\text{Al}_5\text{CuMg}_4$ , have been indicated for the

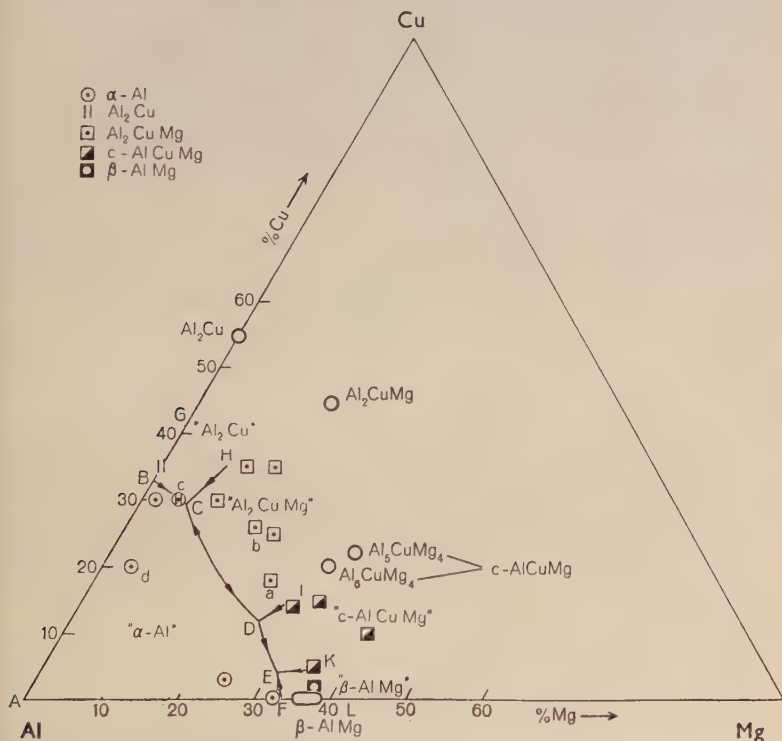


FIG. 2.—The Al-Cu-Mg System. Point *c* indicates an alloy for which it has not been possible to ascertain whether solid aluminium or  $\text{Al}_2\text{Cu}$  is primary.

phase *c*-AlCuMg. Table II lists those phases which, during solidification, separate first from the melt within the different regions of the diagram. Also given are the reactions corresponding to the lines (melt + two solids) and points (melt + three solids) in Fig. 2.

Fig. 3 (Plate LVII) is a photomicrograph of an alloy containing copper 18 and magnesium 23% (point *a* in Fig. 2). On solidification  $\text{Al}_2\text{CuMg}$  separates first from the melt. When the point corresponding to the composition of the melt has reached the line *CD*, solid aluminium

also separates, and the composition of the melt follows the line *CD* towards *D*. At point *D*,  $\text{Al}_2\text{CuMg}$  reacts peritectically with the melt, forming solid aluminium and *c*- $\text{AlCuMg}$ , and is very soon entirely enveloped by *c*- $\text{AlCuMg}$  and unable to take further part in the peritectic reaction. Solid aluminium and *c*- $\text{AlCuMg}$  therefore separate eutectically and the line *DE* is followed towards *E*. At point *E*  $\beta$ - $\text{AlMg}$  also separates, and the solidification of the melt is complete.

TABLE II.—*Phases and Reactions in Al-Cu-Mg System.*

Region, Line, or Point	Primary Phase, or Equilibrium Reaction
<i>ABCDEF</i> . . . .	$\alpha$ -Al
<i>GBCH</i> . . . .	$\text{Al}_2\text{Cu}$
<i>HCDI</i> . . . .	$\text{Al}_2\text{CuMg}$
<i>IDEK</i> . . . .	<i>c</i> - $\text{AlCuMg}$
<i>KEFL</i> . . . .	$\beta$ - $\text{AlMg}$
<i>BC</i> . . . . .	Eutectic: Melt $\rightleftharpoons \alpha\text{-Al} + \text{Al}_2\text{Cu}$
<i>CD</i> . . . . .	„ Melt $\rightleftharpoons \alpha\text{-Al} + \text{Al}_2\text{CuMg}$
<i>DE</i> . . . . .	„ Melt $\rightleftharpoons \alpha\text{-Al} + c\text{-AlCuMg}$
<i>EF</i> . . . . .	„ Melt $\rightleftharpoons \alpha\text{-Al} + \beta\text{-AlMg}$
<i>HC</i> . . . . .	„ Melt $\rightleftharpoons \text{Al}_2\text{Cu} + \text{Al}_2\text{CuMg}$
<i>ID</i> . . . . .	Peritectic: Melt + $\text{Al}_2\text{CuMg} \rightleftharpoons c\text{-AlCuMg}$
<i>KE</i> . . . . .	Eutectic: Melt $\rightleftharpoons c\text{-AlCuMg} + \beta\text{-AlMg}$
<i>C</i> . . . . .	Eutectic: Melt $\rightleftharpoons \alpha\text{-Al} + \text{Al}_2\text{Cu} + \text{Al}_2\text{CuMg}$
<i>D</i> . . . . .	Peritectic: Melt + $\text{Al}_2\text{CuMg} \rightleftharpoons \alpha\text{-Al} + c\text{-AlCuMg}$
<i>E</i> . . . . .	Eutectic: Melt $\rightleftharpoons \alpha\text{-Al} + c\text{-AlCuMg} + \beta\text{-AlMg}$

In Fig. 4 (Plate LVII) is shown a photomicrograph of an alloy containing copper 26 and magnesium 17% (point *b* in Fig. 2). The order of solidification is very similar to that described above for the alloy shown in Fig. 3.

Figs. 5 and 6 (Plate LVIII) are photomicrographs of an alloy containing copper 30 and magnesium 5%. This composition corresponds to point *c* in Fig. 2 and is very close to that of the non-variant point *C*. As expected at this composition, the photomicrographs show eutectic complexes of solid aluminium,  $\text{Al}_2\text{Cu}$ , and  $\text{Al}_2\text{CuMg}$ .

Figs. 7 and 8 (Plate LIX) are photomicrographs of an alloy containing copper 20 and magnesium 4% (point *d* in Fig. 2). When this alloy solidifies, solid aluminium separates first, and the content of alloying elements in the melt increases until either the line *BC* or the line *CD* is reached in the immediate neighbourhood of point *C*. Subsequently  $\text{Al}_2\text{Cu}$  or  $\text{Al}_2\text{CuMg}$  also separates. When the point corresponding to the composition of the melt follows *BC* or *CD* towards *C*, a eutectic separation of solid aluminium,  $\text{Al}_2\text{Cu}$ , and  $\text{Al}_2\text{CuMg}$  is almost immediately obtained, and the solidification of the melt is then complete. The





of copper in the  $\text{Al}_6\text{Mn}$  phase. In the system  $\text{Al-Cu-Mn}$  this phase should therefore be denoted  $(\text{Al,Cu})_6(\text{Mn,Cu})$ , but as the copper content of the phase is always small, the formula  $\text{Al}_6\text{Mn}$  will be used.

Fig. 11 gives the compositions of the solid phases according to the present investigation, but the liquidus surfaces according to Petri.<sup>41</sup> In Table III the solid phases which precipitate first from the melt within the different regions of the diagram are listed, together with the mono-variant and non-variant equilibria.\*

TABLE III.—*Phases and Reactions in Al-Cu-Mn System.*

Region, Line, or Point	Primary Phase, or Equilibrium Reaction
<i>ABCDE</i> . . . .	$\alpha$ -Al
<i>FBCG</i> . . . .	$\text{Al}_6\text{Mn}$
<i>GCDH</i> . . . .	$r$ -AlCuMn
<i>HDEI</i> . . . .	$\text{Al}_2\text{Cu}$
<i>BC</i> . . . .	Eutectic: $\text{Melt} \rightleftharpoons \alpha\text{-Al} + \text{Al}_6\text{Mn}$
<i>CD</i> . . . .	" $\text{Melt} \rightleftharpoons \alpha\text{-Al} + r\text{-AlCuMn}$
<i>DE</i> . . . .	" $\text{Melt} \rightleftharpoons \alpha\text{-Al} + \text{Al}_2\text{Cu}$
<i>GC</i> . . . .	" $\text{Melt} \rightleftharpoons \text{Al}_6\text{Mn} + r\text{-AlCuMn}$
<i>HD</i> . . . .	" $\text{Melt} \rightleftharpoons r\text{-AlCuMn} + \text{Al}_2\text{Cu}$
<i>C</i> . . . .	Peritectic: $\text{Melt} + \text{Al}_6\text{Mn} \rightleftharpoons \alpha\text{-Al} + r\text{-AlCuMn}$
<i>D</i> . . . .	Eutectic: $\text{Melt} \rightleftharpoons \alpha\text{-Al} + r\text{-AlCuMn} + \text{Al}_2\text{Cu}$

### 3. *Al-Cu-Fe.*

In addition to the phases belonging to the subsidiary systems  $\text{Al-Cu}$  and  $\text{Al-Fe}$ , two other phases,  $\text{Al}_7\text{Cu}_2\text{Fe}$  and  $(\text{Al,Cu})_6(\text{Fe,Cu})$ ,† have been found.

According to Wiehr,<sup>47</sup> who proposed the formula  $\text{Al}_{12}\text{Cu}_4\text{Fe}$ , the phase  $\text{Al}_7\text{Cu}_2\text{Fe}$  has a tetragonal lattice and unit-cell dimensions  $a_1 = 6.32$ ,  $a_3 = 14.74$  kX. In the present investigation crystals of  $\text{Al}_7\text{Cu}_2\text{Fe}$ , isolated from an alloy containing copper 33 and iron 2.5%,

\* *Note by Editor:* While the present paper was being prepared for publication, Day and Phillips<sup>43</sup> published a study of the system  $\text{Al-Cu-Mn}$  within the ranges copper 0-18, manganese 0-8%, and copper 30-35, manganese 0-2%. The conditions of their investigation correspond not to equilibrium but to a cooling rate of about  $8^\circ\text{C./min.}$  This cooling rate is stated to be intermediate between that likely to occur in chill casting and that in sand casting. Day and Phillips report no phases which form a eutectic with solid aluminium other than those found in the present investigation. For  $r\text{-AlCuMn}$ , which they term  $\alpha(\text{Cu-Mn})$ , their work confirmed the existence of a homogeneity range, the composition in equilibrium with aluminium being copper 19 and manganese 24%. Day and Phillips further state that  $r\text{-AlCuMn}$  is isomorphous with  $\alpha(\text{Mn-Si})$  and  $\alpha(\text{Fe-Si})$  or, as these phases are called in the present investigation,  $c\text{-AlMnSi}$  and  $c\text{-AlFeSi}$ . As reported below, these two phases have a cubic lattice; the last statement is therefore incorrect. For points *C* and *D* in Fig. 11 they found copper 14.85, manganese 0.90%, and copper 32.50, manganese 0.60%, respectively.

† For earlier nomenclature, see Table XXVII (Plate LXXV).

were examined by Westgren,<sup>48</sup> who obtained the lattice spacings  $a_1 = 6.32$ ,  $a_3 = 14.78$  kX. The unit cell contains 28 aluminium, 8 copper, and 4 iron atoms. The arrangement of the atoms in the unit cell is given in an Appendix (p. 552).  $\text{Al}_7\text{Cu}_2\text{Fe}$  crystals appear as grey plates or blades of the form  $\{001\}$ , showing birefringence; the colour may change from dark grey to light grey in polarized light.

The second ternary constituent,  $(\text{Al,Cu})_6(\text{Fe,Cu})$ , was isolated from an alloy containing copper 12, magnesium 7, and iron 1% and the composition was found to be aluminium 70, copper 8, and iron 22%. Magnesium was added to the alloy in order to facilitate isolation of the crystals. The phase has an orthorhombic lattice with unit-cell dimensions  $a_1 = 7.449$ ,  $a_2 = 6.428$ , and  $a_3 = 8.768$  kX. These dimensions correspond very closely to those for  $\text{Al}_6\text{Mn}$ , with which  $(\text{Al,Cu})_6(\text{Fe,Cu})$  is isomorphous. Crystals of  $(\text{Al,Cu})_6(\text{Fe,Cu})$  form rhombic needles and show the same change of colour in polarized light as crystals of  $\text{Al}_6\text{Mn}$ .

To judge from the etching properties,  $\text{Al}_3\text{Fe}$  dissolves some copper. It could therefore be denoted  $(\text{Al,Cu})_3(\text{Fe,Cu})$  in the system Al-Cu-Fe, but will be written  $\text{Al}_3\text{Fe}$ , as the copper content is probably very low.

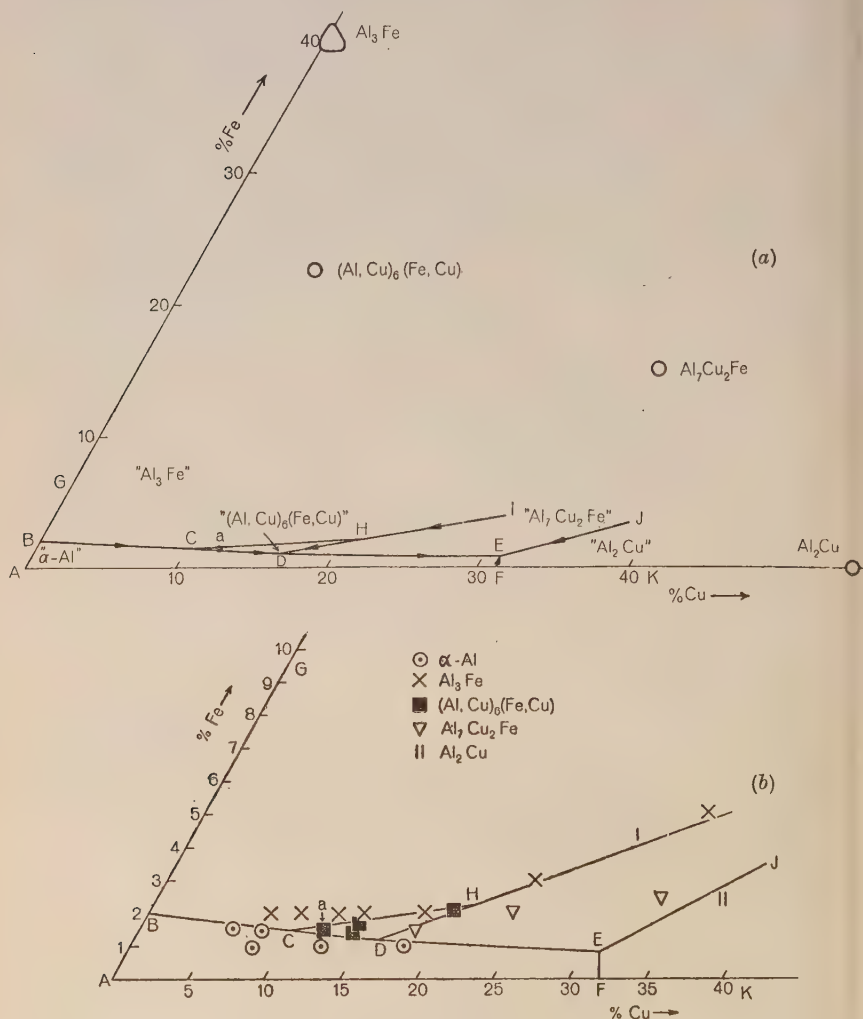
The liquidus surfaces have previously been investigated by Gwyer, Phillips, and Mann<sup>44</sup> and by Yamaguchi and Nakamura.<sup>45</sup> The phase  $(\text{Al,Cu})_8(\text{Fe,Cu})$  was, however, not observed by them.

The results obtained in the present investigation are shown in Figs. 12 (a) and (b). Table IV gives the solid phases which separate

TABLE IV.—Phases and Reactions in Al-Cu-Fe System.

Region, Line, or Point	Primary Phase, or Equilibrium Reaction
<i>ABCDEF</i> . . .	$\alpha\text{-Al}$
<i>GBCHI</i> . . .	$\text{Al}_3\text{Fe}$
<i>CDH</i> . . .	$(\text{Al,Cu})_6(\text{Fe,Cu})$
<i>IHDEJ</i> . . .	$\text{Al}_7\text{Cu}_2\text{Fe}$
<i>JEFK</i> . . .	$\text{Al}_2\text{Cu}$
<i>BC</i> . . .	Eutectic: $\text{Melt} \rightleftharpoons \alpha\text{-Al} + \text{Al}_3\text{Fe}$
<i>CD</i> . . .	„ $\text{Melt} \rightleftharpoons \alpha\text{-Al} + (\text{Al,Cu})_6(\text{Fe,Cu})$
<i>DE</i> . . .	„ $\text{Melt} \rightleftharpoons \alpha\text{-Al} + \text{Al}_7\text{Cu}_2\text{Fe}$
<i>EF</i> . . .	„ $\text{Melt} \rightleftharpoons \alpha\text{-Al} + \text{Al}_2\text{Cu}$
<i>CH</i> . . .	Peritectic: $\text{Melt} + \text{Al}_3\text{Fe} \rightleftharpoons (\text{Al,Cu})_6(\text{Fe,Cu})$
<i>HD</i> . . .	„ $\text{Melt} + (\text{Al,Cu})_6(\text{Fe,Cu}) \rightleftharpoons \text{Al}_7\text{Cu}_2\text{Fe}$
<i>IH</i> . . .	„ $\text{Melt} + \text{Al}_3\text{Fe} \rightleftharpoons \text{Al}_7\text{Cu}_2\text{Fe}$
<i>JE</i> . . .	Eutectic: $\text{Melt} \rightleftharpoons \text{Al}_7\text{Cu}_2\text{Fe} + \text{Al}_2\text{Cu}$
<i>C</i> . . .	Peritectic: $\text{Melt} + \text{Al}_3\text{Fe} \rightleftharpoons \alpha\text{-Al} + (\text{Al,Cu})_6(\text{Fe,Cu})$
<i>D</i> . . .	„ $\text{Melt} + (\text{Al,Cu})_6(\text{Fe,Cu}) \rightleftharpoons \alpha\text{-Al} + \text{Al}_7\text{Cu}_2\text{Fe}$
<i>E</i> . . .	Eutectic: $\text{Melt} \rightleftharpoons \alpha\text{-Al} + \text{Al}_7\text{Cu}_2\text{Fe} + \text{Al}_2\text{Cu}$
<i>H</i> . . .	Peritectic: $\text{Melt} + \text{Al}_3\text{Fe} \rightleftharpoons (\text{Al,Cu})_6(\text{Fe,Cu}) + \text{Al}_7\text{Cu}_2\text{Fe}$

first from the melt within the different regions of the diagrams, together with the reactions occurring at the lines and points of Figs. 12 (a) and (b).



FIGS. 12 (a) and (b).—The Al-Cu-Fe System.

Figs. 9 and 10 (Plate LX) are photomicrographs of an alloy containing copper 12 and iron 1.5% (point *a* in Fig. 12). The phase first separating on solidification is (Al,Cu)<sub>6</sub>(Fe,Cu). This phase separates alone, until the composition of the melt reaches the line *CD*. Solid



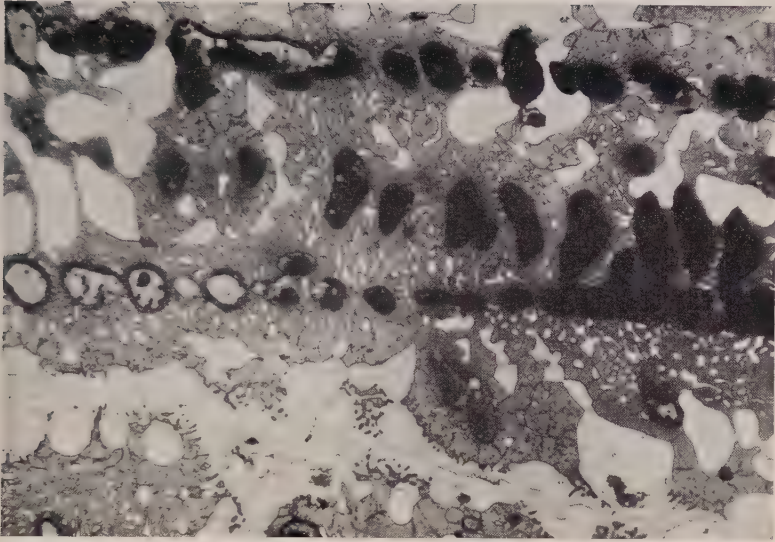


FIG. 3.—Al-18% Cu-23% Mg Alloy cast in a graphite crucible. Etched in phosphoric acid (1 : 10). Al<sub>2</sub>CuMg (grey dendrites usually covered by an easily removable dark deposit), surrounded by dark grey *c*-AlCuMg and a binary eutectic of *c*-AlCuMg and (white) the Al-rich phase.  $\beta$ -AlMg (grey) forms a binary eutectic with *c*-AlCuMg.  $\times 400$ .

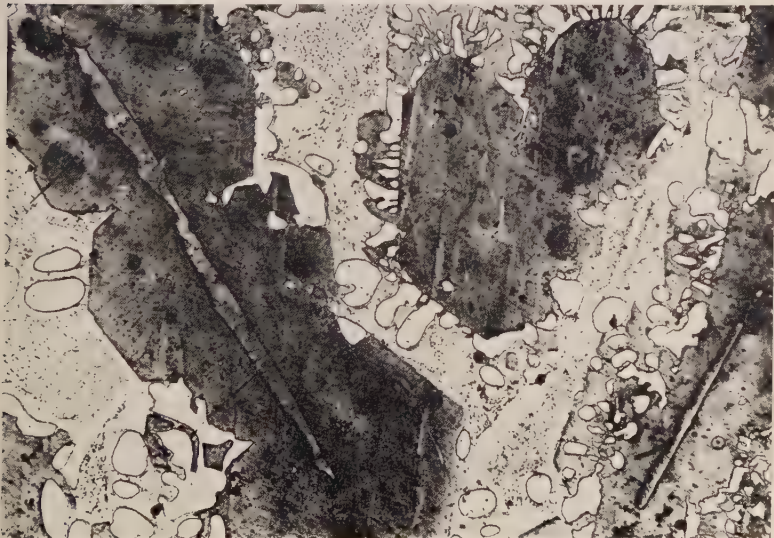


FIG. 4.—Al-26% Cu-17% Mg Alloy cast in a refractory-brick mould. Etched in phosphoric acid (1 : 10). Needles of Al<sub>2</sub>CuMg enveloped by *c*-AlCuMg (darkly etched), and a degenerate eutectic of *c*-AlCuMg and the (white) Al-rich phase;  $\beta$ -AlMg (grey). The dotted grey region is probably a binary eutectic of *c*-AlCuMg and  $\beta$ -AlMg.  $\times 120$ .





FIG. 5.—Al-30% Cu-5% Mg Alloy cast in a refractory-brick mould cooled from the top during solidification. Etched in HF (1 : 200).  $\text{Al}_2\text{CuMg}$  (dark grey);  $\text{Al}_2\text{Cu}$  (light grey); Al (white).  $\times 400$ .



FIG. 6.—Same Alloy as Fig. 5, etched in 1% NaOH.  $\text{Al}_2\text{CuMg}$  (white);  $\text{Al}_2\text{Cu}$  (dark); Al (lightly etched).  $\times 400$ .



FIG. 7.—Al-20% Cu-4% Mg Alloy cast in a refractory-brick mould. Etched in HF (1 : 200). Al<sub>2</sub>CuMg (dark grey); Al<sub>2</sub>Cu (light grey); Al (white).  $\times 400$ .

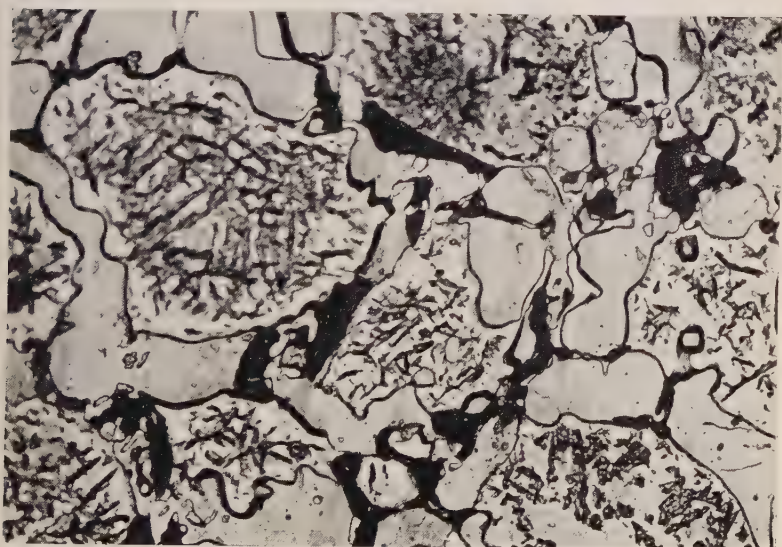


FIG. 8.—Same Alloy as Fig. 7, etched in 1% NaOH. Al<sub>2</sub>CuMg (white); Al<sub>2</sub>Cu (dark); Al (lightly etched).  $\times 400$ .

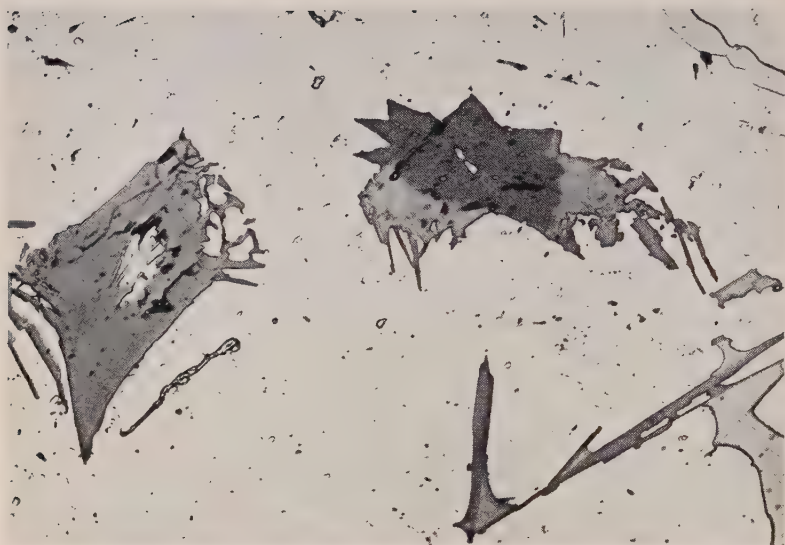


FIG. 9.—Al-12% Cu-1.5% Fe Alloy cast in a refractory-brick mould. Unetched. In the centre star-shaped  $\text{Al}_3\text{Fe}$  (dark grey) enveloped by  $\text{Al}_7\text{Cu}_2\text{Fe}$  (grey). To the left  $(\text{Al,Cu})_6(\text{Fe,Cu})$  (grey) enveloped by  $\text{Al}_7\text{Cu}_2\text{Fe}$  having the same tone as  $(\text{Al,Cu})_6(\text{Fe,Cu})$ .  $\times 400$ .



FIG. 10.—Same field as Fig. 9, etched in 10% ferric nitrate.  $\text{Al}_3\text{Fe}$  (dark grey);  $(\text{Al,Cu})_6(\text{Fe,Cu})$  (somewhat lighter than  $\text{Al}_3\text{Fe}$ );  $\text{Al}_7\text{Cu}_2\text{Fe}$  (darkly etched).  $\times 400$ .



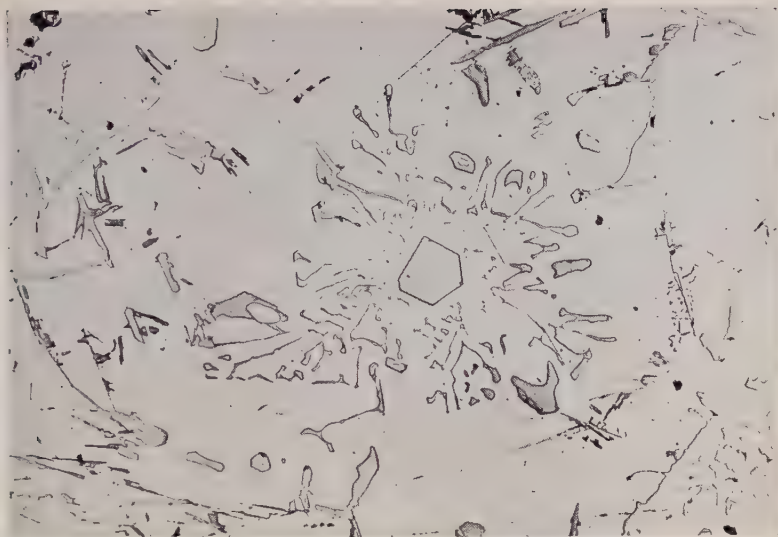


FIG. 20.—Al-2.3% Fe-4.6% Si Alloy cast in a refractory-brick mould. Unetched. In the centre a primary crystal of  $c\text{-AlFeSi}$  surrounded by a eutectic of this phase and solid Al ("Chinese script").  $\times 120$ .



FIG. 21.—Al-3.0% Fe-14.5% Si Alloy cast in a refractory-brick mould. Photographed in polarized light. A section through a large plate of  $m\text{-AlFeSi}$  surrounded by Si and solid Al. Twin lamellæ give the plate a striped appearance.  $\times 120$ .



FIG. 22.—Al-10% Fe-15% Si Alloy cast in a preheated cast-iron mould. Etched in HF (1:200).  $t$ -AlFeSi (light grey) enveloped by  $m$ -AlFeSi (grey); Si (somewhat darker grey); Al (light). In lower left-hand corner a large crystal of Si.  $\times 80$ .



FIG. 23.—Same field as Fig. 22, photographed in polarized light.  $\times 80$ .





FIG. 24.—Al-11.7% Cu-3.0% Mg-1.0% Mn Alloy cast in a refractory-brick mould. Etched in HF (1 : 200). Eutectic of Al and unstable  $\alpha$ -AlCuMgMn between dendrites of Al ( $\alpha$ -AlCuMgMn somewhat darker than Al).  $\times 240$ .

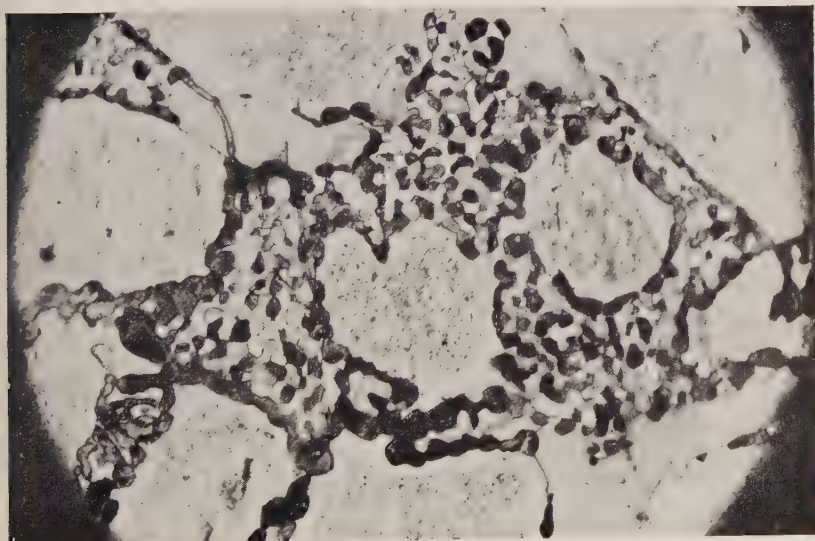


FIG. 25.—Same Alloy as Fig. 24 after heating at 490° C. for 80 hr. Etched in HF. Between dendrites of Al an aggregate of almost unetched  $\text{Al}_2\text{Cu}$  and dark particles (probably mainly  $\text{Al}_2\text{CuMg}$ ).  $\times 240$ .

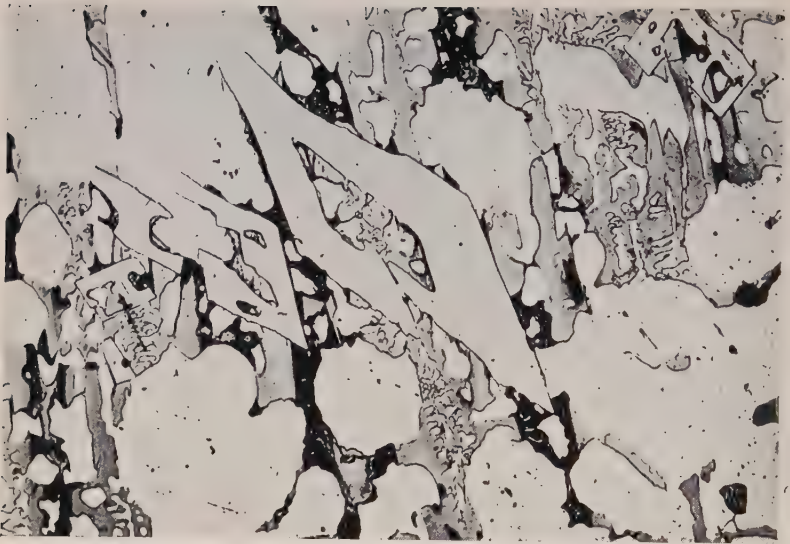


FIG. 26.—Al-9% Cu-9% Mg-2% Mn Alloy cast in a refractory-brick mould. Un-etched. Light grey primary crystals with rhombic intersection are  $\text{Al}_6\text{Mn}$  (grey);  $\text{Al}_2\text{CuMg}$  (darker grey);  $c\text{-AlCuMg}$  (dark); Al (white).  $\times 120$ .

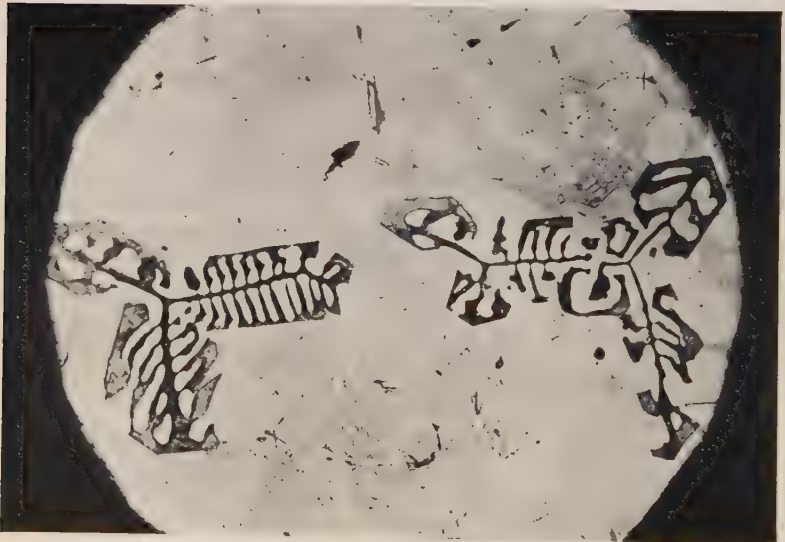


FIG. 27.—Al-26.25% Cu-1.50% Mn-2.25% Si Alloy allowed to cool in furnace after casting. Etched in HF (1:200).  $c\text{-AlMnSi}$  (darkly etched, owing to copper content);  $\text{Al}_2\text{Cu}$  (light grey); Al (almost white) containing small crystals of Si.  $\times 160$ .

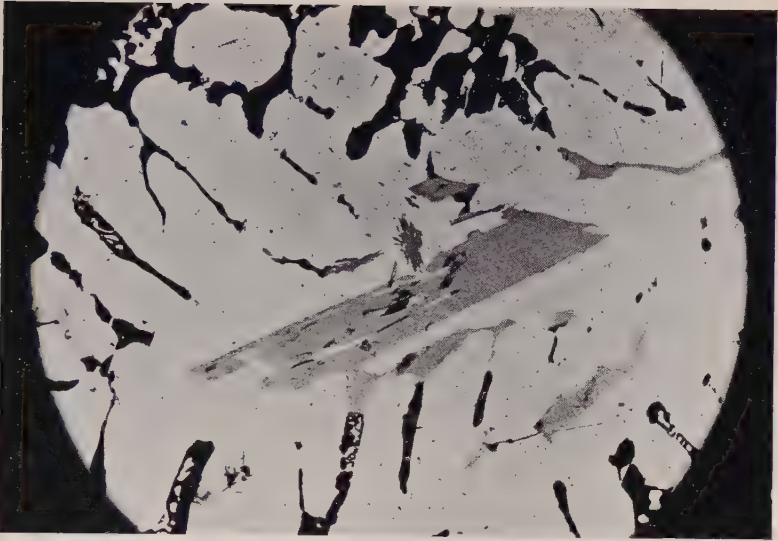


FIG. 34.—Al-12% Cu-7% Mg-1% Fe Alloy cast in a refractory-brick mould. Etched in 10% ferric nitrate. A light grey phase:  $(\text{Al,Cu})_6(\text{Fe,Cu})$ ; small, somewhat darker jagged grains:  $\text{Al}_3\text{Fe}$ ;  $\text{Al}_2\text{CuMg}$  (dark); Al (white).  $\times 160$ .

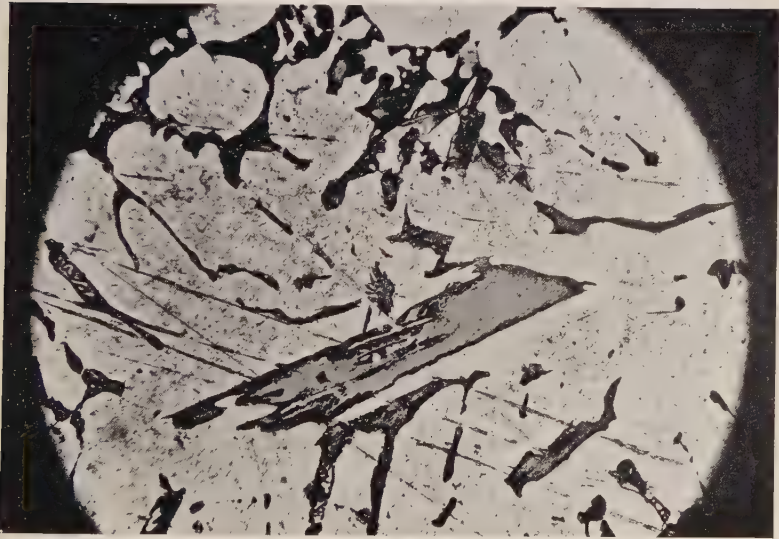


FIG. 35.—Same field as Fig. 34, etched in  $\text{H}_2\text{SO}_4$  (1:4).  $(\text{Al,Cu})_6(\text{Fe,Cu})$  (lightly etched at phase boundary);  $\text{Al}_3\text{Fe}$  (deeply etched and dark).  $\times 160$ .



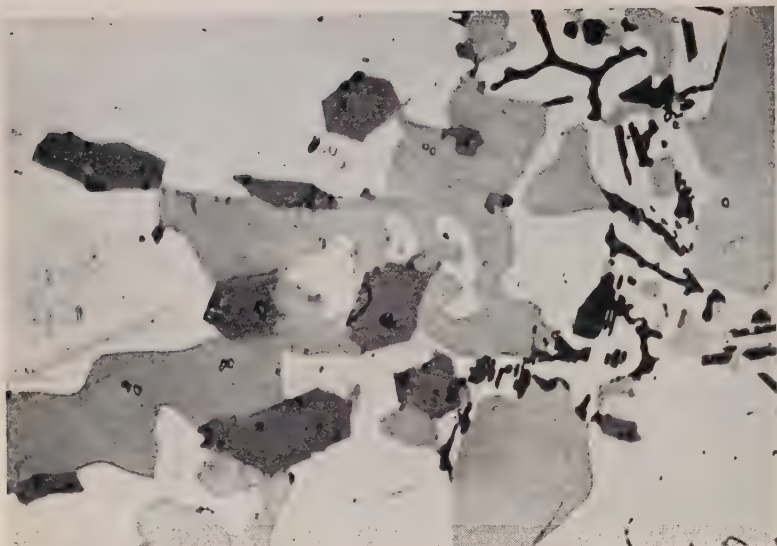


FIG. 36.—Al-14% Cu-2% Mg-4% Si Alloy cast in a refractory-brick mould. Un-etched. A dark grey phase with a hexagonal section: *h*-AlCuMgSi; Al<sub>2</sub>Cu (light grey but darker than Al); Si (dark).  $\times 400$ .

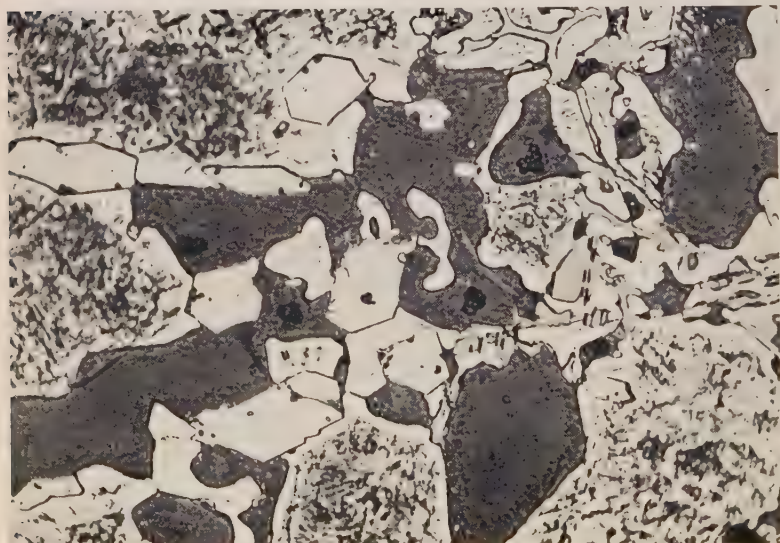


FIG. 37.—Same field as Fig. 36, etched in 1% NaOH. *h*-AlCuMgSi (white); Al<sub>2</sub>Cu (dark grey); Si (light grey).  $\times 400$ .

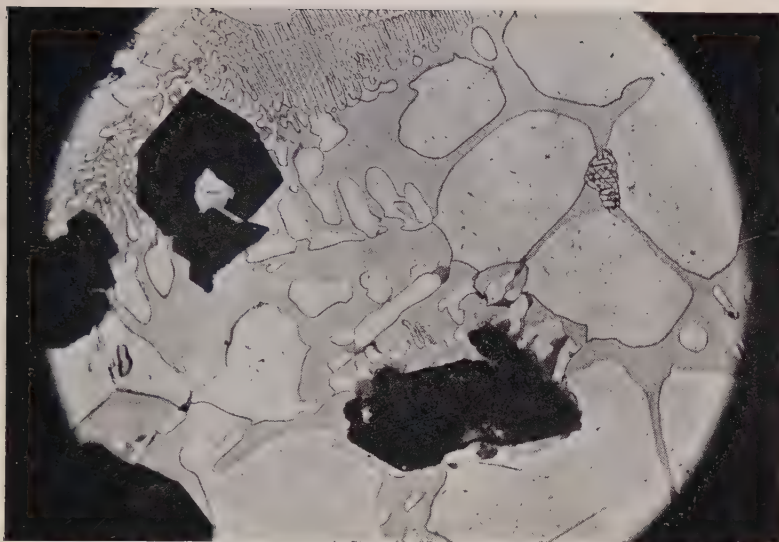


FIG. 38.—Al-18% Cu-1.6% Mn-0.4% Si Alloy cast in a refractory-brick mould. Etched in HF (1 : 200). Dark phase with straight-line contours:  $r$ -AlCuMn;  $Al_2Cu$  (light grey); Al (white);  $c$ -AlMnSi (darker grey than  $Al_2Cu$ ) seems to envelop  $r$ -AlCuMn in certain cases.  $\times 160$ .

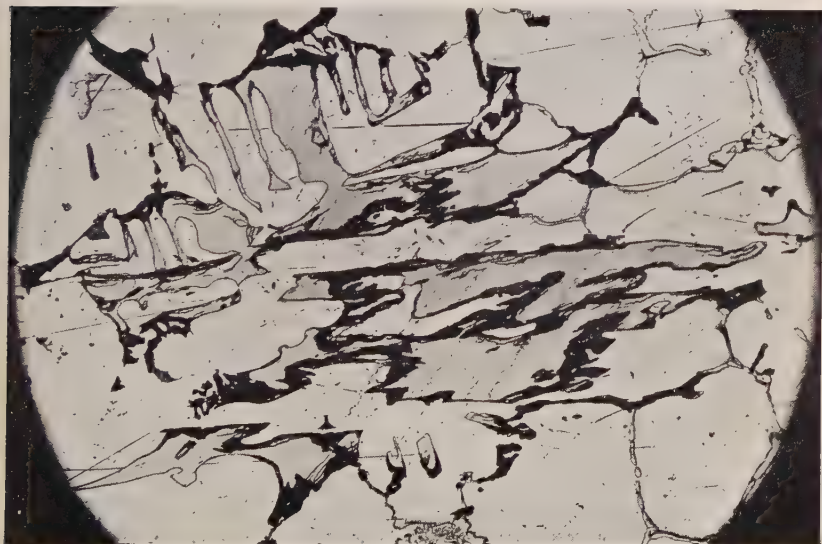


FIG. 39.—Al-7.5% Cu-2% Mn-0.5% Si Alloy cast in a preheated refractory-brick mould. Etched in HF (1 : 200).  $Al_6Mn$  (light grey) partly enveloped by  $c$ -AlMnSi (darkly etched); Al (light coloured).  $\times 80$ .



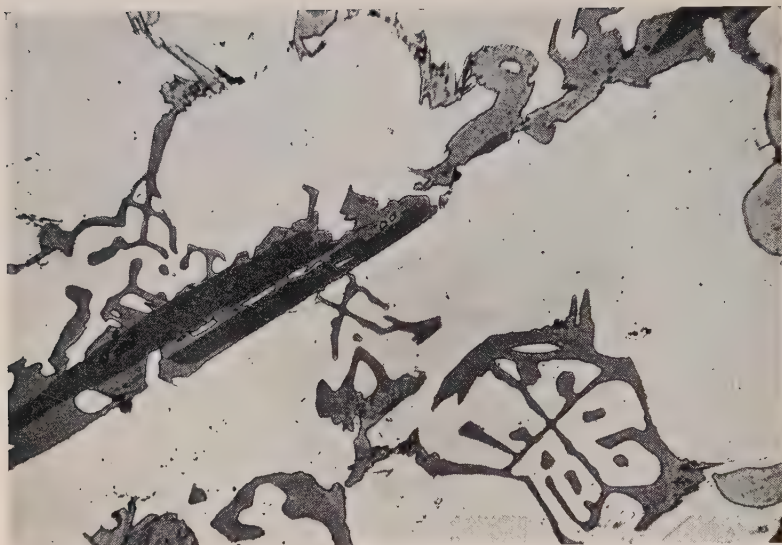


FIG. 40.—Al-12% Cu-1.5% Fe-1.5% Si Alloy cast in a preheated refractory-brick mould. Unetched.  $\text{Al}_3\text{Fe}$  (dark grey) enveloped by  $c\text{-AlFeSi}$  (lighter grey); Al (light);  $c\text{-AlFeSi}$  forming eutectic with Al appears as “Chinese script”.  $\times 240$ .

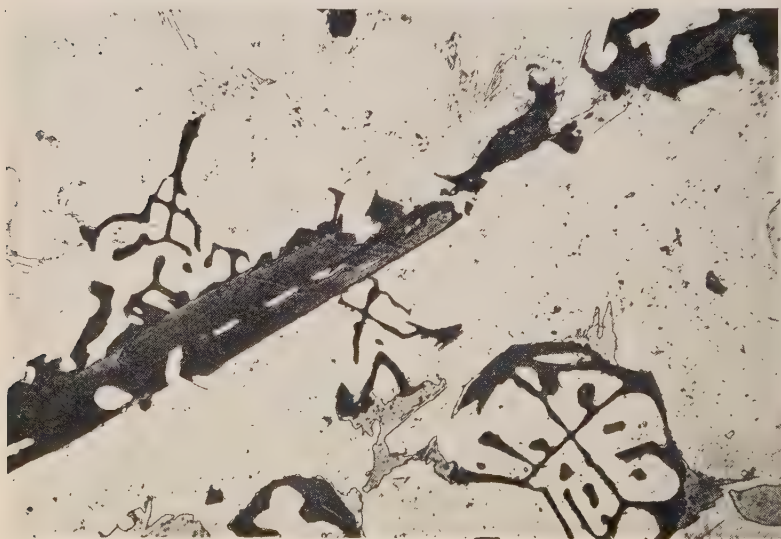


FIG. 41.—Same field as Fig. 40, etched in HF (1:200).  $\text{Al}_3\text{Fe}$  (uneven grey);  $c\text{-AlFeSi}$  (dark coloured) in certain cases enveloped by  $\text{Al}_7\text{Cu}_3\text{Fe}$  (light grey).  $\times 240$ .



FIG. 42.—Another part of same specimen as Figs. 40 and 41, etched in HF (1 : 200).  $\text{Al}_3\text{Fe}$  (uneven grey);  $c\text{-AlFeSi}$  (dark coloured) in certain cases enveloped by  $\text{Al}_7\text{Cu}_2\text{Fe}$  (light grey).  $\times 240$ .

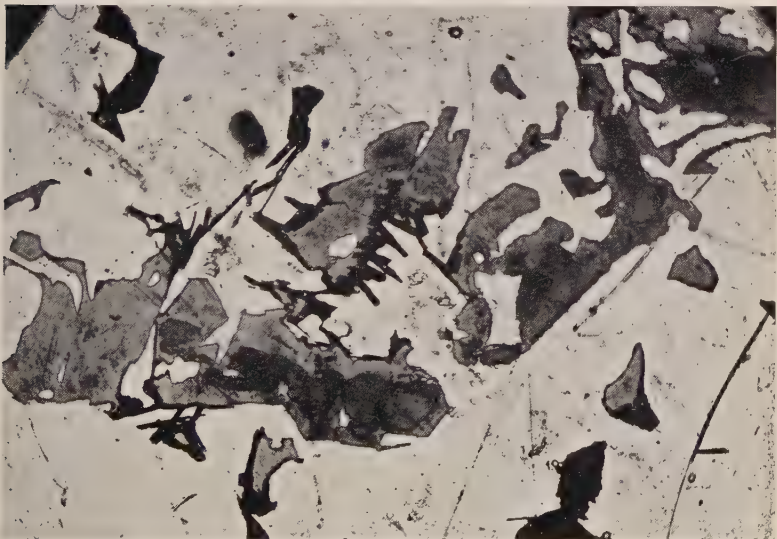


FIG. 43.—Same field as Fig. 42, etched in 10% ferric nitrate.  $\text{Al}_3\text{Fe}$  (dark grey) enveloped by  $c\text{-AlFeSi}$  (lighter grey). Lamellæ of  $\text{Al}_7\text{Cu}_2\text{Fe}$  and rounded grains of  $\text{Al}_2\text{Cu}$  also appear (both dark coloured).  $\times 240$ .

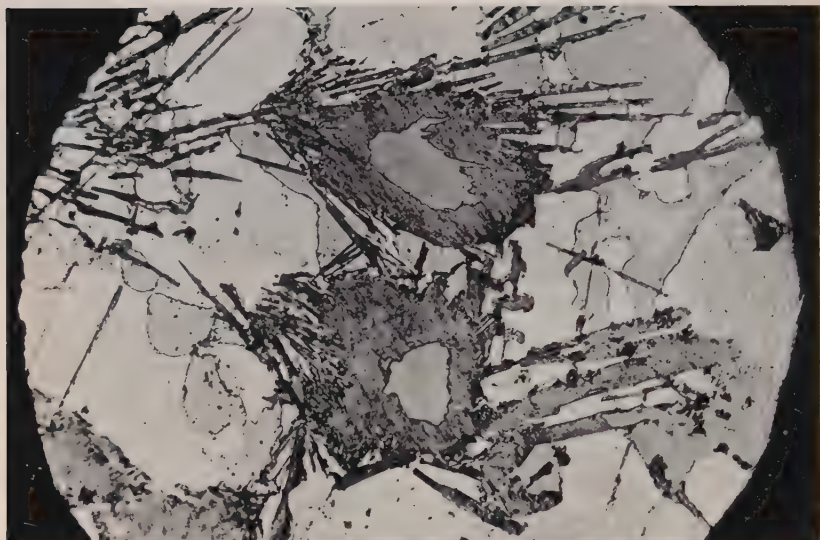


FIG. 44.—Al-20% Cu-1.6% Fe-5.4% Si Alloy cast in a refractory-brick mould. Etched in HF (1 : 200). *c*-AlFeSi (grey) enveloped by *m*-AlFeSi (lamellar and dark grey). Si (grey colour),  $\text{Al}_2\text{Cu}$  (light grey), and Al (very light) also appear.  $\times 240$ .

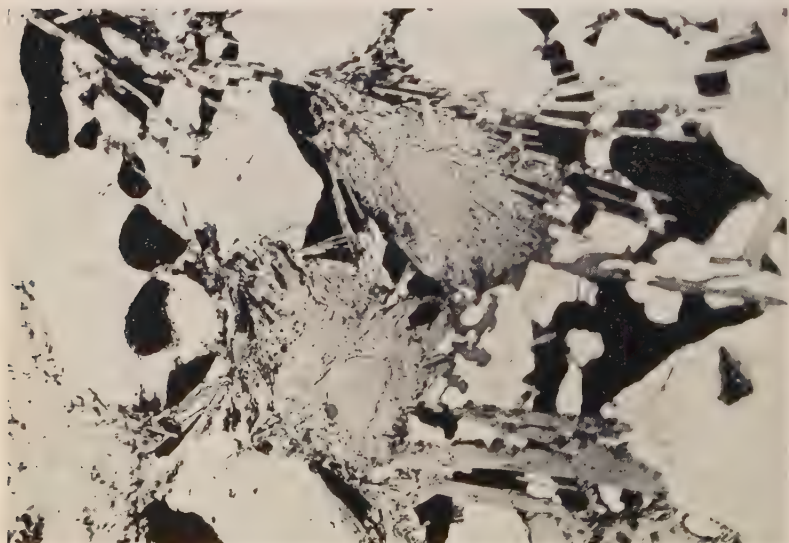


FIG. 45.—Same field as Fig. 44, etched in 10% ferric nitrate.  $\text{Al}_2\text{Cu}$  (darkly etched); *m*-AlFeSi (light grey).  $\times 240$ .



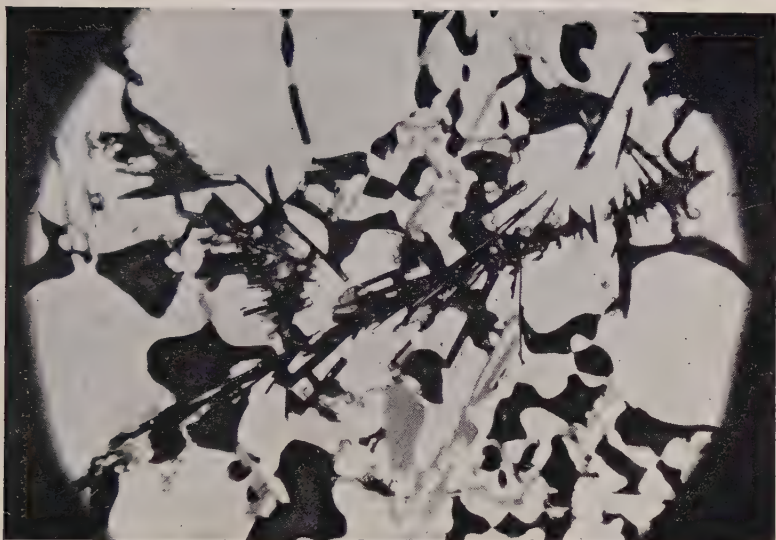


FIG. 46.—Al-15.5% Cu-0.5% Fe-4% Si Alloy cast in a refractory-brick mould. Etched in 10% ferric nitrate.  $\text{Al}_7\text{Cu}_2\text{Fe}$  (dark lamellæ);  $\text{Al}_2\text{Cu}$  (dark grains); Si (grey); Al (white). Arrangement of  $\text{Al}_7\text{Cu}_2\text{Fe}$  lamellæ seems to indicate that they have been formed by transformation of  $m\text{-AlFeSi}$ .  $\times 240$ .

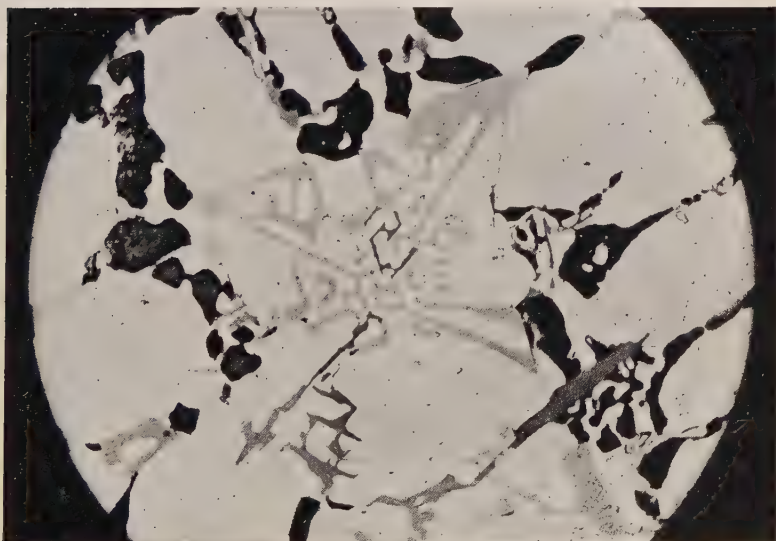


FIG. 47.—Al-14.5% Cu-0.5% Fe-5% Si Alloy cast in a refractory-brick mould. Etched in 10% ferric nitrate.  $c\text{-AlFeSi}$  (grey); Si (dark grey);  $\text{Al}_2\text{Cu}$  (darkly etched grains); Al (light background).  $\times 160$ .



FIG. 48.—Al-6% Mg-0.3% Fe-12% Si Alloy cast in a refractory-brick mould. Unetched.  $h$ -AlMgFeSi ( $\text{Al}_8\text{Mg}_3\text{FeSi}_6$ ): dark, branched particle in middle of field; Si (darker grey than  $h$ -AlMgFeSi);  $\text{Mg}_2\text{Si}$  (dark, owing to polishing); Al (light background).  $\times 160$ .

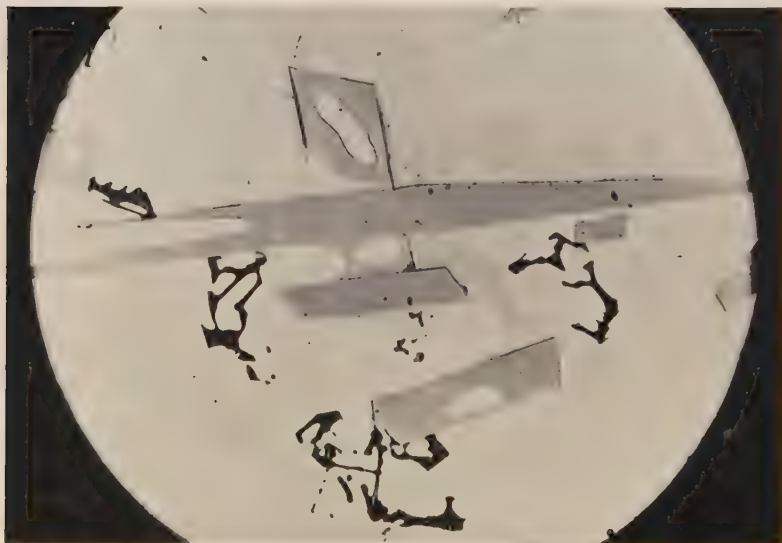


FIG. 49.—Al-10% Mg-1.5% Mn-1% Fe-0.15% Si Alloy cast in a refractory-brick mould. Unetched.  $\text{Al}_3(\text{Mn,Fe})$  (grey needles with rhombic section);  $\beta$ -AlMg (light grey phase with rounded outlines);  $\text{Mg}_2\text{Si}$  (dark); Al (light).  $\times 160$ .



aluminium and  $(\text{Al,Cu})_6(\text{Fe,Cu})$  then separate together, and the composition of the melt follows the line  $CD$  towards point  $D$ , where  $(\text{Al,Cu})_6(\text{Fe,Cu})$  is enveloped by  $\text{Al}_7\text{Cu}_2\text{Fe}$ , which separates peritectically. In both photomicrographs  $(\text{Al,Cu})_6(\text{Fe,Cu})$  is seen to the left, enveloped by  $\text{Al}_7\text{Cu}_2\text{Fe}$ . In the centres, however,  $\text{Al}_7\text{Cu}_2\text{Fe}$  envelops a constituent which in Fig. 10 has the same grey colour as  $(\text{Al,Cu})_6(\text{Fe,Cu})$  but which

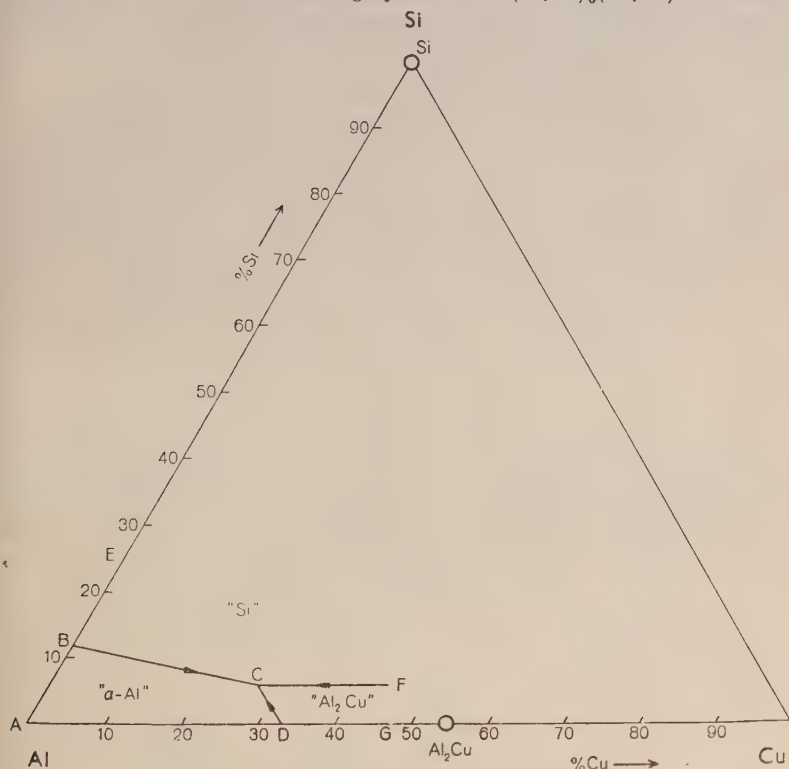


FIG. 13.—The Al-Cu-Si System (according to Hisatsune <sup>50</sup>).

in Fig. 9 is somewhat darker than  $(\text{Al,Cu})_6(\text{Fe,Cu})$ . This phase is  $\text{Al}_3\text{Fe}$ . As the point  $a$  is situated fairly close to the line  $CH$ , such separation of  $\text{Al}_3\text{Fe}$  is not entirely excluded by the diagram. It ought, however, to be peritectically enveloped by  $(\text{Al,Cu})_6(\text{Fe,Cu})$ , which should separate until it becomes enveloped by  $\text{Al}_7\text{Cu}_2\text{Fe}$  during a second peritectic reaction. In Figs. 9 and 10  $\text{Al}_3\text{Fe}$  is enveloped only by  $\text{Al}_7\text{Cu}_2\text{Fe}$ . This deviation from the diagram is explicable by undercooling. A tendency to undercooling could also partly explain why  $(\text{Al,Cu})_6(\text{Fe,Cu})$  has not been previously observed.

4. *Al-Cu-Si.*

In this system no phases occur other than those belonging to the subsidiary systems Al-Cu and Al-Si.

The system has been investigated by Gwyer, Phillips, and Mann,<sup>44</sup> and by Hisatsune,<sup>50</sup> with good agreement in the parts of the diagram which are of interest to the present work. Hisatsune's results are reproduced in Fig. 13. Table V indicates the significance of the regions, lines, and points in this figure.

TABLE V.—*Phases and Reactions in Al-Cu-Si System.*

Region, Line, or Point	Primary Phase, or Equilibrium Reaction
<i>ABCD</i> . . . . .	$\alpha$ -Al
<i>EBCF</i> . . . . .	Si
<i>FCDG</i> . . . . .	$\text{Al}_2\text{Cu}$
<i>BC</i> . . . . .	Eutectic: $\text{Melt} \rightleftharpoons \alpha\text{-Al} + \text{Si}$
<i>DC</i> . . . . .	„ $\text{Melt} \rightleftharpoons \alpha\text{-Al} + \text{Al}_2\text{Cu}$
<i>FC</i> . . . . .	„ $\text{Melt} \rightleftharpoons \text{Si} + \text{Al}_2\text{Cu}$
<i>C</i> . . . . .	Eutectic: $\text{Melt} \rightleftharpoons \alpha\text{-Al} + \text{Si} + \text{Al}_2\text{Cu}$

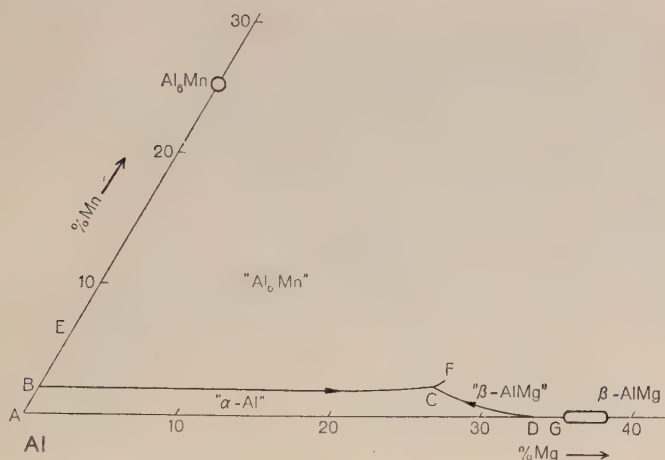
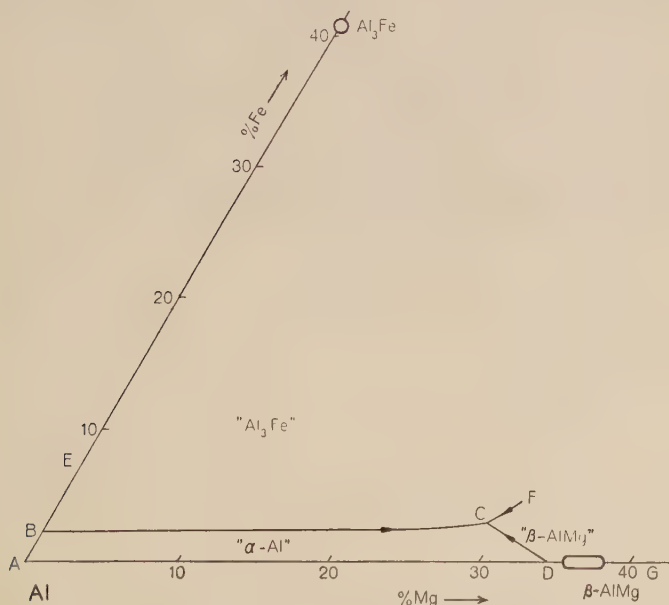
5. *Al-Mg-Mn.*

According to Leemann<sup>51</sup> no phases are present in this system other than those belonging to the subsidiary systems Al-Mg and Al-Mn. Fig. 14 shows Leemann's diagram, and Table VI gives the significance of the regions, lines, and points in this figure.\*

TABLE VI.—*Phases and Reactions in Al-Mg-Mn System.*

Region, Line, or Point	Primary Phase, or Equilibrium Reaction
<i>ABCD</i> . . . . .	$\alpha$ -Al
<i>EBCF</i> . . . . .	$\text{Al}_6\text{Mn}$
<i>FCDG</i> . . . . .	$\beta$ -AlMg
<i>BD</i> . . . . .	Eutectic: $\text{Melt} \rightleftharpoons \alpha\text{-Al} + \text{Al}_6\text{Mn}$
<i>CD</i> . . . . .	„ $\text{Melt} \rightleftharpoons \alpha\text{-Al} + \beta\text{-AlMg}$
<i>CF</i> . . . . .	„ $\text{Melt} \rightleftharpoons \text{Al}_6\text{Mn} + \beta\text{-AlMg}$
<i>C</i> . . . . .	Eutectic: $\text{Melt} \rightleftharpoons \alpha\text{-Al} + \text{Al}_6\text{Mn} + \beta\text{-AlMg}$

\* *Note by Editor:* While the present paper was in course of preparation Wakeman and Raynor<sup>67</sup> published a study of the system Al-Mg-Mn with special reference to ternary-compound formation. They found that equilibrium in solid aluminium-rich alloys involves solid aluminium, the  $\text{Al}_6\text{Mn}$  and  $\beta\text{-AlMg}$  phases, and a ternary compound  $T(\text{MnMg})$  which was previously unknown. From the form of an isothermal diagram based on the results of 204 days' annealing at 400° C. the composition of  $T(\text{MnMg})$  was found to be  $(\text{Mn}, \text{Mg})_3\text{Al}_{10}$ , or nearly  $\text{MnMg}_2\text{Al}_{10}$ . The examination of slowly cooled alloys suggested that  $T(\text{MnMg})$  was formed peritectically from  $\text{MnAl}_6$  and from  $\text{MnAl}_4$ , but the fields of primary separation were not examined in detail.

FIG. 14.—The Al-Mg-Mn System (according to Leemann <sup>51</sup>).FIG. 15.—The Al-Mg-Fe System (according to Barnick and Hanemann <sup>52</sup>).

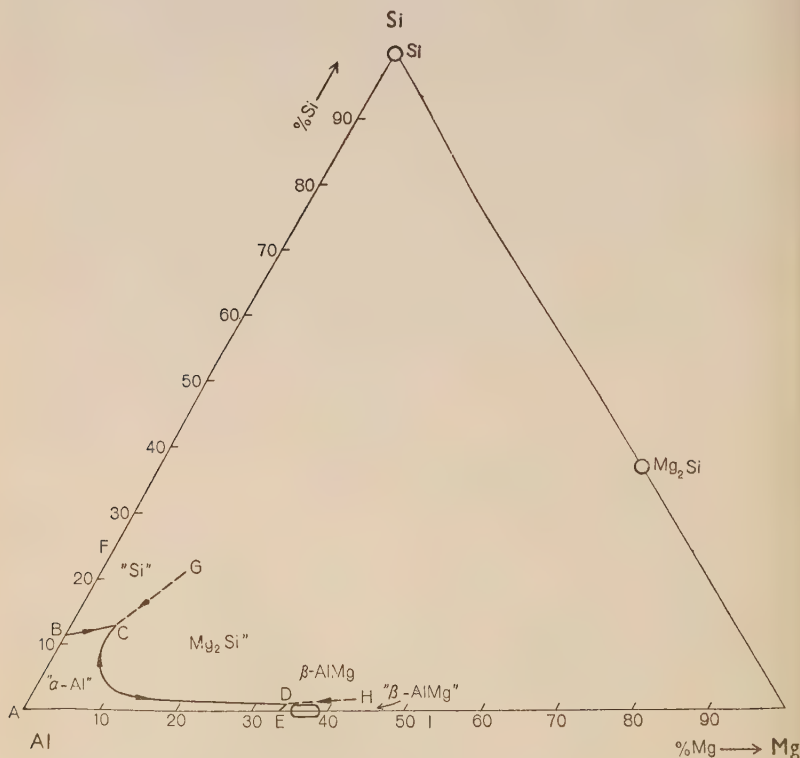
### 6. Al-Mg-Fe.

In this system, which has been investigated by Barnick and Hanemann,<sup>52</sup> no phases occur except those belonging to the subsidiary

systems Al-Mg and Al-Fe. Their diagram is given in Fig. 15. Table VII lists the regions, lines, and points.

TABLE VII.—*Phases and Reactions in Al-Fe-Mg System.*

Region, Line, or Point	Primary Phase, or Equilibrium Reaction
<i>ABCD</i> . . . . .	$\alpha$ -Al
<i>EBCF</i> . . . . .	$\text{Al}_3\text{Fe}$
<i>FCDG</i> . . . . .	$\beta$ -AlMg
<i>BC</i> . . . . .	Eutectic: $\text{Melt} \rightleftharpoons \alpha\text{-Al} + \text{Al}_3\text{Fe}$
<i>CD</i> . . . . .	„ $\text{Melt} \rightleftharpoons \alpha\text{-Al} + \beta\text{-AlMg}$
<i>FC</i> . . . . .	„ $\text{Melt} \rightleftharpoons \text{Al}_3\text{Fe} + \beta\text{-AlMg}$
<i>C</i> . . . . .	Eutectic: $\text{Melt} \rightleftharpoons \alpha\text{-Al} + \text{Al}_3\text{Fe} + \beta\text{-AlMg}$

FIG. 16.—The Al-Mg-Si System (according to Hanson and Gayler <sup>54</sup>).

## 7. Al-Mg-Si.

Aluminium-rich alloys in this system contain  $\text{Mg}_2\text{Si}$  in addition to the phases belonging to the subsidiary systems Al-Mg and Al-Si.

$\text{Mg}_2\text{Si}$ , the composition of which closely corresponds to the simple formula, has a cubic unit cell ( $a_1 = 6.391$  kX.) containing 12 atoms arranged in a lattice of the fluorite type.<sup>53</sup> Crystals of  $\text{Mg}_2\text{Si}$  take the form of octahedra, somewhat blunted by cube faces. The crystals, having cubic symmetry, are not birefringent. The diagram in Fig. 16 is that given by Hanson and Gayler.<sup>54</sup> Table VIII shows the solid phases which separate first within the different regions of the diagram, and the corresponding three- and four-phase equilibria.

TABLE VIII.—Phases and Reactions in Al-Mg-Si System.

Region, Line, or Point	Primary Phase, or Equilibrium Reaction
<i>ABCDE</i> . . . . <i>FBCG</i> . . . . <i>GCDH</i> . . . . <i>HDEI</i> . . . .	$\alpha\text{-Al}$ $\text{Si}$ $\text{Mg}_2\text{Si}$ $\beta\text{-AlMg}$
<i>BC</i> . . . . <i>CD</i> . . . . <i>DE</i> . . . . <i>CG</i> . . . . <i>DH</i> . . . .	Eutectic: $\text{Melt} \rightleftharpoons \alpha\text{-Al} + \text{Si}$ „ $\text{Melt} \rightleftharpoons \alpha\text{-Al} + \text{Mg}_2\text{Si}$ „ $\text{Melt} \rightleftharpoons \alpha\text{-Al} + \beta\text{-AlMg}$ „ $\text{Melt} \rightleftharpoons \text{Si} + \text{Mg}_2\text{Si}$ „ $\text{Melt} \rightleftharpoons \text{Mg}_2\text{Si} + \beta\text{-AlMg}$
<i>C</i> . . . . <i>D</i> . . . .	Eutectic: $\text{Melt} \rightleftharpoons \alpha\text{-Al} + \text{Mg}_2\text{Si} + \text{Si}$ „ $\text{Melt} \rightleftharpoons \alpha\text{-Al} + \text{Mg}_2\text{Si} + \beta\text{-AlMg}$

## 8. Al-Mn-Fe.

This system contains only the phases belonging to the subsidiary systems Al-Mn and Al-Fe.

According to Degischer<sup>55</sup> the homogeneity range of  $\text{Al}_6\text{Mn}$  extends to the composition iron 13 and manganese 14%. From a melt containing manganese 1.5 and iron 2.5% the  $\text{Al}_6\text{Mn}$  phase deposits as a secondary separation, in equilibrium with  $\text{Al}_3\text{Fe}$ . In the present investigation, the lattice spacings of the  $\text{Al}_6\text{Mn}$  phase in an alloy of the above composition were determined as  $a_1 = 7.483$ ,  $a_2 = 6.482$ , and  $a_3 = 8.819$  kX. The values for  $a_1$  and  $a_3$  in particular deviate considerably from the corresponding values for the same phase in the system Al-Mn, which confirms that  $\text{Al}_6\text{Mn}$  dissolves iron. From a melt containing manganese 1.5 and iron 2% the  $\text{Al}_6\text{Mn}$  phase separates primarily. As this composition differs only slightly from that at which the melt is in equilibrium with the phases  $\text{Al}_6\text{Mn}$  and  $\text{Al}_3\text{Fe}$ , the  $\text{Al}_6\text{Mn}$  phase in this alloy can be considered as saturated with iron. Crystals



of  $\text{Al}_6\text{Mn}$  isolated from the alloy contained manganese 12.0 and iron 14.6%, in substantial agreement with Degischer.\* The  $\text{Al}_6\text{Mn}$  phase will therefore be denoted  $\text{Al}_6(\text{Mn},\text{Fe})$  in this system.

X-ray photographs obtained from a powdered specimen of the  $\text{Al}_3\text{Fe}$  phase, isolated from an alloy containing manganese 0.5 and iron 3.5%, were very similar to those of the  $\text{Al}_3\text{Fe}$  phase in the binary system. Certain deviations were, however, evident, indicating that  $\text{Al}_3\text{Fe}$  dissolves some manganese. As, however, the solubility is probably very low, the formula  $\text{Al}_3\text{Fe}$  will be used in preference to  $\text{Al}_3(\text{Fe},\text{Mn})$ .

The liquidus surfaces for the phases mentioned have been investigated by Degischer<sup>55</sup> and by Phillips,<sup>56</sup> who disagree over the position of the boundary between the liquidus surfaces for  $\text{Al}_6(\text{Mn},\text{Fe})$  and  $\text{Al}_3\text{Fe}$ . The results obtained in the present investigation confirm those published by Phillips (CF in Figs. 17 (a) and (b)) rather than those of Degischer (CF). Table IX shows the phases which separate first from the melt within the different regions of the diagram, and the equilibrium reactions for the boundary lines.

TABLE IX.—*Phases and Reactions in Al-Mn-Fe System.*

Region, Line, or Point	Primary Phase, or Equilibrium Reaction
$ABCD$ . . . . $EBCF$ . . . . $FCDG$ . . . .	$\alpha\text{-Al}$ $\text{Al}_6(\text{Mn},\text{Fe})$ $\text{Al}_3\text{Fe}$
$BC$ . . . . $CD$ . . . . $CF$ . . . .	Eutectic: $\text{Melt} \rightleftharpoons \alpha\text{-Al} + \text{Al}_6(\text{Mn},\text{Fe})$ " $\text{Melt} \rightleftharpoons \alpha\text{-Al} + \text{Al}_3\text{Fe}$ { Peritectic: $\text{Melt} + \text{Al}_3\text{Fe} \rightleftharpoons \text{Al}_6(\text{Mn},\text{Fe})$ Eutectic: $\text{Melt} \rightleftharpoons \text{Al}_3\text{Fe} + \text{Al}_6(\text{Mn},\text{Fe})$
$C$ . . . .	Eutectic: $\text{Melt} \rightleftharpoons \alpha\text{-Al} + \text{Al}_3\text{Fe} + \text{Al}_6(\text{Mn},\text{Fe})$

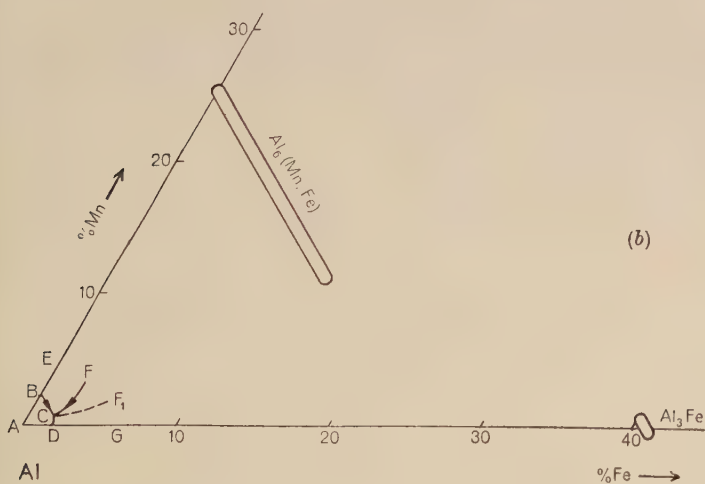
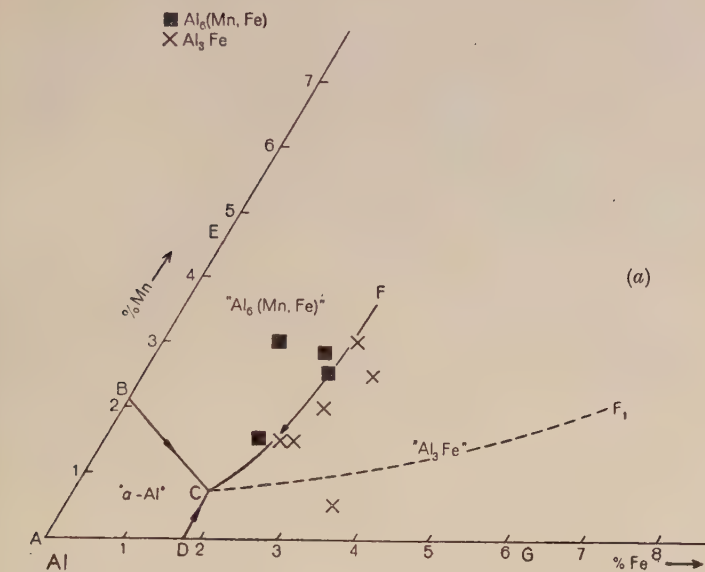
Both a peritectic and eutectic reaction have been given for  $CF$ . The latter may be valid in the immediate neighbourhood of the ternary eutectic  $C$ .

### 9. *Al-Mn-Si.*

In this system the ternary phase  $c\text{-AlMnSi}$  has been found in addition to those belonging to the subsidiary systems  $\text{Al-Mn}$  and  $\text{Al-Si}$ .

$c\text{-AlMnSi}$  corresponds to the phase termed  $\alpha(\text{Mn-Si})$  by Phillips,<sup>56</sup> and  $T$  by Bückle<sup>57</sup>; according to the latter it has a variable composition but contains approximately manganese 40 and silicon 15%. During the present investigation  $c\text{-AlMnSi}$ , isolated from an alloy containing manganese 4 and silicon 4%, was found to contain manganese 26.6 and

\* These results have also been confirmed by Raynor.<sup>42</sup>



FIGS. 17 (a) and (b).—The Al-Mn-Fe System.

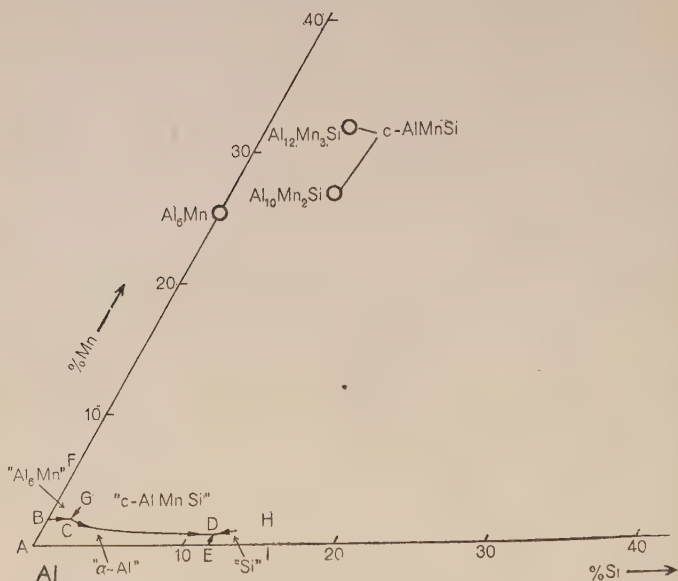
FIG. 18.—The Al-Mn-Si System (liquidus lines according to Phillips <sup>56</sup>).

TABLE X.—Phases and Reactions in Al-Mn-Si System.

Region, Line, or Point	Primary Phase, or Equilibrium Reaction
ABCDE . . . . .	$\alpha$ -Al
FBCG . . . . .	$\text{Al}_6\text{Mn}$
GCDH . . . . .	$c\text{-AlMnSi}$
HDEI . . . . .	Si
BC . . . . .	Eutectic: $\text{Melt} \rightleftharpoons \alpha\text{-Al} + \text{Al}_6\text{Mn}$
CD . . . . .	„ $\text{Melt} \rightleftharpoons \alpha\text{-Al} + c\text{-AlMnSi}$
DE . . . . .	„ $\text{Melt} \rightleftharpoons \alpha\text{-Al} + \text{Si}$
CG . . . . .	Peritectic: $\text{Melt} + \text{Al}_6\text{Mn} \rightleftharpoons c\text{-AlMnSi}$
DH . . . . .	Eutectic: $\text{Melt} \rightleftharpoons c\text{-AlMnSi} + \text{Si}$
C . . . . .	Peritectic: $\text{Melt} + \text{Al}_6\text{Mn} \rightleftharpoons \alpha\text{-Al} + c\text{-AlMnSi}$
D . . . . .	Eutectic: $\text{Melt} \rightleftharpoons \alpha\text{-Al} + c\text{-AlMnSi} + \text{Si}$

silicon 8.0%, corresponding approximately to the formula  $\text{Al}_{10}\text{Mn}_2\text{Si}$ . An X-ray investigation showed that  $c\text{-AlMnSi}$ , isolated from an alloy with manganese 7.5 and silicon 7.0%, is cubic ( $a_1 = 12.625$  kX.). When the possible atomic positions, which have not been determined, are considered, a composition corresponding to the formula  $\text{Al}_{12}\text{Mn}_3\text{Si}$  seems probable; this would necessitate 24.6% manganese and 6% silicon. Crystals of  $c\text{-AlMnSi}$  form light grey cubes which are not birefringent.

Separating as a eutectic with solid aluminium, *c*-AlMnSi forms dendrites which because of their appearance are often called Chinese script.

The investigations of the liquidus surfaces by Bückle<sup>57</sup> and by Phillips<sup>56</sup> agree very well over the positions of the lines along which the melt is in equilibrium with solid aluminium and one other solid phase. Fig. 18 has been based on data taken from Phillips's investigation. Table X shows the solid phases which precipitate first from the melt within the different regions of the diagram, and contains descriptions of the reactions which occur along the lines and at the points in Fig. 18.

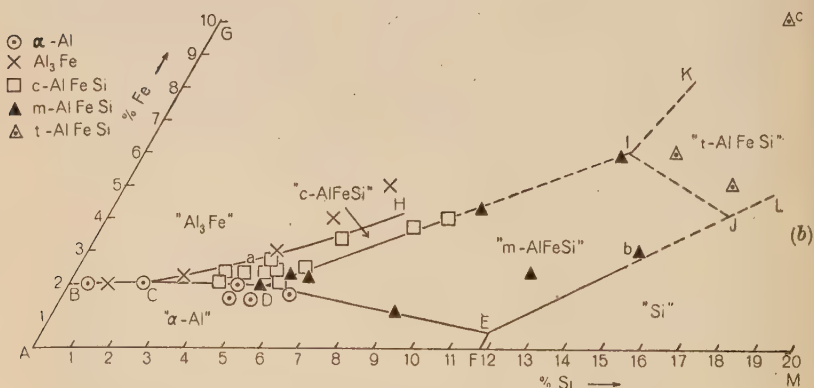
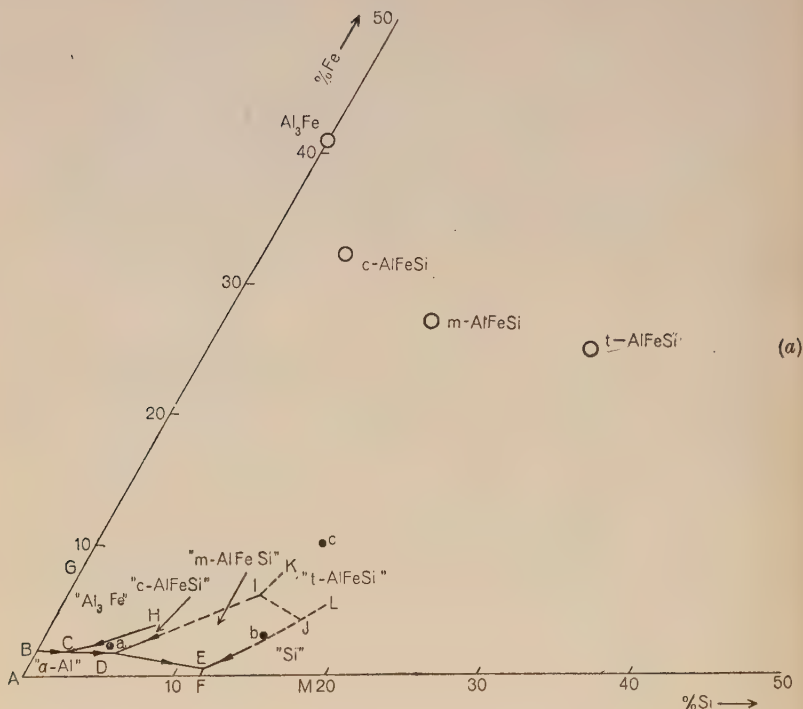
#### 10. Al-Fe-Si.

As well as the phases belonging to the subsidiary systems Al-Fe and Al-Si, two more phases have been found, which may form eutectic complexes with solid aluminium. These two phases will be called *c*-AlFeSi and *m*-AlFeSi. Reference will also be made to another phase, *t*-AlFeSi, since it is often confused with *m*-AlFeSi, although it cannot form a eutectic with solid aluminium.

*c*-AlFeSi corresponds to the phase which Gwyer and Phillips<sup>58</sup> designated  $\beta$ , and Dix and Heath<sup>2</sup> and Phillips and Varley<sup>59</sup>  $\alpha(\text{Fe-Si})$ . According to Dix and Heath this phase contains iron 30 and silicon 8%. In the present investigation *c*-AlFeSi was isolated from an alloy with iron 4 and silicon 5%. X-ray investigation showed cubic symmetry ( $a_1 = 12.523$  kX.). The lattice spacing corresponds closely to that for *c*-AlMnSi, with which *c*-AlFeSi is isomorphous. Analysis of crystals of *c*-AlFeSi isolated from the above alloy gave the composition iron 31.9, silicon 5.57, and aluminium 62.4%. A formula approximating to this composition is  $\text{Al}_{20}\text{Fe}_5\text{Si}_2$ . As, however, *c*-AlFeSi is isomorphous with *c*-AlMnSi, a composition corresponding to  $\text{Al}_{12}\text{Fe}_3\text{Si}$  seems more probable. Crystals of *c*-AlFeSi appear as rhombic dodecahedra, i.e. they have the form {110}. They are light grey in colour and are not birefringent. As a eutectic with solid aluminium, *c*-AlFeSi forms dendrites similar to those of *c*-AlMnSi and generally described as Chinese script.

Fink and Van Horn<sup>61</sup> concluded that *c*-AlFeSi should be a solid solution of silicon in the  $\text{Al}_3\text{Fe}$  phase, because they found that X-ray photographs of *c*-AlFeSi were very similar to those of  $\text{Al}_3\text{Fe}$ . This cannot be correct, however, since the crystal structure is quite different for the two phases.

*m*-AlFeSi corresponds to the phase which Gwyer and Phillips<sup>58</sup> designated *X*, and Dix and Heath<sup>2</sup> and Phillips and Varley<sup>59</sup>  $\beta(\text{Fe-Si})$ . Dix and Heath gave the composition of this phase as iron 27, silicon 15, and aluminium 58%. *m*-AlFeSi was, in the present work, isolated



FIGS. 19 (a) and (b).—The Al-Fe-Si System.



from two alloys (iron 4, silicon 9%, and iron 3, silicon 10%, respectively) which had been cast in insulating-brick moulds. In the first case the isolated phase contained aluminium 58.2, iron 27.4, and silicon 13.6%, and in the second aluminium 59.3, iron 27.2, and silicon 13.5%. In both cases the composition corresponds closely to the formula  $\text{Al}_9\text{Fe}_2\text{Si}_2$ . For X-ray investigation crystals were isolated from an alloy cast in a refractory-brick mould and containing iron 2 and silicon 12%. The lattice was found to be monoclinic with unit-cell dimensions  $a_1 = a_2 = 6.11$ ,  $a_3 = 41.4$  kX. and  $\alpha_2 = 91^\circ$ . The positions of the atoms have not been determined. Crystals of *m*-AlFeSi form pseudo-tetragonal blades in which the dominating faces belong to the {001} group. The crystals form twin lamellæ, the twinning planes belonging to the {001} group. The crystals show birefringence, and the twin lamellæ are therefore distinctly visible in polarized light. In ordinary light the crystals are yellowish grey.

*t*-AlFeSi appears to correspond to the phase which Gwyer and Phillips<sup>58</sup> termed  $\delta$ . Jäniche,<sup>60</sup> who gave the formula  $\text{Al}_4\text{Si}_2\text{Fe}$ , found the lattice to be tetragonal with unit-cell parameters  $a_1 = a_2 = 6.15$  and  $a_3 = 9.47$  kX. From an alloy cast in a refractory-brick mould and containing iron 15 and silicon 20%, crystals of *t*-AlFeSi were isolated.\* Jäniche's results were confirmed, and the following parameters were determined for the tetragonal lattice:  $a_1 = a_2 = 6.11$ ,  $a_3 = 9.46$  kX. The crystals form tetragonal plates with faces belonging to the {001} and {110} groups; they have an appearance similar to the crystals of *m*-AlFeSi, but the plates are thicker. The crystals show birefringence, and therefore exhibit changing colours in polarized light. In ordinary light they are pale grey.

The liquidus surfaces were investigated by Gwyer and Phillips,<sup>58</sup> and later re-examined by Phillips and Varley<sup>59</sup> within the range iron 0.6 and silicon 0–12%. In both cases the conditions studied correspond to a cooling rate of about 8° C./min. The results of the present work, which are summarized in Figs. 19 (a) and (b), are in good agreement with the two investigations mentioned. Table XI shows the phases which separate first from the melt within the different regions of the diagram, and also the liquidus lines and non-variant points.

Fig. 20 (Plate LXI) is a photomicrograph of an alloy containing iron 2.3 and silicon 4.6% (point *a* in Fig. 19). *c*-AlFeSi is the first solid phase to separate on freezing, and later, when the composition of the melt has reached the line *CD*, a eutectic of this phase and solid aluminium is formed. In Fig. 20 a primary crystal of *c*-AlFeSi is seen surrounded by a eutectic of this phase and solid aluminium.

\* Jäniche isolated this phase from an alloy of the same composition.

TABLE XI.—*Phases and Reactions in Al-Fe-Si System.*

Region, Line, or Point	Primary Phase, or Equilibrium Reaction
<i>ABCDEF</i> . . . .	$\alpha$ -Al
<i>GBCH</i> . . . .	$\text{Al}_3\text{Fe}$
<i>HCDI</i> . . . .	$c\text{-AlFeSi}$
<i>IDEJ</i> . . . .	$m\text{-AlFeSi}$
<i>KIJL</i> . . . .	$t\text{-AlFeSi}$
<i>LJEFM</i> . . . .	Si
<i>BC</i> . . . .	Eutectic: $\text{Melt} \rightleftharpoons \alpha\text{-Al} + \text{Al}_3\text{Fe}$
<i>CD</i> . . . .	„ $\text{Melt} \rightleftharpoons \alpha\text{-Al} + c\text{-AlFeSi}$
<i>DE</i> . . . .	„ $\text{Melt} \rightleftharpoons \alpha\text{-Al} + m\text{-AlFeSi}$
<i>EF</i> . . . .	„ $\text{Melt} \rightleftharpoons \alpha\text{-Al} + \text{Si}$
<i>HC</i> . . . .	Peritectic: $\text{Melt} + \text{Al}_3\text{Fe} \rightleftharpoons c\text{-AlFeSi}$
<i>ID</i> . . . .	„ $\text{Melt} + c\text{-AlFeSi} \rightleftharpoons m\text{-AlFeSi}$
<i>IJ</i> . . . .	„ $\text{Melt} + t\text{-AlFeSi} \rightleftharpoons m\text{-AlFeSi}$
<i>JE</i> . . . .	Eutectic: $\text{Melt} \rightleftharpoons m\text{-AlFeSi} + \text{Si}$
<i>LJ</i> . . . .	„ $\text{Melt} \rightleftharpoons t\text{-AlFeSi} + \text{Si}$
<i>C</i> . . . .	Peritectic: $\text{Melt} + \text{Al}_3\text{Fe} \rightleftharpoons \alpha\text{-Al} + c\text{-AlFeSi}$
<i>D</i> . . . .	„ $\text{Melt} + c\text{-AlFeSi} \rightleftharpoons \alpha\text{-Al} + m\text{-AlFeSi}$
<i>E</i> . . . .	Eutectic: $\text{Melt} \rightleftharpoons \alpha\text{-Al} + m\text{-AlFeSi} + \text{Si}$
<i>J</i> . . . .	Peritectic: $\text{Melt} + t\text{-AlFeSi} \rightleftharpoons m\text{-AlFeSi} + \text{Si}$

Fig. 21 (Plate LXI) is a photomicrograph of an alloy containing iron 3.0 and silicon 14.5% (point *b* in Fig. 19). Such an alloy solidifies as follows:  $m\text{-AlFeSi}$  first separates from the melt and later, when the composition of the melt has reached the line *JE*, solid silicon also separates. During the latter separation, *JE* is followed towards *E*. At point *E*, solid aluminium also separates, in addition to  $m\text{-AlFeSi}$  and solid silicon, until the alloy is solid.

In Figs. 22 and 23 (Plate LXII) photomicrographs are shown of an alloy containing iron 10 and silicon 15% (point *c* in Fig. 19). The order of solidification for such an alloy is probably as follows. First  $t\text{-AlFeSi}$  separates until the line *IJ* is attained, when this phase reacts peritectically with the melt. During this reaction  $m\text{-AlFeSi}$  is formed, which envelops  $t\text{-AlFeSi}$  and thereby terminates the peritectic reaction.  $m\text{-AlFeSi}$  then separates from the remaining melt. The subsequent course of the solidification process is the same as that already described in connection with Fig. 21.

#### V.—QUATERNARY SYSTEMS.

In order to describe graphically systems with four components, projections of the kind described on pp. 492 and 493 have been used. In these diagrams, liquid in equilibrium with solid aluminium and three other phases is represented by a point, liquid in equilibrium with solid

aluminium and two other solid phases by a line, and liquid in equilibrium with solid aluminium and one other solid phase by a two-dimensional region. The relative contents of the alloying elements form the co-ordinates in these diagrams. The relative amounts of alloying constituents in the melt, as well as in the solid phases which are in equilibrium with the melt and with solid aluminium, are shown. The discussion will, however, in general be limited to the conditions in the melt.

Points drawn in these diagrams mark the composition of the alloys investigated and of the phases which appear to be primary or (when solid aluminium precipitates first) secondary. At every such point the number specifies the total aluminium content of the alloy. If the alloy phase appears to be primary a bar is placed below this number; if the aluminium phase appears to separate out first and the solid alloy phase second, the bar is placed above the number. The points along the sides of the triangular diagrams indicate the relative contents at which the melt is in equilibrium with solid aluminium and one or several other solid phases for total aluminium contents of 95, 90, 85%, &c. This enables some idea to be obtained of the position of the surfaces which, in the polythermal tetrahedral diagram, correspond to melt in equilibrium with solid aluminium and one other solid phase. It is also possible in most cases to judge how close to these surfaces the alloys investigated have been.

Equilibria between melt, solid aluminium, and one other phase have been found to be eutectic in all the quaternary systems investigated.

### 1. *Al-Cu-Mg-Mn.*

In this system only one unstable phase has been found in addition to the phases belonging to the subsidiary ternary systems. This phase is designated  $\alpha$ -AlCuMgMn; it is light grey and does not show birefringence.

The results obtained in this investigation for the system Al-Cu-Mg-Mn are summarized in Fig. 28, which consists of 6 different regions. Within each of these regions solid aluminium and one other phase separate eutectically from the melt. Table XII shows the reactions involved in the regions (melt + two solids), along the boundary lines (melt + three solids), and at the points (melt + four solids) of Fig. 28.

Fig. 24 (Plate LXIII) is a photomicrograph of an alloy containing copper 11.7, magnesium 3.0, and manganese 1.0%, or, in relative contents, copper 73, magnesium 20, and manganese 7% (point *a* in Fig. 28). On solidification aluminium appears first. The following order of solidification seems probable. The primary separation of solid aluminium is followed by the separation of a eutectic complex of

$\alpha$ -Al +  $r$ -AlCuMn, and later, when the point representing the relative contents of alloying constituents has reached the line  $ML$ ,  $Al_2CuMg$  also separates.  $ML$  is now followed towards  $M$ . At point  $M$ , solid aluminium,  $r$ -AlCuMn,  $Al_2CuMg$ , and  $Al_2Cu$  separate, until the alloy is solid. In Fig. 24 a eutectic of solid aluminium and the unstable

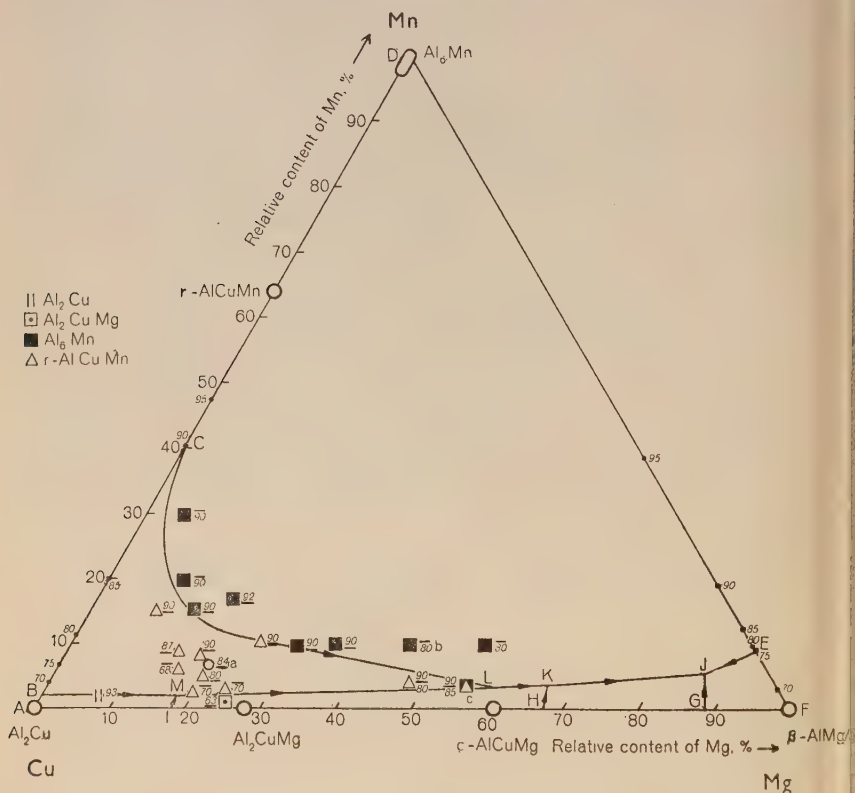


FIG. 28.—The Al-Cu-Mg-Mn System. The point  $c$  represents two alloys, one containing 85% aluminium, in which  $Al_6Mn$  is primary, and the other containing 90% aluminium, in which  $r$ -AlCuMn is secondary.

$z$ -AlCuMgMn phase is seen between the rounded aluminium dendrites. By heating at  $490^\circ C.$  for 80 hr., however,  $z$ -AlCuMgMn is decomposed. After this treatment a eutectic similar to that shown in Fig. 24 attains the appearance seen in Fig. 25 (Plate LXIII). Between the dendrites of solid aluminium an aggregate is seen, consisting of almost unetched  $Al_2Cu$  and dark particles, which are probably mainly  $Al_2CuMg$ . It is not possible to discern whether the dark particles also contain  $r$ -AlCuMn.

TABLE XII.—*Equilibrium Reactions in Al-Cu-Mg-Mn System.*

Region, Line, or Point	Equilibrium Reaction
<i>ABMI</i> . .	Eutectic: $\text{Melt} \rightleftharpoons \alpha\text{-Al} + \text{Al}_2\text{Cu}$
<i>IMLKH</i> . .	„ $\text{Melt} \rightleftharpoons \alpha\text{-Al} + \text{Al}_2\text{CuMg}$
<i>HKJG</i> . .	„ $\text{Melt} \rightleftharpoons \alpha\text{-Al} + c\text{-AlCuMg}$
<i>GJEF</i> . .	„ $\text{Melt} \rightleftharpoons \alpha\text{-Al} + \beta\text{-AlMg}$
<i>BCLM</i> . .	„ $\text{Melt} \rightleftharpoons \alpha\text{-Al} + r\text{-AlCuMn}$
<i>CDEJKL</i> . .	„ $\text{Melt} \rightleftharpoons \alpha\text{-Al} + \text{Al}_6\text{Mn}$
<i>BM</i> . .	Eutectic: $\text{Melt} \rightleftharpoons \alpha\text{-Al} + \text{Al}_2\text{Cu} + r\text{-AlCuMn}$
<i>IM</i> . .	„ $\text{Melt} \rightleftharpoons \alpha\text{-Al} + \text{Al}_2\text{Cu} + \text{Al}_2\text{CuMg}$
<i>ML</i> . .	„ $\text{Melt} \rightleftharpoons \alpha\text{-Al} + \text{Al}_2\text{CuMg} + r\text{-AlCuMn}$
<i>LK</i> . .	„ $\text{Melt} \rightleftharpoons \alpha\text{-Al} + \text{Al}_2\text{CuMg} + \text{Al}_6\text{Mn}$
<i>HK</i> . .	Peritectic: $\text{Melt} + \text{Al}_2\text{CuMg} \rightleftharpoons \alpha\text{-Al} + c\text{-AlCuMg}$
<i>KJ</i> . .	Eutectic: $\text{Melt} \rightleftharpoons \alpha\text{-Al} + c\text{-AlCuMg} + \text{Al}_6\text{Mn}$
<i>GJ</i> . .	„ $\text{Melt} \rightleftharpoons \alpha\text{-Al} + c\text{-AlCuMg} + \beta\text{-AlMg}$
<i>EJ</i> . .	„ $\text{Melt} \rightleftharpoons \alpha\text{-Al} + \beta\text{-AlMg} + \text{Al}_6\text{Mn}$
<i>CL</i> . .	Peritectic: $\text{Melt} + \text{Al}_6\text{Mn} \rightleftharpoons \alpha\text{-Al} + r\text{-AlCuMn}$
<i>M</i> . .	Eutectic: $\text{Melt} \rightleftharpoons \alpha\text{-Al} + \text{Al}_2\text{Cu} + r\text{-AlCuMn} + \text{Al}_2\text{CuMg}$
<i>L</i> . .	Peritectic: $\text{Melt} + r\text{-AlCuMn} \rightleftharpoons \alpha\text{-Al} + \text{Al}_2\text{CuMg} + \text{Al}_6\text{Mn}$
<i>K</i> . .	„ $\text{Melt} + \text{Al}_2\text{CuMg} \rightleftharpoons \alpha\text{-Al} + c\text{-AlCuMg} + \text{Al}_6\text{Mn}$
<i>J</i> . .	Eutectic: $\text{Melt} \rightleftharpoons \alpha\text{-Al} + c\text{-AlCuMg} + \beta\text{-AlMg} + \text{Al}_6\text{Mn}$

TABLE XIII.—*Equilibrium Reactions in Al-Cu-Mg-Fe System.*

Region, Line, or Point	Equilibrium Reaction
<i>ABKJ</i> . .	Eutectic: $\text{Melt} \rightleftharpoons \alpha\text{-Al} + \text{Al}_2\text{Cu}$
<i>JKLMI</i> . .	„ $\text{Melt} \rightleftharpoons \alpha\text{-Al} + \text{Al}_2\text{CuMg}$
<i>BCLK</i> . .	„ $\text{Melt} \rightleftharpoons \alpha\text{-Al} + \text{Al}_7\text{Cu}_2\text{Fe}$
<i>CDNML</i> . .	„ $\text{Melt} \rightleftharpoons \alpha\text{-Al} + (\text{Al,Cu})_6(\text{Fe,Cu})$
<i>IMNOH</i> . .	„ $\text{Melt} \rightleftharpoons \alpha\text{-Al} + c\text{-AlCuMg}$
<i>HOFG</i> . .	„ $\text{Melt} \rightleftharpoons \alpha\text{-Al} + \beta\text{-AlMg}$
<i>DEFON</i> . .	„ $\text{Melt} \rightleftharpoons \alpha\text{-Al} + \text{Al}_3\text{Fe}$
<i>BK</i> . .	Eutectic: $\text{Melt} \rightleftharpoons \alpha\text{-Al} + \text{Al}_2\text{Cu} + \text{Al}_7\text{Cu}_2\text{Fe}$
<i>JK</i> . .	„ $\text{Melt} \rightleftharpoons \alpha\text{-Al} + \text{Al}_2\text{Cu} + \text{Al}_2\text{CuMg}$
<i>CL</i> . .	Peritectic: $\text{Melt} + (\text{Al,Cu})_6(\text{Fe,Cu}) \rightleftharpoons \alpha\text{-Al} + \text{Al}_7\text{Cu}_2\text{Fe}$
<i>KL</i> . .	Eutectic: $\text{Melt} \rightleftharpoons \alpha\text{-Al} + \text{Al}_2\text{CuMg} + \text{Al}_7\text{Cu}_2\text{Fe}$
<i>LM</i> . .	„ $\text{Melt} \rightleftharpoons \alpha\text{-Al} + \text{Al}_2\text{CuMg} + (\text{Al,Cu})_6(\text{Fe,Cu})$
<i>IM</i> . .	Peritectic: $\text{Melt} + \text{Al}_2\text{CuMg} \rightleftharpoons \alpha\text{-Al} + c\text{-AlCuMg}$
<i>MN</i> . .	Eutectic: $\text{Melt} \rightleftharpoons \alpha\text{-Al} + (\text{Al,Cu})_6(\text{Fe,Cu}) + c\text{-AlCuMg}$
<i>DN</i> . .	Peritectic: $\text{Melt} + \text{Al}_3\text{Fe} \rightleftharpoons \alpha\text{-Al} + (\text{Al,Cu})_6(\text{Fe,Cu})$
<i>NO</i> . .	Eutectic: $\text{Melt} \rightleftharpoons \alpha\text{-Al} + c\text{-AlCuMg} + \text{Al}_3\text{Fe}$
<i>HO</i> . .	„ $\text{Melt} \rightleftharpoons \alpha\text{-Al} + \beta\text{-AlMg} + c\text{-AlCuMg}$
<i>FO</i> . .	„ $\text{Melt} \rightleftharpoons \alpha\text{-Al} + \beta\text{-AlMg} + \text{Al}_3\text{Fe}$
<i>K</i> . .	Eutectic: $\text{Melt} \rightleftharpoons \alpha\text{-Al} + \text{Al}_2\text{Cu} + \text{Al}_2\text{CuMg} + \text{Al}_7\text{Cu}_2\text{Fe}$
<i>L</i> . .	Peritectic: $\text{Melt} + \text{Al}_7\text{Cu}_2\text{Fe} \rightleftharpoons \alpha\text{-Al} + \text{Al}_2\text{CuMg} + (\text{Al,Cu})_6(\text{Fe,Cu})$
<i>M</i> . .	„ $\text{Melt} + \text{Al}_2\text{CuMg} \rightleftharpoons \alpha\text{-Al} + (\text{Al,Cu})_6(\text{Fe,Cu}) + c\text{-AlCuMg}$
<i>N</i> . .	„ $\text{Melt} + (\text{Al,Cu})_6(\text{Fe,Cu}) \rightleftharpoons \alpha\text{-Al} + c\text{-AlCuMg} + \text{Al}_3\text{Fe}$
<i>O</i> . .	Eutectic: $\text{Melt} \rightleftharpoons \alpha\text{-Al} + c\text{-AlCuMg} + \beta\text{-AlMg} + \text{Al}_3\text{Fe}$



Fig. 26 (Plate LXIV) is a photomicrograph of an alloy containing copper 9, magnesium 9, and manganese 2%, or, in relative contents, copper 45, magnesium 45, and manganese 10% (point *b* in Fig. 28).

## 2. Al-Cu-Mg-Fe.

No phases have been found in this system other than those belonging to the subsidiary systems Al-Cu-Mg, Al-Cu-Fe, and Al-Fe-Mg.

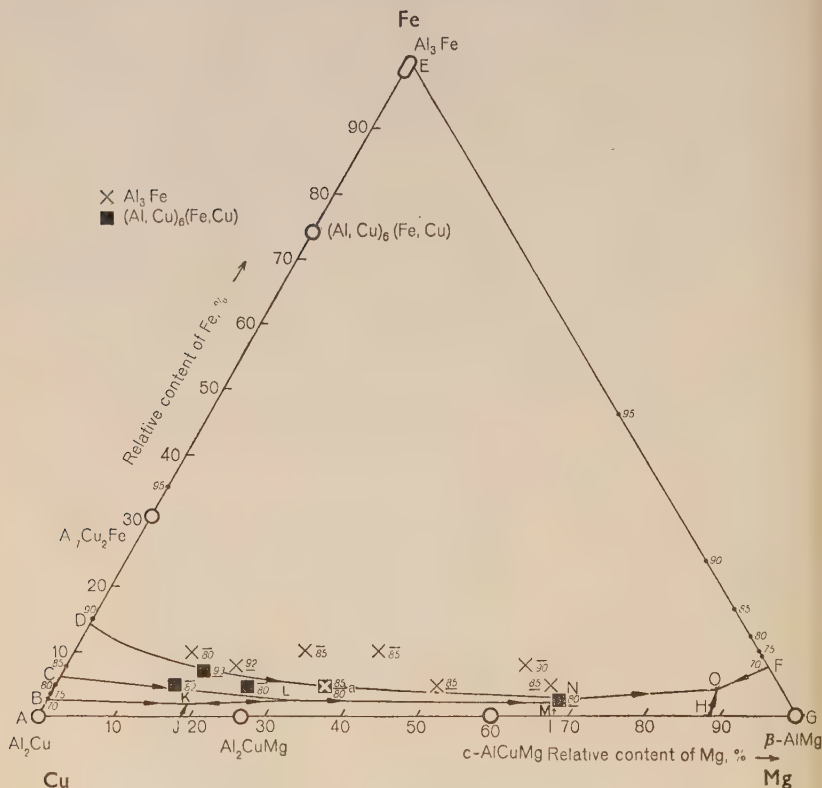


Fig. 29.—The Al-Cu-Mg-Fe System. The point *a* represents two alloys, one containing 80% aluminium, in which  $\text{Al}_3\text{Fe}$  is primary, and the other containing 85% aluminium, in which  $(\text{Al,Cu})_6(\text{Fe,Cu})$  is secondary.

The results obtained in the present investigation are shown in Fig. 29. Table XIII lists the equilibria corresponding to the regions, lines, and points of Fig. 29.

Figs. 34 and 35 (Plate LXV) are photomicrographs of an alloy containing copper 12, magnesium 7, and iron 1%, or, in relative contents,

copper 60, magnesium 35, and iron 5% (point *a* in Fig. 29). During the solidification of this alloy,  $(\text{Al,Cu})_6(\text{Fe,Cu})$  and  $\text{Al}_3\text{Fe}$  probably separate from the melt before solid aluminium.

### 3. Al-Cu-Mg-Si.

One phase has been found in this system besides those belonging to the subsidiary ternary systems. This phase is termed *h*-AlCuMgSi,



FIG. 30.—The Al-Cu-Mg-Si System.

and corresponds to the phase which Dix, Sager, and Sager<sup>62</sup> have called AlCuMgSi and which Petrov<sup>63</sup> named  $\text{Al}_x\text{Cu}_4\text{Mg}_5\text{Si}_4$ . In the present work, crystals of this phase were isolated from an alloy containing copper 13.8, magnesium 24.8, and silicon 22.2%, or, in relative contents, copper 23, magnesium 40, and silicon 37%. Analysis of these crystals gave the composition aluminium 19.9, copper 20.6, magnesium 31.8,

and silicon 31.4%, in fairly close agreement with the formula  $\text{Al}_5\text{Cu}_2\text{Mg}_8\text{Si}_6$  (aluminium 21.6, copper 20.3, magnesium 31.1, silicon 27.0%). X-ray investigation shows that  $h\text{-AlCuMgSi}$  has a hexagonal structure; the unit-cell dimensions are  $a_1 = a_2 = 10.30$  kX. and  $a_3 = 4.04$  kX. The crystals form hexagonal needles which are grey in ordinary light and show intense polarization colours.

The results of the present work are indicated in Fig. 30. Table XIV shows the reactions associated with the different regions, lines, and points of the diagram.

TABLE XIV.—*Equilibrium Reactions in Al-Cu-Mg-Si System.*

Region, Line, or Point	Equilibrium Reaction
<i>ABLKJI</i> . . .	Eutectic: Melt $\rightleftharpoons \alpha\text{-Al} + \text{Al}_2\text{Cu}$
<i>IJNH</i> . . .	" Melt $\rightleftharpoons \alpha\text{-Al} + \text{Al}_2\text{CuMg}$
<i>HNOG</i> . . .	" Melt $\rightleftharpoons \alpha\text{-Al} + c\text{-AlCuMg}$
<i>GOEF</i> . . .	" Melt $\rightleftharpoons \alpha\text{-Al} + \beta\text{-AlMg}$
<i>JKMDEON</i> . . .	" Melt $\rightleftharpoons \alpha\text{-Al} + \text{Mg}_2\text{Si}$
<i>KLM</i> . . .	" Melt $\rightleftharpoons \alpha\text{-Al} + h\text{-AlCuMgSi}$
<i>BCDML</i> . . .	" Melt $\rightleftharpoons \alpha\text{-Al} + \text{Si}$
<i>BL</i> . . .	Eutectic: Melt $\rightleftharpoons \alpha\text{-Al} + \text{Al}_2\text{Cu} + \text{Si}$
<i>LK</i> . . .	" Melt $\rightleftharpoons \alpha\text{-Al} + \text{Al}_2\text{Cu} + h\text{-AlCuMgSi}$
<i>KJ</i> . . .	" Melt $\rightleftharpoons \alpha\text{-Al} + \text{Al}_2\text{Cu} + \text{Mg}_2\text{Si}$
<i>JI</i> . . .	" Melt $\rightleftharpoons \alpha\text{-Al} + \text{Al}_2\text{Cu} + \text{Al}_2\text{CuMg}$
<i>JN</i> . . .	" Melt $\rightleftharpoons \alpha\text{-Al} + \text{Al}_2\text{CuMg} + \text{Mg}_2\text{Si}$
<i>HN</i> . . .	Peritectic: Melt + $\text{Al}_2\text{CuMg} \rightleftharpoons \alpha\text{-Al} + c\text{-AlCuMg}$
<i>NO</i> . . .	Eutectic: Melt $\rightleftharpoons \alpha\text{-Al} + c\text{-AlCuMg} + \text{Mg}_2\text{Si}$
<i>GO</i> . . .	" Melt $\rightleftharpoons \alpha\text{-Al} + c\text{-AlCuMg} + \beta\text{-AlMg}$
<i>EO</i> . . .	" Melt $\rightleftharpoons \alpha\text{-Al} + \beta\text{-AlMg} + \text{Mg}_2\text{Si}$
<i>KM</i> . . .	Peritectic: Melt + $\text{Mg}_2\text{Si} \rightleftharpoons \alpha\text{-Al} + h\text{-AlCuMgSi}$
<i>LM</i> . . .	Eutectic: Melt $\rightleftharpoons \alpha\text{-Al} + \text{Si} + h\text{-AlCuMgSi}$
<i>MD</i> . . .	" Melt $\rightleftharpoons \alpha\text{-Al} + \text{Si} + \text{Mg}_2\text{Si}$
<i>J</i> . . .	Eutectic: Melt $\rightleftharpoons \alpha\text{-Al} + \text{Al}_2\text{Cu} + \text{Al}_2\text{CuMg} + \text{Mg}_2\text{Si}$
<i>K</i> . . .	Peritectic: Melt + $\text{Mg}_2\text{Si} \rightleftharpoons \alpha\text{-Al} + \text{Al}_2\text{Cu} + h\text{-AlCuMgSi}$
<i>L</i> . . .	Eutectic: Melt $\rightleftharpoons \alpha\text{-Al} + \text{Al}_2\text{Cu} + h\text{-AlCuMgSi} + \text{Si}$
<i>M</i> . . .	Peritectic: Melt + $\text{Mg}_2\text{Si} + \text{Si} \rightleftharpoons \alpha\text{-Al} + h\text{-AlCuMgSi}$
<i>N</i> . . .	" Melt + $\text{Al}_2\text{CuMg} \rightleftharpoons \alpha\text{-Al} + c\text{-AlCuMg} + \text{Mg}_2\text{Si}$
<i>O</i> . . .	Eutectic: Melt $\rightleftharpoons \alpha\text{-Al} + c\text{-AlCuMg} + \beta\text{-AlMg} + \text{Mg}_2\text{Si}$

Fig. 36 (Plate LXVI) is a photomicrograph of an alloy containing copper 14, magnesium 2, and silicon 4% (point *a* in Fig. 30). On solidification aluminium separates first, the subsequent order being probably as follows. As the point *a* is situated within the region *KLM*,  $h\text{-AlCuMgSi}$  separates secondarily as a eutectic with aluminium. The point representing the relative alloy contents in the melt moves, during this separation, towards the line *LK*. When this line is reached,  $\text{Al}_2\text{Cu}$  separates together with aluminium and  $h\text{-AlCuMgSi}$ . *LK* is now

followed towards point *L*, where a eutectic of aluminium, *h*-AlCuMgSi, Al<sub>2</sub>Cu, and silicon precipitates until the alloy has completely solidified.

#### 4. Al-Cu-Mn-Fe.

The only phases found are those belonging to the subsidiary ternary systems.

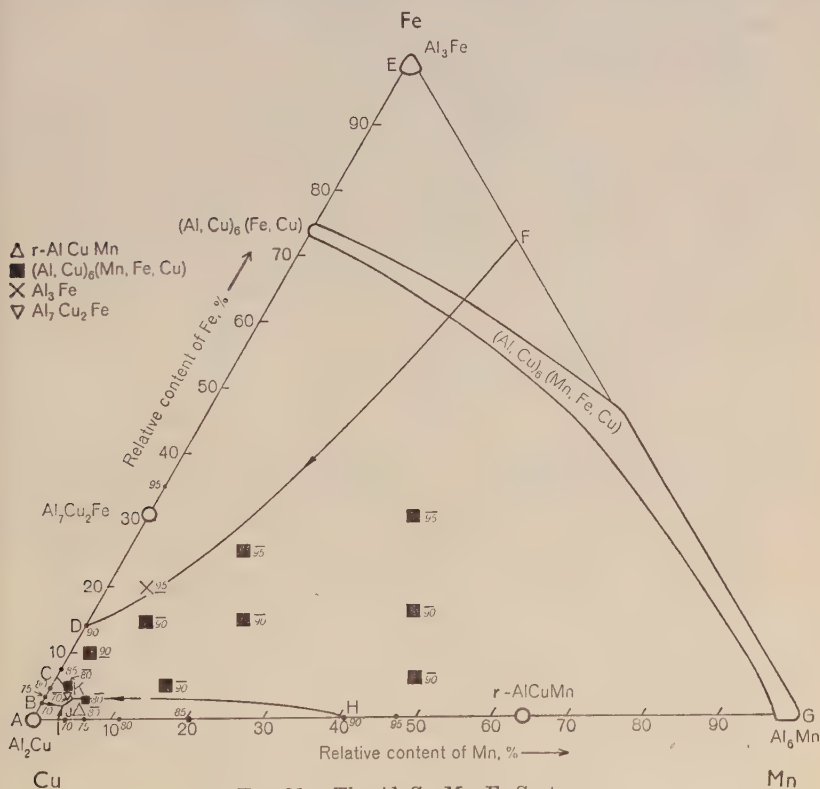


FIG. 31.—The Al-Cu-Mn-Fe System.

From an alloy which contained copper 7.75, manganese 0.75, and iron 1.5%, crystals were isolated and investigated by X-rays. They were orthorhombic, with lattice spacings  $a_1 = 7.473$ ,  $a_2 = 6.452$ , and  $a_3 = 8.794$  kX. These values are in fair agreement with the corresponding data for Al<sub>6</sub>(Mn,Fe) and (Al,Cu)<sub>6</sub>(Fe,Cu), although deviations are evident. The composition of these crystals by analysis was copper 1.9, manganese 8.5, and iron 18.7% (in relative contents copper 7, manganese 29, and iron 64%). The phases Al<sub>6</sub>(Mn,Fe) and

(Al,Cu)<sub>6</sub>(Fe,Cu) thus belong to the same homogeneity range and are the same phase. This phase will be designated (Al,Cu)<sub>6</sub>(Mn,Fe,Cu).

The results obtained are collected in Fig. 31. Table XV shows the relevant polyphase equilibria.

TABLE XV.—*Equilibrium Reactions in Al-Cu-Mn-Fe System.*

Region, Line, or Point	Equilibrium Reaction
<i>ABJI</i> .	Eutectic: Melt $\rightleftharpoons$ $\alpha$ -Al + Al <sub>2</sub> Cu
<i>IJKH</i> .	„ Melt $\rightleftharpoons$ $\alpha$ -Al + <i>r</i> -AlCuMn
<i>BJKC</i> .	„ Melt $\rightleftharpoons$ $\alpha$ -Al + Al <sub>7</sub> Cu <sub>2</sub> Fe
<i>CDFGHK</i> .	„ Melt $\rightleftharpoons$ $\alpha$ -Al + (Al,Cu) <sub>6</sub> (Mn,Fe,Cu)
<i>DEF</i> .	„ Melt $\rightleftharpoons$ $\alpha$ -Al + Al <sub>3</sub> Fe
<i>BJ</i> . .	Eutectic: Melt $\rightleftharpoons$ $\alpha$ -Al + Al <sub>2</sub> Cu + Al <sub>7</sub> Cu <sub>2</sub> Fe
<i>IJ</i> . .	„ Melt $\rightleftharpoons$ $\alpha$ -Al + Al <sub>2</sub> Cu + <i>r</i> -AlCuMn
<i>KJ</i> . .	„ Melt $\rightleftharpoons$ $\alpha$ -Al + Al <sub>7</sub> Cu <sub>2</sub> Fe + <i>r</i> -AlCuMn
<i>CK</i> . .	Peritectic: Melt + (Al,Cu) <sub>6</sub> (Mn,Fe,Cu) $\rightleftharpoons$ $\alpha$ -Al + Al <sub>7</sub> Cu <sub>2</sub> Fe
<i>HK</i> . .	„ Melt + (Al,Cu) <sub>6</sub> (Mn,Fe,Cu) $\rightleftharpoons$ $\alpha$ -Al + <i>r</i> -AlCuMn
<i>DF</i> * .	{ Eutectic: Melt $\rightleftharpoons$ $\alpha$ -Al + Al <sub>3</sub> Fe + (Al,Cu) <sub>6</sub> (Mn,Fe,Cu) Peritectic: Melt + Al <sub>3</sub> Fe $\rightleftharpoons$ $\alpha$ -Al + (Al,Cu) <sub>6</sub> (Mn,Fe,Cu)
<i>J</i> . .	Eutectic: Melt $\rightleftharpoons$ $\alpha$ -Al + Al <sub>2</sub> Cu + Al <sub>7</sub> Cu <sub>2</sub> Fe + <i>r</i> -AlCuMn
<i>K</i> . .	Peritectic: Melt + (Al,Cu) <sub>6</sub> (Mn,Fe,Cu) $\rightleftharpoons$ $\alpha$ -Al + Al <sub>7</sub> Cu <sub>2</sub> Fe + <i>r</i> -AlCuMn

\* For the line *DF* two reactions have been given, since the equilibrium reaction along this line in the direction from *F* to *D* changes from eutectic to peritectic.

### 5. *Al-Cu-Mn-Si.*

Only the phases belonging to the subsidiary ternary systems have been found.

The etching reactions indicate that the phase which, in the subsidiary system Al-Mn-Si, has been called *c*-AlMnSi dissolves copper. Although the phase might thus be designated *c*-Al(Mn,Cu)Si in this system, it will be written *c*-AlMnSi, as the copper content is probably very low.

The results obtained are shown in Fig. 32. Table XVI gives the phases which may separate eutectically, together with solid aluminium, within the different regions in the diagram, and contains the equilibria corresponding to the boundaries and points in Fig. 32. As it has not been possible to decide whether the reaction for the line *JK* is eutectic or peritectic, or both, the two alternatives are given in the Table.

Fig. 27 (Plate LXIV) is a photomicrograph of an alloy containing copper 26.25, manganese 1.50, and silicon 2.25% (point *a* in Fig. 32), which was allowed to cool in the furnace. On solidification, the first phase to separate is *c*-AlMnSi and the second is aluminium. As soon as aluminium starts to separate, the system can be considered to



be in equilibrium with this phase and with the melt. The following order of solidification may be deduced from the diagram. During the separation of *c*-AlMnSi (primary, as well as in a eutectic with solid aluminium) the point representing the relative contents of alloying elements in the melt moves towards the line *JI*. When this line is reached,  $\text{Al}_2\text{Cu}$  separates together with *c*-AlMnSi and aluminium. In

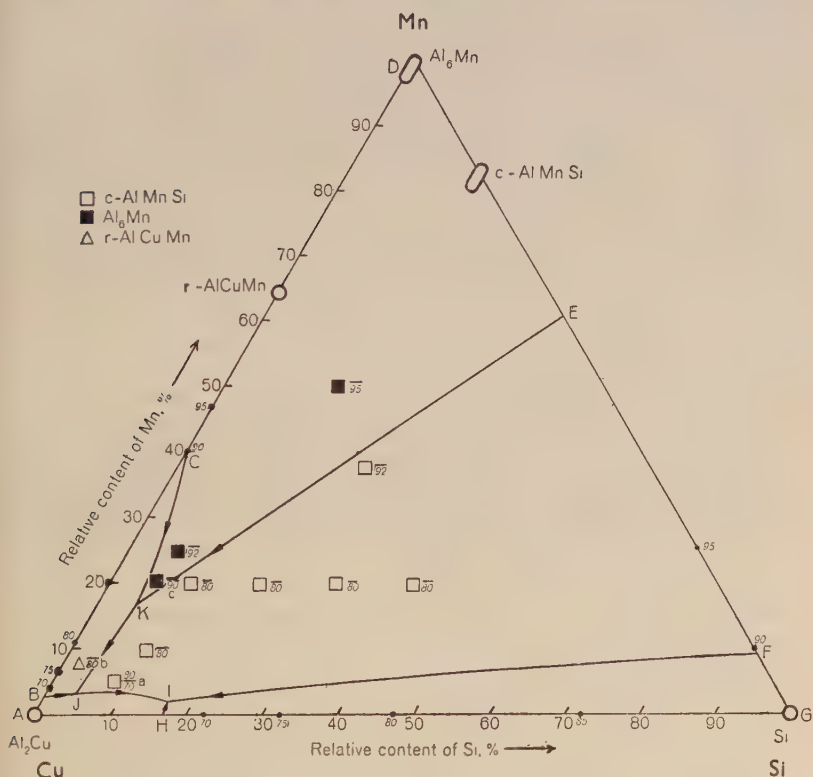


FIG. 32.—The Al-Cu-Mn-Si System.

the course of this separation, the composition of the melt follows the line *JI* towards point *I*, where a eutectic, containing solid aluminium, *c*-AlMnSi,  $\text{Al}_2\text{Cu}$ , and silicon, separates until the alloy is solid.

Fig. 38 (Plate LXVII) shows an alloy containing copper 18, manganese 1.6, and silicon 0.4% (point *b* in Fig. 32). A molten alloy of this composition, on cooling, deposits first *r*-AlCuMn, and then aluminium. When solid aluminium appears, the system may be considered to be in equilibrium with this phase and with the melt.

TABLE XVI.—*Equilibrium Reactions in Al-Cu-Mn-Si System.*

Region, Line, or Point	Equilibrium Reaction
<i>ABJIH</i> .	Eutectic: Melt $\rightleftharpoons$ $\alpha$ -Al + $\text{Al}_2\text{Cu}$
<i>HIFG</i> .	„ Melt $\rightleftharpoons$ $\alpha$ -Al + Si
<i>BCKJ</i> .	„ Melt $\rightleftharpoons$ $\alpha$ -Al + $r\text{-AlCuMn}$
<i>CDEK</i> .	„ Melt $\rightleftharpoons$ $\alpha$ -Al + $\text{Al}_6\text{Mn}$
<i>EFIJK</i> .	„ Melt $\rightleftharpoons$ $\alpha$ -Al + $c\text{-AlMnSi}$
<i>BJ</i> . .	Eutectic: Melt $\rightleftharpoons$ $\alpha$ -Al + $\text{Al}_2\text{Cu}$ + $r\text{-AlCuMn}$
<i>JI</i> . .	„ Melt $\rightleftharpoons$ $\alpha$ -Al + $\text{Al}_2\text{Cu}$ + $c\text{-AlMnSi}$
<i>HI</i> . .	„ Melt $\rightleftharpoons$ $\alpha$ -Al + $\text{Al}_2\text{Cu}$ + Si
<i>JK</i> . .	{ „ Melt $\rightleftharpoons$ $\alpha$ -Al + $r\text{-AlCuMn}$ + $c\text{-AlMnSi}$
<i>FI</i> . .	{ Peritectic: Melt + $r\text{-AlCuMn}$ $\rightleftharpoons$ $\alpha$ -Al + $c\text{-AlMnSi}$
<i>CK</i> . .	Eutectic: Melt $\rightleftharpoons$ $\alpha$ -Al + Si + $c\text{-AlMnSi}$
<i>EK</i> . .	Peritectic: Melt + $\text{Al}_6\text{Mn}$ $\rightleftharpoons$ $\alpha$ -Al + $r\text{-AlCuMn}$
	„ Melt + $\text{Al}_6\text{Mn}$ $\rightleftharpoons$ $\alpha$ -Al + $c\text{-AlMnSi}$
<i>I</i> . .	Eutectic: Melt $\rightleftharpoons$ $\alpha$ -Al + $\text{Al}_2\text{Cu}$ + $c\text{-AlMnSi}$ + Si
<i>J</i> . .	Peritectic: Melt + $r\text{-AlCuMn}$ $\rightleftharpoons$ $\alpha$ -Al + $\text{Al}_2\text{Cu}$ + $c\text{-AlMnSi}$
<i>K</i> . .	„ Melt + $\text{Al}_6\text{Mn}$ $\rightleftharpoons$ $\alpha$ -Al + $r\text{-AlCuMn}$ + $c\text{-AlMnSi}$

The following order of solidification is deduced from the diagram. During the separation of  $r\text{-AlCuMn}$ , as a primary phase or as a eutectic mixture with aluminium, the point representing the relative contents of alloying elements in the melt moves towards the line *BJ*. When this line is reached,  $\text{Al}_2\text{Cu}$  separates in addition to  $r\text{-AlCuMn}$  and aluminium. During this reaction *BJ* is followed towards the point *J*. At this point  $r\text{-AlCuMn}$  reacts peritectically with the melt. In addition to aluminium and  $\text{Al}_2\text{Cu}$ ,  $c\text{-AlMnSi}$  now appears. The latter phase probably envelops the  $r\text{-AlCuMn}$ . The melt remaining after the interruption of the peritectic reaction yields a precipitate of aluminium,  $\text{Al}_2\text{Cu}$ , and  $c\text{-AlMnSi}$ . The point which represents the relative content of the melt now follows the line *JI* towards point *I*, where a eutectic of aluminium,  $\text{Al}_2\text{Cu}$ ,  $c\text{-AlMnSi}$ , and silicon is deposited, until the melt has solidified completely. Fig. 38 shows  $r\text{-AlCuMn}$ ,  $\text{Al}_2\text{Cu}$ , and aluminium;  $r\text{-AlCuMn}$  appears in certain cases to be enveloped by  $c\text{-AlMnSi}$ . Silicon has also been observed in this structure, but is not present in the photomicrograph.

An alloy which contains copper 7.5, manganese 2, and silicon 0.5% (point *c* in Fig. 32) is illustrated in Fig. 39 (Plate LXVII). On solidification the first precipitate is  $\text{Al}_6\text{Mn}$ ; this reacts peritectically with the melt and is enveloped by  $c\text{-AlMnSi}$ .

#### 6. *Al-Cu-Fe-Si.*

No phases have been found in this system other than those belonging to the subsidiary ternary systems.

According to Gwyer, Phillips, and Mann,<sup>44</sup>  $\text{Al}_7\text{Cu}_2\text{Fe}$  and  $m\text{-AlFeSi}$  (or, as those authors term them,  $N$  and  $X$ ) are linked by a homogeneity range and thus should constitute the same phase. Since the present investigation has shown that  $\text{Al}_7\text{Cu}_2\text{Fe}$  and  $m\text{-AlFeSi}$  are not iso-

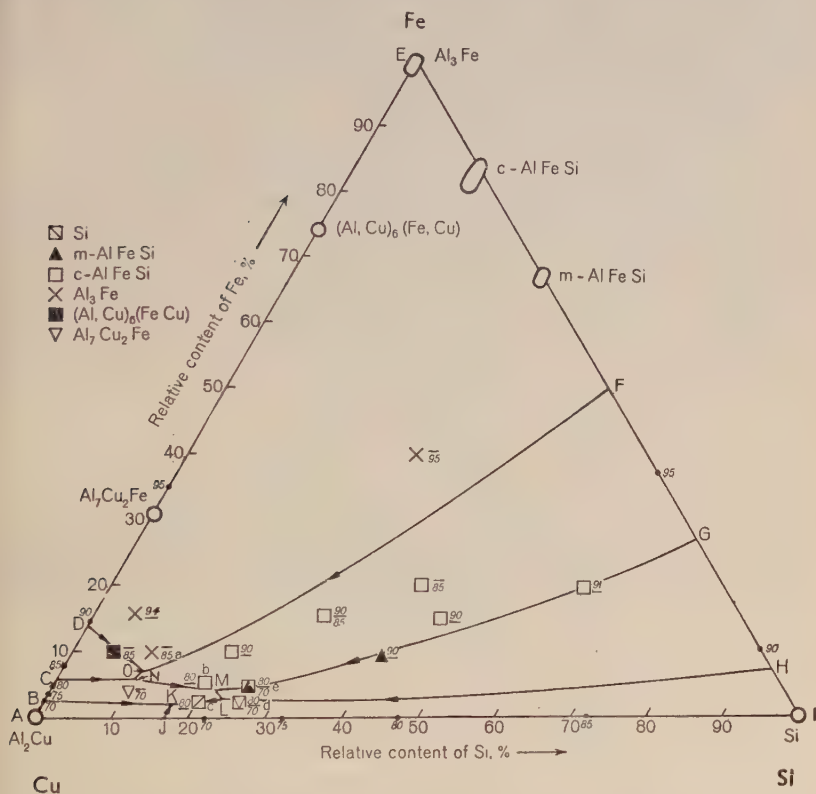


FIG. 33.—The Al-Cu-Fe-Si System. The point  $d$  represents two alloys, one containing 70% aluminium, in which  $\text{Al}_7\text{Cu}_2\text{Fe}$  is primary, and the other containing 80% aluminium, in which  $c\text{-AlFeSi}$  is secondary. The point  $e$  represents two alloys, one containing 70% aluminium, in which  $c\text{-AlFeSi}$  is primary, and the other containing 80% aluminium, in which  $m\text{-AlFeSi}$  is secondary.

morphous, this is not correct.  $\text{Al}_7\text{Cu}_2\text{Fe}$  does not show changes in etching properties, or in lattice-spacing values, indicative of a homogeneity range. On the other hand, it seems possible that a slight solubility of copper in  $m\text{-AlFeSi}$  may exist, as very small changes in the etching reactions have been observed.

Crystals isolated from alloys containing copper 6, iron 3, and silicon 6%, have a cubic lattice ( $a_1 = 12.501$  kX.). This value differs only slightly from the lattice spacing of  $c\text{-AlFeSi}$ , isolated from alloys belonging to the Al-Fe-Si system ( $a_1 = 12.523$  kX.), suggesting that the crystals consist of  $c\text{-AlFeSi}$  which has dissolved some copper. In this system the  $c\text{-AlFeSi}$  phase might therefore be designated  $c\text{-Al(Fe,Cu)Si}$ , but the term  $c\text{-AlFeSi}$  will be retained as the copper content is probably very low.

TABLE XVII.—*Equilibrium Reactions in Al-Cu-Fe-Si System.*

Region, Line, or Point	Equilibrium Reaction
<i>ABKJ</i> . .	Eutectic: Melt $\rightleftharpoons \alpha\text{-Al} + \text{Al}_2\text{Cu}$
<i>BCNMLK</i> . .	„ Melt $\rightleftharpoons \alpha\text{-Al} + \text{Al}_7\text{Cu}_2\text{Fe}$
<i>JKLHI</i> . .	„ Melt $\rightleftharpoons \alpha\text{-Al} + \text{Si}$
<i>LMGH</i> . .	„ Melt $\rightleftharpoons \alpha\text{-Al} + m\text{-AlFeSi}$
<i>CDON</i> . .	„ Melt $\rightleftharpoons \alpha\text{-Al} + (\text{Al,Cu})_6(\text{Fe,Cu})$
<i>NOFGM</i> . .	„ Melt $\rightleftharpoons \alpha\text{-Al} + c\text{-AlFeSi}$
<i>DEFO</i> . .	„ Melt $\rightleftharpoons \alpha\text{-Al} + \text{Al}_3\text{Fe}$
<i>BK</i> . .	Eutectic: Melt $\rightleftharpoons \alpha\text{-Al} + \text{Al}_2\text{Cu} + \text{Al}_7\text{Cu}_2\text{Fe}$
<i>JK</i> . .	„ Melt $\rightleftharpoons \alpha\text{-Al} + \text{Al}_2\text{Cu} + \text{Si}$
<i>KL</i> . .	„ Melt $\rightleftharpoons \alpha\text{-Al} + \text{Al}_7\text{Cu}_2\text{Fe} + \text{Si}$
<i>HL</i> . .	„ Melt $\rightleftharpoons \alpha\text{-Al} + \text{Si} + m\text{-AlFeSi}$
<i>ML</i> . .	{ „ Melt $\rightleftharpoons \alpha\text{-Al} + \text{Al}_7\text{Cu}_2\text{Fe} + m\text{-AlFeSi}$
<i>CN</i> . .	{ Peritectic: Melt + $m\text{-AlFeSi} \rightleftharpoons \alpha\text{-Al} + \text{Al}_7\text{Cu}_2\text{Fe}$
<i>NM</i> . .	„ Melt + $(\text{Al,Cu})_6(\text{Fe,Cu}) \rightleftharpoons \alpha\text{-Al} + \text{Al}_7\text{Cu}_2\text{Fe}$
<i>GM</i> . .	„ Melt + $c\text{-AlFeSi} \rightleftharpoons \alpha\text{-Al} + \text{Al}_7\text{Cu}_2\text{Fe}$
<i>ON</i> . .	{ Eutectic: Melt $\rightleftharpoons \alpha\text{-Al} + (\text{Al,Cu})_6(\text{Fe,Cu}) + c\text{-AlFeSi}$
<i>DO</i> . .	{ Peritectic: Melt + $(\text{Al,Cu})_6(\text{Fe,Cu}) \rightleftharpoons \alpha\text{-Al} + c\text{-AlFeSi}$
<i>FO</i> . .	„ Melt + $\text{Al}_3\text{Fe} \rightleftharpoons \alpha\text{-Al} + (\text{Al,Cu})_6(\text{Fe,Cu})$
	„ Melt + $\text{Al}_3\text{Fe} \rightleftharpoons \alpha\text{-Al} + c\text{-AlFeSi}$
<i>K</i> . .	Eutectic: Melt $\rightleftharpoons \alpha\text{-Al} + \text{Al}_2\text{Cu} + \text{Si} + \text{Al}_7\text{Cu}_2\text{Fe}$
<i>L</i> . .	Peritectic: Melt + $m\text{-AlFeSi} \rightleftharpoons \alpha\text{-Al} + \text{Al}_7\text{Cu}_2\text{Fe} + \text{Si}$
<i>M</i> . .	„ Melt + $c\text{-AlFeSi} \rightleftharpoons \alpha\text{-Al} + \text{Al}_7\text{Cu}_2\text{Fe} + m\text{-AlFeSi}$
<i>N</i> . .	„ Melt + $(\text{Al,Cu})_6(\text{Fe,Cu}) \rightleftharpoons \alpha\text{-Al} + \text{Al}_7\text{Cu}_2\text{Fe} + c\text{-AlFeSi}$
<i>O</i> . .	„ Melt + $\text{Al}_3\text{Fe} \rightleftharpoons \alpha\text{-Al} + (\text{Al,Cu})_6(\text{Fe,Cu}) + c\text{-AlFeSi}$

Phase diagrams for this system have been given by Gwyer, Phillips, and Mann,<sup>44</sup> who took no account of the presence of the phase  $(\text{Al,Cu})_6(\text{Fe,Cu})$ , nor of the fact that  $\text{Al}_7\text{Cu}_2\text{Fe}$  and  $m\text{-AlFeSi}$  are not isomorphous. The results obtained in the present investigation are given in Fig. 33. Table XVII shows the phases which may separate eutectically with solid aluminium within the different regions of the diagram, together with the appropriate equilibrium reactions associated

with the lines and points. It has not been possible to decide whether the reactions along the lines *ML* and *ON* are eutectic or peritectic, or both. Two alternatives are therefore given for these lines.

Figs. 40–43 (Plates LXVIII and LXIX) are photomicrographs of an alloy containing copper 12, iron 1.5, and silicon 1.5% (point *a* in Fig. 33). The following order of solidification may be suggested. First,  $\text{Al}_3\text{Fe}$  separates from the melt. This phase then reacts peritectically with the melt to form *c*- $\text{AlFeSi}$ , which envelops  $\text{Al}_3\text{Fe}$  and interrupts the peritectic reaction. The remaining melt deposits *c*- $\text{AlFeSi}$  and, later, aluminium also. *c*- $\text{AlFeSi}$  then reacts peritectically with the melt, to form  $\text{Al}_7\text{Cu}_2\text{Fe}$ , which envelops the *c*- $\text{AlFeSi}$ , interrupting the peritectic reaction. The remaining melt precipitates aluminium and  $\text{Al}_7\text{Cu}_2\text{Fe}$  and later  $\text{Al}_2\text{Cu}$  as well. Finally, a eutectic of solid aluminium,  $\text{Al}_7\text{Cu}_2\text{Fe}$ ,  $\text{Al}_2\text{Cu}$ , and silicon forms.

Figs. 44 and 45 (Plate LXX) are photomicrographs of an alloy containing copper 20, iron 1.6, and silicon 5.4% (point *b* in Fig. 33). This alloy solidifies in the following sequence. *c*- $\text{AlFeSi}$  first separates from the melt, and reacts peritectically with it to form *m*- $\text{AlFeSi}$ . During this reaction *c*- $\text{AlFeSi}$  is enveloped by *m*- $\text{AlFeSi}$  and the peritectic reaction is interrupted. The remaining melt deposits *m*- $\text{AlFeSi}$  and later aluminium also, followed by silicon. Finally, a eutectic of *m*- $\text{AlFeSi}$ , aluminium, silicon, and  $\text{Al}_2\text{Cu}$  is formed. In Fig. 45, where the etching reagent was ferric nitrate,  $\text{Al}_2\text{Cu}$  appears dark and *m*- $\text{AlFeSi}$  light grey. If the lamellar phase had consisted of  $\text{Al}_7\text{Cu}_2\text{Fe}$  it would have etched dark. According to the diagram only  $\text{Al}_7\text{Cu}_2\text{Fe}$  could form a eutectic with aluminium, silicon, and  $\text{Al}_2\text{Cu}$ .

In Fig. 46 (Plate LXXI) the alloy contained copper 15.5, iron 0.5, and silicon 4% (point *c* in Fig. 33). On solidification solid aluminium appears first. According to Fig. 33, the following order of solidification would be expected. Since point *c* is located on the line *KL*, silicon,  $\text{Al}_7\text{Cu}_2\text{Fe}$ , and aluminium should be deposited simultaneously, following the primary separation of the aluminium. The point representing the relative contents of alloying constituents in the melt follows the line *KL* to point *K*. At this point a eutectic of aluminium, silicon,  $\text{Al}_7\text{Cu}_2\text{Fe}$ , and  $\text{Al}_2\text{Cu}$  should separate until everything has solidified. In Fig. 46 dark lamellæ of  $\text{Al}_7\text{Cu}_2\text{Fe}$ , dark grains of  $\text{Al}_2\text{Cu}$ , grey silicon, and white aluminium are seen. The arrangement of the  $\text{Al}_7\text{Cu}_2\text{Fe}$  lamellæ seems to indicate that they have been formed by transformation of *m*- $\text{AlFeSi}$ .

Fig. 47 (Plate LXXI) is a photomicrograph of an alloy containing copper 14.5, iron 0.5, and silicon 5% (point *d* in Fig. 33). When this alloy solidifies, aluminium is the first phase to appear. According to Fig. 33 the order of solidification should be as follows. As point *d* is



situated in the region *JKLHI*, silicon separates together with aluminium after the primary separation of the latter. During this separation the point representing the relative contents of alloying elements in the melt moves towards the line *KL*. When this line is reached,  $\text{Al}_7\text{Cu}_2\text{Fe}$  appears in addition to solid aluminium and silicon, and the line is followed towards point *K*. Finally, a eutectic of aluminium, silicon,

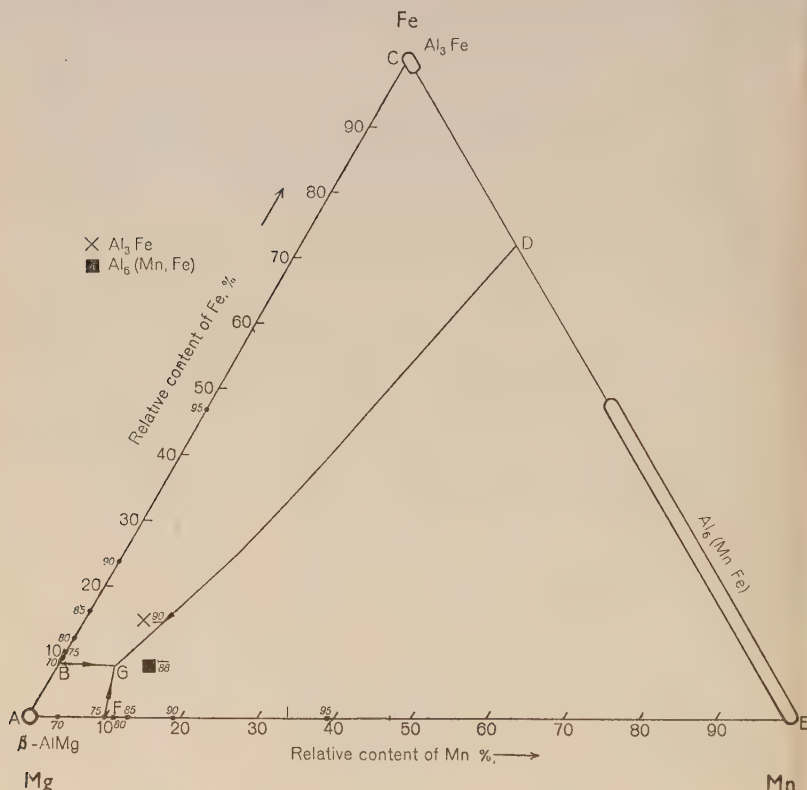


FIG. 50.—The Al-Mg-Mn-Fe System.

$\text{Al}_7\text{Cu}_2\text{Fe}$ , and  $\text{Al}_2\text{Cu}$  is formed. In Fig. 47 grey *c*- $\text{AlFeSi}$ , dark grey silicon, darkly etched grains of  $\text{Al}_2\text{Cu}$ , and a light background of aluminium can be seen.  $\text{Al}_7\text{Cu}_2\text{Fe}$ , which according to Fig. 33 ought to appear in this alloy, seems to have been replaced by *c*- $\text{AlFeSi}$ .

The photomicrographs discussed show that the order of solidification for alloys belonging to the system Al-Cu-Fe-Si may deviate considerably from that indicated by the diagram. According to Gwyer, Phillips, and Mann<sup>44</sup> the power of nucleation is low for  $\text{Al}_7\text{Cu}_2\text{Fe}$ . This phase

is likely, therefore, to be prone to undercooling, which would explain the apparent discrepancies.

### 7. Al-Mg-Mn-Fe.

No phases have been found in this system except those belonging to the subsidiary ternary systems. The results obtained are shown in Fig. 50. Table XVIII gives the reactions associated with the regions, lines, and point of this figure.

TABLE XVIII.—*Equilibrium Reactions in Al-Mg-Mn-Fe System.*

Region, Line, or Point	Equilibrium Reaction
ABGF . .	Eutectic: Melt $\rightleftharpoons$ $\alpha$ -Al + $\beta$ -AlMg
CDGB . .	„ Melt $\rightleftharpoons$ $\alpha$ -Al + Al <sub>3</sub> Fe
DEFG . .	„ Melt $\rightleftharpoons$ $\alpha$ -Al + Al <sub>6</sub> (Mn,Fe)
BG . .	Eutectic: Melt $\rightleftharpoons$ $\alpha$ -Al + $\beta$ -AlMg + Al <sub>3</sub> Fe
DG . .	„ Melt $\rightleftharpoons$ $\alpha$ -Al + Al <sub>3</sub> Fe + Al <sub>6</sub> (Mn,Fe)
FG . .	„ Melt $\rightleftharpoons$ $\alpha$ -Al + Al <sub>6</sub> (Mn,Fe) + $\beta$ -AlMg
G . . .	Eutectic: Melt $\rightleftharpoons$ $\alpha$ -Al + $\beta$ -AlMg + Al <sub>3</sub> Fe + Al <sub>6</sub> (Mn,Fe)

### 8. Al-Mg-Mn-Si.

In this system the only phases found are those belonging to the subsidiary ternary systems. Fig. 51 gives the results obtained and Table XIX shows the phases which may form a eutectic with solid aluminium within the different regions of the diagram, and the reactions corresponding to univariant lines and non-variant points.

TABLE XIX.—*Equilibrium Reactions in Al-Mg-Mn-Si System.*

Region, Line, or Point	Equilibrium Reaction
ABIH . .	Eutectic: Melt $\rightleftharpoons$ $\alpha$ -Al + $\beta$ -AlMg
HIJKG . .	„ Melt $\rightleftharpoons$ $\alpha$ -Al + Mg <sub>2</sub> Si
GKEF . .	„ Melt $\rightleftharpoons$ $\alpha$ -Al + Si
BCDJI . .	„ Melt $\rightleftharpoons$ $\alpha$ -Al + Al <sub>6</sub> Mn
DEKJ . .	„ Melt $\rightleftharpoons$ $\alpha$ -Al + $c$ -AlMnSi
BI . . .	Eutectic: Melt $\rightleftharpoons$ $\alpha$ -Al + $\beta$ -AlMg + Al <sub>6</sub> Mn
HI . . .	„ Melt $\rightleftharpoons$ $\alpha$ -Al + $\beta$ -AlMg + Mg <sub>2</sub> Si
JI . . .	„ Melt $\rightleftharpoons$ $\alpha$ -Al + Al <sub>6</sub> Mn + Mg <sub>2</sub> Si
DJ . . .	Peritectic: Melt + Al <sub>6</sub> Mn $\rightleftharpoons$ $\alpha$ -Al + $c$ -AlMnSi
KJ . . .	Eutectic: Melt $\rightleftharpoons$ $\alpha$ -Al + Mg <sub>2</sub> Si + $c$ -AlMnSi
GK . . .	„ Melt $\rightleftharpoons$ $\alpha$ -Al + Mg <sub>2</sub> Si + Si
EK . . .	„ Melt $\rightleftharpoons$ $\alpha$ -Al + Si + $c$ -AlMnSi
I . . .	Eutectic: Melt $\rightleftharpoons$ $\alpha$ -Al + $\beta$ -AlMg + Al <sub>6</sub> Mn + Mg <sub>2</sub> Si
J . . .	Peritectic: Melt + $c$ -AlMnSi $\rightleftharpoons$ $\alpha$ -Al + Al <sub>6</sub> Mn + Mg <sub>2</sub> Si
K . . .	Eutectic: Melt $\rightleftharpoons$ $\alpha$ -Al + Mg <sub>2</sub> Si + $c$ -AlMnSi + Si

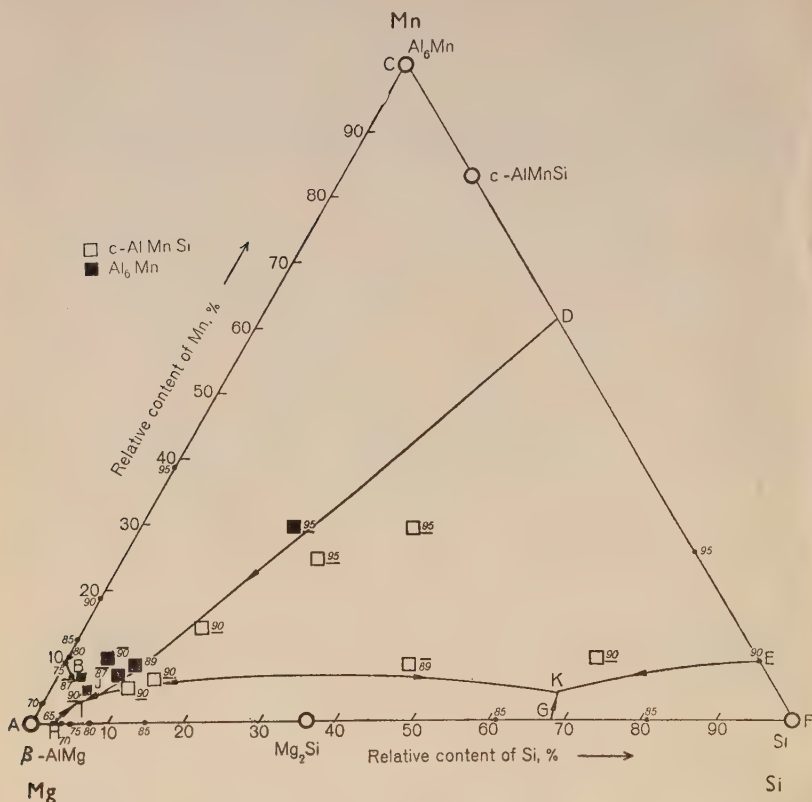


FIG. 51.—The Al-Mg-Mn-Si System.

9. *Al-Mg-Fe-Si*.

In this system one additional phase, designated *h*-AlMgFeSi, has been found besides those belonging to the subsidiary ternary systems. Crystals of *h*-AlMgFeSi were isolated from an alloy containing magnesium 6, iron 0.3, and silicon 12%. The composition found was aluminium 40.0, magnesium 15.6, iron 12, and silicon 33.8%. This corresponds to the formula  $\text{Al}_{7.2}\text{Mg}_{3.2}\text{Fe}_{1.1}\text{Si}_{6.0}$ . According to Perlitz and Westgren<sup>64</sup> this phase has an hexagonal unit cell with dimensions  $a_1 = 6.62$  and  $a_3 = 7.92$  kX. The cell contains 8 aluminium, 3 magnesium, 1 iron, and 6 silicon atoms. The arrangement of the atoms is given in an Appendix, p. 552. The formula should thus be written  $\text{Al}_8\text{Mg}_3\text{FeSi}_6$ . Crystals of this phase form trigonal plates which are white in ordinary light, but which in polarized light appear purple to blue. In eutectic mixture with aluminium, the phase shows a branched appearance.

The results obtained for the system are given in Fig. 52. Table XX shows the phases which may form a eutectic with solid aluminium within the different regions of the diagram, and the corresponding equilibrium reactions.\*

Fig. 48 (Plate LXXII) is a photomicrograph of an alloy containing magnesium 6, iron 0.3, and silicon 12% (point *a* in Fig. 52). When this

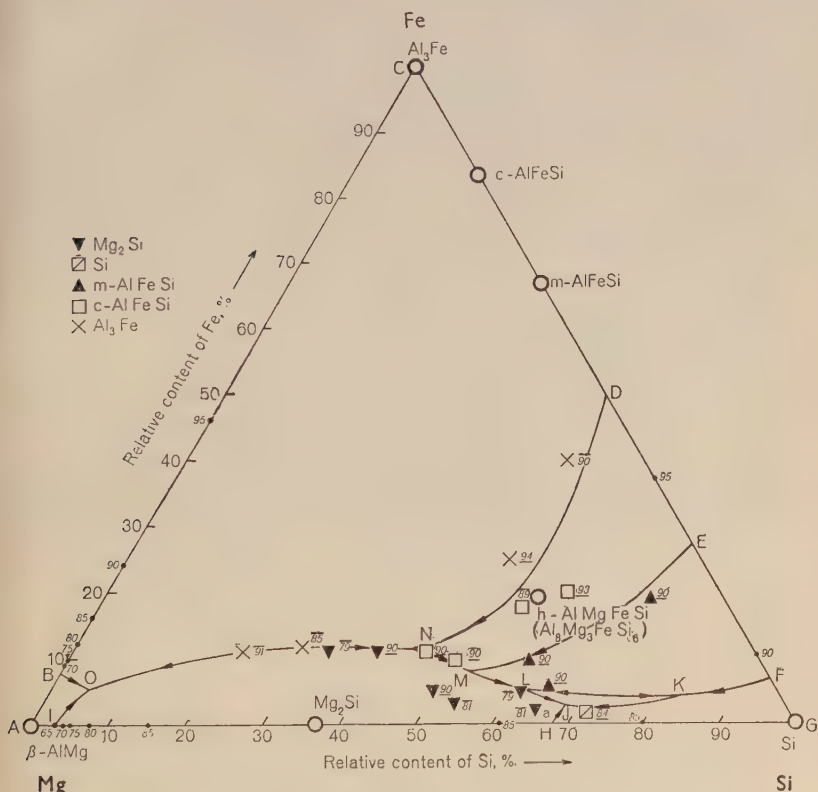


FIG. 52.—The Al-Mg-Fe-Si System.

alloy solidifies,  $Mg_2Si$  is the first phase to separate, and solid aluminium follows. From Fig. 52 it cannot be deduced with certainty whether  $h-AlMgFeSi$  will be the next phase to appear, together with aluminium

\* Note by Editor: While this work was being prepared for publication, a study of the system Al-Mg-Fe-Si was published by Phillips,<sup>65</sup> whose results are in good agreement with those obtained in the present work.

and  $\text{Mg}_2\text{Si}$ . The solidification process should, however, end with a eutectic separation of aluminium,  $\text{Mg}_2\text{Si}$ , Si, and  $h\text{-AlMgFeSi}$ . In Fig. 48,  $h\text{-AlMgFeSi}$  is seen in the middle of the field as a dark, branched phase. Also present are darker grey silicon, dark  $\text{Mg}_2\text{Si}$ , and aluminium, which forms the light background.

TABLE XX.—*Equilibrium Reactions in Al-Mg-Fe-Si System.*

Region, Line, or Point	Equilibrium Reaction
<i>ABOI</i> . .	Eutectic: Melt $\rightleftharpoons \alpha\text{-Al} + \beta\text{-AlMg}$
<i>BCDNO</i> . .	" Melt $\rightleftharpoons \alpha\text{-Al} + \text{Al}_3\text{Fe}$
<i>DEMN</i> . .	" Melt $\rightleftharpoons \alpha\text{-Al} + c\text{-AlFeSi}$
<i>EFKLM</i> . .	" Melt $\rightleftharpoons \alpha\text{-Al} + m\text{-AlFeSi}$
<i>FGHJK</i> . .	" Melt $\rightleftharpoons \alpha\text{-Al} + \text{Si}$
<i>HIONMLJ</i> . .	" Melt $\rightleftharpoons \alpha\text{-Al} + \text{Mg}_2\text{Si}$
<i>KJL</i> . .	" Melt $\rightleftharpoons \alpha\text{-Al} + h\text{-AlMgFeSi}$
<i>BO</i> . .	Eutectic: Melt $\rightleftharpoons \alpha\text{-Al} + \beta\text{-AlMg} + \text{Al}_3\text{Fe}$
<i>IO</i> . .	" Melt $\rightleftharpoons \alpha\text{-Al} + \beta\text{-AlMg} + \text{Mg}_2\text{Si}$
<i>ON</i> . .	" Melt $\rightleftharpoons \alpha\text{-Al} + \text{Mg}_2\text{Si} + \text{Al}_3\text{Fe}$
<i>DN</i> . .	Peritectic: Melt + $\text{Al}_3\text{Fe} \rightleftharpoons \alpha\text{-Al} + c\text{-AlFeSi}$
<i>NM</i> . .	Eutectic: Melt $\rightleftharpoons \alpha\text{-Al} + \text{Mg}_2\text{Si} + c\text{-AlFeSi}$
<i>EM</i> . .	Peritectic: Melt + $c\text{-AlFeSi} \rightleftharpoons \alpha\text{-Al} + m\text{-AlFeSi}$
<i>ML</i> . .	Eutectic: Melt $\rightleftharpoons \alpha\text{-Al} + \text{Mg}_2\text{Si} + m\text{-AlFeSi}$
<i>LK</i> . .	Peritectic: Melt + $m\text{-AlFeSi} \rightleftharpoons \alpha\text{-Al} + h\text{-AlMgFeSi}$
<i>KF</i> . .	Eutectic: Melt $\rightleftharpoons \alpha\text{-Al} + m\text{-AlFeSi} + \text{Si}$
<i>LJ</i> . .	" Melt $\rightleftharpoons \alpha\text{-Al} + \text{Mg}_2\text{Si} + h\text{-AlMgFeSi}$
<i>KJ</i> . .	" Melt $\rightleftharpoons \alpha\text{-Al} + \text{Si} + h\text{-AlMgFeSi}$
<i>HJ</i> . .	" Melt $\rightleftharpoons \alpha\text{-Al} + \text{Mg}_2\text{Si} + \text{Si}$
<i>O</i> . .	Eutectic: Melt $\rightleftharpoons \alpha\text{-Al} + \beta\text{-AlMg} + \text{Al}_3\text{Fe} + \text{Mg}_2\text{Si}$
<i>N</i> . .	Peritectic: Melt + $\text{Al}_3\text{Fe} \rightleftharpoons \alpha\text{-Al} + \text{Mg}_2\text{Si} + c\text{-AlFeSi}$
<i>M</i> . .	" Melt + $c\text{-AlFeSi} \rightleftharpoons \alpha\text{-Al} + \text{Mg}_2\text{Si} + m\text{-AlFeSi}$
<i>L</i> . .	" Melt + $m\text{-AlFeSi} \rightleftharpoons \alpha\text{-Al} + \text{Mg}_2\text{Si} + h\text{-AlMgFeSi}$
<i>K</i> . .	" Melt + $m\text{-AlFeSi} \rightleftharpoons \alpha\text{-Al} + \text{Si} + h\text{-AlMgFeSi}$
<i>J</i> . .	Eutectic: Melt $\rightleftharpoons \alpha\text{-Al} + \text{Mg}_2\text{Si} + \text{Si} + h\text{-AlMgFeSi}$

10. *Al-Mn-Fe-Si.*

In this system no phases were distinguished other than those belonging to the subsidiary ternary systems.

Crystals having the form of rhombic dodecahedra were isolated from two separate alloys with the following compositions: manganese 4, iron 2, silicon 3%, and manganese 3, iron 3, silicon 3%. The crystals from the first alloy contained manganese 15.7, iron 16.1, silicon 6.8%, and those from the second manganese 18.8, iron 11.7, and silicon 7.1%. X-ray investigation of crystals from the first alloy showed the symmetry to be cubic ( $a_1 = 12.63 \text{ kX.}$ ). This value agrees well with the corresponding values for  $c\text{-AlMnSi}$  (12.625 kX.) and  $c\text{-AlFeSi}$  (12.523 kX.). These should therefore be regarded as parts of the same

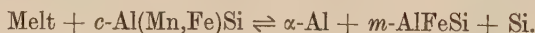




TABLE XXI.—*Equilibrium Reactions in Al-Mn-Fe-Si System.*

Region, Line, or Point	Equilibrium Reaction
<i>ABJI</i> . .	Eutectic: Melt $\rightleftharpoons \alpha\text{-Al} + \text{Al}_6(\text{Mn,Fe})$
<i>BCDJ</i> . .	„ Melt $\rightleftharpoons \alpha\text{-Al} + \text{Al}_3\text{Fe}$
<i>DEKHIJ</i> . .	„ Melt $\rightleftharpoons \alpha\text{-Al} + c\text{-Al}(\text{Mn,Fe})\text{Si}$
<i>EFK</i> . .	„ Melt $\rightleftharpoons \alpha\text{-Al} + m\text{-AlFeSi}$
<i>FGHK</i> . .	„ Melt $\rightleftharpoons \alpha\text{-Al} + \text{Si}$
<i>BJ</i> . .	Eutectic: Melt $\rightleftharpoons \alpha\text{-Al} + \text{Al}_6(\text{Mn,Fe}) + \text{Al}_3\text{Fe}$
<i>DJ</i> . .	Peritectic: Melt + $\text{Al}_3\text{Fe} \rightleftharpoons \alpha\text{-Al} + c\text{-Al}(\text{Mn,Fe})\text{Si}$
<i>IJ</i> . .	„ Melt + $\text{Al}_6(\text{Mn,Fe}) \rightleftharpoons \alpha\text{-Al} + c\text{-Al}(\text{Mn,Fe})\text{Si}$
<i>EK</i> . .	{ Eutectic: Melt + $c\text{-Al}(\text{Mn,Fe})\text{Si} \rightleftharpoons \alpha\text{-Al} + m\text{-AlFeSi}$
<i>FK</i> . .	„ Melt $\rightleftharpoons \alpha\text{-Al} + c\text{-Al}(\text{Mn,Fe})\text{Si} + m\text{-AlFeSi}$
<i>HK</i> . .	„ Melt $\rightleftharpoons \alpha\text{-Al} + m\text{-AlFeSi} + \text{Si}$
<i>J</i> . .	„ Melt $\rightleftharpoons \alpha\text{-Al} + c\text{-Al}(\text{Mn,Fe})\text{Si} + \text{Si}$
<i>K</i> . .	{ Peritectic: Melt + $c\text{-Al}(\text{Mn,Fe})\text{Si} \rightleftharpoons \alpha\text{-Al} + m\text{-AlFeSi} + \text{Si}$

$\alpha$  or  $\alpha(\text{MnSiFe})$  corresponds to  $c\text{-Al}(\text{Mn,Fe})\text{Si}$ . For the point *K* they reported the reaction to be peritectic:



## VI.—QUINARY SYSTEMS.

Systems with five components are represented either by projections of the kind described on p. 494, or by sections through these projections for a certain relative content of one of the alloying elements. These projections are given in the shape of regular tetrahedra, the sides of which are the corresponding projections for the subsidiary systems with four components. The sections through these projections have the shape of equilateral triangles. The tetrahedral models shown in perspective in the following figures have all been drawn as viewed from an infinitely distant point. In order to indicate that the lines in these diagrams are at varying distances from the observer, nearer lines have been drawn more heavily than distant ones. In the tetrahedral models the representation of melt in equilibrium with solid aluminium and four other phases is a point, that of melt in equilibrium with solid aluminium and three other phases is a line, melt in equilibrium with aluminium and two other solid phases corresponds to a surface, and melt in equilibrium with solid aluminium and one other solid phase is represented by a space region. The equilibria occurring in the systems with five components between melt, solid aluminium, and one other solid phase are all eutectic. The method used to represent points,

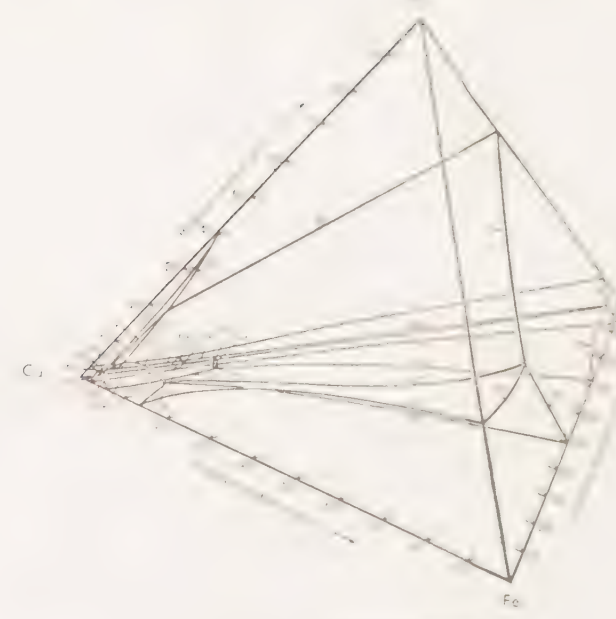
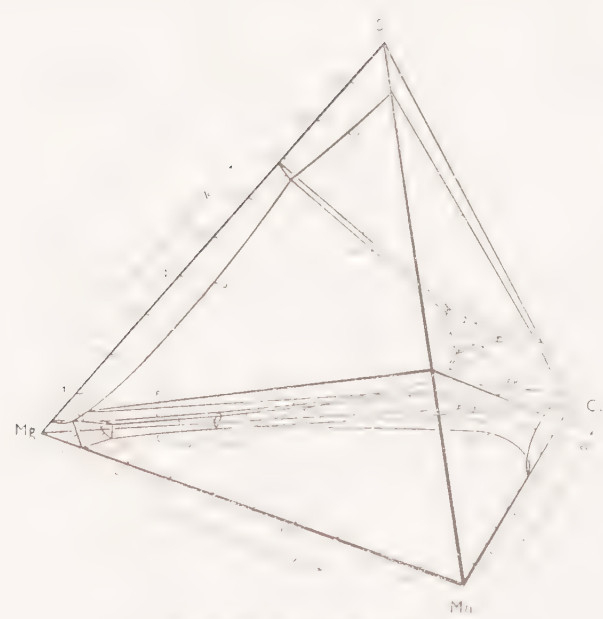
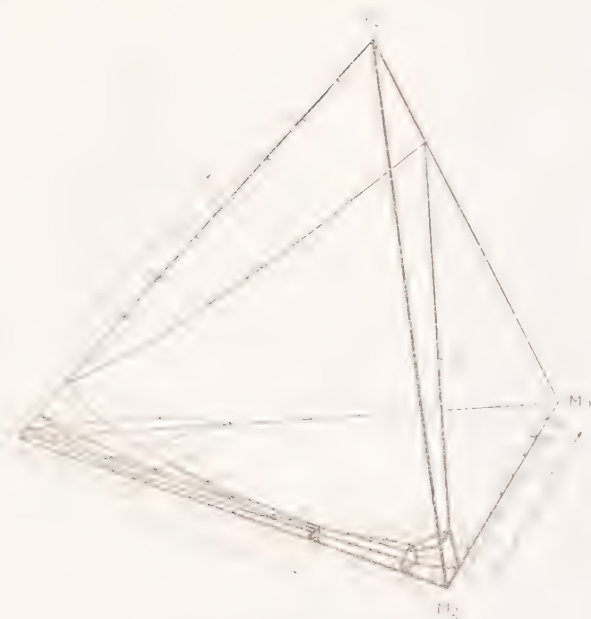


FIG. 60.—The Al-Cu-Mg-Mn-Si System.

FIG. 62.—The Al-Cu-Mn-Fe System.

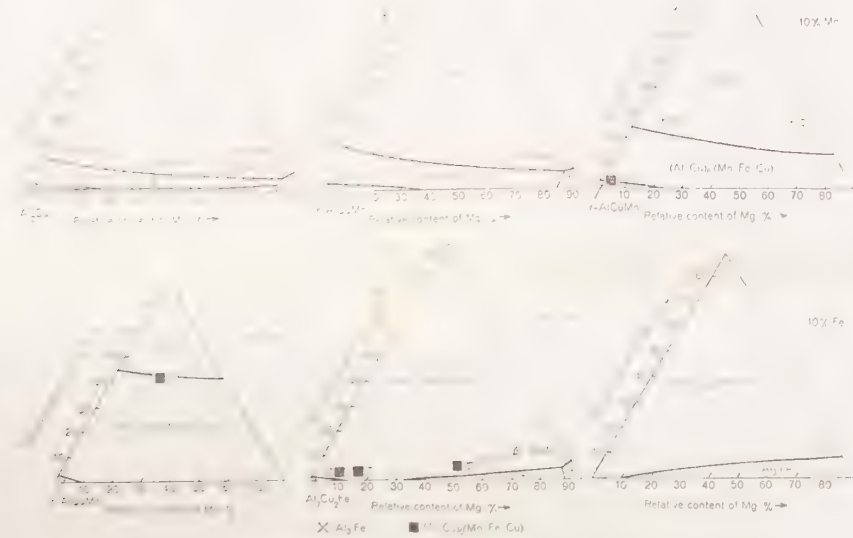


FIG. 59.—The Al-Cu-Mg-Mn-Fe System. Sections for various relative manganese or iron contents.

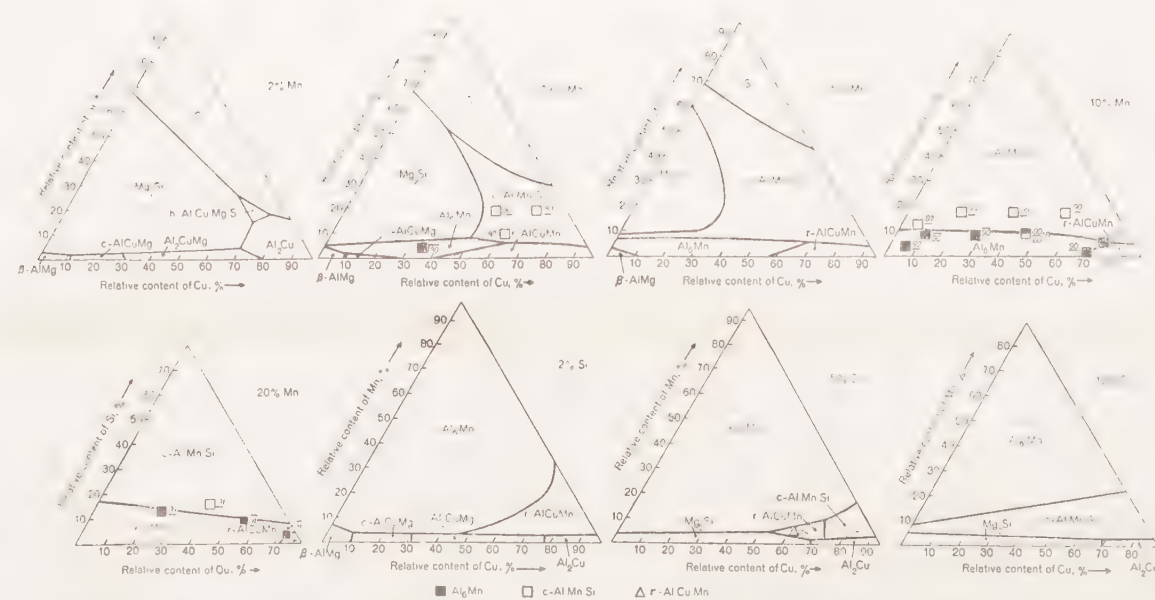
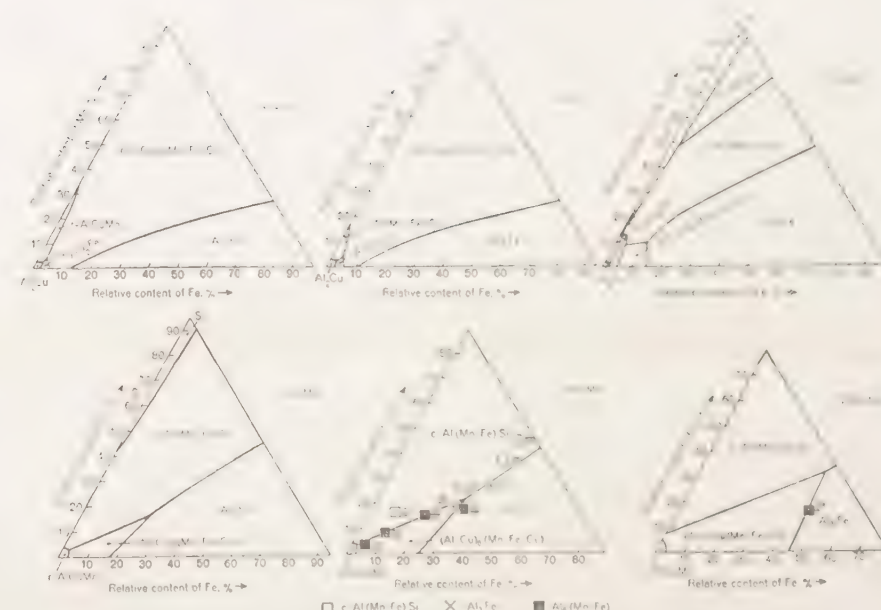
FIG. 61.—The Al-Cu-Mg-Mn-Si System. Sections for various relative manganese or silicon contents. Point *a* in the section for 10% manganese represents two alloys, one containing 80% aluminium, in which *c*-AlMnSi is primary, and the other containing 90% aluminium, in which *c*-Al<sub>6</sub>Mn is secondary.

FIG. 63.—The Al-Cu-Mn-Fe-Si System. Sections for various relative manganese or silicon contents.

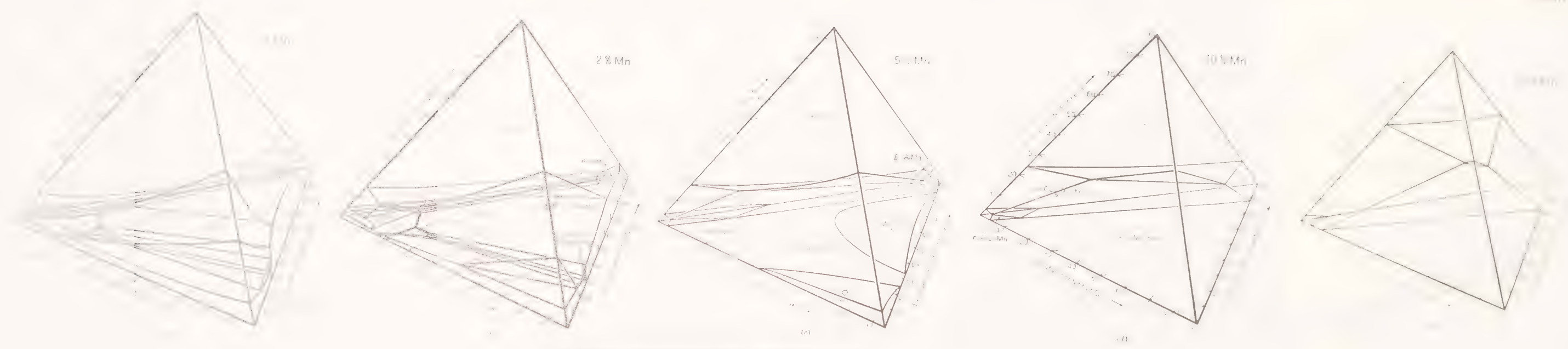


Fig. 58. Al-Cu-Mn phase diagrams for various relative manganese content.

Phases of  
the surface  
the Al-Cu  
the quinar  
the belong  
The solid phases  
to dissolve  
from the se  
quinary sys  
example,  
containing copper  
and the followi  
these 7-8, a  
to save space  
constituents have  
In some cases  
ered in the p  
amty. No cl  
diagrams sh  
The alloys stu  
base or conce  
primary—are sh  
these diagrams  
systems.

Fig. 58 (Plate  
Al-Cu-Mg-Mn-Fe  
subsidiary system  
Al-Mg-Mn-Fe. A  
phases in equilibri  
in the diagram ha  
from Fig. 58 and  
of its own. By n  
identify surfaces a  
melt in equilibrium  
For instance, the s  
ABG, and ABF, co  
Al<sub>3</sub>Fe, and (Al,Cu  
(see Key to Table  
the surface would  
symbol for alumin  
specify the surface  
used to indicate th  
VOL. LXXVII.



lines, and surfaces in the diagrams will be described in connection with the system Al-Cu-Mg-Mn-Fe.

In the quinary systems no solid phases have been found other than those belonging to the corresponding subsidiary quaternary systems. The solid phases occurring in the systems with five components do not seem to dissolve other alloying constituents to any considerable extent, apart from the solubility exhibited by the corresponding phases in the quaternary systems. The phase  $(\text{Al,Cu})_6(\text{Mn,Fe,Cu})$  may be mentioned as an example. Needles of this phase were isolated from an alloy containing copper 4.32, magnesium 0.72, manganese 0.8, and iron 2.16%, and the following analysis was found: aluminium 73.8, copper 1.2, manganese 7.8, and iron 19.2%, but no magnesium. For this reason and to save space in the diagrams, the relative contents of the alloying constituents have not been indicated for the solid phases.

In some cases the order of solidification in the quinary systems covered in the present investigation could not be determined with certainty. No claim is therefore made for accuracy in detail, but the diagrams given should show the main features.

The alloys studied and observations made concerning the primary phase—or concerning the secondary phase when aluminium is primary—are shown in the sectional diagrams. The notation adopted in these diagrams is similar to that employed in the case of quaternary systems.

### 1. *Al-Cu-Mg-Mn-Fe.*

Fig. 58 (Plate LXXIII) shows the tetrahedral model for the system Al-Cu-Mg-Mn-Fe. The faces of the tetrahedron correspond to the subsidiary systems Al-Cu-Mg-Mn, Al-Cu-Mg-Fe, Al-Cu-Mn-Fe, and Al-Mg-Mn-Fe. As far as space would permit, the names of the solid phases in equilibrium with solid aluminium and melt along each line in the diagram have been printed next to that line. As may be seen from Fig. 58 and Table XXII, each phase has been assigned a symbol of its own. By means of lines indicated in this way it is possible to identify surfaces and space regions in the diagram which correspond to melt in equilibrium with solid aluminium and one other solid phase. For instance, the surface which in Fig. 58 is bounded by the lines *AB*, *ABG*, and *ABF*, corresponds to melt in equilibrium with solid aluminium,  $\text{Al}_3\text{Fe}$ , and  $(\text{Al,Cu})_6(\text{Mn,Fe,Cu})$ . The symbols for these three phases (see Key to Table XXII) are  $\alpha$ , *A*, and *B*, so that the full symbol for the surface would be  $\alpha AB$ . There is no need, however, to include the symbol for aluminium, and the shortened symbol *AB* is sufficient to specify the surface. In a similar manner the symbol *ABF* may be used to indicate the line in which the three surfaces *AB*, *AF*, and *BF*



intersect, and *ABFG* the point of intersection of the four lines *ABF*, *ABG*, *AFG*, and *BFG*.

In Table XXII are listed first the surfaces, lines, and points associated with peritectic reactions, indicating the solid phase which, on cooling, reacts with the liquid. Thus *BC* is associated with a reaction between melt and  $(\text{Al,Cu})_6(\text{Mn,Fe,Cu})$  (*B*) to form  $\alpha\text{-Al} + \text{Al}_7\text{Cu}_2\text{Fe}$  (*C*). The various surfaces, lines, and points associated with eutectics are listed subsequently.

In the case of *AB*, it is uncertain whether the reaction is eutectic or peritectic; it seems to be eutectic when the copper content is low, but otherwise peritectic. A similar uncertainty exists in respect of the lines *ABF* and *BDH*. In both cases, low copper contents appear to favour the eutectic reaction.

TABLE XXII.—*Equilibrium Reactions in Al-Cu-Mg-Mn-Fe System.*

Key		Surfaces		Lines		Points	
Symbol	Phase Denoted	Peritectic	Solid Reactant	Peritectic	Solid Reactant	Peritectic	Solid Reactant
<i>a</i>	$\alpha\text{-Al}$	<i>AB</i> *	<i>A</i>	<i>ABF</i> *	<i>B</i>	<i>BCDH</i>	<i>C</i>
<i>A</i>	$\text{Al}_3\text{Fe}$	<i>BC</i>	<i>B</i>	<i>BCD</i>	<i>B</i>		
<i>B</i>	$(\text{Al,Cu})_6(\text{Mn,Fe,Cu})$	<i>BD</i>	<i>B</i>	<i>BCH</i>	<i>C</i>		
<i>C</i>	$\text{Al}_7\text{Cu}_2\text{Fe}$	<i>FH</i>	<i>H</i>	<i>BDH</i> *	<i>D</i>		
<i>D</i>	$r\text{-AlCuMn}$			<i>BFH</i>	<i>H</i>		
<i>E</i>	$\text{Al}_2\text{Cu}$						
<i>F</i>	$c\text{-AlCuMg}$						
<i>G</i>	$\beta\text{-AlMg}$						
<i>H</i>	$\text{Al}_2\text{CuMg}$						
		Eutectic		Eutectic		Eutectic	
		<i>AF, AG, BH, BF, BG, CD, CE, CH, DE, DH, EH, FG</i>		<i>ABG, AFG, BFG, CDE, CDH, CEH, DEH</i>		<i>ABFG, CDEH</i>	

\* May be eutectic.

Fig. 59 (Plate LXXIII) gives sections through the tetrahedral model of Fig. 58 for relative contents of 2, 5, 10, and 20% manganese, and 5 and 10% iron. It shows the solid phases which may be in equilibrium with solid aluminium and melt in the different regions of the diagram.

## 2. *Al-Cu-Mg-Mn-Si.*

Fig. 60 (Plate LXXIII) represents the tetrahedral model for the system  $\text{Al-Cu-Mg-Mn-Si}$ . Table XXIII gives the key to the symbols used and indicates the reactions involved.

TABLE XXIII.—Equilibrium Reactions in Al-Cu-Mg-Mn-Si System.

Key		Surfaces		Lines		Points	
Symbol	Phase Denoted	Peritectic	Solid Reactant	Peritectic	Solid Reactant(s)	Peritectic	Solid Reactant(s)
<i>B</i>	Al <sub>6</sub> Mn	<i>BD</i>	<i>B</i>	<i>BDH</i>	<i>D</i>	<i>BDJK</i>	<i>B, K</i>
<i>D</i>	<i>r</i> -AlCuMn	<i>BK</i>	<i>B</i>	<i>BDJ</i>	<i>B</i>	<i>BDHJ</i>	<i>D</i>
<i>E</i>	Al <sub>2</sub> Cu	<i>DK</i> *	<i>D</i>	<i>BDK</i>	<i>B</i>	<i>BFHJ</i>	<i>H</i>
<i>F</i>	<i>c</i> -AlCuMg	<i>FH</i>	<i>H</i>	<i>BFH</i>	<i>H</i>	<i>DEJK</i>	<i>K</i>
<i>G</i>	$\beta$ -AlMg	<i>JL</i>	<i>J</i>	<i>BJK</i>	<i>K</i>	<i>EJKL</i>	<i>J</i>
<i>H</i>	Al <sub>2</sub> CuMg			<i>DEK</i>	<i>D</i>	<i>IJKL</i>	<i>I, J</i>
<i>I</i>	Si			<i>DJK</i>	<i>K</i>		
<i>J</i>	Mg <sub>2</sub> Si			<i>EJL</i>	<i>J</i>		
<i>K</i>	<i>c</i> -AlMnSi			<i>FHJ</i>	<i>H</i>		
<i>L</i>	<i>h</i> -AlCuMgSi			<i>IJL</i>	<i>I, J</i>		
				<i>JKL</i>	<i>J</i>		
		Eutectic		Eutectic		Eutectic	
		<i>BF, BG, BH, BJ, DE, DH, DJ, EH, EI, EJ, EK, EL, FG, FJ, GJ, HJ, IJ, IK, IL, JK, KL</i>		<i>BFG, EFJ, BGJ, BHJ, DEH, DEJ, DHJ, EHJ, EIK, EIL, EJK, EKL, FGJ, IJK, IKL</i>		<i>BFGJ, DEHJ, EILK</i>	

\* May be eutectic.

Fig. 61 (Plate LXXIII) shows sections through the tetrahedral model (Fig. 60) for the relative contents of 2, 3.6, 5, 10, and 20% manganese, and of 2, 5, and 10% silicon. In the figure the solid phases which may be in equilibrium with solid aluminium and melt have been indicated for the different regions.

### 3. Al-Cu-Mg-Fe-Si.

In Fig. 54 is shown the tetrahedral model for the system Al-Cu-Mg-Fe-Si. Table XXIV gives the equilibrium reactions for the surfaces, lines, and points which correspond to melt in equilibrium with solid aluminium and two, three, and four other phases, respectively.

Fig. 55 shows sections through the tetrahedral model (Fig. 54) for relative contents of 2, 5, 10, and 20% iron. It indicates the phases which within the different regions of the diagram may be in equilibrium with solid aluminium and melt.

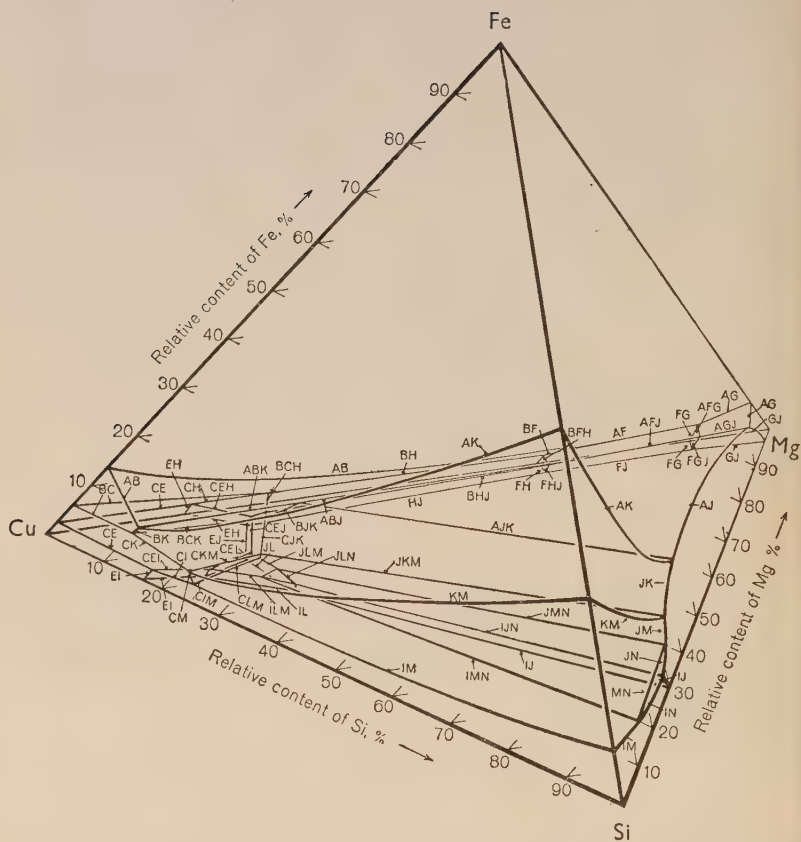


FIG. 54.—The Al-Cu-Mg-Fe-Si System.

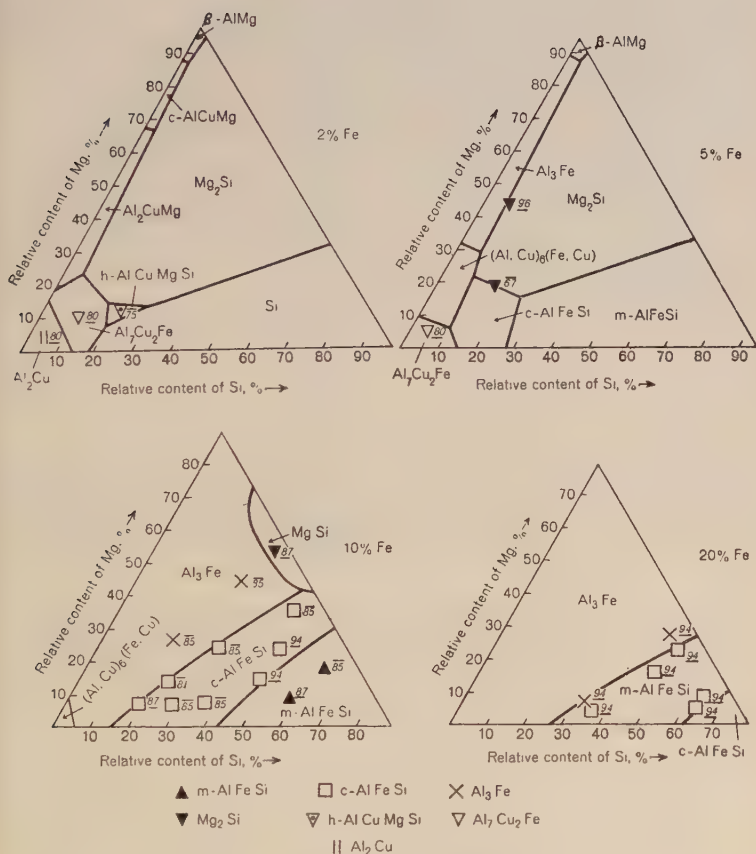


FIG. 55.—The Al-Cu-Mg-Fe-Si System. Sections for various relative iron contents.

TABLE XXIV.—*Equilibrium Reactions in Al-Cu-Mg-Fe-Si System.*

Key		Surfaces		Lines		Points	
Symbol	Phase Denoted	Peritectic	Solid Reactant	Peritectic	Solid Reactant(s)	Peritectic	Solid Reactant(s)
<i>A</i>	Al <sub>3</sub> Fe	<i>AB</i>	<i>A</i>	<i>ABF</i>	<i>B</i>	<i>ABJK</i>	<i>A</i>
<i>B</i>	(Al,Cu) <sub>6</sub> (Fe,Cu)	<i>AK</i>	<i>A</i>	<i>ABJ</i>	<i>A</i>	<i>ABFJ</i>	<i>B</i>
<i>C</i>	Al <sub>7</sub> Cu <sub>2</sub> Fe	<i>BC</i>	<i>B</i>	<i>ABK</i>	<i>A</i>	<i>BCHJ</i>	<i>B</i>
<i>E</i>	Al <sub>2</sub> Cu	<i>BK</i> *	<i>B</i>	<i>AJK</i>	<i>A</i>	<i>BCJK</i>	<i>B (K)</i>
<i>F</i>	c-AlCuMg	<i>CK</i>	<i>K</i>	<i>BCH</i>	<i>B</i>	<i>BFHJ</i>	<i>H</i>
<i>G</i>	β-AlMg	<i>CM</i> *	<i>M</i>	<i>BCJ</i>	<i>B</i>	<i>CEJL</i>	<i>J</i>
<i>H</i>	Al <sub>2</sub> CuMg	<i>FH</i>	<i>H</i>	<i>BCK</i>	<i>B</i>	<i>CILM</i>	<i>M</i>
<i>I</i>	Si	<i>JL</i>	<i>J</i>	<i>BFH</i>	<i>H</i>	<i>CJLM</i>	<i>M, J</i>
<i>J</i>	Mg <sub>2</sub> Si	<i>KM</i>	<i>K</i>	<i>BJK</i> *	<i>K</i>	<i>CJKM</i>	<i>K</i>
<i>K</i>	c-AlFeSi	<i>LN</i> *	<i>N</i>	<i>CIM</i>	<i>M</i>	<i>IJLN</i>	<i>I, J</i>
<i>L</i>	h-AlCuMgSi	<i>MN</i>	<i>M</i>	<i>CJK</i>	<i>K</i>	<i>ILMN</i>	<i>N</i>
<i>M</i>	m-AlFeSi			<i>CJL</i>	<i>J</i>	<i>JLMN</i>	<i>J, N</i>
<i>N</i>	h-AlMgFeSi			<i>CJM</i>	<i>M</i>		
				<i>CKM</i>	<i>K</i>		
				<i>CLM</i>	<i>M</i>		
				<i>EJL</i>	<i>J</i>		
				<i>FHJ</i>	<i>H</i>		
				<i>IJL</i>	<i>I, J</i>		
				<i>ILN</i> *	<i>N</i>		
				<i>IMN</i>	<i>M</i>		
				<i>JKM</i>	<i>C</i>		
				<i>JLM</i>	<i>J</i>		
				<i>JLN</i>	<i>J (N)</i>		
				<i>JMN</i>	<i>M</i>		
				<i>LMN</i>	<i>N</i>		
		Eutectic		Eutectic		Eutectic	
		<i>AF, AG, AJ,</i> <i>BF, BH, BJ,</i> <i>CE, CH, CI,</i> <i>CJ, CL, EH,</i> <i>EI, EJ, EL,</i> <i>FG, FJ, GJ,</i> <i>HJ, IJ, IL,</i> <i>IM, IN, JK,</i> <i>JM, JN, LM</i>		<i>AFG, AFJ,</i> <i>BFJ, BHJ,</i> <i>CEH, CEI,</i> <i>CEJ, CEL,</i> <i>CHJ, CIL,</i> <i>EHJ, EIL,</i> <i>FGJ, IJN,</i> <i>ILM</i>		<i>AFGJ, CEHJ,</i> <i>CEIL</i>	

\* May be eutectic.

4. *Al-Cu-Mn-Fe-Si.*

The tetrahedral model is reproduced in Fig. 62 (Plate LXXIII). Table XXV gives the equilibrium reactions at the surfaces which, in Fig. 62, correspond to melt in equilibrium with solid aluminium and two other solid phases. For the surface *AB* a eutectic and a peritectic reaction have been given; the eutectic reaction is probably valid at a high relative content of iron.

Fig. 63 (Plate LXXIII) shows sections through the tetrahedral model



TABLE XXV.—*Equilibrium Reactions in Al-Cu-Mn-Fe-Si System.*

Key		Surfaces		Lines		Points	
Symbol	Phase Denoted	Peritectic	Solid Reactant	Peritectic	Solid Reactant(s)	Peritectic	Solid Reactant(s)
<i>A</i>	Al <sub>3</sub> Fe	<i>AB</i> *	<i>A</i>	<i>ABK</i>	<i>A (B)</i>	<i>BCDK</i>	<i>B</i>
<i>B</i>	(Al,Cu) <sub>6</sub> (Mn,Fe,Cu)	<i>AK</i>	<i>A</i>	<i>BCD</i>	<i>B</i>	<i>CIKM</i>	<i>M</i>
<i>C</i>	Al <sub>7</sub> Cu <sub>2</sub> Fe	<i>BC</i>	<i>B</i>	<i>BCK</i>	<i>B</i>		
<i>D</i>	<i>r</i> -AlCuMn	<i>BD</i>	<i>B</i>				
<i>E</i>	Al <sub>2</sub> Cu	<i>BK</i>	<i>B</i>	<i>BDK</i>	<i>B</i>		
		<i>CK</i> *	<i>K</i>	<i>CDK</i> *	<i>C</i>		
<i>I</i>	Si	<i>CM</i> *	<i>M</i>	<i>CIM</i>	<i>M</i>		
<i>K</i>	<i>c</i> -Al(Fe,Mn)Si	<i>DK</i> *	<i>D</i>	<i>CKM</i>	<i>K (M)</i>		
<i>M</i>	<i>m</i> -AlFeSi	<i>KM</i> *	<i>K</i>	<i>DEK</i>	<i>D</i>		
				<i>IKM</i> *	<i>K</i>		
		Eutectic		Eutectic		Eutectic	
		<i>CD, CE, CI, DE, EI, EK, IK, IM</i>		<i>CDE, CEI, CEK, CIK, EIK</i>		<i>CEIK</i>	

\* May be eutectic.

(Fig. 62) for relative contents of 2, 5, 10, and 20% manganese, and for 2 and 5% silicon. The phases which may be in equilibrium with solid aluminium and melt within the different regions of the diagram have been indicated.

TABLE XXVI.—*Equilibrium Reactions in Al-Mg-Mn-Fe-Si System.*

Key		Surfaces		Lines		Points	
Symbol	Phase Denoted	Peritectic	Solid Reactant	Peritectic	Solid Reactant(s)	Peritectic	Solid Reactant
<i>A</i>	Al <sub>3</sub> Fe	<i>AK</i>	<i>A</i>	<i>ABJ</i>	<i>A, B</i>	<i>ABKJ</i>	<i>K</i>
<i>B</i>	Al <sub>6</sub> (Mn,Fe)	<i>BK</i>	<i>B</i>	<i>AJK</i> *	<i>A</i>	<i>IKMN</i>	<i>M</i>
<i>G</i>	$\beta$ -AlMg	<i>KM</i> *	<i>K</i>	<i>BJK</i>	<i>K</i>	<i>JKMN</i>	<i>M</i>
<i>I</i>	Si	<i>MN</i>	<i>M</i>	<i>IKM</i> *	<i>K</i>		
<i>J</i>	Mg <sub>2</sub> Si			<i>IMN</i>	<i>M</i>		
<i>K</i>	<i>c</i> -Al(Mn,Fe)Si			<i>JKM</i>	<i>K</i>		
<i>M</i>	<i>m</i> -AlFeSi			<i>JMN</i>	<i>M</i>		
<i>N</i>	<i>h</i> -AlMgFeSi			<i>KMN</i>	<i>M</i>		
		Eutectic		Eutectic		Eutectic	
		<i>AB, AG, AJ, BG, BJ, GJ, IJ, IK, IM, IN, JK, JM, JN, KN</i>		<i>ABG, ABJ, AGJ, BGJ, IJK, IJN, IKN, JKN</i>		<i>ABGJ, IJKN</i>	

\* May be eutectic.

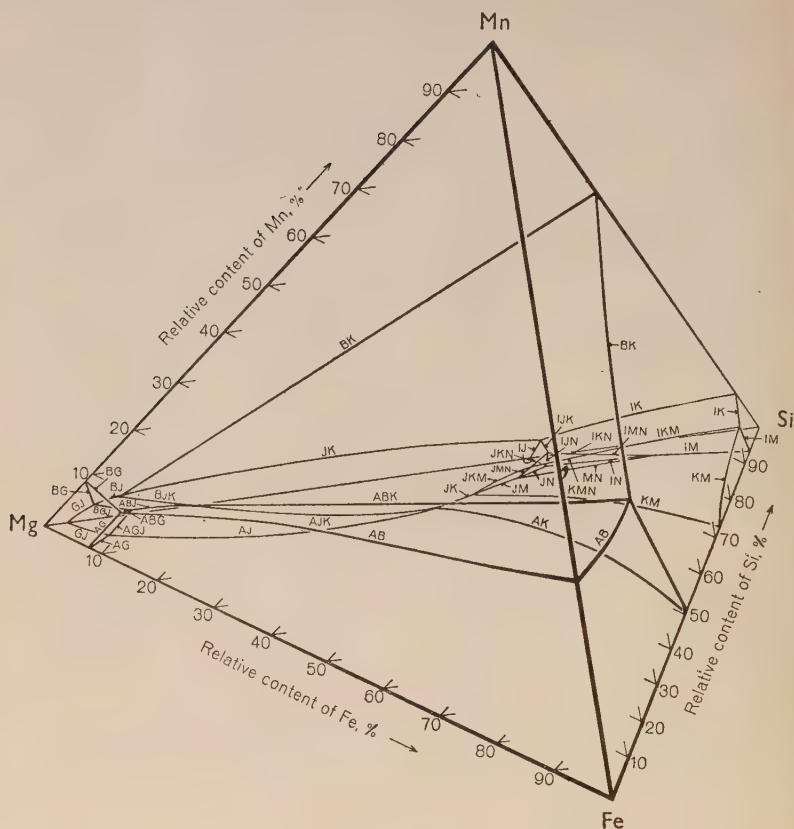


FIG. 56.—The Al-Mg-Mn-Fe-Si System.

### 5. *Al-Mg-Mn-Fe-Si.*

Fig. 56 shows the tetrahedral model for this system. Table XXVI gives the key and indicates the equilibrium reactions involved.

In Fig. 57 are given sections through the tetrahedral model (Fig. 56) for relative contents of 2, 5, 10, and 20% manganese. The phases have been indicated which may be in equilibrium with solid aluminium and melt in the different regions.

Fig. 49 (Plate LXXII) is a photomicrograph of an alloy containing magnesium 10, manganese 1.5, iron 1, and silicon 0.15%, or, in relative contents, iron 7.9, magnesium 79.0, manganese 11.9, and silicon 1.2%. The phase which first separates from the melt is probably  $Al_6(Mn,Fe)$ .

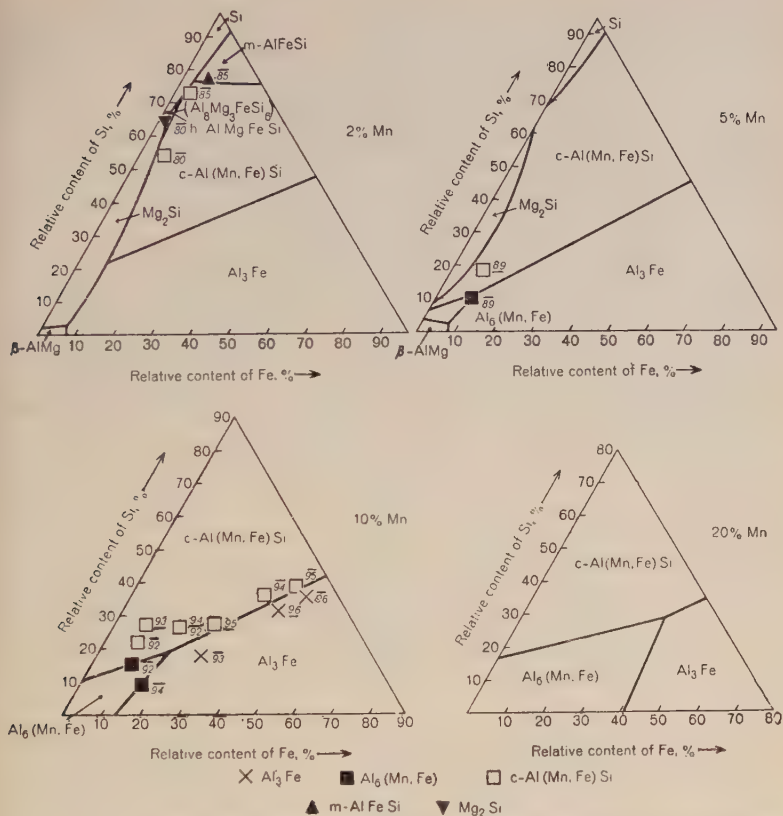


FIG. 57.—The Al-Mg-Mn-Fe-Si System. Sections for various relative manganese contents.

## VII.—SENARY SYSTEM.

### *Al-Cu-Mg-Mn-Fe-Si.*

In the system Al-Cu-Mg-Mn-Fe-Si no phases other than those occurring in the subsidiary systems with five components have been found. The investigation has, however, been limited to those aluminium alloys in which firstly copper, and secondly magnesium and manganese (in certain cases also silicon) form the main alloying constituents.

To describe the system, diagrams have been used which may be considered as sections through projections of the kind described on p. 494. Equilibrium between melt, solid aluminium, and one other phase corresponds to a space region, while melt, aluminium, and two

other phases coexist over a surface; melt, aluminium, and three other phases are in equilibrium along a line, and melt, aluminium, and four other phases at a point. For certain special sections it is, however, possible that a surface degenerates into a line which then corresponds to melt and aluminium in equilibrium with four other phases; and, similarly, that a line is reduced to a point, which then represents melt and aluminium in equilibrium with five other phases. In the diagrams only the relative contents of the melt have been shown.

The difficulty of determining the order of solidification, which was appreciable with five components, is considerably enhanced when the number of components is increased to six. No great degree of accuracy can therefore be claimed for the diagrams here proposed for the system Al-Cu-Mg-Mn-Fe-Si. It should, however, be sufficient to allow the order of solidification to be estimated in the alloys to which this investigation was limited.

No detailed attempt was made to study the six-component system experimentally. The order of solidification was, however, studied in two alloys, both cast in a refractory-brick mould. One of these contained copper 8.6, magnesium 3.0, manganese 1.0, iron 0.8, and silicon 0.6%. Primary crystals of  $(\text{Al,Cu})_6(\text{Mn,Fe,Cu})$  were observed, and also relatively large crystals of  $\text{Mg}_2\text{Si}$ . In eutectic mixture with aluminium rather large grains of  $\text{Al}_2\text{Cu}$  appeared, together with fine-grained  $\text{Al}_2\text{Cu}$  and  $\text{Al}_2\text{CuMg}$ . The other alloy contained copper 8.2, magnesium 2.3, manganese 2.1, iron 0.8, and silicon 1.2%. Small needles of  $(\text{Al,Cu})_6(\text{Mn,Fe,Cu})$  and grains of  $c\text{-Al}(\text{Mn,Fe})\text{Si}$  appeared to have recrystallized before solid aluminium. Between the dendrites  $\text{Mg}_2\text{Si}$ ,  $\text{Al}_2\text{Cu}$ , and  $\text{Al}_2\text{CuMg}$  were observed. Figs. 64 (a)–(e) (Plate LXXIV) show the sections for the senary system for relative manganese contents of 0, 2, 5, 10, and 20%. The section for 0% manganese has been included in order to facilitate the interpretation. For every bounded region in the diagram the corresponding phase in equilibrium with melt and solid aluminium has been indicated. The equilibria which occur in this system between melt, solid aluminium, and one other solid phase are probably in all cases eutectic. The equilibrium reactions correspond to the equilibria in the subsidiary systems with five components where such a correspondence is possible.

## VIII.—DISCUSSION.

### 1. *Etching and Other Properties of Phases.*

The etching properties found for the various phases in the present investigation, and their colour in ordinary and polarized light, are

given in Table XXVII (Plate LXXV). This table also shows which phases correspond to those appearing in the etching tables published by Keller and Wilcox,<sup>9</sup> by Schrader,<sup>10, 11</sup> and by Mondolfo.<sup>66</sup>

The data included in Table XXVII with regard to the colours of the phases in polarized light were obtained by means of observations made with a Reichert microscope with crossed Nicol prisms, using objective Epilum 15 and ocular 10  $\times$ . As vertical illuminator a transparent glass mirror was used, and as illuminating source an A.C. carbon arc. Practically identical results were obtained in some corresponding observations made with a Zeiss Neophot microscope, using a D.C. carbon arc as the illuminating source (objective Achromate 18  $\times$  and ocular 10  $\times$ ).

For a phase with a range of homogeneity, the etching properties may vary with the composition. According to Table XXVII (Al,Cu)<sub>6</sub>(Mn,Fe,Cu) and *c*-Al(Mn,Fe)Si show such variations in their etching properties. Al<sub>6</sub>Mn is generally not attacked by hydrofluoric acid (1 : 200) under the conditions given in the table, while (Al,Cu)<sub>6</sub>(Mn,Fe,Cu) is slightly etched and acquires a light brown colour. Further, hydrofluoric acid (1 : 200), employed as described, does not attack *c*-AlMnSi, but *c*-Al(Fe,Cu)Si is coloured light brown. (Al,Cu)<sub>6</sub>(Mn,Fe,Cu) and *c*-Al(Mn,Fe)Si have very wide homogeneity ranges. Table XXVII shows, however, that the etching reaction may vary considerably also for a phase with a narrow homogeneity range, such as Al<sub>3</sub>Fe. When free from copper, this phase is not etched by hydrofluoric acid, but with copper in solution it presents a spotted brown appearance.

In certain cases variations in the etching properties have been found which probably do not depend on variations in the composition of the phase in question, but rather on differences in the composition of the aluminium phase. From Table XXVII it seems clear that the magnesium content, in particular, of the aluminium phase may have some influence on the etching properties. Thus, *c*-AlFeSi is not etched by hydrofluoric acid (1 : 200) if the magnesium content of the alloy is low, but it is slightly etched if the magnesium content is higher.

The results obtained in this investigation concerning crystal system, crystal form, lattice dimensions, and density of the different phases have been collected in Table XXVIII, which contains also references to data on the atomic arrangements where these are known.

## 2. *Commercially Important Alloys.*

In Table XXIX are listed some commercially important alloys representative of the type of alloy to which this investigation has been



TABLE XXVIII.—*Crystal Structure*

Phase	Analyses of Phases with Extended Homogeneity Range					Crystal System
	Cu, %	Mg, %	Mn, %	Fe, %	Si, %	
Si	...	...	...	...	...	Cubic
Al <sub>2</sub> Cu	...	...	...	...	...	Tetragonal
Al <sub>2</sub> CuMg	...	...	...	...	...	Orthorhombic
c-AlCuMg	...	...	...	...	...	Cubic
β-AlMg	...	...	...	...	...	Cubic
Mg <sub>2</sub> Si	...	...	...	...	...	Cubic
Al <sub>7</sub> Cu <sub>2</sub> Fe	...	...	...	...	...	Tetragonal
r-AlCuMn	...	...	...	...	...	Orthorhombic
h-AlMgFeSi (Al <sub>8</sub> Mg <sub>3</sub> FeSi <sub>6</sub> )	...	...	...	...	...	Hexagonal
h-AlCuMgSi	...	...	...	...	...	Hexagonal
Al <sub>8</sub> Mn	...	...	...	...	...	Orthorhombic
Al <sub>8</sub> (Mn,Fe)	...	...	12.0 *	14.6 *	...	
(Al,Cu) <sub>8</sub> (Mn,Fe,Cu)	1.9	...	8.5	18.7	...	
(Al,Cu) <sub>8</sub> (Fe,Cu)	8.0	0.0	...	22.8	...	
Al <sub>2</sub> Fe	...	...	...	...	...	Orthorhombic
c-AlMnSi	...	...	26.6	...	8.0	Cubic
c-Al(Mn,Fe)Si	...	...	15.7	16.1	6.8	
c-AlFeSi	...	...	...	31.9	6.6	
m-AlFeSi	...	...	...	...	...	
t-AlFeSi	...	...	...	...	...	Monoclinic (pseudo-tetragonal)
						Tetragonal

\* The analytical data were obtained on crystals of Al<sub>8</sub>(Mn,Fe) isolated from an alloy containing iron 2 and manganese 1.5%; while the crystals of the same phase, from which the lattice dimensions given in the table were obtained, were isolated from an alloy containing iron 2.5 and manganese 1.5%. The Al<sub>8</sub>(Mn,Fe) phase is probably in both cases saturated with iron.

TABLE XXIX.—*Commercially Important Alloys.*

Al- loy	Content, %					Relative Content, %					Phases Likely to Occur
	Cu	Mg	Mn	Fe *	Si *	Cu	Mg	Mn	Fe	Si	
16S	2.2	0.3	...	0.3	0.3	70.0	10.0	...	10.0	10.0	c-AlFeSi, Al <sub>7</sub> Cu <sub>2</sub> Fe, Si, Al <sub>2</sub> Cu, h-AlCuMgSi
17S	4.0	0.5	0.5	0.3	0.3	71.0	9.0	9.0	5.5	5.5	(Al,Cu) <sub>8</sub> (Mn,Fe,Cu), c-Al(Mn,Fe)Si, Al <sub>2</sub> Cu, Al <sub>7</sub> Cu <sub>2</sub> Fe, Mg <sub>2</sub> Si, Al <sub>2</sub> CuMg
22S	4.0	0.5	0.5	0.3	1.25	61.0	7.7	7.7	4.6	19.0	c-Al(Mn,Fe)Si, Mg <sub>2</sub> Si?, h-AlCuMgSi, Si, Al <sub>2</sub> Cu, Al <sub>7</sub> Cu <sub>2</sub> Fe
24S	4.2	1.5	0.5	0.3	0.3	61.5	22.0	7.5	4.5	4.5	(Al,Cu) <sub>8</sub> (Mn,Fe,Cu)?, † c-Al(Mn,Fe)Si, Mg <sub>2</sub> Si, Al <sub>2</sub> Cu, Al <sub>2</sub> CuMg, Al <sub>7</sub> Cu <sub>2</sub> Fe
26S	4.4	0.4	0.8	0.3	0.8	66.0	5.5	12.0	4.5	12.0	c-Al(Mn,Fe)Si, Al <sub>2</sub> Cu, Mg <sub>2</sub> Si?, h-AlCuMgSi, Si, Al <sub>7</sub> Cu <sub>2</sub> Fe

\* The alloys were assumed to contain 0.3% each of iron and silicon as impurities.

† Hofmann<sup>22</sup> has found (Al,Cu)<sub>8</sub>(Mn,Fe,Cu) in ingot metal.

## Data and Density of Phases.

Crystal Form	Lattice Constants				Atomic Arrangement	Density, g./c.c.
	$a_1$ , kX.	$a_2$ , kX.	$a_3$ , kX.	$\alpha_4$		
Octahedra {111}.	5.147	...	...	...	Known	...
Needles {110}.	6.052	...	4.878	...	Known (20, 21)	...
Needles {010} and {021} combined.	4.00	9.23	7.14	...	Known (40), see Appendix	...
Rhombic dodecahedra {110} modified by cubes {100}.	14.28	...	...	...	Unknown	...
Octahedra {111}, sometimes modified by cubes {100}.	28.16	...	...	...	Unknown	2.24
Plates or lamellae {001}.	6.391	...	...	...	Known (53)	...
Needles. Often twins.	6.32	...	14.78	...	Known (48), see Appendix	>4.1
Trigonal tablets bounded by {001} and {100}.	...	...	...	...	Unknown	3.70
Needles.	6.62	...	7.92	...	Known (64), see Appendix	2.82
Needles {110} bounded at the ends by {001}.	10.30	...	4.04	...	Unknown	2.79
Flat needles bounded by {110} and {100}. Needle axis [001]. Often twins on {110}.	6.485	7.525	8.840	...	Unknown	3.27
	6.482	7.483	8.819	...		...
	6.452	7.473	8.794	...		...
	6.428	7.449	8.768	...		3.56
Cubes {100}.	48.04	15.59	8.10	...	Unknown	3.83
Rhombic dodecahedra {110}.	12.625	...	...	...	Unknown	3.55
"	12.63	...	...	...		...
"	12.523	...	...	...		3.61
Pseudo-tetragonal plates or lamellae {001}. Twins on {001}.	6.11*	6.11	41.4	91°	Unknown	3.39
Tetragonal plates bounded by {001} and {110}.	6.11	...	9.46	...	Unknown	3.43

The numbers in parentheses relate to the references at the end of the paper.

TABLE XXX.—Metastable and Stable Phases.

Alloy	Metastable (Enveloped) Phases	Stable Phases
16S	$c$ -AlFeSi	$Al_2Cu$ , $Al_7Cu_2Fe$ , Si, $h$ -AlCuMgSi
17S	$(Al,Cu)_6(Mn,Fe,Cu)$ , $c$ -Al(Mn,Fe)Si	$Al_2Cu$ , $Al_7Cu_2Fe$ , $Al_2CuMg$ , $Mg_2Si$
22S	$c$ -Al(Mn,Fe)Si, $Mg_2Si$	$Al_2Cu$ , $Al_7Cu_2Fe$ , Si, $h$ -AlCuMgSi
24S	$(Al,Cu)_6(Mn,Fe,Cu)$ , $c$ -Al(Mn,Fe)Si	$Al_2Cu$ , $Al_7Cu_2Fe$ , $Al_2CuMg$ , $Mg_2Si$
26S	$c$ -Al(Mn,Fe)Si, $Mg_2Si$	$Al_2Cu$ , $Al_7Cu_2Fe$ , Si, $h$ -AlCuMgSi

limited. The phases which, according to Figs. 54 and 64, may be expected to occur in these alloys are also indicated in the table. These are: silicon,  $Al_2Cu$ ,  $Al_2CuMg$ ,  $Mg_2Si$ ,  $Al_7Cu_2Fe$ ,  $h$ -AlCuMgSi,  $(Al,Cu)_6(Mn,Fe,Cu)$ , and  $c$ -Al(Mn,Fe)Si.\* As the solidification process proceeds, some of these phases will be practically enveloped by other

\*  $h$ -AlMgFeSi is probably present in a casting alloy with silicon 7 and magnesium 0.3%, or in the alloy 51S with silicon 1 and magnesium 0.6%, since in both cases the alloy contains some iron.

phases, which will be in equilibrium with the last portions of aluminium to solidify. The metastable and stable phases in the alloys in question may be tentatively listed as shown in Table XXX.

Without a knowledge of the composition of the solid aluminium phase in the senary alloys, it is difficult to say whether  $(\text{Al,Cu})_6(\text{Mn,Fe,Cu})$  and  $c\text{-Al}(\text{Mn,Fe})\text{Si}$  are metastable or stable.

#### ACKNOWLEDGEMENTS.

The extensive research work reported in this paper was conducted by the late Mr. Gösta Phragmén, partly at the Metallografiska Institutet, Stockholm, and partly at Fingspöngs Metallverk, now the Svenska Metallverken, Finspång, where he was assisted by Mr. Å. Josefsson. The preparation of the paper was undertaken by Mr. Per Spiegelberger, Lic.Phil., of the Metallografiska Institutet, Stockholm, in collaboration with former colleagues of Mr. Phragmén's. The English translation, which was made by Mr. E. Öhman, now at Jernkontoret, Stockholm, has been revised and edited for publication by Mr. H. W. L. Phillips, M.A., and Professor G. V. Raynor, M.A., D.Sc., to whom the Publication Committee expresses its warm thanks.

Professor E. G. Rudberg, Ph.D., Mr. Phragmén's successor as Director of the Metallografiska Institutet, submitted the paper for publication.

#### REFERENCES.

1. F. Keller and C. M. Craighead, *Trans. Amer. Inst. Min. Met. Eng.*, 1936, **122**, 321.
2. E. H. Dix, Jr., and A. C. Heath, Jr., *Trans. Amer. Inst. Min. Met. Eng., Inst. Metals Div.*, 1928, 164.
3. W. Fraenkel and L. Marx, *Z. Metallkunde*, 1929, **21**, 2.
4. K. L. Meissner, *Z. Metallkunde*, 1929, **21**, 328.
5. W. Koeh and F. W. Nothing, *Aluminium*, 1935, **17**, 535.
6. H. Y. Hunsicker, *Symposium on Age-Hardening of Metals (Amer. Soc. Metals)*, 1940, 56.
7. K. L. Dreyer and H. J. Seemann, *Metallwirtschaft*, 1941, **20**, 625.
8. E. H. Dix, Jr., and W. D. Keith, *Proc. Amer. Soc. Test. Mat.*, 1926, **26**, (II), 317.
9. F. Keller and G. W. Wilcox, *Metal Progress*, 1933, **23**, (2), 44; (4), 45; (5), 38.
10. A. Schrader, "Ätzheft", p. 15.\* Berlin: 1939 (Gebrüder Borntraeger).
11. T. Berglund (revised by A. Meyer), "Handbuch der metallographischen Schleif-, Polier- und Ätzverfahren", pp. 244-245. Berlin: 1940 (Julius Springer).
12. A. Wilm, *Metallurgie*, 1911, **8**, 225.
13. R. Vogel, "Die heterogenen Gleichgewichte" ("Handbuch der Metallphysik", Band II), p. 669. Leipzig: 1937 (Akademische Verlagsgesellschaft m.b.H.).
14. H. W. Bakhuys Roozeboom, *Z. physikal. Chem.*, 1894, **15**, 145.
15. N. Parravano and G. Sirovich, *Gazz. Chim. Ital.*, 1912, **42**, (I), 113.

\* In a later edition (Berlin, 1941) some minor changes have been made concerning the phases which are of interest in connection with the present work. The designations *N* (Al-Cu-Fe) and *Q* (Al-Cu-Mg-Si) have been replaced, respectively, by *N* ( $\text{Al}_6\text{Cu}_2\text{Fe}$ ) and *Q*<sub>Si</sub> (Al-Cu-Mg-Si).

16. N. Parravano and G. Sirovich, *Gazz. Chim. Ital.*, 1912, **42**, (I), 630.
17. A. Schrader and H. Hanemann, *Z. Metallkunde*, 1943, **35**, 185.
18. F. Wöhler, [*Liebigs*] *Ann. Chem.*, 1860, **115**, 102.
19. G. Phragmén, *J. Inst. Metals*, 1933, **52**, 117 (discussion).
20. E. R. Jette, G. Phragmén, and A. Westgren, *J. Inst. Metals*, 1924, **31**, 193.
21. J. B. Friauf, *J. Amer. Chem. Soc.*, 1927, **49**, 3107.
22. Gmelins "Handbuch der anorganischen Chemie", System-Nummer 35, "Aluminium", Teil A, Lief. 5, p. 645. Berlin: 1937 (Verlag Chemie G.m.b.H.).
23. G. Grube, *Z. anorg. Chem.*, 1905, **45**, 225.
24. D. Hanson and M. L. V. Gayler, *J. Inst. Metals*, 1920, **24**, 201.
25. M. Kawakami, *Kinzoku-no-Kenkyu*, 1933, **10**, 532.
26. T. Halstead and D. P. Smith, *Trans. Amer. Electrochem. Soc.*, 1926, **49**, 291.
27. W. L. Fink and L. A. Willey, *Metals Handbook* (Amer. Soc. Metals), 1939, 1226.
28. W. L. Fink and L. A. Willey, *Trans. Amer. Inst. Min. Met. Eng.*, 1937, **124**, 78.
29. N. S. Kurnakov and V. I. Mikheeva, *Izvest. Sek. Fiziko-Khim. Anal.*, 1940, **13**, 209.
30. K. Riederer, *Z. Metallkunde*, 1936, **28**, 312.
31. H. Perlitz, *Nature*, 1944, **154**, 606.
32. E. H. Dix, Jr., W. L. Fink, and L. A. Willey, *Trans. Amer. Inst. Min. Met. Eng.*, 1933, **104**, 335.
33. W. Hofmann, *Aluminium*, 1938, **20**, 865.
34. E. Bachmetew, *Z. Krist.*, 1934, [A], **88**, 179, 575.
35. A. J. Bradley and A. Taylor, *Proc. Roy. Soc.*, 1938, [A], **166**, 353.
36. H. Hanemann and A. Schrader, "Atlas Metallographicus", Band III, Teil 1, p. 69. Berlin: 1941 (Gebrüder Borntraeger).
37. F. Laves, K. Löhberg, and H. Witte, *Metallwirtschaft*, 1936, **14**, 793.
38. H. Nishimura, *Mem. Coll. Eng. Kyōtō Imp. Univ.*, 1937, **10**, 18.
39. F. Laves and H. Witte, *Metallwirtschaft*, 1936, **15**, 15.
40. H. Perlitz and A. Westgren, *Arkiv Kemi, Min. Geol.*, 1943, [B], **16**, (13).
41. H.-G. Petri, *Aluminium-Archiv*, 1939, (14).
42. G. V. Raynor, *J. Inst. Metals*, 1944, **70**, 531.
43. M. K. B. Day and H. W. L. Phillips, *J. Inst. Metals*, 1948, **74**, 33.
44. A. G. C. Gwyer, H. W. L. Phillips, and L. Mann, *J. Inst. Metals*, 1928, **40**, 318.
45. K. Yamaguchi and I. Nakamura, *Rikwagaku Kenkyū-jo Ihō*, 1932, **11**, 815.
46. A. J. Bradley and H. J. Goldschmidt, *J. Inst. Metals*, 1939, **65**, 389.
47. H. Wiehr, *Aluminium-Archiv*, 1940, (31).
48. A. Westgren, private communication.
49. H. Töllner, *Aluminium-Archiv*, 1940, (34).
50. C. Hisatsune, *Mem. Coll. Eng. Kyōtō Imp. Univ.*, 1935, **9**, 18.
51. W. G. Leemann, *Aluminium-Archiv*, 1938, (9).
52. M. Barnick and H. Hanemann, *Aluminium*, 1938, **20**, 533.
53. E. A. Owen and G. D. Preston, *Proc. Phys. Soc. (Lond.)*, 1924, **36**, 341.
54. D. Hanson and M. L. V. Gayler, *J. Inst. Metals*, 1921, **26**, 321.
55. E. Degischer, *Aluminium-Archiv*, 1939, (18).
56. H. W. L. Phillips, *J. Inst. Metals*, 1943, **69**, 305.
57. H. Bückle, *Aluminium-Archiv*, 1939, (13).
58. A. G. C. Gwyer and H. W. L. Phillips, *J. Inst. Metals*, 1927, **38**, 29.
59. H. W. L. Phillips and P. C. Varley, *J. Inst. Metals*, 1943, **69**, 317.
60. W. Jäniche, *Aluminium-Archiv*, 1936, (5).
61. W. L. Fink and K. R. Van Horn, *Trans. Amer. Inst. Min. Met. Eng., Inst. Metals Div.*, 1931, 383.
62. E. H. Dix, Jr., G. F. Sager, and B. P. Sager, *Trans. Amer. Inst. Min. Met. Eng.*, 1932, **99**, 119.
63. D. A. Petrov, *Acta Physicochim. U.R.S.S.*, 1937, **6**, 505.
64. H. Perlitz and A. Westgren, *Arkiv Kemi, Min. Geol.*, 1942, [B], **15**, (16).
65. H. W. L. Phillips, *J. Inst. Metals*, 1946, **72**, 151.
66. L. Mondolfo, "Metallography of Aluminium Alloys". New York: 1943 (John Wiley and Sons).
67. D. W. Wakeman and G. V. Raynor, *J. Inst. Metals*, 1948-49, **75**, 131.

## APPENDIX.—Atomic Arrangement of Ternary and More Complex Phases.

 $Al_2CuMg$ . Orthorhombic,  $a_1 = 4.00$ ;  $a_2 = 9.28$ ;  $a_3 = 7.14$  kX.Space group  $D_{2h}^{17} - Cmc$  (000;  $\frac{1}{2}\frac{1}{2}0$ ) +8 Al in 8 (f):  $0y_1z_1$ ;  $0\bar{y}_1\bar{z}_1$ ;  $0, y_1, \frac{1}{2} - z_1$ ;  $0, \bar{y}_1, \frac{1}{2} + z_1$ .4 Cu in 4 (c):  $0y_2\frac{1}{4}$ ;  $0y_2\frac{3}{4}$ .4 Mg in 4 (c):  $0y_3\frac{1}{4}$ ;  $0y_3\frac{3}{4}$ .With  $2\pi y_1 = 128^\circ$ ;  $2\pi z_1 = 20^\circ$ ;  $2\pi y_2 = -80^\circ$ ;  $2\pi y_3 = 26^\circ$ . $Al_7Cu_2Fe$ . Tetragonal,  $a_1 = 6.32$ ;  $a_3 = 14.78$  kX.Space group  $D_{4h}^6 - P4/mnc$ .4 Al in 4 (e):  $00z_1$ ;  $00\bar{z}_1$ ;  $\frac{1}{2}, \frac{1}{2}, \frac{1}{2} + z_1$ ;  $\frac{1}{2}, \frac{1}{2}, \frac{1}{2} - z_1$ ;  $2\pi z_1 = 44^\circ$ .4 Fe in 4 (e):  $00z_2$ ;  $00\bar{z}_2$ ;  $\frac{1}{2}, \frac{1}{2}, \frac{1}{2} + z_2$ ;  $\frac{1}{2}, \frac{1}{2}, \frac{1}{2} - z_2$ ;  $2\pi z_2 = 108^\circ$ .8 Cu in 8 (h):  $x_3y_30$ ;  $\bar{x}_3\bar{y}_30$ ;  $\frac{1}{2} + x_3, \frac{1}{2} - y_3, \frac{1}{2}$ ;  $\frac{1}{2} - x_3, \frac{1}{2} + y_3, \frac{1}{2}$ ;  
 $\bar{y}_3x_30$ ;  $y_3\bar{x}_30$ ;  $\frac{1}{2} + y_3, \frac{1}{2} + x_3, \frac{1}{2}$ ;  $\frac{1}{2} - y_3,$   
 $\frac{1}{2} - x_3, \frac{1}{2}$ ;  $2\pi x_3 = 100^\circ$ ,  $2\pi y_3 = 33^\circ$ .8 Al in 8 (g):  $x_4, \frac{1}{2} + x_4, \frac{1}{4}$ ;  $\bar{x}_4, \frac{1}{2} - x_4, \frac{1}{4}$ ;  $\frac{1}{2} + x_4, \bar{x}_4, \frac{1}{4}$ ;  $\frac{1}{2} - x_4,$   
 $x_4, \frac{1}{4}$ ;  
 $x_4, \frac{1}{2} + x_4, \frac{3}{4}$ ;  $\bar{x}_4, \frac{1}{2} - x_4, \frac{3}{4}$ ;  $\frac{1}{2} + x_4, \bar{x}_4, \frac{3}{4}$ ;  
 $\frac{1}{2} - x_4, x_4, \frac{3}{4}$ ;  $2\pi x_4 = 60^\circ$ .16 Al in 16 (i):  $x_5y_5z_5$ ;  $\bar{x}_5\bar{y}_5\bar{z}_5$ ;  $\frac{1}{2} + x_5, \frac{1}{2} - y_5, \frac{1}{2} + z_5$ ;  
 $\frac{1}{2} - x_5, \frac{1}{2} + y_5, \frac{1}{2} + z_5$ ;  
 $x_5y_5\bar{z}_5$ ;  $\bar{x}_5\bar{y}_5z_5$ ;  $\frac{1}{2} + x_5, \frac{1}{2} - y_5, \frac{1}{2} - z_5$ ;  
 $\frac{1}{2} - x_5, \frac{1}{2} + y_5, \frac{1}{2} - z_5$ ;  
 $\bar{y}_5x_5z_5$ ;  $y_5\bar{x}_5z_5$ ;  $\frac{1}{2} + y_5, \frac{1}{2} + x_5, \frac{1}{2} + z_5$ ;  
 $\frac{1}{2} - y_5, \frac{1}{2} - x_5, \frac{1}{2} + z_5$ ;  
 $\bar{y}_5x_5\bar{z}_5$ ;  $y_5\bar{x}_5\bar{z}_5$ ;  $\frac{1}{2} + y_5, \frac{1}{2} + x_5, \frac{1}{2} - z_5$ ;  
 $\frac{1}{2} - y_5, \frac{1}{2} - x_5, \frac{1}{2} - z_5$ ;  
 $2\pi x_5 = 73^\circ$ ,  $2\pi y_5 = 149^\circ$ ,  $2\pi z_5 = 36^\circ$ . $h-AlMgFeSi$ . Hexagonal,  $a_1 = 6.62$ ;  $a_3 = 7.92$  kX.Space group  $D_{3h}^3 - C\bar{6}2m$ .

1 Fe in 1 (a): 000.

1 Al in 1 (b):  $00\frac{1}{2}$ .3 Al in 3 (f):  $x_100$ ;  $0x_10$ ;  $\bar{x}_1\bar{x}_10$ ;  $2\pi x_1 = 145^\circ$ .3 Mg in 3 (g):  $x_20\frac{1}{2}$ ;  $0x_2\frac{1}{2}$ ;  $\bar{x}_2\bar{x}_2\frac{1}{2}$ ;  $2\pi x_2 = 160^\circ$ .4 Al in 4 (h):  $\frac{1}{3}, \frac{2}{3}z_4$ ;  $\frac{1}{3}, \frac{2}{3}\bar{z}_4$ ;  $\frac{2}{3}, \frac{1}{3}z_4$ ;  $\frac{2}{3}, \frac{1}{3}\bar{z}_4$ ;  $2\pi z_4 = 83^\circ$ .6 Si in 6 (i):  $x_30z_3$ ;  $0x_3z_3$ ;  $\bar{x}_3\bar{x}_3z_3$ ;  $2\pi x_3 = 270^\circ$ . $x_30\bar{z}_3$ ;  $0x_3\bar{z}_3$ ;  $\bar{x}_3\bar{x}_3\bar{z}_3$ ;  $2\pi z_3 = 80^\circ$ .



Phase Nomenclature According to Authorities Named

Colour in :

Etching Reactions

For convenience of reference	Schröder (10), (11)	Keller and Wilcox (8)	Monbaliu (12)	Ordinary Light	Polarized Light	20 ml. H <sub>2</sub> SO <sub>4</sub> (sp. gr. 1.84), 80 ml. H <sub>2</sub> O, 70° C., 30 sec.	0.5 ml. HF (40%), 100 ml. H <sub>2</sub> O, 20° C., 15 sec.	0.5 ml. HF (40%), 1.5 ml. HCl (sp. gr. 1.19), 2-3 ml. HNO <sub>3</sub> (sp. gr. 1.40), 95-50 H <sub>2</sub> O, 20° C., 15 sec.	10 ml. H <sub>2</sub> PO <sub>4</sub> (sp. gr. 1.70), 100 ml. H <sub>2</sub> O, 20° C., 2 min.	25 ml. HNO <sub>3</sub> (sp. gr. 1.40), 75 ml. H <sub>2</sub> O, 70° C., 10 sec.	100 g. Fe (SiO <sub>2</sub> 0.3), 200 ml. H <sub>2</sub> O, 20° C., 20 sec.	1 g. NaOH, 100 ml. H <sub>2</sub> O, 50° C., 15 sec.	10 g. NaOH, 100 ml. H <sub>2</sub> O, 70° C., 5 sec.
Si	Si	Si	Si	Dark violet. Transparent.	Does not change.	None.	None.	None.	None.	None.	None.	None.	None.
Al <sub>2</sub> O <sub>3</sub>	Al <sub>2</sub> O <sub>3</sub>	Al <sub>2</sub> O <sub>3</sub>	Al <sub>2</sub> O <sub>3</sub>	Light.	Orange greenish-blue.	None.	None.	None.	None.	Heavily attacked. Coloured dark brown.	Coloured dark brown.	Coloured greyish-brown to violet-brown.	Coloured yellowish-brown to violet-brown.
Al <sub>2</sub> O <sub>3</sub> Mg	8 (Al <sub>2</sub> O <sub>3</sub> Mg <sub>2</sub> ) (38)	Al <sub>2</sub> O <sub>3</sub> Mg	Cu <sub>2</sub> Mg <sub>3</sub> Al <sub>4</sub>	Darkens on polishing.	Purple-yellowish-grey.	Coloured dark brown.	Often coloured brown.	Coloured brown.	Coloured brown.	Heavily attacked. Coloured dark brown.	Coloured dark brown.	None.	Generally coloured light brown.
Al <sub>2</sub> O <sub>3</sub> Mg	7 (Al <sub>2</sub> O <sub>3</sub> Mg <sub>2</sub> ) (38)	...	Cu <sub>2</sub> Mg <sub>3</sub> Al <sub>4</sub>	Light. Darkens on polishing.	Does not change.	Heavily attacked. Dark coloured.	Heavily attacked. Darkened.	Heavily attacked. Darkened.	Coloured intense brown.	Heavily attacked.	Darkened.	None.	None.
β-AlMg	β-Al <sub>2</sub> Mg <sub>3</sub>	β-AlMg	Mg <sub>2</sub> Al <sub>3</sub>	Light.	Does not change.	Heavily attacked.	Slightly attacked.	Slightly attacked.	Slightly attacked.	Slightly attacked.	Slightly attacked.	None.	None.
Mg <sub>2</sub> Si	Mg <sub>2</sub> Si	Mg <sub>2</sub> Si	Mg <sub>2</sub> Si	Light. Blue after wet polishing.	Does not change.	Heavily attacked.	Heavily attacked. Darkened.	Heavily attacked. Darkened.	Heavily attacked. Darkened.	Heavily attacked.	Heavily attacked. Darkened.	Slightly attacked.	Slightly attacked.
Al <sub>2</sub> O <sub>3</sub> Fe	Y (Al <sub>2</sub> O <sub>3</sub> -Fe) (14)	β-Al <sub>2</sub> O <sub>3</sub> Fe	Cu <sub>2</sub> FeAl <sub>3</sub> (45) (46)	Grey.	Dark grey.	Brown striations.	Sometimes coloured light brown.	Coloured brown.	None.	Generally not attacked.	Coloured brown.	Sometimes coloured light brown.	Coloured light brown.
Al <sub>2</sub> O <sub>3</sub> Mn	7 (Al <sub>2</sub> O <sub>3</sub> -Mn) (11)	Al <sub>2</sub> O <sub>3</sub> Mn	Al <sub>2</sub> O <sub>3</sub> Mn	Light grey.	Distinct change.	Slightly etched. Not coloured.	Coloured brown.	Coloured dark brown.	None.	Slightly attacked.	None.	Sometimes uneven brown colour.	Vari-coloured.
Al <sub>2</sub> O <sub>3</sub> MgSi	Q (Al <sub>2</sub> O <sub>3</sub> -Mg-Si) (19)	...	Al <sub>2</sub> O <sub>3</sub> MgSi	Light.	Bright yellow-light blue.	None.	None.	None.	None.	None.	None.	None.	None.
Al <sub>2</sub> O <sub>3</sub> MgSi	...	Q (Al <sub>2</sub> O <sub>3</sub> -Mg-Si) (19)	Cu <sub>2</sub> Mg <sub>3</sub> Si <sub>4</sub> Al <sub>4</sub>	Dark grey.	Dark purple-light yellow.	Not etched. Sometimes coloured light brown.	Not attacked. Sometimes varicoloured.	Slightly attacked. Sometimes blue.	None.	Heavily attacked. Darkened.	Heavily attacked. Darkened.	None.	None.
Al <sub>2</sub> O <sub>3</sub> Mn	...	Al <sub>2</sub> O <sub>3</sub> Mn	MnAl <sub>2</sub>	Light grey.	Brownish-yellow-bluish-grey.	None.	Attacked only when Mg content high.	None.	None.	None.	None.	Slightly attacked. Sometimes varicoloured.	Attacked. Vari-coloured.
Al <sub>2</sub> O <sub>3</sub> MnFe	...	Al <sub>2</sub> O <sub>3</sub> Mn (55)	Al <sub>2</sub> O <sub>3</sub> Mn	Light grey.	Brownish-yellow-bluish-grey.	Sometimes discoloured.	Slightly attacked.	Slightly attacked. Sometimes coloured brown.	None.	None.	None.	Slightly attacked. Sometimes slightly coloured.	Attacked. Vari-coloured.
Al <sub>2</sub> O <sub>3</sub> Mn,Al,Fe,Cu	Al <sub>2</sub> O <sub>3</sub> Mn,Al,Fe,Cu	...	...	Light grey.	Brownish-yellow-bluish-grey.	None.	Sometimes coloured light brown.	Slightly attacked. Sometimes coloured brown.	None.	None.	None.	Slightly attacked. Sometimes slightly coloured.	Dark and varicoloured.
Al <sub>2</sub> O <sub>3</sub> Fe	Al <sub>2</sub> O <sub>3</sub> Fe (30) *	α-Al <sub>2</sub> O <sub>3</sub> Fe	α-(Al <sub>2</sub> O <sub>3</sub> Fe) (10) FeAl <sub>3</sub>	Light grey.	Brownish-yellow-bluish-grey.	Attacked. Not coloured.	Coloured light brown.	Darkened.	None.	Slightly attacked.	None.	Coloured brown.	Darkened. Vari-coloured.
Al <sub>2</sub> O <sub>3</sub> Mn,Fe,Cu	Al <sub>2</sub> O <sub>3</sub> Mn,Fe,Cu	Al <sub>2</sub> O <sub>3</sub> MnFe	Al <sub>2</sub> O <sub>3</sub> MnFe	Light grey.	Brownish-yellow-bluish-grey.	None.	Slightly attacked. Generally coloured light brown.	Slightly attacked. Sometimes coloured brown.	None.	None.	None.	Varicoloured.	Intense darkening. Varicoloured.
Al <sub>2</sub> Fe	Al <sub>2</sub> Fe	Al <sub>2</sub> Fe	FeAl <sub>3</sub>	Grey.	Changes somewhat.	Heavily attacked. Dark coloured.	None.	None.	None.	None.	None.	Sometimes coloured light brown.	Intense brown colour.
Al <sub>2</sub> Fe	(Al <sub>2</sub> O <sub>3</sub> ) <sub>2</sub> Fe <sub>2</sub> O <sub>3</sub>	Al <sub>2</sub> Fe	FeAl <sub>3</sub>	Grey.	Changes somewhat.	Heavily attacked. Dark coloured.	Mottled brown colour.	Darkened.	None.	None.	None.	Coloured brown.	Coloured brown.
Al <sub>2</sub> Fe	Al <sub>2</sub> (Fe,Mn)	...	...	Grey.	Changes somewhat.	Heavily attacked. Dark coloured.	Coloured brown.	Slightly attacked.	None.	None.	None.	Coloured light brown.	Coloured brown.
α-AlMnSi	T (Al-Mn-Si) (57)	AlMnSi	α-(AlMnSi)	Light grey.	Does not change.	None.	None.	None.	None.	None.	None.	Sometimes varicoloured.	Varying colour.
α-AlMn,CuSi	...	...	...	Light grey.	Does not change.	Almost unattacked, but etching pits at cracks. Not coloured.	Uneven brown colour.	None.	None.	None.	None.	Sometimes coloured light brown.	Varying colour.
α-AlFeSi	...	α-AlFeSi	α-(AlFeSi)	Light grey.	Does not change.	Slightly etched. Coloured light brown.	Slightly attacked, especially in alloys containing Mg.	Sometimes coloured light brown.	None.	None.	None.	None.	Intense brown colour especially in alloys containing Mg.
α-AlFe,CuSi	...	...	...	Light grey.	Does not change.	Heavily attacked. Dark coloured.	Coloured light brown.	Coloured brown.	None.	None.	None.	Sometimes coloured light brown.	Coloured brown.
α-Al(Fe,Mn)Si	P (Al-Fe-Mn-Si) (49)	...	α-(AlMnFeSi)	Light grey.	Does not change.	Slightly etched.	Sometimes coloured light brown.	Coloured light brown.	None.	None.	Slightly attacked. Coloured yellowish-grey.	None.	None.
α-Al(Mn,Fe,Cu)Si	...	...	...	Light grey.	Does not change.	Fairly deeply attacked. Slightly darkened.	Coloured light brown.	None.	None.	None.	None.	None.	None.
m-AlFeSi	...	β-AlFeSi	FeSiAl <sub>3</sub>	Yellowish-grey.	Distinct change.	Fairly deeply attacked. Darkened.	Coloured light brown.	None.	None.	None.	None.	Varying colour.	Light brown colour especially in alloys containing Mg.
l-AlFeSi	...	T (Al <sub>2</sub> Si <sub>2</sub> Fe) (60)	δ-(AlFeSi)	Light grey.	Distinct change.	Attacked.	None.	None.	None.	Coloured brown, greyish-brown.	None.	None.	None.
r-AlCuMgMn	...	...	...	Light.	Does not change.	Coloured light brown.	None.	Coloured brown.	None.	Heavily attacked. Darkened.	Heavily attacked. Darkened.	None.	None.

\* (Al<sub>2</sub>O<sub>3</sub>)<sub>2</sub>Fe<sub>2</sub>O<sub>3</sub> probably corresponds to the phase which Tollner has designated "Q Fe" (Al<sub>2</sub>O<sub>3</sub>?Mg?Fe?) (49).

The numbers in parentheses relate to the references at the end of the paper.

Section 10.1.1. The following is a list of the

1. The first part of the

2. The second part of the

3. The third part of the

4. The fourth part of the

5. The fifth part of the

6. The sixth part of the

7. The seventh part of the

8. The eighth part of the

9. The ninth part of the

10. The tenth part of the

11. The eleventh part of the

12. The twelfth part of the

13. The thirteenth part of the

14. The fourteenth part of the

# THE CONSTITUTION OF URANIUM-MOLYBDENUM ALLOYS.\*

1263

By P. C. L. PFEIL,† B.Sc., Ph.D., STUDENT MEMBER.

## SYNOPSIS.

The uranium-molybdenum system has been examined experimentally, using micrographic, X-ray, and thermal-analysis methods. No intermediate phases were recognized in this system. As predicted, the solid solution of molybdenum in  $\gamma$ -uranium is relatively extensive, and is in equilibrium with a molybdenum-rich solid solution containing a small quantity of uranium. With approximately 19 at.-% molybdenum the  $\gamma$  body-centred cubic modification is stabilized down to room temperature. The  $\gamma$  phase can be retained down to room temperature by quenching alloys containing above approximately 9 at.-% molybdenum, but with lower molybdenum contents decomposition to  $\alpha$  by a martensitic type of reaction occurs. The solid solubility of molybdenum in  $\beta$ -uranium is restricted, whilst that in the  $\alpha$ -modification is intermediate between that in the  $\beta$  and  $\gamma$  modifications. This leads to a direct transformation between  $\gamma$ - and  $\alpha$ -uranium, not involving the  $\beta$  phase, in alloys containing more than 2 at.-% molybdenum. The  $\alpha/(\alpha + \gamma)$  phase boundary falls to room temperature with increasing molybdenum contents.

The experimental results, particularly the solid solubility of molybdenum in the three allotropic modifications of uranium, are discussed in terms of the general theory of the alloying behaviour of uranium.

## I.—INTRODUCTION.

As was first shown by specific-heat<sup>1</sup> and electrical-resistivity<sup>2</sup> measurements, there are three allotropic modifications of uranium. The crystal structure of the  $\alpha$  form, stable from room temperature to 665° C., has been shown by Jacob and Warren<sup>3</sup> to be orthorhombic, with  $a = 2.852$ ,  $b = 5.865$ , and  $c = 4.945$  kX. There are 4 atoms per unit cell.  $\beta$ -Uranium, stable between 665° and 772° C., is of complex crystal structure and may also be orthorhombic. The  $\gamma$  modification, stable between 772° C. and the melting point (1133° C.), is body-centred cubic, with a lattice parameter, extrapolated to room temperature, of approximately 3.43 kX.<sup>4, 5</sup>

The probable alloying behaviour of uranium has been considered by Raynor.<sup>6</sup> On the basis of size-factor and Brillouin-zone effects no elements can be expected to form extensive substitutional solid solutions in  $\alpha$ - or  $\beta$ -uranium, but extensive solid solubility in the  $\gamma$  form may be expected of molybdenum and tungsten, among the elements

\* Manuscript received 2 February 1950.

† Metallurgy Division, Atomic Energy Research Establishment, Harwell, Berks.

of Group VI, and appreciable solid solubility of vanadium, niobium, and tantalum, among the elements of Group V. The general effect of these elements on the transformation temperatures of uranium would be to stabilize the  $\gamma$  phase down to lower temperatures, possibly to room temperature.

As a test of part of these suggestions an experimental investigation of the uranium-molybdenum system by means of micrographic, X-ray, and thermal-analysis methods has been undertaken.

## II.—EXPERIMENTAL METHODS.

### (a) *Materials Used.*

The uranium used for the preparation of the alloys was of purity greater than 99.95%. The principal impurities were carbon, silicon, iron, aluminium, and oxygen. The purity of the molybdenum was better than 99.97%. Spectrographic analysis showed that, in general, not only was there no pick-up of impurities, but the iron and silicon contents were appreciably reduced.

### (b) *Preparation of Alloys.*

In preliminary experiments powder-metallurgy methods for the preparation of the alloys were tried but proved unsatisfactory because the resulting compacts contained large quantities of oxide particles. Vacuum melting was therefore adopted, using an apparatus built by Mr. P. J. Bowles who prepared the first few ingots with it. Alloys were made up in quantities of from 200 to 300 g., by melting together the appropriate quantities of uranium and molybdenum under a vacuum of below  $10^{-3}$  mm. pressure. The charge consisted of a single piece of uranium placed on top of a piece of molybdenum; as the density of molybdenum is much less than that of uranium, some mixing was obtained by the molybdenum rising through the liquid uranium.

High-frequency induction heating was employed for melting, the generator available being of the valve type with a maximum output of 5 kW. at a frequency of 5 mc./s. Although a rapid initial rate of heating could be obtained, there were serious disadvantages in the use of this generator. Because of the high frequency and the high voltage (5–10 kV.) on the output coil of the generator, a discharge passed through bursts of gas emitted from the charge as it melted. This discharge absorbed most of the power, thus preventing the charge from heating up further until the gas was pumped away. Although the speed of the pumping system, in comparison with the size of the system evacuated, was relatively rapid, melting was slow, often taking 2–3 hr. to complete.

Although excellent mixing of the charge is characteristic of induction-melting methods when the frequency is less than 100–200 kc./s., the frequency in this case was too high and the alloys showed marked longitudinal segregation. In an attempt to prepare unsegregated ingots, the apparatus was modified to permit a molybdenum stirrer to be introduced into the melt. This was agitated through a Wilson seal. While the charge was completely molten the stirrer was removed, and the alloy allowed to cool. This stirring reduced the amount of segregation considerably. Without stirring, for example, an alloy intended to contain 7.0 wt.-% molybdenum, showed 11.2% at the top, 8.6% at the centre, and 4.0% molybdenum at the base. With the stirring arrangements described, an alloy intended to contain 12.0 wt.-% molybdenum gave on analysis 15.0% at the top, 14.7% at the centre, and 14.0% molybdenum at the base of the ingot. Although the longitudinal segregation was considerably reduced by this method, the composition of the final alloy was between 1 and 3 wt.-% richer in molybdenum than was intended. Alloys of critical composition could not therefore be prepared by this method.

Through the kindness of Dr. N. P. Allen, critical alloys were prepared without mechanical stirring, in the Metallurgy Division of the National Physical Laboratory, using a spark-gap type of generator giving an output of up to 14 kW. at a frequency which varied between 30 and 50 kc./s. Segregation in alloys prepared in this way was very small; for example, five samples taken from various parts of an alloy nominally containing 9.0 wt.-% molybdenum all gave analyses between 8.90 and 9.10% molybdenum.

In preliminary experiments pure thoria, alumina, and beryllia were used as crucible materials. At temperatures below 1350° C. none of these materials was attacked. Beryllia proved satisfactory at the highest temperature investigated (approximately 1700°–1800° C.), but alumina and thoria were attacked at temperatures of approximately 1400° and 1500° C., respectively. Since temperatures of the order of 1600° C. were necessary to dissolve molybdenum with reasonable speed, beryllia crucibles were used in this investigation.

### (c) *Annealing Techniques.*

Uranium oxidizes very readily in air; above 350° C. oxidation is extremely rapid. In most cases specimens were enclosed in hard-glass or silica tubes, evacuated before final sealing-off. Reaction between the sample and the glass or silica was prevented by enclosing the specimen in a thin-walled pure alumina crucible. Tubular resistance furnaces, automatically controlled to within  $\pm 1^\circ$  C. of the



required temperature by a resistance-thermometer controller, were used for the annealing experiments. Temperatures were measured with a standardized platinum/platinum-13% rhodium thermocouple. At the end of the annealing treatments, specimens were plunged into a bath of cold water and the containing tube broken to ensure a rapid quench.

In some experiments involving annealing periods of relatively short duration, or at temperatures above that at which silica is non-porous to air, samples were suspended in a vertical annealing furnace through which a gentle current of purified argon was passed. Temperatures were measured with a platinum/platinum-13% rhodium thermocouple introduced into the furnace, with the tip near the sample. Quenching was effected by fusing a portion of the tungsten suspension wire, thus allowing the specimen to fall into a bath of low-vapour-pressure oil, cooled to just above its freezing point. At the higher temperatures, contact between the tungsten wire and the specimen was prevented by means of a few small pieces of beryllia.

(d) *Thermal Analysis.*

Investigation of the effects of molybdenum on the  $\alpha \rightleftharpoons \beta$  and  $\beta \rightleftharpoons \gamma$  transformations of uranium was attempted by means of thermal-analysis experiments. The apparatus, constructed by Mr. J. M. North, was arranged so that both direct temperature/time curves and differential curves based on the difference in temperature between the specimen and a standard copper block near the specimen, could be obtained at the same time. The specimen, thermocouples, and copper block were placed inside a heavy copper tube and the whole inserted in a silica tube which was continuously evacuated. Initial measurements on uranium-molybdenum alloys were made by Miss J. R. Murray; these, together with subsequent experiments, are described in Section IV.

(e) *X-Ray Methods.*

Copper  $K_{\alpha}$  radiation from a Metropolitan-Vickers demountable X-ray set was used in the X-ray investigations. Exposure times of from 5 to 10 hr. were necessary with an output of 20 m.amp. at 40 kV. Both "glancing-angle" and "powder" methods were used for the X-ray examination of specimens at room temperature.

(f) *High-Temperature X-Ray Work.*

A Unicam high-temperature camera with minor modifications was found satisfactory for these experiments. Filings were prepared after

the alloy had been heat-treated to produce a homogeneous single-phase structure, if possible, so as to avoid complications of the type described by Hume-Rothery and Raynor.<sup>7</sup> After removal of iron, the filings (unsieved) were inserted in a silica capillary of 0.4 mm. bore and 0.02 mm. wall thickness, and sealed-off under a vacuum of approximately  $10^{-5}$  mm. pressure. The high-temperature camera was evacuated, and temperatures were maintained constant to within  $\pm 2^\circ$  C. In general, a period of 16 hours' annealing was allowed for the specimen to approach equilibrium before an exposure was taken. Only two or three satisfactory patterns could be obtained before the lines became spotted, owing to sintering of the powder.

(g) *Analytical Methods.*

(i) *Chemical.*—Critical microspecimens and X-ray specimens, were analysed for molybdenum by Mr. M. Gibson of the Chemistry Division, A.E.R.E., while representative alloys were spectrographically examined for possible pick-up of impurities. Molybdenum was precipitated, using cupferron, and finally weighed as  $\text{MoO}_3$ . When only small samples were available, for example, X-ray powder specimens, molybdenum was determined absorptiometrically.

(ii) *Autoradiographic.*—Experiments to determine the composition of a second phase by autoradiographic methods were tried. A flat surface of the specimen was positioned a very short distance away from an  $\alpha$ -sensitive nuclear emulsion. After making allowances for the different absorption of  $\alpha$  particles by uranium and molybdenum, it was possible to determine differences in composition from the varying numbers of  $\alpha$ -particle tracks in the emulsion. The technique has not yet been perfected, but an accuracy better than  $\pm 10\%$  of the quantity of  $\alpha$ -active material present is readily obtainable.

### III.—MICROGRAPHIC EXAMINATION.

(a) *Preparation of Specimens.*

Fresh sections were prepared for micrographic examination by the usual procedure of grinding on successively finer emery papers, followed by polishing with aqueous suspensions of alumina, magnesia, and chromic oxide on blanket felt. As uranium is a relatively hard metal, polishing was slow. For the softer alloys, Selvyt cloth or chamois leather was more satisfactory than blanket felt. In some cases a final electrolytic polish was given.

In spite of the relatively high purity of the alloys, small quantities of uranium oxide and carbide particles were always observed.

*(b) Identification of Phases.*

No intermediate phases were found in the alloys of uranium and molybdenum, but solid solutions based on  $\alpha$ -,  $\beta$ -, and  $\gamma$ -uranium and on molybdenum were recognized. The metallographic characteristics of these phases were as follows:

(i) *Molybdenum*.—In alloys containing more than 28 at.-% molybdenum, primary crystals were observed. X-ray and contact-autoradiographic experiments showed that these consisted of molybdenum with some uranium in solid solution. Recognition of the molybdenum-rich solid solution in the unetched condition was not difficult, but a useful confirmatory etching reagent was an aqueous solution containing 5% potassium hydroxide and 5% potassium ferricyanide, which stained the phase brown.

(ii)  *$\gamma$ -Uranium*.—In the "as polished" condition this phase appeared yellowish in colour and could readily be distinguished in the unetched condition from a solid solution based on  $\alpha$ -uranium. An etching reagent containing 50% nitric acid and 50% acetic acid by volume, darkened this phase slowly. The grains were clearly delineated. Although when containing less than 9 at.-% molybdenum in solid solution the  $\gamma$  phase decomposed to  $\alpha$  on quenching, the original  $\gamma$  grain boundaries could still be clearly recognized.

(iii)  *$\alpha$ -Uranium*.—Under all conditions in which the  $\alpha$  and  $\gamma$  solid solutions are in equilibrium, the  $\alpha$  phase is harder than the  $\gamma$ , and in the unetched condition appears very light grey in slight relief. Etching reagents containing nitric acid have little effect on the appearance of this phase. In general, however, finely divided mixtures of the  $\alpha$  and  $\gamma$  phases etched very rapidly in these solutions.

(iv)  *$\beta$ -Uranium*.—The extension of the  $\beta$  phase into the uranium-molybdenum equilibrium diagram is very restricted. Its micrographic characteristics were similar to those of the  $\alpha$  phase, though there were slight differences which enabled the  $\beta$  phase to be recognized. The constituents of a two-phase ( $\alpha + \beta$ ) alloy were heavily outlined on etching for 30 sec. in 50% nitric, 50% acetic mixed acids.

#### IV.—THE CONSTITUTIONAL DIAGRAM.

The uranium-molybdenum equilibrium diagram is illustrated in Figs. 1 and 2. For convenience in presentation of the evidence on which the diagrams are based, the constitution of the alloys in the "as melted" condition is first described, followed by an account of the experimental results relating to each main phase field. Conditions approximating to equilibrium in alloys containing less than 19 at.-%

molybdenum (as indicated by micrographic and high-temperature X-ray experiments) are described before the results of thermal analysis and complementary micrographic work.

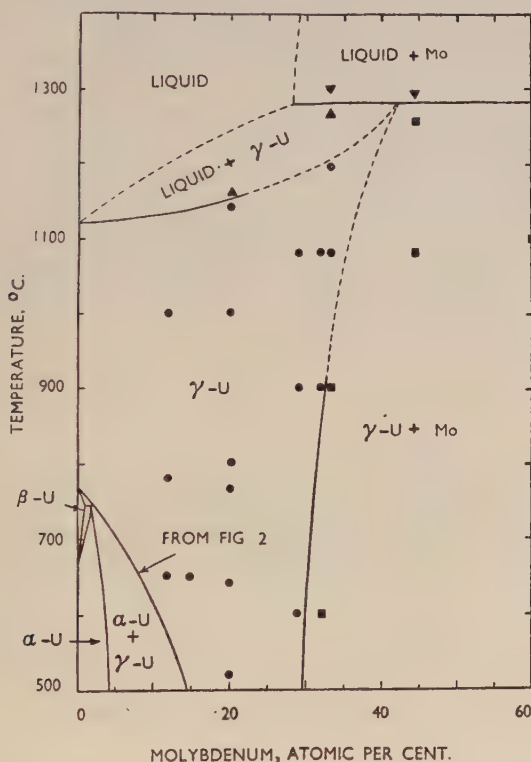


FIG. 1.—The Uranium-Molybdenum Equilibrium Diagram.

KEY.

- $\gamma$ -U.
- $\gamma$ -U + Mo.
- ▲ Liquid +  $\gamma$ -U.
- ▼ Liquid + Mo.

All alloys are represented by analysed compositions.

### 1. Constitution of "As Melted" Alloys.

In the "as melted" condition, alloys containing more than 28.9 at.-% molybdenum showed primary crystals of molybdenum-rich solid solution in a cored solid solution based on  $\gamma$ -uranium (see Fig. 3, Plate LXXVI, which is unetched). Ingots containing between 13.7 and 28.9 at.-% molybdenum showed only cored  $\gamma$ -uranium solid solution, as illustrated in Fig. 4 (Plate LXXVI). No sharp demarcation

line suggestive of a phase boundary was visible under high magnification. Alloys containing slightly less molybdenum showed a two-phase structure in the slowly cooled condition. With 8.2 at.-% molybdenum or less a microstructure suggestive of a transformation in the solid state was obtained (see Fig. 5, Plate LXXVI). In no alloy was there any suggestion of a eutectic between the molybdenum- and uranium-rich solid solutions.

### *2. $\gamma$ -Uranium + Molybdenum Field.*

Alloys containing primary crystals of molybdenum were annealed at 1080° C. for periods of 1, 4, and 8 weeks. Those samples with 33.1 at.-% molybdenum or less, which contained undissolved particles of molybdenum after 1 week's annealing, became homogeneous after annealing for 4 weeks. A sample with 44.4 at.-% molybdenum was not homogeneous after 4 weeks' annealing, and no change was observed after heat-treatment for a further 4 weeks, making a total of 8 weeks at 1080° C. The solubility of molybdenum in uranium is therefore probably between 33.1 and 44.4 at.-% at 1080° C. The solubilities at 900° and 600° C. were investigated by re-annealing previously homogenized alloys for periods of 3 or 6 weeks at these lower temperatures. None of these experiments suggested the existence of an intermetallic compound between uranium and molybdenum, nor did further experiments which consisted of annealing samples containing unmelted molybdenum for periods extending up to 8 weeks at temperatures in the range 500°–1000° C., show any indication of rimming of the molybdenum.

### *3. The Molybdenum-Rich Solid Solution.*

X-ray examination showed the presence of only two body-centred cubic phases, one of lattice parameter approximately 3.370 kX. and the other 3.146 kX., in an alloy containing 31.7 at.-% molybdenum slowly cooled to room temperature. Pure molybdenum is body-centred cubic with a lattice parameter of 3.140 kX. The presence of a body-centred cubic structure of parameter 3.146 kX. confirms the micrographic identification of a molybdenum-rich solid solution.

Because the difference in parameters is small, the solubility of uranium in molybdenum is probably limited. In a contact autoradiographic experiment, those parts of the nuclear emulsion in contact with the primary crystals of molybdenum in an alloy containing 44.4 at.-% molybdenum, after annealing at 1080° C., showed a much lower density of  $\alpha$  tracks than those parts of the plate in contact with uranium-rich solid solution. The amount of uranium contained



within these particles of molybdenum is estimated to be  $4.5 \pm 0.6$  at.-%. This is probably the limit of solid solubility of uranium in molybdenum at  $1080^{\circ}\text{C}$ . As far as can be judged from the evidence available it seems unlikely that this limit decreases very markedly in the range  $1080^{\circ}$ – $600^{\circ}\text{C}$ .

#### 4. Formation of $\gamma$ by Peritectic Reaction.

The fact that the primary crystals present in alloys containing between 28.9 and 33.1% molybdenum dissolved on subsequent annealing at  $1080^{\circ}\text{C}$ ., suggests the existence of a peritectic relationship between the uranium- and molybdenum-rich solid solutions and the liquid phase. Annealing and quenching experiments on a sample containing 19.9 at.-% molybdenum, showed that at  $1140^{\circ}\text{C}$ . there was no sign of melting having taken place, but after quenching from  $1160^{\circ}\text{C}$ ., it was obvious that the specimen had been semi-liquid. As the melting point of 99.99% pure uranium is  $1133^{\circ} \pm 2^{\circ}\text{C}$ .,<sup>8</sup> these experiments indicate that the solidus temperature of this alloy is above the melting point of uranium, which is consistent with the existence of a peritectic reaction.

A specimen containing 33.1% molybdenum showed only the  $\gamma$  phase of uranium after annealing and quenching from  $1195^{\circ}\text{C}$ . After quenching from  $1265^{\circ}\text{C}$ ., the specimen had been in the semi-liquid condition but no particles of molybdenum were visible. After quenching from  $1300^{\circ}\text{C}$ . particles of molybdenum were found. The oxide skin on the surface of these specimens preserved their shape approximately, even when semi-liquid. Similarly, an alloy containing 44.4 at.-% molybdenum showed the  $\gamma$ -uranium-rich and molybdenum-rich solid solutions after quenching from  $1255^{\circ}\text{C}$ . After quenching from  $1292^{\circ}\text{C}$ ., the sample had been partially melted, while more molybdenum-rich solid solution was present than at  $1255^{\circ}\text{C}$ .

The existence of a peritectic reaction involving the liquid and molybdenum-rich solid solution phases to form the  $\gamma$ -uranium-rich solid solution is therefore confirmed. The temperature of the peritectic horizontal lies within the limits of  $1265^{\circ}$  and  $1292^{\circ}\text{C}$ . The maximum solid solubility at this temperature is certainly between 33.1 and 44.4 at.-%, and from the proportion of molybdenum present after annealing the 44.4% sample at  $1255^{\circ}\text{C}$ . it is probably between 41 and 43 at.-% molybdenum.

#### 5. The Homogeneous $\gamma$ Field.

No molybdenum was precipitated in a sample containing 21.4 at.-% molybdenum, after homogenization and very slow cooling, over a period of 2 weeks, to room temperature.

Thermal-analysis experiments up to a temperature of 900° C., showed no transformations in an alloy containing 19.9 at.-% molybdenum. Specimens annealed at and quenched from temperatures between 400° C. and 1140° C. and slowly cooled gave in all cases a single-phase microstructure, characteristic of  $\gamma$ -uranium. X-ray evidence confirmed that the body-centred cubic  $\gamma$  structure, with a lattice parameter of 3.410 kX., had been retained down to room temperature.

Wilson and Rundle,<sup>5</sup> in a letter concerning the structures of uranium metal, quote the lattice parameters of  $\gamma$ -uranium containing different amounts of molybdenum in solid solution. Table I gives their results and those of the present author.

These lattice parameters are an approximately linear function of composition and extrapolate to the lattice parameter of molybdenum, 3.140 kX. (see Section V).

TABLE I.—*Lattice Parameters of  $\gamma$ -Uranium.*

Molybdenum, at.-%		Lattice Parameter, kX.
Wilson & Rundle <sup>5</sup>	Pfeil	
17.3	...	3.412
...	19.9	3.410
22.8	...	3.394
24.2	...	3.385
29.4	...	3.376
31.2	...	3.365
...	31.7	3.370

#### 6. *Effect of Molybdenum on Allotropic Modifications.*

The effect of molybdenum on the allotropic modifications of uranium was studied by (a) thermal analysis; (b) micrographic examination of annealed and quenched samples; and (c) high-temperature X-ray work. At an early stage preliminary results of the thermal-analysis and micrographic experiments appeared to be in contradiction. Subsequent work indicated that these discrepancies should be ascribed to differences between equilibrium and non-equilibrium conditions.

#### 7. *Alloys in Which Conditions Approximate to Equilibrium.*

In general, the alloys represented in Fig. 2, particularly those used to determine the  $\gamma/(\alpha + \gamma)$  phase boundary, were homogenized by annealing at a convenient temperature in the single-phase  $\gamma$  region. At 800° C., for example, periods of the order of 2–14 days, depending

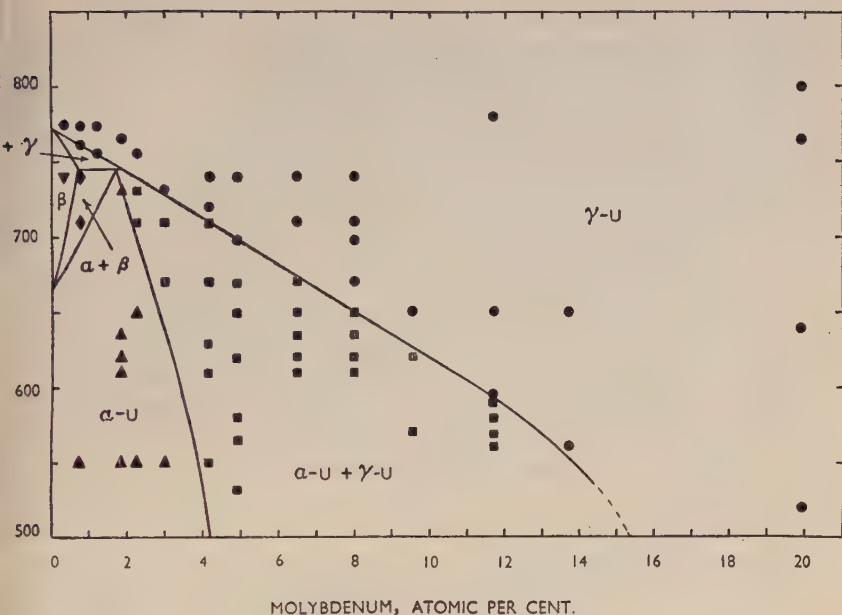


FIG. 2.—The Effect of Molybdenum on the Allotropic Modifications of Uranium.



All alloys are represented by analysed compositions. Details of the annealing treatments and microstructures of alloys represented in Fig. 2 have been deposited in the Institute Library.

on the composition, were found to be necessary. These samples were then annealed at successively lower temperatures, sufficient time being allowed for precipitation to be completed, as tested by further annealing at the same temperature. The times necessary for complete precipitation increased from less than 2 days above 700° C. to 1–2 weeks below 600° C. At the higher temperatures, precipitation of the  $\alpha$  phase on a coarse scale occurred preferentially at the grain boundaries, but much finer microstructures were produced at the lower temperatures with less tendency to form preferentially at the boundaries.

The general appearance of the fine precipitate at first suggested that it had been formed as a result of eutectoid decomposition rather than by precipitation. The appearance of the 11.7% alloy, illustrated in Fig. 6 (Plate LXXVI), is typical of microstructures obtained with alloys containing between 9 and 15 at.-% molybdenum, though this sample is not in equilibrium since on further annealing at 588° C. more pre-

cipitation occurred. The microhardness of the light phase in low relief is 140, whereas the dark phase with an appearance similar to that of pearlite has a hardness of approximately 440. Annealing and quenching experiments showed that when quenched from 595° C., or above, a single-phase structure characteristic of the  $\gamma$  phase was obtained, with a hardness of 140. X-ray experiments confirmed that this was the  $\gamma$  phase which had been retained down to room temperature by quenching.

The existence of a eutectoid implies that there must be a third phase in this region, in addition to the  $\alpha$  and  $\gamma$  phases, but X-ray diffraction patterns, taken both at room temperature on the quenched sample and at 588° C., showed the presence of only the  $\alpha$  and  $\gamma$  structures. Less of the  $\gamma$  phase was present after annealing and quenching from 568° C., and when quenched from 560° C. only the dark material was present. This dark material is interpreted as a finely divided mixture of the two phases, and is regarded as having been formed by the breakdown of the  $\gamma$  phase containing 11.7% molybdenum in solution, into an  $\alpha$  phase containing less molybdenum and a  $\gamma$  phase with more molybdenum.

When samples were extremely slowly cooled over the temperature range 600°–570° C. the structure of the dark material was much coarser, and was clearly two-phase in nature. One phase was light in colour while the other was dark. The dark phase was continuous with the soft  $\gamma$ -uranium, while there was a sharp boundary between this phase and the light phase in the dark material. This is consistent with the suggestion that the dark material is composed of a finely divided mixture of the  $\alpha$  and  $\gamma$  phases. Although an X-ray diffraction pattern showed only the  $\alpha$  structure, when very slowly cooled to room temperature the specimen consisted entirely of the dark material considered to represent a finely divided mixture of the two phases. It could not be expected, however, that small quantities of the  $\gamma$  phase would be recognizable, as the first four lines of the body-centred cubic structure occur at similar spacings to lines from the orthorhombic  $\alpha$ -uranium structure. Synthetic mixtures of the two phases showed that, under the conditions of the experiments, it was necessary for at least 10–15% of the body-centred cubic phase to be present, before it could be recognized.

With less than 9 at.-% molybdenum in solution, the  $\gamma$  phase could not be retained by quenching. The micrographic appearance of the 4.9 at.-% alloy quenched from 740° C., for example, indicated that the specimen had been quenched from a single-phase  $\gamma$  solid-solution field, but X-ray diffraction experiments revealed only the  $\alpha$  structure,



which indicated that the  $\gamma$  phase had decomposed on quenching. Further etching revealed the transformation structure of needles reproduced in Fig. 7 (Plate LXXVI). Another sample of the same alloy quenched from 717° C. after 5 days' annealing, showed the presence of a trace of another phase around the grain boundaries, as illustrated in Fig. 8 (Plate LXXVI). Further etching again revealed the needle-like transformation structure. This sample was not in equilibrium, for on further annealing at 717° C. it became homogeneous  $\gamma$ . Specimens quenched from the temperature range judged to be that of a homogeneous  $\beta$ -phase field, by preliminary thermal-analysis work (see p. 566) showed indications that they had been quenched from a two-phase field, the proportion of the white phase increasing with decreasing temperature (see Figs. 9 and 10, Plate LXXVII).

High-temperature X-ray experiments with an alloy containing 4.9% molybdenum, showed the  $\gamma$  structure only at 720° C.; a mixture of the  $\gamma$  and  $\alpha$  structures at 700° and 680° C., with a larger proportion of  $\alpha$  at the lower temperature; while only the diffraction pattern characteristic of the  $\alpha$ -uranium structure was found at 665° C., 600° C., and room temperature. This evidence indicates that equilibrium in this alloy involves only the  $\gamma$  and  $\alpha$  solid solutions and not the  $\beta$  phase, in agreement with the micrographic work.

In these high-temperature experiments only the  $\alpha$  phase was detected at 665° or at 600° C., whereas under equilibrium conditions, as shown in Fig. 2, substantial quantities of the  $\gamma$  phase would be present. Although, before making an exposure, 16 hours' annealing *in situ* was allowed for the approach of specimens to equilibrium, which was approached from the low-temperature direction, it is probable that the annealing period was insufficient to attain true equilibrium. Very much longer annealing periods could not be given except at the expense of the quality of the X-ray diffraction pattern, because of the sintering of the powder. An additional reason for the discrepancy is that if precipitation of  $\gamma$  from  $\alpha$  was in the form of tiny particles, which seems probable under the conditions of these experiments, it is not unlikely that even larger amounts than 10-15% of the  $\gamma$  phase would fail to be recognized.

These experiments identify the two phases observed micrographically as  $\alpha$  and  $\gamma$ .

The position of the  $\gamma/(\alpha + \gamma)$  phase boundary determined micrographically by precipitation, was confirmed by annealing samples at a constant temperature for long periods until no change of microstructure was observed on further annealing. Thus equilibrium was approached from both directions.



The  $\alpha/(\alpha + \gamma)$  phase boundary was not determined so accurately, because annealing periods of 12–16 weeks at 550° C. were necessary for equilibrium to be attained. Previous annealing at other temperatures was not found to be helpful for approaching equilibrium more rapidly. Figs. 11–14 (Plate LXXVII) illustrate the microstructure of a series of alloys annealed at 650° C. for 14 days. Further annealing, however, changed the proportions of the two constituents. Again, further annealing at 650° C. of the sample represented by Fig. 10 caused more  $\alpha$  to precipitate.

Micrographic evidence indicates that while the  $\gamma/(\alpha + \gamma)$  phase boundary is at a higher temperature, in the 4.2 and 4.9% molybdenum alloys, than the  $\alpha \rightleftharpoons \beta$  transformation temperature of pure uranium, the  $\alpha/(\alpha + \gamma)$  phase boundary is at a lower temperature. This suggests the possibility that a peritectoid reaction between solid solutions based on  $\beta$ - and  $\gamma$ -uranium, to form a solid solution based on  $\alpha$ -uranium, may occur with lower molybdenum contents. This possibility is supported by the microstructures of annealed and quenched specimens containing less than 2 at.-% molybdenum (see Fig. 2). From the proportion of  $\alpha$  present in the 0.77% alloy quenched from 740° C., the maximum solid solubility is estimated at approximately 0.7 at.-% molybdenum. Alloys containing between 0.7 and 1.9 at.-% molybdenum undergo a peritectoid reaction at approximately 745° C., where solid solutions based on  $\beta$ - and  $\gamma$ -uranium react to form a solid solution based on  $\alpha$ -uranium.

#### 8. Thermal Analysis and Supporting Experiments.

##### *The 11.7 At.-% Alloy.*

The typical behaviour of alloys containing from 9 to 14 at.-% molybdenum is represented by the behaviour of the 11.7 at.-% alloy. This alloy showed one transformation, which starts at 580° and finishes at 640° C. on heating, and starts at 600° and finishes at 515° C. on cooling. The temperatures of the beginning of this transformation compare reasonably well with those indicated by micrographic work (see Fig. 2). Under relatively rapid rates of cooling some  $\gamma$  could be retained down to room temperature. On reheating, this transformed to  $\alpha$  in the temperature range 350°–450° C., transforming back to  $\gamma$  at a higher temperature.

##### *The 4.9 At.-% Alloy.*

The behaviour of the 4.9 at.-% alloy is typical of the range of compositions from 2 to 9 at.-% molybdenum.

Thermal-analysis experiments with a 4.9 at.-% molybdenum alloy

on heating or cooling at a rate of between  $0.5^{\circ}$  and  $4^{\circ}$  C./min. showed two transformations at the approximate temperatures given in Table II.

TABLE II.—*Transformation Temperatures in a 4.9 At.-% Molybdenum Alloy.*

	Transformation No. 1		Transformation No. 2	
	Start	Finish (approx.)	Start	Finish (approx.)
Heating . . .	636° C.	674° C.	742° C.	769° C.
Cooling . . .	612° C.	535° C.	717° C.	665° C.

The original interpretation of these results was that the first transformation was from  $\alpha$  to  $\beta$  and the second from  $\beta$  to  $\gamma$ . This interpretation is contradicted both by micrographic examination of samples of the alloy after annealing and quenching from various temperatures, when only two phases were recognized, and by high-temperature X-ray experiments when the  $\alpha$  and  $\gamma$  phases and not the  $\beta$  phase were detected.

A possible explanation of the two transformations observed in thermal-analysis experiments is that, with the cooling rates used, not all the  $\gamma$  phase had decomposed into  $\alpha$  by processes involving nucleation and growth before the temperature had fallen sufficiently to reduce diffusion to a very low rate, at which further growth of the  $\alpha$  precipitate would be insignificant. At this stage the specimen consists of the precipitated  $\alpha$  containing less than 4.9% molybdenum in a matrix of retained  $\gamma$ , richer in molybdenum. On further cooling another transformation takes place, where the retained  $\gamma$  transforms directly into  $\alpha$  of the same composition, by a martensitic or diffusionless type of reaction.

At room temperature, therefore, a slowly cooled alloy of this composition would consist of two  $\alpha$  phases of different compositions plus a trace of retained  $\gamma$ . In agreement with this hypothesis, the lines of the X-ray diffraction pattern due to  $\alpha$ -uranium were doubled, while those lines due to uranium oxides remained single. The small quantity of retained  $\gamma$  could not be detected for the reasons explained earlier.

Further experiments showed that the precipitation of  $\alpha$  from homogeneous  $\gamma$  in the temperature range  $700^{\circ}$ – $650^{\circ}$  C. is a process which depends upon the duration of the precipitation treatment as well as on the temperature of annealing. The amount of  $\alpha$  precipitated increased in a succession of specimens of the same composition with

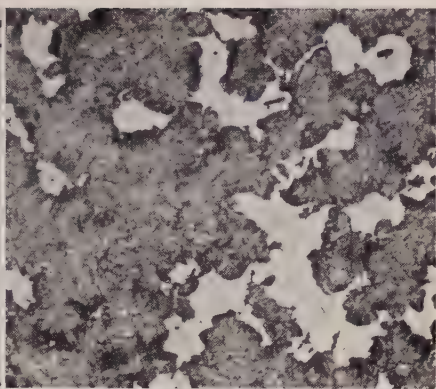
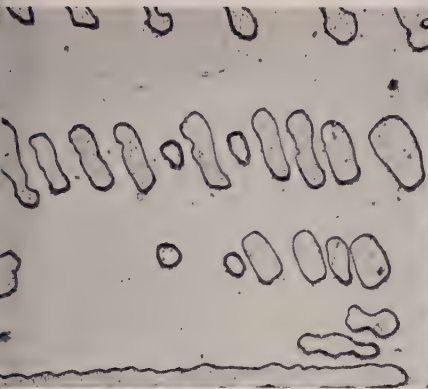
otherwise the same previous history, but with increasing annealing times at 670° C. Above 72 hours' annealing at 670° C. no further effects were observed. These observations are consistent with a reaction, involving diffusion, depending on the nucleation-and-growth type of kinetics. It is of interest to note that, particularly at the higher temperatures,  $\alpha$  was first precipitated along the grain boundaries and only at a later stage within the grains.

The micrographic appearance of alloys quenched both from the  $\gamma$  and  $(\gamma + \alpha)$  phase fields (see, for example, Fig. 7, Plate LXXVI, and Fig. 9, Plate LXXVII), is entirely consistent with a martensitic type of reaction having taken place on quenching. This decomposition could not be prevented by the fastest rates of quenching attainable. The first of the two transformations on reheating a slowly cooled sample of the 4.9 at.-% alloy is probably the martensitic transformation in reverse, though it may be caused by the molybdenum-rich portions of the sample transforming into  $\gamma$  by nucleation and growth mechanism.

The results of further thermal-analysis experiments supply additional confirmation that, under equilibrium conditions, there should be only one transformation in this alloy. A specimen was cooled through the temperature range of the first transformation, which was observed, and annealed at 650° C. overnight. On further cooling the second transformation was very much weaker than without intermediate annealing. On subsequent reheating at a steady overall rate of 1° C./min. the transformation in the temperature range 636°–674° C. was much weaker than that at the higher temperature. On extending the annealing period at 650° C. to 48 hr., but keeping the conditions otherwise the same, only one transformation was detected on cooling or on subsequent reheating. The thermal transformations of Table II have been disregarded in Fig. 2 because they refer to non-equilibrium conditions. Nevertheless the temperatures of the start of transformation No. 2 of this table are not inconsistent with the transformation temperatures established micrographically.

#### *9. Confirmatory Evidence Using Segregated Alloys.*

Annealing and quenching experiments at 14 different temperatures were performed with longitudinally segregated specimens, covering the composition range 2.0–21.4 at.-% molybdenum. The results of these experiments showed that no other phase had been overlooked, confirming the work with alloys of uniform compositions, and in addition demonstrated that  $\alpha$ , precipitating from a homogeneous  $\gamma$  solid solution, gives rise to a progressively finer microstructure the lower the temperature.



- Fig. 3.—44.4 at.-% Mo. As melted. Unetched. Primary crystals of Mo.  $\times 200$ .  
 Fig. 4.—23.7 at.-% Mo. As melted. Etched 2 min. Cored solid solution.  $\times 100$ .  
 Fig. 5.—4.9 at.-% Mo. As melted. Etched 2 min.  $\times 250$ .  
 Fig. 6.—11.7 at.-% Mo. Annealed for 5 hr. at  $588^{\circ}\text{C}$ . Etched 30 sec.  $\times 40$ .  
 Fig. 7.—4.9 at.-% Mo. Annealed for 2 days at  $740^{\circ}\text{C}$ . Etched 2 min. Decomposed  $\gamma$ .  
 $\times 200$ .  
 Fig. 8.—4.9 at.-% Mo. Annealed for 5 days at  $717^{\circ}\text{C}$ . Etched 30 sec.  $\gamma + \alpha$  (light).  
 $\times 150$ .

Etching reagent : 50% nitric, 50% acetic mixed acids.

[To face p. 568.



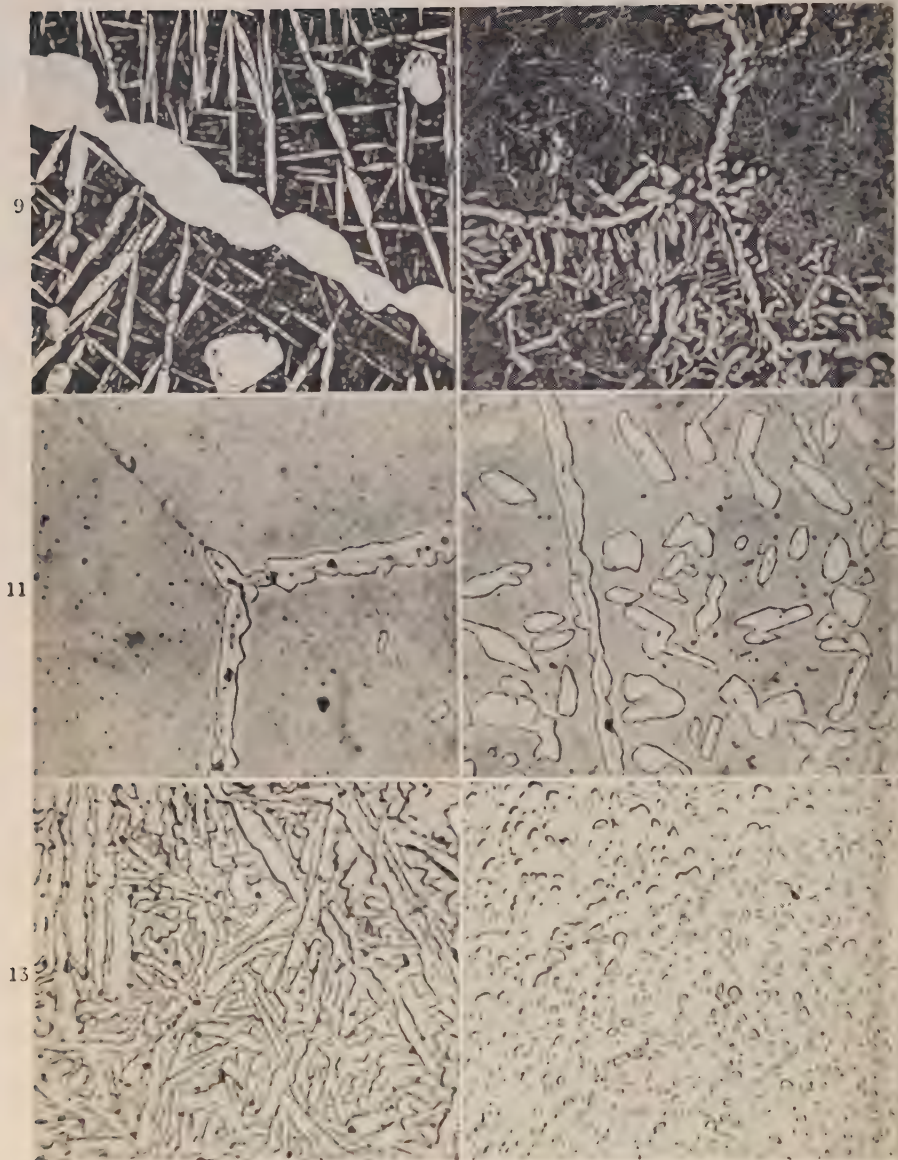


FIG. 9.—4.9 at.-% Mo. Annealed for 3 days at 740° C., then 4 days at 670° C. Etched 2 min.  $\times 200$ .

FIG. 10.—4.9 at.-% Mo. Annealed for 3 days at 740° C., then 7 days at 650° C. Etched 2 min.  $\times 150$ .

FIG. 11.—8.1 at.-% Mo. Annealed for 14 days at 650° C. Etched 30 sec.  $\gamma + \alpha$  (in grain boundaries).  $\times 400$ .

FIG. 12.—6.2 at.-% Mo. Annealed for 14 days at 650° C. Etched 30 sec.  $\gamma + \alpha$ .  $\times 400$ .

FIG. 13.—5.1 at.-% Mo. Annealed for 14 days at 650° C. Etched 30 sec.  $\alpha + \gamma$ .  $\times 400$ .

FIG. 14.—3.9 at.-% Mo. Annealed for 14 days at 650° C. Etched 30 sec.  $\alpha + \gamma$ .  $\times 400$ .

Etching reagent: 50% nitric, 50% acetic mixed acids.



## V.—DISCUSSION.

In many cases where metals or intermediate phases are found to possess complex crystal structures, these structures correspond to a Brillouin zone which can just accommodate the number of valency electrons per atom. This leads to a decrease in the contribution of the electronic energy to the free energy of the structure. It is possible, therefore, that the  $\alpha$  and  $\beta$  modifications of uranium correspond to structures with almost full Brillouin zones.

Raynor<sup>6</sup> has considered the forms of the Brillouin zone arising from combinations of the (110), (021), (002), (111), and (112) planes, all of which give rise to intense lines on the X-ray diffraction pattern of  $\alpha$ -uranium. A combination of the (021) and (110) planes gives rise to a zone which can contain 2.66 electrons per atom. Since it is unlikely that the effective valency for uranium is as low as 2.66, this zone can probably be regarded as a completely filled inner zone for  $\alpha$ -uranium. Planes of the form (111) can enclose a volume in  $k$ -space by themselves; calculations show that this volume can contain 4.09 electrons per atom. A combination of (111) and (110) planes gives a volume which can hold 3.62 electrons, while planes of the form (112) give rise to a Brillouin zone which can contain 8.97 electrons. Since this number is too large to correspond to the valency electrons of uranium, it must represent an outer zone which is not filled. If  $\alpha$ -uranium is characterized by an almost full Brillouin zone, then it is probable that the valency in this modification is four, and that the nearly full zone is that bounded by planes of the form (111) which can contain a maximum of 4.09 electrons. The crystal structure of  $\alpha$ -uranium is such that each atom has two nearest neighbours in the  $bc$  plane at a distance of 2.76 Å., making an angle of 127° with each other, and two neighbours at a slightly greater distance of 2.85 Å., vertically above and below a given atom along the  $a$  axis. Pauling<sup>9</sup> has shown that this structure is consistent with the presence of four covalent bonds and one inert pair. The form of the Brillouin zones for  $\beta$ -uranium is not at present known. In contrast to the relative complexity of the  $\alpha$  and  $\beta$  structures, the  $\gamma$  structure is typically metallic in which the full group valency of six may be acting.

The extensive solid solubility of molybdenum in  $\gamma$ -uranium, which attains a maximum of approximately 43 at.-% at 1280° C., is in agreement with the predictions of Raynor<sup>6</sup> (see Introduction). This solubility, combined with the fact that the lattice parameters, which are a linear function of composition, extrapolate to that of pure molybdenum (3.140 kX.), favours the view that the valency of

uranium in the  $\gamma$  form is the same as that of molybdenum, i.e. six; otherwise some deviation might be expected (see Raynor).<sup>10</sup> The theory that  $\alpha$ -uranium is quadrivalent, with an almost full Brillouin zone, is supported by the lack of an extensive solubility of molybdenum in this modification of uranium. The very restricted solubility of molybdenum in the  $\beta$  modification suggests that the valency of  $\beta$ -uranium is different from six and that like the  $\alpha$  form,  $\beta$  is characterized by an almost full Brillouin zone. The fact that molybdenum has a higher solubility in  $\gamma$ -uranium than in the  $\alpha$  or  $\beta$  modifications, results, as predicted, in the stabilization of the  $\gamma$  form down to lower temperatures. With approximately 19 at.-% molybdenum in solid solution, the  $\gamma$  body-centred cubic modification of uranium is stable from room temperature up to the solidus temperature.

The existence of a direct  $\gamma \rightleftharpoons \alpha$  transformation of the martensitic type in uranium-molybdenum alloys is of interest, as it suggests the possibility that if pure uranium were quenched rapidly enough from above the  $\beta \rightleftharpoons \gamma$  transition temperature, the  $\gamma$  phase might decompose directly into  $\alpha$ , without first forming  $\beta$ .

#### ACKNOWLEDGEMENTS.

The author wishes to express his thanks to the Director of the Atomic Energy Research Establishment for permission to publish this paper; to Mr. J. D. Grogan and Mr. R. J. Pleasance of the Metallurgy Division of the National Physical Laboratory for the preparation of many of the alloys used in the investigation; and to Dr. T. S. Hutchinson of the Diffraction Group, A.E.R.E., for much valuable assistance and advice in connection with the high-temperature X-ray work. Grateful acknowledgement is also made to Mr. C. H. Thomas for help with the experiments and to Mr. H. Haines for skilful assistance with the photomicrography. To Professor G. V. Raynor and to Dr. H. M. Finniston, particular thanks are due for their interest and for helpful discussions during the course of the work.

#### REFERENCES.

1. G. E. Moore and K. K. Kelley, *J. Amer. Chem. Soc.*, 1947, **69**, 2105.
2. A. I. Dahl and M. S. Van Dusen, *J. Research Nat. Bur. Stand.*, 1947, **39**, 53.
3. C. W. Jacob and B. E. Warren, *J. Amer. Chem. Soc.*, 1937, **59**, 2588.
4. J. Chipman, *U.S. Atomic Energy Commission Publ.*, 1946, (MDDC-539).
5. A. S. Wilson and R. E. Rundle, *Acta Cryst.*, 1949, **2**, 126.
6. G. V. Raynor, private communication.
7. W. Hume-Rothery and G. V. Raynor, *J. Sci. Instruments*, 1941, **18**, 74.
8. A. I. Dahl and H. E. Cleaves, *J. Research Nat. Bur. Stand.*, 1949, **43**, 513.
9. L. Pauling, "The Nature of the Chemical Bond and the Structure of Molecules and Crystals", p. 143 (2nd edn.). Ithaca, N.Y.: 1940 (Cornell University Press).
10. G. V. Raynor, *Trans. Faraday Soc.*, 1949, **45**, 698.

## THE URANIUM-IRON SYSTEM.\*

1264

By J. D. GROGAN,† B.A., MEMBER.

WITH AN APPENDIX ON

## AN X-RAY EXAMINATION OF URANIUM-IRON ALLOYS.

By C. J. BIRKETT CLEWS,† B.Sc., Ph.D.

(Communication from the National Physical Laboratory.)

## SYNOPSIS.

The solubility of iron in solid uranium increases with temperature from about 0.004 wt.-% (0.018 at.-%) at 600° C. to about 0.35 wt.-% (1.5 at.-%) at 805° C., the temperature at which the solid-solubility curve meets both the solidus and a peritectic horizontal line where liquid reacts with solid uranium to form the compound  $U_6Fe$ . No discontinuous change in solubility has been detected at the transformation of  $\alpha$ - into  $\beta$ -uranium, but at the transformation of  $\beta$  into  $\gamma$  the solubility increases from 0.1 to 0.2 wt.-% (0.4–0.8 at.-%). The liquidus meets the peritectic horizontal at about 5 wt.-% (18 at.-%) iron. The compound  $U_6Fe$  forms with another compound ( $UFe_2$ ) a eutectic which contains about 11 wt.-% (34 at.-%) iron and melts at 725° C. The compound  $UFe_2$  melts at 1230° C. and forms, with iron, a eutectic which contains about 47 wt.-% (78 at.-%) iron and melts at 1055° C.

X-ray examination has confirmed the existence of these two compounds. The structure of  $UFe_2$  is discussed.

THIS paper describes an examination of the uranium end of the uranium-iron system and a brief survey of the remainder. After this work had been completed a paper by Gordon and Kaufman,<sup>1</sup> covering the same subject, was published in the U.S.A. The conclusions reached in the two papers are very similar.

## I.—EXPERIMENTAL.

*Materials Used.*—The iron used in this investigation was metal of 99.98% purity prepared at the National Physical Laboratory. The uranium, which was provided by the Ministry of Supply, Division of Atomic Energy, was also of high purity.

*Alloying.*—Alloys were prepared by melting charges of 200–300 g. in a H.F. induction furnace *in vacuo*. Alloying took place readily; heating and cooling curves were taken by the methods described by Adcock.<sup>2</sup>

*Polishing.*—The Vickers hardness number of uranium is about 200.

\* Manuscript received 11 February 1950.

† Metallurgy Division, National Physical Laboratory, Teddington, Middlesex.

The metal, though not hard, rapidly blunted the usual steel hacksaw blade; consequently, pieces for polishing were generally cut off by means of a high-speed diamond wheel. The particles detached on cutting ignited in air. The metal is toxic, and to prevent these particles from escaping into the air the work was copiously flooded with water and slitting was carried out behind a screen. Surfaces for polishing were ground on emery paper flooded with paraffin. Grinding was continued to Hubert 00 paper. The metal was polished first on a revolving pad with chromic oxide, which was carefully washed to remove any traces of chromic acid, and was finished by hand-polishing with magnesia on Selvyt cloth. The polished surface tarnished rapidly in air, particularly when the weather was warm.

An electrolytic bath was sometimes used for the final polishing; this produced a brilliant finish and emphasized the different phases present without colouring them in the very short time employed. The bath was composed of equal volumes of absolute alcohol, ethylene glycol, and orthophosphoric acid (density 1.5). The cathode was of carbon; the voltage 15–20 V. The time needed was a few seconds; longer exposure generally caused the destruction of one of the phases when the material being polished was duplex. The oxide  $\text{UO}_2$  was particularly rapidly attacked.

*Etching.*—The agent used was nitric acid diluted with an equal volume of water or acetic acid. Both solutions behaved in a very similar manner. Uranium was slowly attacked by this agent. The compound  $\text{U}_6\text{Fe}$  was gradually coloured a pale yellow on long treatment and when in contact with the uranium phase the boundary became strongly outlined. Prolonged etching for a period of 15–45 min. was required to develop the structure of  $\text{U}_6\text{Fe}$  precipitated from solid solution in  $\beta$ -uranium (Fig. 7, Plate LXXIX). The peculiar attack of the etching reagent on the compound  $\text{UFe}_2$  is described later in the paper. The oxide  $\text{UO}_2$ , which was present in all the phases of the system except the free iron phase, was rapidly eaten out during etching and was represented by black holes in the etched material.

## II.—THE CONSTITUTIONAL DIAGRAM.

### 1. The Uranium-Rich Area.

*The Liquidus.*—The melting point of the uranium used in this investigation was  $1125^\circ\text{C}$ . On addition of iron the liquidus fell to  $1084^\circ\text{C}$ . at 0.4 wt.-% (1.7 at.-%) and to  $805^\circ\text{C}$ . at 5 wt.-% (18 at.-%). At low iron concentrations the liquidus was detected by thermal analysis, but at concentrations above 1.8 wt.-% no arrests due to the liquidus were

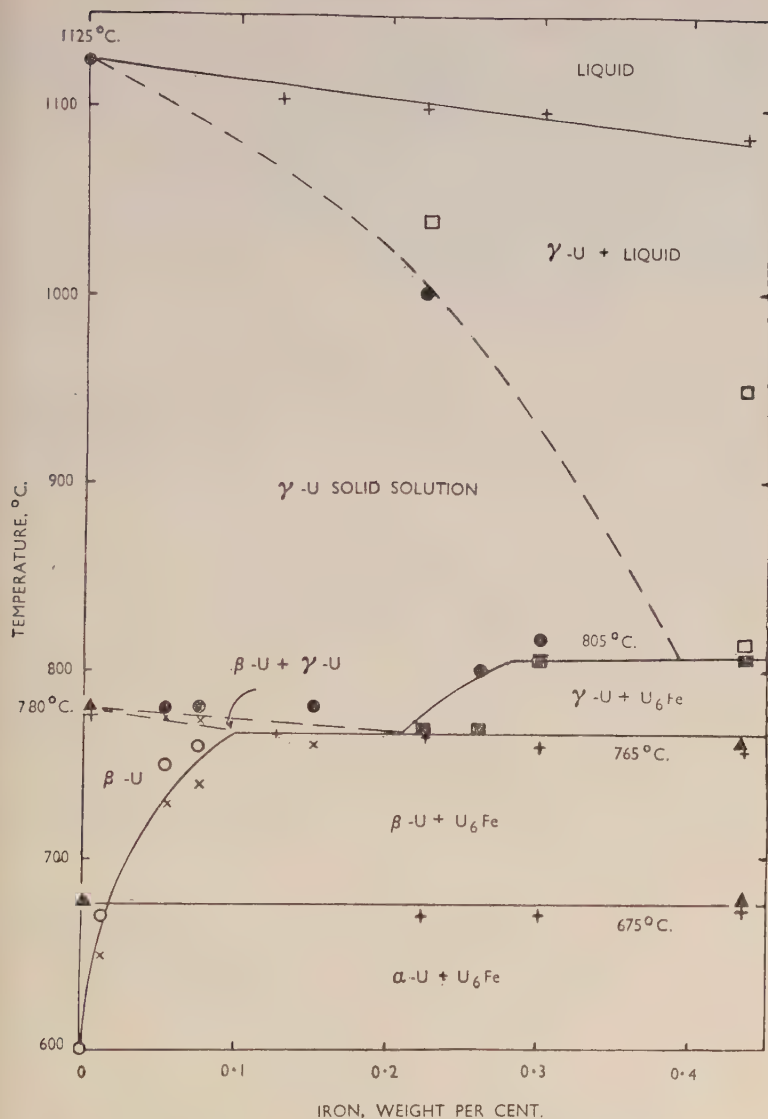


FIG. 1.—Uranium-Rich Area of the Uranium-Iron Equilibrium Diagram.

## KEY.

- + Thermal arrests.
- ▲ Dilatometer arrests.
- Liquid.
- Single-phase  $\gamma$ .

- Single-phase  $\alpha$  or  $\beta$ .
- × Duplex  $\alpha$  or  $\beta$  +  $U_6Fe$ .
- Duplex  $\gamma$  +  $U_6Fe$ .



seen in thermal curves until compositions were reached in which the peritectic reaction no longer occurred. From there to the eutectic composition the liquidus arrest again appeared. Fig. 1 gives the shape of the liquidus, solidus, and solid-solubility curves.

*The Solidus.*—The solidus falls very rapidly with increase of iron. At 0.43 wt.-% (1.85 at.-%) iron it occurs at 805° C., the temperature of the peritectic reaction. Its form was determined approximately by quenching experiments; Fig. 3 (Plate LXXIX) shows a small amount of chilled liquid in an alloy containing 0.42 wt.-% (1.85 at.-%) iron quenched in mercury from 815° C.

*Changes in the Solid State.*—Uranium exists in three allotropic modifications,  $\alpha$ ,  $\beta$ , and  $\gamma$ . The changes from  $\alpha$  to  $\beta$  and from  $\beta$  to  $\gamma$  are accompanied by sudden expansions, and thus can easily be detected by dilatometric measurements. They take place with considerable absorption of heat and so can be detected also by thermal analysis. Both transformations occur on cooling at lower temperatures than on heating and are accompanied by a recalescence which is insufficient in amount to raise the temperature to that of the transformation on heating; the latter has been accepted as the equilibrium transformation temperature in the construction of the equilibrium diagram.

*The  $\beta \rightleftharpoons \gamma$  Change.*—This change occurred in the purest available samples of uranium at 780° C. on heating and at 770° C. on cooling; the change on cooling occurred regularly with a recalescence of 2°–3° C. The addition of 0.22 wt.-% iron lowered the change on heating to 765° C. and on cooling to 750° C. Further addition of iron altered these temperatures very little. The values obtained by thermal analysis agreed fairly well with those obtained by dilatometric measurements, but were rather lower. X-ray examination at room temperature has shown only  $\alpha$ -uranium in material quenched from elevated temperatures. Quenching therefore does not suppress the  $\gamma$ - $\beta$  and  $\beta$ - $\alpha$  transformations. Material of low iron content quenched from the  $\gamma$  range developed on etching the structure shown in Fig. 4 (Plate LXXIX). This structure is typical of material quenched from the  $\gamma$  range and did not occur in material quenched from the  $\beta$  or  $\alpha$  range. The  $\gamma$ - $\beta$  change in pure uranium does not occur over a range of temperature. The addition of iron produces a range over which  $\gamma$  and  $\beta$  exist together (see Fig. 1). Fig. 5 (Plate LXXIX) shows an alloy (iron 0.15 wt.-%) quenched in this range. In this figure the clear areas are the  $\beta$  phase and the striated ones the decomposed  $\gamma$ . The black spots are uranium oxide,  $\text{UO}_2$ . Fig. 6 (Plate LXXIX) shows the same material slowly cooled through the  $\gamma$ - $\beta$  change and illustrates the mode of precipitation of the iron as  $\text{U}_6\text{Fe}$  from  $\gamma$  solid solution at the  $\gamma$ - $\beta$  eutectoid transformation.

*The  $\alpha \rightleftharpoons \beta$  Change.*—The solubility of iron in  $\beta$ -uranium decreases with temperature. The compound  $U_6Fe$  separates in lamellar form (Fig. 7, Plate LXXIX) from this phase. On annealing, this structure aggregates into larger particles (Fig. 8, Plate LXXIX).

In the purest available uranium the  $\alpha \rightleftharpoons \beta$  transformation occurred at 675° C. on heating and at 660° C. on cooling, with a recalescence of a few degrees on cooling. No alteration of transformation temperature due to the presence of iron has been detected; as the solid solubility of iron in uranium at this temperature is only about 0.01 wt.-%, any change in solubility at this temperature is likely to be so small as to evade detection.

The solubility of iron in the  $\alpha$  range decreases with temperature, and Fig. 8 shows that it is less than 0.014 wt.-% at 650° C. No free  $U_6Fe$  was detected at room temperature in the purest sample of uranium available; this contained 0.0036 wt.-% iron.

## 2. The Compound $U_6Fe$ and Peritectic Area (Fig. 2, Plate LXXVIII).

Primary uranium separates from the liquid until the iron content reaches about 5 wt.-% (18 at.-%). At 805° C. solid uranium and liquid react to form the compound  $U_6Fe$ . On cooling, this reaction occurs with recalescence, which may be very marked; the temperature has been observed to fall over 30° C. below the peritectic temperature before the reaction started; in all cases, except when the iron content was very low (0.43%), the heat evolved was sufficient to raise the temperature to 805° C. by recalescence. In these alloys the free uranium appeared as very characteristic rounded particles in a network of compound (Fig. 9, Plate LXXX). In the range of composition from approximately 2.5 to 3.8 wt.-% iron, the reaction between solid and liquid was not complete, free uranium,  $U_6Fe$ , and the eutectic  $U_6Fe-UFe_2$  appearing together in the metal (Fig. 10, Plate LXXX). Segregation occurred in this range, the metal becoming richer in iron towards the top of the ingot, and chemical analyses of samples from different areas varied considerably from one another. In alloys higher in iron agreement was very satisfactory. Alloys containing from 4 wt.-% (15 at.-%) iron to the eutectic composition at about 11 wt.-% (34 at.-%) show pseudo-primary or primary  $U_6Fe$  and  $U_6Fe-UFe_2$  eutectic (Fig. 11, Plate LXXX). Near the eutectic composition the primary  $U_6Fe$  developed a columnar structure (Fig. 12, Plate LXXX).

## 3. The $U_6Fe-UFe_2$ Eutectic (Fig. 2, Plate LXXVIII).

The liquidus was not detected on thermal curves in alloys of composition near to that of the compound  $U_6Fe$ . When the peritectic area

was passed, arrest points due to the liquidus occurred. The liquidus fell with increasing iron content to 725° C. at the eutectic composition, about 11 wt.-% (34 at.-%) iron. The positions of this eutectic and of that between  $\text{UFe}_2$  and Fe have not been fixed with accuracy; the liquidus in these areas has been drawn in broken curves to indicate this.

In alloys containing 4–6 wt.-% (15–21 at.-%) iron, arrest points not represented by a line on the diagram (Fig. 2, Plate LXXVIII) were detected on thermal analysis at about 750° C. On cooling, the arrest was sharp; on heating, it spread over 10° C. or more. This may represent some change occurring in the compound  $\text{U}_6\text{Fe}$ . Alloys in the region of that compound burst their containers on cooling. It is difficult to assign this fact to a change in volume due to the peritectic reaction at 805° C., and it may be associated with these points. Alloys of composition near to  $\text{U}_6\text{Fe}$  were very brittle and cracked badly (Fig. 13, Plate LXXX). This cracking also may be due to the same change.

#### 4. *The Compound $\text{UFe}_2$* (Fig. 2, Plate LXXVIII).

As the iron content of the alloys increases above 11 wt.-% the liquidus rises to 1230° C. at the melting point of the compound  $\text{UFe}_2$ . This compound, which like  $\text{U}_6\text{Fe}$  has a white metallic colour when polished, possesses peculiar etching properties; when attacked for a short time, about 30 sec., by 50% nitric acid it is coloured a deep black. On longer exposure it again becomes colourless (Figs. 14 and 15, Plates LXXX and LXXXI). No alloy of composition near to  $\text{UFe}_2$  has been prepared free from both  $\text{U}_6\text{Fe}$  and Fe (Fig. 16, Plate LXXXI). This suggests that the range of composition of the phase  $\text{UFe}_2$  is small; no annealing treatments have been carried out to explore the range.

#### 5. *The $\text{UFe}_2$ -Fe Area* (Fig. 2, Plate LXXVIII).

With increasing iron content the liquidus falls to 1055° C., the melting point of the  $\text{UFe}_2$ -Fe eutectic. This contains about 47 wt.-% (78 at.-%) iron (Figs. 17, 18, and 19, Plate LXXXI). At room temperature the iron is present as  $\alpha$  and the alloys are highly magnetic. The influence of uranium on the  $\alpha$ - $\gamma$  change has not been investigated. In the one alloy submitted to thermal analysis an arrest occurred on heating at 935° C. This arrest may be associated with the  $\alpha$ - $\gamma$  change. No corresponding arrest was observed on cooling.

The solid solubility of uranium in iron has not been investigated. The presence of a slight Widmanstätten structure in the iron phase suggests that there may be some solubility (Fig. 20, Plate LXXXI); it is not sufficient, at room temperature, to change the lattice parameter of  $\alpha$ -iron significantly.

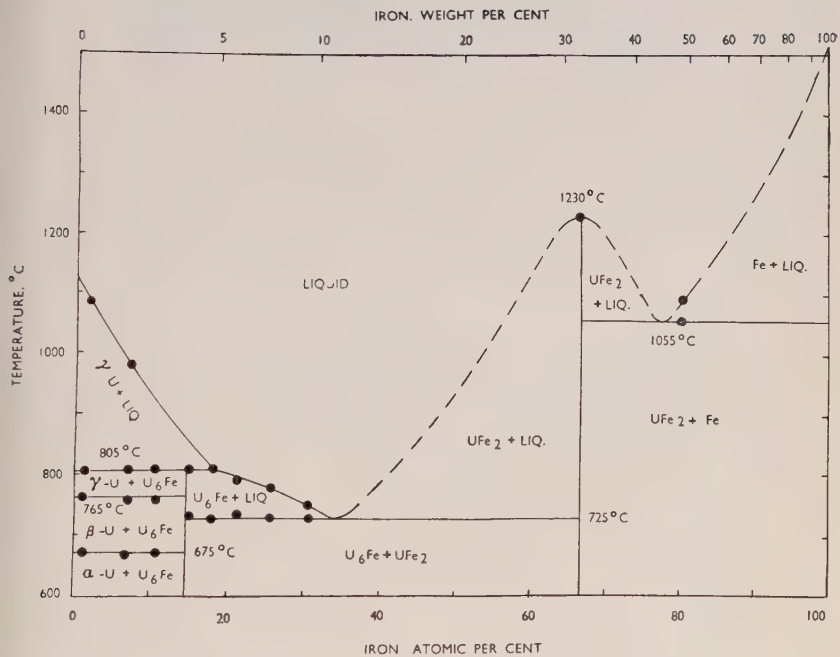
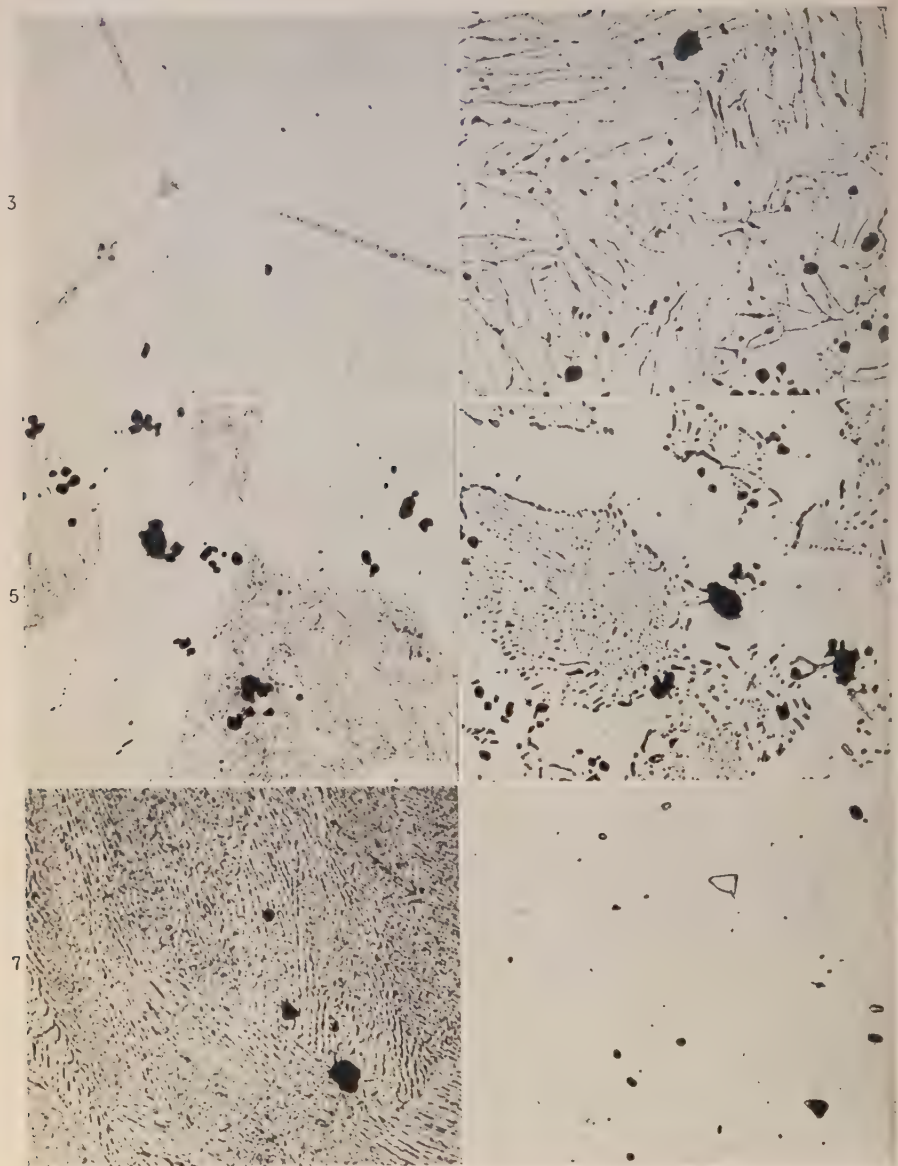


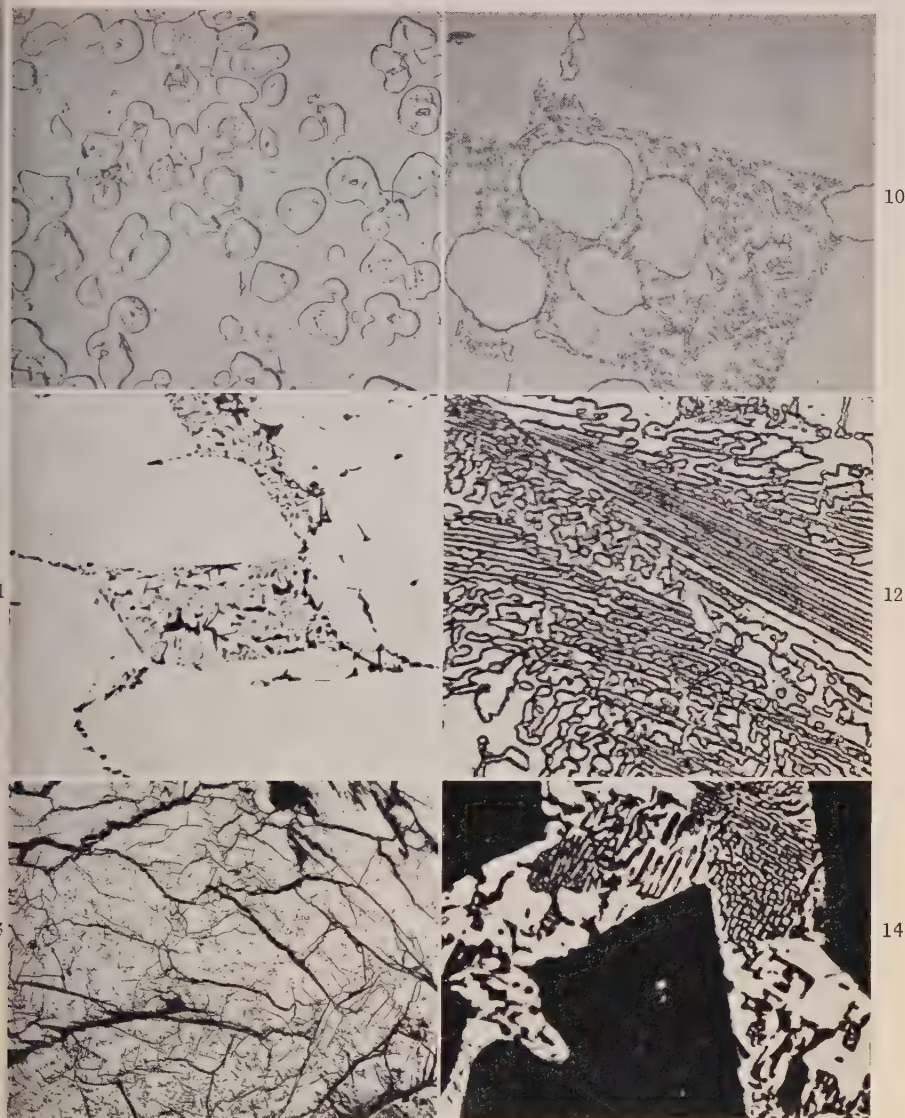
FIG. 2.—The Uranium-Iron Equilibrium Diagram.



FIGS. 3-8.—PHOTOMICROGRAPHS OF URANIUM-IRON ALLOYS.

- FIG. 3.—0.42 Wt.-% (1.85 at.-%) iron. Quenched from 815° C.  $\gamma$  + liquid.  $\times 500$ .  
 FIG. 4.—0.15 Wt.-% (0.65 at.-%) iron. Quenched from 777° C. Deeply etched. Decomposed  $\gamma$  and  $\text{UO}_2$  (black).  $\times 150$ .  
 FIG. 5.—0.15 Wt.-% (0.65 at.-%) iron. Quenched from 770° C.  $\beta$  (clear areas);  $\gamma$  (striated);  $\text{UO}_2$  (black).  $\times 150$ .  
 FIG. 6.—0.15 Wt.-% (0.65 at.-%) iron. Quenched from 600° C.  $\text{U}_6\text{Fe}$  precipitated from decomposed  $\gamma$ ;  $\text{UO}_2$  (black).  $\times 150$ .  
 FIG. 7.—0.052 Wt.-% (0.22 at.-%) iron. Furnace-cooled from 900° C. Deeply etched.  $\times 500$ .  
 FIG. 8.—0.014 Wt.-% (0.06 at.-%) iron. Annealed for 72 hr. at 649° C. and quenched.  $\alpha$ ;  $\text{U}_6\text{Fe}$ ;  $\text{UO}_2$  (black).  $\times 500$ .





FIGS. 9-14.—PHOTOMICROGRAPHS OF URANIUM-IRON ALLOYS.

Fig. 9.—1.8 Wt.-% (7.0 at.-%) iron. Finished electrolytically. Rounded U in  $U_6Fe$ .  $\times 150$ .  
 Fig. 10.—3.2 Wt.-% (12.5 at.-%) iron. Finished electrolytically. Rounded U and  $U_6Fe-UFe_2$  eutectic in  $U_6Fe$ .  $\times 500$ .

Fig. 11.—4.0 Wt.-% (15 at.-%) iron. Etched in  $HNO_3$ .  $U_6Fe-UFe_2$  eutectic in  $U_6Fe$ .  $\times 150$ .

Fig. 12.—9.2 Wt.-% (30 at.-%) iron. Finished electrolytically. Mainly  $U_6Fe-UFe_2$  eutectic.  $\times 500$ .

Fig. 13.—4.0 Wt.-% (15 at.-%) iron. Showing spontaneous cracking of ingot. Photomacrograph.  $\times 4$ .

Fig. 14.—20.0 Wt.-% (51 at.-%) iron. Etched 15 sec.  $UFe_2$  (black);  $U_6Fe$  (white).  $\times 500$ .



FIGS. 15-20.—PHOTOMICROGRAPHS OF URANIUM-IRON ALLOYS.

- FIG. 15.—As Fig. 14 (Plate LXXX), etched 2 min.  $U_6Fe$  and  $UFe_2$  (both white).  $\times 500$ .
- FIG. 16.—30.0 Wt.-% (64 at.-%) iron. Unetched. Mainly  $UFe_2$ , with a little  $U_6Fe-UFe_2$  eutectic.  $\times 500$ .
- FIG. 17.—40.0 Wt.-% (74 at.-%) iron. Etched 30 sec.  $UFe_2$  (black) and  $UFe_2-Fe$  eutectic.  $\times 500$ .
- FIG. 18.—50 Wt.-% (81 at.-%) iron. Finished electrolytically.  $Fe$  and  $UFe_2-Fe$  eutectic.  $\times 500$ .
- FIG. 19.—As Fig. 18, etched 30 sec.  $UFe_2-Fe$  eutectic.  $\times 2000$ .
- FIG. 20.—As Fig. 18. Finished electrolytically. Showing Widmanstätten structure in  $Fe$ .  $\times 2000$ .

## APPENDIX.

AN X-RAY EXAMINATION OF URANIUM-IRON ALLOYS, AND A DISCUSSION OF THE STRUCTURE OF  $\text{UFe}_2$ .

By C. J. BIRKETT CLEWS, B.Sc., Ph.D.

A series of ten uranium-iron alloys has been examined by the X-ray diffraction method. The alloys contained from 1 to 50 wt.-% iron. All the samples containing 4% and more of iron were prepared by pounding in a steel pestle. They were made from unannealed ingots and were not necessarily in equilibrium. The powder samples were not annealed. The constituents of these alloys, as determined by the X-ray method, are summarized in Table I. Apart from impurities in the form of uranium oxide, only four phases were observed, the iron and uranium phases and "A" and "B" phases.

TABLE I.—*Constituents of Uranium-Iron Alloys as Determined by X-Ray Diffraction Method.*

Sample	Fe, wt.-%	Constituents				
		U	"A" ( $\text{U}_6\text{Fe}$ )	"B" ( $\text{UFe}_2$ )	Fe	Uranium Oxides
X23 . . .	1.1	Present	Present	...	...	...
UF18 . . .	1.8	"	"	...	...	...
UF40 . . .	4	...	95%	Trace ?	...	< 5%
UF50 . . .	5	...	< 95%	Trace ?	...	5%
UF70 . . .	7	...	> 70%	25%	...	< 5%
UF80 . . .	8	...	65%	30%	...	> 5%
UF100 . . .	10	...	30%	50%	...	20%
UF200 . . .	20	...	10%	85%	...	> 5%
UF300 . . .	32	...	?	95%	5%	...
UF500 . . .	50	...	...	70%	25%	5%

The diffraction lines belonging to the "A" phase, which from metallurgical evidence is the compound  $\text{U}_6\text{Fe}$ , were in all cases very broad and diffuse. Line broadening may be attributable either to lattice distortion giving rise to variations in the lattice parameter, or to small particle size. From the observed behaviour of alloys of composition near to  $\text{U}_6\text{Fe}$  the former explanation is the more likely, the broadening being due to stresses in the material. The crystal structure of this compound \* is tetragonal. The principal spacings are listed in Table II.

The "B" phase gave sharp diffraction lines, and with increase in iron content there was a very small but definite decrease in the spacings. This phase, which has a cubic diamond type of structure, has a com-

\* A further study <sup>3</sup> of this compound appeared after the present paper had been submitted for publication.

TABLE II.—*Diffraction Line Spacings and Intensities for Phase "A" ( $U_6Fe$ ).*

Spacings, Å.	Intensity	Spacings, Å.	Intensity
3.15	m	1.46	w
2.60	m-w	1.43	s
2.50	s	1.36 <sub>5</sub>	s
2.25	w	1.31	s
2.10	vw	1.27 <sub>5</sub>	m-w
2.02	m-w	1.22	m-w
1.83	w	1.17 <sub>5</sub>	m-s
1.72	w	1.13 <sub>5</sub>	w
1.60	w	1.09 <sub>5</sub>	w
1.49	m-s		

position corresponding to the compound  $UFe_2$ ; it is isomorphous with the uranium-aluminium compound  $UAl_2$ . The respective lattice parameters are  $UFe_2$  7.04<sub>2</sub> Å., and  $UAl_2$  7.74<sub>1</sub> Å. The parameter value for  $UFe_2$  has been determined from the spacings given by the alloy corresponding most closely in composition to that of the pure compound.

The lattice parameter and the line intensities of the compound  $UAl_2$  measured at the National Physical Laboratory, are in close agreement with the values quoted by Rundle and Wilson.<sup>4</sup> The structure type in the nomenclature of the "Strukturbericht" is C15 ( $Cu_2Mg$  structure). The spacings, indices, and intensities of the "B" ( $UFe_2$ ) phase are listed in Table III, and the calculated intensities for  $UAl_2$ , taken from

TABLE III.—*Diffraction Line Spacings, Indices, and Intensities for Phase "B" ( $UFe_2$ ).*

Indices	Spacings, Å.	Observed Intensities	Calculated Intensities for $UAl_2$ *
(111)	4.05	m	78
(200)	...	...	0
(220)	2.50	s	314
(311)	2.11 <sub>3</sub>	s	375
(222)	...	...	10
(400)	1.76	w	100
(331)	1.61 <sub>5</sub>	m	170
(420)	...	...	0
(422)	1.44	s	429
(333) (511)	1.35 <sub>9</sub>	s	375
(440)	1.25 <sub>5</sub>	s	293
(531)	1.19 <sub>5</sub>	m	254
(442) (600)	...	...	0
(620)	1.12	s	334
(533)	1.08	s	216

\* According to Rundle and Wilson,<sup>4</sup>



Rundle and Wilson, are included for comparison. It will be noted that the agreement is satisfactory.

The atomic positions in the face-centred lattice are :

8 U atoms in (000;  $\frac{1}{4}\frac{1}{4}\frac{1}{4}$ );  
16 Fe atoms in ( $\frac{5}{8}\frac{5}{8}\frac{5}{8}$ ;  $\frac{6}{8}\frac{6}{8}\frac{6}{8}$ ;  $\frac{7}{8}\frac{7}{8}\frac{7}{8}$ ;  $\frac{3}{8}\frac{3}{8}\frac{3}{8}$ ).

The interatomic distances are :

- (a) About each U atom, 4 U at 3.05 Å. and 12 Fe at 2.92 Å.
- (b) About each Fe atom, 6 Fe at 2.48 Å. and 3 U at 2.92 Å.

The U-Al interatomic distances given by Rundle and Wilson appear to be in error and should be 3.23 Å. and not 2.58 Å.

In several recent papers (Pauling,<sup>5</sup> Pauling and Soldate,<sup>6</sup> Zachariasen<sup>7</sup>) the structures of intermetallic compounds have been discussed in the light of Pauling's resonating-valence-bond theory (Pauling<sup>5, 8</sup>).

From the equation :

$$R(1) - R(n) = 0.300 \log n,$$

where  $R(1)$  is the single-bond radius and  $R(n)$  is the experimentally observed radius, it is possible to calculate  $n$ , the bond number or the number of shared electron pairs involved in the bond. Taking Pauling's single-bond radii for uranium and iron and the radii determined from the  $\text{UFe}_2$  structure, the bond numbers are 0.45, 0.54, and 0.28 for the U-U, Fe-Fe, and U-Fe bonds, respectively. These give valencies of a little over 5 for uranium and about 4.5 for iron, compared with the normal Pauling valency for transition elements of 5.78 (or 6). If, following Pauling, the bond numbers are expressed as simple fractions,  $\frac{1}{2}$ ,  $\frac{1}{2}$ , and  $\frac{3}{10}$ , the calculated valencies become 5.60 for uranium, in good agreement with the normal valency, and 3.90 for iron, indicating a valency of 4. The bond lengths calculated from these modified bond numbers are U-U 3.02 Å., Fe-Fe 2.51 Å., and U-Fe, 2.90 Å.

A similar calculation for the compound  $\text{UAl}_2$  leads to valencies of 2.8 ( $\approx 3$ ) for aluminium and 2.0 for uranium. This low value of the uranium valency has been found for a number of uranium silicides by Zachariasen,<sup>7</sup> and Pauling and Ewing<sup>9</sup> found it necessary to assume that some of the uranium atoms in the  $\text{UH}_3$  structure have a valency of 2.3.

The difference in valency behaviour of the uranium atoms in these two compounds with the same crystal structure is striking. It would appear that whereas the iron atoms adjust their valency to allow the uranium atoms to have their normal valency, in the  $\text{UAl}_2$  structure it is



## 580 *An X-Ray Examination of Uranium-Iron Alloys*

the aluminium atoms which have normal valency and the uranium valency is adjusted to permit this. At this stage it is not possible to draw conclusions; a great deal more needs to be known before the full significance of the resonating-bond theory as applied to intermetallic compounds is understood.

### ACKNOWLEDGEMENTS.

The work described above was carried out in the Metallurgy Division of the National Physical Laboratory as part of the programme of the Division of Atomic Energy, Ministry of Supply. This paper is published on the recommendation of the Division of Atomic Energy and by permission of the Director of the Laboratory.

The author wishes to acknowledge the assistance given by Mr. R. J. Pleasance who prepared all the microsections and photomicrographs and carried out much of the observational work. The X-ray patterns were prepared by Miss B. R. Brown, B.Sc.

### REFERENCES.

1. P. Gordon and A. R. Kaufman, *U.S. Atomic Energy Commission Publ.*, 1949, (AECD-2683); also *Trans. Amer. Inst. Min. Met. Eng.* (in *J. Metals*), 1950, **188**, (1), 182.
2. F. Adcock, *J. Iron Steel Inst.*, 1931, **124**, 114; 1937, **135**, 282.
3. N. C. Baenziger, R. E. Rundle, A. I. Snow, and A. S. Wilson, *Acta Cryst.*, 1950, **3**, 34.
4. R. E. Rundle and A. S. Wilson, *Acta Cryst.*, 1949, **2**, 148.
5. L. Pauling, *J. Amer. Chem. Soc.*, 1947, **69**, 542.
6. L. Pauling and A. M. Soldate, *Acta Cryst.*, 1948, **1**, 212.
7. W. H. Zachariasen, *Acta Cryst.*, 1949, **2**, 94.
8. L. Pauling, *Proc. Roy. Soc.*, 1949, [A], **196**, 343.
9. L. Pauling and F. J. Ewing, *J. Amer. Chem. Soc.*, 1948, **70**, 1660.

# DEFORMATION TEXTURE OF DRAWN FACE-CENTRED CUBIC METAL WIRES.\* 1265

By WALTER R. HIBBARD, Jr.,† A.B., D.Eng., MEMBER.

## SYNOPSIS.

Theoretical considerations indicate that the deformation texture of drawn face-centred cubic metal wires should be a single [111] orientation rather than the double [111], [100] orientation previously reported. X-ray analyses of wires drawn 98% show essentially a single [111] texture for lead, nickel, copper, aluminium, silver, and gold, in support of this theory.

## I.—INTRODUCTION.

A DEFORMATION texture has been defined as the crystal orientation with respect to the stress axis which is eventually attained by most of the grains of a polycrystalline aggregate and is such that the required type of strain may occur without changing this orientation. Since during slip the slip direction is that in which the metal flows, the texture orientation must contain active slip directions suitably oriented to accommodate the imposed strain. For example, in a drawn wire, the texture orientation must contain at least three active slip directions symmetrically disposed about the wire axis in order to retain the circular cross-section of the wire during drawing, and these must be less than  $45^\circ$  from the wire axis in order to extend the wire in the drawing direction and reduce its diameter by the action of shear on planes in which the component of axial force resolved in the slip direction is greater than the associated normal component (in the plane containing the axis and the slip direction). Otherwise, the orientation of the crystals will change during deformation. For face-centred cubic metals, the only orientation meeting these requirements is a [111] direction parallel to the wire axis.

This analysis suggests that the double [111], [100] wire texture which has been reported for most face-centred cubic metal wires for the last twenty-five years or so <sup>2, 3, 4, 5</sup> is actually not the final texture but an intermediate one. In support of this suggestion, it has been found <sup>6</sup> that after sufficient deformation (about 96% reduction in dia.), copper and copper alloy wires lose their [100] component, leaving essentially a single [111] texture as predicted by theory.<sup>1, 7</sup> The single [111] texture is a favourable one theoretically, for, although mechanisms have

\* Manuscript received 1 December 1949.

† Assistant Professor of Metallurgy, Yale University, New Haven, Conn., U.S.A.

been described <sup>8</sup> for obtaining the [100] component in the wires, there is no theory which can account for the varying amounts of it in different metals.

This development leaves some doubt as to the accuracy of Table I, which was originally published by Schmid and Wassermann <sup>4</sup> in 1927, and reproduced frequently thereafter.

TABLE I.—*Percentage of Crystals with Direction Parallel to the Wire Axis.*

Metal	Parallel to [100] Axis	Parallel to [111] Axis
Aluminium . . . .	0%	100%
Copper . . . . .	40%	60%
Gold . . . . .	50%	50%
Silver . . . . .	75%	25%

In fact, a careful study of Schmid and Wassermann's paper reveals the following points which suggest that their results should be further investigated:

- (1) The wires were extensively etched before X-ray analysis.
- (2) The amount of deformation was not recorded.
- (3) The "gold" actually contained 75% gold, 16% silver, and 9% copper.

(4) Cylindrical-film X-ray techniques were used rather than the directed-beam transmission methods more recently used for determining pole figures.

Earlier papers by Ettisch, Polányi, and Weissenberg <sup>2, 3</sup> reported a double [111], [100] texture for copper, aluminium, and palladium, but also did not give the amount of deformation. Greenwood's analysis <sup>5</sup> indicating double texture for nickel was based on wire drawn about 85%, which is believed to be insufficient to develop the final texture. In support of this belief, it is interesting to note that for metals where a single [111] texture has been reported, the amount of deformation was at least 90%; namely, in aluminium <sup>9</sup> 98.2%, in copper <sup>6</sup> 96.4%, and in lead <sup>10</sup> 90%, although the "lead" actually contained 2% antimony.

The present paper reports the results of texture determinations of drawn face-centred cubic metal wires in an attempt to evaluate the points raised in this introduction.

## II.—EXPERIMENTAL PROCEDURE AND RESULTS.

The metals used in the investigation are listed in Table II. Rods approximately 6.4 mm. in dia. were drawn by hand through wire

dies until a wire dia. of 0.127 mm. was obtained (98% reduction in dia.). Several wires were laid side by side on transparent tape and Debye X-ray transmission photographs using (111) and (002) rings were taken with unfiltered copper  $K_\alpha$  radiation directed at an angle approximately  $(90 - \theta)$  from the wire axis, where  $\theta$  is the average Bragg angle for these two planes. In this way the photograph indicates directly the presence of (111) and (100) planes perpendicular to the wire axis, or [111] and [100] directions parallel to the wire axis. Since the orientation of the grains about the wire axis is random, no further analysis is necessary to describe the texture.

TABLE II.—*Purity and Sources of Materials.*

Metal	Purity	Source
Copper . .	Phosphorus-deoxidized electrolytic	Scovill Manufacturing Company, Waterbury, Conn.
Aluminium . .	99.994%	Aluminum Company of America, New Kensington, Pa.
Silver . .	99.993%	R. F. Miller and W. E. Milligan. <sup>11</sup>
Gold . .	"High purity"	H. M. Day and C. H. Mathewson. <sup>12</sup>
Nickel . .	99.31%	International Nickel Company, New York City.
Lead . .	99.999%	American Smelting and Refining Company, Barber, N.J.

For all the wires essentially a single [111] deformation texture was obtained, as illustrated in Fig. 1 (Plate LXXXII) for nickel and in Fig. 2 (Plate LXXXII) for copper. The aluminium, silver, and lead showed evidences of room-temperature recrystallization. In fact, in several places the lead wire was one grain in diameter. There was a surprisingly large number of randomly oriented grains in the silver, and particularly in the gold, as indicated by a weak complete diffraction ring with higher-intensity spots which define the texture.

The aluminium wire contained a minor [100] component, as shown in Fig. 3 (Plate LXXXII) for a specimen drawn 98%. This [100] component is believed to be the result of room-temperature recrystallization for the following reasons :

(1) Aluminium of this purity is known to recrystallize at room temperature with large amounts of deformation.<sup>13</sup>

(2) The [100] component on the X-ray photograph is characteristic of diffraction from large recrystallized strain-free grains (i.e. it is "spotty" rather than diffuse).

(3) The [100] component increased in intensity with increasing deformation above 90%. The condition at 98% is as shown in Fig. 3.

Increasing recrystallization with increasing deformation would be expected.

(4) The deformation texture of less pure aluminium wire has been reported previously as a single [111] component.<sup>4, 9</sup>

The disturbing element is the fact that the recrystallized texture of drawn aluminium wire has been previously reported to be the same as the deformation texture.<sup>9, 14, 15, 16</sup> However, in the present work, the [100] texture is a minor component, probably less than 5%, and it appears that the aluminium wire deformation texture is primarily [111].

### III.—CONCLUSION.

The deformation texture of drawn face-centred cubic metal wires is primarily a [111] direction parallel to the wire axis, as predicted by a theory<sup>1</sup> based on slip and flow. The [100] fibre-texture component previously reported in the literature<sup>2, 3, 4, 5</sup> is an intermediate orientation which disappears with extensive deformation.

### ACKNOWLEDGEMENTS.

Professor C. H. Mathewson stimulated and encouraged this investigation, and critically read the manuscript. The manuscript was also read by Drs. R. M. Brick, F. H. Wilson, and L. W. McKeehan, and by Mr. M. L. Kronberg. The author wishes to thank the suppliers of the metals, previously indicated in Table II.

### REFERENCES.

1. W. R. Hibbard, Jr., and M.-K. Yen, *Trans. Amer. Inst. Min. Met. Eng.*, 1948, **175**, 126.
2. M. Ettisch, M. Polányi, and K. Weissenberg, *Z. Physik*, 1921, **7**, 181.
3. M. Ettisch, M. Polányi, and K. Weissenberg, *Z. physikal. Chem.*, 1921, **99**, 332.
4. E. Schmid and G. Wassermann, *Z. Physik*, 1927, **42**, 779; *Z. Metallkunde*, 1927, **19**, 325.
5. G. Greenwood, *Z. Krist.*, 1929, **72**, 309; 1930, **73**, 442.
6. W. R. Hibbard, Jr., *Trans. Amer. Inst. Min. Met. Eng.* (in *J. Metals*), 1949, **185**, (9), 598.
7. F. Wever, *Trans. Amer. Inst. Min. Met. Eng., Inst. Metals Div.*, 1931, **51**.
8. W. Boas and E. Schmid, *Z. techn. Physik*, 1931, **12**, 71.
9. G. Sachs and E. Schiebold, *Z. Metallkunde*, 1925, **17**, 400.
10. W. Hofmann, *Z. Metallkunde*, 1937, **29**, 266.
11. R. F. Miller and W. E. Milligan, *Trans. Amer. Inst. Min. Met. Eng.*, 1937, **124**, 229.
12. H. M. Day and C. H. Mathewson, *Trans. Amer. Inst. Min. Met. Eng.*, 1938, **128**, 261.
13. W. G. Burgers, *Nature*, 1947, **159**, 203.
14. E. Schmid and G. Wassermann, *Z. techn. Physik*, 1928, **9**, 106.
15. G. Greenwood, *Z. Krist.*, 1931, **80**, 481.
16. (Frhr.) v. Göler and G. Sachs, *Z. Metallkunde*, 1927, **19**, 90.



DEBYE TRANSMISSION X-RAY PHOTOGRAPHS OF WIRE DRAWN 98%, SHOWING  
(111) (INNER) AND (002) DIFFRACTION RINGS.

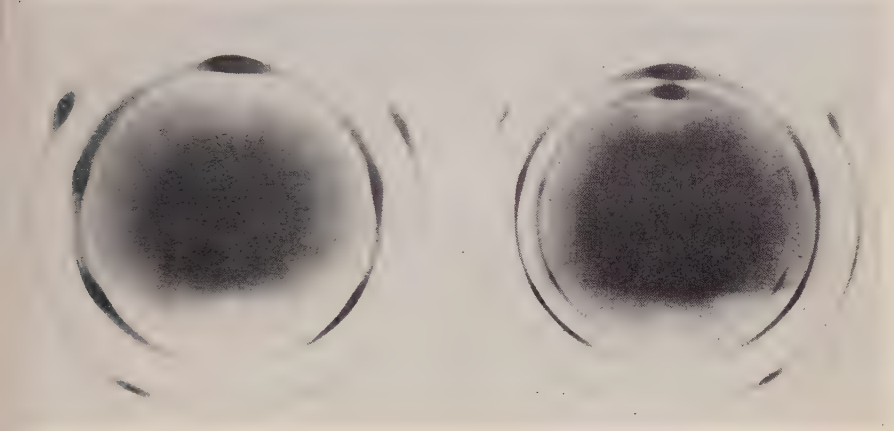


FIG. 1.—Nickel Wire. Unfiltered  $\text{CuK}_\alpha$  radiation directed at an angle of  $65^\circ$  to the wire axis (vertical).

FIG. 2.—Copper Wire. Unfiltered  $\text{CuK}_\alpha$  radiation directed at an angle of  $67^\circ$  to the wire axis (vertical).

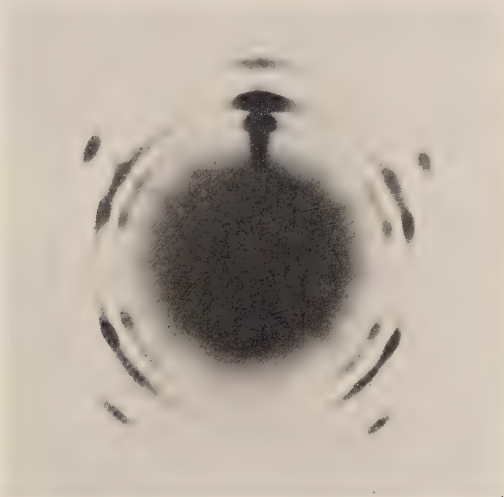


FIG. 3.—Aluminium Wire. Unfiltered  $\text{CuK}_\alpha$  radiation directed at an angle of  $69^\circ$  to the wire axis (vertical).



# LATTICE PARAMETERS OF BINARY NICKEL-COBALT ALLOYS.\*

By A. TAYLOR,† Ph.D., F.Inst.P., F.I.M., MEMBER.

## SYNOPSIS.

Cobalt and nickel are mutually soluble in each other in all proportions. In general, increasing the cobalt content increases the lattice spacing of face-centred cubic nickel in a non-linear manner, producing an inflection in the spacing/composition curve in the region of  $\text{Ni}_3\text{Co}$ , and a second inflection near  $\text{NiCo}_3$ , beyond which point face-centred cubic and hexagonal close-packed forms coexist in randomly occurring ratios. The effect of nickel additions to cobalt within this anomalous region is to reduce both the  $a$  and  $c$  parameters of the hexagonal structure, while causing the mean atomic volume to fall at the same rate as for the cubic form. The transformation from the cubic to the hexagonal structure of equivalent composition involves a decrease of nearly 0.6% in atomic volume.

## I.—INTRODUCTION.

THE nickel-cobalt system is very simple, nickel and cobalt forming from about 477° C. to the solidus temperature a continuous series of face-centred cubic solid solutions from pure cobalt to pure nickel.<sup>1-5</sup> Below 477° C. cobalt transforms to the hexagonal form<sup>6,7</sup> and frequently displays a "mistakes" structure,<sup>8,9,10</sup> with an intimate mixture of hexagonal and cubic forms. The addition of 30% of nickel to cobalt depresses the transformation temperature from 477° to 0° C.

The only extensive X-ray examination of the nickel-cobalt binary system is that of Osawa,<sup>11</sup> which was carried out using Mond nickel containing iron 0.1, carbon 0.037, sulphur 0.019, silicon 0.006, and copper 0.013%, and electrolytic cobalt containing 0.18% iron. The Debye-Scherrer photographs were taken in a 5.7-cm.-dia. camera with iron  $K_\alpha$  radiation. The lattice parameters computed from the individual reflections were averaged, not extrapolated to the value for an angle of 90°, as is normal practice, with the result that an error of 1 part in 350 was present in the final parameters. The room-temperature lattice parameters of the face-centred cubic phase were expressed by the relation:

$$a_w = 3.508 + 0.00017145 \times C \text{ kX.}$$

where  $C$  is the percentage cobalt content. In the hexagonal structure, which according to Masumoto<sup>6</sup> can exist alone over the range 70–100%

\* Manuscript received 11 February 1950.

† The Mond Nickel Co., Ltd., Birmingham.

cobalt, the  $a$  parameter was stated to remain constant at 2.492 kX. while the  $c$  parameter falls rapidly from 4.056 kX. for pure cobalt to 4.036 kX. at 80% cobalt.

In a brief description of the nickel-cobalt system, Lacy,<sup>12</sup> states that the lattice parameter of an alloy containing 70% nickel, 30% cobalt is 3.530 kX., and that the hexagonal phase present in an 80% cobalt alloy gives  $a = 2.489$  kX.,  $c/a = 1.621$ , while pure cobalt has  $a = 2.502$  kX.,  $c/a = 1.6233$ . Ellis and Greiner<sup>13</sup> give, for pure cobalt in the cubic form,  $a_w = 3.5368$  kX., and for the hexagonal modification,  $a = 2.5020$ ,  $c = 4.0611$  kX. Bradley, Jay, and Taylor<sup>14</sup> give the value of  $a_w = 3.5169$  kX. for Hilger nickel powder filings slowly cooled from 900° C., 3.5170 kX. for powder quenched from 700° C., and 3.5168 kX. for powder quenched from 800° and 900° C., respectively.

A series of very approximate density determinations on a range of nickel-cobalt alloys was made by Bloch.<sup>2</sup> It was decided, in view of the availability of suitable specimens, to carry out a fresh series of measurements and compare them with densities computed from the X-ray data.

## II.—MATERIALS EXAMINED.

All but three of the nickel-cobalt binary alloys used in the present survey were already available from a concurrent investigation. They had been made from Mond nickel and cobalt as 14-lb. heats, chill-cast and subsequently forged and rolled to  $\frac{5}{8}$ -in.-dia. bar. Small pieces, about 2 in. long, were sawn from the bars and used for the X-ray investigation. As a check on the parameter measurements on these alloys, three alloys of higher purity and containing approximately 25, 50, and 75% cobalt, were made as 50-g. melts under an atmosphere of hydrogen in a high-frequency induction furnace in crucibles lined with pure alumina. When the metals were thoroughly mixed, the hydrogen was pumped off while the alloys were still molten, after which they were allowed to solidify and cool *in vacuo*. Chemical analyses of the samples are given in Table I.

The spectrographic analyses of various samples of cobalt obtained for X-ray examination are listed in Table II.

## III.—EXPERIMENTAL PROCEDURE.

All the samples from the rolled bars were lump-annealed in air for 2 days at 1200° C. to ensure homogeneity, and quenched. The special 50-g. melts were vacuum-annealed at 1200° C. for 2 days and also quenched. About 0.040 in. of the surface of the samples was ground

TABLE I.—Summary of X-Ray Data on Nickel-Cobalt Alloys from Measurements Made at 20° C.

Alloys	Analysis, wt.-%						Structure		Lattice Parameters, kX. (at 20° C.)			Atomic Volume, kX. <sup>3</sup> , for Slowly Cooled Alloys	Density, g./c.c.	
	O	Si	Fe	Mn	Ti	Ni	Co (balance)	Slowly Cooled from 900° C.	Quenched from 900° C.	17 hr. at 750° C. and Rapidly Cooled	Quenched from 900° C.	Slowly Cooled for 14 days from 900° C.	Calculated from X-Ray Data	Observed
Ni	0.01	0.061	0.06	Trace	0.00	99.96	0.97	Cubic	Cubic	3.5169	3.5168	3.5169	8.907	8.907
KOI	0.01	0.06	0.06	0.02	0.02	90.2	19.35	"	"	3.5184	...	3.5184	8.899	8.90
KOI	0.01	0.07	0.21	0.05	0.05	75.2	24.44	"	"	3.5202	...	3.5201	8.891	8.87
KJD	0.01	0.02	0.02	0.05	0.005	74.4	25.5	"	"	3.5222	3.5239	3.5215	8.882	8.87
No. 82	...	0.07	0.10	0.01	0.00	71.0	28.82	"	"	3.5226	...	3.5233	8.869	8.87
KOK	0.01	0.06	0.12	Trace	0.01	62.4	37.4	"	"	3.5249	...	3.5249	8.861	8.86
KOL	0.01	0.07	0.21	0.03	0.07	50.7	48.9	"	"	3.5258	3.5268	3.5266	8.853	8.85
KOM	0.02	0.07	0.04	0.06	0.005	49.3	50.6	"	"	3.5283	3.5273	3.5274	8.841	8.83
No. 83	0.02	0.06	0.22	0.02	0.07	41.1	58.51	"	"	3.5314	...	3.5306	8.827	8.83
KON	0.01	0.08	0.36	0.03	0.07	31.1	68.35	50% cubic	50% cubic	...	3.5312	3.5316	8.822	8.82
KOO	0.01	0.07	0.21	0.02	0.05	25.9	73.74	50% hexagonal	50% hexagonal	3.5314	3.5314	$a = 2.4950$ $c = 4.0569$	8.822	8.82
KSE	0.01	0.07	0.21	0.02	0.05	25.9	73.74	50% hexagonal	50% hexagonal	3.5314	3.5314	$a = 2.4950$ $c = 4.0569$	8.822	8.82
No. 84	...	0.08	0.06	0.08	0.005	23.18	76.6	Cubic	Cubic	...	3.5314	3.5319	8.820	8.82
KOP	0.01	0.09	0.37	0.07	0.00	21.7	77.76	Cubic + trace hexagonal	Cubic + little hexagonal	3.5319	3.5323	3.5322	8.802	8.80
KOQ	0.01	0.12	0.54	0.11	0.00	10.63	88.59	50% cubic	50% cubic	3.5489	...	3.5354 $a = 2.5006$ $c = 4.0605$	8.802	8.80
KSF	0.01	0.13	0.63	0.13	0.00	0.35	98.75	50% hexagonal	50% hexagonal	...	Rapidly cooled	...	8.872	...
	0.01	0.13	0.63	0.13	0.00	0.35	98.75	Rapidly cooled cubic + hexagonal	Rapidly cooled cubic + hexagonal	...	3.5381	...	8.872	...



TABLE II.—Summary of X-Ray Data on Different Varieties of Cobalt from Measurements Made at 20° C.

Cobalt	Spectrographic Analysis, %						Condition	Structure	Lattice Parameters, kX. (at 20° C.)	Atomic Volume, kX. <sup>3</sup>
	Ni	Fe	Mn	Ti	Cu	Mg				
Glydach reduced oxide (Lab. Mark KSF)	0.45	0.63	0.13	0.00	...	...	Cast and forged bar. Filings annealed at 900° C. for 1 day and rapidly cooled.	Cubic + hexagonal	3.5381	11.073
Glydach reduced oxide (Lab. Mark M17)	1.0	0.10	0.10	...	0.10	...	Fine powder, as received.	Cubic	3.5373	11.064
Glydach special reduced oxide	0.005	0.01	0.16	0.01	0.02	0.02	Fine powder, as received.	Cubic + trace hexagonal	3.5365	11.058
Inco electrolytic	0.3	Trace	...	...	0.01	...	Filings annealed at 900° C. for 100 hr. and quenched. Filings annealed at 900° C. for 2 days and slowly cooled to room temperature in 14 days.	Cubic + hexagonal Cubic + hexagonal	3.5381 3.5384	11.073 11.075
Matthey "Specpure" cobalt	Trace	Trace	Trace	Trace	Trace	Trace	Powder, as received. Powder, quenched from 900° C.	Cubic + hexagonal Cubic + hexagonal	3.5370 $a = 2.5014$ $c = 4.0616$ 3.5371 $a = 2.5012$ $c = 4.0615$	11.062 11.004 11.063 11.002
Hillger spectroscopically pure	Trace	Trace	Trace	Trace	Trace	Trace	Filings slowly cooled from 900° to 400° C. in 3 days, held at 400° for 2 days, and quenched.	Cubic + hexagonal	3.5370 $a = 2.5022$ $c = 4.0616$	11.062 11.011 <sub>3</sub>

away and then samples of fine filings which could pass through a 200-mesh sieve were taken from the homogeneous interior of the samples. These filings were sealed in  $\frac{1}{8}$ -in.-dia., evacuated, thin-walled silica tubes and then heated for 2 days at 900° C., followed by slow cooling to room temperature in 14 days. Further samples were heated at 900° C. for 2 days and quenched by dropping the silica tubes into water. In a number of cases, powders were heated at 750° C. for 17 hr. and rapidly cooled by pulling the tubes from the furnace and allowing them to cool on a metal plate.

Copper radiation, which is normally employed in X-ray crystallographic work for nickel-rich alloys, proved quite unsuitable for this series owing to the proximity of the cobalt absorption edge to the copper  $K_\alpha$  wave-length. Instead, filtered manganese radiation ( $\lambda_{a_1} = 2.09751$ ,  $\lambda_{a_2} = 2.10149$  kX.), was used for taking the Debye-Scherrer photographs. An extremely high degree of accuracy in parameter measurement was obtained with this radiation, since the 311 reflection of the face-centred cubic phase falls at a Bragg angle of approximately 82°. Over the range 0-70% cobalt, where the alloys are all cubic, a 9-cm.-dia. Debye-Scherrer camera was used which could record spectra up to 86°. Over the range 70-100% cobalt the alloys frequently consist of a mixture of cubic and hexagonal phases, the spectrum lines of which overlap. In particular, the cubic 311 reflection is overlapped by the hexagonal  $11\bar{2}2$ ,  $220$  by  $11\bar{2}0$ , and  $111$  by  $0002$ . For these alloys a 19-cm.-dia. camera and iron  $K_\alpha$  radiation ( $\lambda_{a_1} = 1.932076$ ,  $\lambda_{a_2} = 1.936012$  kX.), was employed, by means of which the cubic  $222$  reflection was clearly separated from the hexagonal  $0004$  at approximately 72°, and in the lowest orders it was just possible to resolve  $111$  from  $0002$ .

Accurate values of the parameters of the cubic alloys were obtained by extrapolating the computed values against the function  $\frac{1}{2}(\cos^2\theta/\theta + \cos^2\theta/\sin \theta)$  as described by Taylor and Sinclair<sup>15</sup> and by Nelson and Riley,<sup>16</sup> and finally making a small correction for refractivity. A similar procedure for the hexagonal alloys, using reflections of the form  $000l$  and  $hkio$ , was employed to determine the  $c$  and  $a$  parameters.<sup>17</sup>

The densities of a number of the alloys in the form of bar were measured by the Archimedes method, using pure toluene as the immersion fluid.

#### IV.—EXPERIMENTAL RESULTS.

The lattice-parameter and density measurements made at 20° C. are summarized in Tables I and II. The values of  $a_w$  for the cubic phase

are probably correct to 1 part in 50,000. The values of  $c$  for the hexagonal structures are also accurate to 1 part in 50,000, but  $a$  is only accurate to about 1 part in 10,000 owing to the diffuseness and weakness of the 2020 reflection on which the accuracy of the extrapolated  $a$  parameter largely depends. In general, the parameters from the purer

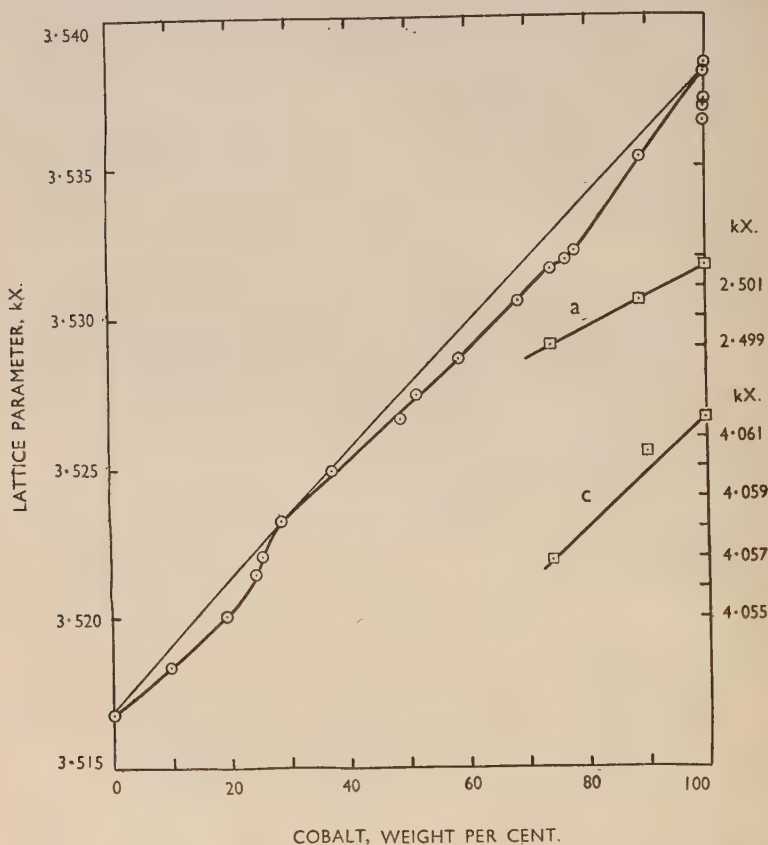


FIG. 1.—Lattice Parameters of Nickel-Cobalt Alloys Annealed at 900° C. and Slowly Cooled to Room Temperature in 14 Days.

50-g. melts confirm the trends in parameter exhibited by the large heats. The lattice-parameter measurements for the slowly cooled alloys are plotted in Fig. 1 which shows a well-marked inflection in the parameter/composition curve in the region of 30% cobalt and a second inflection in the neighbourhood of 74% cobalt.

Owing to the variability of the lattice parameter of cobalt, resulting

from its origin and thermal treatment, it is not easy to decide on a reference line joining the parameter of pure nickel to that of cobalt on the parameter/composition diagram. It was decided to adopt the value  $a_w = 3.5381$  kX. for the parameter of cobalt, since this particular

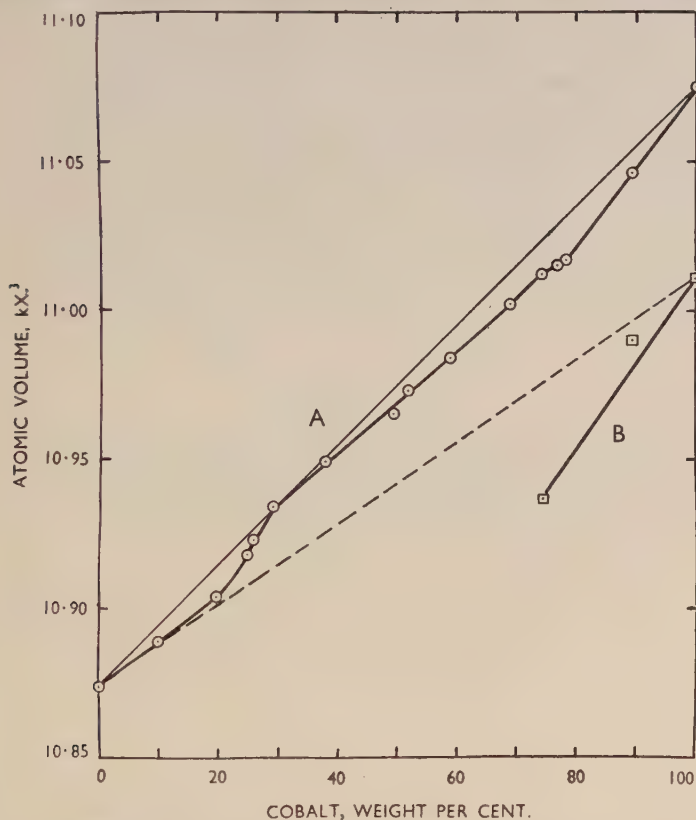


FIG. 2.—Atomic Volumes in kX.<sup>3</sup> of Nickel-Cobalt Alloys Annealed at 900° C. and Slowly Cooled to Room Temperature in 14 Days. A = Face-centred cubic lattice. B = Hexagonal close-packed lattice in equilibrium with face-centred cubic lattice.

spacing corresponds to the one for Inco high-purity electrolytic cobalt, and also for the Clydach cobalt used in making the 14-lb. heats which were subsequently forged down into  $\frac{5}{8}$ -in. bar. With this choice of datum line, all the parameters of the alloys exhibit the commonly observed contraction from the simple rule of mixtures, with the exception of 29% cobalt which lies on the line near the inflection point.

The  $a$  and  $c$  parameters of the hexagonal phase coexisting with the cubic structure are plotted in Fig. 1. Both these parameters decrease with increasing nickel content, contrary to the findings of Osawa,<sup>11</sup> who stated that the  $a$  parameter remains constant. The variation of atomic spacing in this region is best brought out by the atomic volume/composition curves plotted in Fig. 2. Curve A corresponds to the atomic volumes of the face-centred cubic phase, while curve B corresponds to the atomic volumes of the coexisting hexagonal structures. It is interesting to note that both curves have roughly the same slope over the range 75–100% cobalt, indicating that the addition of nickel influences both structures equally. At the nickel-rich end, where there is a marked initial downward deviation of the atomic-volume curve, it appears that the volume of the solute cobalt atoms approximates to the hexagonal value rather than the cubic one.

The parameters of some of the alloys seem to be influenced by the heat-treatment given to the filings. In the region of  $\text{Ni}_3\text{Co}$ , filings quenched from 900° C. have a higher lattice parameter than when slowly cooled, which is indicative of a disorder–order transformation on cooling. Alloys given a prolonged anneal at 750° C., followed by a rapid cool to room temperature by pulling the silica tubes out of the furnace, tended to give even lower spacings than the slow cool over 14 days from 900° C. This would point to the critical temperature of ordering as lying in the region of 750°–800° C., and would imply that the equilibrium in the slowly cooled alloys lagged behind the temperature.

In the hexagonal + cubic region, the proportions of the coexisting structures seem to be independent of thermal history, since, in a series of powders heat-treated simultaneously, the alloy containing 23.4% nickel was entirely cubic, although its immediate neighbours on both sides contained quantities of hexagonal structure. Alloy *KSE* with 25.9% nickel contained approximately equal amounts of cubic and hexagonal structures, while *KOP* with 21.7% nickel contained only a small trace of hexagonal structure. It would appear from the few slow-cooling and quenching experiments that have been carried out, that the amounts of the hexagonal and the cubic structures coexisting do not vary steadily as the cobalt content is increased beyond 70%, but rather that the hexagonal structure tends to appear quite suddenly in the region of  $\text{NiCo}_3$  and to be present in the various cobalt-rich alloys in random quantities. No obvious explanation of this can be given.

Cobalt from different sources also tends to give wide variations in the proportions of the structures present and in the lattice parameters (see Table II). It would seem that heat-treated filings from cobalt in massive form, whether prepared electrolytically or as cast ingot, give



somewhat higher lattice parameters than powders which have been directly prepared by hydrogen-reduction of the oxide and examined by X-rays in the "as-received" condition. It may be that the fine powders prepared by reduction consist of imperfectly formed crystals which have odd atoms missing from the lattice. These defects could conceivably cause the neighbouring atoms to crowd in towards them, thereby producing an overall decrease in parameter analogous to the fall in parameter observed when an element takes into substitutional solution atoms of smaller radius. On the other hand, it is possible that melting in air or in hydrogen atmosphere, or preparation by electrolysis, enables sufficient gas to be absorbed to influence the parameter values significantly.

The results of the density measurements which were made on a number of the forged bars differed considerably from those published by Bloch,<sup>2</sup> but were in excellent agreement with values computed from the lattice-parameter measurements of the face-centred cubic phase.

#### V.—CONCLUSIONS.

(1) Over the range of binary nickel-cobalt alloys from pure nickel to 70 wt.-% cobalt the crystal structure remains close-packed face-centred cubic. Beyond 70% cobalt, the alloys are either face-centred cubic or a mixture of face-centred cubic and hexagonal close-packed structures in which the proportions of the two structures do not seem to be systematically dependent on heat-treatment or composition.

(2) In general, the lattice parameters of both the face-centred and hexagonal structures increase with increasing cobalt content, but there is a marked inflection in the parameter/composition curve in the region of 30% cobalt, and a second inflection in the region of 74% cobalt, the latter being associated with the coexistence of hexagonal and cubic structures.

(3) Density measurements made on a number of the alloys agreed well with densities computed from the lattice-parameter measurements.

(4) Alloys in the region of  $\text{Ni}_3\text{Co}$  when quenched from 900° C. have appreciably higher lattice parameters than alloys which have been slowly cooled. This suggests that  $\text{Ni}_3\text{Co}$  is capable of superlattice formation, although superlattice lines are not observed owing to the very great similarity in the X-ray-scattering factors of nickel and cobalt atoms.

(5) The crystal structure and lattice parameters of unalloyed cobalt seem to be considerably influenced by the method of its preparation, vacuum-annealed filings giving appreciably higher lattice parameters than powders obtained directly from hydrogen-reduced cobalt oxide.

(6) In general, the atomic volumes of the hexagonal structures lie approximately 0.6% below those of the corresponding cubic values, thus indicating a lattice contraction during the transformation from the cubic to the hexagonal phase.

## ACKNOWLEDGEMENT.

The author wishes to thank The Mond Nickel Company, Ltd., for permission to publish this paper.

## REFERENCES.

1. W. Guertler and G. Tammann, *Z. anorg. Chem.*, 1904, **42**, 353.
2. O. Bloch, *Arch. Sci. Phys. Nat.*, 1912, **33**, 293.
3. R. Ruer and K. Kaneko, *Metallurgie*, 1912, **9**, 419.
4. M. Waehlert, *Österr. Z. Berg- u. Hüttenwesen*, 1914, **62**, 341.
5. T. Kasé, *Sci. Rep. Tôhoku Imp. Univ.*, 1927, [i], **16**, 492.
6. H. Masumoto, *Sci. Rep. Tôhoku Imp. Univ.*, 1926, [i], **15**, 449.
7. A. W. Hull, *Phys. Rev.*, 1921, [ii], **17**, 571.
8. O. S. Edwards and H. Lipson, *Proc. Roy. Soc.*, 1942, [A], **180**, 268; *J. Inst. Metals*, 1943, **69**, 177.
9. A. J. C. Wilson, *Proc. Roy. Soc.*, 1942, [A], **180**, 277.
10. A. R. Troiano and J. L. Tokich, *Trans. Amer. Inst. Min. Met. Eng.*, 1948, **175**, 296.
11. A. Osawa, *Sci. Rep. Tôhoku Imp. Univ.*, 1930, [i], **19**, 109.
12. C. E. Lacy, *Metals Handbook (Amer. Soc. Metals)*, 1948, 1192.
13. W. C. Ellis and E. S. Greiner, *Metals Handbook (Amer. Soc. Metals)*, 1948, 1136.
14. A. J. Bradley, A. H. Jay, and A. Taylor, *Phil. Mag.*, 1937, [vii], **23**, 545.
15. A. Taylor and H. Sinclair, *Proc. Phys. Soc.*, 1945, **57**, 108.
16. H. B. Nelson and D. P. Riley, *Proc. Phys. Soc.*, 1945, **57**, 160.
17. A. Taylor and R. W. Floyd, *Acta Cryst.*, 1950, **3**, 285.

# DISCUSSION ON THE PAPER BY MR. R. W. RUDDLE: "A PRELIMINARY STUDY OF THE SOLIDIFICATION OF CASTINGS."

(*J. Inst. Metals*, this vol., p. 1.)

DR. E. W. FELL\* (Member): The diagrams in Mr. Ruddle's paper showing cooling curves and isotherms are very interesting. My contribution is concerned with the calculation of the solidification times of the castings; in particular, I wish to draw attention to certain mathematical methods by which (a) the influence on the calculation of somewhat troublesome corner and end effects may be regarded as negligible, and (b) account may be taken of surface curvature. These refinements, by making the calculation more exact, should result also in a better understanding of any discrepancies between the calculated and observed solidification times.

The macrostructure of an aluminium cylinder casting, seen in Fig. 16 (Plate I) of the paper, shows prominent corner and end effects. As far as the calculation of solidification times is concerned, corner and end effects may be ignored by choosing the dimensions of the cylinder casting so that its length is large in proportion to its diameter. There should then be a part of the cylinder, sufficiently removed from the ends, in which the direction of flow of heat may be regarded as purely normal to the cylinder axis. For example, supposing that end effects extended a distance of 4 in. from each end, a cylinder 14 in. long would be free from them over a length of 6 in. The observed solidification times could also be determined in this particular central length of the cylinder by means of thermocouples, for purposes of comparison.

The metal/mould interface is taken to be a plane, in the paper, in order to calculate the total heat absorbed by the mould in time  $t$ , but the area of the curved part of the surface of the 5-in.-dia. cylinder casting is in fact a large proportion of its total surface area. Accordingly, we may consider the infinite medium bounded internally by the circular cylinder of radius  $r = a$ , where the initial temperature of the medium is zero and the surface  $r = a$  is at constant temperature  $V$ . The flux at the surface of the cylinder is:

$$f = -K \left[ \frac{\partial v}{\partial r} \right]_{r=a} = \frac{4VK}{a\pi^2} \int_0^\infty e^{-\kappa u^2 t} \frac{du}{u[J_0^2(au) + Y_0^2(au)]} \quad \dots (1)$$

where  $K$  is the thermal conductivity of the medium, and  $\kappa (= K/\rho c)$  its thermal diffusivity,  $t$  the time,  $u$  a variable, and  $J_0(au)$  and  $Y_0(au)$  are Bessel functions of the first and second kinds, respectively, of order zero. Thus the quantity of heat passing into the medium in time  $t$  is:

$$\int_0^t f dt \quad \dots \dots \dots (2)$$

Numerical values of the integral (1) have been tabulated and are shown graphically,† from which  $f$  is obtainable as a function of  $t$ . We might now proceed as follows. The graph for  $f$  with respect to  $t$  having been drawn, the

\* Senior Assistant in Metallurgy, Technical College, Bradford.

† H. S. Carslaw and J. C. Jaeger, "Conduction of Heat in Solids", p. 283, Fig. 32. London: 1947 (Oxford University Press).

value of the integral (2), for an arbitrary value of  $t$ , is found by measuring the area below the curve. The same operation is repeated for other arbitrary values of  $t$ . It is convenient to draw a further graph relating the areas to their respective values of  $t$ , and then the time necessary for any given quantity of heat to be conducted away from the cylinder  $r = a$  may be read directly off it. Here, the cylindrical surface  $r = a$  represents the metal/mould interface, and the medium represents the mould material. In making this particular calculation, the surface area of the casting may be taken simply as  $2\pi al$ , where  $l$  is the central length of the cylinder casting that is judged to be free from end effects according to the method of the previous paragraph.

The AUTHOR (*in reply*): I should like to thank Dr. Fell for his comments on my paper. I quite agree with him that the calculations of solidification times given in the paper could be made more exact by taking into account the corner, end, and surface-curvature effects, and I have read with interest his suggested method of calculating the heat extraction by moulds with curved surfaces.

In view of the evident inaccuracies in the solidification-time calculations in the paper, one of my colleagues and I have carried out some further work in which we have attempted to deal with the question of the heat extraction by the corners and curved surfaces of moulds, using a combination of experimental and mathematical methods. The results of this work are being published by the Institute.\* It may interest Dr. Fell to know that in this later work we have determined experimentally the rate at which a cylindrical mould surface extracts heat, and also calculated it by a method similar to that proposed by him.

\* R. W. Ruddle and R. A. Skinner, *J. Inst. Metals*, 1951, **79**, 35.

JOINT DISCUSSION ON PAPERS BY DR. W. A. WOOD AND MR. N. DEWSNAP: "ATOMIC DISPLACEMENTS ASSOCIATED WITH ELASTICITY IN PLASTICALLY DEFORMED METALS"; BY PROFESSOR A. H. COTRELL AND DR. V. AYTEKIN: "THE FLOW OF ZINC UNDER CONSTANT STRESS"; BY DR. W. A. WOOD AND MR. R. F. SCRUTTON: "MECHANISM OF PRIMARY CREEP IN METALS"; BY DR. G. B. GREENOUGH AND MRS. E. M. SMITH: "THE MECHANISM OF CREEP AS REVEALED BY X-RAY METHODS"; AND BY MR. E. A. CALNAN AND MR. B. D. BURNS: "SOME X-RAY OBSERVATIONS ON THE NATURE OF CREEP DEFORMATION IN POLYCRYSTALLINE ALUMINIUM."

(*J. Inst. Metals*, this vol., pp. 65, 389, 423, 435, 445.)

MRS. E. M. SMITH\*: We should like to emphasize again that we feel that it is of great importance to relate all the experimental work which has been done in connection with the mechanism of creep to some underlying theory. The main experimental fact previously established is that in pure aluminium creep at about 300° C. causes a breakdown of the original annealed grains into strain-free fragments, whereas rapid deformation causes considerable distortion of the metal lattice which is still evident after prolonged soaking at 300° C. We have now shown that similar perfect fragments are produced during creep when the specimens are initially cold worked instead of annealed, and that in aluminium of commercial purity creep does not produce the perfect fragments. The explanation which we have given in terms of dislocations and based on the phenomenon of polygonization fits these results, and at the moment this seems to be the only attempt that has been made to explain them in terms of fundamental concepts. We are well aware that there are difficulties in the way of accepting these ideas as they stand, but it is hoped that some of these difficulties may be removed in the course of discussion.

There is one point in particular upon which opinions would be welcome; that is the question of the homogeneity or otherwise of the creep deformations which give rise to cell formation. As stated in our paper there is a certain amount of evidence to show that the deformation of grains in a polycrystalline specimen subjected to tensile loading is inhomogeneous, and the results de-

\* Remarks made in introducing the paper for discussion at the Autumn Meeting of the Institute held in Bournemouth, September 1950.



scribed by Calnan and Burns support this view, since the apparent directions of splitting which they observed were different in adjacent areas of the same grain. We should like to know, however, whether there is any reason why deformation by creep should be more inhomogeneous than a fast deformation, as if this were so, it would certainly be in keeping with the experimental facts.

We should also like to discuss briefly a point raised by Wood and Scrutton in their paper. They claim that the process of cell formation during creep cannot be identified with that of polygonization, since it takes place without any intermediate disordering of the structure. Although we suggest that the final structure obtained is the same as that reached in polygonization, it is not necessary to assume that the two processes are identical. It is quite conceivable that an array begins to form during the early stages of creep, and dislocations produced later are continuously absorbed, so that there is never a sufficient number scattered at random through the material to cause much disordering. Wood and Scrutton have shown that when the deformation is very slow the reflection spots break up without showing much blurring, but since the normal back-reflection X-ray technique is relatively insensitive, this does not necessarily mean that there is not *any* intermediate disordering of the lattice. Moreover, one certainly cannot say that the grains never pass through a distorted stage before dissociating into cells. In their paper specimen B, for instance, has broken down into cells after a strain of 6% (see Fig. 15, Plate XLVII), but there is definite distortion at earlier stages of the deformation (see Figs. 13 and 14, Plates XLVI and XLVII). It is clear, therefore, that the cell mechanism can sometimes be associated with intermediate disordering of the structure, and it seems of little significance that the degree of the latter is found to vary.

DR. A. J. BRADLEY,\* F.R.S. (Member): The existing theories of the deformation of metals are unsatisfactory because they do not take into account

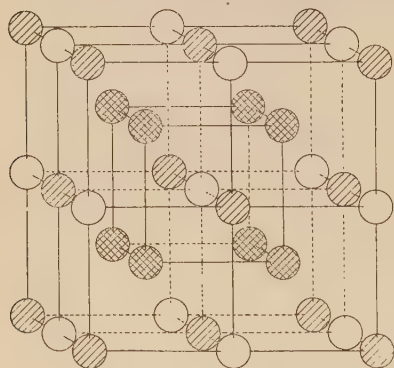


FIG. A.—Electronic Structure of Aluminium (Bradley).

the outer structure of the atom. It was pointed out at Amsterdam † in 1948 that a metallic crystal consists essentially of a space lattice of positive ions interpenetrated by one or more subsidiary lattices to form special sites for the free valence electrons. The electronic structure of metallic aluminium is on this basis extremely simple, and is illustrated in Fig. A.

The unit 'cell' contains in all sixteen sites in the form of a body-centred cubic superlattice. Four of these sites, taken separately, constitute the usual face-centred cubic space-lattice of aluminium, as it is revealed by X-rays.

Each atom is triply ionized, the free valence electrons being inserted interstitially. A second face-centred cubic lattice in this way provides four new sites for those valence electrons which are in the  $p$  state. Taken together, the  $\text{Al}^{3+}$  ions and the  $p$  sites form a structure of the rock-salt type. At the

\* B.S.A. Group Research Centre, Sheffield.

† A. J. Bradley, *Physica*, 1949, 15, 170.

centre of each small cube there are eight more interstitial sites for those electrons which are in the  $sp$  state; thus the whole arrangement resembles the structure of  $\text{Fe}_3\text{Al}$ , the Fe atoms being replaced by the valence electrons.

Each  $\text{Al}^{3+}$  ion is surrounded by eight of the  $sp$  sites arranged at the corners of a simple cube as in the Lewis-Langmuir theory, while the six neighbouring  $p$  sites are distributed octahedrally as in Pauling's wave-mechanical theory. The electropositive ion with the ten electrons of the  $K$  and  $L$  shells constitutes the atomic core. It is enclosed within a sphere of radius  $0.5 \text{ \AA}$ , whereas the whole aluminium atom is allotted a radius of  $1.43 \text{ \AA}$ . Thus over 90% of the atomic volume is occupied by the valence electrons only.

There are three free electrons per atom; these are by no means equivalent. In full agreement with Pauling's exclusion principle, each acts independently of the other two. One of them ( $3p$ ) is able to travel freely between all of the  $sp$  and  $p$  sites, but does not ever penetrate the atomic core; the other two ( $3s^2$ ) are more restricted in their motions. The first of these  $s$  electrons can travel only between the atomic core and one neighbouring electronic site of either type ( $sp$  and  $p$ ). It is completely barred from five out of six  $p$  sites and seven out of eight  $sp$  sites. Finally, the second of the  $3s^2$  electrons is even more tightly bound to the atomic core, being permitted to wander only as far as one adjacent  $sp$  site. It cannot in any normal circumstances pass to a  $p$  site.

In short, the 13 electrons of the aluminium atom may be subdivided into two distinct groups:

$1s^2 + 2s^2 + 2p^6$ : 10 electrons inside the atomic core constituting the  $\text{Al}^{3+}$  ion.

$3s^2 + 3p$ : 3 electrons which pass most of their time between the ions, and help to link together neighbouring atoms.

DR. J. C. CHASTON,\* B.Sc., A.R.S.M., A.Inst.P., F.I.M. (Member): In discussions on creep in recent years it has become fashionable to consider that deformation may take place by two mechanisms which can be briefly described as slip on the crystal planes and viscous flow at the grain boundaries.

It seems worth while to emphasize that this view, admittedly an oversimplification, is extremely difficult to reconcile with such facts as the observations of Calnan and Burns on the inhomogeneity of deformation within the crystals, particularly if the term "grain boundary" is considered to imply a transition region a few atoms thick from one lattice to another. It appears evident that when earlier workers have referred to "flow at the grain boundaries" they have been describing a process which would now seem to be much more accurately characterized as a localized deformation of the crystals in the neighbourhood of the grain boundaries. Only a little reflection is needed to make it clear that the irregularly shaped crystals in a polycrystalline metal cannot rotate or slip simply by movement at a thin boundary layer. It is inevitable that an appreciable volume of each crystal must be deformed when adjacent crystals change their relative orientations. The idea that crystals can glide over one other at the crystal boundaries must be abandoned. It is becoming abundantly clear that large deformations must occur on each side of the boundary, or the crystals will part.

DR. G. B. GREENOUGH†: I would like to comment on the paper by Wood and Dewsnap separately from any discussion of the creep papers, since it deals with a different aspect of the general work on the deformation of metals. Wood and Dewsnap are of the opinion that Heyn stresses are small compared

\* Deputy Research Manager, Johnson, Matthey and Co., Ltd., Wembley.

† Metallurgy Department, Royal Aircraft Establishment, Farnborough, Hants.

with the stresses that they are measuring. If that were true, then the stresses that they deduce from their experimentally observed strains would be substantially correct and would have a real meaning. However, the authors have not recorded any results to substantiate their opinion, and it is, therefore, essential to examine the matter closely.

Table A shows the residual lattice strains observed in a direction normal to the specimen surface after the plastic extension of fine-grained mild-steel specimens. Three different diffraction lines have been examined. In order to show that the values are reproducible, not only from specimen to specimen but also from observer to observer, values are quoted that were obtained by three authors. It should be noted that Finch's \* values are relative ones, while those due to Garrod † (taken from his figure for a stress of 23.8 tons/in.<sup>2</sup>) and myself ‡ are absolute values.

TABLE A.—*Residual Lattice Strain in Plastically Extended Mild-Steel Specimens.*  
(No applied stress.)

Plane Reflecting	Residual Lattice Strains		
	Finch *	Garrod †	Greenough ‡
	$\times 10^{-5}$	$\times 10^{-5}$	$\times 10^{-5}$
310 . . . . .	+20	+34	+24
211 . . . . .	+1	+16	+7
110 . . . . .	-24	-13	-25
Plastic Extension, % . . . . .	19	...	19
Stress Previously Applied, tons/in. <sup>2</sup> .	30	23.8	27.4

Heyn stresses are responsible for the variation in the residual lattice strain with the plane reflecting, and the above table shows how remarkably good is the agreement between the *relative* values observed by the three authors, and with my own earlier values.§ It is clear that the relative values obtained are truly representative of the Heyn stresses in the specimens. Actually other stresses also exist, but attention is here concentrated on the Heyn components.

The mean value of the difference in lattice strain shown by the 310 and 220 diffraction lines is  $47 \times 10^{-5}$ . In order to make this figure comparable with the figures quoted by Wood and Dewsnap I have converted this strain into a stress, using the normal macroscopic values of Poisson's ratio and Young's modulus (although this is not entirely justifiable). This shows that the average difference between the total biaxial stress sum in the grains giving rise to a 310 diffraction line and those giving rise to a 220 diffraction line is 21 tons/in.<sup>2</sup>. It is abundantly clear that the stress in a grain depends on its orientation with respect to the direction of plastic extension, and that the difference between the stresses in the grains is large.

In their experiments, Wood and Dewsnap use one diffraction line and measure the lattice strains observed in each of two cases, (a) when the incident beam is perpendicular to the surface, and (b) when the beam makes an angle to the surface. Fig. B illustrates the two cases, the reflecting normals making

\* L. G. Finch, *Nature*, 1950, **166**, 508.

† R. I. Garrod, *ibid.*, 1950, **165**, 241.

‡ G. B. Greenough, *ibid.*, 1950, **166**, 509.

§ G. B. Greenough, *Metal Treatment*, 1949, **16**, 58.

angles  $\beta = 90^\circ$  and  $\beta = 45^\circ$  with the surface. It will be seen that the grains diffracting in the two cases are not the same, and that they have different orientations with respect to the direction of plastic extension. Wood and Dewsnap assume that the stress in the two families of reflecting grains is the same, and calculate the component of the stress  $S_y$  from the difference in the strains shown in the two cases. It is clear, however, from the figures quoted above for the Heyn stresses that the assumption might be completely false, and, therefore, that the values deduced for  $S_y$  are not reliable. Since Wood and Dewsnap use the value of  $S_y$  in calculating  $S_x$ , this must also be unreliable. It must be emphasized that the error in the values is not necessarily small; it could be as much as 100%.

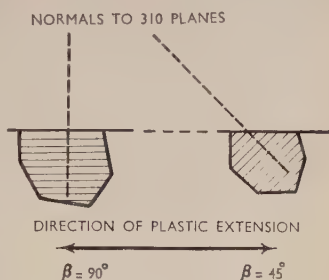


FIG. B.—Orientation of Grains Reflecting in Two Exposures, Used to Determine  $S_y$  (Greenough).

MR. R. C. GIFFKINS \*: Dr. Greenough and Mrs. Smith refer in their paper to some creep tests with lead, and suggest that they found no difference in the effects of fast and slow straining either because the temperature of the tests was too low or because the impurities in the lead were too great. While it is certain that these factors, particularly the former, can be of great importance in determining the mechanism of creep, it is probable that in this case all the rates of strain used were too great for anything but diffuse X-ray reflections to be obtained—that is, slip was the predominant mechanism operating. I have made observations using X-ray and metallographic techniques on a number of specimens during the course of creep tests with high-purity lead and its alloys. In the case of the pure lead, slip and consequently diffuse X-ray reflections are obtained when the rate of strain is such that 4% extension occurs in 220 hr.; this rate is less, by a factor of 8, than the slowest—4% in 28 hr.—used by Greenough and Smith. In this test I found microscopical evidence of some sub-division of grains, as well as slip, boundary movement, and grain rotation. At a much slower rate of strain—4% in 140 days—there was some sub-division of X-ray reflections, but microscopical examination was not possible owing to tarnishing of the specimen.

It is therefore evident that the comparatively high rates of strain used by Greenough and Smith would all give rise to effects which would not reveal any tendency to deform by mechanisms other than slip.

With the tests using high-purity lead, an added difficulty is the recrystallization which takes place at about 4% strain; this, and the problem of retaining a polish have been avoided by using a single-phase lead-thallium alloy, and it is hoped to publish some observations on this work shortly.

DR. W. H. HALL,† M.A. (Member): Dr. Greenough and Mrs. Smith have advanced an interesting explanation of the changes in back-reflection X-ray patterns during deformation in terms of the dislocation hypothesis. Mr. Williamson and I have recently obtained more detailed evidence from Debye-Scherrer patterns which confirms their interpretation. Observations of the diffraction patterns of the isotropic metals aluminium and tungsten were made, and the line shapes and intensities and the diffuse background scattering after cold-working and annealing treatments were compared. The apparatus used

\* Ballieu Laboratory, University of Melbourne, Australia.

† Lecturer in Metallurgy, Birmingham University.



was a Geiger-counter spectrometer employing monochromatic radiation and divergent-beam geometry, an evacuated specimen chamber being used to prevent diffuse air scattering. Filings of aluminium of high purity (99.99%) and of a commercial grade (about 99.7%) were examined, and although after annealing the diffraction patterns were identical, on cold working the commercial aluminium exhibited much greater line broadening, confirming the results of Dr. Greenough and Mrs. Smith. It was found that besides causing line broadening, cold working significantly increased the diffuse background scatter throughout the spectrum, the backgrounds from both filed specimens being about 15 counts higher than that from an annealed specimen. Simultaneous measurements of the Debye-Scherrer lines showed that their integrated intensities were correspondingly reduced after filing, and the total diffracted intensity was found to remain constant within 1%.

Comparison of the line-broadening and diffuse-scattering measurements reveals an important result. Although the line breadths of the filed pure aluminium were very little greater than the annealed breadths, the increase in background scatter was fully as great as that for the specimen of commercial purity, which exhibited much greater broadening. The similarity of the backgrounds of the two cold-worked specimens indicates that the amounts of short-range disturbance were about the same in both, but the line-broadening results show that the long-range order was far greater in the pure aluminium than in the impure material. If dislocations are assumed to be responsible for the diffraction effects, the diffuse scattering must originate largely in the severe localized distortions near to the dislocation lines, and the background measurements show that the total numbers of dislocations in the two specimens must have been approximately equal. Dislocation theory regards recovery as the migration and rearrangement of dislocations produced during deformation to form arrays of minimum strain energy. Such migration is assisted by a rise in temperature and resisted by impurities, which form stable "atmospheres" round the dislocations and impede their movement. The experimental results are thus fully explained if the numbers of dislocations initially produced by filing were the same, but redistribution occurred only in the pure aluminium, recovery in the commercial aluminium being retarded by the impurities present.

These results were confirmed by measurements on tungsten of 99.9% purity filed and annealed at various temperatures. Annealing up to 1150° C. caused recovery, characterized by considerably diminished line-broadening without any change in background level. Recrystallization on annealing at 1300° C. further decreased the line breadths very slightly, implying little additional increase in long-range order, but the background level dropped significantly, as previously found for aluminium, indicating the elimination of the localized lattice imperfections. It is considered that these results offer strong support to the dislocation hypothesis, for it is difficult to postulate any other reasonable model which explains both the long-range and short-range diffraction effects so simply, but much more theoretical and experimental work will be necessary before a fully quantitative explanation is obtained. A paper describing the investigations in more detail is in course of publication.

DR. R. W. K. HONEYCOMBE,\* M.Sc. (Member): In discussing the nature of the cold-worked metal, Wood and Scrutton point out that the X-ray reflections obtained from lightly deformed specimens occur as smeared-out arcs of reflection in which strong and often sharp reflection spots can be seen. They suggest that this effect is found because the lattice is made up of relatively perfect fragments separated by regions of crystallite debris ( $10^{-4}$  cm.) and they

\* Cavendish Laboratory, Cambridge.



reject the possibility that the lattice is continuous though distorted. While I would not deny the possibility of fragmentation in a *heavily* cold-worked metal, I think that in the early stages of deformation—that is, 1–5% extension as considered by Wood and Scrutton—there is no direct evidence for fragmentation. There is, on the other hand, fairly direct evidence that the lattice is continuous although distorted in certain regions. Lightly deformed aluminium crystals and coarse-grained polycrystals give rise to the same X-ray effects as those mentioned by Wood and Scrutton, and I have shown recently \* that these can be explained by the presence in the crystals of narrow bands of lattice curvature or *kink bands*. Under favourable conditions these can be detected microscopically. The occurrence of the bands is widespread and has been studied by X-ray micrography by which means they can be detected at small strains (1% elongation). This work has revealed a second source of lattice disorientations which may be even more important at high temperatures, namely bands of secondary slip which are regions in which the predicted slip system does not operate but a second set of slip planes can be observed. These bands are also usually on a microscopic scale and although they are not primarily regions of lattice distortion, they are regions of local disorientation which could give rise to maxima in X-ray asterisms.

I contend that these inhomogeneities play an important part in slow deformation at elevated temperatures, and although they may not develop to the same degree because of the intrusion of other phenomena such as polygonization, I think they have a primary role in the observed fragmentation. The development of the above types of inhomogeneity during creep would result in a two-stage process; first, large disoriented regions would form, which later would become further fragmented by polygonization, i.e. diffusion of dislocations in distorted regions. Calnan and Burns subscribe to this view on the basis of their experiments, whereas Wood and Scrutton consider that a fine crystalline debris is first produced and is later absorbed to form larger fragments.

At very slow rates of deformation and at very high temperatures a direct fragmentation of the crystals appears to occur, and it is only by considering the process in terms of the migration of dislocations that a reasonable mechanism can as yet be suggested. The evidence for the formation and migration of dislocations in deformed and subsequently annealed metals, although indirect, is strong, and it seems reasonable to assume that they are present in a very mobile state in aluminium slowly deformed at elevated temperatures. This means that such inhomogeneities as kink bands are short lived as such, because the lattice curvatures (regions with excess dislocations of one sign) are continuously removed as they form. The inhomogeneities are simply a source of dislocations for polygonization, and the mobility of the resultant dislocation walls quickly removes any evidence of their origin in the crystal.

DR. A. LATIN,† M.Eng. (Member): I was particularly interested in Professor Cottrell's paper on creep of zinc and his attempts at developing a theory of quasi-viscous creep flow. Any theory put forward has to account for the exponential type of relationship between  $\kappa$  and the applied stress in the application of the Andrade equation. Neither the energy barrier nor the hardening/recovery theories account adequately for this. With regard to the latter, the argument may be advanced that to say hardening is balanced by recovery during the creep process is simply to state that neither occurs. Consequently I think Professor Cottrell might well consider whether a more direct approach to the problem of quasi-viscous creep ought not to be made. Essentially the process can be looked upon as a stress-directed, thermally

\* R. W. K. Honeycombe, *Proc. Phys. Soc.*, 1950, [A], 63, 673.

† British Insulated Callender's Cables, Ltd., London.

activated diffusion of disordered regions through an ordered lattice. Disordered regions may consist of full line-dislocations, which move, as I have suggested previously, by a combination of glides and jumps, &c., or more localized regions, which move by processes analogous to "diffusion of vacancies". The general type of motion envisaged, taking place in a disordered structure, leads to a Newtonian form of viscous flow. In taking place through an ordered structure, I would suggest that it would be found to lead to the exponential flow constant/applied stress relationship. In applying such a theory to a polycrystalline structure, the difference in action at the grain boundaries and within the grains themselves would correspond, at least to some degree, with the difference in amounts of disorder in these regions.

DR. A. H. SULLY,\* M.Sc. (Member): I am confining my comments to the four papers which are concerned primarily with the mechanism of slow deformation. These papers are of considerable significance because they all have very much the same theme and all demonstrate the complexity of the mode of deformation of a polycrystalline metal. They also show more clearly than has previously been done how the mode of deformation varies with the rate of strain.

Cottrell and Aytakin list four processes which accompany the deformation of polycrystal specimens: slip, twinning, cell formation, and displacement along grain boundaries. Except for high strain rates in a few metals I think that we can eliminate twinning as an important factor in creep deformation at practically important strain rates and focus our attention on the other three, namely slip, cell formation, and grain-boundary flow.

It is quite clear from the X-ray papers that, at a particular temperature, the rate of deformation determines which of these processes is predominant. Thus at fast rates of strain deformation is mainly by slip, at slower rates cells are formed and are involved as units in the deformation process, while at very slow rates it is not improbable that the units of structure are the grains themselves, and creep occurs primarily by viscous flow at the grain boundaries.

It is also quite plain that there is no clear-cut distinction between these processes. There must be a gradual transition from one to the other as the strain rate is decreased at a given temperature or the temperature is raised at a given strain rate. Furthermore, as is mentioned in at least two of the papers, the deformation is inhomogeneous and the process of deformation may vary from crystal to crystal and, as is shown by Calnan and Burns, even in different parts of the same crystal. The particular process which predominates depends not only on the strain rate but also on the metal under test. This is clearly shown by Greenough and Smith, who note a considerable difference between the creep deformation of 99.25% aluminium and 99.92% aluminium. For a rather large creep rate in both cases of about 10% in 50 hr. the high-purity material showed mainly cell formation, while the metal of lower purity showed considerable diffuseness of the diffraction spots, suggesting that slip processes were also operative. The apparent discrepancy between Wood and Scrutton's results and those of Calnan and Burns may similarly be due to the differences in purity of the material, 99.4% in the case of Calnan and Burns, who found slip with later cell formation, and 99.98% in the case of Wood and Scrutton, whose specimens showed little signs of slip at a corresponding rate of deformation.

I find particularly interesting the synthesis by Cottrell and Aytakin of the constant-barrier and recovery theories of constant-state creep. This formalized theory accounts very successfully for their experimental observations on creep transients and recovery. The authors have not claimed that steady-state

\* Principal Physicist, Fulmer Research Institute, Ltd., Stoke Poges, Bucks.

creep in polycrystals can be accounted for on the basis of this theory. Indeed they are at pains to point out the complexity of deformation of polycrystals. Here I think they might have been bolder. I see no reason why this theory cannot account for steady-state creep under conditions where grain-boundary viscous effects are relatively unimportant, that is at relatively high strain rates and relatively low temperatures.

One may consider the primary or transient stage of the creep curve to result from that stage of the deformation in which the strength seeks to achieve homogeneity from an initially very inhomogeneous condition. At high strain rates this is achieved by slip and strain-hardening, varying from crystal to crystal. At low strain rates the inhomogeneity is relieved by the diffusion of dislocations to form cell boundaries or perhaps out of the crystals altogether—leaving the crystals as the units of deformation. One is tempted therefore to construct the following table which is to a large extent a synthesis of existing knowledge of the various processes of creep deformation.

TABLE B.—Processes of Creep Deformation.

	Predominant Mechanism in		
	Transient Creep	Steady-State Creep	"Tertiary" Creep
Single Crystals	Slip (Twinning)	Recovery	Necking
Polycrystals:			
(a) Low temp.; high strain rates	Slip	Recovery	Necking
(b) High temp.; low strain rates	Slower dislocation movements giving cell formation or exhaustion creep	Grain- and cell-boundary viscous movements	Grain separation

The distinction between deformation mechanisms (b) and (a) is practically of great importance. In (b) the whole emphasis at low strain rates moves to the crystal boundary and the properties of the crystals are relatively unimportant. This explains why in precipitation-hardened alloys, the overaged condition may be much more resistant to creep at very low rates than the normally aged material which has the maximum strength in tensile tests at the creep temperature.

There is only one point of criticism which I have to offer on any of these excellent papers. This relates to the paper by Wood and Scrutton. I am not convinced that the X-ray evidence enables them to differentiate with such apparent certainty between a mechanism of cell formation from a structure previously disordered and cell formation directly without prior distortion. It seems to me that such a conclusion is unjustified unless it is based upon a much more comprehensive correlation of the structure with time of application of stress than that which the authors have made. As was pointed out by Crusard\* in the discussion of Wilms and Wood's paper at the Paris meeting last October and also by Greenough and Smith, in their paper, cells must form by the migration of dislocations present in the lattice, and this motion must result in an increasing perfection of the crystalline units. The initial state of disorder may vary in degree and must depend on the initial strain rate at the beginning of the test, but the distinction is only one of degree and does not justify Wood and Scrutton's conclusion that two distinct mechanisms are operating.

\* *J. Inst. Metals*, 1948-49, 75, 1125.



MR. B. WALTERS,\* (Member): On behalf of the Imperial Smelting Corporation, Ltd., I would like to thank Professor Cottrell and Dr. Aytekin for the recognition they have given to the Corporation as suppliers of the zinc used in their work. I would, however, mention that the description "spectroscopically pure" which the authors use is not correct. The zinc produced on a laboratory scale for research purposes has a purity of the order of 99.999%; we do not consider it to be spectroscopically pure, and usually quote impurity contents.

DR. W. A. WOOD † (Member): My colleagues and I note with interest that Dr. Greenough and Mrs. Smith have repeated and confirmed our observations on what we termed the cell mechanism of deformation in aluminium. Their X-ray photographs from the pure metal, however, do not appear to show the cell structure so clearly as in our experience it can be shown. This experimental deficiency seems partly to have coloured their interpretation.

Presumably the main purpose of this paper was to interpret the cell mechanism in terms of dislocation theory. As the authors point out, we have felt that such an interpretation at the present stage of our knowledge of dislocations would be premature. And despite the very interesting hypotheses now put forward, it is still difficult to avoid the feeling that, for some time yet, more facts will prove of greater value than more theory. Indeed it is doubtful whether the proposed interpretation is good enough to stand up to the facts already available.

One recent observation may be quoted. It was established in our earlier work that at a given temperature the cell size is a function of the rate of strain, being larger the slower the strain rate. Suppose we take a specimen and, by an appropriate rate of strain at a fixed temperature, cause the grains to break up into cells of quite a small size, such as would produce a large number of sharp secondary X-ray reflection spots. Suppose now we reduce the rate of strain, keeping the temperature the same, and then re-examine the cell size. It is found that the small cells in each grain grow into large cells, of a size corresponding to the new slower rate of strain. This is the new observation, which we are terming "cell growth". Then if desired, by increasing the rate of strain we can break the cells down again, and so on. Apparently therefore, deformation breaks down the grains or cells. Heating produces cell growth. What we observe is the resultant.

It is clear that this phenomenon of "cell growth" is directly opposed to the basic postulate of Greenough and Smith that heating a deformed grain causes it to break down or, to use their terminology, "polygonizes" it. Indeed, I find it difficult to accept the idea of polygonization at all, even in the sphere of "recovery", where it seems first to have been introduced. It seems much more natural to suppose that heating produces healing and growth, not disruption of a grain. Therefore we remain rather sceptical of the authors' conclusion that "by adopting the theory of polygonization put forward by Cahn, it is possible to explain all the observations made by Wilms and Wood, and by Wood and Rachinger".

Messrs. Calnan and Burns have performed a useful task in showing the special behaviour of large crystals of aluminium under prolonged stress. I should like to make the point that although it is a special case, the large crystal fits naturally into the general scheme when we consider the influence of grain-size on creep characteristics. We have examined the behaviour of a whole range of grain-sizes, from a fine polycrystalline aggregate to a single-crystal specimen; and we find that at a given temperature, the effect of increasing the grain-size is virtually equivalent to increasing the rate of strain; that is,

\* Imperial Smelting Corporation, Ltd., Avonmouth.

† Baillieu Laboratory, University of Melbourne, Australia.

the internal breakdown of the grains becomes more drastic. The evident reason is that the fewer grain boundaries there are available, the more the interior itself of the grain has to be responsible for external changes in shape of a specimen.

Thus at an appropriate elevated temperature and rate of strain, we find that a sufficiently fine-grained specimen deforms mainly by grain-boundary movements, with no detectable internal breakdown. With a specimen of coarser grain, the interior of the grain is affected and breakdown occurs into a coarse cell size. As the grain-size is made still larger the cell size becomes finer. Ultimately with a very large grain-size or single crystal, as the authors observe, we approach the more drastic stage of slip.

A further comment on the work is that for systematic results, a material of reasonable purity is to be preferred. It is unfortunate that the authors confined their attention to material of such a low standard as 99.4% purity.

PROFESSOR A. H. COTTRELL (*in reply*): I cannot accept Dr. Latin's statement that the hardening/recovery theory of steady creep does not account for the exponential increase of creep rate with stress. If, during the recovery of a strain-hardened specimen, the internal stress decreases logarithmically with time, as our experiments on recovery suggest, then the hardening/recovery theory leads directly and unambiguously to the exponential creep law. Moreover, the logarithmic recovery law is very reasonable, since it requires only that the activation energy for recovery should be a smoothly decreasing function of the internal stress. Arguments such as "that to say hardening is balanced by recovery is simply to state that neither occurs" could be dangerous, and I doubt whether Dr. Latin would want to go so far as to aver, regarding the free fall of a body through the earth's atmosphere, that the opposing forces of gravity and air resistance no longer occur when they are balanced. The view of steady creep which Dr. Latin takes, that of the "stress-directed thermally-activated diffusion of disordered regions through an ordered lattice", may well be correct. What I would like to know is the direction along which he would wish to develop the view into a complete theory. Would it be developed as a constant-barrier theory or as a hardening/recovery theory? It has to be the one or the other.

Dr. Sully has invited us to consider extending the recovery theory of creep to polycrystals. There is one difficulty that needs clearing up first. We do not yet know whether the rate of recovery in a polycrystal is independent of the mechanical history. If it does depend on the history, one may expect a recovery creep whose rate is not constant. The theoretical analysis and experimental study of such a creep would be difficult. In one respect, however, I would go further than Dr. Sully in applying the theory to polycrystals. Suppose that creep takes place slowly at high temperatures in a polycrystalline specimen. Then, as Dr. Sully points out, the predominant mechanism of flow is the viscous movement along grain boundaries. But the process that eventually controls the rate of this grain-boundary flow may in fact be recovery within the grains. For, as the boundaries slide past each other, stress concentrations are set up at the corners where different grains interlock. These stress concentrations gradually increase until they reach the elastic limit of the grains. Plastic flow then occurs near the boundaries and the material in these regions strain-hardens. If this hardening went on indefinitely the creep would eventually be brought to a standstill. However, if recovery occurs in the strain-hardened regions the hardening could not increase indefinitely and creep would therefore continue. Thus, although the predominant mechanism of flow would be the sliding along grain boundaries, the rate of flow might be determined by the rate of recovery inside the grains.

On behalf of Dr. Aytekin and myself I must apologize for the fact, pointed



out by Mr. Walters, that our description of the zinc we used was not correct. We called it spectroscopically pure because the amounts of impurity it contained were too small to be measured by the spectroscope, and I am sorry that we overlooked the fact that the suppliers were more careful in their description.

DR. GREENOUGH and MRS. SMITH (*in reply*): We were pleased to hear of Dr. Hall's results and to learn that they support our own. However, there is the important difference that whereas his work indicates that polygonization occurs in pure aluminium at room temperature, we observe it only after creep at 300° C. It is becoming increasingly obvious that the sensitivity of the X-ray technique employed often determines whether or not polygonization is observed, so that direct comparisons can only be made when the same technique is used. Dr. Hall, by measuring line breadths, can differentiate between dislocations at random and arranged regularly to give "cells" about  $10^{-5}$  cm. across, while our cruder technique only shows separate diffraction spots from "cells" about  $10^{-3}$  cm. in size or greater. In view of Dr. Hall's work, it appears probable that a pure aluminium specimen pulled quickly at 300° C. does polygonize, but that the polygonized units formed are either too small or too imperfect to give discrete X-ray reflections. In this case, our explanation, although still generally applicable, would require some modification.

Dr. Honeycombe has mentioned that kink bands play an important part in the plastic flow of metals. We agree, but we are not yet sure whether they are merely examples of inhomogeneous deformation and important because they provide regions where there is a concentration of dislocations of one sign, or whether they are of more fundamental interest.

We were most interested to hear that Mr. Gifkins has observed sub-division of the X-ray reflections from pure lead after slow deformation at room temperature. Since the strain rate required to produce the effect was considerably slower in this case than in that of aluminium deformed at 300° C., it seems probable that the temperature of deformation was effectively (as well as actually) lower for the lead, since the effects of strain rate and temperature are to some extent interchangeable. Our own recent work on lead of about 99.99% purity indicates that polygonization probably takes place at about 100° C. at rates of strain similar to those employed in experiments with aluminium at 300° C. Hirst\* also observed some splitting of the reflection spots from lead during slow creep at room temperature, but in this case the reflections after creep were much more diffuse than in the case of aluminium.

We are sorry that Dr. Wood finds our illustrations inferior to his own; we must agree that they have lost a little in clarity during reproduction. Perhaps, with more experience, we shall become as adept as he in providing convincing pictures. However, our explanation is not based solely on our own results, and we think that the published work of Dr. Wood and his collaborators is completely in accord with our ideas.

In his further remarks, Dr. Wood states that he considers facts to be of greater value than theory at this stage of our knowledge, but his comments on polygonization illustrate clearly the dangers of paying too little attention to the latter. When polygonization occurs in a deformed crystal, the total number of dislocations, i.e. of lattice imperfections, present in the crystal remains unchanged, but they become so arranged that the degree of long-range order in the crystal increases. The process represents an increase rather than a decrease in the perfection of the crystal, and it is a complete misconception to view the process as a "disruption" of the crystal.

We are very interested in Dr. Wood's latest observations and look forward

\* H. Hirst, *Proc. Austral. Inst. Min. Met.*, 1941, [N.S.], (121), 11.

to learning more details of them. It does not appear at first sight that they should prove to be incompatible with our views.

DR. WOOD, MR. DEWSNAP, and MR. SCRUTTON (*in reply*): It is clear that for some time the effects of deformation will be interpreted according to two distinct schools of thought; this is perhaps a good thing. One view, based on polygonization, holds that the deformed metallic lattice first exists in a metastable distorted shape, and then becomes broken up into discrete cells only if sufficiently heated. The other view is that the distortion and dissociation are for all practical purposes instantaneous with deformation; the effects of subsequent heating or straining are then changes in a grain already broken down. The changes may involve further breakdown, or they may involve growth of the debris within the main grain boundaries. This second view is essentially that put forward many years ago by Gough and Wood, and usually referred to as the fragmentation theory. The term fragmentation is not very apt, because there is no more fragmentation than there is at a grain boundary in a metal; but it seems to have come to stay, and will serve.

The above remarks will make it easier to reply to the discussion on our papers. Thus, in reply to Mrs. Smith and also to Dr. Sully, we suggest that they will overlook a significant point if they see no difference between a cell structure formed direct and one formed from a previously disordered structure. This applies whichever of the above theories is used, but is clearer in terms of the fragmentation theory. The removal of the disordering (by growth of the debris) reduces the resistance of the metal to plastic flow; whereas the direct dissociation of annealed grains to cells, virtually the production of a finer-grained structure, increases the resistance to flow. These are two opposing processes. We attach some importance to this aspect, and have followed it up in extended experiments, about to be published. In these we have separated the two processes and measured the resistance to deformation while the disordering is being removed and the resistance while direct dissociation is taking place. The results clearly confirm our prediction of two opposing mechanisms.

In reply to Dr. Honeycombe's theories, we view with some distrust his statement that "there is fairly direct evidence that the lattice is continuous but distorted" after deformation; this is the type of assertion that just cannot be proved directly by the physical techniques at our disposal. There is nothing in such evidence that cannot be explained equally well by the fragmentation theory; thus the lattice disorientations and kinks that he observes could equally well arise from disoriented fragments of submicroscopic size.

Dr. Greenough's remarks refer to our paper (Wood and Dewsnap) on the rather different subject of internal strains. We should like to say, firstly, that as far as we are aware the earliest systematic stress/strain curves for the metallic lattice were those published by Smith and Wood now many years ago; we are therefore familiar with the experimental geometry. Diagrams almost identical with the one Dr. Greenough uses to illustrate the relevant factors will be found in the papers just mentioned. A point we have always made in this and the earlier work is that the only reliable measurement in this type of experiment is measurement of strain, not stress; thus a change in lattice parameter of, say, 0.1% has a definite meaning and represents a definite abnormality in a grain, whatever it may mean in terms of internal stress. We have also pointed out, as in the present paper, that conversion to internal stresses depends on what theory of stress/strain relation is adopted for the individual grains in an aggregate. It can hardly be claimed that any theory is fully reliable, in view of the complex interaction of one grain with another. The conversion is virtually arbitrary. Dr. Greenough claims that a particular relationship can be chosen which proves that the internal strains

are due to Heyn stresses. If this is so, the strains as well as the internal stresses should behave in a regular manner related to the nature of the external deformation applied to a specimen. That they do behave in a regular manner with *fine-grained* material was one of the chief points made by Smith and Wood in their earlier work; the figures quoted by Dr. Greenough in support of this point merely confirm what has been known for some time. But the present paper shows that in *coarse-grained* aggregates, the internal strains do not behave in a regular manner. Therefore, the Heyn-stress theory, as interpreted by Greenough, cannot have it both ways.

DISCUSSION ON PAPER BY DR. N. THORLEY :  
 "THE CALCULATION OF THE ACTIVATION ENERGIES OF RECOVERY AND RECRYSTALLIZATION FROM HARDNESS MEASUREMENTS ON COPPER."

(*J. Inst. Metals*, this vol., p. 141.)

DR. MAURICE COOK\* (Member of Council) and DR. T. LL. RICHARDS† (Member): By a fully rigorous theoretical treatment the author has in his very interesting paper developed our two-stage conception of recrystallization in such a way that it can now be generally applied without making any restrictive assumptions. It is unfortunate, however, that Dr. Thorley has made the successful application of his treatment to the analysis of our results dependent on the determination of the exact slope of the final straight portion of the  $\ln 1/1 - x$  versus  $t$  relationship. If, as is quite probably true for heavily rolled copper strip, the actual relationship is similar to that of the hypothetical curve in Fig. 1 of the paper, then the truly linear part begins only towards the end of the recrystallization stage, which makes the exact determination of the slope difficult. Indeed, it would seem from Fig. 2 (p. 151), in particular, that he has chosen the slope rather arbitrarily. In our opinion it would be preferable to derive the constants  $A$  and  $\beta$  of the general equation (3) algebraically from the corresponding values of  $\ln 1/1 - x$  and  $t$  taken at points on the non-linear portion of the curve, thus preserving the general character of the treatment.

Nevertheless, the author has by his analysis succeeded in obtaining approximate values of the separate activation energies of recovery and recrystallization, and it is interesting to note that within experimental error they have the same value. This observation explains the difficulty that is experienced in dissociating the two effects in H.C. copper. We should mention, however, that, contrary to the statement made on p. 142, we do not hold the view that the two stages are necessarily characterized by different activation energies. Although it so happens that the values of the activation energies derived either from equations (4) and (5) or directly from hardness figures are similar, it should be pointed out that theoretically the latter procedure is valid only when based on differences between intermediate and final hardness values and not on relative hardness values as used by Dr. Thorley.

DR. V. A. PHILLIPS,‡ A.R.S.M., L.I.M. (Junior Member): Dr. Thorley is to be congratulated on his stimulating paper, which takes the two-stage theory of the recrystallization of heavily cold-rolled copper a step further. He has shown how separate activation energies can be calculated for the two stages postulated in the theory of Cook and Richards. Although that theory conforms fairly well with the observed time dependence of the rate of recrystallization, this does not prove beyond doubt that two physically distinct processes

\* Director, Imperial Chemical Industries, Ltd., Metals Division, Birmingham.

† Research Physicist, Imperial Chemical Industries, Ltd., Metals Division, Birmingham.

‡ British Non-Ferrous Metals Research Association, London.



do in fact exist; however, the point should be capable of proof or disproof by suitably devised experiments in the near future. Until such experiments have been carried out one can do little more than speculate about the physical nature of the processes involved. At present all that can be said is that the rate of recrystallization is describable in terms of two stages governed by activation energies of  $P$  and  $Q$  respectively. Whether  $P$  and  $Q$  are to be identified with activation energies for so called "recovery" and "recrystallization", or for nucleation and growth, or for some other processes, is uncertain.

The author states on p. 149 that equation (3) predicts that the rate of growth of the crystals is higher at the later period, when  $\ln\left(\frac{1}{1-x}\right)$  is linear with  $t$ . Perhaps it would be better to say, rather, that the rate of recrystallization is greater, since published work points to the fact that the rate of growth is constant with time when the grains are large enough to be measured.

Two interesting conclusions may be drawn from equation (3) (p. 149) which avoids the approximation made by Cook and Richards. This equation may be written :

$$\ln\left(\frac{1}{1-x}\right) = A\left[t + \frac{1}{\beta}(e^{-\beta t} - 1)\right] \quad . \quad . \quad . \quad (1)$$

Consider conditions at  $x = \frac{1}{2}$ , where  $e^{-\beta t}$  is small compared with 1, that is  $t_s$  (half-recrystallization time) is within the straight portion of the  $\ln\left(\frac{1}{1-x}\right)$  versus  $t$  plot.

$$\text{Then} \quad \ln 2 = A\left(t_s - \frac{1}{\beta}\right)$$

$$\begin{aligned} \text{or} \quad t_s &= \frac{1}{\beta} + \frac{\ln 2}{A} \\ &= \frac{1}{\beta} \cdot e^{P/RT} + \frac{\ln 2}{a} \cdot e^{Q/RT} \quad . \quad . \quad . \quad (2) \end{aligned}$$

Differentiating (1) :

$$\frac{1}{1-x} \cdot \frac{dx}{dt} = A(1 - e^{-\beta t})$$

or, at  $x = \frac{1}{2}$ , neglecting  $e^{-\beta t}$  again :

$$\begin{aligned} \left(\frac{dx}{dt}\right)_{x=\frac{1}{2}} &= \frac{1}{2}A \\ \left(\frac{dx}{d(\ln t)}\right)_{x=\frac{1}{2}} &= \frac{1}{2}At_s \\ &= \frac{1}{2}\left(\ln 2 + \frac{a}{\beta} \cdot e^{\frac{P-Q}{RT}}\right) \text{ from (2).} \end{aligned}$$

Thus the slope of the  $x$  versus  $\ln t$  plot is independent of temperature if, and only if,  $P = Q$ . Consequently, the family of curves obtained when the rate of recrystallization is measured for a particular material at different temperatures and the fraction recrystallized is plotted against the logarithm of the annealing time, do not superimpose in general according to the theory when displaced along the  $\ln t$  time axis, but only as a special case when  $P = Q$ .

For an oxygen-free alloy containing 0.005% arsenic, based on 99.999% purity copper and rolled 95% from an average grain-size of 0.013 mm., I have obtained values of  $P$  and  $Q$  calculated according to the Thorley method of 27 and 42 kg.cal./mol. The slope of  $x$  versus  $\ln t$  ( $t$  in hours) plots increased



with temperature from 0.35 at  $10^3/T = 2.564$  (corresponding to 117.0° C.) to 6.5 at  $10^3/T = 2.046$  (corresponding to 215.8° C.), measuring the slope between  $x = 0.2$  and  $x = 0.8$ ; whereas the slopes calculated according to the theory were 0.47 and 5.4 respectively. Because of the large difference between  $P$  and  $Q$ , this material would be much more suitable than pure copper for the investigation of the physical significance of the two stages.

A second conclusion is also of interest. Putting  $1/T = \phi$  into the previous equation (2) and differentiating :

$$\begin{aligned}\frac{d}{d\phi}(\ln t_s) &= \frac{\frac{Q}{R} \cdot \frac{\ln 2}{a} \cdot e^{\frac{Q}{R} \cdot \phi} + \frac{P}{R} \cdot \frac{1}{b} \cdot e^{\frac{P}{R} \cdot \phi}}{\frac{\ln 2}{a} \cdot e^{\frac{Q}{R} \cdot \phi} + \frac{1}{b} \cdot e^{\frac{P}{R} \cdot \phi}} \\ &= \frac{Q}{R} - \frac{Q-P}{R} \cdot \frac{1}{1 + \frac{b \ln 2}{a} \cdot e^{\frac{Q-P}{R} \cdot \phi}}\end{aligned}$$

Therefore if  $Q > P$ , as  $\phi \rightarrow \infty$ , the slope of the  $\ln t_s$  (half-recrystallization time) versus  $1/T$  plot  $\rightarrow \frac{Q}{R}$  and increases to this value.

Alternatively since :

$$\frac{d}{d\phi}(\ln t_s) = \frac{P}{R} - \frac{P-Q}{R} \cdot \frac{1}{1 + \frac{a}{b \ln 2} \cdot e^{\frac{P-Q}{R} \cdot \phi}}$$

if  $P > Q$ , as  $\phi \rightarrow \infty$ , the slope  $\rightarrow \frac{P}{R}$  and increases to this value.

Hence the theory predicts that the slope of the  $\ln t_s$  versus  $1/T$  plot should not be linear except as an approximation when  $1/T \rightarrow \infty$ , that is when  $T$  gets small. It is necessary to evaluate the second term in order to decide whether it can be neglected in a given case.

The author's Table I shows that  $\frac{P-Q}{RT}$  is  $\gg 1$  in several cases, and hence in these instances Cook and Richards's results are not a good approximation for  $2Q$  as suggested on p. 155.

I am greatly indebted to Mr. D. Glenmow, M.A., Trinity College, Cambridge, for mathematical assistance.

The AUTHOR (*in reply*): I am glad to have the comments of Dr. Cook and Dr. Richards on my paper, as they were responsible for the experimental work on which it is based, and it must be stressed again that although the theory applies well to their work on cold-rolled copper, using hardness as the criterion of recrystallization, it is not correct to say that it can be generally applied as the two-stage conception of recrystallization. Other properties may follow a different course in relation to the structural changes in the metal.

It is true that the theory would be more strongly supported if it were possible to use the non-linear parts of the  $\ln 1/(1-x)$  versus  $t$  curves to determine  $A$  and  $\beta$ , but unfortunately there are insufficient experimental data in this region for most of the curves and the method cannot be successfully applied. Specimen A4 was chosen for illustration in Fig. 2 because it was this specimen that was so fully dealt with in Cook and Richards's original paper and in the subsequent discussion on it. Furthermore, nothing is known about the experimental error associated with each measurement.

With regard to the final point, it is admitted that the only justification for

using hardness figures without calculating the corresponding degrees of recrystallization is in the agreement with the values of  $P$  and  $Q$  obtained from the  $\ln 1/1-x$  versus  $t$  curves. As Dr. Cook and Dr. Richards point out, this direct method has no theoretical foundation, and whether the agreement is fortuitous for these particular experiments or is generally true for other physical and mechanical properties of cold-worked metals cannot yet be decided.

In thanking Dr. Phillips for his valuable contribution, I must especially compliment him on the neat way in which he has derived expressions for the slopes of the  $x$  versus  $\ln t$  and the  $\ln t_s$  versus  $1/T$  plots and so facilitated the discussion of these curves. This has revealed several new and interesting features of the problem with which I shall deal later.

It is agreed that while the present theory gives two separate activation energies it is not absolutely certain what exact physical processes they energize. This also applies to other methods in which an approximate value of 22,000 cal. is obtained for the "activation energy" of copper measured from the linear  $\ln t_s$  versus  $1/T$  plots. The importance of the present work is that *two* activation energies are derived.

With regard to the first of Dr. Phillips's conclusions, on the slope of the  $x$  versus  $\ln t$  curves, it is interesting to note that his experimental results agree so well with the theory. It is evident that there is no master curve for the hardness isothermals. The addition of so small a percentage of arsenic causes  $P$  and  $Q$  to diverge by much more than one would have thought, and this points essentially to the future use of such alloys in this type of experiment.

A fact rather overlooked so far is that one must take into account the numerical values of  $a$  and  $b$  as well as  $P$  and  $Q$ . It is true that the slope of the isothermals will be independent of temperature if  $P = Q$ , mathematically, but this is also true if:

$$\frac{a}{b} \cdot e^{\frac{P-Q}{RT}} \longrightarrow 0, Q \gg P,$$

assuming that  $a$  and  $b$  are temperature-independent constants and that the temperatures involved are the ordinary temperatures met with in these isothermal experiments. The values of  $a/b$  I have derived are of the order of 0.01, and  $|P-Q|$  is about 2000 cal., so that the above expression

becomes  $\frac{1}{100} e^{\pm \frac{1000}{T}}$ . Hence, when  $Q \gg P$  this expression is negligible and the isothermals are all parallel for the temperature range of the experiments, but when  $P > Q$  the slope does depend on the temperature of the anneal.

In his second point Dr. Phillips concludes that the slopes of the  $\ln t_s$  versus  $1/T$  curves should only be constant as  $T \longrightarrow 0$ . The fact is, of course, that all such published curves are linear at ordinary or even higher temperatures, so that this conclusion must not be taken to imply that these curves are linear only at exceptionally low temperatures. The second term of Dr. Phillips's expression can usually be neglected in practice.

The reason for this difference is again in the numerical values of  $a$ ,  $b$ ,  $P$ , and  $Q$ , previously mentioned. Dr. Phillips's statement is quite correct if:

$$\frac{b}{a} \cdot \ln 2 \cdot e^{\frac{Q-P}{RT}} \longrightarrow \infty \text{ for } Q > P,$$

and if

$$\frac{a}{b \ln 2} \cdot e^{\frac{P-Q}{RT}} \longrightarrow \infty \text{ for } P > Q.$$

In each case we must consider the expression as a whole, not merely from the temperature point of view. Taking  $b/a = 100$  approximately, as before, we see that this also affects the numerical values of these expressions and that the several possibilities must be considered individually.

Case I.

If  $Q$  is slightly greater than  $P$ , then :

$$\text{slope} = \frac{Q}{R} - \frac{N}{R}$$

where

$$N = (Q - P) \cdot \frac{1}{1 + 70e^{\frac{Q-P}{RT}}}$$

Since the minimum value of the exponential is 1, as  $T \rightarrow \infty$  or  $Q - P \rightarrow 0$ , the maximum possible value of this deviation  $N$  is given by :

$$N_{\max.} = \frac{1}{71} (Q - P).$$

This maximum error is about 60 cal. for specimen A2 and is well within the experimental error. At ordinary temperatures, e.g.  $T = 300^\circ \text{K.}$ , the deviation is only about 1 cal. The slope of the  $\ln t_s$  versus  $1/T$  plot is in practice quite constant in this case, irrespective of the value of  $T$ .

Case II.

If  $P$  is slightly greater than  $Q$ , then :

$$N = (P - Q) \cdot \frac{1}{1 + \frac{e^{\frac{P-Q}{RT}}}{70}}$$

and the maximum value of  $N$  is given by

$$N_{\max.} = (P - Q) \text{ as } T \rightarrow \infty \text{ or } P - Q \rightarrow 0.$$

For specimen A4,  $N_{\max.}$  is about 1100 cal. at  $300^\circ \text{K.}$ , so that in the work described the slope gives an energy between  $P$  and  $Q$  with an error of about 5% of  $P$  itself.

When  $P > Q$ , the slope does deviate appreciably from the assumed  $P/R$  and only approaches this value as  $T \rightarrow \infty$ . However, this difference is never greater than  $P - Q$ , and in the work of Cook and Richards is not of very great importance.

Case III.

If  $Q$  is much greater than  $P$ , as in Dr. Phillips's own experiments with arsenical copper, assuming that  $b/a$  is still about 100, the exponential term is so large that even for comparatively high temperatures  $N$  is very small. In this case, therefore, the curves should always be linear.

Case IV.

If  $P$  is much greater than  $Q$  we have the same conclusion as in Case III.

These considerations show that the greatest error is found when  $P > Q$ , and even then this can be of the same order as the experimental error. When  $Q > P$  the slopes give  $Q$  quite accurately. Hence, Cook and Richards's results should be values of  $Q$  for  $Q > P$ , and approximately  $\frac{1}{2}(P + Q)$  for  $P > Q$  or, at any rate, less than  $P$ .

It will be seen from Table I of the paper that the agreement with this theory is not uniform for all specimens, indicating the necessity of more accurate isothermal measurements before it can be tested further.

The fact that the  $\ln t_s$  versus  $1/T$  curves quoted in the literature are quite linear, even at temperatures as high as  $500^\circ \text{K.}$ , could be explained if  $Q \gg P$  for these experiments.

## DISCUSSION ON THE PAPER BY MR. G. A. MELLOR: "THE CONSTITUTION OF MAGNESIUM-RICH ALLOYS OF MAGNESIUM AND ZIRCONIUM."

(*J. Inst. Metals*, this vol., p. 163.)

DR. E. F. EMLEY,\* B.Sc., A.I.M., F.R.I.C. (Member): This is a very useful paper. Mr. Mellor has made an independent investigation of the magnesium-zirconium system and has obtained sufficient data to construct a tentative constitutional diagram which shows important departures from recently published work by Sauerwald † and by Siebel. ‡

Some of the many practical difficulties attending the investigation of the liquidus have been indicated by Mr. Mellor. He rightly mentions that an important function of the "chloride master alloy" is to provide a reservoir of active zirconium from which zirconium can dissolve and diffuse into the body of the melt faster than it can be precipitated from solution through pick-up of impurities or in other ways. It is, I think, important to realize that the provision of such an active reservoir of zirconium is an essential feature of any successful zirconium alloying process; once the alloy is transferred away from its reservoir of alloying reaction product loss of zirconium occurs. The equilibrium which Mr. Mellor has studied differs fundamentally therefore from other metallurgical equilibria in that it is essentially dynamic and not static, and can only be maintained in the presence of an excess of alloying agent. The problem of making an alloy with about 0.7% zirconium in solution is in fact analogous to that of filling a bath containing eight holes from one tap connected to a slowly falling head of water. The activity of the zirconium reservoir decreases with time, particularly if the melt is not stirred and a fresh surface of alloying residue thereby brought into contact with the body of the metal.

Some inherent difficulties of the method employed by Mr. Mellor to fix the liquidus appear worth considering because of their bearing on the probable accuracy of the results. In investigating the magnesium-manganese alloys, Grogan and Haughton || used a settling period of 10 min., and the much smaller size of particles in the magnesium-zirconium alloys suggests that longer times should be used in the present case, as was done by Mr. Mellor. The excess of alloying agent forming the zirconium reservoir must be sufficient to maintain saturation of the melt with zirconium during the whole of the settling period without the necessity for stirring the melt; otherwise low results may be obtained. On the other hand, the use of too much alloying agent will introduce considerable amounts of undissolved pure zirconium particles and thereby give high results, since complete separation by chemical methods of the zirconium present in the dissolved and undissolved states is not practicable. Grogan and Haughton alloyed their melts at about 900° C. and held the melts at successively lower temperatures for 10-min. periods. In a number of cases the manganese contents did not fall appreciably with temperature in the early

\* Metallurgist, Magnesium Elektron, Ltd., Clifton Junction, nr. Manchester.

† F. Sauerwald, *Z. anorg. Chem.*, 1947, **255**, 212; *Z. Metallkunde*, 1949, **40**, 41.

‡ G. Siebel, *Z. Metallkunde*, 1948, **39**, 22.

|| J. D. Grogan and J. L. Haughton, *J. Inst. Metals*, 1943, **69**, 241.



stages, thereby enabling results relating to unsaturated conditions to be rejected. No such check appears possible with magnesium-zirconium alloys because of the steepness of the liquidus. However, the degree of grain refinement of a 1-in. chill-cast bar appears to depend, over a wide range of metal and mould temperatures, only on the dissolved zirconium content of the alloy, and examination of such a bar in fact forms a convenient way of controlling the zirconium alloying procedure. It seems therefore that for any given alloying temperature the true liquidus should correspond closely to the minimum analysed zirconium content in a group of melts giving the maximum degree of grain refinement in the control bar. The effects of small amounts of suspended zirconium particles\* on the analysed zirconium contents of melts would, however, tend to offset slight departures from complete saturation, and it is not thought that Mr. Mellor's procedure of taking the average analysed zirconium content of his melts has given rise to high results. In fact our own results, using the method indicated, give about 0.65% for the true solubility of zirconium at 800° C., in comparison with Mr. Mellor's figure of 0.58%. It should be borne in mind, however, that the exothermic salt-reduction processes used to obtain the figure of 0.65% might conceivably introduce more zirconium at a given alloying temperature than the chloride-master-alloy process used by Mr. Mellor, in which no appreciable heat is evolved.

We have been interested in Mr. Mellor's important inference from his work that the precipitate forming in the cored areas on heat-treating magnesium-zirconium alloys in air is largely hydride. In the course of subsequent work carried out in the laboratories of Magnesium Elektron, Ltd., by P. A. Fisher and D. J. Whitehead, the presence of  $ZrH_2$  was confirmed by X-ray analysis. They found that with adequate surface protection very few signs of precipitation were visible on heat-treating at 500° C. an alloy containing (by analysis) 0.68% soluble zirconium, and they infer that, since the soluble zirconium content of the cored areas must exceed the average content for the specimen, the true solid solubility of zirconium at 500° C. is somewhat greater than Mr. Mellor proposes and may well exceed 0.7%. There seems little doubt that hydride formation during heat-treatment accounts for the absence of solid solubility below 500° C. found by Sauerwald.

One feature of Sauerwald's diagram which Mr. Mellor does not appear to have specially investigated is the very high solid solubility of 4.5% at the melting point. While I am sure that Mr. Mellor is right in doubting Sauerwald's interpretation of the chemical analysis of alloys made by heat-treating magnesium containing a high concentration of metallic zirconium particles, it does appear that Sauerwald also obtained high solid-solubility figures on alloys made by prolonged stirring of zirconium powder with magnesium sheet under argon. The existence of the zirconium-rich coring in the alloys appears to require a considerable extension of the solid solubility at temperatures near the melting point, and diffusion of zirconium can evidently take place readily under such conditions, since we have found that prolonged heat-treatment at 600° C. removes coring without giving rise to precipitation.

The figures for zirconium in solution in cast alloys derived from the resistivity measurements (Table V, p. 172) seem to us to be very low, and probably Mr. Mellor would wish these figures to be interpreted with caution, since a resistivity method standardized on solution-treated wrought material might not be directly applicable to a strongly cored as-cast structure.

\* In preparing the chloride master alloy for Mr. Mellor's experiments great care was taken to avoid as far as possible all impurities which could give rise to insoluble compounds with zirconium. His alloys would therefore be abnormally free from zirconium-rich particles.



DR. F. A. FOX,\* F.I.M. (Member): This paper is of interest from several points of view, not least in that it shows how difficult some constitutional work can be. The author was faced with a binary system as perverse as any this side of uranium; also he—a single worker—undertook the task at a time when alloying methods had not been standardized even in the specialist laboratory which was working practically full time on the problem. Evidences of both these sources of difficulty are visible in the paper; however, before dealing with some of them, it might perhaps be useful to recall why this particular alloy system was of interest.

The alloying elements which by 1939 had been found to have any practically-based utility for magnesium were aluminium, zinc, manganese, cerium, and tin, with cadmium and silver of doubtful value. The impetus given to research on magnesium by the 1939-45 war led to a close re-investigation of the possibilities of all elements which might prove useful. One of the early tasks was the establishment of a criterion of usefulness in an alloying element; general consideration of the physical metallurgy of magnesium led to the view that refinement of the grain of the cast alloy would be a valid first indication of likely merit. In an examination of the grain-size of as-cast metal, zirconium quickly showed itself the most powerful grain-refining element tested; when other properties of the magnesium-zirconium alloys were investigated, these were also promising. Interest quickly developed, since considerably improved mechanical properties seemed to be attainable, particularly in the presence of zinc as a third element. The practical exploitation of the zirconium-containing alloys was, however, soon seen to be difficult of realization because of serious non-uniformity in alloying behaviour in the zirconium-containing alloying materials then available. The Germans had proposed alloys of this kind before the war, and it was evident why the proposals had not been followed up. No two batches behaved alike, and every refinement in technique or materials produced only a temporary improvement; eluding difficulty *A* led only to trouble *B*.

It was at a stage of this kind that the author began his task; some account of the parallel developments which were to take place in the laboratories of Magnesium Elektron, Ltd., have been given by Emley,† and Ball‡ has reviewed the progress made in the eventual commercial production of the zirconium-containing magnesium-base alloys. In commenting on the paper, therefore, full allowance must be made for the great development of the subject that has taken place since the work at the National Physical Laboratory was begun.

It is to be noted that the title of the paper refers to "constitution" and that at the bottom of p. 172 the author refers to Fig. 4 as a "diagram", and does not call it an "equilibrium diagram"; in the middle of p. 167 and at the top of p. 169, there are references to the importance of the presence of excess zirconium in the melt. In spite of these points, however, the author does not make it clear, as he should, that his work is not concerned with equilibrium as ordinarily understood. Fig. 4 is certainly a "diagram"; the general reader, not knowing the reasons for the choice of wording, might well suppose it to be an equilibrium diagram. Under the conditions under which the author's work was done, it is, however, evidently an "unstable-equilibrium diagram". The author admits by implication that if he holds his melt for a time long enough for the excess undissolved zirconium in it to be dissipated, he will lose soluble zirconium; his diagram will then gradually

\* Deputy Technical Manager, H. J. Enthoven and Sons, Ltd., London; former Chief Metallurgist, Magnesium Elektron, Ltd., Clifton Junction, nr. Manchester.

† E. F. Emley, *J. Inst. Metals*, 1948-9, 75, 481.

‡ C. J. P. Ball, *Metallurgia*, 1947, 35, 125, 211.

collapse on to its axes. Fig. 4 no doubt has some value; but readers of the paper should clearly appreciate what it is, and what it is not. It is not an equilibrium diagram.

It might be possible to determine the true equilibrium diagram of the magnesium-zirconium alloys; such a piece of work would probably be expensive and would require conditions very far removed from those of the practical use of the alloys. The basic difficulties are those of purity, atmosphere, and crucible material. With triple-distilled magnesium, with high-purity "chloride master alloy", with a crucible of high-purity metallic zirconium, and with an atmosphere of purified argon, true equilibrium conditions might be established, and a new, possibly distinctly different, Fig. 4 be drawn.

In face of this major criticism, much detailed comment is superfluous. However, one or two further points seem relevant.

The author refers to the difficulty of distinguishing between zirconium merely present in the alloy and that in solution in the alloy. This difficulty is a serious one, but he does not say how he dealt with it; how, for example, are the figures in Table II arrived at, and how is he able to say that accuracies of the order of 0.02% zirconium are effectively obtained? In this connection, it is not clear how the last column of Table V is derived.

There seems to be a half-suggestion on p. 170 that although hydride formation would vitiate microscopic methods of determining the solubility limits, this determination can be properly made by resistivity methods, although the alloys were to be similarly exposed to hydride-forming conditions. On p. 171 the presence of hydride in resistivity specimens is, in fact, recognized; however, the basis of the choice of resistivity method and its efficiency might perhaps be made clear.

Finally, should not the phrase on p. 174 "solid solubility as determined by electrical resistivity", read "solid solubility as *estimated* by electrical resistivity"?

The AUTHOR (*in reply*): Dr. Emley's contribution is valuable because it gives an independent and expert opinion on the accuracy and reliability of the results. I am grateful for what is in effect an addition to the paper. Only two points need comment. A solid solubility of 0.7% at 500° C. is not in disagreement with my own results, and the solubility line in Fig. 4 could be drawn accordingly. The figures in the last column of Table V were derived from resistivity results and were intended to be indications of the amount of zirconium in solution rather than determinations.

Thanks are due to Dr. Fox for giving the historical background of the subject. I cannot agree that Fig. 4 should be called an "unstable-equilibrium diagram". The limitations in the accuracy of the present work have been discussed in the paper and in Dr. Emley's contribution. Such limitations are not so great as to lead me to think that the "true equilibrium diagram" would be very different from Fig. 4. I suggest that, along with most published constitutional diagrams, it might be called the "most probable form of the magnesium-zirconium equilibrium diagram".

The figures given in Table II were obtained by chemical analysis of zirconium soluble in 15% hydrochloric acid. It is nowhere stated that "accuracies of the order of 0.02% zirconium are effectively obtained". The more cautious statement on p. 167 reads "... it would be unwise to claim that the above figures are accurate to limits closer than  $\pm 0.03\%$  zirconium". In the last column of Table V the figures were derived from resistivity results as described for Fig. 3 on p. 171.

Dr. Fox would like more light on the reasons why solid solubility was *estimated* by means of electrical resistivity rather than by microscopical examination. When the latter was attempted it was found impossible to say

whether zirconium particles were present in the annealed specimens, not only on account of hydride formation but also because the zirconium particles were extremely small. In cast alloys zirconium particles are identified by the surrounding coring. If the coring disappears on annealing no one can say whether the particles have disappeared also. Rolled material proved to be too difficult to prepare for microscopical examination, but was the most convenient form for resistivity experiments. It seemed to be less subject to hydride formation on annealing than was the cast material. Furthermore, as described on pp. 170-172, any drop in resistivity due to hydride formation could be recognized from the fact that the value could be restored by subsequent heat-treatment at 600° C.

# DISCUSSION ON THE PAPER BY DR. W. ROSTOKER: "THE EFFECT OF APPLIED LOAD IN MICRO-INDENTATION TESTS."

(*J. Inst. Metals*, this vol., p. 175.)

MR. A. R. G. BROWN,\* M.Sc., L.I.M. (Student Member): A survey of the instruments available for hardness testing at low loads is at present being carried out for the Mechanical Methods Sub-Committee of the British Iron and Steel Research Association New Techniques Committee. Information concerning the variation of hardness with applied load which has so far been accumulated does not appear to corroborate the results reported by Dr. Rostoker.

It is convenient to express the variation of hardness with applied load by means of the index  $n$  in the expression:

$$L = aD^n$$

where  $L$  = load in g.,  $D$  = length of diagonal, and  $a$  and  $n$  are constants.

Meyer investigated this relationship for static ball-hardness tests, and  $n$  has become known as the "Meyer Index". In work with diamond-pyramid indenters, however, it is thought that this terminology is confusing, and that  $n$  is better referred to as the "Logarithmic Index".

In the survey undertaken by B.I.S.R.A. two copper specimens were included, one (*A*) being in the annealed condition, the other (*B*) being 50% cold-worked. The logarithmic indices obtained in eight co-operating laboratories are given in Table A.

TABLE A.—*Logarithmic Indices for Copper Specimens.*

Specimen	Laboratory							
	1	2	3	4	5	6	7	8
<i>A</i> . . .	2.46	1.95	1.95	1.90	1.93	1.92	1.86	1.84
<i>B</i> . . .	2.52	1.99	2.03	1.93	2.00	1.97	1.90	1.88

The logarithmic indices reported by Laboratory 1 approach most nearly those given by Dr. Rostoker, and it is significant that the instrument employed has a loading arrangement similar to that of the Bergsman tester. The falling off of hardness at low loads reported by Laboratory 1 has been attributed to inertia effects in the instrument, although this has not yet been proved. Only one other laboratory reports an index exceeding 2 for either specimen, and again the instrument concerned is of the Bergsman type.

The results in Table A show little change in the logarithmic index occasioned by the 50% cold work on specimen *B*. Certainly no effect of the order reported by Dr. Rostoker is found.

Of a further six specimens used in the survey it may be stated that in no case do the logarithmic index values depart from the value 2.0 by more than 0.5, and excluding Laboratory 1 the total range is 1.78–2.21.

\* Metallurgy (General) Division, British Iron and Steel Research Association, London.



Four reasons are given by Dr. Rostoker in explanation of the low apparent hardness values obtained at low loads.

The question of inertia appears to be inadequately considered, and some confusion with kinetic-energy effects seems to exist. Surely the balancing test described by Dr. Rostoker indicates that the accuracy of loading under ideal conditions would be  $\pm 50$  mg., not that inertia effects may be ignored. A detailed treatment of the effects of inertia has been given by Girschig,\* who points out that the inertia effects, which are due to the total mass of the moving parts of the tester, are closely connected with the velocity of loading. It is, in fact, likely that the inertia of this type of instrument may have an appreciable influence at low loads.

The presence of a soft surface layer after mechanical preparation is suggested by the work of Bowden on friction between surfaces. It is possible that such a surface layer may not be wholly removed by electrolytic polishing, and some workers claim to find evidences of the existence of such a layer on hardness testing at very small loads. It is not likely, however, that the layer would be sufficiently thick to affect the results at a load of 25 g. in the case of the relatively soft materials investigated.

The question of elastic recovery requires further attention. Contrary to Dr. Rostoker's postulation, it has been shown that in the case of Knoop indentations at low loads elastic recovery leads to high apparent hardness values owing to a reduction of indentation size.†

Two further factors, not mentioned by Dr. Rostoker, have been found to play an important part in causing low apparent hardness values at low loads. The first, vibration, is very difficult to eliminate. All hardness testers using loads below 200 g. should certainly be mounted on some type of shock-absorber mechanism, although even when so mounted it has been found that adjacent working machinery may cause appreciable errors (5–10% of the mean hardness at loads below 10 g.). Secondly, the instrument used in Dr. Rostoker's test was a standard Bergsman, and presumably electrical contact was indicated by a filament lamp. Such lamps consume appreciable amounts of current, and considerable arcing may occur at the contacts at the moment of break, giving a "kick" just as the full load is applied to the indenter. This has been shown to give rise to multiple or enlarged indentations, besides causing excessive contact wear, and rendering detection of full loading difficult. Perhaps this was what Dr. Rostoker experienced when he reports that a double indentation effect occurred at loads below 25 g.

MR. E. R. W. JONES,‡ B.A., A.I.M. (Member), and Mr. B. W. MOTT,‡ M.A. (Member): This paper is important in that Dr. Rostoker shows that the microhardness values he obtains vary with load and draws certain inferences from his results which suggest that microhardness values may be used to assess work-hardening capacity.

Before one can place any confidence in these results it is necessary to demonstrate, firstly, that the data are typical, and secondly, that the inferences drawn are more probable than other possible inferences.

With regard to the first point we would like to stress that microhardness tests are extremely sensitive to slight maladjustments in the apparatus. As an example, the data plotted in Fig. A on two samples of copper-base alloys and two samples of steel show an effect similar to that of Rostoker, though of opposite sign. The tests were made with a Tukon machine fitted with a

\* R. Girschig, *Rev. Mét.*, 1946, **43**, 95.

† L. P. Tarasov and N. W. Thibault, *Trans. Amer. Soc. Metals*, 1947, **38**, 331.

‡ Metallurgy Division, Atomic Energy Research Establishment, Harwell, Berks.



Vickers diamond. By plotting (diagonal)<sup>2</sup> against load, as in Fig. B, a family of straight lines is obtained cutting the load axis at one point. This suggests that the variation in apparent hardness with load is due to a zero error in

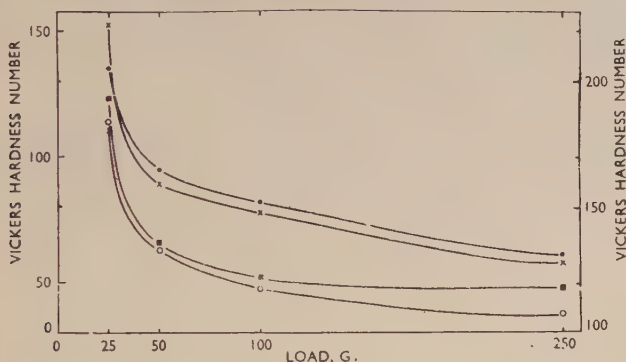


FIG. A.—Apparent Variation of Hardness with Load. Using Tukon machine with Vickers diamond.

× Copper, mechanically polished (left-hand scale).    ■ Copper, annealed (left-hand scale).  
● Mild steel, mechanically polished (right-hand scale).    ○ Mild steel, annealed (right-hand scale).

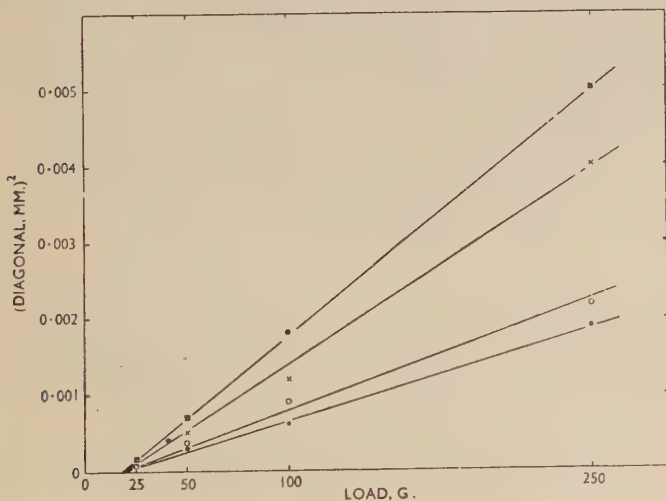


FIG. B.—Same data as Fig. A replotted.

load of about 20 g. On investigation, it was found that the full load was not being applied because of failure of the micro-switch operating the solenoid; when this was repaired, the results plotted in Fig. C showing constant hardness were obtained.

On the second point we would remark that there seems to have been no

critical examination of the exponential equation used to fit the data. Exponential equations are deservedly popular as a means of representing data, but there is a fundamental difference between an equation, which represents data, and the law the data obey. To the statistician, in fact, there is an infinity of equations which may be used to fit data, and all he can say is that one equation fits better than another.

To make this point clearer, the parameters of an equation :

$$L = a_0 + a_1d + a_2d^2$$

have been calculated for two of Rostoker's materials (copper 84% R.A. and annealed aluminium). These are plotted in Fig. D and the corresponding exponentials in Fig. E. By eye, there is little to choose between the two equations, though in fact the exponentials are slightly better on the "least squares" criterion. However, the difference is not significant and, if one

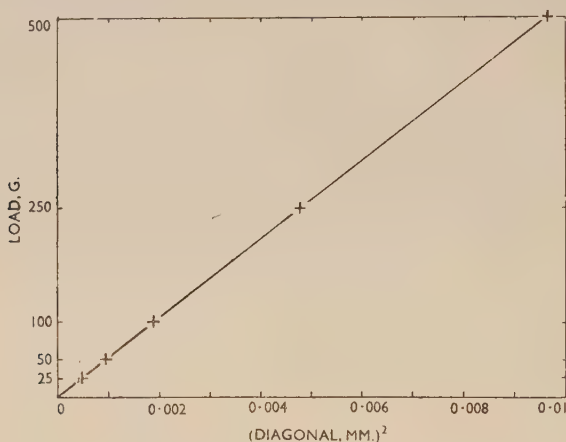


FIG. C.—Similar to Fig. B after adjustments to machine.  
Material: soft copper.

chose to use the polynomial for any reason, that decision could not be gainsaid from the data.

While we do not suggest that the power series is the correct form to use, it has various merits. First, it leads to constant hardness at high loads, which is more consistent with technical testing than Rostoker's equation, and secondly, the terms in it are capable of physical interpretation as follows :

- (i)  $a_0$  represents the zero error in loading ;
- (ii)  $a_1$  represents the net effect of terms which are linear in  $d$  (these may include "chisel tip", variation in pyramid angle with depth, "piling-up", or "sinking-in"; and
- (iii)  $a_2$  represents the hardness term.

With these considerations in mind, we suggest that the use of an exponential law for microhardness tests, which implies that the "law of similarity" does not hold, is unjustified on the data given.

There is one further point. Rostoker has mentioned a number of possible causes of his observed effects, but there is one possibility that occurs to us which has not been included. In the description of the instrument by the

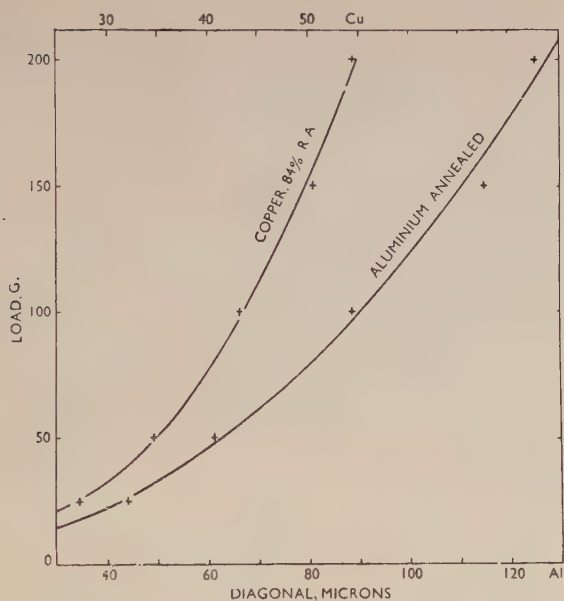


FIG. D.— $L = a_0 + a_1d + a_2d^2$ . Rostoker's data.

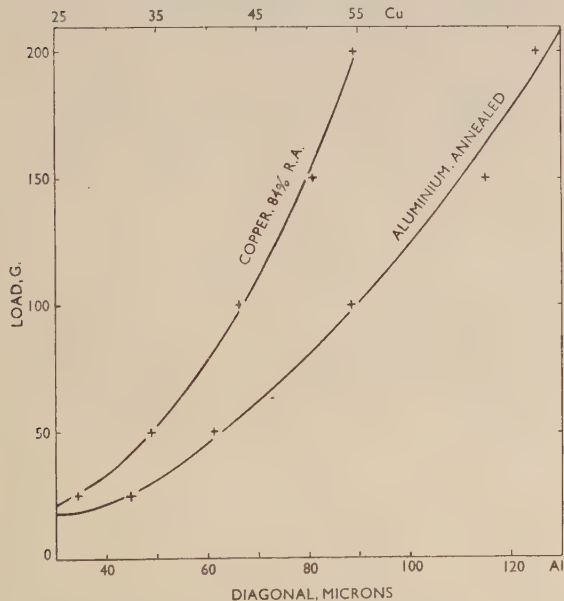


FIG. E.— $L = ad^n$ . Same data as Fig. D.

designer reference is made to an axle about which the beam pivots. We suggest that friction at this pivot should be considered, since the load on the beam varies with the applied load, and the beam does move on this pivot.

Thanks are due to the Director, A.E.R.E., for permission to publish these comments and to Miss Z. R. Craig and Mr. S. D. Ford for the calculations and experimental results, respectively.

PROFESSOR H. O'NEILL,\* D.Sc., M.Met., F.I.M. (Vice-President): The paper is useful, firstly, because it examines a cold-worked series of metals, and secondly, because it again draws attention to the non-applicability of the principle of similarity to these micro-indentations. There is no doubt that the usual macro-impressions produced at different loads by a cone or a pyramid always give a logarithmic index of 2.0 whatever the condition of the metal. The  $n$  values in Rostoker's Table I (p. 181) show that for the Bergsman system the pyramid index is seldom 2.0, and furthermore, that it *increases* to values of about 3.0 as a metal is progressively cold worked. This unexpected state of affairs has rightly surprised the author and does not appear to be explained by a recent communication from Finniston, Jones, and Madsen † suggesting that changes in (ball)  $n$  value are more a function of crystal anisotropy than of anything else.

The results in Table I for quenched and tempered eutectoid steel indicate, by analogy with the cold-worked specimens, that martensite has a lower work-hardening capacity than sorbite. I must point out that not only in the reference quoted by Dr. Rostoker, ‡ but in earlier and later work, the ball  $n$  value for martensite is shown to be higher than that for sorbite. The brittleness of martensite does not necessarily mean that it cannot be work-hardened considerably. If a ball indentation is made in a quench-hardened steel, then exploration of its surface by the Vickers test will show that the martensite has been strain-hardened appreciably. Quench-hardened razor blades can be strain-hardened in diamond dies, while martensitic surfaces can be cold worked by such treatments as the "Cloudburst" process.

If diamond-pyramid tests at normal loads between, say, 30 and 100 kg. are made on martensitic steels, then it is known that the logarithmic index is 2.0.§ The observation that the index for the Bergsman microtest on similar material is 3.34 is due either to some defect in the instrument or to the inapplicability of the rule of geometrical similarity. The latter view has been advocated for some time by German workers,|| who have variously suggested that surface friction causes trouble or that some of the indenting force is lost in making "internal surfaces". Using his own microtest, Hanemann reported  $n = 2.0$  for tetragonal martensite and 2.2–2.3 for austenite.

MR. L. E. SAMUELS, ¶ B.Met.E. (Member): At the time Dr. Rostoker's most interesting paper arrived in Australia, we had just noted the same phenomena in the microhardness testing of hand-mechanically-polished hardened steel, using a 136° diamond-pyramid indenter in a Wilson "Tukon" microhardness machine. These results, which are shown in the first line of Table B (each figure being the arithmetic mean of five determinations), provide

\* University College, Swansea.

† H. M. Finniston, E. R. W. Jones, and P. E. Madsen, *Nature*, 1949, **164**, 1128.

‡ H. O'Neill, *Proc. Inst. Mech. Eng.*, 1944, **151**, 125.

§ H. O'Neill, *Carnegie Schol. Mem., Iron Steel Inst.*, 1926, **15**, 233.

|| See F. Schultz and H. Hanemann, *Z. Metallkunde*, 1941, **33**, 124.

E. O. Bernhardt, *Z. Metallkunde*, 1941, **33**, 135.

W. Bischof and B. Wenderott, *Arch. Eisenhüttenwesen*, 1942, **15**, 497.

¶ Defence Research Laboratories, New South Wales Division, Australia.

confirmation of Dr. Rostoker's results on an entirely different type of machine. The specimen on which these results were obtained was specially selected for uniformity of hardness. At first it was thought that the effect might have resulted from a tempered surface layer produced during preliminary grinding; repeated careful checks on the preparation technique have convinced me that this is not so, and that the effect is inherent in the test, as concluded by Dr. Rostoker.

TABLE B.

Line Ref. No.		Indenting Load, g.				
		1000	500	200	150	100
1	Hardness Number : 136° Pyramid Indenter.	790	790	750	705	660
2	Hardness Number : Knoop Indenter.	750	750	790	795	800
3	Depth of Impression (136° Pyramid) : Measured Depth, $\mu$ . Decrease in Depth, %.	6.8 7	4.5 12	2.5 25	2.3 25	2.0 20
4	Hardness Number : Calculated from Depth and Diagonal of Impression.	795	795	774	724	673

Tests were made simultaneously on the same sample and under the same conditions with a Knoop diamond-pyramid indenter. These measurements show no decrease in hardness number with load, but rather the increase in apparent hardness at small loads which has often previously been reported (see line 2, Table B). Since no appreciable recovery occurs in the longer measured diagonal of the Knoop impression, the Knoop hardness number being based on the unrecovered projected area of the impression, this comparison suggests that the anomalous results with the 136° indenter are attributable to elastic recovery of the impression. The comparison also establishes that the anomalous results are not attributable either to unsatisfactory operation of the hardness machine or to unsatisfactory preparation of the surface.

An attempt was made to measure the depth of the 136° pyramid impressions by focusing with a high-aperture objective alternately on the edge and tip of the impression and reading the fine-focus micrometer of the microscope. This method is not very sensitive, but should be accurate to within at least  $\pm 0.5 \mu$ . The arithmetic mean of these measurements, together with the percentage difference between this value and the depth calculated for a 136° pyramid from the diagonal measurement, are shown in line 3 of Table B. The measured depth is, in all cases, less than the calculated, and the percentage decrease grows appreciably greater with decrease in load.

These measurements throw some light on Dr. Rostoker's suggested explanation of the anomaly, namely, that the decrease in depth of the impression during recovery is accompanied by an outward movement at the specimen surface. If we assume, first, that the recovered pyramidal area of the impression is equal to the original unrecovered pyramidal area, and, secondly, that the recovered impression is still a square-based pyramid, then, knowing the diagonal and depth of the impression, the true pyramidal recovered area can be calculated. Division of the indenting load by this area should give a corrected hardness number based on the unrecovered area of the impression. The results of such calculations are shown in line 4 of Table B.



This correction compensates for only a small fraction of the apparent decrease in hardness. Furthermore, similar calculations indicate that a decrease in depth of impression of approximately 60% would be necessary to account fully for the results obtained with a 200-g. indenting load. Even though the method of measuring the depth of impression was not very satisfactory, it is felt that it would certainly have distinguished between a 25% and a 60% decrease in depth. More convincing, similar calculations show that, even if the projected area of the recovered impression was equal to the pyramidal area of the unrecovered impression (100% recovery of the impression), the correction would not fully account for the anomalous hardness measurement with the 100-g. indenting load.

It is probable that neither of the above assumptions is strictly correct. With respect to change of pyramidal area during recovery, it should be noted that an increase in area would be necessary to explain the anomaly; such an increase would appear to be impossible. As pointed out by Dr. Rostoker, the recovered impression at small indenting loads is not a square, but shows appreciable outward bulging of the sides. Crow and Hinsley \* have developed a method of correcting for this bulging, but the correction is in the wrong direction to account for the present anomaly, i.e. a correction for bulging would further reduce the hardness number.

It would seem unlikely, therefore, that the effect is entirely, or even largely, attributable to elastic recovery of the impression. The conclusion seems inescapable that the unrecovered impression at small indenting loads is larger than would be anticipated. In this event, it would appear that the mode of penetration of the indenter changes at lower indenting loads, the change presumably being associated both with the properties of the material under test and the shape of the indenter.

The AUTHOR (*in reply*): The contributions to the discussion provide further illustration of the conflicting experiences with microhardness testers.

The results of the survey quoted by Mr. Brown are certainly not in agreement with those reported in the paper. Proper discussion, however, must await publication of a fuller account of testing conditions and instruments used.

I do not feel that the origin of the anomaly described can be attributed to inertia effects. Mr. Brown is quite correct in drawing attention to the more complicated nature of the dynamic contribution to the applied load. The balancing test is a measure only of the resistance to movement of the beam pivot. The contribution due to acceleration of the beam system is difficult to evaluate, and undoubtedly could influence the apparent hardness. However, experiments with the Bergsman instrument on the manual variation of loading velocity did not reveal any pronounced differences in apparent hardness. One further point can be made. If the logarithmic index were truly independent of the degree of strain-hardening, then inertia could certainly not be the cause of the distinct apparent dependence reported, for an inertial increment to each applied load would increase the logarithmic index by the same amount for any condition of the specimen.

The double-indentation effect reported was subsequently shown definitely to be due to slight loose alignment in the rack-and-pinion mechanism of the projection microscope. Correction of this trouble permitted satisfactory testing at any load. The arcing effect at the contact points has not been noted.

The suggestion of Messrs. Jones and Mott that a parabolic relationship exists between the applied load and the measure of the diagonal of the resultant

\* T. B. Crow and J. F. Hinsley, *J. Inst. Metals*, 1946, 72, 461.

impression is very interesting. Calculation of the three constants based on curves best fitting the data on copper are summarized in Table C.

TABLE C.

Percentage Reduction	$a_0$	$a_1$	$a_2$
0	-23.8	+ 417	20,310
14	- 4.8	- 643	54,900
40	+22.0	-2871	102,375
58	+46.5	-4300	124,000
84	+45.0	-4137	126,145

If  $a_0$  were to represent the zero error in loading, then it is to be expected that it should have approximately the same value in all equations. It is evident that this is not the case. Further, the magnitude of the suggested zero loading is far greater than is conceivable for the Bergsman instrument.

I would not conclude from these calculations that the parabolic law has been proved not to apply, but rather that the range of applied loads used does not provide a range of data wide enough to permit an accurate evaluation. In view of the above calculations, it would seem that the validity of the apparent deviation from the "law of similarity" is still an open question.

The microhardness measurements on soft copper should not be construed as evidence contrary to the results presented in the paper, for it has been amply demonstrated that a completely annealed structure does, indeed, exhibit microhardnesses which are almost independent of the applied load. The metallurgical condition of the copper-base alloys has not been given, and so no comment can be made.

In reply to Professor O'Neill, I must apologize if I seemed to imply that a martensite structure was incapable of plastic deformation. I sought only to suggest that the results of the microhardness measurements indicated that martensite was capable of considerably less plastic deformation than a sorbitic structure. Professor O'Neill has not presented evidence to the contrary. I would like to thank Professor O'Neill for drawing attention to the previous work of German investigators on this subject.

Mr. Samuels's experiences with the "Tukon" machine are very interesting. In particular, the comparison of the behaviour of the Knoop and the 136° pyramid indenter is valuable in emphasizing the influence of the indenter shape in hardness-testing phenomena.

If a  $\log P/\log d$  plot is made from the data on line 1 of Table B, it will be seen that the points really fall on two intersecting straight lines. The line joining points corresponding to the three smallest loads has a slope of 2.5-2.7. This is in quite close agreement with the results on heat-treated steels reported in the paper. The line joining the points for 1000- and 500-g. loads has the slope of 2 which normal macrohardness testing exhibits. These results give further support to the suggestion that deformation under light loads by a 136° pyramid indenter is of an unusual nature.

Mr. Samuels furnishes convincing evidence that the origin of the effects reported cannot be fully accounted for by any simple elastic-recovery mechanism.

## DISCUSSION ON THE PAPER BY MR. E. DAVIS AND MR. E. HOLMES : " THE PRESSURE- WELDING CHARACTERISTICS OF SOME COPPER-BASE ALLOYS."

(*J. Inst. Metals*, this vol., p. 185.)

DR. J. C. CHASTON,\* B.Sc., A.R.S.M., A.Inst.P., F.I.M. (Member): The phenomenon of pressure welding, which Mr. Davis and Mr. Holmes have examined so effectively by simple tests is of considerable interest in many metallurgical applications and is, of course, essentially the cause of the cohesion of metal particles in powder metallurgy operations.

The authors' conclusion that " deformation of the weld interface was the most significant variable " affecting weld strength is of special importance. This conclusion, incidentally, is supported by the results of tests carried out in America, in which it was found that welding was assisted by twisting in opposite directions two bars forced together to form a butt joint, or by forcing a conical plug into a conical cavity. These observations help to provide a better understanding of the mechanism of the operation of sheath rolling which has recently received a great deal of attention as a method of consolidating powders of such metals as titanium, chromium, or beryllium. If the normal techniques of powder metallurgy are employed, these metals are troublesome to fabricate, but it is found that if the powders are surrounded by an iron sheath they may be rolled and worked without undue difficulties. In these instances it would seem that partial welding of the particles may well be assisted by the slight rubbing of the particles together in their envelope.

Of particular interest in the paper is the strength of the welds of 93 : 7 aluminium bronze in spite of the presence, clearly revealed in the photomicrographs, of a considerable amount of oxide at the weld interface. It was at one time widely believed that sound welds could be obtained only in the complete absence of oxide or gas films. This assumption was tacitly accepted in many of the early works on powder metallurgy. It is becoming evident, however, that in many instances the presence of an oxide film is not necessarily a deterrent to adhesion by sintering or welding processes. In some systems, no doubt, the oxide is partially soluble in the basis metal, and in others it may be possible to form a firm key between oxide layers and the metal lattice. It would seem that sintering and welding in the presence of oxide films would be well worth a detailed experimental study.

MR. A. J. FIELD, † M.C., B.Sc., F.I.M. (Member): The cladding of aluminium alloys, which is a hot solid-pressure-welding process, is carried on quite extensively in industry for the production of aircraft sheets. The process involves making a sandwich of aluminium alloy with two thin plates of pure aluminium on the outer surfaces. This is then heated and passed through a rolling mill, and should weld up on the first pass. One has, therefore, in the normal cladding process, two soft covers and a hard core, and, as might be expected, in the first pass through the rolling mill the soft covers can be seen

\* Deputy Research Manager, Johnson, Matthey and Co., Ltd., Wembley, Middlesex.

† Manager, Falkirk Rolling Mills, The British Aluminium Co., Ltd.

to move over the core, owing to their being deformed to a greater extent. It appears from experience that, if there were not that relative movement, a satisfactory weld would not result. The weld has to be obtained in the first pass, or, at most, in the second pass, if it is to be complete.

It is peculiar, but true, that it is very much easier to clad a hard alloy than it is to clad pure aluminium. It has been found very difficult to clad aluminium with aluminium by the rolling process, as the rolls exert a curling effect on the metal. This is exerted on the solid metal, as on the sandwich. If the solid metal were not solid, the rolls would make it sprout out in front of the gap, but the tensile stresses in the solid block normally hold it together, and this permits rolling to take place satisfactorily. In the case of a sandwich of pure aluminium cover-plates and a pure aluminium core, there is little relative movement in rolling, and satisfactory welding is not usually obtained. The pressures are high enough, for the force exerted by a heavy rolling mill may be up to 1000 tons, and some hundred tons may be applied on a width of perhaps 48 in. and a length of 1 in., which is well in excess of the pressures quoted for the cold welding of copper.

Again, in the hot rolling of hard aluminium alloys, trouble is sometimes experienced with the cracking of the front edge of the block, which is called "crocodiling" in this country, or "alligatoring" in the U.S.A., following the fauna of the hemispheres, because the two halves of the block, originally solid, open out in front like the mouth of a crocodile. This phenomenon is referred to in a paper by Thomas and Fowler,\* and is due to the action of the force exerted by the rolls within the metal. One can roll the block back through the rolls if it crocodiles, and while it is still hot, and the two halves distort together but they will not unite.

In addition to the factor of relative movement which favours welding in the cladding process for aluminium, there is also operative, in the examples mentioned, the factor of dissimilarity of composition, which exists when pure aluminium cover-plates are satisfactorily welded to an alloy core, but not in the unsatisfactory welding of pure aluminium to pure aluminium or alloy to alloy. This may exercise an important influence, but against this conclusion is the fact that, in the case of shaft journals and their bearings, dissimilar metals have less tendency to seize or weld than similar metals. This would indicate that interfacial abrasion due to relative movement is a factor that assists the welding.

MR. R. F. TYLECOTE,† M.A., M.Sc., A.I.M. (Member): I welcome this paper particularly, since the authors have employed a technique similar to that used in work on the pressure-butt welding of light alloy bar,‡ and it therefore permits a comparison of the relative weldability of the two metals and their alloys.

It is interesting to note that extremely small deformation is required by copper as compared with aluminium for satisfactory welding, i.e. failure remote from the weld. For example, using Davis's definition of deformation, we get the following:

	Deformation, %
Aluminium-manganese alloy . . . . .	75
Deoxidized copper . . . . .	10
Aluminium alloys . . . . .	80
Copper-base alloys . . . . .	30-80

Presumably the effect of the various alloying elements on copper is connected with the type of oxide films formed. Nickel and tin apparently have

\* W. J. Thomas and W. A. Fowler, *J. Inst. Metals*, 1948-49, 75, 921.

† I.C.I. Research Fellow, Royal School of Mines, London.

‡ R. F. Tylecote, *Weld. Research* (in *Trans. Inst. Weld.*), 1949, 3, (1), 28.



the least effect on weldability, while, as might be expected, zinc, silicon, and aluminium exercise the greatest influence.

I notice that in the opinion of the authors good welds were not obtained until recrystallization across the interface had occurred. It would be interesting to know whether the recrystallization process itself is responsible for the elimination of the interface, or whether this elimination occurs only when the temperature is high enough for a large proportion of the residual oxide to be dispersed by diffusion during the welding period.

Work on light alloy welds made at room temperature shows that it is almost impossible to get grain growth across the interface by annealing at any temperature after welding (see Fig. A, Plate LXXXIII). In the case of similar welds in copper and steel grain growth across the interface is readily obtainable (see Fig. B, Plate LXXXIII). This suggests that the reason for the difference in behaviour is due to oxide solubility and not recrystallization *per se*. The authors' results on aluminium bronze show the difficulty of eliminating an interface containing an alumina film.

This leads to another point. Is the elimination of an interface by recrystallization and oxide solution (where possible) absolutely necessary for a satisfactory weld? Davis's results show that an ultimate tensile stress of 27.2 tons/in.<sup>2</sup> and 36% elongation can be obtained in aluminium bronze, presumably without the elimination of the interface. The same applies to aluminium and its alloys, and also to many other metals welded at room temperature.

The authors found that an emiered surface was better than a pickled surface on the high-strength bronzes. The superiority of a mechanically roughened surface is in line with my own work on aluminium and other metals, where a scratch-brushed surface proved the best. This is probably due to the high pressure intensity produced where the asperities meet, and which results in the break-up of oxide films and metal/metal contact.

Whitehead,\* in work on friction, has put forward a possible explanation why a greater deformation is required to weld copper at room temperature than to weld aluminium. This is based on the relative hardness of oxide and metal. The hardness of alumina is about 4 times that of aluminium (Mohs' scale), whereas the hardness of copper oxide is of the same order as that of copper. Whitehead suggests that during the deformation of aluminium, the underlying metal readily deforms, leading to the cracking of the brittle alumina film on the surface and its intermingling with the metal. On the other hand, copper and copper oxide deform together, thus preventing metal/metal contact until a much higher degree of deformation has been attained than in the case of aluminium.

At higher temperatures the relative position of copper and aluminium seems to be reversed and it is suggested that the picture may be rather different. Work carried out at the B.N.F.M.R.A.† shows that at high temperatures the oxide film on copper becomes quite soft and ductile. It would be expected that under high pressures this film would be readily squeezed away from the points of contact. For example at 700° C. copper oxide has a tensile strength of about 1 ton/in.<sup>2</sup> and an elongation of 20%, and according to Davis and Holmes pressures of the order of 1—2.5 tons/in.<sup>2</sup> are required for welding deoxidized copper at this temperature.

DR. A. LATIN ‡ (Member): The energy required to form a pressure weld is, say,  $W$ , expressed in the usual way of work per unit volume (in this case per unit volume of the metal actually undergoing the deformation and welding

\* J. R. Whitehead, *Proc. Roy. Soc.*, 1950, [A], 201, 109.

† R. F. Tylecote, *J. Inst. Metals*, 1950–51, 78, 301.

‡ British Insulated Callender's Cables, Ltd., London.



process). Is  $W$  simply given by the sum of two terms, one expressing the work required for plastic deformation and the other frictional losses (both internal and external) incurred? Or should a third term expressing the true welding energy be added, in which case  $W = W_p + W_f + W_1$  ( $W_p$  and  $W_f$  being the plastic deformation and frictional losses, respectively, and  $W_1$  the welding energy). The two first terms then represent energy loss and the aim in practice is to obtain maximum (or optimum) efficiency (measured by  $W_1/W$ ) which corresponds to maximum strength with minimum deformation.

I suggest further that the term  $W_1$  is itself made up of three terms; one of these expresses the energy required to overcome the effect of the asperities mentioned by Mr. Tylecote and bring the two surfaces into point-to-point contact, and the second expresses the energy required to displace the oxide or other interfering film. The final term is one which expresses the surface-energy charge during the process and which is negative.

DR. V. A. PHILLIPS,\* A.R.S.M., L.I.M. (Junior Member): The term "pressure welding" might be considered to include any welding process brought about by pressure and heat, where actual melting of an appreciable portion of the metal does not occur. The terms "pressure" and "heat" would be regarded in the broadest sense; thus the welding together of lead under its own weight at room temperature and even, hypothetically, the welding of mercury at temperatures below its melting point would be included. Unlike the authors I would include the manufacture of wrought iron in the smithy. It is surprising that no mention is made in the introduction of the manufacture of Alclad and other clad materials which provide a very important commercial example of the phenomenon.

I feel that the authors have somewhat inevitably had to choose between trying on the one hand to produce a sound pressure weld and, on the other hand, to evaluate by an arbitrary procedure the pressure-weldability of different materials. There seems to be no fundamental reason why any of the materials investigated should not be satisfactorily welded if the right conditions and techniques are found. Nevertheless the authors are to be congratulated on the valuable data which they have made available.

In order to facilitate welding it would seem desirable to localize deformation at the interface as far as possible, for then films on the surfaces will be most effectively removed, recrystallization will be encouraged where it is wanted, and metal wastage will be reduced. In the technique used this is to some extent achieved by playing the ring of heating flames on the line circumference. I would like to ask the authors whether they found that the higher thermal conductivity of the pure copper led to a significantly greater temperature gradient, which might partially account for its ease of welding? If so, then a further improvement might be obtained by tapering the test-pieces to reduce the volume of metal near the interface. It might be possible with tapered test-pieces to use ohmic heating, passing a high current directly through them. Would not the beneficial action of a suitable flux outweigh the disadvantage of occasional residual inclusions? It would be interesting to see whether the welding of the hard copper-base alloys could be more easily accomplished if a thin layer of pure copper was inserted at the interface.

The AUTHORS (*in reply*): We agree with those contributors to the discussion who state that relative movement of the interface during pressure welding assists joint formation. The importance of interface movement has been demonstrated recently by Cooke and Levy,<sup>†</sup> who succeeded in making

\* British Non-Ferrous Metals Research Association, London.

† V. W. Cooke and A. Levy, *J. Metals*, 1949, 1, (11), 28.

pressure welds between aluminium alloys and stainless steel by rotating the former in contact with the stainless steel under pressure at elevated temperatures. Pressure welding of dissimilar materials varying widely in response to deformation under load at a given temperature was impracticable under the conditions which we used, owing to lack of movement at the interface, the least deformable material merely penetrating under the welding load into the softer alloy.

Although under the conditions defined in the paper the strongest joints were those in which complete recrystallization had occurred, we would not suggest that such a mechanism was essential. Strong pressure welds could be made with aluminium alloys at room temperature, and between dissimilar copper-base alloys at elevated temperatures, and in neither case would recrystallization occur across the interface. As pointed out by Mr. Tylecote oxide films interfere with recrystallization without necessarily lowering the joint strength, and in this connection we note with interest his views on the effect of the strength of the oxide film on the relative ease of welding by pressure aluminium and copper at room and elevated temperatures.

Dr. Phillips has erred in suggesting that the higher thermal conductivity of copper as compared with those of its alloys would lead to a significantly greater temperature gradient in the former instance, for surely the reverse is the case. Interposing a thin film of copper between copper-base alloys does in some instances facilitate pressure welding, but unless the film is very thin joint strength is more nearly that of the copper than that of the alloy employed.

Finally, we are grateful to those contributors who have pointed out an obvious omission in the applications of pressure welding detailed in the introduction, namely the production of clad metals of many types.

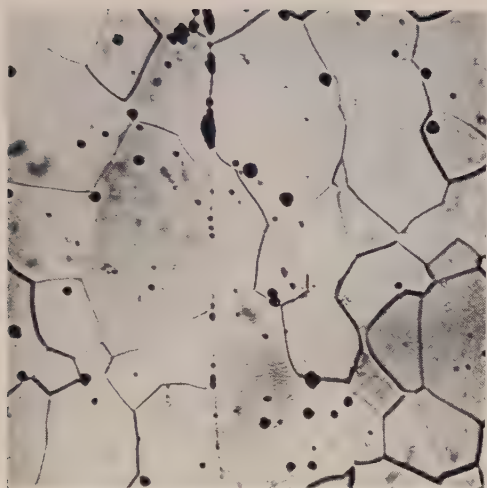


FIG. A.—Weld in 99.5% Aluminium, made at room temperature with 70% deformation and heat-treated at 450° C. for  $\frac{1}{2}$  hr.  $\times 220$ .

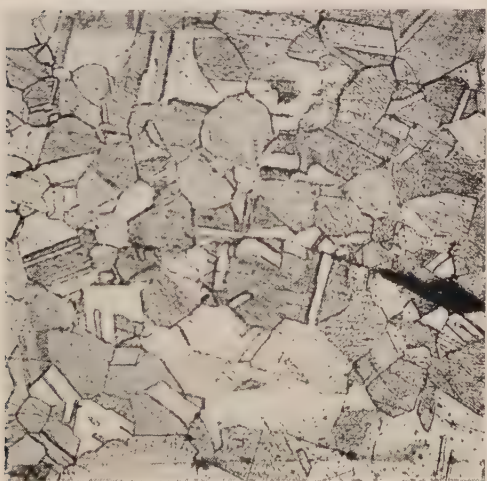


FIG. B.—Weld in Deoxidized Copper, made at room temperature with 70% deformation and annealed at 700° C. for  $\frac{1}{2}$  hr.  $\times 220$ .



JOINT DISCUSSION ON THE PAPERS BY MR. E. C. W. PERRYMAN AND MR. S. E. HADDEN: "STRESS-CORROSION OF ALUMINIUM-7% MAGNESIUM ALLOY"; BY DR. P. T. GILBERT AND MR. S. E. HADDEN: "A THEORY OF THE MECHANISM OF STRESS-CORROSION IN ALUMINIUM-7% MAGNESIUM ALLOY"; AND BY MR. E. C. W. PERRYMAN AND MR. J. C. BLADE: "RELATIONSHIP BETWEEN THE AGEING AND STRESS-CORROSION PROPERTIES OF ALUMINIUM-ZINC ALLOYS."

(*J. Inst. Metals*, this vol., pp. 207, 237, 263.)

DR. U. R. EVANS,\* F.R.S. (Member): Corrosion damage may be divided into four groups of increasing virulence. First, we have uniform corrosion, which is relatively harmless. Next, we have pitting, which (for an equal destruction of material) produces more damage, since it can lead to premature perforation, although probably not to great mechanical weakening. Thirdly, if there is a specially sensitive material present along the grain boundaries as a result of unfortunate heat-treatment, there may be mechanical weakening, although if the whole of the grain boundaries are attacked—irrespective of direction—the loss of strength will be relatively slow. If, however, tensile stress is applied during the corrosive action, so that the attack is concentrated on a limited number of grain boundaries—namely, those which provide paths roughly at right angles to the stress direction—the loss of strength may occur much more rapidly. This is the fourth, and most dangerous, type of attack.

There is reason to think that cracking will often progress more quickly along paths which run roughly at right angles to the general stress direction than along potential paths leading in other directions. For along such a path, if a bridge of chemical-resistant material (joining two grains) should hold up the advance of the intergranular attack, the stress may rupture the bridge so that advance will begin again; conversely, if a mechanically strong bridge is encountered, the chemical action should destroy it. Provided that the mechanically strong bridges and the chemically strong bridges are not identical, the probability of a permanent hold-up will be negligible (the product of two small quantities is very small). The experimental results reported in the papers under discussion provide evidence of the two types of hold-up; the mechanical hold-ups are shown by jerks in the extension curves, and the chemical hold-ups by jerks in the potential curves. If the two types are uncorrelated, intergranular attack with simultaneous application of stress will cause cracking to progress faster than when intergranular attack and stress are applied one

\* Reader in the Science of Metallic Corrosion, Cambridge University.



at a time. But if the types are correlated, or if (in the extreme case) the two sorts of bridges are identical, then stress-corrosion (as defined in the papers) will be less serious, or possibly even absent. This may explain why some materials which suffer intergranular attack are not seriously prone to stress-corrosion.

MR. A. J. FIELD,\* M.C., B.Sc., F.I.M. (Member): Messrs. Perryman and Blade have dealt with the series of binary aluminium-zinc alloys which, though not used in industry at the present time on account of their moderate strength, are of considerable scientific interest and may assume a more direct commercial importance. The authors are to be congratulated on the observations which they have made and on the clarity of their photographs, but it may be thought that they had been unduly exercised to align their findings and observations with previous published work. Their findings with regard to the binary aluminium-zinc system should not be connected out-of-hand with aluminium-magnesium-zinc alloys, as the authors indicate in the paper. Complex aluminium alloys containing smaller quantities of zinc (5-6%) are now becoming very important commercially as being those of highest strength, and it would not seem that the authors' conclusions would be applicable to them, as these alloys have demonstrated their reliability in service.

In this connection, reference may be made to the production in the 1920s of some of the higher-zinc aluminium-zinc alloys in wrought form, similar in composition to the old German or L5 alloys, which at one time were widely used industrially in the form of extruded rods, possessing very good machining properties though they were not free machining. It was found that when these rods were supplied in the extruded and cold-drawn condition, in some cases they developed what in earlier days was called season-cracking. The alloy in question was not a binary zinc alloy, but contained 10-13% zinc and 2½% copper, the latter being essential to provide adequate strength. There seemed to be a line of demarcation in the zinc content at about 11%, for cracks appeared only in alloys containing above that percentage. The old 3% copper, 20% zinc alloy, which was similarly supplied on occasion, has also been known to develop season-cracks.

Exception is taken to the expression "hydrostatic tension", used in the paper in explaining the mechanism of fracture, as being a contradiction in terms. "Hydro" connotes a liquid of low viscosity, which is not here in question, and such a fluid is not capable of transmitting tensile stress but could only transmit pressure. Moreover, "static" is not compatible with the idea of slip involved before fracture, which implies motion.

Another case where too hasty an analogy seems to have been drawn with previous work is the comparison of the plunging of cold steel into water, with a resultant loss of strength, with what happens to the aluminium-zinc alloy when exposed to moist air. I do not think that that is a fair comparison. Moreover, the authors' reference to the precipitation of zinc from this system can hardly be valid from consideration of the equilibrium diagram.

In conclusion, it may be emphasized that zinc is itself rather a peculiar metal, and its use presents many complications. It is opportune to recall that, about 1930, Committee B-6 of the American Society for Testing Materials did a great deal of work on die-cast alloys, including zinc alloys, and it was then that the necessity was first recognized of employing 99.99% zinc in die-castings, if dimensional growth was to be avoided. The present authors have avoided that pitfall by using zinc of the required purity, as well as 99.99% aluminium.

\* Manager, Falkirk Rolling Mills, The British Aluminium Co., Ltd.

DR. H. K. HARDY,\* M.Sc., A.R.S.M., A.I.M. (Member): Although I do not intend to discuss the stress-corrosion side of this series of papers it is, perhaps, not inappropriate to consider some details of the ageing mechanisms, since these largely control the stress-corrosion behaviour.

Fig. 5 (p. 217) of Perryman and Hadden's paper gives the ageing times at different temperatures to cause equal degrees of stress-corrosion susceptibility. Thus, it is probably essentially similar to graphs for time/temperature relationships to other points on the ageing curves such as peak hardness, incubation period, &c. Unfortunately, the experimental points plotted in Fig. 5 cover only the range of ageing temperatures between 80° and 160° C., and I would like to ask the authors whether they are in a position to extend this up to the solubility curve at 325° C. Comparison with Fig. 4 (p. 215), which I assume also covers material stretched 10%, strongly suggests that the time/temperature/transformation or reciprocal-rate curve may well consist of two interpenetrating C-curves. This is shown in Fig. A, in which I have inverted the

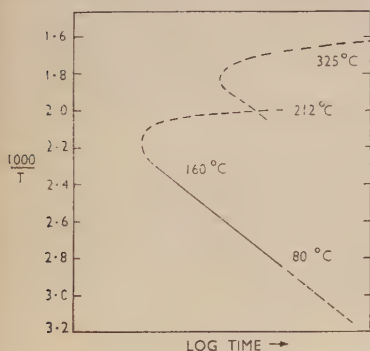


FIG. A.—Time/Temperature Relationships for a Constant Stress-Corrosion Life of Aluminium-7% Magnesium Alloy Commercially Annealed and Stretched 10% Before Ageing. (Hardy.)

Full line from Fig. 5 (p. 217 of paper by Perryman and Hadden).

Dotted line covers extensions suggested by the stress-corrosion life/temperature relationship of Fig. 4 (p. 215).

authors' Fig. 5 to allow for easier comparison with Fig. 4. If the authors are able to confirm that the reciprocal-rate curve has this shape over the full temperature range, it very strongly suggests that two distinct methods of decomposition occur, corresponding to each of the C-curves which I have drawn. One of these may involve recrystallization due to the cold working. The growing divergence from the straight-line part of the curve is due to an additional activation energy which increases as the temperature is raised.†‡ I shall be much interested to learn how the intersection point at 212° C. is influenced by cold work before ageing, as recrystallization may be introduced by long ageing times. The authors have found that small additions of zinc shifted the lower C-curve to longer ageing times, and I should like to know whether the upper C-curve has been affected. Complete proof that two distinct methods of decomposition have occurred would be obtained if similar reciprocal-rate curves were given by plotting the times to other stages of the decomposition process, such as maximum hardness. I have applied this method of analysis to ageing curves of aluminium-copper alloys in a paper now in the press.‡

The authors have referred to the work of Robertson § on the stress-corro-

\* Head of the Physical Metallurgy Section, Fulmer Research Institute, Stoke Poges, Bucks.

† H. K. Hardy, *J. Inst. Metals*, this vol., p. 457.

‡ H. K. Hardy, *J. Inst. Metals*, 1951, 79, in the press.

§ W. D. Robertson, *Trans. Amer. Inst. Min. Met. Eng.*, 1946, 166, 216.

sion of 24S alloy (copper 4.5%, magnesium 1.5%), but I am unable to agree with their deduction that no correlation existed between the stress-corrosion susceptibility and the ageing curve; Robertson found that the maximum susceptibility occurred at the beginning of the rise in strength. Very similar results have been reported by Logan, Hessing, and Francis.\* The explanation for this system is that precipitation takes place first in the grain boundaries, and maximum susceptibility to stress-corrosion occurs when there is a maximum difference in potential between the anodic film of copper-poor material immediately adjacent to the grain boundaries and the undecomposed grain centres, to give a maximum current density. Conditions are, of course, different in the aluminium-magnesium alloy, in which the precipitate represents the anodic phase.

I do not feel completely satisfied about the interpretation given by Perryman and Blade for the ageing curves of aluminium-zinc alloys. Guinier † has shown that the first stage in the ageing process at room temperature in alloys with a high degree of supersaturation is the formation of spherical clusters of solute atoms, the so-called Guinier-Preston zones, for this system. These segregates can be accounted for, ‡ since the system probably possesses free-

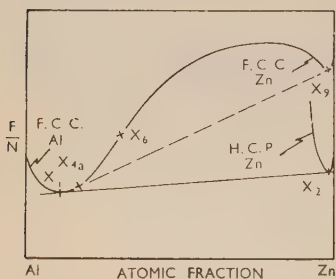


FIG. B.—Hypothetical Free-Energy/Composition Curves for Aluminium-Zinc Alloys at Room Temperature. (Hardy.)

Alloys quenched to the right of  $x_{2a}$  would show segregation within the solid solution, although an activation energy would be required initially for alloys between  $x_{2a}$  and  $x_2$  (the inflection point on the curve).

Alloys quenched to supersaturations between  $x_1$  and  $x_{2a}$  would decompose by precipitation without forming segregates. (Hardy, *J. Inst. Metals*, this vol, p. 457 and 1951, 79, in the press.)

energy relationships essentially similar to those shown in Fig. B. According to Borelius and Larsson,§ the minimum at  $x_2$  should be closer to 60 at.-% zinc. It seems very reasonable to associate the initial rise in hardness with the Guinier-Preston zones, of free energy and composition such as  $x_2$ , rather than with the formation of platelets as quoted by the authors. The softening on ageing at elevated temperatures is probably due to reversion, and the second rise in hardness is due to the formation of platelets. According to Geisler, Barrett, and Mehl ¶ these will at first be coherent with the matrix.

I have shown very recently, by a theoretical approach, ‡ that the first-formed Guinier-Preston zones will be forced to redissolve in the immediate neighbourhood of the particles of the next, more stable, decomposition product. The change in etching characteristics due to this re-solution of the Guinier-Preston zones could well account for the "light phenomenon", both in this system and in aluminium-copper alloys.\*\* This change will occur first at the

\* H. L. Logan, H. Hessing, and H. E. Francis, *J. Research Nat. Bur. Stand.*, 1947, **38**, 465.

† A. Guinier, *Métaux, Corrosion, Usure*, 1943, **18**, 209; *Bull. Lab. d'Essais*, 1947, No. 23.

‡ H. K. Hardy, *J. Inst. Metals*, this vol., p. 457.

§ G. Borelius and L. E. Larsson, *Arkiv Mat., Astron. Fysik*, 1948, [A], **35**, (13).

¶ A. H. Geisler, C. S. Barrett, and R. F. Mehl, *Trans. Amer. Inst. Min. Met. Eng.*, 1943, 152, 201.

\*\* M. L. V. Gayler, *J. Inst. Metals*, 1946, **72**, 243.

grain boundaries, and the authors' very clear demonstration of the light phenomenon in aluminium-zinc alloys is in pleasing agreement with the theoretical work, if we accept the validity of the Guinier-Preston zones in this system. The light phenomenon does not occur where the degree of supersaturation is low; the aluminium-13% zinc alloy showed the effect on ageing at 125° C., whereas the aluminium-10% zinc alloy did not. Presumably any Guinier-Preston zones formed in the latter alloy at room temperature were completely redissolved by reversion before the platelets were formed.

It is this re-solution effect which probably accounts for the lattice-parameter effects characterizing discontinuous precipitation.\* This does not require recrystallization, but, as I have indicated earlier,† it will be facilitated when the lattice strain is sufficiently great to lead to recrystallization.

Finally, I would like to congratulate the authors of these papers. They are a veritable mine of information and greatly repay a close study.

MR. P. F. THOMPSON ‡: The authors are to be congratulated on their efforts to correlate the applications of stresses and corrosion phenomena. Often in the past much work has been put into the mechanical aspects of the matter and but little into the fundamentals of the corrosion processes associated therewith. The authors have endeavoured to fill the hiatus, but unfortunately they seem to have retained some of those older ideas on corrosion which have been a hindrance to the proper appreciation of its electrochemical nature.

The use of the salt spray as a "corrosive agent" is not entirely satisfactory. However carefully determined the mechanical and metallographical factors may be, no study of the combined effects of stress and corrosion can be of real value when the vital electrochemical factors of the electrolyte are so disordered and ill-defined as in the application of the salt spray, particularly under variable conditions of humidity. Apart from the effects of the chloride ion *per se*, the important potential differences due to differential aeration cannot be scientifically assessed during such a haphazard application.

Again, sodium chloride or any neutral non-oxidizing salt cannot be regarded as a "corrosive agent" in the sense that the authors appear to use it. The idea that any reagent "attacks" a metal is fundamentally wrong. The term "attack" is a colloquialism or a piece of jargon suitable for the man in the street, but it has little meaning for those who fully appreciate the true mechanism of the corrosion cell. Sodium chloride—or more exactly the chloride ion—has no oxidizing properties; it therefore cannot function at the cathode of a cell as a cathogen or agent which raises the positive potential of this electrode sufficiently to ionize the metal at the anode. At the anode the chloride ion may form negatively-charged complex ions of the type  $(M(Cl)_4)^{-}$  and if these are sufficiently stable two concomitant processes are possible: (1) dissolution of the solid corrosion products or films resulting therefrom, if the solubility product of the compounds permits; (2) slightly accelerated corrosion due to the depression of the positive potential of the metal caused by the disappearance of the metal ions into the complex. These effects, however, must await anodic-ion emission which remains at a standstill unless a cathodic process is functioning elsewhere.

Apart from the above and an increase in conductivity of the liquid which is of little moment when the anodic and cathodic distances are small, a neutral salt such as sodium chloride cannot play any notable part in the corrosion cell.

In a heterophase alloy, however, oxide layers on the surface and possibly

\* H. K. Hardy, *J. Inst. Metals*, 1951, **79**, in the press.

† H. K. Hardy, *J. Inst. Metals*, 1948-49, **75**, 707.

‡ Senior Research Officer in Corrosion, Aeronautical Research Laboratories, Department of Supply, Melbourne, Australia.



around grains may be dissolved by sodium chloride solutions, thus allowing access to phases previously shielded from the electrolyte.

No such dissolution of aluminium hydroxide takes place and that of magnesium hydroxide is probably very small. I have shown that a marked reduction of potential occurs on copper, zinc, and their alloys when immersed in 3% sodium chloride solution and a still greater reduction in saturated salt solution. This indicates that if oxides or hydroxides of these metals were present, they would be dissolved and fissures opened so that corrosion by differential aeration would be promoted. Such oxide layers would become more accessible under stress and, even if complex ion dissolution did not take place, the more or less porous mass would absorb the electrolyte and set up the differential aeration required for the oxygen-ionization type of corrosion.

In this connection it is not necessarily the more electronegative phase which becomes the anode, but the surface which happens to be in contact with that part of the electrolyte which has the lowest oxidation potential, normally the least aerated. I have shown elsewhere that even a platinum electrode in fully de-aerated water can be more negative (anodic) than a fully filmed and aerated aluminium micro-electrode in the same liquid.

From the mechanical point of view the authors have emphasized the concentration of stresses at the bottom of a cavity, but they do not seem to have made clear that there must also be a considerable concentration of electrical energy or current density at the bottom of a de-aerated cavity. The number of coulombs poured into a microscopical area from the very large cathodic surface of the test-pieces used and exposed to the liquid thoroughly aerated must be very considerable. A rough calculation will show that oxygen diffusion to cathodes of the size of the test-pieces used would corrode about 4 mm.<sup>3</sup>/day of magnesium on a fully de-aerated anode.

In the case of aluminium the corrosion rate in fissures is such that the corrosion products are extruded in long filaments and often hydrogen bubbles make their appearance, each bubble depositing the hydroxide in a crater-like pustule. Once this process is initiated, it may go on indefinitely, with the bubbles rising at the rate of about one a minute with great regularity. Though a breaking or bending stress increases the hydrogen evolution, such a stress does not seem necessary for its initiation. If the cavity is opened up to the aerated liquid, hydrogen evolution ceases; hence it may be taken that oxygen initiates or inhibits hydrogen evolution, depending on the point of application.

In the case of magnesium a relatively clean surface under tap-water sets up hydrogen evolution at appropriate points of low overpotential, without any scratching of the film being necessary. Again, magnesium or high-magnesium-aluminium phases would not require much if any stress to set the hydrogen-evolution type of corrosion going.

I have suggested elsewhere the possibility that compounds of the "spinel" type may form tougher and more protective films than those produced from the single hydroxides. If this is the case for aluminium-magnesium and aluminium-zinc hydroxides, certain alloy compositions may be critical in this respect, so that the corrosion products can form films which have the maximum resilience and resistance to fracture under the various forms of stress.

The determinations of potential as made by Messrs. Gilbert and Hadden are subject to some comment. The use of large electrodes for the determination of the electrolytic potential of a metal or alloy is rarely satisfactory. I have never obtained reasonable results without the use of a uniplanar electrode of so small an area that differential effects in the solution and on the metal are reduced to a minimum.

It seems clear that the potential values of  $-1.3$  to  $-1.4$  V. obtained by



these authors for unprepared surfaces are a resultant of many potentials, mostly due to differential aeration. When cavities are opened up to some extent by electropolishing or pickling, aeration must become more uniform, and thus the less negative value of  $-1.0$  to  $-0.8$  V. is obtained. This, however, seems somewhat positive for a non-oxidizing solution said to be de-aerated. I suspect that the method of de-aeration practised by the authors is not effective. Evacuation over the surface and "saturation" with nitrogen of doubtful freedom from oxygen is not enough. I have found that commercial nitrogen is not to be trusted, so I always use a purifying train to ensure complete removal of oxygen. Since the change of its potential is proportional to the log of the 4th root of its partial pressure, a very small amount of oxygen still has a marked oxidizing potential; hence the necessity for scrupulous care in its removal. With purified nitrogen it takes about 3 hours' steady passage of the gas at room temperature to effect practically complete de-aeration of about 50 ml. of water. Conversely, it takes a considerable time to saturate the liquid again by the passage of air.

No electrochemical experiments on aeration and de-aeration are trustworthy unless an inert micro-electrode of platinum or gold is used in the liquid as a check. A minus value of  $0.50$ – $0.55$  V. on the saturated calomel scale in a non-oxidizing or non-reducing neutral solution is sufficiently indicative of complete de-aeration, and about  $+0.00$  to  $+0.10$  V. on the same scale may be taken as representing complete aeration from the atmosphere. Raising the temperature over about  $80^{\circ}\text{C}$ . with the passage of pure nitrogen de-aerates a liquid much more rapidly, and this provides a useful technique, since the intrinsic potential of the electrode varies but little with rise of temperature.

In Perryman and Blade's paper, again, the possibility of oxide films occurring at grain boundaries does not appear to have been taken into account. The effects of sodium chloride on the life of the specimen as found by these authors is quite consistent with the complex-ion-forming properties of zinc hydroxide or oxide. Further, the possibility of oxide formation actually during the heat-treatment, in conjunction with the separation of the zinc-rich phase, should not be overlooked.

Another matter open to criticism is the use of such substances as dichromated lanolin, which is presumably an emulsion of dichromate solution and *adeps llanæ* or wool grease. Owing to the high oxidizing potential of the dichromate, the potential of a test-piece partly covered with this preparation would be much higher than normal, and any conclusions drawn from it would be fallacious.

I have drawn up a chart summarizing the work done on aluminium in Melbourne in respect of hydrogen evolution and its limits imposed by aeration and over-potential.\*

Despite any deficiencies in their electrochemical technique, the authors have undoubtedly made a notable contribution to the metallographical side of the subject.

The AUTHORS (*in reply*): We are in general agreement with the ideas put forward by Dr. U. R. Evans, but we feel that the detailed interpretation of such generalizations may vary from case to case. Thus, for aluminium-7% magnesium alloy with  $\beta$  at the grain boundaries, there is evidence that although various parts of the grain boundary differ in their susceptibility to corrosion in salt solution, every part is to some extent susceptible. Likewise, every part of the grain boundary has some limit of mechanical strength. We have endeavoured to emphasize that the rate of corrosion of a given element in a

\* P. F. Thompson, *Australian Council for Aeronautics, Rep. No. ACA24, 1946.*

crevice is dependent not only on its composition and metallurgical structure, e.g. whether it consists of  $\beta$  phase or is a solid-solution "bridge", but also on other factors such as composition and pH of the electrolyte in contact with the element, the nature of the film, if any, on it, accessibility of oxygen, &c. Similarly, whether or not the element will fail mechanically will depend on local circumstances such as depth of crevice, radius of curvature at the base, orientation of crevice with respect to the direction of stress, &c., as well as on the mechanical properties of the material at the point in question. It is the essence of the theory of stress-corrosion of aluminium-7% magnesium alloy put forward, that both the corrosive conditions and the local stress distributions are continually changing, so that the rate of penetration varies even though the composition of the grain-boundary material is constant throughout. If the nature of this material changes, other considerations are involved. Thus, consider a stress-corrosion crevice which is temporarily halted at a solid-solution bridge. This bridge is for the moment relatively both mechanically and chemically resistant. Eventually it will fail either because it is corroded away, even though at a rate much slower than that at which the  $\beta$  phase corrodes, or because it becomes unable to resist the local stresses, which may be augmented and redistributed owing to the progress of corrosion along the  $\beta$  phase at other parts of the grain boundary. On the other hand, it is conceivable that the bridge might delay the advancement of the crevice for such a long time that another crevice would catch up and pass the original one, and become the crevice which eventually leads to failure. It therefore appears that the presence of a small number of bridges, very resistant to both chemical and mechanical failure, would not necessarily prevent stress-corrosion.

In connection with Dr. Evans's reference to material susceptible to intercrystalline corrosion but not to stress-corrosion, we have recently observed an outstanding example. If aluminium-7% magnesium alloy aged for 24 hr. at 125° C. after solution-treating and overstraining 10%, i.e. with more or less continuous grain-boundary films of  $\beta$  phase, is immersed in 5% phosphoric acid, attack at the grain boundaries occurs uniformly all over the surface; in due course the individual grains fall out, and eventually most of the piece is converted to a heap of crystals which themselves are attacked only very slowly in the acid. If a stressed loop is immersed in the acid *exactly the same thing happens* and no other corrosion cracking occurs. It is our view that when intercrystalline attack occurs in phosphoric acid the conditions in the crevices which lead to a diminution—or even cessation—of attack on the  $\beta$  phase are established much more quickly than in, say, hydrochloric acid, owing no doubt, to the different effects of phosphate and chloride ions at the anode. The result is that one crevice never advances sufficiently beyond the others for the stress concentration to exceed the value required to cause mechanical breakdown. Stress-corrosion thus never begins, and attack proceeds only when crystals fall away and allow access of more strong acid to the base of the crevices.

With reference to Mr. Field's objection to the term "hydrostatic tension", we consider its use is legitimate because it is the generally accepted term for describing a state of uniform triaxial tension, i.e. a state where no shear forces are present. As shown on p. 278 of Perryman and Blade's paper, such is the state of affairs at the grain boundaries perpendicular to the applied stress in the aluminium-zinc alloys.

Benedicks's work on the effect of liquids on the tensile strength of metals was referred to because this effect may well be playing a part in the mechanism of failure in the aluminium-zinc alloys. It is known that when sustained tensile tests are carried out on glass, the failure time for a given stress is much longer in vacuum than in moist air. As shown in Table VI (p. 276) of Perryman and Blade's paper, moisture has a pronounced effect on the failure time,

and it is possible that this is not a corrosion effect but an effect similar to that for glass described above.

Although the equilibrium phase precipitated in the aluminium-zinc system is a zinc-rich solid solution containing up to 0.4% aluminium, the small pits seen together with the light phase during ageing cannot represent the equilibrium zinc-rich precipitate, for the reasons given on p. 268 of the paper. It was therefore inferred that they were zinc-rich zones of an unknown composition coherent with the aluminium lattice. We have nowhere suggested that precipitation of zinc occurs during the ageing of these alloys. We are surprised at Mr. Field's suggestion that we connect "out-of-hand" the aluminium-zinc alloys with the commercially-used aluminium-magnesium-zinc alloys, for Perryman and Hadden were careful to refrain from suggesting that there is necessarily similarity in the behaviour of these two types of alloys.

With reference to Dr. Hardy's remarks, we do not agree that Fig. 5 in the paper by Perryman and Hadden is similar to curves obtained from hardness measurements, &c. Whereas hardness values give a measure of the properties of the material as a whole, i.e. grains and grain boundaries, the stress-corrosion susceptibility, for a wide range of ageing temperatures, appears to be governed by the continuity of second phase at the grain boundaries, and as shown in the paper, when a continuous grain-boundary network of  $\beta$  phase had been formed, further precipitate within the grains did not significantly affect the stress-corrosion life. Therefore, as pointed out by Perryman and Hadden, each line in their Fig. 5 represents an equivalent state in the precipitation process at the grain boundary. At higher ageing temperatures than those used to obtain the lines in Fig. 5, however, the stress-corrosion life is no longer correlated directly with the observed continuity of  $\beta$  at the grain boundary, and the interpretation of the extension of these lines is therefore more complex. Using stress-corrosion results for ageing temperatures up to 240° C., we can obtain graphs of  $1/T$  against ageing time apparently consisting of one *C*-curve and half another, intersecting at about 210° C. The data available, however, are really too scanty for this to be put forward with assurance, and it is not possible to decide, for instance, whether the temperature of intersection is independent of stress-corrosion life, as it should be if Dr. Hardy is correct in his suggestion that the two *C*-curves indicate two different methods of decomposition. We are unable to give any further information on the effect of cold work on the intersection of the two *C*-curves.

Dr. Hardy says we found that small additions of zinc shifted the lower *C*-curve to longer ageing times. Actually, insufficient results were obtained on these zinc-bearing alloys to establish the presence of a *C*-curve, although it is probable that such a curve would be found and that it would be displaced to longer ageing times. We cannot say, however, how any upper *C*-curve might be affected by the zinc additions.

Regarding the correlation between the stress-corrosion susceptibility and the ageing curve, it is unfortunate that the statement on p. 230 of the paper by Perryman and Hadden is badly worded. What is meant is that maximum stress-corrosion susceptibility does not occur at maximum hardness, which accords with Robertson's results for aluminium-4.5% copper-1.5% magnesium alloy. We agree that there is a correlation between the stress-corrosion susceptibility of aluminium-copper alloys and the microstructural changes that take place during ageing. Gayler's observation that the "light phase" in aluminium-4% copper alloy first appeared at the beginning of the second hardness rise agrees well with Robertson's stress-corrosion results.

While Dr. Hardy's explanation of the light phenomenon is very interesting, we do not think that it is in complete keeping with the experimental observations. First, according to Dr. Hardy the light phenomenon would not be expected to be seen until a precipitate had been formed from the segregates



(Guinier-Preston zones). As is shown in Perryman and Blade's paper, the light phenomenon is observed long before the equilibrium precipitate appears. In fact, it is the formation of such precipitate that prevents the light phase from further advancement into the grain. Similar results were found for aluminium-4% copper alloy by Gayler, who first observed the light phase at the beginning of the second hardness rise and did not observe the intermediate precipitate  $\theta'$  until after maximum hardness. Secondly, according to Dr. Hardy's theory, when the segregates (Guinier-Preston zones) are forced to dissolve there would be a concentration gradient between the separated particles.\* If such a concentration gradient was responsible for the light phase, then sharp boundaries would not be expected. This is not in keeping with our micrographic observations, which showed clearly that both in aluminium-zinc and aluminium-copper alloys the light phase has two sharp boundaries.

Mr. Thompson has criticized the use of the salt spray. This was a reasonable test to adopt in the early stages of the work, when the emphasis was on obtaining data on the life to be expected from aluminium-7% magnesium alloy in various metallurgical conditions and under various stresses, when exposed in service in corrosive (particularly marine) environments. To obtain good reproducibility this test needs to be applied under controlled conditions of humidity and this has been adopted as standard practice for some time. Mr. Thompson does not appear to appreciate, however, that for the later and more fundamental side of the work, for instance whenever electrochemical measurements were made, the specimens were completely immersed in salt solution. Chromated lanolin, which was applied to protect direct-tensile stress-corrosion test specimens that were sprayed with salt solution, was not used on the immersed specimens for electrochemical measurements.

The authors regard the phrase "attack by sodium chloride solution" as synonymous with "corrosion in sodium chloride solution" and fully appreciate all that this implies when one accepts an electrochemical theory of corrosion, e.g. the effects of the presence of dissolved oxygen (which is normally assumed to be present in a solution unless it is specifically stated to be absent). As we understand Mr. Thompson, his principal point is that sodium chloride takes no part in the stress-corrosion process, and in particular that chloride ions, having no oxidizing power, cannot take part in the cathodic reaction. We are not clear whether Mr. Thompson is of the opinion that we have stated that chloride ions do so function, but we hasten to say that we agree with him on this point and add that nothing in our papers is intended to suggest the contrary. We have, in fact, pointed out that the cathodic reaction will be either evolution of hydrogen or reduction of dissolved oxygen, according to the circumstances. In conditions where the former is not possible, removal of dissolved oxygen prevents corrosion. On the other hand, we cannot agree that sodium chloride is taking no part in the process. It should not be necessary to point out that sodium and chlorine ions carry practically all the current in the corrosion cells when the electrolyte is 3% sodium chloride solution, and that chloride ions will tend to accumulate at the anode. The presence of chloride can certainly modify the corrosion process, since it may lead to the formation of soluble corrosion products at the anode and the continuation of corrosion which might otherwise be stifled by insoluble products. We do not wish to pursue this matter further here, but would mention that in a recent paper Hoar † has discussed in some detail the "film-rupturing" power of chloride and other ions. There can be no doubt that sodium chloride plays a part, since if it is eliminated no stress-corrosion (as defined by us) occurs in distilled water. We therefore feel justified in saying that "attack" occurs in sodium chloride solution (aerated), since we are merely referring to

\* H. K. Hardy, *J. Inst. Metals*, this vol., Fig. 11(c), p. 479.

† T. P. Hoar, *Trans. Faraday Soc.*, 1949, 45, 683.

the corrosion observed in those circumstances, and we imagine it is agreed that this has taken place.

There can be little question that the initial intercrystalline corrosion of the alloys in question is attributable essentially to the potential differences between the grain boundaries and the grain bodies; the latter are the cathodes, at which reduction of dissolved oxygen occurs, dissolution at the anodes being due to the undermining and disrupting of protective films owing to the presence of chloride. Differences in oxygen concentration over the specimen surface probably have negligible effects at this stage. Subsequently, however, when crevices deepen, oxygen-concentration gradients undoubtedly exist. This is recognized in the discussion in Section VII.3 of the paper by Gilbert and Hadden.

We do not see the relevance of Mr. Thompson's calculation of the rate of corrosion of magnesium corresponding to the amount of oxygen that could diffuse to the test-pieces concerned, since the rate of corrosion is limited, of course, by anodic polarization. We have pointed out how very large currents may flow if the anode surface is bare, e.g. when a new surface is exposed immediately after a local mechanical breakdown, though when this occurs in a stress-corrosion crevice most of this large current may flow to cathodes inside the crevice with the evolution of hydrogen. However, rapid polarization of the anode as films re-form will limit the amount of attack that can occur at this very fast rate, possibly to only a small part of the whole. These views emphasize the importance of films on the electrodes (and we are therefore surprised to see a suggestion in Mr. Thompson's contribution that we do not take into account films at the grain boundaries) and they receive support from the fact that cracking in hydrochloric acid—when oxide or hydroxide films must play a much smaller part, if any at all—is much more rapid than in sodium chloride solution.

It is not claimed that the electrochemical measurements made during this work are of a refined nature or of the highest accuracy. The effects obtained, however, were large and definite, and in our opinion the interpretations given are not vitiated by minor effects due to the particular size and shape of the specimens used.

With regard to the method of de-aeration, it is not claimed that this is the best possible. Since, however, the method used brought about a conclusive result, i.e. prevention of stress-corrosion cracking in aluminium-7% magnesium alloy, the use of more refined techniques was unnecessary. The values of  $-1.3$  to  $-1.4$  V. for the potential of loops with unprepared surfaces and of  $-0.8$  to  $-1.0$  V. for loops with electropolished or pickled surfaces were for aerated solutions, and we cannot trace the statement attributed to us by Mr. Thompson that they were de-aerated.



JOINT DISCUSSION ON PAPERS BY MR. T. H. ROGERS: "A METHOD FOR ASSESSING THE RELATIVE CORROSION BEHAVIOUR OF DIFFERENT SEA-WATERS"; BY DR. I. G. SLATER, MR. L. KENWORTHY, AND MR. R. MAY: "CORROSION AND RELATED PROBLEMS IN SEA-WATER COOLING AND PIPE SYSTEMS IN H.M. SHIPS"; BY MR. R. MAY AND MR. R. W. DE VERE STACPOOLE: "THE JET-IMPINGEMENT APPARATUS FOR THE ASSESSMENT OF CORROSION BY MOVING SEA-WATER"; AND BY MR. H. S. CAMPBELL: "PITTING CORROSION IN COPPER WATER PIPES CAUSED BY FILMS OF CARBONACEOUS MATERIAL PRODUCED DURING MANUFACTURE."

(*J. Inst. Metals*, 1949-50, 76, 597, and this vol., pp. 309, 331, 345.)

DR. MAURICE COOK,\* F.I.M. (Member of Council): Dr. Slater, Mr. Kenworthy, and Mr. May are to be congratulated on a very informative paper in which they have gathered together much useful matter of interest to those concerned with the manufacture, handling, and maintenance of cooling systems and their components, as well as to producers of materials used in their construction. Over the years much headway has been made in investigations into the many problems involved and considerable success has been achieved in the development of materials with improved resistance to the various types of corrosion which occur in cooling systems, so much so, in fact, that as far as condenser tubes are concerned, as the authors have pointed out, the corrosion problem is virtually solved, unless and until any further design development substantially increases the severity of operating conditions. Condenser tubes, however, represent only one type of component in the systems, and there still remain other problems to be solved and there is, in consequence, still room for improvements. This welcome paper is largely in the nature of a factual record and is not much concerned with speculative or conjectural matters of a debatable character. While, therefore, there is little, if anything, in the paper with which I find myself in any degree at variance, there are one or two points on which I would like to comment.

Of the materials currently in use for condenser tubes no one is likely to question the superiority of cupro-nickel, aluminium brass, and the more recently

\* Director, Imperial Chemical Industries, Ltd., Metals Division, Birmingham.

introduced high-tin bronze alloys over 70 : 30 or Admiralty brass, but in case any one might infer from the authors' observations that they are immune from attack under conditions of partial obstruction, it should, perhaps, be pointed out that even in tubes of these materials corrosion from this cause can, and does, occur, even to the point of perforation, under severe conditions.

The paper has rightly stressed the importance of the design of the water-intake system and the inlet boxes, but little mention has been made of the method of fitting condenser tubes. To minimize impingement attack and inlet-end corrosion, flush-fitting, bell-mouthed ferrules (that is, radiused at the inlet edge) are to be preferred to the so-called shoulder type which stand proud of the tube plate. The effects illustrated in Figs. 12 and 14 of the paper (Plates XXVII and XXVIII) are, therefore, not surprising. From the appearance of the sides of the ferrules, where the threads can in some instances be clearly seen, it would appear as if these were, in fact, intended to be fitted flush with the tube plate, and they are, moreover, not radiused at the inlet edge. Whilst it is true, as the authors state, that aluminium brass ferrules give satisfactory service, they have a tendency to bind in the tube plate, and their removal after a relatively lengthy period of service is generally a somewhat difficult operation. Cupro-nickel ferrules are free from this disadvantage and for this reason their use is greatly to be preferred, especially as they can safely be coupled with aluminium brass or Admiralty brass tubes.

The authors have not made any reference to the use of inserts at the inlet end of condenser tubes for the purpose of protection against impingement attack, and whilst this may not have been a Naval practice, it is one which has been commonly resorted to in other marine condensers and condensers in land installations. For this purpose, metallic inserts have been used, and whilst they were successful in protecting the tubes as long as they lasted, their removal not uncommonly proved to be anything but an easy matter. The use of inserts of plastic material has been shown to afford excellent protection and they can, moreover, be simply and easily fitted and removed.

The thermal conductivity of aluminium brass is  $0.22 \text{ cal./cm.}^2/\text{cm./}^\circ\text{C./sec.}$  as compared with 0.06 for cupro-nickel, and while it is, in consequence of this difference, a common practice with designers to allow extra surface in condensers fitted with cupro-nickel tubes, it is a moot point whether in service this difference in conductivity of the alloy does appreciably affect the thermal efficiency of the unit. Both soon become coated inside and outside with films of material of low conductivity, which inevitably reduces thermal efficiency.

Although not mentioned by the authors, the advantages of regular cleaning of condenser tubes as a contribution to efficient functioning and the minimizing of corrosion cannot be too strongly emphasized. How this is best done is determined by particular circumstances, but any method which is used should achieve the removal of most of the deposit and at the same time leave a relatively thin homogeneous film on the sides of the tubes and avoid exposing areas or patches of bare metal.

Practical experience certainly indicates that steel protector plates, if correctly fitted, are effective in reducing the incidence of corrosion in tube-plates and ferrules in condensers with gun-metal water boxes. Where, as is much more usual nowadays, the boxes are of steel or cast iron, protector plates are not necessary, but in these circumstances there is the attendant risk of large, loose masses of rust forming and becoming detached and lodged in the tubes, thus causing premature failure by deposit attack or by impingement following partial obstruction, unless, as the authors have pointed out, the steel or iron surfaces can be adequately protected against corrosion.

The copper alloy containing small percentages of nickel and iron seems undoubtedly to be a very promising piping material, and apart from its capacity for withstanding impingement attack, it can be more readily mani-

pulated by copper-smithing techniques and more easily joined, by welding, for example, than some of the other materials which have been considered for this purpose.

The subject under discussion naturally deals with the effect of sea-water, but failure in cooling systems may occasionally originate on the steam side and it would be of interest to know whether in their experience the authors have encountered this to any extent.

As the authors have remarked, useful information can be obtained with small experimental condensers and model circulating systems, since with these it is often possible to approximate more closely to service conditions than it is with many of the more usual types of laboratory corrosion tests. The latter none the less have proved of undoubted value and both methods of testing have their place in the evaluation of materials of construction for cooling systems.

DR. U. R. EVANS,\* F.R.S. (Member): These papers record past achievements, provide information about the present position, and afford hope for the future.

The information given as to the materials and protective processes that have proved satisfactory is most valuable; it comes from users, and will therefore be welcomed by other users. It should also be studied by salesmen, in order that they may know the circumstances in which they can recommend their materials or processes with confidence, and those in which they should withhold recommendations. Nothing is more harmful to a good material or process than that it should be applied to a purpose for which it is unsuitable, for that will discredit it and prevent its use in cases where it would be valuable.

The statement in the paper by Slater, Kenworthy, and May that the condenser problem is virtually solved is a tribute to the Institute of Metals Committee of which Sir Harold Carpenter was so long Chairman and Dr. G. D. Bengough Senior Experimenter. Mr. May, one of the present authors, was a prominent member of the group in its most fruitful period.

The value of zinc protector blocks in inlet tubes is questioned in that paper; it is stated that the blocks get loose and do mischief. It might, however, be worth while to experiment with zinc-rich paints, taking care to select a situation where failure to obtain protection would not be fatal. Paints consisting of metallic zinc powder in an organic vehicle, e.g. polystyrene, give coats containing 95% of metallic zinc. Other paints with an inorganic (cementiferous) matrix yield coats less rich in metallic zinc but show better adhesion. Such paints confer protection, even at places where the steel base has been exposed at a scratch-line, for periods exceeding a year in sea-water; the protection is sacrificial at the outset, but the cathodic action produces a film on the steel base, so that protection continues without rapid consumption of zinc and lasts a long time. Success cannot be guaranteed, but trials would be worth making.

Mr. Campbell's outstanding research explains why copper pipes often give good results in natural waters of a type which might be expected to attack copper; the waters, he shows, contain an unidentified, and hitherto unsuspected, inhibitor. It appears hardly satisfactory to rely on the chance presence of an unidentified substance, and hope may be expressed that the inhibitor will be identified, and a simple test for it provided. The important effect of a carbonaceous coat, which causes pitting by acting either as a cathode, or an oxygen-screen, or both, is of great interest. A large cathode (the carbonaceous coat) combined with the small anodes (the copper exposed at discontinuities in the coat) must concentrate on small points the corrosion which would otherwise be well spread out, thus causing intensified attack.

\* Reader in the Science of Metallic Corrosion, Cambridge University.



The question may be asked : If carbonaceous deposits can be avoided, is it advisable to use copper pipes for waters which do not contain the inhibitor? Mr. Campbell's views on that question would be welcome.

It is suggested that chlorides stimulate attack, because the small solubility of cuprous chloride keeps low the copper-ion concentration, and thus shifts the potential in a direction favouring corrosion. On the other hand, it might well be expected to favour the production of a protective film. As to whether the small solubility will stimulate attack or prevent it, this presumably depends on the nucleation number. If vast numbers of cuprous chloride nuclei are quickly formed, one may hope for a fine-grained film which becomes protective whilst still thin; if few nuclei appear, the film cannot cover the whole surface until it has become so thick that cracking (due to misfit stresses) becomes probable, with adverse results.

I understand that Mr. May and Mr. Campbell have been considering the possibility that the unknown inhibitor is effective because it affects the nucleation rate. Would it be possible for them to make their views available? Do they, for instance, consider that the inhibitor is adsorbed on the tiny cuprous chloride crystals and prevents them from growing, so that fresh crystals are produced? Such a mechanism might lead to the production of a fine-grained film which would cover the whole surface and give protection whilst still thin.

DR. R. GENDERS,\* M.B.E. (Member) : These papers are especially welcome in that they describe applications which have resulted from a wide range of research work carried out in the past. It is surprising that, in engineering, frequent cases are still to be found where metals are placed in juxtaposition, in blatant contravention of the rules laid down broadly by the electrochemical series. It is surely the responsibility of the engineer to see that his use of metals is as far as possible in line with up-to-date knowledge. On the other hand, the investigator should always bear in mind the viewpoint of the maker and user industries in presenting his work.

The development of aluminium brass was a direct by-product of a research with which I was concerned, carried out for the B.N.F.M.R.A. at the Research Department, Woolwich. The matter began with a visit to Mouy-Bury in France, to inspect the methods being used by Gaston Durville for the casting of aluminium bronze strip ingots for French coinage. The surfaces of those ingots were extremely good, and it was decided to investigate the Durville method for casting ordinary brass strip ingots. It was found, however, that the presence of aluminium in the alloy was a considerable factor in the success of the method and it therefore became necessary to carry out a comprehensive study of the casting, working properties, and mechanical properties of the copper-zinc-aluminium alloys. The results of that investigation were published in the *Journal of the Institute*.† It was observed that alloys containing about 2% aluminium were resistant to corrosion and to discoloration on heating. On the suggestion of Dr. R. S. Hutton, the corrosion-resisting properties were further investigated and, in accordance with the available knowledge at that time, a small percentage of arsenic was added to minimize dezincification. The composition originally selected for the first condenser-tube trials has not since been improved upon. This selection was based on 2% aluminium, the proportions of copper and zinc being arranged to give an  $\alpha$  alloy with the same working and mechanical properties as 70 : 30 brass. Thus the introduction of aluminium brass was entirely an application of research observations, together with knowledge available from a vast amount of earlier corrosion research.

\* Consultant Metallurgist, London.

† *J. Inst. Metals*, 1930, 43, 163.

Referring to the paper by Slater, Kenworthy, and May, it would be interesting to have some amplification of the views of the authors regarding the particular advantages of aluminium brass for distillation plant and the specific properties of the alloy which they have in mind in that connection. The authors have not mentioned an occasional type of failure which takes the form of a sharply localized perforation in ordinary brass tubes at a position well away from the ends and presumably out of range of any disturbance that would cause impingement. The cause of such failures is often obscure. In amplification of the brief reference made in the paper to brazing metals, it might be mentioned that aluminium brass is susceptible to intercrystalline penetration by brazing metals at any temperature above their melting points. If parts are brazed under conditions which impose even slight stresses on the joint while the brazing metal is liquid, this can lead to severe penetration and possibly the formation of cracks. Crevice attack at such positions can lead to ultimate perforation.

The authors of all the papers are to be congratulated on bringing forward valuable information on a difficult and important field of application which deserves wide publicity, especially among metal users who suffer from corrosion problems.

MR. W. H. RICHARDSON,\* B.Sc. (Member): The information presented in the paper by Slater, Kenworthy, and May is of an extremely valuable nature, but the absence of all reference to aluminium bronze unfortunately makes it incomplete.

Aluminium bronze of the type which complies with specifications D.T.D. 412 and B.S. No. 1400-AB2 in the cast condition and D.T.D. 197A in the wrought condition is undoubtedly an extremely satisfactory material for use under the most severe conditions of sea-water corrosion. Cavitation-erosion tests carried out by Beeching† have demonstrated that such an alloy is far superior to all the other copper alloys commonly used for this type of application, e.g. manganese bronze, gun-metal, phosphor bronze, &c.

Aluminium bronze to specification D.T.D. 412 was approved by the Admiralty for sea-water circulating-pump impellers during the war, and since that time has been used extensively. In this period it has given excellent service which has supplied the strongest practical evidence of its superiority over the gun-metals and phosphor bronzes. It is therefore surprising to read in the paper that "Phosphor bronze, which is commonly used for such impellers, normally gives reasonable service. Alternative alloys for more severe conditions are Monel metal and stainless steel, though perhaps with some risk to adjacent parts owing to the highly cathodic nature of these alloys", since experience suggests that aluminium bronze can replace the two latter materials without the same risk to adjacent parts.

Evidence that aluminium bronze is highly resistant to impingement attack has also been obtained, and in this connection it would be interesting to hear whether the authors can produce any laboratory test results to demonstrate the resistance of aluminium bronze to this form of attack in comparison with the behaviour of other materials examined.

It is, of course, appreciated that the use of aluminium bronze (of the type under consideration) in sea-water cooling systems has been largely confined to pump impellers, and since this particular component received only brief mention in the paper there is some excuse for omitting all reference to it. Nevertheless, I feel that had the success of this material received due consideration by the authors it would probably have suggested itself as a

\* Chief Metallurgist, Langley Alloys Ltd., Langley, Bucks.

† R. Beeching, *Trans. Inst. Eng. Ship. Scotland*, 1942, 85, 210.



promising material for other components in the system, e.g. valves, condenser-tube plates, ferrules, &c.

In any case I think that this type of alloy should be subjected to the various laboratory tests discussed by the authors, since, as stated in the paper, "... most of the available materials and alloys are not regarded as perfect; the majority have their weaker points and tend to undergo some corrosion of one type or another". Consequently an alloy such as aluminium bronze, which shows every indication of being a highly satisfactory material for applications requiring high resistance to attack by sea-water and related phenomena, should not be overlooked in an investigation of this nature.

In conclusion, I would like to point out that the Admiralty engineers are by no means unfamiliar with the merits of this type of aluminium bronze for applications demanding high resistance to sea-water corrosion and are, in fact, preparing a new specification to control its composition in such a manner as to ensure maximum resistance to the various forms of attack encountered in marine applications.

DR. W. H. J. VERNON,\* O.B.E. (Member): The papers are to be welcomed as valuable contributions to the general effort directed towards the combating of corrosion. It may be observed that the complexity of the subject is no longer a serious obstacle to a reasonable understanding of corrosion mechanism. Naturally, in a field so vast there is ample room, as in the analogous field of preventive medicine, for more extended fundamental research. But it cannot be too strongly urged that there already exists a store of knowledge still far from fully applied by engineers and metallurgists. Many of the corrosion failures and much of the wastage in industry might be avoided by attention to principles already well established. This indeed is excellently illustrated in the paper by Slater, Kenworthy, and May.

In one important respect the analogy between the fields of corrosion prevention and preventive medicine breaks down completely, namely, in the number of practitioners available to apply existing knowledge to the struggle against metallic corrosion and human disease, respectively. In this country the number of trained "corrosion practitioners" is lamentably, even hopelessly, small and is at striking variance with the growing realization, both in industry and in public undertakings, of the importance of corrosion as a major economic factor. This growing realization is borne out by the increasing number of enquiries received, the key-note of which is frequently the hold-up of production.

The picture here presented is in marked contrast with that which obtains in the United States, where the study of corrosion phenomena enters into the curricula of a number of Universities and Colleges, where there is a large and growing army of "corrosion engineers" engaged wholly in the field of corrosion prevention, and where there is a flourishing National Association of Corrosion Engineers, whose activities include the organization of meetings and the publication of a monthly journal devoted entirely to matters of corrosion. It is clear that there exists in this country nothing approaching the counterpart of such a system. The urgent need for intensifying the guidance and assistance to industry in dealing with corrosion problems, and particularly in making available to industry the results of corrosion research, cannot be questioned; but such shortcomings as there are cannot fairly be laid at the door of the handful of corrosion workers who at present are bearing the heavy burden of attempting to put across existing information to industry—a task entirely incommensurate with their numbers and one

\* Chemical Research Laboratory, Department of Scientific and Industrial Research, Teddington, Middlesex.

which must frequently necessitate the curtailing of research in the very fields in which further knowledge is urgently required.

Among many other things emphasized in the paper by Slater, Kenworthy, and May is the importance of design. The examples quoted are necessarily highly specific, but the matter itself is undoubtedly of much wider significance; it suggests, in fact, one of several broad generalizations that may be drawn from the group of papers as a whole. Although it is true that the more resistant the materials at one's disposal the less important such factors as design must become, nevertheless even good material can be sacrificed by errors both of design and of assembly. Available evidence confirms that these two factors represent a common and avoidable source of failure in service.

A second generalization, also suggested by the paper of Slater, Kenworthy, and May, concerns the influence of water speed. The authors observe that the higher water speeds and increased speed of working generally were largely responsible for a greatly increased incidence of corrosion under war conditions. This is significant, because precisely the same point was made in Bengough's reports following the first World War. Those earlier increased demands had been largely met by the work of Dr. Bengough and his associates, and it is evident from the present paper that the deficiencies that have been more recently revealed have also been very largely made good. As before, the importance of the matter extends beyond Service practice; for example, in land installations the tendency is to employ higher speeds and higher temperatures and pressures—again leading to the introduction of new problems, or to the intensification of old ones.

Incidentally, the authors mention that no really satisfactory high-duty coating has been found during the work. I think, however, they will agree that, in the search for the ideal coating which the Admiralty required, a good deal of progress was made in the development of coatings for general purposes. This is reflected in the work with the C.R.L. rotor apparatus to which the authors have referred. In the early days of the C.R.L. work the acceleration factor of that apparatus was sufficiently high to provide for a fairly rapid test of available protective coatings, but with increasing efficiency of protection the period of test became extended until finally we were reduced to the necessity of considering means of making the test more severe, i.e. because of the advances made in methods of protection.

A further generalization to be drawn from the papers is that of the importance of surface films. That emerges from all four papers, whether one is considering the formation of protective films on new metal surfaces, the breakdown of such films by impingement attack or otherwise, or even the deposition of harmful films from extraneous sources.

Passing from the general to the particular, I should like briefly to refer to the paper by May and Stacpoole, which provides a most welcome description of the latest form of May's original jet test. Here the entrained air is regarded as serving a dual purpose, being responsible both for the production of surface films and for their breakdown. Possibly even now the picture of the mechanism is not entirely complete. Can the action of the air bubbles be stated more precisely; to what extent can impingement attack be induced in the absence of air bubbles, and in what way does such attack, if any, differ from that produced in their presence?

May and Stacpoole use in their tests a limited volume of sea-water that is circulated continuously around the apparatus. In the counterpart of the method as employed by our American friends at Kure Beach, N.C., an unlimited volume of sea-water flows through continuously, the apparatus being connected up to the ocean itself. As a matter of interest I should like to ask what difference in results, if any, is produced by this difference in technique?

The paper by Mr. Rogers reveals some striking results concerning the

corrosiveness of sea-water in relation to the period and mode of storage. One wonders to what extent the variations described are due to aerobic or anaerobic organisms, possibly operating alternately. For example, in the case of stagnant sea-water there is the question whether the results would be affected by the amount of free air space in the carboy? Would anaerobic organisms become active when the carboy is completely filled and air supply at the minimum? The author mentions that biological activity, and hence the corrosiveness of the water, is affected by temperature. Is there also any effect of light, i.e. would the results be influenced by storage of the sea-water in the dark, the temperature remaining constant?

DR. F. WORMWELL,\* M.Sc. (Member): Fig. 4 (Plate XXIII) of the paper by Slater, Kenworthy, and May is an illustration of failure of rivet heads in steel connected to non-ferrous metal. I would like to ask whether the failure of the steel was particularly on the rivet heads, as it appears to be. This is a matter of some general interest.

In the same paper (p. 316), there is a reference to the fact that rust assists in forming a protective coating on condenser tubes. This recalls the protective action of zinc corrosion products on steel. A statement on p. 318 implies that aluminium brass might behave better than cupro-nickel at high temperatures. I would like the authors to confirm that, and if possible to suggest the basis for their belief. On p. 321 they refer to the importance of the conditions during the early life of structures—a factor that often crops up in corrosion work. The early period of exposure of metal to a corrosive environment is often very critical, and good conditions at that stage can help a great deal.

There is a reference on p. 325 of the paper to service tests being essential, a conclusion that will be generally accepted. However hard one may try in the laboratory, one can never be quite sure of reproducing the conditions of service, and laboratory tests can best be regarded as a means of sorting out materials or coatings, which must be applied eventually in service before complete confidence can be placed in them. As regards the acceleration of laboratory tests, the principles put forward by the authors are very sound. It is unwise to introduce any new factor into a test merely for the purpose of accelerating it. The authors, however, are perhaps a little over-cautious, in that they are not prepared to intensify any factor known to be present to an extent beyond that occurring in the most severe cases in practice. That is no doubt sound, but I think it is sometimes possible to go further. If it is not possible to do so, it merely indicates gaps in the knowledge available.

On p. 327 the reproducibility of results is discussed. In our own work at Teddington we have found that even with a plain sodium chloride solution it is extremely difficult to reproduce the conditions of rapid movement and aeration from test to test, and in particular we have evidence, not yet complete, that the influence of temperature is much greater than previously suspected. In this connection, I should appreciate any further opinions which Dr. Slater and his colleagues care to give on the influence of temperature on the problems which they are studying. One would also welcome a general description of the results obtained by the test described in the paper by May and Stacpoole.

With regard to the paper by Rogers, I wonder whether it can be assumed that changes in sea-water will necessarily affect all alloys, and even all copper-bearing alloys, in the same way as copper itself. Copper was used in the test to examine sea-water, but can it be assumed that the corrosion rates of the alloys would vary in the same way as the corrosion rates of copper when the sea-water changed?

Another point is whether it has been established that the reproducibility

\* Chemical Research Laboratory, Department of Scientific and Industrial Research, Teddington, Middlesex.



of the test is sufficient to be quite certain that all these apparent changes are significant. It is very difficult to reproduce conditions of aeration by bubbling and, if the authors have really succeeded in doing so, they are to be congratulated on overcoming many experimental difficulties.

MR. CAMPBELL (*in reply*): In answer to Dr. Evans's question on the advisability of using copper pipes for waters that do not contain inhibitor, even if the pipes are free from carbonaceous deposits, I would say that, provided also that they do not contain the vitreous type of cuprous oxide scale referred to in the paper, there is little danger of cold-water pitting corrosion.

The copper corrosion inhibitor, present in many waters, has not yet been isolated or identified, but several simple tests for it have been developed. In view of the great practical importance of carbonaceous films, the present paper was published before work on the inhibitor was sufficiently advanced for publication. I agree that the inhibitor probably operates by affecting the nucleation of cuprous chloride or cuprous oxide at the anode, in some such way as Dr. Evans suggests; I have observed that anodically formed cuprous oxide is produced as large crystals in the absence of inhibitor but as a fine-grained film in the presence of inhibitor. This and other aspects of the copper corrosion inhibitor will, however, be discussed in a subsequent paper.

MR. MAY, MR. ROGERS, and MR. STACPOLE (*in reply*): As regards the point raised by Dr. Vernon, we have found that it is possible for impingement attack to occur on materials which do not form very strong protective films, even when no air bubbles are detectable, providing the turbulence in the water stream is great enough. Thus, in the jet-impingement apparatus, if no air is added, copper is usually considerably attacked at jet speeds over about 10 ft./sec., and 70 : 30 brass is liable to attack at speeds over about 15 ft./sec. When air bubbles are present both materials may undergo impingement attack at jet speeds as low as 7 or 8 ft./sec. With a material such as aluminium brass on which the protective film heals very rapidly, impingement attack rarely if ever occurs, whether air bubbles are present or not. However, breakdown sometimes does occur if contaminating substances in the sea-water interfere with the formation of the protective film, particularly if the water speed is higher than 15 ft./sec., but the resulting attack takes the form of intense pitting. With a material susceptible to impingement attack, such as copper, there is no marked difference in the attack which occurs in the absence and in the presence of air bubbles.

For laboratories situated away from the sea coast it is necessary to use a limited volume of sea-water, which is recirculated in the jet test throughout a run. This procedure has certain drawbacks and necessitates some precautions, particularly in the selection of alloys to be tested together in the same batch of sea-water. We have no experience of using sea-water flowing continuously through, but we are in touch with Mr. LaQue and his colleagues and hope to be able to arrive at some conclusions as to the effects of this factor.

The processes going on during the storage of sea-water are extremely complicated, as the biological literature on the subject shows, and it is not possible to mention more than one or two points here. The effect of light is only one of the factors to be considered, and while its presence or absence will have an effect on the quantity and type of organisms present, we have little evidence about the resulting effect on the corrosive properties of the water. It is our normal practice to transport sea-water in carboys closed with a rubber bung, usually with a small air space. In such conditions it is possible for the dissolved oxygen content to be reduced and conditions favourable for the growth of anaerobic bacteria established. Very occasionally we receive a

carbonyl in which sulphate-reducing bacteria have become active, producing  $H_2S$ , but this is unusual.

In reply to Dr. Wormwell, there is little doubt that the changes which affect the corrosion of copper do *not* affect all copper alloys in the same way. We have found that the correlation between copper corrosion index and depth of attack on 70 : 30 cupro-nickel containing no iron is reasonably high, and this appears to be generally true for materials that undergo impingement attack. But with materials such as aluminium brass, which break down only occasionally and then suffer pitting, we believe that the index gives an indication of the probability of breakdown rather than of the expected depth of attack. Thus, the index gives some general indication of the corrosive properties of a sea-water sample; we believe its chief value would be to aid in comparison of tests carried out at different times or at different places. Although the reproducibility of the copper corrosion index determinations in themselves is reasonably good, the foregoing will indicate that the interpretation of the results is not easy. For this reason little significance can be attributed to small variations, but the index serves to give a broad classification of the corrosiveness of sea-water samples. Even this has previously not been possible.

DR. SLATER, MR. KENWORTHY, and MR. MAY (*in reply*): First of all, we should like to say how gratified we are that our paper was received so favourably and that it evoked such a useful discussion, to which leading corrosion experts contributed.

With regard to Dr. Cook's contribution, we are surprised that he should have inferred from the paper that the more resistant condenser-tube materials are immune from attack under conditions of partial obstruction. We devoted a small section to tube obstruction (see pp. 322-323) in which the statement is made that where tube obstructions occur "even the most resistant tube alloys might well fail".

We thank Dr. Cook for referring to the importance of fitting ferrules flush with the tube-plate, a point which should have been made in the paper. Nowadays, this practice is usual, but the photographs in question (Figs. 12 and 14, Plates XXVII and XXVIII) illustrate the tube-plate of one of our older cruisers, ten years ago. The ferrules were, however, bell-mouthed, although this may not appear so from the photographs.

With regard to Dr. Cook's statement that aluminium brass ferrules tend to bind in the tube-plate, rendering their removal difficult after a lengthy period of service, we have gone to considerable pains to get confirmation of this view. After extensive enquiries, not one single authentic case could be brought to our notice of this having taken place. In order to make quite certain, however, tests were put in hand in the drain coolers of certain of H.M. ships and on experimental models. In the former case, no difficulty was experienced in removing the ferrules after extensive periods of service. In the latter, small naval brass packing boxes were fitted with standard packings, with graded clearances between ferrules and packing boxes, as wide as would be met with in service. After  $2\frac{1}{2}$  years, during which time the assemblies were immersed under half-tide conditions, the aluminium brass ferrules were removed as readily (as measured with a Maseeley torsion wrench) as cupro-nickel or Admiralty brass ferrules.

Only limited use has been made of condenser-tube-inlet inserts in H.M. Service and these have been of the non-metallic variety. They have been resorted to only in the rare cases where inlet-end corrosion has occurred.

With regard to the difference in thermal conductivity between aluminium brass and cupro-nickel, to which brief reference was made in the paper, we should not like to comment in detail at this stage, as the subject is at present



undergoing investigation. It would appear, however, that notwithstanding the reduction in conductivity caused by scale formation, there may still be a significant difference in practice in favour of aluminium brass.

On the subject of the material for water-boxes, it should be remembered that the paper deals with practice in H.M. ships, where iron and steel doors, which were introduced as an emergency measure, are now relatively few, whilst those that remain are being coated with rubber.

A final point made by Dr. Cook concerns failures originating on the steam side of coolers. At one time failures due to the erosive action of steam and water from auxiliary steam inlets to condenser were fairly common, but they are now rare owing to the care taken in arranging baffles to prevent direct impingement on the tubes. Very occasional instances of trouble have also been encountered in air-ejector condensers and distiller condensers from a corrosive condensate caused by incorrect venting of incondensable gases.

We thank Dr. Evans for his kind remarks and for his suggestion of using zinc-rich paints instead of zinc protector blocks in inlets.

In reply to Dr. Genders, aluminium brass tubes were first used in distillers as a substitute for tin-coated tubes in order to save tin. They were chosen after experiment had shown that when the protective film had formed, the amount of copper passing into solution in the condensate was satisfactorily low.

With regard to Dr. Genders's point concerning an occasional type of failure in ordinary brass condenser tubes, we feel that this is probably due to localized impingement set up by partial obstructions, as pointed out on p. 317 (Section II. 1(j)). It should be appreciated, however, that ordinary brass condenser tubes are not now used in H.M. ships.

We are grateful to Dr. Genders for drawing attention to the effect of brazing metals on stressed aluminium brass. This is a factor that should have been mentioned, although we did not encounter such failures in the cooling systems examined.

We are particularly happy to have Dr. Vernon's views on the lack of technical support in this country on matters relating to corrosion and its prevention. Although we do not lack the originality of thought which is the inspiration of the best fundamental work, there seems to be a profound apathy on the part of our engineers in orienting this work to practical and economic ends. One is thus inclined to the view that corrosion research has but doubtful virtues which are not fit subjects for discussion in our "old world" environment. It is hoped that this appeal for help in publicizing corrosion information will not go unheeded.

We would apologise to Dr. Vernon for not making clear that although no high-duty coating proved at the time of the investigations to be really satisfactory for the service in question, the C.R.L. rotor apparatus played a very great part in the development and selection of paints which not only proved highly successful for other purposes, but which also provided at least a valuable temporary measure in minimizing corrosion in condenser systems, particularly in the early days of the war.

In reply to Mr. Richardson, we agree that aluminium bronze should have been included in the possible materials for use as pump impellers, but we would hasten to assure him that we have not overlooked the possibilities of its use for other components. On the contrary, one of us (L.K.) has been responsible for instigating a thorough investigation of this class of alloy which has led to a revision of the specification to which Mr. Richardson refers in his last paragraph.

In reply to the first point raised by Dr. Wormwell, the corrosion in the ship-builder's tube was particularly severe on the rivet heads but was not entirely confined to these, very considerable attack of the plating having taken place at the point of contact with the gun-metal.

With regard to the relative merits of aluminium brass and cupro-nickel under hot conditions, it has been shown that hot clean moving sea-water forms a particularly good protective film on aluminium brass with little precipitation of corrosion products in the liquid. Under the same conditions cupro-nickel develops a protective film but more basic salt appears in the liquid and continues to do so for a longer period. Over a number of years the use of aluminium brass in hot conditions has become well established, especially in drain coolers, in which the temperature may be up to boiling point. Very few failures have come to light and these have all been associated with contamination, deposits, and local stagnation. Fewer cupro-nickel tubes have been used in hot conditions and few failures have been experienced, but as the relative numbers in use are not known, a reliable comparison between the two materials based on practical results is not possible.

In reply to Dr. Wormwell's final query concerning the effect of temperature, the greatest influence of rise in temperature as mentioned in the previous paragraph, is an increased tendency for film formation, apparently owing to the speeding up of the initial attack upon which film formation depends. Provided film formation is not hampered by such factors as contamination of the water, or the settlement of precipitated corrosion products and other deposits owing to stagnation of the liquid, a higher temperature may result in a lower rate of corrosion. This is notably the case where impingement attack is concerned, and it has been found essential to cool the water used in the jet-impingement apparatus for this reason. It might be mentioned that by film formation in hot sea-water under ideal laboratory conditions it is possible to make 70 : 30 brass resist impingement almost as well as aluminium brass, but only so long as the film is not mechanically damaged.

DISCUSSION ON THE PAPER BY MR. J. J. HOBEN AND MR. J. F. MULVEY: "THE NEW CONTINUOUS BRASS MILL OF THE SCOVILL MANUFACTURING COMPANY, WATERBURY, CONN., U.S.A."

(*J. Inst. Metals*, this vol., p. 357.)

MR. W. F. BRAZENER,\* J.P. (Member): Members will be appreciative of the fact that a paper of this description has been submitted to the Institute of Metals rather than to one of a number of other Institutes to whom it will be of considerable interest. Mechanical, electrical, and production engineers will no doubt study the paper as keenly as will metallurgists. In point of fact, one of the great lessons to be learned from it is the importance of the closest collaboration between all these groups in the development of the metal industry.

Taking the paper as a whole, the majority of metallurgists will display the greatest interest in the continuous-casting process. This method can obviously only be warranted where it is possible to manufacture on mass-production lines. The growth and development of the Scovill Manufacturing Company has placed it in such a position that mass production has become the order of the day. Although from an economic standpoint the casting of ingots is a relatively small part of the total production cost of strip brass, yet the Management of this Company has deemed it advisable to start its continuous production right from the beginning of the manufacturing process.

In the ordinary way, to cope with a production of, say, 10 tons/hr. of brass slab ingots, one envisages a lay-out of ten 1-ton-capacity Ajax-Wyatt furnaces pouring into water-cooled moulds of the Junkers type. This, of course, is fairly common practice in other plants in the U.S.A. The quantity of 10 tons has been assumed, since it is likely that at the Scovill plant two of the feeding furnaces are in use, whilst the third is either under repair or being held in reserve. From the data given, the output from two furnaces will be approximately 10 tons/hr. Undoubtedly the Scovill Manufacturing Company has taken into full consideration all the metallurgical and economic factors before embarking on this process of continuous casting for increasing its productivity rate.

The problem of maintaining a sufficient supply of molten metal to the holding furnace has been overcome by a typical American adventure. The Ajax-Scomet furnaces, with their large holding capacity and rapid melting rate, make it possible for the continuous-casting machine to function with little fear of interruption. Amongst the many new features included in the construction of these furnaces, one of the most interesting developments is the embodying of a straight-channel design with two inductors set between the three channels which extend from the bottom channel. The claim is made that the efficiency, according to experience to date, is higher than has been obtained in any other type of furnace. It will be interesting to learn whether electric-furnace builders agree with the conclusion of the authors that this is due to the fact that a great amount of power is concentrated in a small space,

\* Managing Director, The Mint, Birmingham, Ltd., Birmingham.

or whether there may be some other reason connected with the pattern of the channels and the location of the induction units. The question is whether there is anything in the fundamental design of this type of furnace to give it a greater efficiency, in terms of units per ton of brass melted, than is the case with the Ajax-Wyatt L.F. induction type of furnace. When these furnaces have been longer in operation, it will be of considerable interest to know what life is obtained from the linings, particularly in view of their construction from pre-fired shapes and standard bricks.

The continuous method of casting, with its careful control of temperature and rate of pouring, can be expected to produce an ingot whose internal structure will be equal to that of any ingot poured in the orthodox way under the best possible conditions. One of the interesting features of the process, and one which has an important bearing on the soundness of the ingot, is the relatively slow rate of transfer of molten metal from the holding furnace to the mould. Assuming that in the continuous process a mould giving an ingot 24 in. wide  $\times$  2½ in. thick is producing 20,000 lb. of metal/hr., approximately 5½ lb. of metal/sec. is being poured into the mould, which means in effect a rise of approximately  $\frac{1}{4}$ – $\frac{1}{3}$  in. of metal/sec. in the mould. Pouring from an Ajax-Wyatt furnace into a single Junkers-type water-cooled mould of similar cross-sectional dimensions ( $24 \times 2\frac{1}{2}$  in.) the rate of pour would be, on an average, at the rate of 1 in. rise/sec. Excluding feeding time, which is essential in the latter method, it appears that in the continuous process the molten metal is transferred to the mould at only about one-third the rate which is common to the normal practice of pouring from a single furnace into a single mould.

In view of the fact that in the continuous process mould lubrication can only be achieved by oil impingement on the mould wall at the surface of the molten metal, it is not to be anticipated that the surface of the ingot will be entirely satisfactory. One expects in practice that the surface of an ingot cast from a single furnace into a Junkers-type water-cooled mould which has been properly cleaned and lubricated will be superior to the surface of the continuously-cast product. Now the most common practice for the production of brass strip from the ingot is by initial hot-rolling, whereas in the process described the ingots are cold rolled. As the hot-rolling process tends to create a much inferior surface on the strip as compared with the results from cold rolling, it is quite probable that at the run-down stage there is very little difference in the surface quality achieved by the two methods. Also, in view of the subsequent milling which applies to both the hot and the cold process, minor surface imperfections are not of vital importance.

Whilst it may be conceded, as is claimed by the authors, that by melting large quantities of metal at one time there is little variation in composition, it can, of course, be readily visualized that the fortuitous introduction of some deleterious element such as bismuth can affect a very large tonnage of metal before it is detected.

Another interesting feature of this continuous-casting unit is the use of chrome iron in tubular form as a medium for conveying the molten metal from the holding furnace to the mould. Presumably, also, the needle valve is of the same composition. It would be interesting to have more detail regarding this pouring device. To many of us it is something novel to find that there is an alloy capable of resisting the action of molten brass. If the authors could furnish us with the composition of the alloy, the actual dimensions of the distributor, and its length of service, it would be appreciated.

For those who are interested in having more information on the continuous-casting process, it is perhaps worth while calling the attention of members to a recent description \* of the Rossi continuous-casting machine installed at the

\* J. H. Hyde, *Iron Age*, 1949, 164, (23), 80.



Bristol Brass Corporation. This article describes the operation of continuous casting at greater length than the authors have been able to do in the present paper, and although the product is a billet for extrusion purposes the essential features are very similar to the continuous-casting process at Scovill.

Turning to the rolling side, the breaking-down rolling is surprisingly (for an ingot of this size) carried out as a cold-rolling operation. The probable reason for this is that it would be difficult for such an immense industrial concern as the Scovill Manufacturing Company to guarantee that all the scrap metal which has to find its way back to the melting furnace had been segregated so as to be free from those impurities which render the hot-rolling operation in an  $\alpha$ -brass impossible. I have particularly in mind lead, which if present in excess of about 0.02% will cause failure in hot rolling. This handicap—if it can be called a handicap—is largely, if not entirely, overcome by the high-powered cold-rolling mill and the mechanical handling devices ancillary to it. A very brief description of the Scovill rolling mill, accompanied by a well-illustrated flow chart, has recently been published.\* The latter gives an indication of the methods employed to make this mill live up to its description of being a "continuous" strip mill.

\* No really true impression, however, can be given by a mere verbal, or printed, description of this rolling mill. It has, so to speak, to be seen to be believed. One gets an impression of perpetual motion with only occasional human intervention. The treatment of the metal is in accordance with good metallurgical practice; and if there are any doubts raised by the somewhat revolutionary methods employed, the quality of the finished product is the answer. Those who have seen this plant in operation cannot fail to be impressed both by the immensity of it, and also by the thought and ingenuity which have been displayed in its mechanization, not to mention the courage needed to embark on such a project.

MR. A. J. FIELD,† M.C., B.Sc., F.I.M. (Member): The paper is of the utmost interest to members in the aluminium industry, as well as to those in the copper and brass trade. In aluminium mills, rolling is developing on at least as great a scale.

Those who come from Birmingham will be interested to hear of the ubiquity of the Birmingham craftsmen who contributed to the start of the Scovill plant many years ago. It was interesting to learn recently that former citizens of Birmingham also contributed to the starting up, about the year 1730, of the Carron Ironworks at Falkirk in Scotland, one of the oldest in the country.

The paper gives a clear description of a most excellently engineered plant, the keynotes of which are simplicity and efficiency. It is questionable if the term "continuous" can properly be applied to the rolling mills, where it usually connotes tandem-stand rolling, but it is certainly applicable to the casting.

With regard to the Ajax-Scomet 1000 kW. L.F. induction furnace ("Scomet" presumably implying that it was designed by the metallurgical department of Scovill) the claim for superior efficiency may possibly arise from compactness of design, and, as all electrical losses are utilized in the melting of the metal in induction furnaces, the high efficiency may be attributed to the reduction of the thermal losses from the chamber.

With regard to the changing of the inductor units, which are most ingeniously fixed to the furnace body, it is stated in the paper that any inductor can be changed while leaving two others working. It is difficult to see how that can be done in the case of the middle inductor. When the furnace is

\* L. S. Sperry, *Iron Age*, 1949, **164**, (25), 59.

† Manager, Falkirk Rolling Mills, The British Aluminium Co., Ltd.



tilted to change this inductor, the inductor on one side of it would also be above the metal level, and therefore empty and on open circuit. Perhaps the authors could say whether, if only one inductor is working when the middle one has to be changed, this is sufficient to maintain the metal in the bath molten. A second question with regard to the furnace is whether the power is shut off during tapping. If not, it seems that when the furnace is tilted the upper inductor would come to a point where it open-circuited and might overheat the metal or arc in those channels.

The tapping arrangements on the furnace are not entirely clear from the drawing, where it appears that, when the furnace is tilted, the metal would not run out of a spout in the middle of the front edge but from a hole in the side wall. If that is so, it would be a little complicated to deliver the metal into the 5000-lb. transfer ladle, and there must be a fair amount of fall, since it is not a lip-axis but a centre-axis furnace. There might be a 3-ft. drop, so that some kind of launder would be necessary in addition to the equipment shown in the drawing.

The Rossi casting machine is properly called a continuous-casting machine, though in the aluminium industry it has been customary to call a static-mould, limited-stroke, casting machine a continuous one, before the recent introduction of the designation "semi-continuous." As Mr. Brazener has pointed out, there would be a metal delivery of something like 300-500 lb./min. into the mould. The vibration or rate of reciprocation of the mould would be about one oscillation per 2-4 sec. The metal is stated to descend at anything from  $\frac{3}{16}$  to  $1\frac{3}{4}$  in./min., but to get the output required the figure would have to be near the top of that range.

The illustrations in the paper give some assurance in respect of the surface quality of the ingot, as does also the fact that there is no mention of the scalping of the cast ingot previous to rolling it on the cold-rolling mills. It would be interesting to have further information about this point, and in particular as to whether oscillation every 2 sec. or so gives rise to discontinuities on the surface, or to any seam or particular segregation, including inverse segregation. This is frequently encountered in the continuous casting of aluminium, and invariably with aluminium alloys, and has to be removed before rolling.

In the case of the brass and copper cast by the chill-casting and by the continuous processes, is any metallurgical difference found in the resulting strip materials? Do they both behave in exactly the same way when formed by the press-worker and spinner?

Mr. Brazener has referred to the life of the mould and its lubrication, and these are points of considerable interest, as is also the thickness of the mould material. The material is copper, but is it just ordinary copper? The depth of the mould appears to be about 3 ft., which is much greater than is generally used for aluminium.

There is a point of practical importance to strip rollers in the cold-rolling operation and that concerns the nature of the edges of the strip. It is found in strip rolling, particularly at thin gauges, that any crack, even minute, on the edges of the strip causes grave risk of ripping across under tension, thus reducing output and increasing cost. It would be interesting to know whether any method is adopted at Scovill to suppress edge cracking, or to remove it by a trimming process, which is not very economical, or whether the material is so good that, with the benefit of the frequent anneals which it receives, it just does not crack at all at the edges.

The annealing is carried out in a simple and quite logical manner, but there is one small practical point on which further information is desirable. The coils are passed through a roller-hearth furnace on edge. Does that have any damaging effect on the lower edge of the coils? Here again slight damage means a great deal in strip rolling. From the illustration, it appears that the

coils are simply loaded upright direct on to the rollers. Can an assurance be given that no damage is thereby caused to the metals used?

The description of the slitting machines, though not directly a metallurgical matter, is of very great interest to those who have to control the operation of a rolling mill. Could the authors confirm that no back tension, other than that from the unwinding drum, is applied as regards the lighter slitters? In the case of the heavy slitter, mention is made of a metal wiper, which is presumably there to provide a tension. Particulars of the facing and lubrication of the metal wiper would be of interest.

Another very ingenious machine is the strip-inspection machine, by which a proportion of the coils are run through and inspected, and, presumably on a statistical basis, the remainder of the product is passed, rejected, or re-inspected. That machine operates at 60-240 ft./min. What means, if any, are adopted for gauge checking?

Another interesting item is the leader bar for joining succeeding coils together in the continuous-processing machines, such as the pickling machine and the strip-inspection machine. It is possible to gather from the text an idea of how this operates, but it would be very helpful if a sketch could be added, and perhaps a little amplification of the description.

The adoption of vacuum-suction lifts is of great practical importance and seems to be the perfect solution of the problem which Scovill has to face. There are two points about this. The line of cups under the lifting beam must sometimes project beyond the end of the strip, and in such cases, some cups are rendered inoperative, either locally or from the hoist operator. Is that control automatic, or, if not automatic, is it time-consuming? Does the apparatus take effective charge of strips and slabs which might not be quite flat, but wavy, and is there any trouble with the apparatus unexpectedly letting go of the piece it is lifting?

MR. E. ROBSON \* (Member): As one who has been privileged to visit the Scovill plant and other plants in America on a number of occasions, I may be able to give some useful details. Unfortunately it is about two years since I was at Scovill, and the continuous plant there, though in course of erection, was not then in operation. I did, however, go carefully into the Company's continuous-casting practice for extruded billets and strips for strip rolling. Chrome iron was used for the pouring boxes, and also for the needle valves, but I cannot give the composition. They were quite rough castings, generally resting on a centre collar. The needles were crude, and although these plants are most marvellous engineering developments, some of the methods used for controlling the running of the metal would at first sight appear to be quite primitive. The needle valve was completely controlled by one of the operators. I think that the chrome iron feeders used lasted for about two-thirds of a shift. The plants operated on 24-hr. shifts.

With regards to the finish on the slabs, the extruded billets had quite as good a finish as the billet cast in a normal water-cooled mould. I have always found the Americans to be very particular about maintaining that finish throughout the whole of the production range. I would like to emphasize, however, that when I was at Scovill two years ago 45% of the output was being used for finishing in their own plant. They made everything from paper clips to divers' helmets. I was told that within two years they hoped to use nearly 70%. As has already been mentioned, a large part of the output is a low-leaded brass, and cold work is almost essential and always has been.

I do not know whether their automatic strip mill will develop better than their continuous billet casting, but I know that the Chase Company tried

\* General Manager, The Manganese Bronze and Brass Co., Ltd., Ipswich.

the continuous casting of extrusion billets and have given it up. I have watched the huge machine at Scovill, 120 ft. high, casting extrusion billets. It was continuous, but stoppages were quite frequent. I do not think, however, that the Americans are nearly so worried about a stoppage as are people in this country. They have very good maintenance gangs standing by to get things going again. On the other hand, the Chase Company gave it up, and I must confess that, for this form of production, I was much more impressed by a long line of beautifully designed water-cooled moulds at Chase than by the marvellous contraption at Scovill.

On p. 367 of the paper there is a schematic drawing of the slab-casting machine, from which it would appear that the holding furnace is casting direct into the mould, controlled by the needle valve. In the plants which I saw, the holding furnace was casting into a supplementary ladle, and this in turn was casting into the mould box. It is a very difficult problem to control the flow of metal direct out of the holding furnace, and much easier to regulate it when it is passing into a supplementary ladle in the way just described. Perhaps that point could be elaborated.

There is one other point which merits thought. With a continuous mill of the kind in question the storage problem is enormous, and there the Americans, with their tiered-up storage, have an advantage. The coils of strip went up and up, and this saved an enormous amount of floor space, which in America is very expensive. With these huge outputs there would have to be a tremendous revision of British ideas of how to carry stocks of material.

I think that Scovill, with a continuous output, are on the right lines in trying to use as much as possible of it within their own works, because that helps to overcome the trouble of the small order, which is everybody's bugbear.

The AUTHORS (*in reply*): Regarding the composition of the needle valve and the distributor, both are made of approximately 25%-chrome iron. Nickel must be kept at a minimum, as it has been our experience that the higher the nickel, the more rapid the deterioration. During regular operation, we chip the holding furnace once every 24 hr. In order to do this, it is necessary to tilt the furnace back to a vertical position, which, of course, interrupts the operation and raises the distributor clear of the mould. During this period the distributor is removed and replaced with a clean one. The interior of the one removed is then sand-blasted to dislodge the oxides that build up on the interior. It is then ready to be used again. The average total life of one of these distributors is 60-70 hr. of operation.

Mr. Field says: "The metal is stated to descend at anything from  $\frac{3}{16}$  to  $1\frac{3}{4}$  in./min." He probably meant per oscillation, which would be approximately correct. The surface of these bars, as cast, compares very favourably with static-mould-cast material, both with respect to the surface and the edges. The bars are rolled, as cast, from  $2\frac{1}{2}$  to 0.400 in. (with two intermediate anneals), they are then overhauled or scalped in the conventional manner. As to the possible formation of discontinuities owing to the oscillation of the mould, these do not occur during normal operation. They can be formed by stopping the mould momentarily and then starting up again; otherwise they present no problem.

The mould used in this operation is an ordinary large-diameter copper tube, purchased from one of our competitors (as we do not make large-diameter tubing) which has been re-formed to the shape of a rectangle. It is 25 in. long, while the walls are  $\frac{3}{16}$  in. thick, chromium-plated on the inside. We are not in a position to say what the ultimate life of these moulds will be. Normally we change them every 24 hr. at the same time as we change the distributor. They are then brushed and wiped clean and are ready to be put back in service. Ultimately the chromium burns off at the molten-metal line. This



occurs when the mould has cast approximately 5,000,000 lb. When this happens, the remaining chromium is stripped off and the mould re-plated. We have done this several times on different moulds and they are all still being used.

We should have been more lucid in our explanation of the probable reason for the higher efficiency of the melting furnaces. We feel that the chief reason for this is the fact that as the size of any container is increased, the increase in the volume is proportional to the cube of any dimension, while the increase in the surface area is only proportional to the square of any dimension. This means that as the size of a furnace increases, there are fewer square inches of surface per pound of metal through which it may lose its heat. Instead of saying as we did in the paper "a great amount of power is concentrated in a small space", we should have said, "a great amount of power is concentrated in a large volume relative to the area through which heat may be lost". Another element which is of considerable significance is the amount of refractory lining. The thickness of the refractory in this furnace is at least twice as great as in our ton furnaces. This fact, added to the point made above, should add up to a considerable reduction in heat losses and consequently greater operating efficiency.

Mr. Field raised a question regarding the problem of changing the middle inductor. When this inductor is changed, two inductors must be drained, putting them out of operation as he thought. However, the one inductor left is adequate to maintain a molten bath in the furnace and melt sufficient metal to satisfy the second inductor when it is rolled back beneath the metal line. The furnace is held at this position until enough metal is melted to supply the third inductor; then the furnace is rolled to its normal operating position. The power is shut off when this furnace is being poured.

Regarding any metallurgical difference in finished strip of continuous-cast versus chill-cast material, we have been unable to distinguish one from the other by any laboratory test. However, in fabricating operations which involve deep drawing, we have very concrete reasons for believing that rejects due to broken cups or shells are far less when continuous-cast material is used than in the case with material cast in either water-cooled moulds or cast-iron moulds. This result we feel is due to the almost total absence of shrinkage cavities in the continuous-cast material.

As pointed out by Mr. Field, the nature of the edges is especially important when rolling thin-gauge material. Breaks at this point can be very expensive from the angle of lost production. For this reason we trim 0.064 in. off all our bars in order to ensure sound edges at subsequent operations. To protect the edges during the annealing operations, each coil is up-ended on to a circular perforated Inconel pan on which it rides through the annealing furnace. Close examination of Fig. 10 (Plate XL) will show a lip extending around the base of each coil; that is the edge of the pan.

Regarding the operation of the vacuum-cup system, each cup has a valve located in its stem. When the length of the bar is such that the use of some cups is unnecessary, these cups are rendered inoperative by simply turning their valves. This is done by hand and takes but a fraction of a second per valve. Occasionally they do drop a bar, but this happens so seldom that it is of no significance. With respect to back-tension used on the light-duty slitters, the equipment is designed to enable us to use up to 1000 lb. Normally we operate with 250-300 lb.

## OBITUARY

### GEORGE BERNARD BROOK.

The death of Mr. George Bernard Brook occurred on 15 October 1950 at his home in Baslow, Derbyshire, 11 days after the celebration of his golden wedding. He was 77 years of age.

Mr. Brook was a son of the late Mr. Heber Alfred Brook of Messrs. Brook Bros., platers, Cambridge Street, Sheffield, and was educated at The Royal Grammar School, Sheffield. His first post after leaving school was an apprenticeship under the Sheffield City Analyst. Mr. Brook then took up a course of training in electrometallurgy at the Birmingham Central Technical College, travelling to Birmingham from Sheffield for each class—surely a very fine example for other students.

He subsequently founded (in 1910) the Department of Non-Ferrous Metallurgy in the Applied Science Department at Sheffield University, St. George's Square, where he remained as senior lecturer until 1920. During the first World War he was appointed metallurgist to the Small Arms Division of the Ministry of Munitions, in which capacity he assisted in the production of millions of cupro-nickel bullet cases each week.

In 1920 Mr. Brook joined The British Aluminium Co., Ltd., as Chief Chemist, with headquarters in Kinlochleven, Argyllshire. For the next 19 years he undertook much research work, covering all phases of aluminium production, until his retirement in 1939. At the outbreak of the last war he again took up active metallurgical work at a Royal Ordnance Factory near Crewe, investigating many metallurgical problems.

Mr. Brook's last years were spent in only semi-retirement, since even up to the time of his death he continued to act as Consultant to Messrs. D. F. Tayler and Co., Ltd., Birmingham. He had had many honours conferred on him during an active and varied career: he was an Honorary Fellow of the Royal Society of Edinburgh, a Fellow of the Royal Institute of Chemistry, and a Fellow of the Institution of Metallurgists.

Mr. Brook was an active member of the Institute, which he joined in 1910, and a regular attendant at its functions. His failing health confined him to his hotel, however, during the recent meeting at Bournemouth. He will be very greatly missed among his many friends; as a father and a scientist his life was an inspiration to all who knew him.

Mr. and Mrs. Brook had four sons, three of whom are still living.

H. H. SYMONDS.

### AUSTIN CROWTHER.

Mr. Austin Crowther of Bawtry Road, Doncaster, died at his home on 15 January, at the age of 64.

After experience with consulting metallurgists in the Midlands and metal production on Tyneside, Austin Crowther joined Peglers Ltd., brass-founders, of Doncaster, over 30 years ago, to take charge of the metal department. Here, he introduced the open-hearth reverberatory, the semi-rotary, and the electric furnaces. In 1936 he joined the Board of the Company and played a considerable part in its rapid progress. By his research and experience he made an outstanding contribution to the study of non-ferrous metal-



lurgy, and he was well known and highly respected throughout the country. He became a member of the Institute in 1914.

Mr. Crowther had a very charming personality, was an interesting conversationalist, unfailingly courteous, and of sterling character. He was a loyal comrade and friend, and his loss will be felt sorely in many circles. He was a very keen worker for the Methodist Church, and could always be relied upon to help in any good cause.

He leaves a widow and two sons, who have the sincere sympathy of a large number of friends.

A. E. EMBERTON.

#### RICHARD BANNER DEELEY.

Mr. Richard Banner Deeley, B.Sc., A.R.S.M., died at Hill End Hospital, St. Albans, on 16 October 1950 in his 50th year. His passing was a sad loss to a wide circle of business associates, a considerable number of whom were close personal friends.

Mr. Deeley was educated at St. Paul's School, and received his scientific training at The Royal School of Mines. From there he went to the British Motor Cycle and Cycle Car Research Association in 1924, where he spent about three years before joining the staff of Lightalloys, Ltd., in 1927 as metallurgist. During the 1939-45 war he occupied the position of Superintendent of Foundries, a post which he filled with considerable distinction, and in July 1948 he was appointed Technical Director of the Company, which position he held at the time of his death.

Mr. Deeley had an infinite capacity for detail, and this, combined with his deep technical knowledge and wide practical experience, made him a very valued member of numerous important technical committees dealing with aluminium and its alloys. In the aluminium foundry industry generally, he will be remembered for his considerable technical attainments, but to those who came in direct contact with him he will leave the happiest recollections of a man whose friendliness and courtesy was equalled only by his anxiety to be of service to those who so often sought his advice.

Mr. Deeley had been a member of the Institute of Metals since 1923. He leaves a widow and a son.

CHAS. J. FEAR.

#### LIEUT.-COLONEL SIR JOHN GREENLY, K.C.M.G., C.B.E.

Sir John Greenly, K.C.M.G., C.B.E., M.A., F.Inst.Met., who, at the time of his retirement owing to illness in July 1950, was Chairman of the well-known firm of Babcock and Wilcox, Ltd., died at his home near Reading on 31 December 1950, at the age of 65.

The second son of the late E. H. Greenly, J.P., D.L., of Titley Court, Herefordshire, John Henry Maitland Greenly was born on 25 July 1885. He was educated at Charterhouse and Trinity College, Oxford, receiving his early training as an engineer with the firm of Sir John Wolfe, Barry and Partners. In 1906 he was commissioned in the Herefordshire Regiment (T.F.) and promoted to Captain in 1912. He served in the 1914-18 war, being appointed to be a Staff Captain and Brigade Major in 1916 and Lieut.-Colonel in 1917. He was twice mentioned in despatches. From 1916 to 1919 he served as Assistant Controller of Inspection of Munitions of War at the Ministry of Munitions, and in 1919 he was made a C.B.E.

In 1920 he was appointed Joint Managing Director of Messrs. William

Foster, Pascoe, Grenfell and Company, copper manufacturers and smelters of London and Swansea, and subsequently Joint Managing Director of British Copper Manufacturers, Ltd. Thus began his association with the non-ferrous metals industry, which he was to serve in a most outstanding manner through his energetic work for the British Non-Ferrous Metals Research Association, of which he became Chairman in 1937, holding that position until the year 1949. For his great services to the non-ferrous metals industry he was awarded the Platinum Medal of the Institute of Metals in 1946.

In 1929 Sir John joined the Board of Directors of the firm of Babcock and Wilcox, Ltd., and it was to this great organization, with its world-wide ramifications, that he subsequently devoted so much of his energies. He was elected Chairman of the Board of Directors of that Company in 1937, in succession to the late Sir John Dewrance, and held this post with great distinction until within six months of his death. His duties with this firm took him all over the world, and he became well known and dearly loved throughout the whole of the Babcock and Wilcox organization. He was an active director of the Associated Babcock Companies in Canada, Germany, and Poland.

Through his active connection with Babcock and Wilcox, Ltd., he became keenly interested in the economic and efficient use of the world's fuel supplies, and served as President of the Institute of Fuel from 1938 to 1941, was a member of Council of the British Coal Utilization Research Association during the years 1938-46, a member of the Fuel and Power Advisory Council 1944-46, and Vice-President of the Coal Utilization Joint Council 1945-46. During the years 1942-47 he was a member of the Fuel Research Board.

Throughout his career Sir John Greenly held many posts of national importance, which reflect his great organizing ability, wide breadth of vision, and industrial experience. Thus, from 1937 to 1943 he was a member of the Advisory Council to the Committee of the Privy Council for Scientific and Industrial Research; a member of the Industrial Advisory Panel to the Air Ministry from 1938 to 1939; Chairman of the Prime Minister's Advisory Panel of Industrialists on Rearmament from 1938 to 1939, and Controller-General of the British Supply Board in Canada and the United States during 1939-40. His services to his country in this sphere of work were recognized in 1941, when he was created a Knight Commander of the Most Distinguished Order of St. Michael and St. George.

After his return from the United States at the end of 1940, he became Deputy Chairman and Administrator of the National Fire Prevention Executive and was a member of the Fire Prevention (Operational) Committee of the Ministry of Home Security.

Sir John was keenly interested in the welfare of Technical Institutions and strongly believed in the benefits which can accrue from the dissemination and discussion of technical information. He joined the Institute of Metals in 1928 and was elected a Member of Council in 1936. He served as a Vice-President from 1939 to 1942 and as President from 1942 to 1944. He was made a Fellow



of the Institute in 1947. As has already been mentioned, he also served for three years as President of the Institute of Fuel, and was a member of the Institution of Mechanical Engineers, the Institution of Engineering Inspection, and a Fellow of the Institution of Metallurgists. The prosecution of industrial research through the means of Research Associations received his strong support, as is well known from his connection with the British Non-Ferrous Metals Research Association, the British Welding Research Association, and the British Coal Utilization Research Association.

Sir John Greenly was a man of outstanding personal charm, great wisdom, and kindness, possessing a vast experience of people and affairs. His death is a great loss to his many friends, to his country, and to the industry which he served so well.

C. H. DAVY.

### ROBERT CROOKS STANLEY.

Robert Crooks Stanley, who died on 12 February 1951, was a man of outstanding accomplishments in many fields—mining, scientific, industrial, financial, and educational. He provided the leadership through which The



International Nickel Company of Canada, Ltd., has emerged as one of the world's leading mining and metallurgical enterprises. Under his guidance ores with which metallurgists had long struggled in an effort to separate the nickel contents, have been made to yield this metal in ever-increasing quantities, as well as copper, platinum, and many by-product metals. International Nickel, of which he had been President from 1922 until February, 1949, and Chairman from 1937 to the time of his death, is today the world's largest producer of nickel and the platinum metals, and is the greatest single producer of copper in the British Empire.

Mr. Stanley was born on 1 August 1876, in Little Falls, New Jersey, the son of Thomas and Ada (Crooks) Stanley. He was for

a time instructor of manual training at nearby Montclair High School to help finance his technical training at Stevens Institute of Technology in New Jersey. Mr. Stanley received a mechanical-engineering degree at Stevens in 1899, and later served as the Institute's Chairman of the Board and Trustee for fourteen years. After his graduation from the Columbia School of Mines as a mining engineer in 1901, Mr. Stanley was employed by the S. S. White Dental Company of Philadelphia to investigate platinum placer sands in British Columbia.

Upon his return from this field trip arrangements were made for him to assay samples at the precious-metals refinery maintained by a predecessor company of International Nickel at Bayonne. This proved to be his introduction to a career of almost fifty years with International Nickel.

In 1905 Mr. Stanley discovered Monel, which has since become one of the



outstanding alloys for applications where strength, corrosion-resistance, and appearance are requisites. He effected numerous advances in nickel metallurgy, and his patented refining process became the basis for recovering nickel by electrolytic refining. As General Superintendent of International Nickel's Orford Works, Mr. Stanley was successful in substantially stepping-up nickel production to meet the demands of World War I, but when he became President of International Nickel in 1922 the industry was at its lowest ebb. Up to that time nickel had been consumed principally in the manufacture of armaments. To promote industrial peace-time uses of the company's products, one of his initial efforts was the formation of a Development and Research Division, through which thousands of commercial peace-time applications for nickel were established. International Nickel thus became one of the first metal companies in North America to pursue research vigorously. It was my great pleasure to join Mr. Stanley and his associates at this time in their initial programme of research.

As a result of the rapid rate of increase in nickel consumption, the development of an adequate and dependable supply of the metal for world industry became an essential part of Mr. Stanley's programme. As early as 1924 he began to prepare his Canadian productive organization on a basis which, only a few years earlier, would have been regarded as fantastically large. A nickel mill and smelter were built at Copper Cliff, Ontario, the Frood Mine was developed into one of the world's largest mines, and an electrolytic copper refinery was built. Outstanding in this programme was the consolidation with The Mond Nickel Company, Ltd., early in 1929 to form the present International Nickel Company of Canada, Ltd.

During the six years of the Second World War, International Nickel, under Mr. Stanley's direction, produced and delivered to the Allied countries for military and essential purposes about one and a half billion pounds of nickel in all forms, together with more than one and three-quarter billion pounds of refined copper and substantial quantities of the platinum metals, so vital to modern warfare.

While meeting the war emergency, International Nickel did not relax its research efforts. In addition to assisting non-essential industries in finding substitute materials for nickel for their products during this period, under Mr. Stanley's guidance the company continued to expand its study of nickel's peace-time potentialities.

In 1937 International Nickel launched a project for the mining of the Frood-Stobie open-pit surface ores and for the construction of larger concentrating, smelting, and refining facilities to utilize these ores. This large pit of surface ores, however, will soon be mined out. In anticipation of this fundamental physical change affecting its production, the Company embarked more than ten years ago on an extended programme to replace open-pit capacity with further underground capacity. When the undertaking is completed the Company will be able to hoist 13,000,000 tons annually, and its underground mining operations will be unmatched in size by that attained by any non-ferrous base-metal mining operation in the world—a fitting monument to a far-seeing leader who piloted his organization successfully through periods of war, depression, and prosperity.

Mr. Stanley's outstanding achievements in the nickel industry brought him wide recognition in other fields. He was a director of a number of prominent United States, British, and Canadian companies and recipient of four honorary degrees in engineering, science, and law.

Among the numerous honours bestowed upon him were: the Thomas Egleston Medal of Columbia University Engineering School's Alumni Association; the First Annual Charles F. Rand Foundation Gold Medal; the American Society for Metals Gold Medal for the Advancement of Research; the Alumni

Award Medallion of the Alumni Association of Stevens Institute of Technology for his "distinguished service to the College"; the rank of Commander of the Order of Leopold by the King of the Belgians in 1937; and the King's Medal for Service in the Cause of Freedom by King George VI in 1947.

Despite his many other interests, Mr. Stanley never lost touch with research and was justly proud of the many accomplishments of International Nickel's extensive Development and Research Division. He was greatly pleased to receive the Institute of Metals (Platinum) Medal for 1948 in recognition of outstanding service to the non-ferrous industries. In expressing his pleasure to the President of the Institute, he wrote: "I wish you could include in this high honour the many technical men in my organization, who have worked hard and long to elevate this Company to its present position".

Mr. Stanley was a member of the Institute of Metals for over twenty years and we who have known him have lost an intimate friend and experienced counsellor.

PAUL D. MERICA.



## NAME INDEX.

- Abdou, Abdou Hanna.** Elected student member, xxii.
- Antelo, Héctor Francisco.** Elected member, xiii.
- Ashen, Frederick Charles.** Elected member, xiii.
- Aust, Karl Thomas.** Elected student member, xiv.
- Aytekin, V.** *See* Cottrell, A. H.
- Ballass, John Thomas.** Elected student member, xxi.
- Bartlett, Kenneth M.** Elected member, xx.
- Bertrandias, Jean Antoine George.** Elected member, xix.
- Bethune, Albert William.** Elected student member, xiv.
- Bhaduri, Sukumar.** Elected member, xiii.
- Bhatnagar, Parmatma Sarup.** Elected member, xix.
- Blade, J. C.** *See* Perryman, E. C. W.
- Bonds, John Douglas.** Elected student member, xxiii.
- Bornemann, Alfred.** Elected member, xxi.
- Bouchaud, Peter.** Elected member, xix.
- Bradley, A. J.** Discussion on "Atomic Displacements Associated with Elasticity in Plastically Deformed Metals"; "The Flow of Zinc Under Constant Stress"; "Mechanism of Primary Creep in Metals"; "The Mechanism of Creep as Revealed by X-Ray Methods"; "Some X-Ray Observations on the Nature of Creep Deformation in Polycrystalline Aluminium", 598.
- Bradshaw, Francis Julian.** Elected member, xix.
- Bramley, George Edward Arthur.** Elected member, xxi.
- Brazener, W. F.** Discussion on "The New Continuous Brass Mill of the Scovill Manufacturing Company, Waterbury, Conn., U.S.A.", 658.
- Brook, George Bernard.** Obituary notice, 665.
- Brown, Arthur James Stephen.** Elected member, xxii.
- Brown, A. R. G.** Discussion on "The Effect of Applied Load in Micro-Indentation Tests", 621.
- Brunner, Hanus.** Elected student member, xxi.
- Bunshah, Rointan Framroze.** Elected student member, xiv.
- Burns, B. D.** *See* Calnan, E. A.
- Calnan, E. A., and B. D. Burns.** Paper: "Some X-Ray Observations on the Nature of Creep Deformation in Polycrystalline Aluminium", 445.
- Campbell, Hector S.** Paper: "Pitting Corrosion in Copper Water Pipes Caused by Films of Carbonaceous Material Produced During Manufacture", 345; reply to discussion, 654.
- Cassavetes, Nicholas John, Jr.** Elected student member, xxi.
- Cesana, Giorgio.** Elected member, xix.
- Chalmers, Bruce.** *See* Thall, B. M.
- Chamberlain, Alan.** Elected member, xix.
- Chang, Wen-Hsiang.** Elected student member, xiv.
- Chaplin, Norman John.** Elected student member, xxii.
- Chaston, J. C.** Discussion on "Atomic Displacements Associated with Elasticity in Plastically Deformed Metals"; "The Flow of Zinc Under Constant Stress"; "Mechanism of Primary Creep in Metals"; "The Mechanism of Creep as Revealed by X-Ray Methods"; "Some X-ray Observations on the Nature of Creep Deformation in Polycrystalline Aluminium", 599; discussion on "The Pressure-Welding Characteristics of Some Copper-Base Alloys", 630.
- Chiaverini, Vicente.** Elected member, xiii.
- Clark, John Beverley.** Elected student member, xx.
- Clark, Robert.** Elected student member, xiv.
- Clews, C. J. Birkett.** *See* Grogan, J. D.
- Coffinberry, Arthur Shotter.** Elected member, xxi.
- Collet, Raoul.** Elected member, xxi.
- Cook, M.** Discussion on "A Method for Assessing the Relative Corrosion Behaviour of Different Sea-Waters"; "Corrosion and Related Problems in Sea-Water Cooling and Pipe Systems in H.M. Ships"; "The Jet-Impingement Apparatus for the Assessment of Corrosion by Moving Sea-Water"; "Pitting Corrosion in Copper Water Pipes Caused by Films of Carbonaceous Material Produced During Manufacture", 646.

- Cook, M., and T. L. Richards. Discussion on "The Calculation of the Activation Energies of Recovery and Recrystallization from Hardness Measurements on Copper", 611.
- Cottrell, A. H., and V. Aytakin. Paper: "The Flow of Zinc Under Constant Stress", 389; reply to discussion, 607.
- Craig, George Black. Elected member, xiii.
- Crowthor, Austin. Obituary notice, 665.
- Curlook, Walter. Elected student member, xiv.
- Daniel, Alan Raymond. Elected student member, xx.
- Danko, Joseph Christopher. Elected student member, xxii.
- Das Gupta, Dhruva Ranjan. Elected member, xix.
- Davidson, Roy Campbell. Elected student member, xxii.
- Davis, Edwin, and Eric Holmes. Paper: "The Pressure-Welding Characteristics of Some Copper-Base Alloys", 185; reply to discussion, 633.
- De Barr, Albert Edward. Elected member, xx.
- Deeley, Richard Banner. Obituary notice, 666.
- Delbart, Georges Robert. Elected member, xx.
- Dewsnap, N. See Wood, W. A.
- Dhavernas, Jean Marie. Elected member, xx.
- Dick, Alexander Walter Henry. Elected member, xix.
- Dixon, Wilfred. Elected member, xix.
- Dodworth, Alfred John. Elected member, xiii.
- Dutt, Asoke Kumer. Elected student member, xx.
- Duval, Robert. Elected member, xxii.
- Eborall, Robert Kenneth. Elected member, xxii.
- Edmonds, Vincent Louvaine. Elected member, xix.
- Edwards, Frank Fryer. Elected student member, xiv.
- Emley, E. F. Discussion on "The Constitution of Magnesium-Rich Alloys of Magnesium and Zirconium", 616.
- Evans, U. R. Discussion on "Stress-Corrosion of Aluminium-7% Magnesium Alloy"; "A Theory of the Mechanism of Stress-Corrosion in Aluminium-7% Magnesium Alloy"; "Relationship Between the Ageing and Stress-Corrosion Properties of Aluminium-Zinc Alloys", 635; discussion on "A Method for Assessing the Relative Corrosion Behaviour of Different Sea-Waters"; "Corrosion and Related Problems in Sea-Water Cooling and Pipe Systems in H.M. Ships"; "The Jet-Impingement Apparatus for the Assessment of Corrosion by Moving Sea-Water"; "Pitting Corrosion in Copper Water Pipes Caused by Films of Carbonaceous Material Produced During Manufacture", 648.
- Failoni, Vittorio. Elected member, xix.
- Fell, E. W. Discussion on "A Preliminary Study of the Solidification of Castings", 595.
- Field, A. J. Discussion on "The Pressure-Welding Characteristics of Some Copper-Base Alloys", 630; discussion on "Stress-Corrosion of Aluminium-7% Magnesium Alloy"; "A Theory of the Mechanism of Stress-Corrosion in Aluminium-7% Magnesium Alloy"; "Relationship Between the Ageing and Stress-Corrosion Properties of Aluminium-Zinc Alloys", 636; discussion on "The New Continuous Brass Mill of the Scovill Manufacturing Company, Waterbury, Conn., U.S.A.", 660.
- Fischer, Peter. Elected student member, xxi.
- Fletcher, John Thomas. Elected member, xx.
- Fox, F. A. Discussion on "The Constitution of Magnesium-Rich Alloys of Magnesium and Zirconium", 618.
- Genders, R. Discussion on "A Method for Assessing the Relative Corrosion Behaviour of Different Sea-Waters"; "Corrosion and Related Problems in Sea-Water Cooling and Pipe Systems in H.M. Ships"; "The Jet-Impingement Apparatus for the Assessment of Corrosion by Moving Sea-Water"; "Pitting Corrosion in Copper Water Pipes Caused by Films of Carbonaceous Material Produced During Manufacture", 649.
- Gifkins, R. C. Discussion on "Atomic Displacements Associated with Elasticity in Plastically Deformed Metals"; "The Flow of Zinc Under Constant Stress"; "Mechanism of Primary Creep in Metals"; "The Mechanism of Creep as Revealed by X-Ray Methods"; "Some X-Ray Observa-

- tions on the Nature of Creep Deformation in Polycrystalline Aluminium", 601.
- Gilbert, P. T., and S. E. Hadden.** Paper: "A Theory of the Mechanism of Stress-Corrosion in Aluminium-7% Magnesium Alloy", 237; reply to discussion, 641.
- Giroudot, Pierre.** Elected member, xx.
- Greenly, (Sir) John.** Obituary notice, 666.
- Greenough, G. B.** Discussion on "Atomic Displacements Associated with Elasticity in Plastically Deformed Metals", 599.
- and **Edna M. Smith.** Paper: "The Mechanism of Creep as Revealed by X-Ray Methods", 435; remarks at opening of discussion, 597; reply to discussion, 608.
- Grogan, J. D.** Paper: "The Uranium-Iron System", with an Appendix (by C. J. Birkett Clews): "An X-Ray Examination of Uranium-Iron Alloys", 571.
- Guest, Joseph Clifford.** Elected member, xxii.
- Hadden, S. E.** See Gilbert, P. T.; Perryman, E. C. W.
- Hall, W. H.** Discussion on "Atomic Displacements Associated with Elasticity in Plastically Deformed Metals"; "The Flow of Zinc Under Constant Stress"; "Mechanism of Primary Creep in Metals"; "The Mechanism of Creep as Revealed by X-Ray Methods"; "Some X-Ray Observations on the Nature of Creep Deformation in Polycrystalline Aluminium", 601.
- Hanser, Klaus.** Elected member, xxi.
- Hardy, H. K.** Paper: "The Thermodynamics and Kinetics of Precipitation in Solid Solutions", 457; discussion on "Stress-Corrosion of Aluminium-7% Magnesium Alloy"; "A Theory of the Mechanism of Stress-Corrosion in Aluminium-7% Magnesium Alloy"; "Relationship Between the Ageing and Stress-Corrosion Properties of Aluminium-Zinc Alloys", 637.
- Hebert, Robert Earl.** Elected student member, xxi.
- Hibbard, Walter R., Jr.** Paper: "Deformation Texture of Drawn Face-Centred Cubic Metal Wires", 581.
- Hoben, J. J., and J. F. Mulvey.** Paper: "The New Continuous Brass Mill of the Scovill Manufacturing Company, Waterbury, Conn., U.S.A.", 357; reply to discussion, 663.
- Hodgson, Brian John Rubery.** Elected student member, xxiii.
- Holmes, Eric.** See Davis, Edwin.
- Holst, Wilhelm.** Elected member, xxi.
- Honeycombe, R. W. K.** Discussion on "Atomic Displacements Associated with Elasticity in Plastically Deformed Metals"; "The Flow of Zinc Under Constant Stress"; "Mechanism of Primary Creep in Metals"; "The Mechanism of Creep as Revealed by X-Ray Methods"; "Some X-Ray Observations on the Nature of Creep Deformation in Polycrystalline Aluminium", 602.
- Houston, David Arthur.** Elected member, xiii.
- Hugony, Eugenio.** Elected member, xx.
- Hulme, Kenneth Gretton.** Elected student member, xiv.
- Ingham, Bertram Hobart.** Elected member, xiii.
- Jarleborg, Martin Holger.** Elected member, xx.
- Johansen, Frederick Charles.** Elected member, xx.
- Johnson, Geoffrey Alan.** Elected member, xxi.
- Jollivet, Léon.** Elected member, xiii.
- Jones, E. R. W.** Discussion on "The Effect of Applied Load in Micro-Indentation Tests", 622.
- Juett, Douglas.** Elected member, xx.
- Kay, Sydney.** Elected member, xxi.
- Kehl, George Louis.** Elected member, xiii.
- Kenaghan, Francis John.** Elected student member, xx.
- Kenworthy, L.** See Slater, I. G.
- Killingworth, Donald.** Elected member, xiii.
- Last, Anthony John.** Elected student member, xiv.
- Latin, A.** Discussion on "Atomic Displacements Associated with Elasticity in Plastically Deformed Metals"; "The Flow of Zinc Under Constant Stress"; "Mechanism of Primary Creep in Metals"; "The Mechanism of Creep as Revealed by X-Ray Methods"; "Some X-Ray Observations on the Nature of Creep Deformation in Polycrystalline Aluminium", 603; discussion on "The Pressure-Welding Characteristics of Some Copper-Base Alloys", 632.
- Lee, Morgan Hamilton.** Elected student member, xiv.

- Lehane, Thomas John. Elected member, xx.
- Lever, Reginald Ernest. Elected member, xxii.
- Livingston, John A. Elected member, xx.
- Lloyd, Lowell Thomas. Elected member, xx.
- Loveday, Kenneth William. Elected student member, xxi.
- MacKenzie, David. Elected member, xxi.
- Markin, Alan. Elected member, xxi.
- Martin, Alfred John. Elected student member, xiv.
- Mason, Henry Robert. Elected student member, xxi.
- May, R. *See* Slater, I. G.
- and R. W. de Vere Stacpoole. Paper: "The Jet-Impingement Apparatus for the Assessment of Corrosion by Moving Sea-Water", 331; reply to discussion, 654.
- Maybrey, (Mrs.) Mary Clarke. Elected member, xxi.
- Mellor, G. A. Paper: "The Constitution of Magnesium-Rich Alloys of Magnesium and Zirconium", 163; reply to discussion, 619.
- Meussner, Russel Allen. Elected member, xxi.
- Moody, John Wentworth. Elected student member, xiv.
- Mulvey, J. F. *See* Hoben, J. J.
- Murad, Abu Bakr. Elected student member, xx.
- Nourse, John Dudley. Elected member, xxii.
- Old, Bruce Scott. Elected member, xx.
- O'Neill, H. Discussion on "The Effect of Applied Load in Micro-Indentation Tests", 626.
- Owen, Charles Penrhyn. Elected member, xxii.
- Pearson, Thomas Gibson. Elected member, xx.
- Penman, Robert Roland. Elected student member, xx.
- Peretti, Ettore A. Elected member, xiii.
- Perkins, Raymond Frank. Elected student member, xxi.
- Perryman, E. C. W. Paper: "Use of Diamond Dust for Polishing Metallographic Specimens of Non-Ferrous Metals and Alloys", 61.
- and J. C. Blade. Paper: "Relationship between the Ageing and Stress-Corrosion Properties of Aluminium-Zinc Alloys", 263; reply to discussion, 641.
- Perryman, E. C. W., and S. E. Hadden. Paper: "Stress-Corrosion of Aluminium-7% Magnesium Alloy", 207; reply to discussion, 641.
- Pfeil, P. C. L. Paper: "The Constitution of Uranium-Molybdenum Alloys", 553.
- Phailbus, Theodore. Elected member, xx.
- Phillips, V. A. Discussion on "The Calculation of the Activation Energies of Recovery and Recrystallization from Hardness Measurements on Copper", 611; discussion on "The Pressure-Welding Characteristics of Some Copper-Base Alloys", 633.
- Phragmén, Gösta. Paper: "On the Phases Occurring in Alloys of Aluminium with Copper, Magnesium, Manganese, Iron, and Silicon", 489.
- Preston, Bryan Wentworth. Elected member, xxii.
- Quadt, Raymond A. Elected member, xxii.
- Randle, Keith Charles. Elected junior member, xxii.
- Reiter, Stanley F. Elected student member, xx.
- Richards, T. Ll. *See* Cook, M.
- Richards, William Gwynfab. Elected member, xiii.
- Richardson, W. H. Discussion on "A Method for Assessing the Relative Corrosion Behaviour of Different Sea-Waters"; "Corrosion and Related Problems in Sea-Water Cooling and Pipe Systems in H.M. Ships"; "The Jet-Impingement Apparatus for the Assessment of Corrosion by Moving Sea-Water"; "Pitting Corrosion in Copper Water Pipes Caused by Films of Carbonaceous Material Produced During Manufacture", 650.
- Ridley, Norman. Elected student member, xiv.
- Ridley, R. W. *See* Thorpe, P. L.
- Robson, E. Discussion on "The New Continuous Brass Mill of the Scovill Manufacturing Company, Waterbury, Conn., U.S.A.", 662.
- Rogers, T. H. Reply to discussion on "A Method of Assessing the Relative Corrosion Behaviour of Different Sea-Waters", 654.
- Rostoker, W. Paper: "The Effect of Applied Load in Micro-Indentation Tests", 175; reply to discussion, 628.



- Roxbee Cox, H. May Lecture: "Industrial Gas Turbines", 287.
- Ruddle, R. W. Paper: "A Preliminary Study of the Solidification of Castings", 1; reply to discussion, 596; paper: "Correlation of Tensile Properties of Aluminium Alloy Plate Castings with Temperature Gradients During Solidification", 37.
- Samuels, L. E. Discussion on "The Effect of Applied Load in Micro-Indentation Tests", 626.
- Scarrott, Derrick Ronald. Elected student member, xiv.
- Scharschu, Charles A. Elected member, xiii.
- Scrutton, R. F. *See* Wood, W. A.
- Seaton, Raymond. Elected student member, xxii.
- Sheppard, Norman John. Elected member, xxii.
- Signora, Mario. Elected member, xxi.
- Slater, I. G., L. Kenworthy, and R. May. Paper: "Corrosion and Related Problems in Sea-Water Cooling and Pipe Systems in H.M. Ships", 309; reply to discussion, 655.
- Slocombe, Harry Eric. Elected member, xxii.
- Slooff, Arnout. Elected member, xxii.
- Smith, Edna M. *See* Greenough, G. B.
- Smith, Robert. Elected member, xxii.
- Smurthwaite, John William. Elected member, xiv.
- Solomon, John Graham. Elected member, xxiii.
- de Souza Santos, Tharcisio D. Elected member, xiv.
- Stacpoole, R. W. de Vere. *See* May, R.
- Stanley, Robert Crooks. Obituary notice, 668.
- Sully, A. H. Discussion on "Atomic Displacements Associated with Elasticity in Plastically Deformed Metals"; "The Flow of Zinc Under Constant Stress"; "Mechanism of Primary Creep in Metals"; "The Mechanism of Creep as Revealed by X-Ray Methods"; "Some X-Ray Observations on the Nature of Creep Deformation in Polycrystalline Aluminium", 604.
- Swaroop, M. Elected member, xxii.
- Sykes, Elwyn Charles. Elected student member, xiv.
- Symonds, John. Elected student member, xiv.
- Tasker, H. S. Presidential Address, 99.
- Taylor, A. Paper: "Lattice Parameters of Binary Nickel-Cobalt Alloys", 585.
- Teghtsoonian, Edward. Elected student member, xiv.
- Thall, Burnett M. Elected member, xiv.
- and Bruce Chalmers. paper: "Modification in Aluminium-Silicon Alloys", 79.
- Thompson, P. F. Discussion on "Stress-Corrosion of Aluminium-7% Magnesium Alloy"; "A Theory of the Mechanism of Stress-Corrosion in Aluminium-7% Magnesium Alloy"; "Relationship Between the Ageing and Stress-Corrosion Properties of Aluminium-Zinc Alloys", 639.
- Thompson, Thomas. Elected member, xxi.
- Thorley, N. Paper: "The Calculation of the Activation Energies of Recovery and Recrystallization from Hardness Measurements on Copper", 141; reply to discussion, 613.
- Thornely, Bernard Norman Heath. Elected member, xiv.
- Thornton, Philip Challis. Elected student member, xxi.
- Thorpe, P. L., G. R. Tremain, and R. W. Ridley. Paper: "The Mechanical Properties of Some Wrought and Cast Aluminium Alloys at Elevated Temperatures", 111.
- Timm, Harold A. Elected member, xx.
- Tipton, Clyde Raymond. Elected member, xxii.
- Tranier, Jean Lucien Marcel. Elected member, xxii.
- Trela, Edward. Elected member, xiv.
- Tremain, G. R. *See* Thorpe, P. L.
- Tucker, Herbert John Charles. Elected member, xiv.
- Tylecote, R. F. Discussion on "The Pressure-Welding Characteristics of Some Copper-Base Alloys", 631.
- de Vere Stacpoole, R. W. *See* May, R.
- Vernon, W. H. J. Discussion on "A Method for Assessing the Relative Corrosion Behaviour of Different Sea-Waters"; "Corrosion and Related Problems in Sea-Water Cooling and Pipe Systems in H.M. Ships"; "The Jet-Impingement Apparatus for the Assessment of Corrosion by Moving Sea-Water"; "Pitting Corrosion in Copper Water Pipes Caused by Films of Carbonaceous Material Produced During Manufacture", 651.



- Wagstaff, Raymond Claude. Elected member, xxiii.
- Walker, David Gaston. Elected student member, xxiii.
- Walters, B. Discussion on: "The Flow of Zinc Under Constant Stress", 606.
- Wauchope, Kenneth Laird. Elected member, xiv.
- Weinberg, Fred. Elected student member, xiv.
- Winegard, William Charles. Elected student member, xiv.
- Winston, John Stanton. Elected member, xxi.
- Wood, W. A. Discussion on "Atomic Displacements Associated with Elasticity in Plastically Deformed Metals"; "The Flow of Zinc Under Constant Stress"; "Mechanism of Primary Creep in Metals"; "The Mechanism of Creep as Revealed by X-Ray Methods"; "Some X-Ray Observations on the Nature of Creep Deformation in Polycrystalline Aluminium", 606.
- Wood, W. A., and N. Dewsnap. Paper: "Atomic Displacements Associated with Elasticity in Plastically Deformed Metals", 65; reply to discussion, 609.
- and R. F. Scrutton. Paper: "Mechanism of Primary Creep in Metals", 423; reply to discussion, 609.
- Wormwell, F. Discussion on "A Method for Assessing the Relative Corrosion Behaviour of Different Sea-Waters"; "Corrosion and Related Problems in Sea-Water Cooling and Pipe Systems in H.M. Ships"; "The Jet-Impingement Apparatus for the Assessment of Corrosion by Moving Sea-Water"; "Pitting Corrosion in Copper Water Pipes Caused by Films of Carbonaceous Material Produced During Manufacture", 653.
- Wright, John Charles. Elected student member, xiv.

PRINTED IN GREAT BRITAIN BY  
RICHARD CLAY AND COMPANY, LTD.,  
BUNGAY, SUFFOLK.

